SOME PIECES OF MY JOURNEY

From my Initial Commitments to my Current Situation

Une vie ne vaut rien, mais rien ne vaut une vie

André Malraux

Volume 1 to Volume 5

Pedro S. Sêco E Pinto

To all my Friends

2024

PREFACE

Biographies of important geotechnical figures are few and far between. Examples are Richard Goodman's excellent volume on Karl Terzaghi, Judith Nieschcial's biography of her father, Sir Alex Skempton, Peter Scarle's book on the Hungarian Karoly Szechy, the volume on Laurits Bjerrum, edited by Kaare Flaate, Elmo DiBiaggio and Kare Senneset, and the volume on Victor de Mello, edited by his son, Luiz Guilherme.

Autobiographies of such figures are even more rare, and I am aware of only two, one by Geoffrey Meyerhof, and the other by T. William Lambe. Both of these have not been published in book form and so are not generally available to the public. Therefore, this present offering by Pedro Seco e Pinto, which I will refer to as a "Memoir", is a welcome addition to this very small body of literature. Although he states that it was not his intention to write an autobiography, he has in fact done just that, and has provided us with a remarkably detailed and interesting history of his evolution from a schoolboy to one of the world's leading geotechnical personalities. The level of detail can be judged by the fact that the memoir is composed of five volumes, which are as follows:

1. From his initial commitments to his current situation.
2. Participation in conferences and meetings.
3. Touring lectures and international seminars.
4. Engineering projects.
5. Selected papers.

What strikes the reader is the remarkable level of detail with which his activities are described. There are many photographs of various aspects of his life, including with his parents and his family, with many other distinguished colleagues, and also with many items of memorabilia from conferences and meetings. Indeed, he has even kept name tags from the conferences he has attended, and one can only marvel at his ability to collect, classify and curate such an impressive array of memorabilia.

It is clear that Pedro has a love of travelling and his attendance at 133 conferences must be a candidate for the Guinness Book of Records! The many photographs from these travels must bring back many happy memories, and for the reader, seeing some of the past giants of our profession provokes bitter-sweet memories of persons who have influenced our profession. Another unique feature of the memoir is the 55 pages of messages from Pedro's colleagues around the world, a measure of the admiration and respect he has enjoyed from his peers during his career.

During his Presidency of the International Society for Soil Mechanics and Geotechnical Engineering (ISSMGE) in the period 2005-2009, Pedro initiated the ISSMGE Bulletin, and set up the Society's own journal, the International Journal of Geotechnical Case Histories. The Bulletin celebrating the 75th anniversary of the Society was a particularly important historical document, as it set out in some detail the history of the Society to the year 2011.

A notable feature of Pedro's career is his commitment to promoting geotechnical activities in developing countries. Volume 3 of his memoir, prefaced by appropriate quotes from both Buddha and Socrates, sets out a remarkable catalogue of visits and lectures to 21 countries that he delivered or organized over a period of 13 years, from 2006 to 2019. Were it not for the Covid virus, this number would no doubt have increased in the succeeding 4 years. One can only speculate how many frequent flyer points he accumulated while undertaking these immensely valuable trips.

The book "A Short History of Western Thought", written by Stephen Trombley, discusses the relationship between science and philosophy, and states: "Philosophy ignores science at its peril, and science without philosophy would lose its way Philosophy provides the questions science tries to answer, and it provides the tools with which those answers are judged". There are two main views on philosophy; one states that knowledge can be gained only by reason, the other that it relies on empirical evidence. In our small corner of science, geotechnical engineering, it has become clear that we rely both on reason and empirical evidence to gain knowledge. We use reason to develop a theory, and then judge this theory by undertaking experiments which provide empirical evidence to support or refute this theory. Pedro's memoir amply demonstrates the application of this dual philosophical approach in his work, and how the theories developed by reason and confirmed by experiment, can be applied to solve real-world problems. It is not only Pedro's knowledge of

philosophy, and its application, that is impressive, but also his knowledge of literature and poetry, in multiple languages. He particularly delights in quoting relevant pieces of poetry to illustrate and bring home the points he makes during his lectures.

Readers of Pedro's memoir cannot but be impressed by the broad range of projects, research topics, geographical adventures, and literary and philosophical musings that it offers. It reflects a life that has clearly been both diverse and stimulating, one that has been of great service to his profession, and one that has engendered a remarkable number of friendships around the world. Long may he continue to contribute his talents to his family, friends, and to the geotechnical profession.

Harry G. Poulos

March 2024

INTRODUCTION

It is not my intention to write a self-biography, because my contribution is very modest and humble in comparison with the lives of politicians and scientists, really giants, that have changed the world.
I tried to make the things better, considering that innovating, growth, evolution and reinvention sustain the life. "*Ad astra per espera*".

I would like to take this opportunity to thank for your great support, for the joy and the happiness that I have lived.
My debt of gratitude is huge.
The life gave me much more that I have deserved and my great sadness is that I was not able to reciprocate in the same scale.

My only purpose is to thank, to honor, to show my gratitude, to stress and to remember the important role of several persons.
Without your support, effort and time this wonderful journey would not be possible.

I decided to compile some pieces of my journey in simple words, and for a better clarification and reading is organized in 5 Volumes.

Volume 1 covers my roots in Goa-India, my secondary education in Lourenço Marques/Mozambique, the quadrilateral Africa/Europe/Asia/ America where I developed my high education, my first steps in professional practice, the entities to whom I worked, namely the industry activity during the period 1971-1972, the army service in Massingir dam (Mozambique), from 1972-1974, my activity at the National Laboratory of Civil Engineering (LNEC) during the period of 1975 to 2005, my involvement with the University teaching from 1977 to 2018, my interaction with the Portuguese Geotechnical Society (SPG) since 1976, my relationship with the Portuguese Institute of Engineers (Ordem dos Engenheiros) since 1972.

My involvement with the International Society for Soil Mechanics and Geotechnical Engineering (ISSMGE), since 1981, in different positions, such as member of Technical Committee, Chairman of Technical Committee, Vice President for Europe, President, Immediate Past President and Appointed Board Member is described. It presents also a brief description how ISSMGE operates.

This Volume ends with some closing remarks and thanks.

Volume 2, divided in 2 Parts due to the extension, describes more than 133 Conferences that I had the privilege to participate in different roles, namely Invited Lecturer, State of the Art Lecturer, General Report, Chairman, Advisory Committee Member, Organizing Committee Member, Delegate with paper, and the lessons that I have learned from this very rich experience.
In a world that moves in the direction of the global village it is very important the universality of the knowledge and the need for a permanent renewing. It is important to communicate, to share experiences, to compare methodologies and to monitor the results. The benefits of an open dialogue between academicians, researchers, practitioners, contractors and owners are huge.

Volume 3 deals with 54 Touring Lectures/International Seminars that I had the privilege to coordinate, with the purpose to divulge the developments on soil mechanics and geotechnical engineering for the Member Societies of developments countries in Africa, Asia, Europe and South America Regions. There are no words to express the support, the generosity and the co-operation that I have received from several experts, colleagues, friends and entities.
I will summarize this rich experience in the following words:
There is still much darkness in the world. But trust me, there is also more light in it than ever. So many people have come to realize that we can curse the darkness or we can have the courage to be one who lights a candle.

We want all of you to make part of our community, to promote our growth and to make you feel that you are contributing for our dream come true.
I enjoy interacting with people, because I believe when people like me, know me and trust me they will help me with new ideas and interesting insights.
I was asked Pedro what keeps you going? What is the source of your energy? Who inspires you? My answer was You. Thank you for the privilege to work together.

Volume 4 is related with the professional practice and describes 28 engineering geotechnical projects that I have selected from 207 projects (consultant activity) that I was involved during my career.
The following issues were covered: laboratory tests, in situ tests, geotechnical design, soil dynamics and earthquake engineering, numerical methods, constitutive laws, quality control, ground improvement, retaining walls, underground structures, maritime structures, environmental studies, embankment dams, power plants, bridge foundations, building foundations, highways, risk analysis and monitoring and safety evaluation.
This Volume combines the theoretical developments of modeling with the applications for geotechnical projects calibrated by performance behavior under static and seismic actions.
In order to turn the reading more attractive a summary of the history of soils mechanics is included, as well a description of recent earthquakes.
We should not forget that failure is an essential ingredient for high achievement. We cannot win without leaving our safety zone and taking calculated risks. The most risks we take to pursuit our dreams, the more we are going to fail. But we should not forget there is nothing so useless as doing efficiency that which should not be done.
I consider that failure helps us to get closer to our dreams, equipped us with more knowledge and that success and failure go hand in hand.
The error shows us the truth, but we should explore carefully this practice.

Volume 5 integrates 17 Papers that I have selected from my list of publications and deserve more divulgation, that cover a large spectrum of topics, namely: Ground Characterization, Embankment Dams, Bridge Foundations, Buildings Foundations, Landslides, Tunneling, Earthquake Engineering, Solid Waste Landfills, Harbour Structures, Eurocodes and Education.

All the 5 Volumes end with some personal comments that shows my way of living and reflecting engineering.

For writing these notes I had to make some options, maybe you agree or disagree, but I ask for your indulgence.
I believe that the graduate students and the young engineers will find some interest in Volume 4 and in Volume 5.
The most senior engineers will re-visit their contributions for ISSMGE and some episodes that they lived when reading the Volume 1 to Volume 3.
Volume 2 and Volume 3 are very easy and light to read, as they are based in photographs, with short legends, to give the possibility to use your imagination when re-visiting those places and remembering your role in those events.

I remind the memorable lines of T.H. Huxley:
"The known is finite
The unknown is infinite
Intellectually we are in the middle of an islet
Surrounded by an immense ocean of inexplicability.
Our business in each generation is to
Reclaim a little more land
To add something to the extent and solitude of our possessions".

The fifth dimension is only possible when the knowledge is raised to a level of the unity of vibration.
Ars longa vita brevis (Seneca).

To all of you my deep gratitude for the kindness, generosity, inspiration and friendship and my thanks for this memorable adventure.

INDEX

Volume 1 — Some Pieces of my Journey - **From my Initial Commitments to my Current Situation**

1. INTRODUCTION ……..2
2. Where All has Begun – Goa/India/Asia……3
3. Secondary and High Education - Lourenço Marques/Mozambique/Africa/Europe/America ……8
4. INDUSTRY ACTIVITY (1971-1972) ……..……..15
5. ARMY SERVICE (1972-1974) ……...18
6. LNEC ACTIVITIES ……28
7. UNIVERSITY ACTIVITIES ……53
8. PORTUGUESE INSTITUTE OF ENGINEERS ….....63
9. SPG - PORTUGUESE GEOTECHNICAL SOCIETY ……..66
10. ISSMGE ACTIVITIES ……..76
10.1. Technical Committees ……77
10.2. Positions ……..82
10.2.1. ISSMGE VP (for Europe) -2001-2005 ……82
10.2.2. ISSMGE President (2005-2009) ……108
10.2.3. IMMEDIATE PAST PRESIDENT (2009-2013) ……159
10.2.4 Appointed BOARD MEMBER (2017-2022) ……174
10.3. INTERNATIONAL CONFERENCES ……182
10. 4. REGIONAL CONFERENCES ……184
10.5. YOUNG GEOTECHNICAL ENGINEERS - The ISSMGE FUTURE ……184
10.5.1. Introduction ……184
10. 5.2. Civil Engineering Education ……185
10. 5.3. Young Geotechnical Engineers Conferences ……188
10. 5.4. My thoughts expressed during IYGEC and RYGEC ……190
10.6. OTHER INTERNATIONAL CONFERENCES ……192
10.7. MEETINGS WITH MEMBER SOCIETIES and GEOTECHNICAL GROUPS ……193
10.8. ISSMGE BULLETIN ……193
10.9. ISSMGE JOURNAL ……198
10.10. ISSMGE – 75 Years Celebration ……199
10.11. TOURING LECTURES/INTERNATIONAL SEMINARS ……205
10.12. Some Challenges ……...206
11. RELATIONSHIP WITH SISTER SOCIETIES AND OTHER SOCIETIES ……207
FEDIGS
12. HTC (HERITAGE TIME CAPSULE) ACTIVITIES ……..219
13. HONNORS AND AWARDS ……..221
14. CONSULTING ACTIVITIES ... …….222
15. SELECTED PAPERS ……228
16.FAMILY EPISODES … ……228
17. CLOSING REMARKS and THANKS ……245
ANNEX 1. CURRICULUM VITAE ……247
ANNEX 2/ Awards and Honors ……284
ANNEX 3 / Statements/ National and International colleagues ……302
ANNEX 4 – Obituary ……360

Volume 2 - SOME PIECES OF MY JOURNEY- **PARTICIPATION IN CONFERENCES AND MEETINGS**.....

1.List of the Conferences..... 366
2.ISSMGE (International Society Soil Mechanics and Geotechnical Engineering) Conferences..... 373
12 th ICSMGE – Rio de Janeiro, 1989.....
13 th ICSMGE – New Delhi, 1994.....
14 th ICSMGE – Hamburg, 1997.....

15 th ICSMGE – Istanbul, 2001 .....
16 th ICSMGE Osaka, 2005 .....
17th ICSMGE – Alexandria, 2009 .....
18th ICSMGE – Paris, 2013 .....
19th ICSMGE – Seoul, 2017 .....
3.Other ISSMGE Conferences 404
4. Other International Conferences 575
5.Miscellaneous Conferences 659
6.Final Remarks..... 726
Annex 1 729

Volume 3 - SOME PIECES OF MY JOURNEY -**TOURING LECTURES - INTERNATIONAL SEMINARS**

1. Introduction …...737
2.Touring Lectures/International Seminars …… 740
3.List of Lectures -Curriculum and Photos …….747
4.Period 2006-2009 …….783
5.Period 2010-2013 …….917
6.Period 2018-2019 ……934
7.Final Remarks ……941

Volume 4 – SOME PIECES OF MY JOURNEY - **ENGINEERING PROJECTS**

1. Introduction ……. 945
2. History of Soil Mechanics and Geotechnical Engineering – Brief Summary 946
3. Background of Earthquakes..... 959
4. Liquefaction Assessment 1007
5. Risk and role of Geotechnics in the Society.....1033
6. Geotechnical Projects……...1064
7. Dams Engineering ……...1071
8 Case History Nº 1 - Jambi-ia- Oma Dam (Angola) ……..1151
Case History nº 2 - Keddar Dam (Argélie).....
Case History nº 3 - Kerrada Dam (Argélie).....
Case Histoty nº 4 - Koudiat Ben Aida Dam(Argelie).....
Case History nº 5 - Moamba-Major Dam (Mozambique) .....
Case History nº 6 - Mapai Dam (Mozambique) .....
Case History nº 7- Kolombizo Dam (Malawi) .....
Case History nº 8 - Sabugal Dam(Portugal) .....
Case History nº 9 - Borde Seco e Las Cuevas Dams (Venezuela) .....
Case History nº 10 - Odelouca Dam (Portugal).....
Case History nº 11 - Tapada de Outeiro powerplant 1371
Case History nº 12 - Carregado Powerplant.....
Case History 13 - Sines Powerplant .....
Case History 14 - LARES Powerplant .....
Case History nº 15 - Edifício Kilamba (Angola) – with Alexandre Pinto (JetSj) .....
Case History nº 16 - Building Foundations -Assessment of Liquefaction .....
Case History 17 - Bata Quay (Guine Ecuatorial) .....
Case History nº 18 - MARINA EXPO (with Alexandre Pinto and Rui Tomasio (JetSj).....
Case History nº 19 - Odelouca tunnel.....
Case History nº 20 - Metro of Porto .....
Case History nº 21 - AlbufeiraTunnel 1531
Case History nº 22 – Portinho Tunnel .....
Case History nº 23 - Vasco de Gama Bridge (Portugal).....
Case History nº 24 - Leziria Tagus River Crossing (Portugal).....

Case History nº 25 - Leixões Portaria.....
Case History nº 26 - Grandola landfill (with L. Lopes & A. Mendonça).....
Case History nº 27 - Evora- Estremoz branch .....
Case History nº 28 - ETAR-Water treatment - Vila Franca 1591
FINAL REMARKS ……. .....…….1600……
Annex 1 – Site Investigation
1641……Annex 2 - Anch1706
Annex 3 Foundation movements ……..1724

Volume 5 SOME PIECES OF MY JOURNEY - SELECTED PAPERS – 1729
- Ground Characterization- 14 th Danube Conference- Invited Lecture …….1731

- 12 Th SZECHY Memorial Lecture, Budapest -Dam Engineering – New Challenges
- 20th Chin Lecture-2010 -1Lessons Learned FROM Dams Behavior under earthquakes
- 4th International Case History Conference, 1998-St. Louis), USA, State of-the Art Lecture
A Recent Difficult Foundation Problem: The Case Of The New Tagus Bridge…….1830
- 3rd Victor de Mello Lecture – 2019- delivered in Goa- India,
- 9th Sukle Lecture, Lublijana, 2008 - Landslides Analysis under Static and Seismic Conditions
……..1896
- Nonveiller Lecture - New Trends In Tunnelling Engineering - Croatia, ……1934
- International Conference on Environmental Geotechnics, Lisbon, 1998, ISSMGE TC 5
Seismic Behaviour of Solid Waste Landfills
- V Earthquake Geotechnical Engineering Conference -2011- Santiago de Chile
STATIC AND SEISMIC ANALYSYS OF SOLID WASTE LANDFILLS - SOA Lecture…..1981
-3rd International Conference on Earthquake Engineering - Berkely-2004 -Special Presentation
CONTROL OF VIBRATIONS CAUSED BY UNDERWATER BLASTING
- International Conference on Earthquake Engineering -Tokyo-2009
Seismic behaviour of geotechnical structures. Past, Present and Future
- Klaipeda Seminar- 2019 - Bata Quay Wall Design-Invited Lecture

- ISSMGE International Seminar – Kuala Lumpur, 2011 Rehabilitation and Reinforcement of Marina EXPO Breakwaters and Quay Wall – Invited Lecture

- XII ECSMGE -Amsterdam-1999 Eurocodes 7 & 8-Special Presentation
- International Conference Gifu (Japan) – 2008 -Interaction between Eurocode 7 – Geotechnical Design and Eurocode 8 – Design for Earthquake Resistance of Foundations
- First Conference on Education in Geotechnical Engineering, Romania (2000).
Education in earthquake geotechnical engineering. Practice and Needs.
- Pan American International Conference on Education (2007 -Havana, Cuba
Futuro da Educación en Europe – Invited Lecture…… 2107

EDUCATION

1965 - 1971 - Licentiate in Civil Engineer (6 years course) (with honors).
1975 - 1977 - Master of Soil Mechanics (with honors)
1979 - 1983 - Specialist in Geotechnique (Ph.D. level) (with honors)
1992 – Director of Research (Full Professor level) (with high honors)

POSITIONS

- ISSMGE Board Member (2017-2022)
- ISSMGE Immediate Past President (2009-2013)
- ISSMGE President (2005-2009)
- ISSMGE Vice President for Europe (2001-2005)
- Full Professor of Geotechnical Engineering of University of Coimbra.
- World Bank Consulting for Dams Safety (2013-2015).
- Invited Professor of Master Courses "Soil Mechanics" and "Engineering Geology" of New University of Lisbon (1983-1995).
- United Nations Consulting for Design and Instrumentation for Dams (1988-1992).
- Invited Guest Lecturer of University of California, USA, (1992-1994).
- Chairman of TC4 "Earthquake Geotechnical Engineer "Committee of ISSMGE (1994-2000).
- President of Portuguese Geotechnical Society (1996- 2000).

Professional Experience

Consulting Engineer of 450 major projects in Dams, Power plants, Bridges, Tunnels, Waste landfills, and Quay Walls, in Portugal, Angola, Argelia, Brazil, Cabo Verde, China, Dominican Republic, Ecuador, Guinea- Bissau, Guinea Equatorial, India, Lebanon, Malawi, Morocco, Mozambique, Senegal, Syria, Tunisia, Uganda, Venezuela and Zambia, covering field and laboratory testing, dynamic analyses, earthquake engineering, numerical analyses, ground improvement, slopes, special foundations, instrumentation and safety evaluation.

Conferences

He has presented more than 350 State-of-the Art Lectures and Special Lectures in 80 countries of the 5 Continents.

Awards and Honours

He has received more than 50 international Awards including American Biographical Institute USA, "Special Volume for the Contributors of Earthquake Engineering, Nagadi Lecture by Indian Geotechnical Society, Széchy Lecture by Hungarian S M Society and Hungarian Academy of Sciences, Nonveiller Lecture- by Croatia Geotechnical Society, Sukle Lecture by Slovenia Soil Mechanics Society, Chin Lecture by Huanzhou University (China), Qian Jia Huan Lecture by Hohai University (China), Chin Fung Kee Memorial Lecture by Institute of Engineers of Malasia, Braja Das Lecture and Victor de Mello Lecture by the Indian Geotechnical Society.

Editorial Boards and Reviewer

- Editor of International Journal of Case Histories
- Co-editor of Geotechnical and Geological Engineering Journal, Springer Publisher
- Member of Editorial Board of several Journals, namely "Geotecnia", "Bulletin of Earthquake Engineering", "Acta de Geotecnia", "International Journal of Geotechnical Engineering".
- Editor of Proceedings of 4 International Conferences.

Publications

He is author or co-author of 500 Technical and Scientific Reports, more than 180 papers for national and international conferences and journals and has contributed to 14 books.

pinto.pss@gmail.com

Volume 4

ENGINEERING PROJECTS

Single Notes

Pedro S. Sêco E Pinto

2024

Arabic Proverb

He who knows not, and knows not that he
Knows not - he is a fool, shun him.
He who knows not, and knows that he
Knows not - he is a simple, teach him.
He who knows, and knows not that he
Knows - he is asleep, wake him.
He who knows, and knows that he knows,
He is wise, follow him.

1. Introduction

A poem begins in delight
And ends in wisdom

Robert Frost

I must confess that I have faced several dilemmas to write this Volume 4- Engineering Projects, namely: (i) what is the interest? (ii) what is the target public? (iii) how to summarize projects with volumes of hundreds of pages? (iv) how to turn the reading of the volume attractive?
My final decision was based to honor and to show my gratitude to several entities that gave me the opportunity to show the beauty of the professional practice.
In addition, the graduate students and the young geotechnical engineers may find some benefit and some source of inspiration when they are initiating their geotechnical projects.
To turn this volume attractive, I used several photos. The majority of the photos are from my personal archive, but a few are from websites and I submit my deep thanks to the authors and also my apologies for not having the opportunity to show personally my dept of gratitude.
Following the challenges that always the geotechnical engineer is facing I believe that I have taken the most representative samples. Maybe, I failed in my purpose and so I asked for your indulgence.
This Volume integrates 8 Chapters and 3 Annexes.
Chapter 1 is an introduction,
Chapter 2 presents a brief summary about the History of Soil Mechanics and Geotechnical Engineering.
Chapter 3 address the lessons learned from recent earthquakes.
Chapter 4 analyses the mechanisms of liquefaction, following their important role in the consequences of the earthquakes.
Chapter 5 discuss the risks and role of geotechnics in the society.
Chapter 6 introduces the geotechnical projects that I was involved.
Chapter 7 address dams engineering, as this was one the favorite topic of my activity.
Chapter 8 analyses 28 Case Histories covering different geotechnical projects.
At the end some final remarks, new challenges and my vision -lessons for tomorrow are presented.
In additions, there are 3 Annexes.
The Annex 1 addresses the specifications for Site Investigation Works and Testing.
The Annex 2 presents foundations movements.
The Annex 3 describes anchors tests.

2. History of Soil Mechanics and Geotechnical Engineering – Brief Summary

"Discovery consists of seeing what everybody

Has seen and thinking what nobody has thought "

(A.Szent-Gyorgoyi, American Scientist, 1971)

2.1 Introduction

I was involved in the amazing history of Engineering and particularly of Engineering Geotechnical, with all their ingredients of intelligence, talent, adventure, pain, spirit of sacrifice and also days of joy and happiness.

This story, since the Egyptians, shows periods of greatness, rise and decline, developments in a discontinuous pattern along the times.

Some of the referred persons in this narrative belongs to the History, or because they are not physically with us, or due to their achievements they have gained the statute of immortality.

2.2 The Beginning

Ancient civilizations have settled along the banks of rivers, such as the Nile (Egypt), the Tigris and Euphrates (Mesopotamia), the Yellow River (China), and the Indus (India). Dykes dating back to about 2000 B.C. were built to protect the people (see Figure 2.1).

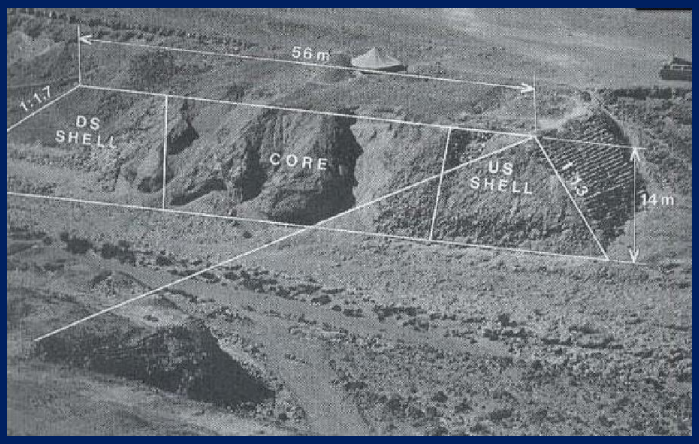

Figure 2.1 The Sadd-el-Kafara Dam photo (from Schnitter courtesy of A.A. Balkema)

Many dykes were built for irrigation purposes, but there is no reliable information about the measures to reinforce the foundations or to protect against the erosion.

In Egypt several pyramids were built in Egypt, by the Pharaohs as tombs with innovative solutions to overcome problems related foundations, slope stability and underground chambers.

In China around 70 A.D., several pagodas were constructed with challenge problems related foundations.

In Mesopotamia, near the Euphrates River the foundations of the monuments were reinforced with mats.

Ancient Greek civilization used isolated pad footings and strip-and-raft foundations for building structures.

The roman arches are well known and still actually we can find some examples.

The Caravan Bridge shown in Figure 2.2, located in Turkey, built by the Romans in 3rd century AD, with 200 m long and a span of 7 m, is still in operation today.

Figure 2.2 View of Caravan Bridge

China is well known for the developments of soil compaction techniques.

The heterogeneity of the foundation material, as well the geometry of the soil layers has caused differential settlements and tilting and leaning Pisa tower is well known.

2.3 First Steps on Soil Mechanics

The first theory on earth pressure was proposed by Henri Gautier (1660–1737) and was adopted by military engineers, In 1729, Bernard de Belidor (1671–1761) extended the theory, which was presented in 1717 by Gautier, for the lateral earth pressure for retaining walls.

Charles Augustin Coulomb (1736– 1806), known from his famous law, where he describes the electrostatic force of attraction and repulsion. In this procedure, Coulomb utilized the laws holding for cohesion and friction of solids. This is one of the earliest published theories in soil mechanics, where the concepts of active and passive pressure are presented. Coulomb is considered as a pioneer in the area of geotechnical engineering for his contribution in the analysis of retaining walls.

In 1820, an extended Coulomb's theory on the active earth pressure of a cohesive fill and also short-term stability of excavated clay slopes, appeared by Henri Navier (1785–1836).

Jean Poncelet (1788–1867), extended Coulomb's theory and define graphically the magnitude of lateral earth pressure on both vertical and inclined retaining walls. Also, he addressed the ultimate bearing capacity for shallow foundations,

William Rankine (1820–1872), analysed the earth pressures and also the stability of retaining walls, in a simple way than Coulomb theory.

Otto Mohr improved Coulomb's theory of impulses, one hundred years later, and developed graphically a 2 D stress-strain situation, introducing the famous Mohr's circle. Both theories were combined later in the well-known theory of Mohr-Coulomb.

Darcy based in the results of laboratory tests in sands defined the well-known hydraulic conductivity for soil, coefficient of permeability k, important soil parameter, in 1856.

Joseph Boussinesq (1842–1929) developed a theory about the way that the stresses distribution in areas under loading in a homogeneous, isotropic, elastic and semi-infinite medium. He computed both the stresses and displacements of the elastic field.

Albert Atterberg (1846–1916) was a Swedish soil scientist and chemist, defined, around in 1908, the clay-size fractions as a by weight percentage of particles, the size of which is less than 2 microns. In 1911, he correlated the cohesion of cohesive soils with the water level of the clay, and defined the limits of shrinkage, plastic and liquid and also defined the index of plasticity as the difference between the limits of plastic and liquid.

W. Fellenius (1876–1957), was involved in studies of the stability of dams and slopes. He extended the 2 D method of slip circle to both cohesive soils and soils with friction and cohesion and proposed for foundations the concept of the safety factor.

However, each of these periods was marked by significant experimental work that was preceded or accompanied by the development of theories that were the necessary tools for engineers in the design and construction of their works. It is therefore scientifically logic to collect measurements and observations, without which progress could not be made.

Leonard Cooling (1903-1977) was the founder of british soil mechanics. Cooling's first degree was in physics, and his early years at the Building Research Station (BRS) were spent in the Physics and Chemistry Divisions, where he worked on the capillary properties of porous materials and on the weathering of building stone.

2.4 Modern Times

The founder of modern soil mechanics Karl Terzaghi (1883–1963) was a brilliant, fearless and enthusiastic man with exemplary work habits: objective, rational, a clear independent thinker, capable of long days and continuous hard work, with high level of intellectual honesty, a sharp observer.
NGI has the privilege of being the custodian of the Terzaghi Library with the largest collections of original manuscripts that documents the birth of a scientific specialty.

Alain Skempton from UK has introduced pore pressure parameters A and B.
Related the history of engineering, Skempton focused on steam engine technology, to a rigorous academic discipline, challenging orthodox assumptions. His major contribution was the study the work of civil engineers, of the eighteenth century. His outstanding ability to reduce a problem to its essentials, independent the type of the work. He was not content to accept what he was told, but he was asking penetrating questions to reach ultimate conclusions and to form his own opinion.

Arthur Casagrande was the inventor of an ingenious worldwide soil testing apparatus, along with fundamental research on seepage and liquefaction.
Arthur Casagrande has said that his interests, in order of their importance, were research, teaching, and practice.

Laurits Bjerrum, former NGI Director, was particularly known by his research on the shear resistance of clays. The various geological processes which can take place with time in the normally-consolidated marine clays, the changes of the geotechnical properties. the effects on the settlement of buildings. The processes considered are: leaching, delayed consolidation, exchange of cations on clay minerals, and bonding of the clay structure by precipitation of cementing agents. The process of delayed consolidation is dealt with in detail.

Ralph Peck worked very closed with Karl Terzaghi. His role related the Chicago underground is very well known.
He has introduced the Observational Method in his famous Rankine Lecture in 1969.
Ralph has been a prolific writer and speaker by his writings and lectures. He is indeed a true master in the art of communication and to transmit his thoughts in a clear, concise and logical manner to any audience, orally or in writing.

The above five mention names were the initial ISSMGE Presidents, from 1936 to 1973.

“The Measurement of Soil Properties in the Triaxial Text” by A. W. Bishop and B. J. Henkel (Arnold, London) in 1957, is very popular. He worked at Imperial College London and was well known for the Bishop's Simplified Procedure to assess slopes stability.

‘Ken’ Harry Roscoe (1914–1970) gave a considerable contribution in critical state models, namely the cam clay model. He has explored the simple shear test and extended the use of triaxial tests.

2.5 Some Ground Improvement Techniques

2.5.1 Surface compaction

Figure 2.3 Surface compaction

2.5.2 Vibrocompaction

This technique consists in the introduction of larger vibrators placed with a certain spacing, performing soil densification to greater depths (Figure 2.4).
This technique was introduced in USA in 1948, and had a growth during 1970´s and 80´s.

Figure 2.4 Vibrocompaction

2.5.3 Dynamic compaction

This technique was proposed by Menard and in this method longitudinal waves, surface waves and transverse waves are created in the soil. The hammer is dropped from a crane and the impact spread over the soils to be processed (Figure 2.5).

Figure 2.5 Dynamic compaction

2.5.4 Electro -osmosis

In this method two electrodes are introduced in the soil and when direct current is connected the pore water begins to move from the anode towards the cathode (Figure 2.6). Due to this physical effect the zone near the anode with low pressure increases with time and with the consolidation of the soil there is an increase of soil strength and a decreased of the compressibility. The electro-osmotic permeability of different soils is very similar, the installation of electrodes is simple and the cost of this technique is low.

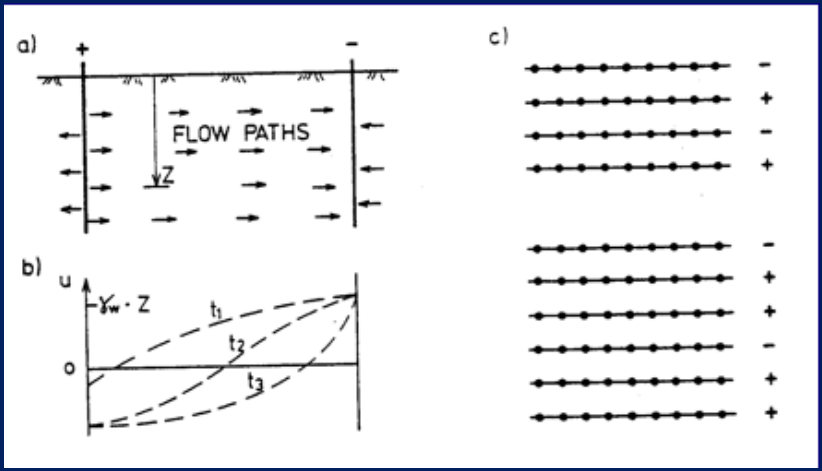

Figure 2.6 Electro-osmosis

2.5.5. Light Weight Materials

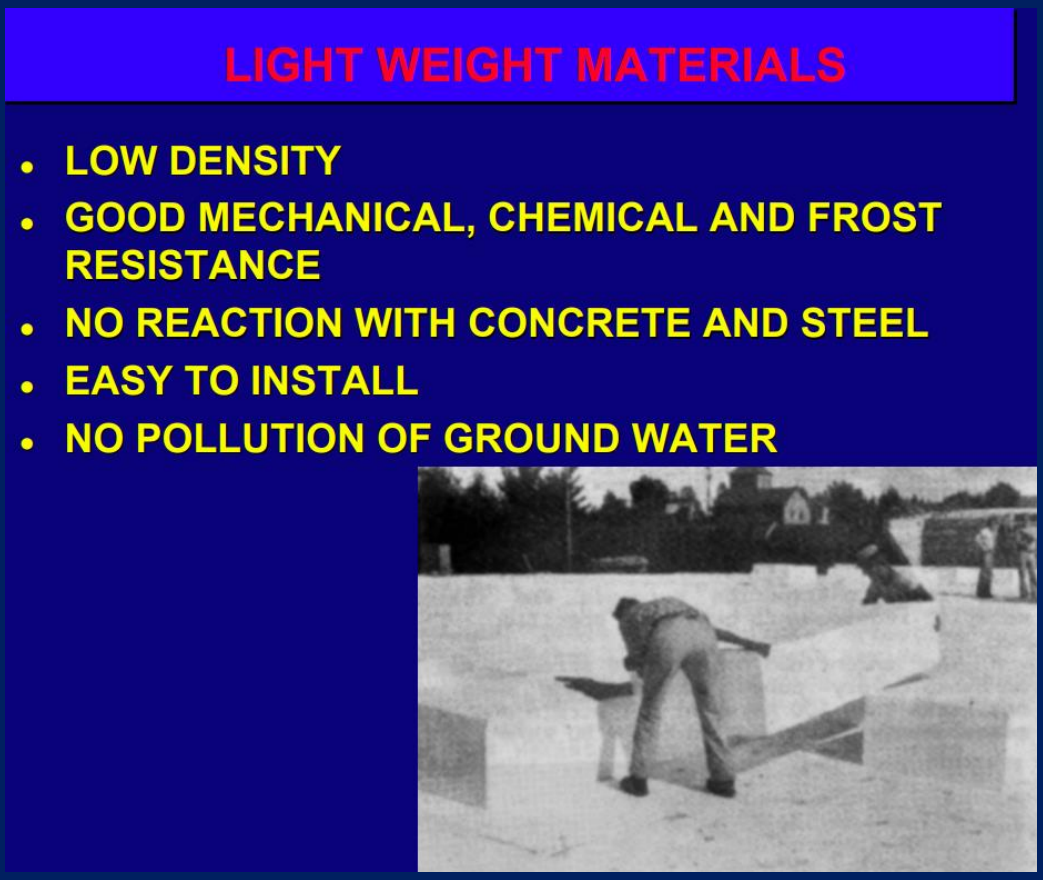

Figure 2.7 Light weight materials

2.5.6 Chemical treatment

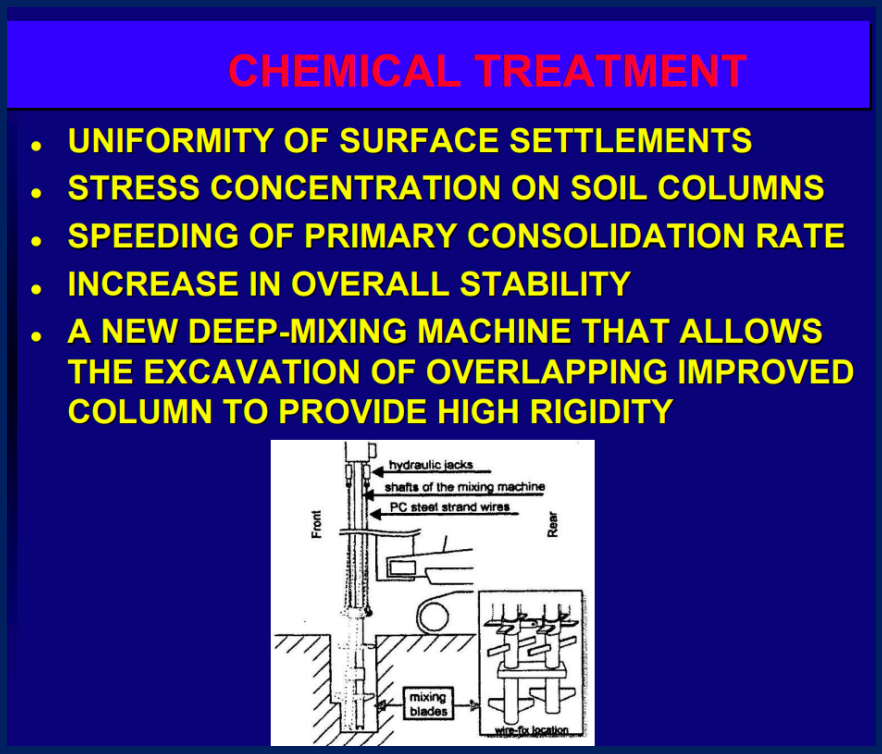

Figure 2.8 Chemical treatment

2.5.7 PVD (Prefabricated vertical drains)

The drains were used to accelerate soil consolidation, to decrease the settlement time, to increase the strength of soft soils (see Figure 2.9). This technique was developed in early 1930´s and was popular in Sweden, Japan and USA.

Figure 2.9 PVD

.

2.5.8 Jet grouting

This technique was developed in Japan in Japan in 1973 and spread to Europe and USA. This technique consists in introducing hydraulic energy to erode the soil and to substitute by an engineering grout to form a solidified concrete column (Figure 2.10).

Figure 2.10 Jet grounting

2.5.9 Micropiles

This technique was conceived in Italy in 1952 by Fernando Lizzi and consists in a small diameter bored, grouted in place pile, with a steel reinforcement (Figure 2.11). The pile can withstand axial and lateral loads. The Federal Highway Administration develop a programme in 1993 to review micropile practice, and also it is important to refer the French research project FOREVER.

Figure 2.11 Micropiles

2.5.10 Ground anchors

This technique consists of a steel bar grouted in a drilled hole and subsequently tensioned to provide lateral or vertical to resist the movements (Figure 2.12). This technique has been used since 19th century and pre-stressed anchors since 1934.

Figure 2.12 Ground anchors

2.5.11 Soil nailing

This technique consists of reinforcement the ground introducing passive inclusions, very closed, to increase the overall soil resistance and to control the displacements (Figure 2.13). It is important to refer to the project CLOUTERRE 1991 developed in France.

Figure 2.13 Soil nailing

2.5.12 Geosynthetics

These materials are manufactured polymer transported to the site and carefully placed.
The current types are: geotextiles, geogrids, geonets, geomembranes geosynthetic liners and geocomposites (Figure 2.14).

Since the advent of geosynthetics in 1970 they are gaining increase attention.

Figure 2.14 Geosynthetics

2.5.13 Stone columns

This technique consists of a penetration of the vibrator to the required depth, the granular material is introduced in the space between vibrator and the annular space and gets down to the tip of the vibrator, where the compaction is performed. The vibrator is then slowly lifted up and down, with little vertical movements, to compact the granular material and to build the stone column (Figure 2.15).

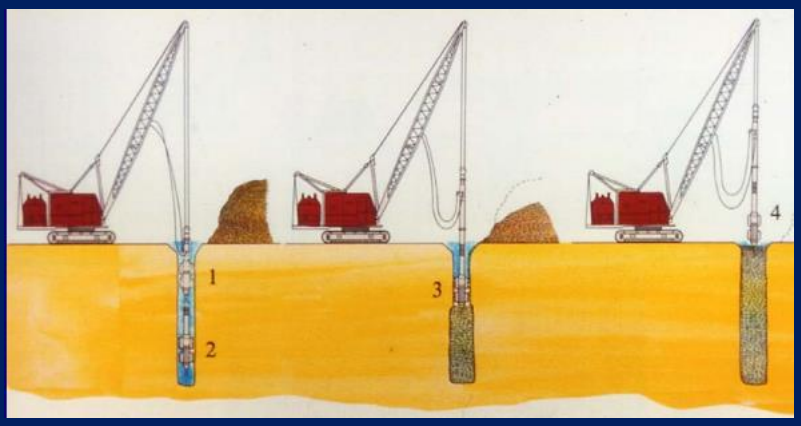

Figure 2.15 Stone columns

2.5.14 Compaction Grouting

This technique has used to improve ground strength and to control ground improvements. There are three modes: (i) permeation grouting in which the grout fills soil pores with no change of volume; (ii) displacement grouting in which a stiff mixture fills voids and compress the surrounding soil, (iii) encapsulation in which natural fragment ground is injected by grout which coats but does not permeate the individual chunks of soil (Figure 2.16).

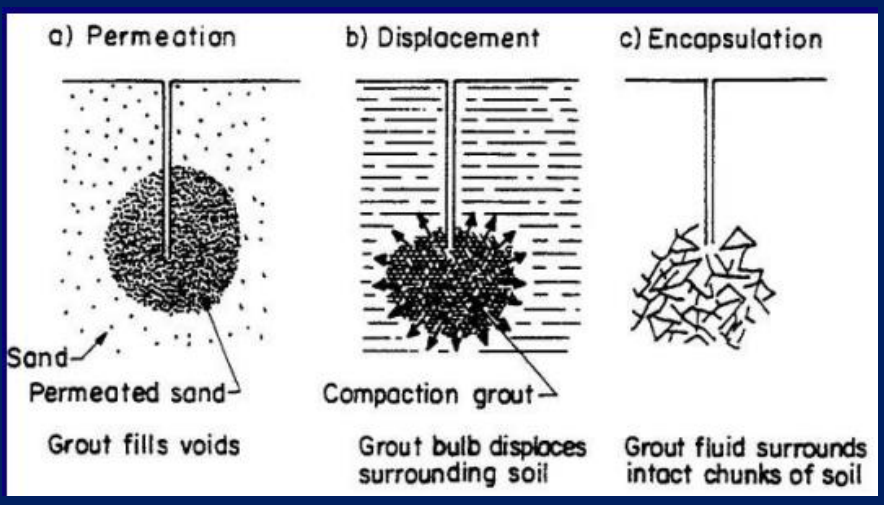

Figure 2.16 Compaction grounting

2.5.15 Reinforced earth

This method was invented by Henry Vidal in early sixties and has three major components: reinforcement, backfill and facing elements (Figure 2.17). The reinforcement materials can be metallic and non metallic and can exhibit the following geometries: strips, sheets, rods and fibers. The granular material used in the embankment aims stress transfer, durability and drainage requirements. Facing elements are used to retain fill material and to prevent erosion of steep faces and in general include precast concrete panels, prefabricated metal sheets and plates, gabions, shotcrete, etc.

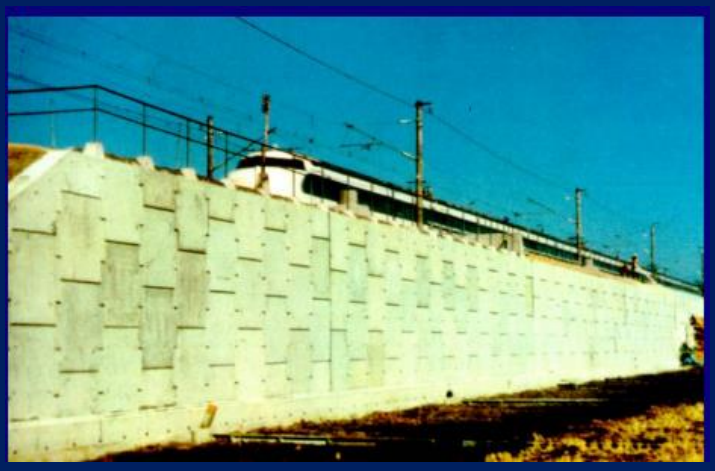

Figure 2.17 Reinforced earth

2.5.16 Blasting

This technique is used to compact loose cohesionless soil layers, saturated with water. The procedure consists: (i) drilling a borehole with bentonite or introducing a casing to the desired depth; (ii) placement of the charge; (iii) backfilling the hole; and (iv) detonation of charges in a carefully sequence (Figure 2.18).
The shock waves generated by blasting provoke the destruction of the initial structure and create a liquefaction condition followed by a rearranging of the particles in a denser packing.

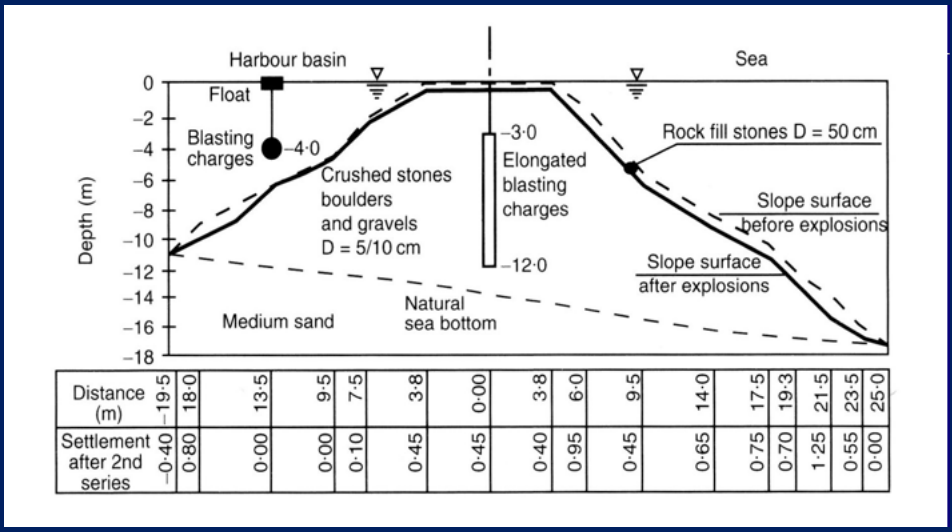

Figure 2.18 Section. Icici breakwater (near Rijeka), Croatia, 1989 – Arrangement of the blasting charges and settlement cross-(after Dembicki, 2005)

2.5.17 Biological reinforcement

This treatment is related with the use of calcifying bacteria with the objective of soil consolidation, in order to create a cementation between the grains of soil skeleton increasing the cohesion (Figure 2.19).

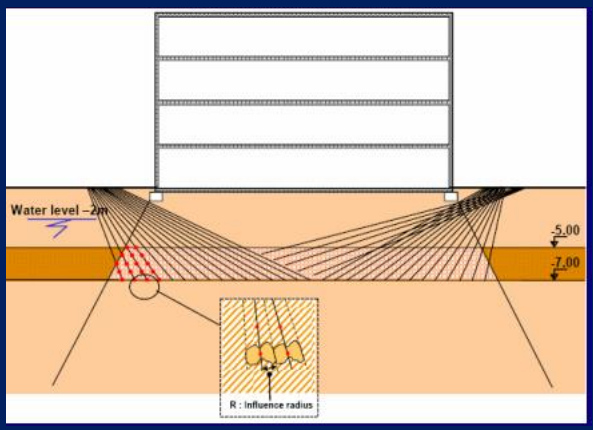

Figure 2.19 Biological reinforcement

2.6 Ethics and Philosophical Approach - Nicomaqueia and Vitruvius

The Philosophy has influenced all the Sciences and its influence in the intellectual formation was absolutely at the beginning, for centuries, and now is relative.

Within this framework the Engineering has explored the Applied Philosophy, using the Ethics and the moral and social principles as driven forces.

This brief item introduces how the ethics in engineering was addressed in the past by the philosophers.

Ética Nicomaqueia written by Aristoteles (year 334 BC) is a set of 10 Books and should be called the character study: the topics are devoted to the man character that we should cultivate and praise or avoid and condemn.

The Book nº I cover the human good and the use of our capacities. A deep discussion of our virtualities is performed in Books nº II to nº IV.
Bokk nº V is devoted to justice.

The Book nº VI covers the virtuality's of thinking, the scientific knowledge, the wisdom, and the comprehension.
The Book VII discuss the nature and value of joy, that is again discussed in Book nº X.

2000 years ago, the Roman architect Marcus Vitruvius Pollio (1st century BC) wrote the ten books on architecture that were translated into many languages. The book offers design principles and is considered as a green pattern book.

A Green Vitruvius is a reference for architects to design and realize sustainable buildings and offers recommendations in the areas of energy and water inputs, materials, indoor air quality and wastes.

The practicing architect has competency in a myriad of areas: building planning, aesthetics, construction technology, programming, building regulations and has to compatibilize the budget, programme, site and timescale.

The information is organized in four independent parts. The sections' structure advice in accordance with the design and construction process, the issues to be considered in green design, the strategies to be adopted and the elements of green design. A fifth section advises on design evaluation.

3. Lessons Learned from Recent Earthquakes

"There `s a fount about to stream
There `s a light about to beam,
There `s a flower about to blow
There `s a warmth about to glow,
There ´a midnight darkness changing
Into grey,
Men of thought and men of action,
Clear the way"

(Charles Mackay, Clear the way)

3.1. Introduction

From the natural hazards it is important to stress that earthquakes play an important role (Figures. 3.1 and 3.2).

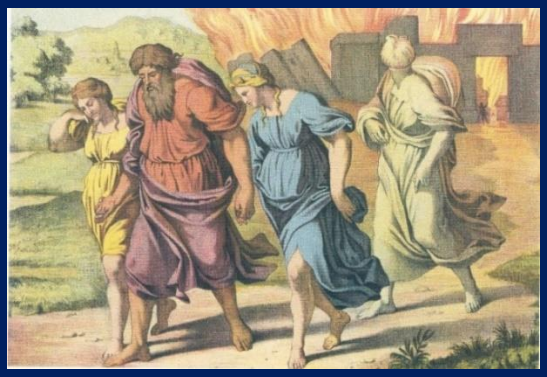

Figure 3.1 Sodoma earthquake

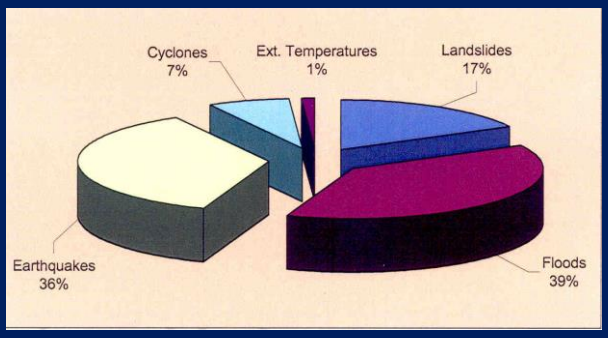

Figure 3.2 Casualties for natural hazards

According to Aristotle (384-322 B.C.) in his book Meteorologica earthquakes were produced by the dried exhalations (spirits or winds) in caves inside the earth which trying to escape make the earth shake

Martin Lister in England and Nicolas Lemery in France in 17th century were the first to propose that earthquakes were produced by large explosions of inflammable material formed by a combination of sulfur, coal, niter and other products accumulated in the interior of earth (Udias and Arroyo, 2005). The explosive theory was also proposed by Newton`s Optics (1718).

In France the world was considered a good place in which everything that happened was viewed to be “for the best” and earthquake was considered with optimism. Voltaire in his novel Candide presented a hard attack to this optimistic view point. Also, Kant and Rosseau defended the optimist position.

The Neotectonics is introduced, the earthquake occurrence is referred, the list of countries stroked by earthquakes is presented and the lessons learned by some important earthquakes are addressed.

3.2 Neotectonics

The tectonic conditions should include tectonic mechanisms, location and description of faults (normal, stryke and reverse) and estimation of fault activity (average slip rate, slip per event, time interval between large earthquake, length, directivity effects, etc.), these factors are important to assess the involved risk.

Determination of neotectonic activity implies first the qualitative geomorphologic analysis of air photos and topographic maps. The GPS system is another powerful means of monitoring the crustal mobility.

The following classification for slip rates: extremely low too low for 0.001 mm/year to 0.01 mm/year, medium to high 0.1 mm/year to 1 mm/year and very high to extremely high 10 mm/year to 100 mm/year.

The most dangerous manifestation concerning the landfill stability and integrity is the surface fault breaking, intersecting the landfill site.

The current practice is the deterministic approach in which the seismic evaluation parameters were ascertained by identifying the critical active faults which show evidence of movements in Quaternary time.

Following (ICOLD, 1989) an active fault is a fault, reasonably identified and located, known to have produced historical fault movements or showing geologic evidence of Holocene (11 000years) displacements

and which, because of its present tectonic sitting, can undergo movements during the anticipated life of man-made structures.

To assess if there is the potential for a significant amount of surface displacement beneath the dam several backhoe trenches are excavated with 3 to 4 meters deep and 30 to 50 meters long and should be inspected and log the exposures geologic features.

Recently a fault investigation method other than trenching has been developed, called the long Geo-slicer method in which long iron sheet piles with a flat U-shaped cross section are driven into an unconsolidated bed, iron plate shutters are inserted to face these iron sheet piles and the piles and shutters are pulled out to take undisturbed samples of strata of a certain width.

This method is advantageous in regard to the ease of securing land for conducting investigations compared with trenching and the ease of bringing the strata samples back to the laboratory for detailed observations (Tamura et.al, 2000).

When active faults are covered with alluvium geophysical explorations such as seismic reflection method, sonic prospecting, electric prospecting, electromagnetic prospecting, gravity prospecting and radioactive prospecting can be used (Takahashi et al., 1997). Of these the seismic reflection method can locate faults if geological conditions are favourable, and confirm the accumulation of fault displacements based on the amount of displacements in strata that increases with strata age.
The tectonic conditions should include tectonic mechanisms, location and description of faults (normal, stryke and reverse) and estimation of fault activity (average slip rate, slip per event, time interval between large earthquake, length, directivity effects, etc.), these factors are important to assess the involved risk.

Determination of neotectonic activity implies first the qualitative geomorphologic analysis of air photos and topographic maps. The GPS system is another powerful means of monitoring the crustal mobility.

Cluff et al. (1982) have proposed the following classification for slip rates: extremely low too low for 0.001 mm/year to 0.01 mm/year, medium to high 0.1 mm/year to 1 mm/year and very high to extremely high 10 mm/year to 100 mm/year.

3.3. Earthquake Occurrence

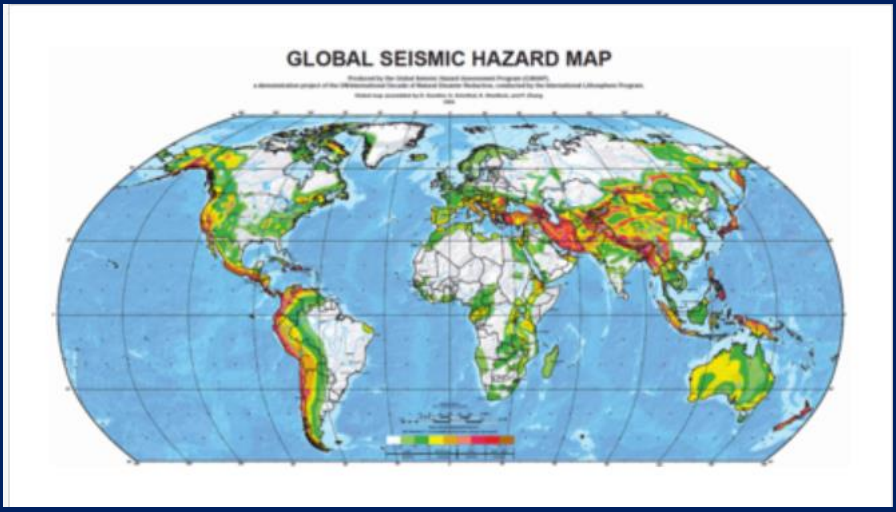

Figure 3.3 Global Seismic Hazard Map

The Global Seismic Hazard Assessment Program was a project by the United Nations that assembled the first consistent, worldwide map of the threat of earthquake shaking (Figure 3.3).

3.4 List by Country with Earthquake Occurrence

The following is the list by countries with earthquake occurrence:

Afghanistan, Albania, Algeria, Argentina, Armenia, Australia, Azerbaijan, Bangladesh, Bosnia and Herzegovina, Brazil, Bulgaria, Canada, Chile, China , Colombia, Costa Rica, Croatia, Cuba, Cyprus, DR. Congo, Dominican Republic, East Timor (Timor Leste), Ecuador, Egypt, El Salvador, Eritrea, Ethiopia, France, Georgia, Germany, Ghana, Greece, Guatemala, Haiti, Iceland, India, Indonesia, Iran, Israel, Italy, Japan, Jordan, Kosovo, Kazakhstan, Kyrgyzstan, Lebanon, Malaysia, Mexico, Morocco, Myanmar, Nepal, Netherlands, New Zealand, Nicaragua, Pakistan, Palestine, Panama, Papua New Guinea, Peru, Philippines, Portugal, Romania, Russia, Saudi Arabia, Slovenia, South Africa, South Korea, Spain, Syria, Taiwan, Tajikistan, Thailand , Turkey, United Kingdom, United States , Venezuela, Yemen.

3.5. Some Important Earthquakes – Lessons Learned

3.5.1. Great 1906 San Francisco Earthquake, 5:12 AM - April 18, 1906

Figure 3.5 San Francisco City Hall after the 1906 Earthquake. (from Steinbrugge Collection of the UC Berkeley Earthquake Engineering Research Center)

The California earthquake of April 18, 1906 ranks as one of the most significant earthquakes of all time, with a rupture around 477 kilometers of the San Andreas fault. The earthquake exhibits large horizontal displacements. Indeed, the significance of the fault and recognition of its large cumulative offset would not be fully appreciated until the advent of plate tectonics more than half a century later.

At almost 5:12 a.m., a foreshock occurred with sufficient force to be felt widely throughout the San
Francisco Bay area and the great earthquake broke some 20 to 25 seconds later, with an epicenter near San Francisco, with violent shocks which lasted some 45 to 60 seconds.

Figure 3.5 illustrates the buildings damages.

3.5.2. Ecuador-Colombia Earthquake (1906)– 8.8

The Ecuador-Colombia earthquake of 1906, with a magnitude 8.8, was a powerful earthquake that occurred on January 31, 1906, along the border between Ecuador and Colombia.
The earthquake caused significant damage, with many buildings being destroyed and also landslides.

The death toll from the earthquake is estimated to be around 1,000 people.
The Ecuador-Colombia earthquake was caused by the movement of the South American Plate and collision with the Nazca Plate and triggered several aftershocks.

cowith the Nazca Plate and generated several aftershocks.

3.5.3 Kamchatka, Russia Earthquake, 1952,

On November 4, 1952, a huge earthquake, magnitude 9, struck off the coast of Kamchatka
Peninsula, and produced a great destructive Pacific-wide tsunami with waves up to 15 meters which caused extensive damage to the Kamchatka

Peninsula and the Kuril Islands and an estimative of 10,000 to 15,000 people dead. The waves traveled as far as Peru, Chile and New Zealand.

3.5.4 Valdivia Earthquake (1960)

Valdivia Earthquake known as the Great Chilean earthquake, 9.5 magnitude it was the most powerful earthquake ever recorded. The earthquake hit on May 22 in the afternoon, approximately 100 miles (160 km) off the coast of Chile, parallel to the city of Valdivia. It lasted approximately 10 minutes and triggered a massive tsunami with waves up to 25 meters (82 feet).

Figure 3.6. Buildings damages

9.2 Magnitude, United States, Alaska. It is the largest earthquake ever recorded in North America and the second largest in history, behind only the 1960 Valdivia earthquake. 131 people were killed, all but nine died from the tsunami.
Figure 3.6 shows the buildings damages.

3.5.6 San Fernando earthquake, USA, 1971

The 1971 San Fernando earthquake occurred in the early morning of February 9 in southern California with a magnitude of 6.5, duration of 12 seconds, with casualties between 58-65 and injured persons between 200-2,000.
Severe damages occurred in San Fernando Valley and surface faulting was extensive to the south of the epicenter in the mountains, as well in the city.

Figure 3.7 illustrates the failure of upstream shell of San Fernando dam.

The death toll of 1960 Valdivia Earthquake is not certain and the number of fatalities has been estimated between 1,000 and 6,000.

3.5.5 Anchorage earthquake, USA, 1964, March 27

Figure 3.7 San Fernando dam

3.5.7 Loma Prieta earthquake, USA, 1989

On October 17, 1989, the San Francisco Bay area of USA was hitted by the Loma Prieta earthquake. The magnitude 6.9 quake was the most powerful since several years.
The Loma Prieta earthquake was triggered by the San Andreas Fault, and Pacific plate moved northwestward and the epicenter slipped up to two meters.
The Loma Prieta earthquake caused 63 deaths, 3,757 injuries, and several damages in transportation routes.

Figure 3.8 shows ground damages provoked by liquefaction.

Figure 3.8 Liquefaction damages

3.5.8 Kobe earthquake, Japan, 1995, January 17

Figure 3.9 Quay wall damages

6,434 people were killed, 43,792 injured and extensive damage occurred in the Kobe area and on Awaji-shima. About 310,000 people were evacuated to temporary shelters. Over 200,000 buildings were damaged or destroyed. Numerous fires, gas and water main breaks and power outages occurred in the epicentral area.
Figure 3.9 illustrates quay wall damages.

3.5.9 Bhuj earthquake 2001, India, January 26,

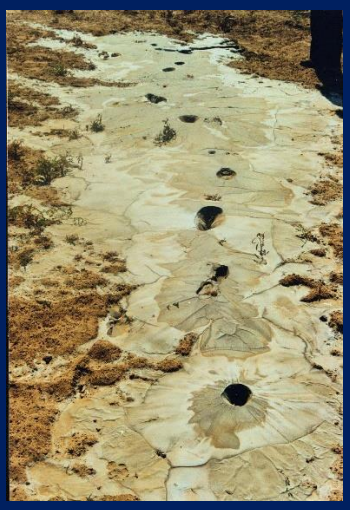

Figure 3.10 Sand boiling

7.7 magnitude, India, 20,085 people were killed, 166,800 people were injured and over a million buildings damaged or destroyed, this was the 3rd largest earthquake in India since 1900.

Figure 3.10 shows the occurrence of sand boiling.

3.5.10 Bande Aceh, Indonesia, 2004, December 26

Figure 3.11 Effects of the tsunamis

On 26 December 2004, at 07:58:53 local time (UTC+7), a major earthquake with a magnitude of 9.1–9.3 M_w struck with an epicenter off the west

coast of northern Sumatra, Indonesia. A rupture of the fault between the Burma Plate and the Indian Plate has triggered the earthquake

A massive tsunami with waves up to 30 m (100 ft) high, devastated communities in 14 countries along coasts of the Indian Ocean, killing an estimated 227,898 people. The devasting effects of the tsunamis are illustrated in Figure 3.11. Is

considered as one of the deadliest natural disasters in recorded history

3.5.11 Haiti Earthquake, 2010, January 13

The earthquake hit at 4:53 PM some 15 miles (25 km) southwest of the Haitian capital of Port-au-Prince. The geographical setting is shown in Figure 3.12. The initial shock registered a magnitude of 7.0 and was soon followed by two aftershocks of magnitudes 5.9 and 5.5. The Haitian government's official count was more than 300,000 and hundreds of thousands of survivors were displaced.

Figure 3.13 illustrates the provoked damages.

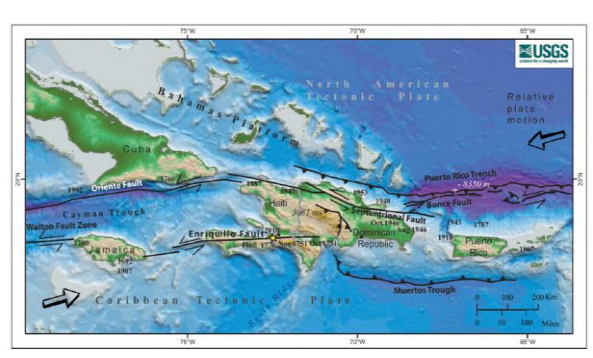

Figure 3.12 Geographical setting (adopted from USGS)

Figure 3.13 Box culvert

The occurred landslides are shown in Figure 3.14.

The buildings damages are illustrated in Figure 3.15.

The earthquake has provoked significant damages in port structures and pedestrian bridge (see Figure 3.16 and Figure 3.17).

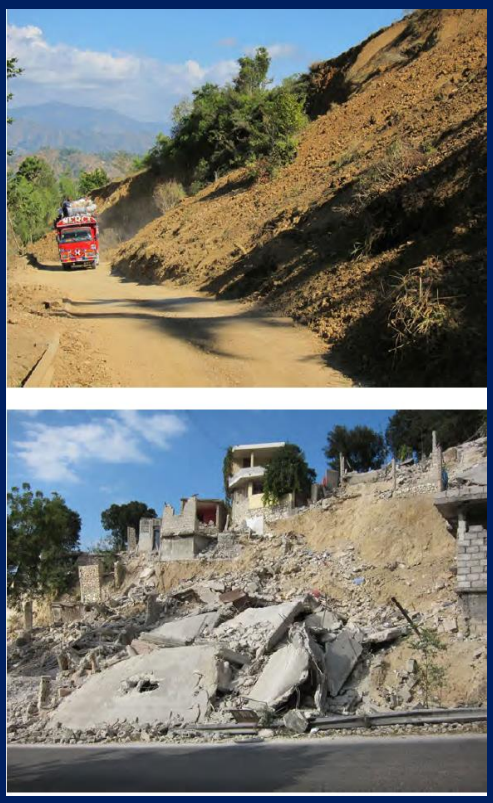

Figure 3.14 Landslides

Figure 3.15 Buildings damages

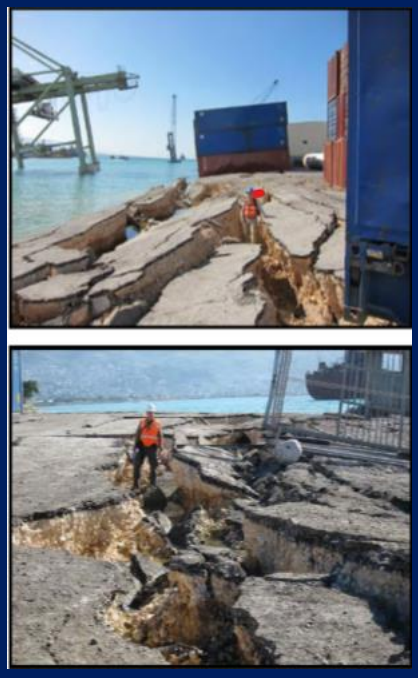

Figure 3.16 Port structures damages by lateral spreading

Figure 3.17 Pedestrian bridges damages

3.5.12 Maule Earthquake, Chile, 2010, February, 27

TECTONIC SETTING

The Maule Earthquake of 27 February 2010 nucleated on the subduction zone that runs along the entire ~5000 km length of the western coastline of South America, known as the Peru-Chile trench (http://earthquake.usgs.gov/). Earthquakes in this region are due to stress buildup resulting from the movement of the oceanic Nazca plate eastward and downward towards the South American plate, as shown in Figure 3.18, at a rate of approximately 70 mm per year. This value can be compared to other subduction zones with slip rates of: ~70 mm/year for Java trench where the Indo-Australian plate subducts beneath the Sunda plate, ~40 mm/year for the Cascadia subduction zone where Juan de Fuca plate subducts beneath the North American plate, and ~20 mm/year for the Himalayan arc region where the Indian plate subducts beneath the Eurasian plate. As shown in Figure 3.19, the dense and heavy oceanic crust (Nazca plate) subducts beneath the lighter continental crust (South American plate). The formation of the Andes Mountain range is related to plate tectonics. It is believed that the thickening of the Andean crust is mostly due to tectonic shortening of the South American plate.

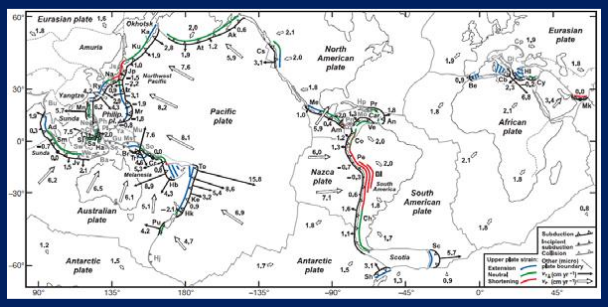

Figure 3.18. Subduction zone between the Nazca and South American plates (Schellart et al., 2007) aries.

HISTORICAL SEISMICITY IN THE REGION

Due to the close proximity to the Nazca-South America subduction zone, Chile has long been subjected to earthquakes of large magnitude. On average, a magnitude 8.0 earthquake occurs every decade and a magnitude 8.7 earthquake or greater is observed within a century

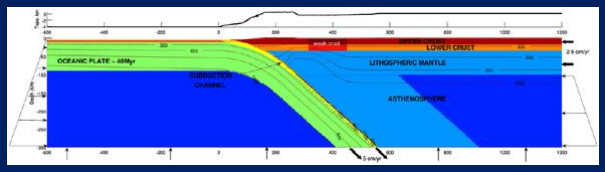

Figure 3.19 Cross-section of the subduction zone (Gerbault et al., 2009)

The map in Figure 3.20 shows recent major earthquakes in Chile alongside seismic gaps. The white circles indicate the rupture for individual events, the red circles show the epicentres and the yellow dots are the aftershocks. From north to south, the Peru-Chile trench has ruptured in several incidents except for three locations that are shown with red lines. The segment of the subduction zone, Concepción gap in Figure 3.20.

THE 27 FEBRUARY 2010 EARTHQUAKE

The Maule earthquake struck Chile on 27 February 2010 at 03:34 a.m. local time. The magnitude of the earthquake is estimated as Mw 8.8. The epicentre was located offshore at 35.909° S, 72.733° W with the following distances to major cities: Chillán 95 km, Concepción 105 km, Talca 115 km, and Santiago 335 km. The hypocentre was 35 km deep (http://earthquake.usgs.gov/earthquakes/eqinthenews/2010/us2010tfan/).

The average slip over the approximately 81,500 km2 rupture area was 5 m, with slip concentrations down-dip, up-dip and southwest, and up-dip and north of the hypocentre.
Relatively little slip was observed up-dip/offshore of the hypocentre. The average rupture velocity was estimated to be in the range of 2.0-2.5 km/sec. The Global Centroid Moment Tensor (GCMT) solution yielded a seismic moment of 1.84 x 1022 Nm, a centroid location of 35.95° S, 73.15° W, and a best double couple fault plane geometry with strike and dip angles of 18°, and a rake angle of 112°.

The simulation of the fault rupture is provided in Figure 3.21. It is seen from the inset in Figure 3.21 that shows the normalized power as a function of time that the duration of the earthquake exceeded 3 min.

However, the significant energy was released within the first the 2 min. It is also concluded by studying the propagation of rupture that the fault was bilateral, spreading away from the epicentre in both the north and south directions.

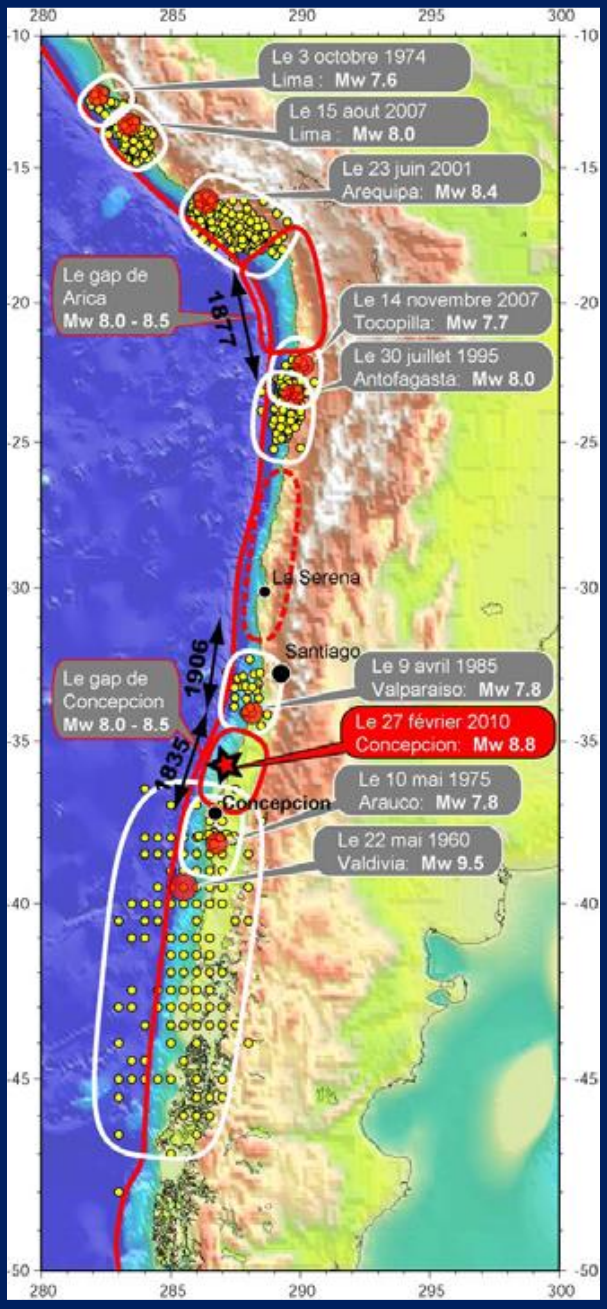

Figure 3.20 Recent major earthquakes in Chile and seismic gaps (Laboratoire de Géologie, Ecole Normale Supérieure (ENS), CNRS, Paris, France, http://www.geologie.ens.fr/~vigny/chili-f.html)

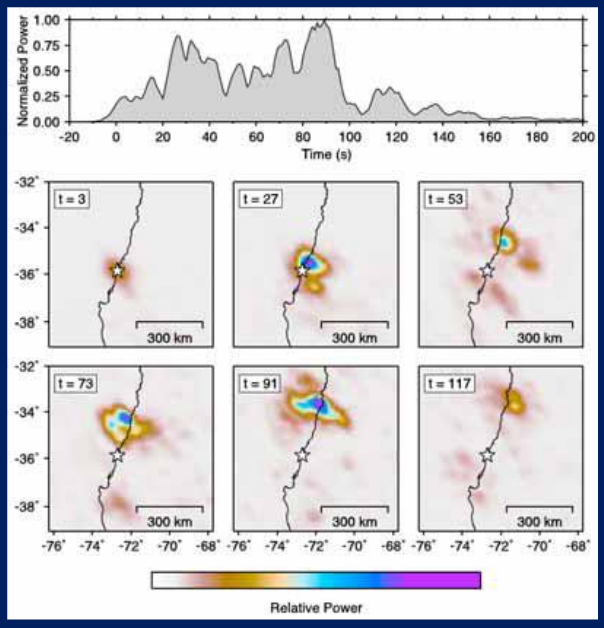

Figure 3.21 Frames from the simulation of the fault rupture (Lay et al., 2010) earthquake (http://researchnews.osu.edu/archive/chilequakemap.htm)

STRONG GROUND MOTION

Ground motions were recorded by two departments at the University of Chile. At the time of writing this report, recordings at 10 stations were available from the Seismological Service at the department of Geophysics and recordings at 9 stations were available from Red National de Acelerografos Departamento de Ingenieria Civil (RENADIC). RENADIC did not provide digital records. However, plots of acceleration time-histories and response spectra were made available. No information is available regarding the site classifications for any of the strong motion stations.

In general, the design spectra from Chilean seismic code match relatively well with the spectra from recorded ground motions.

However, for soil I and II, the spectra of records exceed the design spectra for the intermediate period range. Additionally, the spectra of the records at stations MAIP, CURI, CCSP and MELP, exceed significantly the design spectra for periods shorter than 1 sec. Moreover, the amplifications for these records are 4.26, 4.06, 3.39, and 3.67, respectively, which is an indication of the severity of these records, particularly when compared with the value of 2.70, which is the 84percentile amplification factor used widely. The amplifications of these records are also noteworthy when compared with the amplification factors from the Chilean seismic code, which vary from 2.76 to 3.09 depending on the soil class. Such a feature could result in relatively high demand imposed on short period structures that are designed to conform to code requirements.

-

Therefore, the duration of earthquake shaking is a very important measure of the damage potential of the ground motion. The duration of strong ground motion can vary depending on the magnitude, source distance, and local site conditions. The duration of strong ground motion increases with increasing earthquake magnitude.

The existing attenuation relationships for strong motion duration show that the bracketed duration decreases with increasing distance from the source, while the significant duration increases. This is because the bracketed duration uses the absolute threshold of the amplitude, which decreases with increasing distance from the fault. On the other hand, the significant duration utilizes the relative threshold and thus, is related to the geometry of the accelerogram, regardless of its absolute amplitude. The existing attenuation relationships for a large earthquake like the Chile earthquake are sparse. Therefore, to compare the severity of the durations from the Chile earthquake records, horizontal components of large earthquake records are selected from the Pacific Earthquake Engineering Research (PEER), Next Generation Attenuation (NGA) project database (http://peer.berkeley.edu/nga). The selected records are from relatively large earthquakes (Mw $\geq$ 6.9) with a peak ground acceleration of 0.1 g or more and source distances of less than 100 km.

The available data from the 19 stations in Chile are used to select appropriate attenuation relationships for horizontal ground motions. Attenuation relationships that are developed for subduction zones with thrust mechanisms and large magnitude events, and that utilize a large and uniformly processed data base are selected here.

The five candidate attenuation relationships are
- Zhao et al. (2006)
- Atkinson and Boore (2003)
- Campbell and Bozorgnia (2003)
- Gregor et al. (2002)
- Youngs et al. (1997)

Note that most of the existing attenuation relationships are not developed to account for large magnitude earthquakes such as the 2010 Chile earthquake. Due to lack of soil type information for the ground motion records, comparison of the selected attenuation relationships is made for rock site.

Selection of Records for Back-Analysis of the Case Studies

The records for back-analysis of the case studies are selected amongst the digital recordings available through the Seismological Service at the University of Chile. Most of the stations provided by RENADIC are located north of the rupture plane and none of the stations are within 100 km from case study structures.
Additionally, no digital records from RENADIC are available. Therefore, records from the Seismological Service are considered as seed signals to generate records for back analysis.

GEOTECHNICAL ENGINEERING

The MAE Centre geotechnical team was also the GEER (http://www.geerassociation.org/) Team D, the reconnaissance was a joint activity and the observations are also reported in GEER (2010). For a detailed and extensive set of observations of geotechnical damage during this earthquake the reader is referred to the GEER report.
The visited sites are categorized under (i) landslides, (ii) ports, (iii) roadway embankments, (iv) bridges, (v) bridge embankments, (vi) underground structures, (vii) retaining structures, and (viii) building foundations.

LANDSLIDES AND POTENTIAL TECTONIC MOVEMENTS

A series of landslides along road P22 south of Arauco are illustrated in Figure 3.22 through Figure 3.25. The series of landslides formed a linear feature nearly parallel to the coastline. All along the road vertical offsets were observed in the pavement indicative of deeper movement. This was the case even when the road was further away from the landslide.
It appeared that this was more than a classical "surficial" landslide feature with potentially larger tectonic movement. In our discussions with faculty at the University of Chile they indicated that this linear feature was related to tectonic movement. Additional investigations of this feature would be worthwhile.

Figure 3.22 Arauco landslides/coastal bluff features view 1

Figure 3.23 Arauco landslides/coastal bluff features view 2

Figure 3.24 Arauco landslides/coastal bluff features, April 14, 2010

PORTS

The port of Talcahuano and the surrounding area were inundated by a tsunami caused by the main earthquake shock (Figures 3.26-3.28). The tsunami reached about 0.5 km inland and caused

significant damage to the port facilities. Numerous ships were carried inland or were toppled. The sea walls and port dock were also damaged. The damage appeared to be a result of lateral spreading and liquefaction. However, it was difficult to determine whether this liquefaction was a result of ground shaking or due to the sudden rise in pore water pressure due to dynamic loading resulting from the tsunami induced waves. Most likely, this was a result of a combination of both factors.

Figure 3.25. Arauco landslides/coastal bluff features, note linear feature in the road showing a vertical offset, April 14, 2010

Figure 3.26. Port of Talcahuano, aerial view

Figure 3.27. Tsunami displaced ship, Port of Talcahuano, April 15, 2010

Figure 3.28. Damaged sea wall and dock, Port of Talcahuano, April 15, 2010

The port of Coronel is a major commercial port parts of which experienced damaged due to liquefaction and lateral spreading. A laydown area for container storage, consisted of fill supported by a shallow sheet pile experienced extensive damage. Figure 3.29 through Figure 3.32 show the corresponding photos of the visited areas. The sheet pile wall is embedded about 4-6 m below the ground surface and protrudes about 15-20 m above the ground surface. At waypoint 11 (see Figure 3.30) an outward movement of about 110 cm was measured, while the port officials reported their survey gives about 150 cm. The measurements extended all the way back to the warehouses. At waypoint 12 lateral displacements of about 40 cm was measured, and at waypoint 13, an outward movement of 10 cm was measured. It did not appear that the underlying sands were treated during construction to minimize liquefaction potential.

Figure 3.29 Lateral spreading looking north view 1, Port of Coronel, April 14, 2010

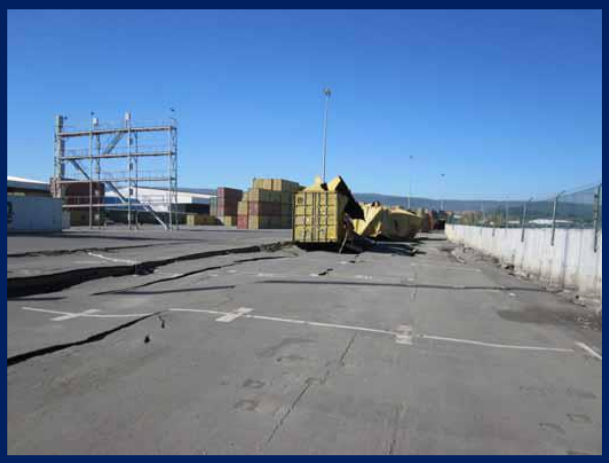

Figure 3.30 Lateral spreading looking south, Port of Coronel, April 14, 2010

Figure 3.31 Sand eject, lateral spreading, Port of Coronel, April 14, 2010

Figure 3.32. Seaside view of the sheet pile wall that experienced lateral spreading, Port of Coronel,

Figures 3.33 and 3.34 show a pier used by fishing boats at Port Lota. The pier appeared undulating likely due to pile settlements. Numerous battered piles with broken connections were observed.

Figure 3.33 View of undulating fishing pier, Port Lota,

Figure 3.34 Typical broken pile connections, Port Lota

Figures 3.35 to 3.37 show a wharf at Port St. Vicente that experienced lateral spreading and failure of a gravity wall resulting in complete loss of section of the wharf or significant lateral movement. The lateral displacement of the wall was measured to be about 167 cm close to the section of the wall that failed and about 63 cm further away. Nearby there were fish processing plants that experienced significant damage due to lateral spreading of the foundations.

ROADWAY EMBANKMENTS

The observations in the sections below regarding the performance of roadway embankments during the earthquake have apparent geotechnical features, therefore included here.

Numerous roadway embankments failed throughout the earthquake-affected zone. This includes a number of embankments along the main north-south highway, Route (Ruta) 5. The failures were due to either failure of the underlying soils or the embankments themselves. Figure 3.38 and Figure 3.39 show a repaired embankment along Route 5. The failed section was bounded by two streams (Figure 3.38) and it is likely that the failure of the embankment was due to loss of strength in the underlying soils (liquefaction) during shaking.

Figure 3.35. Lateral spreading and damage to quay wall, blue fish processing plants in the background damaged by lateral spreading, Port St. Vicente, April 15, 2010

Figure 3.36 Failed section of the quay wall, Port St. Vicente,

Figure 3.37 Measurement of displacement of the wall due to lateral spreading, Port St. Vicente,

Figure 3.38 Roadway embankment ~5km south of Parral,

Figure 3.39 Northboundlane looking south, Repaired Roadway Embankment ~5km south of Parral,

The damages occurred in overpass embankment on the right side of the northbound lane of Route 5 South. are shown in Figures 3.40 and 3.41. The damage of the embankment appeared to be due to shaking of the embankment material. The underlying soil appears to be intact with no evidence of loss of strength. The embankment bulged laterally and settled. The overpass embankment to the left of the northbound lane did not show signs of damage.

Figure 3.40 Damage to overpass embankment, Route 5 South overpass embankment, to Retiro at Tucapel Mill, April 15, 2010

Figure 3.41 Route 5 South overpass embankment, to Retiro at Tucapel Mill,

BRIDGES

The observations are specifically on the geotechnical failures at the Mataquito Bridge.

This bridge crosses the Mataquito River close to the Pacific Ocean. Extensive liquefaction and lateral spreading occurred at the north and south abutments and in the adjacent fields. Figure 3.42 to Figure 3.46 show photos of the bridge and the damage.

The lateral spreading at the south abutment appeared to be more confined due to the topography of the area. However, at the north side, due to existence of large fields around the bridge, extensive lateral spreading was observed (extending ~270 m from the river edge). The lateral spreading from the edge of the abutment wall to the first row of piers was ~54 cm and the total lateral spreading from the edge of the abutment wall to the river's edge was ~180 cm (over a distance of ~65 m). The approach embankment was ~7.6 m high, and settled ~70 cm relative to the bridge deck. The approach embankment experienced outward transverse movement of ~60 cm from the centreline as manifested by cracking of the asphalt along a distance of ~200 m. This appeared due to liquefaction and failure of the underlying soil and was evidenced by compression ridged in the field at the toe of the embankments.

Figure 3.42 Puente Mataquito, looking north (courtesy Google)

Figure 3.43 Lateral spreading on the south end of the bridge, Puente Mataquito,

Figure 3.44 Lateral spreading on the north end of the bridge, Puente Mataquito,

Figure 3.45 Cracking and transverse movement (60 cm on each side) of embankment due to liquefaction of underlying soil, north abutment of the bridge, Puente Mataquito

Figure 3.46 North abutment shoved into bridge deck due to lateral spreading,

UNDERGROUND STRUCTURES

The underground structures appeared to be undamaged by the earthquake shaking. The following types of underground structures were encountered: a. Wide highway box structures (Figure 3.47): these were cut and cover high way box structures with 3 lanes of traffic in one direction. These are constructed in the relatively stiff gravels. The portal of these structures consisting of U-shaped wall sections appeared undamaged. These structures were encountered at two locations and each of them was more than 1 km long.

b. Santiago Metro underground structures (Figure 3.48): no damage was observed in the tunnels and underground stations of the Santiago Metro.

c. Highway Tunnels (Figures 3.49 and 3.50): highway tunnels encountered by the team appeared to be intact. A highway tunnel failure (not observed by the team) was reported on the

northbound lane of Route 5, north of Santiago. It is known as “La Calavera” tunnel near Calera. The tunnel is old and had problems before the earthquake. It was in rock with rock bolts providing support. After the earthquake, rock block was dislodged.
It appeared that well engineered underground structures performed very well even under strong shaking. This is consistent with observations during other earthquakes elsewhere.

Figure 3.47 Highway box structures in Santiago,

Figure 3.48 Santiago Metro, Baquedano Station,

Figure 3.49 Highway tunnel, Route 5 South, April 12, 2010

Figure 3.50 Highway tunnel, Route 5 South, without damages

RETAINING STRUCTURES

Modern retaining wall structures have not exhibited damages. The mechanically stabilized earth walls forming the approach embankment for the two ring road bridges, which have failed, have remained intact as illustrated in Figure 3.51.

Figure 3.51 Mechanically stabilized earth, bridge ring 2, Miraflores Bridge, Santiago,

BUILDING FOUNDATION

A building in Talcahuano, that was tilted, which appeared to be due to failure in the foundation soil is shown in Figure 3.52.

Figure 3.52 Tilting of the Green Building due to bearing soil failure, Talcahuano,

FINAL REMARKS

The Maule earthquake has provoked considerable damage to transportation networks, namely to roads, to bridges, underground structures and to buildings.

3.5.13_Tohoku earthquake, Japan, 2011, March, 11

The 2011 Sendai earthquake and tsunami "Tōhoku region Pacific Ocean offshore earthquake was a 9.0 M_W megathrust earthquake off the coast of Japan that occurred at 14:46 JST (05:46 UTC) on Friday 11 March 2011.

The epicenter was 130 kilometers (81 mi) off the east coast of the Oshika Peninsula, Tōhoku, with the hypocenter at a depth of 32 km (20 mi).

The earthquake triggered tsunami warnings and evacuations along Japan's Pacific coast and in at least 20 countries, including the entire Pacific coast of North America and South America.

The earthquake created extremely destructive tsunami waves of up to 10 meters (33 ft) that struck Japan minutes after the quake, in some cases travelling up to 10 km (6 mi) inland, with smaller waves reaching many other countries after several hours.

The earthquake and tsunami caused extensive and severe damage in Japan, including heavy damage to roads and railways as well as fires in many areas, and a dam collapse. Around 4.4 million households in northeastern Japan were left without electricity and 1.5 million without water.

The main failures on the pavement surface were a result of fill material settlement at bridge approaches, under-drain settlement, embankment slope failures, and lateral spreading of the embankment.

The majority of failed fill areas meet the current specification requirements suggesting an evaluation of current fill standards is necessary. From the field surveys it was concluded the need for developing a standardized condition assessment to evaluate pavement damage after earthquakes.

The lack of communication and reliable information had disastrous consequences in Constitución. As significant portion of the total casualties from the earthquake were from Constitución due to the tsunami.

Many electrical generators were taken down, and at least three nuclear reactors suffered explosions due to hydrogen buildup within the outer containment buildings. According to reports by the International Atomic Energy Agency (IAEA), containment of each of the radioactive cores is intact and no meltdowns have occurred.

Residents within a 20 km (12 mi) radius of the Fukushima I Nuclear Power Plant and a 10 km (6.2 mi) radius of the Fukushima II Nuclear Power Plant were evacuated.

The estimates of the Sendai earthquake's magnitude made it the strongest known earthquake to hit Japan, and one of the five strongest earthquakes in the world overall since modern record-keeping began in 1900.

Japanese Prime Minister Naoto Kan said that "in the 65 years after the end of World War II, this is the toughest and the most difficult crisis for Japan. The earthquake moved Honshu 2.4 m (7.9 ft) east and shifted the Earth on its axis by almost 10 cm (3.9 in), an expected change for an earthquake of that magnitude.

Earthquake

Figure 3.53 Map of the Sendai earthquake and aftershocks

The main earthquake was preceded by a number of large foreshocks, beginning with a 7.2 M_W event on 9 March approximately 40 km (25 mi) from 11 March quake, and followed by another three on the same day in excess of 6 M_W in magnitude One minute prior to the effects of the earthquake being felt in Tokyo, the Earthquake Early Warning system connected to more than 1,000 seismometers in Japan sent out warnings on television of an impending earthquake to millions. This was possible because the damaging seismic S-waves, traveling at 4 kilometers per second, took about 90 seconds to travel the 373 km (232 mi) to Tokyo. The early warning is believed by the Japan Meteorological Agency to have saved many lives.

The earthquake occurred at 14:46 local time in the western Pacific Ocean, 130 km (81 mi) east of Sendai, Honshu, Japan. Its epicenter was 373 km (232 mi) from Tokyo, according to the United States Geological Survey (USGS). Multiple aftershocks were reported after the initial magnitude 9.0 quake. A magnitude 7.0 aftershock was reported at 15:06 local time, 7.4 at 15:15 local time and 7.2 at 15:26 local time. Over five hundred aftershocks of magnitude 4.5 or greater have occurred since the initial quake (Figure 3.53).

Initially reported as 7.9 by the USGS, the magnitude was quickly upgraded to 8.8 and then to 8.9, and then again to 9.0 (Figure 3.54). This earthquake occurred where the Pacific Plate is subducting under the plate beneath northern Honshu; which plate this is a matter of debate amongst scientists. The Pacific plate, which moves at a rate of 8 to 9 cm (3.1 to 3.5 in) a year, dips under Honshu's underlying plate releasing large amounts of energy. This motion pulls the upper plate down until it breaks. The break 130 kilometers (81 mi) off of the coast of Sendai was estimated to be several tens of kilometers long and only 32 kilometers (20 mi) deep, and caused the sea floor to spring up several meters, causing the earthquake. A quake of this size usually has a rupture length of at least 480 km (300 mi) and requires a long, relatively straight fault line. Because the plate boundary and subduction zone in this region is not very straight, it is unusual for the magnitude of an earthquake to exceed 8.5; the magnitude of this earthquake was a surprise to some seismologists. The hypocentral region of this earthquake extends from offshore Iwate to offshore Ibaraki Prefectures. The Japanese Meteorological Agency said that the earthquake may have ruptured the fault zone from Iwate to Ibaraki with a length of 500 km (310 mi) and a width of 200 km (120 mi). Analysis showed that this earthquake consisted of a set of three events. The earthquake may have had a mechanism similar to that of another large earthquake in 869 with estimated magnitude M_s 8.6, which also created a large tsunami. Other major earthquakes with tsunamis struck the Sanriku Coast region in 1896 and 1933.

The quake registered the maximum of 7 on the Japan Meteorological Agency seismic intensity scale in Kurihara, Miyagi Prefecture (Figure 3.55).[Three other prefectures—Fukushima, Ibaraki and Tochigi—recorded an upper 6 on the JMA scale. Seismic stations in Iwate, Gunma, Saitama and Chiba Prefecture measured a lower 6, recording an upper 5 in Tokyo.

The United States' Nuclear Energy Institute released figures indicating the earthquake generated peak ground accelerations of 0.35g (3.43 m/s^2) near the epicenter; with a study by the University of Tokyo indicating some areas experienced accelerations in excess of 0.5g (4.9 m/s^2). On its own, this was not particularly devastating (the New Zealand earthquake of February before caused ground accelerations of up to 2.2g, more than four times as high) with the majority of the damage caused by the resulting Tsunami(Figures 3.56 to 3.57).

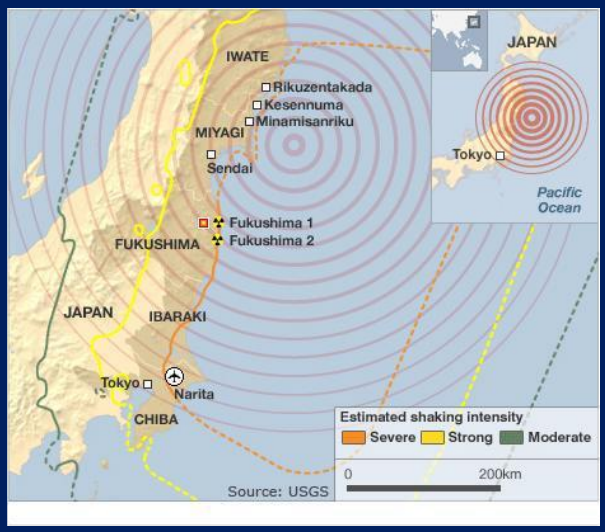

Figure. 3.54 Map of affected areas (Source: USGS)

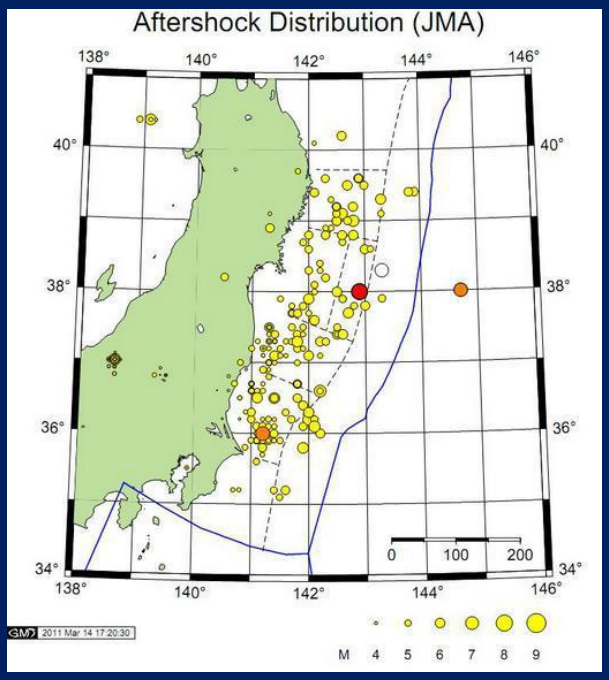

Figure 3.55 Map showing aftershock distribution (Source: Japan Meteorological Agency (JMA))

Figure 3.56 Tsunami affected areas (Source: OCHA, 2011)

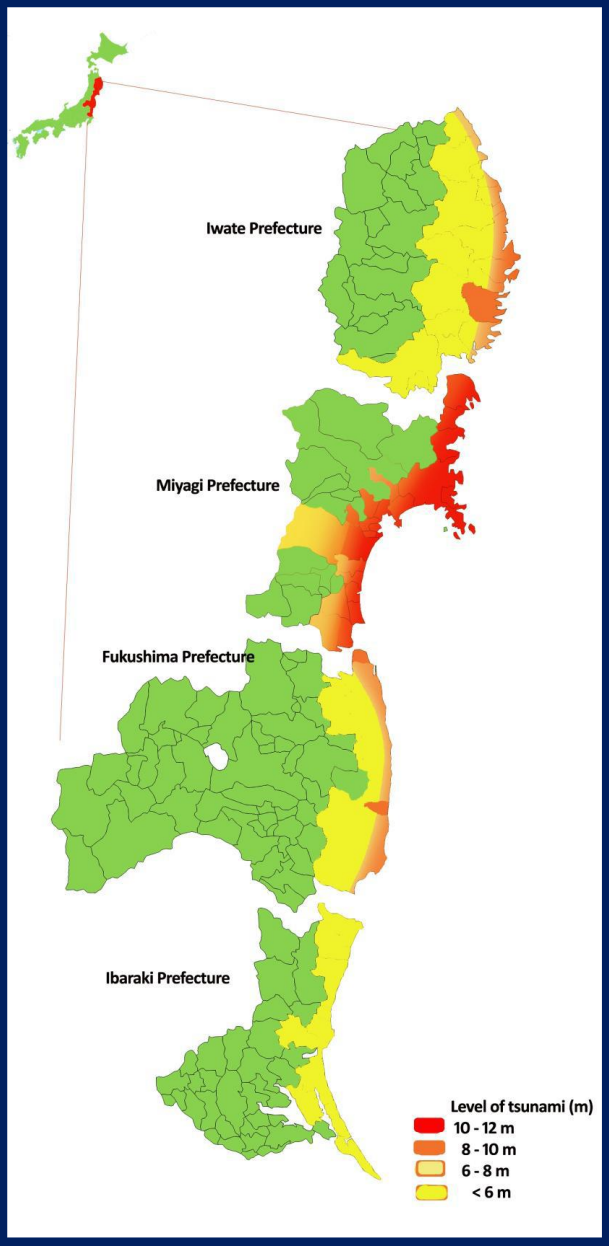

Figure 3.57 Map of local authorities affected by Tsunami (analysed by IEDM, Kyoto University)

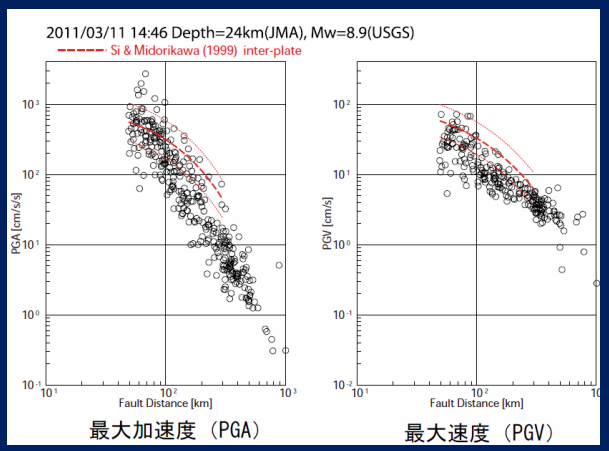

Figure 3.58 Attenuation of PGA (cm/s/s) of the horizontal component and PGV (cm/s); PGA is the measured value and PGV is the computed value converted for the hard foundation with the shear velocity of 600m/s. Data source: NIED

Energy

This earthquake released a surface energy (M_e) of $1.9\pm0.5\times10^{17}$ joules, dissipated as shaking and tsunamic energy, which is nearly double that of the 9.1-magnitude 2004 Sumatran earthquake that killed 230,000 people, and flung the 2,600 ton Apung 1 ship 2 to 3 km (1.2 to 1.9 mi) inland. "If we could only harness the [surface] energy from this earthquake, it would power [a] city the size of Los Angeles for an entire year," USGS director Marcia McNutt said in an interview. The total energy released (M_w) was more than 200,000 times the surface energy and was calculated by the USGS WPhase Moment Solution at 3.9×10^{22} joules, slightly less than the 2004 Sumatra quake. This is equivalent to 9.32 teratons of TNT (approximately 600 million times that of the Hiroshima bomb, or 186,400 times as powerful as man's largest-ever explosive device, Tsar Bomba).

Geophysical impact

Figure 3.59 Soil liquefaction

Soil liquefaction in Koto, Tokyo

The quake moved portions of northeast Japan by as much as 2.4 m closer to North America, making portions of Japan's landmass "wider than before," according to geophysicist Ross Stein. Portions of Japan closest to the epicenter experienced the largest shifts. Stein also noted that a 400 km stretch of coastline dropped vertically by 0.6 m, allowing the tsunami to travel farther and faster onto land The Pacific plate itself may have moved eastwards by up to 20 m, though the actual displacement will have diminished with greater distance from the site of the fault. Other estimates put the amount of slippage at as much as 40 m, covering an area some 300 km to 400 km long by 100 km wide. If confirmed, this would be

one of the largest fault movements ever recorded and accounts for its extreme destructiveness.

According to Italy's National Institute of Geophysics and Volcanology, the earthquake shifted the Earth's axis by 25 centimeters. This deviation led to a number of small planetary changes, including the length of a day and the tilt of the Earth. The speed of the Earth's rotation increased, shortening the day by 1.8 microseconds due to the redistribution of Earth's mass. The axial shift was caused by the redistribution of mass on the Earth's surface, which changed the planet's moment of inertia. Due to the effects of conservation of angular momentum, such changes of inertia result in small changes to the Earth's rate of rotation. These are typical expected "tiny" changes for an earthquake of this magnitude.

Shinmoedake, a volcano in Kyushu, erupted two days after the earthquake. The volcano had erupted in January 2011; it is not known if the later eruption was linked to the earthquake.[1] In Antarctica, the seismic waves from the earthquake were reported to have caused the Whillans Ice Stream to slip by about 0.5 meters.

Tsunami

Tsunami was the most serious type of damage. Because of the sympathy to tsunami victims and their families, engineering societies decided to postpone damage reconnaissance in the affected area unless very necessary. There is, however, minimum information available. First, the height of tsunami was investigated to find that the height was more than 15 m and easily overtopped sea walls that had been constructed against the previously known tsunami height. The destructive power of high tsunami was substantial and removed nearly all the structures in the attacked areas (Figure 3.60). This photograph reminds us of Banda Aceh after tsunami disaster in 2004. In this flat land, there is no place for people to evacuate, even if a tsunami alert is issued properly. In some tsunami-affected areas, the sea water remained on shore for many hours and evacuation was made impossible. There was a huge amount of debris after tsunami attack (Figure 3.61). This debris has to be disposed in an appropriate way, which is a very difficult task.

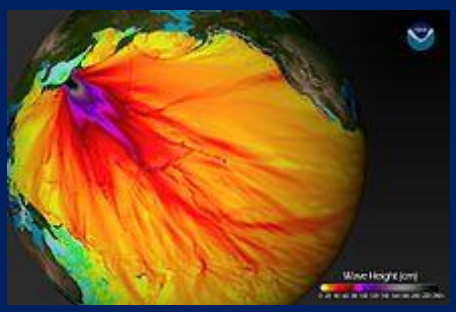

Figure 3.60 Wave height map for the tsunami from NOAA

Figure 3.61 Water column height on 11 March 2011 at DART Station, 690 NM Southeast of Tokyo

The earthquake caused a massive tsunami which wrought massive destruction along the Pacific coastline of Japan's northern islands. The tsunami propagated across the Pacific, and warnings were issued and evacuations carried out in many countries with Pacific coasts, including the entire Pacific coast of North and South America from Alaska to Chile; however, while the tsunami was felt in many of these places, it caused only relatively minor effects. Chile's section of Pacific coast is furthest from Japan (about 17,000 km away-the furthest possible distance on the earth is the semi-circumference, about 20,000 km) but still was struck by tsunami waves up to 2 meters high.

The tsunami warning issued by the Japan Meteorological Agency was the most serious on its warning scale; it rated as a "Major tsunami", being at least 3 m) high. The actual height predicted varied, the greatest being for Miyagi at 10 m high. The earthquake took place at 14:46 JST around 70 km from the nearest point on Japan's coastline, and initial estimates indicated the tsunami would have taken 10 to 30 minutes to reach the areas first affected, and then areas further north and south based on the geography of the coastline. Just over an hour after the earthquake, a tsunami was observed at 15:55 JST flooding Sendai Airport, which is located near the coast of Miyagi Prefecture with waves sweeping

away cars and planes and flooding various buildings as they traveled inland. The impact of the tsunami in and around Sendai Airport was filmed by an NHK News helicopter, showing a number of vehicles on local roads trying to escape the approaching wave and being engulfed by it. A 4-meter-high tsunami hit Iwate Prefecture (Figures 3.62 to 3.77).

Elsewhere across the Pacific

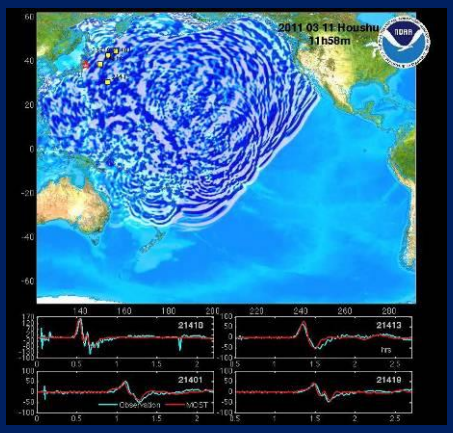

Figure 3.62 NOAA animation of the tsunami's propagation

Shortly after the earthquake, the Pacific Tsunami Warning Center (PTWC) issued tsunami watches and warnings for locations in the Pacific. At 07:30 UTC PTWC issued a widespread tsunami warning for the entire Pacific Ocean. The United States West Coast and Alaska Tsunami Warning Center issued a tsunami warning for the coastal areas of California and Oregon from Point Conception, California, to the Oregon-Washington border. In California and Oregon, up to 2.4 m high tsunami surges hit some areas, damaging docks and harbors and causing over US$10 million of damage. Hawaii estimated damage to public infrastructure alone at $3 million, with damage to private property estimated at tens of millions of dollars. A tsunami warning was also advised for the Canadian province of British Columbia, where the potentially affected areas included British Columbia's north coast and the outer west coast of Vancouver Island; waters around the island were deemed dangerous and all boats were grounded for 12 hours, stranding some island residents in the area.

Figure 3.63 Tsunami waves

Figure 3.64 25. March 14: Rescue workers search for victims in the rubble in Rikuzentakata, northern. Source: REUTERS / Toru Hanai

Figure 3.65. March 16: Braving snow, rescue workers search for survivors in the rubble of tsunami-stricken town of Minamisanriku in

Miyagi Prefecture. (AP Photo/The Yomiuri Shimbun, Hiroaki Ohno)

Figure 3.66 View of the zone before and after the tsunami

Figure 3.67 View of the area before and after the tsunami

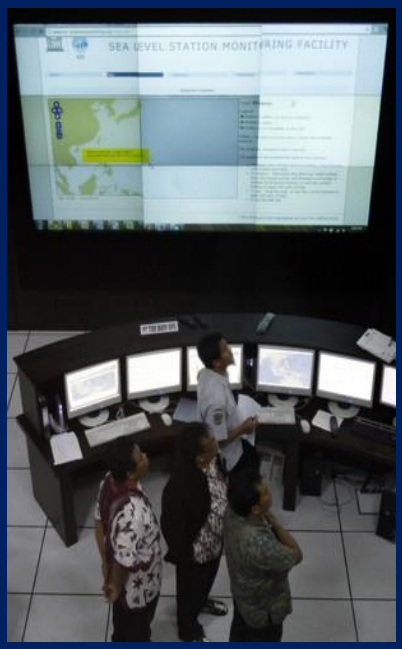

Figure 3.68 Centre in Indonesia to follow the tsunamis

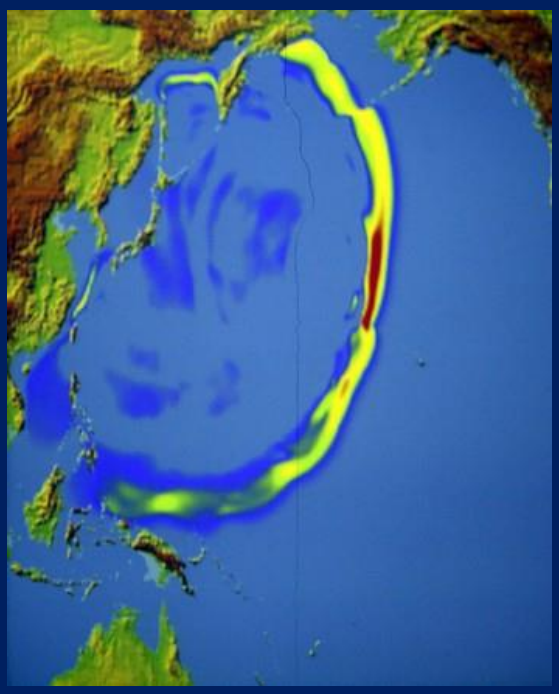

Figure 3.69 Effect of the tsunami in a screen

Figure 3.70 Damages due to the tsunami

Figure 3.71 Tsunami floods (adapted from Live)

Figure 3.72 Tsunami effect

Figure 3.73 Tsunami damages

Figure 3.74 Tsunami floods (adapted from Live)

Figure 3.75 Tsunami floods in coastal area

Figure 3.76 Tsunami effects near Fukushima area

Figure 3.77 Tsunami effects near Ibaraki coast.

Damage and effects

Liquefaction risk is high in sandy ground that is loose, water-saturated, and young in age. Liquefaction occurred at many places of such environment during the present earthquake.
Many artificial islands have been constructed along the coast of Tokyo Bay since 1960s mostly by using dredged seabed sand. Because the risk of liquefaction in such islands has been known for many years, big factories and business buildings have improved subsoil by densification and other methods. During the present earthquake, consequently, most liquefaction problems occurred in the unimproved residential areas where people did not have much knowledge about liquefaction risk.

The degree of damage caused by the earthquake and tsunami combined, most due to the tsunami, is enormous. Film of the worst affected towns show nothing more than piles of rubble, with almost no parts of any structures left standing. The *extent* of the damage was also massive. Estimates of the value of the damage range well into the tens of billions of US dollars; before-and-after satellite photographs of devastated regions show immense damage to many places (Figure 3.78).

Although Japan has invested the equivalent of billions of dollars on anti-tsunami seawalls which line at least 40 per cent of its 22,000-mile coastline and stand up to 12 metres high, the tsunami simply washed over the top of the seawalls, some of which collapsed.

Figure 3.78 Debris washed out to sea

Ports

The Port of Tokyo suffered slight damage; the effects of the quake included visible smoke rising from a building in the port with parts of the port areas being flooded, including soil liquefaction in Tokyo Disneyland's carpark. All of Japan's ports were briefly closed after the earthquake, though the ones in Tokyo and southwards soon re-opened. The north-eastern ports of Hachinohe, Sendai, Ishinomaki and Onahama were destroyed, while Chiba port (which serves the hydrocarbon industry) and Japan's ninth-largest container port at Kashima were also affected though less severely. The ports at Hitachinaka, Hitachi, Soma, Shiogama, Kesennuma, Ofunato, Kamashi and Miyako were also damaged and were expected to be out of action for weeks.

Dam failure

Japanese authorities inspected over 400 dams following the March 11, 2011 M9.0 Tohoku Offshore Earthquake. According to reports by Matsumoto (2011), almost all of these dams withstood minor to severe ground shaking and retained their reservoirs with generally minor to moderate damage. The exception to this was Fujinuma Dam, an embankment dam located in southern Fukushima Prefecture that failed shortly after the earthquake. The failure of the dam

resulted in the uncontrolled release of the entire reservoir, which flowed downstream into a small village and killed 8 people (Matsumoto, 2011; Towhata et al., 2011).

Fujinuma Dam had a maximum height of about 18.5 meters and had a maximum reservoir volume of approximately 1.5 million cubic meters (~1,200 acre-feet) (Figure 3.79). It has sometimes been referred to as Fujinuma-ike, which means it was considered to be a pond-retaining structure because the dam was not on a regulated river (Matsumoto, 2011).

Construction of Fujinuma Dam began in 1937 and was halted during World War II. Following the war, the dam was completed in 1949 (Matsumoto, 2011; Towhata et al., 2011). There were actually two embankment dams retaining the reservoir: an 18.5-meter-high main dam and a ~6-meter-high auxiliary dam. Figure 3.80 presents a general cross section of the main dam obtained from Matsumoto (2011). The main dam had a crest width of 6 meters and an upstream slope which ranged principally between 2.5:1 to 2.8:1, together with small benches and a relatively steep 1.5:1 upper slope. The downstream slope had a general slope of 2.5:1 with a small bench at mid-height (Figure 3.81). It also had a steepened downstream toe, perhaps indicative of a possible rock or gravel toe. It is believed that the auxiliary dam had a similar geometry. The main dam had a crest length of 133 meters.

There are currently no drawings available at the time of this writing to detail the design and construction history of the dam. It is not known what the zoning of the dam was designed to be, although some reports indicate that it was a homogeneous embankment design (Matsumoto, 2011). Nor is there any information currently available regarding what type of and amount of foundation treatment was provided at either the main dam or auxiliary dam.

Figure 3.79 Aerial View of Fujinuma Main Dam and Auxiliary Dam in 2009

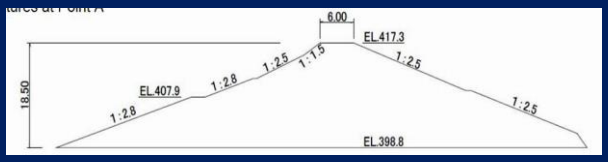

Figure 3.80 Cross Section of Fujinuma Dam (from Matsumoto, 2011)

However, a diagram posted on the left abutment of the main dam indicates that the main dam has had a seepage problem in either the upper foundation or lower embankment materials.

The dam was located approximately 80 kilometres from the fault rupture and directly opposite the approximate middle of the 600-kilometer fault rupture zone. The nearest strong motion seismograph, a surface instrument located 2.8 kilometres away in the community of Naganuma, registered a peak ground acceleration of 0.315g. According to Matsumoto (2011), the reservoir was nearly full when the earthquake occurred. The dam crest reportedly was overtopped. The brief reconnaissance by the GEER team resulted in the following observations of the main dam and the breach within it:

Figure 3. 81 Pre-Earthquake Photograph of Crest and Downstream Slope of Fujinuma Main Dam

Figure 3.82 View of Fujinuma Dam Embankment Fill Layers On Top of Black Organic Foundation Residual Soil Exposed within Downstream Slope at Left Abutment

At least some of the fill was placed in relatively thick lifts (Figure 3.82), so the degree of compaction may have been relatively small compared to the level of compaction required for modern dams. Even though most of the fill material appeared to be cohesive in nature, thick lifts of this material may still be relatively loose, weak, and/or subject to strength losses during a long duration of earthquake shaking

There did not appear to be any filters constructed within the dam embankment or foundation. If the dam deformed significantly during the earthquake shaking, transverse cracks could have developed and promoted internal erosion.

INSTABILITY OF SLOPE AND EMBANKMENT

Shear failure of slopes and embankments occurred at many places. As far as natural slopes are concerned, the size of failures is not very large. Figure 3.83 indicates an example in Ibaraki, north of Tokyo. A bigger slope failure occurred in Shirakawa City of Fukushima Prefecture. This failure developed within a layer of weathered welded tuff and claimed 13 victims. Not worthy is the long distance of runout that suggests the apparent friction angle of 5 degrees approximately. It is necessary to further watch the slope behaviour during aftershocks to come and the rainy season.

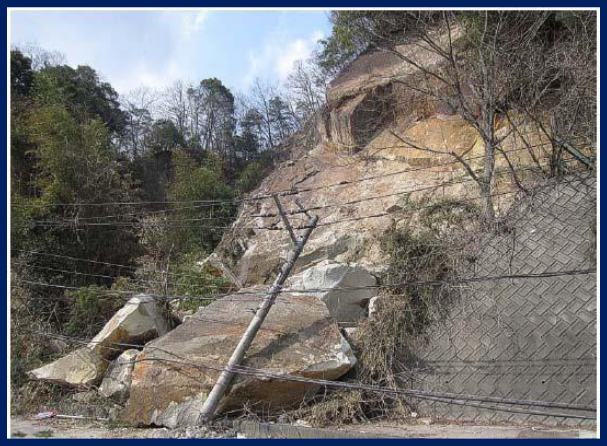

Figure 3.83 Rock fall at Ohgo of Ibaraki

.

Figure 3.84 shows distortion of Shida Bridge approach.

Figure 3.85 illustrates distortion of railway embankment Naruse River, north of Sendai (Joban Line of Japanese Railway East, near Mito, Ibaraki). Distortion of embankment occurred at many places and hindered operation of transportation.

It is particularly remarkable that the bullet trains (Shinkansen) successfully stopped at the onset of earthquake when they were running at a velocity greater than 200 km/h. This success was achieved by combination of many safety technologies.

On the contrary, many problems were detected in artificial earth fills for residential land development in hill areas. A slope failure at Midorigaoka area of Shiroishi City, south of Sendai. Formerly known as Kotobuki-Yama, this development slope failed during the 1978 Miyagiken-Oki earthquake occurred when the earth filling was going on. It appears that engineers in those days judged that the slope would not be perfectly stabilized, and the land was converted to a green park instead of selling it for residence. That decision was right because the upper part of the slope failed once more.

Figure 3.84 Distortion of Shida Bridge approach Naruse River, north of Sendai

Figure 3.85 Distortion of railway embankment (Joban Line of Japanese Railway East, near Mito, Ibaraki

Transport

Japan's transport network suffered severe disruption. Many sections of Tohoku expressway serving northern Japan were damaged All railway services were suspended in Tokyo, with an estimated 20,000 people stranded at major stations across the city (Figure 3.86). In the hours after the earthquake, some train services were resumed (Figures 3.87 and 3.88). Most Tokyo area train lines resumed full service by the next day-12 March. Twenty thousand stranded visitors spent the night of 11–12 March inside Tokyo Disneyland.

A tsunami wave flooded Sendai Airport at 15:55 JST, about 1 hour after the initial quake. Narita and Haneda Airport both suspended operations after the quake, with most flights diverted to other airports for about 24 hours (Figures 3.89 to 3.91). Ten airliners bound for Narita were diverted to nearby Yokota Air Base.

Figure 3.86 Stranded passengers on a Tokyo train. Major disruptions to train travel, as well as car and airplane travel, have occurred in places such as Tokyo and northeastern Japan.

Four trains on coastal lines were reported as being out of contact with operators; one, a four-car train on the Senseki Line, was found to have derailed, and its occupants were rescued shortly after 8 am the next morning. There had been no derailments of Shinkansen bullet train services in and out of Tokyo, but their services were also suspended The Tōkaidō Shinkansen resumed limited service late in the day and was back to its normal schedule by the next day, while the Jōetsu and Nagano Shinkansen resumed services late on 12 March; however, the Tōhoku Shinkansen remained suspended, with visible damage to electrical poles and elevated spans, and the state of the line in harder-hit areas still difficult to ascertain. Services on the Tōhoku Shinkansen partially resumed on 15 March, with one round-trip service per hour between Tokyo and Nasu-Shiobara.

The entirety of JR East's Kesennuma Line was obliterated, save for the platform of Minami-Kesennuma Station.

Figure 3.87 People waiting for transportation

Figure 3.88 People walking due transport disruption

Figure 3.89 Fire in Sendai airport terminal

Figure 3.90 Destruction of Sendai airport due to floods

.

Figure 3.91 Sendai airport are totally flooded

Nuclear power plants

Fukushima I, Fukushima II, Onagawa Nuclear Power Plant and Tōkai nuclear power stations consisting of eleven reactors were automatically shut down following the earthquake. Higashidōri, also on the northeast coast, was already shut down for a periodic inspection. Cooling is needed to remove decay heat for several days after a plant has been shut down. The cooling process is powered by emergency diesel generators, as in the case of Rokkasho nuclear reprocessing plant. At Fukushima I and II tsunami waves overtopped seawalls and destroyed diesel backup power systems, leading to severe problems including two large explosions at Fukushima I and leakage of radiation. Over 200,000 people have been evacuated.

A map showing epicenter of earthquake and position of nuclear power plants is shown in Figure 3.92.

Europe's energy commissioner Guenther Oettinger, in remarks to the European Parliament on 15 March, called the nuclear disaster an "apocalypse", saying that the word was particularly well chosen, and that Tokyo had almost lost control of events at the Fukushima power plant.

Figure 3.92 Epicenter of earthquake and position of nuclear power plants

Fukushima I and II Nuclear Power Plants

Japan declared a state of emergency following the failure of the cooling system at the Fukushima I Nuclear Power Plant, resulting in the evacuation of nearby residents (Figures 3.93 and 3.94).

Figure 3.93 Fukushima Central

Figure 3.94 Before and after images of the explosion at Fukushima I Unit 1 reactor

Officials from the Japanese Nuclear and Industrial Safety Agency have reported that radiation levels inside the plant are up to 1,000 times normal levels, and that radiation levels outside the plant are up to 8 times normal levels. Later, a state of emergency was also declared at the Fukushima II nuclear power plant about 11 km (7 mi) south. This brings the total number of problematic reactors to six.

On March 12, a large explosion, thought to be caused by the buildup of hydrogen gas, blew away the roof and outer walls of the Reactor 1 building, releasing a large cloud of dust and vapor, but the reactor itself was not damaged in the explosion. A BBC journalist reported being stopped 60 km from the blast site by police.

On Sunday, March 13, Japanese authorities admitted that a partial nuclear meltdown could be occurring in Reactors 1 and 3.

Another explosion occurred at Reactor 3 of the Fukushima I plant just after 11:00 local time on March 14. An exterior wall of the building collapsed, but the reactor vessel was not damaged according to a government spokesperson. At 16:29 UTC on Monday 14 March (14 March 01:29 UTC), the Japanese Nuclear and Industrial Safety Agency announced that the explosion had occurred. The local population was advised by the authorities to stay home until the radioactive situation of the environment is totally clarified. Unlike the other five reactor units, reactor 3 runs on mixed uranium and plutonium oxide, or MOX fuel, making it potentially more dangerous in an incident due to the neutronic effects of plutonium on the reactor and the carcinogenic effects in the event of release to the environment.

Additionally, it was reported on 14 Mar at 07:00 EDT that the fuel rods of Reactor 2 at the Fukushima I plant were now fully exposed, and a meltdown of the fuel rods, with the risk of damage to the reactor vessel and a possible radioactive leak, could not be ruled out. As of 14 March, about 160 people have been exposed to dangerous radiation levels near the power stations.

On March 15, at 6:10 a.m. local time an explosion occurred at Reactor 2 of the Fukushima I plant. Radiation "exceeding the legal limit" was detected outside the plant. The government admitted it was "very probable" that the cores of Reactors 1, 2 and 3 had experienced (partial) meltdowns due to high temperatures.

Onagawa Nuclear Power Plant

A fire from the turbine section of the Onagawa Nuclear Power Plant following the earthquake was reported by Kyodo News. The blaze was in a building housing the turbine, which is sited separately from the plant's reactor, and was soon extinguished.

On 13 March the lowest-level state of emergency was declared regarding the Onagawa plant by TEPCO, as radioactivity readings temporarily exceeded allowed levels in the area of the plant TEPCO stated this was due to radiation from the Fukushima I nuclear accidents and not from the Onagawa plant itself.

Tōkai Nuclear Power Plant

The number 2 reactor at Tōkai Nuclear Power Plant was shut down automatically. On 14 March it was reported that a cooling system pump for this reactor had stopped working, but the Japan Atomic Power Company stated that there was a second operational pump and cooling was working, but that two of three diesel generators used to power the cooling system were out of order.

FINAL REMARKS

The huge earthquake of Mw=9.0 on March 11th caused many damages and problems including tsunami tragedies and nuclear accidents. Geotechnical problems are made up of liquefaction in house foundation and river levees.
Due to the mass damage effect, the post-earthquake response and restoration works have been made difficult and delayed. The conventional design philosophy needs further discussion.

The earthquake has provoked significant damage in people's properties; house subsidence due to subsoil liquefaction and slope instability in residential developments in hilly area.

3.5.14 New Zealand earthquake, 2014

INTRODUCTION

Christchurch with a population approximately 377,000 is the second-largest city on the South Island's Canterbury Plains were hit by magnitude 6.3 earthquake, an aftershock from September's magnitude 7.1 tremor. Prior to these two seismic events, Canterbury Plains likely had not experienced an earthquake in thousands of years. In fact, scientists did not even know there was a geologic fault there until it ruptured last year.

The latest Christchurch tremors were not as strong as the original earthquake, but they have caused considerably more damage and claimed dozens of lives, as no deaths occurred during September 2010 quake). The Christchurch epicentre was only 10 kilometres outside of the city, whereas the 2010 event took place about 40 kilometres to the west, in an area that is mostly farmland. In addition, the aftershock struck only about four kilometres in depth below the city, whereas September's temblor originated about 10 kilometres deep.

SEISMIC ACTIVITY

The earthquakes struck an area of New Zealand's South Island where sediments are deposited from the Southern Alps and from the nearby rivers. The sediment deposits reach all the way to the east coast on what is called the Canterbury Plains. During thousands of years, the sediments had been deposited on top.

What defines an "aftershock" as opposed to an earthquake? Does a certain amount of time have to elapse for a seismic event to be considered an earthquake?
It takes many years before seismic activity can be considered an earthquake rather than an aftershock of a previous earthquake. That's a point of debate among seismologists. It takes quite a long time for everything to become quiet again.

It is important to investigate the slip rate, how fast it's moving, whether it's a millimetre per year or a centimetre per year. As plates move, they're building up strain, and is important to estimate how much strain can build up before there is a rupture. Digging trenches along fault lines can be used to study previous seismic activity. As the fault was not previous identified the fault moving was slow, but sufficient to build up toward an earthquake of magnitude 7,
Figures 3.95 to 3.102 show locations of the main shock, aftershocks with magnitude above 3, fault ruptures and earthquake records.

The faults can be mapped and so can be establish some probability of an earthquake happening, but it is not possible to map all faults.

Figure 3.95 Satellite image showing icebergs calved from Tasman Glacier by earthquake
At the Tasman Glacier

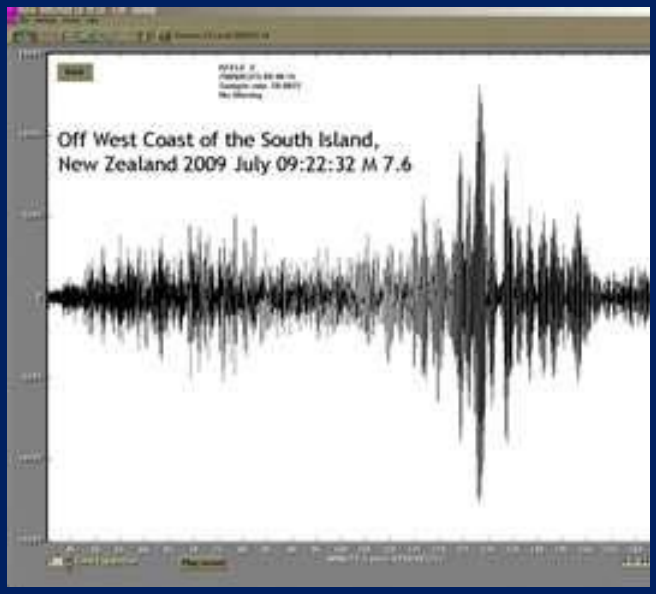

Figure 3.96 New Zealand 2009 earthquake record

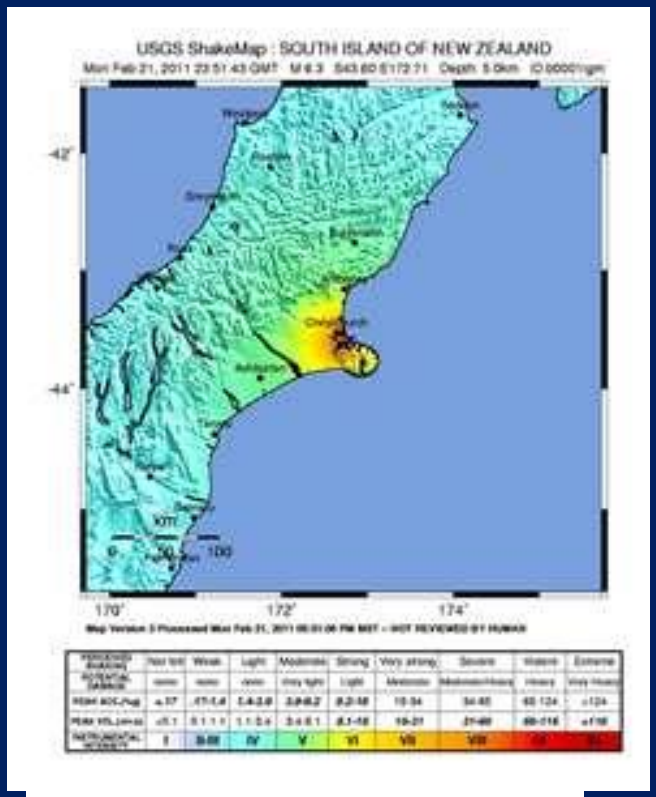

Figure 3.97 New Zealand 2011 earthquake site.

Figure 3.98 Large New Zealand earthquakes.

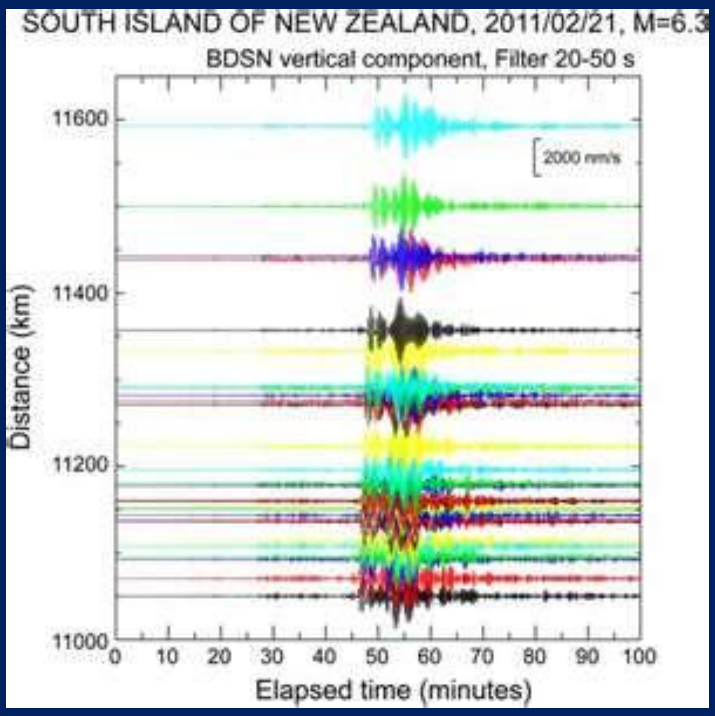

Figure 3.99 New Zealand 2011 earthquake record

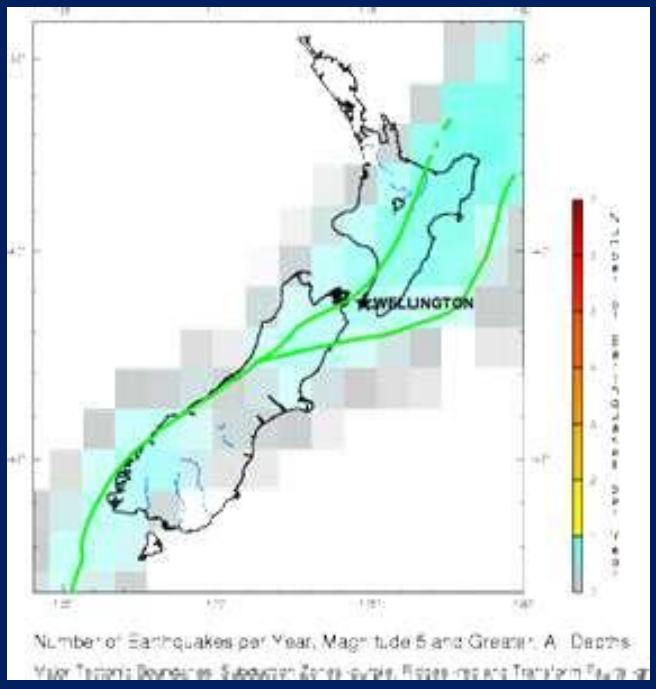

Figure 3.100 New Zealand 2011 earthquake

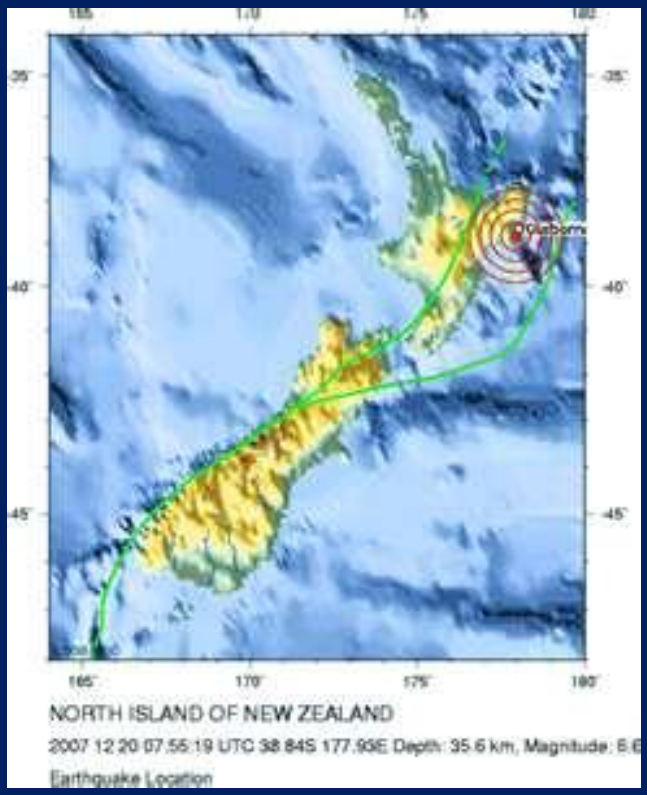

Figure 3.101 New Zealand 2011 earthquake epicentre

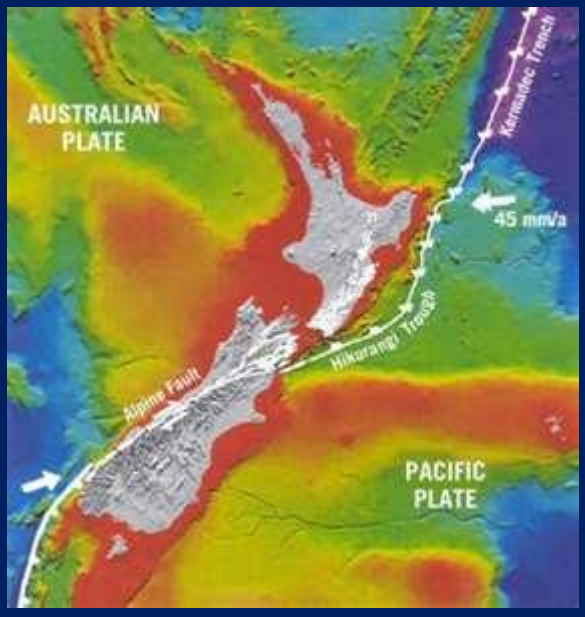

Figure 3.102 Location of plates

ASSESMENT OF BUILDIND BEHAVIOR

New Zealand has some of the strongest building codes in the world, and those building codes are respected. That means you have loss of life, but it's in the dozens or maybe 100 or 200. If the same earthquake were to happen under a city of that size in a developing country, the number of deaths would be in the thousands,

Buildings collapsed around Cathedral Square in central Christchurch. By the afternoon of 3 March, of the 3,000 inspected buildings within the Four Avenues of the central city, 45% had been given red or yellow stickers to restrict access because of the safety problems.

Many heritage buildings were given red stickers after inspections ChristChurch Cathedral lost its spire. The spire's tip had also fallen in earthquakes in 1888 and 1901 but much more fell during the 22 February earthquake.

Figures 3.103 to 3.116 show the damages exhibited by the buildings.

Figure 3.117 shows damages exhibited by the viaduct.

The six-story Canterbury Television (CTV) building collapsed leaving only its lift shaft standing, which caught fire. The building housed the TV station, a medical clinic and an English language school. The school - King's Education -

catered to students from Japan, China, the Philippines, Thailand, Saudi Arabia, Taiwan, and Korea on 23 February police decided that the damage was not survivable, and rescue efforts at the building were suspended. Initially more than 100 people were believed have died in the building. Fire-fighting and recovery operations resumed that night later joined by a Japanese search and rescue squad.

The six-storey PGC House on Cambridge Terrace, headquarters of Pyne Gould Corporation, collapsed, and thirty of the building's two hundred workers were still believed to be trapped within as night fell.

The Forsyth Barr building survived the earthquake structurally, but many occupants were trapped after the collapse of the stairwells, forcing some to abseil out after the quake Search of the building was technically difficult for USAR teams, requiring the deconstruction of 4-tonne stair sets, but the building was cleared with no victims discovered.

Figure 3.103 The Grand Chancellor will be demolished

On 23 February, Hotel Grand Chancellor, Christchurch's tallest hotel, was reported to be on the verge of collapse. The 26-storey building was displaced by half a meter in the quake and had dropped by 1 meter on one side; parts of the emergency stairwells collapsed. The building was thought to be irreparably damaged and have the potential to bring down other buildings if it falls; it was decided the building would be demolished over the following six months.

Figure 3.104 Oxford Terrace Baptist Church

Oxford Terrace Baptist Church was one of many churches damaged by the quake

The historic Canterbury Provincial Council Buildings were severely damaged, with the Stone Chamber completely collapsing.

The Cathedral of the Blessed Sacrament was also severely damaged, with the towers falling, and a decision was made to remove the dome because the supporting structure was weakened. Several other churches have been seriously damaged.

While damage occurred to many older buildings, particularly those with unreinforced masonry and those built before stringent earthquakes codes were introduced, high rises built within the past twenty to thirty years performed well.

Figure 3.105 Canterbury Provincial Council Buildings

Figure 3.106 Cathedral of the Blessed Sacrament

Figure 3.107 Collapse of the building

Figure 3.108 Damage area

Figure 3.109 Collapse of the building

Figure 3.110 Collapse and car damages

Figure 3.111 Collapse of the building

Figure 3.112 Damages exhibited by the church

Figure 3.113 Rotating and collapse of the building

Figure 3.114 Collapse of the building

Figure 3.115 Tilting of the buildings

Figure 3.116 Building collapse

Figure 3.117 Viaduct damages

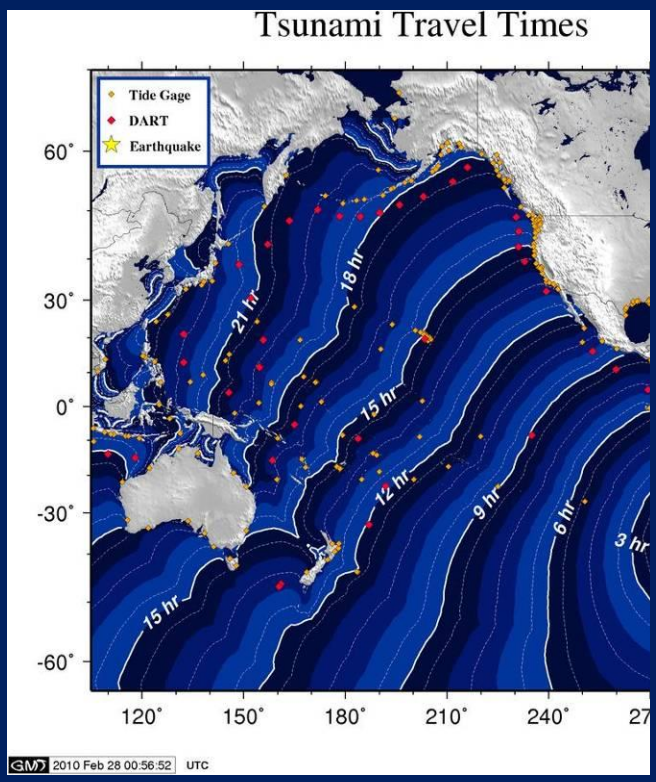

Figure 3.118 Tsunami travel

Figure 3.118 shows the tsunami travel.

Christchurch International Airport

Christchurch International Airport is located 12 km (7 mi) northwest of the city center and was largely unaffected by the earthquake.) (Figure 3.119).

Figure 3.119 Air New Zealand Boeing 777 at Wellington airport

The Christchurch-based national air traffic was closed for a short time while they inspected their facilities.

New Zealand and American research operations in Antarctica have been badly affected by the earthquake, which occurred close to the end of the summer season. Christchurch acts as the major supply and transportation base for both Scott Base and McMurdo Sound research stations, and would normally be the initial destination for scientists returning from the summer season (the bases operate with reduced numbers in the dark Antarctic winter). The problems are exacerbated by the unusual break-up of sheet ice which is normally used for runways in the Antarctic. Several researchers linked to US Antarctic Research are among those missing in Christchurch as a result of the earthquake.

Suburbs

On 7 March, Prime Minister John Key said that around 10,000 houses would need to be demolished, and liquefaction damage meant that some parts of Christchurch could not be rebuilt on

Lyttelton

Buildings in Lyttelton sustained widespread damage, with 60% of the buildings in the main street had been severely damaged No lives were believed to be lost in the town, but two people died on local walking tracks after being hit by rockfalls.

LIQUEFACTION

The earthquake caused widespread liquefaction in the eastern suburbs of Christchurch city as well as in Central Business District (CBD). The liquefaction-affected area in Christchurch during this earthquake was much wider than the one in September 2010. While major liquefied sites in the September 2010 earthquake were distributed along the Avon River (northeast of CBD), liquefaction was observed in the 2011 earthquake across a wide area in suburbs north to south of Christchurch city (Figures 3.120 to 125).

Figure 3.120 Lateral spreading

Figure 3.121 Settlements and lateral displacements

Figure 3.122 Differential settlements of the pavement

Figure 123 Soil boiling

Figure 3.124 Opening of trenches

Figure 3. 125 Lateral spreading

LANDSLIDES

During the Christchurch earthquake, numerous slopes and cliffs suffered shallow landslides and rock falls. One of the most severe damages to a cliff was observed in Sumner, located at the north end of Port Hills in the Banks Peninsula, about 12 km south-east of Christchurch. The cliffs in this area were formed by slope erosion of an ancient volcano. Residential houses were constructed on the cliffs as well as on the flat ground underneath. Many residential houses were built at the edge of the cliff.

Landslides occurred in Sumner, crushing buildings Parts of Sumner were evacuated during the night of 22 February after cracks were noticed on a nearby hillside. Three deaths were reported in the Sumner area.

In contrast to the September 2010 earthquake, Redcliffs and the surrounding hills suffered severe damage. The cliff behind Redcliffs School collapsed on to the houses below. Large boulders were found on the lawns of damaged houses

Twelve streets in Redcliffs were evacuated on Thursday night (24 February) after the cliffs and hills surrounding Redcliffs were deemed unstable (Figure 3.126 and 3.127). Residents were allowed back on Monday night (28 February).

Some 200 kilometres (120 mi) from the epicenter, around 30 million tonnes (33 ST) of ice tumbled off the glacier into Tasman Lake, hitting tour boats with tsunami waves 3.5 metres high (Figure 3.128).

Figure 3.126 Raekura Place in Redcliffs was destroyed by rockfall.

Figure 3.127 Hills slope

Figure 3.128 Ice tumbled off the glacier

CONCLUDING REMARKS

Although the collapse of many commercial buildings led to the greatest casualties in the M 6.3 Christchurch earthquake, it is important to stress that the most significant damage to residential buildings and lifelines was the result of liquefaction and associated ground deformations.
Although the M 7.1 Darfield earthquake caused liquefaction in Christchurch and adjacent areas, the M 6.3 Christchurch earthquake induced more widespread liquefaction and caused more serious damage to infrastructure.
Lessons from case histories all over the world have highlighted the effect of liquefaction to buildings and buried structures, but the scale of

damage experienced in Christchurch following the 2011 event was unusual.

3.5.15 Türkiye and Syria earthquakes 2023, February, 6

Turkiye suffers the influence of 3 tectonic plates and in February 6 2023 occurred a main shock M

7.8 provoked by Anatolian fault, followed by an aftershock M 7.7 and several smaller aftershocks.

At least 59,259 people were killed, 107,204 people were injured in Türkiye and Syria.

Figure 3.129 illustrates the February 6, 2023, earthquakes.

Figure 3.130 shows the historic destructive earthquakes last 60 years.

Figure 3.131 presents the location of seismic stations.

Figure 3.132 illustrates (USGS) Tectonic plate and fault map of the region (link).

Figure 3.133 presents the significant buildings damages.

Figure 3.134 shows the distance-dependence of RotD50 PGA, PGV, and PSA (1.0 sec) for the M 7.8, M 7.7, and M 6.3 events. Recorded data are subdivided into three categories: (1) rock (V S30 ≥ 760 m/s), (2) s

The bridges damages are represented in Figure 3.135.

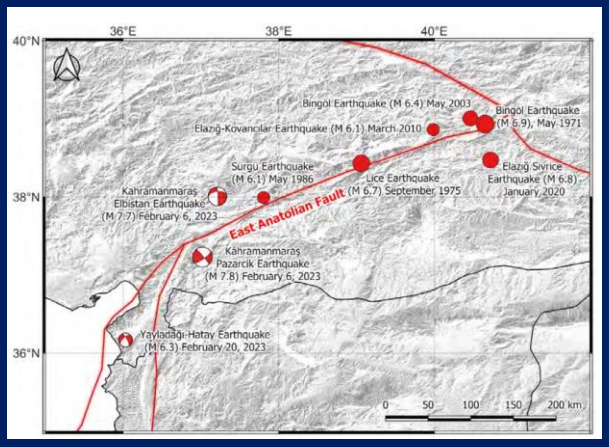

Figure 3.130 Location of last 60 years earthquakes (source GEER, 2023)

Figure 3.129 The February 6, 2023, earthquakes (Google map) (source GEER, 2023)

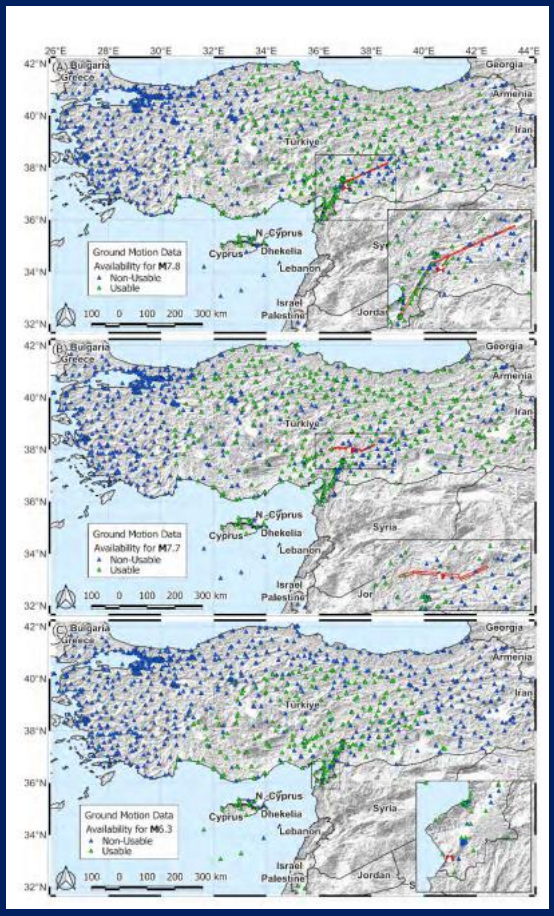

Figure 3.131 Location of seismic stations (source GEER, 2023)

Türkiye, most of which is located on the Anatolian Block, lies at the triple junc

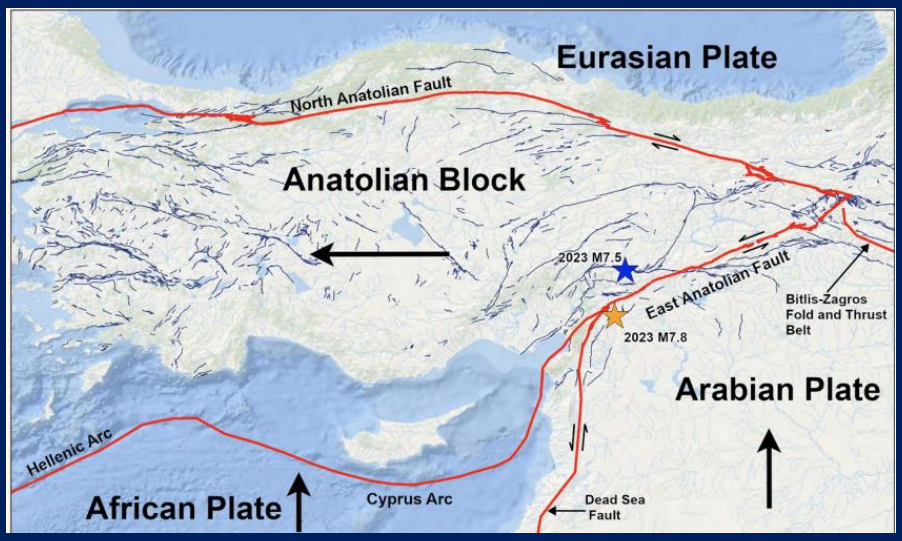

Figure 3. 132 (USGS) Tectonic plate and fault map of the region (link). Red lines denote faults along the plate boundaries. Gray lines denote other faults. (source GEER, 2023)

Figure 3. 133 Building damages (source GEER, 2023)

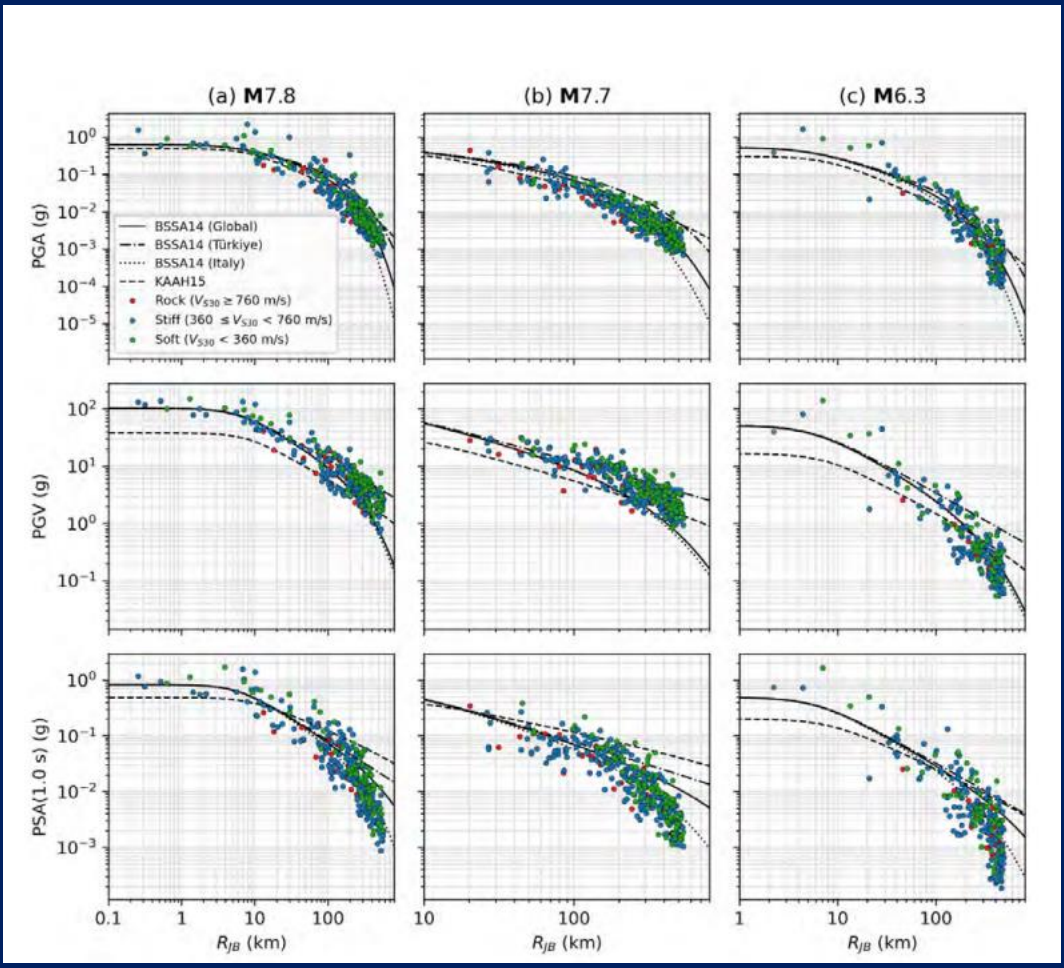

Figure 3.134 Distance-dependence of RotD50 PGA, PGV, and PSA (1.0 sec) for the M 7.8, M 7.7, and M 6.3 events (source GEER, 2023)

Figure 3. 135 Viaduct damages (source GEER, 2023)

Figure 3.136 Liquefaction damages (source GEER, 2023)

Table 3. 1

Level of Damage	**Number of Buildings**
No damage	860,006
Light damage	431,421
Moderate damage	40,228
Heavy damage	179,786
Collapse/Partial collapse	35,355
Urgent need of demolition	17,491
Could not detect	147,895
Total	**1,712,182**

Figure 3.136 illustrates liquefaction damages.

Damage to roadways were observed, namely embankment failure and lateral spreading of roadways as shown in Figure 3.137.

Figure 3.137 Embankment and roadway failure (source GEER, 2023)

The overall performance of dams can be considered good. No significant cracks or deformations were recorded, only minor lateral spreading at the dam crest (see Figure 3.138).

Figure 3.138 Lateral spreading at Kilavusui dam (source GEER, 2023)

The Sultansuyu earth-fill dam was constructed between the years 1986-1992 in Malatya for irrigation purposes. The crest height from the foundation level is almost 60 meters. Crest cracks with varying depths and large cracks on the upstream side were observed after the earthquake. On the crest, cracks with upwards of 2 m lateral deformation (see Figure 3.139).

Figure 3.139 Crest cracking and deformations (source GEER, 2023)

3.5.16 Morrocco earthquake, 2023, September, 8

On 8 September 2023 an earthquake of magnitude 6.8 struck Morocco. The epicenter was in the High Atlas Mountains, several houses have collapsed and other building were reported with structural damage. The earthquake occurred in the African plate.

The earthquake's focus occurred at a depth of 18 km, below the surface, which produced stronger shaking at the surface. The main shock was followed by a magnitude-4.9 aftershock, about 20 minutes later.

A total of 2,122 people is reported to have lost their lives.

More than 380 000 people were affected and 500, 000 people were displaced.

Damage in the earthquake zone was extensive, especially in remote mountain villages in Morocco's Al Haouz province. In this region, nearly all of the houses and other buildings were constructed using unreinforced brick and masonry. Fig. 3.140 illustrates the buildings damages.

In 1960 the city of Agadir was hitted by an earthquake, more than 12,000 people were killed. and led to a revision of building codes that were not respected by the rural houses.

Figure 3.140 Masonry buildings damages

3.6 Final Remarks

The catastrophic effects of the earthquakes raised the attention of the engineers and particularly of the geotechnical engineers to understand better the ground behavior.

The local site conditions, namely the site response, effects of topography, effects of basins, style faulting, ground motions, downhole arrays, attenuation laws have raised deep research to understand better these phenomena.

In summary, from the analysis of the described earthquakes we can say that we have learned some lessons very well, in order to avoid the same mistakes, but unfortunately, we have not given the adequate attention for other situations and so we need to focus in those issues.

In spite of the achievements, we still face a long journey.

4. Liquefaction Assessment

"Little drops of water, little grains of
Sand,
Make the mighty ocean and the pleasant
Land.
So the little minutes, humble though
They be,
Make the mighty ages of eternity"

(Little Things, Julia Carney)

4.1 Introduction

From chapter 3 it was noticed that during the earthquakes occurrence of liquefaction plays an important role, so it seems adequate to introduce this phenomenon in more detail.

The 1964 Niigata (Japan) and the1964 Great Alaskan earthquakes have raised a great interest for a better understanding.

Liquefaction is not a new phenomenon, as it was introduced by Casagrande (1936) for static loads.

The new aspect is that this situation can occur for cyclic loading.

The stress developed in a soil element under cyclic loads depend of the initial stress state that plays an important role in the generation of the pore pressures, during cyclic loads and consequently in the liquefaction likelihood (Figure 4.1).

Following Seed (1976): (i) liquefaction is the condition which the soil continues to exhibit deformations under low or nill residual stress, due to the generation of high pore pressures that will reduce the effective stress and the situation of liquefaction can occur, due to the static or cyclic loads; (ii) initial liquefaction represents a state where during the application of cyclic loads the pore pressures will equalize the confinement pressure without implications in the subsequently deformations; (iii) cyclic liquefaction or cyclic mobility refers to a state where the cyclic loads develop a situation of initial liquefaction and subsequently the cyclic loads provokes limited deformations due to the soil resistance or due the dilatancy and the pore pressures will decrease and the soil will stabilize for the applied loads.

The basic mechanism of a saturated sandy layer liquefaction of low compacity during the earthquake is the progressive development of pore pressure due to the induced cyclic stress and the sandy material becomes more compacted with reduction of effective stress.

For the soil exhibits no volume variation there is an increase of pore pressure (Figure 4.2).

As the value of pore pressure reaches the confining pressure the sand layer exhibits deformations. If the sand is with low compacity can exhibit high deformations near 20% or more and a liquefaction situation.

If the sand is compacted the pore pressures can reach the confinement pressure, but subsequently the soil will exhibit dilatancy, the pore pressure will decrease and no additional deformations will occur.

After the occurrence of liquefaction, the sandy material will settle with withdraw of the water and the sand compacity will increase. The time related with liquefaction depends of the drainage conditions and with the applied cyclic stress.

The duration and intensity of the cyclic loads have influence in the duration of the liquefaction state; if the sandy materials exhibit a high thickness and a fine gradation higher will be the time to dissipate the excess of pore pressure and longer will be the liquefaction state.

The liquefaction risk evaluation is based in the concept of stationary state surface in which the soil deforms under constant load, with an effective minimum stress constant and a volume constant.

The stationary deformation state is reached for large deformations where the initial conditions as fabric, history of stress, deformations and load conditions have dissipated. Consequently, the effective stress of a soil element, that have reached the stationary deformation state, depend only of the compacity state.

The stationary state surface represents the boundary between the conditions that the soil will exhibit a contractile or dilatant behavior during the application of shear loads. Soils with contractile behavior can liquefy under undrained conditions, and soils with dilatant behavior do not liquefy in any condition.

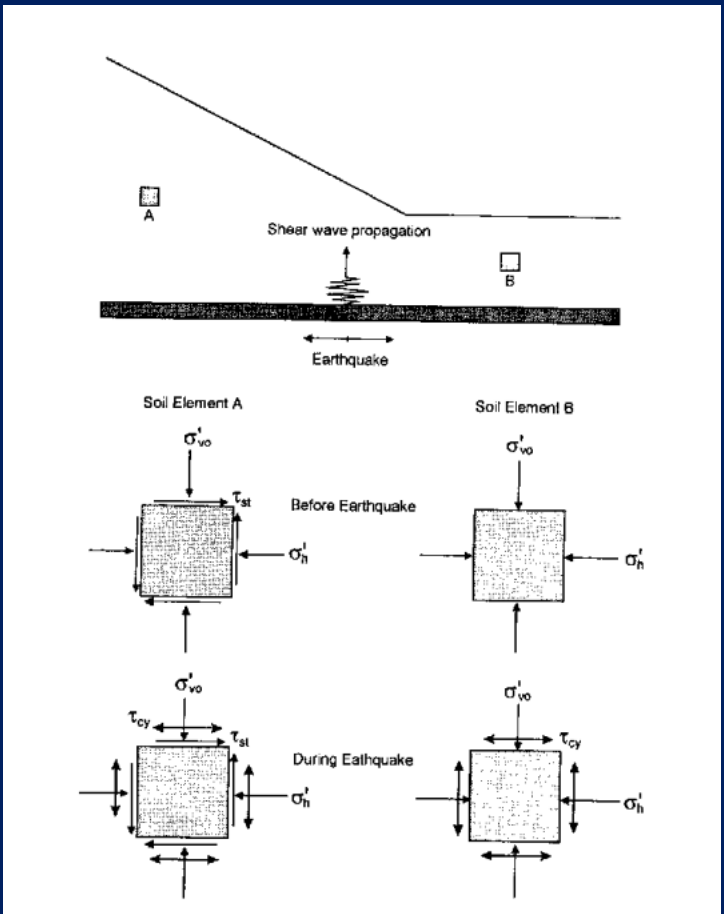

Figure 4.1 Description of liquefaction phenomena

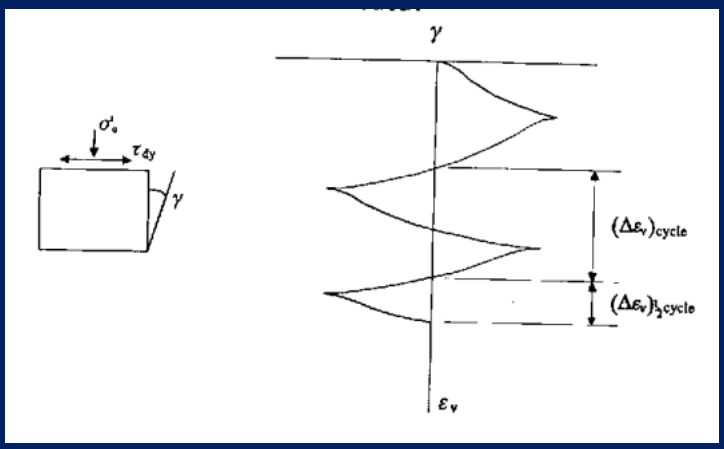

Figure 4.2 Volumetric strain due to cyclic shear strain

Neglecting the liquefaction hazard is also permited when

- α S<0.15 and simultaneously, one or more conditions exists

- The sands have a clay content greater than 20% with plasticity index > 10
- The sands have a silt content greater than 35 % and at the same time N1(60)>20
- The sands are clean with N1(60) >30

4.2 Effects of Liquefaction

The effects of liquefaction on buildings, ground and bridges are shown in Figure 4.3 to Figure 4.5.

Figure 4.3 Effects on buildings

Figure 4. 4 Effects on ground

Figure 4.5 Effects on bridges

4.3 Factors affecting Liquefaction

Seismic History

The seismic history has a great influence in the liquefaction resistance.

Samples with a relative compacity of 54 % and with seismic history exhibit higher liquefaction resistance than samples with 75 % of compacity and without past seismic history.

The following reasons have been pointed:

(i) during the simple shear tests there is a progressive increase of the Ko coefficient related with an increase of liquefaction resistance;
(ii) during the cyclic loading there is a progressive change in the soil structure, with a decrease of volumetric variation with the increase of the number of cycles.

Soil structure

There is evidence that the liquefaction resistance of undisturbed samples from natural deposits is higher than the resistance of samples prepared in laboratory, with the same compacity. One possible explanation is linked with stable structure of natural deposits due to the movements associated with the formation process.

Characteristics of grains

To investigate the influence of the mineralogical characteristics of grains Annakai (1975) have conducted laboratory tests in 4 different sands with the same sieve analysis and relative compacity and concluded that the liquefaction resistance can vary around 20%.

Relative density

The cyclic stress to provoke soil liquefaction depend of the soil relative density.

Soil samples situated higher than the stationary state surface due to their relative density exhibit dilatant behavior without possibility to occur liquefaction.

Confinement Pressure and overconsolidation

Laboratory tests conducted by Finn &Vaid (1977), with cyclic simple shear equipment, and by Seed and Peacock (1971) in overconsolidated sandy samples with OCR between 1 to 8 have shown an increase of liquefaction resistance around 50% for samples with OCR superior to 5.

Cementation Effects

There are evidences that the liquefaction characteristics of in situ deposits depend of the age.

Laboratory tests conducted by Salomone et al. (1978) in triaxial cells and Clough et al. (1989) in cubic samples have demonstrated the effects of cementation increase the liquefaction resistance.

It seems that the increase of liquefaction resistance of sandy natural deposits is associated with the secondary compression of the soil. This increase of resistance can be situated between 25% to 75%.

Effects of fines

Laboratory tests to investigate the effects of fines (material that pass in ASTM sieve 200) have shown that the increase of liquefaction resistance is related with the time needed to mobilize the pore pressure.

This evidence is supported by cyclic triaxial tests conducted by Shen et al., 1977),

Hosri et al. (1984) by laboratory tests and Tokimatsu & Yoshimi (1984) by laboratory and field tests have shown that sands with 20% of clay material and plasticity indexes higher than 10, there was no risk of liquefaction.

4.4 **Triggering of liquefaction**

In general, the assessment of liquefaction potential is essentially deterministic defining the factor of safety (FS) against liquefaction greater than or less than unity. For the risk assessment, the probability associated with the FS is needed. The probability of failure is linked with 3 uncertainties: (i) the ground motion; (ii) the empirical procedures to evaluate liquefaction resistance; (iii) and the natural variability and heterogeneity of the ground.

Probabilistic approaches towards liquefaction assessment have been developed by, amongst others, Cetin et al. [8] and Rodrigue´z-Marek et al. [9], although these are not so widely used as the deterministic methods.

Figure 4.6 shows the flow chart with the input data and decisions required to identify modes of liquefaction-induced ground deformation beneath buildings and the loss estimation (Bird et al, 2006).

The complexities and uncertainties in this process are significant.

The relative likelihood of each mode must be evaluated and the associated magnitude of ground deformation quantified.

Figure 4.7 illustrates the modes of response to ground deformations for any given structural and foundation classification (Bird et al, 2006). For 'rigid body' building response, for determining the damage state it is necessary to accept the system performance.

4.5. **Liquefaction Assessment by laboratory Tests**

Related laboratory tests are used: (i) cyclic triaxial tests; (ii) cyclic simple shear tests; (iii) torsional shear tests. Due to the difficulties to obtain undisturbed samples of high quality, field tests are used, namely SPT tests, CPT tests and seismic cone test.

4.6. Liquefaction Assessment by Field Tests

4.6.1 Liquefaction Assessment by SPT

Following 4.1.3. (2)-Part 5-EC8 "An evaluation of the liquefaction susceptibility shall be made when the foundations soils include extended layers or thick lenses of loose sand, with or without silt/clay fines, beneath the water level, and when such level is close to the ground surface".

Soil investigations should include SPT or CPT tests and grain size distribution (Idriss and Boulanger, 2004). Normalization of the overburden effects can be performed by multiplying SPT or CPT value by the factor $(100/\sigma'_{vo})^{1/2}$ where σ'_{vo} (kPa) is the effective overburden pressure. This normalization factor should be taken not smaller than 0.5 and not greater than 2.

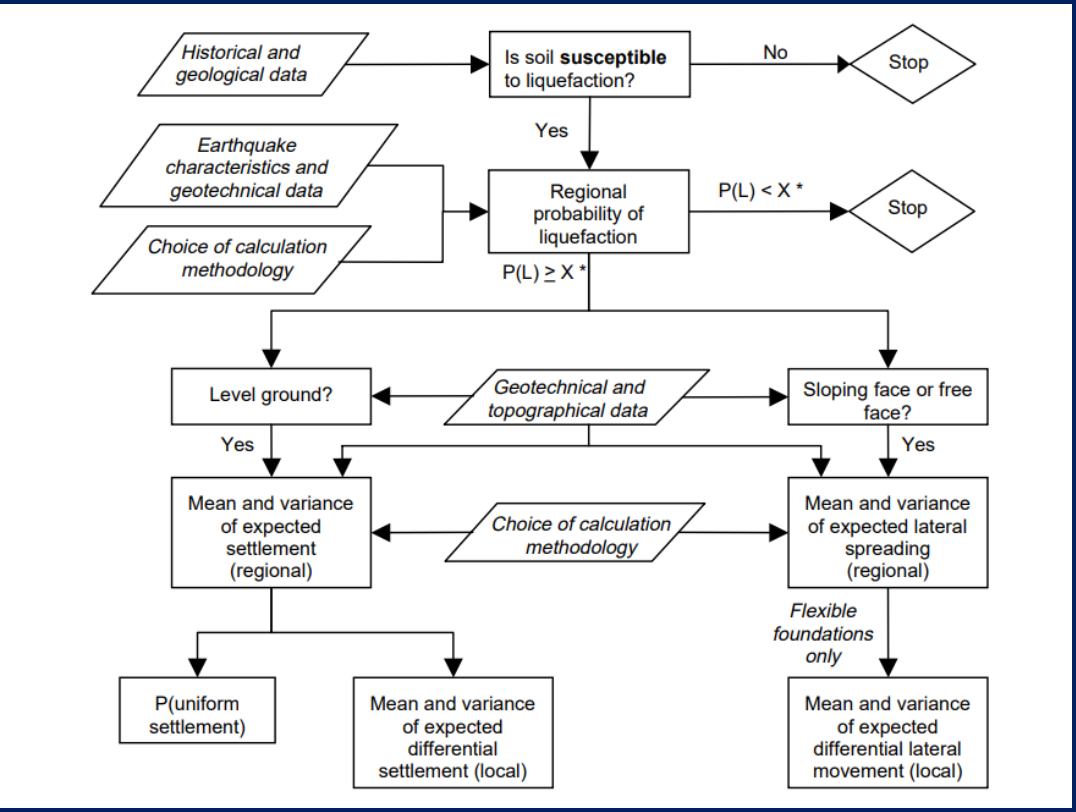

Figure 4.6 Information required for a complete assessment of building vulnerability to liquefaction-induced ground deformations. *X is a predefined value below which the probability of liquefaction is considered negligible (after Bird et al, 2006).

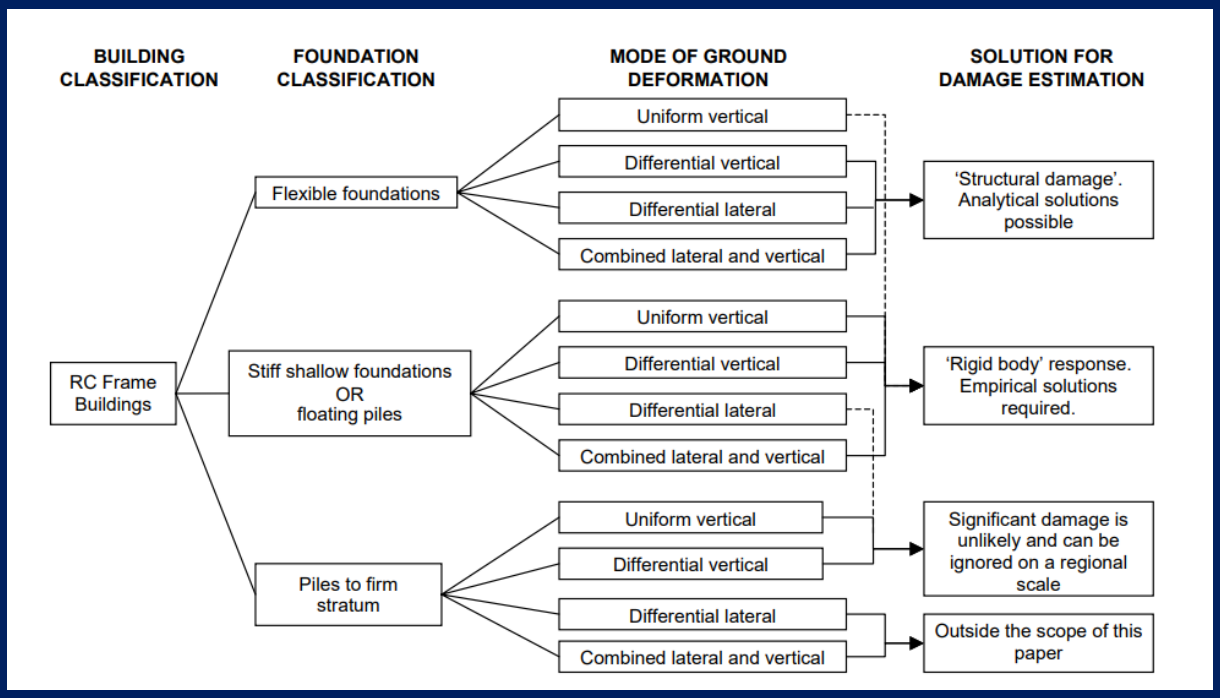

Figure 4. 7. Modes of liquefaction-induced damage within one building classification (after Bird et al, 2006)

The seismic shear stress τ_e can be estimated from the simplified expression:

$$\tau_e = 0{,}65\ \alpha_{gr}\gamma_f\ S\ \sigma_{vo} \qquad (4.1)$$

where α_{gr} is the design ground acceleration ratio, γ_f is the importance factor, S is the soil parameter and σ_{vo} is the total overburden pressure. This expression should not be applied for depths larger than 20 m. The shear level should be multiplied by a safety factor of [1.25].

Seed et al. (1983) proposed the correction of SPT values, taking into account the effective overburden stress, by the relationship $N_1 = C_N . N$, and the C_N values for different relative density values can be obtained by Figure 4.8.

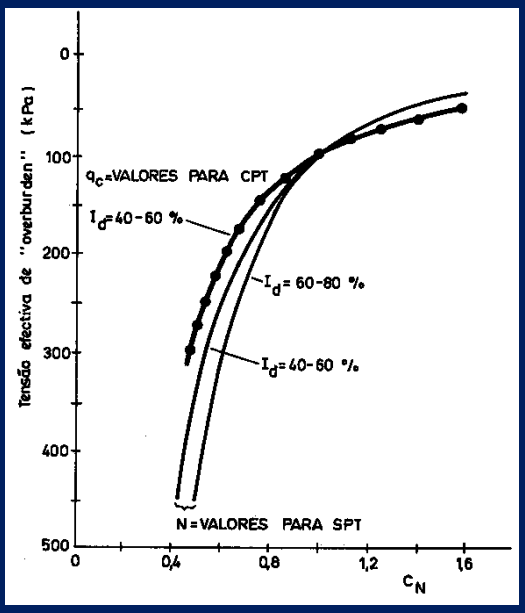

Figure 4.8 SPT and CPT correction values

The magnitude correction factors in EC8 follow the proposal of Ambraseys (1988) and are different from the NCEER (1997) factors. A comparison between the different proposals is shown in Table 4.1.

Table 4.1 - Magnitude scaling factors

Magnitude M	Seed & Idriss (1982)	Idriss NCEER (1997)	Ambraseys (1988)
5.5	1.43	2.20	2.86
6.0	1.32	1.76	2.20
6.5	1.19	1.44	1.69
7.0	1.08	1.19	1.30
7.5	1.00	1.00	1.00
8.0	0.94	0.84	0.67
8.5	0.89	0.72	0.44

Figure 4.9 illustrates the scaling factors.

A new proposal with a summary of different authors presented by Seed et al. (2001) is shown in Figure 4.10.

Figure 4.11 shows the r_d values proposed by Cetin & Seed (2001), based in the analysis of 2600 earthquakes, and incorporates the intensity of vibration, the magnitude and the local stratigraphy.

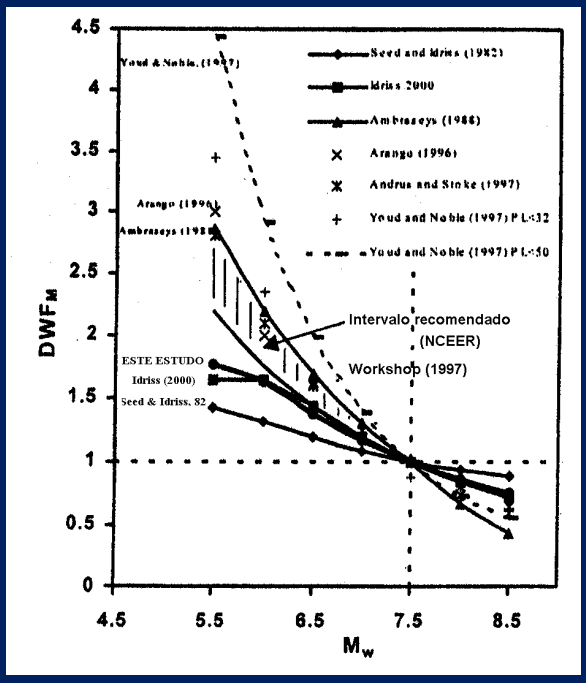

Figure 4.9 Scaling Factors

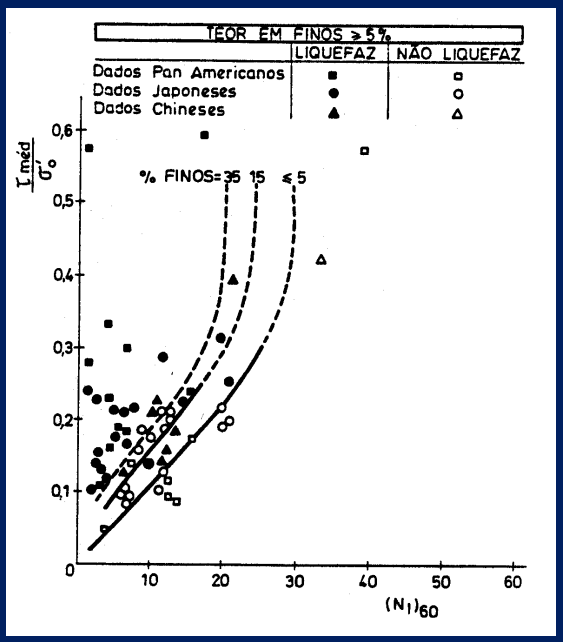

Figure 4.10 Liquefaction potential assessment by SPT tests (after Seed et al, 1985)

A new proposal presented by Cetin et al. (2001) is shown in Figure 4.12 considered advanced in relation with the previous ones, as integrates: (i) data of recent earthquakes; (ii) corrections due the existence of fines; (iii) experience related a better interpretation of SPT test; (iv) local effects; (v) cases histories related more than 200 earthquakes; (v) Baysiana theory.

Bray et al. (2004) have shown that the chinese criteria proposed by Seed and Idriss (1982) was not reliable for the analysis of silty sands liquefaction and have proposed the plasticity index.

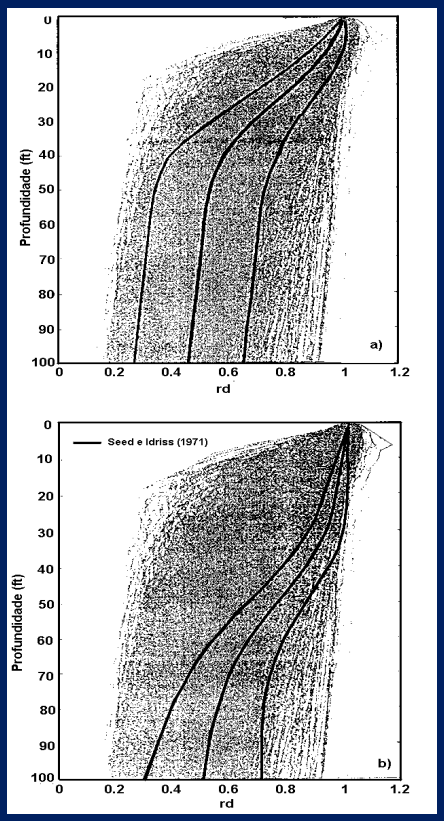

Figure 4.11 r_d values (after Cetin & Seed, 2001)

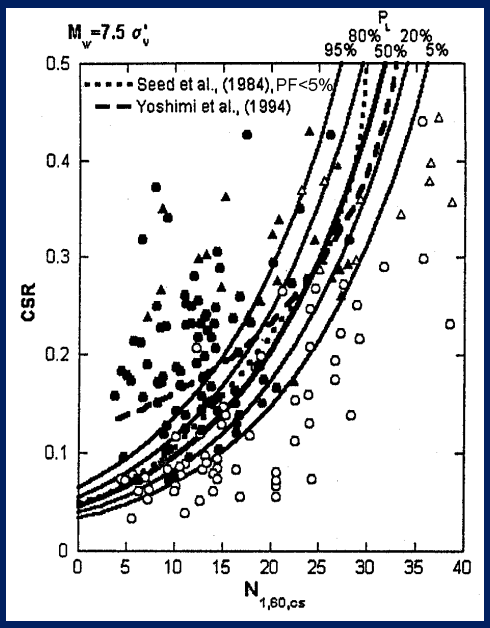

Figure 4.12 Probabilistic approach for liquefaction analysis (after Cetin et al., 2001)

4.6.2 Liquefaction Assessment by CPT tests

The Figures 4.13 and 4.14 illustrates the corrections for CPT tests and also liquefaction assessment by CPT tests.

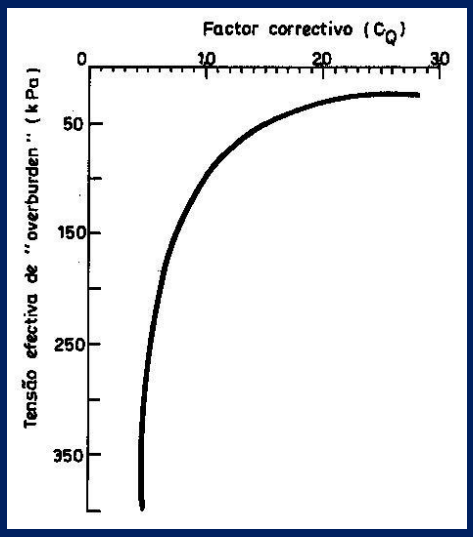

Figure 4. 13 Correlation between C_Q values and overburden effective stress (after Robertson & Campanella, 1985)

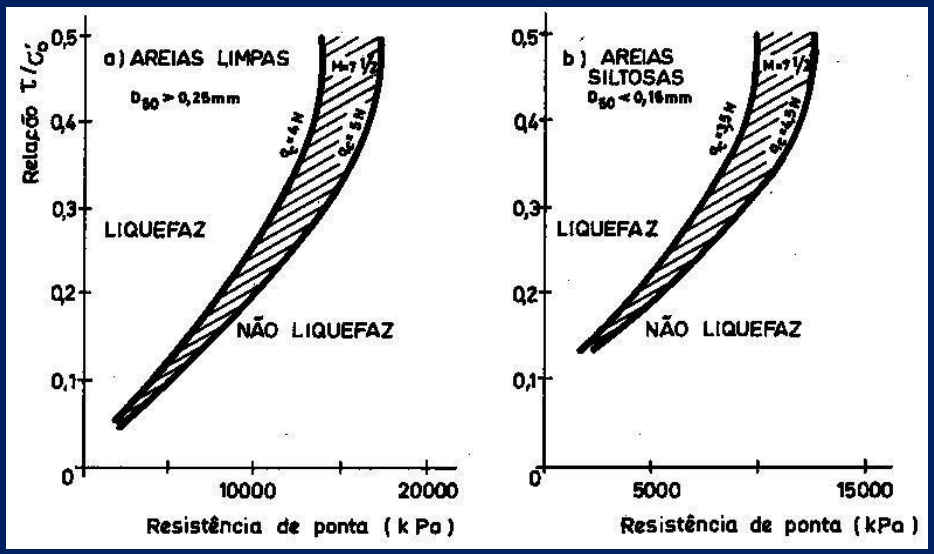

Figure 4.14 Correlation between CPT tests and liquefaction potential of sands (after Seed et al., 1983)

Soil investigations should include SPT or CPT tests and grain size distribution.

The seismic shear stress τ_e can be estimated from the simplified expression:

$$\tau_e = 0{,}65\ \alpha_{gr}\gamma_f S\ \sigma_{vo}$$

where α_{gr} is the design ground acceleration ratio, S is the soil parameter and σ_{vo} is the total overburden pressure.

4.6.3 Assessment of liquefaction by Vs velocities

Empirical liquefaction charts are given with seismic shear wave velocities versus SPT values to assess liquefaction. A comparison between NCEER (1997) and EC8 proposal for pre-standard is shown in Figure 4.15. It is important to refer that the proposal for EC8 is based on the results of Roberston et al. (1992) and the proposal of NCEER (1997) incorporates very recent results.

However, the EC8 standard version considers that these correlations are still under development and need the assistance of a specialist.

The importance of this topic has increased and the assessment of liquefaction resistance from shear wave crosshole tomography was proposed by Furuta and Yamamoto (2000).

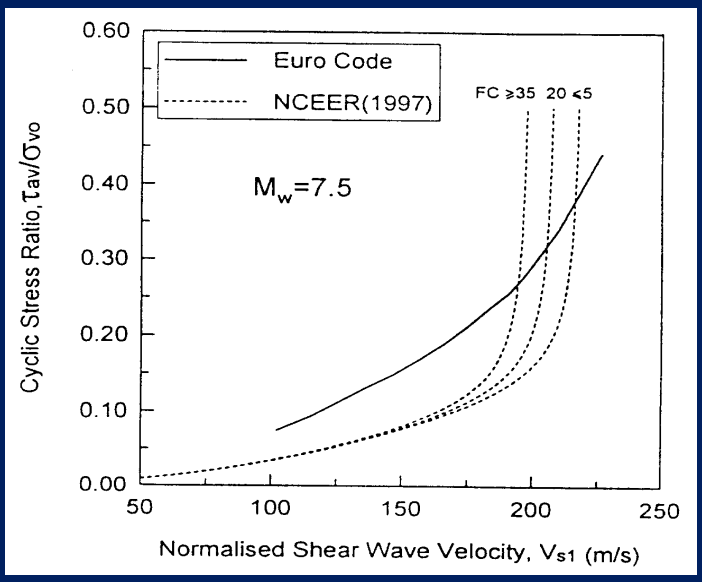

Figure 4.15 Liquefaction potential assessment by NCEER (1997) and EC8 (pre-standard)

4.6.4 Assessment of liquefaction by Plane dilatometer

Vaid et al (1981) proposed for the assessment of liquefaction of sands the angle of dilatancy that can be obtained by triaxial tests or simple shear tests or by pressurometer tests.

Figure 4. 16 illustrates the proposed criteria.

The flat dilatometer allows the definition of the horizontal stress p_0 and so it is possible to define horizontal stress index K_D by the equation proposed by Marchetti (1982):

$$K_D = (p_0 - u)/ \sigma_o \qquad (4.2)$$

where u is the initial pore pressure.

Following Marchetti (1982) the parameter K_D defined by the flat dilatometer in loose sands is more sensible to the effects of pre-consolidation and cyclic loading in comparison with SPT tests or CPT tests, showing, consequently, potentialities in liquefaction evaluation.

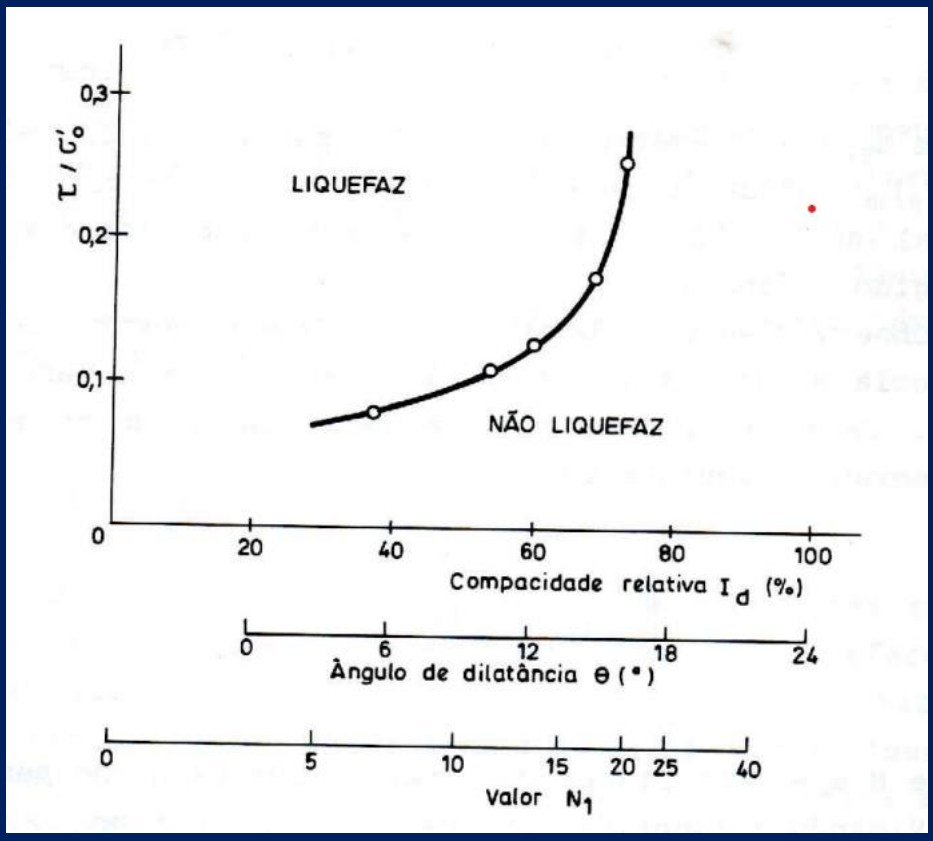

Figure 4.16 Correlation between τ/ σ_o and the angle of dilatancy (after Vaid et al, 1981)

4.6.5 Seismic cone penetrometer

The seismic cone consists of a piezocone below a tri-axial accelerometer array (see Figure 4.17). The Seismic Cone Penetration Test (SCPT) is carried out like a normal CPT but paused at 1m intervals to perform a seismic test. By striking a nylon block anchored to the grounds surface, a seismic shear wave is generated. For greater accuracy and reduction of noise, multiple waveforms can be stacked at each depth.

The accelerometers are more sensitive than conventional geophones and provide larger signal to noise ratios allowing for improved confidence in results and deeper testing.

The direct measurement of shear wave velocity through 1m intervals allows for the reporting of the small strain shear modulus and constrained modulus to a greater degree of confidence than deriving from other ground investigation (GI). As well as producing high quality data, the SCPT is a fast method of GI with typical production rates between 50-70m of testing per day.

Figure 4.17 Seismic cone

4.6.6. Some Comments

The quantity and quality of CPT and SPT case histories has continued to increase with recent earthquake events, including data obtained in the 2010-2011 Canterbury earthquake sequence in New Zealand and the 2011 Mw=9.0 Tohoku earthquake in Japan high-quality case histories representing cases of liquefaction and no liquefaction during the 2010-2011 were compiled. The inclusion of these and other data in liquefaction triggering databases provide an opportunity for re-evaluating liquefaction triggering procedures (Boulanger and Idriss, 2014).

4.7 Assessment of Residual strength

For the assessment of post liquefaction strength, the following variables are important: fabric or type of compaction, direction of loading, void ratio and initial effective confining stress.

A relationship between SPT N value and residual strength was proposed by Seed and Harder (1990) from direct testing and field experience (Figure 4.18).

Ishihara et al. (1990) have proposed a relation of normalized residual strength and SPT tests, based on laboratory tests compared with data from back-analysis of actual failure cases (Figure 4.19). Also, Ishihara et al. (1990) by assembling records of earthquake caused failures in embankments, tailings dams, and river dykes have proposed the relation of Figure 4.20, in terms of the normalized residual strength plotted versus CPT value.

Alba (2004) has proposed Bingham model, based in triaxial tests of large samples, to simulate residual strength of liquefied sands.

4.8 **Evaluation of Settlements**

The topic related with the assessment of post liquefaction strength is not treated in EC8, but it seems that the following variables are important: fabric or type of compaction, direction of loading, void ratio and initial effective confining stress (Byrne and Beaty, 1999).

The susceptibility of foundations soils to densification and to excessive settlements is referred in EC8, but the assessment of expected liquefaction - induced deformation deserves more consideration.

By combination of cyclic shear stress ratio and normalized SPT N-values Tokimatsu and Seed (1987) have proposed relationships with shear strain (Figure 4.21).

To assess the settlement of the ground due to the liquefaction of sand deposits based on the knowledge of the safety factor against liquefaction and the relative density converted to the value of N1 a chart (Figure 4. 19) was proposed by Ishihara (1993).

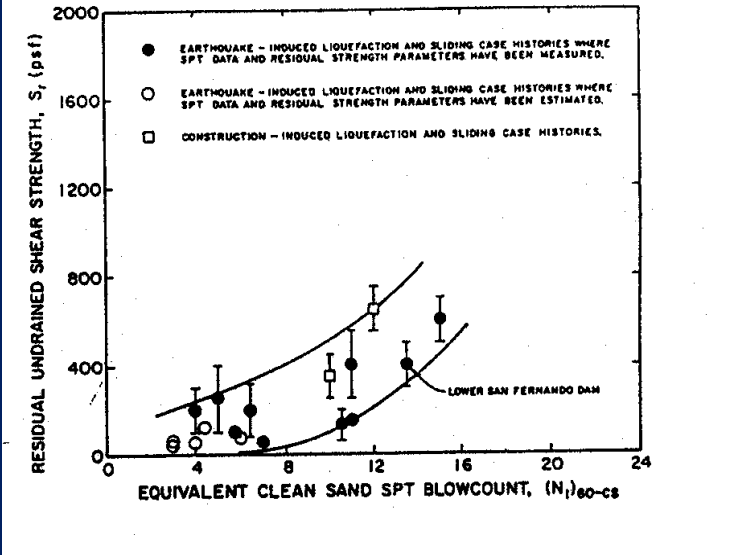

Figure 4.18 Relationship between (N1) 60 and undrained residual strength (after Seed and Harder, 1990)

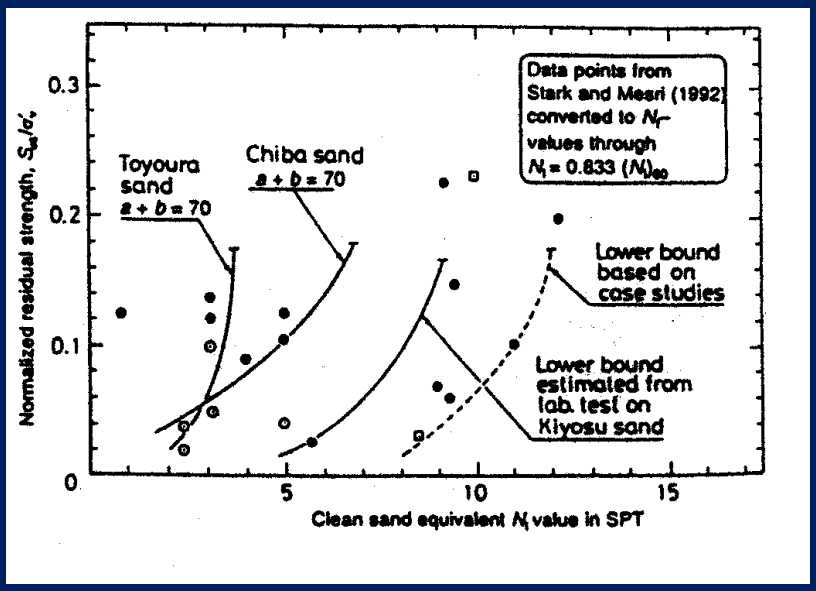

Figure 4.19 Relation of normalized residual strength and SPT tests (after Ishihara et al., 1990)

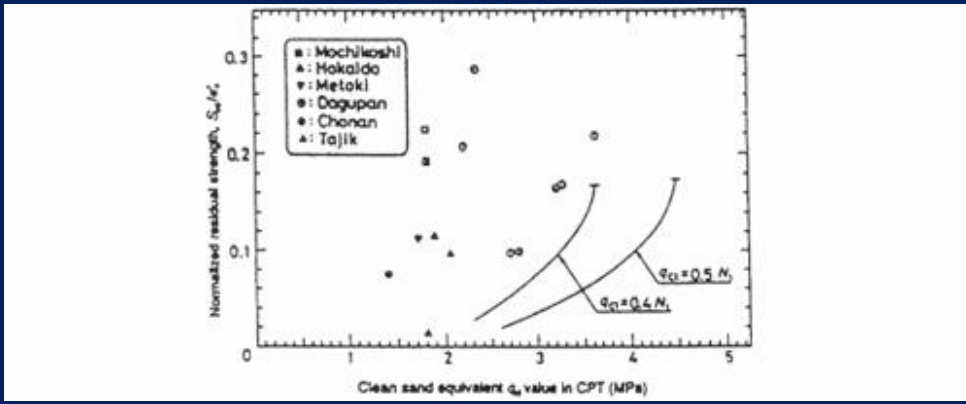

Figure 4.20 Relation of normalized residual strength and CPT tests (after Ishihara et al., 1990)

safety factor against liquefaction and the relative density converted to the value of N1 a chart (Figure 4.21) was proposed by Ishihara (1993).

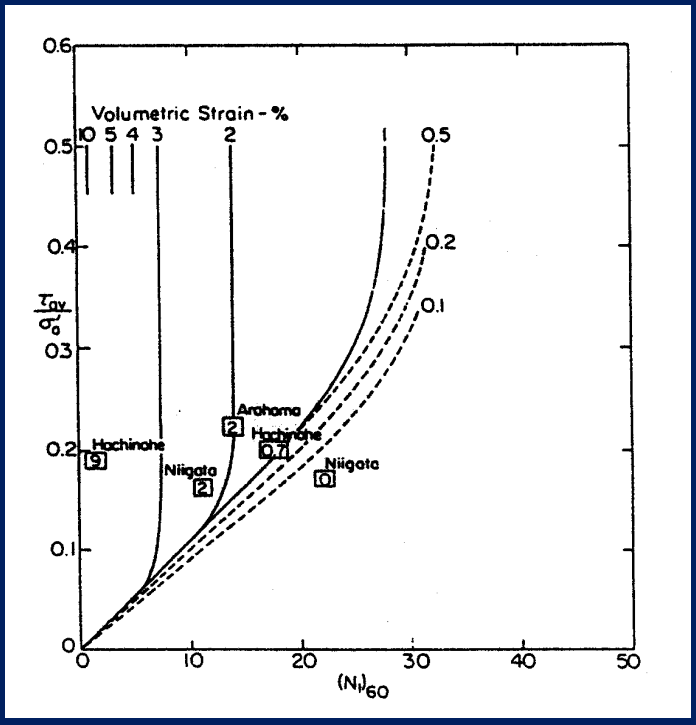

Figure 4.21 Correlation between volumetric strain and SPT (after Tokimatsu and Seed, 1987)

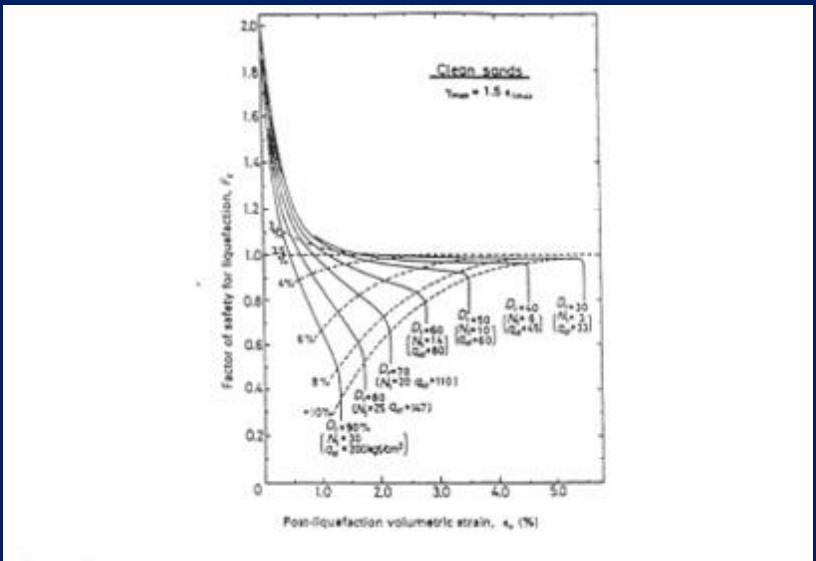

Figure 4.22 Post cyclic liquefaction volumetric strain curves using SPT and CPT tests (after Ishihara et al., 1990)

4.9 **Liquefaction Remedial Measures**

Following EC8 ground improvement against liquefaction should compact the soil or use drainage to reduce the pore water pressure. The use of pile foundations should be considered with caution due the large forces induced in the piles by the liquefiable layers and the difficulties to determine the location and thickness of these layers.

Two categories of remedial measures against liquefaction were proposed (TC4 ISSMGE, 2001; INA, 2001):

(I) Solutions aiming at withstanding liquefaction - Confinement wall (see Figure 4.23): stiff walls anchored in a non liquefied layer (or a bedrock) to avoid lateral spreading in case of liquefaction; Soil reinforcement - transfer of loads to a non-liquefiable layer.
(ii) Solutions to avoid liquefaction: - Soil densification: compaction grouting to minimize the liquefaction potential; - Dewatering: to lower the water table in order to minimize the risk of liquefaction; - Drainage: to facilitate the dissipation of pore pressure; - Fine grouting: to increase the soil cohesion.

The liquefaction prediction/determination methods are covered by the following main japanese standards: (i) Design standards for Port and Harbour Structures, (ii) Design Standards of Building Foundations, (iii) Design Standards for Railway Structures; (iv) Design Specifications for Roads.

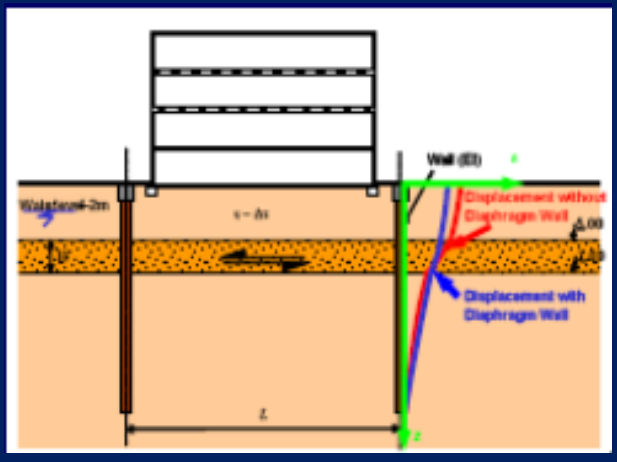

Figure 4.23. Confining wall

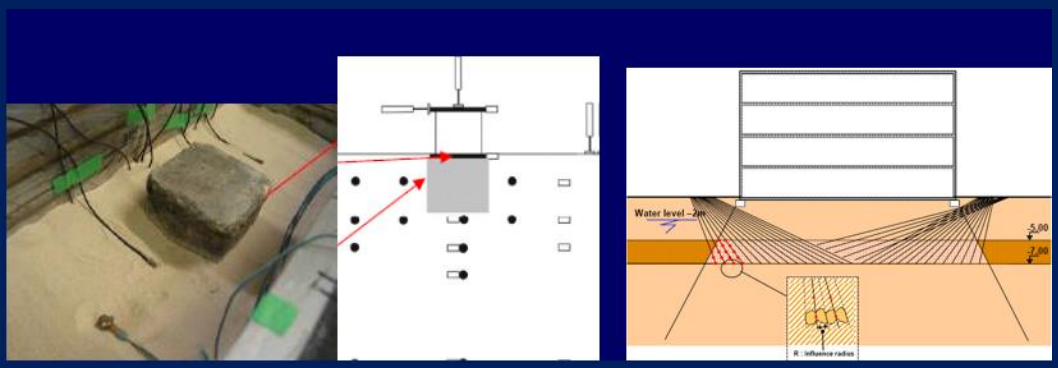

Figure 4. 24 Bacteria treatment

The measures to prevent of occurrence of liquefaction include the improvement of soil properties or improvement of conditions for stress, deformation and pore water pressure. In practice a combination of these two methods is adopted.

The measures to reduce liquefaction induced damage to facilities include (1) to maintain stability by reinforcing structure: reinforcement of pile foundation and reinforcement of soil deformation with sheet pile and underground wall; (2) to relieve external force by softening or modifying structure: adjusting of bulk unit weight, anchorage of buried structures, flattering embankments.

In NEMISREF Project the following criteria for selection was used (Evers, 2005): (i) Potential efficiency; (ii) Technical feasibility; (iii) Impact on structure and environmental; (iv) Cost-effectiveness; (v) Innovation.

Two methods were selected: (i) Soil grouting using calcifying bacteria (see Figure 4.24); (ii) confinement wall.

Related with calcifying bacteria the objective of soil consolidation is to create a cementation between the grains of soil skeleton increasing the cohesion.

With confinement wall even if partial liquefaction could occur the final deformations will be controlled.

The improvement of soil properties, to prevent soil liquefaction, by soil cementation and solidification is performed by deep mix method (Port Harbour Research Institute, 1997), so within this framework the use of bacteria technique is innovative.

The structural strengthening is performed by pile foundation and sheet pile (INA, 2001) and so the confining wall can be considered innovative.

The proposed methods of remediation have an additional advantage minimizing the effects on existing structures during soil improvement.

Comments: It seems that the following items deserve more clarification:
i) Quantification of the values of extended layers or thick lenses of loose sand;
ii) Meaning of ".....when such level is close to the ground surface"? What depth? What is the maximum depth liquefaction can occur?
iii) How to compute seismic shear stress τ_e for depths larger than 20 m;
iv) The use of Becker hammer and geophysical tests to assess the liquefaction of gravely materials should be stressed;
v) The recommended multiplied factor CM for earthquake magnitudes different from 7.5 deserves more explanation. It is important to refer that the well known correlation proposed by Seed et al (1984) for cyclic stress ratio versus N_1 (60) to assess liquefaction and adopted in Annex B of EC8 – Part 5 use different correction factor for earthquake magnitudes different from 7.5.

- Some topics that deserve consideration: residual strength of soil; post – liquefaction settlements; number of cycles versus pore pressures; liquefaction remediation
- Remedial methods against soil liquefaction: (i) the prevention of liquefaction, such as densification method, solidification method, replacement method; and (ii) the reduction of damage to facilities due to liquefaction, such as strengthening of foundation, reduction of lift of structure and control of deformation (TC4 ISSMGE, 2001)

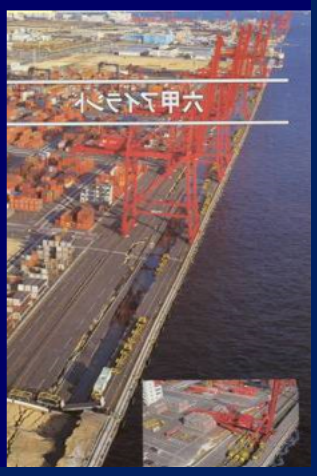

The liquefaction prediction/determination methods are covered by the following main japanese standards: (i) Design standards for Port and Harbour Structures, (ii) Design Standards of Building Foundations, (iii) Design Standards for Railway Structures; (iv) Design Specifications for Roads.

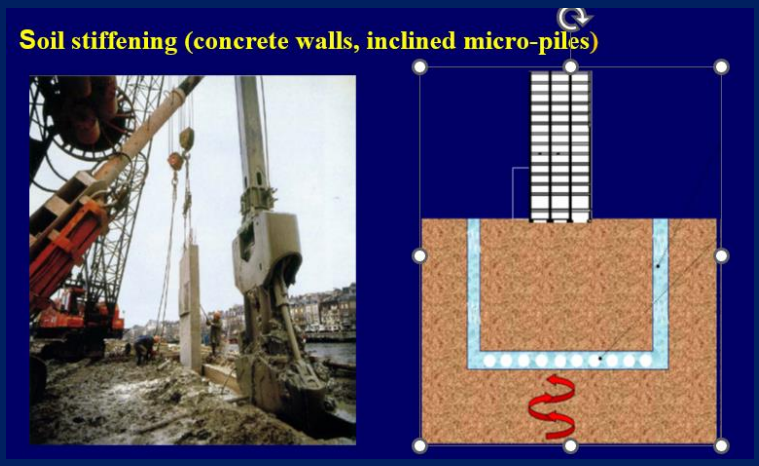

Figure 4.25 Soil stiffening

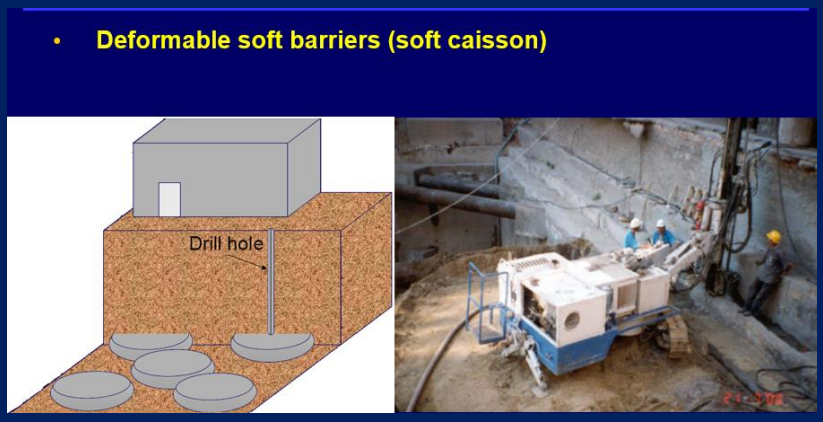

Figure 4.26 Soft barriers

HEAVY TAMPING

- FREE FALL 10-40 m
- RAMMER WEIGHTING 400-1000 kN
- DESTRUCTION OF SOIL FABRIC
- GENERATION OF EXCESS PORE PRESSURE
- PROCESS OF REGAIN THIXOTROPY AND INTER_PARTICLE BONDS WILL TAKE LONG TIME
- LESS EFFECTIVE WHEN CLAY CONTENT IS LARGER THAN 15%

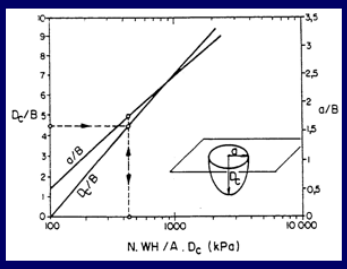

Figure 4.27 Soil densification

The investigations of the decay of free soil vibrations caused by the fall weight after each impact with the compaction degree is getting increase attention. The maximum vertical ground velocity versus distance to the compaction point for a pounder of 16.5 tons from 15 m height is shown in Figure .

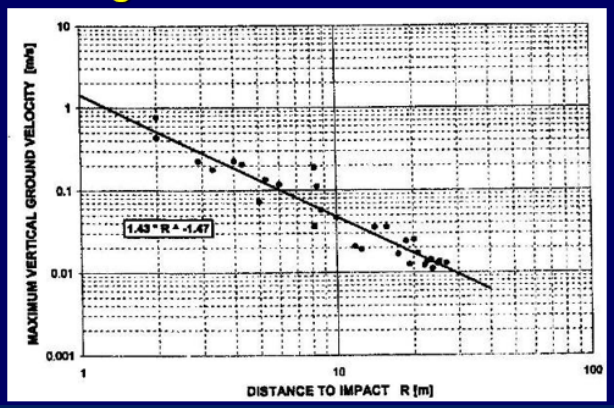

Figure 4.28 Maximum vertical ground velocity versus distance to impact

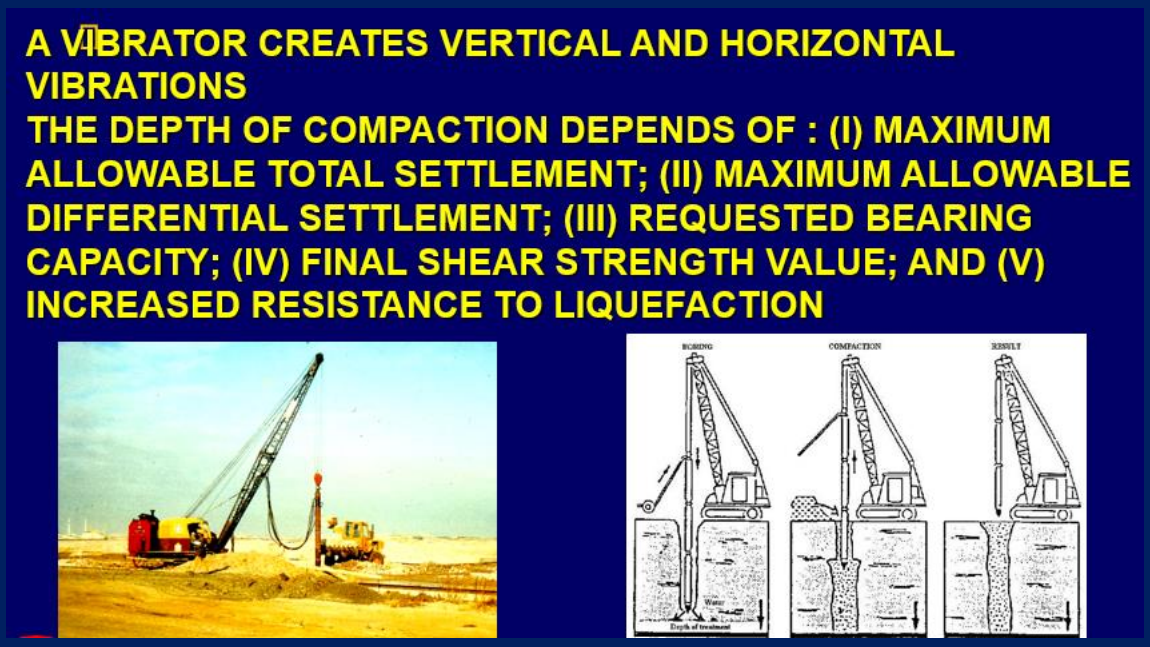

Figure 4.29 Vibroflotation Technique

4.10 Buildings Settlements due to Liquefaction

The settlements of foundations depend of the following factors: (i) thickness of liquefiable layer; (ii) thickness of unliquefiable layer; (iii) density of ground; (iv) grain size; (v) amplitude of acceleration; (vi) number of cyclic loading, (vii) width of footing; (viii) load intensity; (ix) penetration depth.

An excellent summary related with liquefaction induced settlements of buildings was presented by Yasuda et al (2001):

1964 Niigata earthquake

Measurement of settlements of 340 buildings with pile and spread foundations was conducted by Building Research Institute (1965).

For spread foundations buildings the average settlements have shown the following trend (Table 4.1):

Table 4.1 Buildings settlements during Niigata earthquake

Nº Buildings	Settlements (cm)
2	> 200
1	150-200
1	100-150
9	50-100
8	<50

The spread foundations were continuous footing and independent footing and the number of stories of buildings was 1 to 4.
The depth of liquefied layer was 10m.

1990 Philippines earthquake

During the 1990 Luzon Philippines earthquake for spread foundations buildings the average settlements have shown the following trend (Table 4.2):

Table 4.2 Buildings settlements during Philippines earthquake

Nº Buildings	Settlements (cm)
1	> 200
0	150-200
9	100-150
13	50-100
4	<50

The spread foundations were continuous footing and independent footing.

Alluvial loose sand layer has a depth of about 10 m.

1995 Kobe earthquake

The settlements of buildings with spread foundations were not large (Table 4.3):

Table 4.3 Buildings settlements during Kobe earthquake

Site	Maximum settlements (cm)
Naknosshima, Hyogo-ku	5 to 10
Uozakihama, Higashinadaku	54
Uozakimi-namimachi, Higashinadaku 9	20,60

1999 Kocaeli earthquake

Many buildings settled due to liquefaction during 1999 Kocaeli earthquake in Adapazari. The average settlement was 50 cm and the common settlement was 20cm to 40 cm. The buildings were with 2 to 6 stories.

1999 Chi-chi earthquake

In several cities liquefaction has occurred during 1999 Chi-Chi earthquake. The average settlement was 30 cm and the common settlement was 20cm to 40 cm.

Relationship between settlement and inclination
The following relationship can be proposed between average settlement and angle of inclination:

$$I = 0.05\ Sav \qquad (4.3)$$

where I is the angle of inclination(degree) and Sav is the average settlement(cm).

It seems that the settlements of buildings due to liquefaction depend of the grain size of material and decrease with the increase of fines.

From the above analysis it can be concluded that the expected displacements due to liquefaction will be less than 100mm and the rotations less than 1degree.

Based in the analysis of the behavior of 719 buildings that were inspectioned during the occurrence of Kocaeli earthquake (1999), Bray e Stewart (2000) have proposed the Structural Damage Index D1 to D5 (see Table 4.4) and the Ground Failure Index GF0 à GF3 (see Table 4.5).

Table 4.4 Structural Damage Index (after Bray and Stewart, 2000)

Index	Description	Interpretation
D0	Without damages	Without fissures and broken glasses, etc
D1	Ligth damages	Esthetic cracks without damages in structural elements
D2	Moderate damages	Cracking of structural elements without significant displacements around the cracks
D3	High damages	Cracking of structural elements with significant displacements around the cracks
D4	Partial failure	Partial failure of the structure
D5	Failure	Total failure of the structure

Table 4.5 Ground Failure Index (after Bray e Stewart, 2000)

Index	Description	Interpretation
GF0	Without ground failure	Without settlements, rotations and lateral movements
GF1	Light ground failure	Settlements ≤ 10 cm, rotation ≤ 1º, without lateral movements
GF2	Moderate ground failure	Settlements from 10 to 25 cm, rotation from 1º to 3º, lateral movements ≤ 10 cm
Gf3	Significant ground failure	Settlements higher than 25 cm, rotation ≥ 3º, lateral movements ≥ 25 cm

4.11 **Liquefaction of Sandy Gravels Materials**

There have been a number of cases in recent years where liquefaction of gravelly materials has been observed to occur with associated detrimental effects during earthquakes.

Important cases of earthquake-induced liquefaction in gravelly materials include:

(i) The slide in the upstream gravelly-sand shell of Shimen Dam in the 1975 Haicheng earthquake (Wang. [126]); (ii) The liquefaction of gravelly soils in sloping ground causing the Whiskey Springs Slide during the 1984 Mount Borah earthquake (Andrus and Youd (1989); (iii) The slide in the upstream sandy gravel slope protection layer of Baihé Dam in the 1974 Tangshan earthquake (Wang, 1984).

Gravel materials are less vulnerable to liquefaction and laboratory tests conducted under cyclic loading conditions have showed that significantly higher stresses were required, even under undrained cyclic loading conditions, to induce high pore water pressures in gravelly soils than in sands.

Standard methods of in-situ exploration developed for sands, such as the standard penetration test (SPT), the cone penetration test (CPT), the self-boring pressuremeter, etc, give erroneous results in gravels because the soil properties are large compared to the dimensions of the test equipment.

A large-scale type of penetration test in the form of the Becker Penetration Test developed in Canada can be used for exploring the characteristics of deposits containing gravel and cobble-size particles (Figure 4.30).

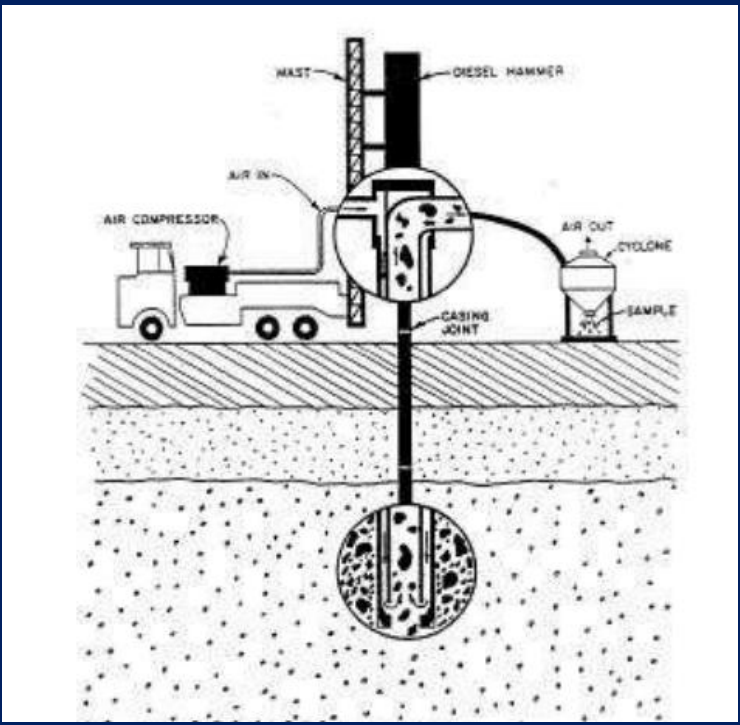

Figure 4.30 Becker Hammer

A comparison between tests with SPT sampler (5.08 cm) and other samplers with higher dimensions, namely japonese with 7.3 cm, italian with 14 cm and american with 7.6 cm, with the purpose to define corrective factors incorporating : (i) the energy transmitted by driven equipment; (ii) using discrete models (DEM) for a better understanding of the crushing effects between the links of particles of gravel materials; (iii) using the theory of waves propagation associated with the records of axial forces, velocity of rods penetration for a better understanding of the particles displacements response and grain dimensions can be summarized in Figure 4.31 and Figure 4.32.

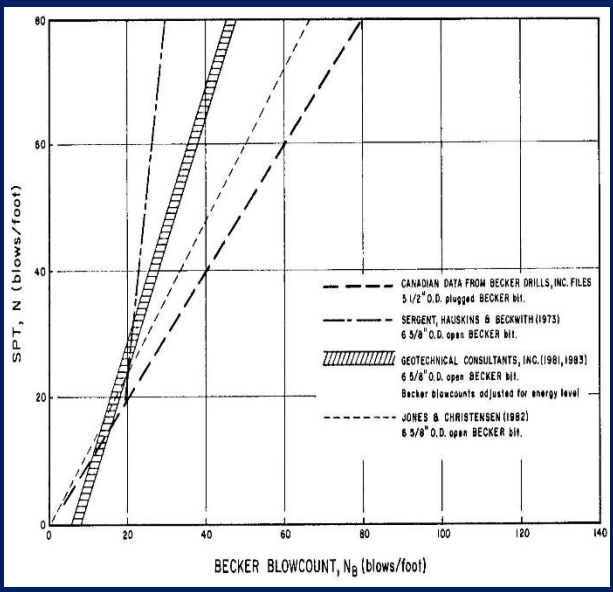

Figure 4.31 Correlations between BPT and SPT values (after Harder and Seed, 1986)

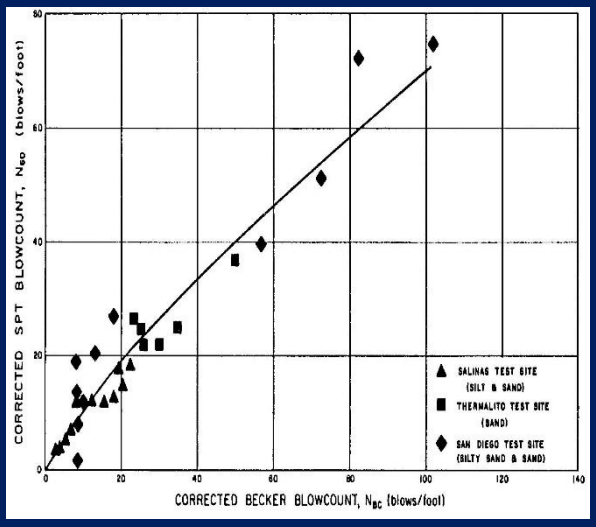

Figure 4.32 Correlations between BPT and SPT modified values (after Harder and Seed, 1986)

Cyclic triaxial tests indicate that undrained liquefaction of gravels can occur in laboratory tests. Membrane compliance plays a significant rule in inhibiting liquefaction in undrained cyclic triaxial tests performed on gravels and there is currently no satisfactory method for accounting this phenomenon. Thus, the non compliant cyclic loading resistance of gravels is not easily determined.

To overcome these difficulties laboratory tests using a shaking table in sandy gravel samples with gravel percentage of 0%, 25%, 50% and 75% and values of relative density of 60% and 85% were recommended (Sêco e Pinto (1991).

Bearing in mind the difficulties related with the preparation of representative samples in laboratory related with parallel gradation curve and ageing effects, complementary shear wave velocities measurement were recommended to provide an approximate correlation between values of stress ratio causing liquefaction in the field and the average shear wave velocity.

4.12 Models to Study Liquefaction

A brief analysis of the models to study liquefaction, namely models in total stress, models in effective stress, endocronic models and probabilistic models is presented.

Models in total stress

The induced shear stress can be computed by a model in total stress.

The development of the pore pressures can be defined by the following methodology:

(i) determination of the induced cyclic stress by the earthquake;
(ii) determination of the number of the equivalent cycles N_e (for 0.65 τ_{max}) induced by the earthquake;
(iii) considering the Figure 4.33 determination of the number of cycles N_l;
(iv) determination of the pore pressure considering the ratio N_e / N_l and the proposal from De Alba et al. (1975) illustrated in Figure 4. 34.

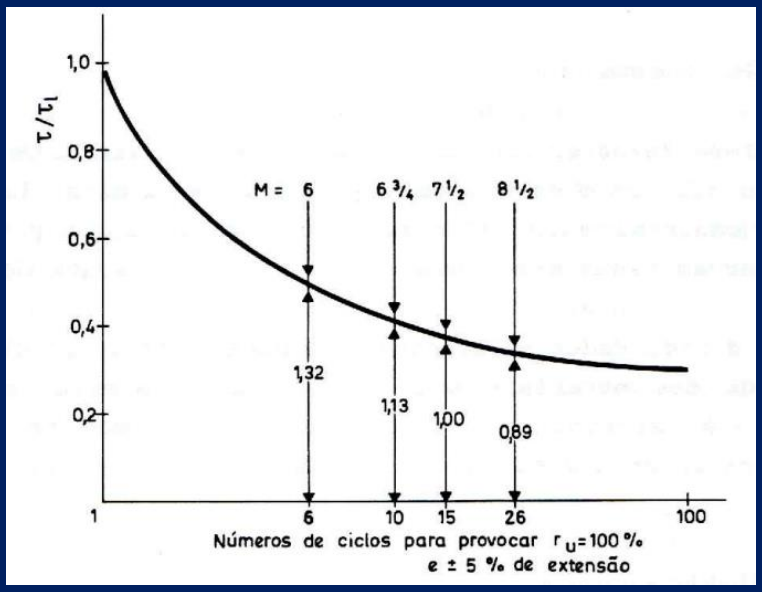

Figure 4. 33 Correlation between τ/τ_l and the number of cycles to reach liquefaction (after Seed et al., 1983)

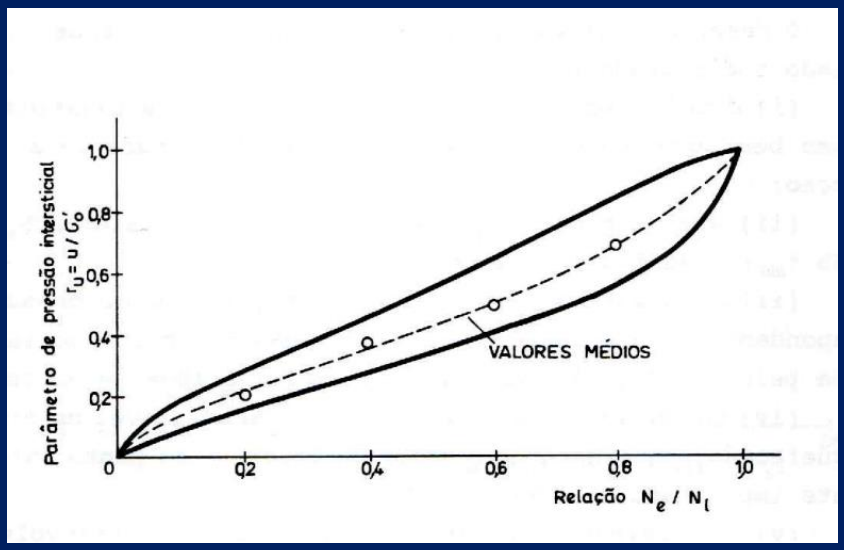

Figure 4. 34 Pore pressures developed in cyclic simple shear tests (after De Alba et al. 1975)

The prediction of pore pressures proposed by this formulation was validated by field observation (Ishihara at al.,1989).

The models in total stress have the following limitations:

(i) the situations of failure before initial liquefaction are not identified;
(ii) hypotheses are necessary to compatibilize the irregular history of stress with the results of irregular cyclic stress;
(iii) do not incorporate the occurrence of the softening due to the generation of pore pressures.

Models in effective stress

The dynamic behavior of loose sands depends of the generation and dissipation of pore pressures.

Due to the seismic loads two types of pore pressures are generated, namely the transient pore pressure and the residual pore pressures.

The latter due to the plasticity deformations of sand soils are only dissipated by drainage and consequently have major influence in the sand resistance.

If there are conditions for sand drainage, during the loading, both generation and dissipation of pore pressure will occur.

Numerical models in effective stress that incorporates the generation and dissipation of pore pressures were proposed by Katsikas & Wylie (1982) and Finn & Bhatia (1981).

Endocronic Models

Bazant and Krizek (1976) introduced the endocronic model to study sands liquefaction and the nonlinear behavior of the material was introduced by the parameter of intrinsic time that depends of the increments of time and increment of deformations.

The authors introduced the following concepts. (i) variation of intrinsic time with hydrostatic pressure; (ii) dilatancy; (iii) softening.

Probabilistic models

Finn (1988) introduced a method to define the probability of liquefaction combining the Seed (1979) with the Cornell in order to include the occurrence of magnitude and acceleration of the earthquake.

Comparison between different Models

From all the described models it is not possible to appoint one model as the best for all the situations.
The models in total stress are acceptable for practical purposes, due to their simplicity.

For important structures analyses in effective stress are necessary as the definition of the seismic history and the prediction of residual displacements are needed for a better understanding of the phenomena.

The endocronic models are very complex and loose the interest for practical applications.

The probabilistic models are getting increase attention, but still are facing difficulties for the characterization of the materials and for the definition of seismic action.

In summary, for practical purposes, simple models can lead to better results in comparison with sophisticated models.

5. **Geotechnical Risk and Safety**

"If a man will begin with certainties, he
Shall end in doubts; but if he will be
Content to begin with doubts, he shall
End in certainties"

(Advancement of Learning, Francis Bacon)

5.1. Introduction

In this chapter my Address in the Opening Ceremony of XIII ECSMGE, Prague, 2003, is presented.

Some additional Reflections -Special Presentation for XX Danube Conference, Passau, 2002, is addressed.

The Eurocodes – 2nd generation are introduced.

5.2 My Address in the Opening Ceremony of XIII ECSMGE, Prague, 2003,

XIII ECSMGE
Opening Address
Souhaite d`Ouverture

On behalf of the International Society of Soil Mechanics and Geotechnical Engineering (ISSMGE) it is for me a great honour and pleasure to address the delegates, on the occasion of XIII th EUROPEAN CONFERENCE ON SOIL MECHANICS AND GEOTECHNICAL ENGINEERING

Au nom de la Société Internationale de Mécanique des Sols et de la Géotechnique c´est pour moi un grand honneur et plaisir souhaiter tous à l`occasion du XIII ème CONGRÈS EUROPÉEN DE MÉCANIQUE DES SOLS ET DE GÉOTECHNIQUE

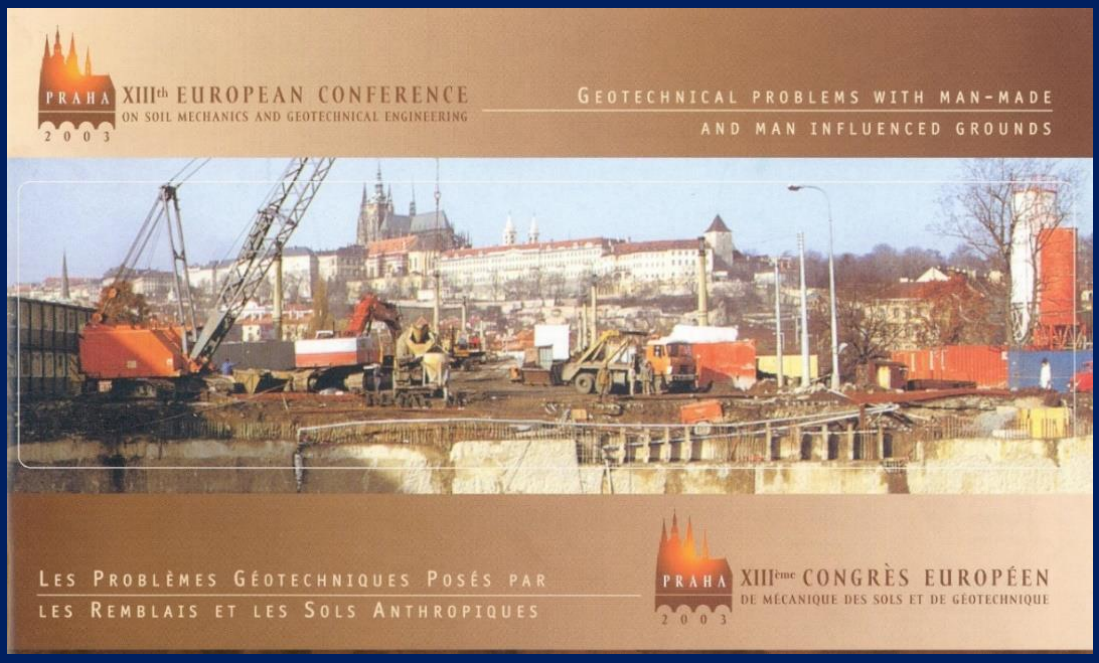

The purpose of this Conference is also to identify future needs for special research in these areas and to promote a cross fertilization between scientists and practitioners.

Within this framework is important to address the role of Geotechnics in our Society

Has the risk related to geotechnical works been minimised successfully by the geotechnical professionals?

Has the geotechnical community explored the best ways for research, design, construction and assessment of geotechnical structures safety?

It is true that the geotechnical structures are vulnerable to accidents and geotechnics follows a similar path to that described by Samuel Butler "Life is the art of drawing sufficient conclusions from insufficient premises"

Developments in sampling and ground characterisation, have been outstanding, from the primitive shear equipment up to modern triaxial equipments, cyclic torsional tests, CPTU tests and borehole TV cameras

Advances in physical modelling using centrifuge and shaking table equipment and in mathematical modelling using elasto-plastic and visco-,plastic models with applications for static design and dynamic design have been enormous

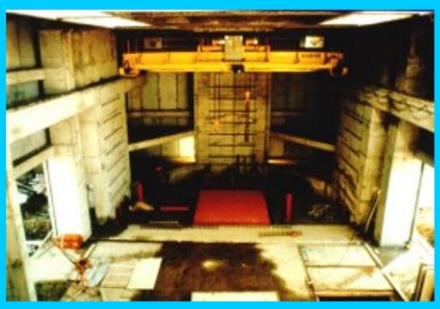

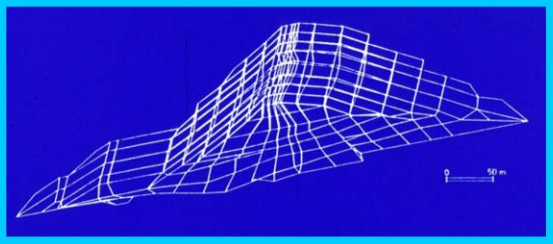

Progress in the use of new technologies for construction has also been spectacular

Monitoring of geotechnical structures to validate models and to assess the structural safety continues to play an important role

In spite of all these progress we feel a great admiration for past engineers who were great giants and have legated us some wonders, nevertheless the existent state of knowledge, such as Pyramids of Egypt, Machupicchu, Mexico Pyramids, Acropolis in Greece, China Wall and Tajmahal Palace in Índia

Nevertheless, accidents such as failures of dams, quay walls, slopes, buildings and bridges, under static or seismic actions, have provoked in geotechnical professionals frustration, pain and shock for the human and materials losses and have raised some questions about the current state of knowledge, showing that there are no definitive solutions and absolute truths

Is nature so complex that it does not allow us to reduce the probability of failure? Or do we need to recognise that failures are the fault of Decision Makers, General Public, Researchers, Professors, Experts and Constructors who are the main actors of this scenario?

Decision Makers should have the courage to accept the opinion of the experts and put the interest of the community above the interest of individuals

The General Public, sometimes with a deficient knowledge of the situation, often forces Decision Makers to take hasty decisions

Experts should accept criticisms to their proposals and should built their reputation on the quality of their opinion and not from their position, while respecting ethical codes

Contractors should not think only about profits, should not shoulder the highest risks and encourage and contribute to smooth dialogue between all project partners

ISSMGE aims to discuss very important questions related with environmental geotechnics, geohazards, education, professional practice, industrial liaison, information technology and role and format of conferences

Through this dialog ISSMGE should like to stress the importance from study of alternative solutions, that different interests and opinions should be considered and past lessons should not be forgotten

Geotechnics is simultaneous complex and a great challenge, but we need to recognize that uncertainties exist, recognise the importance of dialogue and pursue the perfection to reach the optimum solution

We should never forget the words of T.S.Elliot

"Where is the life we lost in living?

Where is the wisdom we have lost in knowledge?

Where is the knowledge we have lost in information"?

The challenge is to cross the threshold between uncertainty and certainty and to find the right answers to these questions

It is my hope that the spirit of cooperation fostered by this Conference will encourage additional projects and will contribute to the advancement of the knowledge in geotechnical engineering

5.3 Additional Reflections -Special Presentation for XX Danube Conference, Passau, 2002

INTRODUCTION

- Casagrande in his Terzaghi Lecture introduced the expression of "calculated risk" related with an estimated risk.
- Peck in his Rankine Lecture has proposed the observational method to control safety
- Whitman in his Terzaghi Lecture "Evaluating Calculated Risk in Geotechnical Engineering " states that it is important to quantify risk, to find a numerical value
- Christian et al. have pointed out that probabilistic methods are important to establish design values of factor of safety and to analyse the effects of uncertainties of the different parameters.
- Ho et al. pointed out that risk is the combination of the probability of occurrence, some unfavorable scenarios and the likelihood of the consequent damages causes

QUANTITATIVE ASSESSMENT OF THE SAFETY

- The quantitative assessment of the safety for each scenario can be done by: (i) methods with a global safety factor; (ii) methods with a partial safety factor; and (iii) probabilistic methods
- The Eurocodes introduce the partial factor method and the limit states (ultimate and serviceability)

$$E_{d,u} < R_{d,u} \quad (4.1)$$

$$F_d = \gamma_f . F_k \quad (4.2)$$

$$X_d = X_k / \gamma_f \quad (4.3)$$

- There are 3 levels on the probabilistic safety factor: semi-probabilistic, probabilistic approximate and exact probabilistic.

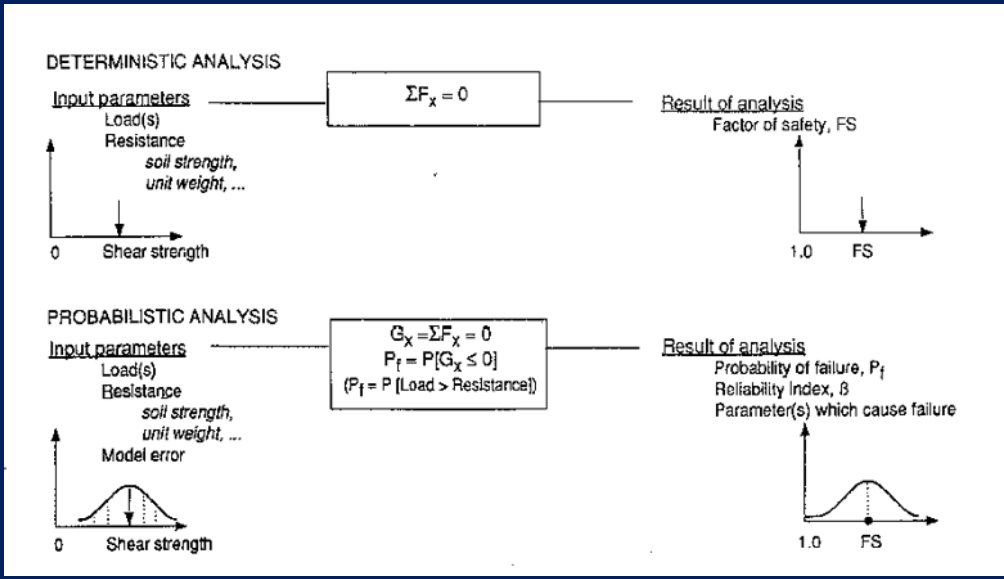

Figure 5.1 Comparison between Deterministic Analysis and Probabilistic Analysis

In the calculation models the uncertainties of the method of analysis and the systematic errors associated with the method of analysis shall be incorporated.

The Bayes´theorem can play an important role to treat this problem.

In the deterministic approach the soil properties are considered with exact values (Figure 5.1). This situation is not correct due the inherent variability of the soils and the inaccuracies and imprecision of the tests (Lumb, 1975).

The role of uncertainties in the factor of safety is presented in Figure 5.2.

Figure 5.3 shows the risk based on soil investigations.

Statistics applications for soils assume the normal or lognormal distributions, although some studies have shown that common soil properties deviate significantly from the normal and would be better characterized by a Beta distribution.

For many practical applications there is no need of all the information contained in a distribution function. The mean value is related with the center of gravity of a probability distribution and to measure the dispersion of a random variable, the variance, the standard deviation and coefficient of variation can be used.

The structure shall be designed and constructed without the occurrence of damage and the associated limitations of use, the costs of which would be disproportionately high in comparison with the costs of the structure itself (Seco e Pinto, 2009b).

Figure 5.4 shows a schematic representation of safety levels (JCSS,1981).

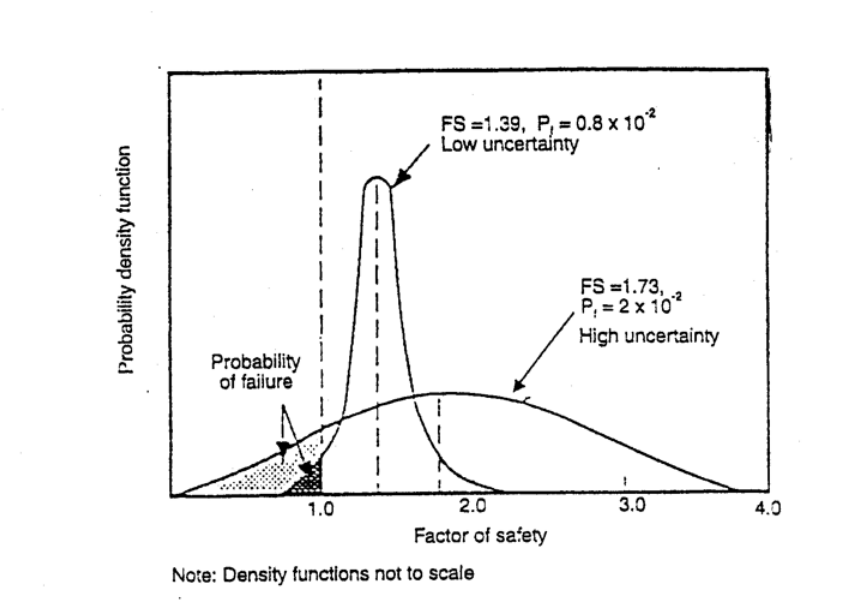

Figure 5.2 Role of uncertainties in the factor of safety

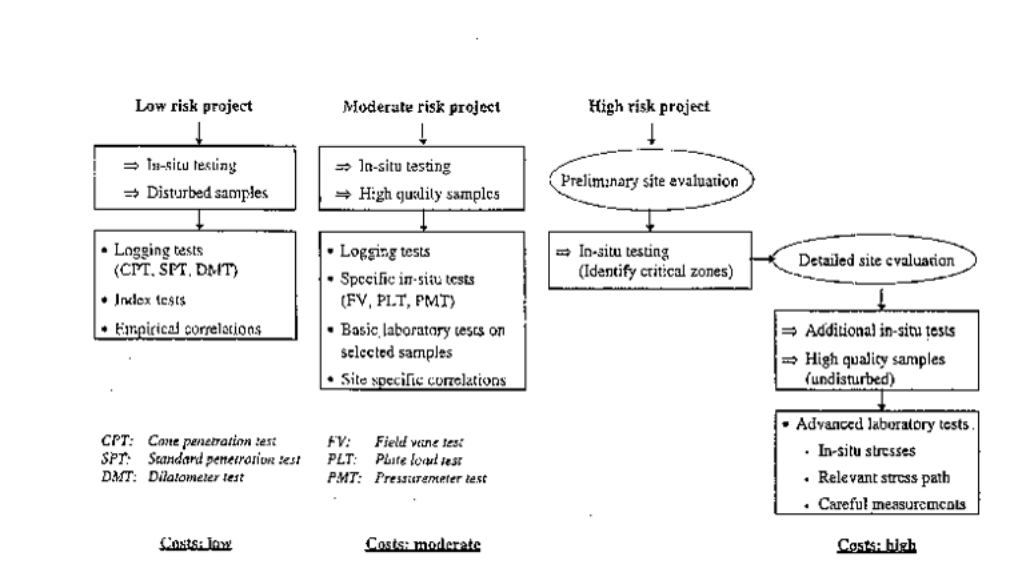

Figure 5.3 Risk based soil investigation

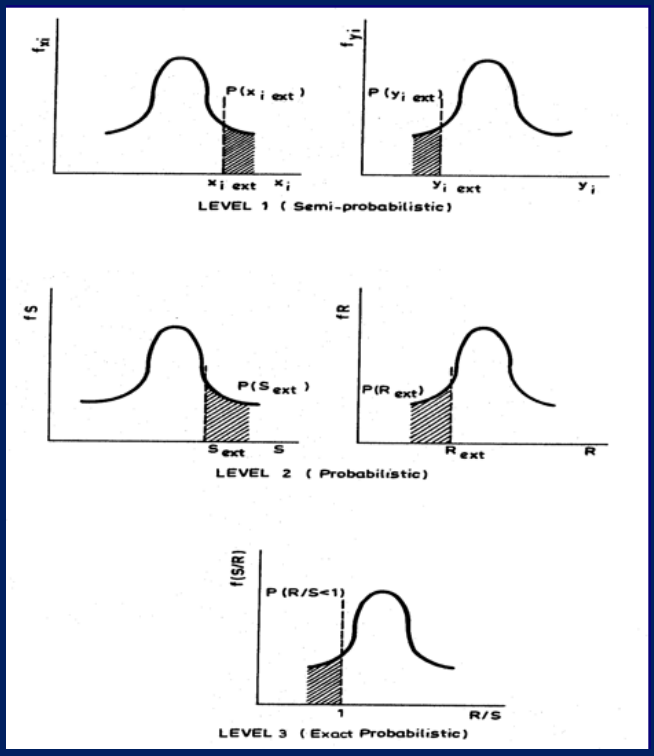

Figure 5.4 Schematic representation of safety levels (after JCSS,1981)

Table 4.1- Applications of Risk Analysis to Geotechnical Problems

Topics	References
Earth slopes	Vanmark (1977b), Christian et al (1994)
Foundations of gravity platforms	Ronold and Bysveen (1992), Nadim and Lacasse (1992)
Liners of landfills	Gilbert and Tang (1995)
Steady state problems of water retaining structures	Griffiths and Fenton (1998)
Pile foundations	Wolf (1993)
Dams (static analysis)	Paté-Cornell (1984), Whitman (1984)
Dams (dynamic analysis)	Yegian et al. (1991)
Landslides	Fell (1994)
Liquefaction	Liao et al. (1988); Haldar and Chern (1988)
Footings on sand	Duncan (2000)

5.3.1 Derived Values

Derived values of geotechnical parameters can be obtained from test results by theory, correlation or empiricism. Figure 5.5 presents the general framework for the selection of derived values.

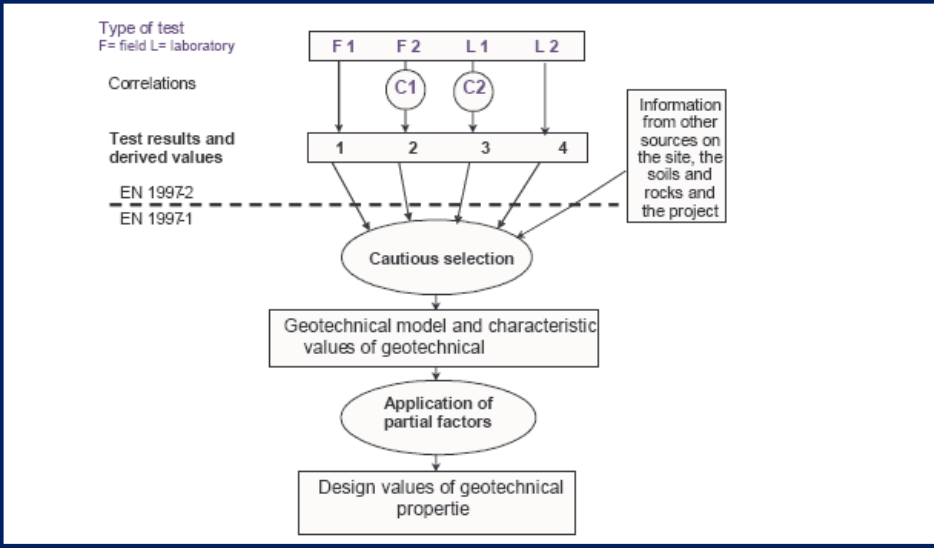

Figure 5.5 General framework for the selection of derived values of geotechnical properties (after EN, 1997-2).

5.3.2 Characteristics Values

The derivation of a characteristic value from tests should take into account (EN 1997-1):

i) the scatter of test data;

ii) statistical uncertainty associated with the number of tests;

iii) prior statistical knowledge.

Three major sources of soil uncertainties can be identified (Vanmarcke, 1977): (i) heterogeneity or in situ variability related with stress history and fluctuations in moisture content; (ii) limited number of soil samples for field or laboratory tests; (iii) errors related with sample disturbance, test imperfections and human factors. The selection of characteristic values for soil or rock materials shall be based on derived values resulting from the results of laboratory and field tests and shall take account of data from previous projects, variability of the ground properties, type and number of samples and the effects of construction activities.

Statistical methods may be employed in the selection of characteristic values for ground material and should allow a priori knowledge of comparable experience with ground properties to be taken into account. The characteristic values should be derived in such a way that the calculated probability of a worse value governing the occurrence of the limit state is not greater than 5%.

The determination of the characteristic values, where the probability of it being exceeded is 5%, is only possible in a very few cases, such as quality control of fills, where the definition of degree of compaction and deviation of water contents can be treated by a statistical approach.

SELECTION OF CHARACTERISTICS VALUES

- **Statistical methods may be employed and the characteristic values should be derived in such a way that the calculated probability of a worse value governing the occurrence of the limit state is not greater than 5%.**
- **Statistics applications for soils assume the normal function or lognormal distributions or would be better characterized by a Beta distribution.**
- **Eurocode 7 has proposed, for the determination of the characteristic value X_k, the following equation:**

$$X_k = X_m [1 - k_n . V_x] \qquad (4.4)$$

where
V_x is the coefficient of variation (standard deviation/mean value)
k_n is a factor depending on the type of statistical distribution and the number of tests.
Based on comparative computations Schneider (1997) has proposed a value of $k_n = 0.5$.

Table 4.2: Values of Coefficient of Variation

Soil property	Coef. of variat.(%)	References
Unit weight	0-10	Harr (12), Eurocode 7 (6)
LL	6-11	Singh (13)
PL	8-18	Singh (13)
PI	5-40	Singh (13)
Water content	6-29	Singh (13)
ϕ`	5-15	Harr (12), Eurocode 7 (6)
C`	30-50	Eurocode 7 (6)
Compressibility modulus	20-70	Eurocode 7 (6)
Undrained shear strength	13-40	Harr (12), Duncan (14)
SPT(N blows)	15-45	Harr (12),
CPT(electric)	5-15	Kulhawy (13)
CPT(mechanical)	15-37	Harr (12)
Dilatometer	5-15	Kulhawy (15)
Vane shear	10-20	Kulhawy (15)

5.3.3 Design Values

The derivation from tests of the design values for a material property, a model parameter or a resistance should be carried out in one of the following ways (EN 0, 1990):

a) by assessing a characteristic value, which is then divided by a partial factor and possibly multiplied if necessary, by an explicit conversion factor;

b) by direct determination of the design value, implicitly or explicitly accounting for the conversion of results and the total reliability required.

The partial factor to be applied to a characteristic value should be taken from the appropriate Eurocode provided there is sufficient similarity between the tests and the usual field of application of the partial factor as used in numerical verifications. It is important to analyse if the response of the structure or structural member or the resistance of the material depends on influences not sufficiently covered by the tests such as:

time and duration effects;

scale and size effects;

different environmental, loading and boundary conditions;

resistance effects, then the calculation model should take such influences into account as appropriate.

5.3.4 Risk Analysis

RISK EVALUATION IN CIVIL ENGINEERING PRACTICE

- The risk of failure incorporates the cost-benefit studies and can be developed by Whitman: (i) an event tree to give structure to the rating process; and (ii) a set of criteria to guide choice of the probabilities at each branch of the event tree.
- The probabilities of the various events may be evaluated partly through analysis, but also by subjective judgment based on past experience.
- The purpose of event trees is to answer two questions: (i) what are the scenarios to be incorporated in the design; (ii) what are the actions to be taken during hazard events.

EVENT TREE

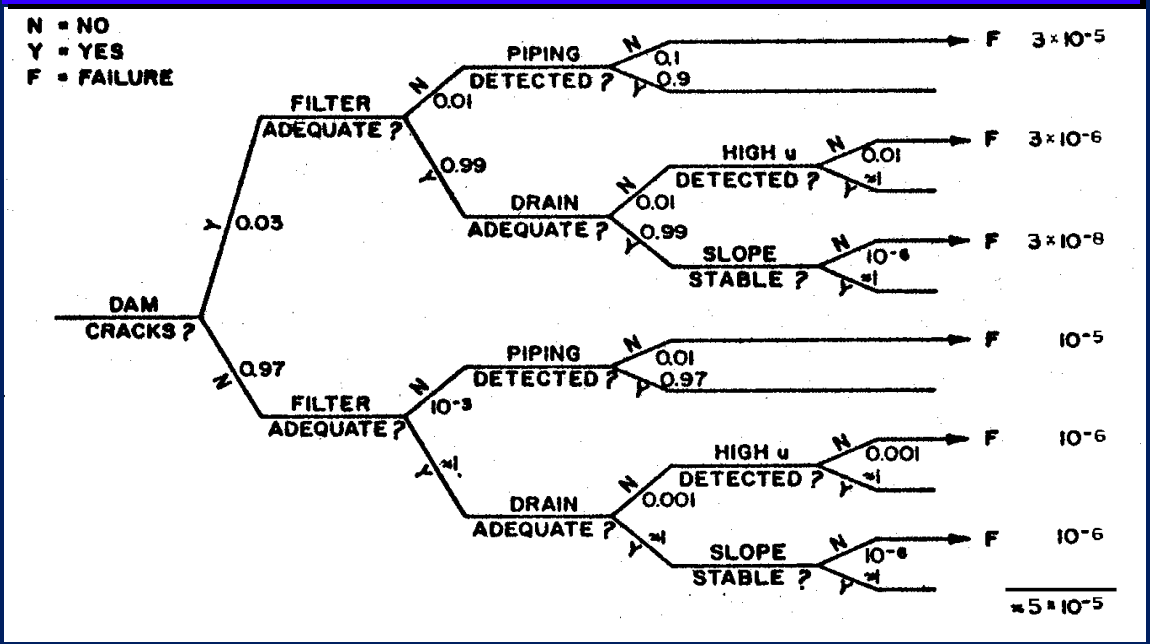

INFLUENCE OF RISK ANALYSIS IN THE DECISIONS (1)

- (i) Identification the loading conditions with the potential to cause dam failure and the estimative of the frequency of occurrence of these events; (ii) identification of the potential modes of failure related with adverse loading events; (iii) evaluation of the likelihood that a particular mode of dam failure will occur for a particular range of loading; (iv) determination of the consequences of failure for each potential failure mode; and (v) determination of the risk cost by summing the product the likelihood of a dam failure mode and the cost of the damages resulting from that failure mode.

INFLUENCE OF RISK ANALYSIS IN THE DECISIONS (2)

- **In practice four categories of risk - decision categories can be identified:**
- **subjective: influenced by political or social factors;**
- **deterministic: one solution is selected and studied with detail, while other alternatives are dismissed;**
- **qualitative: different alternative solutions are ranked without quantification of the risks;**
- **quantitative: different alternative solutions are studied and the costs and benefits are analysed.**
- **The results of a risk analysis can be used to guide future investigations and studies, and to supplement conventional analyses in making decisions on dam safety improvements.**

ROLE OF RISK ANALYSIS IN COST-BENEFIT ANALYSIS

- Assessment of a failure probability, that can be overcome using a statistical observations; (ii) evaluation of potential failure losses of human lives and the economy downstream; and (iii) risk of failure of sequential upstream dams.
- To introduce risk costs in cost-benefit analysis, the failure probability $P_F(t)$ and the cost of failure $C_F(t)$ are estimated each year. The expected value of the cost of failure over the lifetime T of the project, C_F is computed as the sum of annual discounted expected failure costs. These risk costs are subtracted from the benefits.
- The definition of value of life, I.e. what maximum cost of human safety under the considered failure probability is controversy. Values of $200 000 and $1 000 000 were pointed.

FINAL REMARKS (1)

- It is believed that risk analysis, reliability and decision analyses are tools that can help engineers.
- Due to the complexity of the probabilistic approach the advances are slow and the applications are restricted to a few geotechnical structures.
- Probabilistic approach is not a panacea and great efforts should be done for a better characterization of the materials, definition of actions and calibration of models.
- Due to the difficulties to quantify the uncertainties and the increasing of complexity of projects there is a great need for reliability analysis.

FINAL REMARKS (2)

- The probabilistic analysis should be performed with great care analyzing in a critical way the conclusions and should be used in addition to deterministic analysis.
- The probabilistic analysis increases our confidence on the results, allows an optimization of the project considering the risks of failure, can lead to a better cost-effective design and construction, satisfy our personal needs providing a better insight of the different factors of the design and give more confident to our decisions.
- The problematic of structural safety is huge and complex and need the co-operation of the Owners, Official Authorities, Research Institutes, Designers and Constructors.

5.4 Eurocodes – 2nd Generation- Summary of Eurocode 0, Eurocode 1, Eurocode 7 and Eurocode 8

EUROCODES

The Eurocodes consist of the following parts:

EN 1990 Eurocode 0 – Basis of structural and geotechnical design
EN 1991 Eurocode 1 – Actions on structures
EN 1992 Eurocode 2 – Design of concrete structures
EN 1993 Eurocode 3 – Design of steel structures
EN 1994 Eurocode 4 – Design of composite steel and concrete structures
EN 1995 Eurocode 5 – Design of timber structures
EN 1996 Eurocode 6 – Design of masonry structures
EN 1997 Eurocode 7 – Geotechnical design
EN 1998 Eurocode 8 – Design of structures for earthquake resistance
EN 1999 Eurocode 9 – Design of aluminium alloy structures
Eurocode – Glass Structures- Overview of the evoliution

5.4.1 Eurocode 0

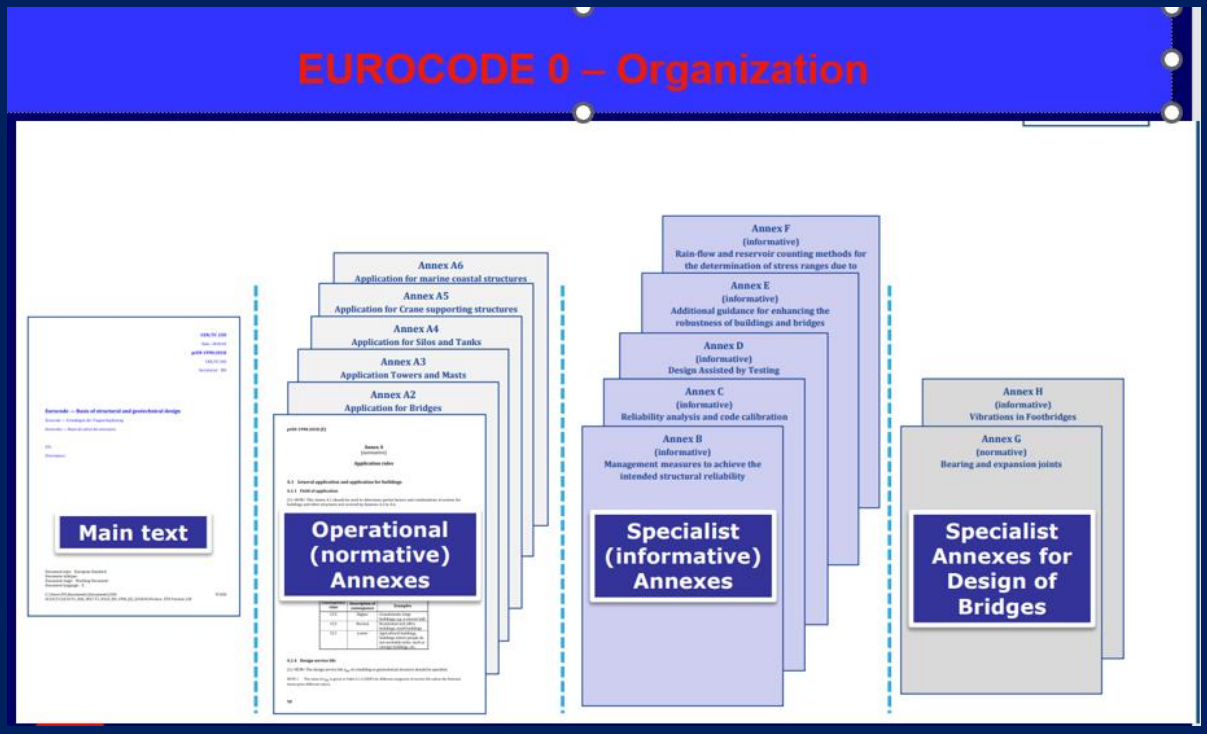

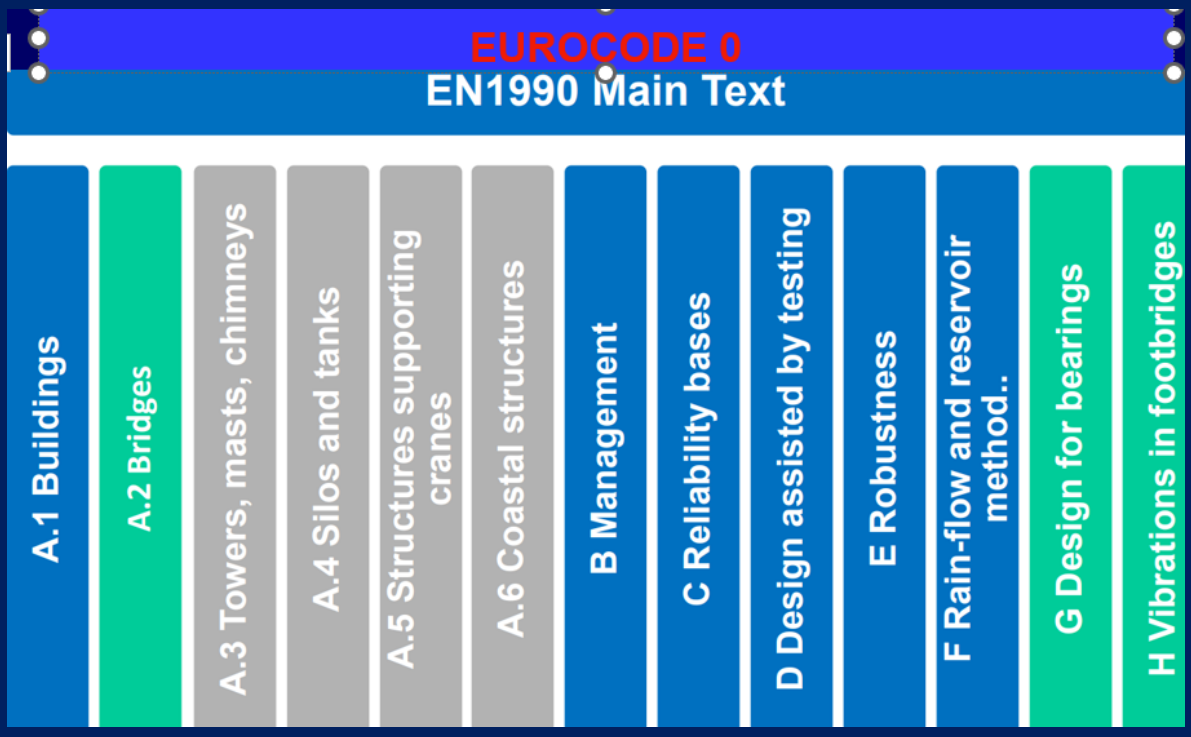

EUROCODE 0 – ULTIMATE LIMIT STATES

6.4 Ultimate limit states

6.4.1 General

(1)P The following ultimate limit states shall be verified as relevant :

a) EQU : Loss of static equilibrium of the structure or any part of it considered as a rigid body, where :
- minor variations in the value or the spatial distribution of permanent actions from a single source are significant, and
- the strengths of construction materials or ground are generally not governing ;

b) STR : Internal failure or excessive deformation of the structure or structural members, including footings, piles, basement walls, etc., where the strength of construction materials of the structure governs ;

c) GEO : Failure or excessive deformation of the ground where the strengths of soil or rock are significant in providing resistance ;

d) FAT : Fatigue failure of the structure or structural members.

EQU

STR/GEO (B)

STR/GEO (C)

EUROCODE 0 – LIMITING FOUNDATIONS MOVEMENTS

Limiting foundation movements

Structural sensitivity class	Description of sensitivity
SSC5	Highest
SSC4	Higher
SSC3	Normal
SSC2	Lower
SSC1	Lowest

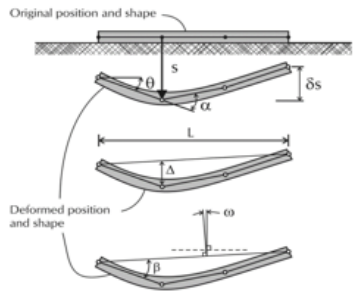

Structural sensitivity class	Description of sensitivity	Maximum differential settlement[a] $\Delta s_{Cd,SLS}$
SSC5	Highest	10 mm
SSC4	Higher	15 mm
SSC3	Normal	30 mm
SSC2	Lower	60 mm
SSC1	Lowest	100 mm

Structural sensitivity class	Description of sensitivity	Maximum angular distortion[a] $\beta_{Cd,SLS}$
SSC5	Highest	0,05 %
SSC4	Higher	0,075 %
SSC3	Normal	0,15 %
SSC2	Lower	0,3 %
SSC1	Lowest	0,5 %

Structural sensitivity class	Description of sensitivity	Maximum tilt[a] $\omega_{Cd,SLS}$
SSC5	Highest	0,1 %
SSC4	Higher	0,2 %
SSC3	Normal	0,3 %
SSC2	Lower	0,4 %
SSC1	Lowest	0,5 %

EUROCODE 0 – CONSEQUENCE CLASSES

- The Eurocodes cover design rules for structures in CC1 to CC3.
- Additional provisions can be needed for CC4, alternative provisions may be used for CC0, elements other than structural may be classified as CC

Consequence class	Indicative qualification of consequences	
	Loss of human life or personal injury[a]	Economic, social or environmental consequences[a]
CC4 – Highest	Extreme	Huge
CC3 – Higher	High	Very great
CC2 – Normal	Medium	Considerable
CC1 – Lower	Low	Small
CC0 – Lowest	Very low	Insignificant

EUROCODE 0 –Table 5.1- Classification of design Situations

Design situation	Conditions	Examples
Persistent	Normal use and exposure	During everyday use
Transient	Temporary use and exposure during a period much shorter than the design service life of the structure	During execution, repair or temporary environmental influence
Accidental	Exceptional conditions or exposure	During flooding, extreme sea water level, fire, explosion, or impact; or local failure
Seismic	Exceptional conditions during a seismic event	During an earthquake
Fatigue	Conditions caused by fatigue actions	Owing to traffic loads on a bridge, wind induced vibration of chimneys, or machinery-induced vibration

5.4.2 Eurocode 1

EUROCODE 1 – ACTIONS on STRUCTURES

Part 1 - 1:
Part 1-2: General actions – Actions on structures exposed to fire
Part 1-3: General actions – Snow loads
Part 1-4:General actions – Wind actions
Part 1-5: General actions – Thermal actions
Part 1-6:
Part 1-7:
Part 1-8: General actions - Actions from waves and currents on coastal structures
Part 1-9: Icing.

Part 2 Traffic loads on bridges and other civil engineering works

Part 4: Silos and tanks.

5.4.3 Eurocode 7

EUROCODE 7- GEOTECHNICAL DESIGN

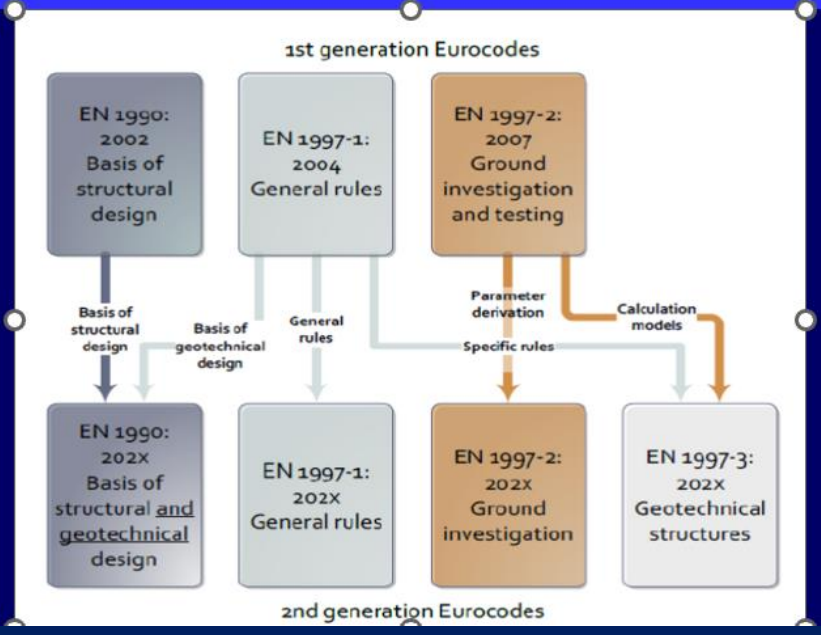

EUROCODE 7- Part 1 - GEOTECHNICAL DESIGN

0. Introduction
1. Scope
2. Normative reference
3. Terms, definitions and symbols
4. Basis of design
5. Materials
6. Groundwater
7. Geotechnical analysis
8. Ultimate limit states
9. Serviceability limit states
10. Implementation of design
11. Testing
12. Reporting

Annexes A, B, & D (informative), Annex C (normative)

Bibliography

. EC7. Part 1. GEOTECHNICAL RELIABILITY

- Zone of influence
- Geotechnical Complexity Class
- Geotechnical Category
- Consequences of failure
- Robustness
- Design service life
- Durability
- Sustainability
- Quality management

EC7. Part 1. GEOTECHNICAL COMPLEXITY CLASSES

Table 4.1(NDP) — Selection of Geotechnical Complexity Class

Geotechnical Complexity Class	Complexity	General features
GCC 3	Higher	**Any** of the following apply: — considerable uncertainty regarding ground conditions — highly variable or difficult ground conditions — significant sensitivity to groundwater and surface water conditions — significant complexity of the ground-structure interaction
GCC 2	Normal	GCC2 applies if GCC 1 and GCC3 are not applicable
GCC 1	Lower	**All** the following conditions apply: — negligible uncertainty regarding the ground conditions — uniform ground conditions — low sensitivity to groundwater and surface water conditions, — low complexity of the ground-structure-interaction
NOTE The terms 'considerable', 'significant', 'highly', etc. are relative to any comparable experience that exists for the particular geotechnical structure, design situation, and ground conditions.		

EC7. Part 1. GEOTECHNICAL CATEGORIES

Table 4.2(NDP) — Relationship between Geotechnical Category, Consequences Class, and Geotechnical Complexity Class

Consequence Class (CC)	Geotechnical Complexity Class (GCC)		
	Lower (GCC1)	Normal (GCC2)	Higher (GCC3)
Higher (CC3)	GC2	GC3	GC3
Normal (CC2)	GC2	GC2	GC3
Lower (CC1)	GC1	GC2	GC2

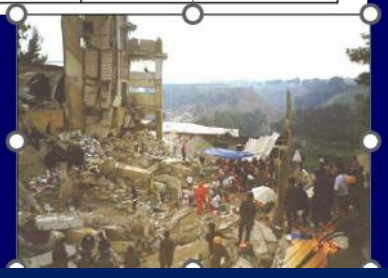

7. Part 1. GEOTECHNICAL CATEGORIES

Geotechnical Category =
Consequence Class x
Geotechnical Complexity Class

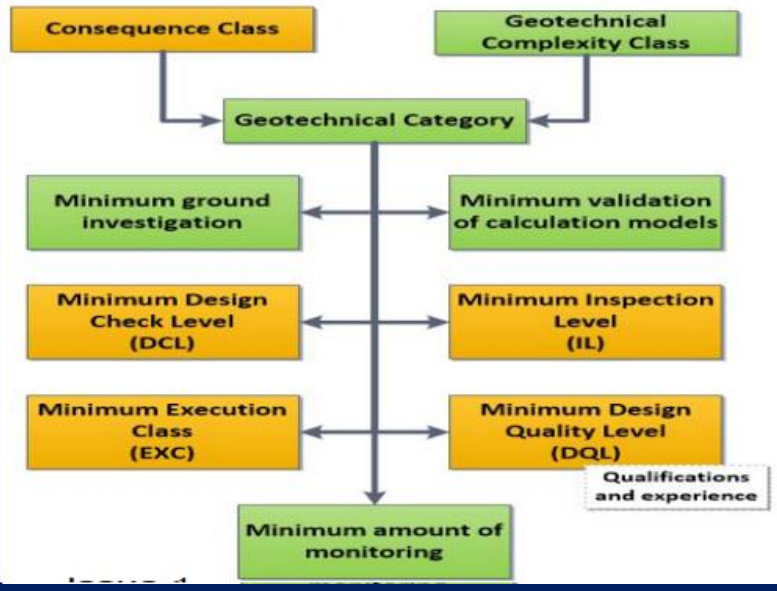

EC7. Part 1. CONSEQUENCES OF CLASSES

Table 4.3(NDP) — Examples of geotechnical structures in different Consequence Classes

Consequence class	Description of consequence	Examples
CC4	Highest	— Critical infrastructures; — Geotechnical structures whose integrity is of vital importance for civil protection[a]; — Areas with significant landslide hazards.
CC3	Higher	— Retaining walls and foundations supporting public buildings, with high exposure; — Man-made slopes and cuts, retaining structures with high exposure; — Major road/railway embankments, bridge foundations that can cause server interruption of service in emergency situations; — Geotechnical structures with a primary navigational function[b]; — Underground constructions with large occupancy.
CC2	Normal	All geotechnical structures not classified as CC1, CC3, or CC4
CC1	Lower	— Retaining walls and foundations supporting buildings with low occupancy; — Man-made slopes and cuts, in areas where a failure will have low impact on the society; — Minor road/railway embankments not vital for the society; — Underground structures with occasional occupancy[c].
CC0	Lowest	Not applicable for geotechnical structures

EC7. Part 1. DESIGN CASES

Action or effect				Partial factors γ_F & γ_E for Design Cases 1-4				
Type	Group	Symbol	Resulting effect	Struct-ural	Static equilibrium and uplift*		Geotechnical design	
				DC1	DC2(a)	DC2(b)	DC3	DC4
Permanent action (G_k)	All	γ_G	unfavourable/ destabilizing	1.35 K_F	1.35 K_F	1.0	1.0	G_k is not factor-ed
	Water	$\gamma_{G,w}$		1.2 K_F	1.2 K_F			
	All	$\gamma_{G,stb}$	stabilizing	not used	1.15		not used	
	Water	$\gamma_{G,w,stb}$			1.0			
	(All)	$\gamma_{G,fav}$	favourable	1.0	1.0		1.0	
Prestress (P_k)		γ_P	See other relevant Eurocodes					
Variable action (Q_k)	All	γ_Q	unfavourable	1.5 K_F	1.5 K_F		1.3	1.1
	Water	$\gamma_{Q,w}$		1.35 K_F	1.35 K_F		1.15	1.0
	(All)	$\gamma_{Q,fav}$	favourable	0				
Effects-of-actions (E)		γ_E	unfavourable	effects are not factored				1.35 K_F
		$\gamma_{E,fav}$	favourable					1.0

EUROCODE 7- Part 2 – GROUND PROPERTIES

0. Introduction
1. Scope
2. Normative reference
3. Terms, definitions and symbols
4. Ground Model
5. Ground Investigations
6. Description and Classification of ground
7. State, Physical
8. Strength
9. Stiffness, Compressibility and Consolidation
10. Cyclic, Dynamic and Cyclic Properties
11. Ground Water and Geohydraulic Properties
12. Geothermal properties
13. Reporting

Annexe A(normative) , Annexes B to C (informative)

Bibliography

EC7. Part 2. Maximum spacing and minimum number of in-situ testing locations for structures in Geotechnical Category 2

Structures		Maximum spacing X_{max}	Minimum number[a] N_{min}
Low-rise structures		30 m	3
High-rise structures	4-10 storeys	25 m	3-4[b]
	11-20 storeys	20 m	3-5[b]
	>20 storeys	15 m	3-6[b]
Estate roads, parking areas and pavements		40 m	2
Silos and tanks		15 m	3
Bridges piers and abutments		1 per pier/base	
Power lines		1 per pylon	
Wind turbines		2 per turbine	
Retaining structures		150 m	-
Slopes and cuttings	< 3 m high	100 m	-
	≥ 3 m high	50 m	-
Embankments and reinforced fill structures	< 3 m high	200 m	-
	≥ 3 m high	100 m	-
Excavations in urban areas > 5 m deep from ground surface		25 m	3

[a] Where no spacing or number of locations is given this should be assessed on a project-specific basis.
[b] Underlined numbers are more appropriate for difficult structures

EC7. Part 3. EUROCODE 7- Part 3

- Clause 4 – Slopes, cuttings, embankments
- Clause 5 – Spread Foundations
- Clause 6- Pile groups and pile rafts
- Clause 7 - Retaining structures
- Clause 8 - Anchors
- Clause 9 - Reinforced fill structures
- Clause 10 - Ground reinforcing elements (Soil nails and rock bolts)
- Clause 11 - Ground Improvement
- Clause 12 - Ground water control

5.4.4. Eurocode 8

EUROCODE 8

Eurocode 8 "Design of Structures for Earthquake Resistant"

- Part 1-1 - Seismic actions & general rules
- Part 1-2 - Buildings
- Part 2 – Bridges
- Part 3 – Buildings and Bridges
- Part 4 – Other Structures
- Part 5 – Geotechnics

EUROCODE 8

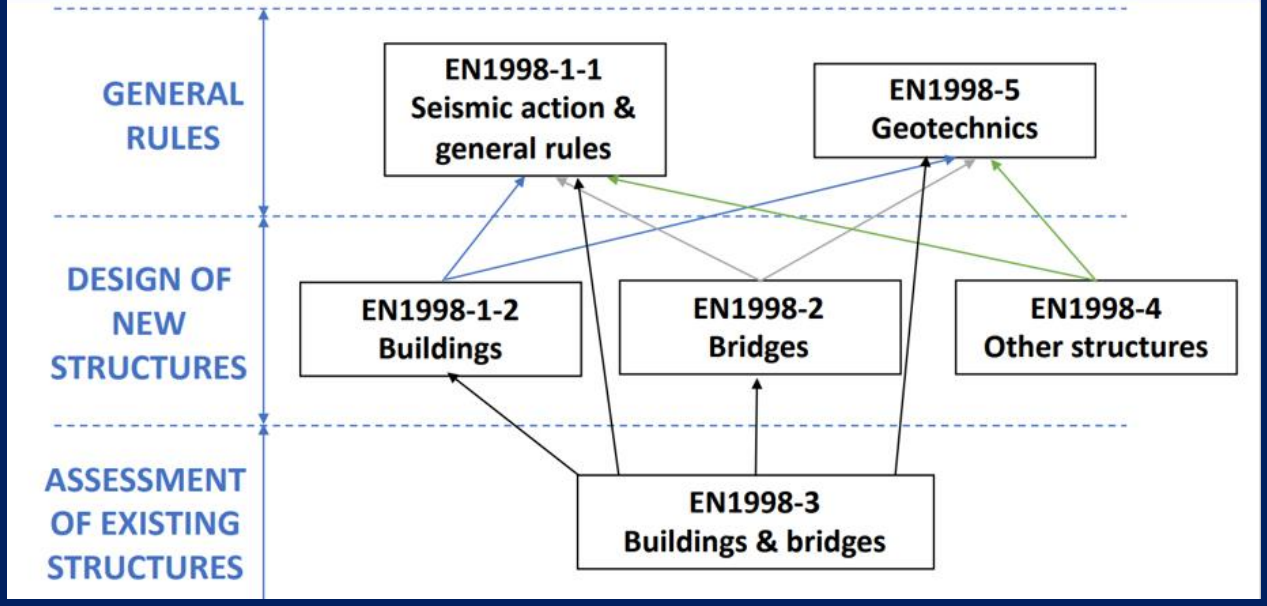

EUROCODE 8 - Simplified description of Site Categories

Site category	Description
A	Rock or other rock-like geological material, including very shallow layers of very dense, dense or medium-dense sand, gravels, very stiff or stiff clay.
B	Deposits consisting prevalently of very dense sand, gravel, or very stiff clay, with representative values of the geotechnical parameters in the range defined in Table B.2 for stiff ground.
C	Intermediate-depth deposits consisting prevalently of dense or medium-dense sand, gravel or stiff clay, with representative values of the geotechnical parameters in the range defined in Table B.2 for medium ground.
D	Intermediate-depth deposits consisting prevalently of loose-to-medium cohesionless soil, or of soft-to-firm cohesive soil, with representative values of the geotechnical parameters in the range defined in Table B.2 for soft ground.
E	Shallow deposits consisting of prevailing alluvium layers, underlain by rock-like materials as described for site category A. Representative values of the geotechnic-cal parameters are in the range defined in Table B.2 for medium or soft ground.
F	Deep deposits consisting of prevailing alluvium layers, with representative values of the geotechnical parameters in the range defined in Table B.2 for medium or soft ground.

EUROCODE 8 - Correspondence between ground class and geotechnical parameters

Test	Parameter		Ground class		
			stiff	medium stiffness	soft
SPT	N_{60} (SPT, ER = 60%) [blows/30 cm]		> 60	30-60	15-30
CPT	q_c – sands (MPa)		> 30	15-30	5-15
	q_c – clays (MPa)		> 6	3-6	1,5-3
FVT or lab tests	c_u (kPa)		> 300	150-300	50-150
PMt	E_m (MPa)		25-100	8-25	4-8
	p_{lim} (MPa)	Sand	2,0-5,0	1,2-2,0	0,4-1,2
		Clay	>1,2	0,7-1,2	0,3-0,7

EUROCODE 8 Topography amplification factors for simple topographic irregularities

Topography description	F_T	Simplified sketch*
Flat ground surface, slopes and isolated ridges with average slope angle $i < 15°$ or height < 30 m	1,0	
Slopes with average slope angle $i > 15°$	1,2	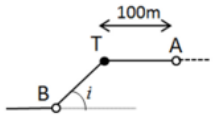
Ridges with width at the top much smaller than at the base and average slope angle $15° < i < 30°$	1,2	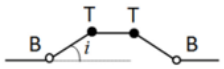
Ridges with width at the top much smaller than at the base and average slope angle $i > 30°$	1,4	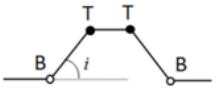

* Values of F_T in the second column refer to the top locations (point T in the simplified sketches). A linear decrease of F_T is considered between point T and point B (base) and point A (located at 100 m distance from T), where $F_T = 1$ applies.

EUROCODE 8 - Part 5- Return periods of seismic actions, in years, for geotechnical structure

Limit State	Consequence class		
	CC1	CC2	CC3
NC	800	1600	2500
SD	250	475	800
DL	50	60	60

EUROCODE 8 - Part 5- Performance factors

Limit State	Consequence class		
	CC1	CC2	CC3
NC	1,2	1,5	1,8
SD	0,8	1,0	1,2
DL	0,4	0,5	0,5

Two roads diverged in a wood and I-I

Took the one less traveled by, and that

has made all the difference

Robert Frost

6.1. Introduction

I have the privilege to be involved in 207 Geotechnical Projects in 20 Countries, during my consulting activity, that have generated around 500 Studies and Technical Reports.

Some of these projects are linked with my assignment with ONU (Organization of United Nations) and other projects with consulting work to the World Bank.

I had the opportunity to interact with Owners (Banco de Portugal, EDP, SMAS, GEAFA, SANEST, Marina EXPO, CM Albufeira), Decision Makers (CM Lisboa, Relacre), Consultants (COBA, KOCH, Grese, Enarco, Atkins, Kaiser-Tycotech, Triede, CESL, Profabril, JetSj, Consulponte, IGC, Proman, Safre, Siemens, Hydra), Clients (TACE, Norinter), and Contractors (BPC, OPCA, Socopol, Hagen, Edifer, Engil, CME, C.C. Lares, Etermar, Nexus, Monte Adriano, Mota-Engil, J. Maurício, Somague, Teixeira Duarte, TACE), sometimes with different perspectives, but always with mutual respect.
I express my deep gratitude for all these entities for giving me the opportunity to live this rich and challenging experience.

I lived without compromises, served my chosen profession to the best of my abilities and without having any regrets, as following Frank Sinatra famous song "My Way".

The following studies were performed, from 1983 to 2019 (a period of 36 years), that covered the following topics:
Feasibility studies, cost-benefit analyses, field and laboratory testing, structural design, soil dynamics, earthquake engineering, numerical analyses, preparation of tender documents, supervision of construction, soil improvement, instrumentation, safety evaluation of the dams, special foundations, harbors, tunnels, powerplants, bridges, landslides, retaining walls, slope stability, highways, residual water treatment stations, environmental studies and other civil engineering works.

6.2 Earth and Rockfill dams, Tailing dams (85 Dams)

ANGOLA (3): Gove, Jambi-oma & Cambambe
The studies were performed by a multidisciplinary design team of COBA, and I collaborated as a geotechnical expert.

ARGELIA (18): HARREZA, SOUANI, LADRAT, KEDDARA, ALI - IZDIHAR, GARGAR, BOUKOURDANE, FOUM EL KHANGA, OUED CHEF, KOUDIAT – ACERDOUNE, Dermoun, Seklafa, Ben Aida, Kerrada, Bouzhoul, Oued Fodda, Ghrib, Bakhada.

Stability analysis (static analysis, seismic analysis), Seepage studies, Analysis stress-stress. Instrumentation, Safety evaluation.
The studies were performed by a multidisciplinary design team of COBA and I collaborated as a geotechnical expert.

Brazil (4): Inhuçu, Passauna, Piraquia & Lontras
The studies were performed by a multidisciplinary design team of COBA and I collaborated as a geotechnical expert.
In addition, a Dams Safety Programme was implemented during the period of 2013-2015 by a Consortium COBA-LNEC, for the World Bank and I was involved in the Dams Safety Evaluation.

CABO VERDE: Small dams

Dominican Republic (5): TAVERA, SABANA YEGUA, SABANETA, HATILLO & BAO (Dams with a length between 1100 m and 1600 m, height between 90 m and 120 m)
The studies covering the instrumentation and safety evaluation were performed by a multidisciplinary design team of COBA and LNEC and I collaborated as a geotechnical expert.

ECUADOR (1): BABA

GUINÉ-BISSAU (1): SALTINHO
The studies were performed by a multidisciplinary design team of COBA and I collaborated as a geotechnical expert.

INDIA (2): THOUBAL PROJECT (L= 1500 m, H=50 m, V= 1.8 x 10 6 m3 and SIPU (L= 1200 m, H=45 m, V= 1.5 x 10 6 m3. Revision of the Design, assignment for the ONU (Organization of United Nations).

LEBANON (1): KFAR SIR
The studies were performed by a multidisciplinary design team of COBA and I collaborated as a geotechnical expert.

MALAWY (1): KHOLOMBIBZO (L=3500 M, H=90 M, V=14 X 10 6 M3), Geotechnical studies, Stability analysis (static analysis, seismic analysis), Seepage studies, Analysis stress-stress. Instrumentation and Safety evaluation.

The studies were performed by a multidisciplinary design team of COBA and I collaborated as a geotechnical expert.

MORROCCOS (1): M'JARA- LABORATORY TESTS

The studies were performed by a multidisciplinary design team of Hidrotecnica Portuguesa and I collaborated in the laboratory tests.

MOZAMBIQUE (5): MASSINGIR, PEQUENOS LIBOMBOS, CORUMANA,
The studies were co-ordinated by LNEC-LEM.

In addition, for Moamba-Major and Mapai dams:
Geotechnical investigation, Stability analysis (static analysis, seismic analysis), Seepage studies, Analysis stress-stress. Instrumentation, Safety evaluation.
The studies were performed by a multidisciplinary design team of COBA and I collaborated as a geotechnical expert.

PORTUGAL (29): MIRA(L= 1500 m, H=84 m , V= 2.5 x 10 6 m3), ODIVELAS(L= 1100 m, H=40 m , V=1.2 x 10 6 m3), ALVITO(L= 1600 m, H=45 m , V=1.8 x 10 6 m3), TOULICA(L= 950 m, H=30 m , V=1.1 x 10 6 m3), Stª MARIA DE AGUIAR(L= 1250 m, H=32 m , V=1.3 x 10 6 m3), CAPINHA, CRATO, COIMBRA(L= 950 m, H=32 m, CRESTUMA(L= 900 m, H=30 m, AZIBO (L= 1600 m, H=45 m , V=1.8 x 10 6 m3), ALIJÓ(L= 1100 m, H=30 m , V=1.1 x 10 6 m3) , and Pisco, Teja, Marzelonas, Boa Vista, Vale de Serra, Enxoé, Maranhão, Pego do Altar, Vale do Gaio.
The studies were co-ordinated by LNEC.

In addition, I was involved in the following studies: Corte Brique, Pico Urze, Alqueva, Michões, Vale do Rossim, Freixeirinha, Ribeiradio, as a geotechnical expert.

Quality control and Instrumentation (17):
MARVÃO(L=1200 m, H=45 m, V=1.6 x 10 6 m3), COVA DA BEIRA (6 dams, namely Peraboa, Peroviseu, Fatela, Monte de Bispo, etc), ODELEITE, MARANHÃO, S. DOMINGOS, FREIXEIRINHA (L=850 m, H=20 m , V =1.2 x 10 6 m3), Odelouca(L=900 m, H=78 m , V=4.1 x 10 6 m3), Abrilongo (L=1200 m, H=40 m , V=1.6 x 10 6 m3), Sabugal(L= 1800 m, H=45 m , V=2.1 x 10 6 m3), Alvorninha, Morgavel, Minutos, Marvão.
Geotechnical investigation, Stability analysis (static analysis, seismic analysis), Seepage studies, Analysis stress-stress. Instrumentation, Safety evaluation.
The majority of these studies were co-ordinated by COBA.

SENEGAL (2): SAMBAGALOU (L= 400 m, H=38 m, V=1.8 X 10 ^{6} m$^{3)}$, AND KALETA (L= 350 m, H=30 m, V=1.2 X 10 ^{6} m3: geotechnical investigation, seismic studies and instrumentation and safety analysis.
The studies were performed by a multidisciplinary design team of COBA and I collaborated as a geotechnical expert.

TUNISIE (1): Al Diar (L= 1300 m, H=45 m, V=1.8 x 10 6 m3),

Geotechnical investigation, Stability analysis (static analysis, seismic analysis), Seepage studies, Analysis stress-stress. Instrumentation, Safety evaluation.
The studies were performed by a multidisciplinary design team of COBA and I collaborated as a geotechnical expert.

UGANDA (1): ORIANG (L= 800 m, H=25 m)
Geotechnical investigation, Stability analysis (static analysis, seismic analysis), Seepage studies, Analysis stress-stress. Instrumentation, Safety evaluation.
The studies were performed by a multidisciplinary design team of COBA and I collaborated as a geotechnical expert.

VENEZUELA (2): BORDE SECO (L= 400 m, H=120 m, V=4.5 x 10 6 m3), LAS CUEVAS (L= 650 m, H=110 m, V=4.0 x 10 6), The studies were performed by a multidisciplinary team of LNEC and my role was co-ordinator of the project.
Geotechnical investigation, Stability analysis (static analysis, seismic analysis), Seepage studies, Analysis stress-stress. Instrumentation, Safety evaluation.

ZAMBIA (2): Kundwika (L= 350 m, H=20 m and Kabwelume (L=500 m, H=25 m
Geotechnical investigation, Stability analysis (static analysis, seismic analysis), Seepage studies, Analysis stress-stress. Instrumentation, Safety evaluation.
The studies were performed by a multidisciplinary design team of COBA and I collaborated as a geotechnical expert.

6.3 Tailing dams (2)- URGEIRIÇA e SINES (geotechnical design and instrumentation).

Special Geotechnical Projects (Foundations Design)

6.4 Bridges (7): Guadiana (2 Km), Arade (1.2 Km, Alcácer do Sal (1.8 Km),
Analysis of pile foundations. The studies were co-ordinated by LNEC.

In addition, the following studies were performed: Vasco de Gama (18 Km), Leziria (11 Km), Ponte de Oeiras, Ponte de Soure.

6.5 Viaducts (6): PORTO (2), LISBOA (2), CALHARIZ, (IP3), CARVALHAL.

6.6 Powerplants (9): Ferrel. The studies were performed under the supervision of LNEC.

In addition, I was involved, as geotechnical expert, in the studies of the following powerplants: Muranzel, Sines, Setubal, Tapada de 0uteiro, Pego, Carregado, Lares e Diar.

6.7 Buildings and Others (12): Edificio Carregado, Complexo Algueirão, Viana de Castelo (the study was performed under the supervision of LNEC), Cidade da Praia (Republica de Cabo-Verde), Mosteiro de S. Clara, Estádio Ponte de Sor, Estádio de Antas, Central Incineradora, Fortaleza do Monte (Macau), Expo Urbe, Edificio Funchal, Edificio Kilamba.
I was involved in the studies as geotechnical expert.

6.8 RESERVOIRS AND TANKS (7): Shell Reservoirs (Banática); Treatment Station (Cabo Ruivo); Petrogal Reservoirs (Porto Brandão). The studies were performed under the supervision of LNEC.

In addition, the following studies were performed: Tanks and Reservoirs - Porto de la Guaira (Venezuela); Reservoirs in Setubal; Reservoirs in Tapada de Outeiro; Tanks and Reservoirs for treatment of water and residual water and Pedrogão station.
I was involved as a geotechnical expert.

6.9 ETARES (Station of Treatment of Residual Water) (7): Loures, Beirolas, Ericeira, Guia, Portinho de Costa, Setubal and Vila Franca.
I was involved in these studies as a geotechnical expert.

6.10 PORT and Maritime structures (9):
LA GUAIRA (VENEZUELA), Praia de Vitória (Azores), MARINA de EXPO, Cais de Malabo, Cais de Contentores, Cais de BATA (Guine Equatorial), Terminal of Seixal, Olhão Port, Transmissor Ilhas de Culatra e Amora.
I was involved in these studies as a geotechnical expert.

6.11 Underground Structures (19)
Metro Lisboa, Coimbra Tunnel and Rossio Tunnel (The studies were performed under the supervision of LNEC);
In addition, the following studies were performed: Tunnel of Gardunha, Tunnel of Sabugal, Metro do Porto (Stations of Campanhã, Heroismo, Trindade, 24 de Agosto, Bolhão, Av. De França), Tunnel of Alfândega, Tunnel of Penalva, Tunnel of Odelouca, Tunnel of Portinho, Pragal Station, Barcarena station, hydraulic tunnels of Lisboa, Albufeira tunnel.
I was involved in these studies as a geotechnical expert.

6.12 Environmental Geotechnics (2):
Residual landfills, Beirolas landfills.

I was involved in these studies as a geotechnical expert.

6.13 Slopes and Retaining Walls (5):

La Josefina (Ecuador),

This study was performed by a multidisciplinary design team of COBA and I collaborated as a geotechnical expert.

Castro d`Aire, Portaria Leixões, Metro de Lisboa-Troço Falagueira, Forum de Almada.

I was involved in these studies as a geotechnical expert.

6.14 Dikes (16):

Mondego Dykes (60 km) and Arade Bridge **(**The studies were performed under the supervision of LNEC).

Upstream and downstream cofferdams of Jambi-o-ma, upstream and downstream cofferdams Moamba Major, dam, upstream and downstream cofferdams of Apertadura dam,

The studies were performed by a multidisciplinary design team of COBA and I collaborated as a geotechnical expert.

In addition, the following studies were performed: Marina Expo, Olhão port, Tejo dykes, Leixões port, Tapada de Outeiro powerplant, Beirolas landfills, Dike of Zezere, Dike of Gâmbia.

I was involved in these studies as a geotechnical expert

6.15 Highways (6): A6, Nó A10-A1, A Sintra, Scut Interior Norte, Ermidas-Sado, Fervença-Lumarinho.

I was involved in these studies as a geotechnical expert.

6.16 Airports (1): Oran (Argelia)

The studies were performed by a multidisciplinary design team of COBA and I collaborated as a geotechnical expert.

6.17 Railways (1): Beni Monsoun-Bejaia (Argelia)

The studies were performed by a multidisciplinary design team of COBA and I collaborated as a geotechnical expert.

6.18 Quarries (2): Campo de Ourique, Alqueva.

I was involved in these studies as a geotechnical expert.

7. Dams Engineering

"The important thing in science is not
So much to obtain new facts as to discover
New ways of thinking about them"

(Sir W. Bragg, British Scientist, 1968)

7.1 Introduction

As 10 of the 28 Case Histories presented in Chapter 8 deals with dams, it seems that justifies a special chapter devoted to these complex and challenging structures.

In this chapter some ancient dams are introduced, the dam's scenarios are addressed, a summary of dam's earthquake performance is presented, the important role of filter and drain materials is stressed, the analysis of dam stability during earthquakes is discussed and the safety of dams is analysed.

7.2 Ancient Dams

Introducing ancient dams in China, India and Iran (see Figure 7.1 to Figure 7.3).

Figure 7.1 Anfenglang reservoir

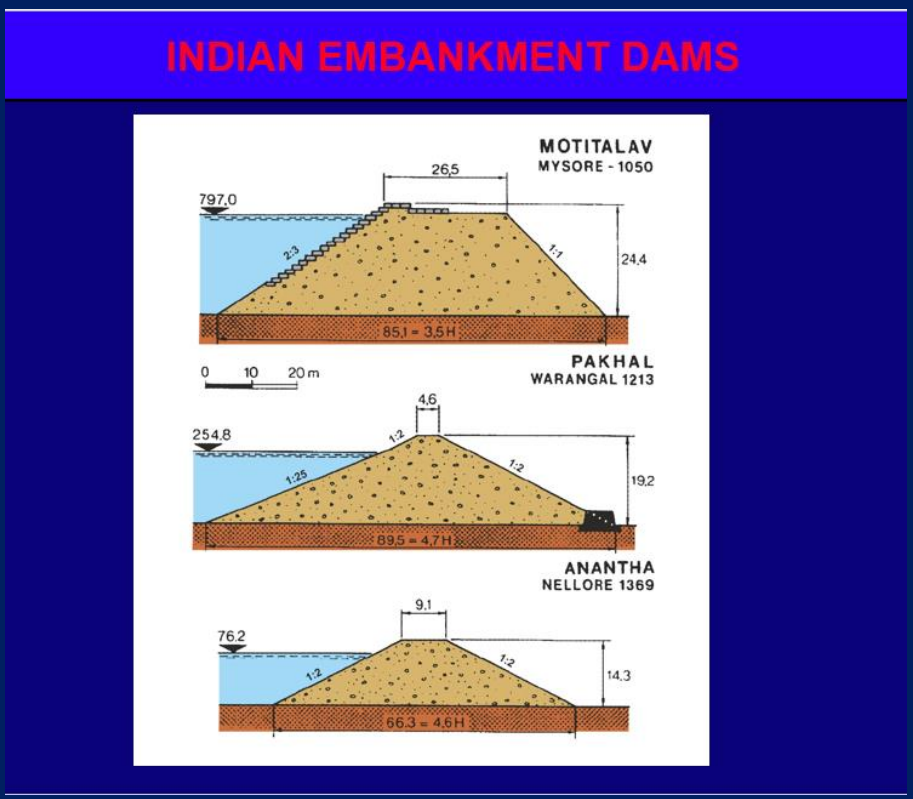

Figure 7.2 Indian dams

Figure 7.3 Iranian dams

7.3 Dams Scenarios

7.3.1 Introduction

The findings of dam failures statistical analysis of data show that (ICOLD, 1995):
the percentage of failure of large dams has been falling over the last four decades, 2,20 % of dams built before 1950 failed, failures of dams built since 1951 are less than 0.5 %;
most failures involve newly built dams. The greatest proportion 70% of failures occur in the first ten years and more especially in the first year after commission.

At the end of XX century, one billion people was living downstream of dams. It seems that millions may be at risk within the next 50 years as a result of dam failures. Although the annual failure probability of dams is lower than 10^{-6} in most cases, it may be higher for dams in seismic areas subject to sudden failures such as tailing dams and hydraulic fill dams.

The potential risk associated with dams consists of structural components and socio-economic components. The structural components of potential risk depend mostly on storage capacity and on the height of the dam, as the potential downstream consequences are proportional to the mentioned values (ICOLD, 1989). Socio-economic risks can be expressed by a number of persons who need to be evacuated in case of danger and by potential downstream damage.

Risk management comprises the estimation of the level of risk and exercising adequate control measures to reduce the risk when the level is not tolerable. The essence of risk management and the role of quantitative risk assessment (QRA) within the context of risk management are shown in Figure 7.4 (Ho et al., 2000).

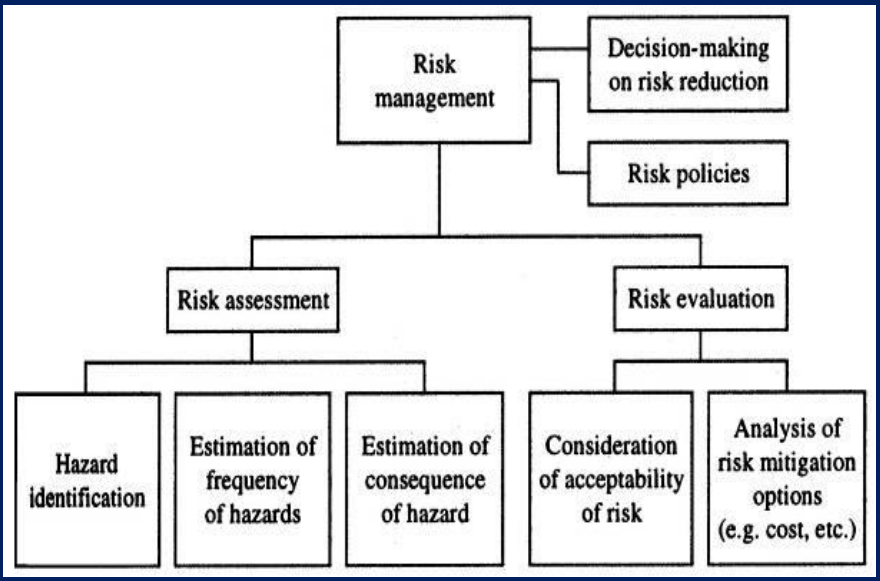

Figure 7.4 Framework for risk management (after Ho et al, 2000)

Consideration of human behavior is essential when assessing the consequence of failures: well organized emergency planning and early warning systems could decrease the number of victims and so the study of human behavior play an important role in assessment of risk analysis (Sêco e Pinto, 1991).

The results of a risk analysis can be used to guide future investigations and studies, and to supplement conventional analyses in making decisions on dam safety improvements. Increasing confidence in the results of risk analyses can lead to a better cost-effective design and construction, satisfy our personal needs providing a better insight of the different factors of the design and give more confident to our decisions (Sêco e Pinto, 2002).

A probabilistic risk assessment addresses three fundamental questions: (I) what can go wrong? (ii) how likely is it?; (iii) what damage will it do?

In general, a society risk of 0.001 lives per year per dam appears to be acceptable. Assuming that the combined probability of failure to a PMF and MCE is approximately 1/100 000 per year, a loss of life of up to 100 people would result in an acceptable risk of 0.001 lives per year per dam.

LESSONS DUE TO CURRENT AND FAILURE SCENARIOS OF DAMS

ICOLD BULLETIN 99

- Deteriorations due to hydraulic structures and operation about 35%
- Deteriorations due to cracking and hydraulic fracturing about 30%
- Slope failure of dams and reservoir about 10%
- Excessive seapage through foundation about 12%
- Inadequate slope protection 7%
- Other situations 6%

LESSONS DUE TO CURRENT AND FAILURE SCENARIOS OF DAMS

ICOLD BULLETIN 99

- 20 % during the construction phase
- 20 % during the filling of reservoir
- 22 % after the construction phase
- 16 % after the period of five years following the construction phase
- 22% no identified cases

7.3.2 DETERIORATIONS DUE TO CRACKING AND HYDRAULIC FRACTURING

Several factors have contributed for the embankment dam cracking (ICOLD, 1997). A description of these factors is presented. Also, the measures that should be incorporated to minimize the occurrence of cracking are referred (Seco e Pinto, 2006).

Differential settlements of foundations

The alluvia foundations with variable thickness can provoke differential settlements, with zones of traction and cracking. It is important to remove this material with poor properties, when its thickness is small.

Foundations singularities

The cracks, joints and faults that occur in the foundations, should be identified and treated during the construction. The weathered material should be removed, the cleaning of the foundation surface should be done with high pressure water, and the cracks should be filled with poor concrete and the first layers adequately compacted, in accordance with the proposals of ICOLD, (1998, 1995).

The hydraulic gradients shall be controlled, to minimize the piping and the occurrence of cracks in the interface fill-foundation, and the springs should be convenient treated.

Dimensions and shape of the valley

Narrow valleys with inclined slopes are favorable for the occurrence of cracks and so the design should incorporate special measures.

The study of shape valley and the development of tension stress can be performed by 2D or 3D analyses.

Liaison embankment-abutment

The liaison embankment-abutment needs special care due to the inclination of the slope, as the slope inclination of abutment can provoke transverse cracks due to differential settlements and the rock discontinuities are favorable to the occurrence of traction zones.

Difference of compressibility between the core and the shell materials

The difference of compressibility and geometry between the core materials and the shell materials favored the occurrence of stress transfer between the core and shell materials. This stress distribution is favorable to the occurrence of longitudinal cracks.

Due to this situation the following effects have occurred: (i) considered settlements during the first filling; (ii) the development of plastic zones that embrace a considerable proportion of the potential shear failure surfaces in the dam, (iii) a reduction in the relative density of the granular materials.

Characterization of fill materials

The characteristics of the fill materials are related with cracking. Some soils have high susceptibility to cracking and can not sustain small differential settlements.

Tests to characterize the edibility of the material, namely flume tests and cylinder rotating tests, should be highly recommended.

Hydraulic fracturing

During the filling of reservoir due to the seepage and buoyancy forces there is a modification of the stress state. When the water pressure is higher than the summation of the effective stress and the traction resistance of the material tension cracks can occurred.

Hydraulic fracturing is defined as the condition to provoke and propagate a physical separation in a soil or rock mass, due to the excessive pore pressure in comparison with the existent stress in the soil and rock mass.

Connection of fills of different ages

The schedule of the works sometimes creates situations with a discontinuous construction of the fills. The exposed surfaces are more vulnerable for the cracking occurrence. When the construction of the fill is rebeginning it is important to remove the material to a depth of 20 cm-40cm, in order to assure a good connection with the existent fill.

Concrete structures incorporated in the embankment

It is difficult to compact the material in the neighboring of conduits and vibratory plates are used. The conduits located inside the embankment favored the stress transference and the cracks formation due the differential settlements. In order to increase the flexibility the placement of wet material in the neighboring of the conduits is recommended.

Speed of filling of the reservoir

The filling of reservoir can provoke the saturation of the foundation and of upstream shell and the redistribution of stress can contribute for the occurrence of transverse and longitudinal cracks.

It is important to control the rate of reservoir filling. Sometimes the hydrological conditions do not allow.

Hydraulic fracturing tests performed in Alvito dam

Hydraulic fracturing tests were conducted in Alvito dam with 50 m high and 1500 m long and 1,5 x 10^6 m3. The core is with clay material and the shell are with schists materials. The dam profile and upstream view are illustrated in Figure 7.5 and Figure 7.6.

During the installation of 19 hydraulic piezometers, located in Figures 7.7 to 7.11, following the instrumentation plan, it was considered a good opportunity to perform hydraulic fracturing tests, as the dam profile integrates a chimney filter, for a better understanding of the mechanisms of this phenomenon.

The drilling equipment and the hydraulic piezometer Geonor are shown in Figure 7.12 and Figure 7.13.

A special equipment to perform the hydraulic fracturing tests, shown in Figure 7.14, was designed by Sêco e Pinto (1983).

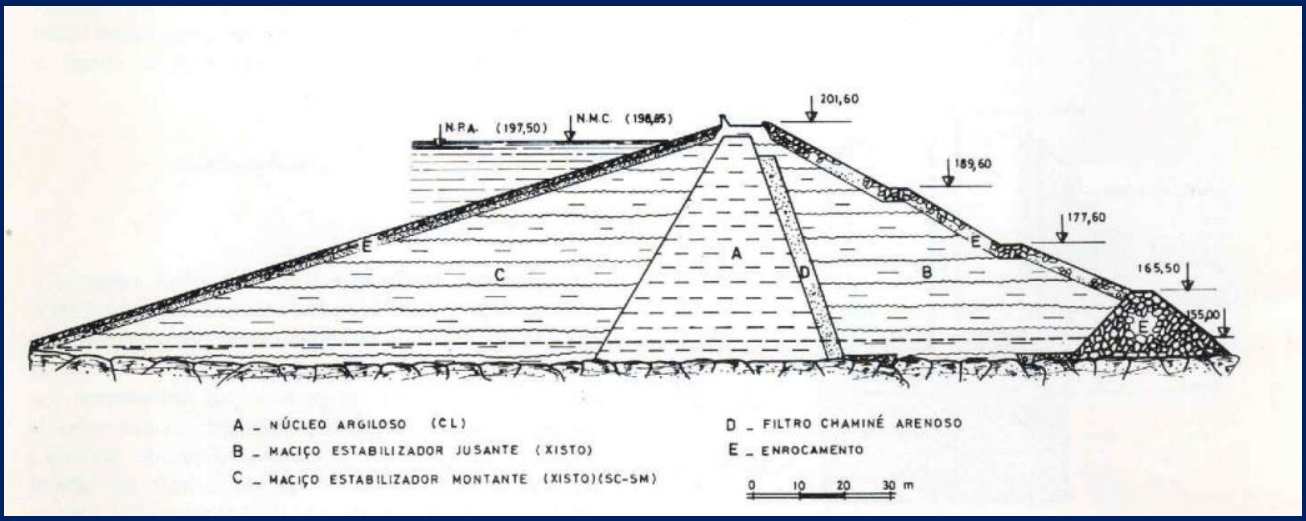

Figure 7.5 Profile of Alvito dam

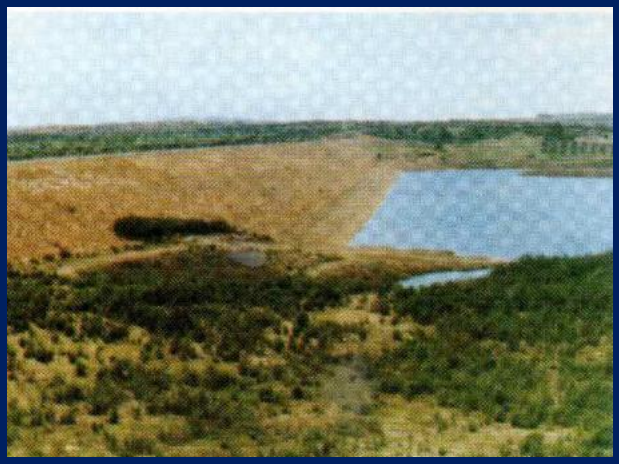

Figure 7.6 Alvito dam upstream side

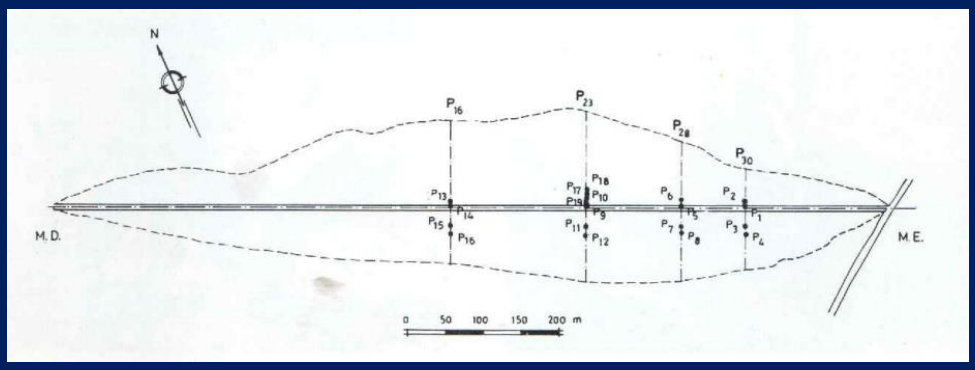

Figure 7.7 Schematic location of the hydraulic piezometers

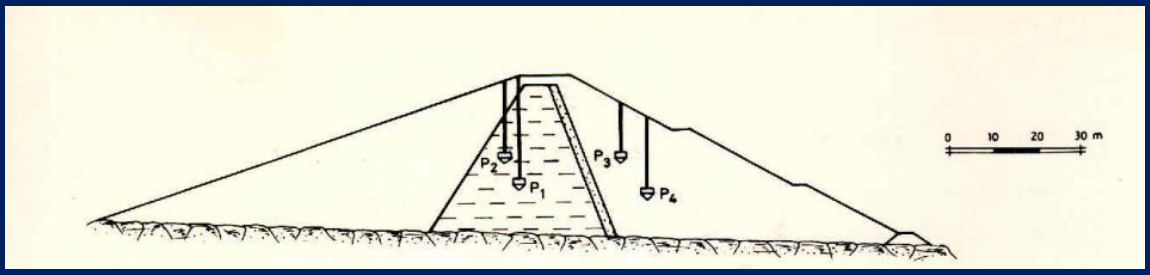

Figure 7.8 Piezometers location in profile P 30

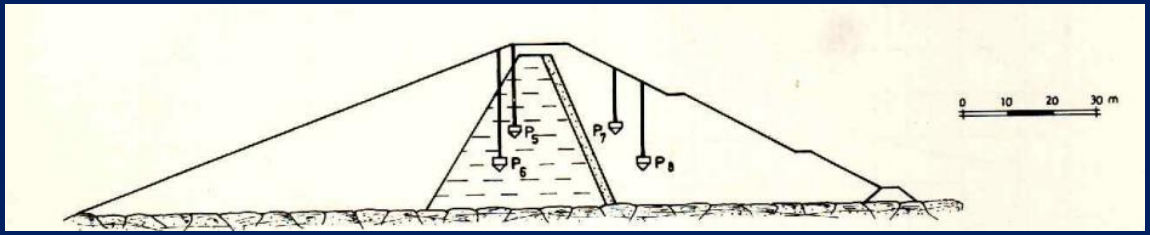

Figure 7.9 Piezometers location in profile P 28

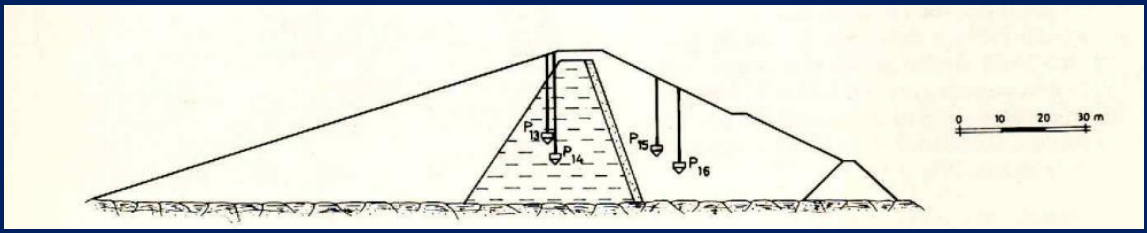

Figure 7.10 Piezometers location in profile P 23

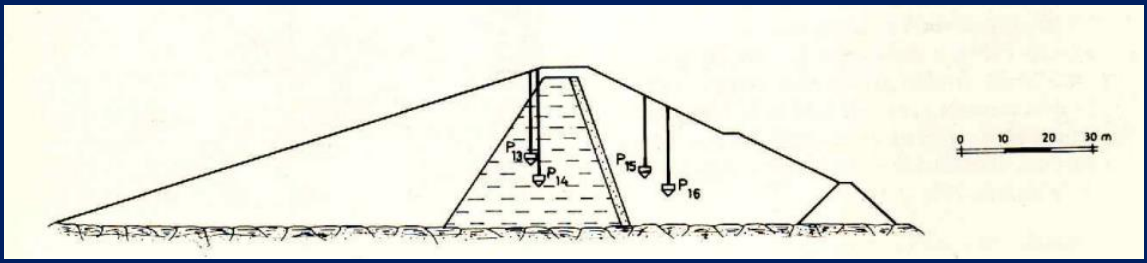

Figure 7.11 Piezometers location in profile P 16

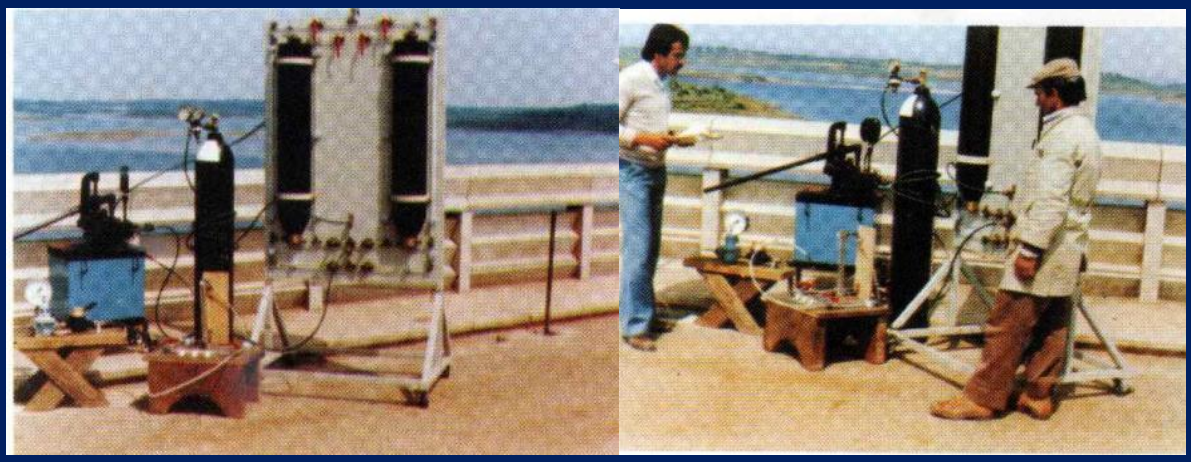

Figure 7.12 View of the equipment

Figure 7.13 Hydraulic piezometer Geonor

Table 7.1 summarizes the obtained results.

Figure 7. 14 illustrates the tests results in piezometer P 5 and it can be noticed a suddenly increase of the flow when the crack has occurred.

Later the permeability test was done to assess the real ground conditions.

A comparison between the results of the hydraulic fracturing tests performed in Alvito dam and the proposals of other researchers is shown in Figure 7.15.

Table 7. 1 Summary of hydraulic fracturing tests results

Piezómetro n.º	Profundidade (m)	Data	Fase de molhagem			Cota da albufeira (m)	Tensão nominal "overburden" (kPa)	Pressão de fractura (kPa)	Pressão de fecho (kPa)	K_0 (campo)	Coef. de permeab. final (m/s)
			Vol. total absorvido (l)	Tempo de molhagem (min.)	Coef. de permeab. inicial (m/s)						
P_2	18	19/3/80	14,4	180	$7,9 \times 10^{-8}$	183	390	280	235	0,60	$9,2 \times 10^{-8}$
P_5	20	15/4/80	38,5	130	$7,1 \times 10^{-8}$	183	430	320	230	0,54	$7,5 \times 10^{-8}$
P_6	26	16/4/80	23,0	120	$8,9 \times 10^{-8}$	183	560	420	340	0,61	$3,6 \times 10^{-8}$
P_9	15	28/3/80	11,0	160	$3,8 \times 10^{-8}$	183	320	240	225	0,70	$5,6 \times 10^{-8}$
P_{10}	35	1/4/80	58,0	180	$5,1 \times 10^{-8}$	183	750	450	390	0,52	$9,7 \times 10^{-8}$
P_{13}	20	2/4/80	10,0	120	$0,8 \times 10^{-8}$	183	430	300	230	0,54	—
P_{14}	26	14/1/80	54,0	180	$6,0 \times 10^{-8}$	183	560	420	320	0,57	$7,7 \times 10^{-8}$
P_{17}	18	9/4/80	30,0	180	$7,0 \times 10^{-8}$	183	390	300	270	0,70	$8,6 \times 10^{-8}$
P_{18}	25	9/5/80	6,0	120	$3,1 \times 10^{-8}$	183	540	430	370	0,69	$3,3 \times 10^{-8}$

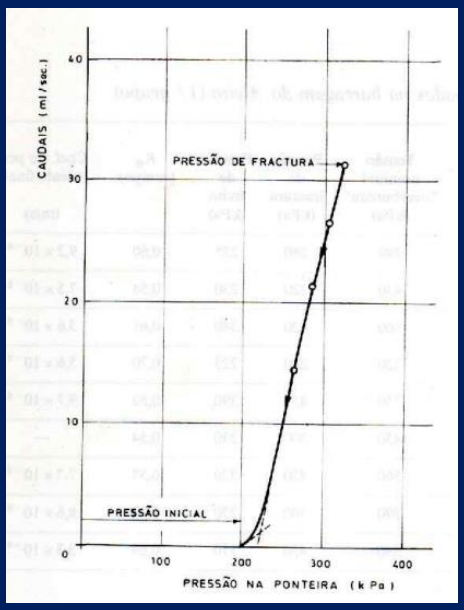

Figure 7. 14 Plot Flows versus Pressures -tests in piezometer P 5

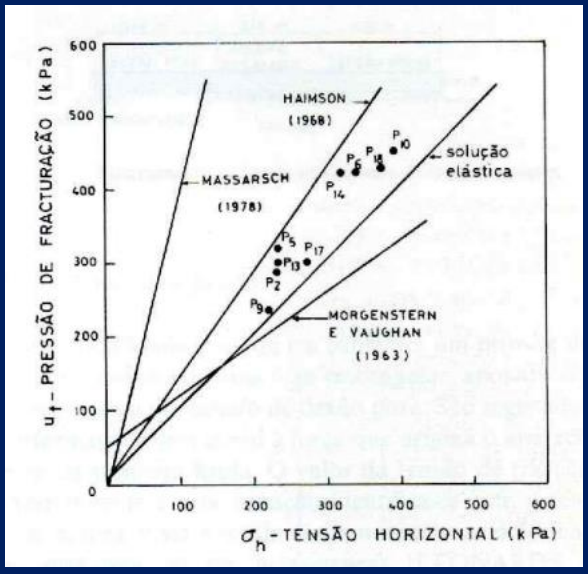

Figure 7.15 Comparative analysis of fracturing tests

Tension strength tests

Considering that the simple tension tests, the bending tests and the diameter compression tests are not adequate for the determination of tensile resistance of soils, special tension strength tests were performed in laboratory in samples of clay (CL) and saibro materials (SM) that are in general placed in the core of the dams constructed in South and in the North of Portugal (Seco e Pinto, 1983).

These special tests had the purpose to investigate the effects of plasticity, water contents, velocity of the tests and degree of compaction in the tensile resistance.

In the samples with 100 mm of diameter and 175 mm height a hole with 5 mm of diameter and 90 mm depth was performed to introduce a plastic tube with 3 mm of diameter with hole in the bottom extension of 20 mm.

Details of the sample's preparation are shown in Figures 7.16 and 7.17.

Figure 7.18 presents the equipment for testing. The samples were placed in triaxial cells and submitted to an isotropic pressure of 100 kPa and 200 kPa during 2 days.

The injected water pressure was increased by a rate of 10 kPa in 12 hours, until the value of the confinement pressure.

Figure 7.19 represents one test results, and the variation of the effective pressure and the variation of the coefficient of the permeability with the increase of the water pressure in the hole.

Figure 7.20 and Figure 7.21 illustrate the visual aspect of the cracks, with vertical tendency.

The obtained results have shown tensile strength values between 10 kPa to 20 kPa and a slightly increase with the increase of the degree of compaction and the water contents.

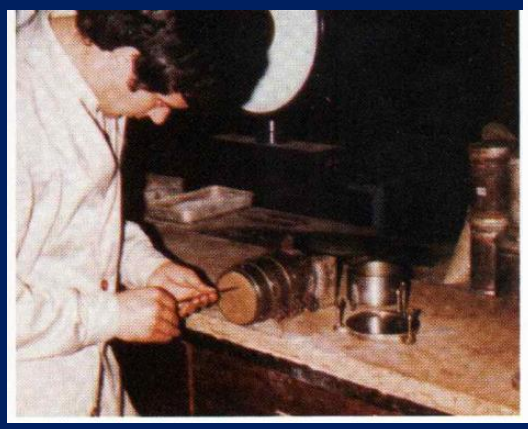

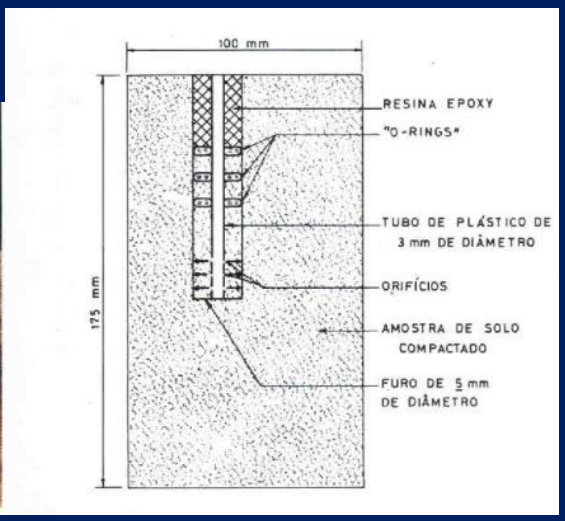

Figure 7.16 Detail of opening of the hole Figure 7.17 Schematic cross section

Table 7.2

Ensaio n.º	Início	Fim	Diâmetro (mm)	Altura (mm)	Teor em água (%)	Peso volúmico seco (kN/m³)	σ_h (kPa)	Lim. de Atterberg: Lim. de liquidez (%)	Lim. de Atterberg: Lim. de plastic. (%)	Resistência à tracção (kPa)	Observações
1	10/10/80	27/10/80	101,6	178,0	14,7	18,2	200	43,7	16,4	20,0	Energia de compactação leve
2	26/8/80	11/9/80	101,6	178,0	12,0	18,6	200	43,2	18,5	20,0	Idem
3	16/9/80	30/9/80	101,6	178,0	8,7	17,6	200	45,5	18,9	10,0	Idem
4	27/2/81	11/3/81	101,6	178,0	10,4	20,1	200	38,3	20,9	20,0	Energia de compactação pesada
5	13/3/81	25/3/81	101,6	178,0	8,9	19,3	200	38,2	18,8	15,0	Idem

Figure 7.18 View of the equipment

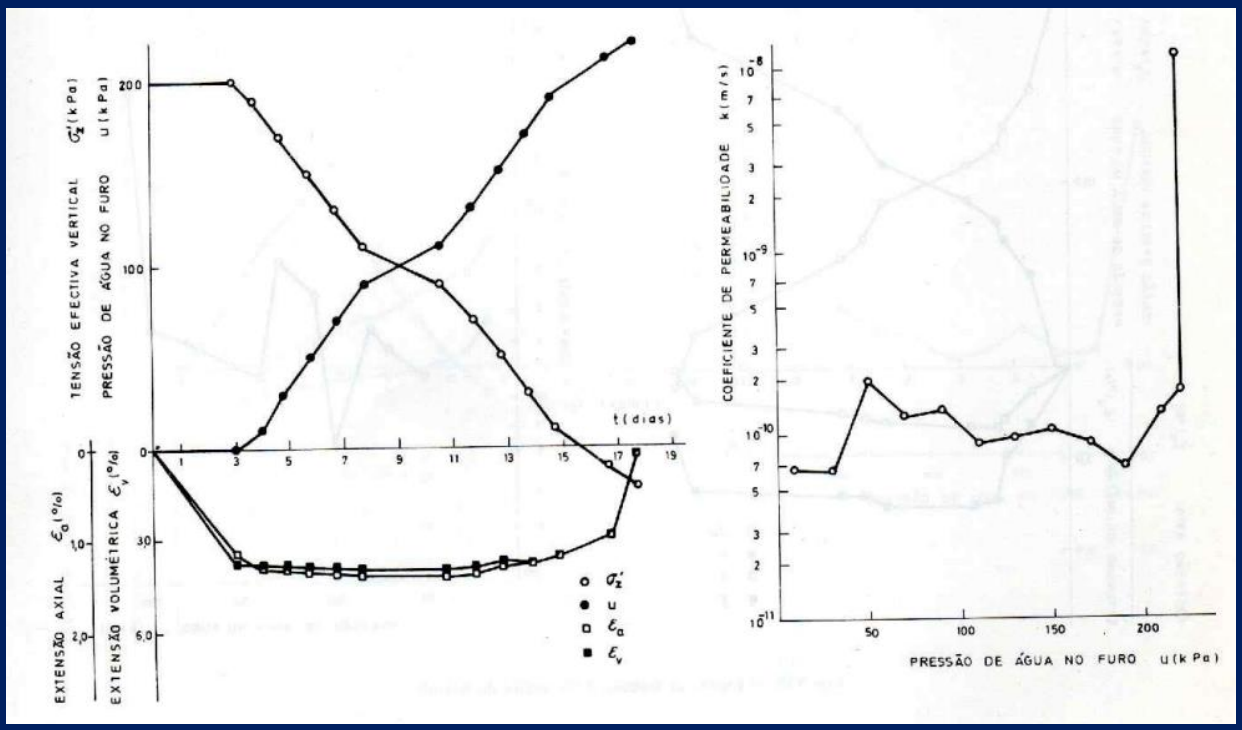

Figure 7.19 Test result

Figure 7.20 Visual aspect of the cracks

Figure 7. 21 Interior view of the sample with the plastic tube

7.4 Filter and Drain Materials

7.4.1 Introduction

Construction control includes placement of filter materials in horizontal lifts, 0.30m thick and compaction by two to three passes of a 10ton vibratory smooth-drum roller. The compaction of filters should be adequate to produce sufficient density to preclude liquefaction, to limit consolidation and to provide adequate strength (ICOLD, 1994b). To avoid contamination, filter materials are placed to a level of 0.5m ahead of adjacent embankment material. Gradation and permeability tests are performed both before and after placement

The characteristics to be fulfilled by filter materials are subsequently analysed.

7.4.2 Characteristics of filter materials

Internal erosion

The filter material to control internal erosion should respect the condition

$$\frac{D_{15(\text{filtre})}}{D_{85}\ (\text{soil})} < 5 \qquad (7.1)$$

where D_{15} and D_{85} are the diameters with 15% and 85%, of material has a lower diameter.

Permeability

To satisfy the permeability condition the material should respect:

$$5 < \frac{D_{15}\ (\text{filtre})}{D_{15}\ (\text{soil})} \qquad (7.2)$$

No cohesion

The filter material should not exhibit cohesion.

Internal stability

The internal stability of filter materials is linked with the capacity to maintain the fine particles during the dam life.

Filter segregation

The placement and compaction of filter materials should be carefully done in order to avoid the segregation.

Following USBR (1987) the coefficient of uniformity should be between 6 and 8.

A summary is presented in Table 7.2

Table 7.2 Proposals for sieve characteristics

Proposals	Sieve characteristics
US Army Corps of Engineers (1941)	D_{max}= 25 d_{50}
Karpoff (USBR,1955)	Dmax= 3” (75mm)
US Army Corps of Engineers (1955)	D_{60}/D_{10}<20
Sherard et al (1984)	Dmax=2” (50mm)

7.4.3 Experimental filter studies

Extracts from the paper published by Sêco e Pinto, P.S. and Teresa Santana in XII ICSMGE, Rio de Janeiro, 1989

Figure 7. 22 illustrates a schematic view of the equipment.

Figure 7.23 shows the particle size distribution Santa Clara dam.

Several tests were conducted with three base materials varying the water content (dry side and wet side of Proctor test), the compaction energy and using six different filter materials. Conventional filter tests, slot tests and hole tests were carried out. A different type of test named "crack erosion test" was performed (this test will not be described herein) and the obtained results are given in Maranha das Neves (1987). In the former tests a slice of base material (25 mm thickness) of a Proctor compaction test was placed in a cylinder of 100 mm diameter. Filter material (20 mm thickness) and gravel material were placed downstream and gravel material was placed upstream. A schematic vue of test apparatus is shown in Figure 1.

In the conventional tests and slot tests water pressures acting across the base specimen were increased in steps of 50 kPa until 200 kPa and each step had a duration of 5 minutes. For the hole tests a pressure of 250 kPa was installed suddenly and the test had a duration of 20 – 25 minutes. For the long term tests a water pressure of 50 kPa was installed through the hole during several days.

To evaluate the behaviour of low compaction zones located in the core material, hole tests were performed in some samples of base material with 90% degree of Proctor compaction.

For the interpretation of the tests the following parameters were considered: (1) stability of the base soils; (2) colour of the emerged water; (3) eroded base soil carried through the filter; (4) variation of the flow during the test; (5) velocity through the slot or hole; and (5) final diameter of the hole.

Table 7.3 presents a summary of Santa Clara and filters materials.

Table 7. 4 shows the hole tests results of Santa Clara material.

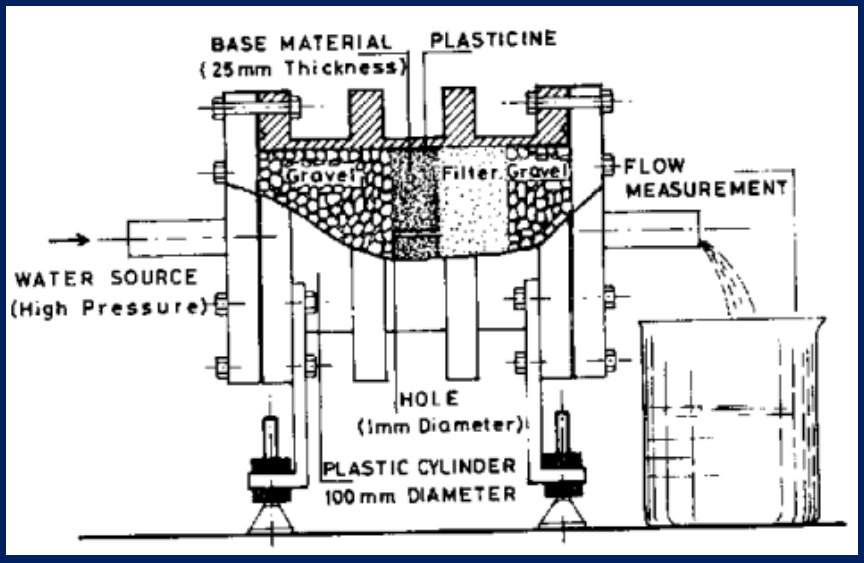

Figure 7. 22 Schematic view of the equipment

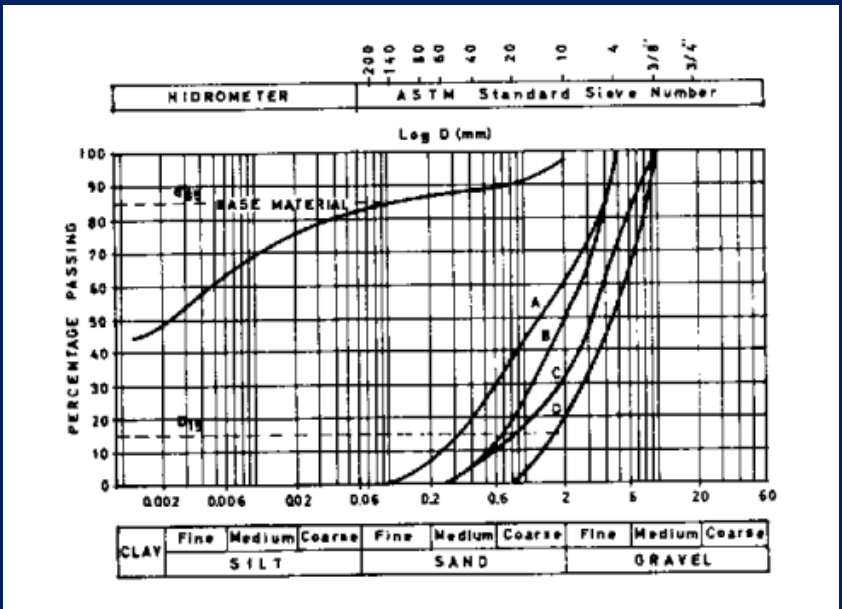

Figure 7.23 Particle size distribution Santa Clara dam

Table 7.3 Summary of Santa Clara and filters materials

Liquid limit (%)	Plastic limit (%)	Optimum water content (%)	Coefficient of permeability (m/s)
50.6	25.5	20.5	10^{-9}
Filters	D_{15} (mm)	D_{15}/d_{85}	Uniformity Coefficient
A	0.35	3.5	8.3
B	0.7	7	4.5
C	0.9	9	6.7
D	1.7	17	3.9

Table 7. 4 Hole tests results -Santa Clara material

Filter	Base material	Q (ml/s)	v (m/s)	Observed behaviour
A	Dry side	19.7 ↓	17.4 ↓	Dirty water $\emptyset_F$ = 1 mm
D_{15}=0.35 mm	w=18.5%	15.8	8.9	Successful
	Wet side	15.8 ↓	14 ↓	Clean water $\emptyset_F$ = 2 mm
D_{15}/d_{85}=3.5	w=22%	21.4	6.8	Successful
B	Dry side	34.4 ↓	22.3 ↓	Dirty water $\emptyset_F$ = 3 mm
	w=18.5%	25.4	3.6	Intermediate
D_{15}=0.7 mm	Wet side	15.5 ↓	10 ↓	Clean water $\emptyset_F$ = 2.5 mm
D_{15}/d_{85}=7	w=21.8%	30.0	6.1	Intermediate
C	Dry side	41.6		Dirty water
	w=18%	-		Failure
D_{15}=0.9 mm	Wet side	13.3 ↓	8.6 ↓	Deficient
D_{15}/d_{85}=9	w=22%	46.7	6.6	$\emptyset_F$ = 3 mm
D	Dry side	96.0		Failure
	w=18%	-		
D_{15}=1.7 mm	Wet side	77.8 ↓		Failure
D_{15}/d_{85}=17	w=22%	105.6		$\emptyset_F$ = 5 mm

Figure 7.24 illustrates the particle size distribution of Marateca dam materials.

Table 7. 5 presents a summary of Marateca and filters materials.

Table 7. 6 condenses the hole tests results of Marateca material.

Table 7.7 summarizes the characterization of Alvito and filters materials.

Table 7.8 Hole tests results of Alvito material.

Figure 7.25 shows the particle size distribution of Alvito dam materials.

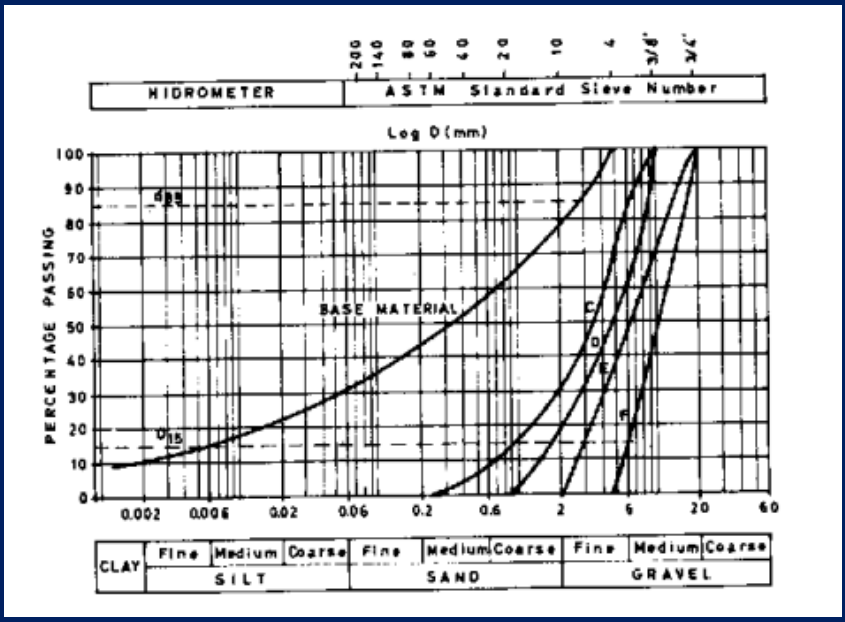

Figure 7.24 Particle size distribution Marateca dam

Table 7.5 Summary of Marateca and filters materials

Liquid limit (%)	Plastic limit (%)	Optimum water content (%)	Coefficient of permeability (m/s)
29.6	25.3	13	10^{-8}
Filters	D_{15} (mm)	D_{15}/d_{85}	Uniformity coefficient
C	0.9	0.3	6.7
D	1.7	0.6	3.9
E	3	1	3.2
F	6	2	2.4

Table 7. 6 Hole tests results -Marateca material

Filter	Base material	Q (ml/s)	v (m/s)	Observed behaviour
C	Dry side w=11.4%	0.73 ↓ 0.33	0.9 ↓ 1.2	Clean water $\emptyset_F$= 1 mm Successful
D_{15}=0.9 mm D_{15}/d_{85}=0.3	Wet side w=14.9	0.03 ↓ 0.03	-	Clean water Clogged Successful
D	Dry side w=11.9%	0.17 ↓ 0.13	-	Clean water Clogged Successful
D_{15}=1.7 mm D_{15}/d_{85}=0.6	Wet side w=13.5%	0.03 ↓ 0.03	-	Clean water Clogged Successful
E	Dry side w=11.9%	52 -	-	Dirty Water $\emptyset_F$= 5 mm Deficient
D_{15}=3 mm D_{15}/d_{85}= 1	Wet side w=14.9%	0.04 ↓ 0.04		Clean water Deficient
F	Dry side w=11.9%	-	-	Failure
D_{15}=6 mm D_{15}/d_{85}=2	Wet side w=14.9%	117	-	Failure

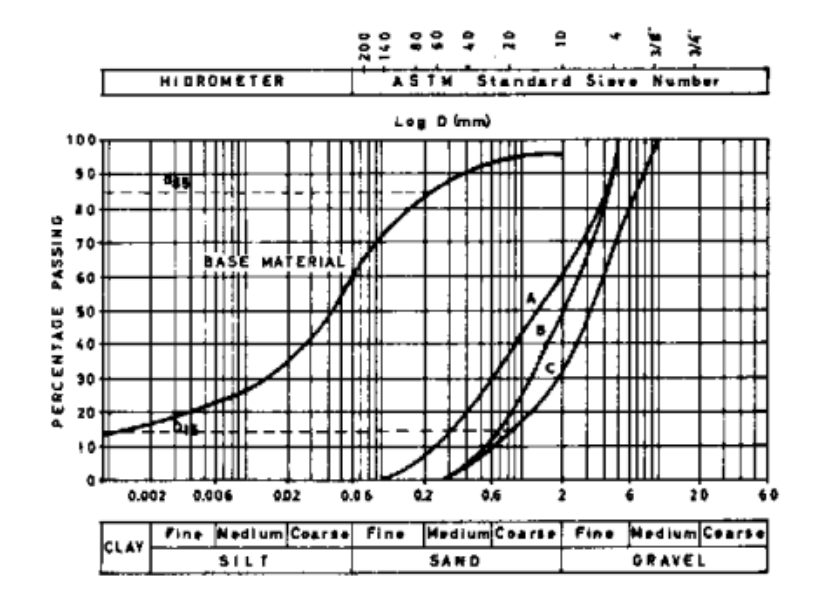

Figure 7.25 Particle size distribution of Alvito dam

Table 7.7 Summary of Alvito and filters materials

Liquid limit (%)	Plastic limit (%)	Optimum water content (%)	Coefficient of permeability (m/s)
41.8	18.7	16.7	10^{-9}

Filters	D_{15} (mm)	D_{15}/d_{85}	Uniformity coefficient
A	0.35	1.4	8.3
B	0.7	2.8	4.5
C	0.9	3.6	6.7

4. ANALYSES AND INTERPRETATION OF THE RESULTS

A comparison with the criteria proposed by other au - thors for the three materials is shown in Figures 5 and 6.

The following conclusions can be drawn:

- for CH soils (Santa Clara) and CL soils (Alvito) Wolski et al. (1970) and Sherard et al. (1984) criteria gave coarser filters, mainly the Wolski one. According to the Vaughan & Soares (1982) criterion the filter should be finer.
- for SM soil (Marateca) the application of Vaughan & Soares (1982), Sherard et al. (1984) Paré et al. (1982) and Kjaernsli et al. (1982) criteria gave finer and less uniform filters (lower D_{15} values).

Table 7.8 Hole tests results -Alvito material

Filter	Base material	Q (ml/s)	v (m/s)	Observed behaviour
A	Dry side w=14.4%	0.32 ↓ 0.33		Dirty water Clogged Successful
D_{15}=0.35 mm				
D_{15}/d_{85}=1.4	Wet side w=18.4%	2.3 ↓ 2.1	2.9 ↓ 2.6	Clean water $\emptyset_F$= 1 mm Successful
B	Dry side w=15.8%	56.3 ↓ 57.3	28 ↓ 8.1	Dirty water $\emptyset_F$= 3 mm Intermediate
D_{15}=0.7 mm				
D_{15}/d_{85}=2.8	Wet side w=17.5%	33.1 ↓ 35.9	16.5 ↓ 11.4	Clean water $\emptyset_F$= 2 mm Intermediate
C	Dry side w=15.8%	-	-	Failure $\emptyset_F$= 4 mm
D_{15}=0.9 mm				
D_{15}/d_{85}=3.6	Wet side w=17.5%	64.3 ↓ 61	-	Dirty water Deficient $\emptyset_F$= 2 mm

Figure 7.26 shows the filters for Santa Clara and Alvito.

Figure 7.27 represents the filter for Marateca material.

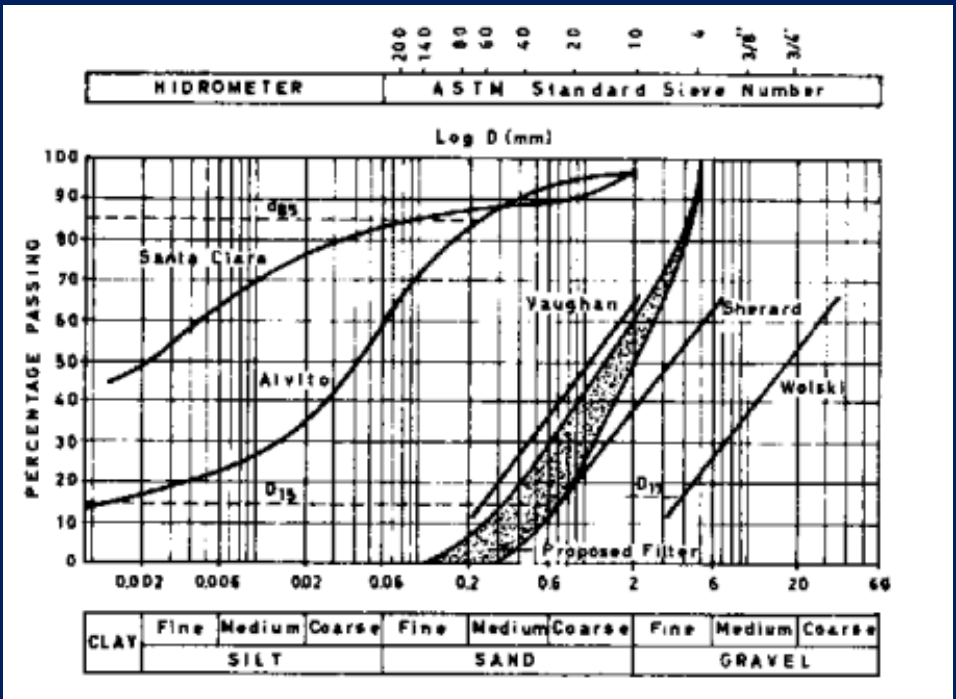

Figure 7.26 Filters for Santa Clara and Alvito

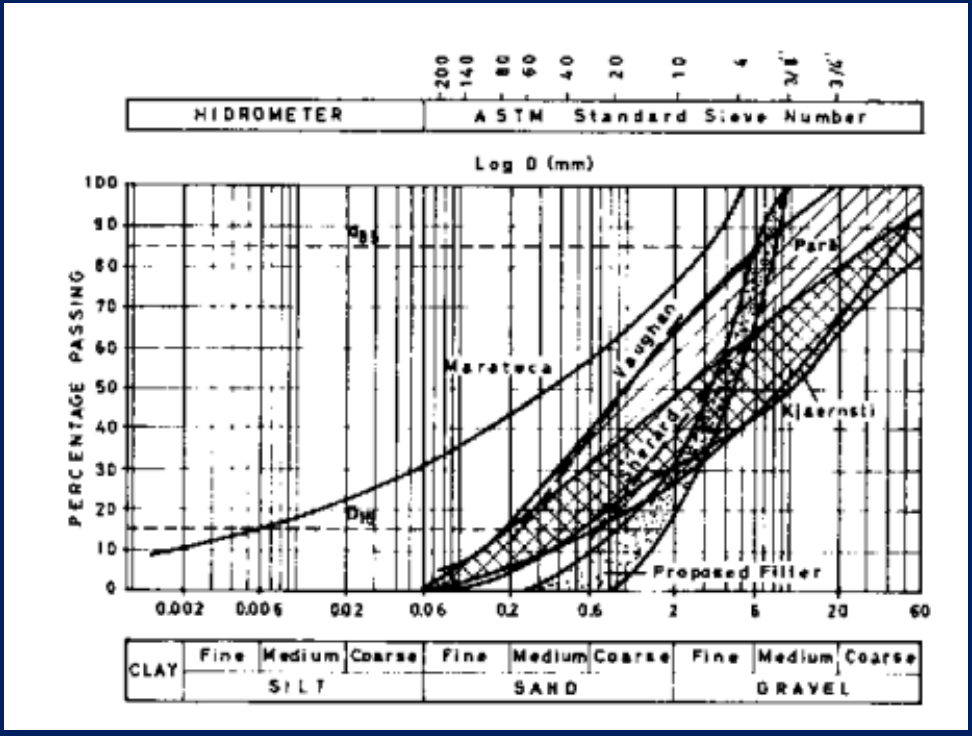

Figure 7.27 Filter for Marateca material

5 SUMMARY AND CONCLUSIONS

The most significant conclusions from this study can be summarized as follows:

(1) Special attention should be drawn in designing downstream core filter material and a risk of core cracking shall be considered.

(2) Conventional tests are useful to verify the stability of base material and filter material.

(3) In the slot tests the calculated velocity was low (about 1 m/s) and was not sufficient to erode the compacted base sample. Clogging has occurred in some base materials.

(4) In the hole tests the final pressure and gradient imposed on the stabilized base specimen are very high. Thus laboratory tests are conservative when compared to the conditions that may exist in a dam which develops a concentrated leak through the core.

(5) For tests with 90% degree of compaction the values of flow were higher than for 100% degree of compaction and the quantity of eroded material was also higher.

(6) In the long term tests with a water pressure of 50 kPa during more than 20 days water emerged clean and no signs of instability of base material were observed.

(7) It seems that the best way to design a filter for silt and clay materials is to perform experimental studies and to compare the results with criteria proposed by other authors.

7.5 Summary of Dams Earthquake Performance

The Mw7.9, 1906 San Francisco Earthquake affected about 30 medium-sized earthfill dams located within 50 km of the fault rupture trace,15 of these being at a distance of less than five km. The majority of these survived the shaking with minimum damage. Such satisfactory performance has been attributed more to the clayey nature of these embankments than to their degree of compaction.

7.9 Kanto, 1923 Japan Earthquake refers of significant damage to Ono Dam, a 122-foot-high earthfill dam, was fractured in many places, a fissure extended down 70 feet along the puddled clay core wall, settled nearly one foot, with longitudinal cracking up to 200 feet long and 10 inches wide.

1985 Mexico Earthquake, Mw 8.0, two large earth-rock and rockfill dams, La Villita (197 feet high) and EI Infiernillo (485 feet high). neither of these dams experienced significant damage during the 1985 earthquake.

In 1987 two events of moderate magnitude, Mw 6.6 Edgecumbe, New Zealand Earthquake, which damaged the 259-foot-high Matahina Dam, and the Mw 6.0Whittier Narrows, California Earthquake, which affected several embankment dams in the greater Los Angeles area, were considered to be significant.

The October 17, 1989, Mw 6.9 Loma Prieta, California Earthquake induced strong shaking to about a dozen embankment dams located within the epicentral area. Over 100 dams of various sizes, mostly embankment dams, were located within 100 km from the epicenter. All but one of the dams concerned performed well,
The exception was Austrian Dam, a 200-foot-high, 700-footcrest length embankment dam constructed in 1950-51, The reservoir was at mid height during the earthquake. The maximum crest settlement and horizontal movements were 2.8 and 1.1 feet, respectively. There was longitudinal cracking and transverse cracking, apparently due to poor compaction of the embankment.

The Northridge, California Earthquake (Mw 6.7) occurred on January 17, 1994, and was centered in the north-central San Fernando Valley, on a blind thrust fault dipping south-southwest below the valley.
The earthquake induced ground motions, sometimes quite severe, at 105 dams located within a 75 km radius of its epicenter (CA DSOD 1994a). These dams included most of those shaken in 1971.Eleven earthfill and rockfill dams experienced some cracking and slope movements as a result of the Northridge Earthquake.

The January 17, 1995, Kobe, Japan, Earthquake Mw 6. No large embankment dams were affected by the Kobe Earthquake, but about 50 dams higher than 40 feet were located within 50 km of the epicenter, including small earth dams, about 266 embankment dams were within that range of distance.

The September 21, 1999, Chi-Chi, Taiwan, Earthquake (Mw 7.6) affected a mountainous area of east central Taiwan. About 2,400 lives were lost,10,000 people injured.
Several medium-size embankment dams were affected and experienced some settlement and surficial cracking. However, they did not leak and otherwise performed satisfactorily.

On January 26, 2001, M 7.7 Bhuj, India Earthquake struck the Gujarat Province in the western part of India. The death toll from the earthquake was estimated at more than20,000 with over three billion dollars in property damage. In this area of India, it is common to find loose sand and silt deposits which may extend to great depths. Where saturated these soils appear to have liquefied during shaking leading to wide spread damage such as sand boils, ground cracking and lateral spreading of ground and embankments. An important aspect of the Bhuj earthquake was the performance of small and moderate size embankment dams. Many dams have been constructed in an effort to store water for irrigation and domestic water supply needs. More than 300 dams were inspected after the earthquake and the following damage classifications were developed to prioritize the repairs

Significant damage – 11 dams
Major damage – 6 dams
Minor Damage – 245 dams

The May 12, 2008 Wenchuan Earthquake was Mw 8 event.
The duration of strong ground motion was up to 120 seconds there were about 300 aftershocks, some over Mw 6. More than 80,000 people were killed by rockfalls and structure collapses.
Twenty- two hundred sixty-six of the 35,601 reservoirs in Sichuan and seven nearby provinces were damaged. There were 69 dam breaks and 331 other highly dangerous situations. Well built dams performed as designed.
Zipingpu Dam, a 512-foot-high concrete faced rockfill dam was 7 km from the fault break, experiencing an estimated peak ground acceleration of 0.5 to 0.6g. The crest settled 3 feet, damaging small parts of the face slab.
Bikou Damis a 335-foot-high central core embankment that experienced an estimate peak ground acceleration of 0.5 g. Its crest settled 9 inches as a result of the shaking.
The January 8, 2009 Costa Rica Earthquake was a Mw 6.1 event
Toro II is an embankment dam 66 feet high with a crest length of approximately 1700 feet, located 11.5 Km from the epicenter. A peak ground acceleration of 0.65g was recorded on the crest of the dam. Damage resulting from the earthquake was limited to longitudinal cracks in the crest of the dam.
Cipreses is an embankment dam approximately 100 feet high with a crest length of approximately1100 feet. A peak acceleration of 0.45g was recorded at a surge tank approximately 10.3Km from the earthquake epicenter. Damage to this embankment also consisted of longitudinal cracks in the crest of the dam.

The Mw 9.0 Tohoku, Japan Earthquake occurred on March 11, 2011, near the north east coast of Japan. The earthquake and tsunami caused enormous damage to Japan.
More than 400 dams were inspected. Generally, dams performed well with minor or moderate cracking occurring at embankment dams.
The crest of Surikawa Dam, a 172-foot-high central core rock fill completed in 2006, settled a maximum of 7 inches, transverse cracking of the crest paving occurred near the abutments and the leakage temporarily increased.

In summary: From the dam behavior during the occurrence of earthquakes can be concluded that dams built of compacted clayey materials on clay or bedrock foundations have historically withstood strong ground motions, in contrast with older embankments built on sandy materials or of insufficiently compacted sands and silts and tailings dams, primarily due to the liquefiable of these materials.
Dams built by modern technique have behaved well.
Rockfill dams have exhibit a good behavior, as due to the high permeability there was a rapid dissipation of pore pressure.

LESSONS FROM DAM BEHAVIOR DURING EARTHQUAKES

- OVERTOPPING DUE TO SLIDES OR ROCKFALLS INTO RESERVOIR
- DISRUPTION OF DAM BY MAJOR FAULT MOVEMENT IN FOUNDATION
- DIFFERENTIAL TECTONIC GROUND MOVEMENTS
- FAILURE OF SPILLWAY OR OUTLET WORKS
- PIPING FAILURE THROUGH CRACKS INDUCED BY GROUND MOTIONS
- LIQUEFACTION OF EMBANKMENT OR FOUNDATION
- SLIDING OR SHEAR DISTORTION OF EMBANKMENT OR FOUNDATION
- TRANSVERSE CRACKS
- LONGITUDINAL CRACKS
- LOSS OF FREEBOARD DUE TO COMPACTION OF EMBANKMENT OR FOUNDATION
- RUPTURE OF UNDERGROUND CONDUITS
- OVERTOPPING DUE TO SEICHES IN RESERVOIR

Selection of Design Earthquakes

The regional geologic study area should cover, as a minimum, a 100 km radius around the site, but should be extended to 300 km to include any major fault or specific attenuation laws.

2 levels for seismic activity, namely MCE (Maximum Credible Earthquake) considering a return period of 500-1000 years and DBE (Design Basis Earthquake) for a return period of 145 years, with a probability of exceeding in 100 years less than 50%, were proposed by ICOLD(1989).

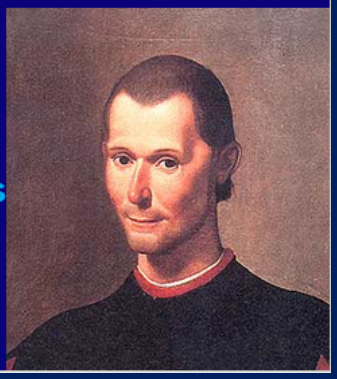

We can not control the natural hazards
but we can minimize the consequences
We should refuse the fate
Nicolau Maquiavel
(1469-1527)
Great political thinker

TECTONIC CONDITIONS

- Following (ICOLD, 1998) an active fault is a fault, reasonably identified and located, known to have produced historical fault movements or showing geologic evidence of Holocene (11 000 years) displacements.
- Surface fault breaking i.e. surface slip along an identified fault zone under the dam is considered as the most dangerous tectonic scenario for dam safety.
- Following Sherard et al. (1974) a concrete dam on active faults or near major active faults is not advisable and if a site with fault movements can not be avoided it is recommended to build an embankment dam

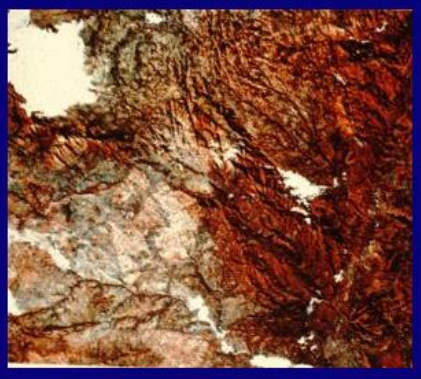

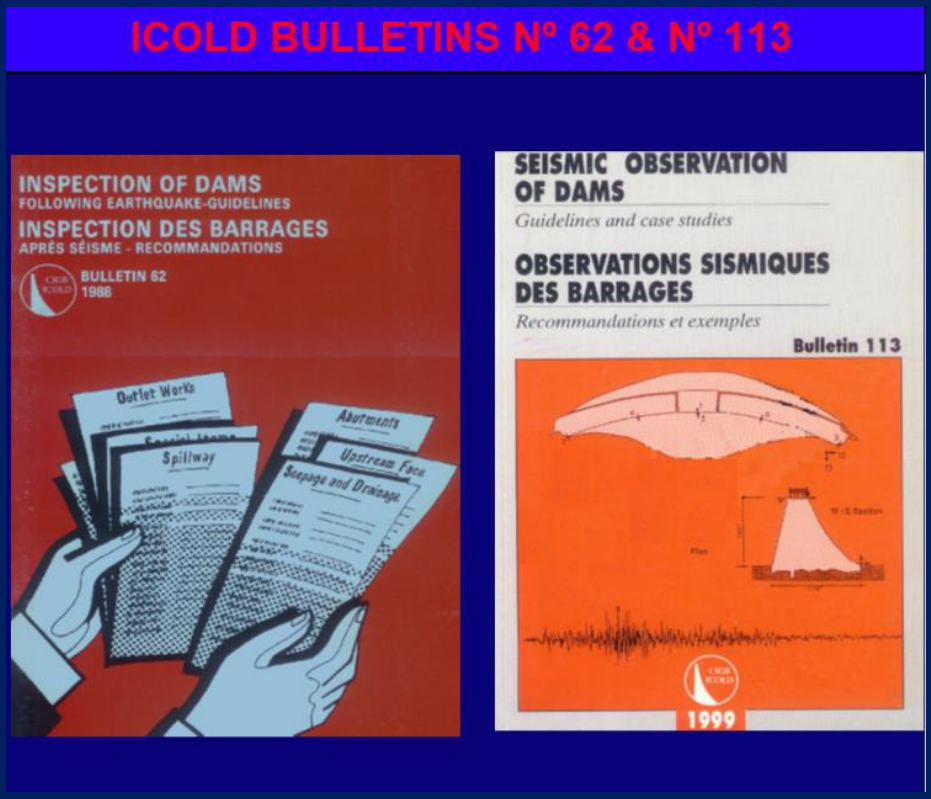

7.6 ANALYSIS OF DAM STABILITY DURING EARTHQUAKES

7.6.1 Introduction

Principles are the fundamental of dam safety. The dam shall safely retain the reservoir and any stored solids and pass environmentally acceptable flows as required for all loading conditions ranging from normal to extreme loads, commensurate with the consequences of failure.

Practices and Procedures suggest methodologies that may be used to meet the Principles.

Table 7.9 presents the seismic criteria probabilistic approach recommended by Canada.

Table 7.9 Seismic Criteria-Probabilistic approach recommended by Canada

Consequence Class of Dam	EQ Design Ground Motion (EDGM-Mean Annual Exceedance Probability
Low	1/500
Significant	1/1000
High	1/2500
Very High	1/5 000
Extreme	1/10 000

New Zealand and UK have suggested a return period of 10 000 years for SEE for Extreme and High risk dams, 3000 years for Moderate risk and 1000 years for Low risk.

. The behaviour of embankment dams during the occurrence of earthquakes can be analysed by experimental methods or mathematical methods.

7.6. Experimental Methods

Experimental methods are used to test predictive theories and to verify mathematical models. Nevertheless some limitations they are useful to understand the mechanisms of dynamic behaviour of embankments. The most common techniques are shaking table and centrifuge models.

Experiments using large shaking table

To analyse the behaviour of embankment dams during earthquakes experiments of models using a large shaking table are sometimes performed. Baba and Nagai (1987) have used dam models with 2.0m high and 6.0m width, with slopes gradients of 1:1.5, 1:2.0 and 1:2.5 and the water was stored by diaphragm walls located at the center of the models.

To measure the response of the dam models during dynamic experiments accelerometers and displacement meters were installed.

From the experiments the following conclusions were obtained:

(i) The natural frequency of the dam model and the acceleration response of the dam have tended to be smaller with storage of water than without.

(ii) Failure of the dam model have started from the vicinity of the upstream crest.

(iii) When there was storage of water the upstream and downstream faces of the dam have indicated different response during earthquake.

(iv) The extension of failure zone depends of amplitude and duration of acceleration.

Error! Bookmark not defined.

Centrifuge tests is a valuable technique to study the response of geotechnical structures to extreme events such as earthquakes. The influence of earthquake intensity on dynamic magnification, the existence of a yield acceleration and a delayed failure can be observed in clay embankments subjected to simulated earthquakes (Kutter and James, 1989). Deformation patterns can be observed by X-ray radiography.

The scaling relations used to interpret model tests in terms of prototype behaviour have to be verified. This is best done by comparing with the prototype. However, prototype monitoring is often too costly and impractical. As an alternative, the concept of modelling of models has evolved to provide a check on the internal consistency of the centrifuge model testing scheme and to validate the scaling relations.

This concept can best be explained by the diagram in Figure 7.28, in which the model size is plotted logarithmically against the gravity level at which the model is tested. All the models that are tested at 1-g conditions are, by definition, prototypes. Consider a 1,000cm prototype, represented by A_1. It can be modelled at 10th scale by a model of 100 cm size (A_2), or at 100th scale by a model of 10cm size (A_3), etc. A_2 and A_3 are not only models of the same prototype A_1, but they are also models of each other. In the absence of the prototype, A_2 and A_3 can be compared with one another and, by using the scaling relations, their behaviour should both extrapolate to the same projected prototype performance (Ko, 1988). It should be noted in passing that A_2 and B_2 are not models of one another; their comparison will delineate size effects in the testing scheme. At the same time, B_2 and A_3 are not models of one another either; their comparisons will determine the effects of increase in the gravity stresses.

Table 7.10 presents the scaling relations between the model and prototype for the different quantities. As can be seen there are conflicts in the scaling relations for time. Whereas the time dynamic event scales by N, the time for diffusion scales by N^2.

The principal arrangements for producing simulated earthquake ground motions are compared in Figure 7.29 (Whitman, 1988).

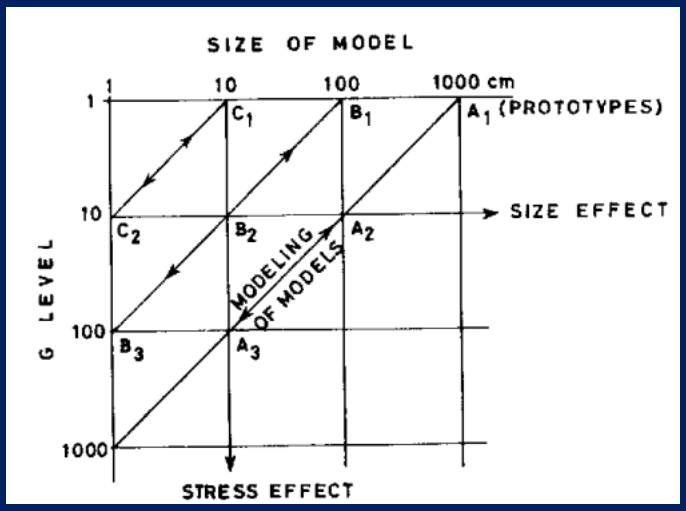

Figure 7.28 Principle of modeling of models (after Ko)

Simplicity refers to equipment and controls required to produce the ground motions. Adjustability refers to the case with which the amplitude, frequency content and duration of the motions can be changed to suit testing requirements. For the frequency range low refers to the prototype frequencies of 0.5 Hz to 2Hz and high corresponds to prototype frequencies of 10 Hz to 20 Hz.

	COST	SIMPLICITY	ADJUST-ABILITY	FREQUENCY RANGE Low High
COCKED SPRING	Very Low	Very Simple	Poor	
PIEZO-ELECTRIC	Low	Simple	Good	
EXPLOSIVE	Low	Simple	Moderate	
BUMPY ROAD	High	Complex	Moderate	
HYDRAULIC	Very High	Very Complex	Very Good	

Figure 7.29 Comparison of various methods for simulating earthquake ground motions on centrifuge (after Whitman (1988).

Table 7.10 SCALING RELATIONS

Can be derived by dimensional analysis, or through analysis of the field equations describing the physical phenomenon (e.g. consolidation)

Quantity	PROTOTYPE	MODEL
	N	1
LENGTH	N^2	1
AREA	N^3	1
VOLUME	1	1
VELOCITY	1	n
ACCELERATION	N^3	1
MASS	N^2	1
FORCE	N^3	1
ENERGY	1	1
STRESS	1	1
STRAIN	1	1
MASS DENSITY	1	1
ENERGY DENSITY	N	1
TIME (DYNAMIC)	N^2	1
TIME (DIFFUSION)	1	1
TIME (CREEP)	1	N
FREQUENCY		

7.6.3 Mathematical Methods

The different methods of dynamic analysis of embankment dams are summarized so that its capabilities as well as its limitations may be better understood.

Pseudo-static methods

Past practice and most current practice in the analysis of embankment stability against earthquake forces involves the computation of the minimum factor of safety against sliding when a static, horizontal force of some magnitude is included in the analysis. The analysis is treated as a static problem and the horizontal force is expressed as the product of a seismic coefficient K, and the weight W, of the potential sliding mass. If the factor of safety approaches unity, the section is generally considered unsafe, although there is no generally recognized limit for the minimum acceptable factor of safety.

Sometimes is assumed that the embankment dam behaves as a rigid body and so the accelerations will be uniform throughout the section and equal at all times to the ground accelerations. The main limitations of this approach are: (1) it is evidence from field tests that all earth dams do not behave as rigid bodies; (2) the maximum acceleration will be developed in an embankment for only a short period of time, so that the deformation resulting from it may be small.

The above deficiencies of a rigid body response have led a number of investigators to propose the use of elastic response solutions for the determination of design seismic coefficients.

The first analysis considering the embankment as a series of infinitely thin horizontal slices connected by linearly elastic shear springs and viscous damping devices was made by Mononobe, Takata and Matumura (1936).

Ambraseys (1960) developed solutions for the case of a truncated wedge of uniform modulus and for a symmetrical wedge of uniform modulus resting in an elastic layer of infinite thickness.

Majumdar (1971) extended Taylor's charts for cohesionless soils to account for horizontal earthquake acceleration.

Koppula (1984) analysed the effects due to earthquakes on purely cohesive slopes by circular failure mechanism including earthquake loading as an equivalent horizontal force.

Ambraseys (1960) presented solutions for a dam profile symmetric, truncated and founded in an elastic layer of infinite thickness.

For the evaluation of the seismic coefficient has proposed:

(i) a seismic coefficient at depth equal to the square root of the summation of the square seismic coefficients for the peak response of the first four modes

$$\bar{k}\{y\} = \left[\sum_{n=1}^{n=4} \{k_n\{y\}^2\}\right]^{\frac{1}{2}} \quad (7.3)$$

e *(ii)* seismic coefficient at each depth equal to the maximum value at that depth, for any modal distributions, i.e.:

$$k\{y\} = [k_n\{y\}]_{mx} \quad (7.4)$$

Both equations represent an attempt to estimate the distribution of the maximum seismic coefficient acting in any instant during the earthquake.

The computed seismic coefficient can be incorporated in slope stability analysis based in the limit equilibrium, e.g. Bishop (1954) simplified method, including the inertia forces and generation of pore pressures.

.

Considering the resistance parameters c' and Φ' in effective stresses the shear resistance is given by the equation:

$$\tau = \frac{c'}{F} + (\sigma_n - u)\frac{tg\,\phi'}{F} \quad (7.5)$$

Where σ_n represents the normal total stress to the potential slipping surface and u is the pore pressure.

The condition of the moment's equilibrium is represented by the equation:

:

$$\rightarrow \quad F = \frac{1}{\sum W\,sen\alpha + Wk_s(\cos\alpha - \frac{z}{R_c})} \sum \left[\{c'\,b + [W - (u + \Delta u_s)b]tg\phi'\}\frac{\sec\alpha}{1 + tg\alpha.tg\phi / F}\right] \quad (7.6)$$

(7.6)

Where:

F – safety factor

W – total weight of the slices

b – width of the slice

I a – angle between the vertical trough the average point at the slice base and the normal of sloping surface that contains I in this point.

Rc – radius of cylinder surface

ks – seismic coefficient

z -vertical distance between the centre of gravity of the slice and the base of the slice.

h -height of the slice I

It is important to stress that these methods consider that seismic coefficient acts in one direction for an infinite time, when in reality inertia forces are reversible after a period of 0.25 to 0.5 seconds and so the factor of safety can drop below unity a number of times, but only for brief periods of time. During such periods permanent displacements will occur and thus the magnitude of the deformations that develop will depend on the time-history of the inertia forces.

Comment: Pseudo-static analyses have severe limitations and were not capable to predict failure of Shefield and S. Fernando dams.

Simplified procedures for estimating induced deformations

-Introduction

Considering the limitations of the pseudo-static methods for the prediction of embankment behavior during the earthquakes new methods were developed based in the determination of deformations.

Following the recommendations of ICOLD (1975) "High embankment dams whose failure may cause loss of life or major damage should be designed by conventional method at first, followed by a dynamic analysis in order to investigate any deficiencies which may exist in the pseudo-statical design of the dam" simplified procedures for estimating induced deformations are presented.

Newmark Method

Newmark (1965) has suggested an approach suitable for rigid-plastic material involving the determination of a yield acceleration, K_{yg}, at which sliding will begin to occur and the computation of the displacements which develop when this acceleration is exceeded. The procedure is illustrated in Figure 7.30. If the acceleration pattern acting on a potential sliding mass is similar to that shown in the Figure 7.30, then no displacement will occur until time t_1, when the induced acceleration reaches the yield acceleration for the first cycle K_{y1}. If the yield acceleration is assumed to remain constant throughout the first cycle, it may be marked off as shown in Figure 7.30, and the variation in velocity of the sliding mass may be computed by integration over the shaded area. The velocity will continue to increase until time t_2 when the acceleration again drops below the yield value, and the velocity is finally reduced to zero at time t_3, as the direction of acceleration is reversed. The rate of displacement of the sliding mass may then computed by integration of the velocity versus time relationship.

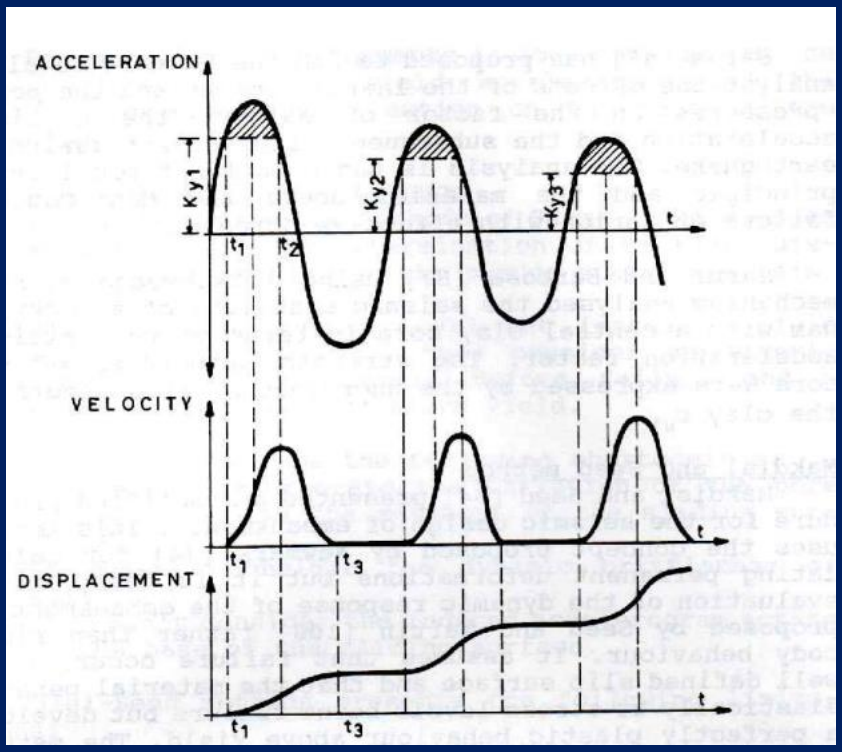

Figure 7.30 Integration of accelerograms to determine downslope displacements (after Newmark, 1965)

Sarma method

Sarma (1973) has proposed a method of computing the critical horizontal acceleration that is required to bring the mass of soil bounded by the slip surface to a state of limiting equilibrium. This critical acceleration is therefore a measure of the static factor of safety.

Sarma (1975) has proposed to use the Newmark model to analyse the effects of the inertia forces and the pore--pressures on the factor of safety, the critical acceleration and the subsequent displacement during an earthquake. The analysis is based on limit equilibrium principle and the material obeys the Mohr-Coulomb failure criterion with effective stresses.

There are two possible ways by which the factor of safety may be reduced to one or below one during an earthquake. First embankment dams when subjected to strong ground motion will be set into vibration which will produce inertia forces on the structure. This together with the pre-earthquake static forces may bring the factor of safety to a value below one. But if the strength of the soil remains unchanged and if the displacement of the failed mass is not large enough to change the configuration of the structure, the factor of safety after the earthquake will be the same as that before the earthquake. Second, it is known that pore-pressures within the soil mass of an earth dam may increase during earthquake loading.

Thus, the increase of inertia forces as well as the decrease of total strength due to pore-water pressure may reduce the factor of safety of the structure to unity at some time during an earthquake. Any further increase of the inertia force will produce displacement of the soil mass along the failure surface relative to the main body of the dam. The behaviour of the pore-pressure along the slip surface during such displacement is unknown but may be assumed to be constant and equal to that at the time when the factor of safety was one.

Sarma and Barbosa (1985) using a two-wedge sliding mechanism analysed the seismic stability of a rockfill dam with a central clay core in terms of the critical acceleration factor. The strength properties of the core were expressed by the undrained shear strength of the clay c_u.

Composite surfaces can be analysed and the convergence is rapid, in general 3 iterations are sufficient.

It is important to analyse the physical condition of the solution, in order to avoid the violation of the failure criteria by the internal forces and the existence of the traction forces in the interior of the failure surface.

The following equations are considered

$$K = (S_1 - \lambda S_4) / \Sigma W_i \quad (7.7)$$

$$\lambda = \frac{S_2}{S_3} \quad (7.8)$$

where

$$S_1 = \Sigma D_i \quad (7.9)$$

$$S_2 = \Sigma W_i (x_i - x_g) + \Sigma D_i (y_i - y_g) \quad (7.10)$$

$$S_3 = \Sigma F_i [(y_i - y_g) tg(\phi_{i'} - \alpha_i) + (x_i - x_g)] \quad (7.11)$$

$$S_4 = \Sigma F_i tg(\phi_{i'} - \alpha_i) \quad (7.12)$$

$$D_i = W_i tg(\phi_{i'} - \alpha_i) + (c_{i'} b_i \cos\phi_{i'} - R_{ui} W_i sen\phi_{i'}) \sec\alpha_i / \cos(\phi_{i'} - \alpha_i) \quad (7.13)$$

where

Kc – horizontal critical acceleration needed to bring the potential sloping surface to an equilibrium condition

bi – width of the slice

ai -inclination of the slice

Xi'Yi – co-ordinates of the medium point of the slice nº i base

Xg, Yg -co-ordinates of the gravity center of the sloping mass

Ni – normal force at the slice base

Wi – weight of each slice

KWi – horizontal force at the gravity center of the slice

c` e ϕ` - soil strength parameters in effective stress at the slice base

Rui – pore pressure coefficient = u/γhi

hj -height of each slice

y – unit weight of the material

If the seismic acceleration is higher than Kcg, the safety factor is less than the unity and the sloping of the soil mass will continue until the seismic acceleration reaches a value less than Kcg.

Assuming the equilibrium of the stable and unstable forces and no variation of pore pressure during the displacement, the following equation can be considered:

$$\ddot{x} = g \frac{\cos(\beta - \theta - \phi')}{\cos\phi'} (K - K_C) \qquad (7.14)$$

where:

X – acceleration of the soil mass

B – inclination of the sloping surface

ϑ – inclination of the inertia force with the horizontal

ϕ'- friction angle in effective stress

Kc – critical seismic coefficient related with a safety factor of unit of the failure surface

K – seismic coefficient

g- acceleration of gravity

The implications related the variation of the direction of the inertia forces are small for rectangular pulses and soils with initial pore pressure nil. Different situations needed further research.

The search of the critical surface and consequently of the minimum Kc' value is simple.

The computation of the displacement of the failure surface is performed when the seismic acceleration at the base of the critical surface is superior to Kc (see Figure 7. 31).

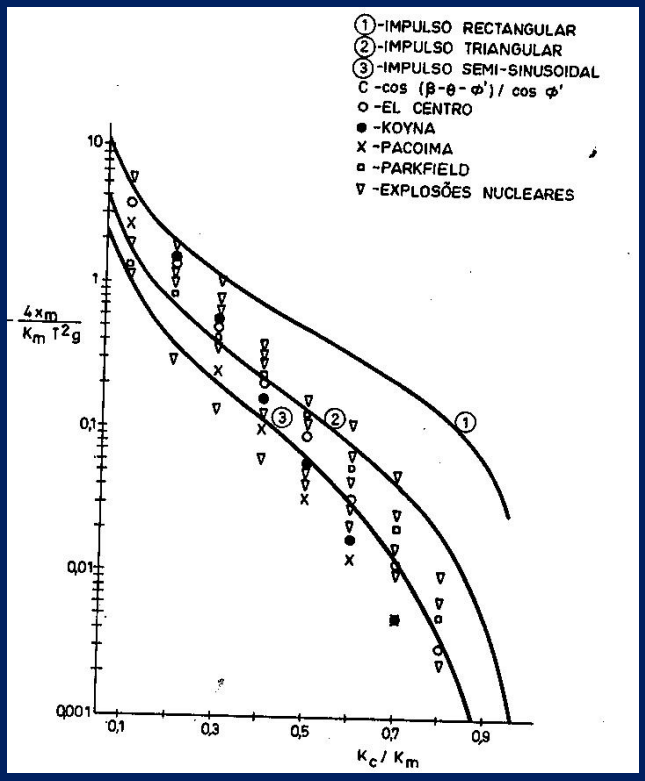

Figure 7.31 Variation of displacement with the ratio Kc/Km

Makdisi and Seed method

Makdisi and Seed (1977) presented a simplified procedure for the seismic design of embankments. This method uses the concept proposed by Newmark (1965) for calculating permanent deformations but it is based on an evaluation of the dynamic response of the embankment as proposed by Seed and Martin (1966) rather than rigid body behaviour. It assumes that failure occurs on a well defined slip surface and that the material behaves elastically at stress levels below failure but develops a perfectly plastic behaviour above yield. The method involves the following steps:

1) A yield acceleration i.e. an acceleration at which a potential sliding surface would develop a factor of safety of unit is determined.
2) Earthquake induced accelerations in the embankment are determined using dynamic response analyses. From these analyses time-histories of average acceleration for various potential sliding masses can be determined.
3) Evaluation of displacements by a simple double integration procedure when the induced acceleration exceeds the calculated yield surface for a given potential sliding mass.

Determination of the yield acceleration

For soils without great deformations and no high development of pore pressures and that maintains their initial resistance after the earthquake occurrence, the yield acceleration can be defined by the methods of limit equilibrium, e.g. Bishop (1954) method or Janbu (1957) method.

Determination of induced acceleration

The determination of the induced acceleration can be performed by a 2D f.e.m analysis using an equivalent elastic model (Chopra, 1966). In each time step the forces at the boundary of the failure surface are computed by the normal and shear stress of finite elements placed along the boundary (see Figure 7. 32). The forces resultant divided by the weight of the surface gives the value of the average induced acceleration in

that instant. This procedure is repeated for each time step for the complete definition of the history of accelerations.

A comparison between the history of crest accelerations with the average acceleration history for different depths of failure potential surfaces shows that the frequencies are apparent and the amplitudes decrease with the increase of the failure surfaces depth.

Considering the maximum crest acceleration u_{max} and the maximum acceleration K_{max} of the potential failure surface, at depth y, the correlations of the variation of the ratio K_{max}/ u_{max} with depth, for different situations of seismic actions, can be stablished.

The maximum crest acceleration and the natural dam period can be defined by f.e.m (Clough and Chopra, 1966) or by method of shear beam (Seed and Martin, 1966). For practical purposes a simplified method for the determination of deformations by an iterative procedure that allows the determination of the shear deformations and the damping ratio, following Figure 7.33, can be used.

Determination of the average shear deformation

The shear beam theory allows the determination of the shear deformation in different levels of the embankment based in time.

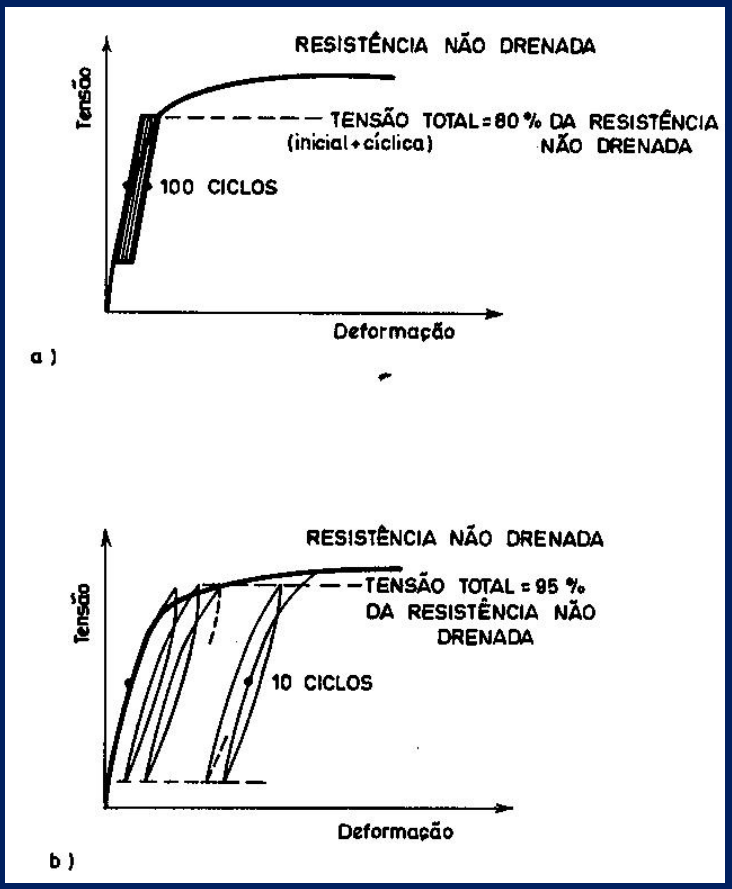

Figure 7. 32 Definition of dynamic resistance (after Makdisi and Seed, 1977)

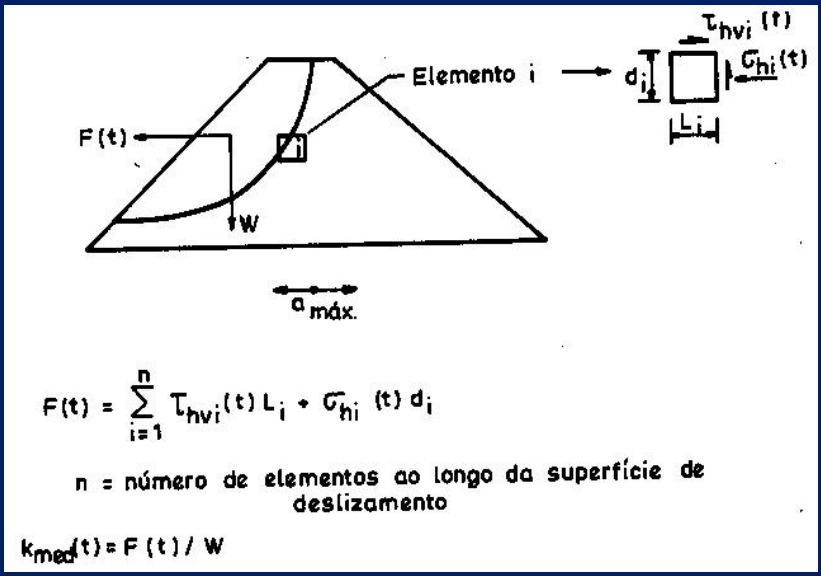

Figure 7. 33 Computation of the induced seismic acceleration (after Makdisi and Seed, 1977)

Computation of permanent displacements

Considering the yield acceleration and the induced acceleration for a potential failure surface the displacements can be computed. Based in Figure 7.34 the yield acceleration can be defined and with the first fundamental period of the dam To and the earthquake magnitude the permanent displacement can be computed by Figure 7.35.

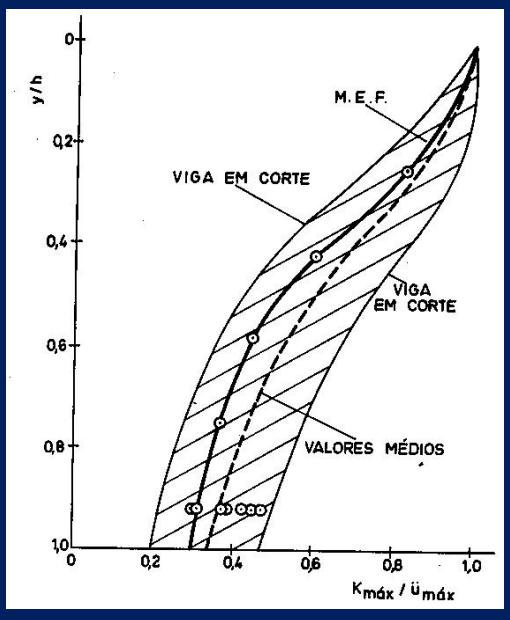

Figure 7.34 Calculation of the yield acceleration (after Makdisi and Seed, 1977)

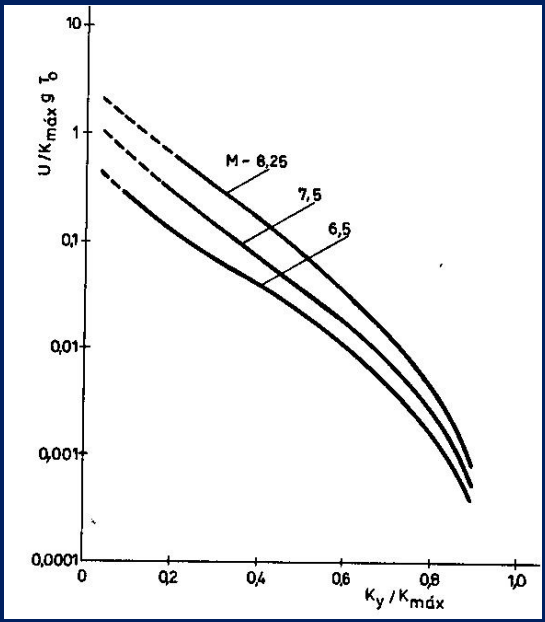

Figure 7. 35 Displacements versus yield acceleration (after Makdisi and Seed, 1977)

Mineiro method

Mineiro (1975, 1979) has proposed a method that takes into account the dynamic brittleness of soils and the excess pore pressures generated during an earthquake.

The method considers the following steps:

1) The initial yield acceleration is determined with the static strength of the material and taking into account the excess pore pressures during the occurrence of the earthquake and the brittleness of the material the residual yield acceleration is computed.
2) Earthquake induced accelerations in dam body are calculated by f.e.m. assuming an elastic linear behaviour with viscous damping for the material.
3) Evaluation of displacements is done considering the value of residual yield acceleration and the induced accelerogram acting on the base of the sliding surface.

Comparison of different methods

The latter described methods of Sarma, Makdisi-Seed and Mineiro allow the determination of residual displacement in opposition to the pseudo static analysis.

They use the Newmark model but instead a rigid behaviour of the material they consider an elastic behaviour for stress levels before failure and a perfect plastic behaviour above yield.

Sarma method presents the following shortcomings:

- It doesn't incorporate the variation of the pore pressures during the movement of the sliding surface;
- It doesn't consider the dynamic brittleness of soils;
- It doesn't consider the induced accelerogram acting on the base of the sliding surface.

Makdisi-Seed methods presents the following limitations:

-For soils which do not develop large cyclic strains or pore pressures and maintain most of their original strength after earthquake shaking;

- The design curves are averages based on a limited number of cases analysed and should be updated.

Mineiro method presents the following simplifications:

- Assumes an elastic behaviour with viscous damping for the material;

Doesn't incorporate the vertical component of the earthquake.

7.6. DYNAMIC ANALYSIS PROCEDURES

7.6.4.1 Introduction

The most widely used method of dynamic analysis for embankment dams involves the following steps (Seed et al., 1975):

1) Determination of the initial stresses in the embankment before the earthquake.
2) Selection of an appropriate acceleration time history, expected to develop in the rock foundation of the dam, for each earthquake under consideration.
3) Evaluation of the embankment response to the base rock excitation which includes the computation of induced shear stress-time histories and requires the determination of the dynamic soil properties.
4) Dynamic testing of representative soil samples to the combination of pre-earthquake stress conditions, and super-imposed dynamic stress applications in order to determine the seismic strength and deformation characteristics of the soil.
5) Comparison of the laboratory cyclic shear stresses required to cause selected levels of strain with the computed shear stresses induced by the earthquake motions.
6) Evaluation of the overall strain potentials, deformations, and stability of cross sections of the embankment.

7.6.4.2 Determination of Initial Stresses

Finite element method is an important tool to determine the stresses and deformations of a dam during the construction phase and normal operation. The method permits the simulation of: (i) embankment construction by layers; (ii) the subsequent loading of the embankment due to reservoir filling and steady-state seepage; (iii) the nonlinear stress-dependent behaviour of the embankment soils.

In simulating the construction of a dam, the loads applied during each increment represent the weights of the added elements. The weight of each element is distributed equally among its nodes, in accordance with the usual procedures for applying gravity loads.

During reservoir filling the following effects may be distinguished (Nobari and Duncan, 1972): (1) the water-load on the core causes downstream and downward movements; (2) the water-load on the upstream foundation causes upstream and downward movements; (3) the buoyant uplift forces in the upstream shell causes upward movements within this zone and downstream rotation of the dam, and (4) collapse of the upstream shell due to wetting causes downward movement within this zone and upstream rotation of the dam. In addition, seepage forces, S, are calculated using the expression

$$S = i \gamma_w A \qquad (7.15)$$

in which S = seepage force, g_w = unit weight of water, and A = area of an element. These forces act in the direction of the hydraulic gradient, and are distributed equally among the nodes of each element within the zone of seepage.

7.6.4.3 Material properties

A - Nonlinear models

K - G model

In the K - G model (Naylor, 1975) K and G are assumed to vary linearly with stress invariants.

$$K = K_1 + a_K p \tag{7.16}$$

$$G = G_1 + q_G p' + \beta_G q_3 \tag{7.17}$$

in which

$$p' = \frac{1}{3}(\sigma_{1'} + \sigma_{2'} + \sigma_{3'}) \tag{7.18}$$

and

$$q^2 = \sigma_1 (\sigma_1 - \sigma_2) + \sigma_2 (\sigma_2 - \sigma_3) + (\sigma_3 - \sigma_1) \tag{7.19}$$

q is related to the second deviatoric invariant, J_2 (= 1/3 q^2) and to the octahedral shear stress, t_{oc} by q = (3/Ö_2) t_{oct}.

The constants can be evaluated by consolidated drained triaxial tests.

M - G model

The constrained modulus M is defined as the ratio of stress to strain for one-dimensional loading (Drnevich, 1975):

$$M = \frac{E(1 - \nu)}{(1 + \nu)(1 - 2\nu)} \tag{7.20}$$

in which E = Young's modulus; and n = Poisson's ratio.

The shear modulus G is defined as the ratio of shear stress to shear strain or as the modulus of rigidity. In terms of Young's modulus and Poisson's ratio it is given by

$$G = \frac{E}{2(1 - \nu)} \tag{7.21}$$

The shear modulus associates the unit angular deformation of an element to applied shear stress.

The modulus can be defined by one-dimensional compression tests and simple shear tests. This formulation intents to minimize the uncertainties associated with the values of Young's modulus and Poisson's ratio.

Hyperbolic model

Hyperbolic stress-strain curves of the type shown in Figure 7.36 can be expressed in the form (Kondner and Zelasko, 1963).

$$\sigma_1 - \sigma_3 = \frac{\epsilon}{\frac{1}{E_i} + \frac{\epsilon}{(\sigma_1 - \sigma_3)_{ult}}} \qquad (7.22)$$

in which E_i = initial tangent modulus, and $(s_1 - s_3)_{ult}$ = asymptotic value of stress difference approached by the hyperbola at infinite strain. These values can be determined readily for a given test by plotting the data as shown in the lower part of Figure 7.7 and fitting a straight line through the data.

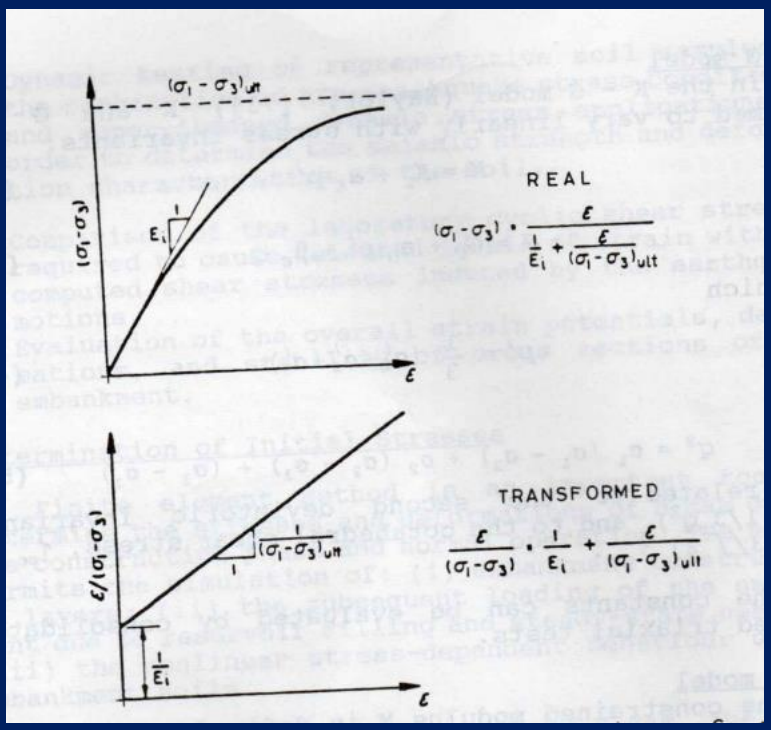

Figure 7.36 Hyperbolic representation of a strain-stress curve

If values of E_i and $(s_1 - s_3)_{ult}$ are determined for a series of tests on the same soil at different confining pressures, the values of both parameters will usually be found to increase with increasing confining pressure s_3.

The variation of E_i with s_3 can be represented conveniently by an equation of the form suggested by Janbu (1963):

$$E_i = Kp_a \left(\frac{\sigma_3}{P_a}\right)^n \qquad (7.23)$$

in which K = modulus number, n = modulus exponent, s_3= = minor principal stress, and P_a = atmospheric pressure expressed in the same units as E_i and s_3. Both the modulus number and the modulus exponent are dimensionless.

The variation of $(s_1 - s_3)_{ult}$ with s_3 can be accounted for conveniently by relating this asymptotic stress difference to the strength $(s_1 - s_3)_f$, which is defined as the maximum value of stress difference in a given test.

The value of strength can be related to the asymptotic stress difference by the following equation

$$(\sigma_1 - \sigma_3)_f = R_f (\sigma_1 - \sigma_3)_{ult} \qquad (7.24)$$

in which R_f = failure ratio, a dimensionless parameter whose value is always less than unity.

Then the stress-dependency of $(s_1 - s_3)_{ult}$ can be accounted for using the Mohr-Coulomb failure criterion.

$$(\sigma_1 - \sigma_3)_{ult} = \frac{1}{R_f} \left\{ \frac{2\,c\,\cos\phi + 2\sigma_3\,\sin\phi}{1 - \sin\phi} \right\} \qquad (7.25)$$

in which c = cohesion intercept, and f = angle of internal friction.

The variation of axial strain with radial strain may be represented by a hyperbolic equation of the form:

$$\varepsilon_a = \frac{-\varepsilon_r}{\nu_i - d\,\varepsilon_r} \qquad (7.26)$$

in which e_a = axial strain, e_r = radial strain, n_i = initial tangent Poisson's ratio, and d = a dimensionless parameter. The values of n_i and d can be determined by plotting data from a given test as shown in the lower part of Figure 7.37, and fitting a straight line to the data.

The variation of the value n_i with confining pressure can be represented by an equation of the form:
in which G = value of n_i at a confining pressure of one atmosphere, and F = reduction in Poisson's ratio for a ten-fold increase in confining pressure.

$$\nu_i = G - F \log_{10}\left(\frac{\sigma_3}{p_a}\right) \qquad (7.27)$$

Using the foregoing equations, Young's modulus and Poisson's ratio are given by the following equations (Wong and Duncan, 1974):

$$E_t = \left[1 - \frac{R_f\,(1 - \sin\phi)\,(\sigma_1 - \sigma_3)}{2c\cos\phi + 2\sigma_3\sin\phi}\right]^2 Kp_a \left(\frac{\sigma_3}{p_a}\right)^n \qquad (7.28)$$

$$\nu_t = \frac{G - F\log\left(\frac{\sigma_3}{p_a}\right)}{\left[1 - \frac{d\,(\sigma_1 - \sigma_3)}{Kp_a\left(\frac{\sigma_3}{P_a}\right)^n\left[1 - \frac{R_f\,(\sigma_1 - \sigma_3)\,(1 - \sin\phi)}{2c\cos\phi + 2\sigma_3\sin\phi}\right]}\right]^2} \qquad (7.29)$$

In the incremental analysis each step is analysed twice, the first time using values of E_t and n_t based on the stresses at the beginning of the incremental, and the second time using values of E_t and n_t based on the average stresses during the increment.

Unloading - reloading modulus can be given by the following equation:
in which K_{ur} = unloading - reloading modulus number n = modulus

$$E_{ur} = K_{ur}\,p_a \left(\frac{\sigma_3}{p_a}\right)^n \qquad (7.30)$$

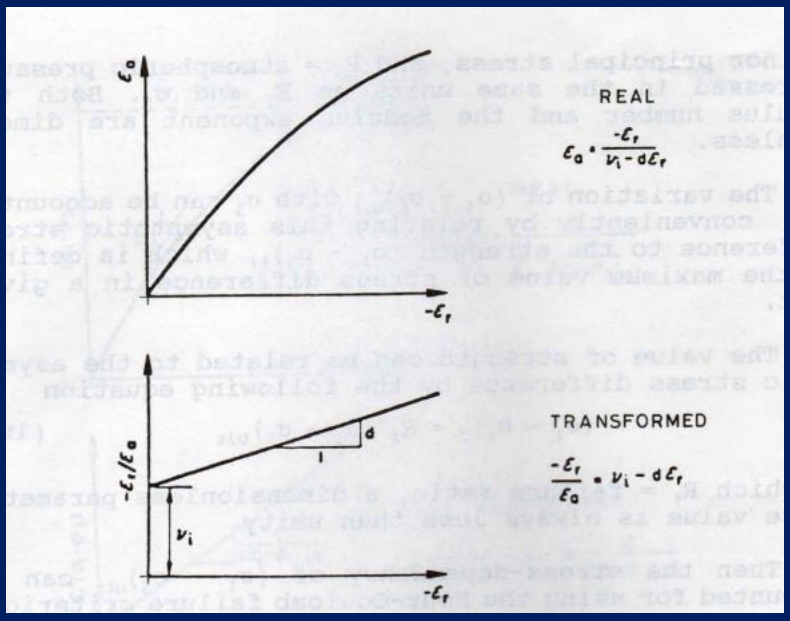

Figure 7.37 Hyperbolic axial strain-radial strain curves

exponent. Figure 7.38 shows the excellent agreement which can be obtained between the hyperbolic model and laboratory tests for the clay core material of Alvito dam (Sêco e Pinto, 1983):

The hyperbolic parameters for the materials of Alvito dam are summarized in Table 7.11.

The hyperbolic relationships have the following limitations:

(i) Based on the generalized Hooke's law they do not represent the behaviour of soils at and after failure.

(ii) They do not incorporate the effect of dilatancy.

(iii) The parameters are not fundamental soil properties, but only values of empirical coefficients which represent the behaviour of the soil under a limited range of conditions.

In spite of these limitations, the hyperbolic relationships are useful for the following reasons:

(i) The parameter values can be determined from the results of conventional triaxial compression tests.

(ii) The same relationships can be used for effective stress analyses and total stress analyses.

A typical example of static stress distribution for Alvito dam is shown in Figures 7.39 to 7.41. Figure 7.39 shows the finite element mesh and Figures 7.40 and 7.41 show the distribution of stresses and displacements at the end of construction and reservoir filling.

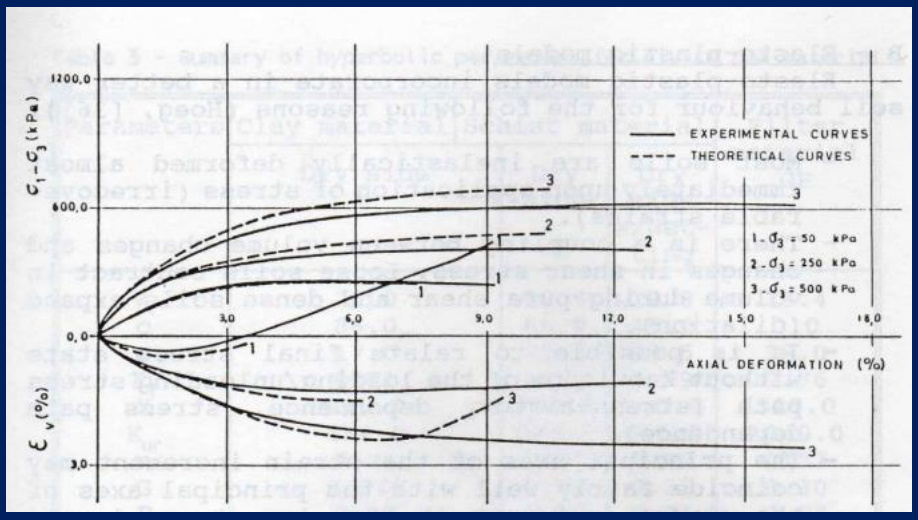

Figure 7.38 Comparison between theoretical and experimental curves (after Sêco e Pinto, 1983)

Table 7.11 Summary of hyperbolic parameters for Alvito dam material

Parameters	Clay material	Schist material		Filter material GP
	Dry side	Dry side	Dry side w/Wetting	
g_t	20.0	19.9	19.8	18.4
c	86.0	66.0	45.0	0.0
f	17.0	25.7	24.5	38.0
R_f	0.81	0.71	0.79	0.76
K	240.0	290.0	330.0	520.0
K_{ur}	480.0	580.0	660.0	1040.0
n	0.34	0.57	0.32	0.37
G	0.315	0.30	0.31	0.30
F	0.19	0.17	0.21	0.08
d	6.0	6.5	8.0	2.5
s_{3t}	-	-	0	-
b	-	-	0	-
s_t	10	0	0	0

g_t - Total unit weight (kN/m^3) G - Poisson's ratio parameter
c - Cohesion (kPa) F - Poisson's ratio parameter
f - Friction angle d - Poisson's ratio parameter
R_f - Failure ratio s_{3t} - Threshold stress
K - Modulus number b - Isotropic collapse coefficient
K_{ur} - Unloading and reloading modulus s_t - Tension strength
n - Modulus

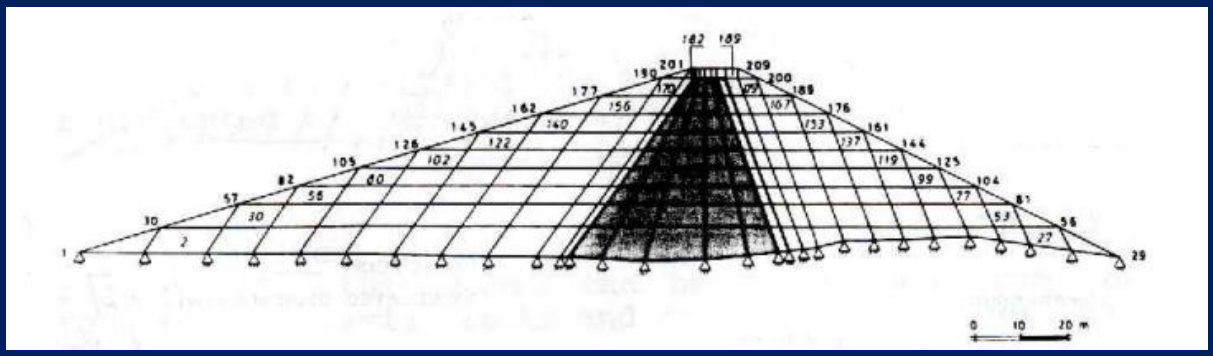

Figure 7.39 Finite element mesh

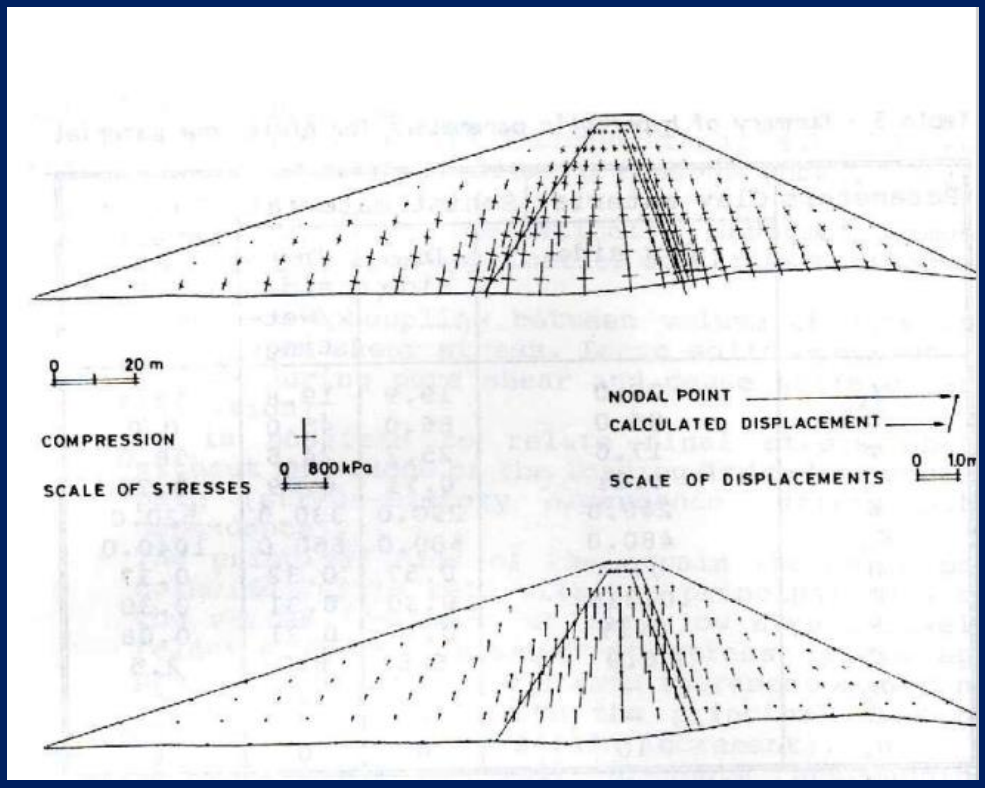

Figure 7.40 Distribution of stresses and displacements at the end of construction (after Sêco e Pinto, 1983)

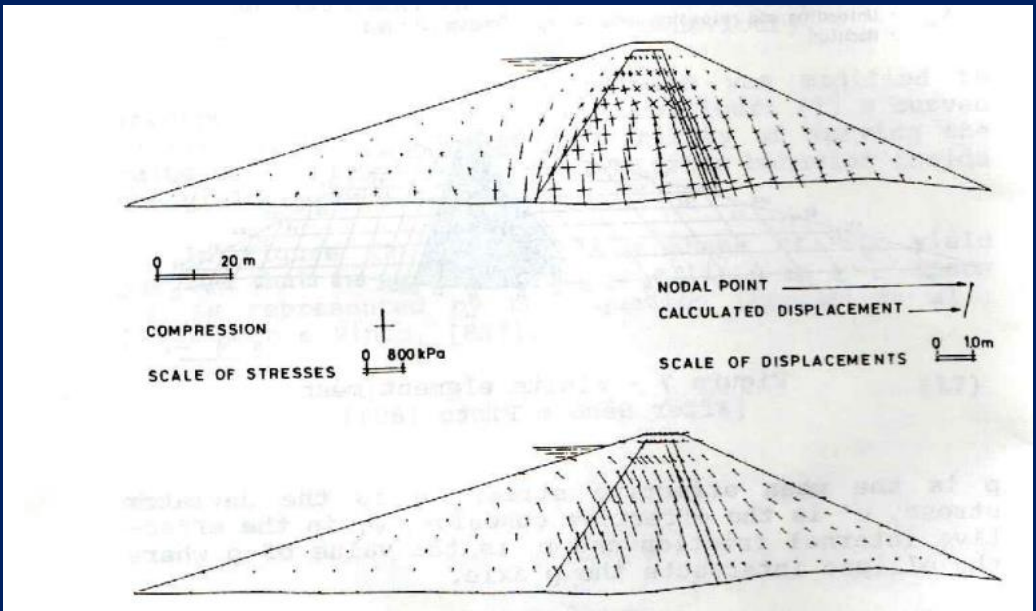

Figure 7.41 Distribution of stresses and displacements - full reservoir (after Sêco e Pinto,1983)

Elasto-plastic models

Elasto-plastic models incorporate in a better way soil behaviour for the following reasons (Höeg, 1978):

- Most soils are inelastically deformed almost immediately upon application of stress (irrecoverable strains).
- There is a coupling between volume changes and changes in shear stress. Loose soils contract in volume during pure shear and dense soils expand (dilation).
- Is possible to relate final stress state without knowledge of the loading/unloading stress path (stress-history dependence, stress path dependence).
- The principal axes of the strain increment may coincide fairly well with the principal axes of the stress increment at very low stress levels (elastic range). However, at stress levels approaching failure, the strain increment axes tend rather to coincide with the principal axes of stress (direction of strain increment).
- The straining of soil elements approaching failure is clearly anisotropic (stress-induced anisotropy during yielding).
- Many soils experience a decrease in strength with further straining after a peak strength has been reached (strain-softening behaviour).

The original Cambridge version was modified to incorporate the following soil behaviour: (i) a curved failure surface; (ii) the possibility of varying the value of l; (iii) a nonlinear elastic behavior inside the yield surface.

In Figure 7.42 is shown the shape of the yield surface that is assumed to be an ellipse in q-p' space and is represented by the equation (Duncan et al., 1981); Sêco e Pinto, 1983):

$$\left(1 + \frac{\eta^2}{M^2}\right)(p + p_r) - p_r = p_{o'} \qquad (7.31)$$

Where

$$p_r = c' \, cotg \, \phi' \tag{7.32}$$

$$M = \frac{6 \, sen \, \phi'}{3 - sen \, \phi'} \tag{7.33}$$

$$\eta = \frac{q}{p + p_r} \tag{7.34}$$

p is the mean effective stress, q is the deviator stress, c' is the effective cohesion, f, is the effective internal friction and p_o is the value of p where the ellipse intersects the p axis.

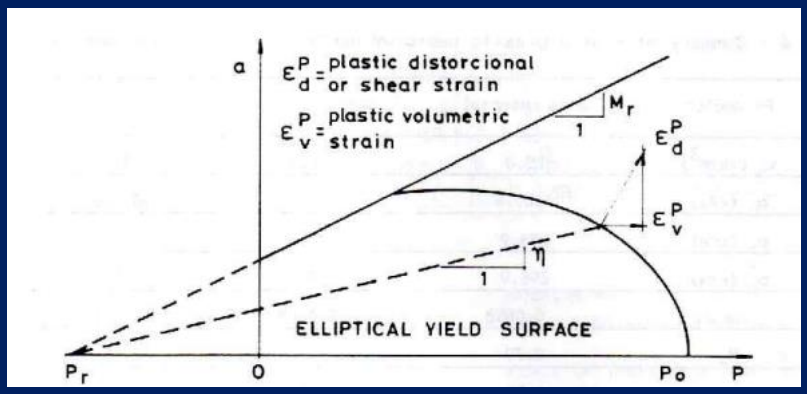

Figure 7.42 The yield surface

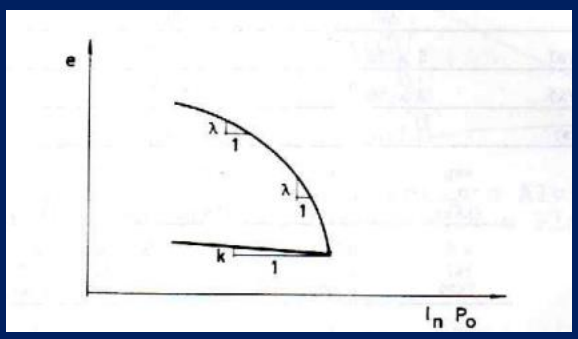

Figure 7.43 Void ratio - In pressure curve

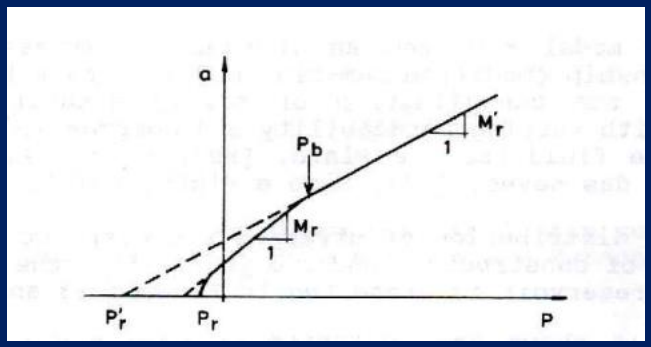

Figure 7.44 The failure surface

The magnitude of the volumetric strain is controlled by the value of the parameter l. This model provides the capability of varying the value of l with changes of p' values (Figure 7.43.

The failure surface which is shown in Figure 7.44 is represented by the equation

$$q = M_r (p + p_r) \qquad (7.35)$$

The values of all the stress-strain parameters required for this model can be determined from the results of triaxial tests and one-dimensional consolidation tests.

The summary of parameters for the materials used in the analysis of Alvito dam is given in Table 7.12.

Table 7.12 Summary of elasto-plastic cam-clay parameters for Alvito dam materials

Parameter	Core material	Shell material	Filter material
g_t (kN/m^3)	20.0	22.5	18.4
p_b (kPa)	1000.0	1000.0	1000.0
p_r (kPa)	296.9	99.8	0
p (kPa)	296.9	99.8	0
k	0.0058	0.0058	0.0059
M_r	0.79	1.17	1.55
M	0.79	1.17	1.55
e_o	0.5	0.40	0.45
S_o	67	70	70
K_{hs} (m/s)	5 x 10^{-7}	10^{-5}	10^{-4}
K_{vs} (m/s)	2 x 10^{-8}	10^{-5}	10^{-4}
s_t (kPa)	10.0	0	0
	avg p_o (kPa) l	avg p_o (kPa) l	avg p_o (kPa) l

432	0.026	299	0.0069	323	0.026
747	0.068	671	0.0271	982	0.044
1329	0.096	1278	0.0581	1746	0.066
p (kPa)	n	p (kPa)	n	p (kPa)	n
100	0.32	100	0.29	100	0.15
300	0.37	300	0.33	300	0.32
600	0.41	600	0.37	600	0.39

The analysis of Alvito dam for the construction stage, the reservoir filling stage and long term seepage is presented in Figures 7.45 to 7.47.

The model provides an incremental stress-strain relationship (modified cam-clay model), and takes into account the consolidation of partly saturated clay soils with varying permeability and compressibility of the pore fluid (Sêco e Pinto, (1983); Sêco e Pinto and Maranha das Neves (1985); Sêco e Pinto (1987).

The distribution of stresses and displacements at the end of construction and two years after the filling of the reservoir is presented in Figures 7.45 and 7.46.

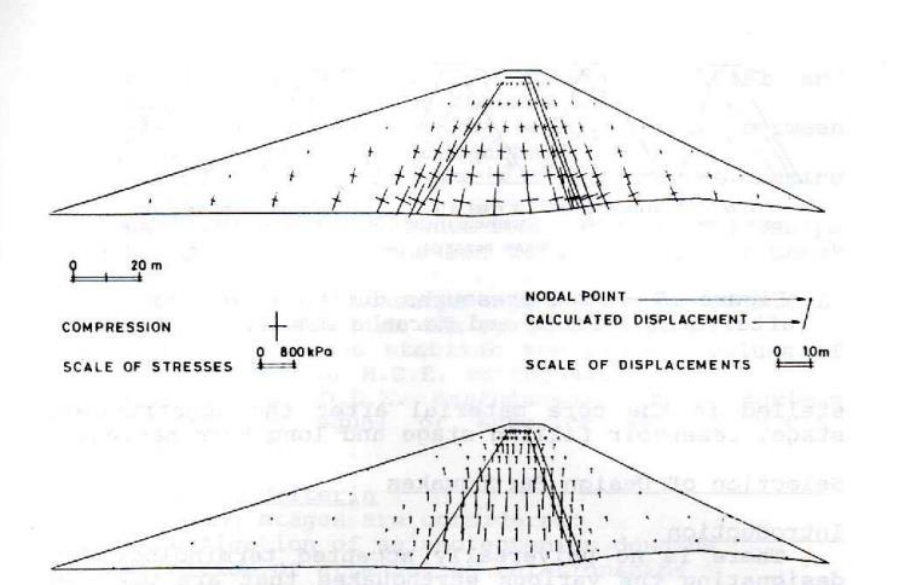

Figure 7.45 Distribution of stress and displacements at the end of construction

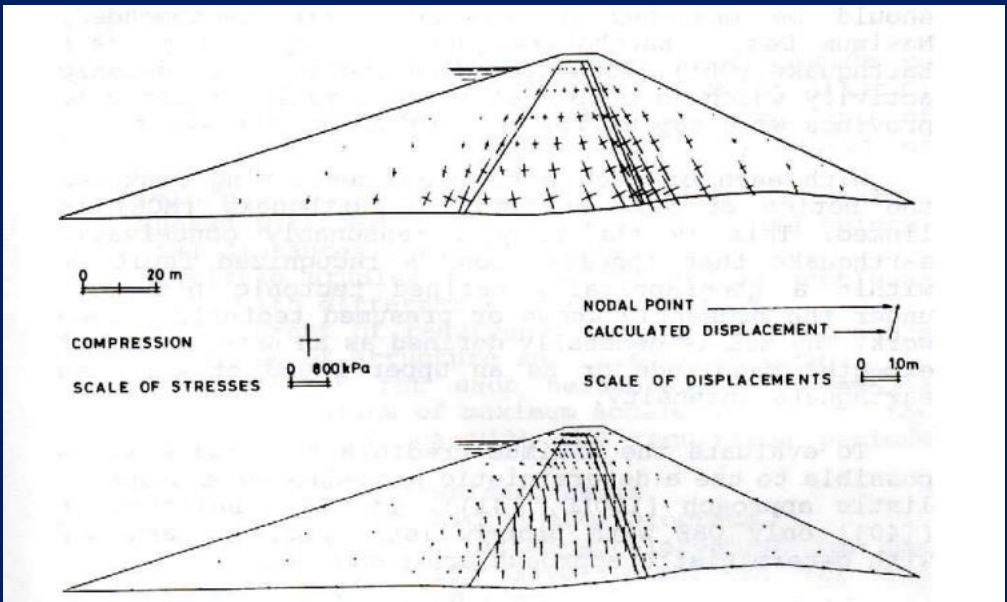

Figure 7.46 distribution of stress and displacements 2 years after the filling of reservoir

Figure 7.47 shows the evolution of pore pressures installed in the core material after the construction stage, reservoir filling stage and long term seep.

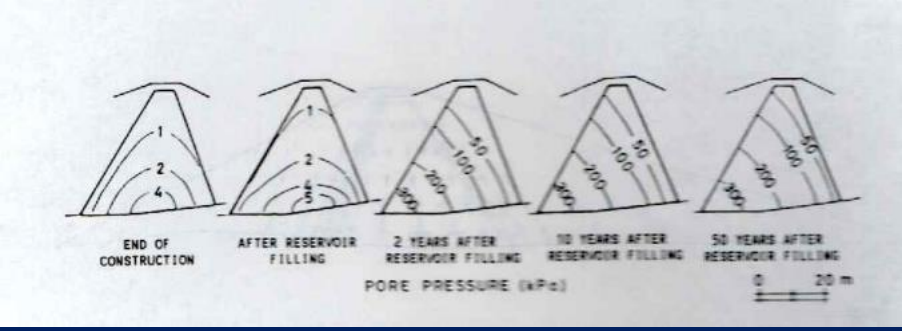

Figure 7.47 Pore pressure during long term

7 6.4. Selection of Design Earthquakes

Introduction

There is no universally accepted terminology for designating the various earthquakes that are used in defining the levels of earthquake motion for which a structure should be designed or evaluated.

Two definitions of earthquake for which the dam should be designed or evaluated are recommended: Maximum Design Earthquake (MOE) and Operating Basis Earthquake (OBE). Both depend on the level of seismic activity which is displayed at each fault or tectonic province with capability of originating the event.

With each of such earthquake generating features the notion of Maximum Credible Earthquake (MCE) is linked. This is the largest reasonably conceivable earthquake that appears along a recognized fault or within a geographically defined tectonic province, under the presently known or presumed tectonic framework. The MCE is generally defined as an upper bound of expected magnitude or as an upper bound of expected earthquake intensity.

To evaluate the Maximum Credible Earthquake it is possible to use a deterministic procedure or a probabilistic approach (ICOLD, 1989). In ICOLD Bulletin 46 (1988) only OBE with probabilistic approach and MCE with deterministic approach are mentioned.

Deterministic Criteria

1 - Definition of the geological conditions and tectonic faults and identification of ground conditions which may affect within 320 km seismic shaking.

2 - Recognition and understanding of the seismotectonics of the dam environs, interpretation of local networks in relation to possible spatial and temporal changes in earthquake activity.

3 - Tentative establishment of a correlation between seismic epicenters and faults.

4 - Definition of a M.C.E. series of earthquakes choosing the most intensives.

5 - Establishment of magnitude recurrence relationships and empirical attenuation relationships to check risk assessments.

6 - With these relationships and the series of M.C.E. earthquakes stablish the worst conditions.

7 - With correlations stablish the highest values of acceleration for M.C.E. earthquakes.

8 - Selection of O.B.E. earthquakes with a maximum acceleration equal or superior 50% of M.C.E. earthquakes.

Probabilistic Criteria

The following stages are considered:

1 - Identification of seismotectonic domains

2 - Definition of attenuation relationships

In general attenuation laws are given by equation:

$$a_m\, x = a_1\, e^{a_2 M}\, R^{a_3} \qquad R = \sqrt{x^2 + h^2 + c^2} \tag{7.36}$$

Where

a_{max}: maximum acceleration (function of magnitude M, epicentral distance x, focal distance h and constant C; a_1, a_2 and a_3 are constants that are functions of focal mechanisms and conditions of propagation of seismic waves.

3 - Determination of acceleration values for earthquakes with magnitudes higher than 4 and epicentral distances lower than 300 km.

4 - Statistic studies to stablish maximum accelerations with different recurrence periods.

5 - Establishment of recurrence periods in accordance with type of structure and life of structure.

6 - Determination for each seismotectonic domains predicted values of maximum accelerations for the site in accordance with the recurrence periods stablished.

7 - Selection of real seismogrammes.

8 - Generation of artificial accelerograms.

9 - Normalization of selected accelerograms for the maximum acceleration level predicted for the adopted recurrence periods.

The statistical studies should be calibrated with deterministic studies.

For the MCE earthquakes probabilistic studies should be done carefully taking into account the geo-technical conditions and the local time acceleration histories.

The generation was done by methodology proposed by Jervis et al. (1977) and consists of: (i) generation of power spectra related with response spectra: (ii) generation of accelerograms based in power spectra by

7.6.4.5 Selection of Soil Properties for Dynamic Analysis

The following properties must be established for each material modeled by the finite element analysis:

1- Total unit weight
2- Maximum shear modulus
3- 3- Variation of maximum shear modulus with effective principal stress
4- Variation off shear modulus with shear strain
5- Variation of damping ratio with shear strain
6- Poisson ratio.

Total unit weights are determined from in situ tests or from laboratory compaction tests.
Maximum shear moduli are obtained by geophysical tests or reasonant column tests.
The variation of shear modulus G and damping ratio with shear strain can be derived by laboratory tests for different techniques are shown in Figure 7.48.
The maximum shear moduli may be obtained by geophysical tests or resonant column tests or by equations proposed by several authors.
Seismic tests to measure compression and shear tests were performed 5 years after the filling of Beliche dam (Sêco e Pinto, 1993)
The dam is 550 m long and 55m high.

LABORATORY TECHNIQUES FOR MEASURING DYNAMIC SOIL PROPERTIES

	Shear Modulus	Young's Modulus	Material Damping	Cyclic Stress Behaviour	Attenuation
Resonant Column	x	x	x		
With adaptation					x
Ultrasonic pulse	x	x			x
Cyclic Triaxial		x	x	x	
Cyclic Simple Shear	x		x	x	
Cyclic Torsional Shear	x			x	
Shake Table	x			x	

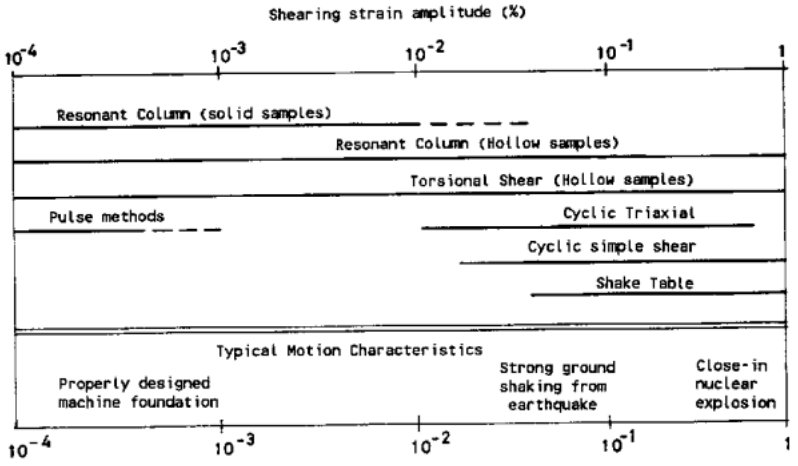

Figure 7.48 Laboratory techniques for measuring dynamic soil properties

.

The cross section is shown in Figure 7.49, as well the two holes with 20 m depth.
The position of the holes was determined by an inclinometer.
Both techniques downhole and crosshole were used for the determination of compression and shear waves, but the latter was more successful.
The obtained by crosshole technique is shown in Table 7.13.
Some details related the energy sources and the recording equipment are shown in Figures 7.50 to Figure 7.52.
Figure 7.53 represents the recorded S waves for 11m depth.

To analyse the seepage and time effects on wave velocities similar tests were also performed 35 years after Maranhão dam operation (Sêco e Pinto and Portugal, 1991).
The dam is 205 m long and 55 m high. The dam cross section is shown in Figure 7. 54 and the obtained results are shown in Table 7.14.

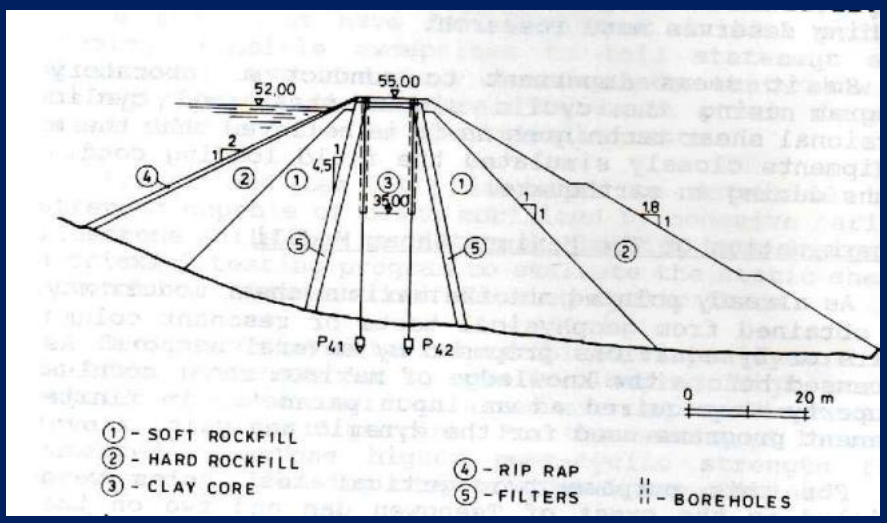

Figure 7.49 Cross section Beliche dam

Table 7.13 Beliche dam -summary of cross hole tests results

Depth	Distance (m)	Time (ms)		Propagation Velocities (m/s)		ν_{din}	G_{din} (MPa)	E_{din} (MPa)
		P wave	S wave	P wave	S wave			
3.00	6.82	---	20.0	900	341	0.42	250	709
5.00	6.78	7.4	19.0	916	357	0.41	274	771
7.00	6.72	8.3	18.5	809	363	0.37	283	775
9.00	6.66	8.6	17.0	774	392	0.33	330	878
11.00	6.62	7.3	16.5	907	401	0.38	345	953
13.00	6.59	6.4	16.0	1030	412	0.40	364	1020
15.00	6.55	6.1	16.0	1074	409	0.42	359	1020
17.00	6.49	7.0	15.0	927	432	0.36	401	1090
19.00	6.44	6.2	16.0	1039	403	0.41	349	983

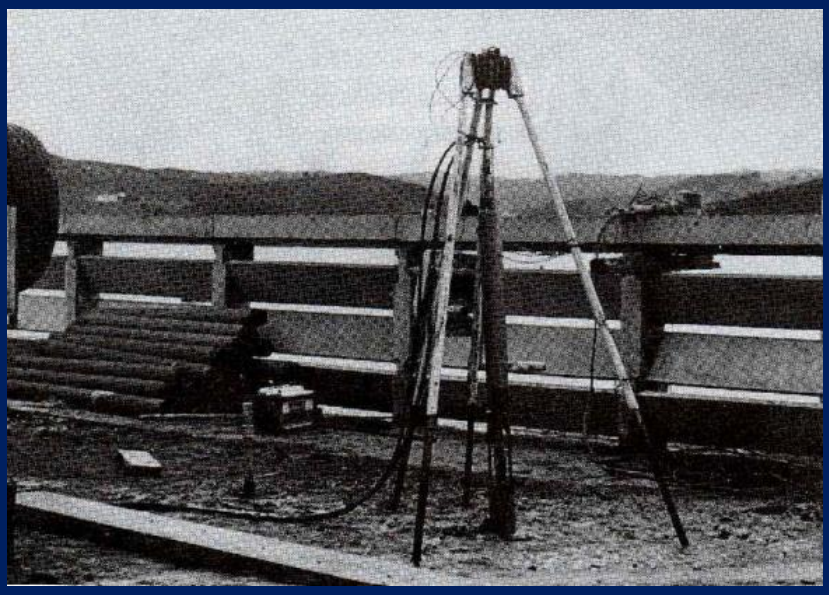

Figure 7.50 Shear wave hammer used in crosshole test

Figure 7.51 Impact device used in downhole technique

Figure 7.52 Recording system

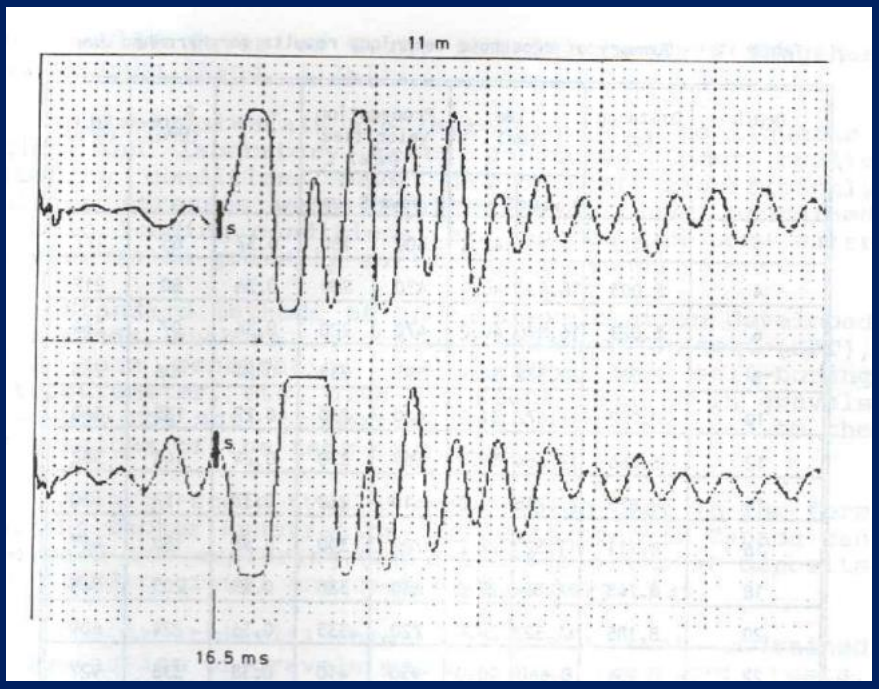

Figure 7.53 S waves recorded values at 11m depth

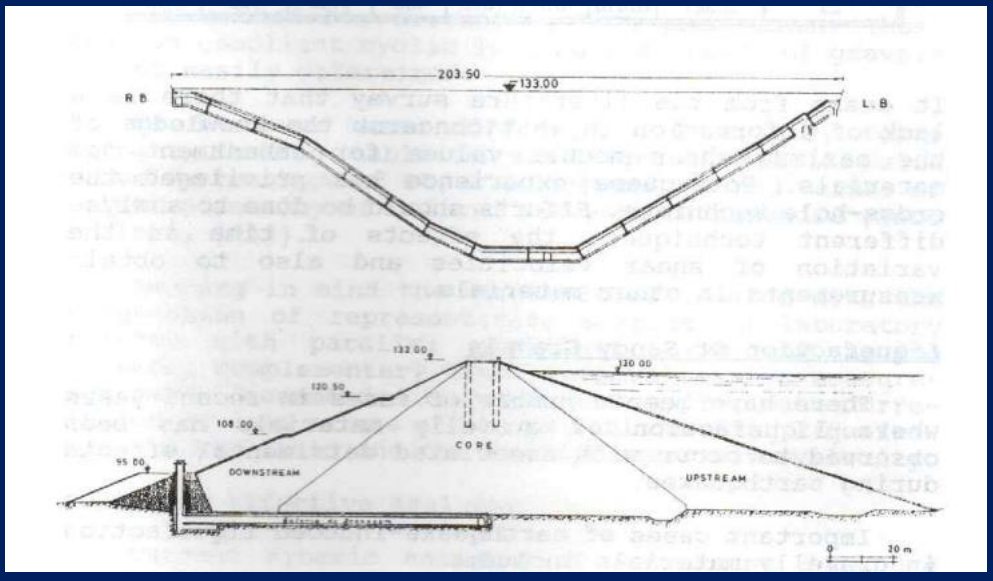

Figure 7.54 Location of boreholes in Maranhão dam

Table 7.14 Summary of crosshole technique results for Maranhao dam

Depth	Distance (m)	Time (ms)	Propagation Velocities	n_{din}	G_{din} (MPa)	E_{din} (MPa)

				(m/s)				
		P wave	S wave	P wave	S wave			
2	7.977	19.942	42.2	400	180	0.37	65	177
4	8.003	18.432	40.4	430	200	0.36	80	217
6	8.023	16.896	40.0	470	220	0.36	97	264
8	8.037	20.362	34.4	395	230	0.24	106	263
10	8.052	17.472	31.2	460	260	0.27	135	343
12	8.066	17.664	30.0	460	270	0.24	146	362
14	8.078	13.248	28.8	610	280	0.37	157	430
16	8.111	11.520	27.2	700	300	0.38	180	497
18	8.148	12.864	25.6	630	320	0.33	205	545
20	8.185	11.328	24.4	720	335	0.36	224	609
22	8.234	8.640	20.0	950	410	0.38	336	927
24	8.290	9.216	18.0	900	460	0.32	423	1116
25	8.321	8.016	18.0	1040	460	0.38	423	1167

7.6.4.5 Deformation Evaluation and Seismic Stability

For the comparison of the earthquake-induced stress conditions and the laboratory data there are two ways:

(i) Determine the irregular non-uniform cyclic stress pattern induced by the earthquake and submit test samples exactly to the same pattern.

However, this procedure has the following limitations:
-if more than one possible earthaquake motion is required multiple series of tests are needed;
- if the design earthquake is changed after the test programme new data are necessary;
-testing equipment to apply programmed stress patterns with special time histories is considerably expensive

(ii) Convert the irregular series of earthquake-induced cyclic stress to an equivalent series of uniform stress cycles to be compared directly with laboratory tests data.

The irregular shear stress-time history can be represented by an equivalent number of uniform cycles (ENUC) as shown in Figure 7.57.

The conversation from the irregular shear stress time history to its uniform equivalent is made by means of a weighting curve as proposed in Figure 7.58.

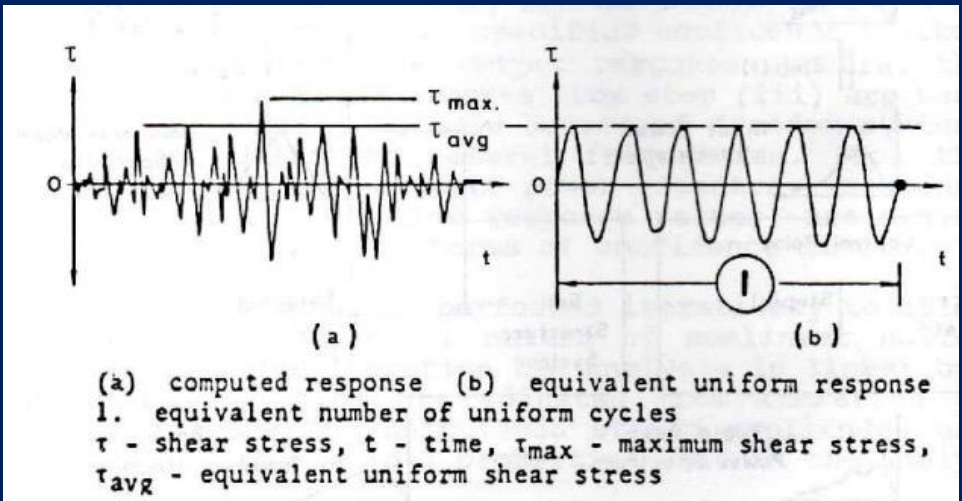

Figure 7.57 Computed and equivalent element shear stress histories

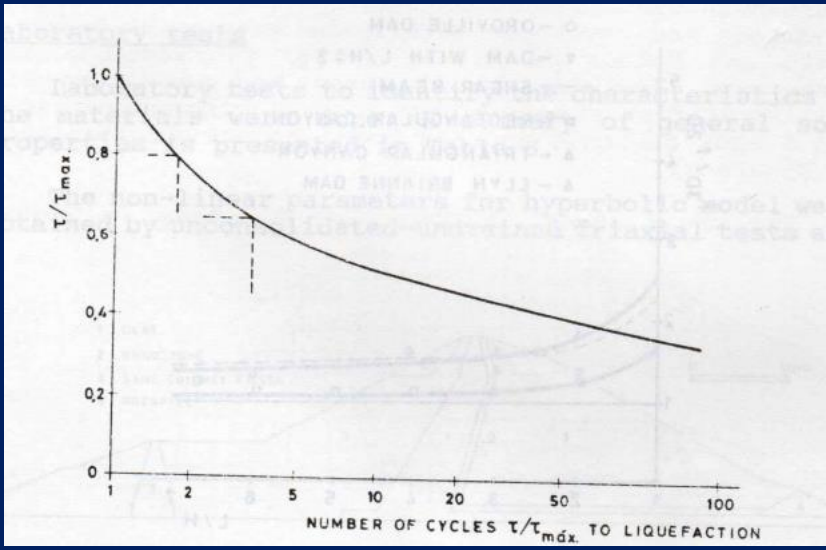

Figure 7.58 Proposed standard weighting curve

Deformation Analysis

For the analysis of seismic induced deformations different methods were used:
Seed et al (1975) proposed to assess dam deformation at the top, the product of the average shear strain to the height of the section.
Lee proposed an approach by a finite element analysis using a nonlinear stress-strain for the soil

The approaches have given reasonable agreement with the measured displacements.

Example of application is shown for Las Cuevas dam (see Case History nº 9).

7.6.5 Computer Programs

Total stress models

Several finite element computer programs assuming an equivalent linear model in total stress have been developed for 1D –SHAKE code (Schanabel et. al., 1972), QUAD 4(Idriss et al.1972), 2D –LUSH code (Idriss et. al., 1973; Lysmer et al., 1974) and pseudo 3D TLUSH code (Lysmer et al., 1975).
All these programs treat nonlinear behavior by iterative linear elastic procedures.
The equation of motion is solved in the frequency domain.

Since these models are essentially elastic the permanent deformations cannot be computed by this type of analysis and are estimated from static and seismic stresses with the aid of strain data from laboratory tests (cyclic triaxial tests or cyclic simple shear tests) (Sêco e Pinto, 1993).
For embankment dams a value of 5% axial strain is used as allowable deformation.

Effective stress models

To overcome these limitations, nonlinear hysteretic models with pore water pressure generation and dissipation have been developed using incremental elastic or plasticity theory.
The nonlinear models can be divided in two categories: incremental elastic model and models using plasticity theory.

The incremental elastic models have assumed a nonlinear and hysteretic behaviour for soil and the unloading-reloading has been modelled using the Masing criterion and incorporate the effect of both transient and residual pore-water pressures generated by seismic loading implemented in TARA 3 and DESRA codes (Lee and Finn, 1978; Finn, 1987) (see Figure 7.59).

For the models based on the theory of plasticity two particular formulations appear to have a great potential for multidimensional analysis: the multi-yield surface model implemented in DYNAFLOW code (Prevost, 1993) and the two-surface model (Mröz et al., 1979).

A modified cam-clay model for cyclic loading taking into account that when saturated clay is unloaded and then reloaded the permanent strains occur earlier than predicted by the cam-clay model was proposed by Carter et al. (1982). The predictions exhibit many of the same trends that have been observed in laboratory tests involving the repeated loading of saturated clays.

For the definition of the constitutive laws the following laboratory tests are used for embankment dams: resonant column tests, cyclic simple shear tests, cyclic triaxial tests and cyclic torsional shear tests.

Figure 7.60 illustrates the Flowchart

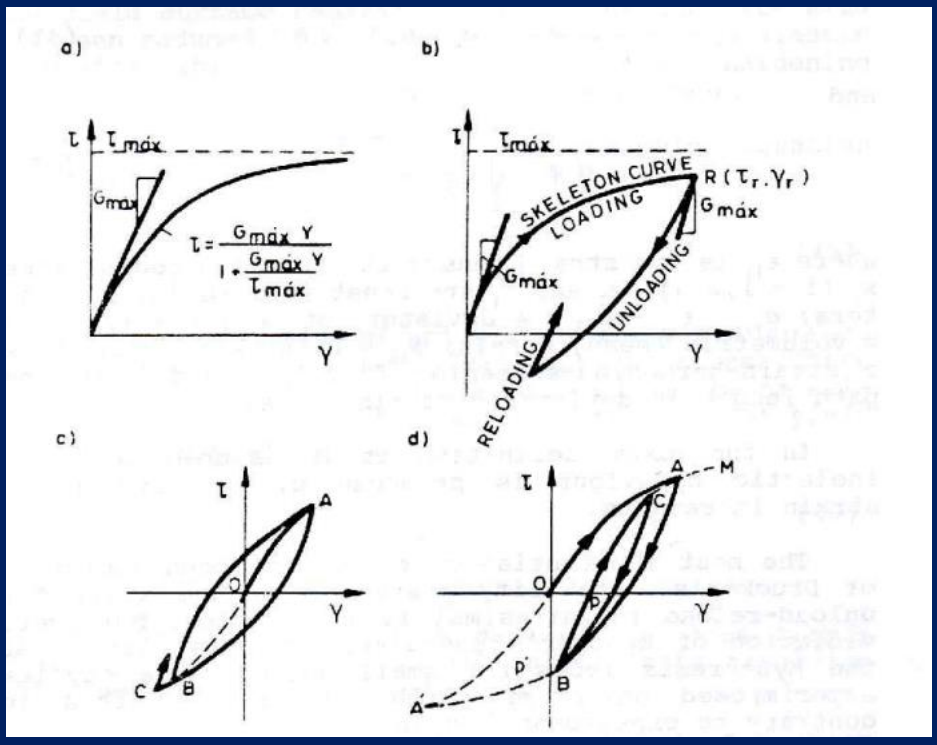

Figure 7.59 (a) Initial loading curve, (b) Masing stress-strain curves for unloading and reloading (after Finn,1985)

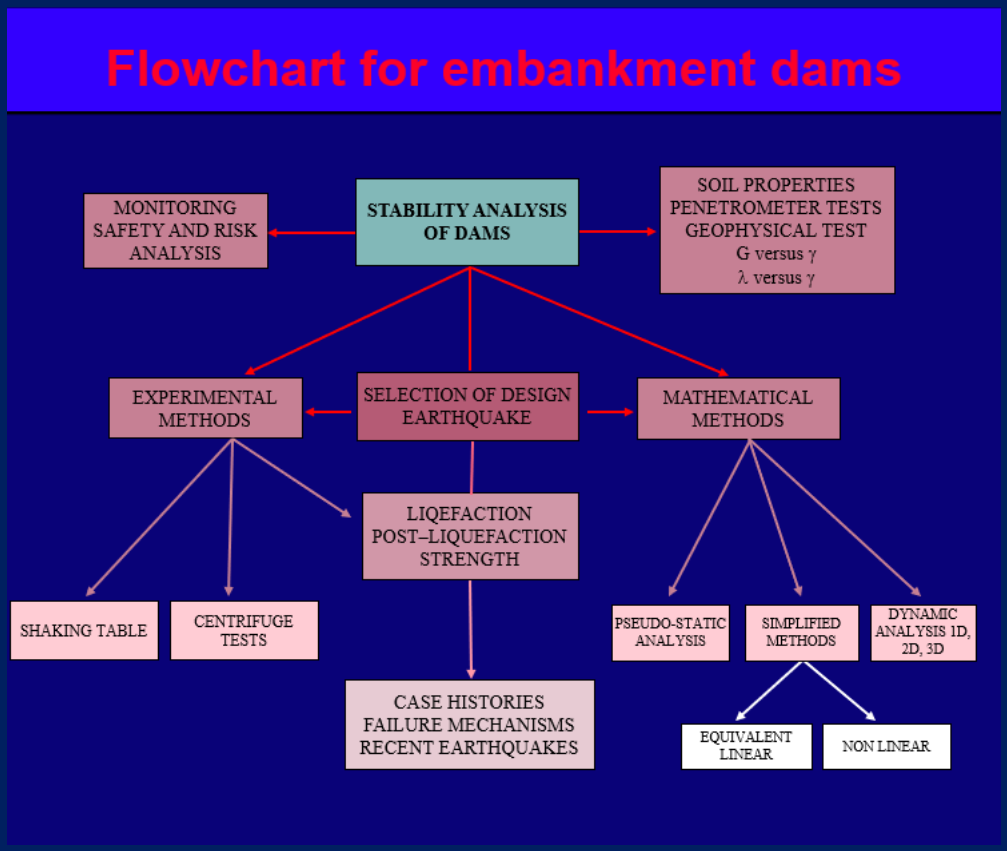

Figure 7.60 Flowchart

7.6.6. Verification and Validation of Models

The need of model and code validation is getting increased attention.

Sargent (1990) has introduced the concepts of verification and validation and the relations established between the three entities: the physical problem; the conceptual model; and the computer model and its numerical implementation are illustrated in Figure 7.61.

Verification intends to ensure that the computer program is correct and it represents faithfully the conceptual model and validation applies essentially to the conceptual model, and its ability to reproduce satisfactorily the physical phenomena.

A slightly different terminology is adopted by ICOLD (1994a) that considers that the numerical modeling process for dams should be checked in order to avoid unreliable results considering the following aspects:

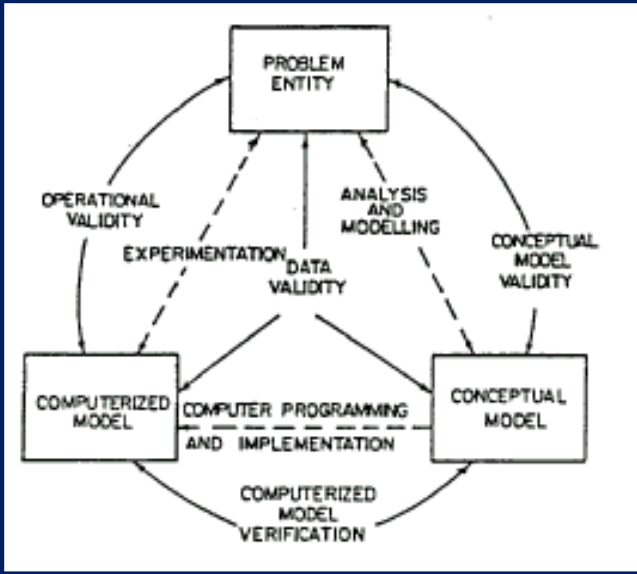

Figure 7.61 Relations between physical problem, conceptual model and computer model (after Sargent, 1990)

i) justification of the whole modeling method (the relevance to physical reality);
ii) validation of the computer code;
iii)quality assurance of the whole computation process.

7.6.7 Future Developments

7.6.7.1 Nonlinear Effective Analyses

Current dynamic analyses of embankment dams use total stresses and treat nonlinear behaviour by iterative linear-elastic procedures. These analyses do not require prohibitively time computer costs and are valid when pore water pressures do not exceed 30% of the effective overburden pressure. As they can not provide information on permanent displacements and deformations, since they are elastic methods, strong interest has developed in nonlinear effective stress methods.

In the nonlinear analysis the soil moduli and damping ratios are updated at several points along the time axis, in contrast with the single after-the-analysis updating of the equivalent linear scheme.

These methods can be divided in two categories, those based on nonlinear hysteretic stress-dependent stress-strain relations and those based on the concept of an elastoplastic constitutive equation based on multi-surface kinematic plasticity theory.

A pore water pressure generation and dissipation model can be coupled with the nonlinear equations of motion.

Nevertheless, the high values of time computer costs of nonlinear effective analyses they provide a very clear overall picture of the dam response to the design earthquake as well as helping the designer with all the details necessary in zones of potential concern.

More gained experience of application of these models is necessary and for their calibration centrifuge models seem very useful.

7.6.7.2 Foundation effect

In most dynamic analyses of dams, the bedrock below the dam is considered rigid, although the earthquake motion is due to travelling seismic waves propagation. In a study of the response of earth dams to travelling seismic waves, Dibaj and Penzien (1969) showed that if the ratio of base width of the dam to the shear wave velocity in the bedrock is less than 0.2 seconds, i.e.

$$\frac{B}{v_s} _ 0.2 \text{ seconds} \qquad (7.37)$$

then the dynamic response of dam to travelling wave will be similar to the response to rigid base motions.

The major difficulty that arises in defining the earthquake input is that the structure interacts with the support medium in its dynamic response; thus, the base motion history with the structure in place is not the same as the "free-field" motion that would have occurred had the structure not been built up.

The formulation of dynamic foundation-structure interaction of a two-dimensional dam idealization may be carried out conveniently by treating the system as two substructures. With this concept the dam may be idealized by the finite element methods. Thus, taking advantage of its ability to handle systems of arbitrary geometry. At the same time the foundation rock may be treated as an elastic half-space, an approach, which is ideally suited to its simplified boundary conditions and semi-infinite extent, and which is computationally more efficient than a finite element idealization (Clough and Zienkiewicz, 1975).

7.6.7.3 Coupled models

The coupled vibration of the dam-foundation and the reservoir systems can be mathematically solved by: (i) the Navier equations for the dam-foundation system in terms of displacements, boundary conditions being prescribed values of displacements (and its derivatives with respect to time) on part of the boundary surface, and values of the dynamic water pressures on the interface between both systems, and (ii) by the equations of propagation of pressure waves in water in terms of dynamic pressures boundary conditions being prescribed values of pressures (and its derivates) on the boundary surface, and values of normal components of the acceleration on the interface between both systems.

Discretization of the above equations yields a system of equations which may be written

$$\begin{bmatrix} \overline{M} & \rho G^T \\ 0 & M \end{bmatrix} \begin{Bmatrix} \ddot{P} \\ \ddot{u} \end{Bmatrix} + \begin{bmatrix} \overline{C} & 0 \\ 0 & C \end{bmatrix} \begin{Bmatrix} \dot{P} \\ \dot{u} \end{Bmatrix} + \begin{bmatrix} \overline{K} & 0 \\ -G & K \end{bmatrix} \begin{Bmatrix} P \\ u \end{Bmatrix} = \begin{Bmatrix} \overline{F} \\ F \end{Bmatrix} \quad (7.38)$$

where M, C and K are the mass, the damping and the stiffness matrices of the dam-foundation system, and M , C, and K are the corresponding matrices of the reservoir system: ü,u and u represent accelerations, velocities and displacements at nodal points, and P ,P and P represent dynamic water pressures and their time derivatives at nodal points; G is an iteration matrix, relating water pressures and forces on the interface between dam-foundation and the reservoir systems; F and F are applied forces and r is the unit specific mass of water.

The coupled problem dam-foundation-reservoir requires prohibitive computational effort for practical problems.

The more effective approach is to treat the dam-water system as composed of two substructures-dam and fluid domain-coupled through the interaction forces and appropriate continuity conditions at the face of the dam.

The dam and foundation region are considered as two substructures of the complete system. The dam may be idealized as a finite element system which has the ability to represent arbitrary geometry and material properties. The foundation rock or soil region may be idealized as a viscoelastic half space.

The dam -reservoir interaction can be analysed by the Westaergaard method combined with the Galerkin method.

A hypothetical example of a concrete face rockfill dam with 100m high is illustrated in Figure 7.62.

The finite element mesh is shown in Figure 7.63.

The construction stage was simulated in 7 layers and the reservoir filling in six steps.

The non linear parameters for hyperbolic model were considered in Table 7.14.

The characteristics of design earthquakes are summarized in Table 7. 15.

The shear stress distribution at the end of reservoir filling is presented in Figure 7. 64.

A parametric study was done exploring the following parameters: (i) effect of the upstream concrete face;(ii) interaction of the reservoir;(iii) effect of the vertical component. The main results are presented in Table 7.16.

The shear stress time histories for three selected elements located at upstream face (see Figure 7. 63) are shown in Figure 7.65.

The maximum acceleration response in both horizontal and vertical directions for selected points located at the upstream face (see Figure 7.63) are presented in Figure 7.66.

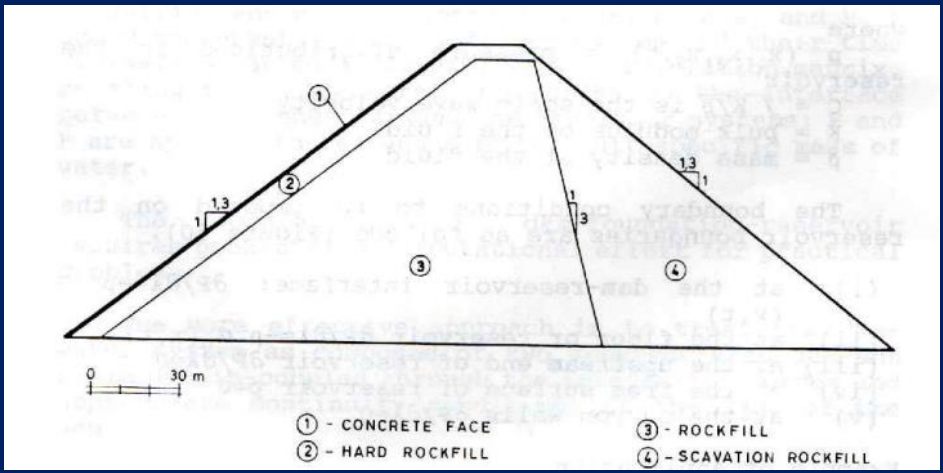

Figure 7.62 Concrete face rockfill dam section

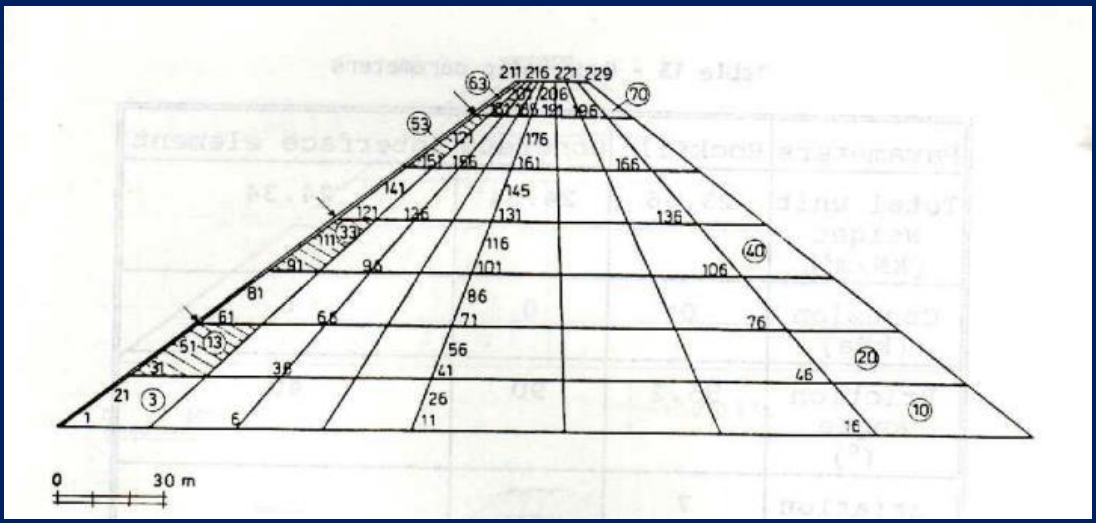

Figure 7.63 Finite element mesh

Table 7.14 Hyperbolic parameters

Soil type Parameter	Symbol	Clay Core	Shell material		Filter	Rockfill	
			Dry	Wet		Dry	Wet
Cohesion (kPa)	C	250	110	30	0.0	0	0
Friction angle at σ_3 = 1 atm (degrees)	ϕ	20,5	35	35	51.0	51.0	49.0
Reduction in ϕ per log cycle (degrees)	$\Delta\phi$	0	0	0	0.0	5.0	6.0
Modulus number	K	840	770	468	690	720	670
Unloading-Reloading Modulus No.	Kur	4200	3900	1404	2070	3600	3350
Failure Ratio	R_f	0.78	0.725	0.772	0.590	0.63	0.62
Modulus Exponent	n	0.17	0.441	0.668	0.450	0.55	0.49
Poisson´s Ratio Parameters	G	0.36	0.43	0.47	0.14	0.40	0.3
	F	0.16	0.15	0.23	0.10	0.14	0.12
	d	9.20	9.80	13.80	27.30	1.01	0.94
Threshold Confin. pressure (kPa)	σ_{3t}	---	350	---	---	---	---
Coef. of Isotropic collap. (kPa^{-1})	ß	---	$2.25x10^6$	---	---	---	---

Total unit weight (kN/m^3)	23.56	24.34	24.34
Cohesion (kPa)	0	0	0
Friction angle (°)	55.2	90	40
Variation of friction angle	7	___	___
Failure ratio	0.58	0.76	0.58
Modulus number	1700	280700	900
Unloading and reloading modulus	7000	280700	5000
Modulus	0.31	0.31	0.31
Poisson's ratio parameter (G)	0.5	0.2	0
Poisson's ratio parameter (F)	0.2	0	0
Poisson's ratio parameter (d)	13.1	0	___

Table 7.15 Design earthquakes characteristics

Characteristics	Near source
Period of life (years)	100
Probability of exceeding the ground acceleration (gal)	10
Ground acceleration (gal)	406
Duration of earthquakes	21

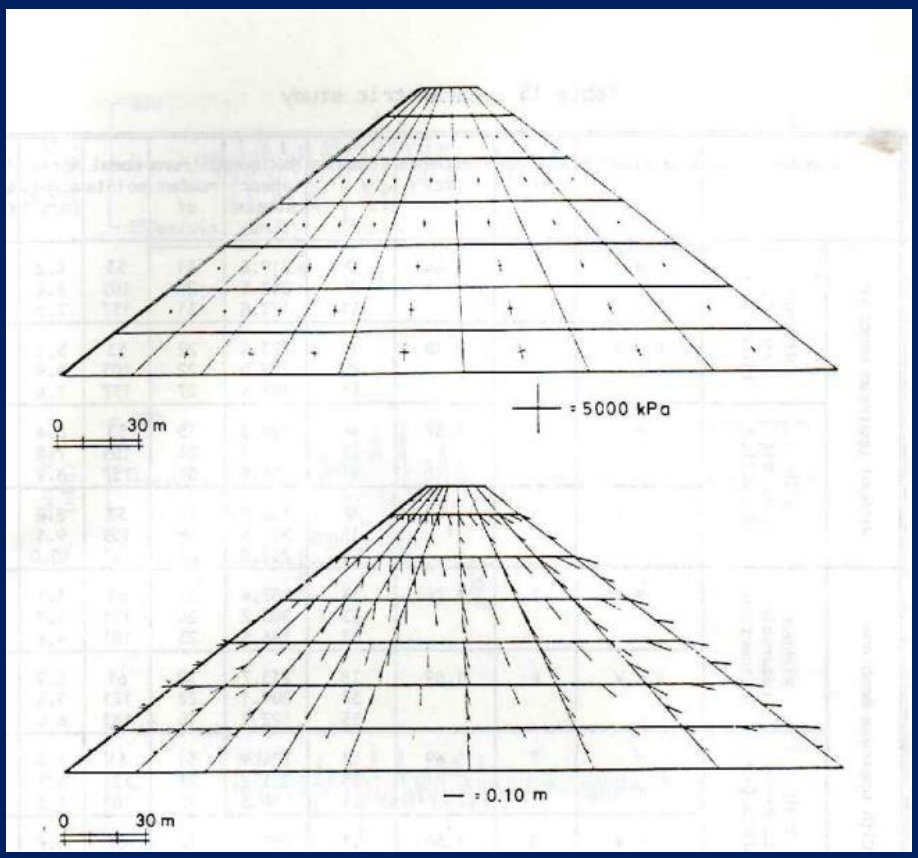

Figure 7.64 Stress distribution

Table 7.16 Parametric study

Examples		Acceleration	Analyse nº	Frequence (Hz)	Elements	Maximum shear stress (kPa)	Uniform number of cycles	Nodal points	Horiz. accel. (m/s^2)	Vert. accel. (m/s^2)
Without upstream membrane	Without reservoir interaction	H	1	1.64	9	219.8	31	53	4.2	0.44
					25	252.5	29	105	4.4	1.8
					41	173.8	31	157	7.2	4.6
		H + V	2	1.58	9	273.4	22	53	5.1	3.1
					25	278.8	22	105	5.9	6.0
					41	192.4	27	157	7.4	8.6
	With reservoir interaction	H	3	1.57	9	328.3	15	53	8.4	0.76
					25	299.7	24	105	7.8	2.0
					41	206.8	31	157	8.9	5.2
		H + V	4	1.52	9	363.0	14	53	8.6	3.2
					25	331.6	18	105	9.1	9.1
					41	242.8	21	157	10.0	10.0
With upstream membrane	Without reservoir interaction	H	5	1.74	13	187.4	39	61	1.1	1.1
					33	203.7	24	121	1.7	1.7
					53	106.5	23	181	4.6	4.6
		H + V	6	1.69	13	213.7	32	61	2.9	2.9
					33	209.1	22	121	5.4	5.4
					53	122.5	15	181	6.0	8.0
	With reservoir interaction	H	7	1.69	13	224.9	31	61	6.3	1.5
					33	221.3	23	121	6.1	2.4
					53	114.3	15	181	7.3	5.4
		H + V	8	1.64	13	259.2	22	61	6.7	2.7
					33	220.3	26	121	7.8	7.5
					53	142.1	12	181	7.5	9.1

H - horizontal acceleration V - vertical acceleration

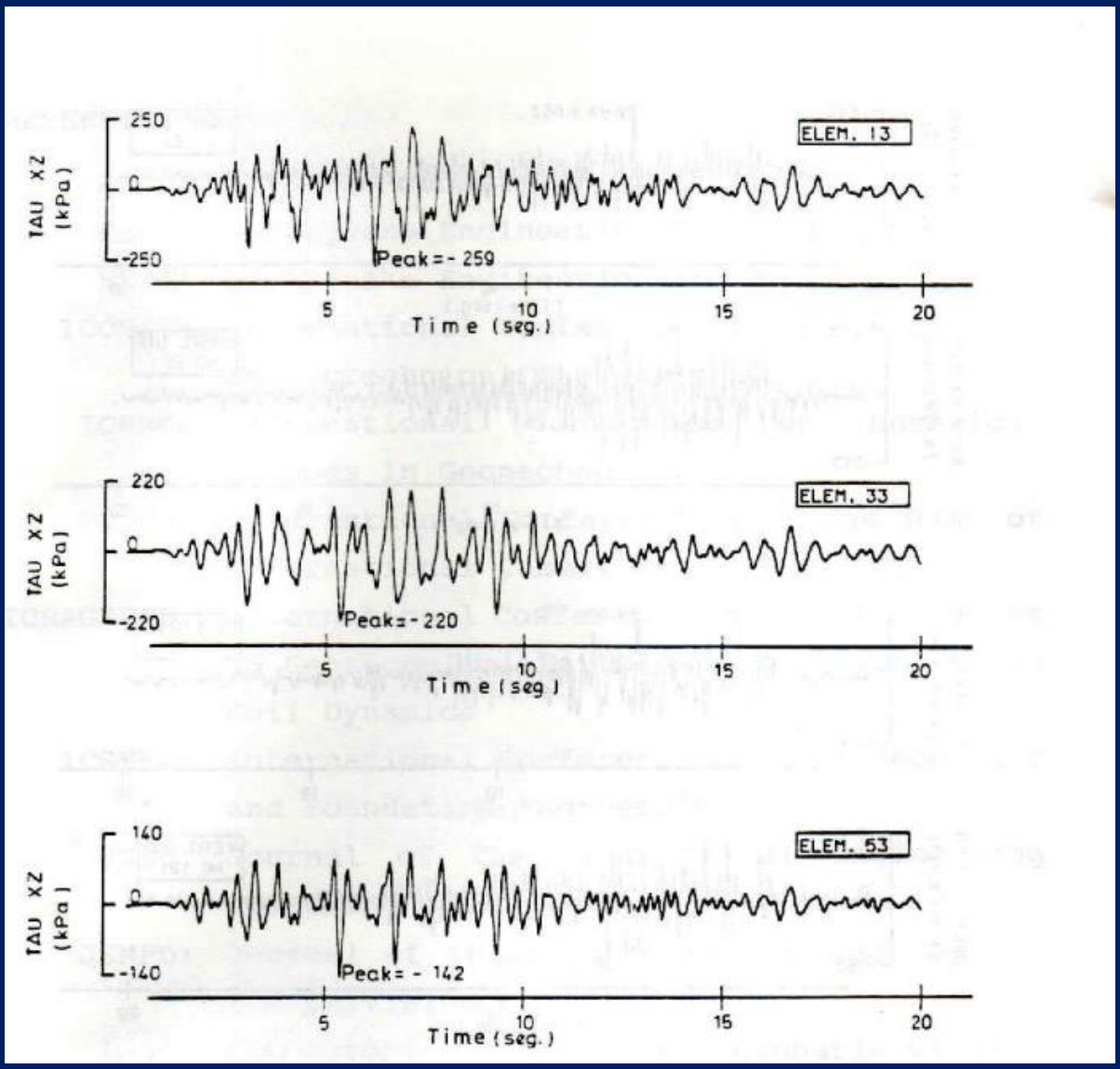

Figure 7.65 Shear stress -time history for finite elements n 13,33 and 53

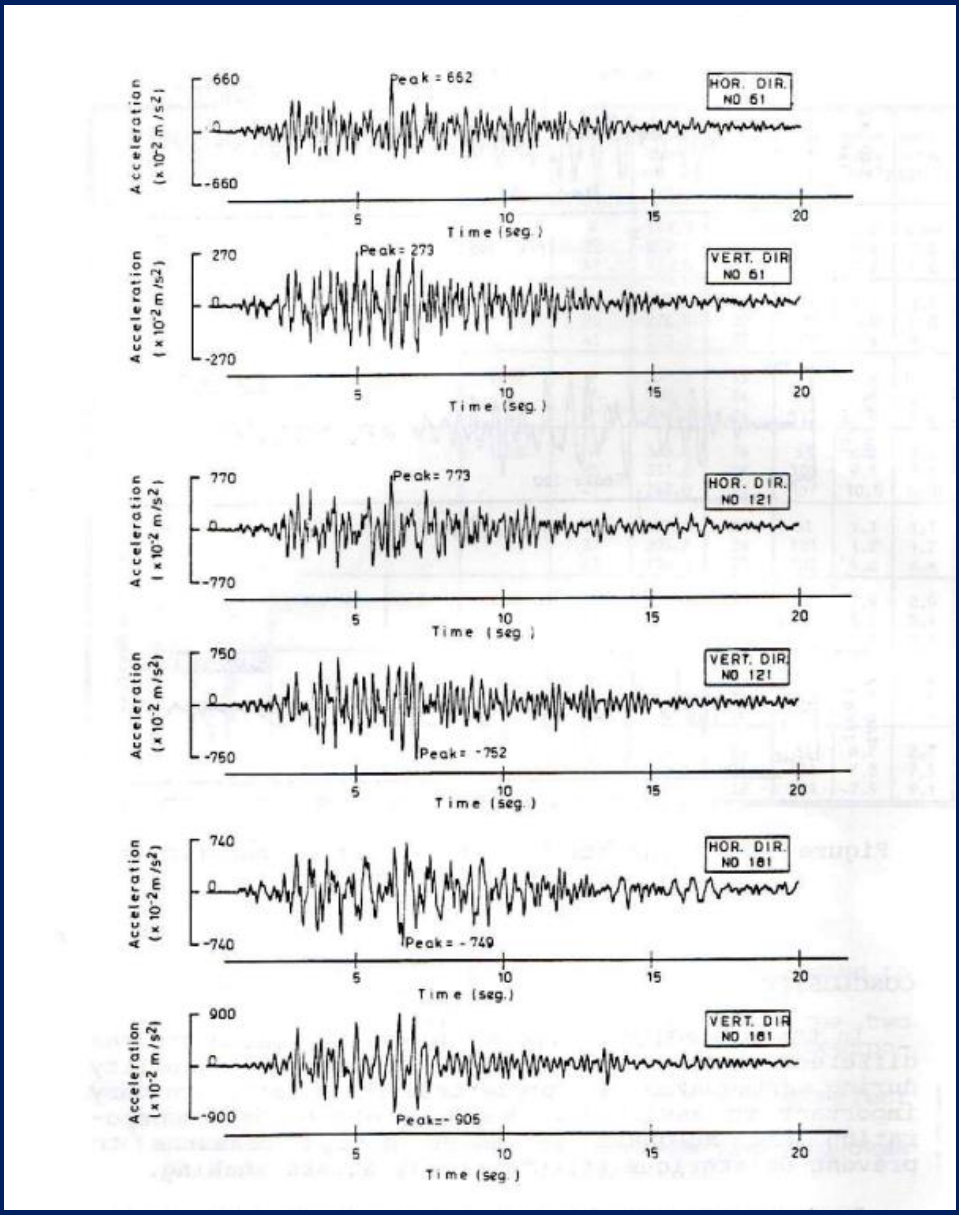

Figure 7.66 Horizontal and vertical accelerations for nodal accelerations for nodal points nº 61, 121 and 181

7.7 Safety of Dams

7.7.1 Introduction

The monitoring and inspections of dams are addressed, the visual inspections are analysed, the monitoring and safety evaluation are discussed, the dam monitoring plan and the risk potential assessment are presented.

Figure 7.36 Monitoring

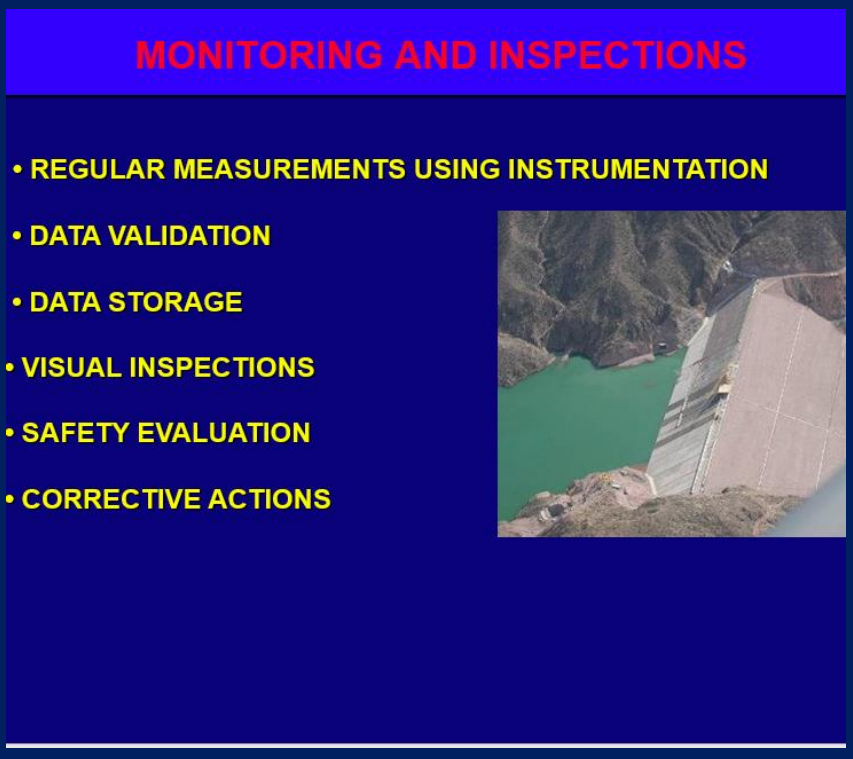

Figure 7.67 Monitoring and inspections

Figure 7.68 Visual inspections

7.7.2 Monitoring and Safety Evaluation

7.7.2.1 Introduction

Safety control is the group of measures taken in order to have an up-to-date knowledge of the condition of the dam and to detect in due time the occurrence of any anomalies to define actions to correct the situation or, at least, to avoid serious consequences.

New systems to deal with automatic data acquisition, very flexible, that allows users to perform treatment of the information integrating tests and analysis, behavior models, visual inspections, documents data by any computer connect with Internet visualization were developed.

The safety control of a dam involves the construction phase and the first filling of water and the long term.

Experience has shown that the rational and systematic control of dam safety should consist of several tasks:

frequent visual inspection by staff in charge of the observation system;

periodic visual inspection by specialist;

regular instrumentation measurements;

data validation;

- data storage;
- visual inspections;
- safety evaluation;
- corrective actions

7.7.2.2 DAM MONITORING PLAN

Dam behaviour during construction and operation is monitored to make it possible to check methods, results of analyses and model tests in order to analyse the dam performance and the dam safety against deterioration of failure (ICOLD, 1981).

Dam potential risk for monitoring proposes

The potential risk associated with dams depends on its storage capacity, height of the dam, potential downstream damage and evacuation requirements (ICOLD, 1989). These risk factors are separately weighted as low, moderate, high and extreme.

The detailed definition of the monitoring scheme cannot be made on the solid basis of the features of the dam, because many external factors are to be taken into account when safety problems are considered.

Usually, the risk factors are classified in three classes, which are referred respectively to actions, to the structure itself or to values affected by hazards. The arithmetic average of all indices falling in a given class forms an overall risk factor for the class. In this way we define, respectively:

- an environmental factor ***E***;
- a reliability factor ***F***;
- a potential human/economic hazard factor ***R***.

Lastly a global risk index a_g, is developed by taking the product of the three partially factors ***E***, ***F***, ***R***, (ICOLD, 1981).

Following the Table 7.17 for the definition of the Global Risk Index, we find for the Mapai Dam these estimated values:

E = (2+2+3+3+3)/5 = 2.6

F = (3+3+1+3)/4 = 2.5

R = (5+3)/2 = 4

a_g = 26 (Global Risk Index)

TABLE 7.17 PROPOSED RISK CONDITIONS EVALUATION (ICOLD, 1981)

External, or Environmental, Conditions (Factor E)					Dam Condition / Reliability (Factor F)				Human / Economic Pote
Seismicity	**Danger of reservoir bank slides**	**Danger of floods higher than design floods**	**Reserv. Func. (type of storage, management)**	**Aggressive environment actions (climate, water)**	**Structural proportioning**	**Foundations**	**Flood outlet equipment**	**Maintenance conditions**	**Reservoir storage volume (m^3)**
(1)	**(2)**	**(3)**	**(4)**	**(5)**	**(6)**	**(7)**	**(8)**	**(9)**	**(10)**
inimal or null V < 4 cms^{-1})	Minimal or null	Very low probability (concrete dams)	Pluriannual, annual or seasonal storage	Very weak	Adequate	Very Good	**Reliable**	Very Good	< 10^5
Low < V < 8 cms^{-1})	**Low**	---	---	Weak	---	Good		Good	10^5 - 10^6
Middle < V < 16 cms^{-1})		**Very low probability (landfill dams)**	**Weekly storage**	**Middle**	**Acceptable**	**Acceptable**		**Satisfactory**	10^6 - 10^7
Strong < V < 32 cms^{-1})			Daily storage	Strong					10^7 - 10^9
Very strong V > 32 cms^{-1})			Pumped Storage	Very Strong		Poor			> 10^9
	Danger of big slides	High Probability			Inadequate	Poor or bad	Insufficient not operational	Unsatisfactory	

(a) Abnormal conditions; technically unavailable intervention

$$E = \frac{1}{5}\sum_{i=1}^{5} \alpha_i \; F = \frac{1}{4}\sum_{i=6}^{9} \alpha_i \; R = \frac{1}{2}\sum_{i=10}^{11} \alpha_i$$

Global index: α_g = E x F x R.

7.7.2.3 Types of measuring devices

Instruments for dam behaviour monitoring should have the following characteristics: (i) sufficient accuracy; (ii) long-term reliability; (iii) low maintenance requirements; (iv) compatibility with construction techniques; (v) low cost; and (vi) simplicity.

For Mapai dam and following the Table , it seems adequate to install: surface movement measuring devices; vertical internal measurements devices; horizontal internal measurement devices; pore water pressures; total pressure cells; seismographs; vertical pendulums (plumb lines); extensometers; joint devices; piezometers; temperature transducers; seepage devices and water levels.

TABLE 7.18 PROPOSED MONITORING INSTALLATIONS AND SURVEILLANCE SCHEME (LANDFILL DAMS) (ICOLD, 1981)

	Type A		Type B			Type C				Others		
Dam height (m)	**Simple visual inspection**	**Seepage discharge (including turbidity)**	**Piezometric measurements**	**Surface displacements**	**Meteorology**	**Internal displacements**	**Total stresses**	**Pore pressures (quick response)**	**Strain measurements**	**Seismological**	**Automatic recording**	**Alarm**
(1)	**(2)**	**(3)**	**(4)**	**(5)**	**(6)**	**(7)**	**(8)**	**(9)**	**(10)**	**(11)**	**(12)**	**(13)**
< 15	X	X Total discharge If α_g > 10 or R ≥ 1	X If α_g > 10 or R ≥ 1	X If α_g > 15 or R > 3						X If α_g > 9 with α_i = 5		
15 to 30	X	X Total discharge	X	X If α_g > 10 or R ≥ 3	(X)	X If α_g > 20		X If α_i = 5		X If α_i = 5	(X) If α_g > 20	(X) If α_g > 25 or α_i > 3
30 to 50	X	X Partial discharge If R ≥ 1	X	X	X If R ≥ 3	X If α_g > 10 or R > 3	(X)	X If α_i ≥ 4		X If α_i ≥ 4	(X)	(X)
50 to 100	**X**	**X Partial discharge**	**X**	**X**	**X**	**X**	**X**	**X**	**X If Global Index α_g > 10 or Factor R > 3**	**X If any numerical index, α_i ≥ 3**	**(X)**	**(X)**
> 100	X	X Partial discharge	X	X	X	X	X	X	X	X	(X)	(X)

X – Installation must be present; (X) – Installation is optional

NOTE: Tables are presented exclusively as guidelines

7.7.2.4 Data Acquisition

An automatic system with teletransmission in comparison with manual readings allows a rapid data processing of a great number of instruments.

Once in operation an automatic system allows a reduction of personal, both in the field and office.

The automatic system and the central data processing allow a quicker updating of the information.

An automatic system implies an increase of complexity, with the electronic equipment to be installed in unfavorable environment of temperature and humidity. A fully automatic system can be destroyed by an event such as an earthquake, or an exceptionally large flood.

7.7.2.5 Data Management

Regarding the data acquisition and processing the software includes the following features (ICOLD, 2000):
- collection of data for some time intervals;
- collection of data for some particular events such as asynchronous transmission of data by a peripheral, using a flag for seismic events or other exceptional conditions;
- collection of data sets following the request of the system operator;
- manual of measurements performed by resident personnel;
- check of data in order to assess the reliability of the measured values, and the malfunction of the instruments;
- data storage and periodic back-up of record files;
- periodic display and print of data and other results of the data processing, following the request of the operator;
- management of anomalies, related with overcoming of allowable limits and the use of alarm signals;
- possibility of communication with remote units;
- display of the measurement points location;
- easy access to the data reduction equations and other logic programs and sets of specific instrument constants.

7.7.2.6 Data Validation and Subsequent Actions

Preliminary check on the raw values (following the execution of function tests on measurement equipment) by comparing the actual values from the sensor readings with the established limits and data reduction (computation of engineering quantities) (Sêco e Pinto, 1998).

For the interpretation of the measurements, it is necessary to establish a procedure, a mathematical model that can be a statistical model, a deterministic model or a hybrid model.

7.7.2.7 Data Storage

It is advisable to design and use a database containing the monitoring data selected to be stored.

The dam safety engineer, or the monitoring personnel at the dam site in case the corresponding software is available locally, shall observe the engineering quantities or/and chronological diagrams with the evolution of these quantities usually plotted versus time and reservoir level, and whenever justified, environmental temperature. The software must be flexible and friendly to produce a list and diagrams with data evolution.

An alarm concerning only a sensor reading will correspond usually to an abnormal situation.

7.7.2.8 Safety Control

Safety control is the group of measures taken in order to have an up-to-date knowledge of the condition of the dam and to detect in due time the occurrence of any anomalies to define actions to correct the situation or, at least, to avoid serious consequences (Post, 1985).

New systems to deal with automatic data acquisition, very flexible, that allows users to perform treatment of the information integrating tests and analysis, behavior models, visual inspections, documents data by any computer connect with Internet visualization are developed (Portela et al, 2005).

7.7.2.9 Visual Inspections

The preliminary inspection before the first filling, with the presence of Owner representative is intended to ascertain the conditions and the functionality of the equipment of appurtenant works and monitoring scheme.

Inspections after the first filling, performed by the Authority with LNEC collaboration and with a Owner representative have the purposes to verify the state of the dam and equipment with implications in decisions to be taken during operation (SRB, 1990b).

Visual inspections are compulsory after exceptional occurrences, such as important earthquakes, big floods and total or nearly total drawdowns of the reservoir (ICOLD, 1988; Sêco e Pinto, 1991).

During inspections the following aspects deserve attention:
Dam Body - (i) upstream face (slope protection, vegetative growth, settlement, debris, burrows and unusual conditions); (ii) downstream face (signs of movement, seepage or wet areas, vegetative growth, condition of slope protection, burrows or unusual conditions); (iii) crest (surface cracking, settlement, lateral movement, camber).

Spillway – (i) approach channel (vegetation, debris, slides, slope protection); (ii) control structures (apron, crest, walls, gates, bridge, chute, stilling basin, outlet channel).

Outlet Works – (i) inlet works, emergency control facility, outlet conduit, service control facility, stilling basin.

Reservoir - Log Boom, landslides, other.

Access Road - Condition of pavement, ditches, bridge.

If an earthquake of moderate or high Richter magnitude occurs an immediate inspection of the dam shall be done following these procedures (ICOLD, 1988):

1) If the dam is damaged to the extent that there is increased or new flow passing downstream immediately implement failure or impending failure procedures as previously planned.
2) If abnormally reduced flow is present at the upstream end of the storage, immediately inspect the river course for possibility of upstream damages due to landslide. If such is the case, implement failure or impending failure procedures.

3) Make an estimate of the characteristics of the earthquake.
4) Immediately conduct a general overall visual inspection of the dam.
5) If visible damage has occurred but has not been serious enough to cause failure of the dam, quickly observe the nature, location and extent of damage and report all the information to the supervisory office for a decision on further actions.
6) Make additional inspections at any time because of possible aftershocks.
7) During inspection the following aspects deserve attention: (i) cracks, settlements and seepage located on abutments or faces of the dam; (ii) drains and seeps for increased flow or stoppage of flow; (iii) outlet works or gate misalignment; (iv) visible reservoir and downstream areas for landslides, new springs and sandboils and rockfalls around the reservoir and in downstream areas; (v) for tunnels and conduits, observe whether silt, sand, gravel, rock or concrete fragments are being carried in the discharge stream.
8) Continue to inspect and monitor the facilities for at least 48 hours after the earthquake because delayed damage may occur.
9) A secondary inspection 2 weeks to a month after the initial inspection should be made.
10) A schedule of very frequent readings should be followed for at least 48 hours after the earthquake.
11) If failure is imminent, warning to downstream residents is essential. All measures should be used to reduce storage in the reservoir.

7.7.2.10 Organization of Monitoring Activities

The obligations of the Owner are: (i) to carry out the first filling of the reservoir; (ii) to submit to the Authority the appointment of a Technical Manager.
The Designer must include a general proposal of the monitoring scheme which should indicate the physical quantities to be monitored, taking into account the hazard scenarios envisaged in the design.
The National Civil Defence Service is responsible for ensuring plans for emergency and coordinating rescue actions.
The Dam Safety Commission is responsible for: (i) proposing to the Authority immediate steps; (ii) ensuring the safety of any dam; (iii) issuing written advices on emerging plans.
The monitoring plan has to be based on the corresponding proposal and be implemented with the collaboration of the different entities involved in the structural safety control. This plan must consider the hazard involved in the construction and operation of the dam and will contain indications about: visual inspections, installation and operating of the monitoring scheme and methods recommended for behavior analysis and safety evaluation of the works
The regulations points to the need up updating the monitoring plan when justified, which is compulsory after construction, first filling, first five years and first twenty years of operation.

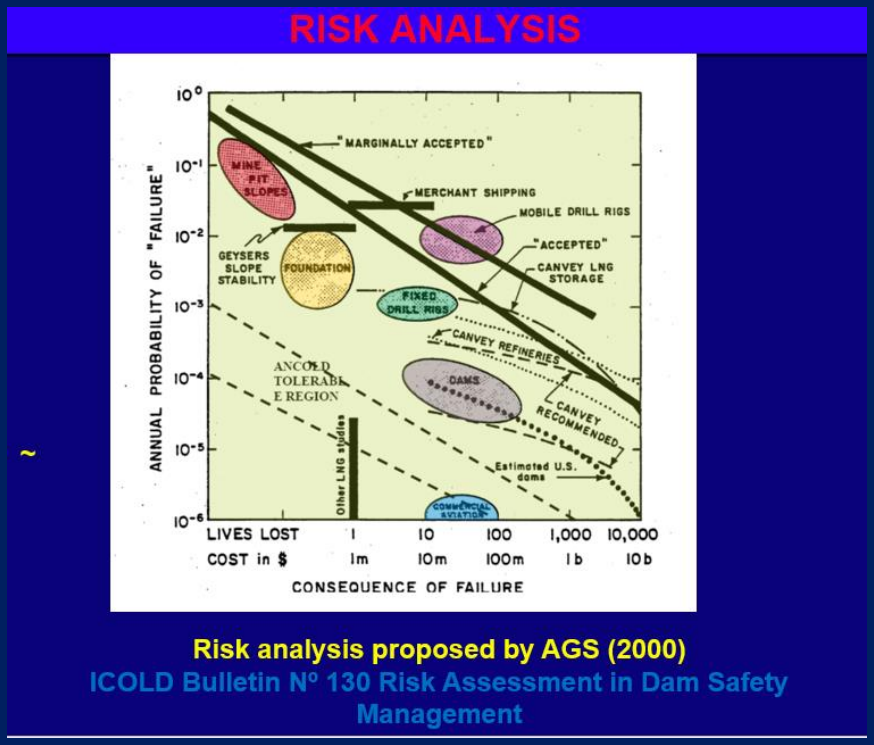

Figure 7.69 Risk analysis

7.7.3 Risk potential assessment

The risk potential is associated with the structural components and with social- economic components. The structural components depend of the reservoir capacity and the height of the dam.

The social economic risks are related with the number of persons that need to be evacuated and with the potential downstream damages.

The risk analysis associated to dams can be defined by Tables 7.19 and 7.20 (WRPT, 1980).

Table 7.19 Risk analysis

Risk factor	**Extreme**	**High**	**Moderate**	**Low**
Contribution for the risk (values)				
Capacity (hm3)	>120 (6)	120-1 (4)	1-0.1 (2)	<0.1 (0)
Height (m)	>45 (6)	45-30 (4)	30-15 (2)	<15 (0)
Nº of persons to be evacuated	>1000 (12)	1000-100 (8)	100-1 (4)	Nill (0)
Potential downstream damages	High (12)	Moderate (8)	Low (8)	Nill (0)

The total risk factor l= Risk factor (capacity)
+ Risk factor (Height)

+ Risk factor (measures for evacuation)
+ Risk factor (Potential downstream damages)

The risk category of the dam can be defined by the total risk factor

Table 7.20 Risk categories

Total Risk factor	Risk Category
(0-6)	I (Low)
(7-18)	II (Moderate)
(19-30)	III (High)
(31-36)	IV (Extreme)

Note: More details related embankment dams can be found in Volume 5.

8. Case Histories- Examples

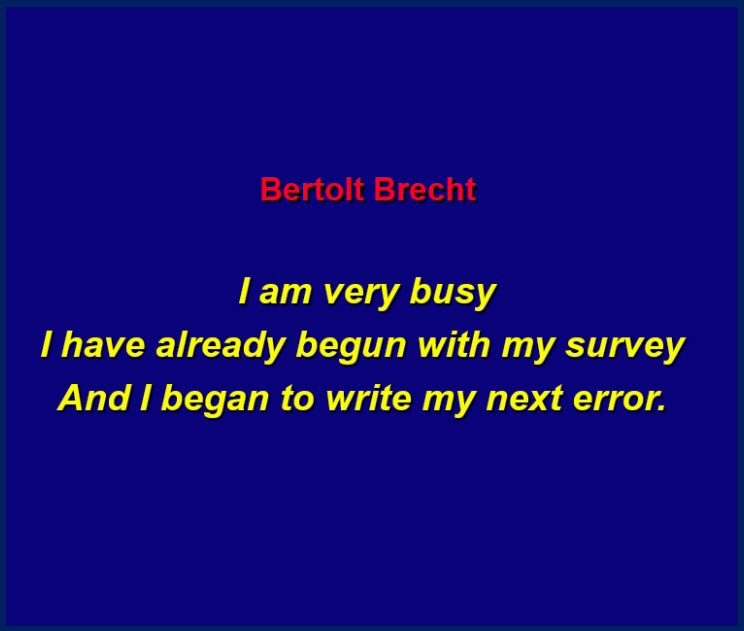

8.1 INTRODUCTION

After an introduction of Case Histories, 28 Case Histories applied to different geotechnical projects such as embankment dams, powerplants, underground structures, buildings foundations, bridges foundations, maritime structures, retaining walls, waste landfills, residual water storage and highways are presented.

The different issues such as: geological studies, site investigation, geotechnical studies, type of structure, seismic studies, stability analysis, seepage analysis, stress-strain analysis, foundation treatment, construction issues, instrumentation and monitoring, construction schedule are analysed.

A Case History to be useful should include the following information:

- Geology of the site
- Seismicity of the area
- Purpose and scope of the geotechnical investigation
- Procedures for sampling
- Description of field equipment
- Data on variation of ground water table
- Results of field and laboratory tests
- Design geotechnical parameters
- Design methodology
- Construction procedures
- Observational data

- Case Histories always give us an opportunity to learn from mistakes and failures. But to take full advantage we must be identify the error and find a better solution. The intellect of man is forced to choose perfection of the life or of the work.
- Failure helps us to get closer to our dreams, equipped us with more knowledge and that success and failure go hand in hand.
- As Bernard Shaw said "By the error we reach the truth, but we should not abuse of this practice".
- Case Histories have remind us the Big Five that have remained unchanged since ancient times:

Conscientiousness
Friendship
Extroversion
Emotional Intelligence
Innovation

- Quoting Karl Terzaghi from the first issue of Geotechnique (1948):

"A well documented case history should be given as much weight as ten ingenious theories".

- Leonard de Vinci has stated that " It seems, though that those sciences which have not been born by experience the mother of all certitude, are vain and full of misconceptions".
- We should not forget that Theory without Practice is a Waste, but Practice without Theory is a Trap.
- Kant has stated that *"Nothing better that a good theory"*, but following Seneca " *Long is the way through the courses, but short through the example*" .
- I would stress that all the past lessons had not deserved total consideration, in order to avoid repeating the same mistakes, and we should preserve the knowledge through a careful analysis of Case Histories.

8.2. EMBANKMENT DAMS

8.2.1 Case History Nº 1 - Jambi-ia- Oma Dam (Angola)

8.2.1.1 Introduction

For Jambi-ia- Oma dam the profile is introduced, the freeboard and the crest width are defined, the geological characteristics are described, the geotechnical characteristics are referred, the definition of design earthquake is discussed, the stability analyses are presented, the seepage studies are analyzed, the stress-strain analyses are addressed and the stability analyses of the excavations are discussed.

8.2.1.2 Dam Profile

The dam is located in Cunene River (Angola) with stored volume of water of 1 088,3 hm^3.
It is a mixed dam, with a concrete section, type gravity with a length of 490.5 m and a height of 46.2 m and an earth section 2 350 m long and with a height of 33.2 m (Figure 8.1).
Slope inclinations: concrete dam 1:0,1 (upstream) and 1:0,8 (downstream) (V:H)
Earth dam, 1:3 (upstream) and 1:2.5 (downstream) (V:H).

It is a frontal spillway with gates and sky jump with 7 spans and a length of 17.25 m.

The outlet allows a flow discharge of 134 m^3/s.
The water intake has a flow of 150 m^3/s.

The hydroelectric powerplant with Francis turbines generates 224 GWh/year.

8.2.1.3 Freeboard

The freeboard was defined by the methodology proposed by Martins (1984) and the following equation:

$$f = f_h + f_s \quad (8.1)$$

where f_h is linked with quantified factors and f_s with factors depending of the failure.

For the definition of f_h the following combinations were considered:

Combination A - NPA + waves due to exceptional wind

Combination B - NMC + waves due to normal wind.

The overflowing F is given by the equation:

$$F = (0.30 + 2.3\ H)\ H_h \quad (8.2)$$

Where

H - inclination of the upstream slope

H_p - height of the project wave

$$H_p = \frac{V^{1.06}\ F^{0.47}}{2.00} \quad (8.3)$$

where

V - is the velocity of normal wind (80 km/h) or exceptional wind (160 km/h)

F - effective fetch in km

Considering a maximum settlement of the dam of 2% results 0.30 m.

Table 8.1 Computation of the effective fetch

θ_i (°)	cos θ_i	F_i	$F_i \cos^2 \theta_i$
42	0.743	-	-
36	0.809	-	-
30	0.866	-	-
24	0.914	-	-
18	0.951	1120	1012.9
12	0.978	1100	1052.1
6	0.995	1220	1207.8
0	1.000	2000	2000.0
6	0.995	750	742.5
12	0.978	880	841.7
18	0.951	620	560.7
24	0.914	480	462.0
30	0.866	500	375.0
36	0.809	460	301.1
42	0.743	400	220.8
$\sum$	**13.512**		**8715.6**

$$F_e = \frac{8715.6}{13512} = 645.0$$

Para $F_e \rightarrow 0.645$ km e 1/2.5 (V/H)

$$A)\ H_s = \frac{80^{1.06} \acute{} 0.645^{0.47}}{200} = 042\ ;$$

$$E_s = \left(0.3 + \frac{2.3}{2.5}\right) \acute{} 0.42 \acute{} 1.25 = 0.64$$

$$B)\ H_s = \frac{160^{1.06} \acute{} 0.645^{0.47}}{200} = 0.88\ ;$$

$$E_s = \left(0.3 + \frac{2.3}{2.5}\right) \acute{} 0.88 \acute{} 1.25 = 1.34$$

Cond.	NPA	NMC	E_s	Δh = 30 cm	Crest
A	27	0.55	0.64	0.30	28.49
B	27	-	1.34	0.30	28.64

So, the crest level was fixed in 29.00 m.

8.2.1.4 Width of the Crest

Following Preece the width of the dam crest is given by:

$$L = 1.1'\sqrt{H' + 1} \quad (8.4)$$

Where H' is the maximum dam height.

Considering H' = 15 m results:

L = 5.16 m

Following the japanese code:

$$L = 3.6\sqrt[3]{H} - 3 \quad (8.5)$$

L = 5.8 m

A value of 6 m was considered for the crest width.

8.2.1.5 Geotechnical Characteristics

The geological materials incorporate porfiroid granites with medium grain and residual soils.

The granite massif is tectonized and divided in blocks of great dimension and exhibits 5 joint families, namely N (50 - 100)ºE, N (0 – 30)º E, N (20 – 55)º W, subvertical, another with the attitude N (10 – 40)º W, N (45 – 65)º SW, and one sub-horizontal.

The site characterization, namely the boreholes along the dam axis have shown that the residual soils have high values of permeability and the quality of the granite massif is increasing with depth.

The geotechnical characterization has included 6 seismic refraction profiles and a zonation was obtained with a superficial zone with a velocity less than 1 000 m/s, and intermediate zone with 2 500 m/s and a deep zone with velocities higher than 3 600 m/s.

In addition, 14 boreholes were performed with Lugeon test in rock materials with high values of permeability in the zone of fractured granite.

As complementary works two additional boreholes were performed.

To characterize the quarry materials 11 electric resistivity profiles were performed and 3 boreholes with a depth of 15 m.

27 trenches were open to characterize the borrow pits and 52 samples were taken to perform identification laboratory tests

Later, in a second campaign 43 samples were taken and compaction tests, shear tests, oedometer tests and permeability tests were performed.

For the characterization of quarry materials resistivity tests and seismic refraction tests were performed.
In addition, 3 boreholes were performed with 15 m depth.

Triaxial tests C.U. with the measurement of pore pressures were performed. The obtained cohesion values were between 0 kg/cm² e 0.35 kg/cm² and the friction angle between 31º and 34.5º.

From the identification tests results the soils were classified in sandy clays (SC), inorganic clays of low plasticity (CL), silty sands (SM) and silts of low plasticity (ML).

Proctor tests have given values of maximum unit weight between 17.1 kN/m3 and 20.5 KN/m3 and optimum contents values between 10.4% and 18.9%.

Direct shear tests have given results of cohesion 0 and 3 kPa and friction angle between 26.5º e 36º.

The consolidation tests gave results of void ratio between 0.37 and 0.76.

The permeability tests performed in boreholes gave results between 10^{-6} a 5 x 10^{-7} m/s.

From the test results it was concluded that the soils materials are good for the construction of an earth dam.

The specifications of site investigation tests are presented in Annex 1.

8.2.1.6 Stability Analysis

The profile type (see Figure 8.1) was defined taking into account the available materials near the dam site and the following mechanical characteristics.

Embankment materials

G = 2.67

γ_h = 21 kN/ m^3 (embankment water content)

γ_s = 22 kN/m^3 (saturated)

c' = 5 kPa

φ' = 28º

Coefficient of permeability (horizontal) 10^{-7} m/s

Coefficient of permeability (vertical) 5x 10^{-8} cm/s.

Filter Materials

Based on past experience the following values were considered:

Coefficient of permeability	k =10^{-4} m/s
Cohesion	c' = 0
Friction angle	= 35°

Rockfill Materials

For the rockfill materials the following values were considered:

Cohesion	c' = 0
Friction angle	= 40°

The sieve analysis of the materials is shown in Figure 8.2.

A computer code SLOPE W was used to analyze the slope stability of the dam profiles.

It is current practice to analyze: construction phase, filling of reservoir and drawdown.

Related with the construction phase both and downstream slope (Figure 8.3) and upstream slope (Figure 8.4) were analyzed.

For the filling of reservoir, the most critical situation is related with the downstream slope (Figure 8.5).

For the drawdown the most critical phase is related with the upstream phase (Figure 8.6).

For the construction phase the design values are summarized in Table 8.2.

For the most critical surface only the cinematic feasible surface was selected

Taking into account the size of the dam a pseudo-static analysis was considered adequate.

The minimum computed safety factor associated to a seismic coefficient of 0.10 was 1.24 (see Figure 8.7).

Table 8.2 Design Values

MATERIAL	UNIT WEIGTH ($kN(m^3)$)	COHESION (kPa)	FRICTION ANGLE (0°)	PIZOMÉTRIC	PARÂMETER R_u
Rip-rap and Filter	20	0	35	0	0
Fill	20	5	32	0	0.1
Downstream rockfill	22	0	40	0	0
Filter and Drain	20	0	35	0	0
Bed-rock	22	200	40	0	0

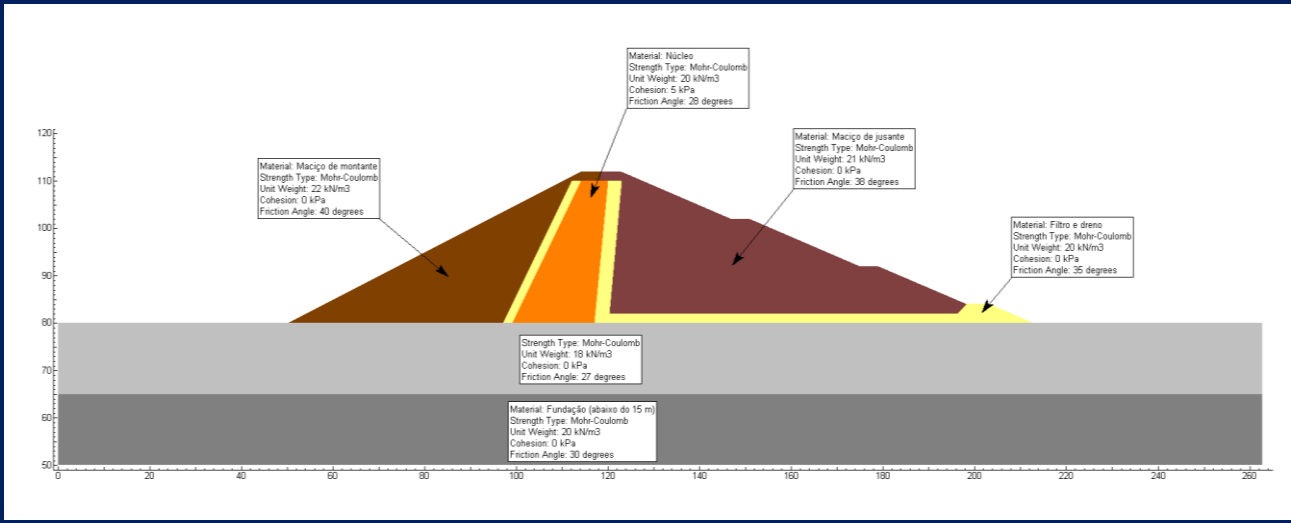

Figure 8.1 Dam Profile

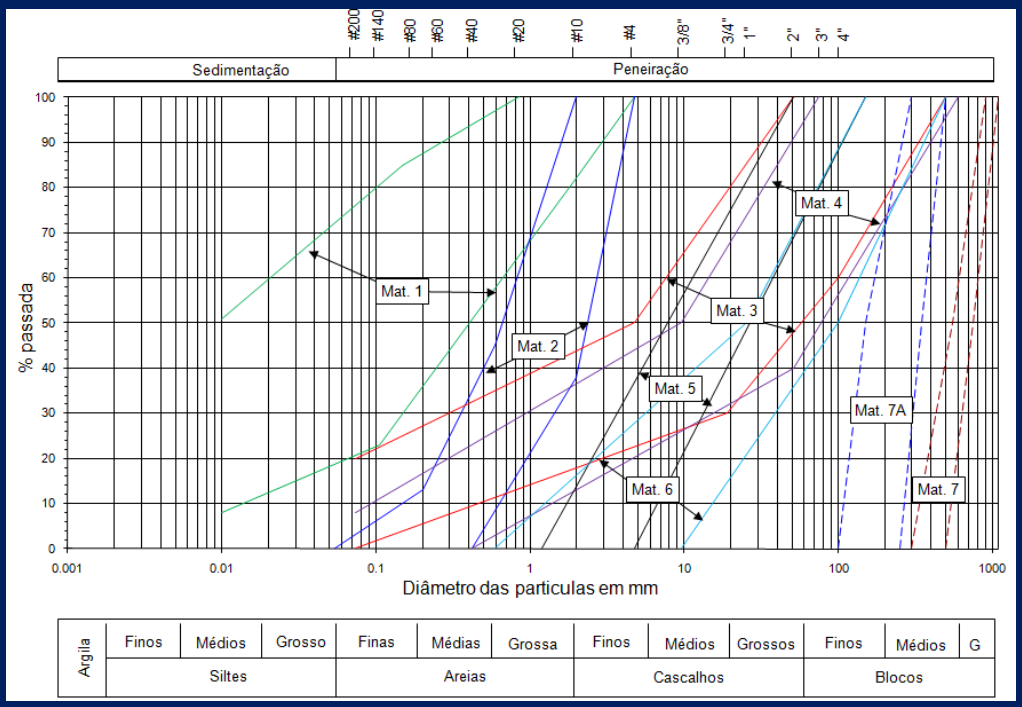

Figure 8.2 Sieve analysis of the materials

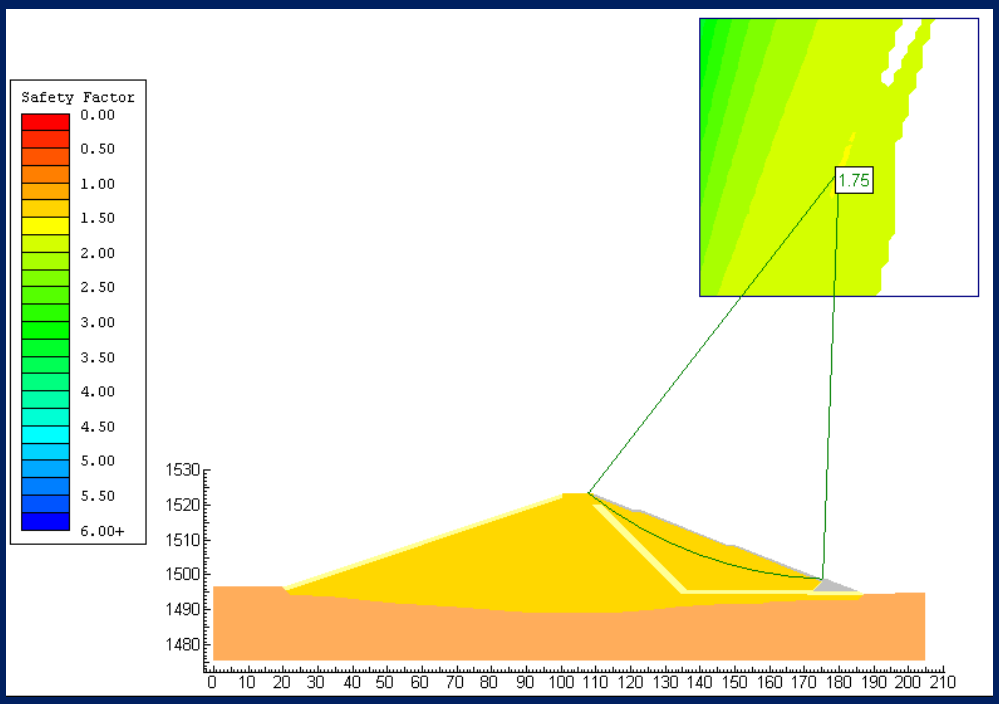

Figure 8.3 Construction phase – Static analysis (minimum safety factor 1.75-downstream shell)

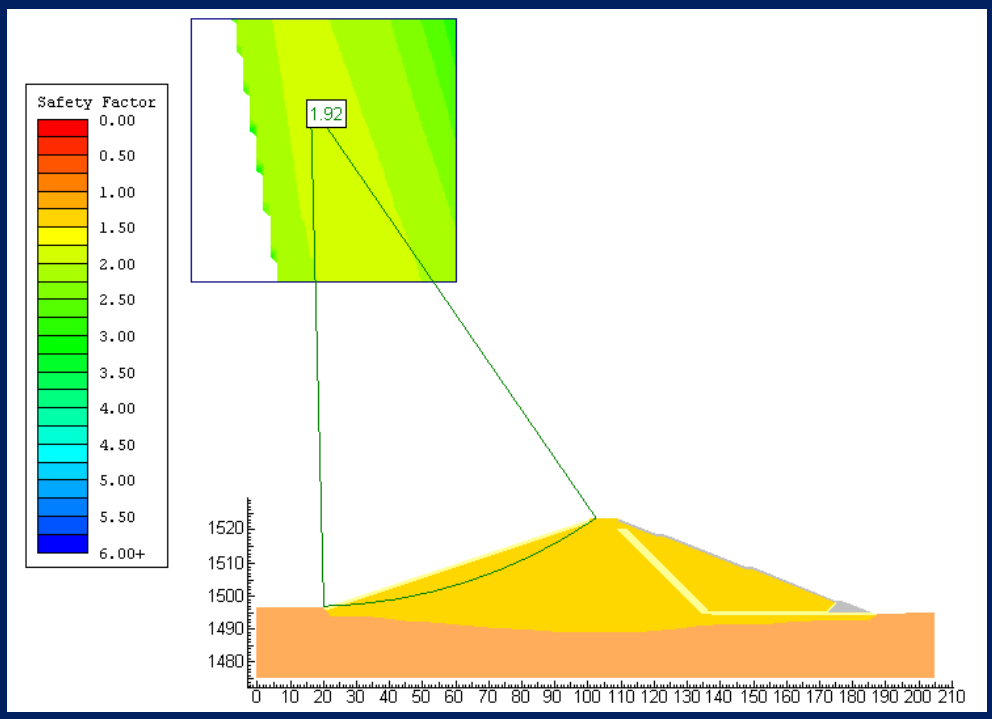

Figure 8.4 Construction phase – Static analysis (minimum safety factor 1.92-upstream shell)

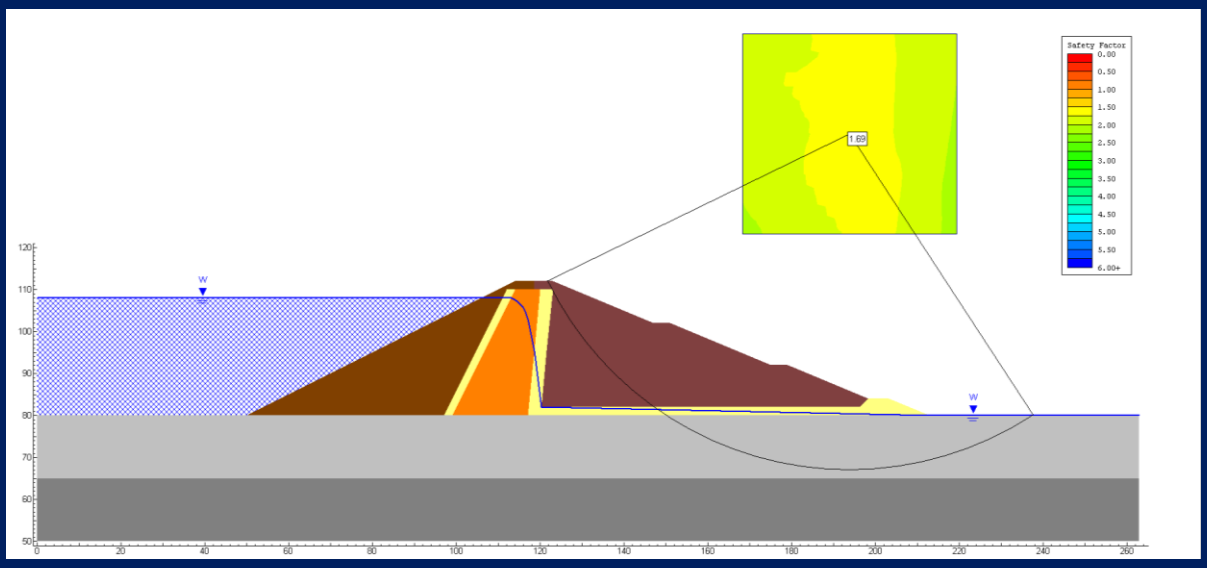

Figure 8.5 Filling Reservoir – Static analysis (minimum safety factor 1.94-downstream shell)

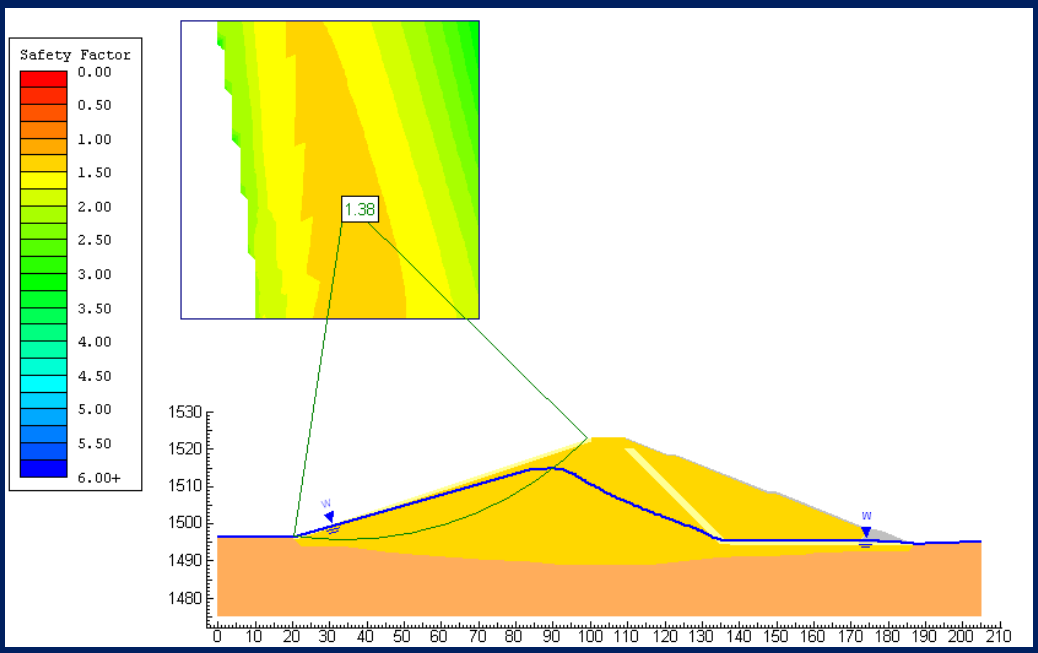

Figure 8.6 Drawdown – Static analysis (minimum safety factor 1.38-upstream shell)

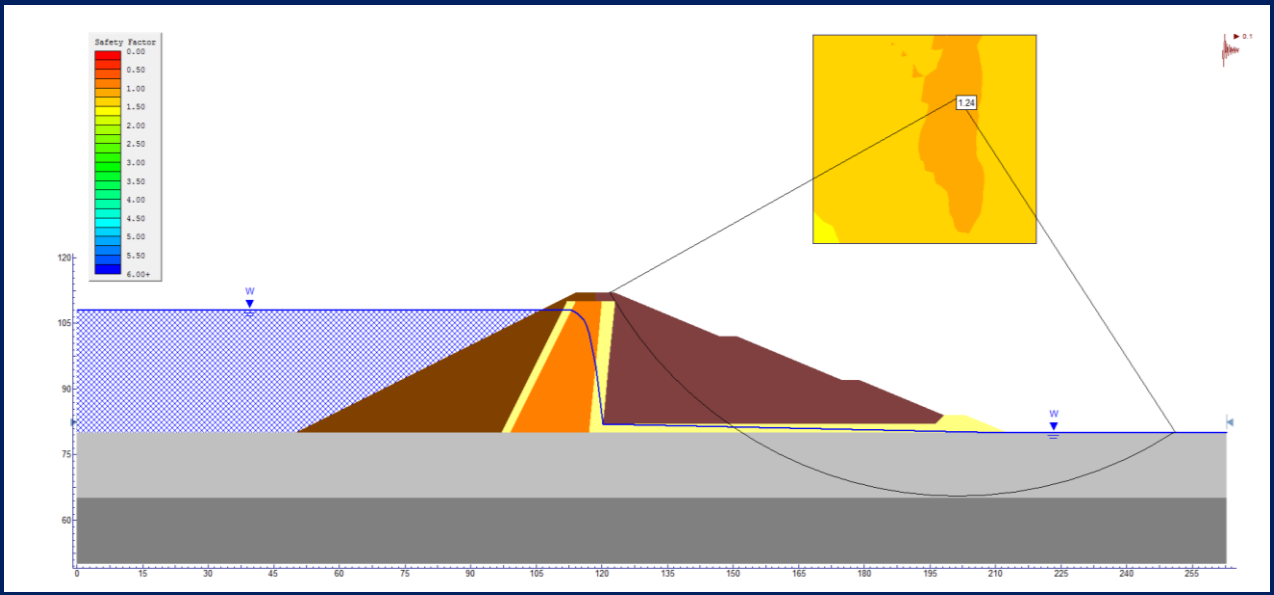

Figure 8.7 Filling Reservoir – pseudo-static analysis (minimum safety factor 1.24-downstream shell)

8.2.1.7 Seepage Studies

The seepage studies were performed using a PLAXIS code and the coefficient of permeability of the materials are shown in Table 8.3. The flows through the dam body and foundation were computed.

The efficiency of a grouting curtain will be analyzed.

The finite element mesh is shown in Figure 8.8.

The equipotentials surfaces are shown in Figure 8.9.

Figure 8.10 illustrates the values of flows computed in critical zones.

Table 8.3 Coefficient of permeability of the materials

Materials	Kv (m/s)	Kh (m/s)
Dam materials (1)	$2x10^{-8}$	10^{-7}
Filters and drains (2), (3)	$1x10^{-4}$	$1x10^{-4}$
Rockfill (4)	3×10^{-2}	3×10^{-2}
Foundation	$5x10^{-6}$	$5x10^{-6}$
Grout curtain	$1x10^{-7}$	$1x10^{-7}$

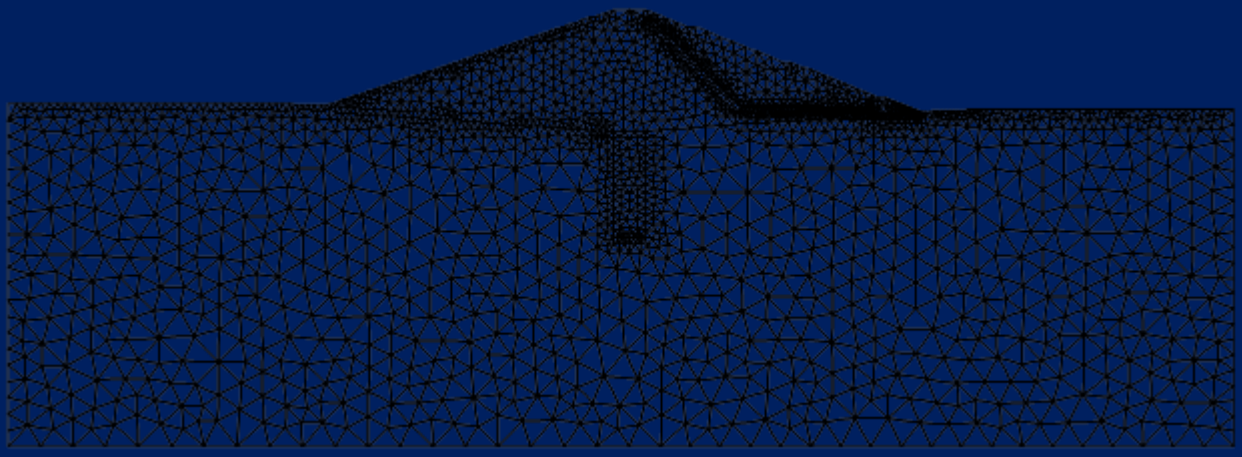

Figure 8.8 FEM mesh

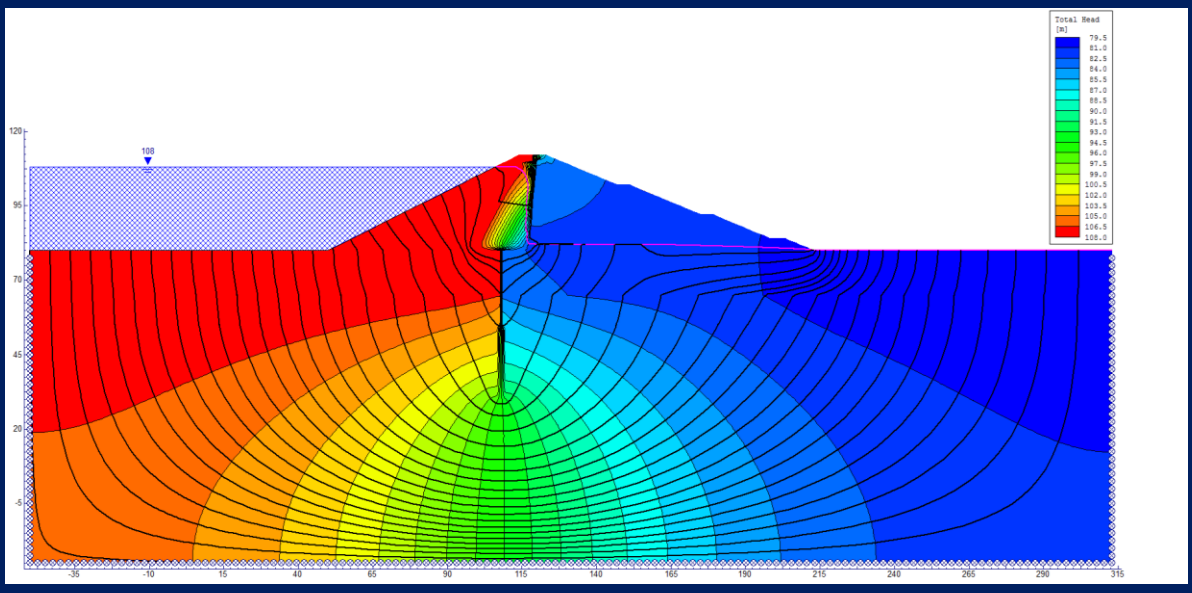

Figure 8.9 Equipotentials Surfaces

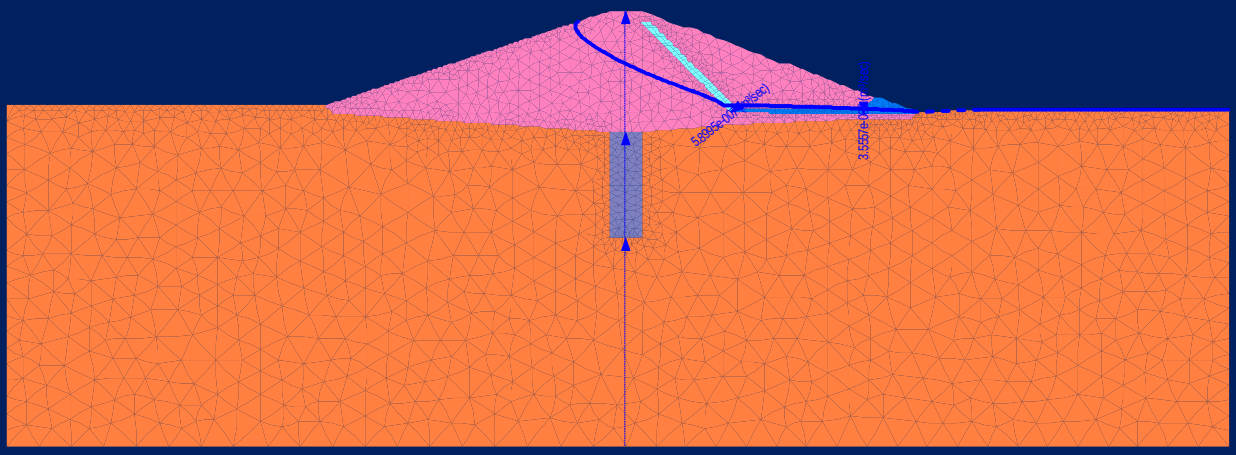

Figure 8.10 Values of flows

8.2.1.8 Stress - Strain Analyses

A stress strain analysis was performed for the construction phase, filling of reservoir and steady state situation. The most critical cross section was analysed.

Different foundations situations were considered.

The purpose of these analyses was to assess the displacements, as well the stress distribution.

An elastic behaviour for the materials were considered, due to the absence of adequate stress-strain curves.

The analyses were performed using the code PLAXIS – version 7.2.

The prediction of the displacements is useful for the definition of the freeboard.

The distribution of the effective vertical stress and the effective horizontal stress for the critical phase of the filling of the reservoir are shown in Figures 8. 11 and 8.12.

The distribution of the vertical displacements and the horizontal displacements for the filling of the reservoir phase are shown in Figures 8.13 and 8.14.

.

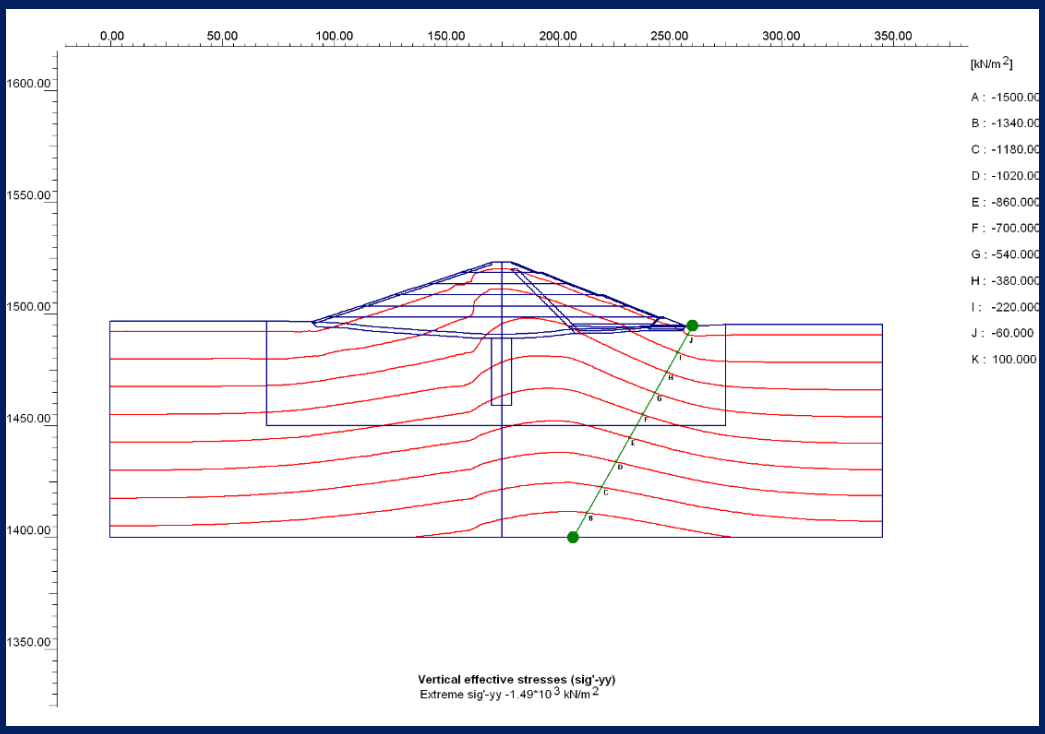

Figure 8.11 Distribution of effective vertical stress – filling reservoir

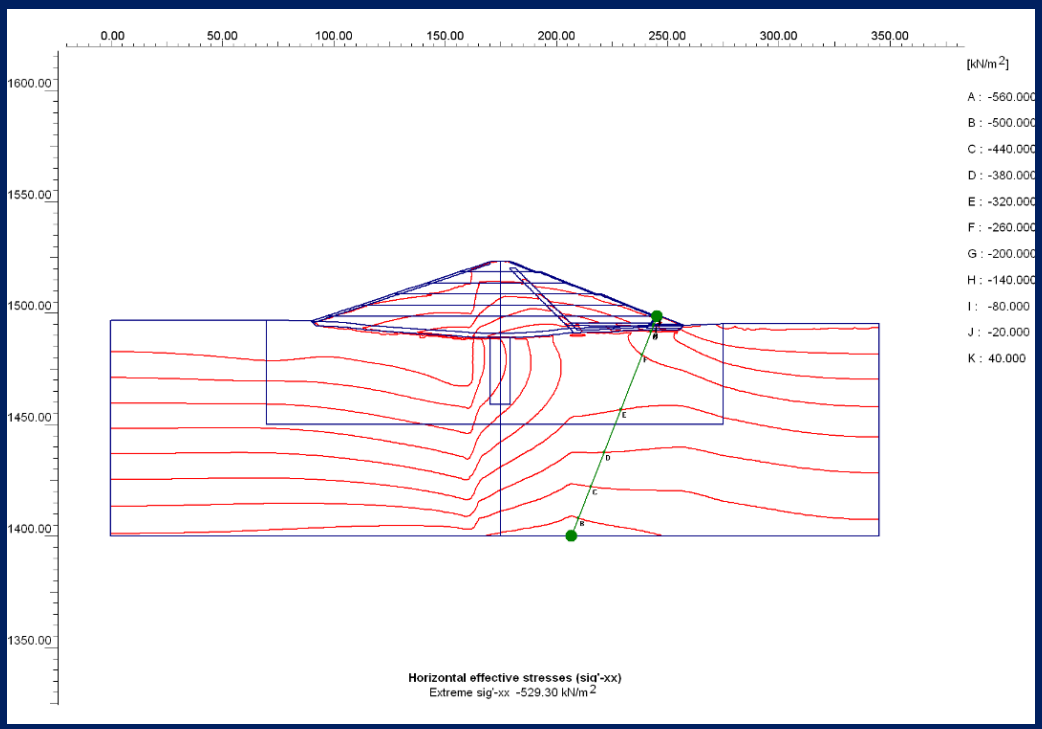

Figure 8.12 Distribution of effective horizontal stress – filling reservoir

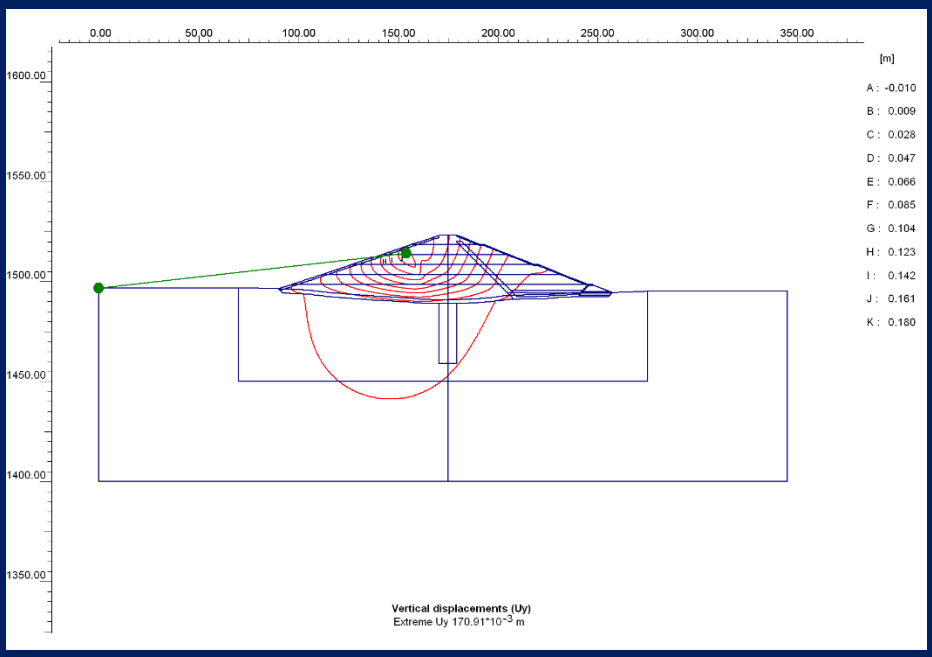

Figure 8.13 Distribution of vertical displacements – filling reservoir

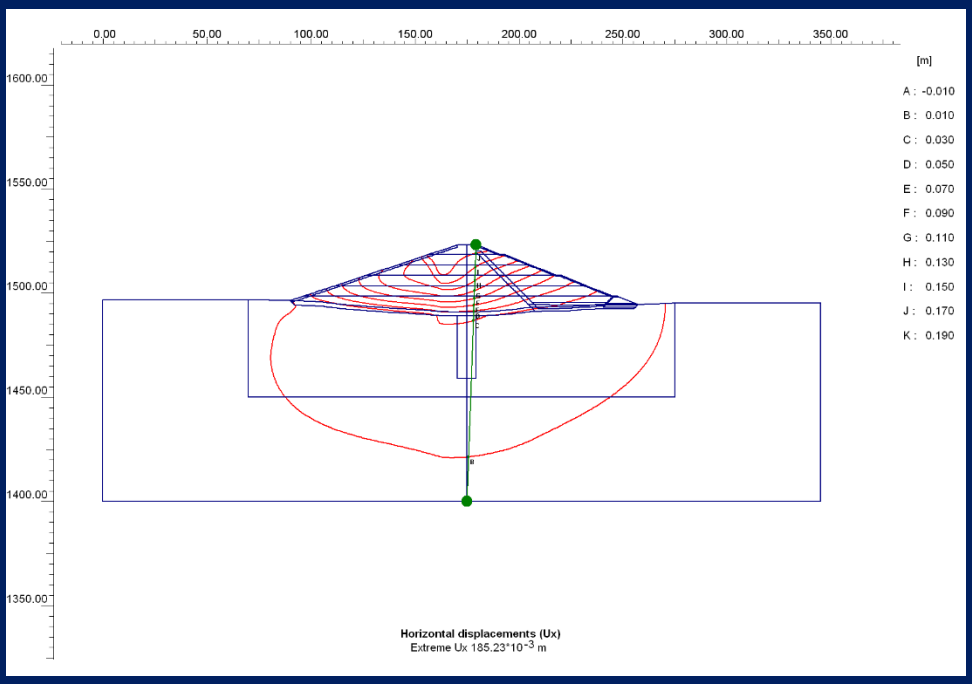

Figure 8.14 Distribution of horizontal displacements – filling of reservoir

8.2.1.9 Selection of Design Earthquakes

The selection of seismic design parameters for dam projects depends on the geologic and tectonic conditions at and in the vicinity of the dam site (Sêco e Pinto, 2004).

The regional geologic study area should cover, as a minimum, a 100 km radius around the site, but should be extended to 300 km to include any major fault or specific attenuation laws.

The probabilistic approach quantifies numerically the contributions to seismic motion, at the dam site, of all sources and magnitudes larger than 4 or 5 Richter scale and includes the maximum magnitude on each source.

The dam should be designed for Design Earthquake (DE) and Maximum Design Earthquake (MDE). Both depend on the level of seismic activity, which is displayed at each fault or tectonic province

For the DE only minor damage is acceptable and is determined by using probabilistic procedures.

For the MDE only deterministic approach was used (ICOLD, 1983) but presently it is possible to use a deterministic and probabilistic approach. If the deterministic procedure is used, the return period of such an event is ignored, if the probabilistic approach is used a very long period is taken (ICOLD, 1989).

Generally speaking, a dam is designed to withstand two different levels of earthquake activity. Hence, two design earthquakes, or series of earthquakes, are specified and are termed "Operating Basis Earthquake" (O.B.E.) and "Maximum Credible Earthquake" (M.C.E.).

An O.B.E. is an event that may reasonable be expected during the lifetime of the structure. The structure must continue to function during and after such an event and thus the loading is classed as "unusual". A full definition of this loading includes a usual static load, because such an earthquake, will occur in combination with self weight, temperature, silt and hydrostatic load.

An M.C.E. event is defined to correspond with the most extreme earthquake action that can reasonably be expected at that site. The structure must withstand the event in such a way that repairs can be undertaken in a reasonable length of time and, more importantly, that no loss of life occurs for example due to a major flood. An M.C.E. event is classed as an "extreme loading".

It was considered the response spectra of Eurocode 8 illustrates in Figure 8.15.

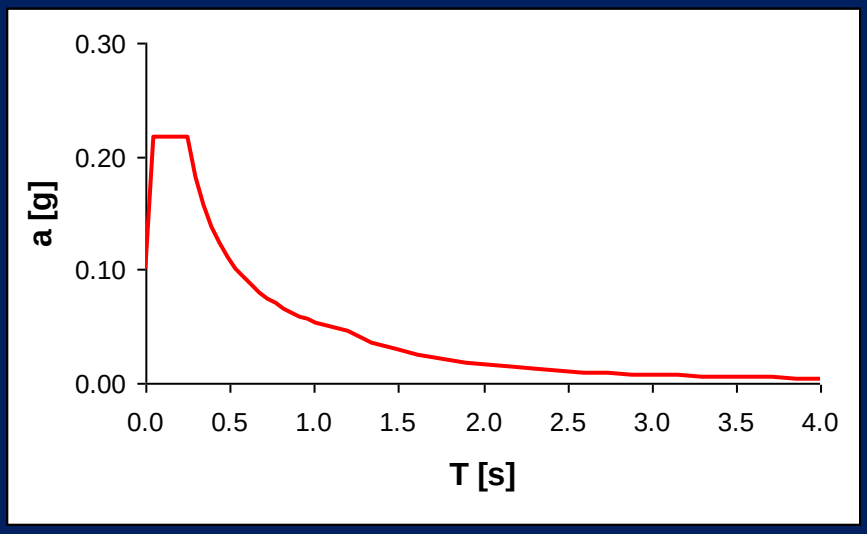

Figure 8.15 Response spectra

8.2.1.10 Stability Analysis of Excavations

The global stability of the excavation of the hydraulic structures was analysed by a parametric study considering anchors of 400 kN, 500 kN e 600 kN and meshes with spacements of 2.0 x 2.0 m, 2.5 x 2.5 m and 3.0 m x3.0 m.

For the verification of rupture modes, the anchors tests are recommended.

For the superficial layers a mesh with nails 3.0 m x 3.0 m apart and 12 m long was considered.

The computed safety factors for the different situations are shown in Table 8.4.

Table 8.4 Computed safety factors

Pre-stressed	**Anchorage mesh [mxm]**					
kN	**2.0 x 2.0**		**2.5 x 2.5**		**3.0 x 3.0**	
400	1.341	Figure 8.16	1.051	Figure 8.17	-	
500	1.624	Figure 8.18	1.176 1.235	Figure 8.19 Figure 8.20	1.042	Figure 8.21
600	1.757	Figure 8.22	1,312	Figure 8.23	1.129	Figure 8.24

For the excavation of the central a mesh of 2.5 x2.5 m with 600 kN anchors can be used or in alternative a mesh of 2.0 x 2.0 m with 400 kN anchors.

For the restitution channel the anchors are definitive and so a mesh of 2.0 x2.0 m with 500 kN anchors is proposed.

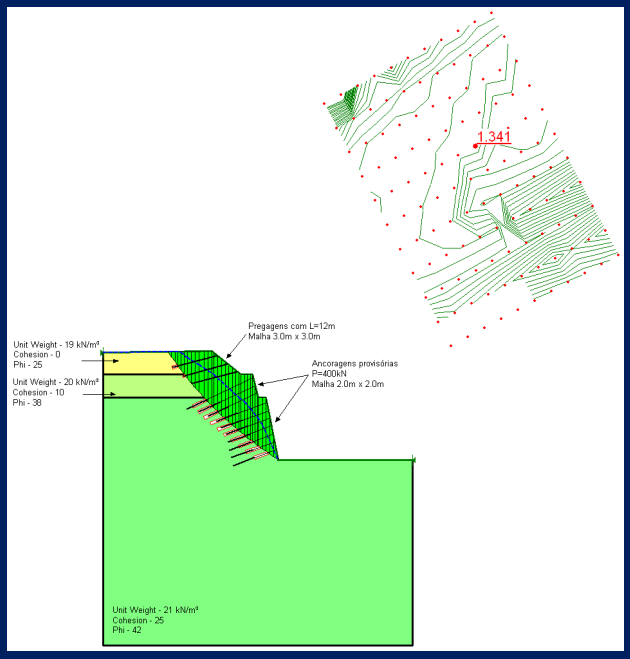

Figure 8.16 Mesh with 2.0 x 2.0 m-anchors of 400 kN

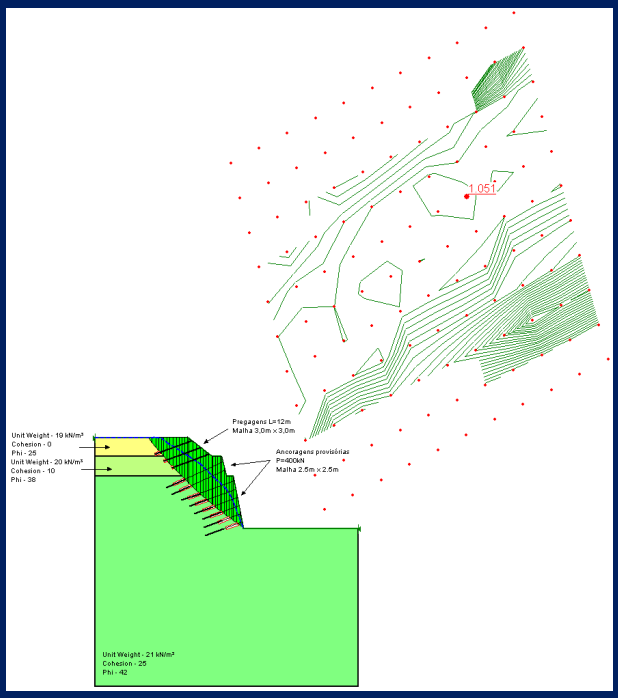

Figure 8.17 Mesh with 2.5 x 2.5 m-anchors of 400 kN

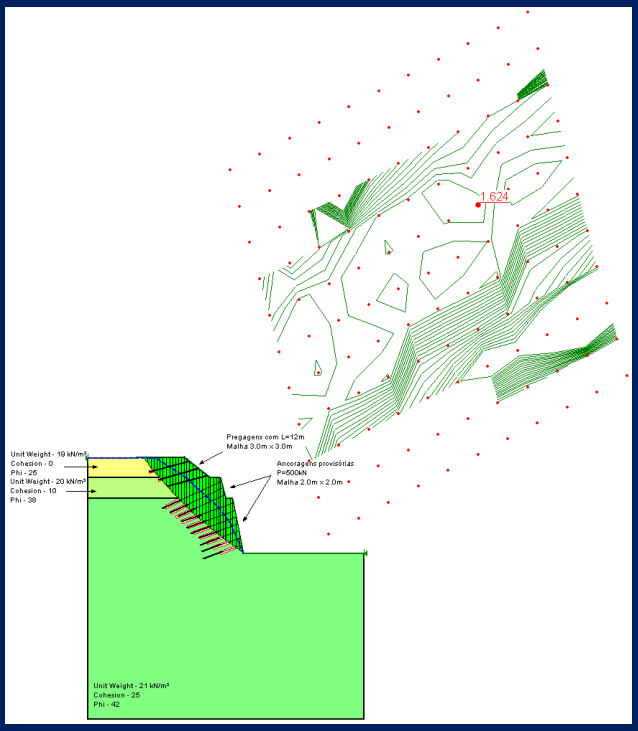

Figure 8.18 Mesh with 2.0 x 2.0 m-anchors of 500 kN

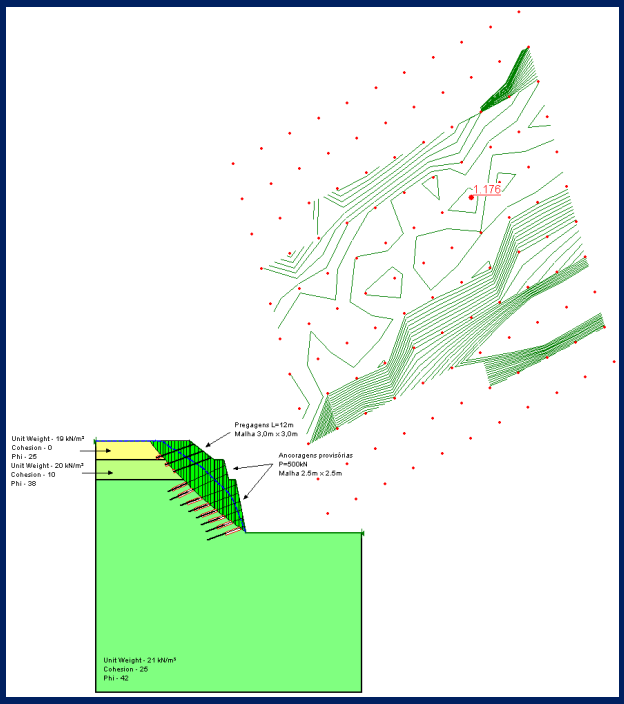

Figure 8.19 Mesh with 2.5 x 2.5 m with 8 anchors of 500 kN

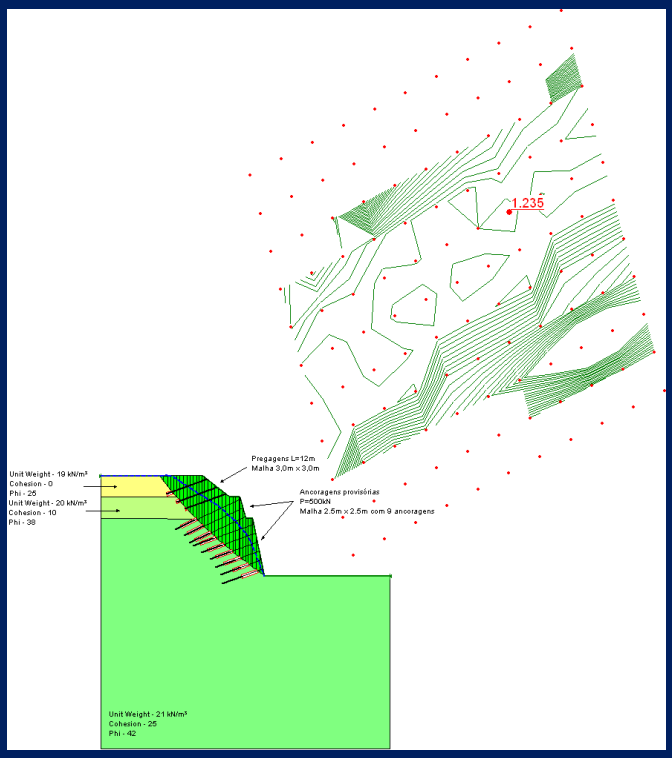

Figure 8.20 Mesh with 2.5 x 2.5 m with 9 anchors of 500 kN

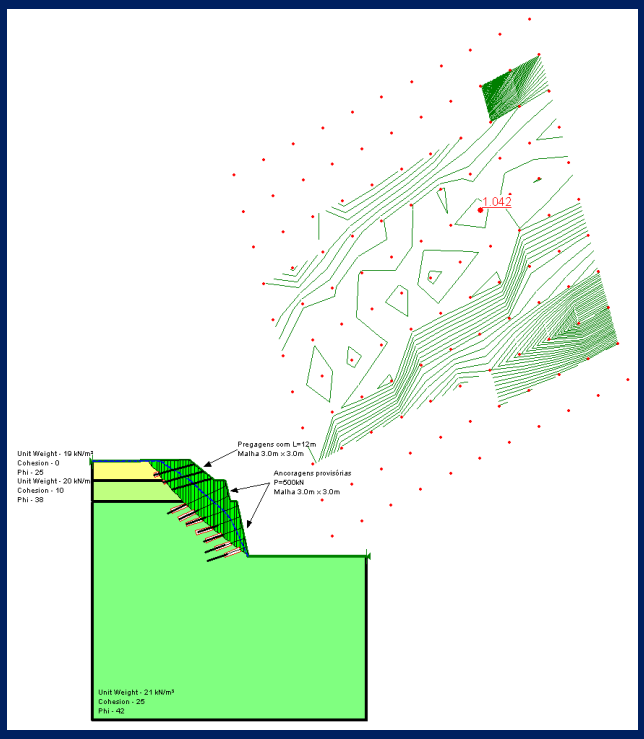

Figure 8.21 Mesh with 3.0 x 3.0 m of 500 kN

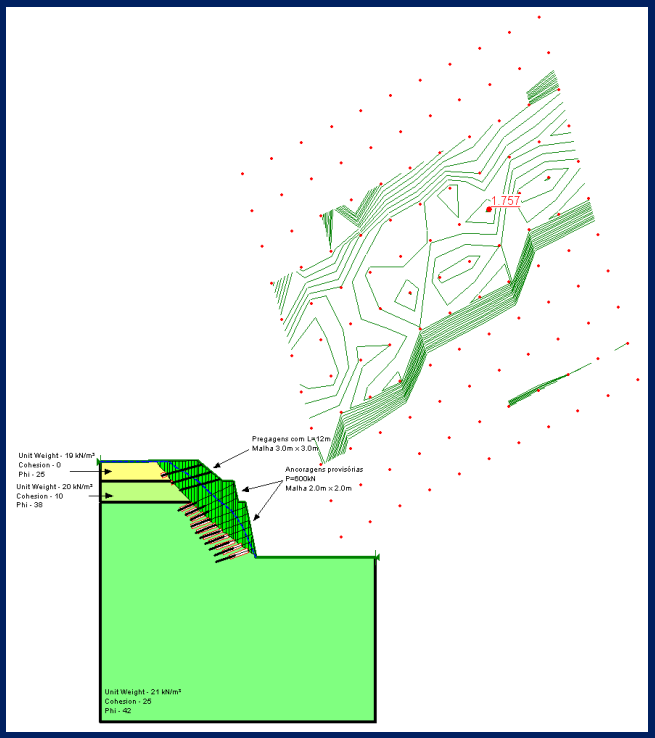

Figure 8.22 Mesh with 2.0 x 2.0 m-anchors of 600 kN

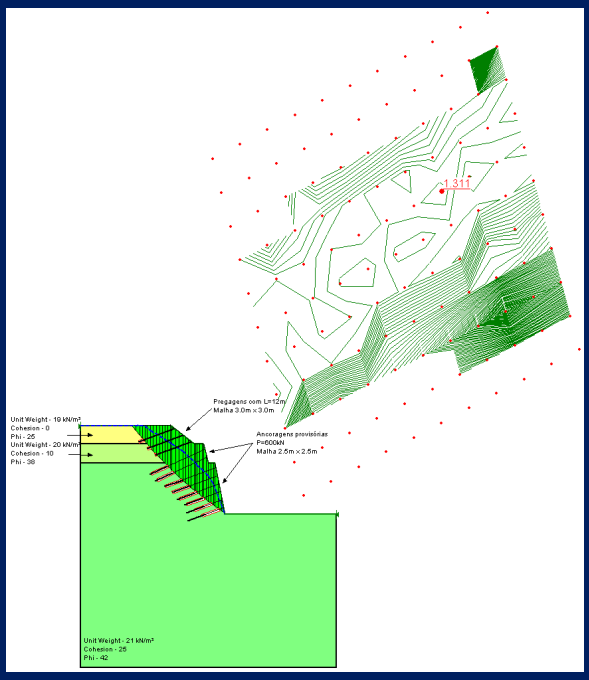

Figure 8.23 Mesh with 2.5 x 2.5 m-anchors of 600 kN

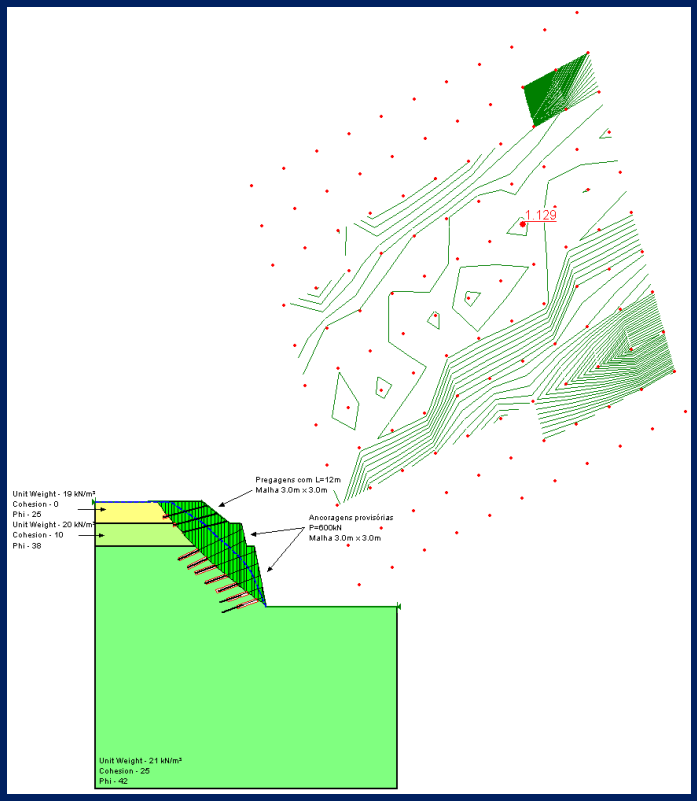

Figure 8.24 Mesh with 3.0 x 3.0 m-anchors of 600 kN

Details related anchors testing is given in Annex 2.

Lesson nº 1: Related to the dam projects the site investigation and geotechnical characterization depend of the available budget and the thigh schedule that the design team face and so, in general, the characterization is "the possible" and not the "desirable" by the design team.

The options that were taken had the goal to reach the optimum solution, in order to assure the absence of incidents for the Jamba-Ia-Oma dam, and a failure probability lower than 10^{-5}, following the recommendations of ICOLD.

Note: The dam project was conducted by a multidisciplinary COBA team and the author was involved in the geotechnical design.

.

8.2.2 Case History nº 2 - Keddar Dam (Argélie)

8.2.2.1 Introduction

The geological and geotechnical characteristics were described.
The seismic studies are presented, the simplified displacements analyses are addressed.
The instrumentation plan is described.
The dam behavior during the 25 May 2003 earthquake is referred.

8.2.2.2 Geological and Geotechnical Characteristics

The rock materials were namely schists and micaschists.

The geotechnical characterization included seismic refraction profiles, trial pits, 61 boreholes (with SPT tests and Lugeon water tests), open trenches and galleries, and laboratory tests of disturbed samples taken in the trial pits.

The site investigation works envisaged geological and geotechnical characterization works, namely the foundation conditions.

The works proposed included the execution of borehole drilling and seismic refraction profiles. Taking into account the results of this site investigation works, it was possible to elaborate an interpretative geological and geotechnical model.

The definition of the geotechnical zones was made considering basically the physical and mechanical characteristics of the occurring formations, such as the weathering and fracturing state of the rock mass, and the quality indexes obtained from the analysis of the boreholes undertaken (percentage of RQD and recovery and N_{SPT}).

The quarries near the dam were explored for the rockfill, drains, filter materials, as well for the concrete.

Echan-tillon	Poro-sité %	Masse volumique (kg/m^3)			Vitesse sonique (m/s)		Contrainte de rupture (MPa)	
		réelle	appa-rente	appa-rente saturée	sec	saturé	sec	saturé
KC	0,68	2710	2690	2700	5460	5960	85,3	71,1
KV	2,7	2730	2650	2680	4830	4930	82,0	23,2
	1,8	2730	2680	2700				
KE	1,2	2730	2700	2710	4900	5380	78,7	60,9
KVA	5,7	2710	2550	2610	4830	4630	-	70,2

The colluvial clay material and the alluvial silt material to be used for the core exhibit liquid limit between 29.7% and 36%, limit of plasticity between 16.5% and 17.1% and index of plasticity between 12.6% and 19.5%.

The elasticity modulus obtained from oedometer tests were between 7 MPa to 14 MPa.

Triaxial tests (CU) gave the following values in effective stresses, cohesion = 51 kPa and friction angle = 21.3º.

In a zone near the dam cofferdam experimental fills for rockfill materials were performed.

The materials were carefully spready with a bulldozer to avoid segregations.

- The rockfill material was saturated with more than 150 l/m³.

After the spreading and humidification, the rockfill material was compacted.

To obtained a relative density of 70%, 3 to 5 passes of a vibrator roller were needed.

- Macro tests for the definition of dry density, water content and sieve analyses were performed.
- Bench marks were installed to assess the correlation between the settlements and the number of passes.
- After a careful analysis 6 passes of the vibrator roller were recommended for layers with 1.0 m of thick.

8.2.2.3 Seismic Studies

Figure 8.25 represents the geodynamic of the basin and the influence of the Eurasian plate and the African plate.
Figure 8.26 ilustrates the Geodynamic context of the North -Africaine site. Model Level 1.
Table 8.5 shows the historic seismic activity.
Figure 8.27 presents the historic and instrumental seismicity in Argelie (NEIC).
The Earthquake instrumentation network is indicated in Figure 8.28.
Following A.S. 55 the seismic zones are ilustrated in Figure 8.29.
Figure 8.30 shows the isoacceleration curves for a return period of 1000 years (Mortgat et Shah, 1978).

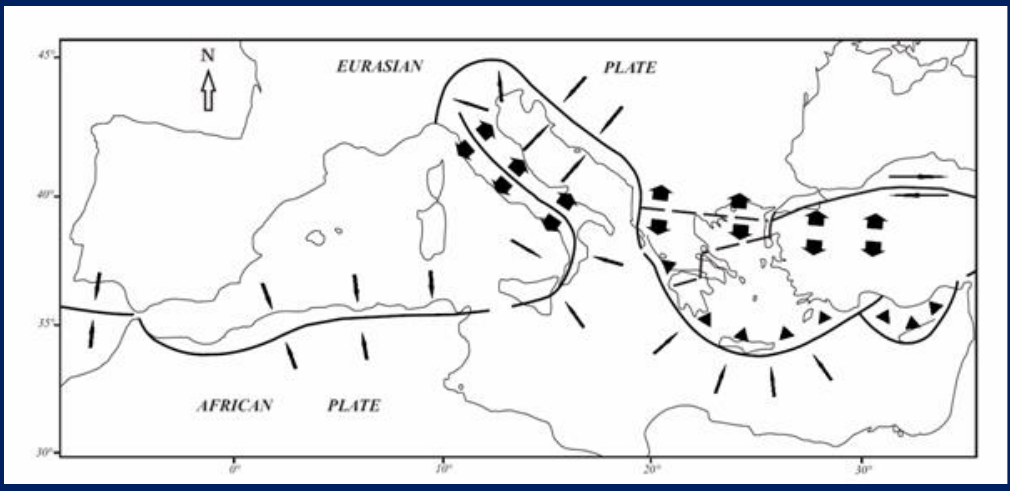

Figure 8.25 Géodynamique of the Méditerranéen basin (Ayadi)

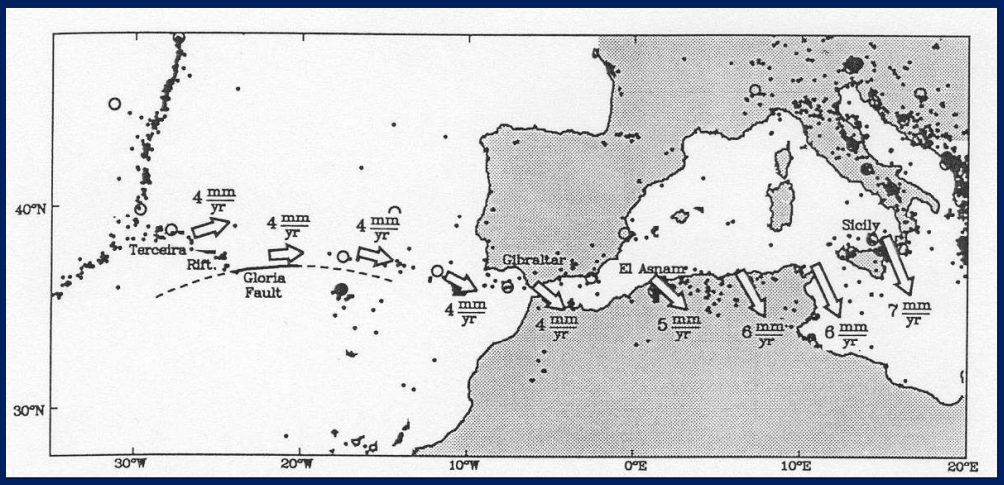

Figure 8.26 Geodynamic context of the North -Africaine site. Model Level 1 (Argus et. al., 1991 Issu de eost.ustrasbg.fr, M. Megrahoui)

Table 8.5 Activité sismique historique (Bezzeghoud et al, 1994)

Localité	Date	I_0	M	Victimes	Observations
Alger	**03-01-1365**	**Forte**	**Forte**	**Plusieurs**	Destructeur : **Alger complètement détruite. 100 répliques pendant la nuit. Une partie d'Alger fut inondée.**
Alger	**10-03-1673**	**Forte**	**Forte**	**??**	Destructeur : **Comparable au séisme de 1716, avec 71 répliques.**
Atlas Métidjéen	**03-02-1716**	**X**	**7.5**	**20000**	**Destructeur : Alger il y a eu plusieurs maisons détruites. Plusieurs répliques (4, 5, et 26 février ainsi qu'en mai et juin).**
Alger	**29-11-1722**	**Forte**	**Forte**	**Plusieurs**	**Violent choc à Alger. Peu de dégâts. A *75* km au SW d'Alger: plusieurs maisons détruites. Plusieurs des personnes tuées. Similaire au séisme de 1716.**
Oran	**09-10-1790**	**IX-X**	**6.5-7.5**	**2000**	Destructeur : **Dégâts au pied des monts de Murdjajo. 3 importantes répliques :19 octobre (I_0=V) ; 21 octobre (I_0=V), 25 octobre (I_0=VI-VII). Ressenties à Malte.**
Mascara	**??-03-1819**	**IX**	**6.5**	**??**	**Dégâts importants à Mascara. Oran peu de dégâts.**
Blinda	**02-03-1825**	**X-XI**	**7.5**	**7000**	**Destruction de Blida et peu de dégâts à Alger. 11 importantes répliques ont été ressenties entre le 2 et 6 mars.**
Djidjelli	**22-08-1856**	**X**	**7.5**	**??**	Destructeur : **Un raz de marées a été observé le long du littoral (Alger, La Calle, Batna, Nice, St. Pierre de Sardaigne, Mahon, ...). Le précurseur du (21 août) et le choc principal ont détruit les 3/4 des habitations à Djijelli et le reste de la ville a connu de sérieux**

					dégâts. les répliques ont été ressenties jusqu'en Octobre. La réplique la puis importante a atteint une intensité I_0=VIII.
Kherba	**09-03-1858**	**IX**	**6.5**	**??**	Destructeur : **La région située entre El Attaf et Aïn Defla a été complètement détruite et les dégâts se sont même étendus jusqu'au Nord-Est de Oued Chellif. Ce séisme a été fortement ressenti à au moins 110 km et jusqu'a la plaine de la Mitidja. Répliques: 12 mars et 14 mai.**
Mitidja	**02-01-1867**	**X-XI**	**7.5**	**100**	Destructeur : **Mouzaïa a été complètement détruite. 160 blessés. Ressenti à Blida, El Affroun, Oued Djer, Bourkika, Koléa, Boufarik, Cherchel, Tipasa, Marengo, Douéra, Alger, Médéa, Duperré… Des traces de surfaces ont été constatées à Djebel Nador. Plusieurs répliques.**
Aurès Biskra	**16-11-1869**	**IX**	**8.5**	**30**	**Dégâts Biskra et ses alentours. Ressenti à Batna et Sétit. Mouvement vertical observé. 11 répliques ressenties du 16 au 20 novembre.**
El Kalaâ	**29.11.1887**	**IX-X (VIII)**	**6.5-7.5**	**20**	Destructeur : **El Kalaâ et Dehba : une mosquée ainsi que plusieurs maisons ont été détruites. Thiouanet: importants dégâts (80 maisons ont été complètement détruites). Ressenti à Oran, Arzew, Relizane, Mostaganem et Mascara. Forte réplique ressentie quelques minutes après**
Gouraya	**15.01.1891**	**X**	**7.5**	**38**	Destructeur : **Dégâts importants: Gouraya et Villebourg ont été complètement détruites. 53 immeubles et maisons détruis ou endommagés. Dégâts à Cherchell, kherba, Blida, El-Affroun, Mouzaia, Miliana et Orléansville. Mouvement vertical observé à Gouraya. Ressenti à Saida et Djelfa. Fortes répliques. Rayon macrosismique 200 Kms**

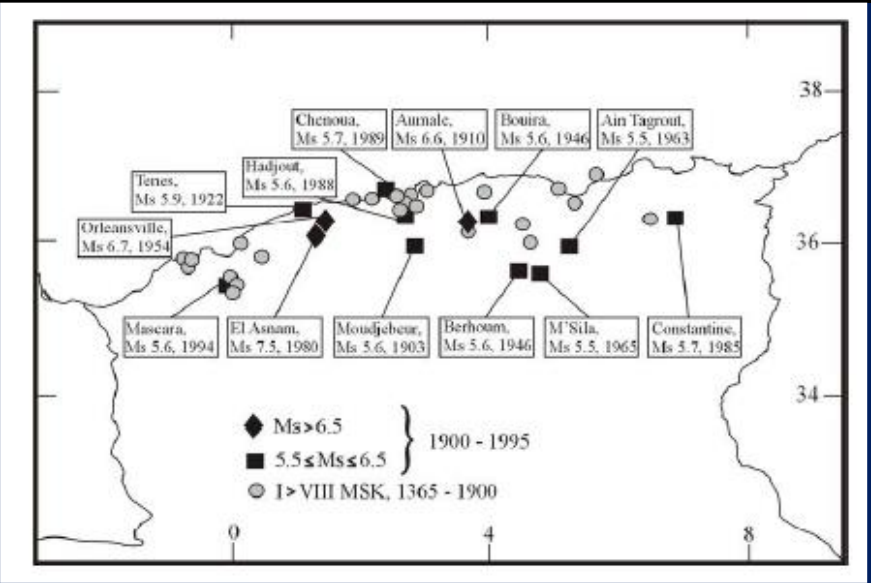

Figure 8.27 Historic and instrumental seismicity in Argelie (NEIC)

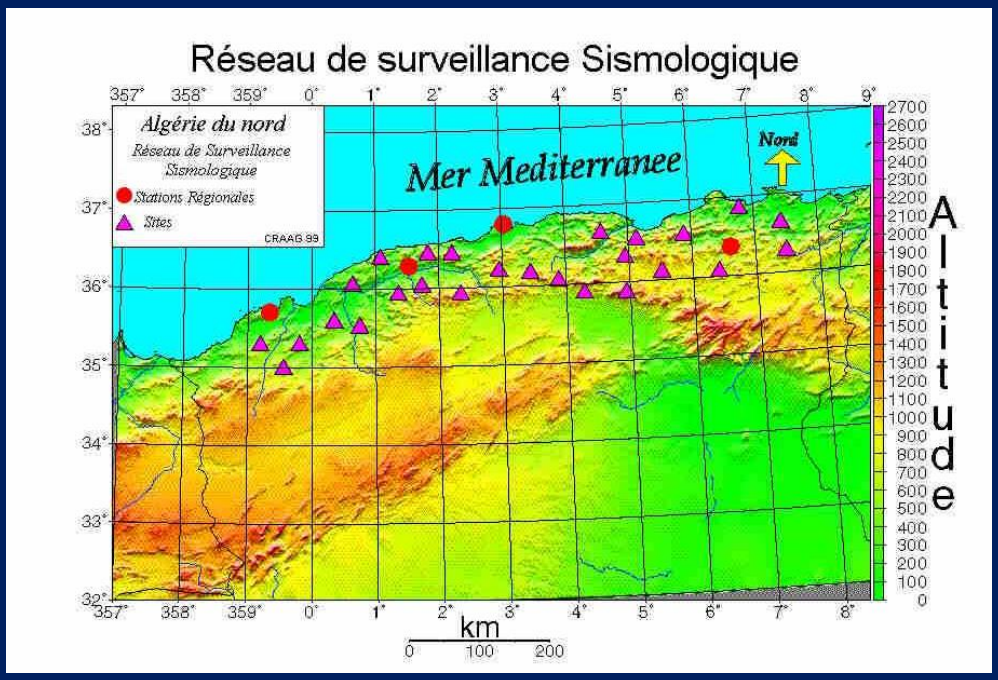

Figure 8.28 Earthquakes instrumentation network

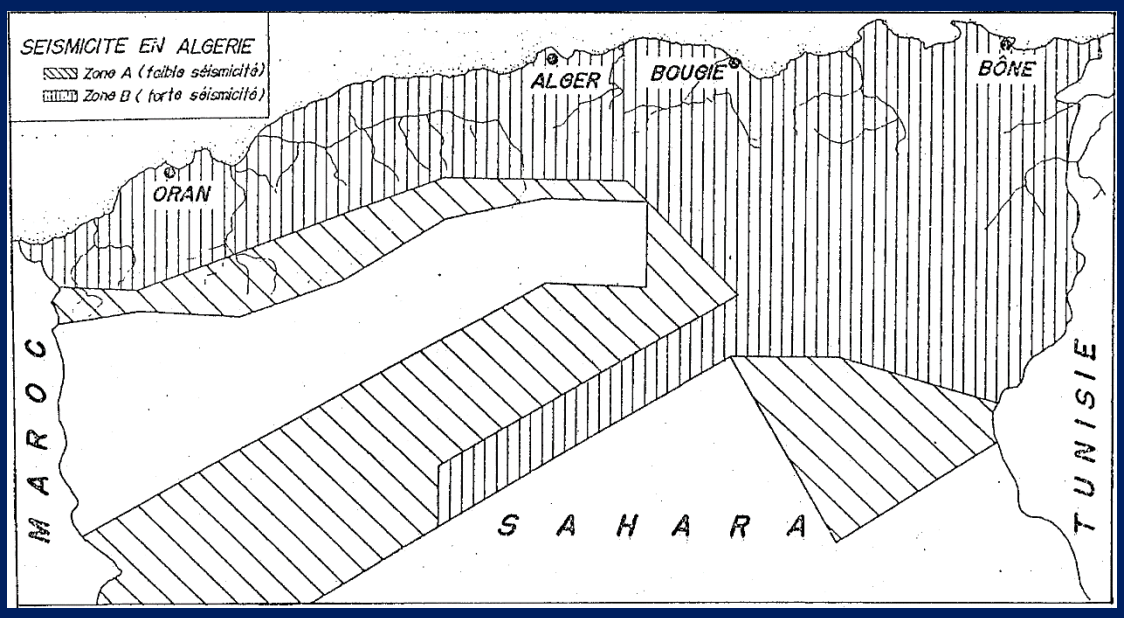

Figure 8.29 Seismic zones from A.S. 55.

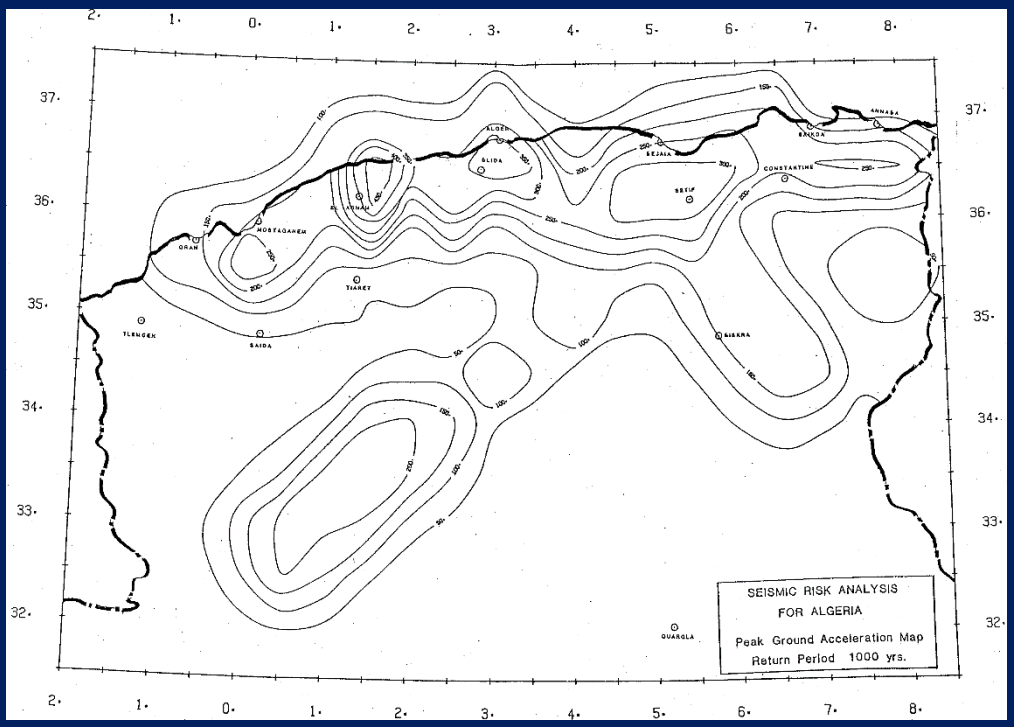

Figure 8.30 Isoacceleration curves for a return period of 1000 years (Mortgat et Shah, 1978).

In summary : It was considered for the OBE (Operating Basis Earthquake) a value defined in the Algerian Code (RPA 99) and for MCE (Maximum Credible Earthquake) a higher value.

Table 8.6 presents a summary of the maximum acceleration values for earthquakes OBE and MCE.

Table 8.6 Maximum acceleration values

Earthquake	Acceleration [g]
OBE	0.15
MCE	0.25

The pseudo-static analyses assuming elastic behavior for the material were performed and the computed safety factors were higher than 1.

8.2.2.4 Simplified Displacements Analyses

Sarma (1975) method and Makdisi and Seed (1977) method, described in item 7. 6.3, were used to compute the displacements.

8.2.2.5 Dam Lay-out

The dam lay-out is illustrated in Figure 8.31.

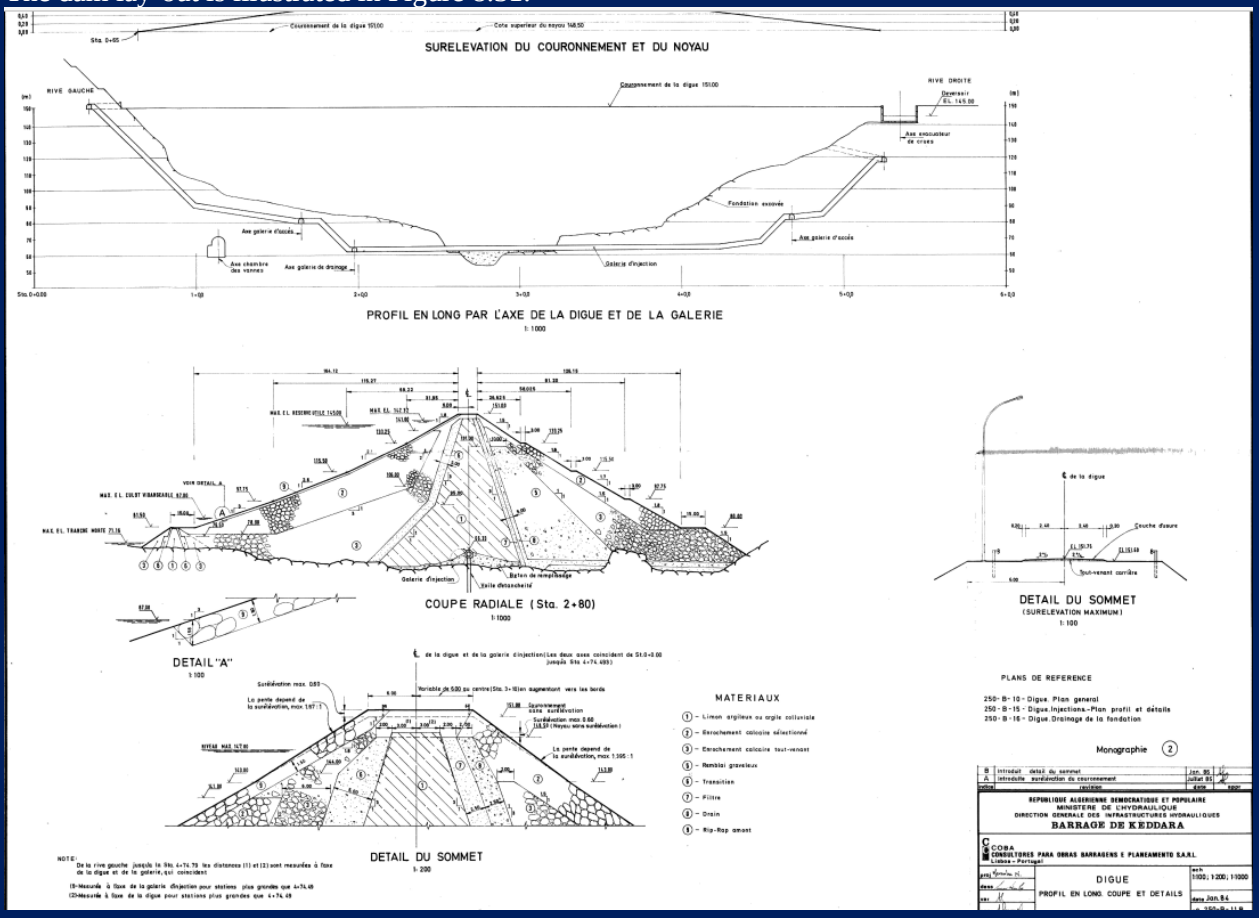

Figure 8.31 dam layout

Figure 8.32 Dam view

Figure 8.32 illustrates the dam view.

8.2.2.6 Instrumentation

The instrumentation plan has included:

- bench marks
- hydraulic piezometers in the embankment;
- hydraulic piezometers in the gallery
- total cells;
- electric pore pressures;
- inclinometers;
- meteorological station;
- flow devices;
- Devices for measurement of reservoir level;
- Devices for measurement of temperature, wind, precipitation and evaporation;
- 1 central measurements station.

The frequency of the measurement was also defined following the reccomendations of ICOLD (Bulletin 41).

8.2.2.7 25 May 2003 earthquake

On May 2003 an earthquake of magnitude 6.8, with a depth of 10 km, occurred 40 km East Alger, provoking 2270 deaths. The earthquake record is presented in Figure 8.33.
The earthquake occurred in the boundary region between the Eurasian plate and the African plate. Along this section, the African plate is moving northwestward against the Eurasian plate with a velocity of about 6 mm per year. The relative plate motions create a compressional tectonic environment, in which earthquakes occur by thrust-faulting and strike-slip faulting.

In Keddar rockfill dam, with 106 m high, located 30 km from the fault, only 1 longitudinal crack and transverse cracks were observed at the dam crest and no leakage were observed in the gallery, as illustrated in Figure 8.34.
A value of 0.34 g was recorded in rock.
.

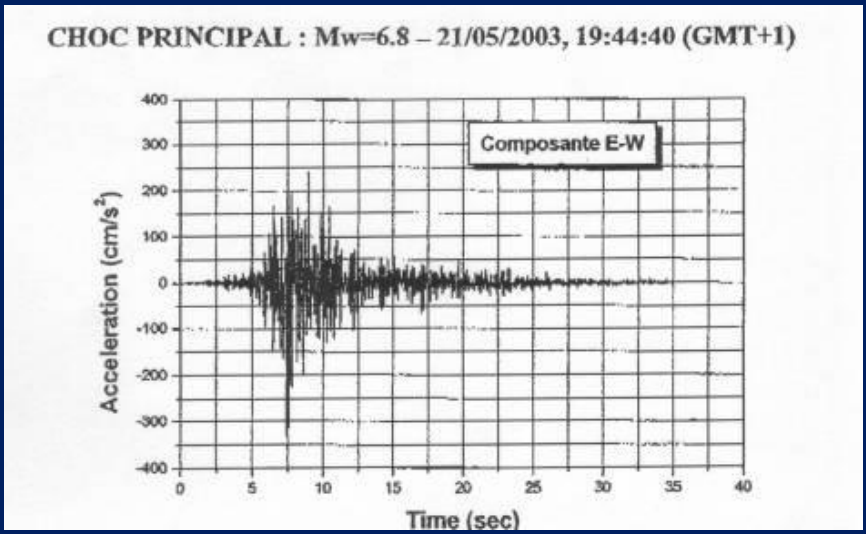

Figure 8.33 Earthquake record

Figure 8.34 (a) Observed transversed cracks at dam crest

Figure 8. 34(b) No leakage inside the gallery

In summary: The dam behaviour during the May 2003 earthquake was in good agreement with the results of pseudo-static analysis and with the predicted displacements values by Sarma and Makdisi-Seed methods.

Lesson nº 2: The statistics of dam behaviour during the occurrence of earthquakes presented by the ICOLD has shown that well designed and constructed rockfill dams exhibit a good behaviour for strong ground motions.

Past experience demonstrates that compacted rockfill dams with powerful vibrators rollers exhibit a good behaviour during the occurrence of earthquakes.

Note: The dam project was conducted by a multidisciplinary COBA team and the author was involved in the seismic design.

8.2.4 Case History nº 3 - Kerrada Dam (Argélie)

8.2.4.1. Introduction

For Kerrada dam the geotechnical characteristics are referred, the tectonic characteristics are described, the definition of design earthquake is discussed, the performance based design is analyzed, the dam profile is introduced, the stability analyses are presented, the dynamic analysis is addressed and the foundation treatment is discussed.

8.2.4.2 Geotechnical Characterization

For Kerrada Dam 26 boreholes were performed with collecting of undisturbed samples for laboratory tests.
The boreholes have allowed the characterization of the rock materials related the weathering and fracturation and also the execution of Lugeon tests.
Laboratory tests were performed namely identification tests and shear tests.

The materials for the core will be submitted to identification test (sieve analyses and Atterberg limits) and Proctor tests.
In addition, direct shear tests and triaxial shear tests were performed in order to define the strength parameters c (cohesion) and ϕ'(friction angle).

A great number of rock properties were defined by the index properties. These properties show the reaction of the rock for the exterior actions and can be used for design purposes.
The index properties are easily defined by conventional laboratories, allow the classification of rock materials and are useful for design purposes. The index properties are very attractive for the researchers and practitioners due its simplicity. The index properties are defined by the following tests: porosity, density, absorption water content, velocity of elastics waves, compression tests, crushing tests, point load strength test, slake durability test and expansibility test.

The ground investigation report has included the Presentation of Geotechnical Information and Evaluation of Geotechnical Information.
The Presentation of Geotechnical Information with documentation of the methods procedures and results has included all relevant reports of: the field investigations, like sampling, field tests and groundwater measurements and of the laboratory tests.

The Evaluation of the Geotechnical Information has included:
- a review of the field and laboratory work.
- a review of the derived values of geotechnical parameters;
- the range and any grouping of derived values of the geotechnical data for each stratum.

8.2.4.3 Tectonic Conditions

The tectonic conditions should include tectonic mechanisms, location and description of faults (normal, inverse, stryke and reverse) and estimation of fault activity (average slip rate, slip per event, time interval between large earthquake, length, directivity effects, etc.), these factors are important to assess the involved risk.

Figure 8.35 shows the focal mechanisms of earthquakes located in North of Algérie.

The foundation properties for soil materials are estimated by geophysical tests (crosshole tests, seismic downhole tests and refraction tests), SPT tests, CPT tests, seismic cone and pressurometer tests.

An active fault is a fault, identified and located, known to have produced historical fault movements or showing geologic evidence of Holocene (11 000 years) displacements and which, because of its present tectonic sitting, can undergo movements during the anticipated life of man-made structures.

The current practice is the deterministic approach in which the seismic evaluation parameters were ascertained by identifying the critical active faults which show evidence of movements in Quaternary time.

Dense recording GPS arrays with sampling rate allow determining deformation rates in seismic active regions. Intrinsic properties of rock at depth have to be obtained in situ by deep drilling into active faults. Computational with high resolution model for stress and deformations in communicating fault systems should be developed. A better exploration of microtremors technique, directivity effects and attenuation laws is needed.

Surface fault breaking i.e. surface slip along an identified fault zone under the dam is considered as the most dangerous tectonic scenario for dam safety.

Algérie is located between two tectonic plaques: Eurasienne plaque and Africaine plaque. In general, the earthquakes were generated by an inverse fault related with the compression movement of tectonic plaques Eurasienne and Africaine. It is also important to refer the earthquakes generated by the faults, e.g. Thénia fault responsible for the 21 May 2003 earthquake is illustrated in Figure 8. 36.

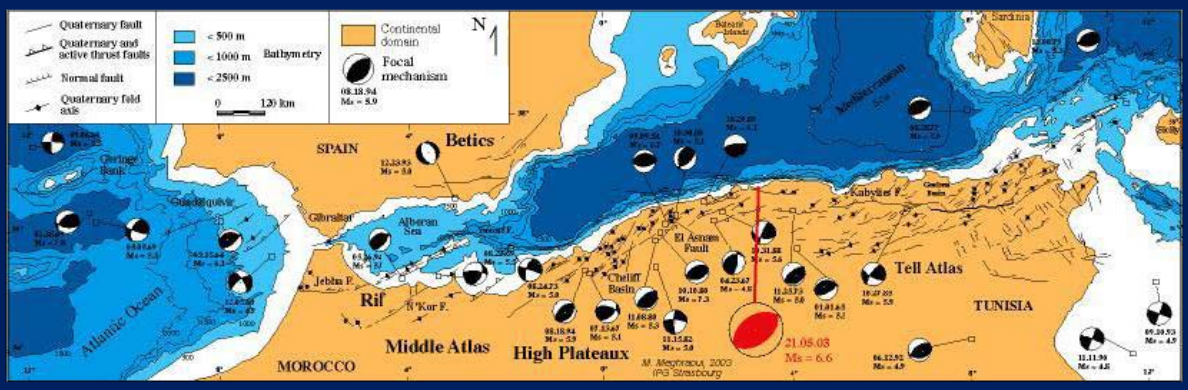

Figure 8.35 Focal mechanisms of earthquakes located in North of Algérie (http:\\eost.u-strasbg.fr)

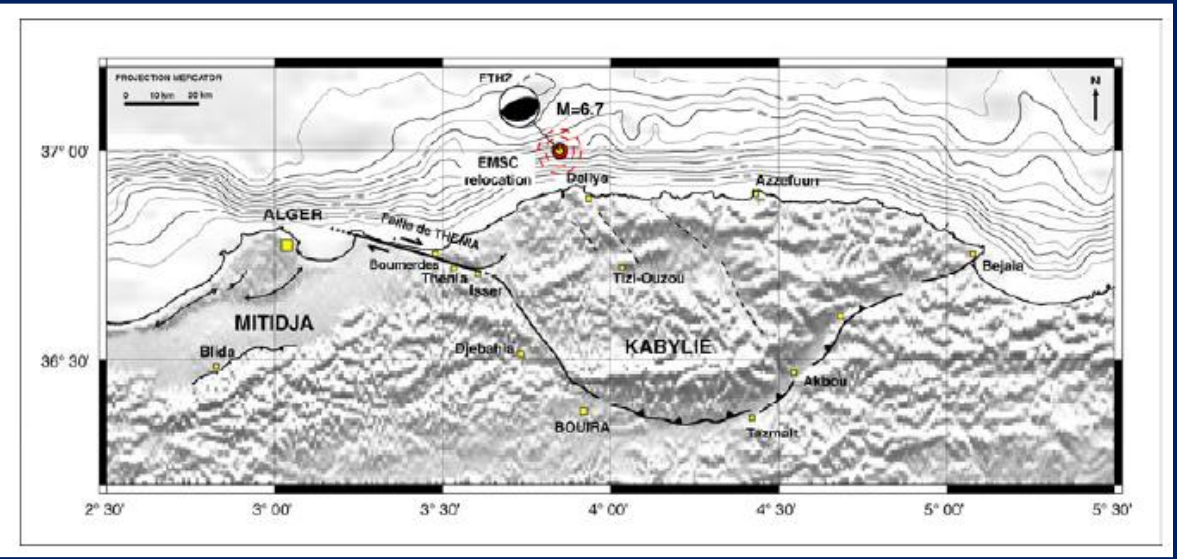

Figure 8.36 Thenia fault and location of 21 May 2003 earthquake (http:\\eost.u-strasbg.fr)

8.2.4.4 Design Earthquake

The definition of design earthquake for Kerrada dam located in the highest seismicity zone of Algérie (R.P.A. 99/version 2003) was performed by probabilistiques methods (Cornell-Mcguire method and experimental method). 7 zones of seismic generation were defined: a) zone 1-Mostaganem and Oran; b) zone 2-El Asnam, c) zone 3-Alger, Sous El Choziane and Bejaia, d) zone 4-Constantine, e) zone 5-Mts of Ksour, f) zone 6-West 1 and g) zone 7-West 2.

SELECTION OF SEISMIC DESIGN ACTION

The selection of seismic design parameters for dam projects depends on the geologic and tectonic conditions at and in the vicinity of the dam site

The regional geologic area should cover, as a minimum, a 100 km radius around the site, but should be extended to 300 km to include any major fault or specific attenuation laws

2 levels, namely MCE (Maximum Credible Earthquake) for a return period of 500-1000 years and OBE (Operating Basis Earthquake) for a return period of 145 years, with a probability of exceeding in 100 years less than 50%,

The definition of design earthquake for Kerrada dam located in the highest seismicity zone was performed by probabilistic and experimental methods. 7 zones of seismic generation were defined: a) zone 1-Mostaganem and Oran; b) zone 2-El Asnam, c) zone 3-Alger and Bejaia, d) zone 4-Constantine, e) zone 5-Mts of Ksour, f) zone 6-West 1 and g) zone 7-West 2.

The seismic design parameters considered for Kerrada dam are summarized in Table 8.7.

Table 8.7 Seismic Design parameters

Type	Earthquake	Acceleration(gals)	Predominant Period(s)
Near	OBE MCE	210 330	0.35 to 0.45 0.35 to 0.45
Far	OBE MCE	150 230	0.55 to 0.80 0.60 to 0.85

8.2.4.5 Performance Basis Design

The new trend for performance basis design is to consider 2 levels of seismic actions and to analyse the situation when the limit of force balance is exceeded for high intensity ground motions associated with a very rare seismic event.

For the design two basic requirements are defined: (i) Non collapse requirement (ultimate limit states) i.e. after the occurrence of the seismic event the structure shall retain its structural integrity, with respect to both vertical and horizontal loads, and adequate residual resistance, although in some parts considerable damage may occur, (ii) Minimization of damage (serviceability limit state) after seismic actions with high probability of occurrence during the design life of the structure some parts can undergo minor damage without the need of immediate repair. The structure shall be designed and constructed without the occurrence of damage and the associated limitations of use, the costs of which would be disproportionately high in comparison with the costs of the structure itself.

Acceptable level of damages in performance based design shown in Table 8.8 are specified by a combination of structural and operational damage.

Table 8.8 Acceptable level of damage in performance based design

Acceptable level	Structural	Operational
Degree I: Serviceable	Minor or no damage	Little or no loss of serviceability
Degree II. Repairable	Controlled damage	Short term loss of serviceability
Degree III: Near Collapse	Extensive damage in near collapse	Long term or complete loss of serviceability
Degree IV Collapse	Complete loss of structure	Complete loss of serviceability

The pseudo-static analyses assume a rigid or elastic behaviour for the material (Ambraseys, 1960) and have the limitation that the seismic coefficient acts in one direction for an infinite time.

8.2.4.6 Dam Profile

Kerrada dam is 760 m long and 85 m height. It is a zoned dam with a clay core and shells with grey materials. There are filter materials at the interfaces between the core and the shells. The inclination of upstream shell is 1/1.1 (V/H) and of downstream shell is 1/1.5(V/H).
The dam profile is shown in Figure 8.37.

The sieve analyses of the different material that integrated the dam profile are illustrated in Figure 8.38.

The Table 8.9 summarizes the mechanical characteristics that incorporates the dam.

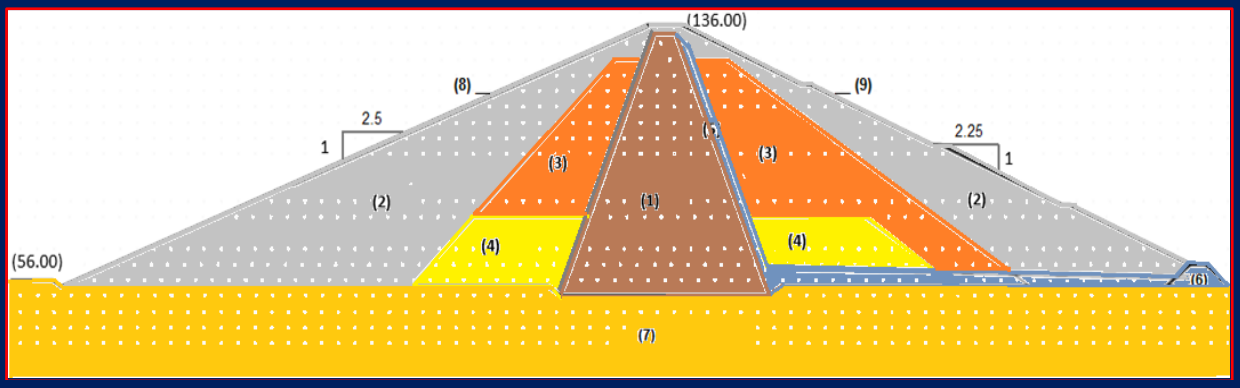

Figure 8.37 Dam profile

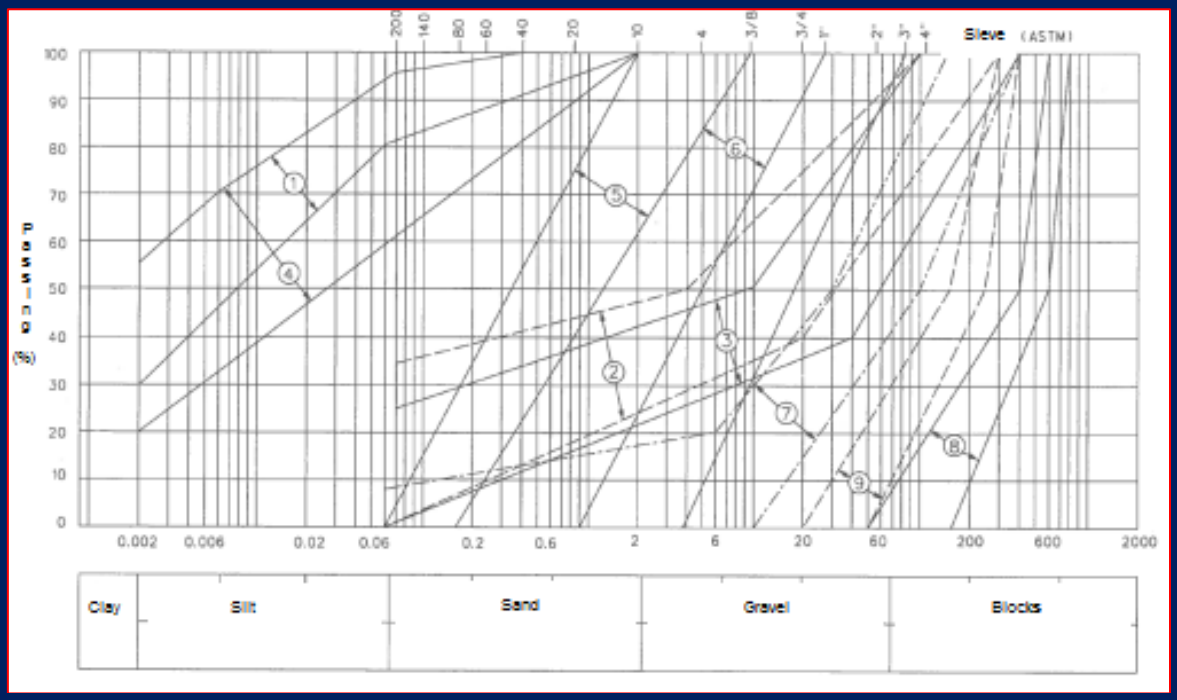

Figure 8.38 Sieve analyses of the different materials

Table 8.9 Mechanical Characteristics of the Materials

Mechanical Characteristics of the Materials

Materials	Density (kN/m3)	Cohesion (kPa)	Friction Angle (°)	r_u
Core (1)	19	5	25	0.3
Marnes and clay of shells (4)	20	0	28	0.3
Soft Grey of shells (3)	21	0	30	0.15
Compact Grey of shells (2)	21	0	36	0.15
Filters and Drains (5)	20	0	35	-
Downstream Toe (6)	22	0	40	-
Foundation (7)	20	50	32	-

8.2.4.7 Stability Analysis

Static Analysis

A computer code SLOPE W was used to analyze the slope stability of the dam profiles.

It is current practice to analyze: construction phase, filling of reservoir and drawdown.

Taking into account the geometry of the dam a pseudo-static analysis was performed.

The obtained safety factors value for the analysis of different phases are shown in Table 8.10.

Table 8.10. Static Safety Factors

Situation	Safety Factor
Construction Phase (Upstream shell)	1.62
Construction Phase (Downstream shell)	1.44
Filling of Reservoir (Downstream shell)	1.67
Rapid Drawdown (Upstream shell)	1.31

For the filling of the reservoir the critical failure surface is shown in Figure 8.39.

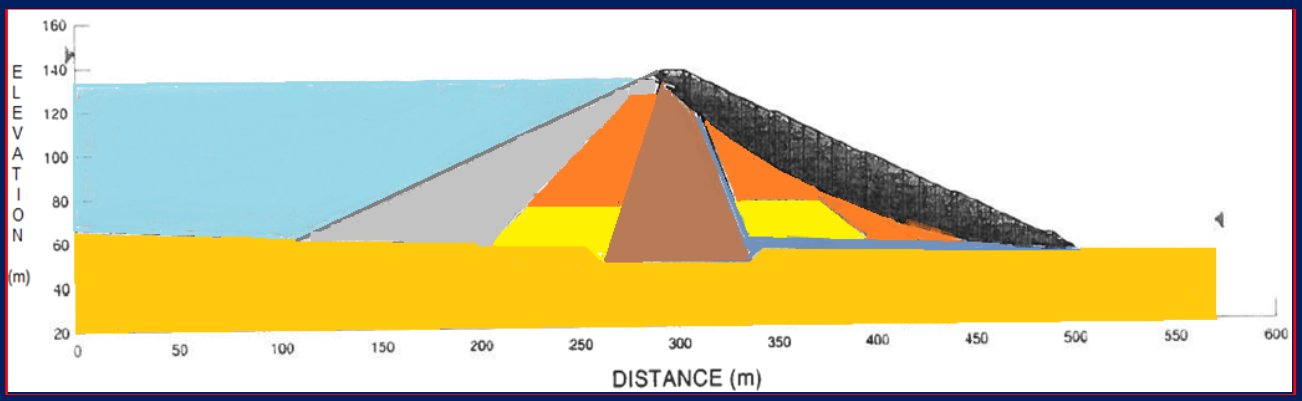

Figure 8.39 Filling of dam reservoir-Minimum safety factor

Pseudo-static Analysis

The pseudo –static analyses for the construction phase, drawdown and filling of reservoir have incorporated the amplification of seismic coefficients and the increment of pore pressure due the seismic actions.

PSEUDO-STATIC SAFETY FACTORS

Situation	Minimum Safety Factor
Construction Phase (Upstream shell)	1.37
Construction Phase(Downstream shell)	1.22
Filling of Reservoir (Downstream shell)	1.0
Rapid Drawdown (Upstream shell)	1.03

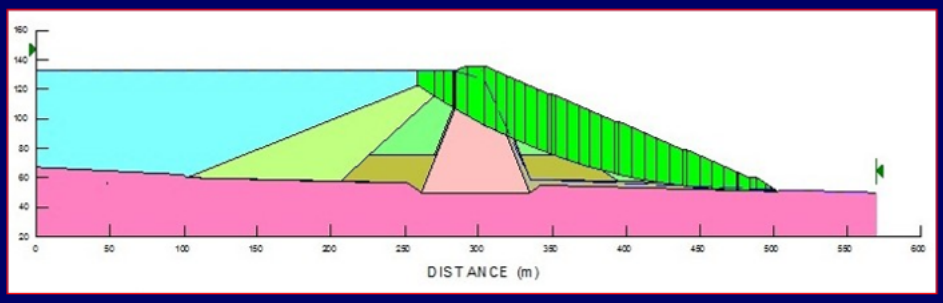

Figure 8.40 Filling of dam reservoir-Minimum safety factor

The critical surface for the pseudo-static analysis related the filling of the reservoir is shown in Figure 8.40.

8.2.4.8 Pseudo- Dynamic Analysis

The formulations of Newmark (1965), Sarma (1975) and Makdisi and Seed (1977) described in item 7.6.3 were used.

Related Makdisi and Seed method for the OBE earthquake the computed displacements for Kerrada dam were:

- for the near earthquake between 129 mm and 167 mm;
- for the far earthquake between 94 mm and 220 mm

For the SSE earthquake the computed displacements were:

- for the near earthquake between 622 mm and 738 mm;
- for the far earthquake between 511 mm and 763 mm.

The Sarma method has given computed displacements of the same order.

8.2.4.9 Dynamic Analysis

The FLAC 6.0 numerical code, with a Mohr-Coulomb model with hysteretic damping (Itasca, 2009), was used to perform the dam response for acceleration time history record of the earthquake that has occurred in Argelie on 23 May 2003. Due to space limitations only, some results are presented.

Figure 8. 41 illustrates the acceleration response at the base, at the middle and at the core crest.

Figure 8. 42 shows the acceleration response at the upstream shell and at the downstream shell.

Figure 8. 43 presents the effective shear stress computed at the middle of the core.

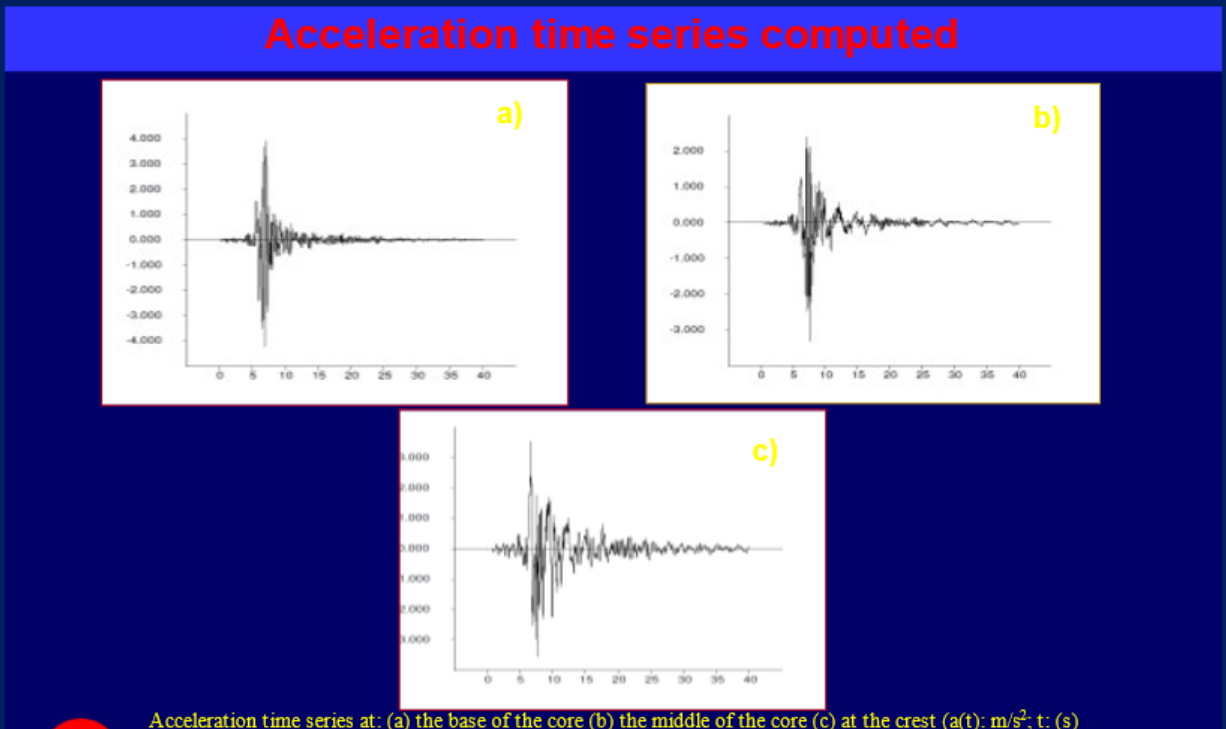

Figure 8. 41 Acceleration response at the base, at the middle and at the core crest

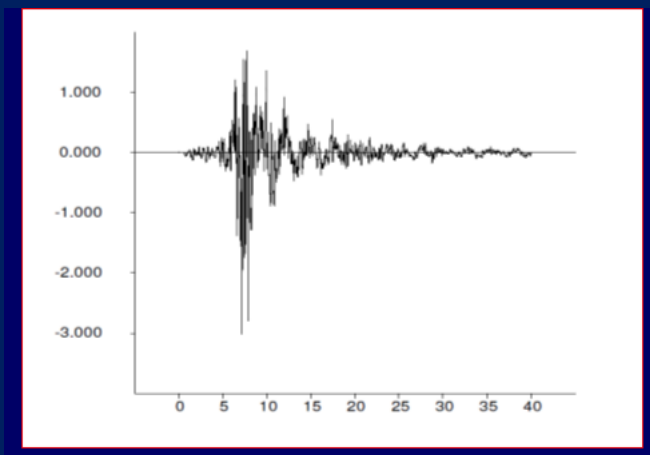

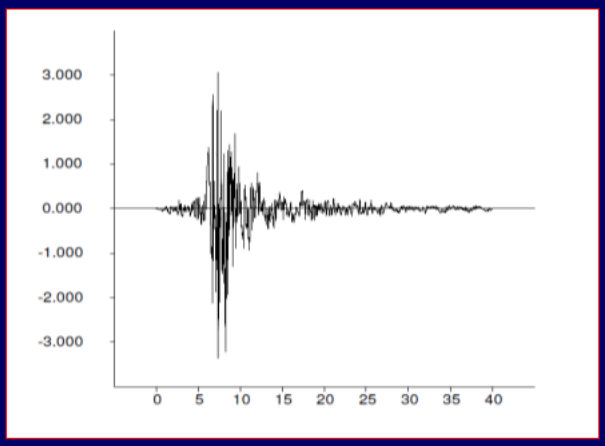

Figure 8. 42 Acceleration response at the upstream shell and at the downstream shell

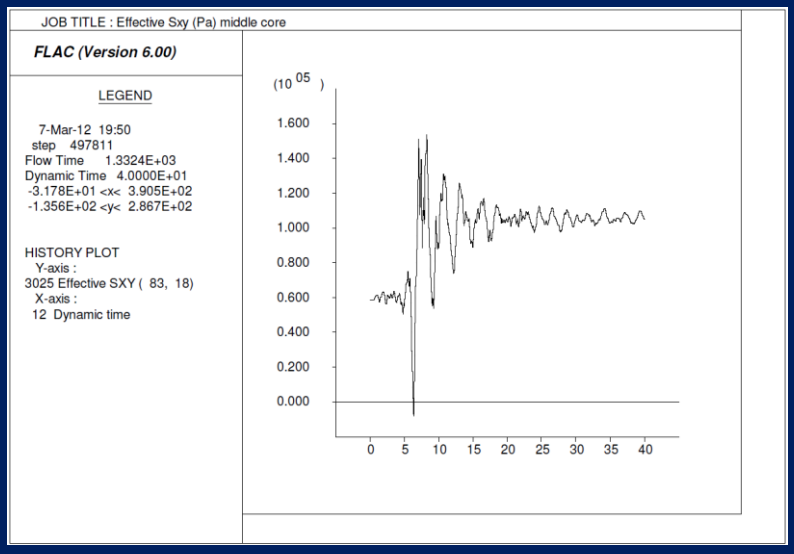

Figure 8. 43 Effective shear stress computed at the middle of the core

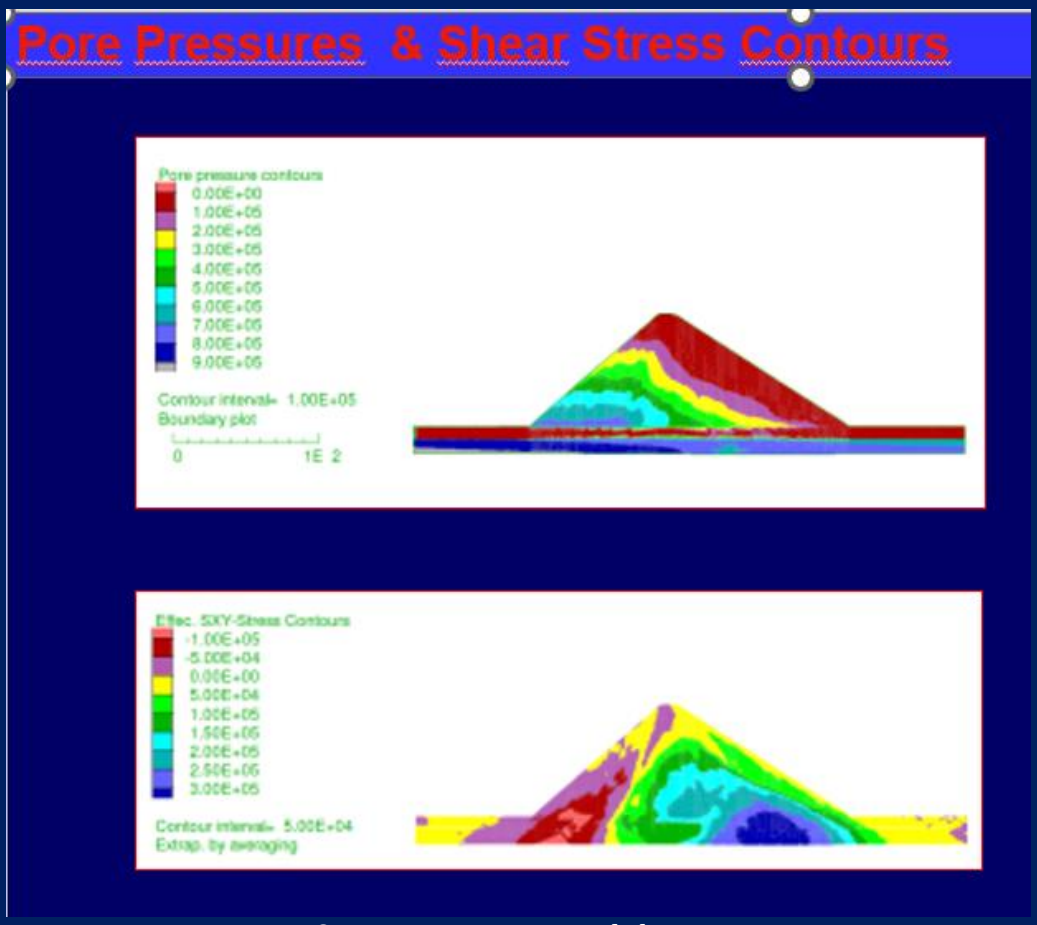

Figure 8.44 Pore pressures and shear contours

Figure 8.44 shows the excess pore pressures fill contours, pointing the deamplification due to the water effects, and the dam effective shear stress contours computed, at the end of the earthquake.

.

CONCLUSIONS

1.The definition of design earthquake for Kerrada dam located in the highest seismicity zone of Algérie was performed by probabilistic methods.

2. Algérie is located between two tectonic plaques: Eurasians plaque and African plaque. In general the earthquakes were generated by an inverse fault related with the compression movement of tectonic plaques Eurasians and African, but it is also important to refer the earthquake generated by Thénia fault responsible for the 21 May 2003 earthquake.

3. The computed static safety factors for the different dam phases were acceptable.

4. The computed safety factors for pseudo static analyses for different dam phases were higher than 1.

5. For the pseudo-dynamic analyses the computed displacements by Makdisi-Seed and Sarma methods were of the same order and were incorporated in the definition of the dam freeboard.

6. The dynamic analysis performed for the real earthquake time history acceleration (Algerie-23 May 2003) gave a better insight related the accelerations and shear stress values and the distribution of the pore water pressures.

8.2.4.10 Foundation treatment

FOUNDATION TREATMENT

- Impermeabilization of foundation due to the existence of thick grey pervious material with impervious marnes materials
- To improve the mechanical strength as the dam is 85 m high
- The foundation treatment has integrated the consolidation treatment and a grout curtain
- The consolidation treatment with 10 to 15 m depth has the purpose to improve the foundation superficial zone with vertical grout holes in quinquonce and 4 m apart. The maximum grout pressure was 4 bars

FOUNDATION TREATMENT

- The grouting equipment should allow a continuous flow and a grounting pressure of 1.0 MPa
- The volumetric mixturer to prepare the mixtures with the desire precision (1 a 2%)
- Equipment of high turbulence to allow a colloidal suspension and the minimum time of mixture was 2 minutes
- The mixture of grout was sent to a reservoir to assure a continuous mechanical agitation
- The grouting pump allows the measurement of the pressure and the value of the flow
- The manometers had an adequate accuracy. The total amplitude of manometers has not exceeded 2 times the maximum allowed pressure
- The packer shall assure the adequate impermeability not allowing seepage between walls of the hole

TYPE OF GROUTS

- The grouts were composed by cement, bentonite, water and additive
- The sand has a percentage of 10% of particles with size less than 0.1mm
- The water has a low percentage of sulphates and other colloidal materials
- The bentonite exhibits an index of plasticity superior to 400%
- The grouts were submitted to viscosity tests, density tests, decantation tests with intervals 5, 15, 30, 60 and 120 minutes, uniaxial strength after 1 day and 7 days and setting time
- The viscosity was assessed by Marsh cone

GROUTING CONTROL

INJECTION GROUTING COMPOSITION

The injection grouting has the following composition, namely:

- Grout I and II (ratio cement: water = 1:0.2) (with 2% of bentonite in weight)
- Grout III (ratio cement: water = 1:1) (without bentonite)
- Grout IV (ratio cement: water = 1:1.5) (with 2% of bentonite in weight)
- Grout V (ratio cement : water = 1:2) (with 3% of bentonite in weight).

INJECTION GROUTING

- The grouts bentonite-cement have not shown decantation higher than 5%, after 1 hour
- The grout curtain was performed from the injection gallery with 3 m high, 2 m width and 680 m long
- The diameter of grout holes was 50mm
- In the right abutment the grout holes were 35 m to 50 m long, in the central part of the dam the grout holes were 35 m to 55 m and in the left abutment the grout holes were 50 m to 90 m
- The gout curtain had one row with the primary holes 24 m apart, the secondary holes 12 m apart, tertiary holes 6 m apart and quaternary holes 3 m apart

Lesson nº 3: Dam behaviour during earthquakes contributes to update and implement national codes.

The two design levels of MCE and OBE is well accepted, but there is still some controversy related the criteria to select the recurrence periods for MCE and OBE.

Are the ICOLD recommendations well accepted?

Note: The dam project was conducted by a multidisciplinary COBA team and the author was involved in the geotechnical design.

8.2.5 Case History nº 4 - Koudiat Ben Aida Dam (Argelie)

8.2.5.1 Introduction

Pour la barrage de Koudiat Ben Aida dam, les characteristics geologiques et sismiques sont decrits, investigation du site est presenté, la definition du seisme du projet est addressé, l´avant projet est analysé, les structure hydrauliques décrits et le plan d`instrumentation et index de risque est presenté.

8.2.5.2 Geologic et Seismique Etudes

Barrage de Koudiat ben Aida est situé dans la région de M'Sila. La chaîne Atlasique est orientée Est-Ouest et s'étend du Maroc à l'Ouest jusqu'à la Tunisie à l'Est; au Nord, est limité par la Méditerranée et, au Sud, par la grande faille Sud-Atlasique (Figure 8.45). C'est une région mobile très plissé, structurée par l'orogénèse alpine, englobant le domaine Tellien, les Hautes Plaines et l'Atlas Saharien (Figure 8.46).

Saharien se compose de dépôts sédimentaires de plateforme épicontinentale jusqu'à 10 000 mètres d'épaisseur, qui ont été moyennement plissées et fracturés. Les roches et matériaux actuels se composent de grès, d'argiles, de marnes et de roches calcaires se situe sur une limite majeure entre deux plaques tectoniques: la plaque Eurasienne et la Plaque Africaine (Figure 8.47).

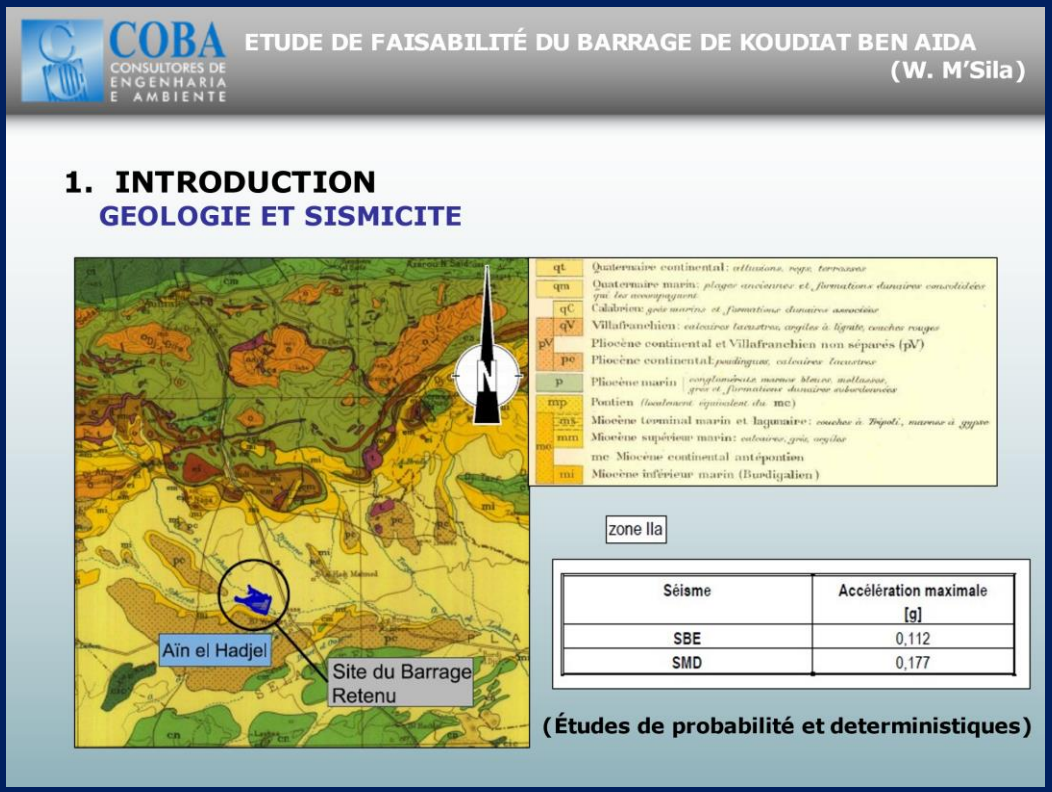

Figure 8.45 Geologie et Sismicité

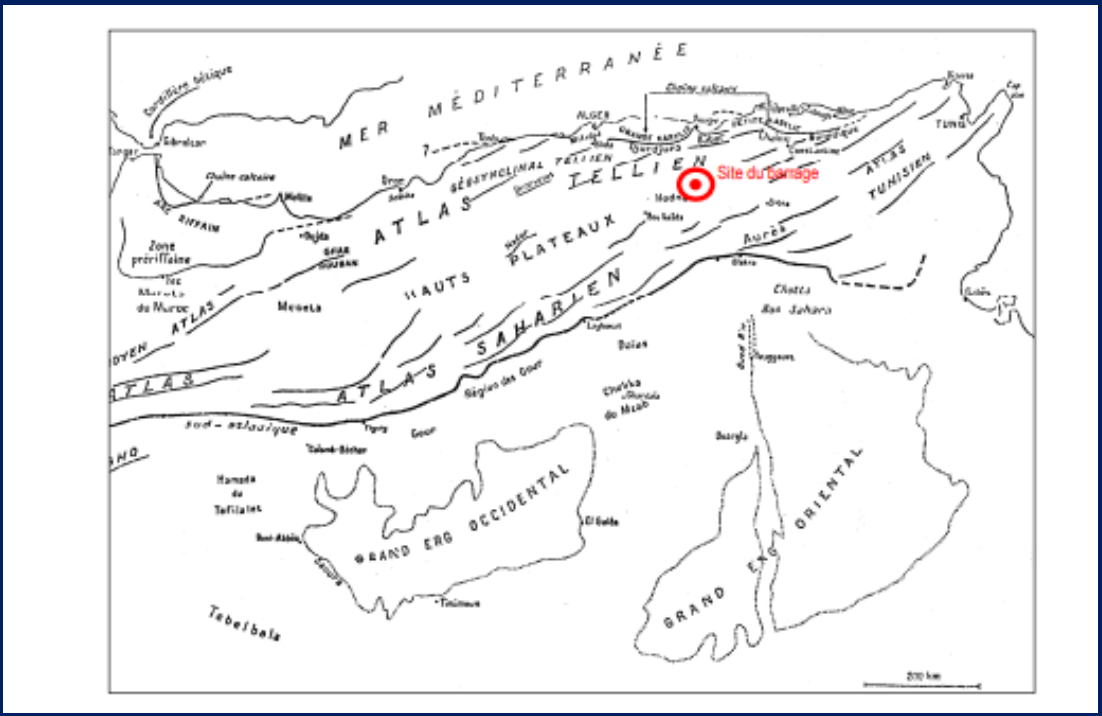

Figure 8.46 Carte des Montagnes d'Atlas et du Sahara Nordique (Hamdache, 1998)

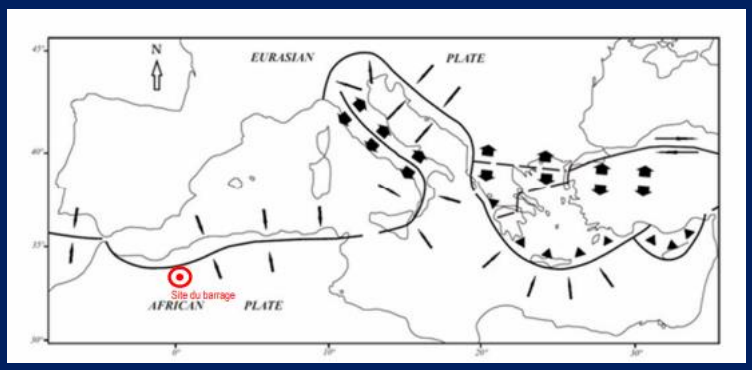

Figure 8.47 Géodynamique du bassin Méditerranéen (Ayadi, 2003)

La Figure 8.48 montre que la zone de M'sila est une dépression plio-quaternaire.

La Figure 8.49 ilustre Carte géologique de la région de M'Sila.

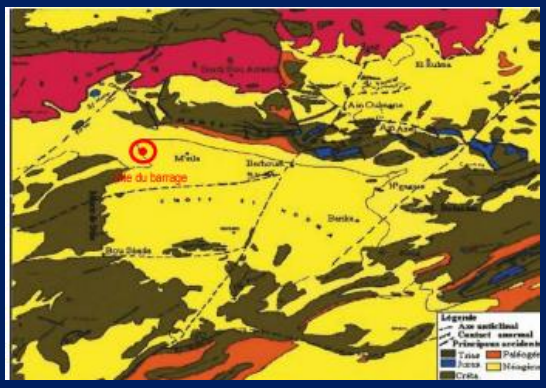

Figure 8.48 Zone de M'sila est une dépression plio-quaternaire

Figure 8.49- Carte géologique de la région de M'Sila – Boussaada avec la zone subsidente Site du barrage

8.2.5.3 Investigation du Site

La Figure 8.50 montre l` investigation du site.

Figure 8.51 ilustre la geometrie du vallée.

Figure 8.52 montre les conditions geologiques de la fondation du barrage.

Figure 8.53 ilustre les materiaux de construction.

Les Figures 8.54 au 8.56 presente le profil du barrage: Variant B1A, Varaint B1B, Variant B1C.

Les Figures 8.57 au 8.59 ilustre le profil du barrage: Variant B2A, Varaint B2B, Variant B2C.

Figure 8. 60 montre les zones sources.

Figure 8.50 Investigation du site

Figure 8.51 La geometrie du vallé

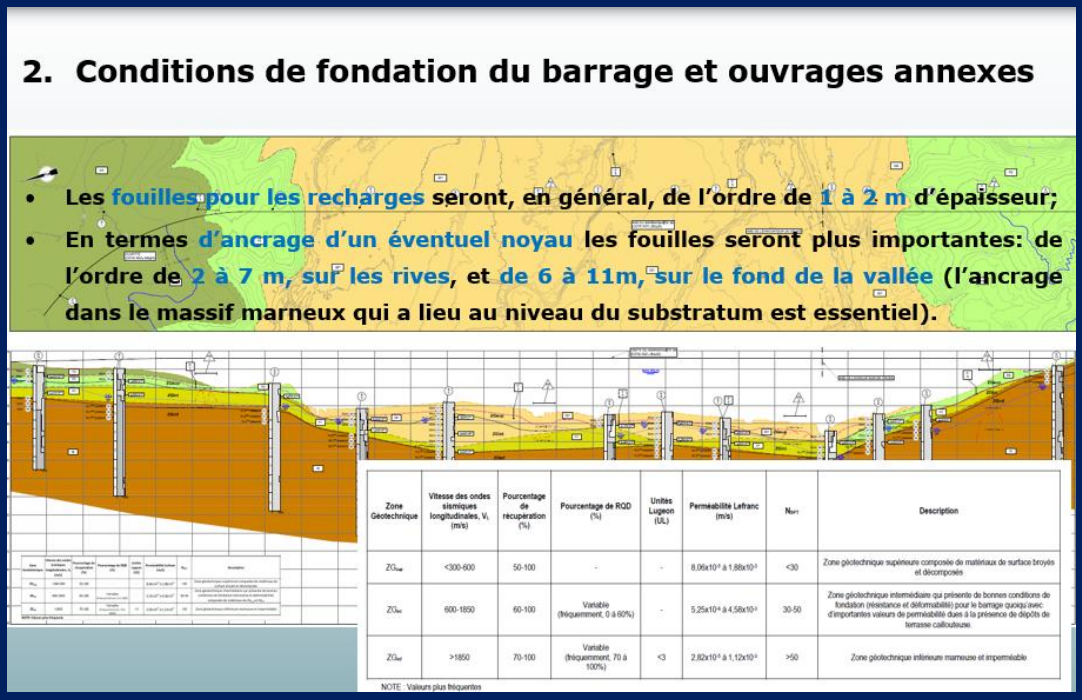

Figure 8.52 Conditions de fondation du barrage

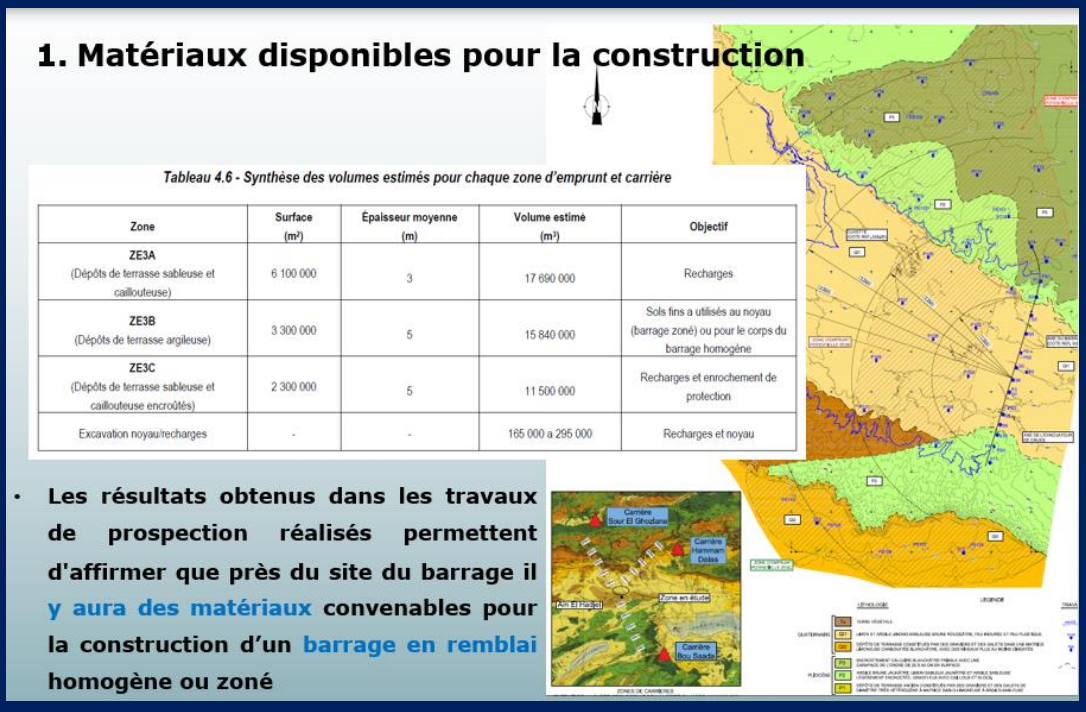

Figure 8.53 Materiaux disponibles pour la construction du barrage

Essais In situ (1)

Sondages
Essai pressiomètrique
Essai dilatomètre

Sondages à laTarrière
Puits de reconnaissance

Essais In situ (2)

- Sondages à percussion ou à rotation avec carottage continue du massif de fondation, appuis et ouvrages hydrauliques annexes
- Sondages avec carottage continue aux zones de carrières

- Essais de perméabilité du type Lefranc
- Essais de perméabilité du type Lugeon
- Essais SPT (Standard Penetration Test)
- Installation de piézomètres

Essais de Laboratoire (1)
Échantillons de Sols

- Analyse granulométrique par tamisage
- Analyse granulométrique par sédimentation
- Essai de dispersivité
- Limites d´Atterberg
- Teneur en eau
- Proctor Normal
- Densité des particules
- Dosage des matières organiques
- Porosité
- Cisaillement direct
- Essais triaxiaux de type consolidé non drainé (CU), avec mesure de la pression interstitielle (3 essais)

Essais de Laboratoire (2)
Échantillons Rocheux

- Essai d'abrasion Los Angeles
- Essai micro Deval sec et humide
- Analyse pétrographique
- Essai Brésilien
- Résistance à la compression simple

Pour bien maîtriser l'influence à long terme de l'eau sur les matériaux rocheux, les deux derniers types d'essai au devront être exécutés sur des échantillons secs et saturés.

8.2.5.4 Variantes du barrage

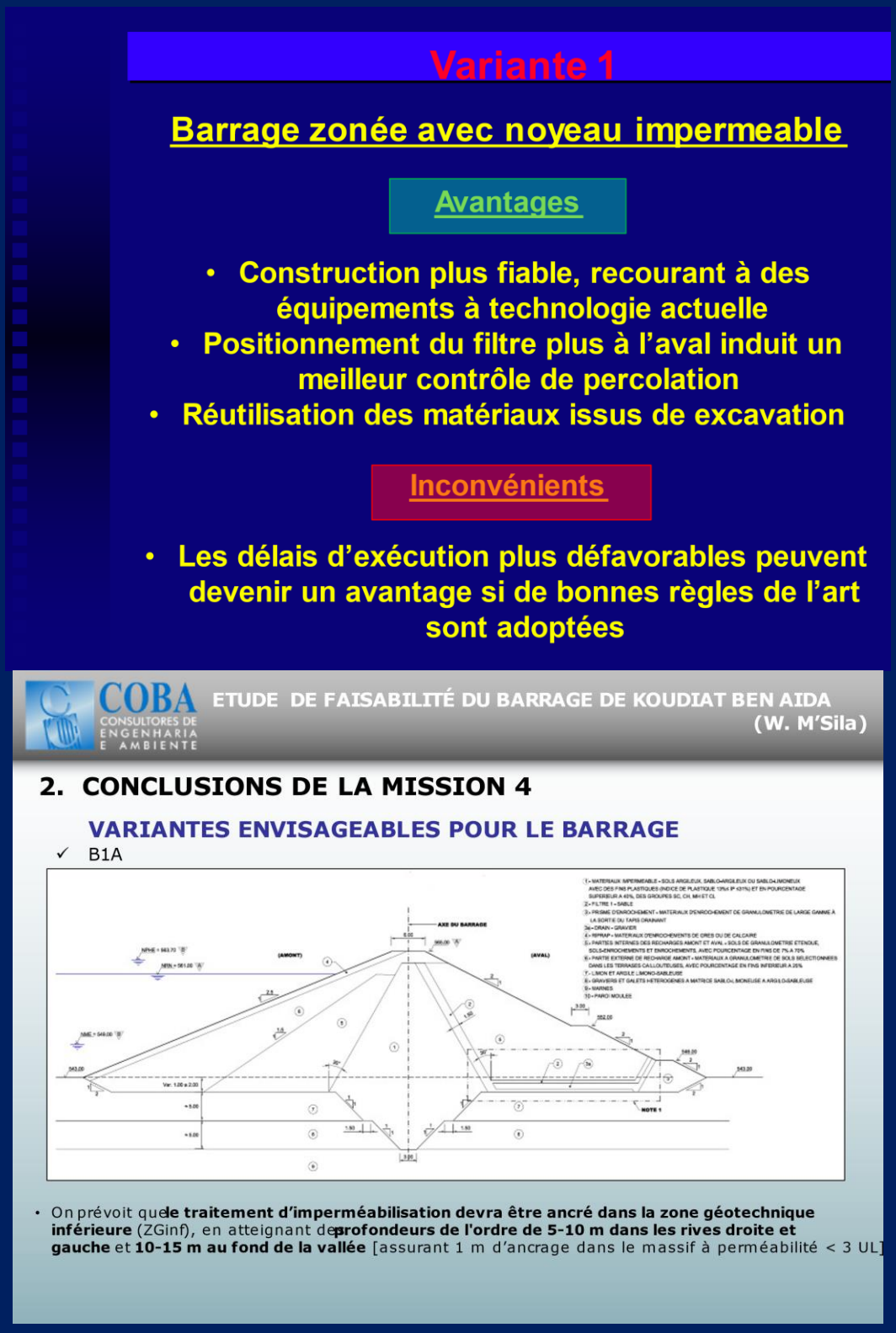

Figure 8.54 Variantes du barrage -Variante B1A

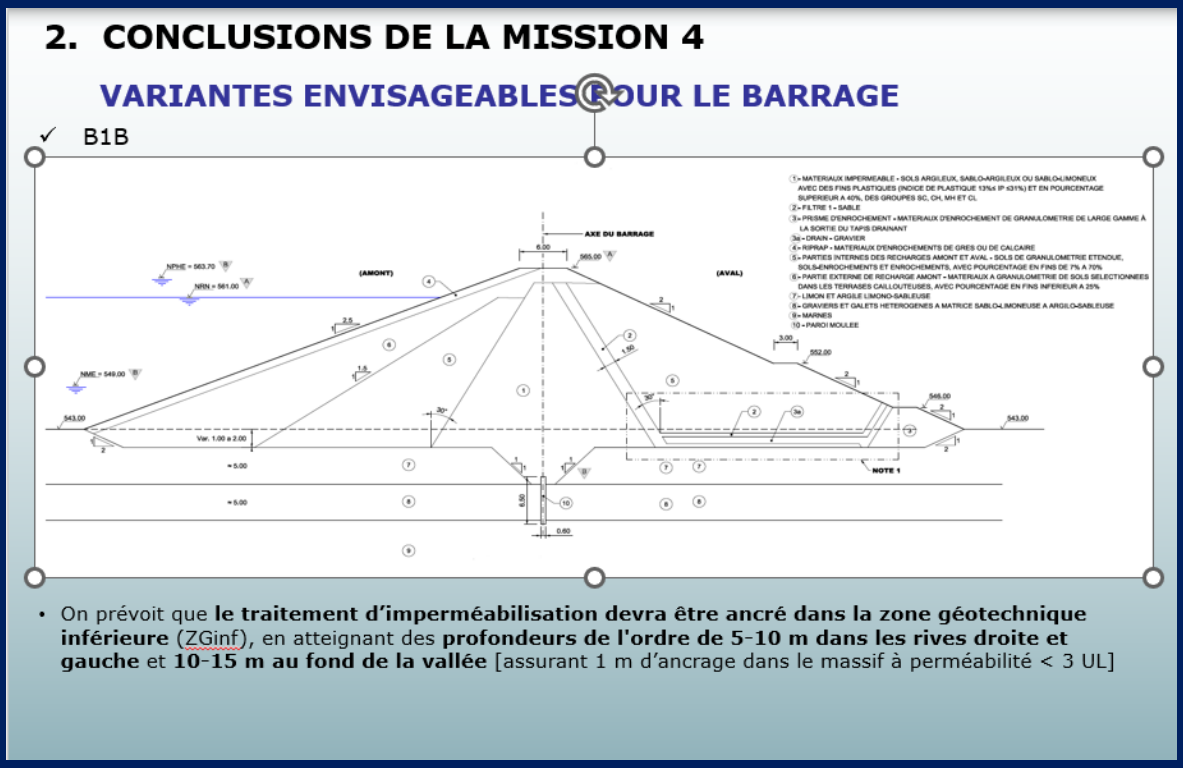

Figure 8.55 Variantes du barrage -Variante B1B

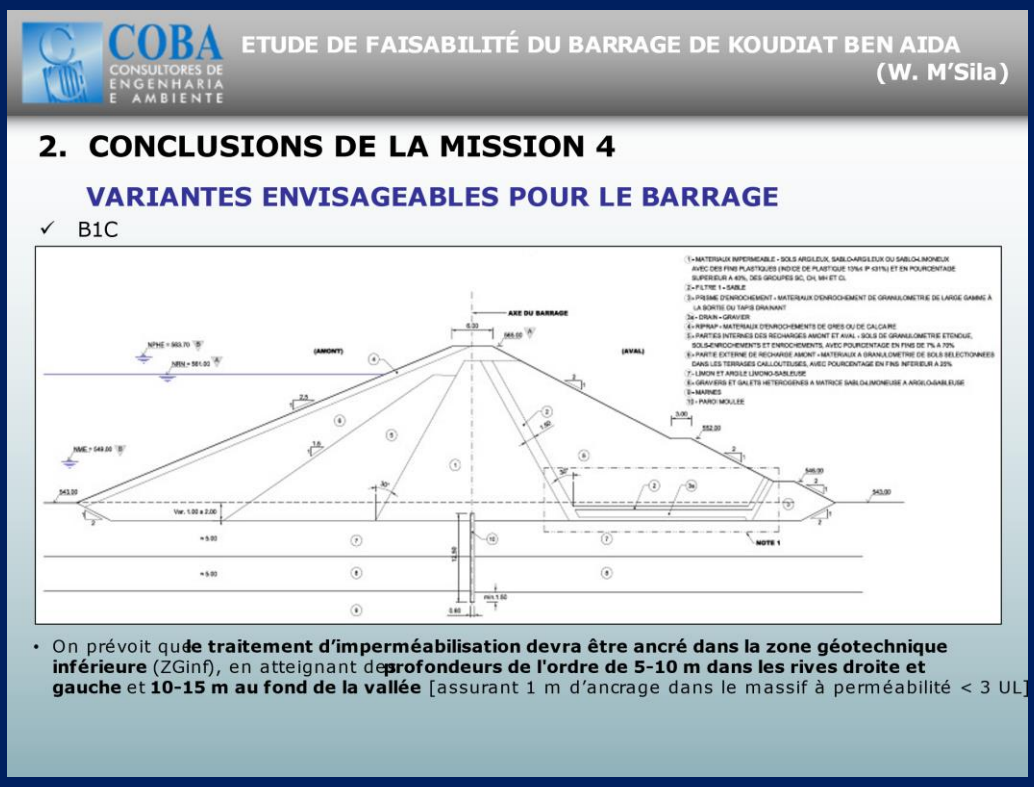

Figure 8.56 Variantes du barrage -Variante B1C

Variante 2

Barrage homogène avec filtre sous vertical et geomembrane au amont

Avantages

Une légère réduction de délais de réalisation des terrassements

Inconvénients

Dispositive imperméable à l`amont est délicat pour garantir l`étanchéité

2. CONCLUSIONS DE LA MISSION 4

VARIANTES ENVISAGEABLES POUR LE BARRAGE

✓ B2A

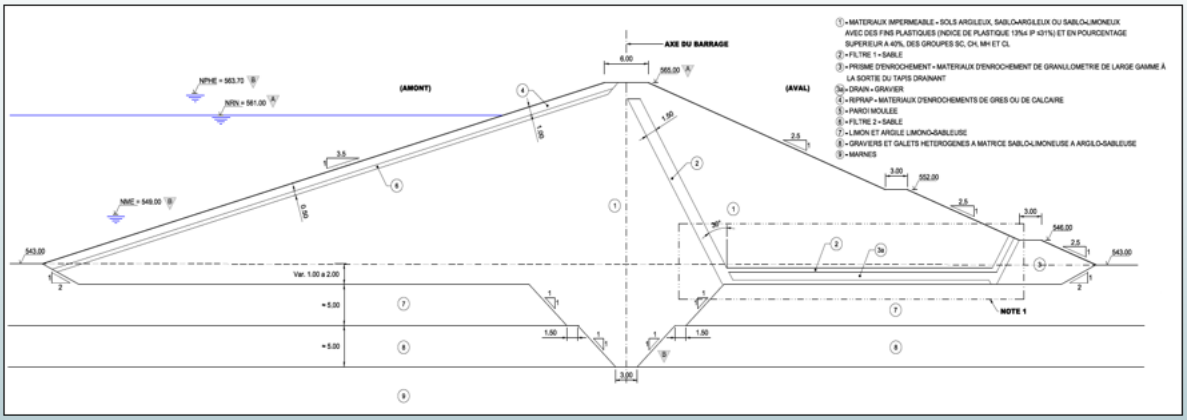

- On prévoit que **le traitement d'imperméabilisation devra être ancré dans la zone géotechnique inférieure** (ZGinf), en atteignant des **profondeurs de l'ordre de 5-10 m dans les rives droite et gauche** et **10-15 m au fond de la vallée** [assurant 1 m d'ancrage dans le massif à perméabilité < 3 UL]

Figure 8.57 Variantes du barrage -Variante B2A

2. CONCLUSIONS DE LA MISSION 4

VARIANTES ENVISAGEABLES POUR LE BARRAGE

✓ B2B

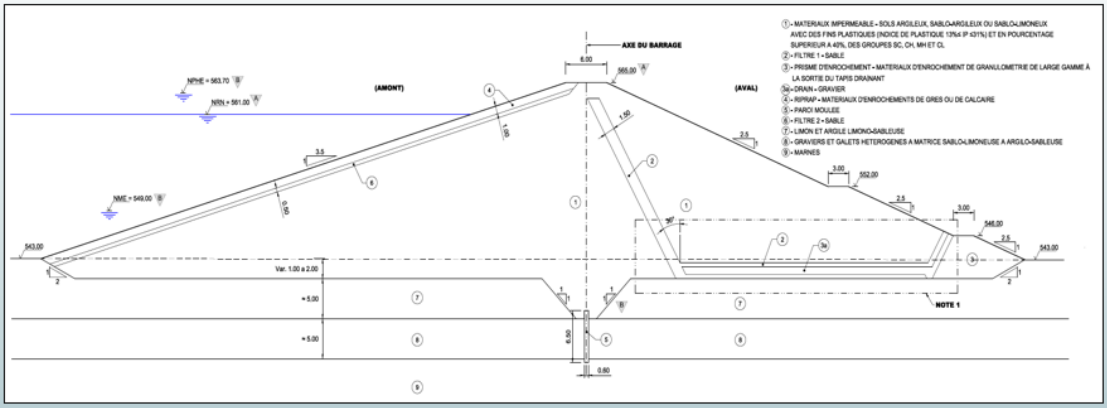

- On prévoit que **le traitement d'imperméabilisation devra être ancré dans la zone géotechnique inférieure** (ZGinf), en atteignant **des profondeurs de l'ordre de 5-10 m dans les rives droite et gauche** et **10-15 m au fond de la vallée** [assurant 1 m d'ancrage dans le massif à perméabilité < 3 UL]

Figure 8.58 Variantes du barrage -Variante B2B

2. CONCLUSIONS DE LA MISSION 4

VARIANTES ENVISAGEABLES POUR LE BARRAGE

✓ B2C

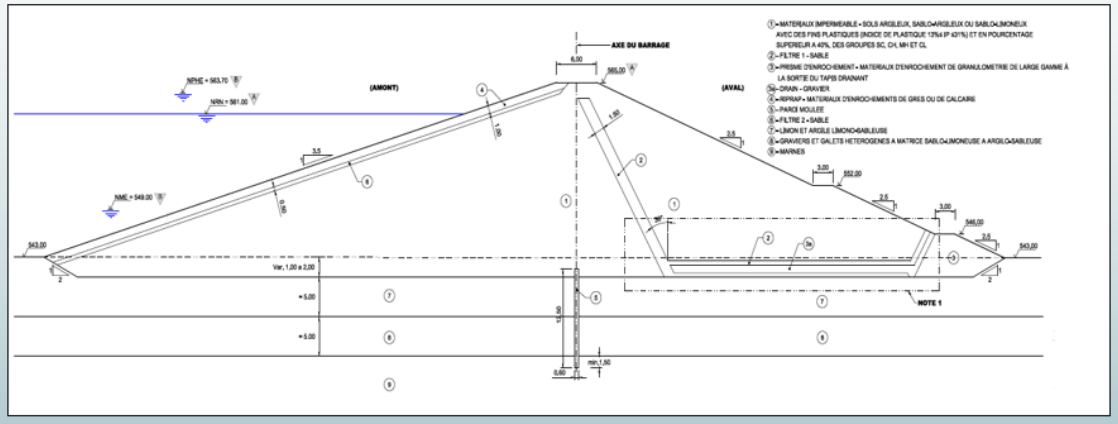

- On prévoit que **le traitement d'imperméabilisation devra être ancré dans la zone géotechnique inférieure** (ZGinf), en atteignant des **profondeurs de l'ordre de 5-10 m dans les rives droite et gauche** et **10-15 m au fond de la vallée** [assurant 1 m d'ancrage dans le massif à perméabilité < 3 UL]

Figure 8.59 Variantes du barrage -Variante B2C

8.2.5.5 Seismic Studies

APPROCHE PROBABILISTE

Basé sur les résultats d'études probabilistes par l'approche probabiliste on cherche à évaluer l'aléa sismique par une loi donnant la probabilité de dépassement sur le site de différentes valeurs de paramètres caractérisant le mouvement du sol. Connaissant les lois de répartition des intensités épicentrales (ou des magnitudes) pour toute zone source ayant une influence sur le site, on modélise l'atténuation de l'énergie depuis chacune d'elles vers celui-ci. L'étape finale consiste à calculer et combiner les effets de toutes zones sources, cherchant à déterminer la probabilité annuelle moyenne de dépassement d'une valeur donnée du mouvement du sol sur le site. L'application de ce calcul à toute une grille de points couvrant une région donnée, permet d'établir des cartes d'aléa sismiques sous différentes formes. Récemment, plusieurs études de ce type on été développées sur le Nord de l'Algérie (Hamdache, 1998; Hamdache et al., 2003, 2004; Peláez et al., 2006). Dans ces études, le territoire a été découpé en 14 zones sources de style sismotectonique homogène: 2 au Maroc (Sm1 et Sm2), 10 en Algérie (Sa1 à Sa10) et 2 en Tunisie (St1 et St2), Figure 8.60. Pour chaque zone source, on été développés des modèles de récurrence de la sismicité, suivant une loi de comportement fréquence-magnitude de forme exponentiel du type Gutenberg-Richter. Les résultats du calcul probabiliste de l'aléa on été représentés sous forme de courbes d'iso-valeur de l'accélération maximal (PGA) susceptible d'être dépassée sur le site pour une période de retour fixée. La Figure 8.61 présente la carte d'aléa sismique régional de la région maghrébine élaboré par Peláez et al. (2006).

Méthode expérimentale L'évaluation probabiliste d'aléa sismique peut être basée sur la méthode expérimentale, utilisant la sismicité concernant la période comprise entre 1365 et 2014, et en considérant, uniquement, les séismes de magnitude supérieure à 5 et distances épicentrales jusqu'à environ de 200 km, comme déjà vu dans la approche déterministe. La méthode expérimentale consiste dans l'analyse statistique des valeurs extrêmes à partir d'un échantillon global relatif à une période de n d'années. La méthode suit marche indiquée au-dessous: i. à partir de l'échantillon global on sélectionne l'événement le plus intense de chaque année, on construit ainsi un échantillon des valeurs plus hautes; ii. on ordonne l'échantillon obtenu, dans le dernier pas, par ordre croissant; iii. à chaque événement on attribue la probabilité n 1 j P + = , où j est le numéro d'ordre de l'échantillon ordonné et n est la dimension de l'échantillon. Cette probabilité (p) peut être rapportée avec la période de retour de l'événement (T) à travers l'expression 1 p 1 T – = . L'extrapolation de la valeur d'accélération associée à toute période de retour est faite en se basant sur l'ajustement de la courbe des paires de valeurs accélération maximale – période de retour. On constate que la représentation des points amax – P en graphique d'extrêmes du type est bien simulée par une courbe parabolique. Au graphique de la Figure 8.62, on a représenté les valeurs de probabilité associées à chaque événement et introduit la courbe qui a un meilleur ajustement au groupe de points. Au Tableau 8.11 et Tableau 8.12 on indique les valeurs de l'accélération maximale dans l'ordre croissant en fonction de la période de retour.

Tableau 8.11 Accélération máximale dans l'ordre croissant en fonction de la période de retour.

a (cm/s²)	T (années)	a (cm/s²)	T (années)	a (cm/s²)	T (années)
3,97	1,01	10,55	1,57	20,64	3,43
4,60	1,03	10,79	1,60	20,69	3,60
4,85	1,04	10,89	1,64	22,11	3,79
5,97	1,06	11,35	1,67	22,38	4,00
6,27	1,07	11,47	1,71	23,68	4,24
6,38	1,09	11,69	1,76	25,87	4,50
6,46	1,11	11,79	1,80	26,25	4,80
6,54	1,13	12,39	1,85	28,11	5,14
6,54	1,14	12,50	1,89	28,20	5,54
6,57	1,16	12,57	1,95	29,73	6,00
6,68	1,18	13,10	2,00	29,89	6,55
6,71	1,20	13,55	2,06	30,04	7,20
6,95	1,22	13,55	2,12	32,63	8,00
7,84	1,24	13,75	2,18	34,34	9,00
8,15	1,26	13,92	2,25	34,76	10,29
8,40	1,29	14,98	2,32	34,98	12,00
8,42	1,31	15,58	2,40	40,38	14,40
8,72	1,33	16,13	2,48	41,08	18,00
8,82	1,36	16,43	2,57	56,07	24,00
9,32	1,38	16,49	2,67	59,85	36,00
9,47	1,41	16,76	2,77	142,44	72,00
9,87	1,44	16,92	2,88		
10,11	1,47	17,68	3,00		
10,35	1,50	17,98	3,13		
10,36	1,53	18,86	3,27		

Tableau 8.12 Accélération maximale

Période de retour [ans]	Accélération maximale [cm/s²]
145	112
1 000	157
5 000	194
10 000	210

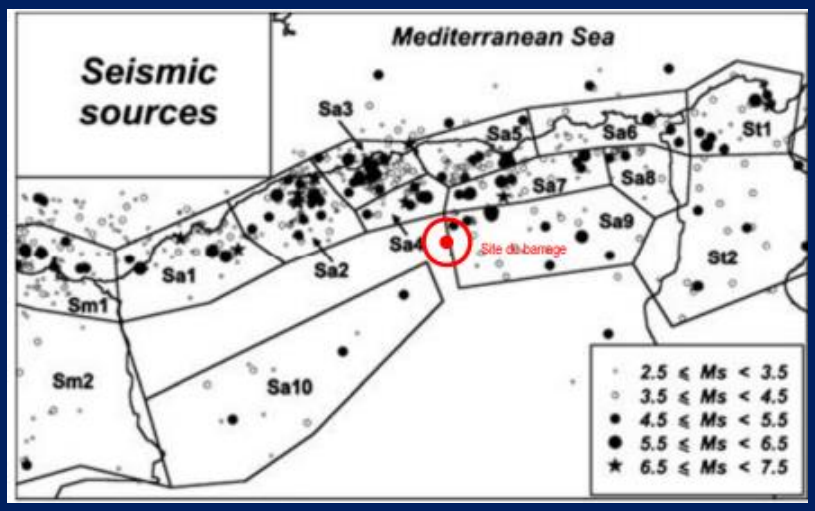

Figure 8. 60 Les zones sources (Peláez et al., 2006)

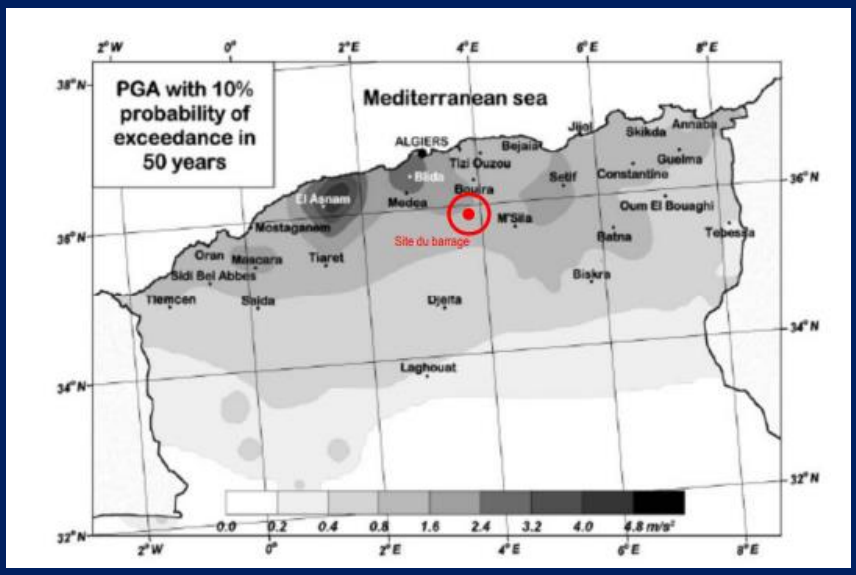

Figure 8. 61 L'accélération maximale (PGA) moyenne pour une probabilité de dépassement de 10% en 50 ans (T= 475 ans) (Peláez et al., 2006)

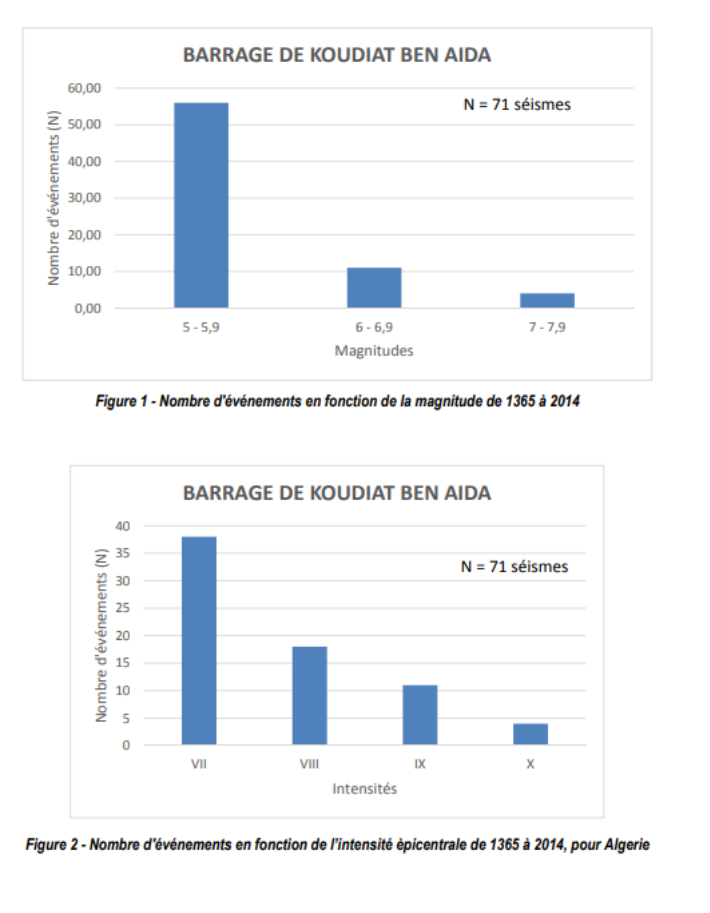

Figure 8.62 Nombre d´événements

8.2.5.6 Avant Projet

La Figure 8.63 et Figure 8.64 ilustre le encadrement geologique et morphologique.

La Figure 8.65 au Figure 8.67 montre la localization des materiaux granulaires disponibles pour la construction du barrage.

Les Figure 8.68 au Figure 8.70 presente la surface critique pour les phases de remplissage du reservoir, vidange du reservoir et pseudo-estatique calcul pour le remplissage du reservoir.

La Figure 8.71 et Figure 8.72 ilustre les structures hydrauliques.

La Figure 8.73 montre le plan de instrumentation.

3. ÉTUDE DE FAISABILITÉ / Mission 5

ENCADREMENT GÉOLOGIQUE ET GÉOMORPHOLOGIQUE

Les formations géologiques rencontrées sur le site sont, essentiellement, les marnes du **Miocène** sous les conglomérats du **Pliocène**. Les formations affleurant au niveau de la plaine sont des limons sableux et alluviaux datés du **Quaternaire**. Sur la rive droite en corniche affleurent des dalles d'encroûtements calcaires très dures.

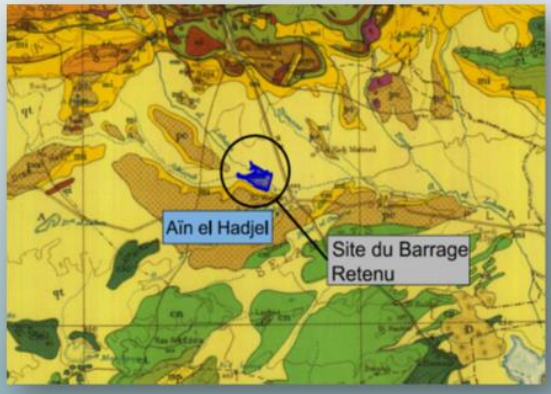

Figure 8.63 Encadrement Geologique et Geomorphologique

3. ÉTUDE DE FAISABILITÉ / Mission 5

ENCADREMENT GÉOLOGIQUE ET GÉOMORPHOLOGIQUE

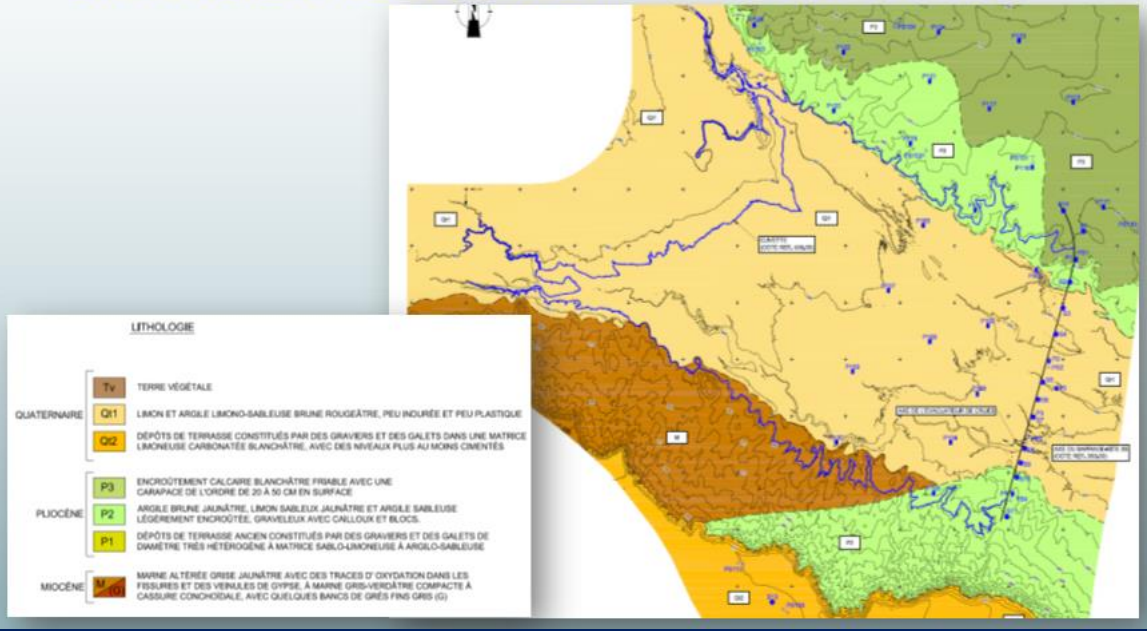

Figure 8.64 Encadrement Geologique et Geomorphologique

3. ÉTUDE DE FAISABILITÉ / Mission 5

ZONAGE GEOTECHNIQUE

Zone Géotechnique	Vitesse des ondes sismiques longitudinales , V_L (m/s)	Pourcentage de récupération (%)	Pourcentage de RQD (%)	Unités Lugeon (UL)	Perméabilité Lefranc (m/s)	N_{SPT}	Description
ZG_{sup}	<300-600	50-100	-	-	$8,06x10^{-5}$ à $1,88x10^{-3}$	<30	Zone géotechnique supérieure composée de matériaux de surface broyés et décomposés
ZG_{int}	600-1850	60-100	Variable (fréquemment, 0 à 60%)	-	$5,25x10^{-6}$ à $4,58x10^{-3}$	30-50	Zone géotechnique intermédiaire qui présente de bonnes conditions de fondation (résistance et déformabilité) pour le barrage quoiqu'avec d'importantes valeurs de perméabilité dues à la présence de dépôts de terrasse caillouteuse.
ZG_{inf}	>1850	70-100	Variable (fréquemment, 70 à 100%)	<3	$2,82x10^{-5}$ à $1,12x10^{-3}$	>50	Zone géotechnique inférieure marneuse et imperméable

Note : (1) –Valeurs plus fréquentes

3. ÉTUDE DE FAISABILITÉ / Mission 5

MATÉRIAUX DISPONIBLES POUR LA CONSTRUCTION

MATÉRIAUX POUR LES FILTRES, DRAINS, AGRÉGATS POUR LE BÉTON ET ENROCHEMENT DE PROTECTION

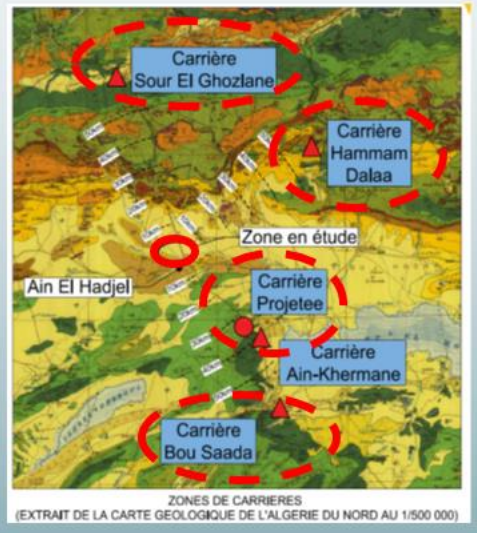

Figure 8.65 Localization de carrières

Figure 8.66 Matériaux pour la construction

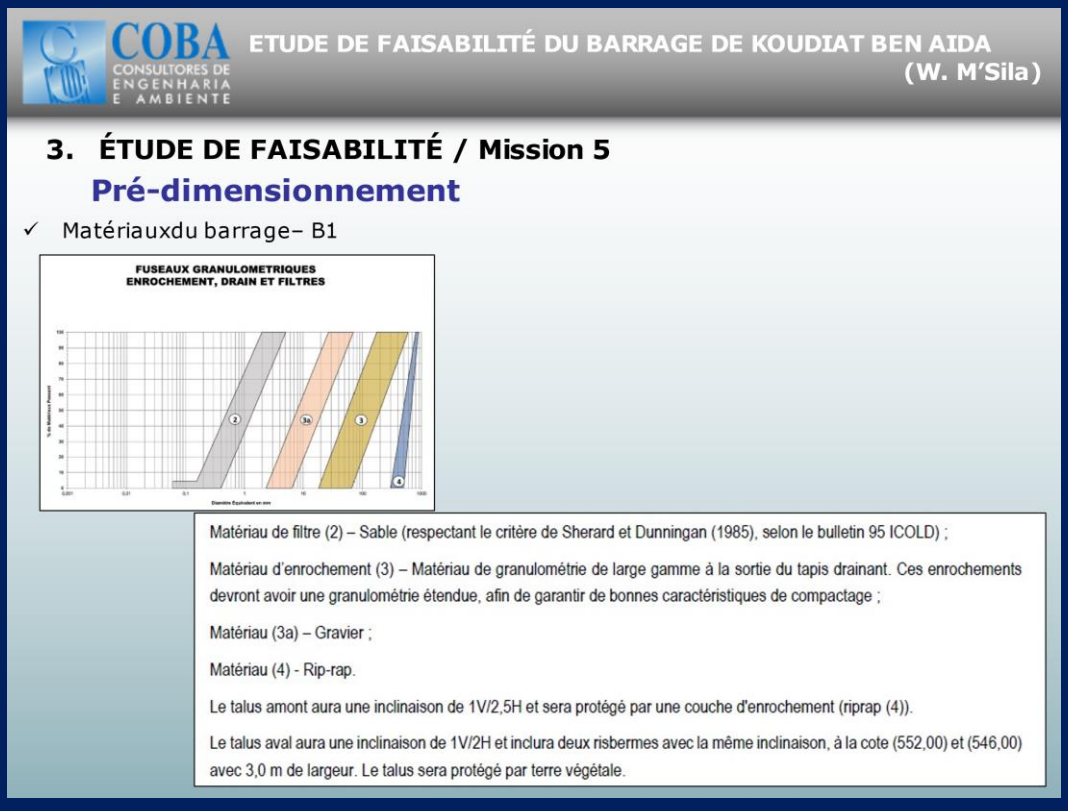

Figure 8.67 Matériaux de filtres, graviers et rip rap

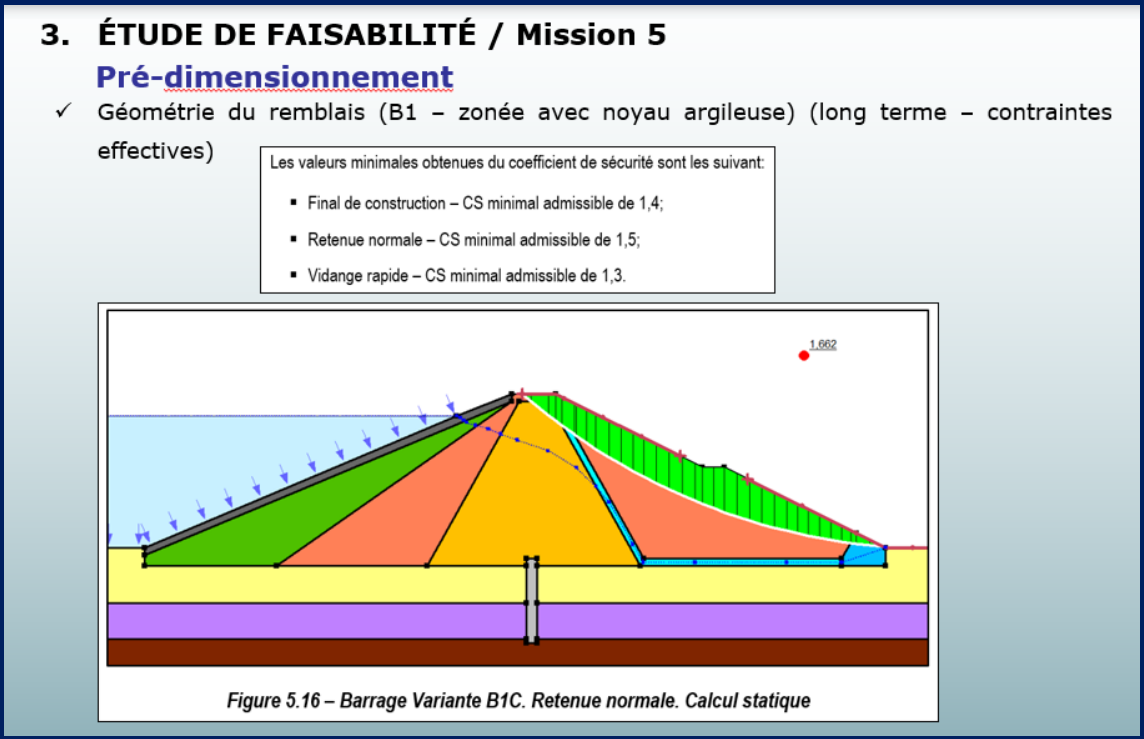

Figure 8.68 Surface critique-retenue normal

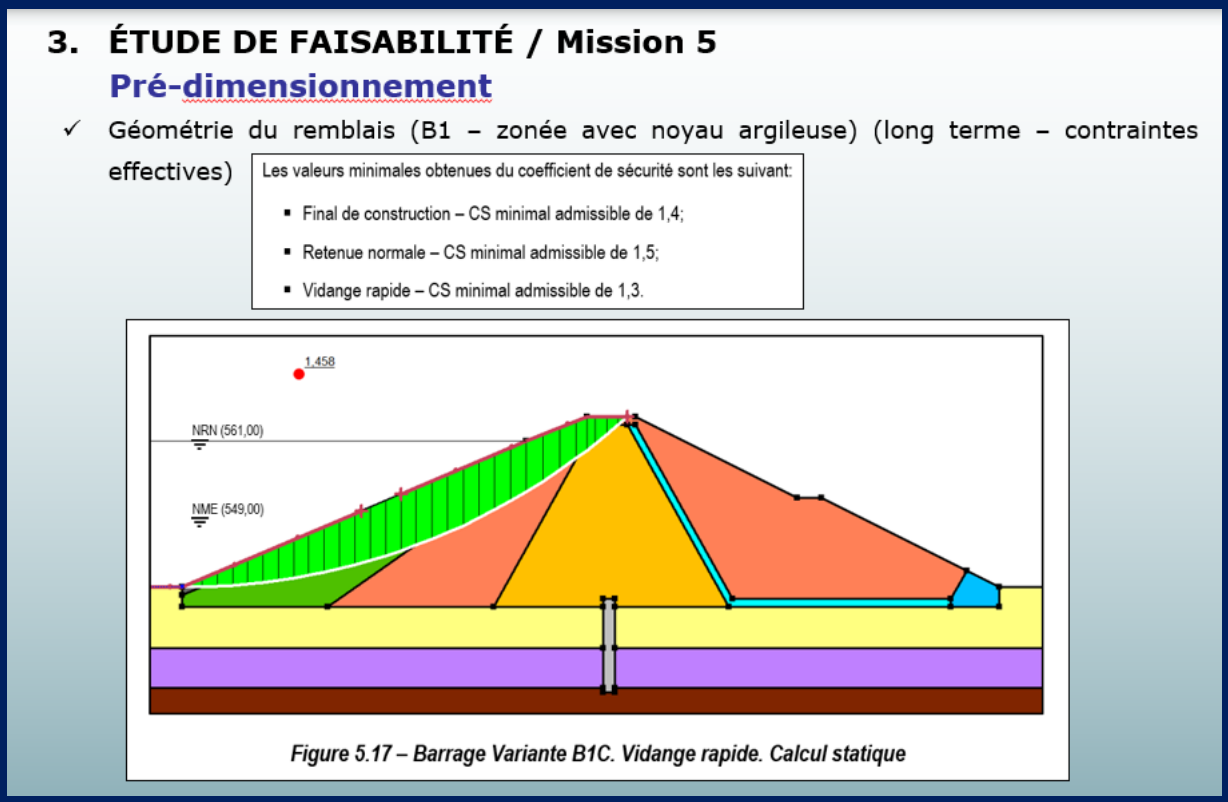

Figure 8.69 Surface critique - vidange rapide

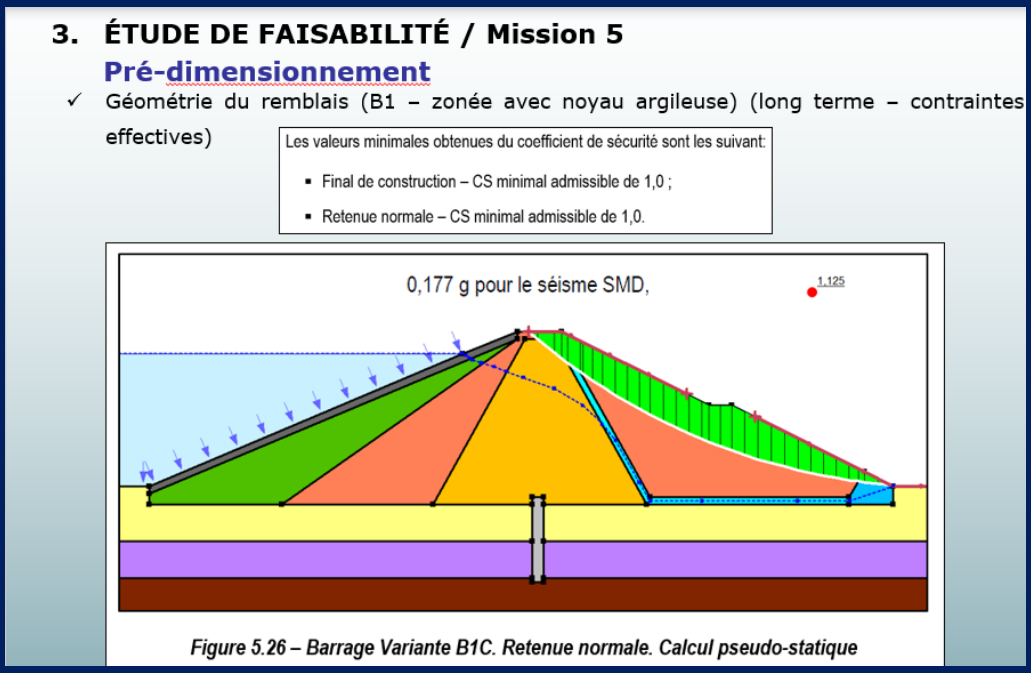

Figure 8.70 Surface critique -retenue normal (calcul pseudo - statique)

8.2.5.7 Ouvrages Hydrauliques

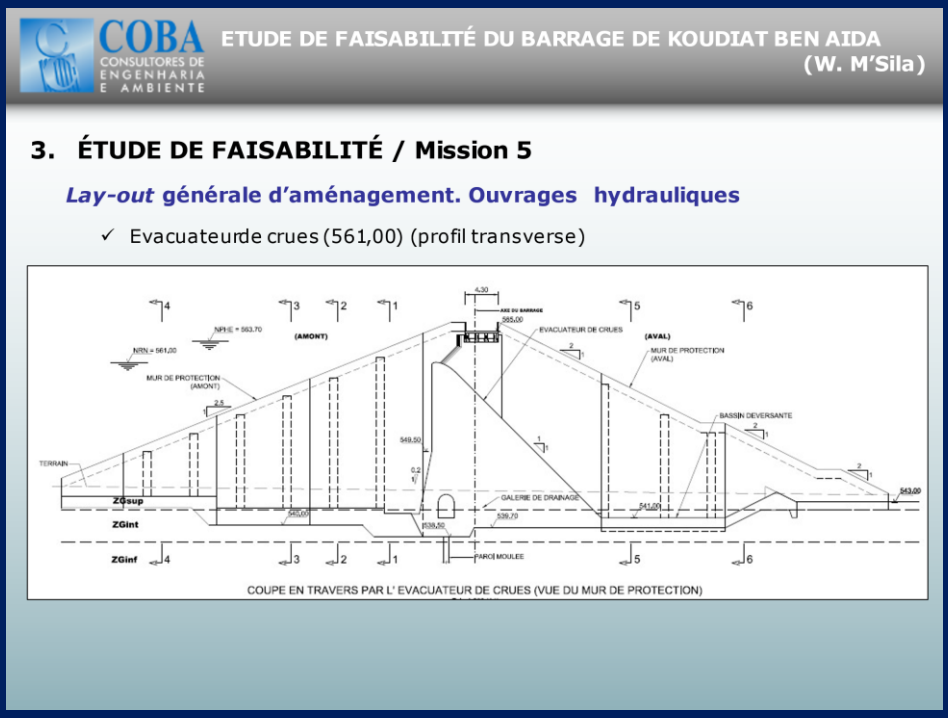

Figure 8.71 Evacuateur de crue

3. ÉTUDE DE FAISABILITÉ / Mission 5

***Lay-out* générale d'aménagement. Ouvrages hydrauliques**

✓ Vidange de fond et Prise d'eau (2 niveaux (547,00) et (554,00))

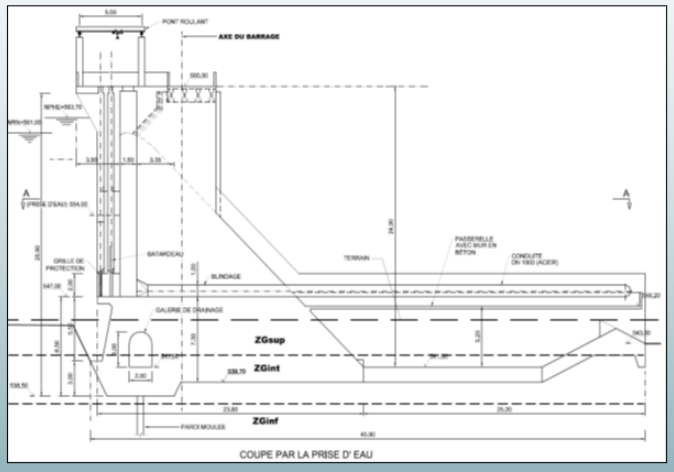

Figure 8.72 Vidange de fond et prise déau

8.2.5.8 Instrumentation-Indice global de risque

Tableau 8.13 Détermination de l`indice global de risque

3. ÉTUDE DE FAISABILITÉ / Mission 5

Pré-dimensionnement

Tableau 1.4 – Détermination de l'indice global de risque

	CONDITIONS EXTERIEURES OU ENVIRONNANTES (Facteur E)					CONDITIONS DE L'OUVRAGE: FIABILITE (Facteur F)				RISQUE POTENTIEL HUMAIN ET ECONOMIQUE (Facteur R)	
	Séismicité	Danger d'éboulis des rivages	Danger de crues supér. à celles du projet	Fonctions de la retenue	Actions agréssives (climat, eau, etc.)	Dimension--nement structurel	Fondations	Equipement (organes d'évacuation)	Entretien	Volume de la retenue (m^3)	Installations en aval
indice α_i	1	2	3	4	5	6	7	8	9	10	11
1	Très faible ou nulle a <0,05g	Très faible ou nul	Très peu probable (barrages de béton)	Pluriannuelle annuelle ou saisonnière	Très faibles	Adéquat	Très bonnes	Fiable	Très bon	$< 10^5$	Zone inhabité et sans valeur économique
2	Faible 0,05 g < a <0,1 g	Faible	---	---	Faibles	---	Bonnes	---	Bon	10^5 - 10^6	Maisons isolées, agriculture
3	Moyenne 0,1 g < a < 0,2 g	---	Très peu probable (barrage en remblais)	Hebdomadaire	Moyennes	Acceptable	Communes	---	Satisfaisant	10^6 - 10^7	Petits villages, agriculture, artisanat
4	Forte 0,2 g < a < 0,4 g	---	---	Journalier	Fortes	---	---	---	---	10^7 - 10^9	Centres moyens; petite industrie
5	Très forte a > 0,4 g	---	---	Pompage	Très fortes	---	Médiocres	---	---	$> 10^9$	Grandes villes; industries; inst. nucléaires
6(a)	---	Grande	Probable	---	---	Insuffisant	Médiocres ou mauvais	Insuffisante non opérationnel	Insatisfaisant	---	

(a) - Conditions anormales - intervention immédiate

$$E = \frac{1}{5}\sum_{1}^{5}\alpha_i \qquad F = \frac{1}{4}\sum_{6}^{9}\alpha_i \qquad R = \frac{1}{2}\sum_{10}^{11}\alpha_i \qquad \text{INDICE GLOBAL } \alpha = EFR$$

3. ÉTUDE DE FAISABILITÉ / Mission 5

Pré-dimensionnement

– Conditions extérieures ou environnantes (Facteur E)

$$E = \frac{1}{5}\sum_{i=1}^{5}\alpha_i = \frac{1}{5}(3+1+3+1+3) = 2,2$$

– Conditions de l'ouvrage : Fiabilité (Facteur F)

$$F = \frac{1}{4}\sum_{i=6}^{9}\alpha_i = \frac{1}{4}(1+3+1+3) = 2,0$$

– Risques humains et économiques (Facteur R)

$$R = \frac{1}{2}\sum_{i=10}^{11}\alpha_i = \frac{1}{2}(4+3) = 3,5$$

La valeur de l'indice global de risque est:

$$\alpha_g = 2,2 \times 2,0 \times 3,5 = 15,4$$

Tableau 1.3 - Quantité de l'auscultation

Auscultation	Quantité
Repère de nivelage	20
Pilier d'observation	2
Piézomètre hydraulique	15
Echelle limnométrique	4
Station météorologique	1
Chambre de mesure de débits	2

3. ÉTUDE DE FAISABILITÉ / Mission 5

Pré-dimensionnement

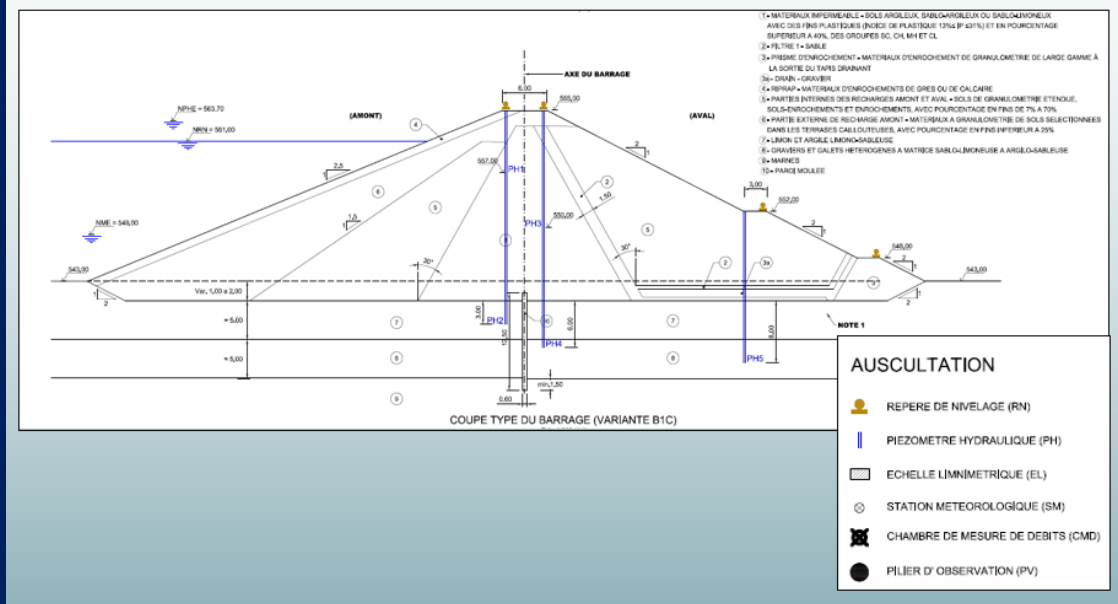

COUPE TYPE DU BARRAGE (VARIANTE B1C)

Figure 8.73 Auscultation du barrage

Lesson nº 4: It is important to stress that a better understanding of embankment dams during the occurrence of earthquakes can only be achieved by a continuous and permanent effort in order to be up-to-date with the last developments in earthquake engineering. It is important that engineers educate themselves and the Public with scientific methods for evaluating risks incorporating the unpredictable human behavior and human errors in order to reduce disasters.

Note: The dam project was conducted by a multidisciplinary COBA team and the author was involved in the geotechnical design.

8.2.6 Case History nº 5 - Moamba-Major Dam (Mozambique)

8.2.6.1 Introduction

For Moamba Major dam the geological characteristics and the geotechnical characteristics are referred, the site investigation is addressed, the width of the crest and the freeboard are defined, the dam the profile is introduced, the definition of design earthquake is discussed, the stability analyses are presented, the seepage studies are analyzed, the stress-strain analyses are addressed and the construction issues are referred.

8.2.6.2 Geological and Geotechnical Characteristics

The Incomati valley integrates two complexes, namely Basalt-dolerític Complex that develops in the neighbor of the dam and part of the reservoir and Riolotic Complex that is located in the rest of the reservoir until South Africa.

The Complex Basalt-dolerític integrates basalts and dolerits that develops from the surface until depths of 30 m and inclinations of 5-15º, with different degrees of weathering. The rocks are covered by colluvial clays, with thickness of 2 to 5 m with gravel materials with thickness of 2 to 6 m.

The valley is filled with alluvial materials with thickness of 25 a 30 m, that integrates sandy materials with high permeability and low compacity.

8.2.6.3 Geotechnical Investigation Programme

The Table 8.14 shows the Geotechnical Investigation Programme and the quantities.

Table 8.15 presents the laboratory tests and the quantities.

Table 8.16 summarizes the characterization of the quarry's samples.

Figure 8.74 illustrates the geological profile.

Figure 8.75 presents the field inspection for searching the materials.

Figure 8.76 shows the assessment of the material.

Figure 8.77 presents the assessment of the trench depth.

Figure 8.78 indicates the survey of rock materials.

Figure 8.79 illustrates the field team.

Table 8.14 Geotechnical Investigation Programme

Activity	Units	Quantitaties
1 – Site investigation	-	VG
2 – Seismic refraction tests	un	7
3 – Trenches	un	165
4 – Holes	un	15
5 – Boreholes		
5.1 – Placement of equipment	un	50
5.2 – Drilling	m	1000
6 – Field tests		
6.1 - SPT tests	un	700
6.2 - CPTU tests	un	12
6.3 - Lugeon tests	un	90
6.4 - Lefranc tests	un	65
7 – Undisturbed tests	un	35
8 – Disturbed tests	un	90
9 – Laboratory tests		
9.1 – Sieve analyses	un	160
9.2 – Atterberg limits (LL and LP)	un	160
9.3 – Water contents and unit weight	un	160
9.4 – Density	un	60
9.5 – Mineralogic analyses and Diffractometry by X Rays	un	7
9.6 – Blue of metilene	un	20
9.7 – Sand Equivalent	un	20
9.8 -Normal Proctor test	un	35
9.9 – Modified Proctor test	un	25

Table 8.15 Geotechnical Investigation Programme – Laboratory tests

Type	Units	Quantitaties
9.10 - C.B.R Test	un	25
9.11 – Expansibility tests	un	10
9.12 – Expansibility tests to determine expansibility potential	un	10
9.13 – Shear direct test	un	20
9.14 – Oedometer test	un	20
9.15 – Triaxial test (CU+U) (samples)	un	45
9.16 – Dispersibility tests	un	10
9.17 – Permeability tests	un	10
10 – Laboratory rocks tests		
10.1 - Porosity, water absortion	un	20
10.2 - Índex of fragmentality	un	10
10.3 – Weathering index / degradability	un	10
10.4 - Expansibility	un	12
10.5 - "Slake-Durability Test"	un	10
10.6 - Los Angeles	un	10
10.7 - "Point Load" tests	un	12
10.8 – Crushing resistance	un	10
10.9 – Uniaxial tests	un	20
10.10 – Brazilian tests	un	10
10.11 - Micro deval	un	10
10.12 – Joint shear test	un	10
10.13 – Velocity of elastic waves	un	12
10.14 – Petroghafic analysis	un	12
10.15 – Reactivity of álcali-sílica	un	6
11 – Tests of water aggressivity	un	12

Table 8.16 Results of laboratory tests of quarry samples (EEO Agrocomplect (1982))

Sample nº	Depth (m)	Rock type	Density	Unit weight (g/cm^3)	Dry unit weight (g/cm^3)	Water absorption (%)	Compression tests (point-load) (MPa)	Mechanical strength	
								Los Angeles (%)	Crushing tests (%)

1	À superfície	Basalto Traqui-andesítico	2,64	2,56	2,51	1,9	-	16	14
2			2,62	2,56	2,52	1,4	56	17	-
3			2,62	2,57	2,55	1,1	123	17	14
4			2,63	2,58	2,54	1,4	70	17	-
5			2,65	2,59	2,55	1,4	255	17	14
6			2,61	2,57	2,54	0,9	99	16	-
7			2,66	2,59	2,54	1,7	100	15	13
8			2,64	2,57	2,53	1,6	65	18	14
9			2,63	2,58	2,55	1,7	120	17	14
10			2,63	2,55	2,50	1,9	-	17	13
11			2,63	2,57	2,53	1,5	54	17	14
Mínimum			2,61	2,55	2,50	0,9	54	15	13
Máxim			2,66	2,59	2,55	1,9	255	18	14
Average			2,63	2,57	2,53	1,5	105	17	14

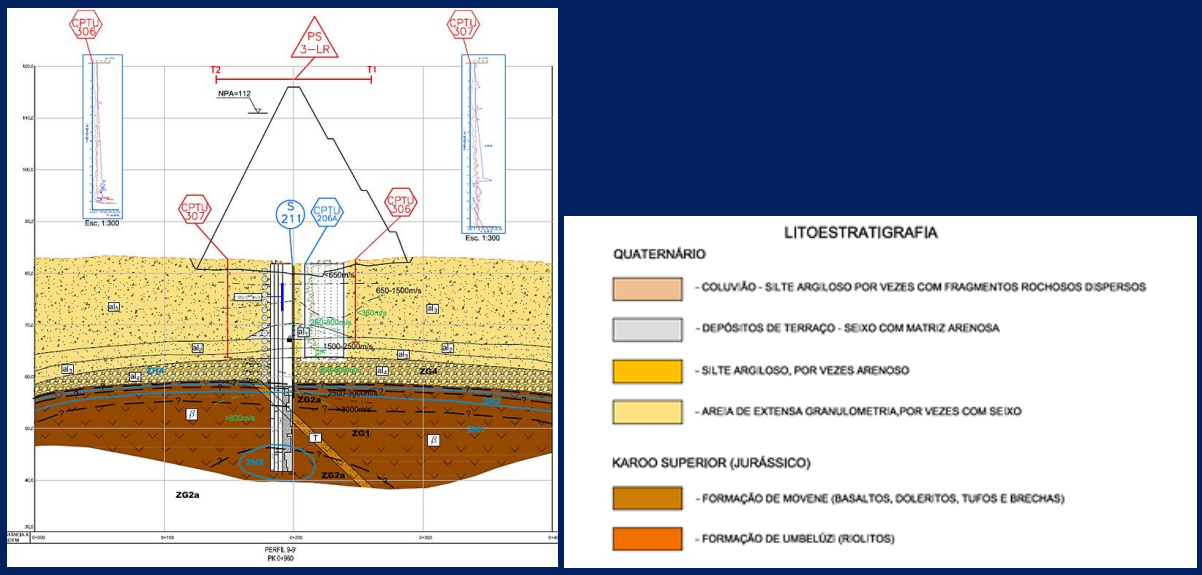

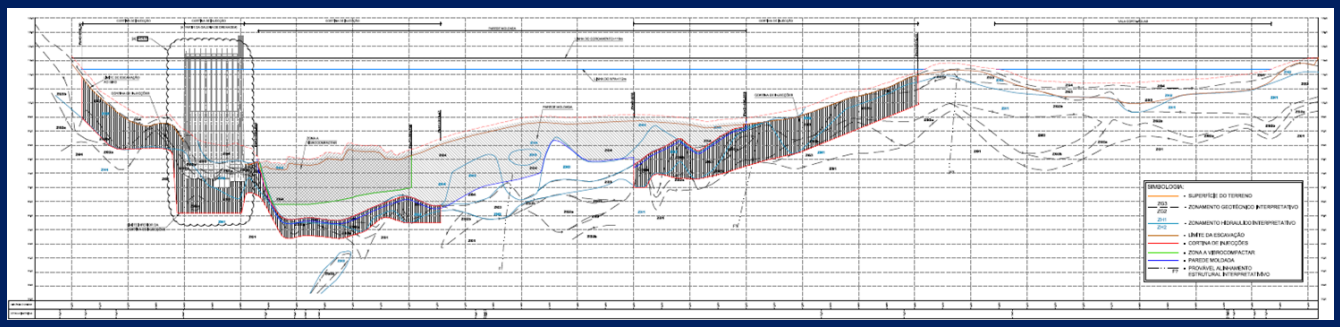

Figure 8.74 Geological Profile

Figure 8.75 Searching for the materials

Figure 8.76 Assessment of the material

Figure 8.77 Assessment of trench depth

Figure 8.78 Survey of rock materials

Figure 8.79 Field team

8.2.6.4 Width of the Crest and Freeboard

Crest width

For the definition of the crest width, it is necessary to consider the dam safety and the exploitation.

Following Preece, considering H = 34 m, results L = 6.5m

Following the japanese code:

$$L = 3{,}6(H)^{1/3} - 3 = 8.7\ m \qquad (8.6)$$

Following spanish code “Comision Interministerial de Normas Sismoresistentes” (1968), for zones of low seismicity, the dam width is given by:

$$L = 3 + 1{,}5(H - 15)^{1/3} = 7\ m \qquad (8.\ 7)$$

Considering these different criteria and that the crest will be used as a roadway to the hydroelectric powerplant, a value of 9 m for the crest was adopted.

Definition of the freeboard

Introduction

Considering equation 8.1 and following the criteria of USBR (1992)

Combination 1: Situation of filling of reservoir associated with waves generated by exceptional wind.

- Combination 2: considering a design flood with a return period of 1 000 years and one gate not operating simultaneously with normal wind
- Combination 3: considering an earthquake with a return period of 1000 years simultaneously with normal wind.

Fetch

The height of the waves generated in the reservoir depend on the wind velocity, on the fetch, i.e on the extension of the free water

The effective fetch is given by the equation (see Figure 8.80):

$$\boldsymbol{Ft = \frac{\sum_{i=1}^{9} Ft_i}{9}} \qquad \textbf{(8.8)}$$

Where:

Ft – effective fetch (km);

Ft_i – radial length i (km).

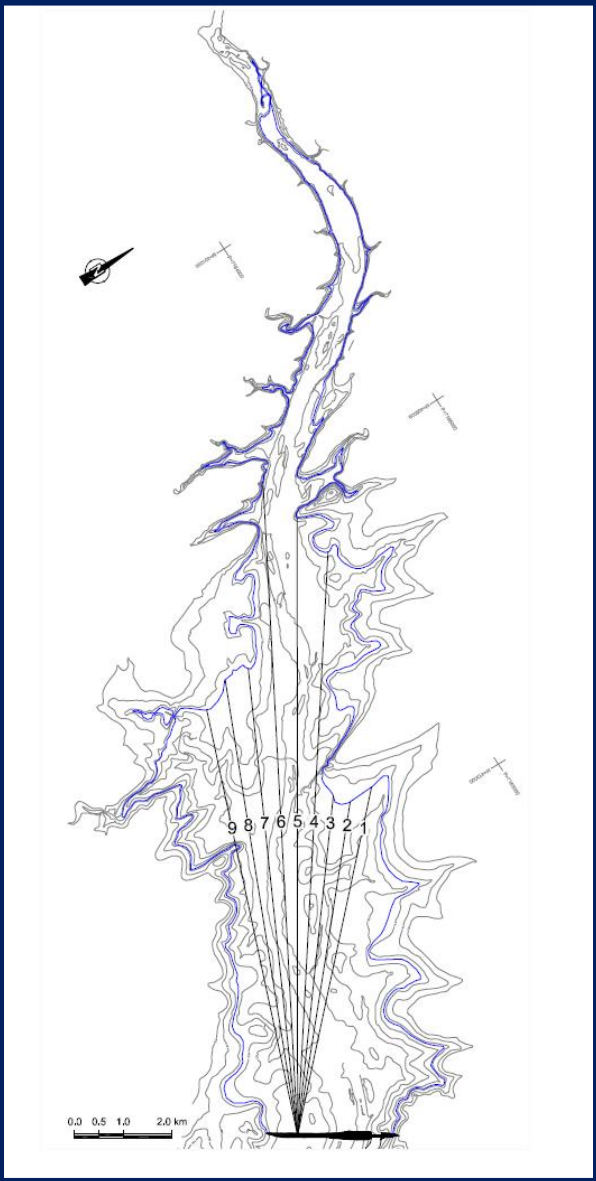

Figure 8.80 Fetch Moamba Major reservoir

For the Moamba-Major reservoir, with water level (108.0), the maximum fetch 3.5 km and the effective fetch 9.9 km (see Table 8 .17).

Table 8.17 Length of the considered radius

i	1	2	3	4	5	6	7	8	9
Ft_i [km]	7.5	7.3	7.4	12.2	12.8	13.5	9.9	9.7	9.1

$$\boldsymbol{Ft = \frac{\sum_{i=1}^{9} Ft_i}{9} = 9.9km} \quad (8.9)$$

Tide due to the wind

The tide generated by the wind can be defined by USBR equation (Zuider Zee):

$$S = \frac{V^2 Ft}{6.3 \times 10^4 \times D} \quad (8.10)$$

where:

S – reservoir elevation (m);

V – wind velocity (km/h);

Ft – effective fetch (km);

D – average depth of the reservoir (m).

~

Considering an effective fetch 9.9 km and average depth of 28 m, and so the tide is

- 0.03 m, for frequent wind (70 km/h);
- 0.08 m, for exceptional wind (120 km/h).

Waves generated by the wind

The wave generated by the wind is given by the equations.

$$Hs = \frac{V^{1.23} \times Ft^{0.5}}{422} \quad \text{USBR (1992)} \quad (8.11)$$

$$Hs = \frac{V \times Ft^{0.5}}{200} \quad \text{Saville, McClendon \& Cochran (1962)} \quad (8.12)$$

where:

H_s – height of the wave (m);

V – wind velocity (km/h);

F_e – effective fetch (km);

The computed values of the waves are in Table 8.18.

Table 8.18 Values of the waves (Hs)

Equation	Exceptional wind	Normal wind
USBR (1992)	2.70 m	1.39 m

Saville, McClendon & Cochran (1962)	1.89 m	1.10 m

For the generated waves were assumed the values of 1.1 e 1.9 m for normal and exceptional wind, respectively:

The length of the wave is:

$$L = 1.56T^2 \quad (8.13)$$

where:

L – length of the wave (m);

T – period of the wave (s);

This value can be obtained by the equation:

$$T = 0.33V^{0.41}Ft^{0.5} \quad (8.14)$$

where:

V – wind velocity (km/h);

F_e – effective fetch (km);

$$R = 1.6 \cdot K \frac{tg(\alpha)}{\sqrt{Hs/L}} \times Hs \quad (8.15)$$

where:

K – Roughness of the upstream slope (value= 0.55);

α – upstream slope inclination = 26.6°;

Hs – height of the waves;

L – length of the wave

The values of the wave generated by the normal and exceptional wind are presented in Table 8.19

Table 8.19 Wave generated by the wind

	Exceptional wind	Normal wind
Hs [m]	1.90	1.10
T [s]	5.01	4.02

L [m]	39.22	25.21
R [m]	3.80	2.32

Wave generated by earthquake

Following spanish code, the height of the wave generated by the equation:

$$h = \frac{K_h \cdot T \cdot \sqrt{g \cdot H}}{2} \quad (8.16)$$

where:

K_h – seismic coefficient;

T – predominant period of the earthquake [s];

g – gravity acceleration [m/s²];

H – upstream maximum water level [m].

Considering H=28 m, a predominant period of 0.45 s, a seismic coefficient of 0.1 g, the height of the wave is 0.37 m.

Crest level

The combinations to compute the fetch are summarized in Table 8.20.

Table 8.20 Combinations to compute the fetch

Combination	**Reservoir level [m]**	**F_Q [m]**	**F_s [m]**	**F_s [m]**	**Crest level [m]**
(1) - C_{PA} = NPA + F_{QPA} + F_S	108	3.87	0.50	4.37	112.37
(2) – C_{MC} = NPA + F_{QMC} + F_S	108	1.50	0.50	2.00	110.00
(3) – C_S = NMC + F_{QS} + F_S	109	2.35	0.50	2.85	111.85

As the crest level is not sufficient to avoid overtopping, a deflector in reinforced concrete at level (113.2) was considered.

8.2.6.5 General Description- Dam Profile

Reservoir: 880 hm3 total storage and 61 km^2 flooded area.

Embankment Dam: 4450 m long and 38 m maximum height.

Figure 8.81 illustrates the dam features. Concrete dam on the left bank, 210 m long including spillway, intake and powerhouse.

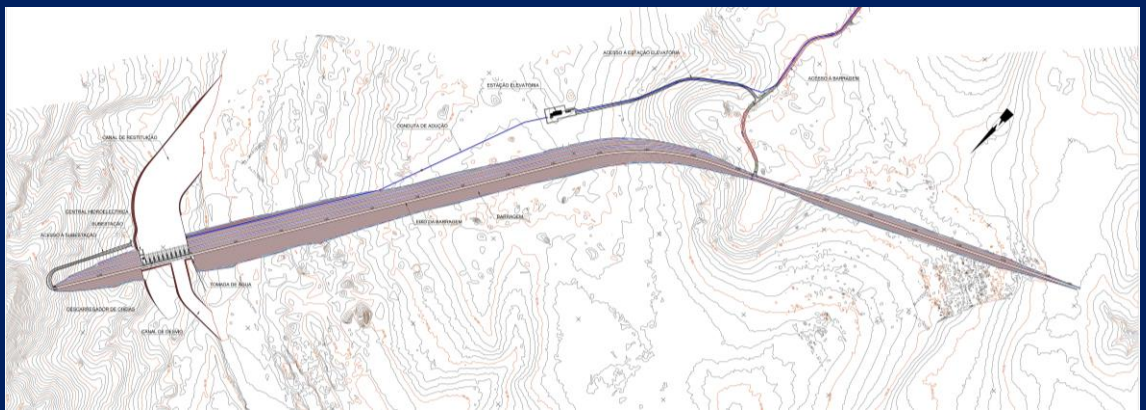

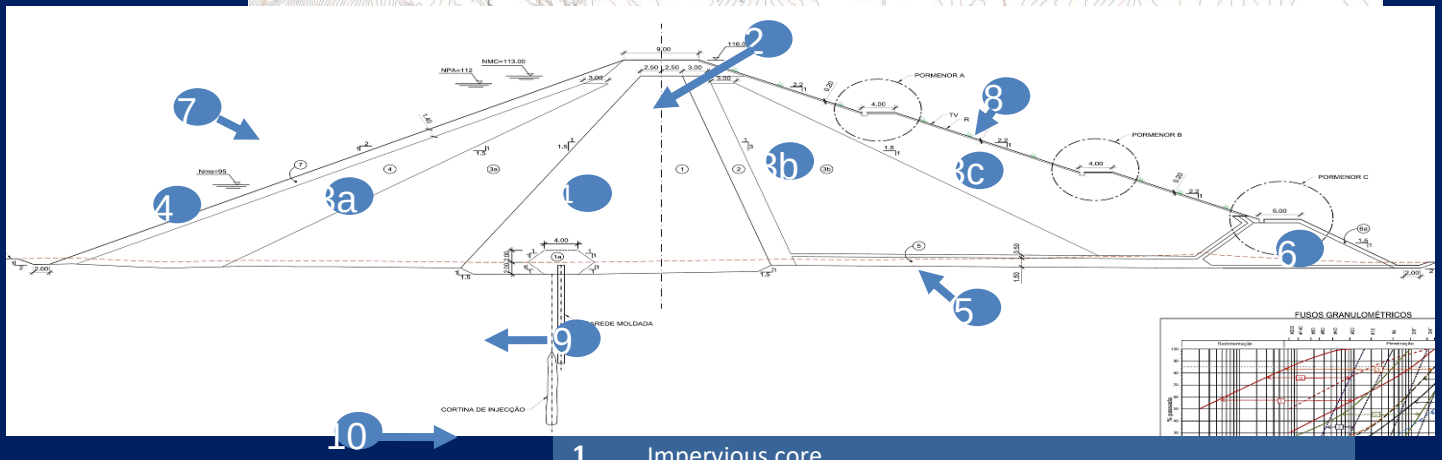

1	Impervious core
2	Filter
3a	Upstream shoulder inner part
3b	Downstream shoulder inner part
3b	Downstream shoulder external part
4	Upstream shoulder external part
5	Drain
6	Rockfill downstream toe

Figure 8.81 Dam Profile

8.2.6.6 Dam Stability Analyses

A computer code SLOPE W was used to analyze the slope stability of the dam profiles.

The geotechnical characteristics of the dam materials are presented in Figure 8.82 and Table 8.21.

It is current practice to analyze: construction phase, filling of reservoir and drawdown.

Related with the construction phase both and downstream slope and upstream slope were analyzed (see Figures 8.83 and 8.84).

As the filling of reservoir is the most critical situation the surface located in the downstream slope with the minimum safety factor is shown in Figure 8.85.

Figure 8.86 illustrates the critical surface for the drawdown phase.

Taking into account the size of the dam a pseudo-static analysis was considered adequate.

The minimum computed safety factor associated to a seismic coefficient of 0.10 was 1.25 (see Figure 8.87).

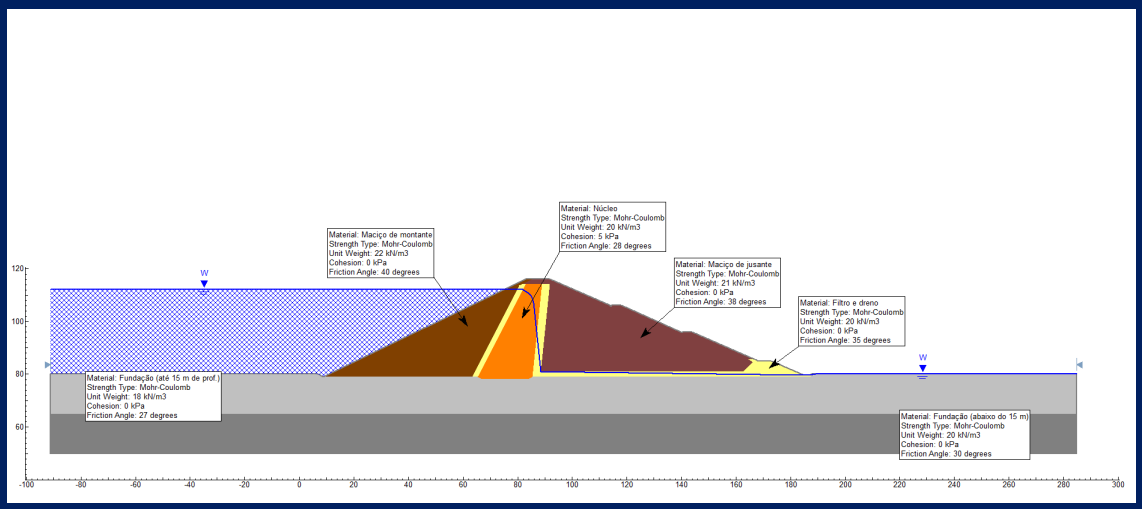

Figure 8.82 Moamba-Major Dam profile- Geotechnical characteristics

Table 8.21 Geotechnical parameters of the Materials

	γ [kN/m^3]	c' [kPa]	ϕ' [°]	E [MPa]	ν [-]	k_v [m/s]	k_h [m/s]
Core (Material Type 1)	20	5	28	15	0,4	5×10^{-10}	10^{-9}
Filtre (Material Type 2)	20	0	35	18	0,3	10^{-4}	10^{-4}
Downstream shell (Material Type 3)	21	0	38	25	0,3	10^{-3}	10^{-3}
Upstream Shell (Material Type 4)	22	0	40	25	0,3	10^{-2}	10^{-2}
Drain (Material Type 5)	20	0	35	15	0,3	10^{-2}	10^{-2}
Rockfill -Downstream toe (Material Type 6)	20	0	35	15	0,3	10^{-2}	10^{-2}
Rip-Rap (Material Type 7 & 7A)	20	0	35	15	0,3	10^{-2}	10^{-2}

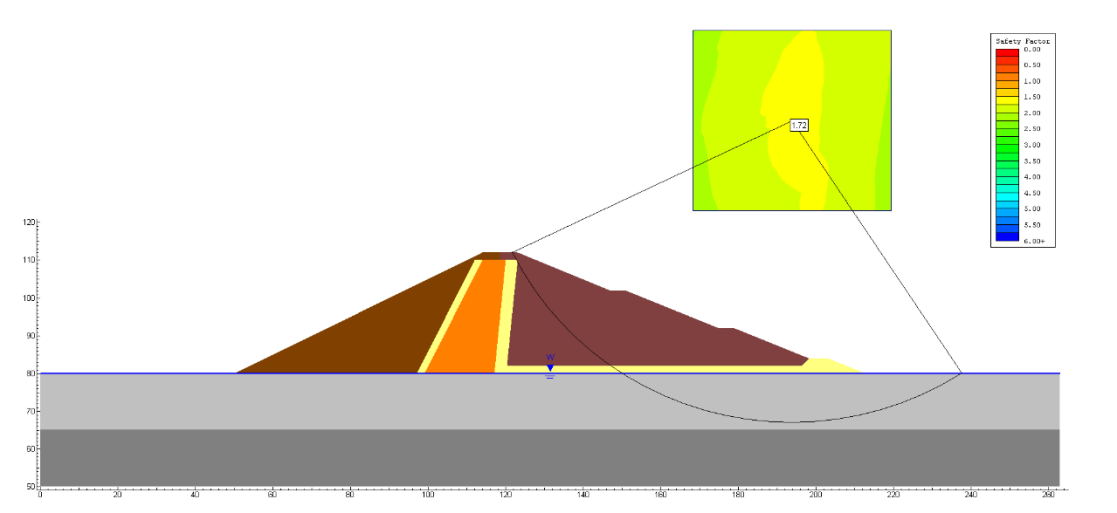

Figure 8.83 Construction phase - downstream slope with the critical surface with the minimum safety factor

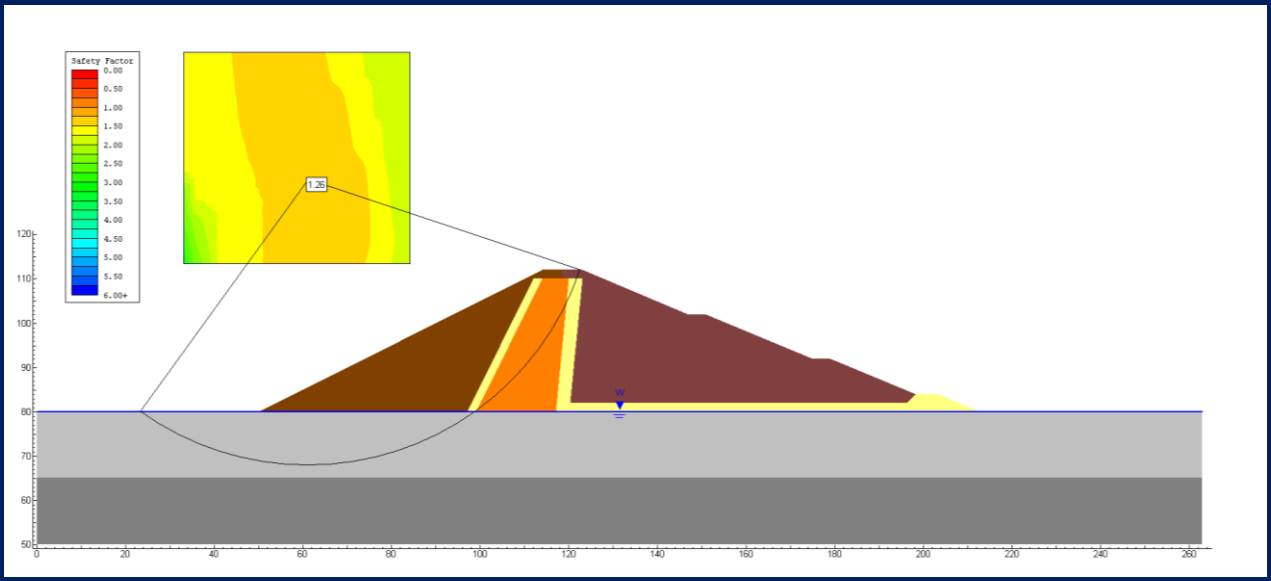

Figure 8.84 Construction phase - upstream slope with the critical surface with the minimum safety factor

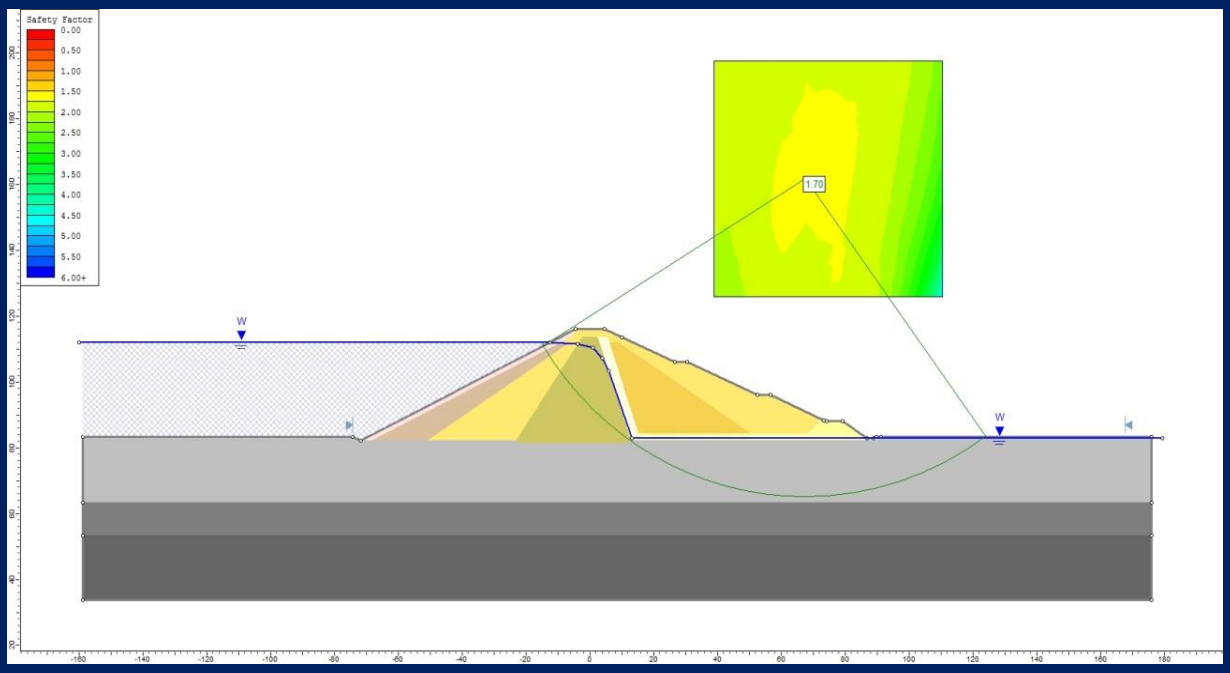

Figure 8.85 Filling of reservoir - downstream slope with the critical surface with the minimum safety factor

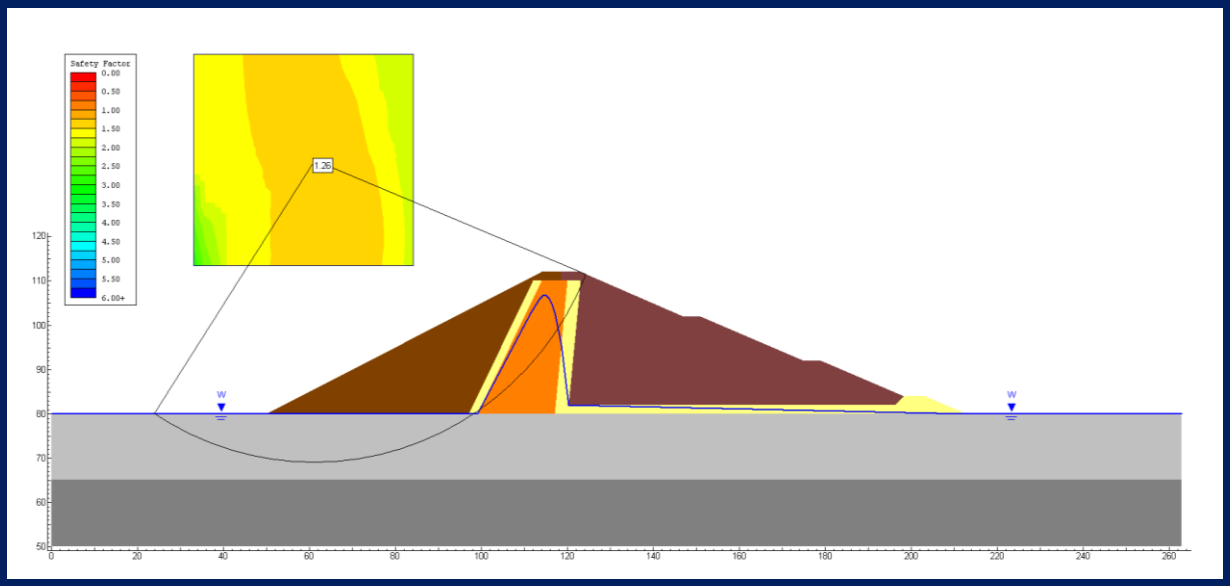

Figure 8.86 Drawdown - upstream slope with the critical surface with the minimum safety factor

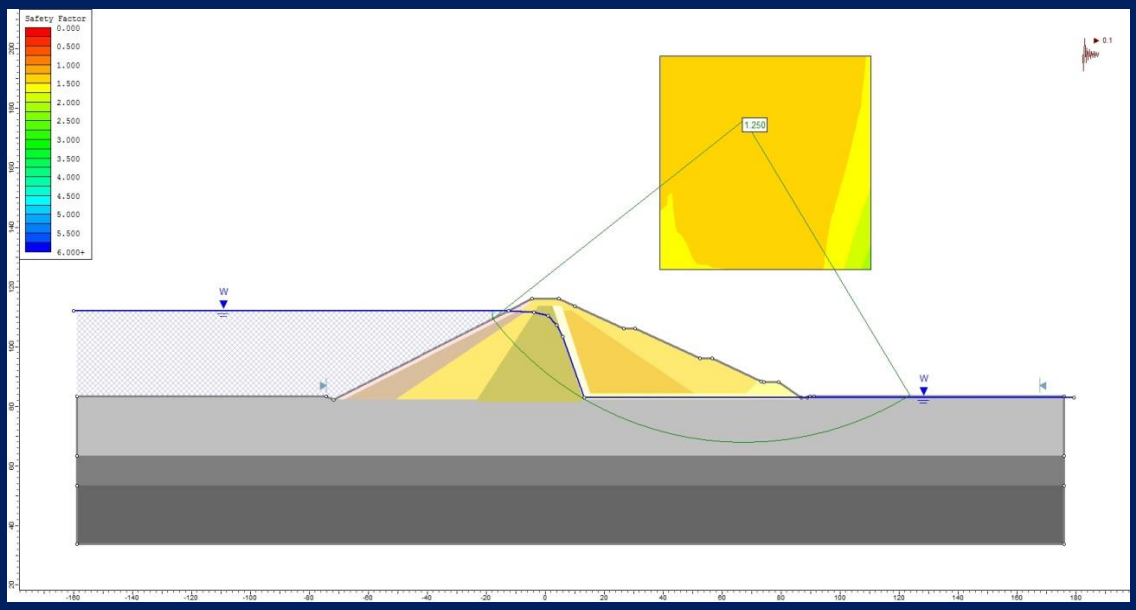

Figure 8.87 (Pk 0+800). Pseudo-static analysis(k=0.1g). Filling of the reservoir. Downstream. Critical surface

8.2.6.7 Seepage Studies

The seepage studies were performed using a PLAXIS code and the fem mesh is shown in Figure 8.88.
The computed flows through the dam body are shown in Table 8.22.
The equipotential surfaces without diaphragm wall and grouting curtain are shown in Figure 8.89.

Figure 8.90 illustrates the equipotential surfaces with diaphragm wall and grouting curtain.

Table 8.22 Computed flows

	Flows [m³/s/m]
Dam body	9.4×10^{-6}
Foundation	7.1×10^{-5}

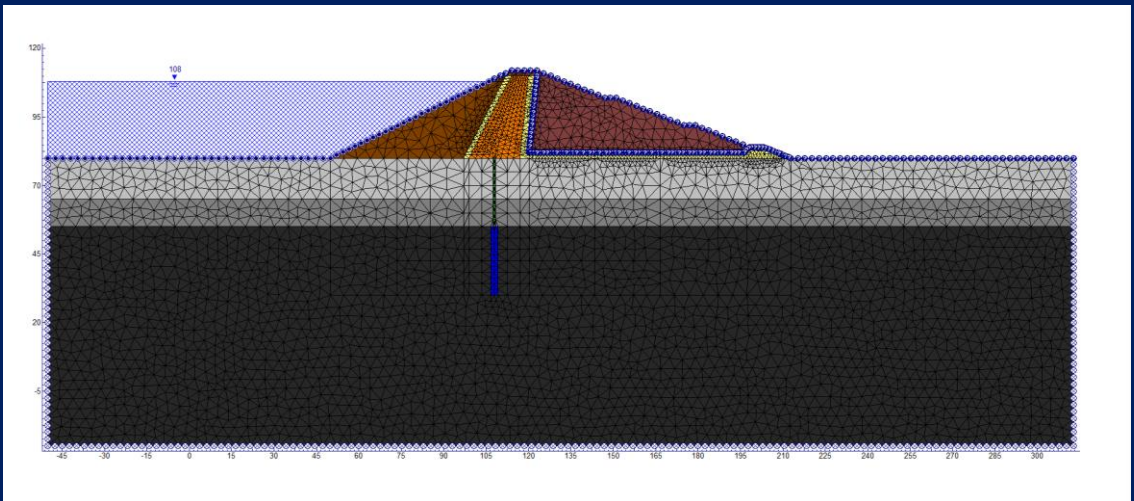

Figure 8.88 Finite element mesh

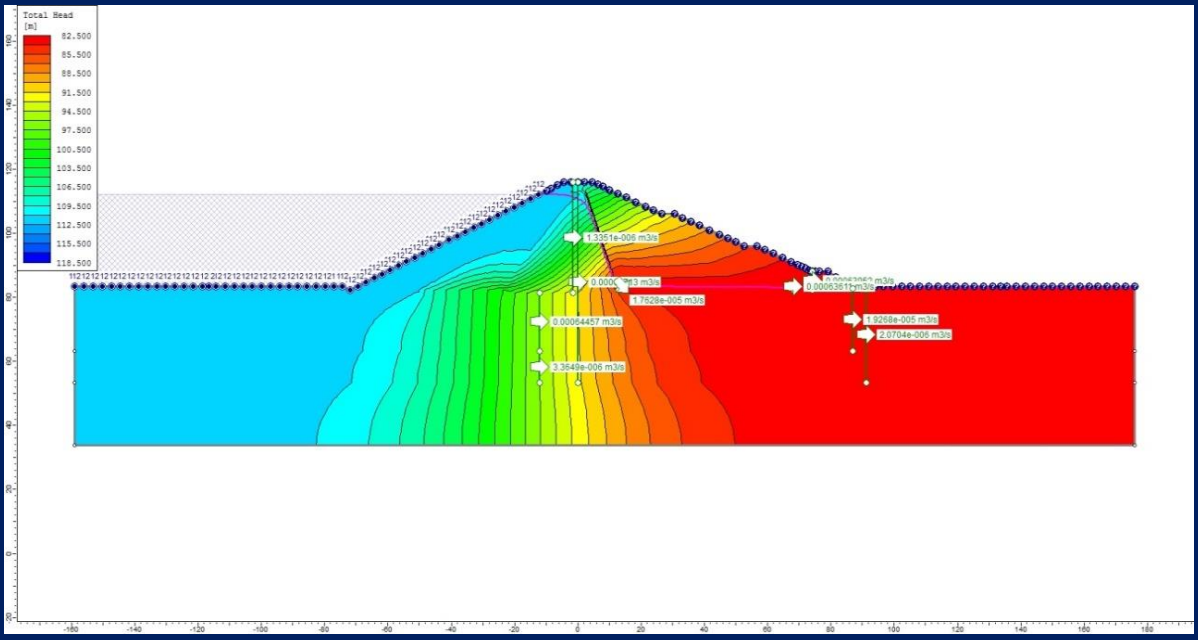

Figure 8.89 Pk 0+800, without diaphragm wall and grouting curtain_– equipotential surfaces and flows

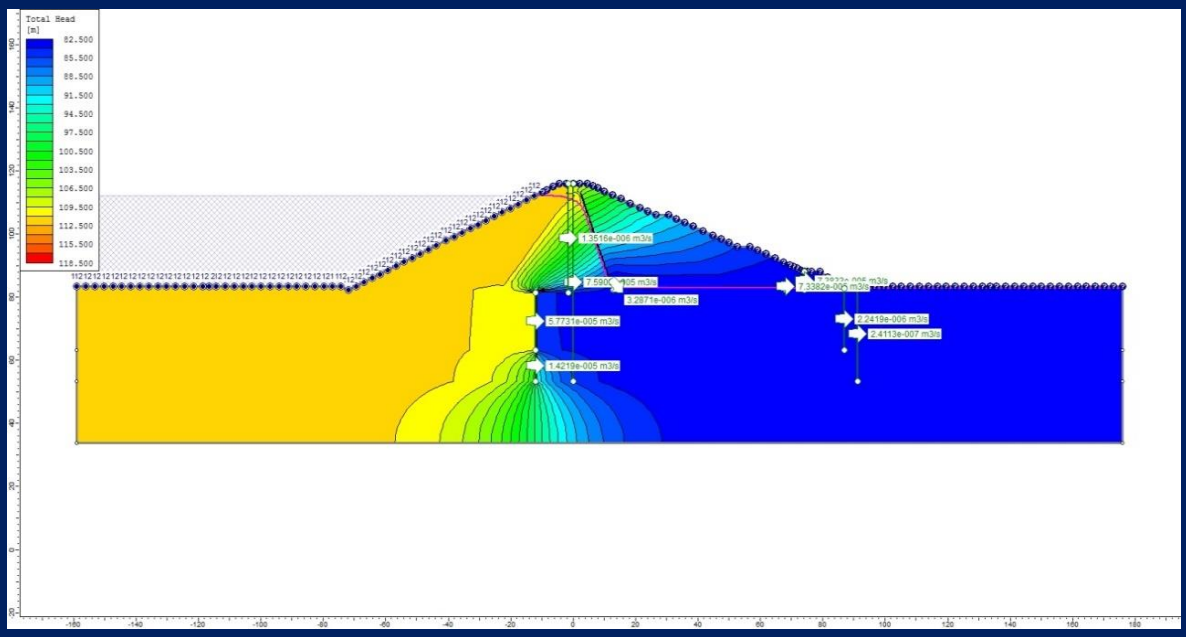

Figure 8.90 Pk 0+800, with diaphragm wall and grouting curtain – equipotential surfaces and flows

8.2.6.8 Filter Design

Introduction

7 Filter Design

Introduction

The filter system and drainage blanket play an important role in the dam behavior.

It is normal to design:

a) Chimney filter

b) Filter and horizontal blanket

c) Filter and rockfill protection of upstream shell.

Flow net

The equation that governs 2D seepage is

$$k_x \frac{\delta^2 h}{\delta k^2} + k_z \frac{\delta^2 h}{\delta z^2} = 0 \qquad (8.17)$$

Where e k_x e k_z are the horizontal and vertical coefficients of permeability and h is the potential

Chimney filter

The value of the flow that reaches the filter is given by:

$$Q_a = k_h \cdot \frac{n_f}{n_d} \qquad (8.18)$$

Where Q_a is the flow, k is the coefficient of permeability, h is the total head, n_f is the number of the flow tubes and n_d is the number of head losses.

Taking into account the flow net results:

$Q_{af} = 9{,}4 \times 10^{-6}\ m^3/s$

Considering the core cracking and a safety factor of 150 results:

$$Q_a = 1.2 \times 10^{-4}\ m^3/s$$

Considering a thickness of 1.5 m for the chimney filter and considering a seepage way around 10 m, the value of the filter coefficient of permeability is given by the equation:

$$k = \frac{Q_a}{\frac{h_c}{L_c} A_c} = \frac{1{,}4 \times 10^{-3}}{\frac{32}{34} \times 3{,}0} = 5{,}0 \times 10^{-4}\ m/s \qquad (8.18)$$

Following the Terzaghi criteria for filters for piping results the condition:

$$\frac{D_{15\,(filtro)}}{D_{85}\,(solo)} < 4 \text{ a } 5 \qquad (8.19)$$

Where D_{15} and D_{85} represents the diameters where 15% e 85%, in weight of the material are particles with less diameter.

For the criteria of permeability, the following equation should be respected

$$5 < \frac{D_{15}(filtro)}{D_{15}(solo)} < 40 \qquad (8.20)$$

And the filter material should exhibit less than 5% of fines (material of size less than ASTM sieve 0.074 mm.

The filter material should respect the Hazen equation:

$$k\ (cm/s) = C_1\, D^2_{10}$$

$$k = 10^{-4}\ m/s \qquad (8.21)$$

This value compared with the value given by equation (8.18), shows that the filter material is adequate.

Horizontal Blanket

The flow that seeps through the horizontal blanket is given by the equation:

$$Q = Q_a + Q_f \tag{8.22}$$

Where

Q_a – is the flow through the dam body

Q_f – is the flow through the foundation

The flow through the foundation is given by the equation:

$$Q_f = Ak_f \frac{h}{L} \tag{8.23}$$

Where

A – area normal to the seepage

h – hydrostatic head

L – seepage length

Considering Figure 8.90 results:

Q_f = 5×10^{-6} m/s

h = 9 m

L = 95 m

A = 10 m^2

Considering equation (8.23) results:

$$k_f = 10 \times 5 \times 10^{-6} \times \frac{9}{95} = 0.5 \times 10^{-5} \cdot m^3/s$$

Considering the effects of the cut-off trench penetration of 60%, the flow value will be reduced of 30%.

$$Q_f = 0.33 \times 10^{-5}\ m^3/s$$

So, the total flow value for the horizontal downstream blanket is:

$$Q = 1.2 \times 10^{-4} + 0.33 \times 10^{-5} = 1.2 \times 10^{-4}\ m^3/s$$

So, the horizontal drain incorporates a filter layer and a drain layer.

Considering a thickness of 0.5 m for the drain the coefficient of permeability of the drain is given by:

$$k_d = \frac{QL}{A^2_b} = \frac{1.2 \times 10^{-4} \times 12.5}{0.5^2} = 6 \times 10^{-3} m/s$$

Considering the Hazen equation (8.21) and the Figure 8.90, the drain material should exhibit a coefficient of permeability of 9×10^{-2} m/s. So, the drain safety factor related the coefficient of the permeability is considerable.

The flow value through the dam is the following:

$$Q = 1,8 \cdot x \cdot 10^{-3} \cdot m^3/s$$

$$Q_t = \frac{325}{2} \times 1.2 \times 10^{-4}\ m^3/s = 19.5 \times 10^{-3} m^3/s$$

So, the drain width is

L = 3.9 m.

For the design it was considered for the drain a width of 12 m to incorporate a safety factor of 3.

Filter and Upstream Rockfill protection

The design of the upstream "rip-rap" protection was based in Corps of Engineers criteria. Considering the height of the reservoir waves of 0.88 m the average rock dimension of D_{50} is 20 cm.

The thickness of the layer is 0.40 m and should incorporate particles of dimensions from 0.40 m to 0.03 m.

To prevent the effect of the wave's erosion a filter with 0.25 m thick was placed between the fill material and the upstream rip-rap.

8.2.6.9 Stress-Strain Analyses

Dam Profile founded on alluvial material

The distribution of effective vertical stress, effective horizontal stress, pore pressures, vertical displacements and horizontal displacements at the end of the construction phase are presented in Figures 8.91, 8.92, 8.93, 8.94 and 8.95.

The distribution of effective vertical stress, effective horizontal stress, pore pressures, vertical displacements and horizontal displacements at the end of the filling of the reservoir are presented in Figures 8.96, 8.97, 8.98, 8.99 and 8.100.

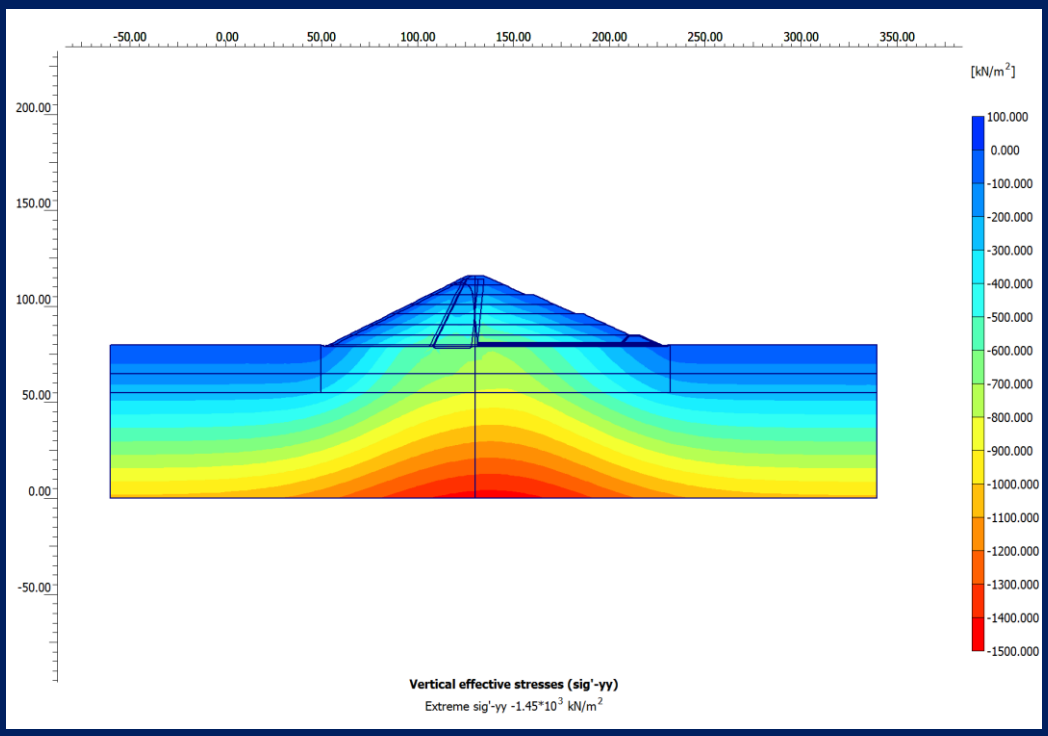

Figure 8.91 Distribution of effective vertical stress (end of the construction)

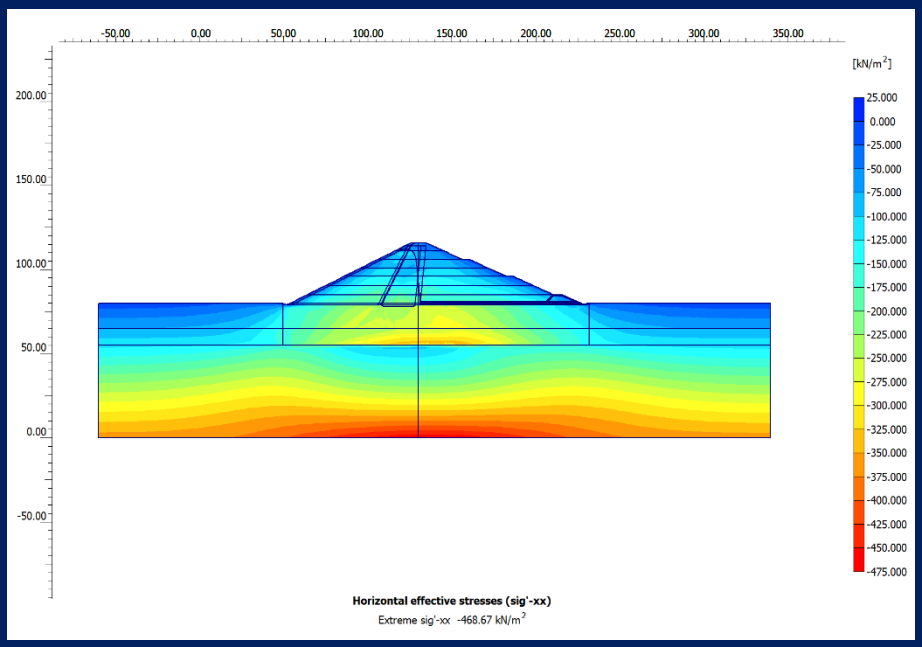

Figure 8.92 Distribution of effective horizontal stress (end of construction)

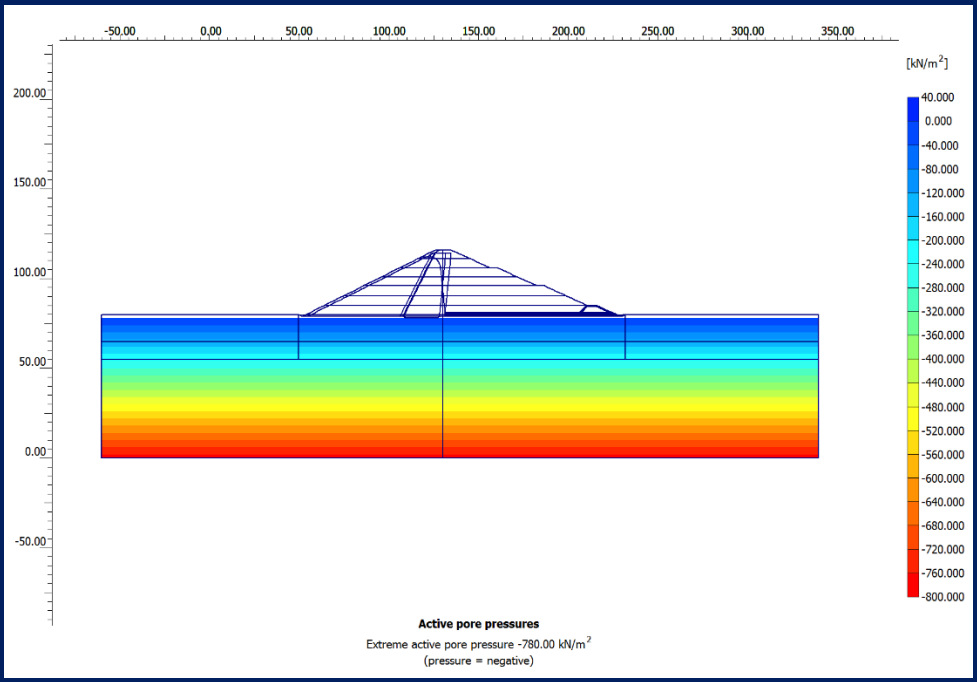

Figure 8.93 Distribution of pore pressure (end of construction)

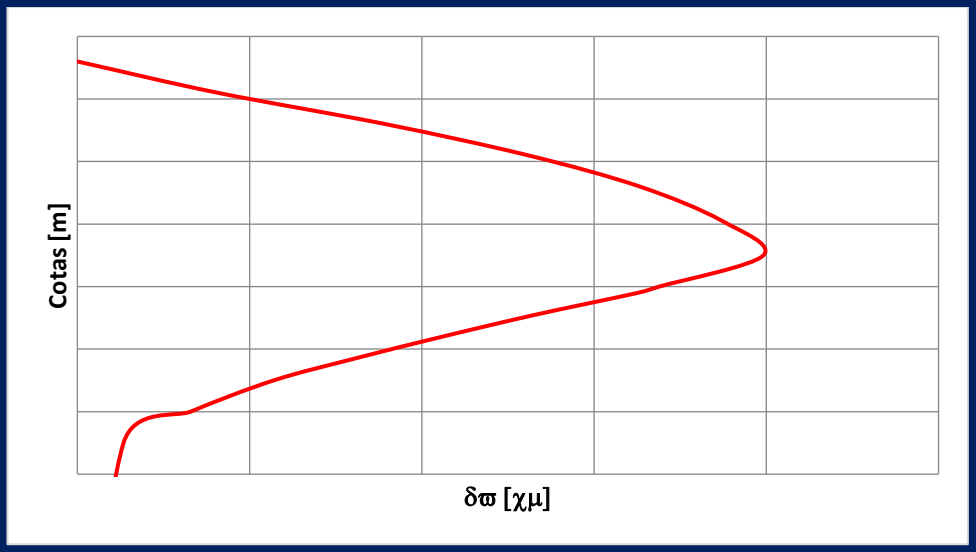

Figure 8.94 Distribution of vertical displacements (end of construction)

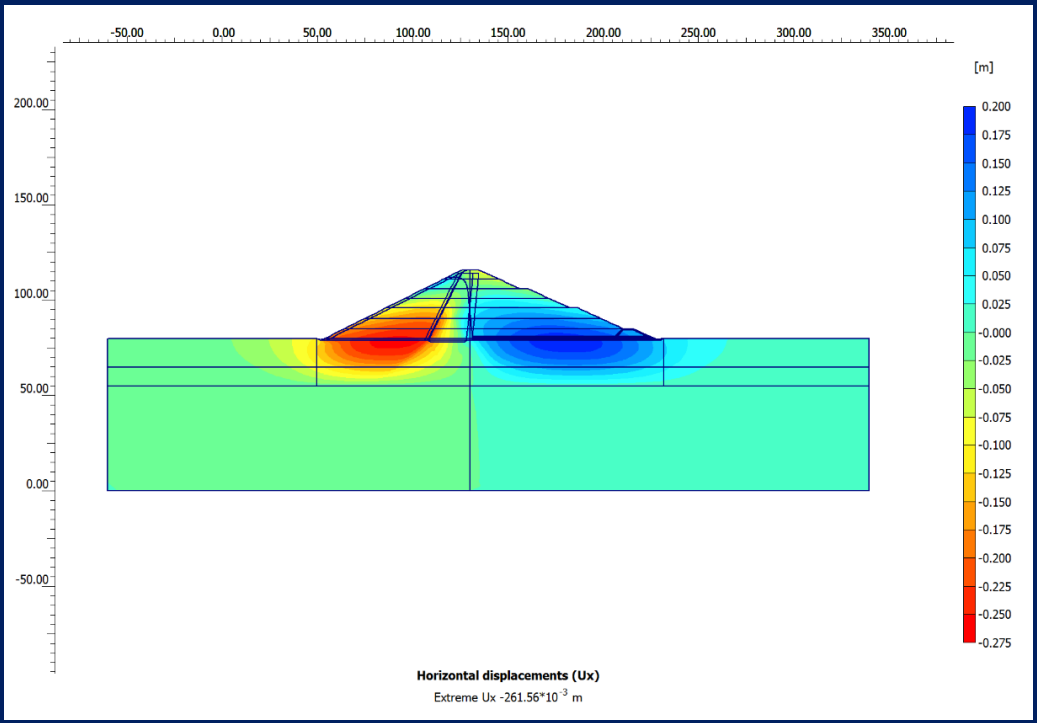

Figure 8.95 Distribution of horizontal displacements (end of construction)

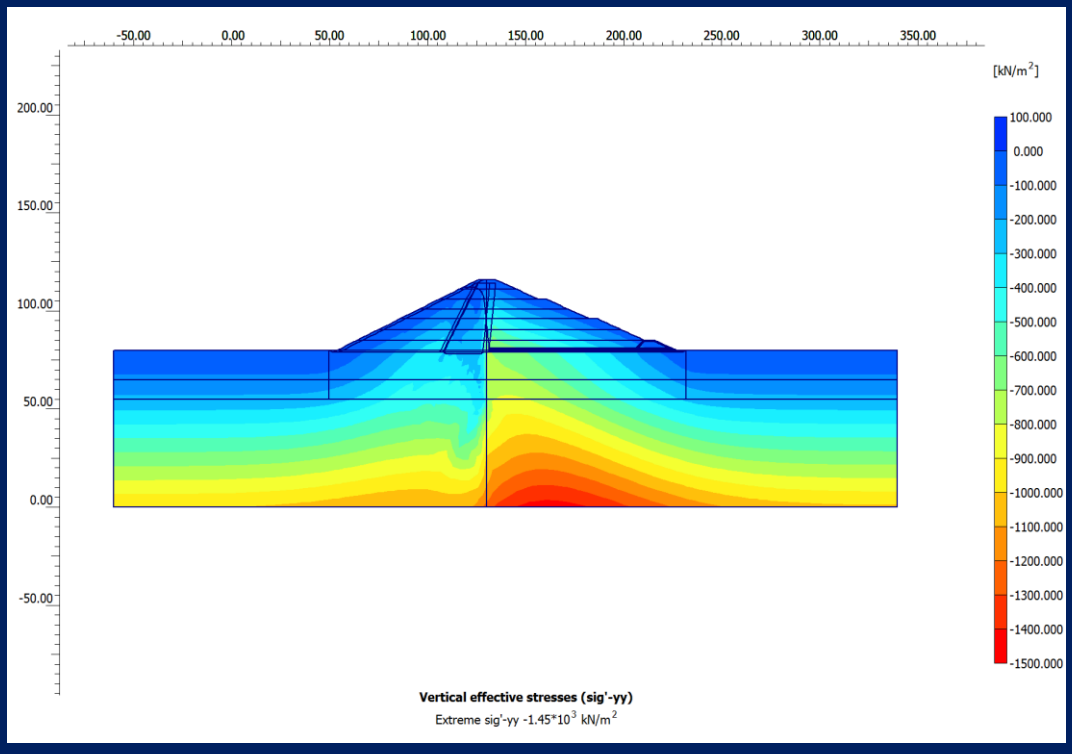

Figure 8.96 Distribution of effective vertical stress (filling of reservoir)

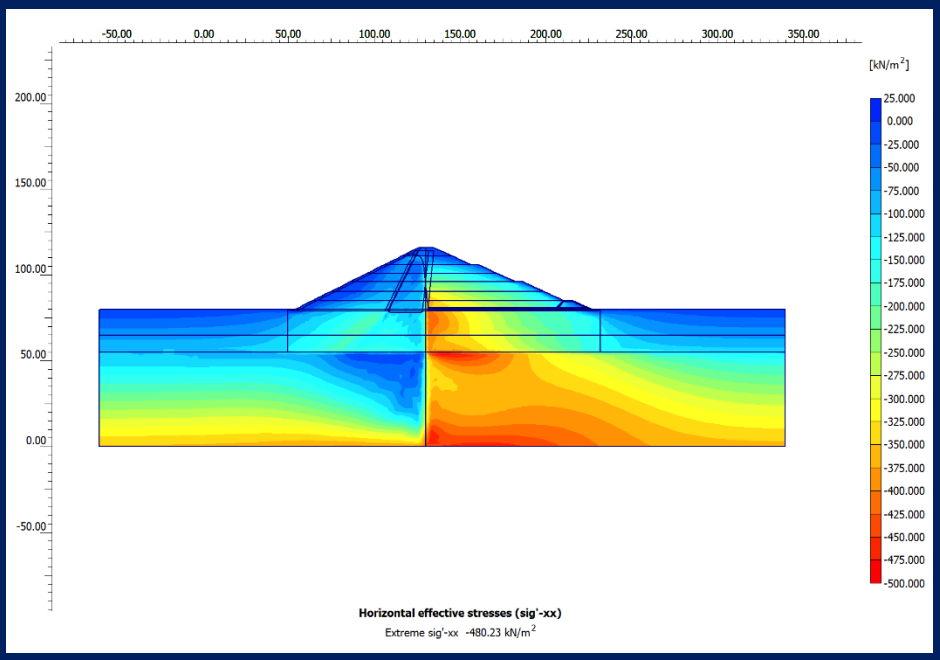

Figure 8.97 Distribution of horizontal effective stress (filling of reservoir)

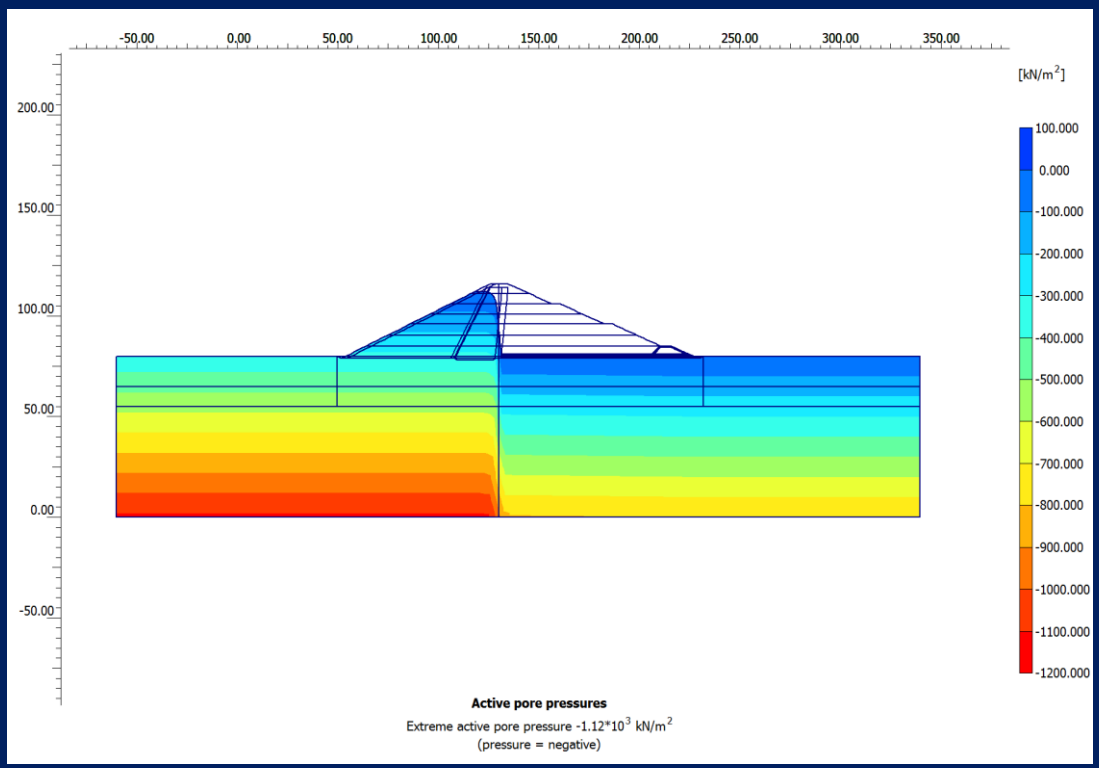

Figure 8.98 Distribution of pore pressures (filling of reservoir)

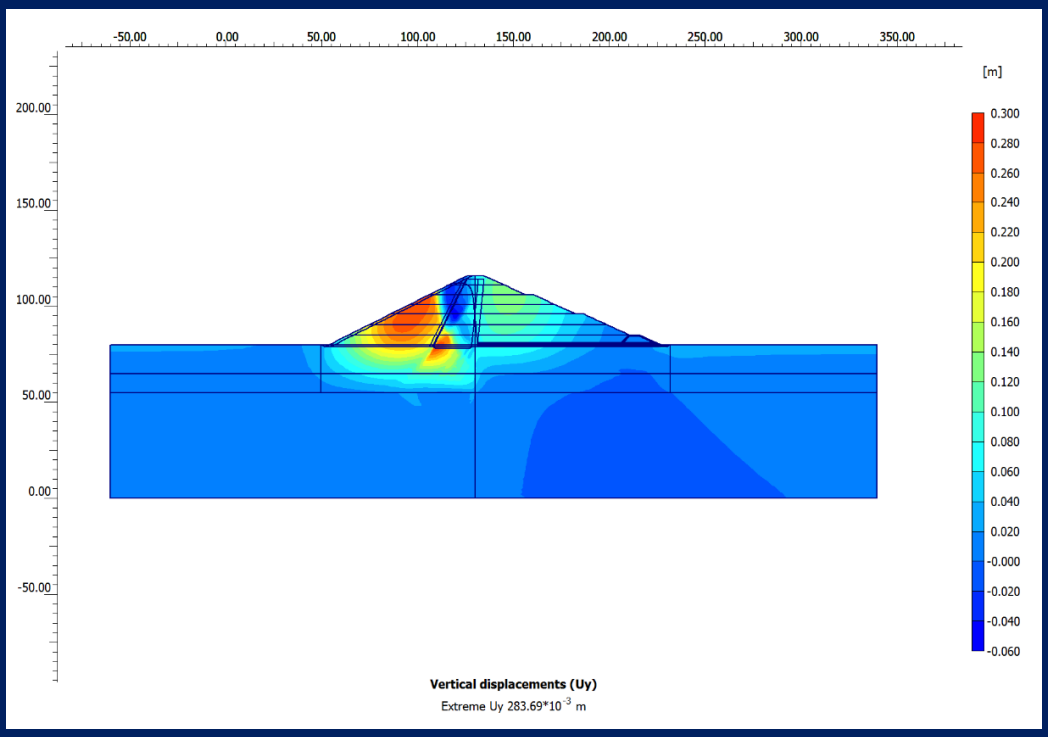

Figure 8.99 Distribution of vertical displacements (filling of reservoir)

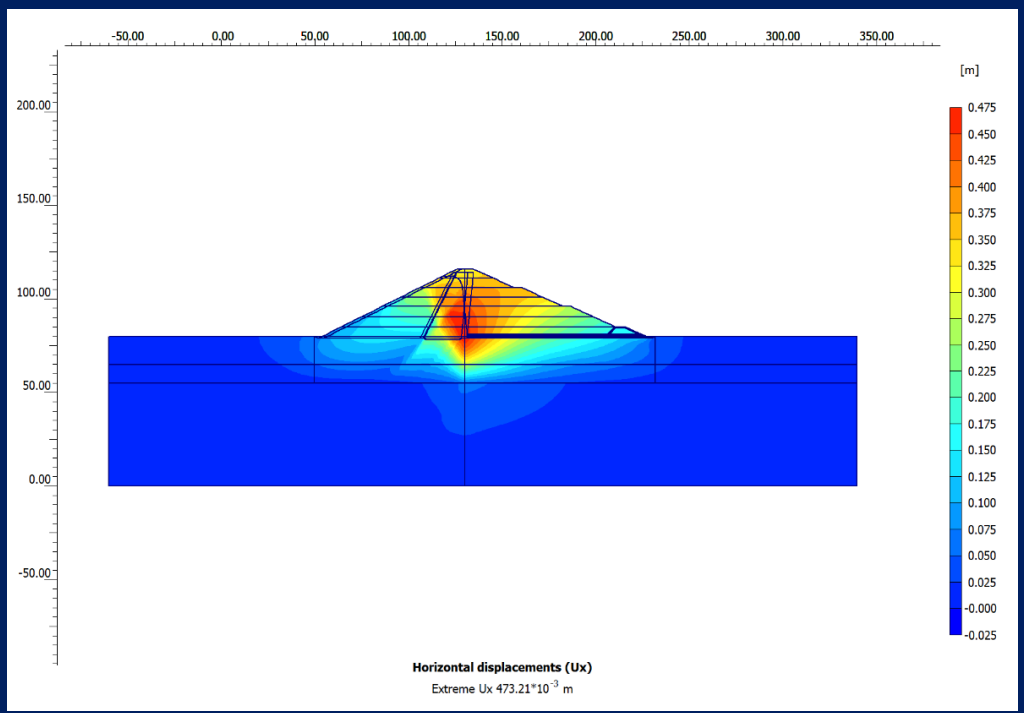

Figure 8.100 Distribution of horizontal displacements (filling of reservoir)

Dam profile founded on bedrock

For the bedrock was considered aa elasticity modulus of 20 MPa.

The distribution of effective vertical stress, effective horizontal stress, pore pressures, vertical displacements and horizontal displacements at the end of the construction phase are presented in Figures 8.101, 8.102, 8.103, 8.104 and 8.105.

The distribution of effective vertical stress, effective horizontal stress, pore pressures, vertical displacements and horizontal displacements at the end of the filling of the reservoir are presented in Figures 8.106, 8.107, 8.108, 8.109 and 8.110.

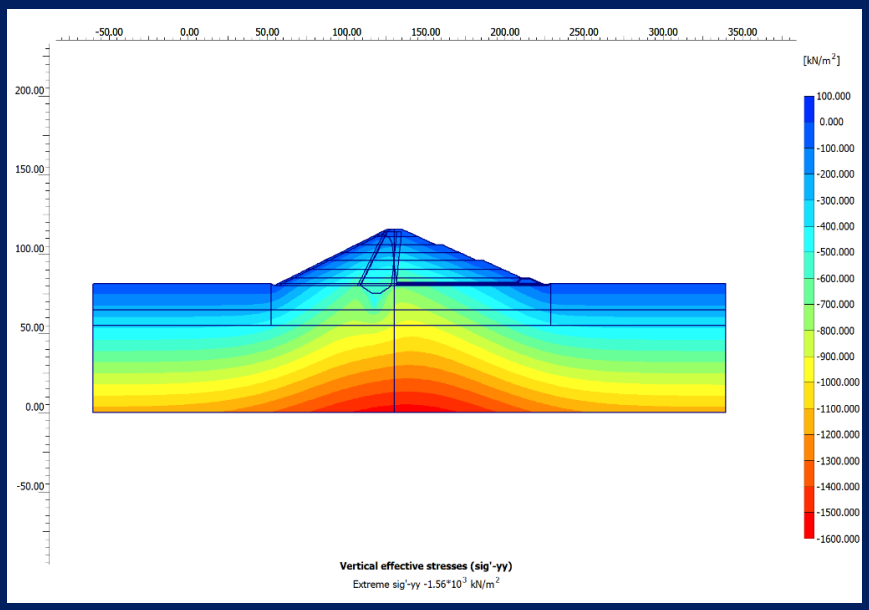

Figure 8.101 Distribution of vertical effective stress (construction phase)

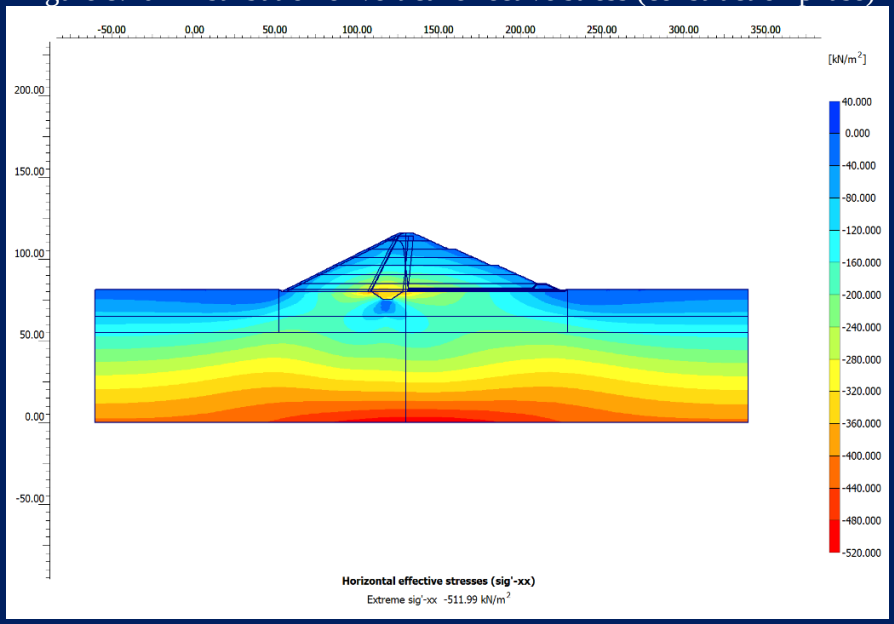

Figure 8.102 Distribution of effective horizontal stresses (construction phase))

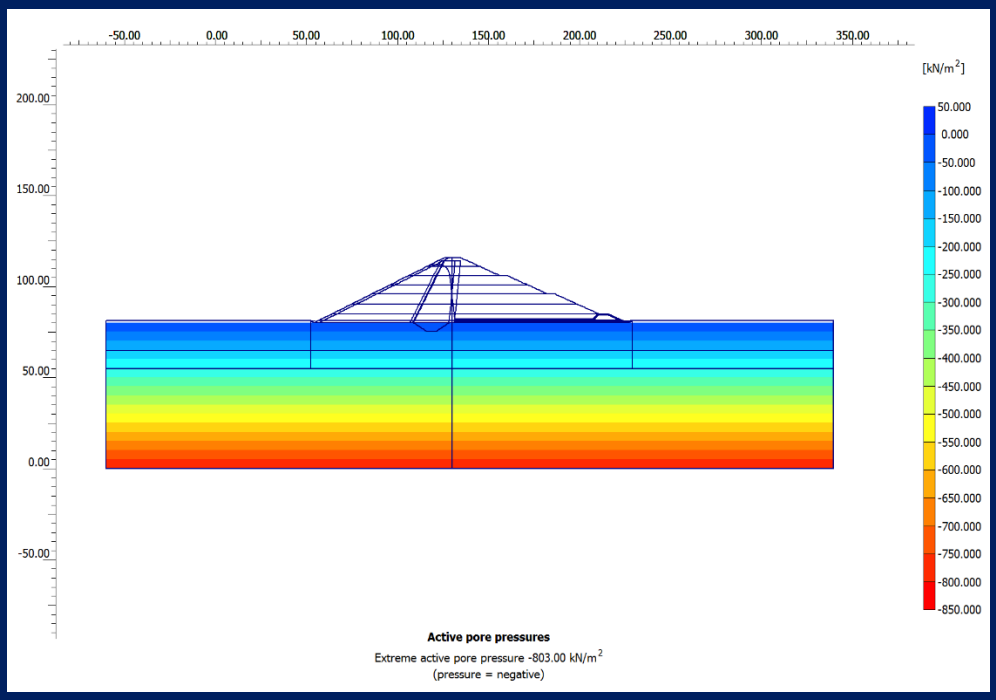

Figure 8.103 Distribution of pore pressures (construction phase)

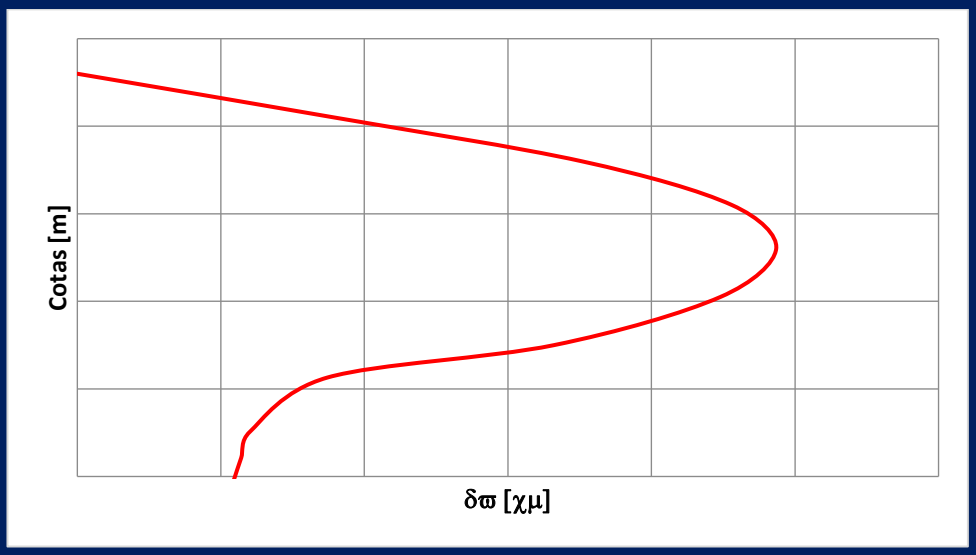

Figure 8.104 Distribution of vertical displacements (construction phase)

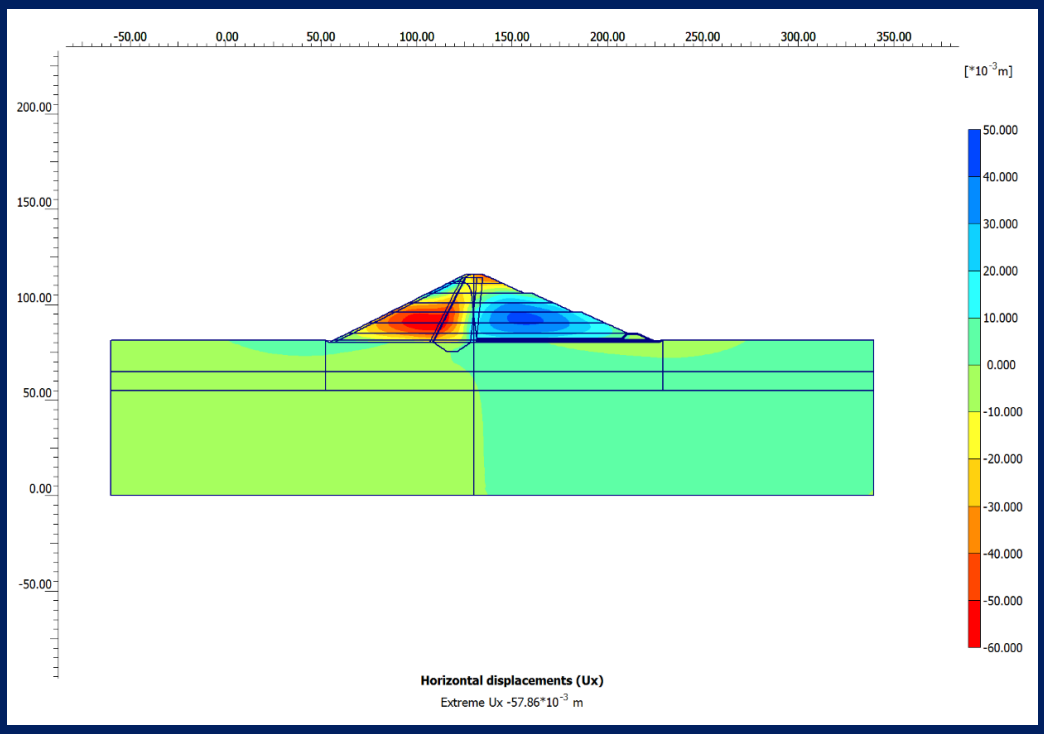

Figure 8.105 Distribution of horizontal displacements (construction phase)

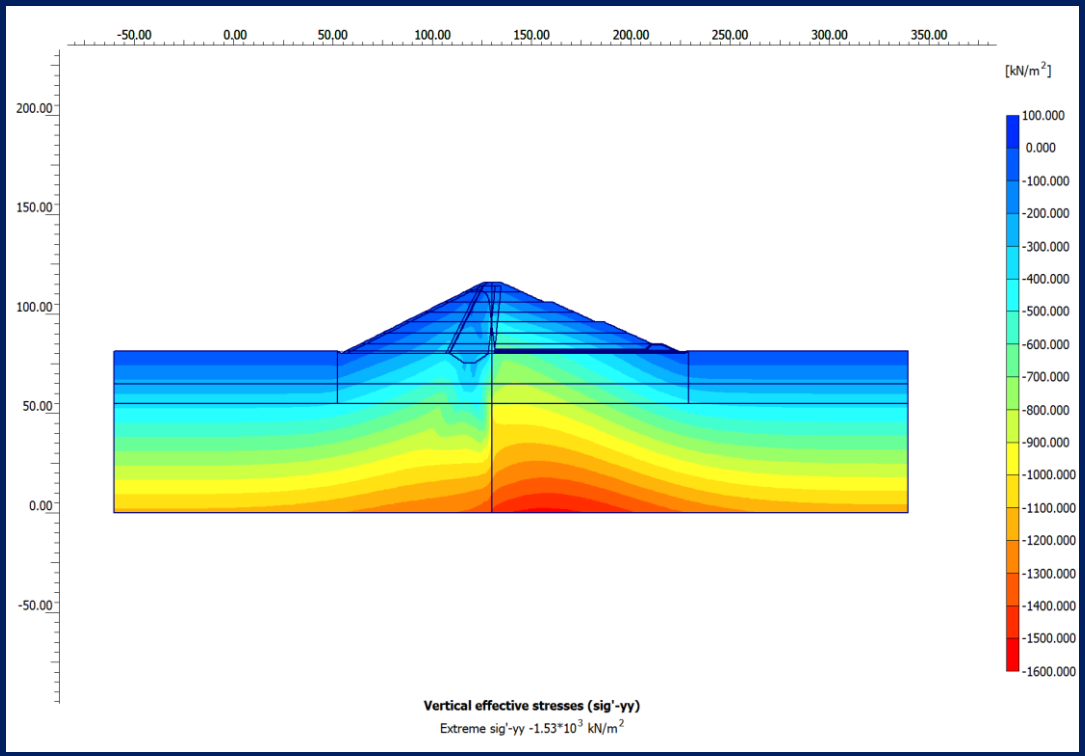

Figure 8.106 Distribution of effective vertical stress (filling of reservoir)

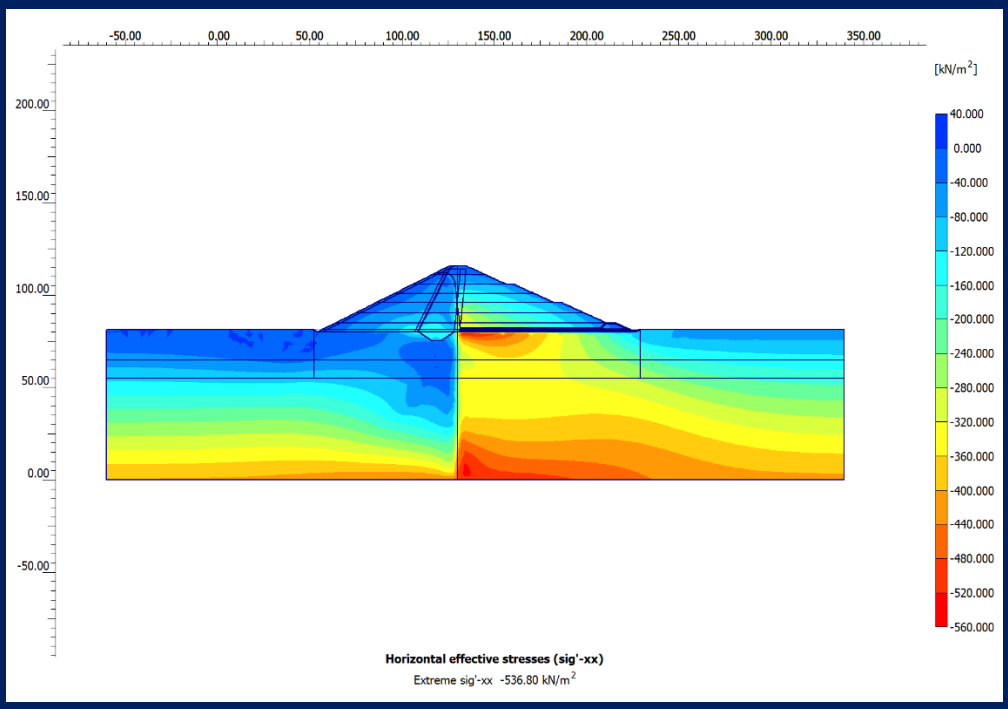

Figure 8.107 Distribution of effective horizontal stress (filling of reservoir)

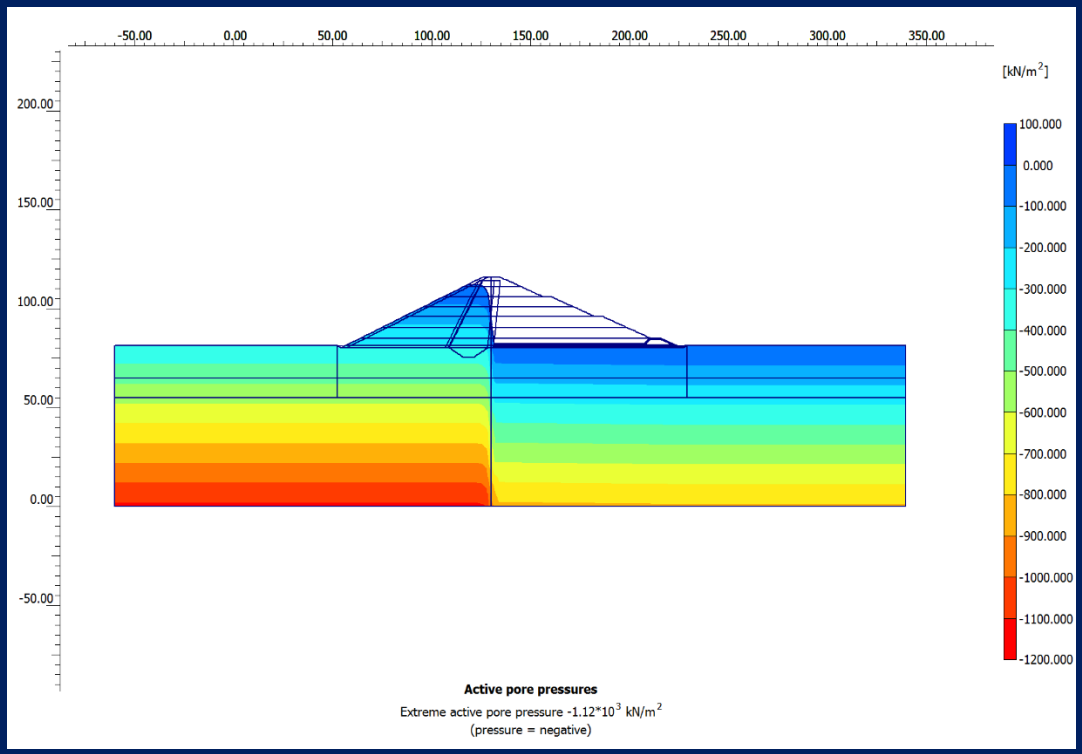

Figure 8.108 Distribution of pore pressures (filling of reservoir)

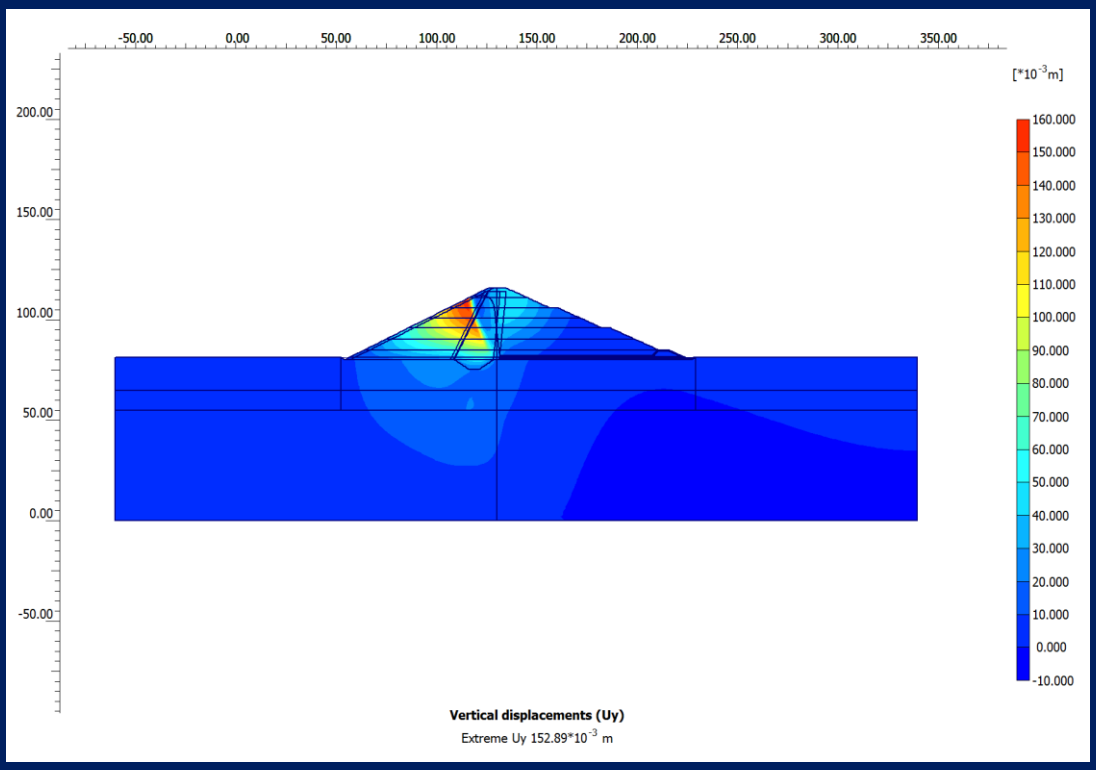

Figure 8.109 Distribution of vertical displacements (filling of reservoir)

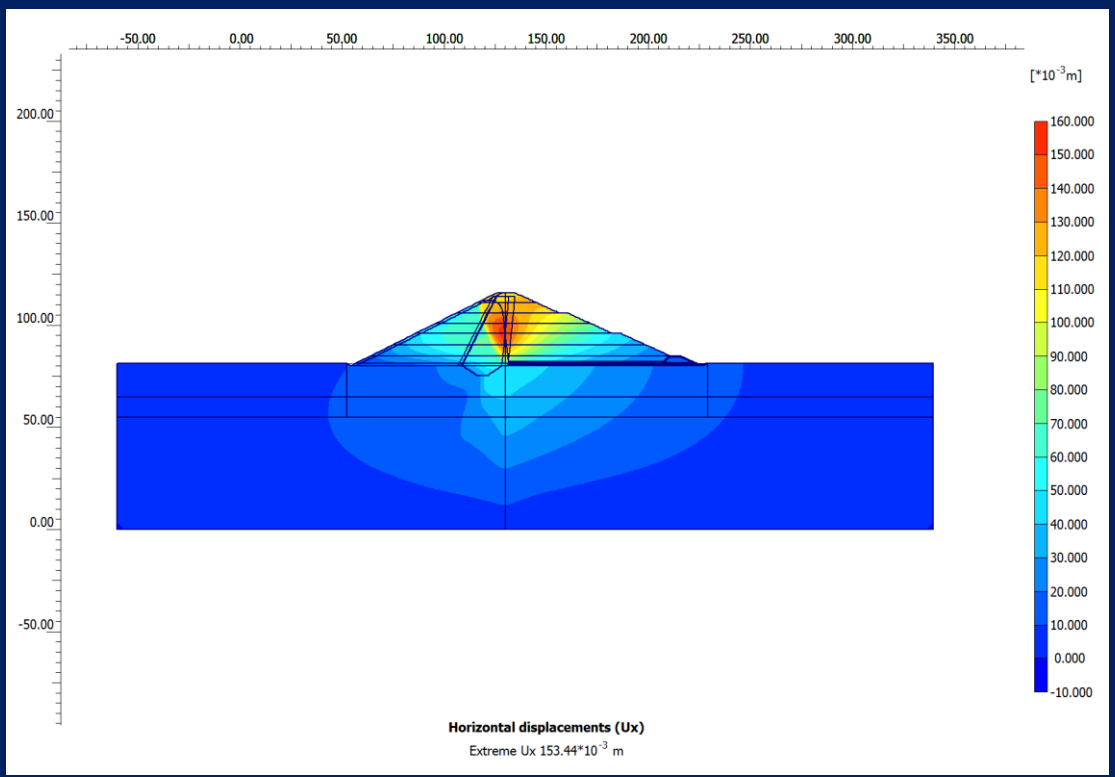

Figure 8.110 Distribution of horizontal displacements (filling of reservoir)

8.2.6.10 Liquefaction Assessment

Liquefaction assessment for the sandy alluvial materials was performed based in SPT tests and CPT tests, following the methodology presented in Figures 4.61 and 4.62.
The interpretation of the results has shown the probability of liquefaction and for the need to increase the compacity of the sandy materials.

Figure 8.111 illustrates the map of locations of earthquakes epicenters in Mozambique.

Figure 8.112 presents the liquefaction assessment.

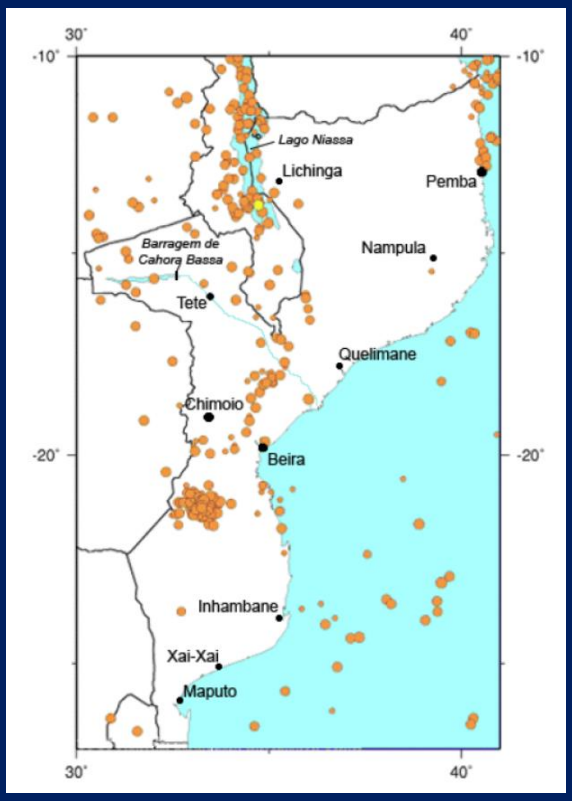

Figure 8.111 Map of locations of earthquakes epicenters in Mozambique

	Prof (m)	σ_0 (kPa)	$\sigma'_{0;\,NA=0m}$ (kPa)	Rd (-)	τ/σ'_0 - $a_{max}/g=0,10$	τ/σ'_0 FS=1,25 $a_{max}/g=0,10$	τ/σ'_0 FS=1,0 $a_{max}/g=0,15$	N_{SPT} S207	C_N (-)	N1 (-)	Potencial liquefacção	q_c (Mpa) CPTU 200	C_Q (-)	Qc (kPa)	Potencial liquefacção	Prof (m)	
P1	1,5	27	12	0,99	0,14	0,18	0,21	4	1,0	4	Liquefaz	1,34	1,0	1339	Liquefaz	1,5	P1
P2	3,0	53	24	0,98	0,14	0,18	0,21	5	1,0	5	Liquefaz	2,24	1,0	2238	Liquefaz	3,0	P2
P3	4,5	80	36	0,97	0,14	0,17	0,21	6	1,0	6	Liquefaz	4,27	1,0	4269	Liquefaz	4,5	P3
P4	6,0	106	48	0,95	0,14	0,17	0,21	5	1,0	5	Liquefaz	2,02	1,0	2025	Liquefaz	6,0	P4
P5	7,5	133	60	0,94	0,14	0,17	0,20	4	1,0	4	Liquefaz	3,04	1,0	3043	Liquefaz	7,5	P5
P6	9,0	159	72	0,93	0,13	0,17	0,20	14	1,0	14	Liquefaz	0,59	1,0	591	Liquefaz	9,0	P6
P7	10,5	186	84	0,89	0,13	0,16	0,19	30	1,0	30	Não liquefaz	1,34	1,0	1339	Liquefaz	10,5	P7
P8	12,0	212	96	0,85	0,12	0,15	0,18	29	1,0	29	Não liquefaz						
P9	13,5	239	108	0,81	0,12	0,15	0,18	60	1,0	60	Não liquefaz						

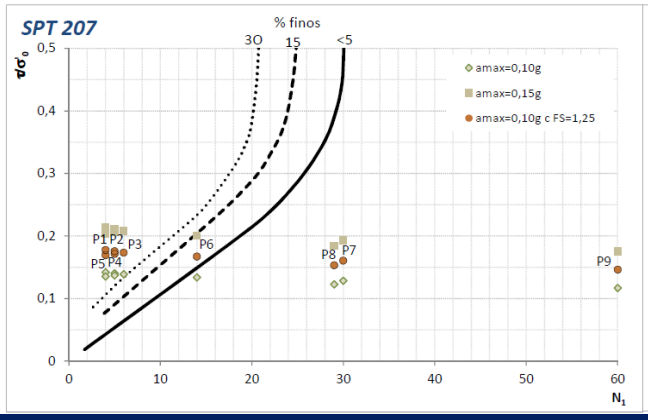

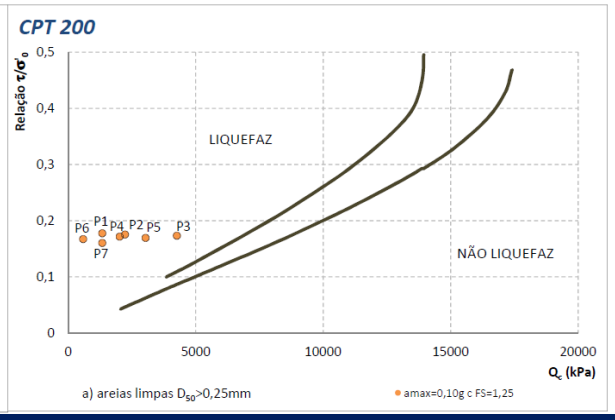

Figure 8.112 Liquefaction Assessment

Vibroflotation

From the different technics for ground improvement and after a careful analysis vibrocompaction was selected to improve the compacity of sand.

Diaphragm Wall

The diaphragm wall shall fulfill the following requirements

a) to full fill the functions.

b) to support the actions.

c) to have adequate durability.

To fulfill these requirements site investigation is needed, detail of the design and constructive procedure.

The ultimate limit states, as well the serviceability limit states shall be verified.

<u>Impervious curtain</u>

An impervious longitudinal curtain, with a depth around 30 m, was considered to control the flows through the dam foundation.

The holes were vertical to intersect the discontinuities families.

For the execution of the grout curtain the following methodology was proposed:

One row of vertical holes 1.5 m apart, with the primary holes, the secondary holes, the tertiary holes and the quaternary holes and the eventually the quinquennia holes, 24, 12, 6, 3 and 1.5 m apart.

In all the primary and secondary holes injection water tests in sections of 5 m shall be performed, followed by the grounting. In other holes Lugeon tests shall be performed only in the last section.

Cut off trench

A cut off trench shall be performed in the foundation's zones with low gradients.

The materials that integrate the cut-off must have a minimum plasticity and water contents between

o W_{op} (optimum content) and W_{op} +2,5% with an average value of Wop +1,5%. The index of plasticity shall not be less than 10% and the percentage of fines higher than 25%.

8.2.6.11 Construction Issues

Figure 8.113 shows the construction of the cofferdam with the core and shell materials.
Figure 8.114 illustrates the quality control tests at the downstream shell.
Figure 8.115 presents the rockfill density test.

Figure 8.113 Cofferdam - Core and Shell

Figure 8.114 Tests at the downstream shell

Figure 8.115 Rockfill density test

Lesson nº 5: During the complementary site investigation programme it is important to characterize the minerology of the clay materials, and their dispersibility. It is important to stress the advantages of a better characterization of the materials during the dam construction, in order to calibrate the design parameters, and this dynamic interaction reminds us that the design only ends with the final dam construction phase.

Note: The dam design project was conducted by a multidisciplinary COBA team and the author was involved in the geotechnical design.

8.2.7 Case History nº 6 - Mapai Dam (Mozambique)

8.2.7.1 Introduction

For Mapai dam the lay-out is addressed, the geotechnical characteristics are referred, the site investigation is addressed, the excavability conditions and slope stability are mentioned, the foundations conditions are described, the freeboard and crest level are defined, the dam the profile is introduced, the definition of design earthquake is discussed, the stability analyses are presented, the seepage studies are analyzed, the stress-strain analyses are addressed, the foundation treatment is analysed, the construction planning is introduced, the risk and monitoring is mentioned and the construction issues are referred.

8.2.7.2 Lay-out

The Mapai dam consists in a 53 m high earthfill dam (above ground terrain level), with a total crest length of 3 360 m (main concrete spillway included) at 173.0 m.a.s.l. The dam, with full supply water level at elevation at 156.4 (NFSWL), impounds a reservoir of 3 000 hm^3 capacity (total storage capacity) and with an inundated area of 228 km^2. The general layout is shown in drawing 40289-FS-IIa-0103-FV-020.

The main spillway of the Mapai Dam is located in the left bank of the Limpopo River and has twelve spans controlled by segment gates that discharge into a concrete canal of rectilinear alignment, ending in a stilling basin.

In the downstream side of the spillway, a concrete waterway in chute canal will be built to carry the flow to the energy dissipation structure.

This channel has a straight axis in plan view, with overall sizes of 248 m length and 295 m wide. Longitudinally the channel has, in its upstream side (164 m length) a constant slope of 308º. In its final length, the slope of the canal is 15.9º.

The height of the side walls is 7.0 m in the upstream side and grows until 27.5 m height in downstream side of the canal.

The bottom outlet structure is located in the right bank of the Limpopo River, and consists in a concrete structure under the embankment dam. This structure also includes an approach channel, an entrance structure and a stilling basin.

8.2.7.3 Geotechnical Characteristics

The Phase I, executed in the Pre-Feasibility Studies, was executed on the sites Nº's 1 (upstream) and 2 (downstream) of Mapai and included seismic refraction profiles, trial pits, boreholes (with SPT tests and Lugeon water tests) and laboratory tests of disturbed samples taken in the trial pits.

The Phase II works, executed in the Feasibility Studies, was executed on the selected dam axis in order to provide more detailed geological and geotechnical information of the dam site. In accordance with the topographic and hydraulic characteristics analysed in both areas of study, Dam Site 2 was considered the best location for the Mapai Dam and its respective auxiliary structures. In this context, the geological and geotechnical site investigation works presented and proposed in the Document 40289-FS-00-00-NT-0003 was carried out throughout the axis of Dam Site 2 and its respective hydraulic structures (Spillway, Powerhouse, Water Intake, Bottom Outlet and Auxiliary Spillway). The site investigation works proposed for this phase of the studies also envisaged geological and geotechnical characterization works, namely the foundation conditions and the assessment of the stability conditions of excavation slopes for implantation of the powerhouse.

The works proposed included the execution of borehole drilling and seismic refraction profiles. Taking into account the results of this site investigation works, it was possible to elaborate an interpretative geological and geotechnical model of the powerhouse site. These site investigation works are available and presented in detail in document 40289-FS-IIa-0102-FV-MDJ.

The geotechnical zoning for the powerhouse foundation was outlined taking into account, essentially, the geological and geotechnical characteristics of the occurring formations, envisaging the foundation conditions of the powerhouse and the corresponding demands upon the foundation ground.

The definition of the geotechnical zones was made considering basically the physical and mechanical characteristics of the occurring formations, such as the weathering and fracturing state of the rock mass, and the quality indexes obtained from the analysis of the boreholes undertaken (percentage of RQD and recovery and N_{SPT}).

This led to the establishment of three geotechnical zones, named ZG1, ZG2 and ZG3. Zone ZG1 was subdivided into ZG1A and ZG1B and zone ZG2 into ZG2A and ZG2B, depending on the lithological type/formation, related to the geological formations $TeAcs_1$ and $TeAcs_2$, respectively, and considering the distinct geotechnical characteristics of the two geological formations.

In order to accommodate the cover soils, even though these are not part of the rock mass and its analysis is based on distinct principles, it was decided to name the surface horizon, which consists of alluvial

deposits and / or colluvio-alluvial deposits, as geotechnical zone ZG4. In general, the worst-case geotechnical zones occur closer to the surface, while the ZG1 and ZG2 zones occur at greater depths.

The geological and geotechnical longitudinal profile is shown in Drawing 40289-FS-IIb-0202-FV-002 according to the alignment of the powerhouse, in which the geotechnical zones are represented. A detailed description of each zone is presented below; the geotechnical characteristics and ranges for each of these zones can be consulted in **Error! Reference source not found.**.

Geotechnical Zone ZG4

Zone ZG4 consists essentially of the cover and filling soils, namely the alluvial deposits and the colluvio-alluvial deposits, where very variable N_{SPT} values were obtained, ranging from 1 to 30 blows.

This horizon has wide-ranging depths; it can reach depths of 47 m in alluvial soils in the central part of the valley.

Geotechnical Zone ZG3

In general, zone ZG3 consists of decomposed material and usually refers to the most weathered, fractured and upper zone of the rock mass. The rock mass is decomposed (W_5) and highly fractured (F_5).

The recovery percentages have very dispersed values, characteristically situated between 0 and 60%, pointing towards a very heterogeneous mass. RQD index values are often null.

Geotechnical Zone ZG2

This zone corresponds to the characteristic domain of the Sandstone / Calcarenitic rock mass, completely weathered to highly / moderately weathered (W_5 to W_{4-3}), with very close to closely spaced fractures (F_{5-4}) and occasional passages in which fractures are located further apart (F_{4-3}).

The recovery percentage is often high, in line with the degrees of weathering and fracturing. The RQD is usually low, where values below 50% are generally observed.

Taking into account the lithological characteristics, this zone was subdivided into zones ZG2A and ZG2B due to the occurrence of the geological formation $TeAcs_1$ and $TeAcs_2$, respectively.

Geotechnical Zone ZG1

This zone corresponds to the Sandstone / Calcarenitic rock mass, predominantly highly/moderately to slightly weathered (W_{4-3} to W_2) and fractured (F_{3-4}), occasionally with moderately widely to widely spaced fractures (F_{3-2}).

The recovery percentage is generally high, normally between 80 and 100%. The RQD index is often greater than 40%.

Taking into account the lithological characteristics, this zone was subdivided into zones ZG1A and ZG1B due to the occurrence of the geological formation $TeAcs_1$ and $TeAcs_2$, respectively.

Figure 8.116 illustrates the crossing the river.
Figure 8.117 shows a river view.

Figure 8.116 Crossing the river

Figure 8.117 River view

8.2.7.4 Foundation Conditions

This item contains some considerations on the geotechnical characteristics of the foundation materials in terms of strength and deformability, namely the foundation conditions of the powerhouse.

At the site where the powerhouse is located, there is a completely weathered rock mass (W_5) whose thickness is approximately 8.2 m, with N_{SPT} values between 29 and of 60 blows falling into geotechnical zone ZG3.

Below this depth the rock mass presents a weathering degree of moderately to slightly weathered (W_{3-2}), and fractures closely to moderately widely spaced (F_{4-3}), and moderately widely to widely spaced fractures (F_{3-2}), with a percentage of RQD between 7 to 38%, up to the depth of 12.0 m, falling within geotechnical zone ZG2A. From this depth the rock mass presents percentage of RQD superior to 60% (geotechnical zone ZG1A and ZG1B).

The powerhouse foundations are intercepted by essentially sandy and calcarenitic formations ($TeAcs_1$) and punctually layers of orange siltstone ($TeAcs_2$).

The powerhouse foundation rock mass is moderately to slightly weathered (W_{3-2}) with fractures moderately widely to widely spaced (F_{3-2}), with a percentage of RQD superior to 82%, and as such falling within the ZG1A geotechnical zone. According to the results of the seismic profiles PS328 and PS329, the powerhouse foundation rock mass presents values of P-wave velocity greater than 2 500 m/s.

Taking into account the demands in terms of strength and deformability, it is expected that the grounds that occurs at the foundation have the required geotechnical conditions. However, in the case of more fractured and weathered zones, excavation and replacement with cyclopean concrete should be performed.

8.2.7.5 Excavability conditions and slope stability

The excavation conditions of the formations that occur at the site of the powerhouse were analysed based on the geotechnical zoning prepared and the results of the survey works undertaken.

These works are located in an area that requires excavations with a depth of approximately until 30 m in relation to the natural ground level.

According to the survey works, it is expected that the area to be excavated for the powerhouse is intercepted by materials with different excavability characteristics. It is therefore considered that when weathered rocks are intersected, excavation can be done with mechanical means. In deeper excavations and when rock mass of better quality is intersected, in particular within geotechnical zone ZG1A, the need to resort to blasting equipment is foreseen.

The explosives should be carefully used so as not to damage the rock mass beyond the intended area. In these situations, the pre-splitting technique must be used since it is fundamental to assure that the slope is correctly cut and according to the recommended geometry, while reducing the propagation of vibrations to the rock mass, in order to avoid the effects of decompression and consequent instability.

The characteristics of the rock mass, as evidenced by the survey works, require slopes with varying inclinations, with smoother inclinations in the surface areas and steeper inclinations in the deeper zones.

Taking into account the geological and geotechnical zoning, the following criteria for slope inclinations were considered for the temporary slopes of the bottom outlet and powerhouse.

8.2.7.6 Freeboard and crest level

In this chapter is presented the analysis and design of freeboard to protect the dam from overtopping as a result of wind-generated wave runup and reservoir setup.

The freeboard should include prevention of any overtopping of the dam by either frequent or infrequent high waves that might interfere with efficient operation of the project, create conditions hazardous to personnel, causes other adverse effects not necessarily associated with the general safety of the structure, or cause a dam breach and failure.

The design of freeboard for dam adhere to concepts and methodologies presented in USBR (1981, 2012).

Freeboard criteria

The freeboard calculation, according with USBR (2012), should consider the following criteria:

- Criteria 1: Crest level > Full supply water level (FSWL) + runup and setup from a 160 kilometres-per-hour wind velocity (highest sustained velocity winds at the site);
- Criteria 2: In this case is considered the design inflow flood (return period of 5 000 years), and the sum of the setup and runup that would be generated by the typical winds that would be expected to occur during large floods.

  Crest level > Maximum reservoir water level (MRWL) + runup and setup from an 80 kilometres-per-hour wind velocity (typical wind at the site).

The minimum freeboard to prevent overtopping should be greater than one meter, 1 m (USBR, 2012).

Wind loadings

The wind blowing over the reservoir causes the temporary setup of the water level and generates wind waves for a given fetch and minimum duration.

The inexistence of site-specific wind data doesn’t allow to determine wind magnitudes with different probability of exceedance.

The following wind speeds are considered to calculate the runup and setup in the reservoir:

- Typical wind expected to occur during large flood: 80 km/h;
- Highest sustained velocity at the site: 160 km/h.

Fetch

The maximum wave heights in a reservoir can be limited by three factors: fetch length (over-water distance the wind blows), wind duration (how long the wind conditions persist) and the wind speed. Generally, the design conditions will be limited by fetch.

The procedure for estimating the fetch over an inland reservoir having an irregularly shaped shoreline consists of constructing nine radials from the dam at 3-degree intervals and extending these radials until they first intersect the shoreline again on the opposite side of the reservoir (see figure below). The length of each radial is measured and arithmetically averaged. This calculation should be performed for several directions (of the central radial) approaching the dam, including the direction where the central radial is normal to the dam axis and also the direction where the total spread results in the longest possible set of radials.

$$F_e = \sum x_i / 9 \qquad (8.24)$$

where:

F_e – effective f*etch*, km;

x_i – length of radial I, km.

The effective fetch calculated for Mapai reservoir are: 13.9 km for the MFWL and 13.2 for the NFSWL.

Wind setup

Wind blowing over a water surface exerts a horizontal shear force on the water, driving it in the direction of the wind. In an enclosed body of water, the wind effect results in a rise in the water level at the downwind end of the fetch. This effect is termed “wind tide” or “wind setup.”

Wind setup in meters, S, is computed as follows (Zuider Zee):

$$S = \frac{V^2 \times F_{\max}}{63000 \times D} \qquad (8.25)$$

where:

S – wind set-up, m;

V – wind speed, km/h;

F_{max} – effective *fetch*, km;

D – average depth of water, m.

The fetch is in NE-SW direction and average depth of water along that direction is:

- 17,5 m for reservoir at MFWL;
- 13,2 m for reservoir at FSWL.

The wind setups (S) in Mapai reservoir calculated for the specified wind loadings are:

- 0,1 m, for a typical wind of 80 km/h;
- 0,4 m, for the highest sustained wind expected at the site of 160 km/h.

Wind generated wave height

Wind-generated waves are not uniform in height, but they consist of a distribution of waves with various heights. The significant wave height (H_s) is defined as the average of the highest one-third of the waves in a wave field.

The fetch limited significant wave height is calculated based on the parameters established in the previous items, namely wind speed and effective fetch of the reservoir, using the following equation (USBR, 2012):

$$H_s = 0.00366 \cdot F_e^{0.5} \cdot V \cdot (1.1 + 0.00969 \cdot V)^{0.5} \quad (8.26)$$

where,

H_s – significant wave height, m;

V – wind speed, km/h;

F_e – effective fetch, km.

The significant wave height (H_s) obtained for the different wind speeds are:

- 1,9 m, for a typical wind of 80 km/h;
- 4,4 m, for the highest sustained wind expected at the site of 160 km/h.

Wave runup

The wave runup in the upstream face of the embankment dam is the vertical distance that the wave travels after hit the dam, measured between the maximum level attained by the wave and the still level.

The computation of the wave runup can be made using the following equation (USBR, 2012):

$$R = H_s(A\xi_p + C)\gamma_r\gamma_b\gamma_h\gamma_\beta \quad (8.27)$$

where:

R – wave runup, m;

H_s – significant wave height, m;

ξ_p – surf similarity factor;

A, C – coefficients dependent on ξ_p;

γ_r – reduction factor related to roughness of the slope;

γ_b – reduction factor for the influence of a berm;

γ_h – reduction factor for the influence of shallow-water conditions;

γ_β – reduction factor for the influence of the direction of the fetch relative to the dam axis.

The factor ξ_p can be calculated using:

$$\xi_p = \frac{\tan\alpha}{\sqrt{s_p}} \tag{8.28}$$

where,

α – slope of angle of the upstream face of the embankment dam with the horizontal;

s_p – steepness of the peak waves.

The s_p parameter can be calculated by:

$$s_p = \frac{2\pi}{g}\frac{H_s}{T^2} \tag{8.29}$$

where,

H_s – significant wave height, m;

T – wave period, s.

The wave period, T, can be determined by:

$$T = 0{,}338 \cdot F_{e^{1/3}} V^{1/3} (1{,}1 + 0{,}0097 \cdot V)^{1/6} \tag{8.30}$$

The application of the equations presented and the coefficients suggested by USBR (2012) allows to estimate a wave runup of 2.2 m and 4,6 m for the waves resulting of a frequent and an exceptional wind, respectively, as presented in the Table 8.23.

Table 8.23 Wave runup in Mapai dam for a frequent and for an exceptional wind

Wind	Frequent	Exceptional	
U_{wind}	80	160	m/s
F_e	13,9	13,2	km
T	3,9	5,1	s
H_s	1,85	4,40	m
tan (α)	0,42		-
s_p	0,08	0,11	-
ζp	1,49	1,27	-
A	1,60		-

Wind	Frequent	Exceptional	
C	0,00		-
$\square_r$	0,55		-
$\square_b$	1,00		-
$\square_h$	1,00		-
$\square_\square$	0,89	0,93	-
R	2,2	4,6	m

Minimum freeboard and dam crest elevation

The Table 8.24 presents the summary of the minimum dam freeboard calculation for the Mapai dam that was carried out accordingly to the methodology proposed by USBR 2012[i].

Table 8.24 Minimum dam freeboard calculation

Parameter	Freeboard above NFSWL	Freeboard above MFWL
Effective fetch	13.2 km	13.9 km
Wind velocity	160 km/h	80 km/h
Significant Wave Height	4.4 m	1.9 m
Wave runup	4.6 m	2.2 m
Wind setup	0.4 m	0.1 m
Minimum freeboard calculation	**5.0 m**	**2.3 m**
Minimum freeboard adopted	**5.0 m**	**3.0 m**
Reference water level	**156.4 m.a.s.l. (NFSWL)**	**170.0 m.a.s.l. (MFWL)**
Minimum dam crest elevation required	**161.4 m.a.s.l.**	**173.0 m.a.s.l.**

The calculation performed points to minimum freeboard values of 5,0 m above the NFSWL (normal full supply water level) and 2,3 m above the MFWL (maximum flood water level). Accordingly, for purposes of establishing the minimum dam crest elevation required, we considered a minimum freeboard of 5,0 m above the NFSWL and 3,0 m above the MFWL.

Taking into account these results, the dam crest elevation was set at 173.0 m.a.s.l.

8.2.7.7 Dam Profile

Figure 8.118 illustrates the Plan of Mapai dam.

Figure 8.119 shows the longitudinal profile of the Mapai dam.

Figure 8.120 presents the geological model at the dam site.

[i] USBR, 2012. "Design Standards No.13 – Embankment Dams", Chapter 6 – Freeboard, U.S. Department of the Interior, Bureau of Reclamation.

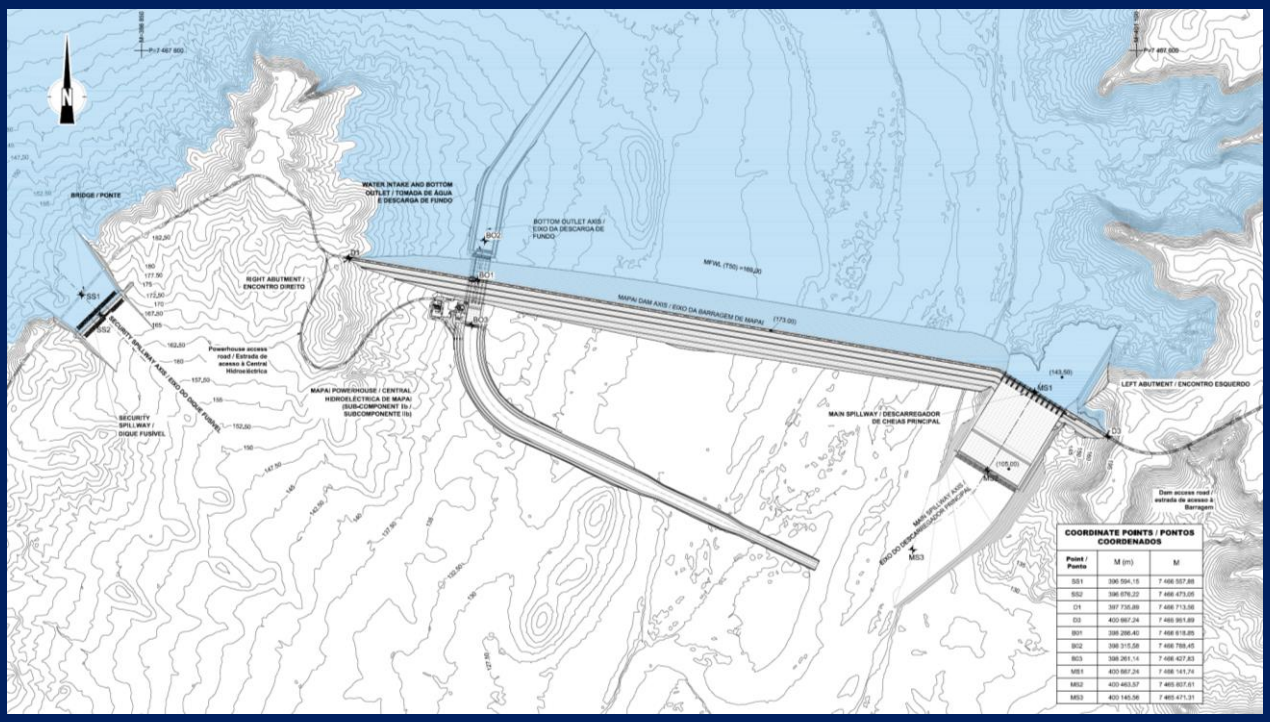

Figure 8.118 Plan of Mapai Dam

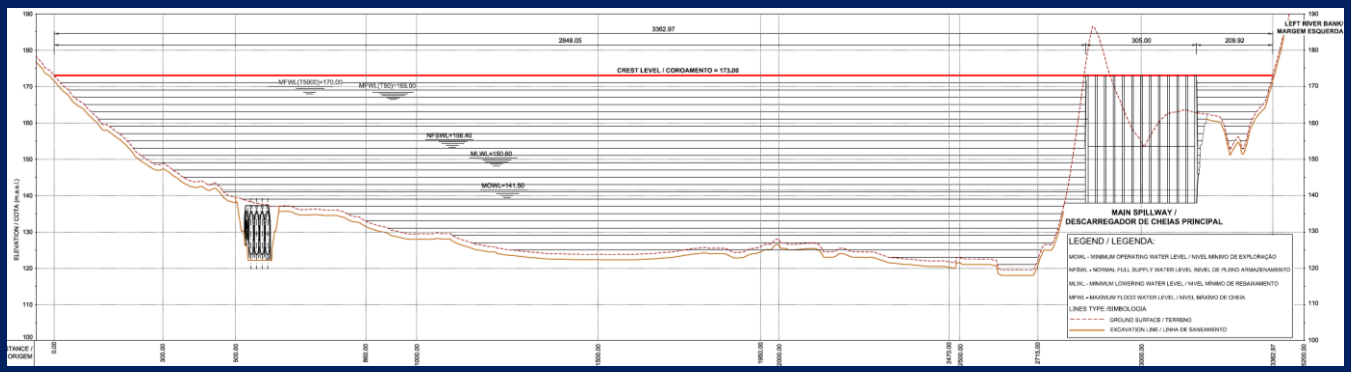

Figure 8.119 Longitudinal Profile of the Mapai Dam

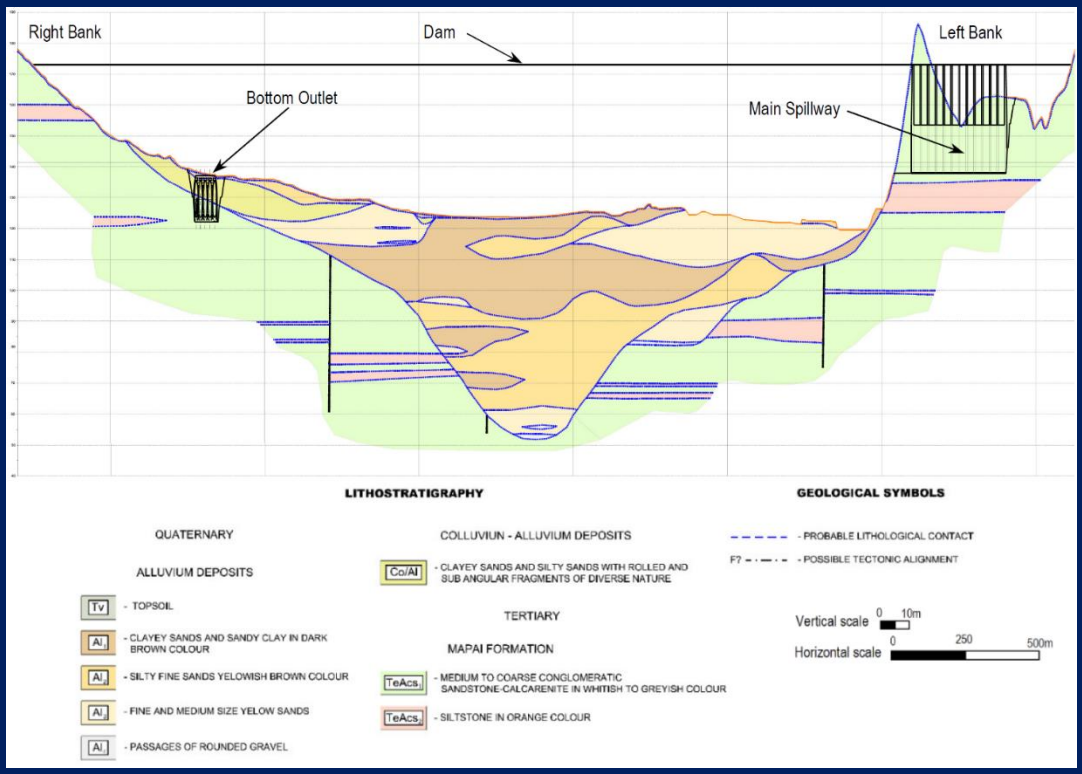

Figure 8.120 Geological model at the Dam Site

Figure 8.121 to Figure 8.123 show the typical cross section nº 1, nº 2, nº3 of the foundation treatment. Figure 8.124 illustrates the dam materials requirements.

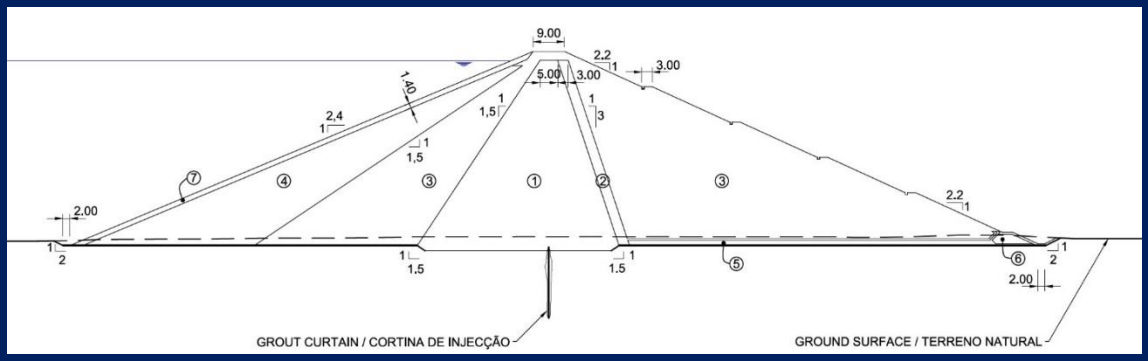

Figure 8.121 Mapai Dam Typical cross section 1 of the foundation treatment

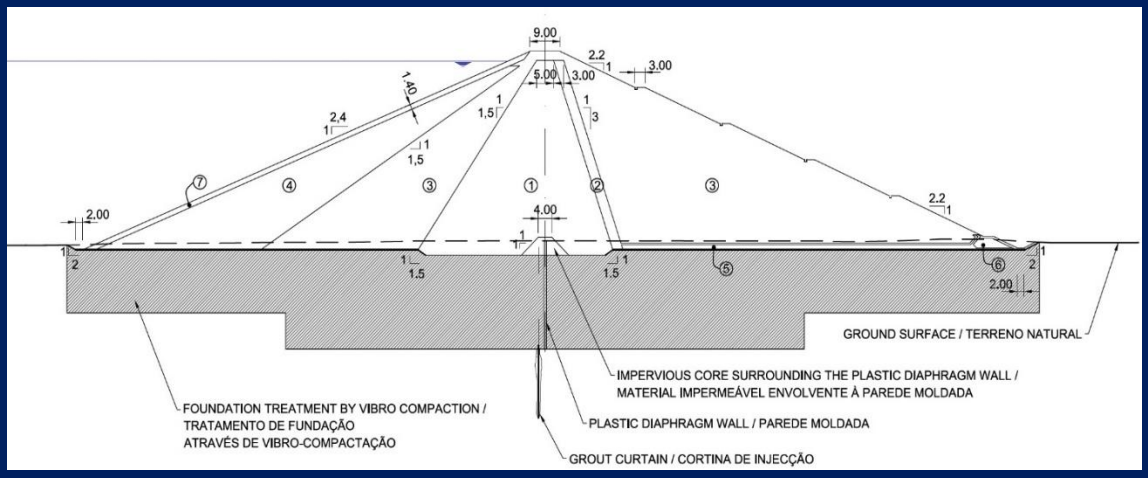

Figure 8.122 Mapai Dam Typical cross section 2 of the foundation treatment

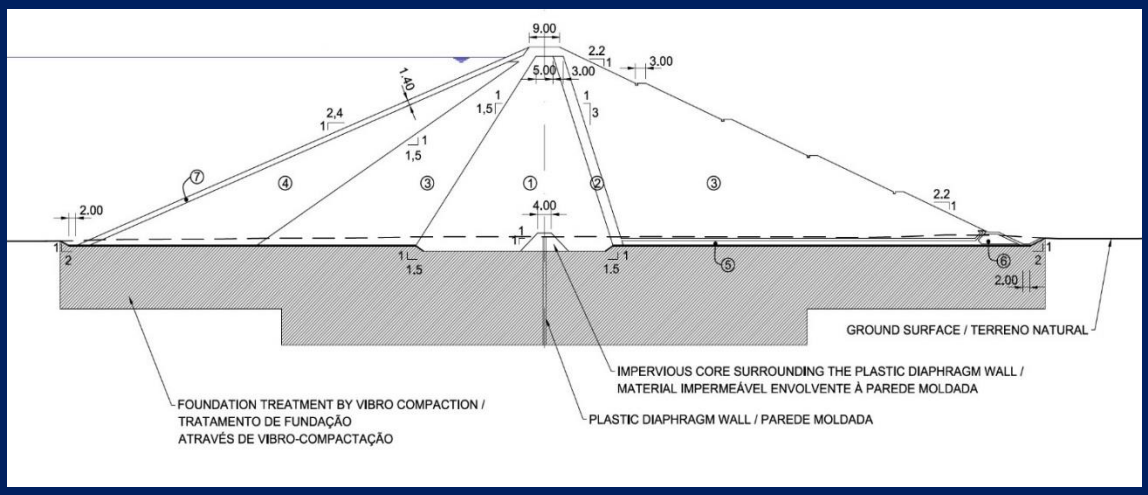

Figure 8.123 Mapai Dam Typical cross section 3 of the foundation treatment

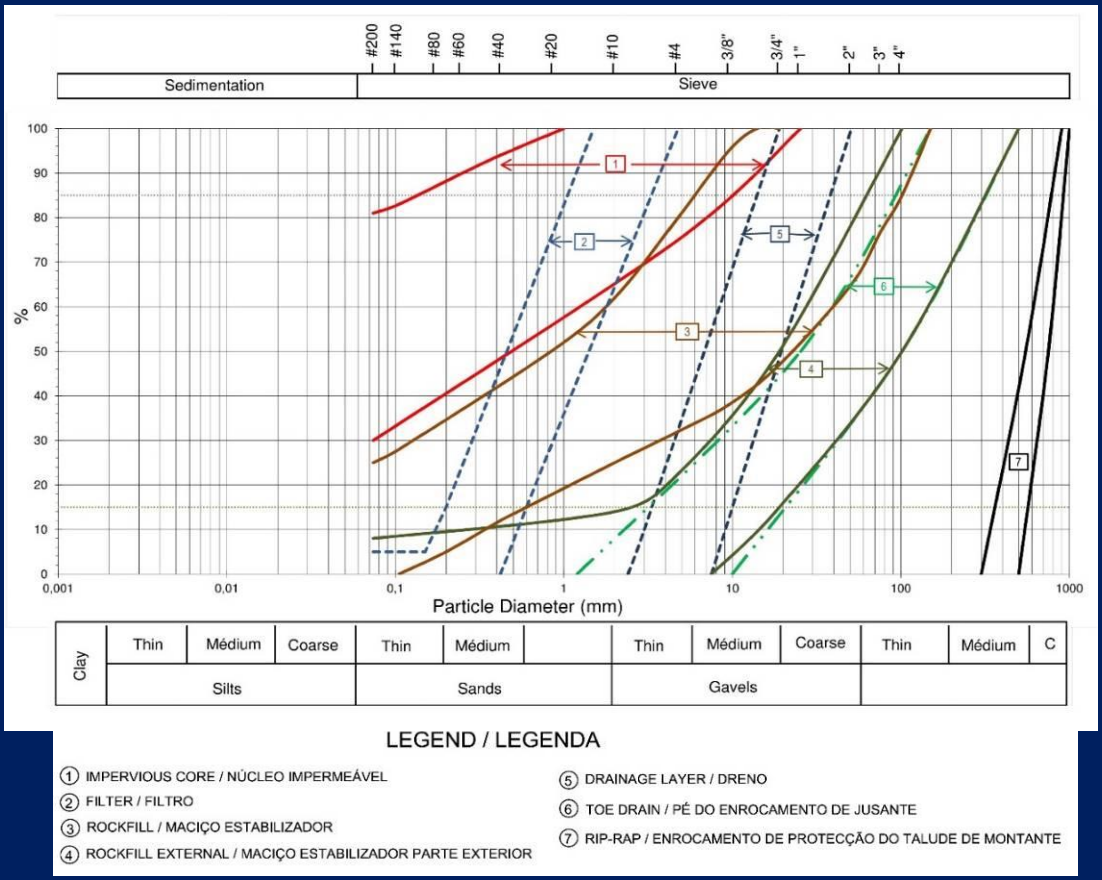

Figure 8.124 Dam materials requirements

8.2.7.8 Stability Analyses

A computer code SLOPE W was used to analyze the slope stability of the dam profiles.

It is current practice to analyze: construction phase, filling of reservoir and drawdown.

For the construction phase the design values are summarized in Table 8.25.

Taking into account the size of the dam a pseudo-static analysis was considered adequate.

Table 8.25 Design Values for the construction phase

MATERIAL	Unit weight (kN/m^3)	Cohesion (kPa)	Friction angle (0°)	Piezometer Surface	R_u
Rip-rap (7)	20	0	40	0	0
Shell material (3)	21	0	38	0	0
Shell material (4)	21	0	42	0	0
Core (1)	20	5	28	0	0.15
Filter	18	0	35	0	0
Foundation (section 1)	20	20	32	0	0
Foundation (sections 2 & 3)	18	0	25	0	0

For the construction phase the most critical surface for the downstream slope has a safety factor of 1.76 (Figure 8.125)

For the construction phase the most critical surface for the upstream slope has a safety factor of 2.129 (Figure 8.126).

The most critical surface for the downstream slope for the filling of the reservoir has a safety factor of 1.754 (Figure 8.127).

The most critical surface for the upstream slope for the drawdown of the reservoir has a safety factor of 1.645 (Figure 8.128).

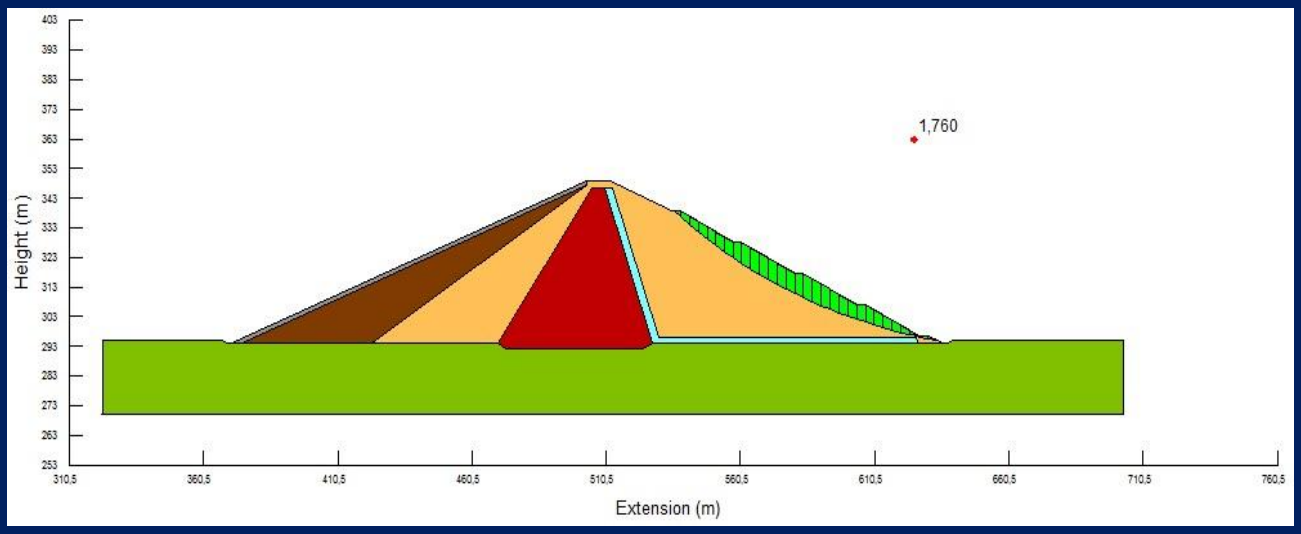

Figure 8.125 Construction Phase Downstream slope. Most Critical surface

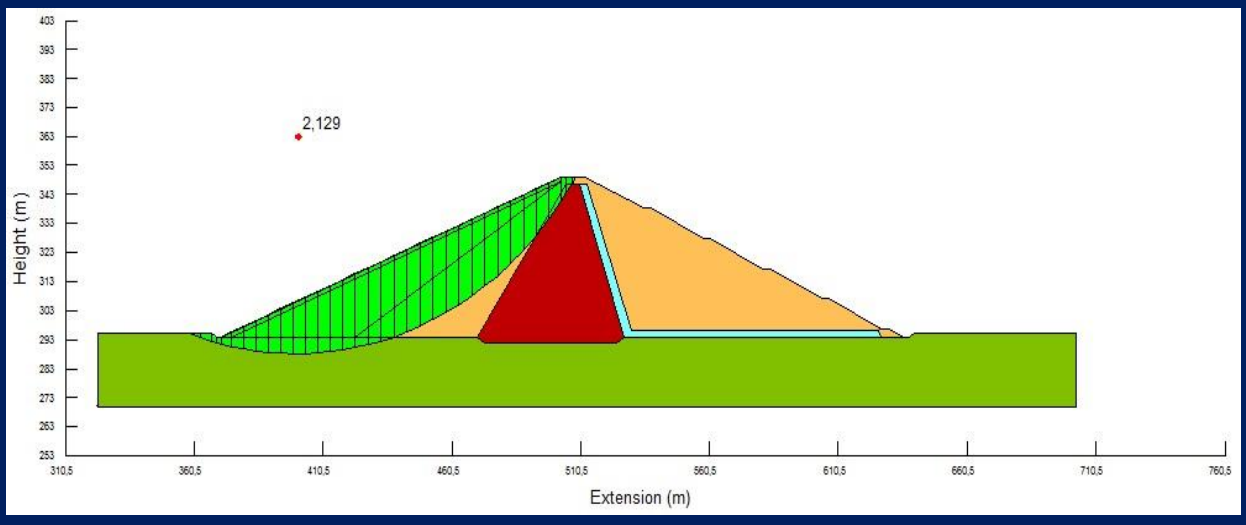

Figure 8.126 Construction Phase Upstream slope. Most Critical surface

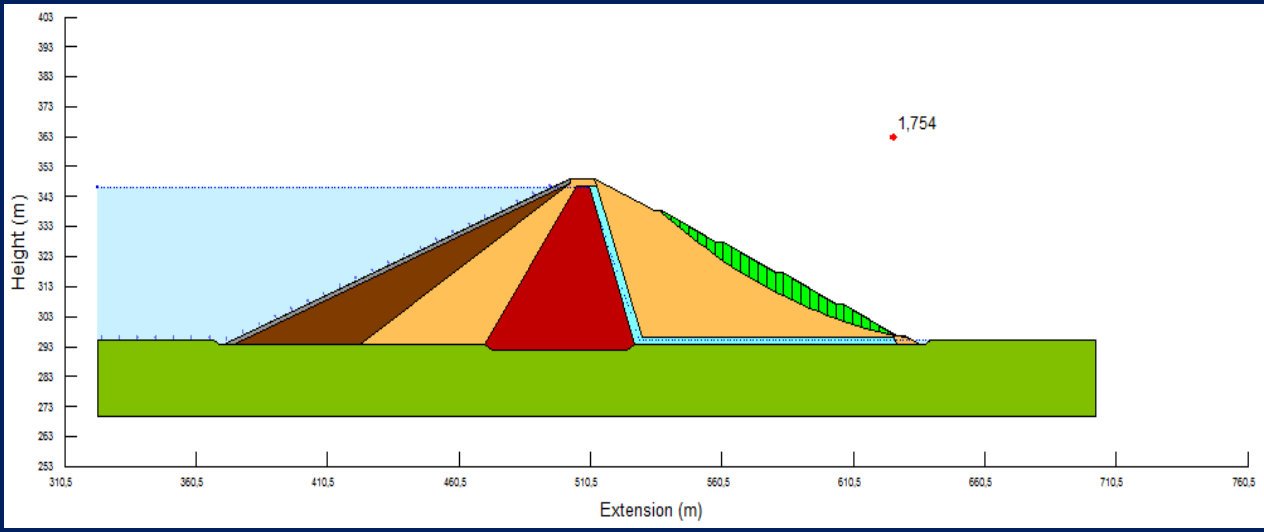

Figure 8.127 Filling of the reservoir Phase Downstream slope. Most Critical surface

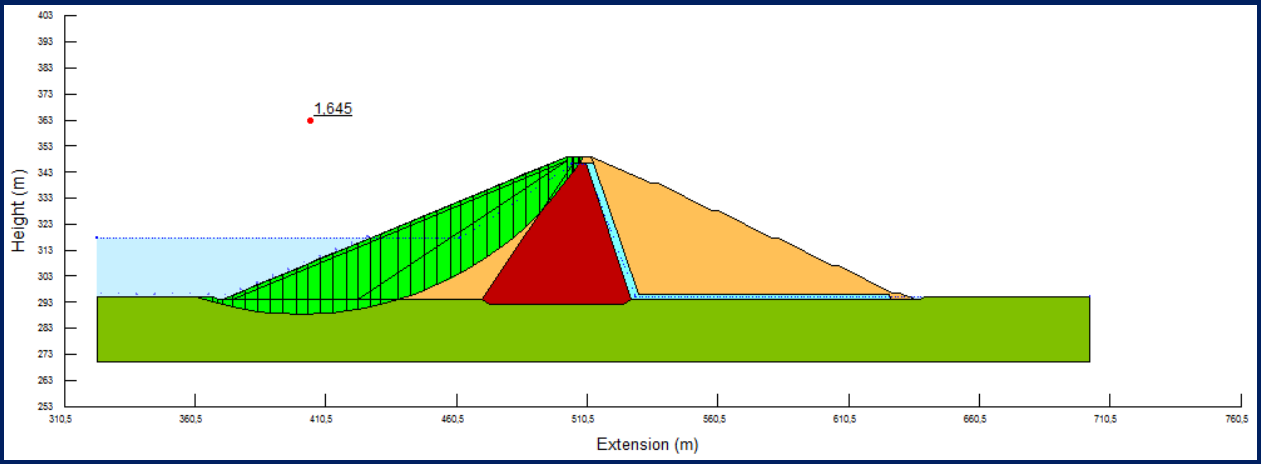

Figure 8.128 Drawdown of the reservoir Phase Upstream slope. Most Critical surface

8.2.7.9 Pseudo-static Analysis

Following the recommendations of ICOLD "High embankment dams whose failure may cause loss of life or major damage should be designed by conventional method at first, followed by a dynamic analysis in order to investigate any deficiencies which may exist in the pseudo-static design of the dam" simplified procedures for estimating induced deformations are presented.

In the present case due to the low seismicity the conventional pseudo-static method is sufficient.

Two situations were analyzed, namely MCE and OBE.

The most critical surfaces for the downstream slope have safety factors of 1.332 and 1.47 (Figure 8.129).

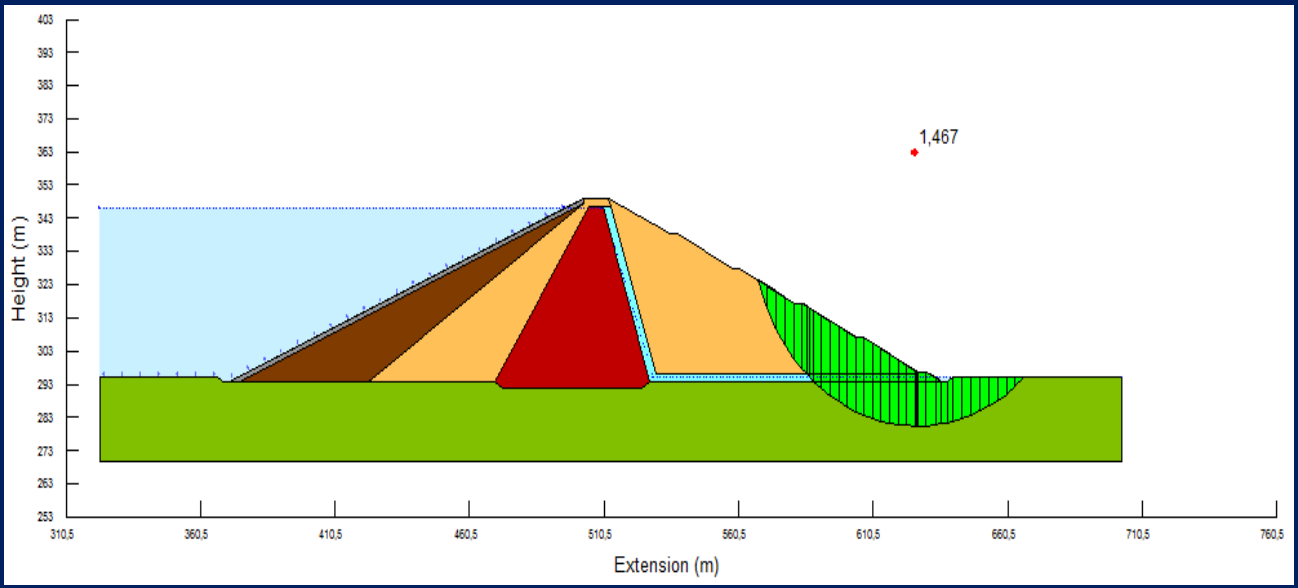

Figure 8.129 Filling of the reservoir Phase –Downstream slope. Most Critical surface (pseudo-static analysis)

8.2.7.10 Stress-Strain Analysis

A stress strain analysis was performed for the construction phase, filling of reservoir and steady state situation.

Different foundations situations were considered.

The purpose of these analyses was to assess the displacements, as well the stress distribution.

An elastic behaviour for the materials were considered, due to the absence of adequate stress-strain curves.

The analyses were performed using the code PLAXIS – version 7.2.

The seepage study was performed by PLAXIS code. The characteristics of the materials are shown in Table 8.26.

Table 8.26 Elasticity modulus of the materials

Materials	E (MPa)	υ
Core (1)	15	0.4
Downstream rockfill (3)	25	0.3
Upstream rockfill 4)	35	0.25
Filters and drains (2), (5)	20	0.3
Rockfill (6)	15	0.25
Foundation (without treatment) (A)	15	0.4
Foundation (vibrocompacted) (B)	50	0.25
Foundation (stone columns) (C)	40	0.3
Foundation (intermediate) (D)	20-45	0.3-0.25
Bedrock (E)	60	0.2

From the large volume of the available information only some results are presented.

Figure 8.130 and 8. 131 show the vertical displacements for step 6 of Case A: Foundation without consolidation treatment and for step 5, Case B: Foundation with vibrocompaction treatment (cross section Type 3A).

Figure 8.132 presents the distribution of effective vertical stress (construction phase) - Case B: Foundation with vibrocompaction treatment (cross section Type 3A).

Figure 8.133 illustrates the distribution of effective horizontal stress (steady state) - Case B: Foundation with vibrocompaction treatment (cross section Type 3A).

Figure 8.134 represents the distribution of horizontal displacements (steady state) - Case B: Foundation with vibrocompaction treatment (cross section Type 3A).

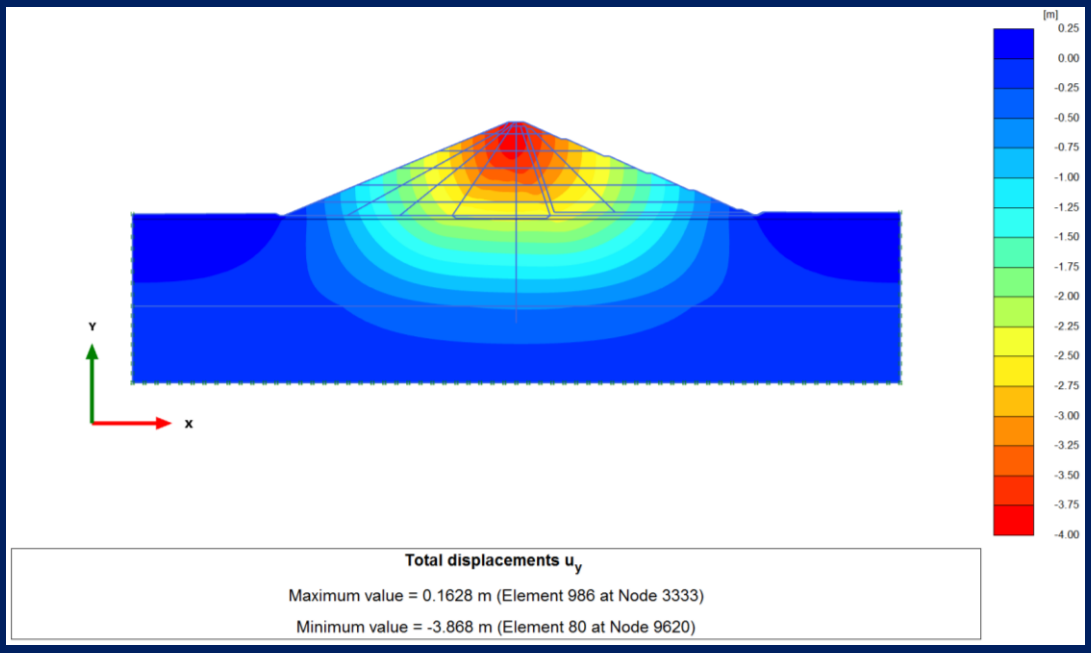

Figure 8.130 Distribution of vertical displacements (step 6) (fill elevation level (173.00)) - Case A: Foundation without consolidation treatment

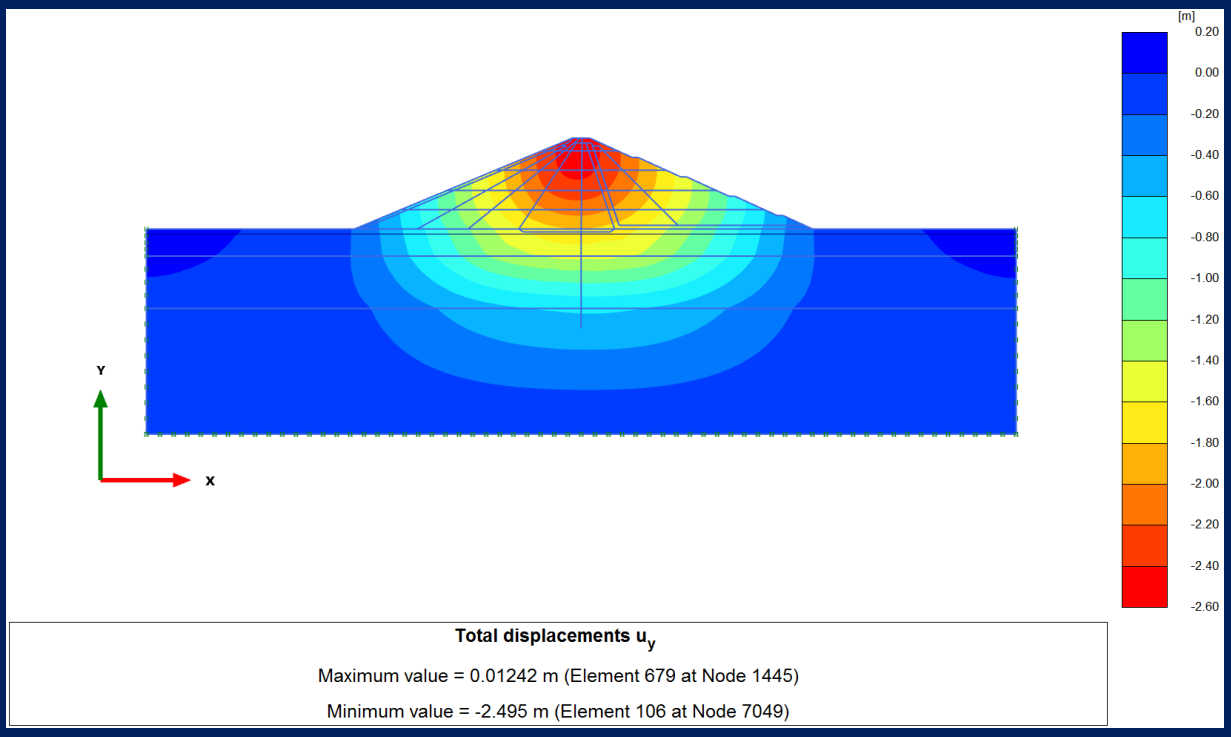

Figure 8.131 Distribution of vertical displacements (step 5) (fill elevation (173.00)) - Case B: Foundation with vibrocompaction treatment (cross section Type 3A)

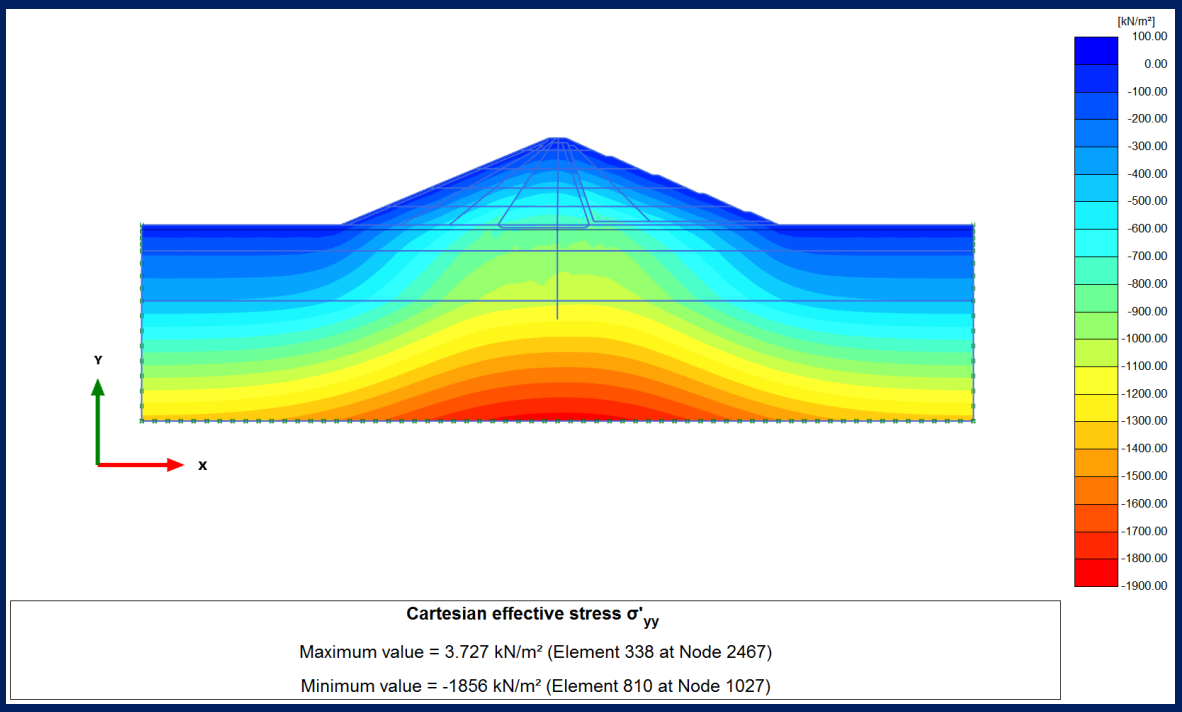

Figure 8.132 Distribution of effective vertical stress (construction phase) - Case B: Foundation with vibrocompaction treatment (cross section Type 3A)

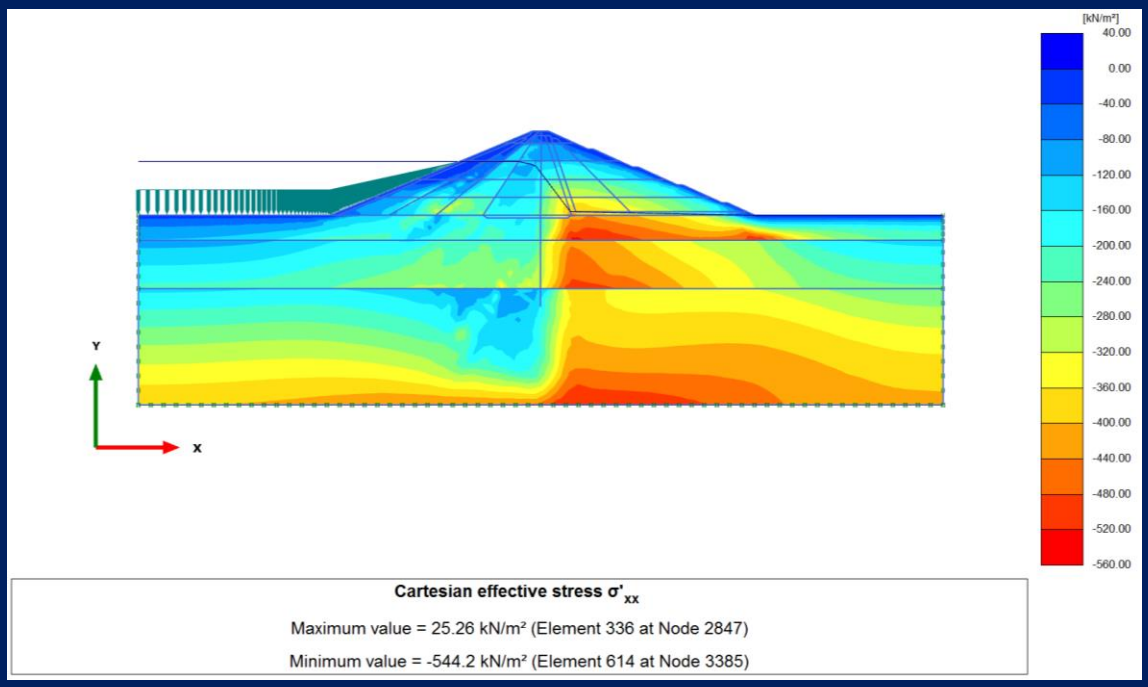

Figure 8.133 Distribution of effective horizontal stress (steady state) - Case B: Foundation with vibrocompaction treatment (cross section Type 3A)

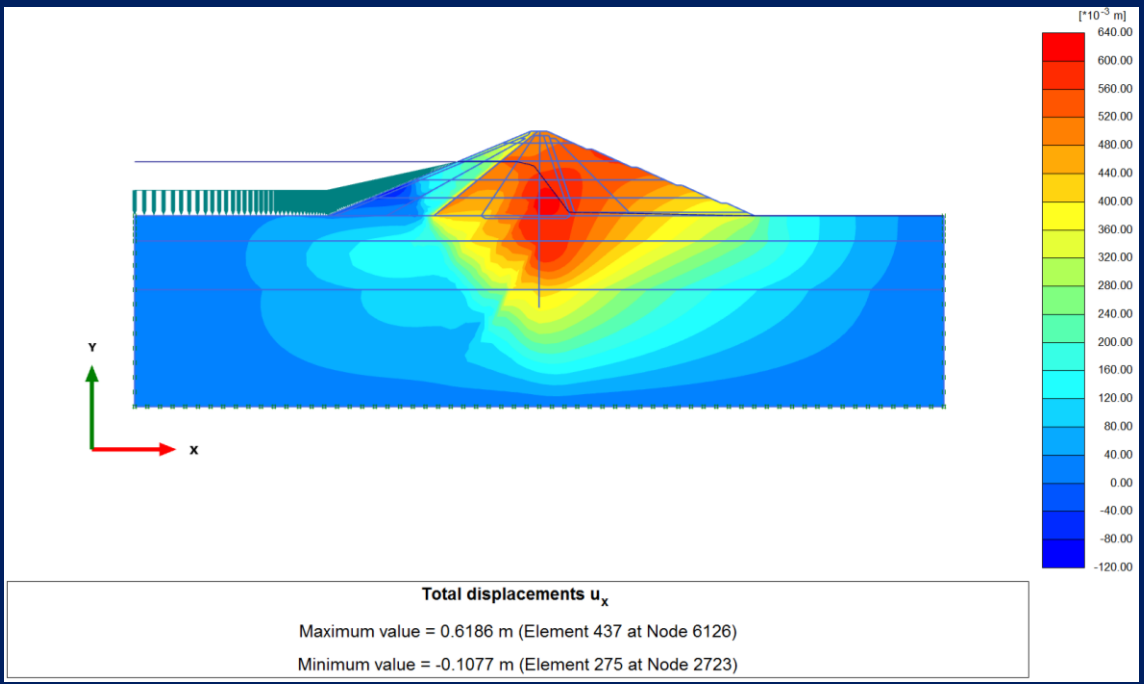

Figure 8.134 Distribution of horizontal displacements (steady state) - Case B: Foundation with vibrocompaction treatment (cross section Type 3A)

8.2.7.11 Seepage Analysis

The seepage studies were performed using a PLAXIS code and the coefficient of permeability of the materials are shown in Table 8.27. The flows through the dam body and foundation were computed.

The efficiency of a grouting curtain will be analyzed.

Figure 8.135 illustrates the equipotential surfaces - 1st Analysis: Without foundation treatment.

Figure 8.136 shows the equipotential surfaces - 2nd Analysis: Cut-off trench (foundation treatment Type 4).

Figure 8.137 presents the equipotential surfaces 3rd Analysis: Cut-off trench and grouting curtain (foundation treatment Type 2).

Figure 8.138 represents the equipotential surfaces 4th Analysis: Diaphragm wall and grouting curtain (foundation treatment Type 3A & 3B).

Table 8.27 Materials coefficient of permeability

Materials	K_v (m/s)	K_h (m/s)
Core (1)	$5x10^{-9}$	10^{-8}
Filter (2)	10^{-4}	10^{-4}

Shell material (3)	10^{-6}	10^{-6}
Shell material (4)	10^{-2}	10^{-2}
Drain (5)	10^{-4}	10^{-4}
Toe drain (6)	10^{-2}	10^{-2}
Rip rap (7)	10^{-2}	10^{-2}
Foundation (without treatment)	10^{-4}	10^{-4}
Foundation (TeAcs1)	10^{-5}	10^{-5}
Foundation (cut off)	10^{-7}	10^{-7}
Diaphragm Wall	10^{-8}	10^{-8}

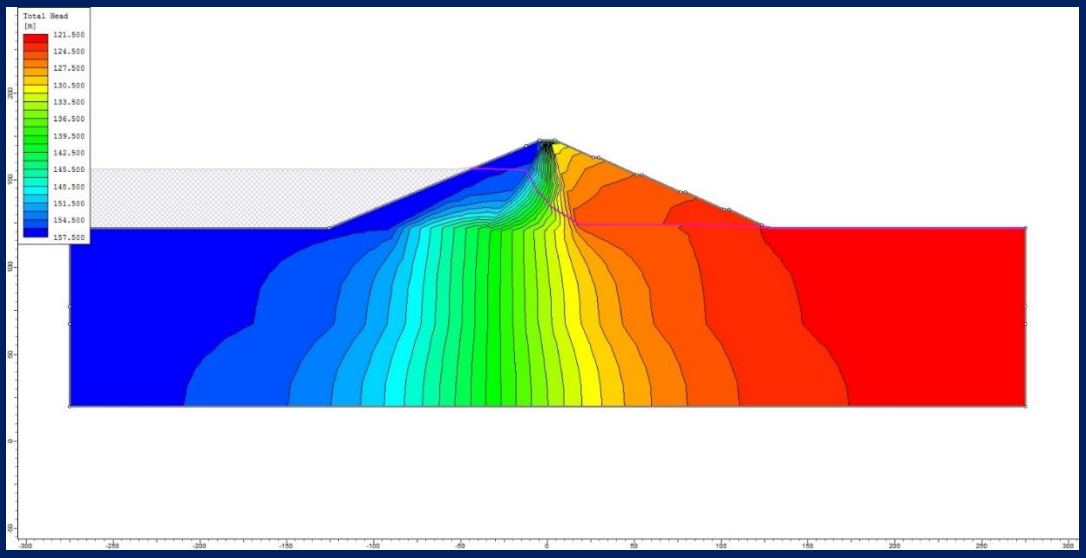

Figure 8.135 Equipotential surfaces - 1st Analysis: Without foundation treatment

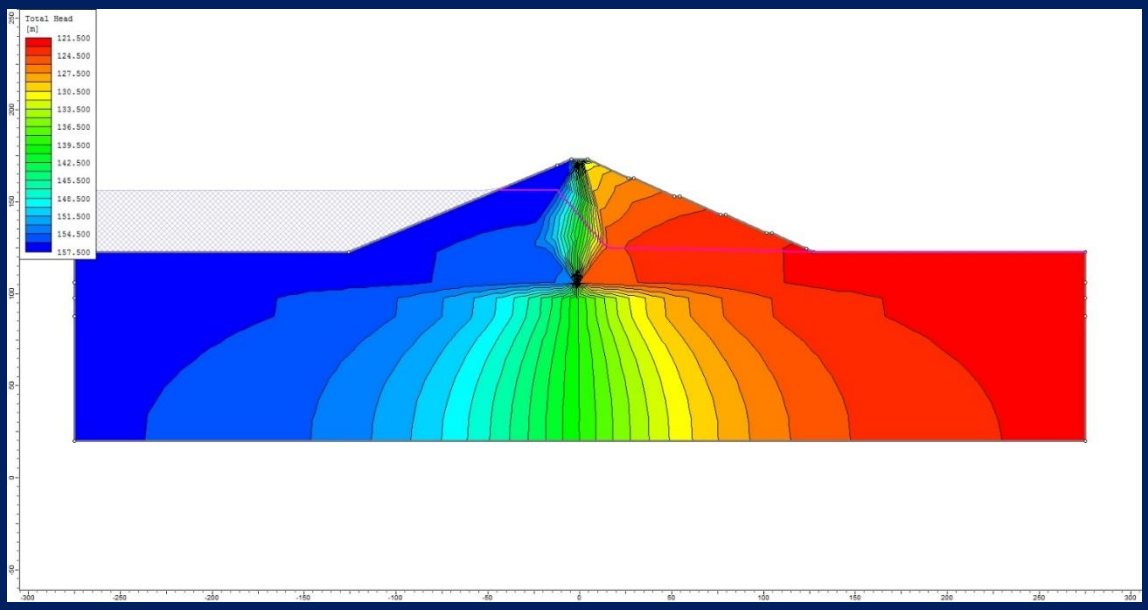

Figure 8.136 Equipotential surfaces - 2nd Analysis: Cut-off trench (foundation treatment Type 4)

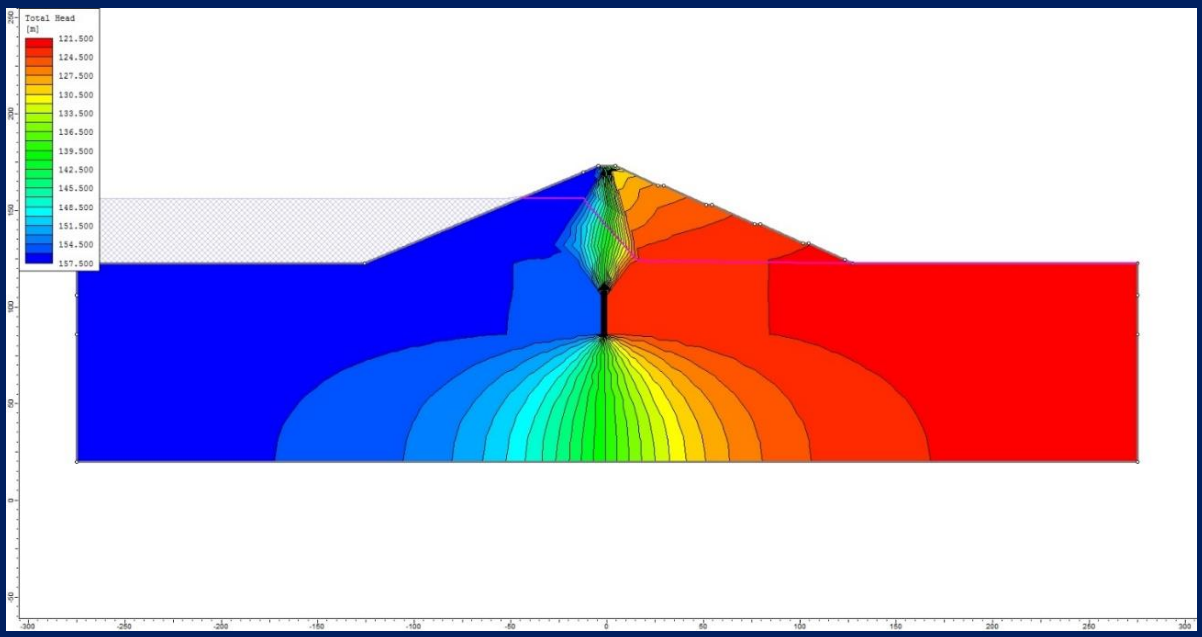

Figure 8.137 Equipotential surfaces 3rd Analysis: Cut-off trench and grouting curtain (foundation treatment Type 2)

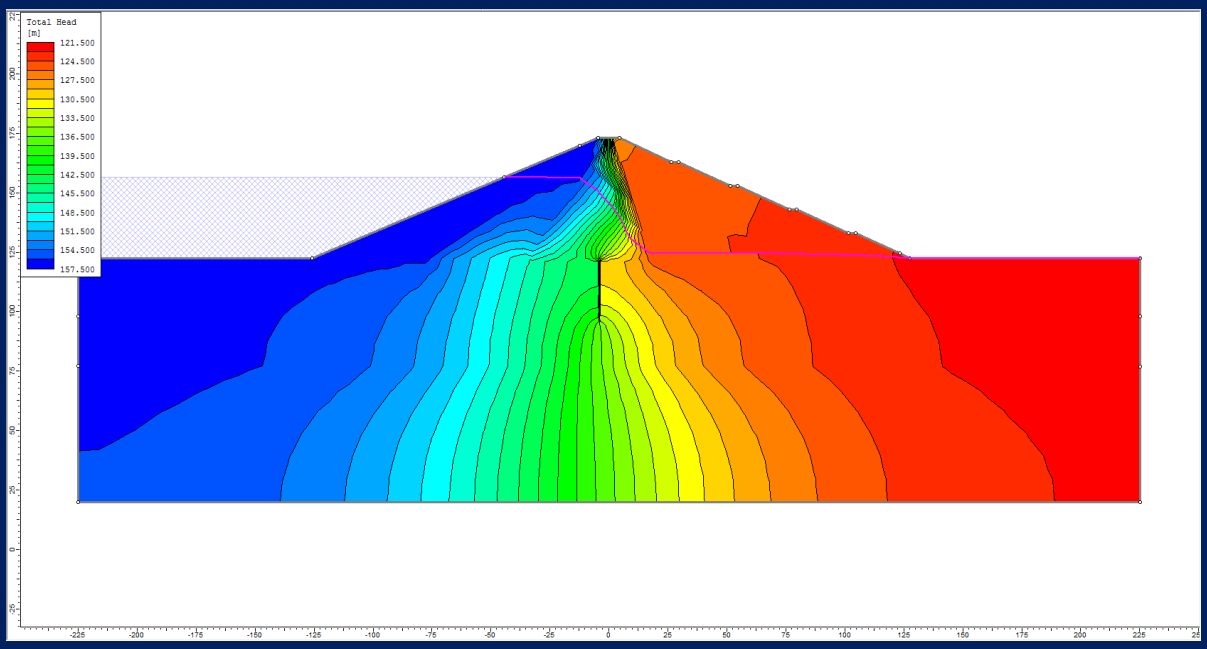

Figure 8.138 Equipotential Surfaces 4th Analysis: Diaphragm wall and grouting curtain (foundation treatment Type 3A & 3B)

8.2.7.12 Foundation Treatment

The following design situations were analysed:

-Liquefaction evaluation;

-Diaphragm wall

- Stone columns

- Grouting.

Introduction

Taking into account the geological and geotechnical interpretative model, an evaluation of possible solutions for the foundation treatment of the alluvial valley was made. In-depth the geological and geotechnical model is complex, with the presence of alluvial deposits with poor geotechnical characteristics, particularly in the central part of the Limpopo River, presenting high thickness.

Taking into account the occurrence of a superficial seismic horizon linked to soil cover with a general P-wave velocity of <500 m/s it is recommended to perform a superficial excavation to ensure better characteristics of deformability of the dam foundation and avoid its treatment.

In addition to control dam foundation seepage there is a need to guarantee a minimum value of a permeability coefficient of $5x10^{-7}$ m/s. Within this framework it is recommended to construct a diaphragm wall crossing the alluvia material, followed by a grouting curtain penetrating in the moderately weathered to slightly weathered rock mass.

The diaphragm wall has the following purposes:

a) to assure the seepage control through the foundation.

b) to support the actions during dam life time.

c) to exhibit adequate durability.

For other dam foundation zones (out of the alluvial valley) it is recommended a cut-off trench with a depth of 4-5 m associated with a grouting curtain. In the dam zones with low hydraulic gradients, it should be constructed a cut-off trench also.

Taking into account the geological scenario described before, the possible location of each of typical cross section of the foundation treatment is presented in Figure 8.139 and in Table 8.28.

The typical cross sections of the foundation treatment are presented in the Figure 8.140 to Figure 8.142.

.

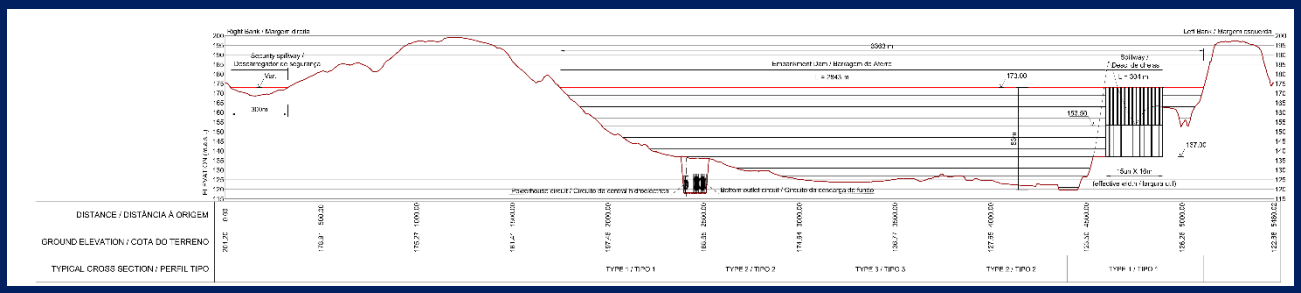

Figure 8.139 Longitudinal profile. Location of typical cross sections.

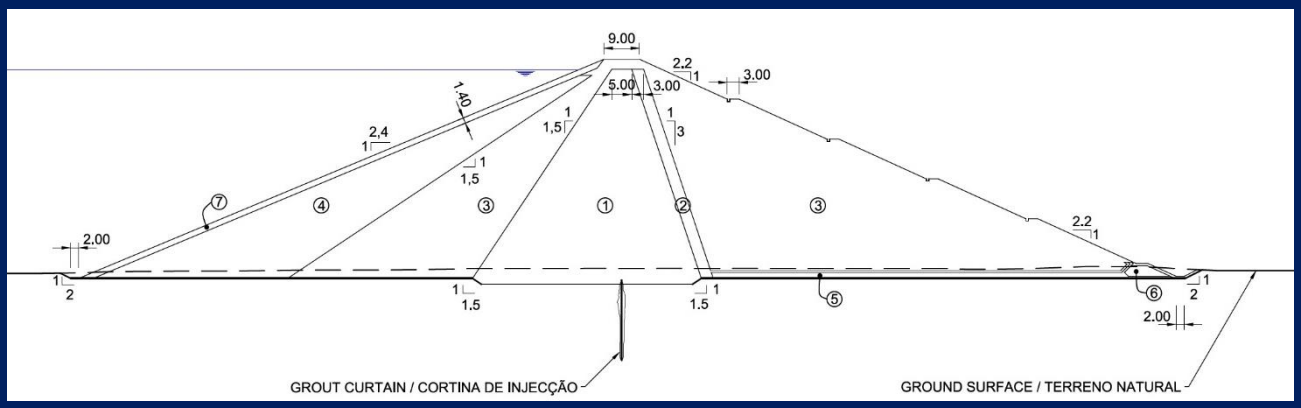

Figure 8.140 Typical cross section 1 of the foundation treatment

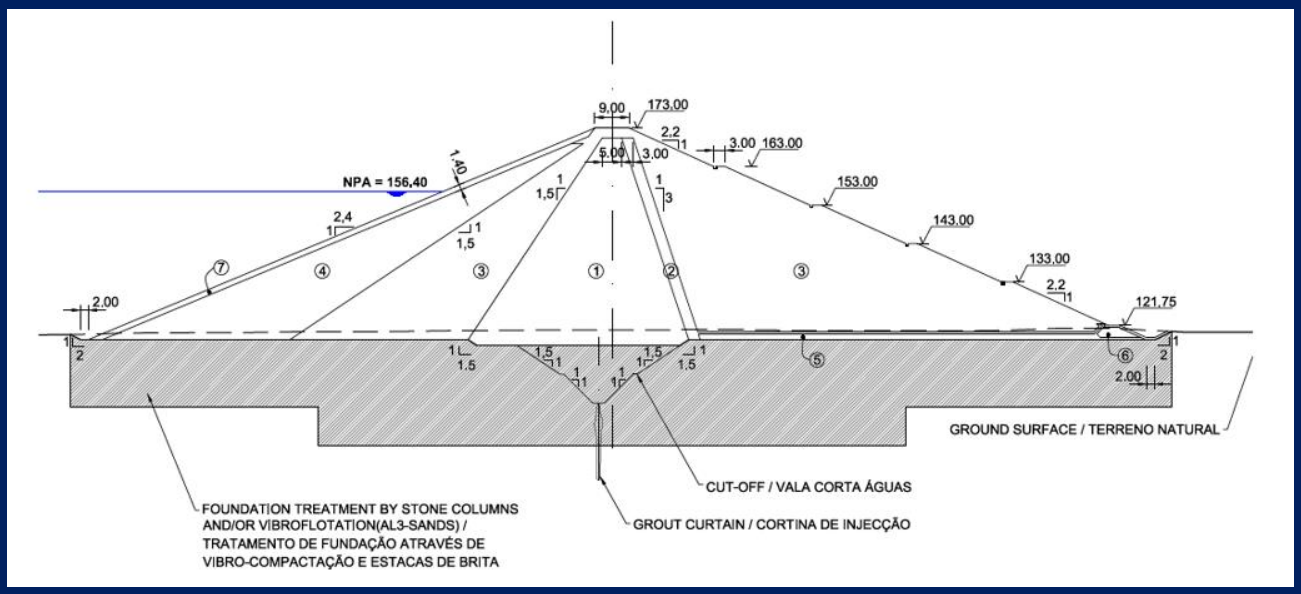

Figure 8.141 Typical cross section 2 of the foundation treatment

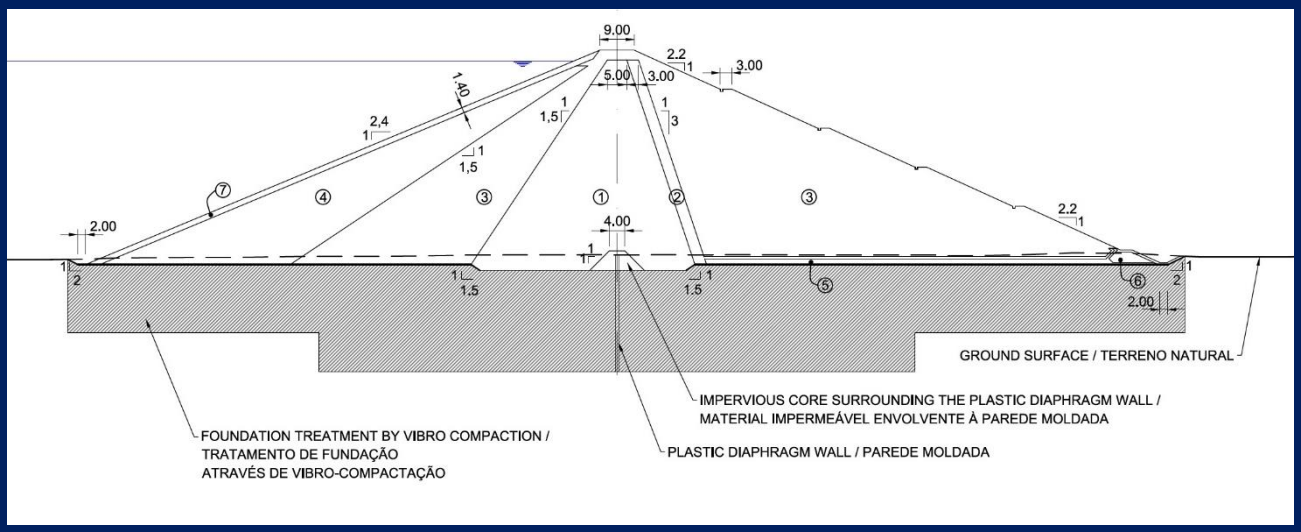

Figure 8.142 Typical cross section 3 of the foundation treatment

Table 8.28 Possible location for the typical cross section of the foundation treatment

Typical cross Section	Foundation treatment solutions	Dam Site
Typical cross Section 1	- superficial excavation - cut-off trench - grout curtain	3+010-3+620 5+660-5+800
Typical cross Section 2	- superficial excavation - cut-off trench - grout curtain Stone columns and /or vibro-compaction(A3)	3+620-4+000 5+000-5+660
Typical cross Section 3	- superficial excavation - cut-off trench - diaphragm wall Stone columns and /or vibro-compaction(A3)	4+000-5+000

Liquefaction Assessment

Considering the expected low compacity of the superficial alluvial sandy materials it could be necessary a vibrocompaction treatment to minimize the occurrence of liquefaction (see Figure 8.143).

Table 8.29 summarizes the liquefaction assessment for borehole S201.

Also due to the low compacity of silty alluvia materials a consolidation by stone columns may be necessary.

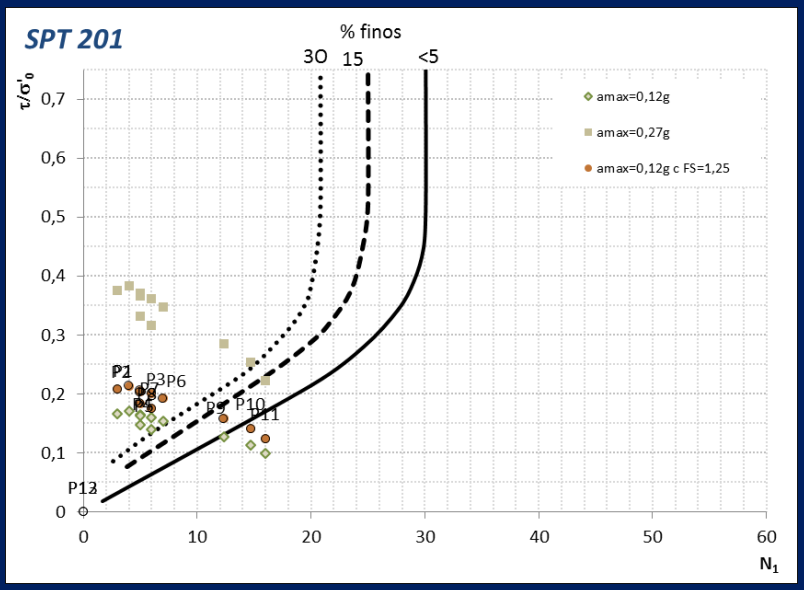

Figure 8.143 Liquefaction assessment for SPT 201

Table 8.29 Liquefaction assessment for borehole S201

	Depth (m)	σ_0 (kPa)	$\sigma'_{0;\ NA=0m}$ (kPa)	Rd (-)	τ/σ'_0 - $a_{max}/g=0,15$	τ/σ'_0 FS=1,25 $a_{max}/g=0,15$	τ/σ'_0 FS=1,0 $a_{max}/g=0,35$	N_{SPT} S201	CN	C_N (-)	N1 (-)	Liquefaction potential
P1	1,5	27	12	0,99	0,21	0,27	0,75	4	1,72	1,0	4	*Liquefy*
P2	4,5	80	36	0,97	0,21	0,26	0,73	3	1,71	1,0	3	*Liquefy*
P3	6,0	106	48	0,95	0,21	0,26	0,72	5	1,57	1,0	5	*Liquefy*
P4	7,5	133	60	0,94	0,20	0,25	0,71	5	1,41	1,0	5	*Liquefy*
P5	9,0	159	72	0,93	0,20	0,25	0,70	6	1,29	1,0	6	*Liquefy*
P6	10,5	186	84	0,89	0,19	0,24	0,67	7	1,20	1,0	7	*Liquefy*
P7	12,0	212	96	0,85	0,18	0,23	0,64	5	1,12	1,0	5	*Liquefy*
P8	13,5	239	108	0,81	0,18	0,22	0,61	6	1,05	1,0	6	*Liquefy*
P9	16,5	292	132	0,73	0,16	0,20	0,55	13	0,95	0,9	12	*Liquefy*
P10	19,5	345	156	0,65	0,14	0,18	0,49	17	0,86	0,9	15	*Liquefy*
P11	22,5	398	180	0,57	0,12	0,15	0,43	20	0,80	0,8	16	*Do not liquefy*

Diaphragm Wall

In Mapai embankment dam a plastic and flexible diaphragm wall is proposed to control the seepage of the foundations due to the existence of alluvial sandy materials with high permeability.

A diaphragm wall with 30 m depth and 0.80 m thick and panels length of 3.0 m is recommended with guide walls with 1.0 m depth and 0.30 m thick.

Overlapping between primary and secondary panels was 0,30 m, with a minimum 1.0-2.0 m penetration of the panels in bedrock. The accepted vertical deviation of the wall is less than 1:133 =0.0075.

In Figure 8.144 the diaphragm wall phases are presented.

For the diaphragm wall slurries, the following composition: Bentonite –liquid limit = 400%, Sand content less 15%, Bentonite/Water = 8%, Cement / Water ratio = 0.25, Admixture NaOH/ Bentonite = 0.6% can be used.

During the excavation the following aspects should be monitored: position of tool, the verticality and continuity between excavation units, ground profile, depth of excavation, self-hardening slurry level, boulders or obstructions in the ground.

The following parameters shall be controlled: self –hardening slurry, density =1.2-1.3, Ph value higher 8, Marsh values =32-35 sec, setting time and bleeding, compressive strength (250-500 kPa 28 days, permeability less 10-8 m/s, axial deformation< 4%, erosion tests for gradients around 75.

To control the diaphragm wall behaviour and efficiency the installation of the following equipment's is recommended: (i) piezometers in the upstream and downstream side of the diaphragm wall and with narrow mesh in the downstream side; (ii) inclinometers in the upstream side of the diaphragm wall; (iii) total pressure cells placed in the cap of the diaphragm wall.

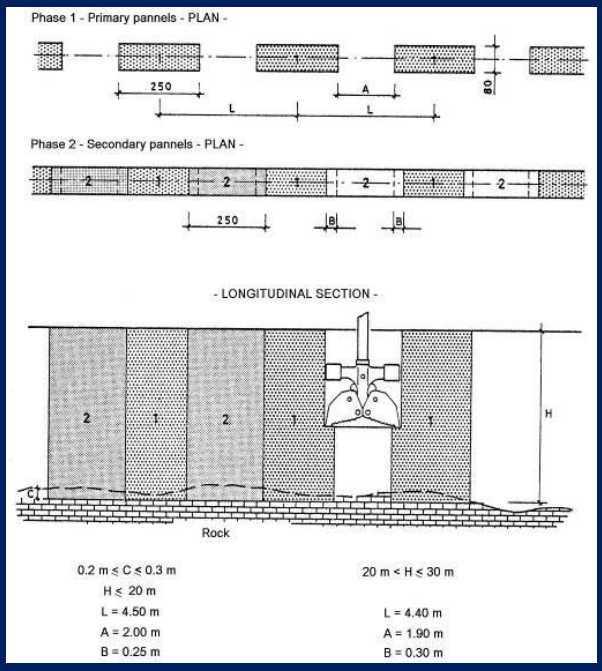

Figure 8.144 Diaphragm wall scheme phases

In summary: (i) To assess the mixtures characteristics a careful control of the components was performed; (ii) For the execution of panels, due to the high temperatures, admixtures to increase the setting time were used; (iii) The quality control of the slurries has shown that the design specifications were fulfilled; (iv) The instrumentation will show the efficiency of the diaphragm wall.

Stone Columns

Due to the existence of silty clay materials with low compacity ground improvement by stone columns is considered,

The execution of stone columns increases the overall safety factor, the ground behaviour and reduces the foundation settlements. This situation results that stone columns are able to support a large part of the load, associated to the high internal friction angle of gravel.

Following Priebe (1995) regarding soil behaviour, where vibro-replacement was applied, it was considered that a rigid foundation transmitting a uniform load is directly supported by an infinite grid of stone columns.

According to the Figure8.145 a stone column, with an A_c section, has an area of influence A that results in $A = A_c + A_s$.

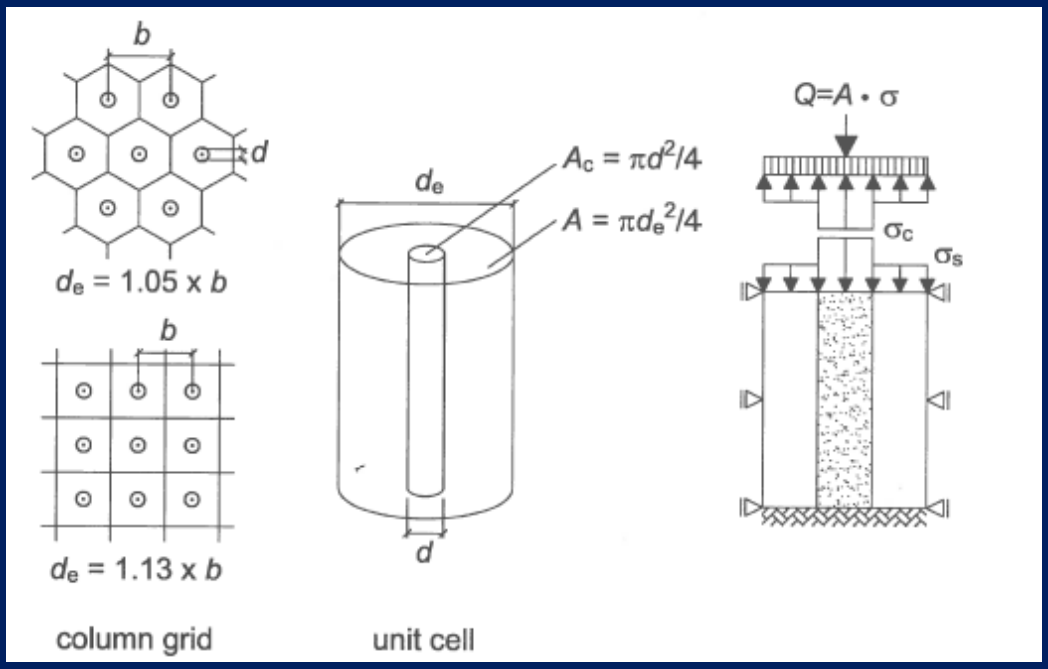

Figure 8.145 Stone Column Influence mesh areas

A stone column is compared to a cylinder that expands radially with stress.

This radial stress comprises the difference between the active impulse of the stone column and the soil horizontal stress at the same depth.

Priebe methodology is based in the following assumptions: i) the column is founded upon a rigid lower stratum; ii) the column material is incompressible; iii) the unit weights of both column and surrounding soil are negligible.

The relationship A/Acol is increased with an additional value A/Acol, that may be observed in Figure 8.146, valid for $\mu_{sol} = 1/3$.

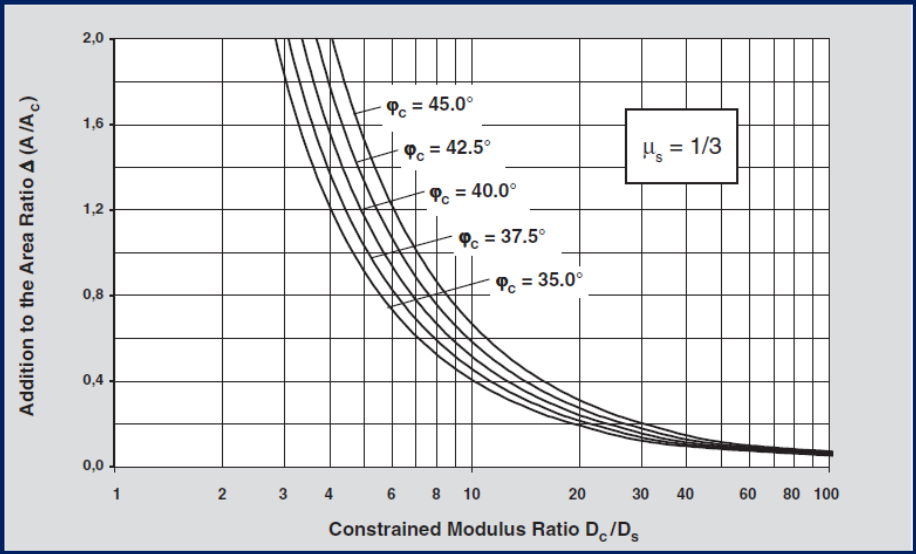

Figure 8.146 Consideration of compressibility effect

Vibroflotation

The vibroflotation techniques for strengthening cohesionless soils by deep compaction probably have their origins on late 1930's (Moseley, 1993).

A steel rod is introduced at the desired depth and a vibrator creates vertical and horizontal vibrations that provoke the compaction of the soil while the rod is slowly withdrawn. A schematic diagram of the equipment and methodology is shown in Figure **Error! Reference source not found.**8.146 a.

The range of suitable soils to be treated by vibroflotation is indicated in Figure 8.147 (Glover, 1982). Particle distributions whiting this zone A can be densified by vibroflotation. For depths higher than 10 m some difficulties are found for soils more than 20% of gravel material.

- Grain size distributions within zone B are excellent soils for densification by vibroflotation.
- For soils with grain size distribution falling within zone C require some modifications of compaction procedures due the presence of silt and excessive fines material (over 15% passing on sieve 200).

The depth of compaction and the spacing depend of the following factors: (i) maximum allowable total settlement; (ii) maximum allowable differential settlement; (iii) requested bearing capacity; (iv) final shear strength value; and (v) increased resistance to liquefaction (Sêco e Pinto and Macedo, 1974).

The treatment efficiency can be evaluated by the following methods: (i) standard penetration test (SPT) by comparing the results before and after the treatment. The well-known limitations of these tests raised some doubts about the results; (ii) static cone penetration (CPT); (iii) pressurometer - the deformation modules can be correlated with the compressibility of the soil; (iv) load tests are carried using in general steel plates with diameter between 300 to 600 mm. Taking into account the size of the plate and the footing the obtained results are limited; and (v) settlement - the efficiency can be assessed by controlling the levels before and after the treatment.

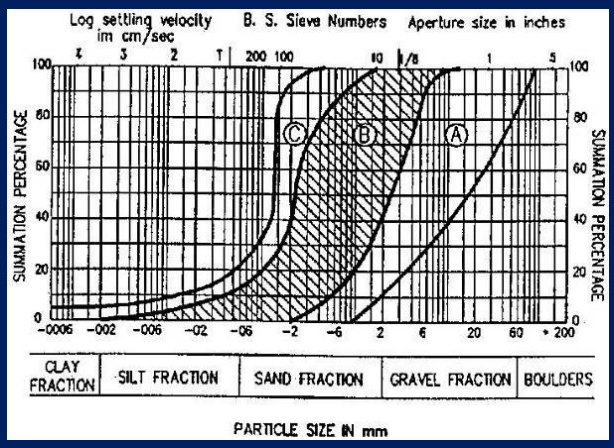

Figure 8.147 (B) Range of soils suitable for improvement by the vibroflotation process (after Glover, 1982)

Grouting

The scheme plan of grout curtain boreholes I presented in Figure 8.148.

Grouting equipment

(i) Grouting records

For each grouting branch a detailed record was presented:

ii. number of the hole;
iii. injected branch;
iv. day and hour of the begin of operation;
v. packer position;
- results of permeability tests before the grouting (if this is the case);
- grouting composition, pressure of grouting, flow and time of variation of these parameters. Also, the grouting quantities were recorded.
- absorption of the total branch;

vi. incidents occurred during the grouting operations;
- tables for each hole, with information about the weight of injected cement and injected pressure for each branch.

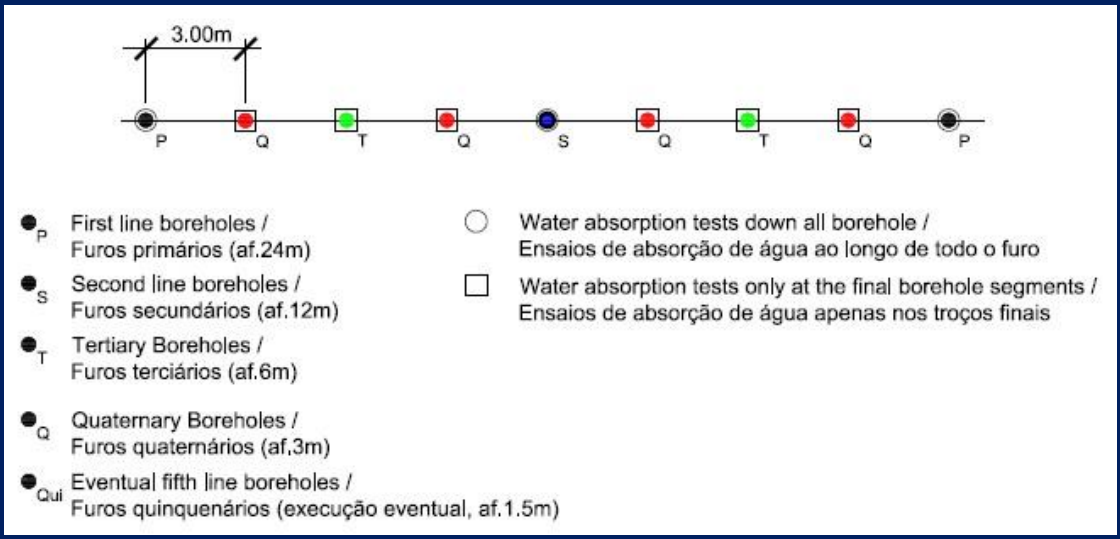

Figure 8.148 Scheme plan of grout curtain boreholes

Drainage curtain

The execution of a drainage curtain to control the uplift effects trough foundation is recommended. This curtain should be executed through the drainage gallery.

The drainage curtain should be executed subsequently the execution of impervious curtain.

The holes for the drainage curtain should be around 76 mm.

8.2.7.13 Construction Planning

In Figures 8.149 to Figure 8.151 are presented the construction phases of Mapai dam.

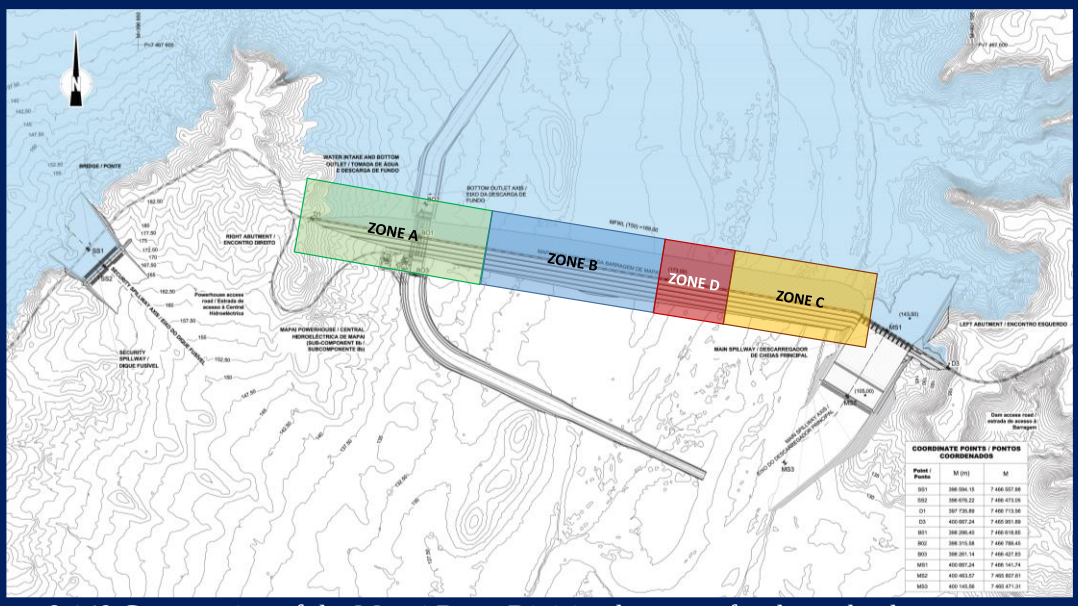

Figure 8.149 Construction of the Mapai Dam. Division by zones for the embankment construction

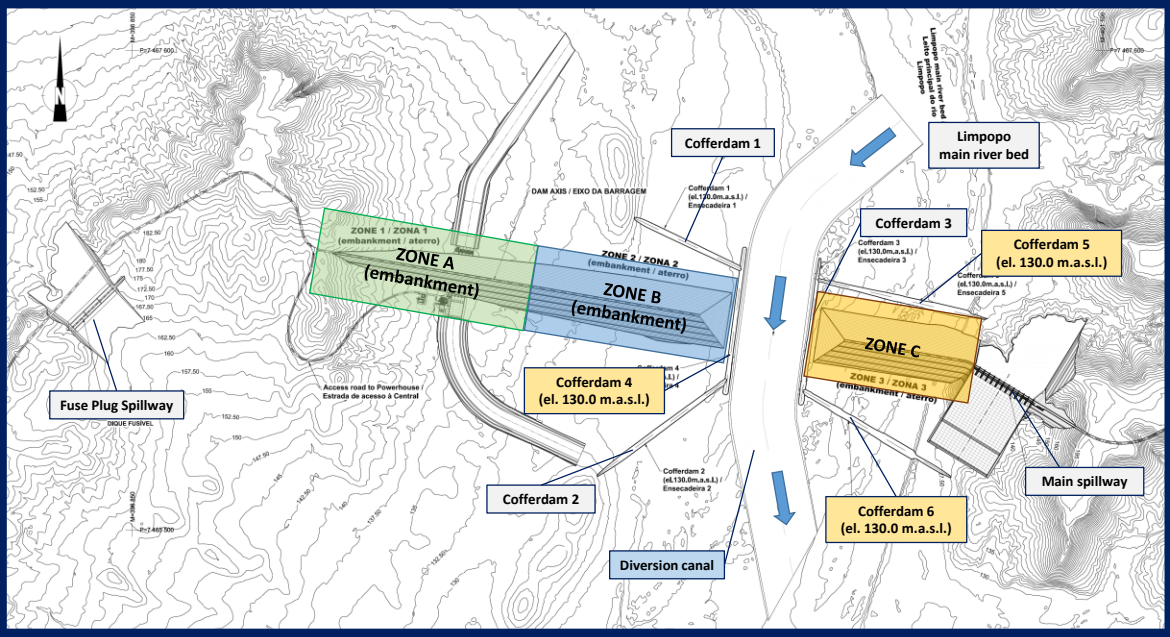

Figure 8.150 Mapai Dam. River diversion works. Phase 2

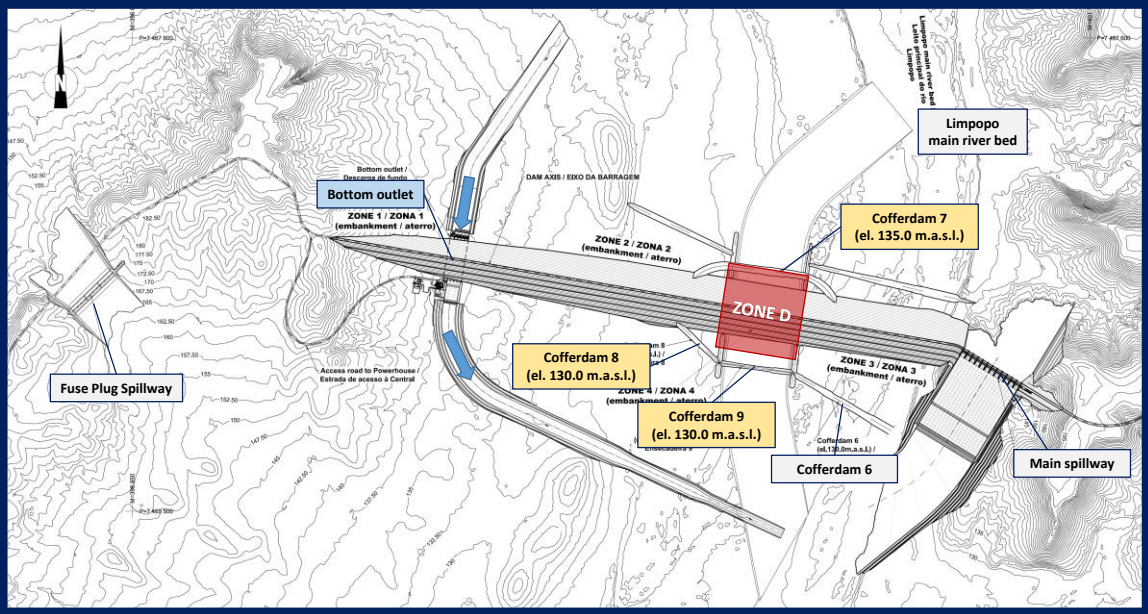

Figure 8.151 Mapai Dam. River diversion works. Phase 3

8.2.7.14 Safety Analysis and Monitoring

Dam potential risk for monitoring purposes

The potential risk associated with dams depends on its storage capacity, height of the dam, potential downstream damage and evacuation requirements (ICOLD, 1989). These risk factors are separately weighted as low, moderate, high and extreme.

Usually, the risk factors are classified in three classes, which are referred respectively to actions, to the structure itself or to values affected by hazards. The arithmetic average of all indices falling in a given class forms an overall risk factor for the class. In this way we define, respectively:

- an environmental factor ***E***;
- a reliability factor ***F***;
- a potential human/economic hazard factor ***R***.

Lastly a global risk index a_g, is developed by taking the product of the three partially factors ***E***, ***F***, ***R***, (ICOLD, 1981).

$$a_g = E \times F \times R \qquad (8.31)$$

8.2.7.15 Time Schedule

The time schedule is presented in Figure 8.152.

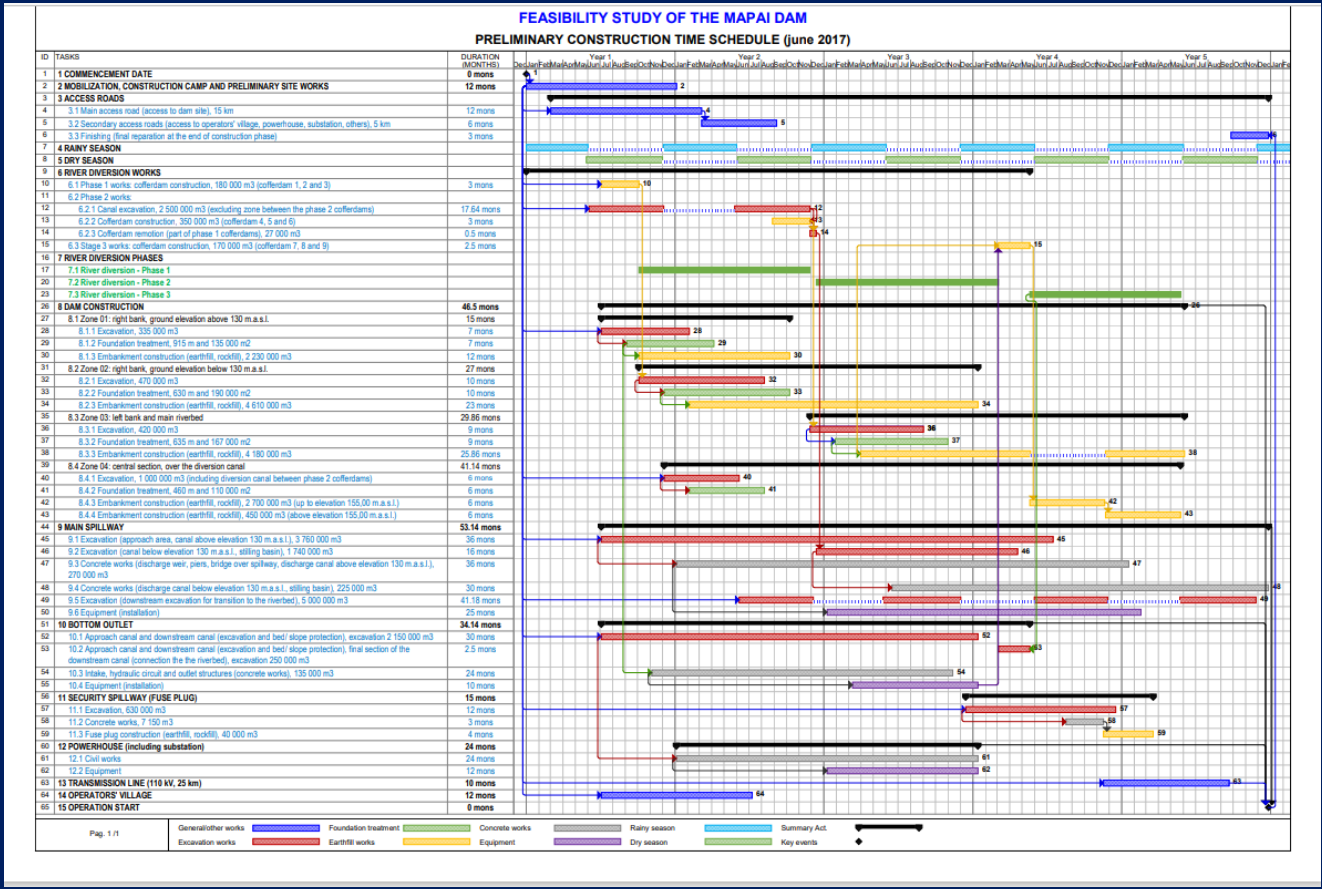

Figure 8.152 Time schedule

Lesson nº 6: Occurrence of liquefaction in a ground with heterogeneous conditions requires a deeper analysis and a better understanding of the phenomena.

It is important the synergy between the Owner, Decision Maker, Designer, Researchers and Constructors in order to share their experience.

It is important to follow the dam codes, the ICOLD recommendations, the State of the Art and the State of the Practice.

Note: This study was conducted under the supervision of COBA and I was involved in the geotechnical design.

8.2.8 Case History nº 7- Kolombizo Dam (Malawi)

8.2.8.1 Introduction

For Kolombizo dam the geological studies are referred, the geotechnical characterization is addressed, the definition of design earthquake is discussed, the dam the profile is introduced, the foundation treatment is analysed, the waterway system is described, the underground structures are mentioned, the construction issues are referred and the monitoring and safety evaluation is mentioned.

8.2.8.2 Geological Studies

Malawi's geology is mainly constituted by igneous and metamorphic rocks of the Basement Complex of Precambrian, both Archean (charnockitic gneiss, granulites, meta-sediments and ultrabasics) and Proterozoic age (meta-sediments and older granitoids).

Overlying volcano-sedimentary sequences, including coals, of Palaeozoic-Mesozoic also occurred in some parts of the country. Karoo strata and Late Jurassic-Cretaceous alkaline igneous intrusive bodies are found in southern Malawi.

Mesozoic and Cenozoic sedimentary rocks are found in narrow belts aligned parallel to Lake Malawi and extensive Quaternary superficial deposits occur along the margins of the lake and the most important rivers.

The geology of the eastern flank of the Shire River is dominated by charnockitic gneisses and granulites rocks as well as by the alluvium/colluvium soils derived from them. The western flank of the Shire River is constituted mostly by the northeastern part of the Shire-Zambezi Karoo outcrop. These rocks are covered by Cenozoic formations as well as by alluvium/colluvium deposits and they overlie the Malawi basement complex formed by hornblende and hornblende-biotite-gneisses.

Figure 8.153 illustrates the extract from geological map Kirk Range-Lisungwe Valley area (scale 1/100 000).

The Kholombidzo Hydropower site is located on the middle Shire River, which flows from Lake Malawi to Zambezi River with a north-south direction. The regional geological setting of Kholombidzo Hidropower site, close to Matope Bridge, is presented.

Site Geological Setting

In the study area it was recognized four geological bedrock units:

Biotite Gneiss – it is the most predominant unit occurring both on right and left banks of the Shire River; it is constituted by dark grey to cream white, medium grained rocks; foliation is well defined as mafic and felsic bands are oriented showing a general trend in a NNE-NE/SSW-SW direction and dip to the SE); some biotite gneiss outcrops show a banded structure well defined.

Figure 8.154 shows the biotite Gneiss outcrop near on left bank of Shire River.

Quartz-feldspathic Gneiss – it occurs preferentially along the right bank; this unit is composed by white to pink, medium to coarse grained rocks; colour variation is imposed by mineral composition and the degree of weathering;

Figure 8.155 presents the quart-feldspathic gneiss outcrops on right bank of Shire River near Matope Bridge.

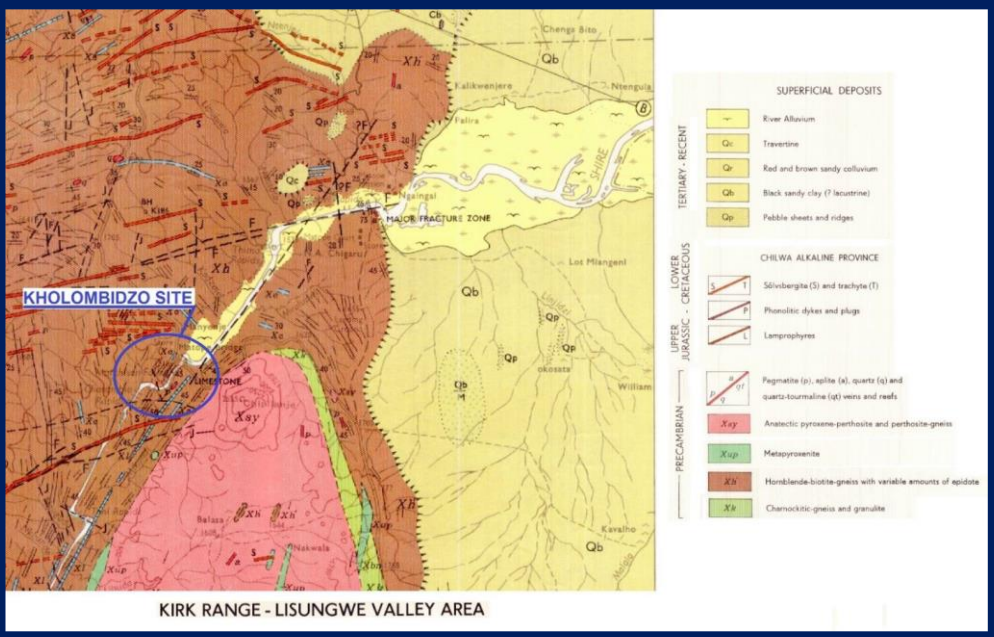

Figure 8.153 Extract from geological map Kirk Range-Lisungwe Valley area (scale 1/100 000).

Figure 8.154 Biotite Gneiss outcrop near on left bank of Shire River

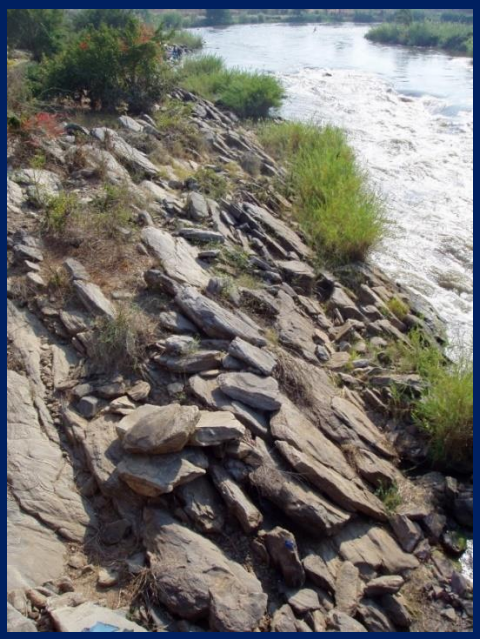

Figure 8.155 Quart-feldspathic gneiss outcrops on right bank of Shire River near Matope Bridge

Marble – this unit is composed by white to light grey, medium-grained rocks; bedding planes show a general trend in a NE-SW direction dipping between 20-40º to NE; outcrops show weathering profiles constituted by sound to slight weathered rocks at 1 to 1.5 m depths.

Figure 8.156 indicates the marble outcrop in the vicinity of SR7.

Syenite – this unit was recognized at the location of seismic refraction profile SR15; however, syenite rocks were not observed in trial pits numbers TP13 and TP14 located near to that profile.

Other bedrock types were encountered in the study area as migmatites which were observed along the Shire River.

The more important geological structure observed in the study area, well-defined in gneissic rocks, is foliation characterized by a general trend in a NNE-NE/SSW-SW direction and dip to the SE. Foliation imparts a flaggy and slabby shape to gneissic rock blocks.

Rock mass jointing is characterized by the occurrence of several sets which are encountered moderately to widely spaced leading to the formation of metric rock blocks observed along the river banks and ridges.

Figure 8.156 Marble outcrop in the vicinity of SR7

8.2.8.3 Geotechnical Characterization

Analysis of the results of site investigation works of phase I

The site investigation works of phase I comprised seismic refraction profiles, trial pits and soil index properties laboratory tests.

The location of field works is presented in Figure 8.157.

Fifteen (15) seismic refraction profiles located at dam sites D1 and D2 as well as along the different alternatives of waterways systems proposed were carried out.

A model of 3 seismic horizons were considered in all profiles. For the superficial seismic horizon with 3.5 m thick values of P-wave velocity of 300 m/s were obtained. The intermediate seismic horizon integrating weathered and fractured rock mass exhibits a value of P-wave velocity of 1 000 m/s. The thickness of this horizon is very variable, it can reach depths of 17 m. The deeper seismic horizon is linked to the sound basement rock mass, being with P-wave velocity greater than 2 000 m/s.

Nineteen (19) trial pits located at dam sites options as well as along the different alternatives of waterways systems proposed were performed. Trial pits were manually excavated from the surface until it was reached a non-digging by hand rock mass which occur at depths lesser than 1.3 m. These results show the shallow nature

of the underlying basement rock.

Figure 8.158 shows the colluvium soil observed at trial pit TR11.
Figure 8,159 illustrates the location of the seismic Lines and trial pits.

22 soil samples were collected from trial pits, for laboratory testing and identification tests, namely particle size determination, Atterberg limits and maximum dry density were performed.

Figure 8.160 presents the foundation geotechnical profile.

Figure 8.161 indicates the gneiss rock mass samples.

A complementary site investigation programme was implemented and has included:

- boreholes with core sampling,
- standard penetration test, SPT,
- Lugeon and Lefranc tests,
- trial pits,
- undisturbed and disturbed soil sampling,
- laboratory testing of soil and rock samples.

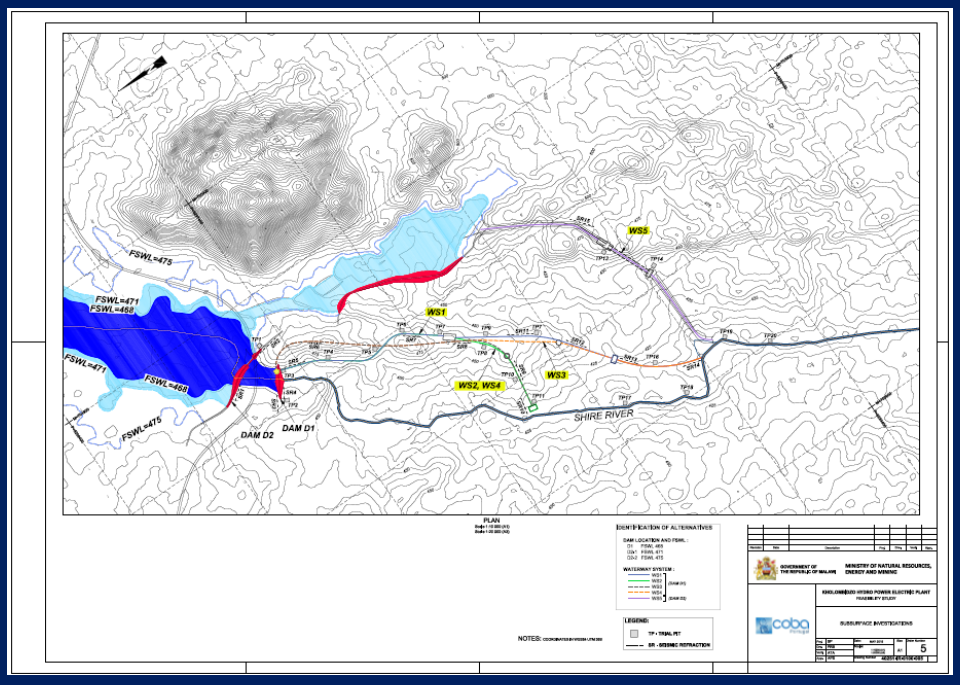

Figure 8.157 Location of the field works – seismic refraction profiles and trial pits

Figure 8.158 Colluvium soil observed at trial pit TR11

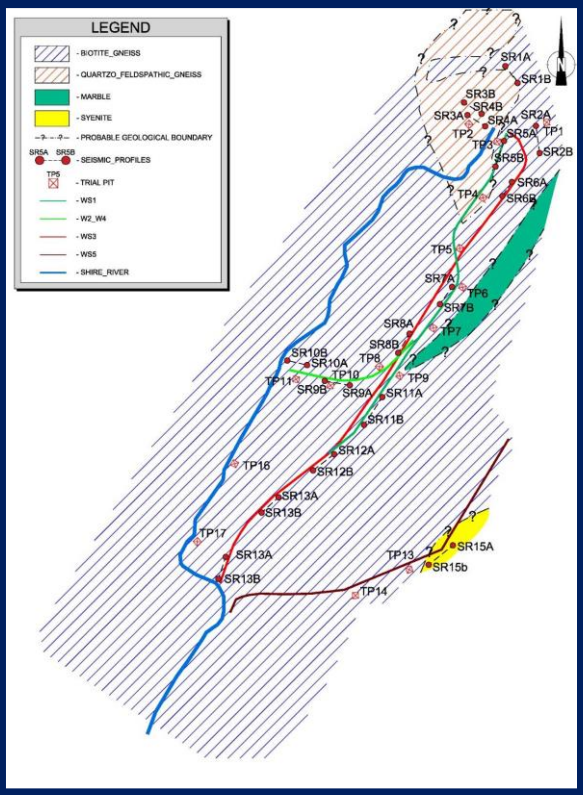

Figure 8,159 Location of the Seismic Lines and trial pits

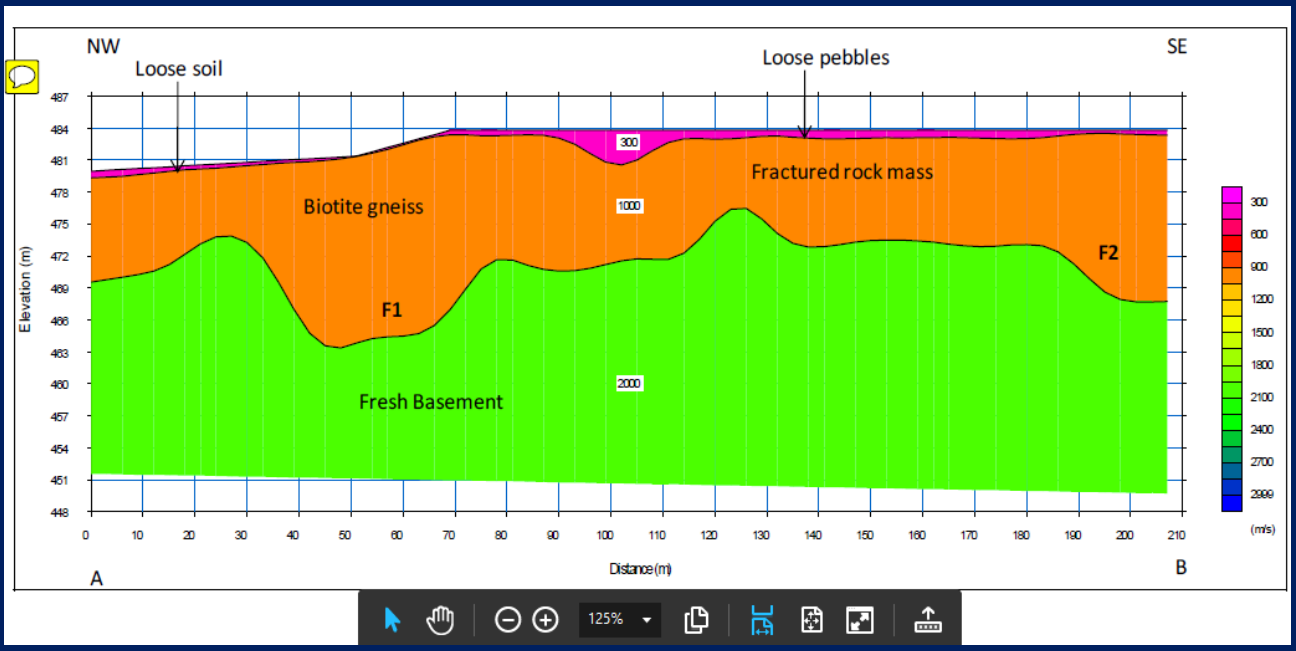

Figure 8.160 Foundation geotechnical profile

Figure 8.161 Gneiss rock mass

8.2.8.4 Seismic Studies

Tectonic

In Malawi, tectonic features fall into two age groups. The first group constitutes Pre Cenozoic age structures. These are faults, shear zones and dyke swarms that are generally of Mesozoic age. The second group of structures is of Cenozoic age. These are faults related to the EARS and are collectively referred to as the Malawi rift. In Malawi, rifting was initiated in Late Tertiary (6-5Ma). Tectonic activity is related to Cenozoic rift structures except where Pre-Cenozoic structures are reactivated.

The Malawi rift extends for about 800km from Rungwe in southern Tanzania to the middle of Shire valley in southern Malawi. The rift structures extend further south by the Shire trough in Malawi and Urema graben in Mozambique. The Malawi rift is largely occupied by the lake which is 40-90km wide. It is composed of curvilinear N-S trending boundary faults which define half grabens and horsts, step faults with riftward tilted blocks and monoclinal structures. Further south in the Shire trough, the rift trend changes from N-S to NW.

Figure 8.162 illustrates the tectonic zone.

Figure 8.163 shows the East African Rift System.

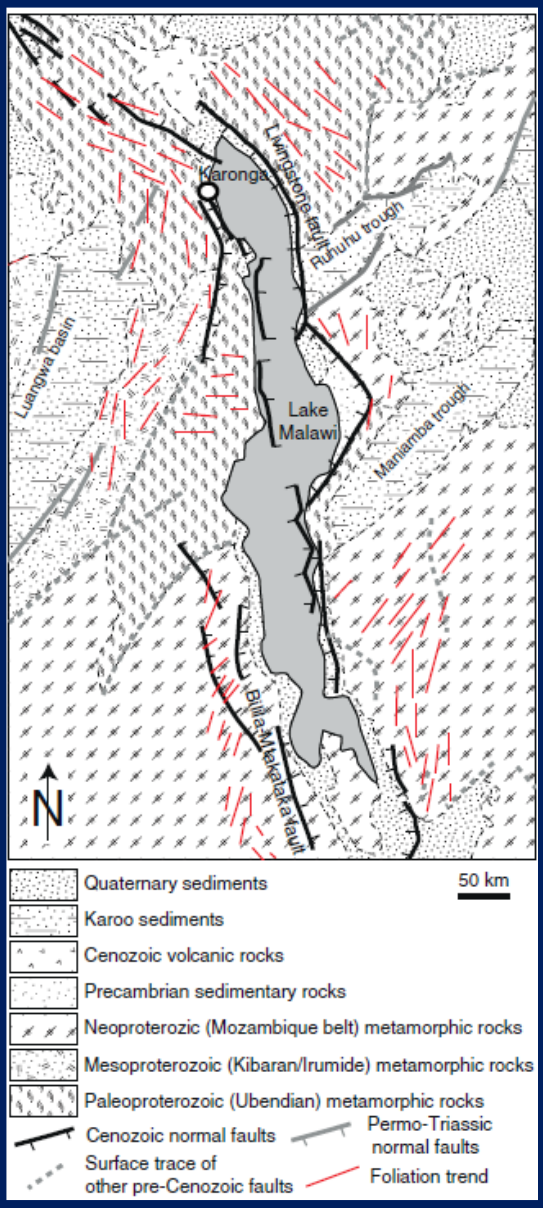

Figure 8.162 Tectonic zone

SE at about latitude 16°S and continues with this trend into Urema graben in Mozambique.

The fault studies should consider various levels: (i) regional investigations should cover 150-200 km radius, in order to form a picture of the general tectonic setup; (ii) local investigations in 50 km radius; and (iii) faults intersecting the dam site with special significance for dam structure.

The Malawi rift is composed of four main types of rift structures: boundary faults, step faults with riftward tilted blocks, half grabens and horsts; and monoclinal structures,

Figure 8.163 East African Rift System

Seismic Map

Figure 8.164 represents the seismicity Map of Africa and Figure 8.165 presents the seismicity Map of Malawi.

Figure 8.166 shows the Karonga earthquake sequence and Figure 8.167 illustrates the sequence of Karonga fault slip.

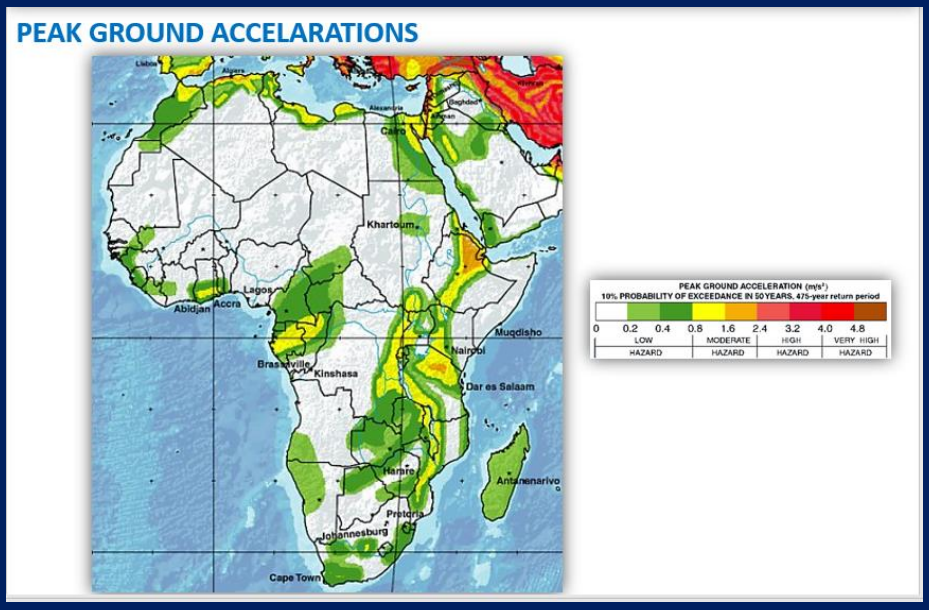

Figure 8.164 Seismicity Map of Africa

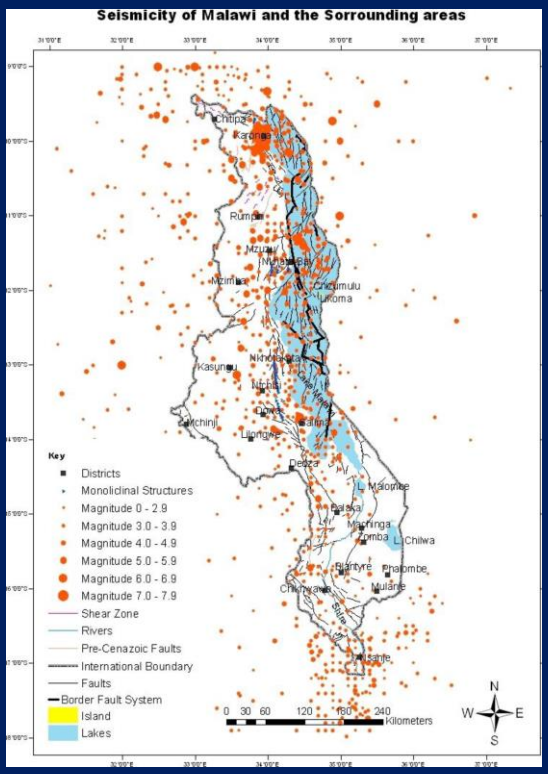

Figure 8.165 Seismicity Map of Malawi

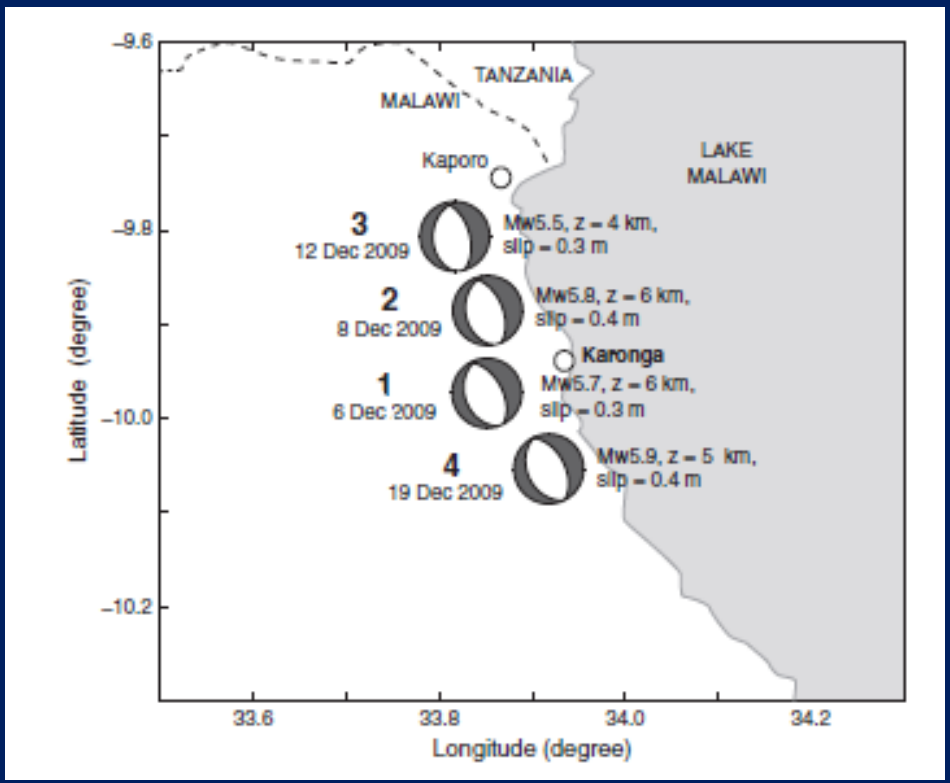

Figure 8.166 Karonga earthquake sequence

Based in the recorded earthquakes for a magnitude higher than 4 and epicentral distances until 500 km, an statistical analysis with extreme values considering a global sample was performed for a period of n years.

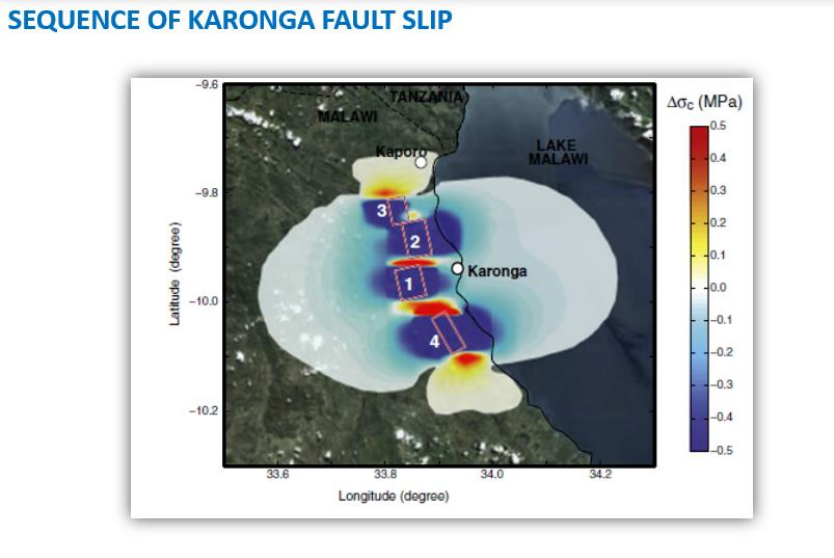

Figure 8.167 Sequence of Karonga fault slip

The methodology has integrated the following steps

Considering the global sample the most intense earthquake in each year was selected and so a sample with the highest values was obtained.

- the sample was organized considering the tendency of increasing values

- for each event was considered a probability of $P = \frac{j}{n+1}$, where j is the number of the organized sample and n is dimension of the sample. This probability (p) can be correlated with the return period of the event (T) considering the equation: . $T = \frac{1}{1-p}$ (8.32)

The extrapolation of acceleration value linked to the return period was based in the ajustment of the curve related with the maximum acceleration values versus return period. The best fit is simulated by a parabolic curve.

Figure shows the probability values associated with each event and the best curve fit to the group of pairs.

Also 4 earthquakes with magnitudes between 4 and 4.8 and short epicentral distances, between 39.6 and 61.64 Km, were considered.

The maximum acceleration values for return periods of 145, 475, 1000, 5000 e 10000 years, for the referred scenarios is shown in Figure 8.168.

The computed values are referred to the bedrock, and so it is important to incorporate the local effects with great importance in the vibration amplitude and spectral richness.

Local effects have a great importance in the amplitude of vibrations and spectral richness.
Taking into account the following factors:

i) uncertainties introduced by incomplete data;
ii) local effects and their consequences for the attenuation relationship;
iii) induced seismicity for earthquakes with small epicentral distance;

Based in the methodology proposed by ICOLD, the available collected data and the low seismicity of the country, the following values of acceleration for the design earthquakes, were considered:

For MCE (Maximum Credible Earthquake), considering a situation of filling of reservoir, a return period of 1000 years, the acceleration value for earthquakes with short epicentral distance is 39.72 cm/s2. This value should be amplified by a factor around 3 to incorporate the local effects and so a peak acceleration value of 0.12 g is obtained.

For OBE (Operating Basis Earthquake) that is linked with a low return period a value of 0.08 g is considered.

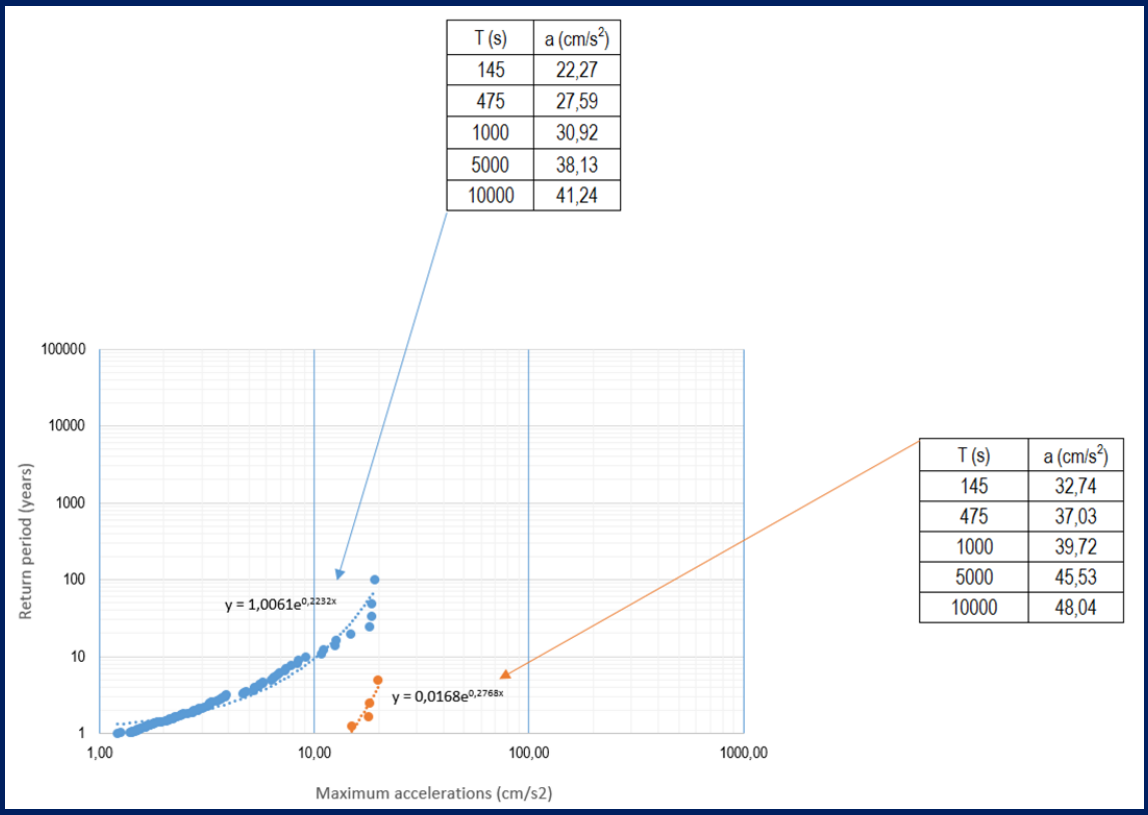

Figure 8.168 Curve related with the maximum acceleration values versus return period

8.2.8.5 Dam Profile

Figure 8.169 shows the dam cross section D2 for a zoned dam solution.

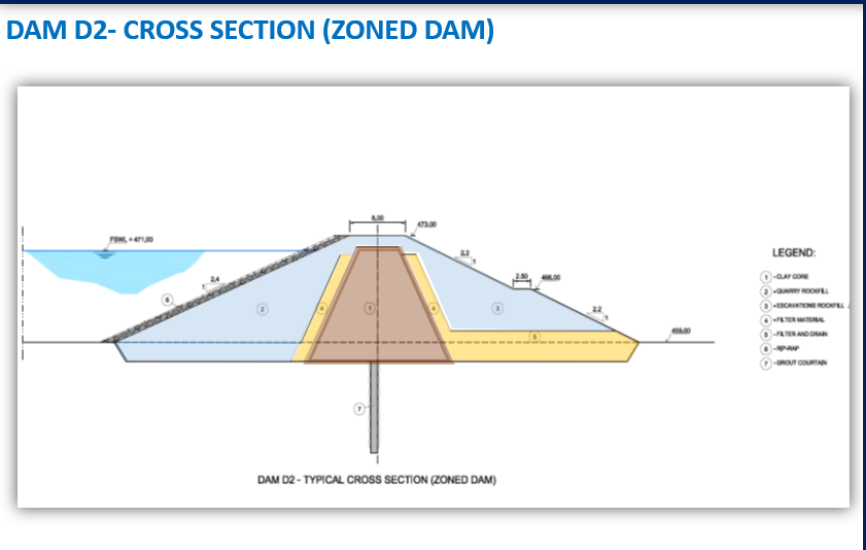

Figure 8.169 Dam cross section D2 (zoned dam)

Figure 8.170 illustrates a dam cross section D2 for a CFRD solution.

Figure 8.171 presents a pre- cofferdam and cofferdam proposed solution.

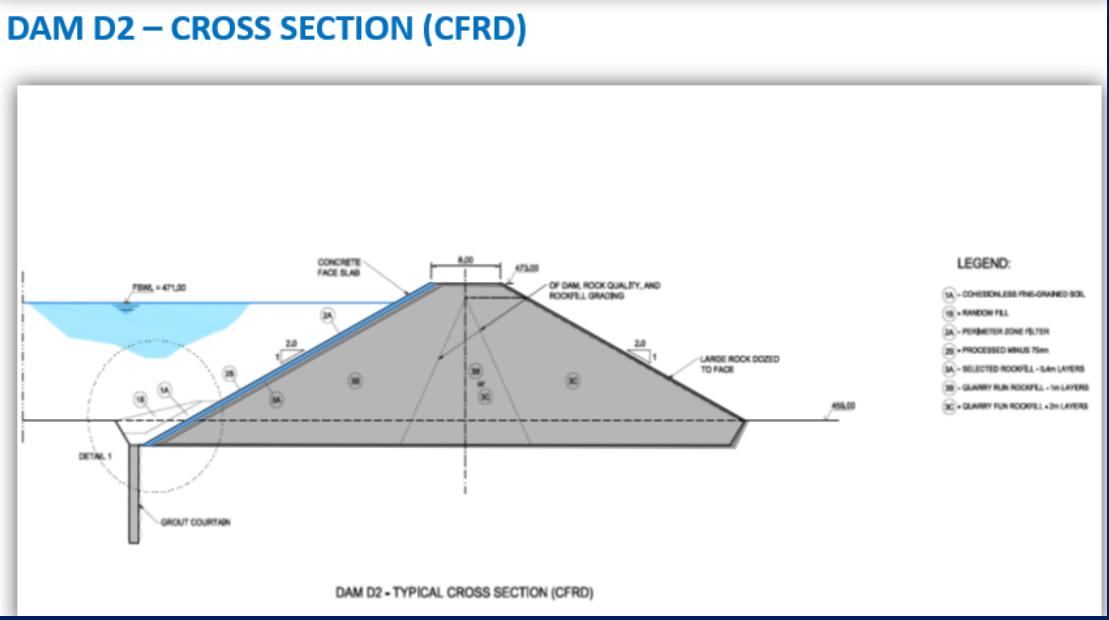

Figure 8.170 Dam cross section D2 (CFRD)

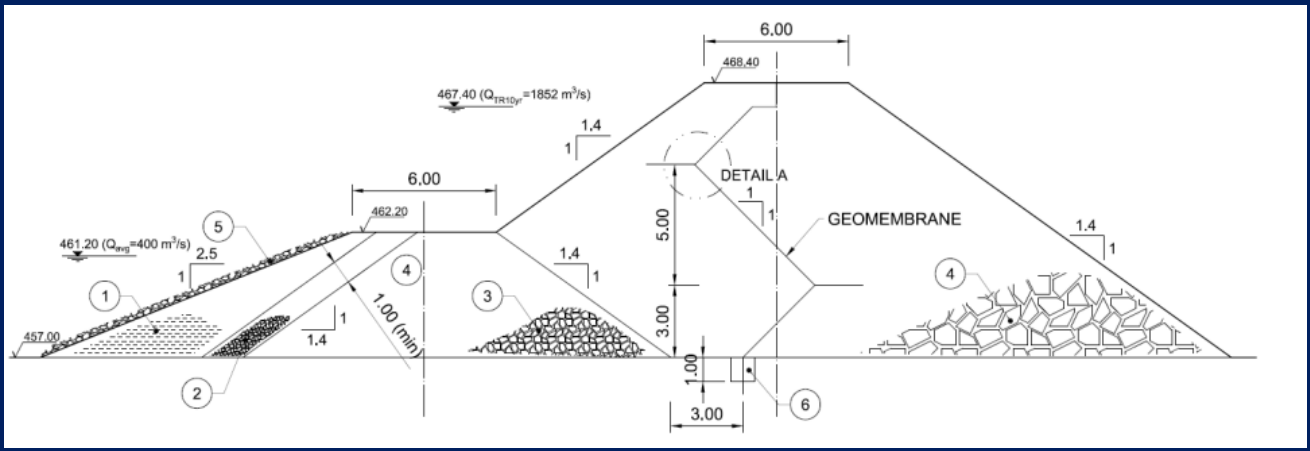

Figure 8.171 Pre- cofferdam and cofferdam proposed solution

DAM PROFILE

The dam D1 is a concrete gravity structure with an expected maximum height above foundation level of 16 m (12 m above ground) and a total crest length of about 300 m and 8.00 m width. The dam develops in a straight alignment and the crest level at elevation (470.00), 2 m above FSWL

The concrete dam profile adopted, is defined by a triangle with one vertex located on the upstream surface at elevation (470.00), corresponding to the crest level, with the upstream surface vertical and the downstream surface sloped 0.8:1.0 (h:v). Taking into account the low height of the dam, it was decided to adopt a concrete gravity undrained profile, with no drainage gallery.

The distance between joints was established at 17.0 m, a value that can be optimized during the following design phases. A preliminary evaluation of the dam profile stability was made, verifying the sliding and overturning stability, according to gravity dam design criteria defined by USACE

Figure 8.172 illustrates the dam profile.

The following verifications were performed:
- Sliding Safety Factor;
- Overturning Safety Factor;
- Foundation Bearing Pressure.

The shear strength design parameters adopted for the interface concrete-rock foundation are 42° friction angle and 35 kPa cohesion.

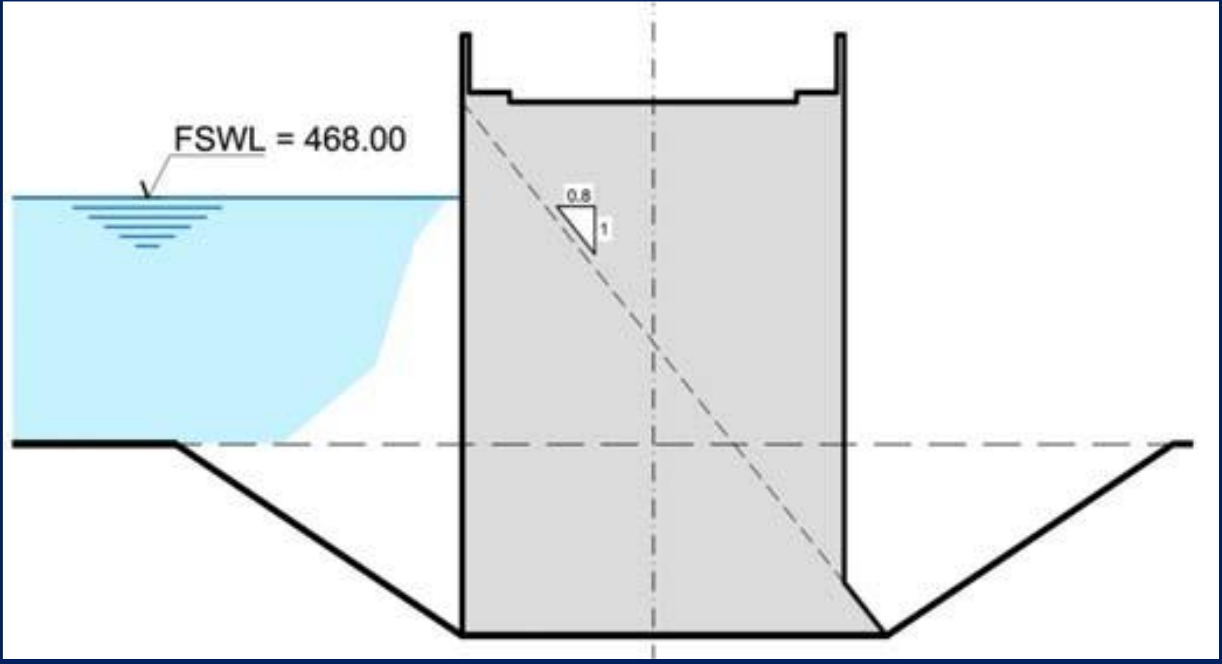

Figure 8.172 Dam Profile

Based on the results of permeability tests (Lugeon tests) for the foundation treatment a grounting curtain in the axial zone of the dam, to guarantee low losses of water, with a maximum depth of 20 m was proposed.

8.2.8.6 DAM FOUNDATION TREATMENT

Introduction

Based on the permeability tests for the foundation treatment a grouting curtain in the axial zone of the dam, to guarantee low losses of water, with a maximum depth of 20 m will be proposed.

A seepage analysis will be performed using the SEEP W code.

The efficiency of the grouting curtain will be analyzed.

Impervious grouting curtain

Related with the impervious grouting curtain the following items will be analyzed:
-characteristics of the equipment's;

- study of the grouting composition;

-laboratory tests for the characterization of viscosity, density and decantation;

- grouting methodology.

Grounting equipment

The grouting equipment should be maintained in good order to control grout volumes and grouting pressures. The equipment should allow a continuous flow and a grouting pressure of 1,0 MPa.

Mixture equipment's

The volumetric mixtures shall allow the preparation of mixtures with the desire precision (1 a 2%).

An equipment of high turbulence shall be used. The velocity of rotation has allowed a colloidal suspension (approximately 1 200 to 1 500 rotations/minute)

The minimum time of mixture shall be 2 minutes.

The mixture of grout was sent for a reservoir to assure a continuous mechanical agitation with a connection with an injector of double injection that has allowed the introduction of the grout in the hole.

The grout mixture shall have an equipment to measure the injected volume.

Grouting pump

The grouting pump shall allow the measurement of the pressure and the value of the flow from zero until the maximum allowed value.

The maximum allowed flow value shall be less than 100 liters/minute and the maximum pressure lower than 1 MPa.

Manometres

The total amplitude of manometers will not exceed 2 times the maximum allowed pressure. The manometers shall have an adequate accuracy.

Grout circuit

The grout circuit shall integrate:

- a bottle of air to minimize the blows of pressure;
- a manometer with direct measurements.

Packers

The packer for grouting shall assure the adequate impermeability not allowing seepage between walls of the hole.

Grouting materials

The grouts will be composed by cement, bentonite, water and additive.

Grouting records

For each grouting branch a detailed record was presented:

- number of the hole;
- injected branch;
- day and hour of the begin of operation;
- packer position;
  - results of permeability tests before the grouting (if this is the case);
  - grouting composition, pressure of grouting, flow and time of variation of these parameters. Also, the grouting quantities were recorded.
  - absorption of the total branch;
- incidents occurred during the grouting operations;
  - tables for each hole, with information about the weight of injected cement and injected pressure for each branch.

8.2.8.7 Waterway System

For the waterway systems it was considered a tunnel construction by NATM method or by a TBM.

NATM Method

The results of core borings that will give information about the degree of rock weathering, thickness of the layers, rock fracturing, rock classification, uniaxial compressive strength of the rock, deformation properties (modulus), effect of water on the rock quality, will be important for the selection of design method combined the empirical methods and the NATM method that includes seven elements:

-
- Exploitation of the strength of native rock mass - Relies on the inherent strength of the surrounding rock mass being conserved as the main component of tunnel support. Primary support is directed to enable the rock to support itself.
- Shotcrete protection - Loosening and excessive rock deformation must be minimized. This is achieved by applying a thin layer of shotcrete immediately after face advance.
- Measurement and monitoring - Potential deformations of the excavation must be carefully monitored. NATM requires installation of sophisticated measurement instrumentation. It is embedded in lining, ground, and boreholes. In the event of observed movements, additional supports are installed only when needed, with a resultant overall economy to the total cost of the project.

- Flexible support - The primary lining is thin and reflects recent strata conditions. Active rather than passive support is used and the tunnel is strengthened by a flexible combination of rock bolts, wire mesh and steel ribs, not by a thicker concrete lining.
- Closing of the invert - Especially crucial in soft ground, the quick closing of the invert (the bottom portion of the tunnel) which creates a load-bearing ring is important, and has the advantage of engaging the inherent strength of the rock mass surrounding the tunnel.
- Contractual arrangements - Since the NATM is based on monitoring measurements, changes in support and construction method are possible, but only if the contractual system enables them.
- Rock mass classification, ranging from very hard to very soft, determines the minimum support measures required and avoids economic waste that comes from needlessly strong support measures. Support system designs exist for each of the main rock classes. These serve as the guidelines for tunnel reinforcement.

The use of different construction techniques, namely: shotcrete, nailing, steel ribs, rockbolds are illustrated in Figures 8.173 to 8. 176.

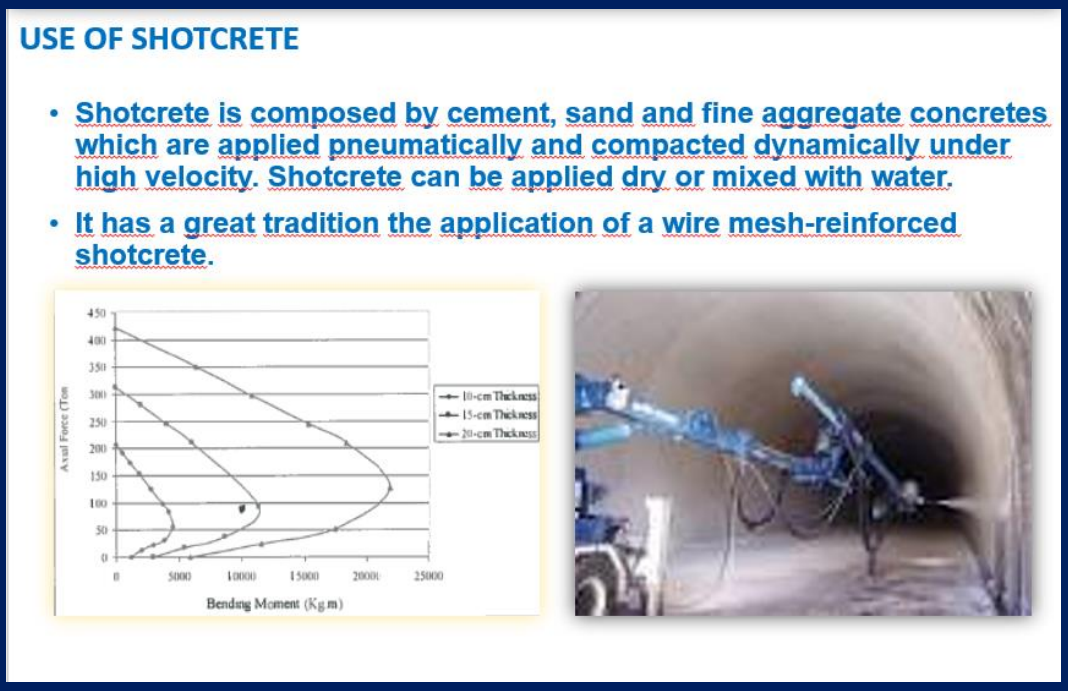

Figure 8.173 Use of shotcrete

Figure 8.174 Use of nailing

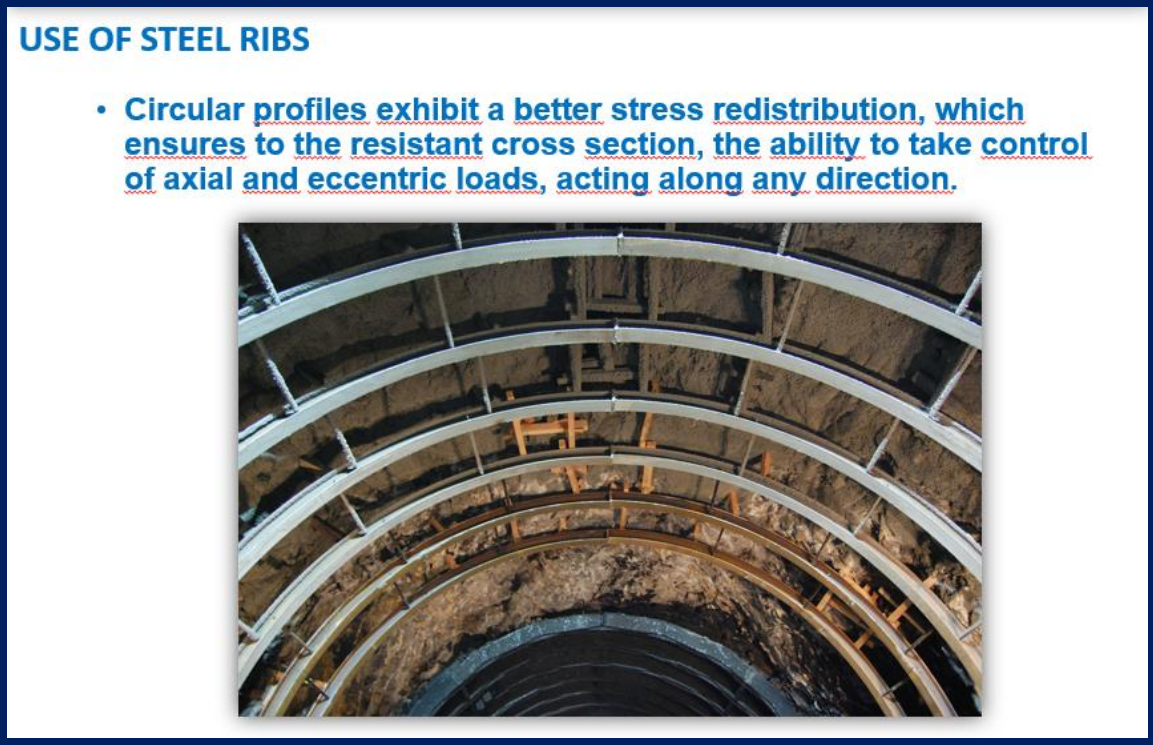

Figure 8.175 Use of steel ribs

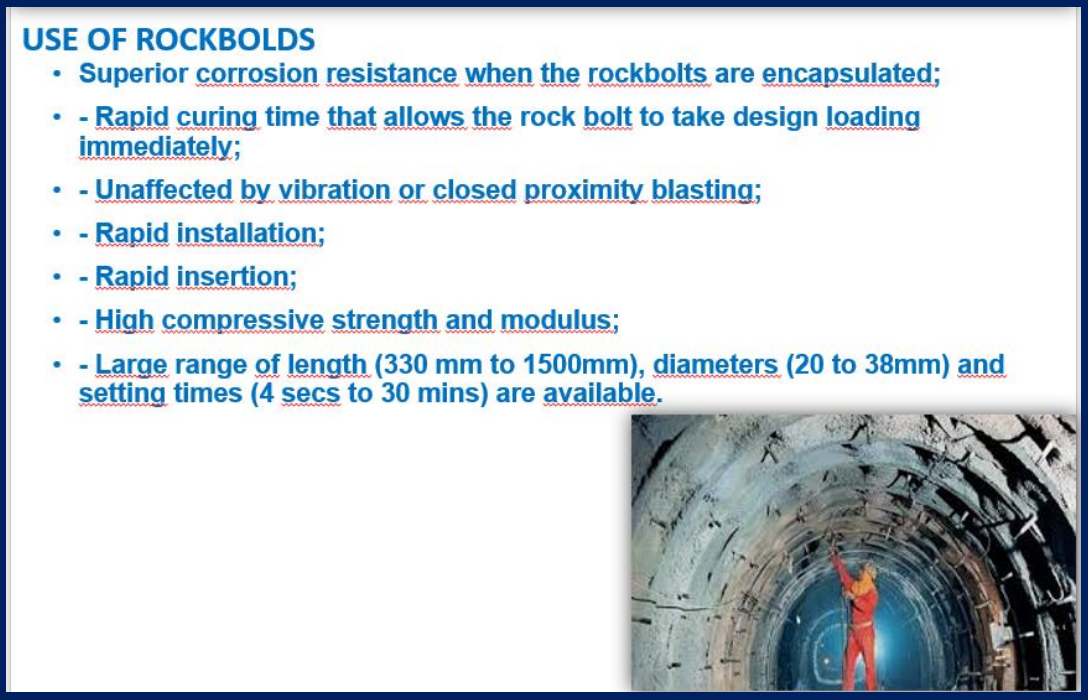

Figure 8.176 Use of rockbolds

ITA Reccommendations

- International Tunnelling Association (ITA) recommendations were followed and so the basics documents for the tunnel design have covered:
- - The geological report presenting the results of the geological and geophysical survey.
- - The hydrogeological report.
- - The geotechnical report on site investigations, including the interpretation of the results of site and laboratory tests with respect to the tunnelling process, soil and rock classification, etc.,
- - Information on line, cross-section, drainage, and structural elements affecting later use of the tunnel.
- - Plans for and a description of the projected excavation or driving procedure, including the different cross-sections related to different ground conditions.
- -Design documents for the types of excavation methods and tunnel supports likely to be applied, considering, e.g. excavation advance and face support (types and number of anchors, shotcrete strength, closure length, etc.).
- - The program for the in-situ monitoring of the tunnel by field measurements.
- - The analysis of stresses and deformations (for unlined tunnels as well as for single-or double-lined tunnels), and the dimensioning of the tunnel support for intermediate phases and final linings. • The design for waterproofing or drainage.
- - Structural documents for the final design of the tunnel project, including the detailing.
- - During and after the excavation, reports on the field measurements and interpretation of their results with respect to the response of the ground and the structural safety of the tunnel.
- - Documentation of the problems encountered during the excavation and measures applied, e.g. strengthening the ground or changing the projected type of support, based on monitoring results.

- Site Investigations. The following aspects were considered for the geological description of each zone: • Name of the geological formation in accordance with a genetic classification. • Geologic structure and fracturing of the rock mass with strike and dip orientations. • Colour, texture and mineral composition. • Degree of weathering. Parameters of the rock mass e.g. in five classes of intervals, including: • Thickness of the layers. • Fracture intercept. • Rock classification. • Core recovery. • Uniaxial compressive strength of the rock, derived from laboratory tests. • Angle of friction of the fractures (derived from laboratory direct shear tests). • Strength of the ground in on-site situations. • Deformation properties (modulus). • Effect of water on the rock quality. • Seismic velocity. Primary stress field of the ground.

  The support systems in circular tunnels are shown in Figure 8.177.

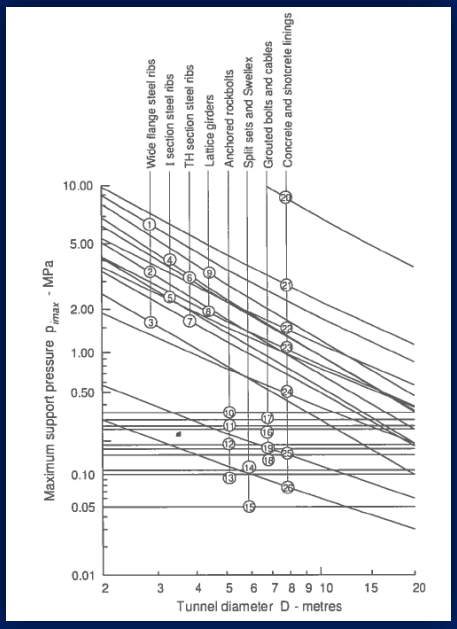

Figure 8.177 SUPPORT SYSTEMS IN CIRCULAR TUNNELS

TBM

Tunneling by TBM is used for the excavation of underground openings under different geological conditions varying from hard rock to soft sedimentary layers.

Procedures used for tunneling by TBM:

- Excavation with a rotating cutter wheel in a cyclic or continuous drilling process;

- Mucking with a mechanical discharging device;

- Placement of primary ground support elements, namely: concrete segments, soil or rock bolts, steel ribs, meshes and shotcrete;

Two different types of TBMs are used according to the expected conditions: open type machines (where the face of excavation is self-standing) and closed type machines.

Tunnelling by TBM is generally appropriate for.

- projects with constant shapes of cross section;

- long tunnels;

- projects with a good accessibility.

The selection of the excavation method for the waterway system will be made based on project requirements, namely:

- Health and safety;

- Environmental aspects;

- Aspects of future operation;

- Design (including Schedule and costs);

- Construction (including Schedule and costs);

- Third parties and existing facilities.

8.2.8.8 Underground Works

The solutions for the underground works of the waterway system of the Kholombidzo HPP are described (primary and definitive supports and excavation methodologies). The underground works comprise the headrace tunnels, the tailrace tunnels, the connection shafts between the surge chambers and the headrace tunnels and, a provisional intermediate access, for constructive proposes, to the headrace tunnels. The main characteristics of the tunnels are indicated in Table 8.30.

The Tunnels Engineering Geological Approach is shown in Table 8. 31.

Table 8.30 Characteristics of the tunnels

	Length (m)	Maximal depth (m)	Geology
Headrace Tunnel 1	2775	50	Biotite Gneiss and Marble
Headrace Tunnel 2	2828	50	Biotite Gneiss and Marble
Intermediate Access	167	45	Biotite Gneiss
Tailrace Tunnels 1 to 4	4 x 72	30	Biotite Gneiss

Table 8.31 Tunnels Engineering Geological Approach

RMR – "Rock Mass Rating"	Litology	Degree of fracturing (ISRM)	Weathering degree (ISRM)	Core Recovery (%)	RQD - "Rock Quality Designation " (%)	Intact rock compressive strength (MPa)
> 70	Biotite gneiss; Marble	F_{1-2}	W_{1-2}	100	> 90	> 100
50 – 70		F_{2-3}	W_{1-2}	100	> 50	> 50
30 – 50		F_3	W_3	> 75	> 50	> 25
< 30	Biotite gneiss; Marble; Tectonic weathered and crushed materials	$F_{3-4\ to}\ F_5$	$W_{3-4\ to}\ W_5$	< 75	< 50	< 25

8.2.8.9 Construction Methods

For the total length of the power waterway, with about 2800 m twin headrace tunnels, and layout with curves near the power intake and the powerhouse, any of the tunnels alone has the sufficient length and geometric characteristics, that the TBM Tunnel Boring Machine, can clearly be pointed as the most economical and recommendable construction method. Both tunnels combined length is, in fact, interesting from a TBM application point of view. However, it implies the recovery, turnaround and re-assembling of the machine.

On the other hand, taking in account the relatively reduced depth of the headrace tunnels (around 50 m maximum), it's relatively easy to open a short (~160 m) intermediate tunnel access, theoretically cutting to a half the excavation duration time. So, even from a schedule point of view, the TBM is not necessarily faster than the conventional tunneling methods, to perform with conventional drill & blast technology. For the intermediate access and the four tailrace tunnels, the envisaged construction method is also the conventional tunneling with drill & blast in rock masses and mechanic excavators and hydraulic hammers in soils and highly weathered rock. It's recommendable for the success of the underground works, that the contractor is well equipped, with appropriate machinery that, in this case, must consider hydraulic drill rigs (jumbos) in sufficient quantity, because after the opening of the intermediate access, up to eight excavation fronts can advance simultaneously (only for the headrace tunnels). For the vertical connection shafts between the surge chambers and the headrace tunnels, the typical mining raise boring method can be used. It consists in drilling a pilot hole from the surface to the adjacent chamber of the headrace tunnel and, from below, enlarge it with an upward reaming.

Tunnels cross sections

As the recommended construction method is drill & blast, an adjustment is made to the previous proposed circular section excavation of the tunnel. The adjustment consisted in increasing the radius in the invert zone of the tunnel, becoming the excavation section more appropriate for the front access to vehicles and better trafficability of rigs and mucking equipment inside the tunnels.

The cross sections for headrace tunnels, intermediate tunnel and tailrace tunnels are shown in Figures 8. 178 to Figure 8. 181.

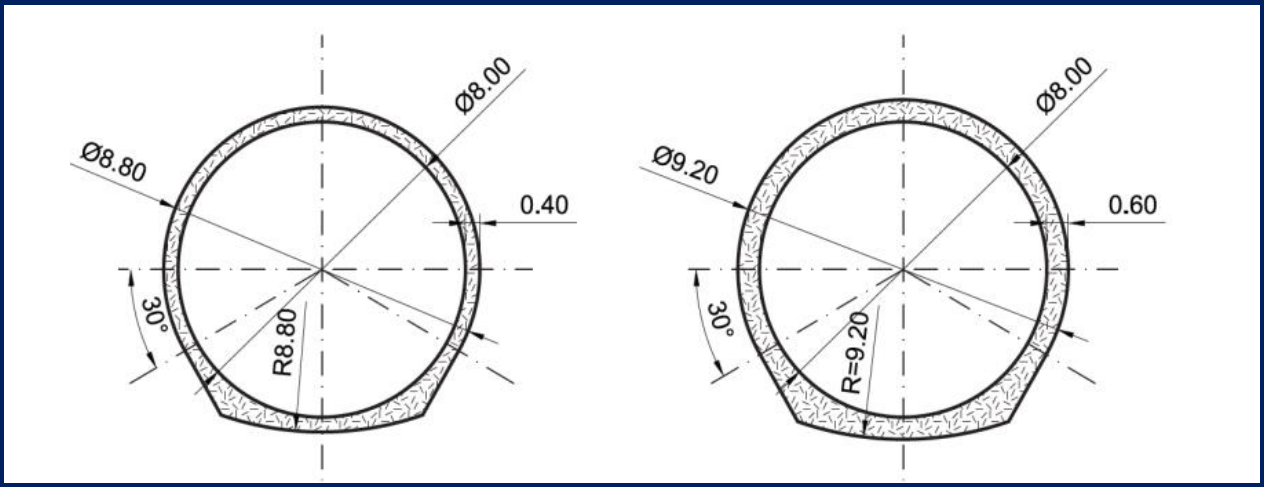

Figure 8.178 Headrace tunnels cross sections. Current section 1 in left, with 0.40m thickness, for RMR values above 50 and at the right side, section 2, with 0.60 m thickness, for RMR values below 50

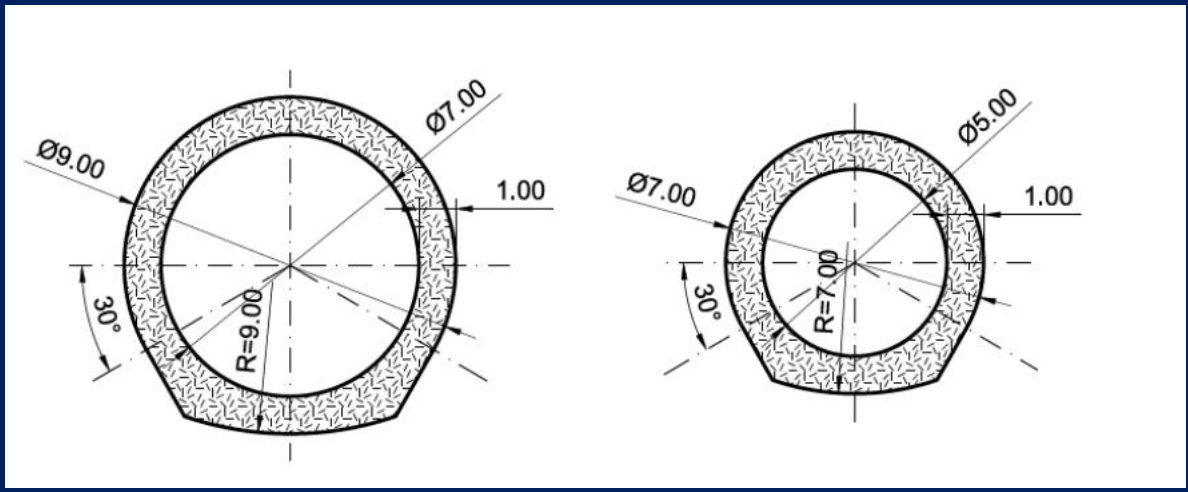

Figure 8.179 Steel lined cross sections 3 and 4. Section 3 in the left for the first 107 m stretch, and section 4 on the right for the final 26 m stretch before the powerhouse

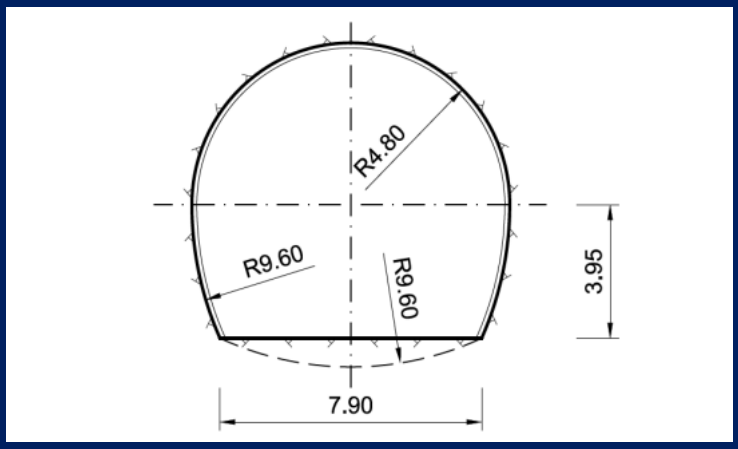

Figure 8.180 Intermediate access tunnel

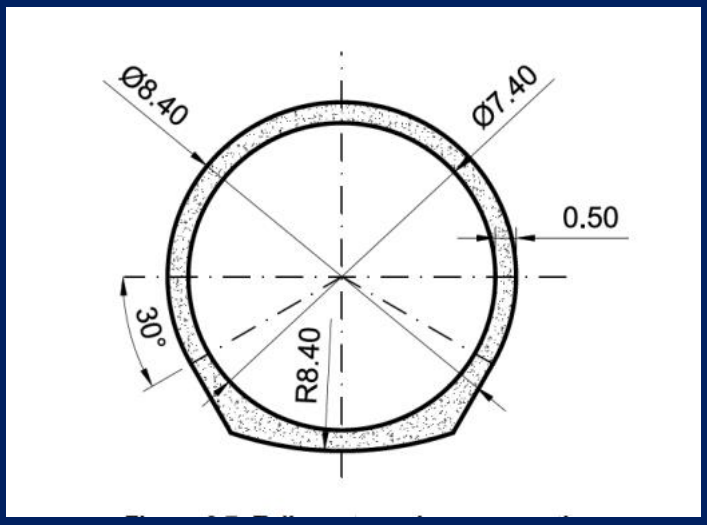

Figure 8.181 Tailrace tunnels cross section

Adopted Primary Supports

The adopted primary supports in headrace tunnels, for different ground conditions, is illustrated in Figure 8. 182.

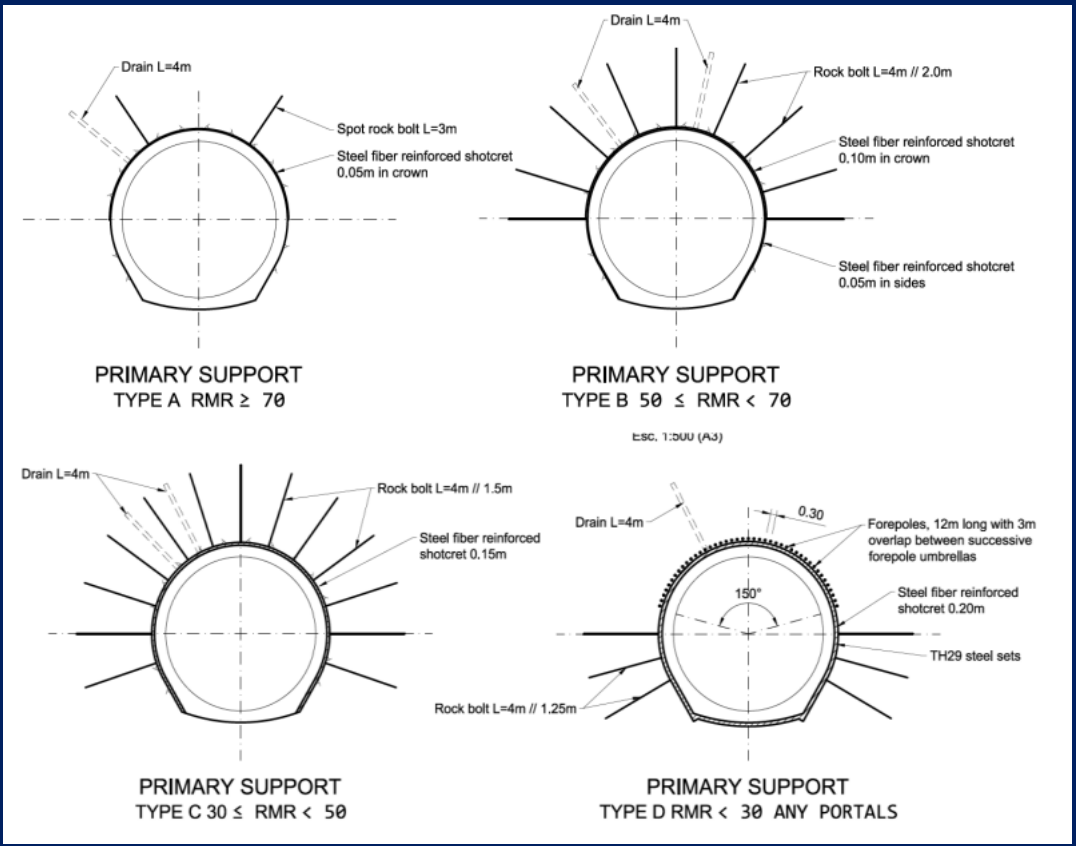

Figure 8.182 Adopted primary supports in headrace tunnels, for different ground conditions

8.2.8.10 Monitoring and Safety Evaluation

MONITORING AND SAFETY CONTROL

- **Frequent visual inspection by staff in charge of the observation system;**
- **Periodic visual inspection by specialist;**
- **Regular instrumentation measurements;**
- **Data validation;**
- **Data storage;**
- **Visual inspections;**
- **Safety evaluation;**
- **Corrective actions.**

Lesson nº 7: The essential steps of good dam analysis, whatever the type of material is involved, shall be performed with a sufficient degree of accuracy that the overall results can be extremely useful in guiding the engineer in the final assessment of static and seismic stability. This final assessment is not made by numerical results but shall be made by experienced engineers who are familiar with the difficulties in defining the actions, namely the design earthquake, and the material characteristics, who are familiar with the strengths and limitations of analytical procedures, and who have the necessary experience gained from studies of past performance.

Note: The dam design project was conducted by a multidisciplinary COBA team and the author was involved in the geotechnical design.

8.2.9 Case History nº 8 - Sabugal Dam

8.2.9.1 Introduction

For Sabugal dam the dam profile studies are introduced, the dam lay-out is addressed, the geological studies are referred, the site investigation is introduced, the geotechnical characterization is addressed, the hydrogeology and tectonic conditions are presented, the definition of design earthquake is discussed, filter and drain conditions are analysed, the construction issues are referred and the monitoring is mentioned.

8.2.9.2 Dam Profile Studies

Introduction

For the definition of dam profile is important to specify:

- Crest width
- Freeboard
- Crest level
- Slope protection.

Crest width

For the crest width the following equation is used:

L = 1,1 $\sqrt{H}$ + 1, H – high of the dam

The Japanese code reccommends :

$L = 3{,}6\sqrt[3]{H} - 3$

Freeboard

For the definition of freeboard, the following actions combinations are used

i) NRN + H_{ve} + Δh + Zm

ii) NPHE + H_{vn} + Δh + Zm

iii) NRN + H_{se} + Δh

where

NRN - Normal water level

NPHE - High water level

H_{ve} - wave height due exceptional wind

H_{vh} - wave height due normal wind

H_{se} - wave height due earthquake

Δh - Dam settlement

Zm - Wave due to wind

a) Settlements

The maximum settlement is obtained at the middle of the dam.

b) Waves due to the wind

Wave height Hs can be defined by equation:

$$Hs = \frac{V^{1.06} F^{0.47}}{2.00} \qquad (8.33)$$

where:

V_V - wind velocity

– F_e - "fetch" effective.

c) Waves due to the earthquakes

Following Spanish code

$$Hse = \frac{Kh.T.\sqrt{gH}}{2} \qquad (8.34)$$

where

Kh - seismic coefficient

T - predominant period (s)

g - gravity acceleration (m/s^2)

H - maximum water level (m)

Slope upstream protection

Following ICOLD Bulletin – "Embankment Dams". Protection of Upstream Slope, Final Draft, December 1991".

$$W_{50} = \frac{H_s^3}{4{,}37\ (Gs-1)^3\ \text{Cotg}\ \phi} \qquad (8.35)$$

where

W_{50} - average weight of rockfill blocks (l_b)
γ_r - rockfill unit weight (lb/ft^3)
H_s - wave height (ft)
G_s - rockfill density
φ - slope inclination

8.2.9.3 Dam Layout

Figures 8. 183 to 8.185 illustrate the dam plan, the longitudinal profile and the dam profile, respectively.

Figure 8.186 presents the sieve analysis of the different materials.

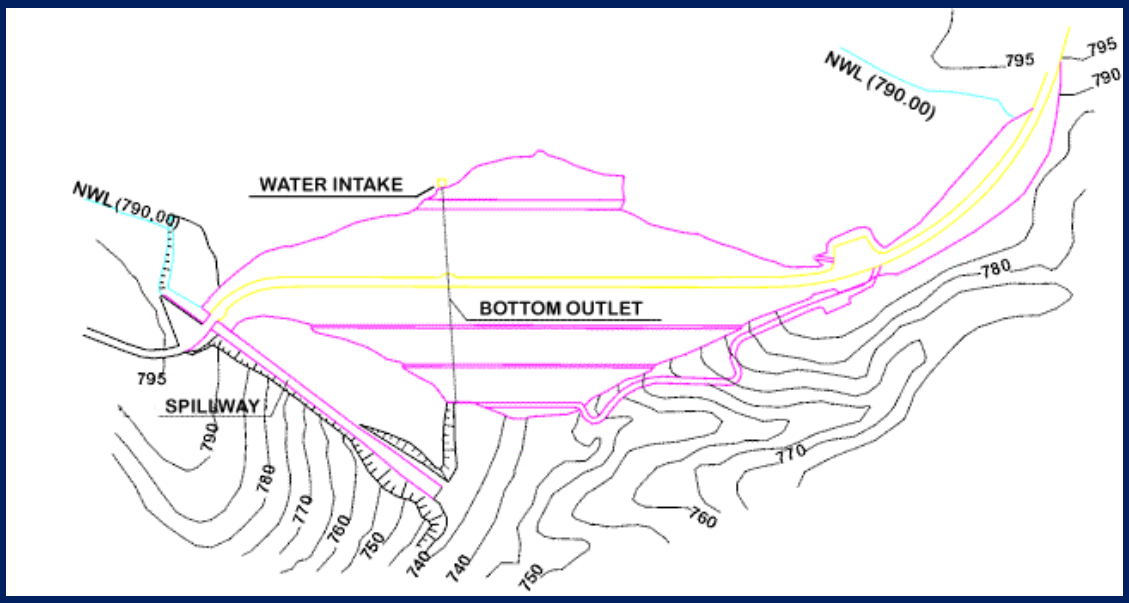

Figure 8.183 PLAN

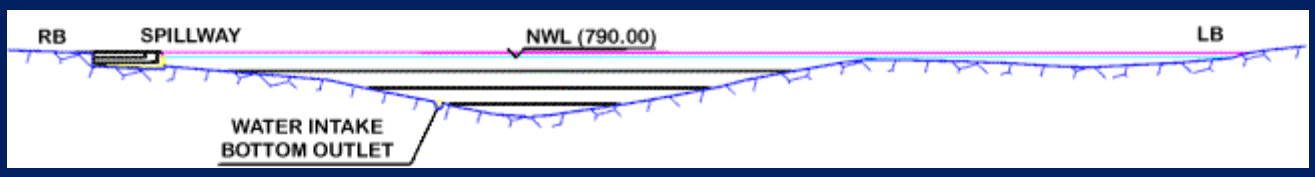

Figure 8.184 Longitudinal Profile

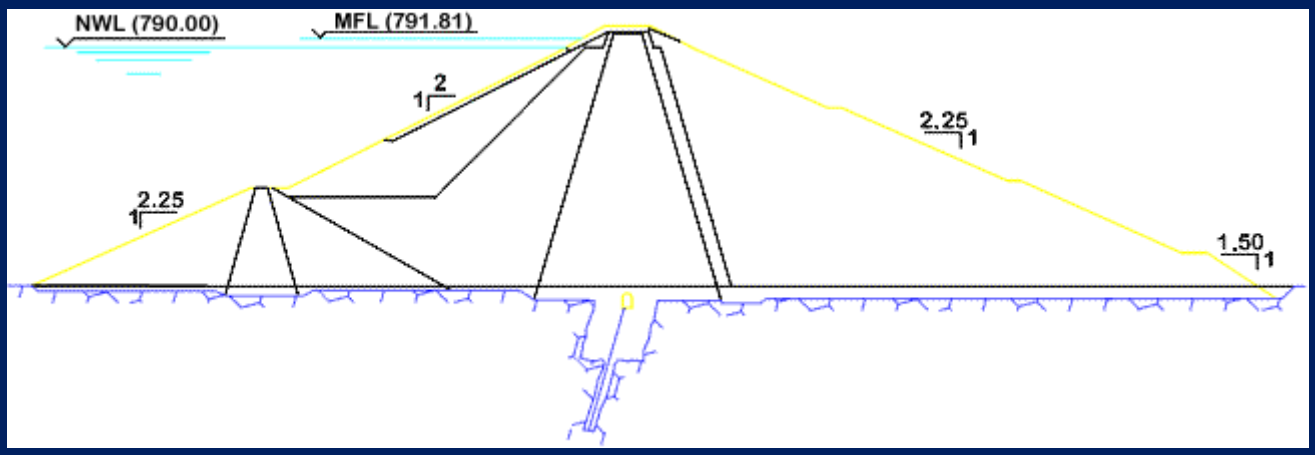

Figure 8.185 Dam profile

The dam has a length of 1005 m and the spillway is located in the right rive.

The maximum dam height is 58.5 m.

The dam profile is zoned with a clay core of clay materials and the shells incorporate schists materials. There is in the upstream shell a section composed by rockfill materials type grauvaques. There is a filter material in the interface between the core and the downstream shell.
The volume of the materials is 1.89 million m3.

The dam crest is located at level (794,00), with a width of 10 m. The upstream slope is 1/2,25 and 1/2 (V/H) and the downstream slope is 1/2,25 V/H and 1.5/1.0.

The levels of maximum flood (NMC) and the filling reservoir (NPA) are, respectively, 791,81 e 790.00.

The impervious core is symmetrical and reaches the maximum level of (793.00), where exhibits a width of 6.0 m. the upstream slope and the downstream slope has an inclination of 1:0,3.

The drainage system incorporates a chimney filter, a longitudinal drainage trench to receive the water that percolates trough the dam and the foundation, by four transversal trenches, by a drainage blanket in contact with the downstream shell and by rockfill material at downstream toe.

The cofferdam shells, the internal zone of the upstream shell, the downstream shell are composed by schist materials.

The external zone of the upstream shell is composed by rockfill material.

The chimney filter at downstream has a thickness of 3.0 m.

The upstream shell is protected by rockfill material 0.9 m thick above level (770) and 0.40 m thick beneath this level. (759,50).

The dam integrates an upstream cofferdam with the crest at level and an exterior berm 8.5 m width.

Taking into account the conditions of the foundation, it was considered important to incorporate a grounting gallery.

The foundation treatment will be executed in two phases, the first phase with a treatment of consolidation and contention and the second phase, after the construction of the grouting gallery, the injection curtain.

The grouting gallery has a length of 647 m with a section of maximum height of 3.0 m.

8.2.9.4 Geological Characteristics

The geological units integrate the superficial deposits (alluvial, colluvial and residual soils), filádios e metagrauvaques that belong to the complex schist-grauvaque.

The alluvial materials are composed by sands, gravels, with thickness varying between 2 to 3 m.

. The coalluvial materials are composed by blocks and gravel with thickness between 2 to 3 m.

The residual soils have thickness between 1 to 3m.

The schist grauvaque is composed by schist and grauvaques interstratificated and exhibit dolerites and quartz materials.

8.2.9.5 Site Investigation

The site investigation has included seismic refraction profiles, boreholes (with SPT tests and Lugeon water tests) and laboratory tests of disturbed samples, taken in the trial pits, namely identification tests, Proctor tests, permeability tests and triaxial tests.

The site investigation was performed in two phases.

In the first phase geophysical tests (profiles and 29 geoelectric boreholes) and 10 rotary boreholes with Lugeon tests.

In the second phase 22 boreholes were performed and 7 seismic refraction profiles, with a length of 60 m.

8.2.9.6 Geotechnical Characteristics

3 geotechnical zones were considered:

The geotechnical zone 3 (ZG3) that integrates the surface deposits and the weathered bedrock with fractures, with RQD values less than 30%, and longitudinal waves less than 1300 m/s. The massif is very permeable and exhibits oxides of iron in the joints.

The geotechnical zone 2 (ZG2) that integrates massif medium weathered, with RQD values between 40% to 80%, and longitudinal waves between 1350 m/s and 3300 m/s. The massif is very permeable with absorption higher than 2 to 3 absorption units and exhibits oxides of iron in the joints.

The geotechnical zone 1 (ZG1) that integrates massif less fractured with RQD values superior to 60% and longitudinal waves superior to 3300 m/s. The massif has low permeabilities absorption less than 2 to 3 absorption units and low evidence of oxides of iron in the joints.

Figure 8.186 illustrates the sieve analyses.

8.2.9.7 Hydrogeology

In the dam site there are two types of aquifers: I) superficial aquifers; and (ii) deep aquifers.

The former are linked with superficial water surfaces and are associated with less productive lands.

The deep aquifers are linked with fissured schist -grauvaque with low permeability and following the results of Lugeon tests with interior drainage (COBA, 1994).

8.2.9.8 Tectonic

This zone belongs to the Iberic Centre and the formations are highly tectonized.
The stratification exhibits 2 attitudes of xistosity.

There are 4 fractured families

Related to the fracturation there are 4 principal families with the following attitude:

(i) A system N72E-80N;
(ii) A system N40E-77S;
(iii) A system N7E-80 N;
(iv) A system N70W-20 N.

Taking into account a bedrock acceleration of 0.10 g, from the seismic risk maps and considering a multiply factor of 1.5 it was considered for SME an acceleration value of 0.15g and for SBP a value of 0.10 g.

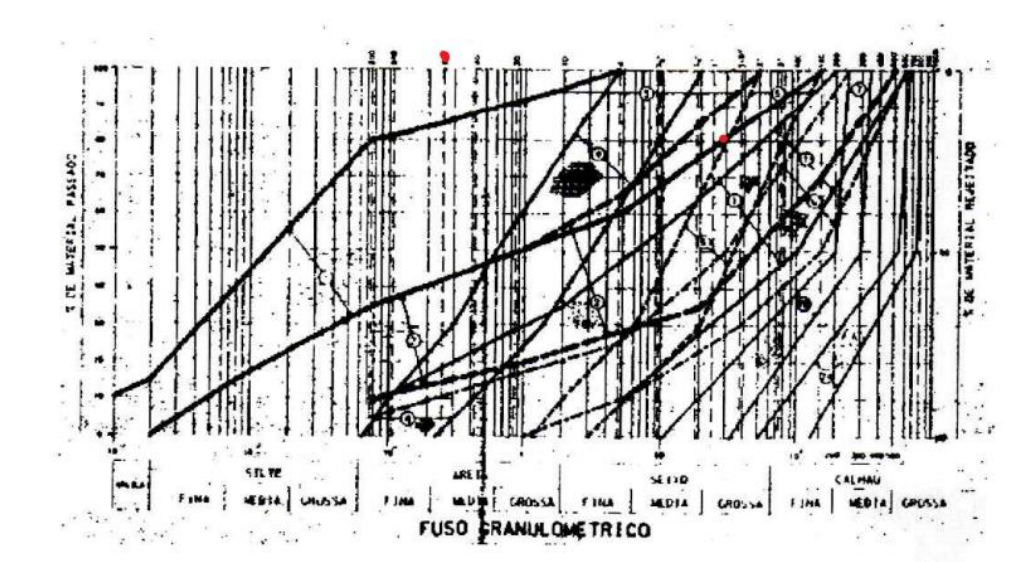

Figure 8.186 Sieve Analyses

8.2.9.9 Filter and Drain Materials

Introduction

The characteristics to be fulfilled by filter materials are subsequently analysed.

Internal erosion

The filter material to control internal erosion should respect the condition

$$\frac{D_{15(\text{filtre})}}{D_{85}\ (\text{soil})} < 5 \qquad (8.36)$$

where D_{15} and D_{85} are the diameters with 15% and 85%, of material has a lower diameter.

Permeability

To satisfy the permeability condition the material should respect:

$$5 < \frac{D_{15}\ (\text{filtre})}{D_{15}\ (\text{soil})} \qquad (8.37)$$

No cohesion

The filter material should not exhibit cohesion.

Internal stability

The internal stability of filter materials is linked with the capacity to maintain the fine particles during the dam life.

Filter segregation

The placement and compaction of filter materials should be carefully done in order to avoid the segregation.

Following USBR (1987) the coefficient of uniformity should be between 6 and 8.

A summary is presented in Table 8.32.

Table 8.32 Proposals for sieve characteristics

Proposals	Sieve characteristics
US Army Corps of Engineers (1941)	D_{max}= 25 d_{50}
Karpoff (USBR,1955)	Dmax= 3” (75mm)
US Army Corps of Engineers (1955)	D_{60}/D_{10}<20
Sherard et al (1984)	Dmax=2” (50mm)

Permeability coefficient

Permeability coefficient of filter materials can be defined by correlations with D_{10} ou D_{15}.

Hazen(1911) has proposed the following equation

$k(cm/s) = 100\ D_{10}^{\ 2}$ (8.38)

where D_{10} é is the effective diameter in centimetres

Sherard (1984) has proposed the following equation

$k= 3500\ D_{15}^{\ 2}$ (8.39)

where k= permeability coefficient in m/s

Construction control

Construction control includes placement of filter materials in horizontal lifts, 0.30m thick and compaction by two to three passes of a 10ton vibratory smooth-drum roller. The compaction of filters should be adequate to produce sufficient density to preclude liquefaction, to limit consolidation and to provide adequate strength (ICOLD, 1994b). To avoid contamination, filter materials are placed to a level of 0.5m ahead of adjacent embankment material. Gradation and permeability tests are performed both before and after placement

8.2.9.10 Instrumentation Plan

The instrumentation plan has included:

- 52 bench marks
- 72 hydraulic piezometers in the embankment;
- 6 hydraulic piezometers at the abutments
- 14 hydraulic piezometers in the gallery
- 64 total cells;
- 29 electric pore pressures;
- 8 inclinometers;
- 1 meteorological station;
- 3 flow devices;
- Devices for measurement of reservoir level;
- Devices for measurement of temperature, wind, precipitation and evaporation;
- 1 central measurements station.

Figure 8.187 shows the placement of an inclinometer tube.

Figure 8.188 illustrates the measurements of internal horizontal displacements.

Figure 8.189 presents the placement of a total cell.

Figure 8.190 shows the gallery piezometers.

Figure 8.191 indicates the flow device.

Figure 8.192 represents the internal gallery.

Figure 8.187 Placement of an inclinometer tube

Figure 8.188 Measurements of internal horizontal displacements

Figure 8.189 Placement of a total cell

Figure 8.190 Gallery piezometers

Figure 8.191 Flow device

Figure 8. 192 Internal gallery

8.2.9.11 Construction Issues

Figure 8.193 shows the clay core compaction.

Figure 8.194 illustrates the weathering of the rockfill material.

Figure 8.195 presents the dam upstream side.

Figure 8.196 represents the dam downstream side.

Figure 8.193 Dam construction -Clay core

Figure 8. 194 Dam construction- weathering of the rockfill material

Figure 8.195 Dam upstream side

Figure 8.196 Dam downstream side

Lesson nº8: There is a need of a better support for the definition of the monitoring plans.

It is important to compare the predicted values of stress and displacements with the observed values, in order to calibrate the model.

Past experience has shown the important role of the monitoring system.

Note: The dam design project was conducted by a multidisciplinary COBA team and the author was involved in the geotechnical design.

8.2.10 Case History nº 9 - Las Cuevas Dams (Venezuela)

8.2.10.1 Introduction

For las Cuevas dam the lay-out is addressed, the geotechnical characterization is introduced, the stress-strain analyses are described, the seepage analyses are mentioned, the definition of design earthquake is discussed and the seismic analyses are presented.

8.2.10.2 Dam Layout

Las Cuevas dam is an earthfill embankment to be constructed in Venezuela, on the Doradas river, in a zone of very high seismicity (Figure 8.197). The dam is 100 m high, 260 m long at the crest, the total embankment volume will be 4.5 x 10^6 m^3 and will impound a reservoir of 1.2 x 10^9 m^3.

The cross section is shown in Figure 8.198 and the upstream slope will be 1:1.8 and the downstream slope 1:1.8. The dam has a sloped narrow core of clay material and two shells of silty-sand material. A chimney-filter located downstream of the core is composed of sand.

The bedrock is composed from a sand-stone with high permeability and for this reason an extensive foundation treatment was recommended.

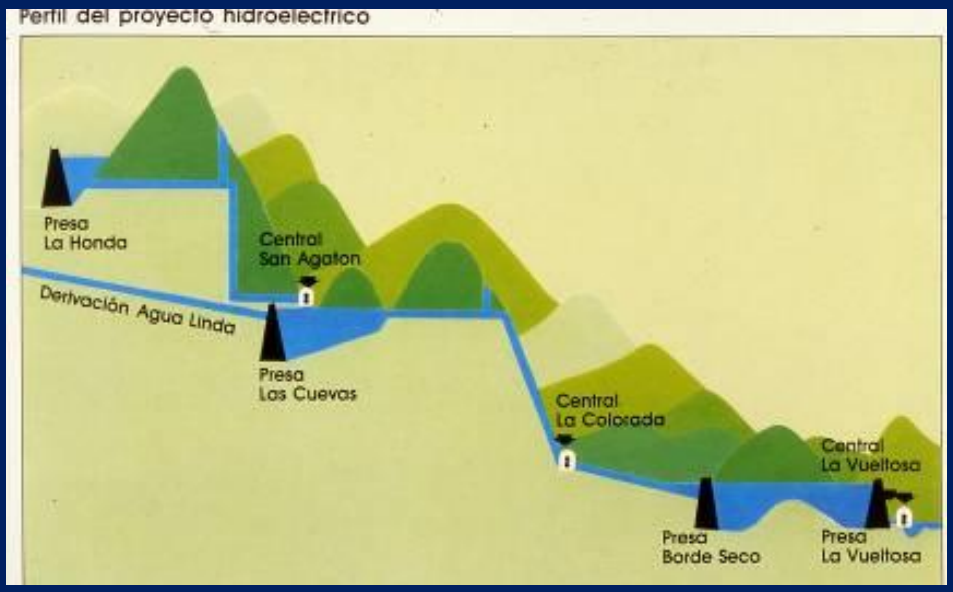

Figure 8.197 Dams location profile

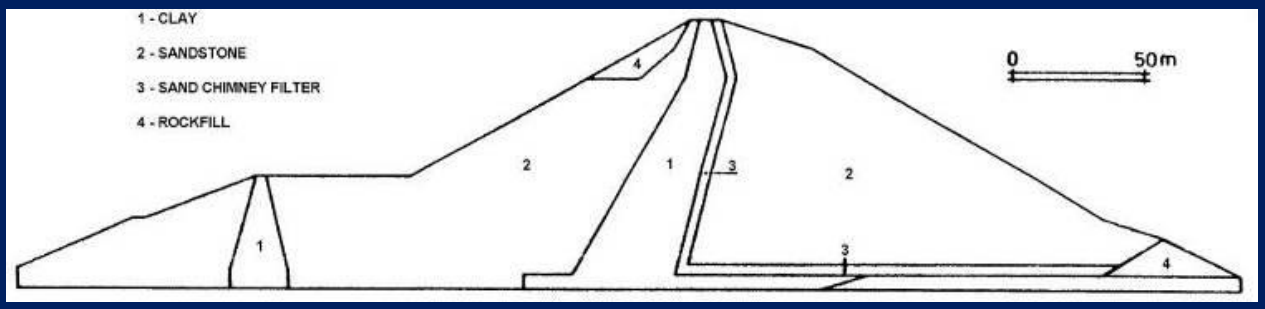

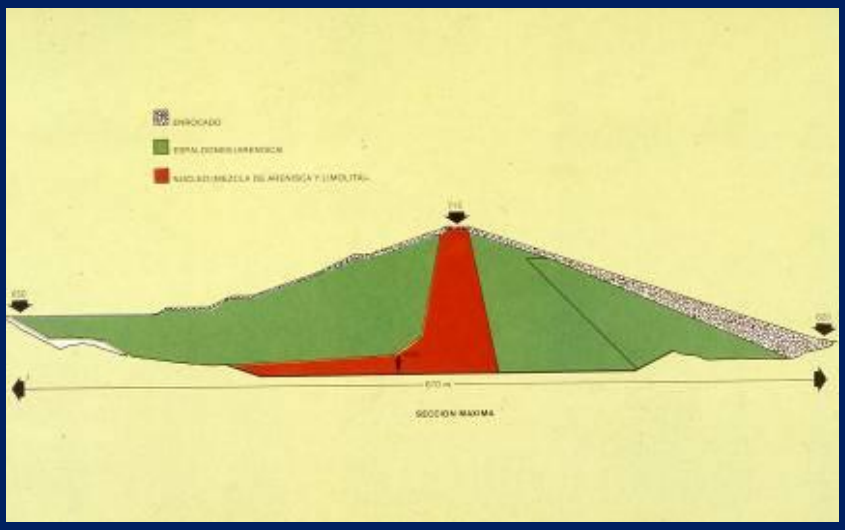

Figure 8.198 Dam cross section

8.2.10.3 Laboratory tests

The results of dam materials -sieve analysis are presented in Figure 8.199.

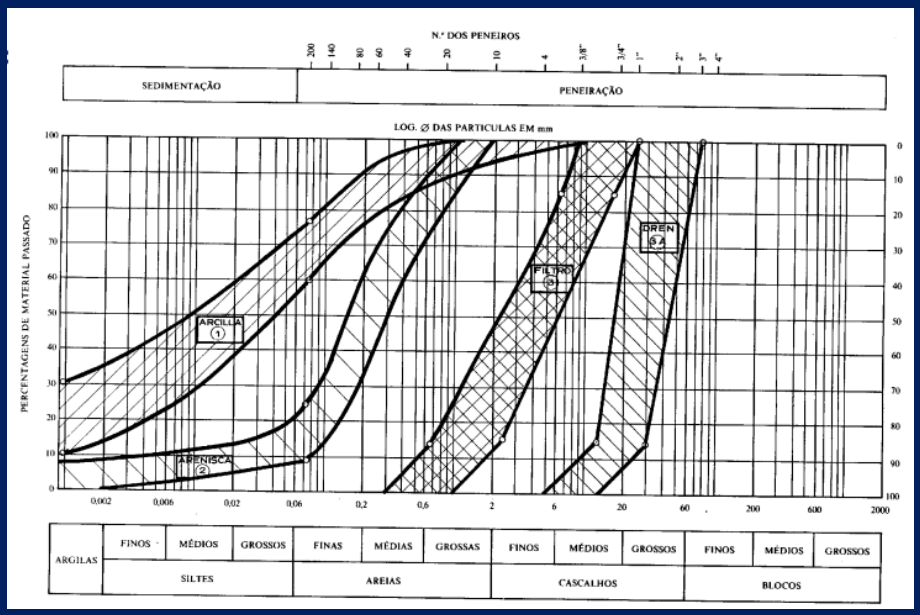

Figure 8.199 Dam materials -sieve analysis

Table 8.33 Summary of laboratory tests

Material type	Proctor test		Atterberg Limits			Unified Classification	Borrow Pit
	Unit weight of dry soil (kN/m³)	Optimum water content (%)	Liquid Limit (%)	Plastic Limit (%)	Plasticity Index (%)		
Core	16.3	22.1	71	37	34	OH	El Porvenir
Core	17.2	20.0	57	31	26	OL	El Porvenir
Core	18.5	16.0	41	22	19	CL	El Porvenir
Shell	17.7	10.8	---	---	---	SM	ICOS 1

8.2.10.4 Stress-Strain Analysis

Figure 8.200 presents the isolines of vertical stress for the final construction phase.

Figure 8.201 illustrates the dam deformations for the final of construction phase.

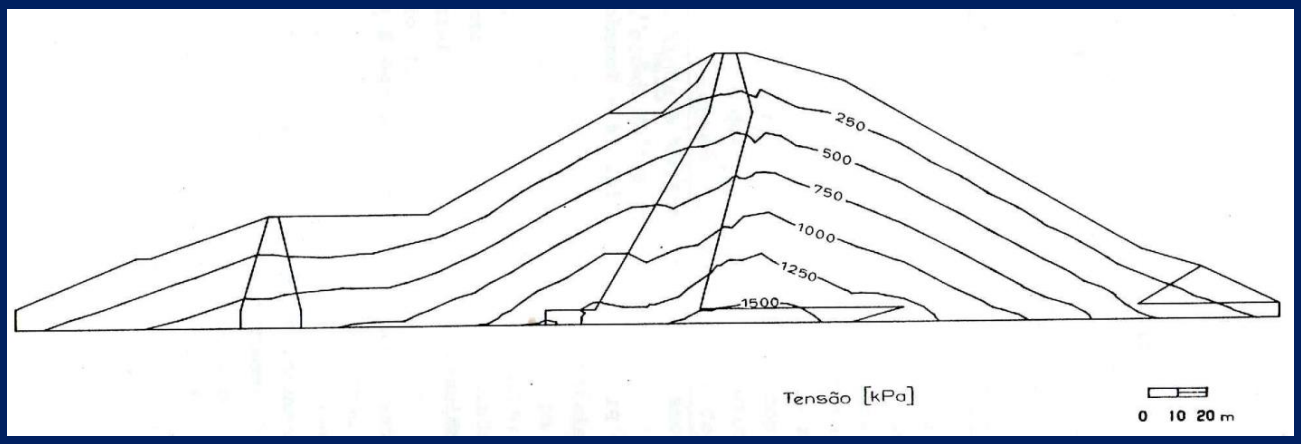

Figure 8.200 Isolines of vertical stress – final construction phase

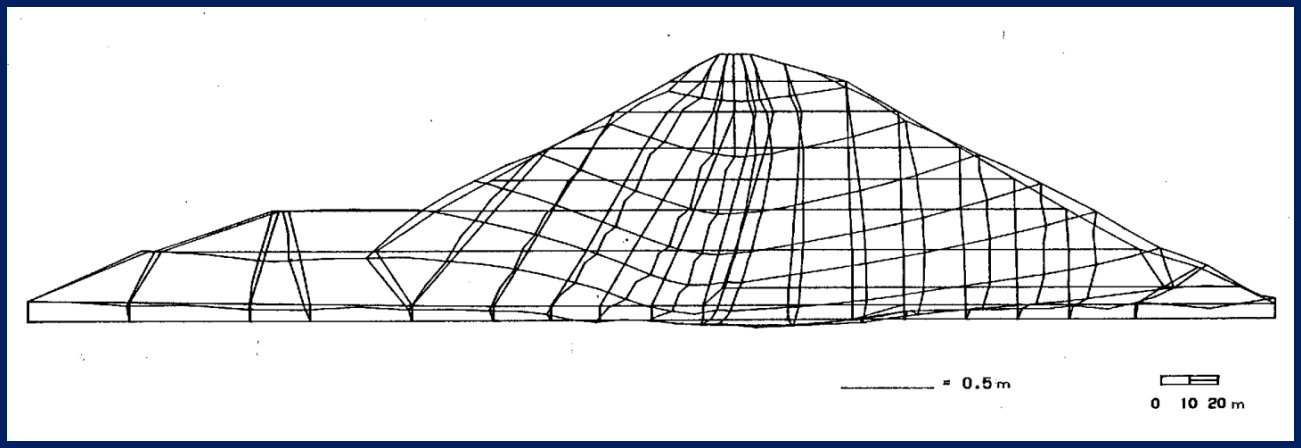

Figure 8.201 Dam deformations- Construction phase

Figure 8.202 represents the isolines of vertical stresses for the filling reservoir phase.

Figure 8.203 shows the dam deformations for the filling reservoir phase.

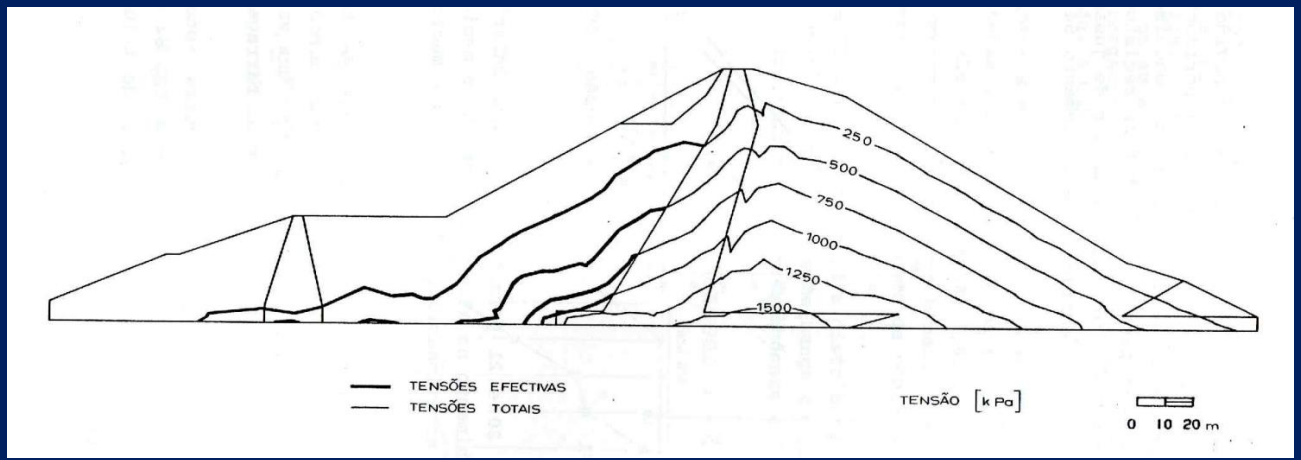

Figure 8.202 Isolines of vertical stresses- Filling reservoir phase

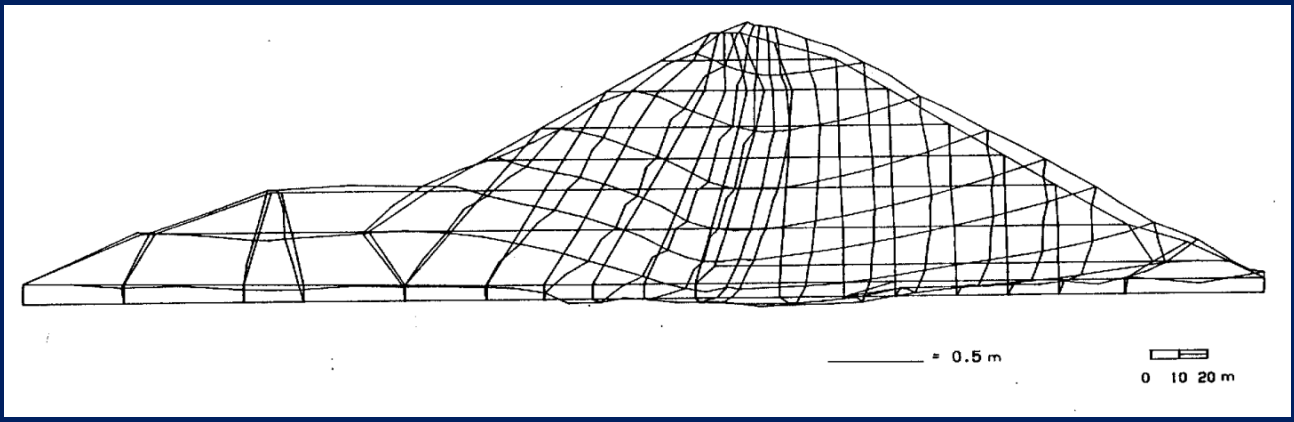

Figure 8.203 Dam deformations- Filling reservoir phase

8.2.10.5 Seepage Studies

Figure 8.204 illustrates the equipotential surfaces and Figure 8.205 shows the distribution of isobarics for the filling of the reservoir.

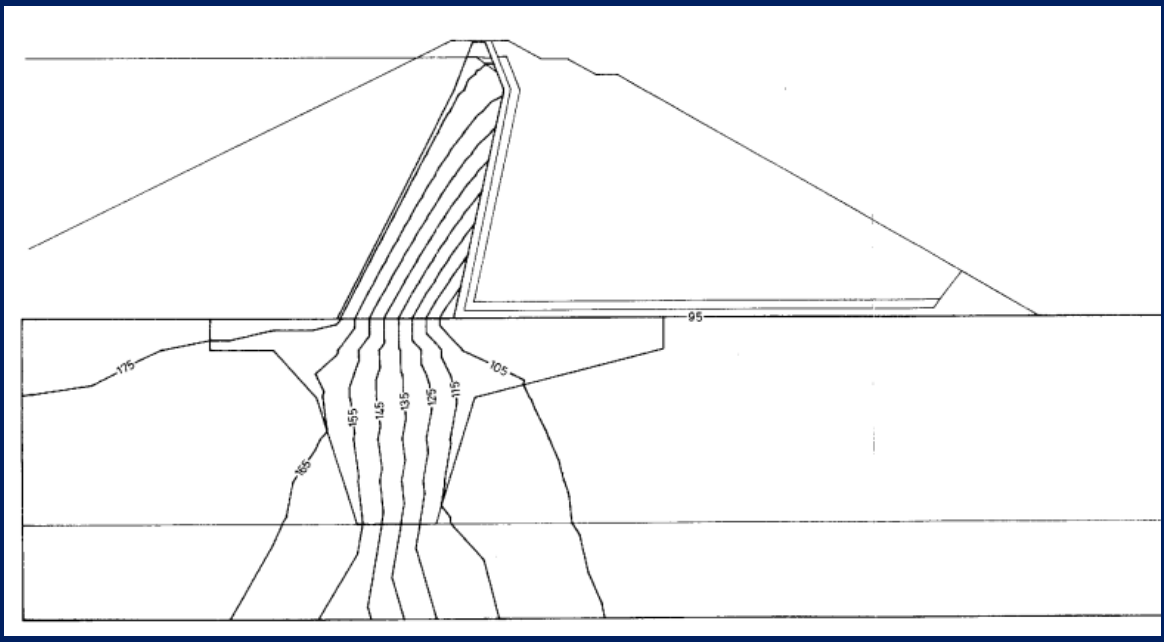

Figure 8.204 Equipotentials surfaces

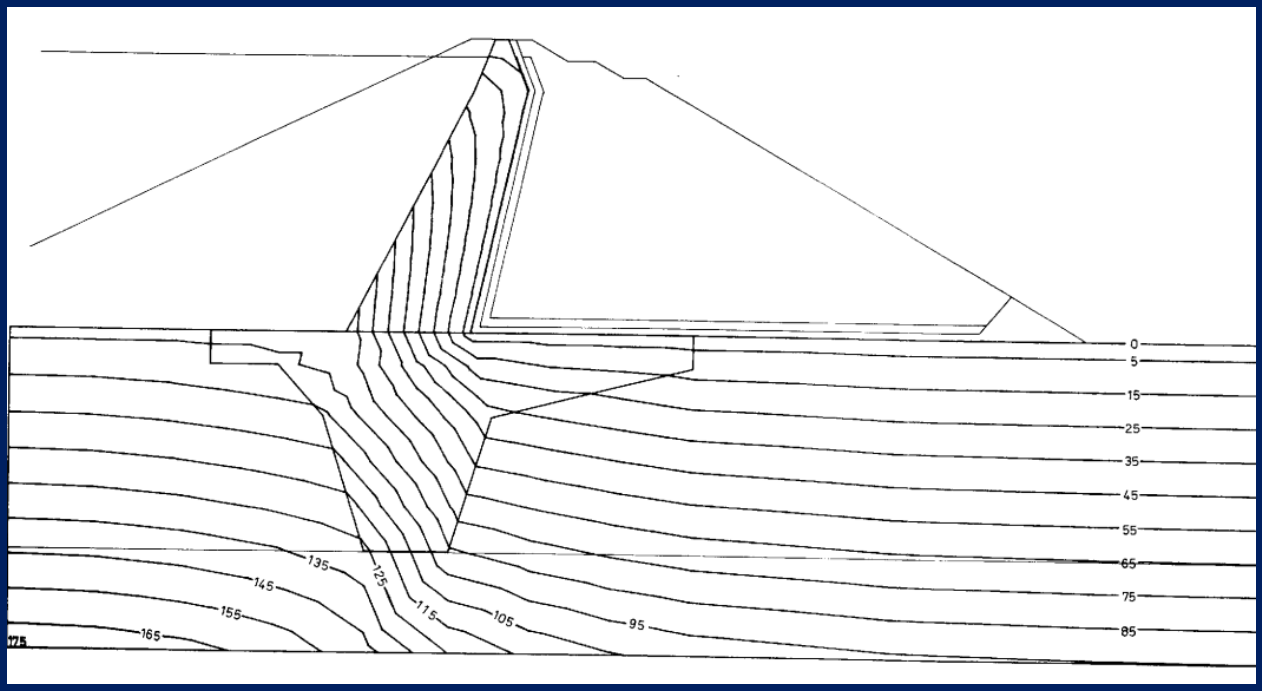

Figure 8.205 Distribution of isobarics

8.2.10.6 Seismic Analysis

Introduction

The results of the cyclic simple shear tests are presented, the definition of pre-earthquake stresses is addressed, the selection of design earthquake is described, the determination of dam seismic response is discussed and the results of the 3 D analysis are shown.

Laboratory Tests

Simple shear tests were performed in samples carefully prepared, with consolidation pressures of 200, 400 and 800 kPa and the friction angle obtained was 29.1º.
In addition, cyclic simple shear tests were performed using Geonor h-12 equipment.

Figure 8.206 and Figure 8.207 compare the results of the tests with the proposals of Seed et al. (1984) and Sun et al. (1988) for the variation of G/G_{max} with shear strain.
Figure 8.208 illustrates the results of the tests with Seed and Idriss (1970) proposal for the variation of damping ratio with shear strain.

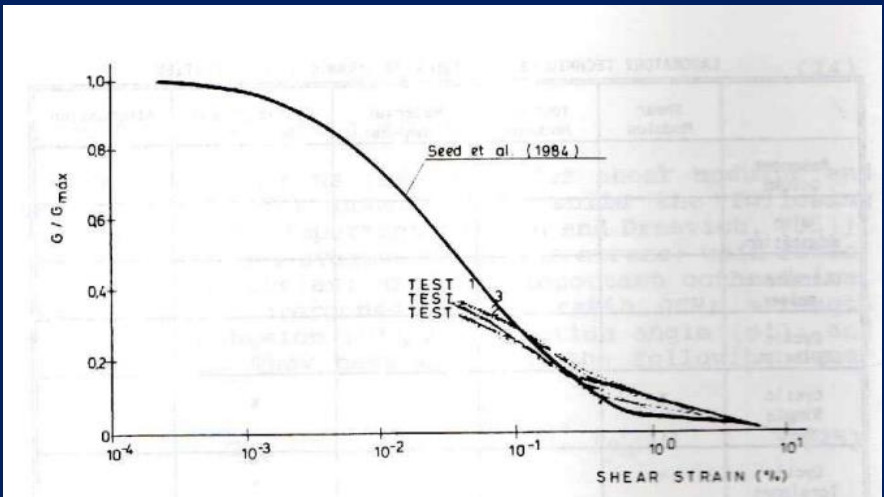

Figure 8.206 Comparison between the tests results with the proposal of Seed et al. (1984)

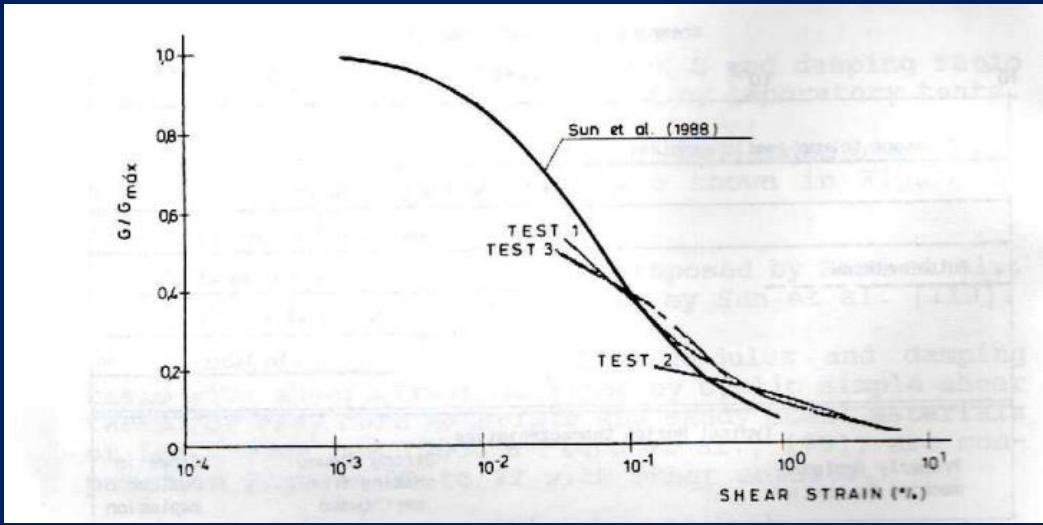

Figure 8.207 Comparison between the tests results with the proposal of Sun et al. (1988)

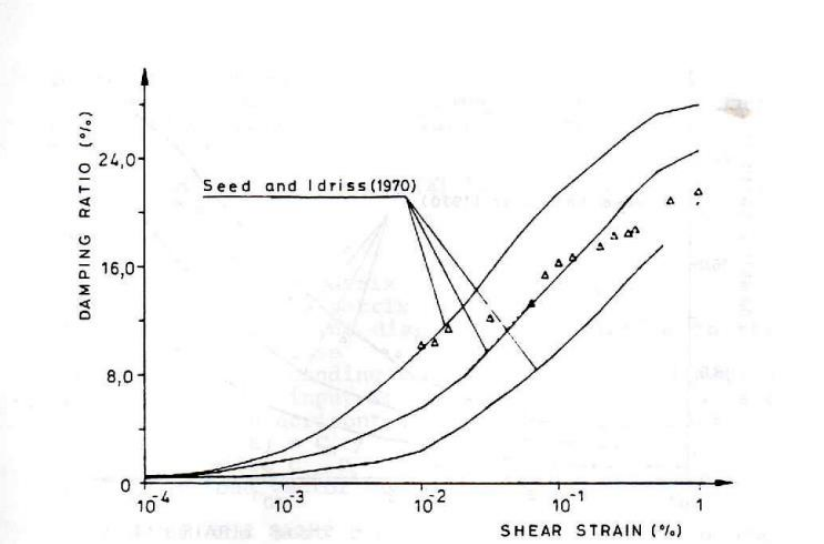

Figure 8.208 Comparison between the tests results with the proposal of Seed and Idriss (1970)

Determination of preearthquakes stresses

Table 8. 34 Summary of hyperbolic parameters for las Cuevas dam materials

Soil type Parameter	Symbol	Clay Core	Shell material		Filter	Rockfill	
			Dry	Wet		Dry	Wet
Cohesion (kPa)	C	250	110	30	0.0	0	0
Friction angle at σ_3 = 1 atm (degrees)	ϕ	20,5	35	35	51.0	51.0	49.0
Reduction in ϕ per log cycle (degrees)	$\Delta\phi$	0	0	0	0.0	5.0	6.0
Modulus number	K	840	770	468	690	720	670
Unloading-Reloading Modulus No.	Kur	4200	3900	1404	2070	3600	3350
Failure Ratio	R_f	0.78	0.725	0.772	0.590	0.63	0.62
Modulus Exponent	n	0.17	0.441	0.668	0.450	0.55	0.49
Poisson´s Ratio	G	0.36	0.43	0.47	0.14	0.40	0.3
	F	0.16	0.15	0.23	0.10	0.14	0.12
Parameters	d	9.20	9.80	13.80	27.30	1.01	0.94
Threshold Confin. pressure (kPa)	σ_{3t}	---	350	---	---	---	---
Coef. of Isotropic collap. (kPa^{-1})	ß	---	2.25×10^6	---	---	---	---

Figure 8.209 represents the 2D finite element mesh (after Sêco e Pinto, 19993).

Figure 8.210 illustrates the preearthquakes stresses (after Sêco e Pinto, 1993).

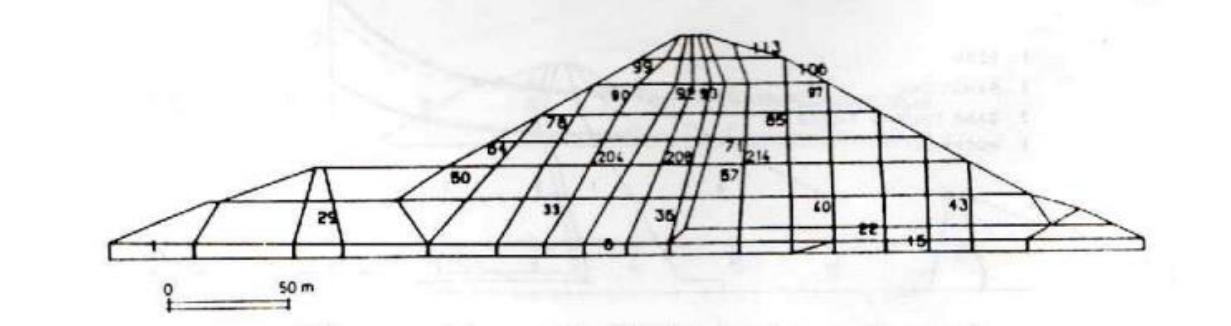

Figure 8.209 2D finite element mesh (after Sêco e Pinto, 1993)

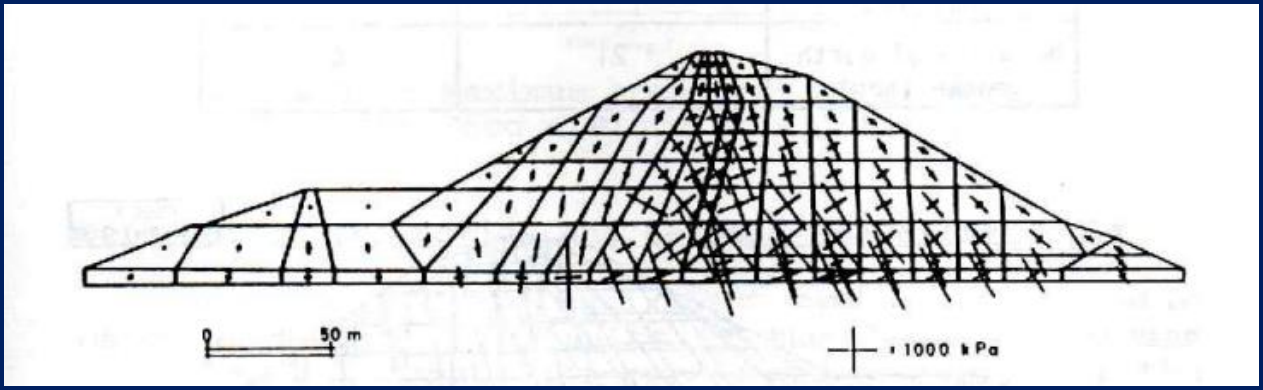

Figure 8.210 Preearthquakes stresses (after Sêco e Pinto, 1993)

Selection of design earthquakes

Las Cuevas Dam is located close to active faults of Caparo and Bocono where generation of very strong motions were recorded.

The characteristics of the main sources of earthquakes are synthesized in Table 8.35.

The maximum acceleration response in both horizontal and vertical directions for selected points located in the upstream shell, core and downstream shell for the near earthquake are presented.

The shear stress time histories for six selected elements located at the upstream shell, core and downstream shell for the near earthquake are shown.

Table 8. 35 Selection of design earthquakes

	Near Source	Far Source
Period of life (years)	100	100
Probability of exceeding the ground acceleration (%)	10	10
Ground acceleration (gal)	406	274
Duration of earthquake (seg)	21	41

Determination of seismic Response

The shear strain potential distribution is presented. It is clear that relatively high values of shear strain potential are concentrated near the surface of the upstream shell.

Since, for dams in narrow canyons, the response of the structure is of a three-dimensional nature and as the crest length to height ratio L/H=2.6 a three-dimensional analysis was performed.

The computer program DYSE52 developed at LNEC was used and the finite element model is shown. The structure was discretized in 555 isoparametric finite element (8 mode cubic element and 6 mode prismatic element) with a total of 648 modal points.

The materials that incorporate the dam were considered continuous and isotropic with the shear modulus and Poisson ratio obtained from the last iteration of the 2D dynamic analysis. A damping viscous coefficient of 10% was assumed.

The first twenty vibration modes were determined with fundamental frequencies between 1Hz and 2Hz.

The first vibration mode is shown in Figure 8. 211.

Figure 8.212 represents the shear stress time history.

Figure 8.213 illustrates the maximum accelerations response.

Figure 8.214 presents a comparison between laboratory shear stresses and equivalent uniform shear stresses (after Sêco e Pinto et al.).

Figure 8.215 indicates the shear potential distribution.

A comparison between natural frequencies computed from 2D and 3D analyses has shown that for 3D analysis the fundamental natural frequencies were 25% higher than those computed from a plane strain analysis.

It was found that a plane strain analysis of the maximum section gave values for the shear stresses that were 50% higher than those computed from a 3D analysis of the dam.

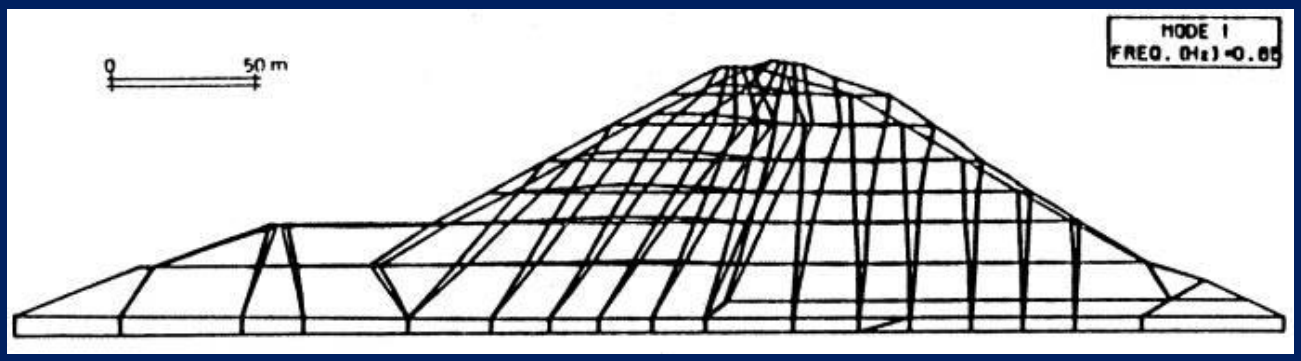

Figure 8.211 2D first vibration mode

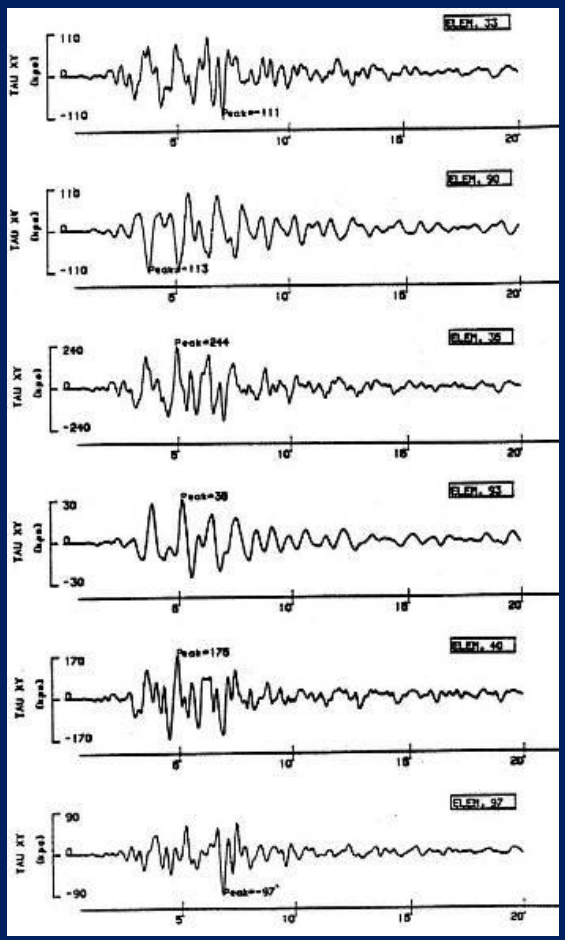

Figure 8.212 Shear stress time history

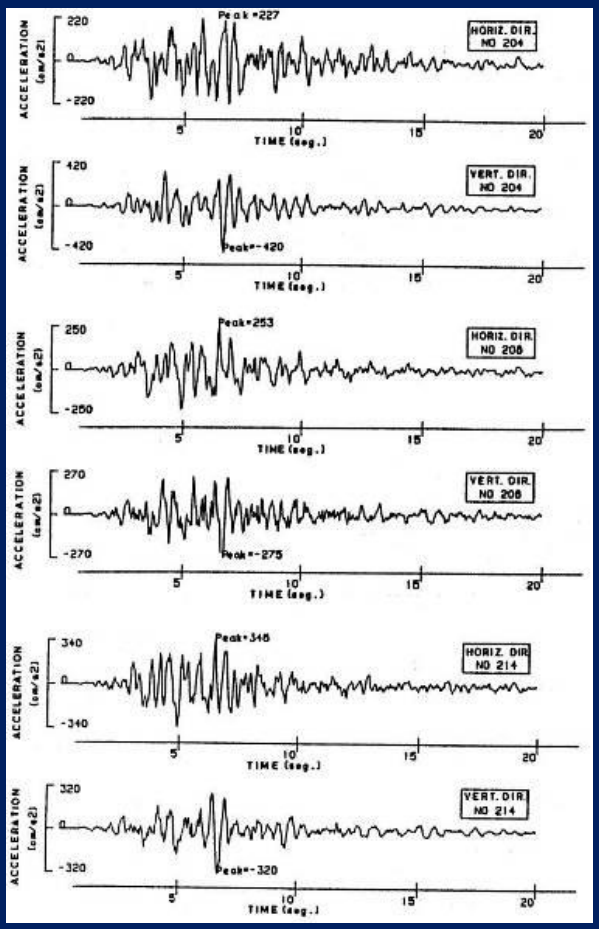

Figure 8.213 Maximum accelerations response

Deformation Evaluation and Seismic Stability

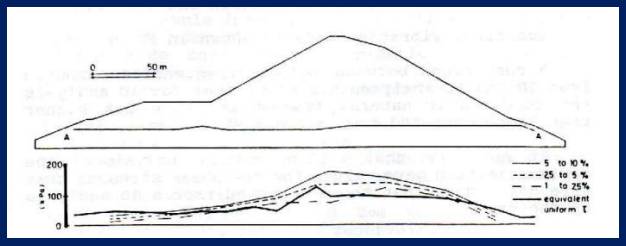

Figure 8.214 Comparison between laboratory shear stresses and equivalent uniform shear stresses (after Sêco e Pinto et al. (1990).

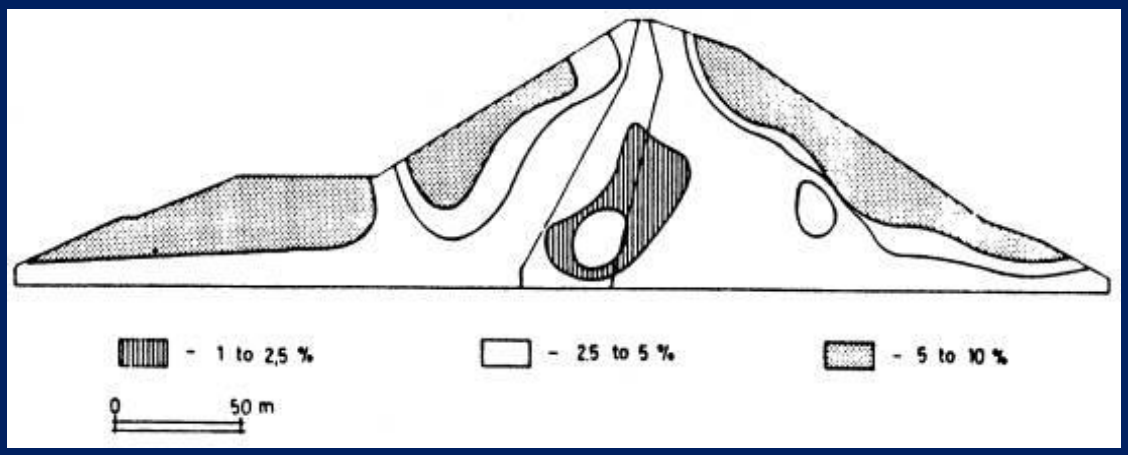

Figure 8.215 Shear potential distribution

Three Dimensional Analysis

Figure 8.216 shows the 3D finite element mesh.

Figure 8.217 illustrates the 3D first vibration mode.

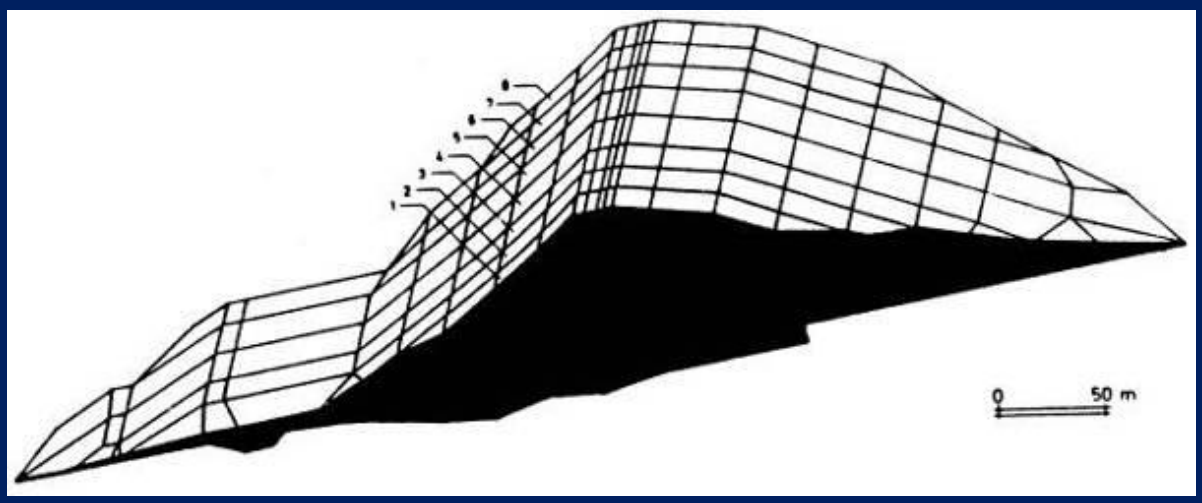

Figure 8.216 3D finite element mesh

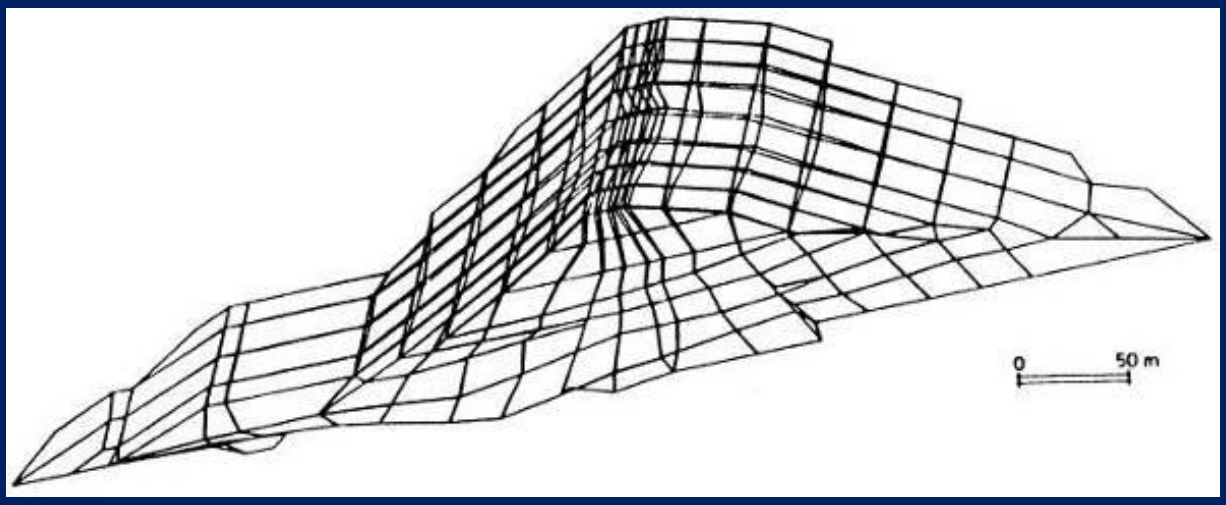

Figure 8.217 3D first vibration mode

Lesson nº 9: Dams located near faults can exhibit a good behaviour for strong motions with only minor cracks.

The identification of tectonic mechanisms, location and description of faults and estimation of fault activity play an important role to assess the involved dam risk.

Note: The studies of the dam were performed by a multidisciplinary LNEC team co-ordinated by Pedro Sêco Pinto. João Marcelino has collaborated in the static analysis and J. Bile Serra and Laura Caldeira in the dynamic studies.
So, this project, in spite of not belonging to my private consultant activity, is included due to his interest.

8.2.11 Case History nº 10 - Odelouca Dam

8.2.11.1 Introduction

Odelouca dam layout is presented, the geotechnical studies are addressed, the experimental fill is described, the execution design is analyzed, the dam quality control is introduced and the instrumentation plan is shown.

8.2.11.2 Dam Layout

Dam profile

The dam has a length of 1005 m and the spillway is located in the right rive.

The maximum dam height is 56.5 m.

Figure 8.218 represents the dam plan.
Figure 8.219 illustrates the longitudinal profile.
Figure 8 220 presents the dam profile.
Figure 8.221 shows the material sieve analysis.

The dam profile is zoned with a core of residual schists and the shells incorporate schists materials. There is in the upstream shell a section composed by rockfill materials type grauvaques. There is a filter material in the interface between the core and the downstream shell.
The volume of the materials is 1.89 million m3.

The dam crest is located at level (794,00), with a width of 10 m. The upstream slope is ½.25 and 1/2 (V/H) and the downstream slope is ½.2 V/H.

The levels of maximum flood (NMC) and the filling reservoir (NPA) are, respectively, 791.81 e 790.00.

The impervious core is symmetrical and reaches the maximum level of (793.00), where exhibits a width of 6.0 m. the upstream slope and the downstream slope has an inclination of 1:0.3.

The drainage system incorporates a chimney filter, a longitudinal drainage trench to receive the water that percolates trough the dam and the foundation, by four transversal trenches, by a drainage blanket in contact with the downstream shell and by rockfill material at downstream toe.

The cofferdam shells, the internal zone of the upstream shell, the downstream shell are composed by schist materials.

The external zone of the upstream shell is composed by rockfill material.

The chimney filter at downstream has a thickness of 3.0 m.

The upstream shell is protected by rockfill material 0.9 m thick above level (770) and 0.40 m thick beneath this level. (759,50).

The dam integrates an upstream cofferdam with the crest at level and an exterior berm 8.5 m width.

Taking into account the conditions of the foundation, it was considered important to incorporate a grounting gallery.

The foundation treatment will be executed in two phases, the first phase with a treatment of consolidation and contention and the second phase, after the construction of the grouting gallery, the injection curtain.

The grouting gallery has a length of 647 m with a section of maximum height of 3.0 m.

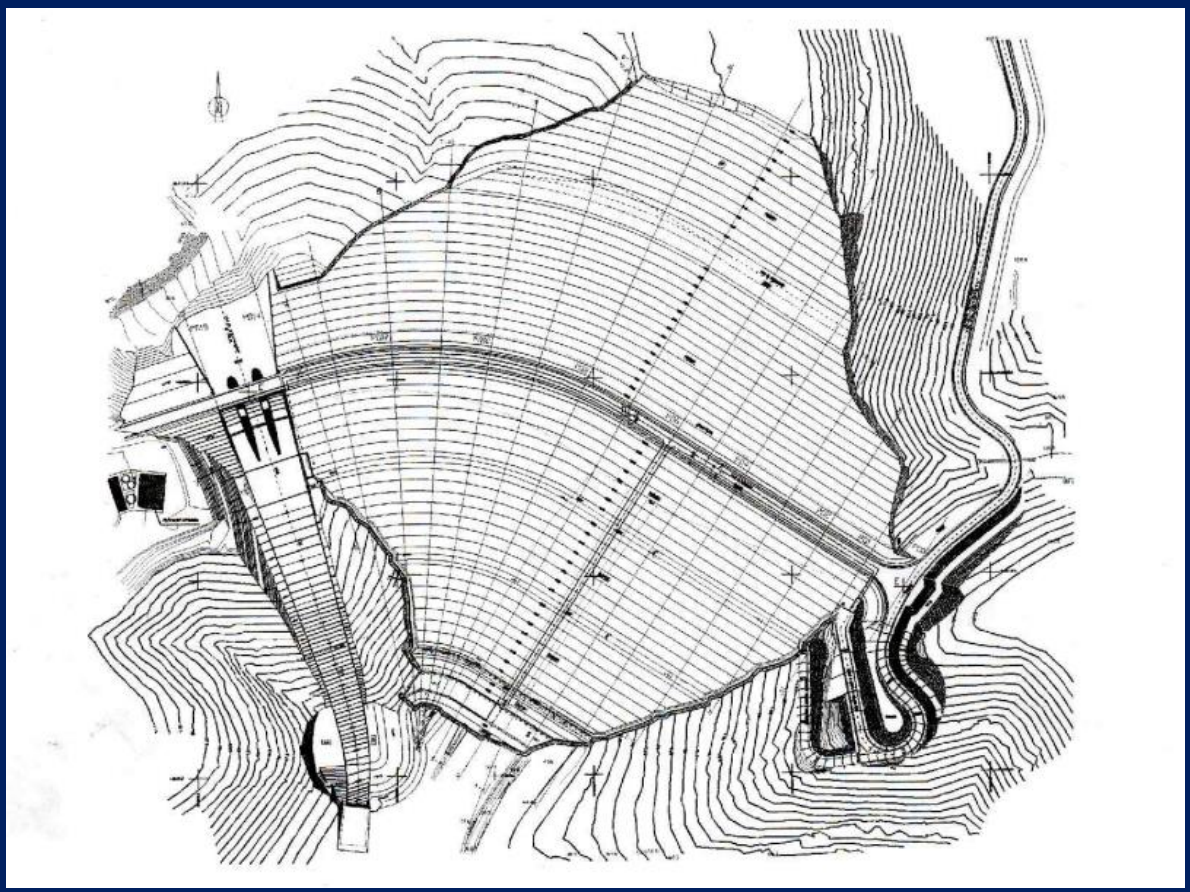

Figure 8.218 Dam plan

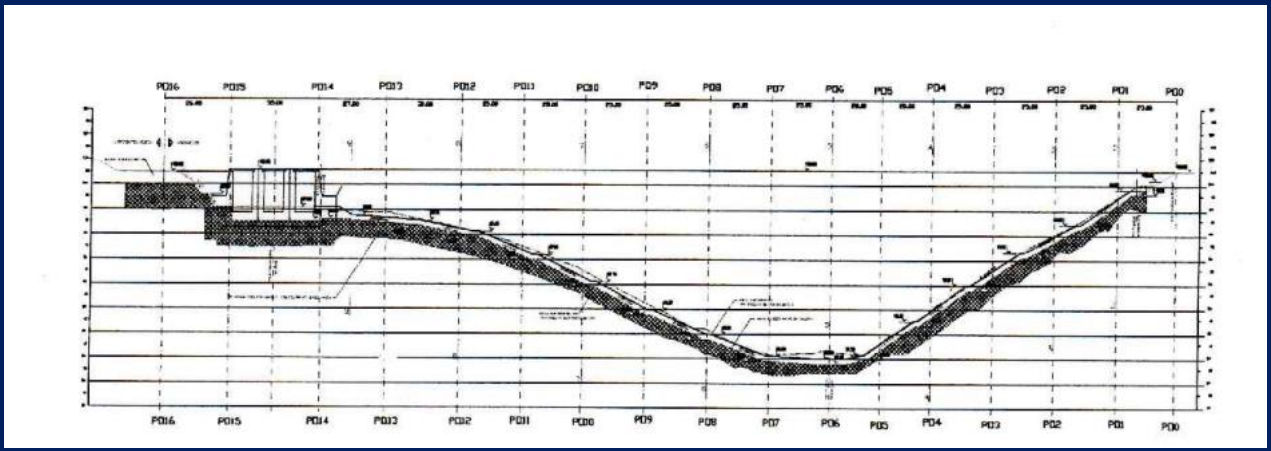

Figure 8.219 Longitudinal profile

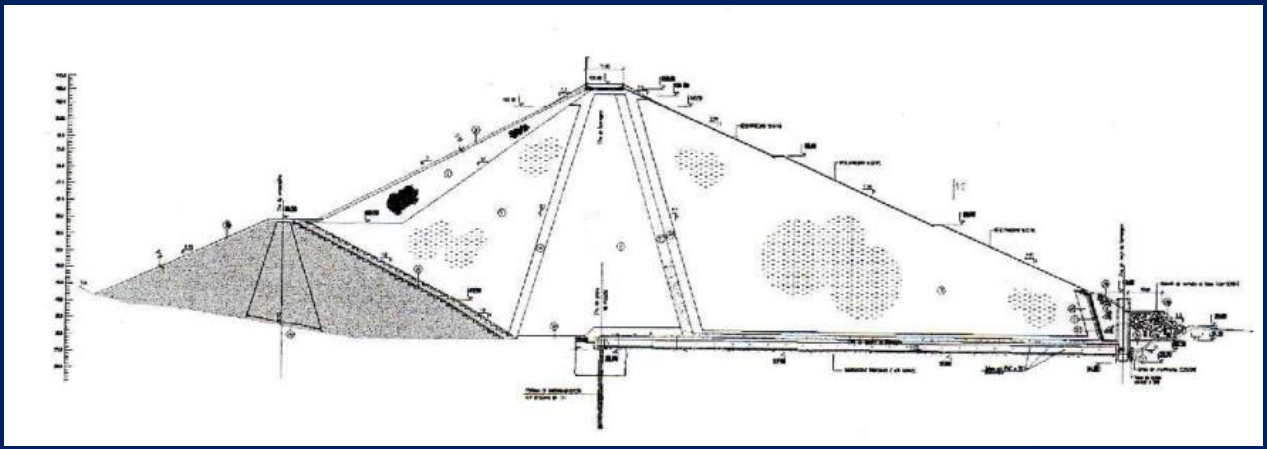

Figure 8 220 Dam profile

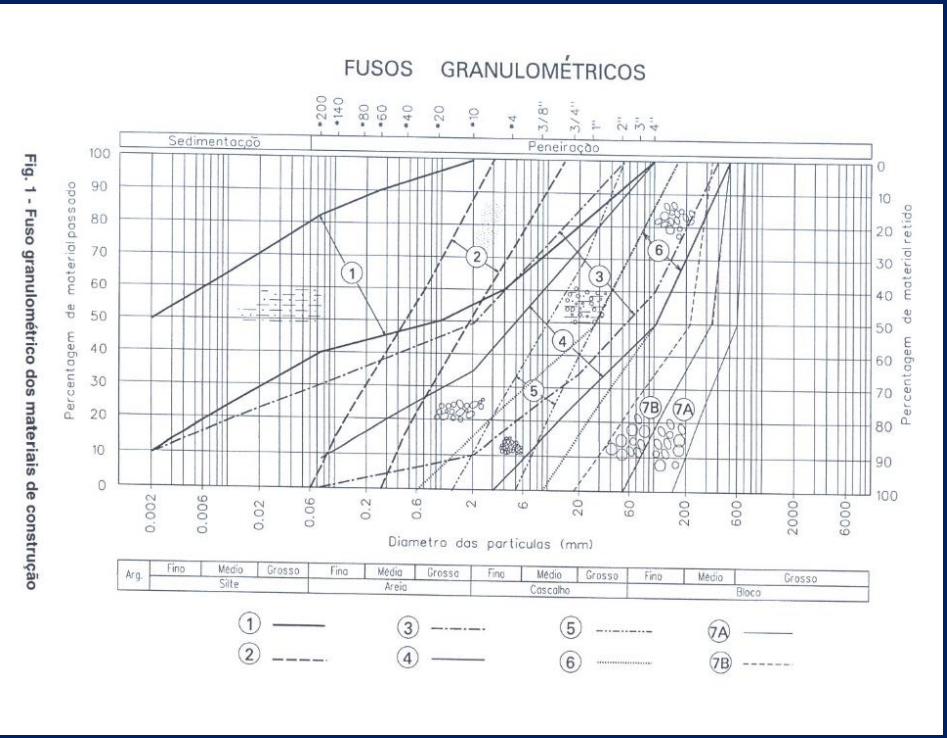

Figure 8.221 Material sieve analysis

8.2.11.3 Geological and Geotechnical Studies

The dam bedrock is from the Series Carbonic for west Algarve essentially composed by filades and metagres interstratificated with Philonian rocks due to the intrusion of Monchique formation. It is intensively tectonized with joints until high depths. The weathering develops to depths between 10 m to 20 m.

The xistosity is N-S, 40ºE,

The principal families of joints are shown in Table 8.35:

Table 8.35 Principals families of joints

Rive	Family	Attitudes of joints

Left	F1	N 47º E, 60º NW
	F2	N 24º W, 72º WSW
	F3	N 66º W, 72º NNE
Right	F1	N 56º E, 65º NNW
	F2	N 14º E, 44º WNW
	F3	E - W, 68º S

The fracturing reaches depths from 15 to 20 metros, and exhibits F_3 and F2 to depths of 30 m.

The permeability tests exhibit high adsorptions until depths from 25 m to 35 m.

So, the dam project proposes a contention curtain with 10 m to 15 m depth, an impervious curtain from the longitudinal gallery.

For the most critical zones inclined boreholes are recommended.

In the dam site and reservoir there are schists materials.

The river valley is fulfilled by fine alluvial materials and also gravel materials grauvaques and sienites.

For the dam core materials with a percentage of fines higher than 40 % and plasticity index between 8% to 25% are recommended.

For the shell materials were used the residual materials of schist and after the compaction the percentage of fines should be less than 30%.

For the determination of mechanical properties of core materials and shell materials triaxial tests were performed.

Also, the quarry of Nave was identified for the materials of the superior part of the upstream shell.

The mechanical and the hydraulic properties of the different material that integrate the dam body are summarized in Table 8.36 and in Table 8.37.

8.2.11.4 Experimental Fill

Figure 8.222 to Figure 8.229 illustrate several details related with construction of the experimental fills and testing.

Figure 8.230 and Figure 8.231 present dam slope views.

Materials 1(core) and 3 (shell) – experimental fills

- A zone near the dam with 30 m long and 20 m width, divided in 4 sections, with 5 m each was selected.

- The materials were previously prepared in the borrow pits.

After the spreading and humidification each of the four sections were compacted following the procedure:

i) Material 1

W = Wop

Layer with 0.20 m thick after compaction, sections 1, 2, 3 and 4 with 6, 8, 10 and 12 passes.

ii) Material 3

W = Wop

Layer with 0.40 m thick after compaction, sections 1, 2, 3 and 4 with 6, 8, 10 and 12 passes.

- For each section with a defined thickness, water content and number of passes, sieve tests, 6 unit weight tests (three tests in 2 depths) were performed.

- The operations were repeated with a water content for the soil of Wop +2,0%.

- The operations were repeated with a water content for the soil of Wop - 2,0%.

The previous operations were repeated for the following thickness:

i) Material 1

Layers with 0.30 and 0.40 m thick.

ii) Material 3

Layers with 0.50 and 0.60 m thick.

The analysis of the results will allow the optimization of the number of passes and the thickness of the layer.

Undisturbed samples were taken from the experimental fills to perform triaxial tests with measurement of the coefficient of permeability.

Material 4

- A zone near the dam with 30 m long and 20 m width, divided in 4 sections, with 5 m each was selected.

- The materials were carefully spready with a bulldozer to avoid segregations.

- The rockfill material was saturated with more than 150 l/m³.

After the spreading and humidification each of the four sections were compacted following the procedure:

- Layer with 0.50 m thick, sections 1, 2, 3 and 4, with 4, 6, 8 and 10 passes.
- Layer with 0.60 m thick, sections 1, 2, 3 and 4, with 4, 6, 8 and 10 passes.
- Layer with 0.70 m thick, sections 1, 2, 3 and 4, with 4, 6, 8 and 10 passes.
- For each layer macro tests for the definition of dry density, water content and sieve analyses, with a minimum of 2, were performed.
- For each layer bench marks were installed to assess the correlation between the settlements and the number of passes.
- The analysis of the results will allow the optimization of the number of passes and the thickness.

- For each layer and number of passes, 6 plate load tests (plate 0.76m) to define the elasticity modulus (load and unload) and sieve analyses were performed.

Figure 8.222 Dumping the material 4

Figure 8.223 Placement of the material 4

Figure 8.224 Compaction of the experimental fill materials

Figure 8.225 Determination of the rockfill grading – material 4

Figure 8.226 In situ density tests

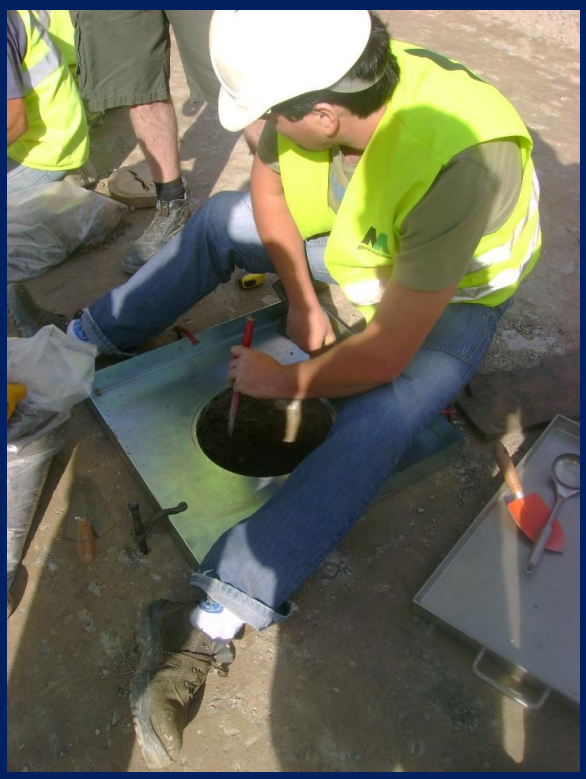

Figure 8.227 In situ density by the sand cone

Figure 8 228 Sand cone test

Figure 8.229 Open trench

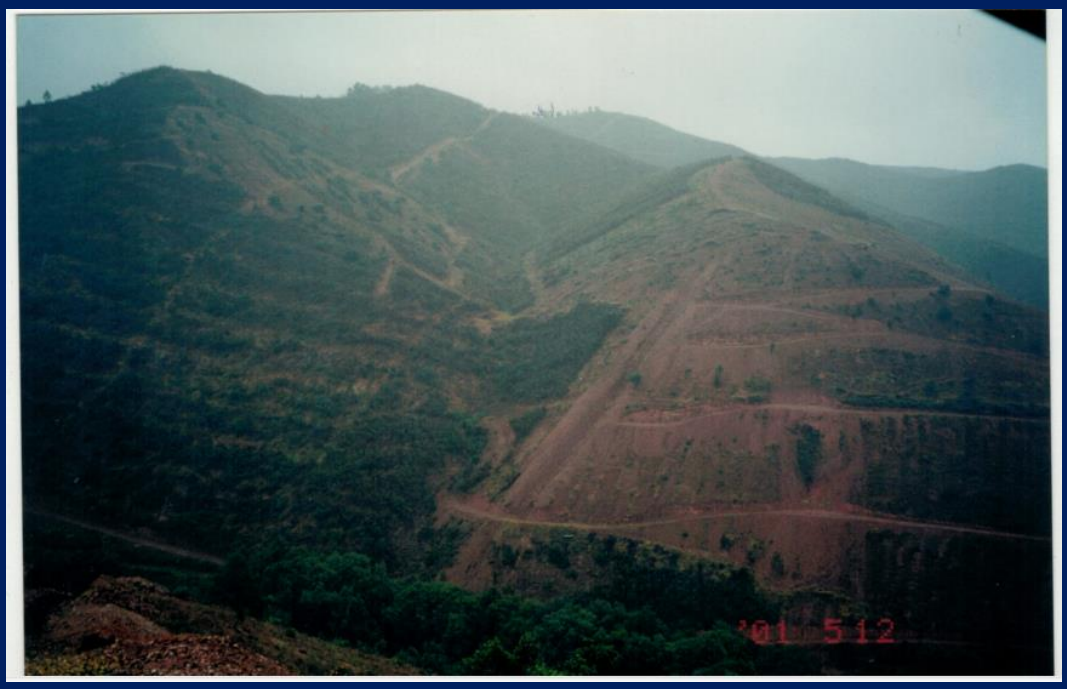

Figure 8.230 Slope view

Figure 8.231 Slope view

8.2.11.5 Construction Issues

The fills quality control of rockfills materials has the purpose to calibrate the values of shear strength, modulus of elasticity and coefficient of permeability considered for the design parameters.
The tests for the determination of unit weights, sieve analysis (definition of percentage of fines) are an indirect methodology.

i) Mechanical resistance

For the definition of the friction angle of rockfill material it is important to explore the different proposals available in the international literature.
In addition, it is important to stress that the laboratory tests performed in LNEC were in samples with an unit weight of 18, 92 kN/m3, much less (around 23%) the average unit weight value of 23,3 kN /m3 given by field tests.

ii) Deformability modulus

Based in the Classification for Rockfillls proposed by Marsal & Resendiz (1975) it can be considered a value of oedometer modulus of E= 63 MPa and a value of deformability modulus of E= 46 MPa higher than the value E= 40 MPa considered in Design COBA (2001).

iii) Permeability characteristics

Taking into account that the samples prepared in laboratory for the triaxial tests generate a percentage of fines that deposits on the base of the sample, the values of obtained coefficient of permeability of magnitude of 10^{-5} m/s are certainly less than the real values.

The values of the obtained in situ coefficient of permeability are doubtful, as there is no correlation between the values of percentage of fines and the values of coefficient of permeability.
.

iv) Unit weight values

The results of the 26 macro tests performed until 17 March 2009 the minimum value was 21,5 kN/m3 and the maximum values was 24, 1 kN/m3, and the average values was 23,3 kN/m3.
All the obtained values are higher than the value 21,5 kN/m3 defined by ADA/Supervisor, and the percentage of rejections is less than 4%.

v) Void ratio

From the 23 tests performed it was concluded that the lowest value was 9.8 and the highest value 24.8 and the average value was 17.6.

vi) Percentage of fines

From the 23 tests performed to determine the percentage of fines (percentage passing at sieve ASTM 200) the lowest value is 3,1 % and the highest value is 6,7%, with na average value of 4,66% (50% less than the maximum value of 8%).

vii) Fragmentability and degradability tests

The maximum values of FR= 2.5 and DG=1.2 were defined by the Supervisor without a solid background and are much less than the French Practice that considers a value of FR<7 for rocks and a value of DG<5 for rocks.
Nevertheless, the tests results satisfy the values defined by the Supervisor.

In summary: It is difficult to understand ADA/Supervisor statement that the material 4 from borrow pit 6 is of less quality the material defined in the Design *(COBA, 2001) and so the cost should be less.*
This statement is not adequately supported taken into account the results of the tests referred above.

Analysis of the situation

Difficulties during the technology control and determination of the water contents of the material.

a) The determination of the superficial water of the gravel material is possible, but i tis necessary to brush and to wash the material, before drying the material in the oven. For the determination of the adsorbed water. The superficial water is the difference between the total water and the adsorbed water.
b) With the method of Donaghe very often ct of the material was dry, but after the application of the method and the corrections the results were showing a wet situation, i.e. the opposite situation.

The Owner gave the instructions to use LNEC recommendations, but with this proposal the situation was inverse, i.e. the layers were exhibiting a situation of wet material, but after the corrections the final result was giving a dry material.

Conclusion

It is important to stress that these TOT materials should exhibit values of percentage retained in sieve ¾ of ASTM between 30 to 55%,
Following the Construction Specifications "the degree of compaction should be a minimum value of 95% of Proctor value to be determined by the Supervisor. The next layer could only be placed with the approval of the last layer.

For the best use of the excavation materials and the available materials located in the vicinity of the dam, the Specifications have assumed for the TOT a percentage of material, retained in sieve 3/4" of ASTM, that could reach values of 65 %.

Dam Portuguese Code

Construction Specifications

Article 61º - Construction Control
For soils and rockfills materials compaction quality control tests should be performed, with a frequency defined by the Supervisor:
a) For soils, the degree of compaction and the deviation of the water related the optimum content;
b) For the rockfills, the unit weight and sieve analysis;
c) *For the filter materials the density and the sieve analysis.*

Dam Design Specification:
Article 31-Study of the Materials s-item 2.d)

Samples should be taken from the borrow pits for the study of compaction characteristics, namely optimum water content, unit weight, unit weight and energy of compaction.

All these articles are general and there is no article related the control of TOT materials.

Bureau of Reclamation Practice

Following the recommendations of Bureau of Reclamation of United States related the design, construction and safety evaluation of dams defined in the Manuals "Earth Dams" e "Design of Small Dams", the frequency for the control of TOT materials is 1 test for a volume of 5000 m3 placed in the dam.

International Practice

The current trend related the design of large dam is the total use of excavations materials and the materials available in borrow pits (with distances less than 2 Km from the dm axis), due to economic reasons (Sherard, 1984; Penman, 1985).

Taken into account the great needed volumes of materials, for example, Oroville dam in United States with, 65 000 000 m3, Tarbela dam in Pakistan, with 142 000 000 m3 and Chicoasen dam, in Mexico, with15 000 000 m3, with high rates of construction, the planning, the operation of borrow pits, the transport, the spreading and compaction of the materials placed in the dam body exhibit a dramatic change.

Following Charles (1997), in his General Report delivered for the last Large Dams Conference, in Firenzi, the layers of the materials should be thick, provided that the total compaction is guaranteed.
The compaction quality control after an adequate balance of the technical and economic aspects, should be practical, and taking into account the modern equipments of transport, spreading and compaction.

ICOLD Recommendations

The increase need for the use of rockfill materials and the recent developments related the characterization and compaction of rockfills are summarized in Bulletin nº92 of ICOLD (1993).

Portuguese Practice

In spite the great use of TOT materials in roads and highways, as well in dams, and some contributions given by LNEC, there are still limitations in the quality control of those materials.

For the control of TOT materials placed in Meimoa dam, Maranha das Neves and Veiga Pinto (1984) proposed the use of 1 D consolidation test in cells of great diameter for the definition of a correlation between unit weight, water content, percentage of gravel and deformability, as following De Mello (1982) due to the characteristics of modern compaction equipments there is no need to assess the shear resistance of rockfills materials.

The Specification E 204-1967 of LNEC defines for the maximum percentage of gravel material retained in sieve 3/4" of ASTM, the value 20%, but a maximum value of 30%, can be acceptable, following the past experience of quality control of Portuguese embankment dams.

The Seminar 249 of LNEC “Quality Control of Earth Works” considers 1 test for a volume of 1500 m3, with a minimum of 1 test for each layer.

In Meimoa dam the percentage of TOT material was between 35% and 60%, with the maximum size of 80mm, and the control was done by Proctor test.

In Azibo dam the percentage of TOT material was around 30%, with the maximum size of 50mm, and the control was done by Proctor test.

In Beliche dam the maximum percentage of TOT material was between 20% to 30%, the maximum size less than 60mm, and the control was done by Proctor test.

Related the thickness of the layers it is important to refer that in Azibo dam a layer with 0.6m thick was compacted with 3 passes of vibrator roller, in Mira dm a layer with 0.8m thick was compacted with 4 passes of vibrator roller and in Monte Rocha a layer of 0.8m thick was compacted with 4 passes.

The vibrator rollers had a weight of 12 tf.

The current trend for the control of TOT materials is the use of Donaghe and Torrey methodology.

Conclusion

The literature survey related the compaction of TOT materials, with high percentage of gravel materials, and the past experience of 50 years of dams portuguese experience gave a better insight for the quality control of shell materials (TOT) of Odelouca dam.

It was stressed for the need of revision of the existent Specifications related the control of TOT materials used for the dam construction.

Also, the frequency of the tests needs to be addressed, as for Odelouca dam, 1 test was performed for a volume of 752 m3 of the material and some situations have occurred with the performance of 2 to 9 test for each layer, following the request of the Supervisor.

Figure 8. 232 presents a dam view during the construction.

Figure 8. 232 Dam view

8.2.11.6 EXECUTION DESIGN

These analyses were performed during the dam construction and the design parameters have taken into account the information given by the experimental fills.

Dam Stability Analysis

A computer code SLOPE W was used to analyze the slope stability of the dam profiles.

It is current practice to analyze: construction phase, filling of reservoir and drawdown.

Related with the construction phase both upstream and downstream slopes were analyzed.

For the filling of the reservoir the most critical situation is related with the downstream slope.

For the drawdown the most critical phase is related with the upstream phase.

Figure 8.233 illustrates for the drawdown situation the shallow critical superficial surface.
Figure 8.234 illustrates for the drawdown situation the deep critical superficial surface.
Figure 8.235 and Figure 8.236 show for drawdown situation the shallow and the deep critical superficial surface for the rockfill permeability of shell material aggravated 5 times K= 10^{-5} m/s.

Figure 8.237 presents for the drawdown situation the critical deep surface, for the rockfill permeability of shell material aggravated 5 times K= 10^{-5} m/s, related the pseudo-static analysis with horizontal seismic coefficient of 0.10g and vertical seismic coefficient of 0.07g.

Seepage Analysis

Figure 8.238 represents the seepage analysis- finite element mesh.
Figure 8.239 illustrates the seepage analysis for the filling reservoir phase.

Figure 8.240 shows the seepage analysis for the drawdown phase.

Stress-Strain Analysis

A stress strain analysis was performed for the construction phase, filling of reservoir and steady state situation.

The purpose of these analyses was to assess the displacements, as well the stress distribution.

Table 8.36 summarizes the materials characteristics.

An elastic behaviour for the materials was considered, due to the absence of adequate stress-strain curves.

The analyses were performed using the code PLAXIS – version 7.2.

Table 8.36 Materials Characteristics

MATERIAL	Dry Unit Weight (kN(m^3))	Saturated Unit Weight (kN(m^3))	Fill Unit Weight (kN(m^3))	Cohesion (kPa)	Friction angle (0°)	Parâmeter R_u
Rockfill material	18,0	22,0	21,5	0	42	0
Shell material	17,5	21,5	21,0	0	36	0,1
Toe rockfill	18,0	22,0	21,5	0	45	0
Filtre	17,0	19,5	19,0	0	35	0
Core	17,5	21,0	20,5	10	29	0,2
Superficial Foundation	18,0	21,0	20,0	50	36	0
Intermediate Foundation	18,0	21,0	20,0	200	38	0
Deep Foundation	18,0	21,0	20,0	500	42	0

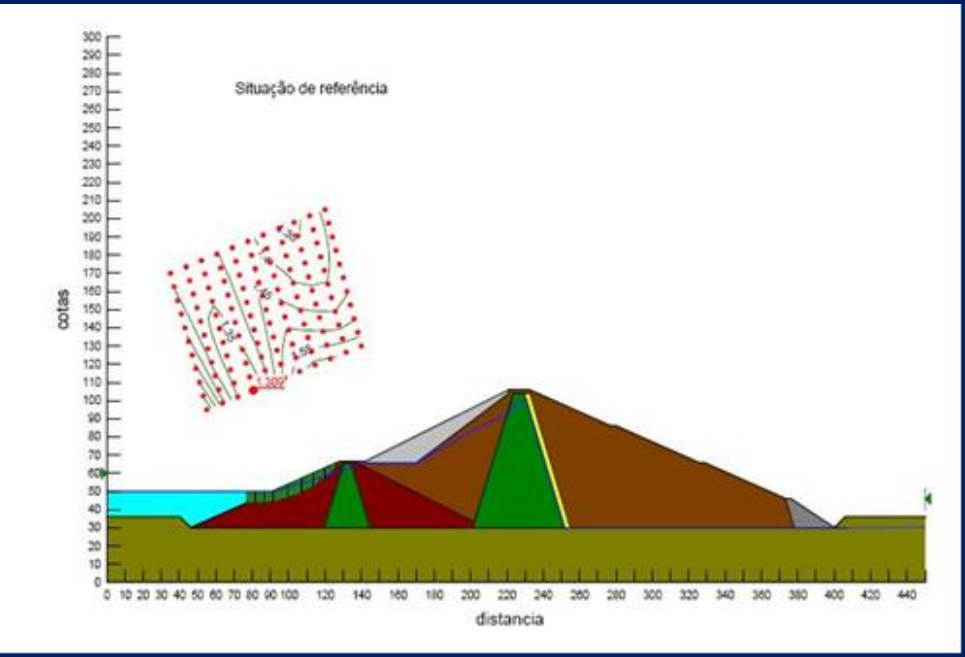

Figure 8.233Drawdown situation- shallow critical superficial surface -same conditions of the initial dam design (SIGMA code)

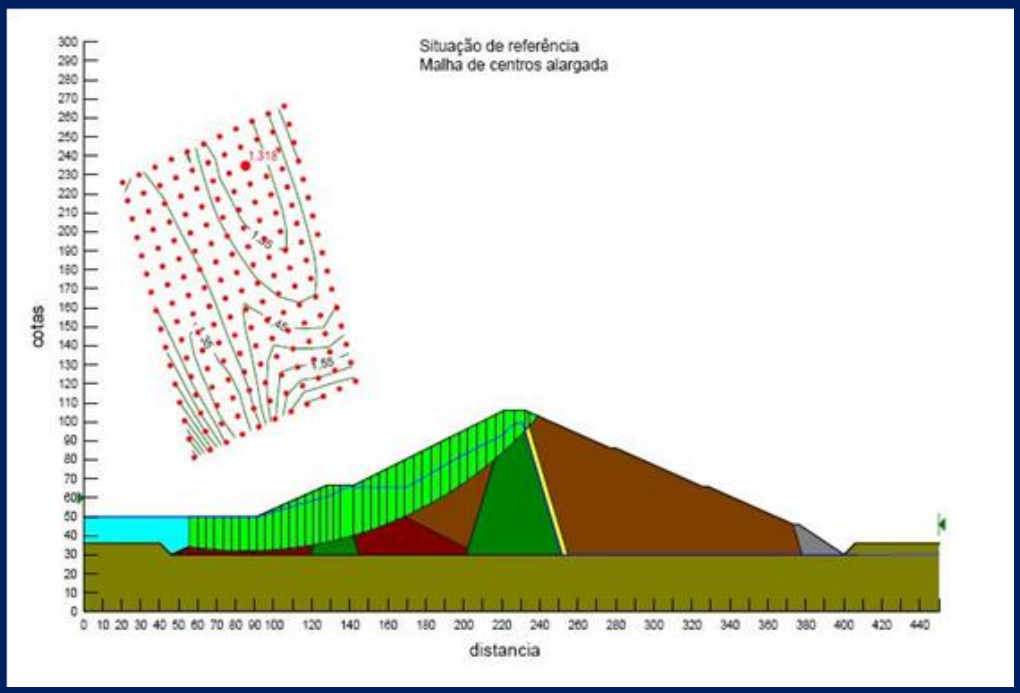

Figure 8.234 Drawdown situation- deep critical deep surface - same conditions as initial dam design (SIGMA code)

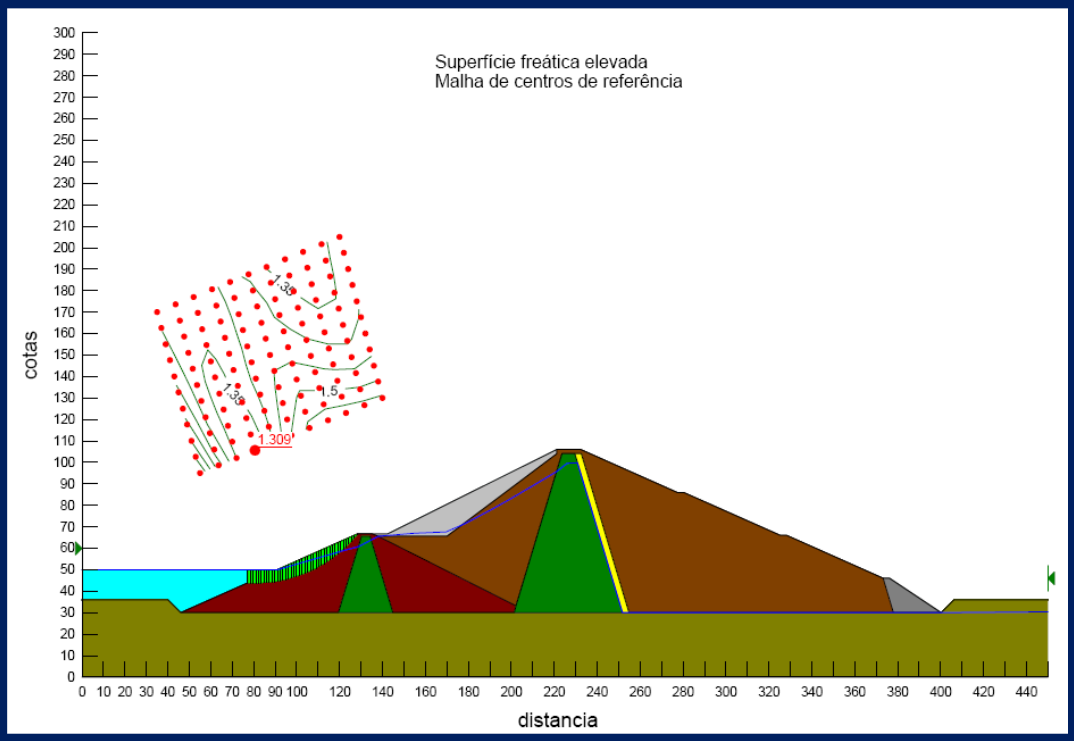

Figure 8.235 Drawdown situation- shallow critical superficial surface -rockfill permeability of shell material aggravated 5 times K= 10-5 m/s (SIGMA code)

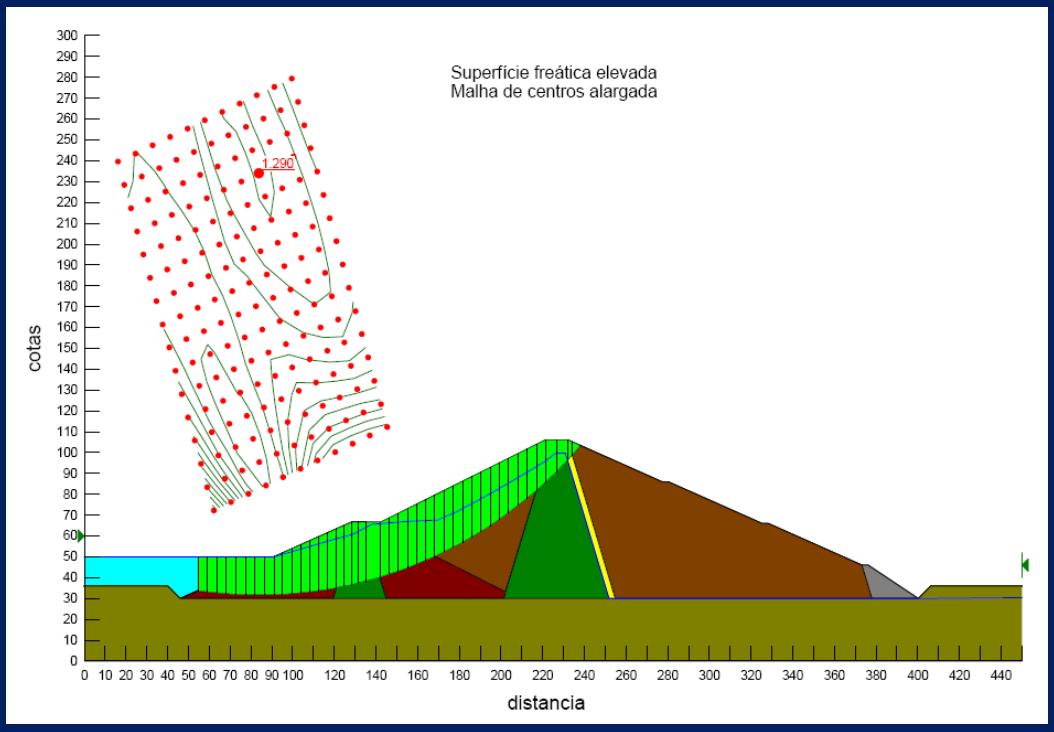

Figure 8.236 Drawdown situation- deep critical deep surface -rockfill permeability of shell material aggravated 5 times K= 10-5 m/s (SIGMA code)

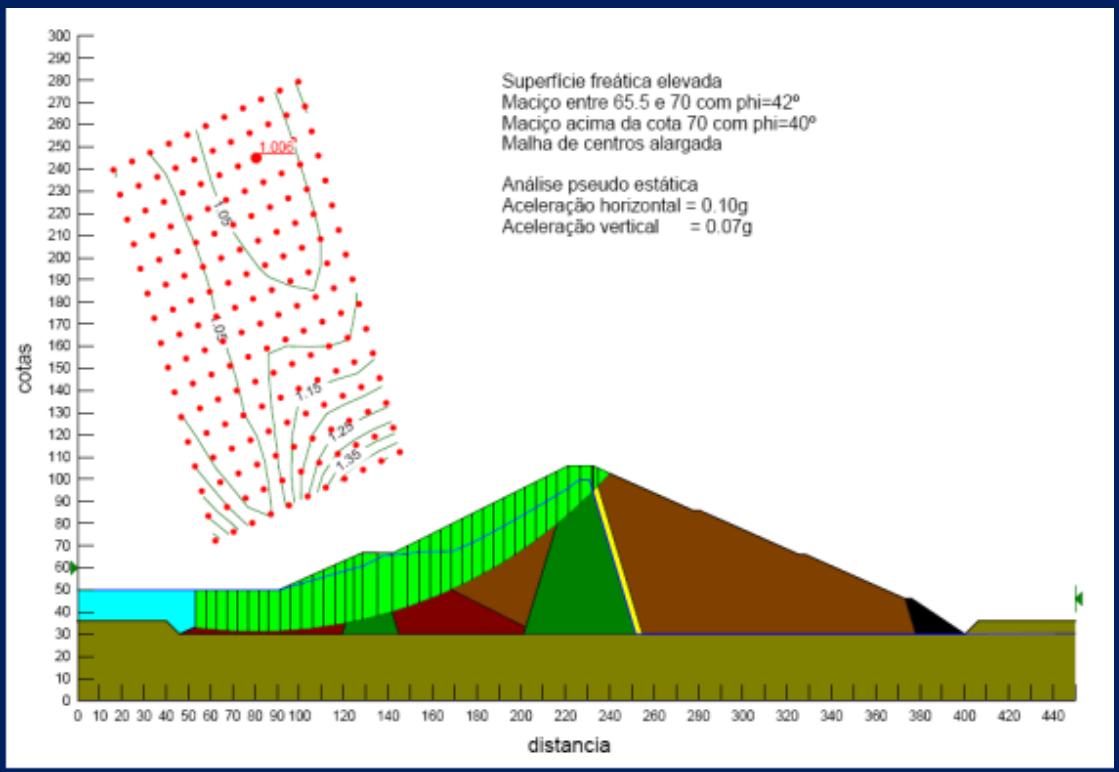

Figure 8.237 Drawdown situation- deep critical deep surface -rockfill permeability of shell material aggravated 5 times K= 10-5 m/s, pseudo-static analysis with horizontal seismic coefficient of 0.10g and vertical seismic coefficient of 0.07g (SIGMA code).

Seepage Analysis

Table 8.37 presents the coefficient of permeability of the materials.

Table 8.37 Coefficient of permeability

MATERIAL	K_x(m/s)	K_y(m/s)	
Rockfill material	10^{-5}	10^{-5}	
Shell material	$5x10^{-6}$	$5x\ 10^{-7}$	
Toe rockfill	$5x\ 10^{-5}$	$5x\ 10^{-5}$	
Filter	10^{-4}	10^{-4}	
Core	$5x10^{-8}$	$5x\ 10^{-9}$	
Superficial Foundation	$5x10^{-6}$	$5x10^{-6}$	
Intermediate Foundation	10^{-6}	10^{-6}	
Deep Foundation	10^{-7}	10^{-7}	

The seepage analysis was performed by SEEPW code.
Figure 8.238 illustrates the seepage analysis- finite element mesh.

The seepage analysis for the filling reservoir phase is presented in Figure 8.239.

The seepage analysis for the drawdown phase is shown in Figure 8.240.

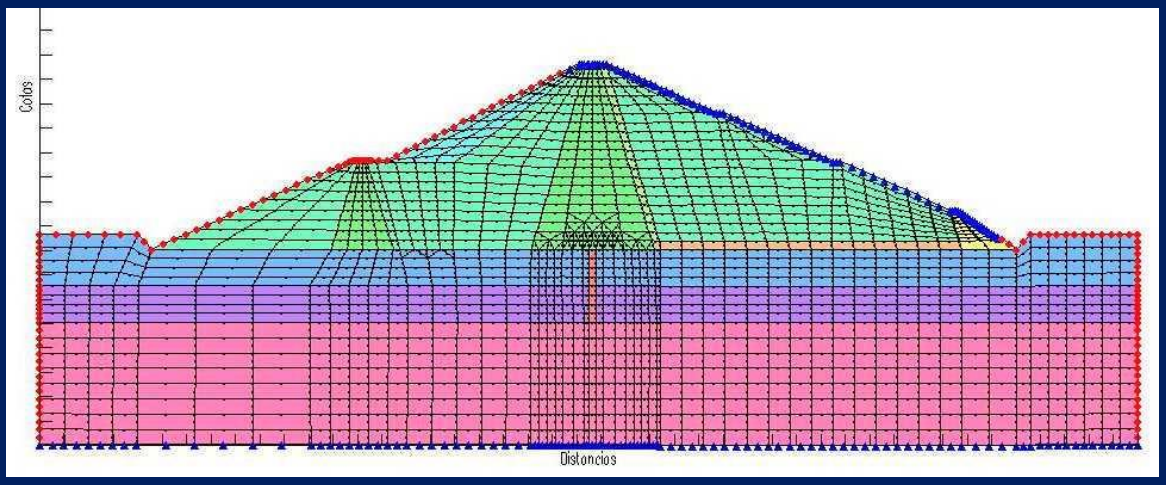

Figure 8.238 Seepage analysis- finite element mesh (SEEPW code)

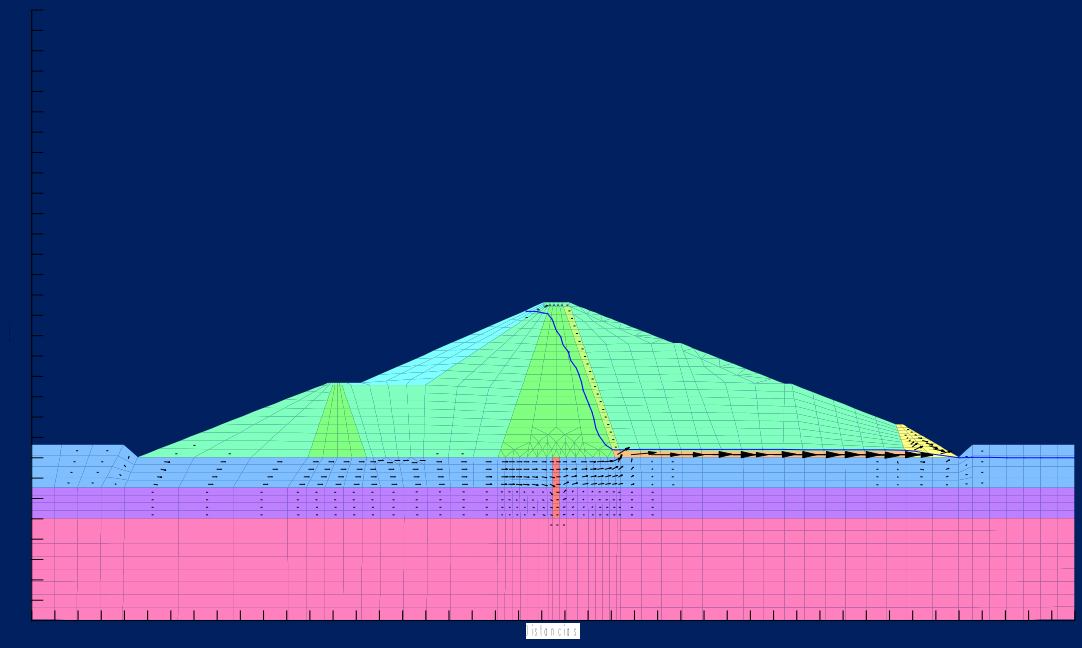

Figure 8.239 Seepage analysis – filling reservoir phase (SEEPW code)

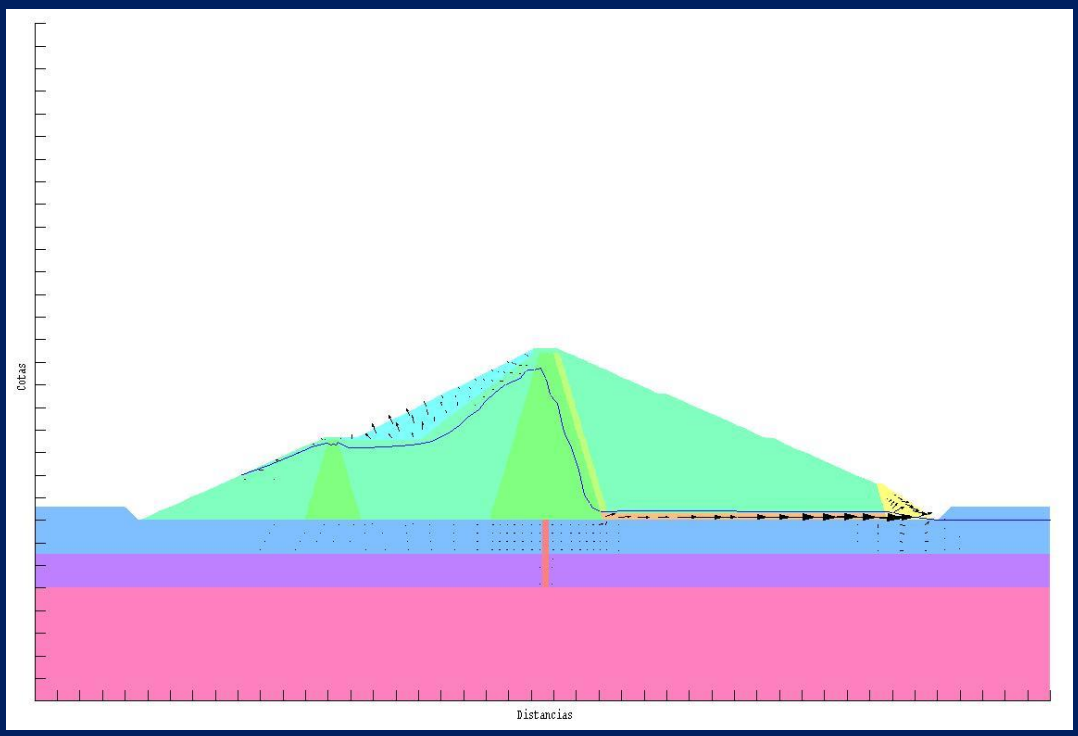

Figure 8.240 Seepage analysis – drawdown phase (SEEPW code)

8.2.11.7 Dam Quality Control

Figure 8.241 shows the clay core- water content deviations.

Figure 8.242 illustrates the clay core- histogram of degree of compactions.

Figure 8.243 presents the sieve analyses-Clay core material.

Figure 8.244 represents the sieve analyses - Filter material.

Figure 8.245 indicates the general dam view.

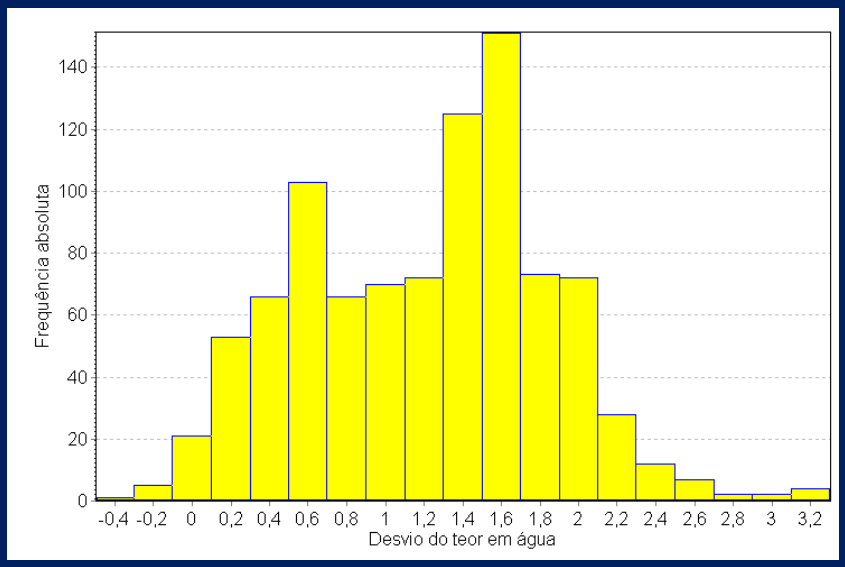

Figure 8.241 Clay core- water content deviations

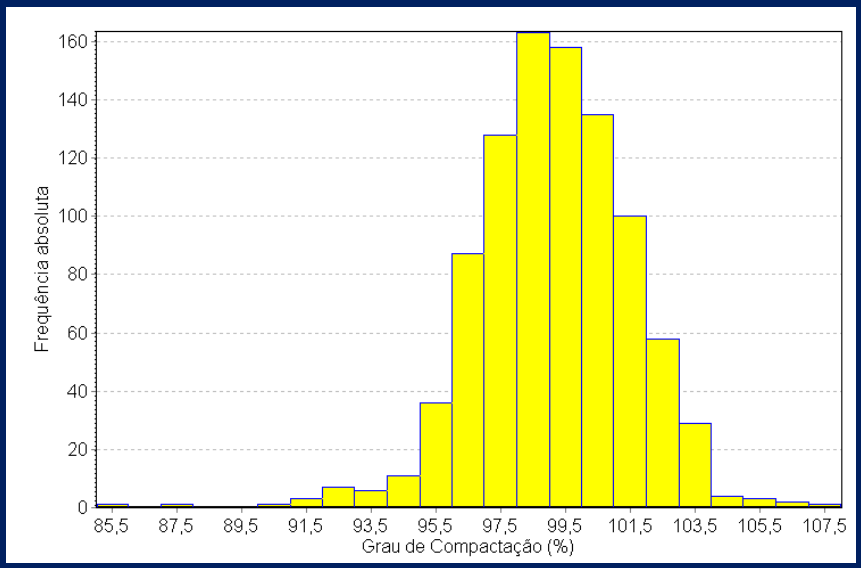

Figure 8.242 Clay core- histogram of degree of compactions

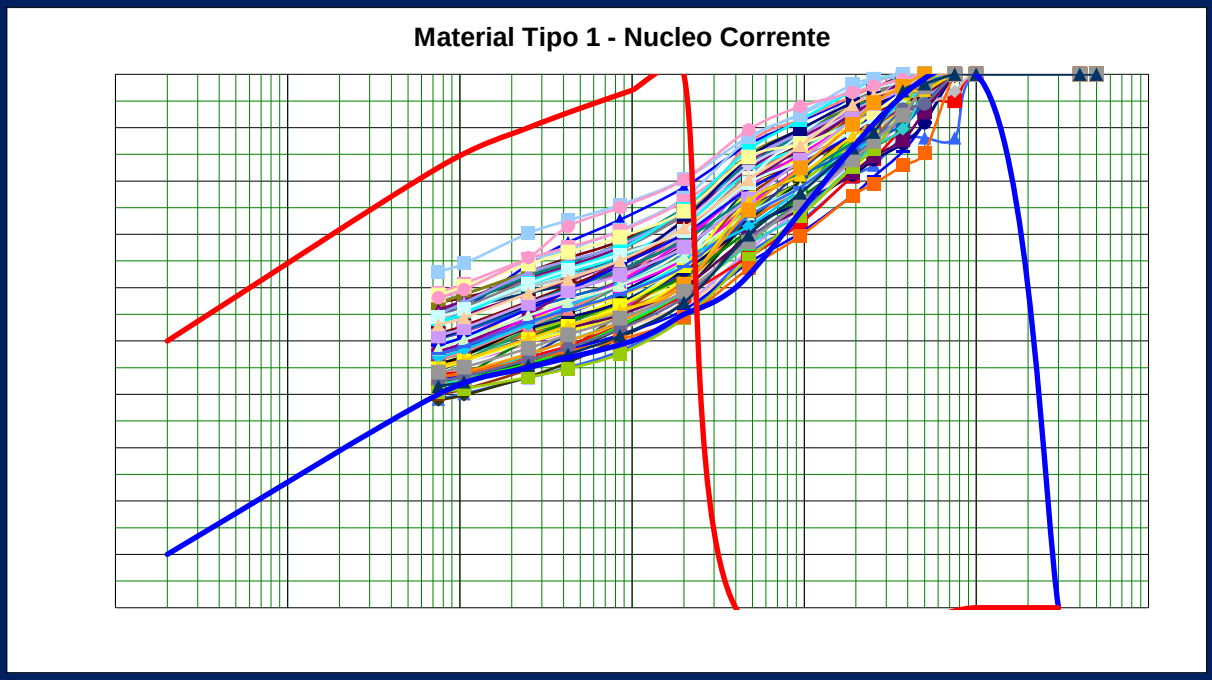

Figure 8.243 Sieve analyses-Clay core material

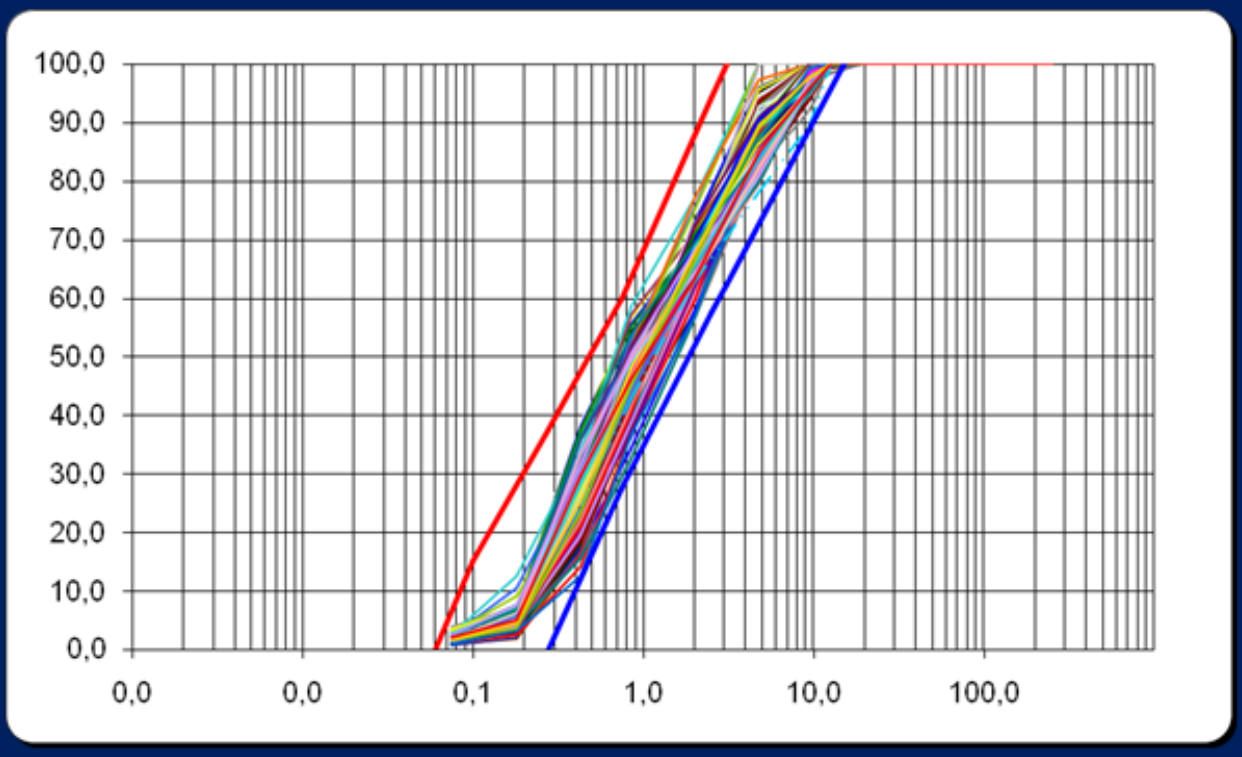

Figure 8.244 Sieve analyses - Filter material

Figure 8.245
General dam view

8.2.11.8 Instrumentation Plan

The instrumentation plan has included:

- 53 bench marks
- 44 hydraulic piezometers in the embankment;
- 45 hydraulic piezometers in the foundation
- 14 cluster of 4 total cells;
- 18 electric pore pressures;
- 6 inclinometers;
- 6 USBR devices for measurement of internal displacements;
- 4 extensometers;
- 5 accelographs;
- 1 meteorological station;
- 25 flow devices;
- Devices for measurement of reservoir level;
- Devices for measurement of temperature, wind, precipitation and evaporation;

1 central measurements station.

Lesson nº 10: Well designed and constructed dams, in spite of severe damages during the earthquakes, have not collapsed, so a good behaviour of Odelouca dam is expected.
There is a need for a better evaluation of residual strength of the clay core material, due to the increase of pore pressure during the earthquakes.

Note. The initial dam design was performed by COBA, further revision was done by Agualogus and I was involved in the dam studies and construction phase for the Consortium Teixeira Dam – Monte Adriano.

COBA (2002), Odelouca Dam. Volume III – Instrumentation Plan.
AQUALOGUS (2005), Odelouca Dam. Execution Design. Volume I – Dam.

Analysis of Embankment Dams

This set of 10 Case Histories covering the dams design and construction justifies some final comments.

The static and dynamic response analysis of embankment dams is a very complex problem. First, dams are large nonhomogeneous structures and the material is a multi-phase solid-fluid medium. Second, the behaviour of the soil skeleton is highly nonlinear, anisotropic and hysteretic. Finally, the interaction of the dam with its boundaries including the underlying foundation and the water in the reservoir further complicates the problem (Sêco e Pinto et al., 1995).

i) For dynamic analyses of embankment dams the nonlinear effective analyses provide a very clear overall picture of the dam response to the design earthquake as well as helping the designer with all the details necessary in zones of potential concern. More experience in the application of these models is necessary and, for their calibration, centrifuge models seem very useful.

ii) Ongoing discussions related with the use of probabilistic methods have the purposes to clarify the following relevant questions (Sêco e Pinto, 2002):

- quantitative assessment of the safety;
- uncertainties of the actions, of the materials and of the models;
- risk evaluation in civil engineering practice;
- influence of risk analysis in the decisions;
- role of risk analysis in cost - benefit analysis.

iii) Dams built on pre-existing landslides have shown that seepage through abutments and open joints and failure surfaces in rock has been the most common negative factor.

iv) Earthquakes risks analyses related with: liquefaction of the dam, reactivation of piping due to shaking, damage of spillway leading to overtopping, collapse of tall slender intake resulting in overtopping and dam overtopping have received great attention.

Lessons for Tomorrow

1. Today there is a need to work in large teams exploring the huge capacity of computers to analyze the behavior of large dams. Innovative methods and new solutions require high reliable information and teams integrating different experts, namely seismologists, geologist, geophysics, geotechnical engineers and structural engineers.
A joint effort between Owners, Decision-Makers, Researchers, Consultants, Professors, Contractors and General Public to face this challenge is needed.

2. It is important to understand the concepts of vulnerability and resilience. Vulnerability is associated with two dimensions, one is the degree of loss or the potential loss and the second integrates the range of opportunities that people face in recovery. This concept received a great attention from Rousseau and Kant (1756). Resilience is a measure of the system`s capacity to absorb recover from a hazardous event. Includes the speed in which a system returns to its original state following a perturbation. The capacity and opportunity to recollate or to change are also key dimensions of disaster resilience. The purpose of assessing resilience is to understand how a disaster can disturb a social system and the factors that can disturb the recovery and to improve it.

3. From the analysis of past dam incidents and accidents occurred during the earthquakes it can be noticed that all the lessons have not deserved total consideration, in order to avoid repeating the same mistakes. We need to enhance a global conscience and to develop a sustainable strategy of global compensation how to better serve our Society. The recognition of a better planning, early warning, quality of evacuation that we should take for extreme events which will hit our civilization in the future.

In dealing with these topics, we should never forget the memorable lines of Hippocrates:

- "The art is long
- -and life is short
- experience is fallacious
- -and decision is difficult".

Future Challenges

The following topics deserve more consideration and can be considered future challenges for a better understanding of seismic dams' behaviour:

1. The main concerns are linked with existing dams, dams that have not designed to sustain earthquakes, or dams built using design criteria and methods of analyses, that are considered as out dated today;
2. Coupled models with nonlinear analyses and pore water pressure generation and dissipation models;
3. Incorporation of fault movements effects in dam foundations behavior;
4. Cost benefit analysis of seismic strengthening of existing dams;
5. The implementation of probabilistic analysis increases our confidence on the results, allows an optimization of the project considering the risks of failure, can lead to a better cost-effective design and construction, satisfy our personal needs providing a better insight of the different factors of the design and give more confident to our decisions;
6. Advantages and limitations of automatic instrumentation;
7. Environmental impacts ;
8. Piping risk analyses-Liquefaction;
9. Rehabilitation-use of geomembranes.

.

8.3 POWERPLANTS

8.3.1 Brief Summary

The first steam turbine was designed in England in 1884 by Sir Charles Algernon Parsons and steam turbines have played an important role since the 19th century.

During the last fifty years steam power plants have been continuously raised in response to the environmental requirements. The design for heat resistant steels in the 20th century, as well as the current status of steel development for power plants, regarding the creep strengthening and enhancement of corrosion resistance, has deserved considerable attention**.**

By 2015 coal was responsible for 39% of world electricity production, and significant deposits exist in South Africa, United States and other countries in Asia and in Australia.
It is important to stress that economies of China, India and United States are based in coal and these countries are the largest producers of electrical energy from coal.
Coal price is low and stable in comparison with alternative fossil fuels and natural gas.
The major disadvantage of the coal is the dirtiest of the fossil fuels and has largest impact in environmental that is getting increase attention.

The global warming was identified and linked with the use of fossil fuels.
How to balance the increase of world population with the electricity demand?

In 1950 nuclear power energy has raised and expand in United States, in UK, in France and other countries, but the Chernobyl disaster and the recent Fukushima accident in 2011 have slow down.

The rising of oil process, with the 1973 crisis, has stimulated other alternative energies as solar power and wind power.

By the end of 20th century hydropower energy and the construction of large dams were critically reviewed due to the environmental problems.

During 1980`s the use of gas for power stations got increase attention in Germany, Sweden and other countries.
In early 1990`s the cost of the gas was cheap, but nowadays is volatile. But the turbine combined cycle with great efficiency and less pollutant than other type of power station has increased the success of gas turbine.
The Middle East has the largest reserves of gas, but also in Europe, in Eurasia, and in other countries as United Staes, Australia, Venezuela, Argelia and Nigeria.

8.3.2 Case History nº 11 - Tapada de Outeiro Powerplant

8.3.2.1 Introduction

For Tapada de Outeiro gas powerplant, located in the North of Portugal, a summary of geological and geotechnical studies is presented, information related the foundations design of the main structures of the powerplant is given, and also Pombal landfill design is referred.
In addition, water intake design is described, the methodology to detect the cavities and also the instrumentation and monitoring of the slope.

8.3.2.2 Geological and Geotechnical Studies

The geological and geotechnical studies were performed in 4 phases during 1990-1994.
The Tapada de Outeiro falls in the massif comprising the Complex xisto -grauvaquico and the formations arr intensely deformed as a consequence of hercyan orogeny. Due to these orogenic movements the embasement rocks exhibit brittle deformation with fracturing and faulting.

The field tests have integrated seismic refraction survey, electric boreholes, drilling and sampling, dilatometer tests, CPT tests and permeability tests (Lugeon and Lefranc tests).

The laboratory tests for the rock materials were unconfined compression tests, triaxial tests, joint slides tests, point load tests and porosity, water absorption and unit weight tests.

For the soil materials, i.e. alluvial materials occurring in the valley, with a thickness of 1,.2 m to 2.5 m only identification tests (sieve analyses and Atterberg limits) were performed.

8.3.2.3 Foundations Design

For the pile capacity for Turbine buildings, UMC, Boiler and Transformer area, piles with 0.8m of diameter with 3000 KN for vertical capacity and piles with 1.0 m of diameter with 4500 KN of capacity were considered determined by Meyerhoff and Poulos methods.

For the horizontal design spring constants were considered.
The ultimate limit states and the serviceability limit states were considered for vertical, horizontal and inclined loads.

For spread foundations the ultimate limit states and the serviceability limit states were verified.
For the quality control of the piles 135 integrity tests were performed in all piles of 30 UMC, Transformer area, Boiler area and Turbine foundations to assess the existence of any discontinuity due to inflow of soil or other defects.

Direct load pile tests were not performed due to the difficulties related with the complexity o reaction frame and also after an evaluation of cost-benefit.

For the water intake the dewatering system was verified for different scenarios.

8.3.2.4 Pombal Landfill- Gabion walls – Drainage System

All the excavated materials were dumped in Pombal valley area and so there was a need to evaluate the stability of this huge landfill with slope 1.8(H) :1(V).

For the stability analysis the most critical 4 profiles were selected, i.e. 2 longitudinal profiles and 2 transverse profiles. The GSLOPE code was used.

For the static analysis the minimum safety factors computed were between 1.3 and 2.3.
For the seismic analysis the minimum safety factors computed were between 1.05 and 1.79.

For the bottom of the landfill gabions walls were selected to assess the stability and for a better paisagistic integration and economic reasons.

The stability of the gabion walls was computed by Coulomb formulation and the computed safety factors for overturning scenario were between 1.59 and 2.34 and for sliding scenario between 2.0 and 2.6.

A drainage system was designed with trenches converging to the existent water line.

8.3.2.5 Water Intake

The water intake of the CCPP Tapada de Outeiro is located on the right riverside of the Rio Douro.
An excavation was executed in the bank, partly in rock and partly in soil to construct this structure. The excavation was performed in dry conditions due to the existence of a cofferdam.

Geological mapping of the slope was performed prior to the excavation (see Figure 2.246 to Figure 2.250).

3 families of discontinuities were identified and the strike and dip of 257 discontinuities were measured during the field work.
A detailed zonification of the slope was performed after a partial excavation, and to assess slope instability risks SMR -Slope Mass Rating by Romana a worldwide known modification of Bieniawasky`s RMR (Rock Mass Rating) was used.
Three zones were identified, namely Zone A= 15 %; Zone B= 25 % and Zone C= 60%

It was recommended: (i) adequate drainage of the rock material by geodrains; (ii) assessment of variation of seepage observed in some discontinuities, (iii) analysis of the installation of heavy equipment such as cranes, tucks near the crest of the slope and the effect in the slope stability.

Figure 8.246 Existing Slope (Frontal View 1)

Figure 8. 247 Existing Slope (Frontal View 2)

Figure 8.248 Existing Slope (Frontal View 3)

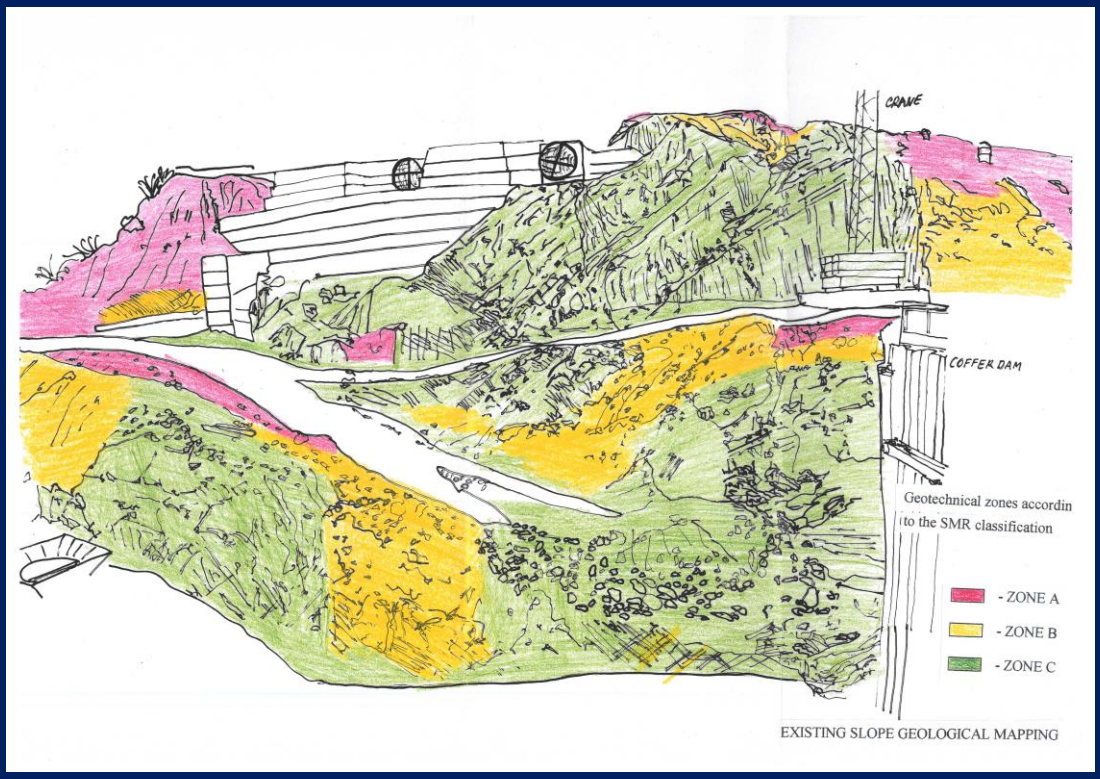

Figure 8. 249 Existing Slope Geological Mapping (1)

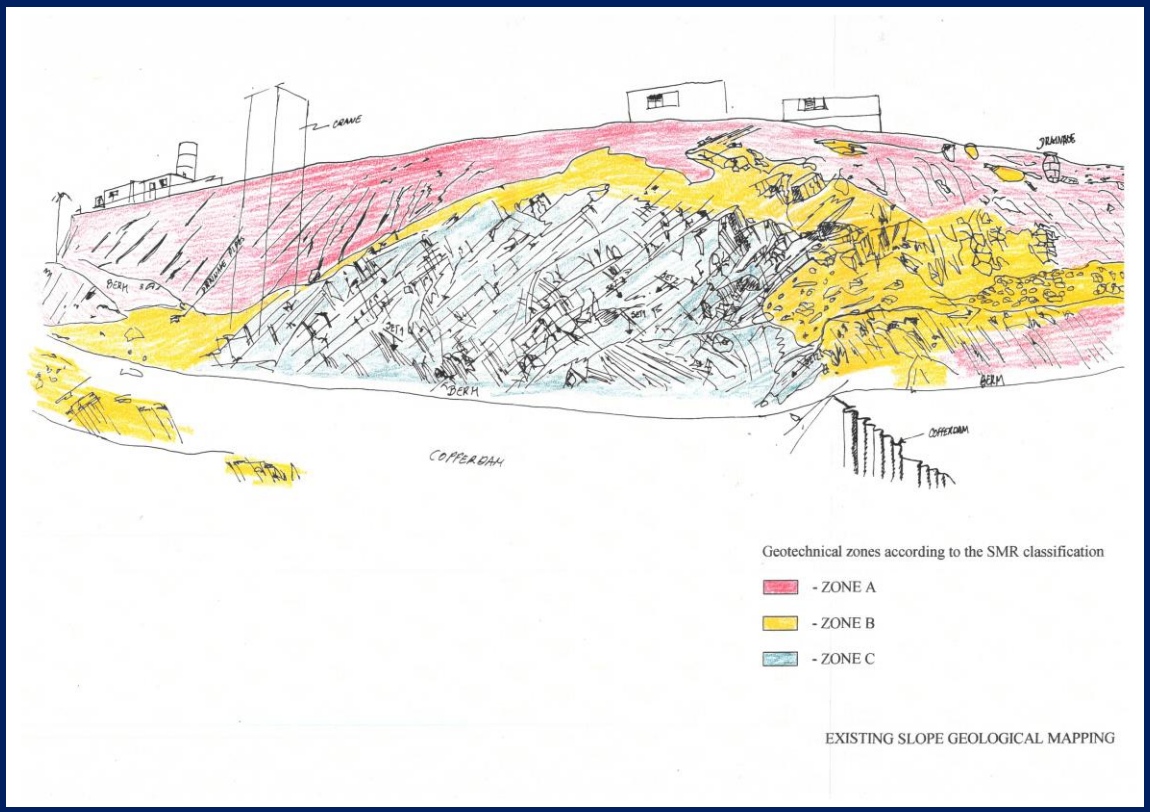

Figure 8. 250 Existing Slope Geological Mapping (2)

Figure 8. 251 Drilling equipment

8.3.2.6 Detection of Cavities

Introduction

During the earthworks of the Combined Cycle Turbogas Power Plant some mine galleries were discovered.

These galleries are related with mining works performed at Medas region to explore gold and antimony since Roman times until 1955.

It is important to stress that field tests performed during four campaigns have not identified the existence of mine galleries.

A balance of the advantages and limitations of different procedures (execution of additional boreholes, georadar and execution of drillholes in selected points) to identify the location of the caves was performed (Seco e Pinto, 1995).

In order to detect veins, possible voids, tunnels, shafts within these veins several geophysical methods (electromagnetics, magnetic, seismic and radar) were used. Based on the results of this geophysical campaign a map with selected areas where additional drilling was necessary was presented by DMT.

This additional drilling program has consisted by the execution of 70 destructive drillholes (performed by Adriano) (Figure 8.247) and 14 boreholes with core sampling (performed by Engil).

This campaign begun on 21st December 1995 and was followed by a team composed by a civil engineer (specialist in geotechnique) and an engineer geologist who performed several visits to the site to give technical assistance to the works.

Methodology

Taking into account the high cost of boreholes with core sampling, it was decided to carry out a large number of drilling holes, 10 to 12 meters deep, distributed all around the area under study.

The boreholes should have been executed with equipment that automatically records some drilling parameters, i.e., that makes continuous logging of physical parameters while drilling (Sêco e Pinto, 1995). The recordable parameters are: drilling velocity, drill feed pressure, impact pressure, rotation pressure, velocity of rotation and reflected percussion.

However, the drilling holes were made with a Hydraulic Drill Rig Roc 642 HC (Figure 8.248), which principal characteristics are described in the next chapter. This equipment doesn't allow a continuous record of some drilling parameters, such as drilling velocity, pressure of the hammer or rotation speed. Therefore, these records have to be done by the operator, who has to record the time required for the penetration of each rod and the pressure variations, marked on the respective manometers, along each rod and for each drilling rod. On the other side, this equipment has an optional system that allows to collect all the material (powder) that results from the drilling. The quantity and type of material collected in each drilling rod comprise two important parameters that represent the quality of the massif and will help to distinguish rock massif from filled areas or cavities.

Considering the equipment used for this work, as well as the purpose of the drilling holes, it was decided to adopt a methodology for execution of the boreholes, consisting of:

- Establish the location for each borehole with a topographer's help;
- Have four men per drilling team, distributed by: drilling commands, dust collector, time record and pressure record;
- Record the drilling parameters for each rod, which means for each 3 meters;
- Collect the material at the end of each drilling rod in a specific plastic bag;
- Identify each plastic bag with the drilling hole number, rod number and depth;
- Record the weight of each bag and store all bags in a safe and not very damp place;
- Observe the material in each bag, register its description and relate it with the massif, filled areas or cavities;
- The drilling team must record all remarkable aspects, such as the presence of water and respective depth of occurrence, brusque variations of drilling parameters, free fall of drill and respective depth of occurrence, difficulties in drill feed, namely due to deflects in the wrong direction of the bit, and all other aspects that seem to be of importance.

The picture of the Front Control Panel is presented in Figure 8.249.

Equipment

The drilling holes were executed with a Hydraulic Drill Rig Roc 642, which is a fully electro-hydraulic drill rig designed for drilling in surface applications, quarries and construction sites similar to the one in question.

Briefly, one can say that the drill rigs consist of some main components, such as a wagon frame with track frames on which the diesel engine is mounted, the carriage body, the dust collector, the hydraulic system, and the air and boom systems.

At the rear of the drill rigs features a platform for the operator. Next to the platform lies the rear control panel where the tramming and winch controls are mounted.

This electro-hydraulic drill rig is powered by a turbo-charged, air-cooled and inter-cooling Dentz diesel engine which is equipped with a monitoring system including auto shut-down functions.

The hydraulically driven dust collector features automatic cleaning and consists of a filter unit, a blower and the blower outlet. The dust collector is, as mentioned earlier, an optional equipment, very useful in this case.

To execute a correct drilling operation without hazards, it is necessary to position correctly the feed control levers and set the feed lever spike steady against the ground. The rock drill must be in the upper position, with a drill rod coupled to the rock drill and the drill bit coupled to the drill rod. Thereafter, and taking into account the characteristics of the rock massif, one must select the correct position of the impact pressure, the dust collector and the flushing air, the drill feed pressure and the lever rotation. The drilling operation begins and must continue until the coupling sleeve reaches the drill steel support. To continue drilling it becomes necessary to add another drilling rod, which is achieved by coupling the rock drill to the new rod and the new rod to the rod below. The drilling operation must continue until the coupling sleeve reaches the drill steel support. Thereafter repeat the above mentioned procedure until the desired hole depth is achieved.

In addition to the time record and the material collected at the end of each drilling rod, there are some pressures to be recorded, which are marked on the Front Control Panel. There are only two features which can be obtained from these manometers, that could, in a certain way, be considered as most important. They are the drill feed pressure and the rotation pressure. However, those pressures are directly related to each other, i.e., there is a system that controls the drill feed pressure by sensing the rotation: when the rotation pressure exceeds the preselected value, the drill feed pressure could decrease to low drill pressure, and due to the drill feed pressure decrease, the rotation pressure drops down, causing the drill feed pressure to increase again to high drill feed pressure. Therefore, although their parameters represent some of the drilling characteristics, and indirectly the massif itself, they cannot be considered useful because the hydraulic system immediately counterbalances any pressure variation due to some hypothetical different characteristics of the massif.

In conclusion, the values read in the manometers were almost constant and the variations recorded comprise no direct relation to the variations of drilling velocity nor to the quantity of recovered material.

Results

Following the previously defined program for execution of the drill holes and the adopted methodology, it was decided to carry out seventy drilling holes, spread out all around the area under study.

Since the purpose of this work consisted in an attempt to identify the exact location of old tunnels and shafts of abandoned mines which are referred to in some documents regarding the subject, and which were partially encountered during the excavation phase of this job, the location of these holes had, as a reference, the DMT - Report, about land geophysics, which identified approximately fifty anomalous points. However, the geophysics methods applied (electromagnetic - EM, magnetic field, seismic, radar

and direct current electrics with multi-electrodes) proved that these are appropriate for the search of the ore veins as well as voids (DMT, 1995).

The execution of destructive boreholes as a method for detection seems to be rather risky, for it does not supply, similarly to the geophysics methods applied, direct results which allow for a clear identification of eventual existing voids.

However, and because of the much higher cost inherent to the execution of one or more boreholes with core sampling per foundation, it was decided to adopt this solution which would have to be carried out much more carefully in order to supply the useful results required for this study.

The methodology applied for the execution of these boreholes implied the presence of a sounding team sensible to the problem in question, and very cautious during the recording of the results obtained.

Table 8. 38 presents the type of information gathered by the sounding team via the execution of these boreholes. Subsequently this data had to be processed. The information obtained for each rod, i.e., per 3 m to 3 m drilling, had to be converted into meter to meter information. This systematization of meter to meter information is based on the assumption that the performance throughout each drilling rod is somewhat homogeneous. In a preliminary phase, the only exceptions are in agreement with some indication obtained from the sounding team regarding brusque performance variations throughout the same rod, and will later be compared with the results of other prospecting works carried out.

Table 8.38 Operator´s Results of Drilling Holes

D200 (rod nº)	Time of drilling (sec.)	Recovered Material (Kg)	Flushing air Pressure (Bar)	Drill Feed Pressure (Bar)	Impact Pressure (Bar)	Rotation Pressure (Bar)
1	0.50	22.3	7	60	160	40
2	1.30	27.4	7	70	160	60
3	2.07	31.3	7	70	160	50
4	2.06	27.2	7	60	160	50

In this way, from the data presented in Table 8.38 we were able to calculate the drilling velocity of each rod, regarding it as invariable, and were able to establish the quantity of material recovered per linear meter of drilling. With these results as a basis, two graphs were produced for each borehole. The first graph presents the drilling velocity and the quantity of recovered material versus the depth, and the second graph indicates the drilling bit advance pressures and rotation versus the depth.

Figure 8.250 shows the graph type for destructive borehole with drilling velocity and recovered material records.

Figure 8.251 illustrates the graph for destructive borehole with drill feed pressure and rotation pressure records.

The records of pressures are not conclusive, for they do not bare a direct relation to the drilling velocity, nor to the quantity of recovered material. However, at first it was considered that the drilling bit advance pressure and rotation could in some way, although not accurately, portray the massif's characteristics, and therefore, these parameters were depicted graphically. However, and as can be observed from the graphs presented in appendix, these parameters are not conclusive. Consequently, the eventual identification of voids through this method can only be accomplished through the brusque variations of drilling speed, the quantity of recovered material, the characteristics of this material and other features detected by the sounding team.

In light of the above, and upon a careful analysis and interpretation of the obtained results, the following scenarios were encountered throughout each borehole:

a) the presence of an area where the drilling speed increased drastically, with an absolute inclination towards open space (in the case where the drilling duration is zero), and where the recovered material is none or almost none.
b) existence of an area where the drilling speed increases, although not so drastically, and where there is a recovery of material very different from the remainder, and generally, inferior.
c) existence of an area where the drilling speed decreases and where, generally, it coincides with an increase of recovered material.
d) absence of brusque variations, with a gradual decrease of drilling speed and an increase of recovered material as the depth increases.

According to the identified scenarios, it was assumed that each described case could correspond to the following situations:

a) the identified variation should correspond to an empty void. Its extent is larger (in depth) as the recovered material decreases and the drilling velocity increases. However, as the registered results refer to 3 m intervals and only by much coincidence could it correspond to a void of equal size, it is observed that there is a brusque variation in the registered values which does not ensure the presence of a void, and much less its geometrical features. This situation was identified as a negative anomaly (A^{--}), i.e., an anomaly that could correspond to the most unfavorable situation, which is the existence of voids.

b) the detected variation probably corresponds to one of the following three situations:

b.1) to a filled hole, which filling material may or not be of the same type of the surrounding massif, but which is generally less compressed, and therefore originates an increase of the drilling velocity and a decrease of the quantity of recovered material.

b.2) to an empty hole, but so small that the average registered values for each 3 m drilling indicate a variation but not so accentuated that it could lead us to admit the existence of a significant cavity.

b.3) to a massif zone which could be weathered and/or cracked, or to an area with water or with a trace of softer material, which therefore originates an increase of drilling velocity and a decrease of recovered material.

These situations were also classified as negative anomalies (A^-). However, the inherent risk is much lower, as either the cavity is filled, or of small dimension to such an extent that the registered variations and observations are not very clear, or there is no cavity and the drilling rod encountered a much softer and decompressed area of the massif, which probably relates to a geological "phenomenon", namely a fault, a vein, a crashing zone or a shear zone resulting from some type of action forces, etc.

c) the identified variation corresponds, in principle, to a harder zone of the massif, and where, consequently, the drilling speed gradually decreases and generally the quantity of recovered material increases. This situation may correspond entirely to a massif of superior quality (undamaged and less cracked) or to a geological "phenomenon", namely a quartz or an ore vein. In either case, this situation was classified as a positive anomaly (A^+), as it does not entail any type of risk or problem to the construction works.

d) this situation was considered as normal (N) and corresponds to drilling in a "conventional" massif, which compacity or quality improves progressively as the depth increases, and thus a constant bias is verified, i.e., of equal signal as the drilling proceeds.

As an exception to the situations referred to above, there are cases where the decrease of drilling velocity does not coincide with areas where there is an increase of recovered material, or vice versa. However, this situation was not considered as very relevant, as there was no indication that could lead us to regard it as some other type of anomaly and, on the other hand, this discrepancy could be due to other factors, such as the presence of surface water or throughout the borehole, which does not enable the correct gathering of powder resulting from the drilling.

All the material collected from the boreholes will be carefully analyzed. Up to date it was only possible to observe a few of them. This observation will allow us to identify the material of the drilled area, and relate it to a schist massif (X) or to embankment materials (A).

In order to better illustrate the results obtained in all the boreholes, and so as to appease the interpretation and comparison of this information with information obtained through the use of other methods, it was indicated in the plan of the site, alongside the identification of each executed borehole, the identified situation type (A^{--}, A^-, A^+ or N), complemented with the identified material type, depth at which the anomaly occurs, in addition to other information regarding the existence of water or the impossibility to gather material.

In view of the above, and in accordance with the results presented in appendix and in the plan, it should be mentioned that up to date, no situation classified as more precarious, i.e., A^{--}, was encountered.

Boreholes with core sampling

Methodology

The data obtained through the geophysics methods and destructive drilling solely allow for an indirect analysis, i.e., only supply data that, upon analysis and interpreted in light of some preselected criteria, permit us to produce of a series of scenarios which are more or less likely to occur.

The need to compare the applicability of the methods used and the preselected criteria originated the execution of some boreholes with core sampling, located in strategic points.

The execution of boreholes with core sampling permits a direct observation of the massif, it's classification according to existing international standards, namely those established by the International Society for Rock Mechanics, and in this way, ensure in those areas the existence or not of deep cavities, where they are filled or not, as well as the type and condition of the filling material.

As a whole, it is foreseen the execution of only 15 boreholes with core sampling, which are to be located in zones with different types of geophysical anomalies. The main purpose of the boreholes with core sampling is to compare the results obtained and eliminate some of the assumptions raised through the analysis of this data. Up to date, only 14 boreholes were carried out. The missing borehole, BH 115, is situated in the northern area next to the gabions wall of smaller dimensions.

The conventional methodology was used for the execution of boreholes with core sampling, and the following operations were carried out:

- Correct identification of the borehole site, with the aid of a topographer;
- Placing of the sampling equipment in its respective place;
- Correct placing and adjustment of the bits to the rod and to the double core sampler;
- Beginning of the drilling with gathering of the test cores at the end of each maneuver;
- Placing of test cores in wooden boxes, approximately 1 m long, arranged from above downwards and from left to right as the drilling advances deeper;
- Identification of all the maneuvers, by separation of the respective test cores with a wooden piece where the maneuver's final depth is marked;
- Identification of the sounding boxes, with inscription of the sounding number, box number, depth of maneuvers and name of job;
- Placing of boxes in a safe place, not exposed to the sun or to large temperature variations and moisture.
- Execution, by the operator, for each borehole, of a daily record where he identifies the borehole, site, job, date and the number and length of maneuvers, lithologic description, the presence of water and its level at the beginning and at the end of the drilling, as well as other observations considered to be important.

The boreholes were executed with conventional equipment which is subsequently described:

Equipment

The sample gathering tests were executed with conventional equipment for rotatory drilling, using a rotatory sampler with double wall. These samplers comprise an exterior tube that acts by rotatory cut and which lower end is provided with hard steel jagged bit. The inner tube - sample carrier - which is maintained fixed because it adheres to the sample, is much longer than the outer tube, enabling the sample to be protected from circulating liquids.

Part of the digging for execution of foundations had already been accomplished by the time the tests were carried out. Consequently, it became necessary to select a much lighter test equipment of smaller dimensions, which could be more easily maneuvered and with easier access to the base of the referred excavations.

Results

For execution of boreholes with core sampling, 15 rotatory drills were carried out, with double sampler and test core recovery.

COMMENTS FOR THE DIFFERENT INVESTIGATION METHODS

As from the overall analysis of the results obtained for all methods of geotechnical prospecting used: geophysics, destructive drilling and boreholes with core sampling, it is possible to establish a few comparisons between this data.

1) According to the DMT report, dated 28/11/1995, during September and November a series of geophysical methods were carried out, namely, electromagnetic samples, determination of the magnetic field, seismic, radar and direct current electrics with multi-electrodes. With the results obtained as a basis, 50 sites with anomalous behaviors at certain depths were identified. These anomalies related to brusque variations and abnormal values of one or more geophysical parameters, such as conductivity of the ground, shear velocities, magnetic field values, radio wave reflections, apparent resistance and induced polarization.

2) These geophysical parameters depend on various factors, the most significant being the type and quality of the massif, namely in terms of mineralogical composition (presence of different mineral concentrations, as well as elements with different conductivity), presence of discontinuities, namely veins, faults or other geological structures, existence or not of water levels, of voids, of old equipment and material related to mine shafts, etc. In other words, although indirectly, these tests may supply information regarding the existence of eventual cavities.

3) The geophysical methods carried out proved to be appropriate for the research of ore veins, as well as voids. However, they do not allow a clear distinction between these two situations, which are so different from each other, and with differences equally important to the work in course.

4) The final analysis of these geophysical campaign made it possible to fix the boundaries between areas with voids and areas where the existence of ore veins or voids is probable, and

that are associated to low values of shear velocity, reflection of radio waves and abnormal conductivity rates or magnetic anomalies.

5)

6) In what refers to destructive drilling, it was observed that these furnish some information regarding the massif type and quality, through some parameters such as drilling velocity and quantity and type of recovered material. With these results as a basis, it is possible to make some conclusions regarding the probably of occurrence of better or worse quality zones, ore veins, voids and eventually some information regarding the latter, namely whether they are filled or not, as well as their approximate location.

7) The boreholes with core sampling were carried out, in a much lesser number. It can be stated that this is the most suitable method for detecting the problem in question. Being this a direct method, it makes it the only one that can safely identify the presence or absence of cavities, filled or not, and the partial geometrical characteristics. If it weren't such an expensive work, one or more boreholes would have been carried out in each foundation site. In this way, it would be possible to define, with absolute accuracy, the eventual sites of cavities.

5 - Conclusions

1) The following conclusions were reached through the interpretation and joint analysis of various samples and works carried out. So as to appease the cross-reference of information, and as was referred in previous chapters, a drawing was made, illustrating all the works carried out and associated anomalous behavior, as well as other observations considered to be of interest.

2) From the analysis of the above drawing, it is possible to detect that the interception of various anomalies, identified and described in previous chapters, lead us to reject the possibility of existence of some cavities until approximately 12 meters deep, i.e., until the studied depth. The existence of small cavities with reduced dimensions and in general filled is of low probability.

3) These conclusions were reached by observing that the majority of the geophysics heterogeneous features identified correspond to harder massif zones, where the drilling speed decreases and the recovered material increases, or in zones with normal behavior in destructive drilling terms or with core sampling, and therefore should relate to other factors such as the presence of ore veins. The negative anomalies (A-) seems to be related with areas of weathered massif, that however correspond, generally, to a good or fair massif.

4) The boreholes executed in the northern area detected the presence of an embankment overlying a schist massif, which was already acknowledged. This embankment is, generally, composed of schist materials, which are sometimes very poorly consolidated. This fact was concluded by the high drilling speeds and reduced recovery, both with the destructive drilling method and the boreholes with core sampling.

5) In spite of the exposed above, it should be stressed that the data and conclusions presented do not include all the programmed boreholes. Therefore, the final conclusions can only be drawn after the execution of all the works, but it is expected that the few missing boreholes to be carried out (9 destructive boreholes and 1 borehole with core sampling) will not change this general trend.

Figure 8.252 View of the drilling equipment

Figure 8.253 Front Control Panel

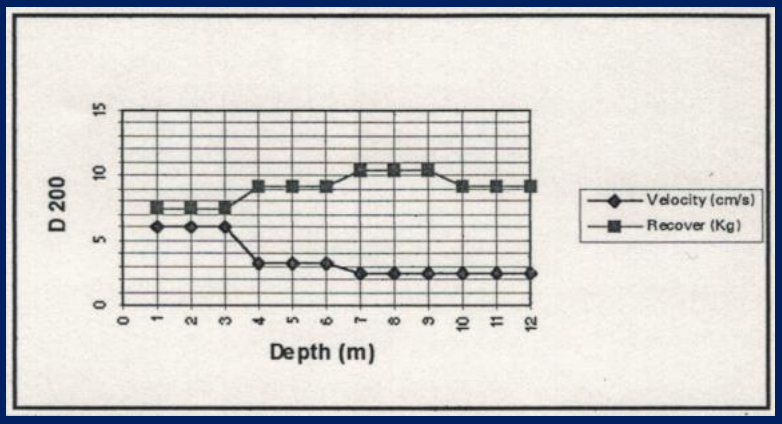

Figure 8.254 Graph for destructive borehole with record of drilling velocity

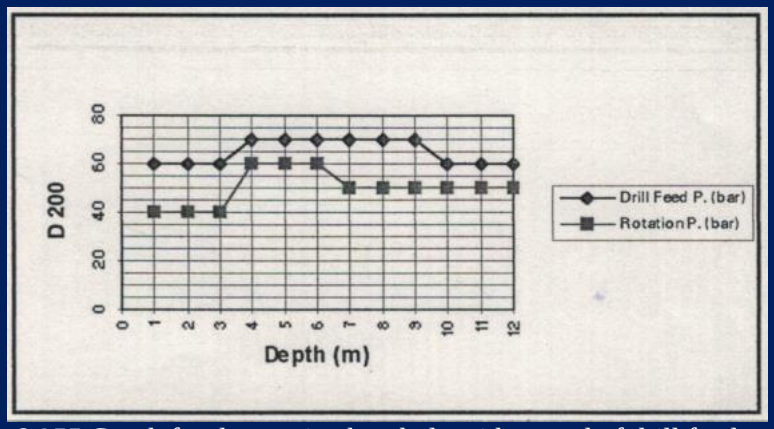

Figure 8.255 Graph for destructive borehole with record of drill feed pressure

8.3.2.7 Instrumentation and Monitoring of the Slope

This stability of this slope with almost 30 m high and slope inclination of 65º was performed by GSLOPE

The following safety factors were computed.

The following actions were taken:

i) Due to the decompression of the rock mass and deficient excavation of the slope Installation of a wire mesh;
ii) Superficial drainage of crest and berms;
iii) Internal drainage of the slope with geo drains;
iv) Instrumentation and monitoring of the slope.

With the purpose to control the phreatic surface in order to calibrate the assumption assumed for the slope stability analysis twelve hydraulic piezometers in vertical drill holes from the crest of the slope were installed. Details of the operations are shown in Figures 8.256 to 8.258.
Also, the behavior of the geodrains was correlated with the measurements of the water level in the piezometers.
For the monitoring of horizontal displacements five inclinometers were placed (see Figure 8.259).
To control the settlements twelve bench marks were placed at the crest.

Figure 8.256 Drilling equipment to install piezometers

Figure 8.257 View of the piezometer tip

Figure 8.258 View of the piezometer cover

Figure 8.259 Cover of the inclinometer tube

For the safety control it was recommended:

- Regular measurements of the installed instruments;
- - Visual inspection of the crest and the berms to detect any recent movement of the slope;
- - In case of any anomaly's actions should be taken to correct the situation or to avoid serious consequences.

Details related the measurements of the piezometers are presented in Figure 8.260 and Figure 8.261.

For the monitoring of horizontal displacements in the inclinometers details related with the wheel mounted sensor and the readings box are shown in Figure 8.262 and Figure 8.263.

Regular site inspections to asses slope stability were performed. So, it was possible to identify that the construction of 3 pipes for electrical cables and 1 pipe for water slope have provoked damages in some geodrains (see Figure 8.264).

Figure 8.260 View of the water level device

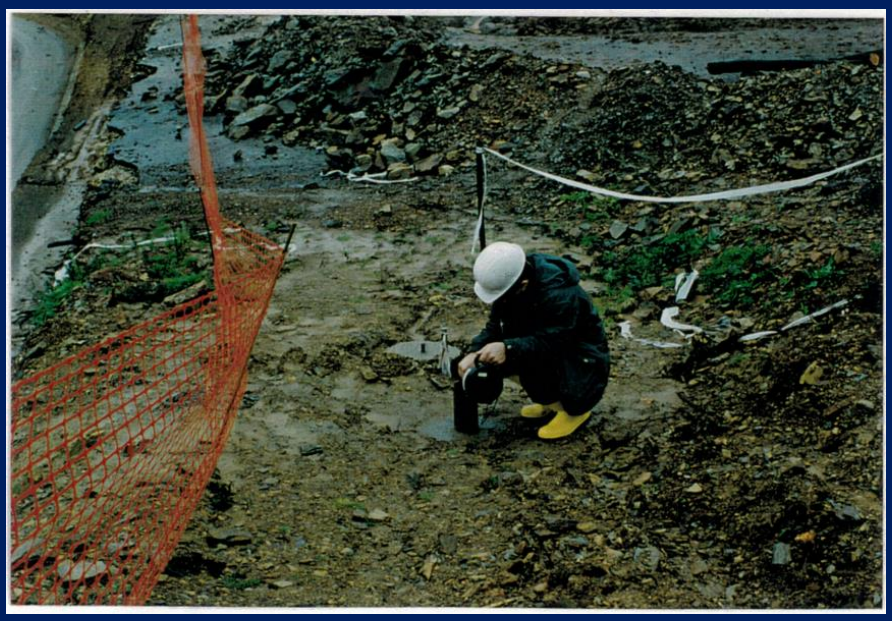

Figure 8.261 Measurement of the water level in the piezometer

Figure 8.262 A view of the inclinometer sensor

Figure 8.263 Measurement of the horizontal displacement in the inclinometer

Figure 8.264 View of the pipes located on the slope

Lesson nº 11: It is very important to analyse the past history of the site, in order to guide the site investigation plan and to identify all the situations that can provoke detrimental effects in the structural safety.

Piles shall be designed to remain elastic, if this is not possible potential plastic hinging shall be considered for: (i) a region of depth 2 d (d-diameter of the pile) from the pile cap; (ii) a region of ± 2 d from any interface between two layers with different shear stiffness (ratio of shear moduli > 6).

Evidence has shown that soil confinement increases pile ductility capacity and increases pile plastic hinge length. Piles have shown the capability to retain much of their axial and lateral capacity even after cracking and experienced ductility levels up to 2.5.

The design of a foundation includes the following steps:

- Project information on superstructure, restriction on settlements, performance requirements
- Specification of geological and geotechnical environment
- Site investigation, idealization of the stratigraphy and determination of soil properties
- Definition of applied loads, including the seismic forces
- Visualization of the type of foundation, or diagnosis of the problem
- Design analysis and safety verifications according with building codes
- Considerations on excavation and construction procedures.

Note. This project was developed for the Consortium Siemens/Koch.

8.3.3 Case History nº 12 - Carregado Powerplant

8.3.3.1 Introduction

For Carregado gas powerplant, located around 35 Km North Lisbon a summary of geological and geotechnical studies is presented, studies related seismic response of ground, information related the foundations design of the main structures of the powerplant, dewatering of the excavations and construction of the cofferdam is given.
In addition, water intake design is referred.
The construction specifications are described.

8.3.3.2 Geological and Geotechnical Studies

The geological and geotechnical studies were performed in 4 phases.

The stratigraphy is the following:

A. Fill material composed by sandy clayed material with a thickness varying from 1 to 3 meters.
B. This unit is composed by silt to very silty clay(mud), dark grey, locally grayish brown, sometimes with fine to medium bands, from holocenic period, with thickness varying from 4 to 6 meters, with low compacity, SPT values between 0 -1, and peak undrained resistance of 20 kPa and residual resistance of 8 kPa, given by vane shear tests.

C. This unit is composed by clay to sandy clay material, dark grey to dark brown, from Plistocenic period, with thickness varying from 12 to 16 meters, SPT values between 4 to 21 blows, and peak undrained resistance between 30 to 40 kPa and residual resistance between 12 -16 KPa, given by vane shear tests.
D. The bedrock under the alluvial material deposits of Miocenic period and the materials includes basically very dense fine to coarse sand, slightly cemented, sometimes slightly silty and/or clayey, usually with fine to coarse gravel. The geological structure of this unit is characterized by a more or less regular stratification, gently towards East, around 3-5 degrees. The SPT values were between 50 to 60 blows.

The field tests performed in 4 campaigns have integrated 32 boreholes with length between 10 m to 26.8m, drilling and sampling, SPT tests, 8 crosshole tests, 11 PCPT tests, 17 Vane shear tests and permeability tests.
In some boreholes piezometers were placed to record the water level.

The laboratory tests identification tests (sieve analyses and Atterberg limits), water content, weight density, porosity, triaxial tests, uniaxial tests and oedometer tests.
Also, water samples were taken to measure aggressivity of water, ph values and alkalinity.

8.3.3.3 Seismic Response of Ground

The seismotectonic analysis is very important for the assessment of earthquake hazard.
Portugal is located in the Eurasian plate about 200 Km north of the Azores-Gibraltar fracture and is affected by the interaction between Eurasian and African plates.
The active faults are shown in Figure 8.265.
In order to assess the influence on seismic hazard of Carregado site some of known earthquakes were selected from the Seismic Catalogue.

The historical seismicity in Portugal is referred in Figure 8.266.

The isoseismic contours maps from the earthquakes of 26 January 1531, 1 November 1755 and 23 April 1969 are shown in Figures 8.267 to 8.269.

The first seismographic station was installed in Coimbra in 1903, the second one in Lisbon in 1910 and the third one in Porto in 1929.
In 28 1969 had occurred in the Gorringe bank and earthquake with a magnitude 7 that was felt from North to South of Portugal and that provoked several damages. The isoseismal contour map of this earthquake is shown in Figure 8.269.
In 2000 the seismographic network has around 30 stations with the high density in the south of Portugal (see Figure 8.270).

The safety of the structures in Portugal should be checked against two seismic actions which represent a moderate earthquake at short focal distance (seismic action type 1) with a duration of 10 seconds and a higher magnitude earthquake at longer focal distance (seismic action type 2) with a duration of 30 seconds.

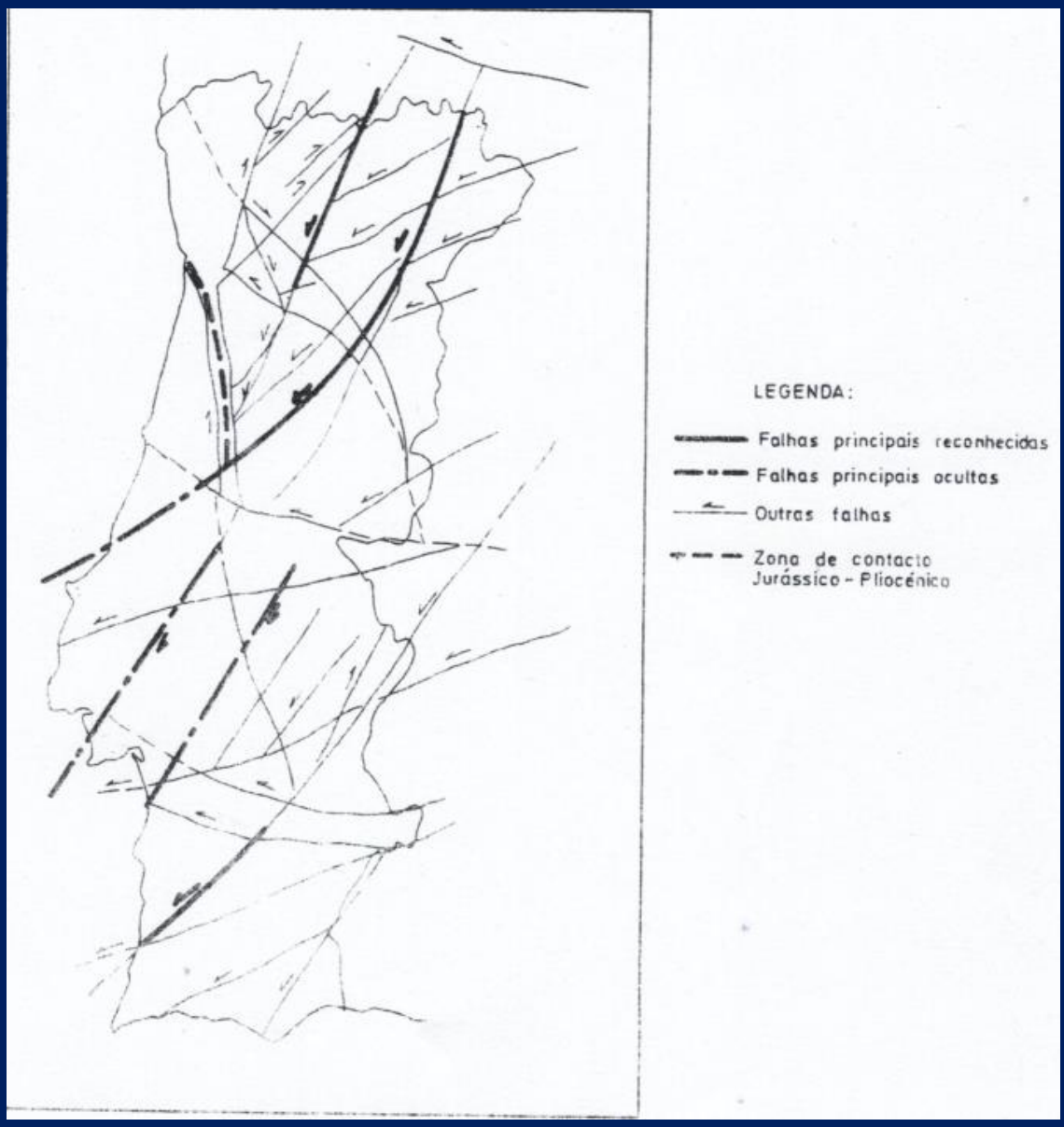

Figure 8.265 Neotectonics model

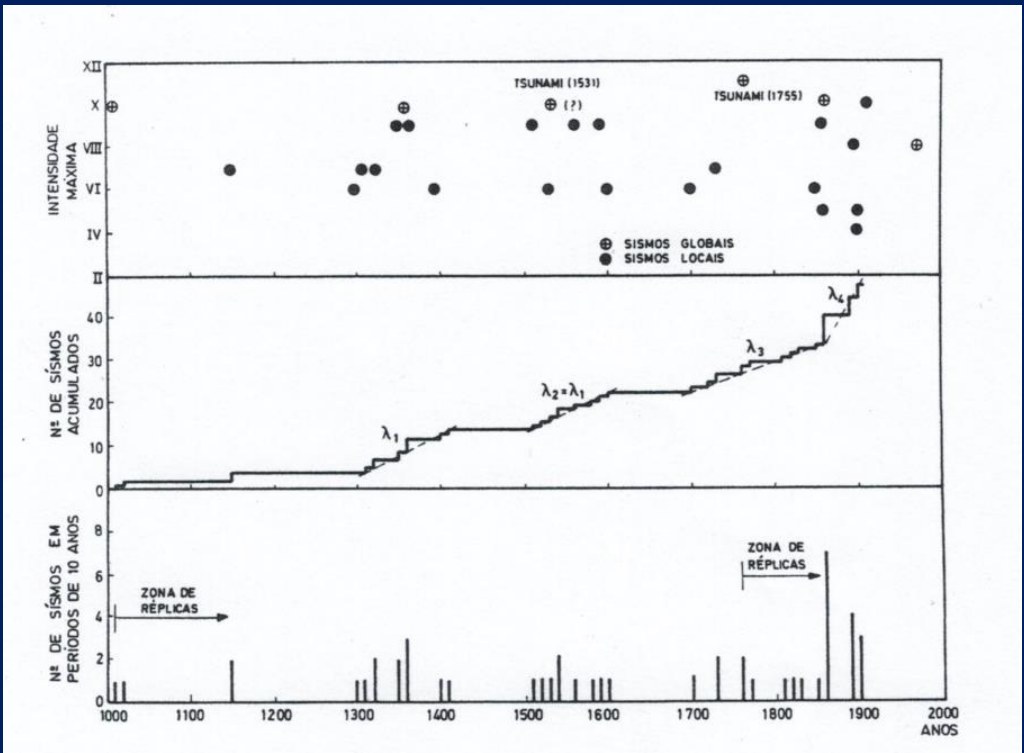

Figure 8.266 Historical seismicity of Portugal

Carregado powerplant was designed to sustain two different levels of activity namely. O.B.E: that is an event that may reasonable be expected during the lifetime of the structure, the structure must continue to function during and after such event and thus the loading is classified as unusual; and MCE that is an event that corresponds with the most extreme earthquake action that can be reasonably expected at the site, the structure must withstand the event in such a way that repairs can be undertaken in a reasonable length of time and more importantly, that no loss of life occurs. And thus, the loading is classified as extreme.

Both determinist and probabilistic approaches were used, as well Eurocode nº 8 for the definition of seismic action.
For the current buildings a pseudo-static analysis was used.
For more complex structures such as turbines, cooling tower and boilers a dynamic analysis was performed incorporating the seismic vibrations and interaction soil-structure.

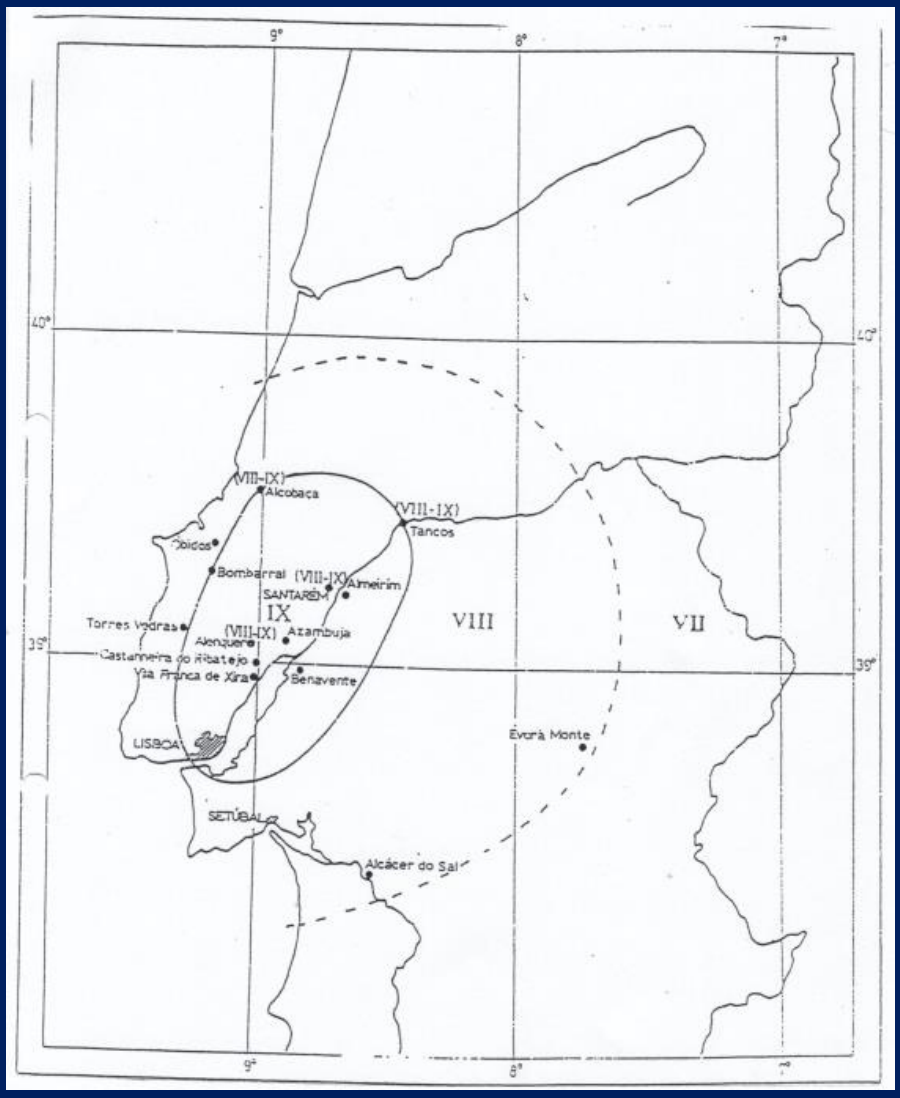

Figure. 8.267 Isoseismal contour map of 26 January of 1531 earthquake

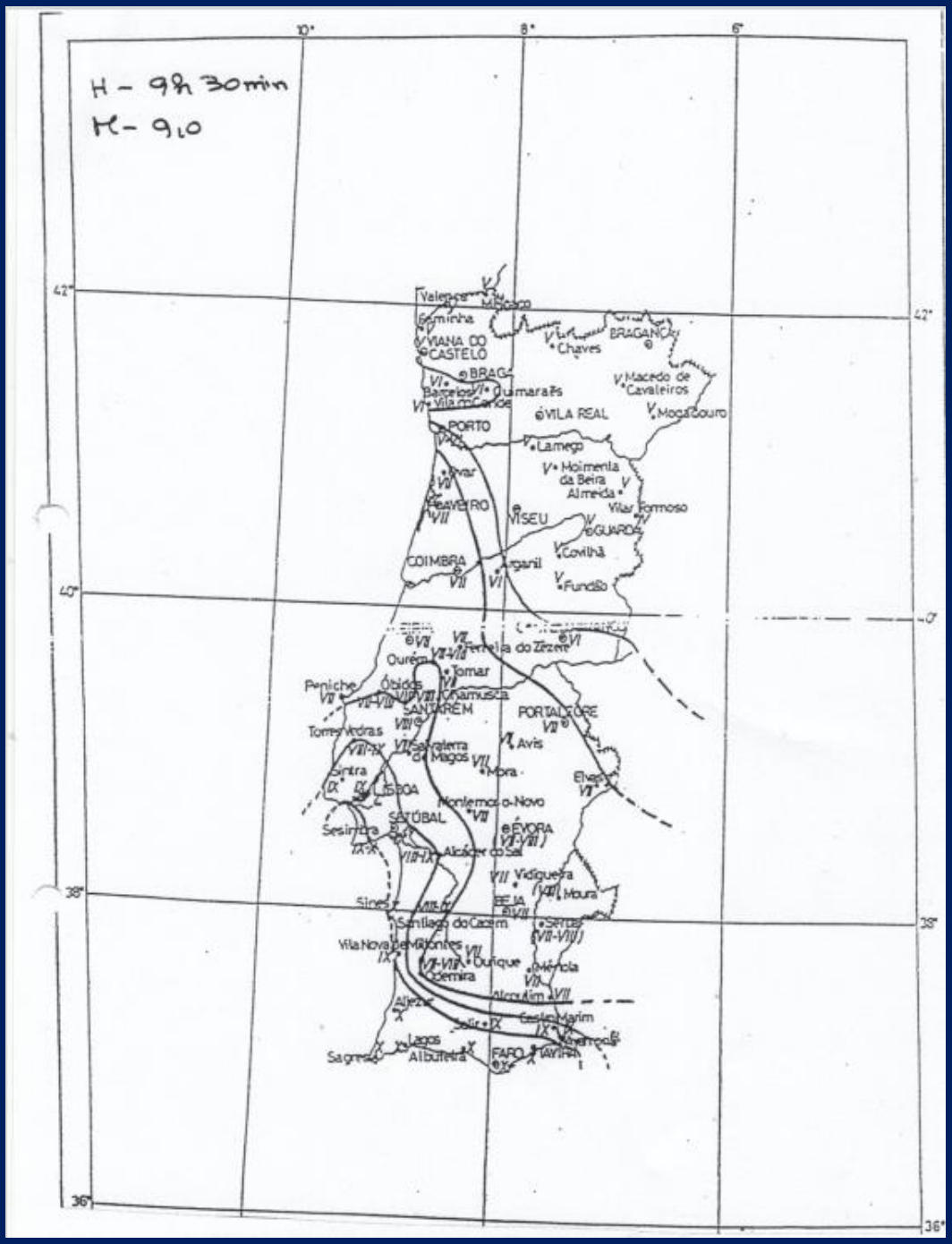

Figure 8.268 Isoseismal contour map of 1 November of 1755 earthquake

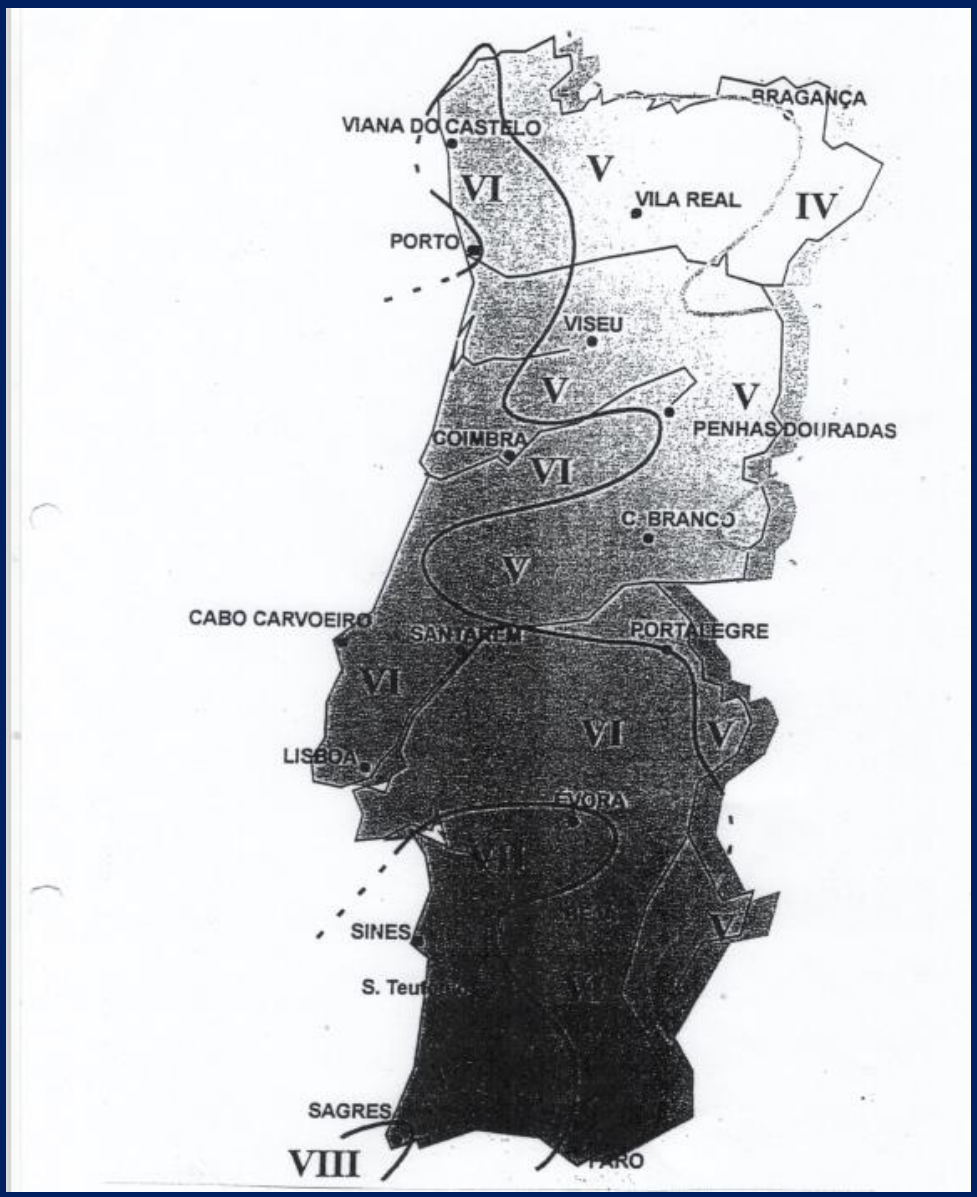

Figure 8.269 Isoseismal contour map of 28 February of 1969 earthquake

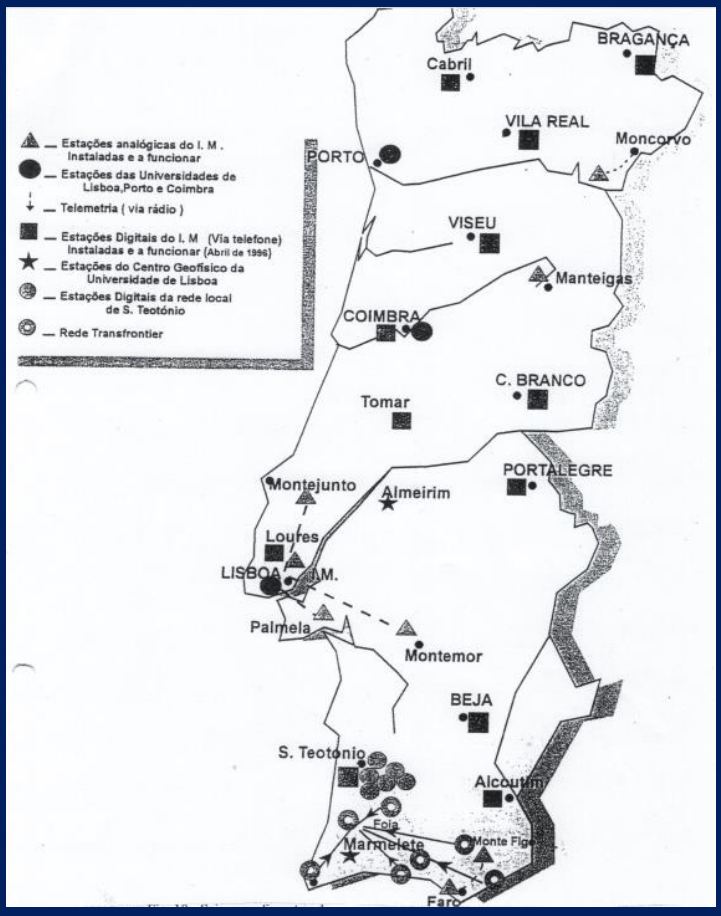

Figure 8.270 Seismographic network

8.3.3.4 Foundations Design

The Raft and Shallow Foundations were designed respecting the ultimate limit states and the serviceability limit states.
Taking into account the characteristics of the structures and the geological and geotechnical characteristics of ground for UGD and UST as the loads transmitted by superstructure is around 50 KPa raft foundations were used.

For other light and less important structures shallow foundations were adopted.

Piles with 0.6 m of diameter with 1815 kN for vertical capacity, piles with 0.8m of diameter with 3154 kN for vertical capacity and piles with 1.0 m of diameter with 4928 kN of capacity were computed using the formulations of Meyerhoff and Poulos methods.

For UMC (main building) piles with 1.0 m of diameter and 24 m long were considered.
Considering a concrete B30 and a steel A400 the following reinforcement was used:
Longitudinal reinforcement 10 bars diameter 20 mm, transversal reinforcement diameter 10 mm double helicoidal with a step of 30 cm.

UMC structure (turbine block) was founded in 27 piles of 0.8m of diameter and 24 m long.

Considering a concrete B30 and a steel A400 the following reinforcement was used:
Longitudinal reinforcement 10 bars diameter 16 mm, transversal reinforcement diameter 10 mm double helicoidal with a step of 30 cm.

URA structure (Cooling tower) was founded in 128 pile of 0.8 m of diameter and 26 m long.
Considering a concrete B30 and a steel A400 the following reinforcement was used:
Longitudinal reinforcement 10 bars diameter 16 mm, transversal reinforcement diameter 10 mm double helicoidal with a step of 30 cm.

UHA structure (boiler) was founded in 32 piles of 1.0 m of diameter and 24 m long.
Considering a concrete B30 and a steel A400 the following reinforcement was used:
Longitudinal reinforcement 10 bars diameter 20 mm, transversal reinforcement diameter 10 mm double helicoidal with a step of 30 cm.

UCA structure (administration building) was founded in 36 piles of 0.8 m of diameter and 24 m long.
Considering a concrete B30 and a steel A400 the following reinforcement was used:
Longitudinal reinforcement 10 bars diameter 16 mm, transversal reinforcement diameter 10 mm double helicoidal with a step of 30 cm.

UST structure (storage building) was founded in 34 piles of 0.8 m of diameter and 24 m long.
Considering a concrete B30 and a steel A400 the following reinforcement was used:
Longitudinal reinforcement 10 bars diameter 16 mm, transversal reinforcement diameter 10 mm double helicoidal with a step of 30 cm.

The computed settlements for 4000 KN were less than 6 mm.

For the horizontal design spring constants were considered.
The ultimate limit states and the serviceability limit states were considered for vertical, horizontal and inclined loads.

For the quality control of the pile's integrity tests were performed in all piles to assess the existence of any discontinuity due to inflow of soil or other defects.

Direct load pile tests were not performed due to the difficulties related with the complexity of reaction frame, the costs and only 1-2 tests could be performed.

Figure 8.271 shows the equipment for piles construction.

Figure 8.272 illustrates a detail of pile reinforcement placement.

Figure 8.271 Equipment for piles construction

Figure 8.272 Detail of pile reinforcement placement

8.3.3.5 Horizontal Pile Load Tests

Test piles with 1.0 m of diameter and embedded in unit C, located near UMC structure were submitted to horizontal tests.
The piles cap had 1.2 x 1.2 x 0.5 m.
In order to avoid the group effects the piles axis were 6 m apart.

Figure 8.273 shows test pile instrumentation.

Integrity pile tests were also performed in order to control the quality of piles and no discontinuity or defects were detected.

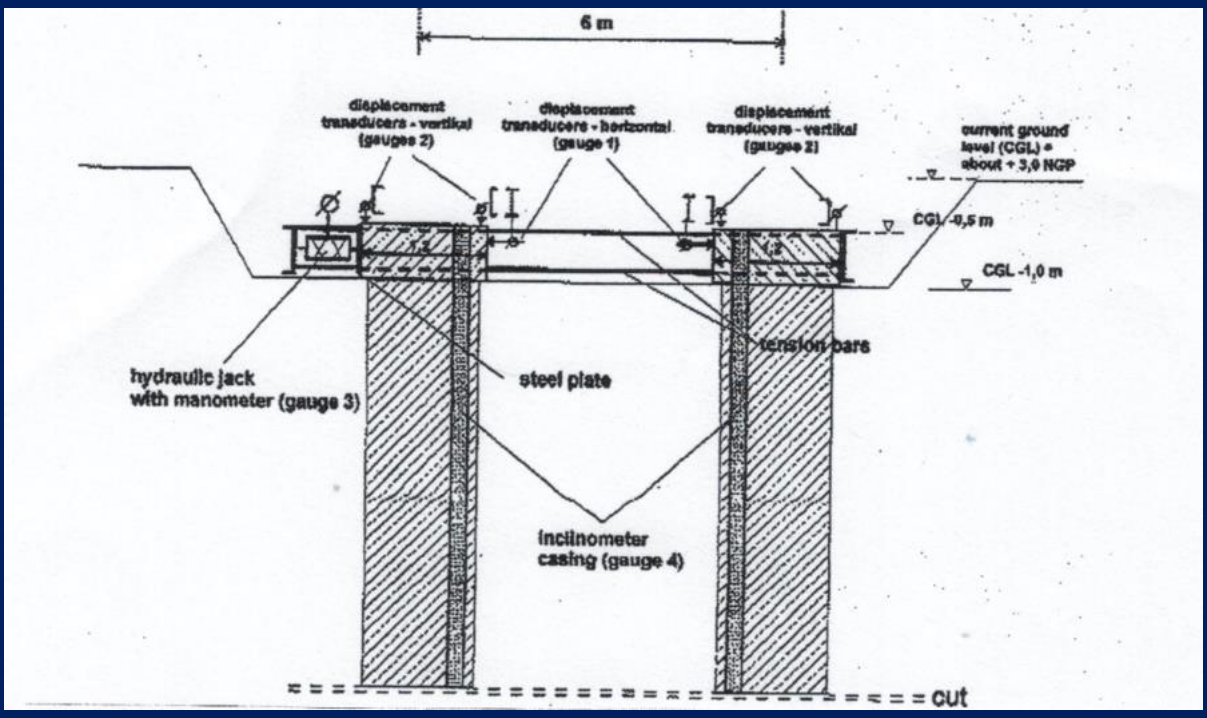

Figure 8.273 Test pile instrumentation

The surface displacements of the piles were determined using two displacement transducers vertical gauges and one displacement transducer horizontal gauge.

The rotation measurements and the determination of horizontal displacements along the shaft were performed by introducing of the digitilt in inclinometer tubed with 76 mm of diameter, attached to the reinforcement of the pile.

The piles have to be pulled towards each other with a tension reaction system and the loads were applied by a hydraulic jack that can reach a maximum values of 1000 bar.

The layout for reaction system and measurements devices is presented in Figure 8.274.

Figure 8.275 shows the results of integrity tests.

A tent was used to protect the measuring devices from wind, rain and sun radiation.

The following conclusions were drawn:

(i) A good behavior of the horizontal and vertical gauges, as well inclinometers were obtained;
(ii) A good agreement was obtained for the pie head horizontal displacements given by the gauges and the inclinometer tubes;
(iii) Due to some lack of pile cap disconnection from the surrounding soil the horizontal values measured by the gauges were different;
(iv) The horizontal load value of 560 kN can be associated to the failure of the pile.

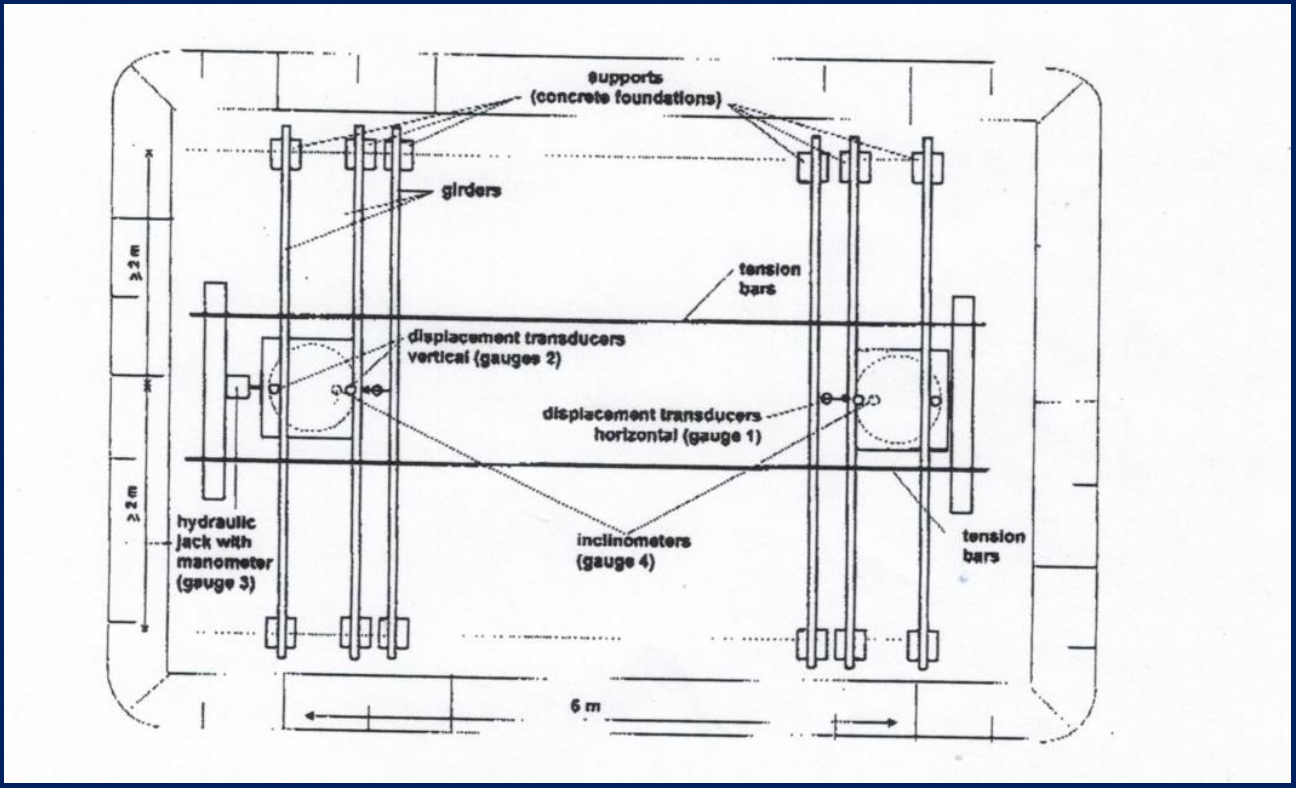

Figure 8.274 Lay-out system

Figure 8.276 illustrates a view of the horizontal pile test.

Figure 8.277 and Figure 8.278 show the system to apply loads to the pile and the measurement of applied loads.

Figure 8.279 exhibits the measurements of pile horizontal displacements with inclinometer.

Figure 8.280 and Figure 8.281 present the results of horizontal pile load tests nº 1and nº 2.

Figure 8.282 shows the pile tests team.

8.3.3.6 Pile Design under Seismic Loads

For the seismic pile design the recommendations of Eurocode 8- Part 5 were adopted and so the inertial forces transmitted to the foundation and the kinematic interaction arising from the dynamic forces loading the piles were separated and finally both effects were superimposed.
The determination of soil properties such as the variation of shear modulus and the damping ratio with shear strain was based in pr0oosals given by literature.
The evaluation of seismic displacement of ground level was based in the seismic response off ground for free field conditions.
The value of the moment computed at the pile head was added with the value transmitted by the superstructure for the design of pile reinforcement.

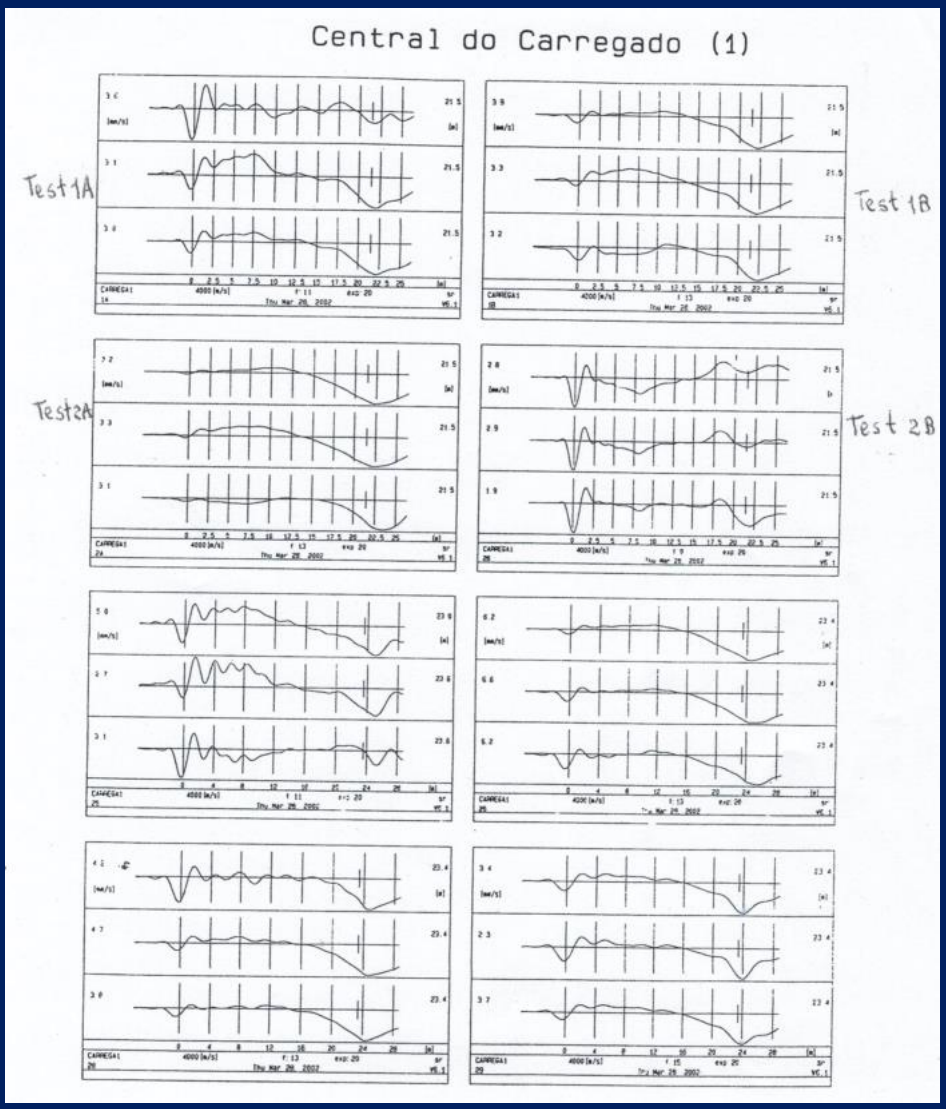

Figure 8.275 Results of integrity tests

Figure 8.276 View of the horizontal pile test

Figure 8.277 System to apply loads to the pile

Figure 8.278 Measurement of loads applied to the piles

Figure 8.279 Measurements of pile horizontal displacements with inclinometer

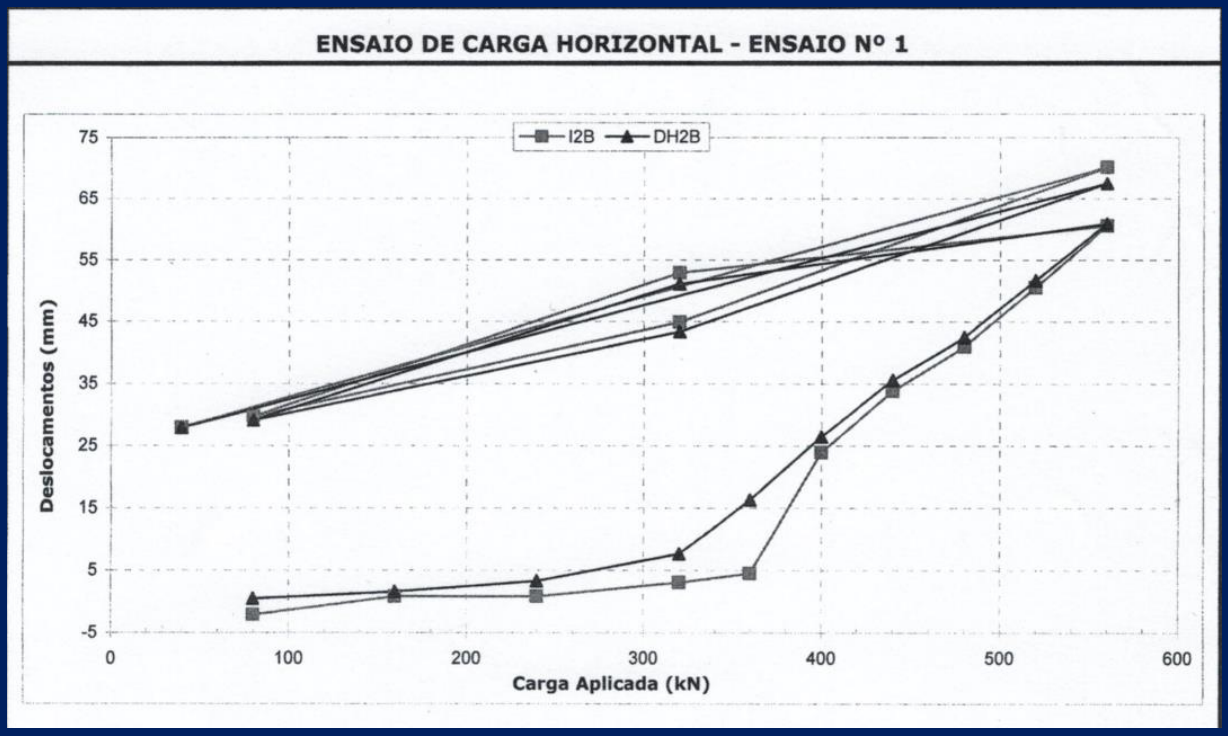

Figure 8.280 Results of horizontal pile load tests nº 1

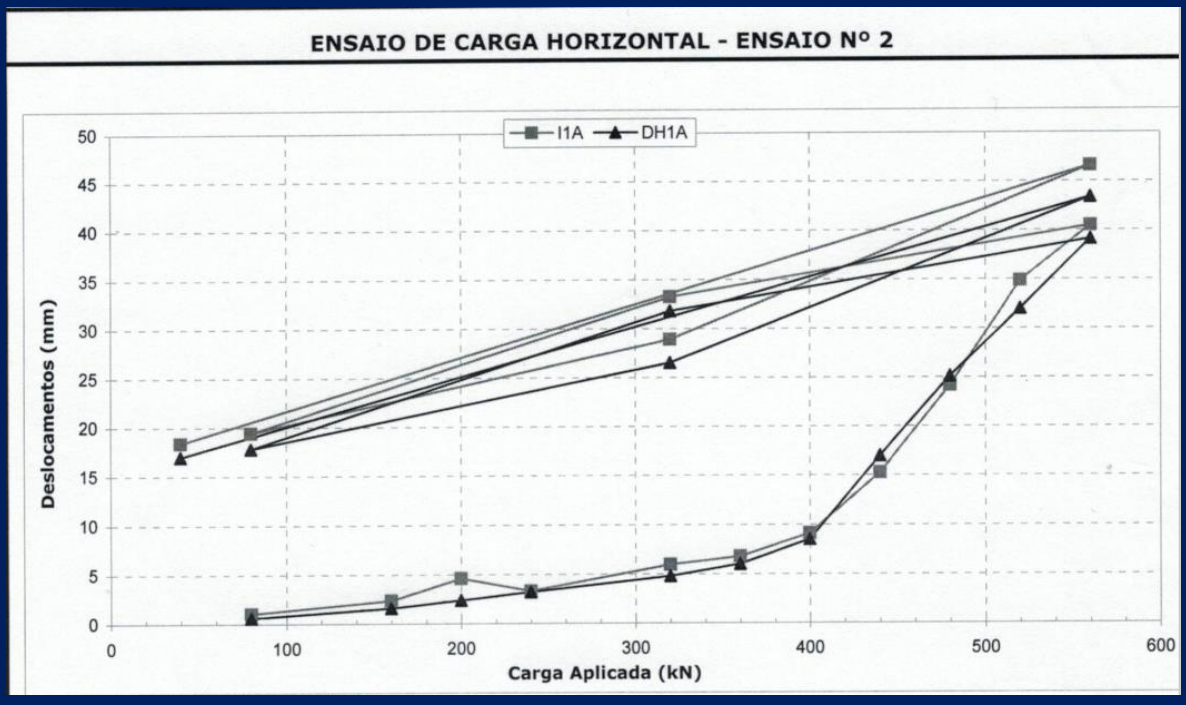

Figure 8.281 Results of horizontal pile load tests nº 2

Figure 8.282 Pile tests team

8.3.3.7 Dewatering of Excavations

The construction of foundations below the water table requires consideration. The dewatering system should be designed to keep the excavation under dry conditions 24 hours a day. The water extraction must be carefully controlled to comply with design situations.

Taking into account the cofferdam a mathematical model was implemented using finite elements in order to stablish the flow net and to compute the flows in different section. To check the assumed assumptions piezometers were installed in sufficient number at various depths to detect the important water changes and be able to control the stability of the foundation excavation.

8.3.3.8 COFFFERDAM

To perform the excavation under dry conditions it is necessary to use sheet -pile wall for lateral support of the excavation banks. The sheet-pile wall should have sufficient water tightness to avoid important percolation of water into the excavation and also should be sufficient rigid to support the earth and water pressures. The material used for the sheet-pile wall should be carefully defined taking into account the characteristics of the problem under consideration i.e. the temporally situation of the cofferdam and that the sheet pile needs to be removed.

The following limit states shall be considered for the design of the sheet – pile (Eurocode 7).

a) -Ultimate limit state design
– loss of overall stability
– failure of a structural element
– combined failure in ground and in structure element
– unacceptable leakage through or beneath the wall
– unacceptable transport of soil grains through or beneath the wall
- unacceptable change to the flow of groundwater.

b) Serviceability limit state design
– movements of the retaining structure which may cause collapse or affect the efficiency of the structure;
– settlements due to vibrations.

In order to reduce the seepage through rock material an impervious curtain shall be necessary.

8.3.3.9 Water Intake

Based in the information given by the boreholes and the CPTU tests, piles with 1.0 m of diameter and 25 m long were proposed for the foundation of water intake structure.
The pile design has combined the inertia forces transmitted by the superstructure with the kinematic forces due the propagation of seismic waves through the pile surrounding soil.

It was proposed the same pile reinforcement trough the length of the pile, due to the connections of the pile with the superstructure and bottom, and also the interfaces between ground material of different characteristics. Due to the increments of horizontal loads related with the seismic movements an increase of pile reinforcement for a length of 3D (D is the pile diameter) for each side of the interfaces is recommended. In summary the same reinforcement trough the length of the pile shall be used.

8.3.3.10 Construction Specifications

Requirements for piling work have covered materials, workmanship, bored piles cast in place, steel piles, pile installation control, pile testing,

Requirements for excavations were referred.

The specifications related the construction of embankments have covered the thickness of the layers, the placing of the materials, the density control and the compaction equipment's, geotextiles characteristics and drainage system.

For the construction control the laboratory and the field equipment's, as well the specifications to be respected were mentioned.

For shallow foundations and raft foundations the specifications for opening the excavations and other construction requirements were referred.

Requirements for piling work, namely materials, tolerances, nuisance and damage, workmanship, pile installation control, pile testing were described**.**

Components and equipment supported on embedded foundations and superstructures are not addressed explicitly in Eurocode nº 8.

Components and equipment directly supported on embedded foundations

For these components, the value of β= 0.32 (see RSA, 1983) can be considered when this equipment is located in current buildings.
For more complex structures such as turbines, cooling tower and boilers the value of power spectra compatible with the frequency value (for action type 1 and action type 2) shall be multiplied by factors related with soil amplification, importance of the structures and partial safety for seismic actions.

Components and equipment supported by superstructures

For the components supported by superstructures (current buildings) a value of β= 0.52 can be considered.
For more complex structures such as turbines, cooling tower and boilers the value of power spectra compatible with the frequency value (for action type 1 and action type 2) shall be multiplied by factors related with soil amplification, importance of the structures and partial safety for seismic actions.

To deal with these high acceleration values the general trend for foundations of machines is to avoid that operating frequencies of machines lie very close to the natural frequencies of the supporting structure in several of the vibrating modes, thus creating possible resonance conditions in the machine-foundation – system. In order to achieve acceptable vibration amplitude, it becomes necessary to make the structure very rigid so that the fundamental frequency of the structural system increase to a value above the operating machine frequency.
Another possibility is to assume an adequate seismic behaviour for the components and equipments.
For the computation of pile inertia forces as well for the lateral displacement of pile and head rotation discrete models can be used (based on Winkler model) or continuous model.

The lateral strength of layers susceptible to liquefaction should be neglected.

Note: This project was done for the Consortium Siemens/Koch.

8.3.4. Case History 13 - Sines Powerplant - Fan Structure Design

8.3.4.1 Introduction

The site investigation programme is described, the geotechnical model is introduced, the seismicity of the zone is presented, the structural types and behaviour factors of concrete buildings and steel buildings is addressed and the design of towers and chimneys is analysed.

8.3.4.2 Site Investigation

The purposes of this site investigation program were the following:

1) Definition and nature of different materials;

2) Seepage conditions through the foundation

3) Definition of soil physical indexes;

4) Determination of mechanical properties of ground materials such as strength and deformability;

5) Chemical analysis of water.

In situ Tests

Around 30 boreholes were performed, with depths between 15-25 m, in the boreholes SPT tests were performed with 1.5 m apart.

Samples were collected from the boreholes for the execution of laboratory tests, namely:

a) disturbed samples for classification tests.

b) water samples for the determination of carbonate content and water aggressivity.

Eleven seismic refraction profiles were performed and longitudinally wave velocities around 1200m/s were obtained above phreatic level and longitudinally wave velocities between 1500-1800 m/s were obtained beneath phreatic level.

Crosshole tests were performed in two zones until a depth of 15 m and the following results were obtained:

Pliocene soils
Shear wave velocities around 200m/s
Longitudinal wave velocities around 800 m/s

Schistous complex
Shear wave velocities between 800-1800 m/s
Longitudinal wave velocities between 1600-2900 m/s

Twelve penetrometers tests were performed in pliocene soils and the obtained values of point resistance were between 20-30 MPa.

Twenty five dilatometer tests distributed by 5 boreholes were performed by LNEC in the chimney and pumping station zones. The values of dilatometer modulus obtained for schist material were between 400 and 1800 MPa.

Six plate load tests were performed by LNEC in Pliocene soils and in spite the dispersion the average elasticity modulus is 24 MPa.

In some boreholes piezometers were placed and have shown a variation of water level around 2-3 m from wet to dry seasons.

Laboratory tests

The following identification tests were performed:
Grain size distribution;
Density;
Porosity;
Water content;
Atterberg limits;
Carbonate content;
Organic matter content.

A triaxial test type CU was performed in one sample from a trench at 4m of depth.

Chemical tests

pH: 8.16-8.36
Ammonia 0-0.17
Magnesium: 8.2-8.5
Sulphates: 21.6-25.3

On rock samples were performed joint tests, unit weight tests and unconfined tests.

8.3.4.3 Geotechnical Model

Pliocene deposits

The sandy materials exhibit a thickness between 2 to 9 m
The most representative SPT values of these deposits were between 20-60. For clay layers SPT ranging 8-15.
Natural water content from between 5.8% to 13.0% with an average value of 9.6%.
Natural unit weight from between 19-23 kN/m3

Unified classification SP-SM
% passing sieve # 200 (ASTM) 2 to 12 %
Liquid limit – No
Plastic index No
Proctor tests Maximum dry density= 18-20 kN/m3
Optimum water contents = 8-11%

Bedrock material

RQD: for schist rock from 20 to 95
Unit weight: 28.2-28.8 kN/m3

Porosity: 10-21%
Unconfined compression: 1.5-4 MPa
Joint tests
Cohesion: 50-80 kPa
Friction angle: 19º-28º
The rock was considered solid.

8.3.4.4 Seismicity

Several seismic risk maps have been developed for different countries and subsequently an application to Portugal is presented (Sousa Oliveira, 1976).
The following methodology was considered.

- Data: magnitude, depth of focus, type of fault mechanism, year, zone of seismicity for 692 earthquakes were recorded.
- For each zone of seismicity Richter's law and Poisson model were used.
- To compute acceleration, velocity, displacement and duration propagation formula according to magnitude, depth, type of fault, pattern of radiation was applied.
- Maximum annual values of displacement, velocity, acceleration and duration of all seismic events felt at the site were computed.
- A comparison of the results with the distribution obtained using the "zone of area sources" concept is done.
- Confidence levels were checked.

Figure 8.283 shows Portugal faults.
Figure 8.284 illustrates the earthquakes epicenters.

Seismic risk map of Portugal for maximum values of accelerations, velocity and displacement for a return period of 1000 years are presented in Figures 8.285 to 8.287.

Soil filtering must be considered in the seismic risk analysis and it requires mainly the determination of the natural frequency of vibration of the soil layers above the bedrock. So, the values of acceleration, velocity and displacement obtained by the above seismic risk maps should be considered at the bed-rock level.

For the definition of the seismicity of the zone the understanding of the seismotectonic model is very important.
For earthquake resistant structural design, it is essential to perform an accurate evaluation of input ground motion combining deterministic and probabilistic approaches.
RSA and Eurocode nº 8 were adopted and for the seismic motion was used for MCE a value of 0.25 g and for OBE a value of 0.15g.

An O.B.E. is an event that may reasonable be expected during the lifetime of the structure. The structure must continue to function during and after such an event and thus the loading is classed as "unusual". A full

definition of this loading includes a usual static load, because such an earthquake, will occur in combination with self-weight, temperature, silt and hydrostatic load.
An M.C.E. event is defined to correspond with the most extreme earthquake action that can reasonably be expected at that site. The structure must withstand the event in such a way that repairs can be undertaken in a reasonable length of time and, more importantly, that no loss of life occurs for example due to a major flood. An M.C.E. event is classed as an "extreme loading".

8.3.4.5 Foundations Design

For the fan structures shallow foundations were used, and ultimate limit states and the serviceability limit states were analysed.

The following limit states were verified:
a) - Ultimate limit state design
   - loss of overall stability
   - bearing resistance failure
   - failure by sliding
b) - Serviceability limit state design
   - settlements: immediate and delayed settlements
   - excessive heave
   - settlements due to vibrations.

For the seismic analysis of fan foundations, a methodology to include the non linear soil behaviour was used.

Because the strict deflection tolerances required usually settlement and deflection considerations rather than bearing capacity govern the allowable foundation stresses on the subsoils. The layout and design foundation are usually governed by the dynamic requirements.

To incorporate accurate frequencies of the machine-foundation system, the effect of soil-structure interaction was taken into account and to represent foundation soil springs were used.

The fundamental objective of a dynamic soil-structure interaction study is to estimate the motions of one or more foundation buildings at a specific site, from a known free field seismic environment. Accordingly, a complete interaction analysis necessarily involves firstly the determination of the temporal and spatial variations of the free field motions and secondly, the evaluation of the motions of the foundation-building system placed in the free field seismic environment.

The interaction between a vibrating foundation-building system and its supporting medium produces basically two mechanisms that modify free field ground motions. One is due to the base shears and overturning moments induced by the structure’s own vibration which, in turn, give rise to soil deformations of increasing magnitude as soil compressibility becomes higher. This mechanism is usually referred to as inertial interaction. The other, known as kinematic interaction, develops when any or a combination of the following conditions exist: i) embedded foundation elements are stiffer than the surrounding soil, ii) inclined wave trains impinge on the foundation, and iii) ground motions are incoherent. The influence of these two interaction mechanisms can be analyzed using either the substructure (impedance or continuum) technique or the complete (direct) approach.

The following 4 modes of vibration were analysed:

Vertical mode :

Horizontal mode

Rocking mode

Torsion mode.

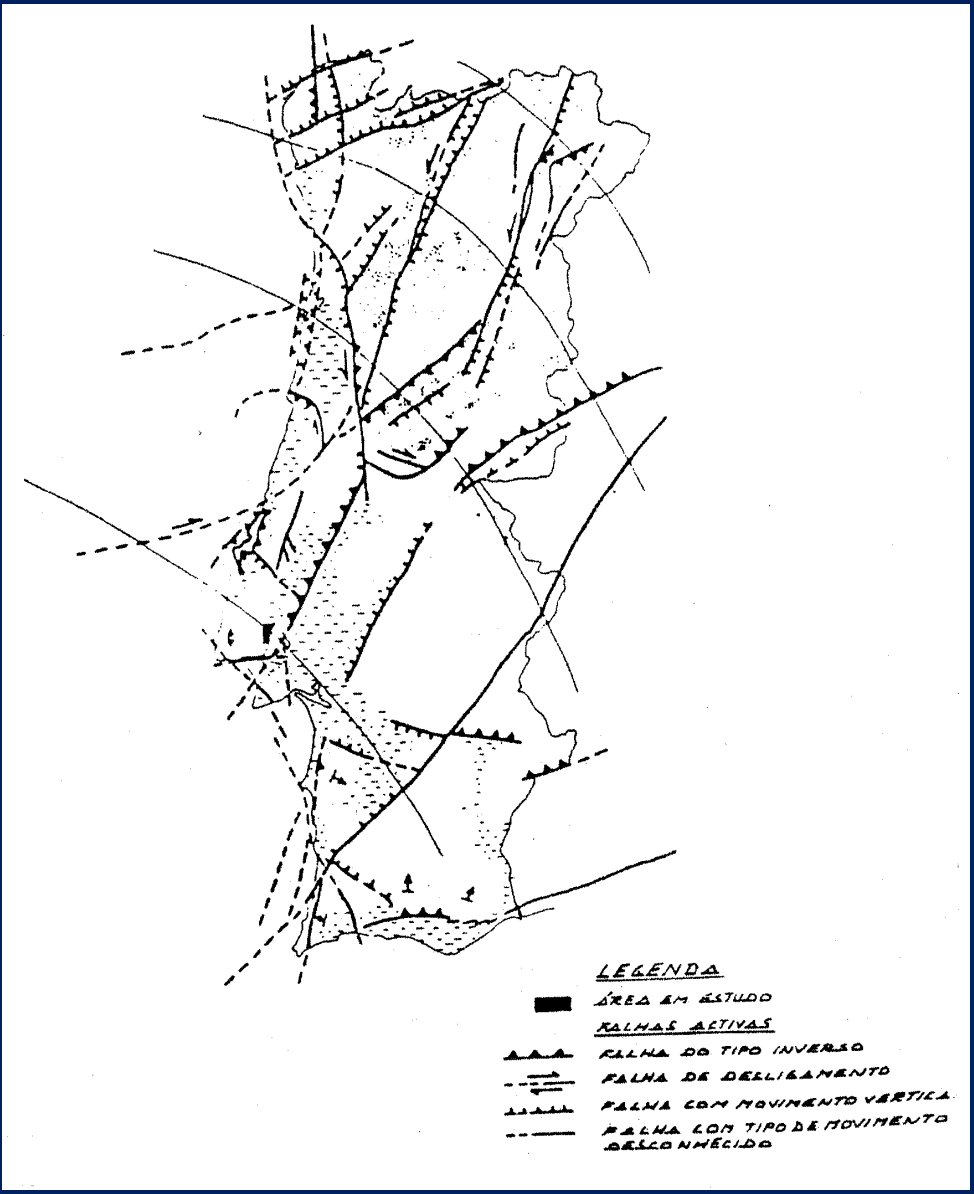

Figure 8.283 Portugal faults (after Sousa Oliveira, 1976)

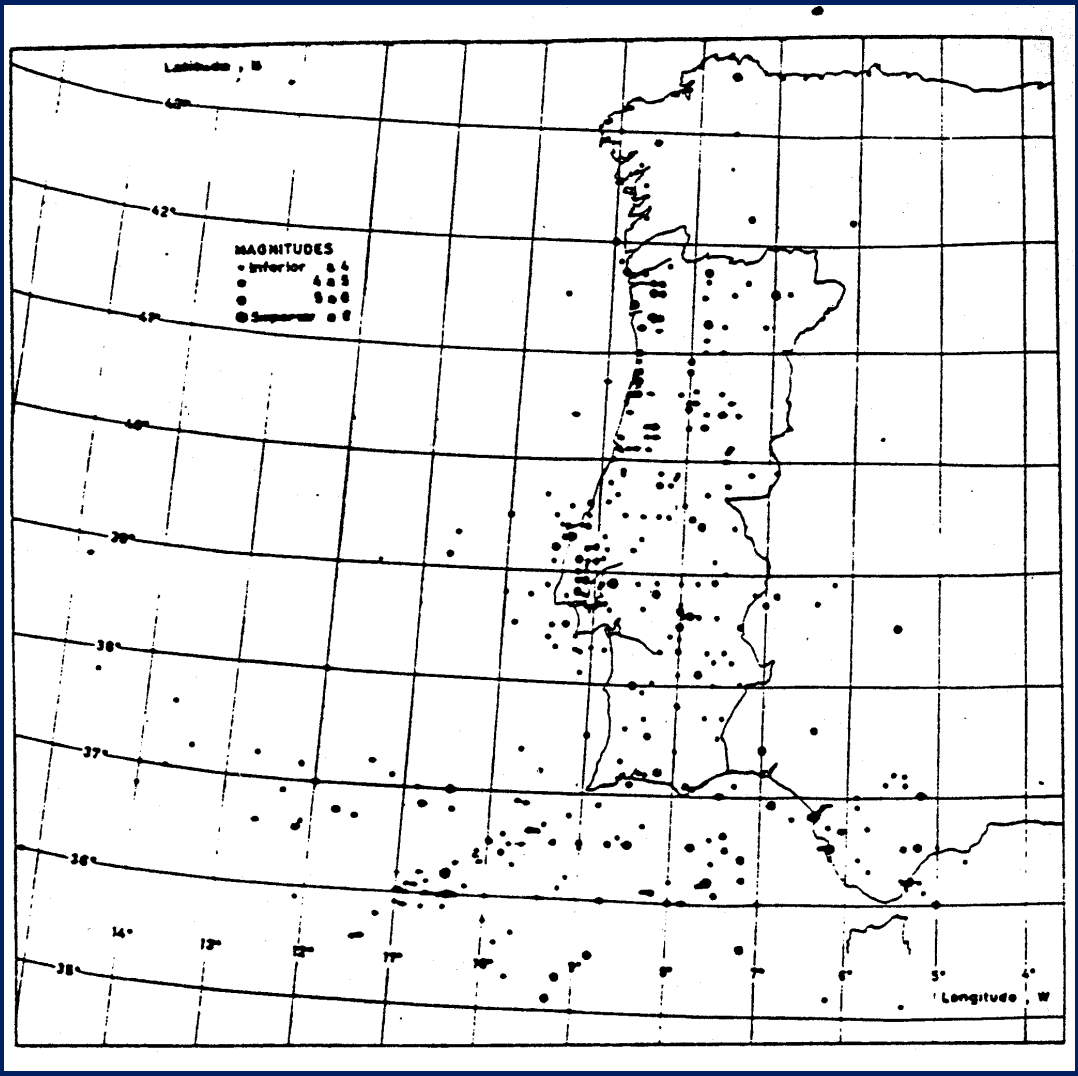

Figure 8.284 Earthquakes Epicenters (after Sousa Oliveira, 1976)

Figure 8.285 Acceleration Map (after Sousa Oliveira, 1976)

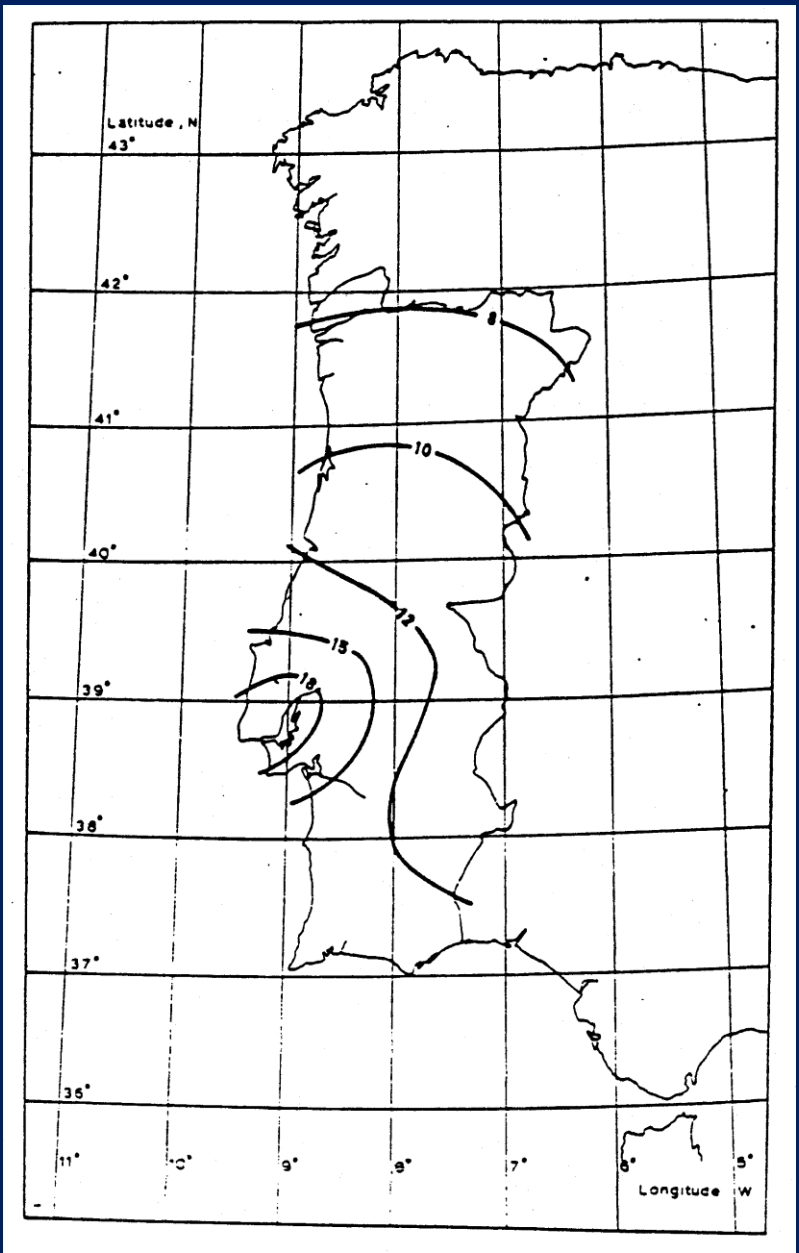

Figure 8.286 Velocity map (after Sousa Oliveira, 1976)

One important task in the foundation design is to avoid a resonant condition between frequencies of machine and machine-foundation system. If a resonant condition occurs the responses of the machine will be greatly amplified.

The effects of the existent neighbouring structures, namely boilers, in order to avoid detrimental effects were analysed.

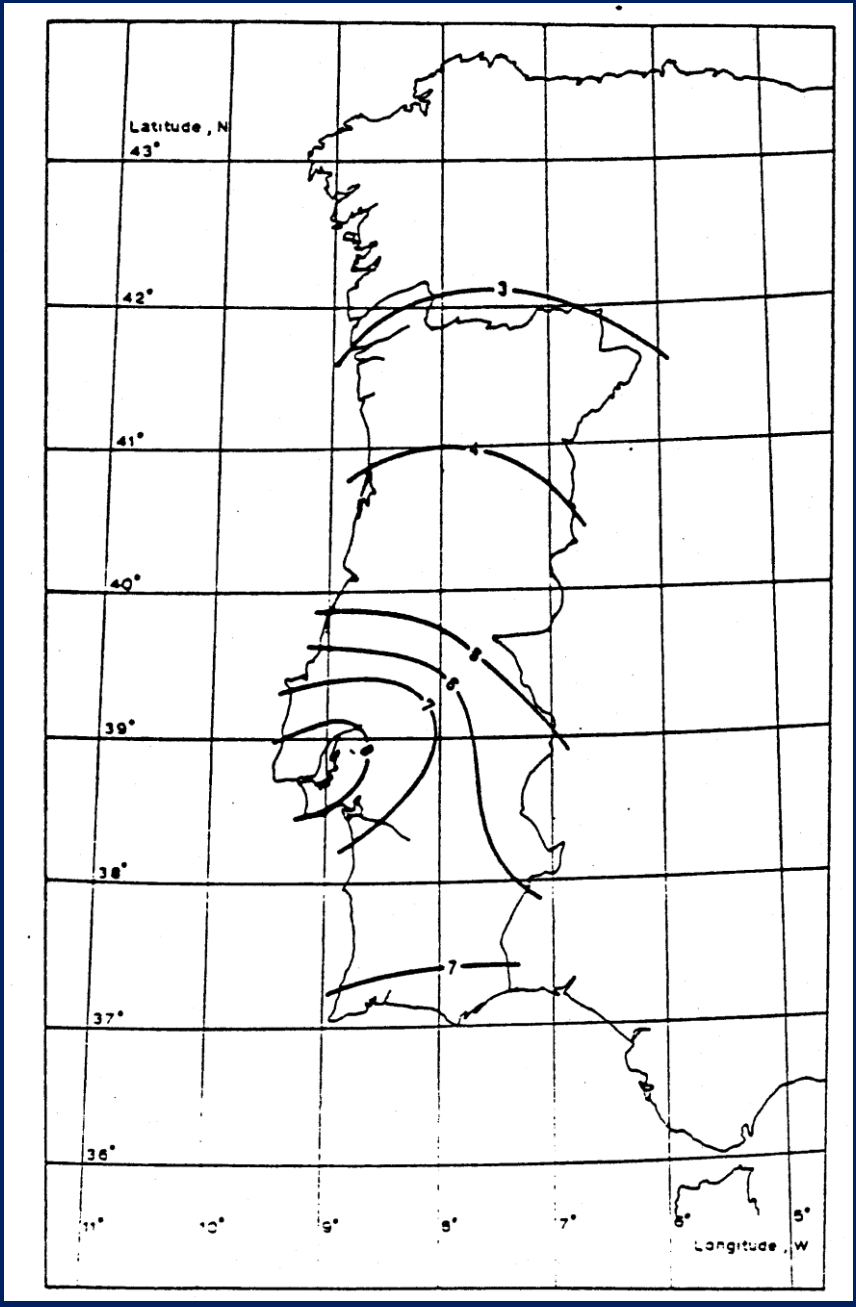

Figure 8.287 Displacement map (after Sousa Oliveira, 1976)

Figure 8. 288 presents the location of structures of Unit 2.

Figure 8. 289 illustrates the location of SCR system.

Figure 8.290 and 8.291 shows the location of foundations related unit 1 and 2 and unit 3 and 4, respectively.

For the concrete buildings and steel buildings the following recommendations should be followed.

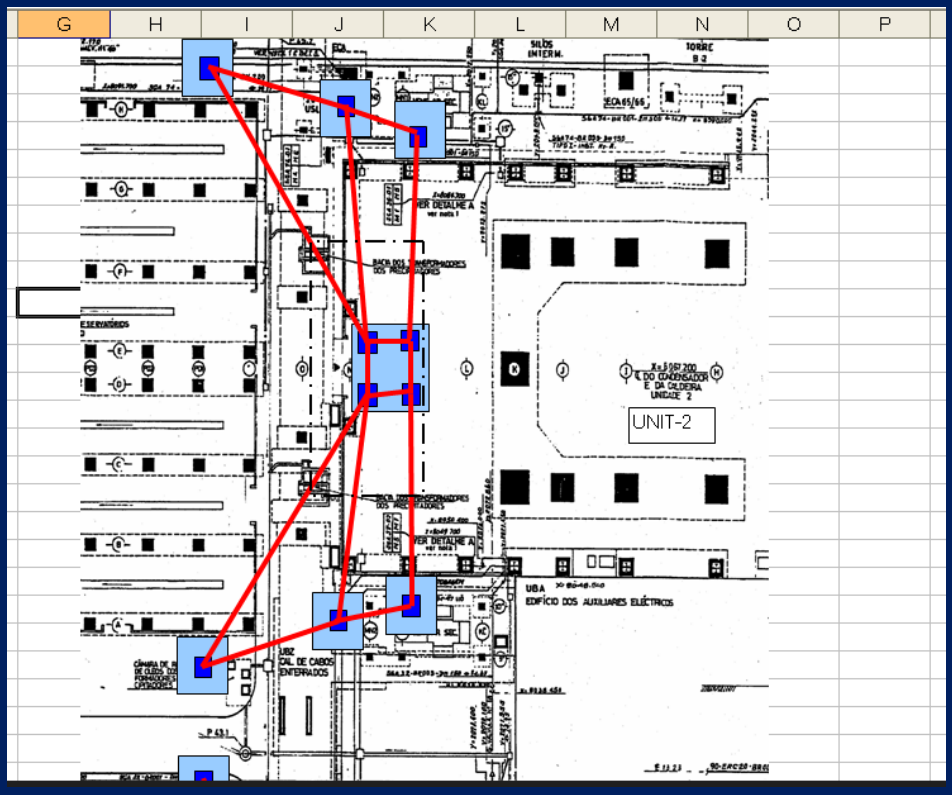

Figure 8. 288 Location of structures of Unit 2

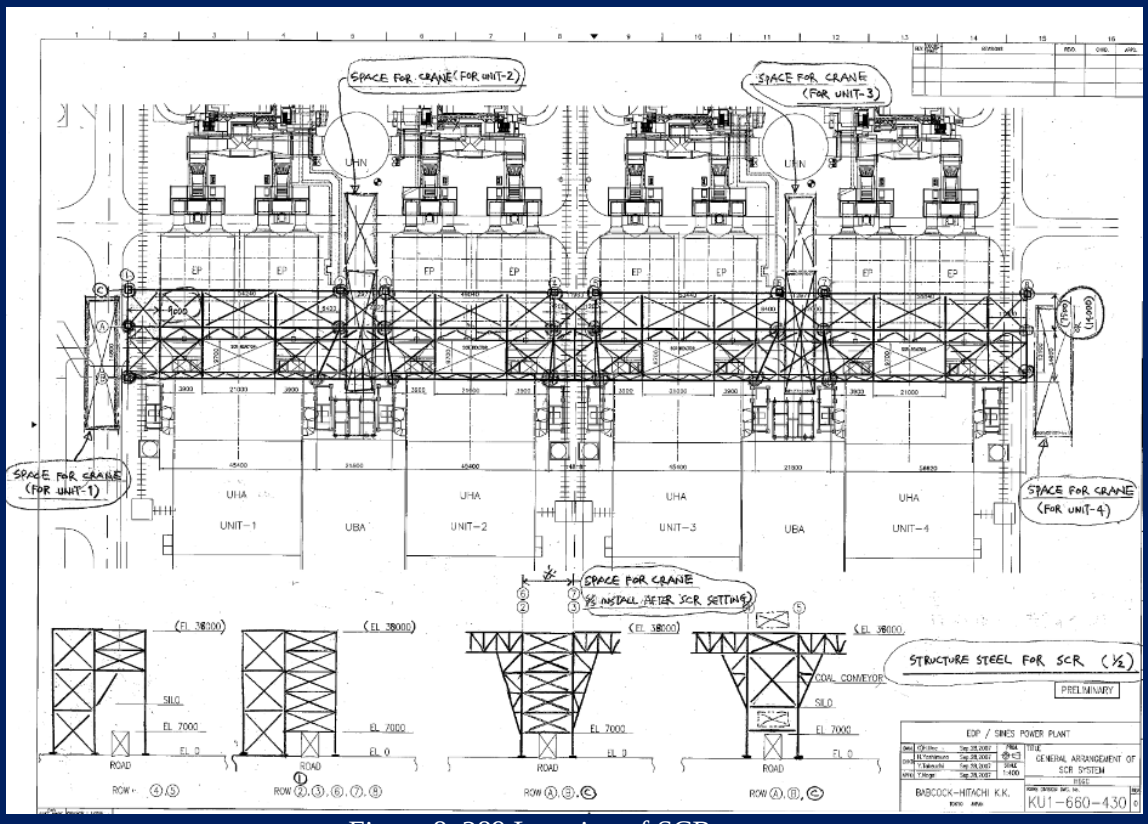

Figure 8. 289 Location of SCR system

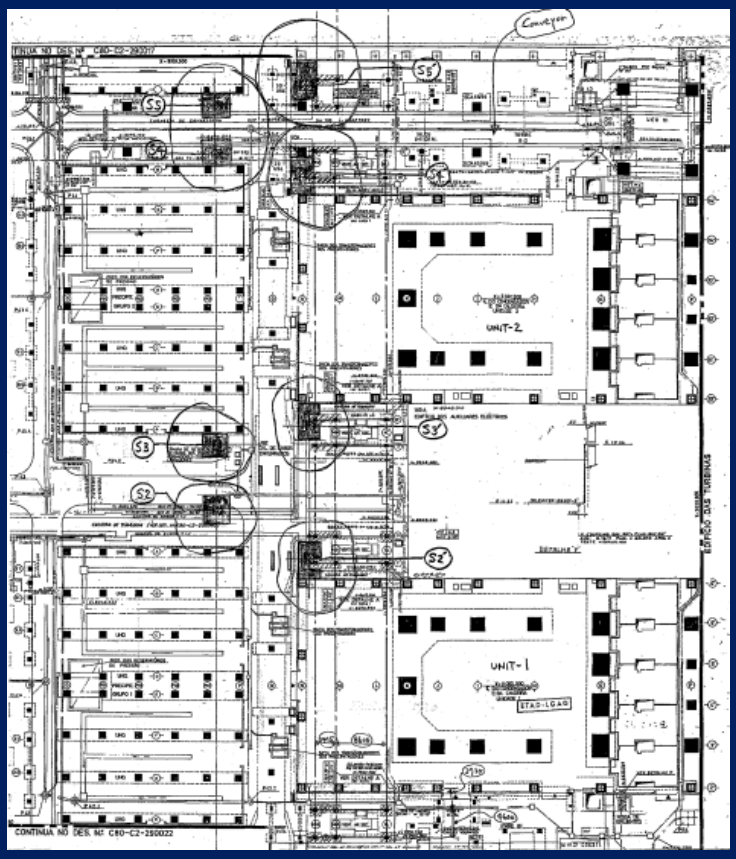

Figure 8.290 Location of foundations – unit 1 and unit 2

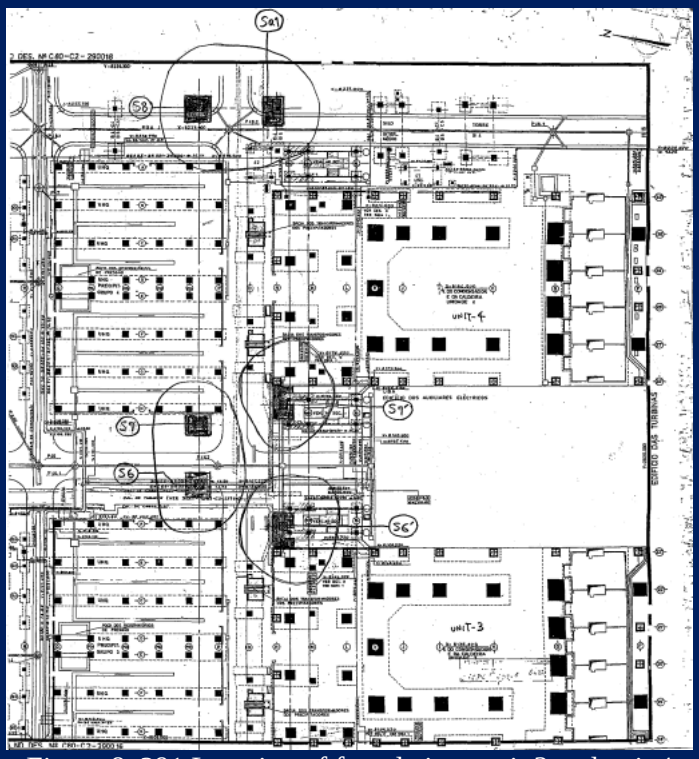

Figure 8. 291 Location of foundations unit 3 and unit 4

8.3.4.6 Concrete buildings

The design of earthquake resistant concrete building shall provide an adequate energy dissipation capacity without substantial reduction of overall resistance against horizontal and vertical loading (Eurocode 8, 1998).

With regard the hysteretic dissipation capacity the following classes can be considered:
(i) DC L –structures design according Eurocode 2 supplemented by rules enhancing available ductility
(ii) DC M – structures design according specific earthquake resistant enabling to enter within the inelastic range under repeated reversed loading without suffering brittle failures,
(iii) DC H- structures designed to seismic excitation to develop stable mechanisms associated with large dissipation of hysteretic energy.

The behavior factor q for energy dissipation capacity shall be obtained by:

$$Q = q_0 \, k_D \, k_R \, k_W > 1{,}5 \qquad (8.40)$$

Where
q_0 is the basis values of behaviour factor
k_D factor reflecting the ductility
k_R factor reflecting the structural regularity
k_W factor reflecting the prevailing mode of failure.

The basic value q_0 of behaviour factor are in Table 8.39.

Table 8.39 Basic values of q_0 of behaviour factor

Structural Type	q_0
Frame system	5.0
Dual system- frame equivalent	5.0
Dual system- wall equivalent, with coupled walls	5.0
Dual system- wall equivalent, with uncoupled walls	4.5
Wall system- with coupled walls	5.0
Wall system- with uncoupled walls	4.0
Core system	3.5
Inverted pendulum system	2.0

The values of k_D shall be taken as the following:
1,0 for DC H
0,75 for DC M
0,50 for DC L

The values of k_R shall be taken as the following:
1,0 for regular structures
0,80 for non regular structures

The values of k_W shall be taken as the following:
1,0 for frame and frame equivalent dual systems
$1/ (2.5\text{-}0.5 \, \alpha_{0)}$ for wall, wall equivalent and core systems

α_0 prevailing aspect ratio height of wall /length of the section

8.3.4.7 Steel buildings

Earthquake resistant steel buildings shall be classified in 2 categories (Eurocode 8):

a) Dissipative structural behaviour- with the capability of parts of structure to resist earthquake actions out of their elastic range. The behaviour factor q is taken greater than 1,0.
b) Non dissipative structural behaviour- the actions effects are calculated on the basis of an elastic global analysis without taking into account non linear material behaviour and the behaviour factor q is taken equal 1,0.

The behaviour factor q for energy dissipation capacity takes the values given in Figs.18 and 19.

If the building is non regular in elevation the q values listed in Figs 18 and 19 shall be reduced by 20%, but not be taken less than 1,0.

For regular buildings in zones of low seismicity having structural systems made from rolled sections or from welded sections a behaviour factor equal to 1,5 may be adopted.

α_1 multiplier of the horizontal design seismic action, while keeping constant all other design actions, which corresponds to the point where the most strained cross-section reaches its plastic moment resistance

α_u multiplier of the horizontal design seismic action, while keeping constant all other design actions, which corresponds to the point where a number of sections reach their plastic moment resistance.

When calculations are not performed in order to evaluate the multiplier α_1 the approximate values of the ratio α_1 / α_u presented in Figs 18 and 19 may be used.

The ratio α_1 / α_u should be limited to 1.6

8.3.4.8 Towers and Chimneys

For ultimate limit state the structures shall be designed in order to retain, with appropriate reliability, its structural integrity with respect both vertical and horizontal integrity, after the occurrence of the design seismic event.

For serviceability limit state the structure shall be designed that in the event of an earthquake, with an intensity of a return period comparable with the design life of the structure, damage shall be prevented in the structural itself, in the non structural elements and in the installed equipment.

The behaviour factor q is given by the equation:

$$Q = q_0 \, k_r > 1,0 \qquad (8.41)$$

where:
q_0 basic behaviour factor

k_r modification factor
Figures 8.292 and 8.293 present the structural types and behaviour factors.

The values of behaviour factor q_0 are shown in Table 8.40 (Eurocode 8, 1998).

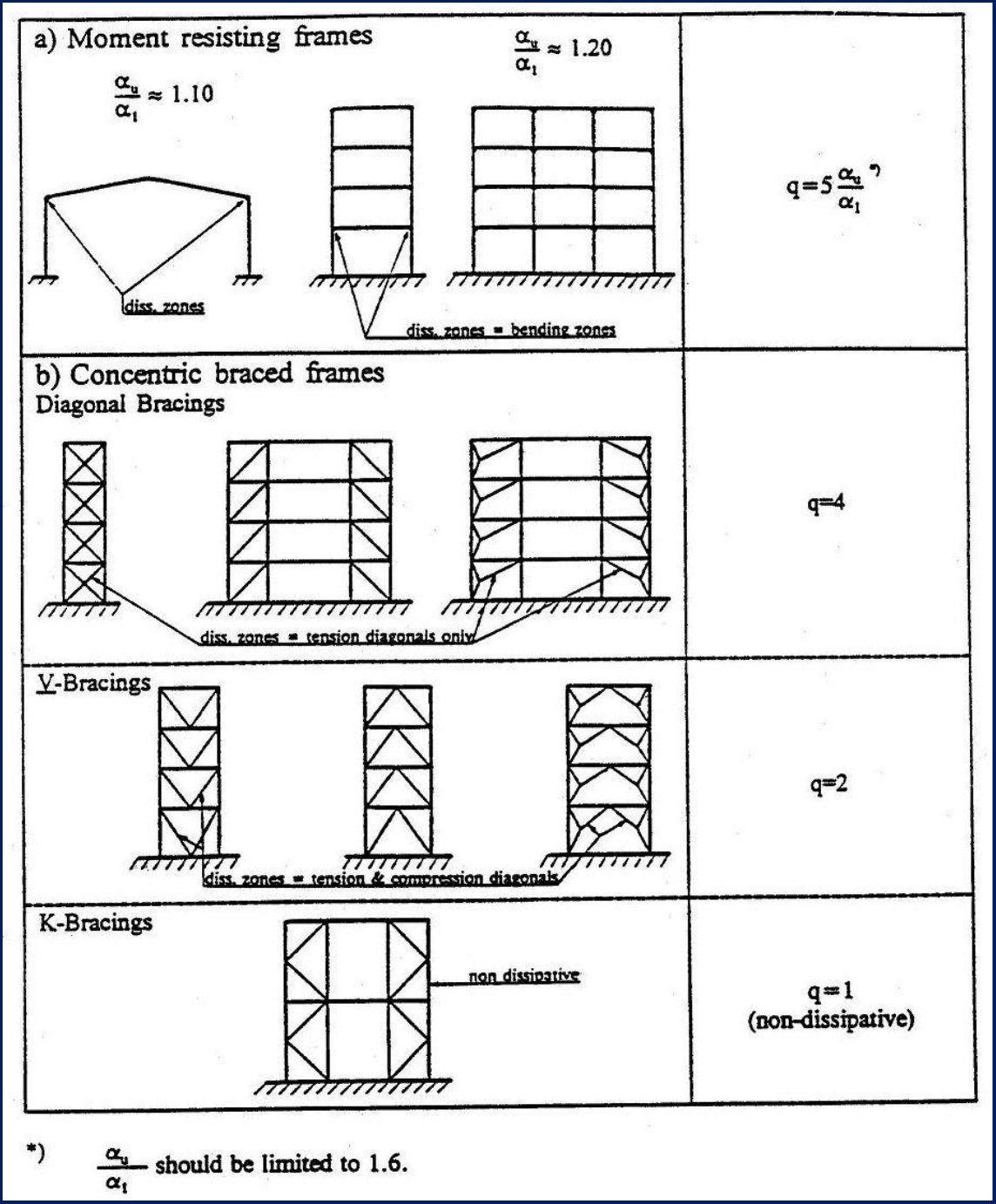

Figure 8.292 Structural types and behaviour factors (after Eurocode 8, 1998)

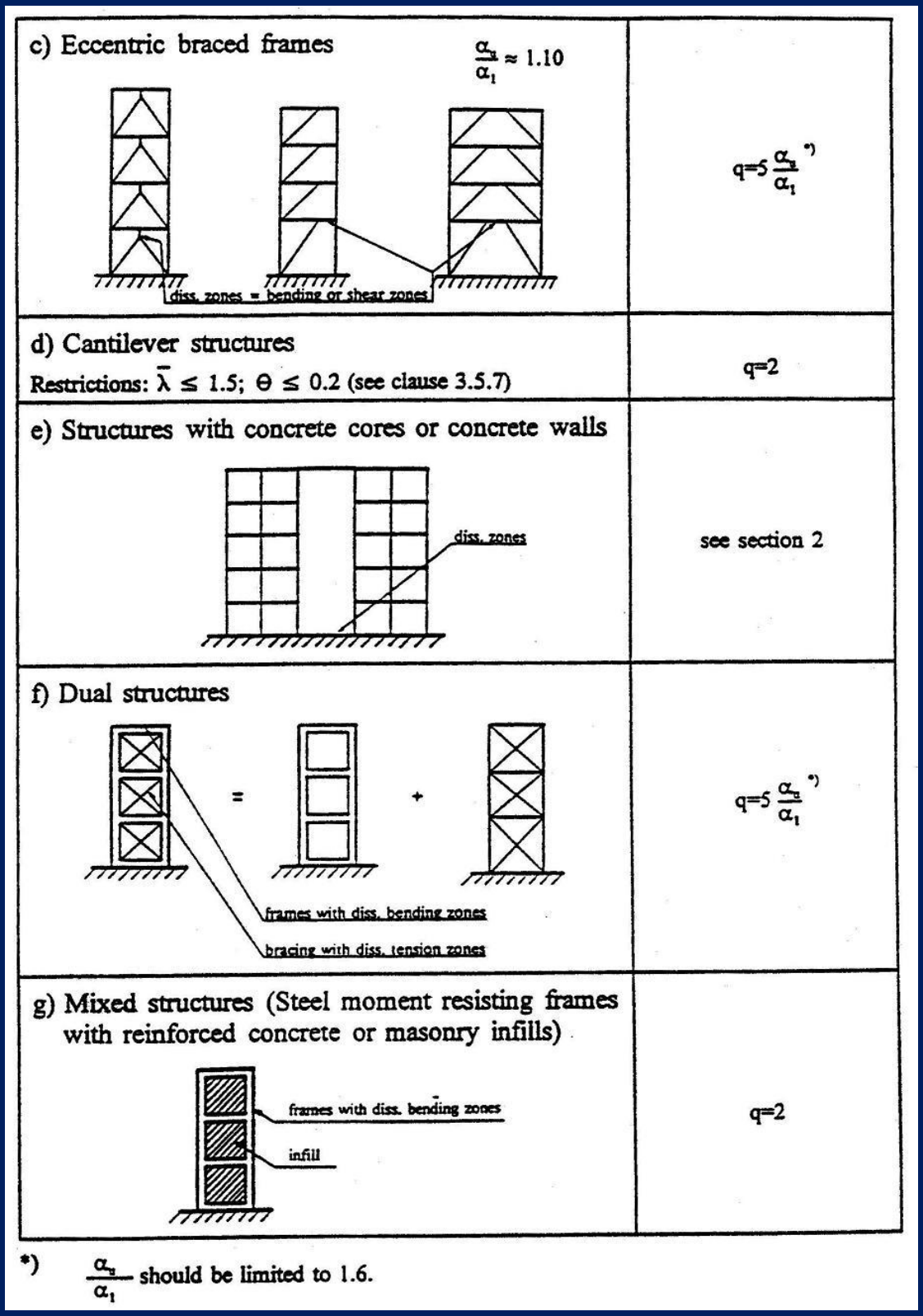

Figure 8.293 Structural types and behaviour factors (after Eurocode 8, 1998)

Table 8.40 Values of basic behaviour factor q_0

Structural Type	q_0
Concrete towers and chimneys when shear type or other brittle failures modes are excluded	3
Concrete towers and chimneys when openings in shafts cause a 30% or larger reduction in bending or shear strength of the cross section in relation to the adjacent ones	1
Steel frames or truss structures of towers designed for dissipative behaviour with moment resisting frames or frames with eccentric bracing	4
Steel frames or truss structures of towers designed for dissipative behaviour for frames with concentric diagonal bracings	3
Steel frames or truss structures of towers designed for dissipative behaviour for frames with V-bracings	2
Structures not designed for dissipative behaviour	1
Structures with cross section satisfying the requirements for plastic global analysis	2
All other structures	1

The values of factor k_r are shown in Table 8.41.

Table 8.41 Values of factor k_r

Horizontal mass eccentricity at a section exceeding 5% of the relevant structure dimension	$k_r = 0.80$
Openings in shaft causing a 30% or larger reduction of the moment of inertia of the cross – section	$k_r = 0.80$
Concentrated mass within the top third of the height contributing 50% or more to the base overturning moment	$k_r = 0.70$
When more than one irregularity is present	k_r equal the product of the two lowest values of k_r

The values related the important factor γ_I are shown in Table 8.42.

Table 8.42 Related the important factor γ_I

For structures whose operation is of strategic importance, in particular if it is a vital component of a water supply system, an electric power plant or a communication facility	$\gamma_I = 1.4$
For structures for the height of which is greater than the distance from the surroundings buildings, for structures built in an area likely to be crowded, or for structures whose collapse may cause shutdown of industries	$\gamma_I = 1.2$

For structures higher than 80 m, not pertaining to the above categories	$\gamma_I = 1.1$
For the remaining cases	$\gamma_I = 1.0$

Towers and chimneys are sensitive to the long components of the seismic excitation.

The model shall include a discretization of the masses so that a suitable representation of the inertia forces is ensured.

The mathematical model shall incorporate: i) rocking and translational stiffness of foundations; (ii) an adequate number of masses and degrees of freedom; (iii) the mass and stiffness of cables and guys; (iv) the relative displacement among supports of equipment or machinery, (v) significant effects such as piping interaction, externally applied structural restraints, hydrodynamic loads; (vi) torsional stiffness of the foundation; (vii) electric transmission towers.

The standard method of analysis is the linear analysis using the q reduced design spectrum either as simplified dynamic analysis or a multimodal analysis.

Nonlinear methods of analysis are also allowed provided that the provisions of EC8 are respected.

The design earthquake motion is defined at the soil surface, i.e. in free field conditions.
The modeling methods of soil structure interaction should consider: (i) the extent of embedment, (ii) the depth of the possible bedrock; (iii) the layering of the soil strata; (iv) the intrinsic variability of the soil moduli in any single stratum, (v) the strain-dependence of soil properties related shear modulus and damping.

Strain dependent, damping and shear moduli for each soil layer should be consistent with the effective shear strain expected during the excitation. Assuming equivalent linear method in each iteration the analysis is linear but the soil properties are adjusted from iteration to iteration in order to compatibilize the soil properties.

Lesson nº 13 The fundamental objective of a dynamic soil-structure interaction study is to estimate the motions of one or more foundation buildings at a specific site, from a known free field seismic environment. Accordingly, a complete interaction analysis necessarily involves firstly the determination of the temporal and spatial variations of the free field motions and secondly, the evaluation of the motions of the foundation-building system placed in the free field seismic environment.

The interaction between a vibrating foundation-building system and its supporting medium produces basically two mechanisms that modify free field ground motions. One is due to the base shears and overturning moments induced by the structure's own vibration which, in turn, give rise to soil deformations of increasing magnitude as soil compressibility becomes higher. This mechanism is usually referred to as inertial interaction. The other, known as kinematic interaction, develops when any or a combination of the following conditions exist: i) embedded foundation elements are stiffer than the surrounding soil, ii) inclined wave trains impinge on the foundation, and iii) ground motions are incoherent.

The influence of these two interaction mechanisms can be analyzed using either the substructure (impedance or continuum) technique or the complete (direct) approach.

In the substructure procedure the soil-structure system is usually divided in two parts: i) a finite region which encircles all the geometric irregularities, the structure, and the nearby soil that might experience inelastic behavior, and ii) the half space that is outside of the generalized soil-structure interface, that is modeled with frequency dependent impedance functions.

Note: This study was performed for EDP (Electricity of Portugal).

8.3.5 Case History 14 - LARES Powerplant

8.3.5. 1 Introduction

The site investigation programme is described, the geological characterization is introduced, the geotechnical characteristics are referred, the definition of design earthquake is presented, the design of spread and raft foundations is addressed, pile design under vertical and horizontal loads is analysed, pile design under seismic loads is presented, the pile quality control, dewatering, liquefaction assessment and slope stability are addressed.

8.3.5.2 Site Investigation

A campaign with 25 boreholes was performed, with boreholes length between 9,0 m to 37,5 m. In 4 boreholes hydraulic piezometers were installed. Also 6 permeability tests.

In these boreholes 358 SPT tests were performed 1.5m apart, the phreatic level was measured and disturbed samples were taken for soil classification.

Also 19 refraction tests and 5 geoelectric tests were performed.

For the determination of the soil pollution two samples were taken in two holes.

Later in July-August 2000, for a better knowledge of ground material to design the foundations of the new powerplant has performed a 2 nd campaign with 5 boreholes with length between 24.05 m to 25.62 m and a total length of 135.38 m.

In these boreholes SPT tests were performed 1.5m apart, the phreatic level was measured and disturbed samples were taken for soil classification.

For each borehole the log presents the following information:

. depth of drilling;
. depth of the water level and its variation;
. depth of different layers;
. depth of soil sampling;
. depth of the SPT tests;
. placement of piezometer (if is the case).

The following identification tests were performed:
Grain size distribution;
Density;
Porosity;
Water content;
Atterberg limits;
Carbonate content ;
Organic matter content.
In addition, uniaxial tests were performed

For the 1D consolidation tests the samples were submitted for the following pressures: 27, 55, 100, 200, 400 e 800 kPa, and each step will be maintained during 24 hours with drainage at top and bottom.

The purposes of this site investigation program were the following:

1. Definition and nature of different materials;
2. Seepage conditions through the foundation
3. Definition of soil physical indexes;
4. Determination of mechanical properties of ground materials such as strength and deformability;
5. Chemical analysis of water.

8.3.5.3 Geological Materials

Industrial wastes

These materials with thickness that can reach 5 m are composed by axes and other wastes sandy-clay materials with gravels.

Fills materials

These materials are composed by sandy gravels with thickness around 2-4m.

Alluvial materials

Are composed by sandy materials and by sandy materials with mud. The thickness of these materials is higher near the river Mondego with a value around 35m.
In the initial first 15 m in general these materials exhibit a very low compacity.

Cretaceous unit

Are composed by calcareous and calcareous with marnes with quality varying from weathered to compact materials.

This unit was considered as bedrock and all the boreholes have terminated.

8.3.5.4 Geotechnical Characteristics.

Industrial wastes

The sandy silty clay materials

Unified classification GP-GM and MH

% passing sieve # 200 (ASTM) 11 to 83%

Liquid limit NP to 82%

Plastic index NP to 12%

Natural water content 9,0 to 17.6%

Alluvial materials

The clay silty sand materials

Unified classification CH, CL-ML

% passing sieve # 200 (ASTM) 76 to 89%

Liquid limit 23 to 98%

Plastic index 5 to 41%

Natural water content 40.4 to 76.5%

Elasticity modulus: 2-6 MPa

Poisson ratio: 0.3-0.35

Cohesion = 0

Friction angle = 24 -28º

k (permeability coefficient) = 10^{-7} m/s.

SPT results were between 1 and 13 blows.

Alluvial sandy material

Unified classification GM-GP
% passing sieve # 200 (ASTM) 5 to 45%
Liquid limit NP
Plastic index NP
Natural water content 9,3 to 44,6%
Cohesion = 0
Friction angle = 26 -32º

k (permeability coefficient) = 10^{-4} to 7.5 x10^{-5} m/s.
SPT results were between 1 and 15 blows.

Cretaceous unit

For this unit by calcareous and calcareous with marnes the SPT values were > 60 blows.

Figure 8.294 shows the geotechnical profile with location of some boreholes.

8.3.5.6 Design Parameters

Introduction

After a balance between the results of the field tests and laboratory tests and based in correlations from literature well accepted the following mechanical properties can be considered.

Alluvial material

The clay silty sand materials

The most representative SPT values of this material are between 1 and 13.

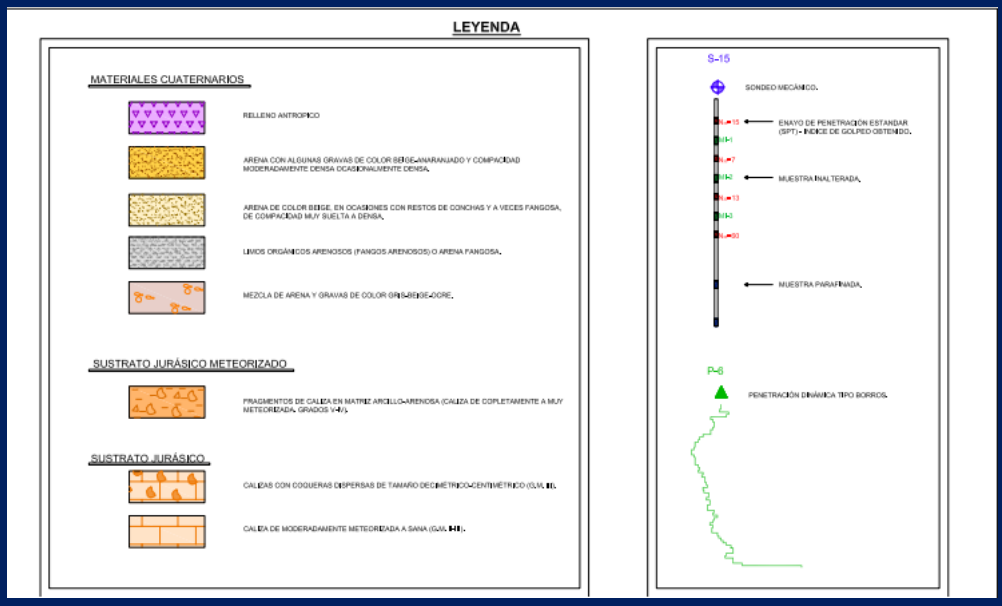

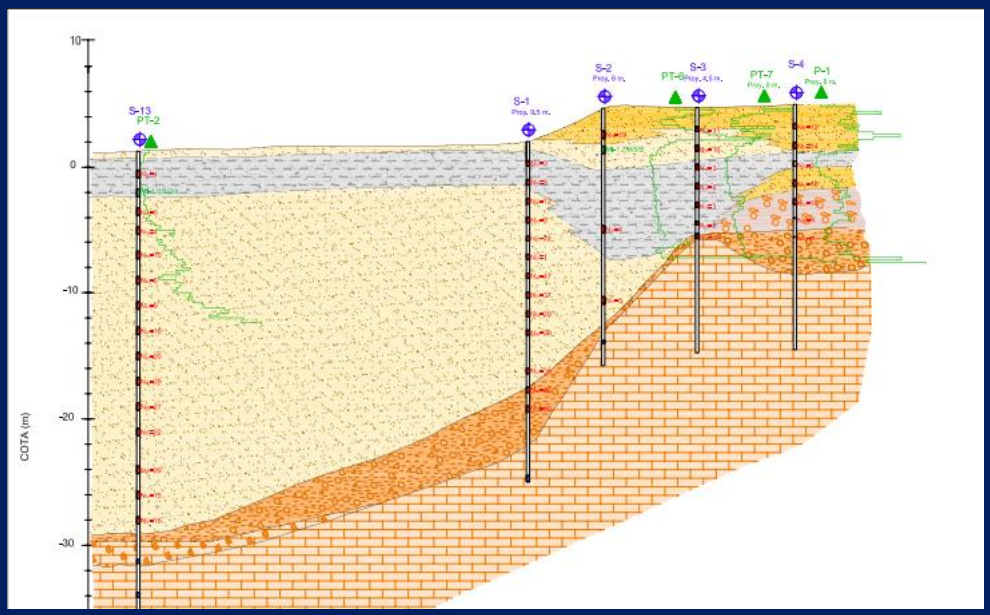

Figure 8.294 Geotechnical profile with location of some boreholes

Friction angle: 24-28º

Elasticity modulus: 2-6 MPa

Shear modulus (dynamic situations) 15-40 MPa

Subgrade reaction: (0.8-1.0) x 10^4 kN/m3 x depth (in meters)
Poisson ratio: 0.35 - 0.4

k (permeability coefficient) = 10^{-7} m/s.

Alluvial sandy material

The most representative SPT values of this material are between 1 and 15.

Friction angle ϕ (in effective stresses) = 26 to 32º

Elasticity modulus: 2-12 MPa

Shear modulus (dynamic situations) 15-80 MPa

Subgrade reaction: (1.0-1.2) x 10^4 kN/m3 x depth (in meters)
Poisson ratio: 0.3 - 0.35

k (permeability coefficient) = 10^{-4} to 7.5 x10^{-5} m/s.

Cretaceous unit

The most representative SPT values of this material are higher than 60.

Friction angle ϕ (in effective stresses) = 38 to 42º

Elasticity modulus: 30 - 50 MPa

Subgrade reaction: (1.1-1.3) x 10^4 kN/m3 x depth (in meters)

Poisson ratio: 0.25 - 0.3

8.3.5.7 DEFINITION OF DESIGN EARTHQUAKE

It seems with a few exceptions that doesn´t exist complete seismic events recorded for a period of time sufficient long that enables a valid extrapolation for the determination of future seismic activity. The complete definition of seismic risk at a proposed powerplant site requires a wide range of quantitative and qualitative information. The former include estimates of relationships between various measures of ground motion, their probabilities of exceedance together with recommendation of appropriate mean return periods to be used for design. The qualitative data include estimates of secondary and tertiary risks associated with seismic shaking.

Generally speaking, a powerplant is designed to withstand two different levels of earthquake activity. Hence, two design earthquakes, or series of earthquakes, are specified and are termed "Operating Basis Earthquake" (O.B.E.) and "Maximum Credible Earthquake" (M.C.E.).

An O.B.E. is an event that may reasonable be expected during the lifetime of the structure. The structure must continue to function during and after such an event and thus the loading is classed as "unusual". A full definition of this loading includes a usual static load, because such an earthquake, will occur in combination with self-weight, temperature, silt and hydrostatic load.

An M.C.E. event is defined to correspond with the most extreme earthquake action that can reasonably be expected at that site. The structure must withstand the event in such a way that repairs can be undertaken in a reasonable length of time and, more importantly, that no loss of life occurs for example due to a major flood. An M.C.E. event is classed as an "extreme loading".

Methodology

Taking into account the rules stablished by U.S.A.E.C. (United States Atomic Energy Commission, 1973), by I.A.E.A. (International Atomic Energy Agency, 1972) it seems reasonable to adapt the following methodology for carrying out seismic risk studies.

Deterministic Criteria

1 - Definition of the geological conditions and tectonic faults and identification of ground conditions which may affect within 320 km seismic shaking.
2 - Recognition and understanding of the seismotectonic of the site, interpretation of local networks in relation to possible spatial and temporal changes in earthquake activity.
3 - Tentative establishment of a correlation between seismic epicenters and faults.
4 - Definition of a M.C.E. series of earthquakes choosing the most intensitives.
5 - Establishment of magnitude recurrence relationship and empirical attenuation relationships to check risk assessments.
6 - With these relationships and the series of M.C.E. earthquakes stablish the worst conditions.
7 - With correlations stablish the highest values of acceleration for M.C.E. earthquakes.
8 - Selection of O.B.E. earthquakes with a maximum acceleration equal or superior 50% of M.C.E. earthquakes.

Probabilistic Criteria

The following stages are considered:

1 - Identification of seismotectonic domains

2 - Definition of attenuation relationships

In general attenuation laws are given by equation:

$$a_m \text{ x} = a_1 e^{a_2 M} R^{a_3} \quad \text{R} = \sqrt{x^2 + h^2 + C^2} \qquad \textbf{8.42}$$

Where

$a_{máx}$: maximum acceleration (function of magnitude M epicentral distance x, focal distance h and a constant C; a_1, a_2 and a_3 are constants that are functions of focales mechanisms and conditions of propagation of seismic waves.

3 - Determination of acceleration values for earthquakes with magnitudes higher than 4 and epicentral distances larger than 300 km.

4 - Statistic studies to stablish maximum accelerations with different recurrence periods.

5 - Establishment of recurrence periods in accordance with type of structure and life of structure.

6 - Determination for each seismotectonic domains predicted values of maximum accelerations for the site in accordance with the recurrence periods stablished.

7 - Selection of real seismograms.

8 - Generation of artificial accelerograms.

9 - Normalization of selected accelerograms for the maximum acceleration level predicted for the adopted recurrence periods.

The statistics studies should be calibrated with deterministic studies.

For the MCE earthquakes probabilistic studies should be done carefully taking into account the geotechnical conditions and the local time acceleration histories.

For the OBE earthquakes studies statistics models can be used as the recurrence periods are of the same order of the adopted periods.

Lares powerplant lies within the zone C of Portugal seismic map.

The ground materials belong to type III.

To obtain the values of peak acceleration and peak velocities the following equations proposed by Idriss et al. (1977) were used:

$$\text{a} = \frac{190.67\, e^{0.823\text{M}}}{(\text{R} + C_1)^{1.56}} \qquad 8.43$$

$$v = \frac{0.836\, e^{1.22}}{(R + C_1)^{1.43}} \qquad 8.44$$

Where

M = magnitude and R = epicentral distance

$C_1 = 0.864\, e^{0.463M}$

Local effects have a great importance in the amplitude of vibrations and spectral richness

Taking into account that we are dealing with an important structure such as a thermal powerplant local effects should be incorporated.

Taking into account the following factors:

i) uncertainties introduced by incomplete data;

ii) local effects and their consequences for the attenuation relationship;

iii) induced seismicity for earthquakes with small epicentral distance;

Based on a simplified approach a value of 0.15 g for peak acceleration shall be adopted for MCE earthquake for a return period of 1000 years and for OBE earthquake a value of 0.10 g shall be considered.

8.3.5.8 DESIGN OF SPREAD AND RAFT FOUNDATIONS

The following limit states shall be considered for spread foundations:

a) - Ultimate limit state design

- loss of overall stability
- bearing resistance failure
- failure by sliding

b) - Serviceability limit state design

- settlements: immediate and delayed settlements
- excessive heave
- settlements due to vibrations

The bearing capacity for a shallow foundation is given by the equation:

$$\sigma_r = (1,3\,cN_c + 1,3\gamma D\,N_q + 0,8\gamma BN\,\gamma) \quad (8.45)$$

where:

γ- unit weight

N_c, N_q e N - capacity factors depending of soil friction angle

D – depth of shallow foundation

2B – width of shallow foundation

c – soil cohesion

For the shallow foundations the following three components of settlement should be considered:

- immediate settlement;
- settlement caused by consolidation;
- settlement caused by creep.

The settlement for a raft foundation can be calculated by the equation:

$$w = \frac{pB}{E1}\, w_{p1}\left(\frac{H}{B}, \frac{H1}{H}, \frac{2}{B}, \frac{e}{B}, \frac{Ep}{E1}, \frac{E1}{E2}, \nu_{.1}, \nu_{.2}\right) \quad (8.46)$$

where for the soil is assumed an elastic (Bescond et al., 1974).

With the symbols defined as:

B - raft width;

E_p elasticity modulus for the raft;

E_1 – elasticity modulus for the first layer;

E_2 – elasticity modulus for the second layer;

H - total height for the two layers;

H_1 – height for the first layer;

H_2- height for the second layer;

e - thickness for the raft;

$\nu_{.p}$- Poisson ratio for the raft material;

$\nu_{.1}$ – Poisson ratio for the first layer;

$\nu_{.2}$ - Poisson ratio for the second layer;

p - applied pressure.

The following limit states were considered:

a) - Ultimate limit state design - loss of overall stability- bearing resistance failure

- failure by sliding

b) - Serviceability limit state design - settlements: immediate and delayed settlements

- excessive heave / - settlements due to vibrations

8.3.5.9 PILE DESIGN

Piles under vertical **loads**

The following limit states were considered:

a) - Ultimate limit state design

- loss of overall stability - bearing resistance failure of the pile foundation

- uplift or insufficient tensile resistance of the pile foundation - failure in the ground due to transverse loading of the pile foundation / - structural failure of the pile in compression, tension, bending or shear /- combined failure in ground and in structure.

b) - Serviceability limit state design

- excessive settlements /- excessive heave / - unacceptable vibrations

For the assessment of the bearing resistance of the piles the following equation can be used:

$$P_u = P_u^{pr} + P_u^{sf} - W \qquad (8.47)$$

where:

P_u - bearing resistance

P_u^{pr} - base resistance

P_u^{sf} - shaft resistance

W - pile weight $W = 25\ \Pi\ d^2\ 1/4$ (kN)

The base resistance can be calculated by the equation proposed by Meyerhoff:

$$P_u^{pr} = r_p^{pr} . A_p \quad (8.48)$$

where A_p is the section of the pile.

The shaft resistance can be calculated by the equation:

$$P_u^{sf} = \frac{1}{200} \sum_i r_{pi}^{sf} A_i^{sf} \quad (8.49)$$

For the definition of allowable pile capacity, a safety factor of 3 is considered and the following equation can be used:

$$N_{adm} = \frac{P_u^{pr}}{3} + \frac{P_u^{sf}}{3} - w \quad (8.50)$$

Following Poulos and Davis (1980) the base resistance can be calculated by the equation:

$$P_u^{pr} = A_p \sigma'_{vb} N_q \quad (8.51)$$

where

σ'_{vb} - overburden effective stress

N_q - bearing capacity factor.

The shaft resistance can be calculated by the equation:

$$P_u^{sf} = \int_0^1 . F_w C \sigma_v' k_s \tan \phi_a' \partial z \quad (8.52)$$

where:

F_W - correction factor

C - perimeter of the pile (C = Πd)

σ'_v - effective overburden pressure

$k_s \tan\emptyset'_a$ - lateral friction value

There is a great variation in theoretical values of Nq derived by different investigators but the values of Meyerhoff (1953) appear to be currently used (see Figure 8.295).

If the influence of cohesion is significant for the base resistance the following contribution can be added:

$$P_u^{pr} = A_p \, c \, N_c \qquad (8.53)$$

The values of N_c can be derived from Figure 8.296 considering the statistical average curve.

For the computation of pile settlements, Poulos and Davis (1980) have proposed the following equation:

$$\delta_p = \frac{Pl}{E_{sp} d} \qquad (8.54)$$

where:

P - axial pile load

E_{sp} - elasticity soil modulus at pile base

d - pile diameter

and

$$I = I_o R_k R_b R_v \qquad (8.55)$$

where: Io, R_k, R_b and R_v are corrective factors.

The values of these constants can be obtained from Figure 8.297.

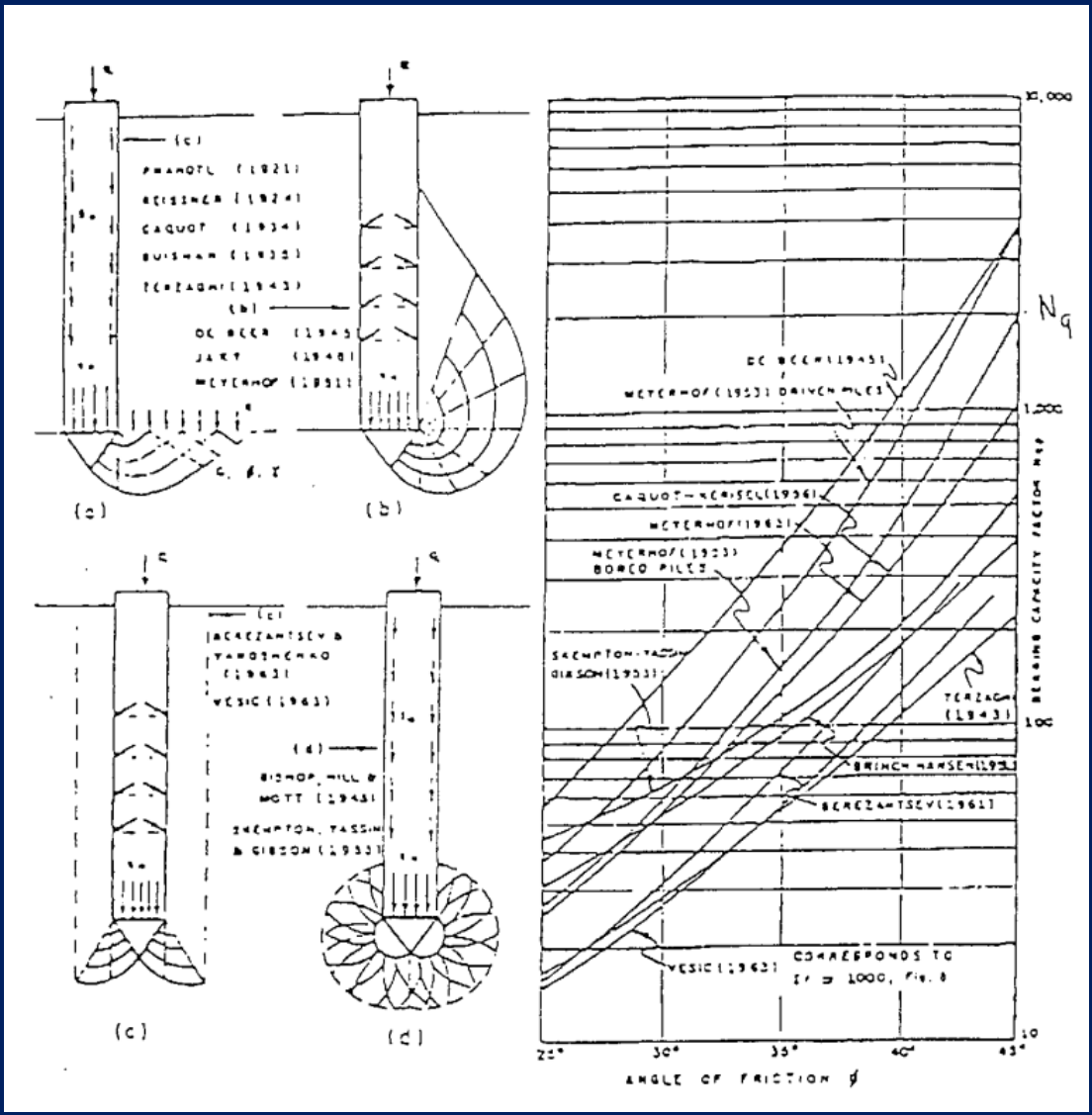

Figure 8.295 Determination of Nq values

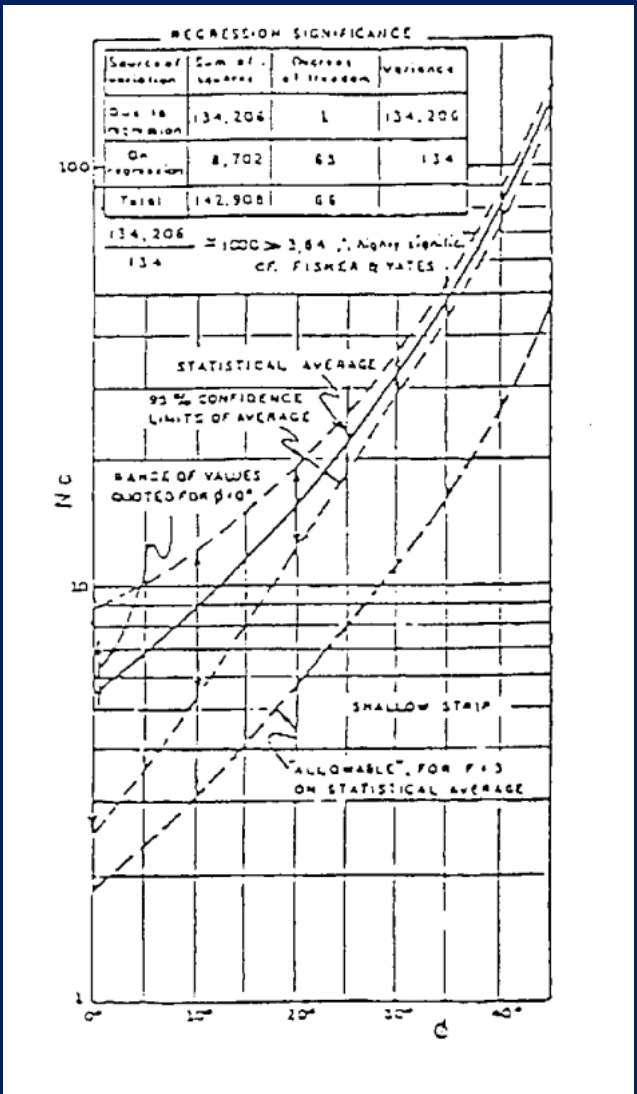

Figure 8. 296 Determination of Nc values

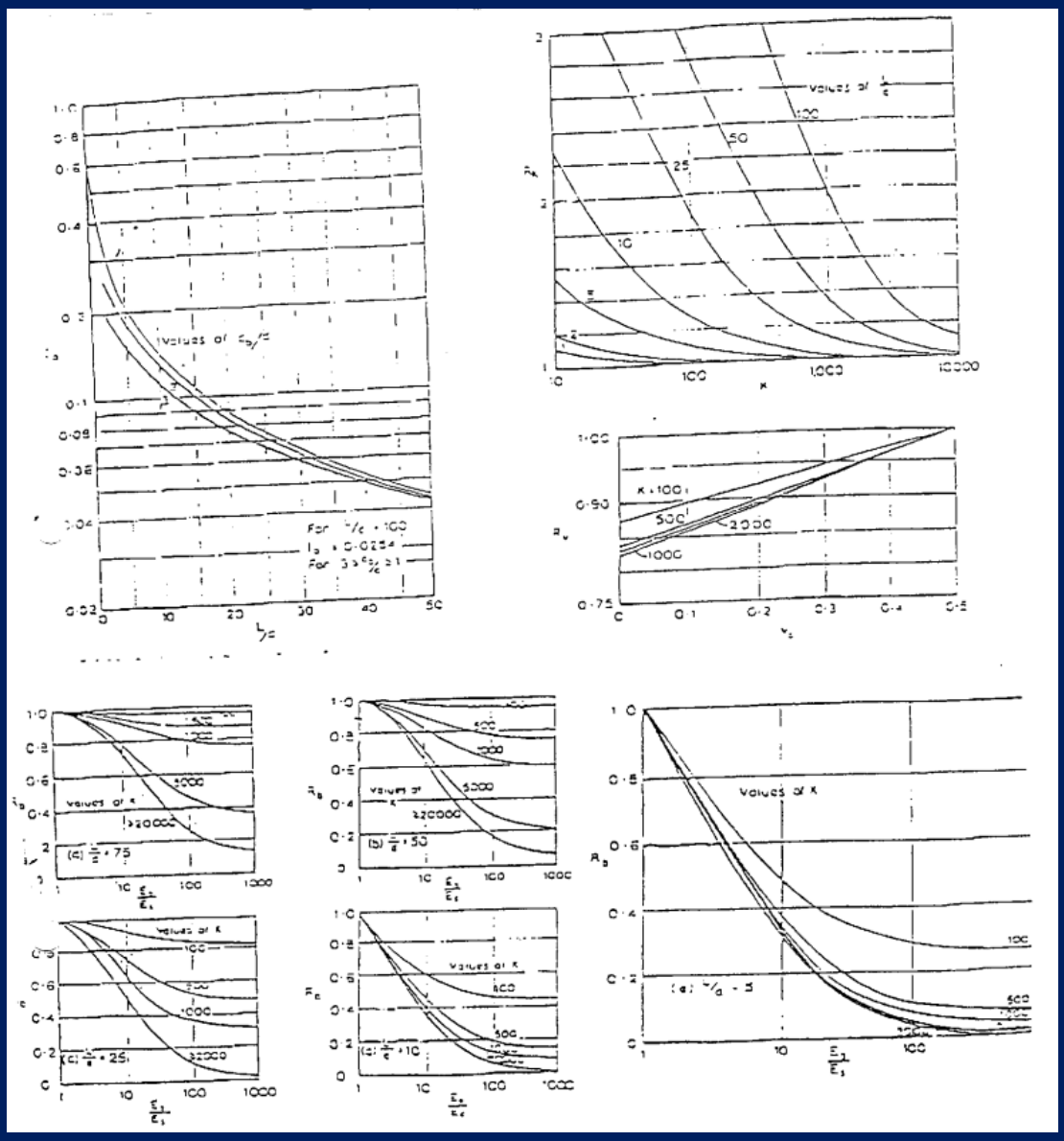

Fig.8. 297 Determination of I_o, R_k, R_b and R_v values

Figure 8.298 illustrates a view of piles.

Figure 8.299 shows the ground material at the bottom of the piles.

Figure 8.298 A view of piles

Figure 8.299 Ground material at the bottom of the piles

13.2 – Piles under horizontal loads

For the analysis of a pile under horizontal loads assuming a value of a constant subgrade reaction or a value of subgrade reaction varying with depth the values of horizontal displacement, rotations, bending moments and shear forces can be determined by the equations E_e – elasticity modulus of pile))

(Castro, 1989):

$$\text{horizontal displacement: } U = Au\ \frac{\lambda^3}{(EI)_e}\ T + Bu\ \frac{\lambda^2}{(EI)_e}\ M \tag{8.56}$$

$$\text{rotation} = \rho = A\rho\ \frac{\lambda^2}{(EI)}\ T + B\rho\ \frac{\lambda}{(EI)_e}\ M \tag{8.57}$$

$$\text{moment} = M = A_M \lambda\ T + B_M\ M \tag{8.58}$$

1 shear force: $T = A_T\ T + B_T \lambda_M^{-1}\ M$

where

$$\lambda = 1{,}65\ \sqrt[4]{\frac{(EI)_e}{(E_s)}} \tag{8.59}$$

1

T - shear force
M - bending moment

The distribution of bending moments, shear forces, rotations and displacements were determined.

Pile foundations with ϕ = 0.60 m, ϕ = 0.80 m and ϕ = 1.0 m will be analysed.

Considering a pile with ϕ = 0.60 m for an average value of SPT = 50 from equation (8.48) results:

$$P_u^{lpoint} = 350\ x\ 50\ x\ \pi\ x\ 0.6^2\ /\ 4 = 4945\ kN$$

considering n = 350

for lateral resistance

$$P_u^{laterra} = 500\ k\ N$$

considering a safety factor of 3 the allowable pile capacity is

$$P_{adm} = \frac{p_u}{3} = 1815 kN \tag{8.60}$$

Considering a pile with ϕ = 0.80 m for an average value of SPT = 50 from equation (8.48) results:

$$P_u^{lpoint} = 350 \times 50 \times \pi \times 0.8^2 / 4 = 8792\ kN$$

considering n = 350

for lateral resistance

$$P_u^{laterra} = 600^k\ N$$

From equation (8.48) results:

considering a safety factor of 3 the allowable pile capacity is

$$P_{\text{adm}} = \frac{p_u}{3} = 3154\text{kN}$$

Considering a pile with ϕ = 1.0 m results

$$P_{\text{adm}} = \frac{p_u}{3} = 4928\text{kN}$$

UMC (main building)

Considering the following loads N= 4000 kN, T= 30 kN e M= 400 kNm applied at the head of a pile with ϕ = 1.0 m and a length of 24 m (based in boreholes SP1 and SP3), the distributions of horizontal displacements, rotations, bending moments and shear forces are computed.

a) Distribution of horizontal displacements:

for z = 0
u = 19.2 x 10^{-3} m

for z = 5
u = 3.7 x 10^{-3} m

for z = 10 m
u = -2.0 x 10^{-3} m

for z = 15 m
u = -2.6 x 10^{-3} m

for z = 20 m
u = -1.6 x 10^{-3} m

b) Distribution of rotations

for z = 0
ñ= -36.1 x 10^{-4}

for z = 5 m
ñ = -14.0 x 10^{-4}

for z = 10 m
ñ = -6,4 x 10^{-4}

for z = 15 m
ñ = -2.1 x 10^{-4}

for z = 20 m
ñ = -1.6 x 10^{-4}

c) Distribution of bending moments

for z = 0
M = 400 kN m

for z = 5 m
M = 391.7 kN m

for z = 10 m
M = 227.9 kN m

for z = 15 m
M = 90.5 kN m

for z = 20 m
M = 30.5 kN m

d) Distribution of shear forces

for z = 0
T = 30 kN

for z = 5 m
T = -23.5 kN

for z = 10 m
T = -31.2 kN

for z = 15 m
T = -20.9 kN

for z = 20 m
T = -13.2 kN

The computed settlements for N= 4000 kN considering the equations (10) and (11) are less than 6 mm.

Considering a concrete B30 and a steel A500 for the loads at pile head N = 4000 kN and M = 400 kNm for a pile with ϕ = 1,0 m and a length of 24 m the following reinforcement can be considered

longitudinal reinforcement 10 ϕ 20 mm

transversal reinforcement ϕ=10 mm double helicoidal with a step of 30 cm.

It is important to stress that this is only an example and the correct values of axial load, bending moment and horizontal load transmitted by the superstructure and applied at the top of the pile are needed for a reliable design of the pile.

For the pile design it is important to combine the inertia forces transmitted by the superstructure with the kinematic forces due the passage of seismic waves through the pile surrounding soil.

UMC structures (turbine block)

These structures can be founded in 27 piles of ϕ = 0,80 m with a length of 24m (based in boreholes SP1 and SP3).

The computed settlements for N= 2500 kN considering the equations (8.50) and (8.51) are less than 4 mm.
Considering a concrete B30 and a steel A500 for the loads at pile head N = 2500 kN and M = 400 kNm for a pile with ϕ = 0.8 m the following reinforcement can be considered

longitudinal reinforcement 10 ϕ 16 mm

transversal reinforcement ϕ=10 mm double helicoidal with a step of 30 cm.

URA Structure (Cooling tower)

This structure can be founded in 128 piles of ϕ = 0.80 m and a length of 26 m following SP5 and SP6, that does not agree with S5 (campaign of August 2000).

The computed settlements for N= 2200 kN considering the equations (8.50) and (8.51) are less than 4 mm.

The following reinforcement can be considered

longitudinal reinforcement 10 ϕ 16 mm

transversal reinforcement ϕ=10 mm double helicoidal with a step of 0.30 m.

UHA Structure (Boiler)

This structure can be founded in 32 piles of ϕ = 1.0 m and a length of 24 m (considering SP2 and SP4).

The computed settlements for N= 1600 kN considering the equations (8.50) and (8.51) are less than 4 mm.

The following reinforcement can be considered

longitudinal reinforcement 10 ϕ 20 mm

transversal reinforcement ϕ=10 mm double helicoidal with a step of 30 cm.

UCA Structure (Control and administration building)

This structure can be founded in 36 piles of ϕ = 0.80 m and a length of 24 m (considering SP 13).

The computed settlements for N= 2000 kN considering the equations (8.50) and (8.51) are around 3 mm.

The following reinforcement can be considered

longitudinal reinforcement 10 ϕ 16 mm

transversal reinforcement ϕ=10 mm double helicoidal with a step of 0.30 m.

UST Structure (Workshop and storage building

This structure can be founded in 34 piles of ϕ = 0.80 m and a length of 24 m (CPTU 6).

The computed settlements for N= 1600 kN considering the equations (8.50) and (8.51) are around 2 mm.

The following reinforcement can be considered:

longitudinal reinforcement 10 ϕ 16 mm

transversal reinforcement ϕ=10 mm double helicoidal with a step of 0.30 m.

It is important to stress that the pile reinforcement should be the same through the length of the pile. The main reason for that is related with the connections of the pile with the superstructure and bottom, and also with the interfaces between ground materials of different characteristics. Due the increments of horizontal loads related with the seismic movements an increase of pile reinforcement for a length of 3D (D is the pile diameter) for each side of the interfaces is recommended. In summary the same reinforcement through the length of the pile shall be used and this requirement will also simplify the construction of pile reinforcement.

Following the Siemens request it was computed for piles of ϕ=.8m and ϕ=1.0m of diameter and for two values of action at the pile head T= 100 kN or M= 100 kNm, the values of horizontal displacements, rotations, bending moment and shear forces, at depth 0, for the determination of horizontal spring values.

Considering a pile with ϕ= 0.8m and T= 100kN

a) horizontal displacement:

for z = 0
$u = 2.9 \times 10^{-2}$ m

b) rotation value

for z = 0
$\tilde{n} = -4 \times 10^{-3}$

c) bending moment

for z = 0
M = 0

d) shear force

for z = 0
T = 100 kN

Considering a pile with ϕ= 0.8m and M= 100kNm

a) horizontal displacement:

for z = 0
$u = 4 \times 10^{-3}$ m

b) rotation value

for z = 0

ñ= -10^{-3}

c) bending moment

for z = 0
M = 100 kNm

d) shear force

for z = 0
T = 0

Considering a pile with ϕ= 1.0 m and T= 100kN

a) horizontal displacement:

for z = 0
u = 2.5×10^{-2} m

b) rotation value

for z = 0
ñ= -2.9×10^{-3}

c) bending moment

for z = 0
M = 0

d) shear force

for z = 0
T = 100 kN

Considering a pile with ϕ= 1.0 m and M= 100 kNm

a) horizontal displacement:

for z = 0
u = 2.9×10^{-3} m

b) rotation value

for z = 0
ñ= -0.7×10^{-3}

c) bending moment

for z = 0

M = 100 kNm

d) shear force

for z = 0
T = 0

Taking into consideration that it is an elastic formulation the values of horizontal displacements can be computed for different combinations of shear forces and bending moments applied at pile head, for the determination of horizontal spring values. For vertical spring values hundred times higher can be considered.

It is important to verify the ultimate limit states and the serviceability limit states for the computed horizontal displacement values and rotations values.

Piles under horizontal loads

For the analysis of a pile under horizontal loads a value of a constant subgrade reaction or a value of subgrade reaction varying with depth were considered for the calculation of the values of horizontal displacement, rotations, bending moments and shear forces.

8.3.5.10 PILE DESIGN UNDER SEISMIC LOADS

Elastic solution in a homogenous media

$G / G_{máx} = S_s^2 / S_{máx}^2$

Considering that equivalent cyclic shear strain is approximately 65% of the maximum average shear strain then (Makdisi and Seed, 1979):

$$(\gamma_m)_{eq} = 0{,}65\ (\phi_1{}'.)_m\ (h/S^2)\ S_{al} \qquad (8.61)$$

where:

S = shear wave velocity

S_{a1} = spectral acceleration

$(Ø'_1)_m$ = mode participation factor

Characteristics of the materials

For the determination of $S_{máx}$ and $G_{máx}$ the following equations were considered:

$$S_{máx} = 81{,}4\ (N_{SPT})^{0{,}34}\ m/s \qquad (8.62)$$

$$G_{máx} = \rho S_{máx}^2 \qquad (8.63)$$

$$G / G_{máx} = S_s^2 / S_{máx}^2 \qquad (8.64)$$

S_S is the shear wave velocity compatible with the level of cyclic equivalent distortion.

Base on the geotechnical characteristics of mud material, it was considered in a simplified way a layer with a thickness of 12 m and a value of $S_{máx}$ = 120 m/s.

Calculation

For the first iteration of computations an initial value of shear modulus G is assumed that allows the determination of a pair of values of $G/G_{máx}$ and λ that are used for the determination of seismic response of the ground and a new value of shear strain is determined that allows the determination of a new set of modulus and damping values. The process usual converges in 3 iterations.

The poweplant is located in zone A and taking into account the SPT results the ground is from type III: For the seismic response of ground, it was considered a power spectrum for seismic action 2, associated with earthquakes of large magnitude and epicentral distance (Mineiro, 1988).
Taking into account the RSA (1983) the power spectra is defined by:

	Hz_1	Frequency	,04	,6	,2	,4	,8	,6	0,0
(f)	(cm/ $s^2)^2$/Hz	Power spectra density of acceleration (comp. horizontal)		20	00	50	5	0	

Considering for the ground material a value of $S_{máx}$ = 118 m/s.

1st iteration

$(\gamma_{m)} = 0,005$

$G/G_{máx} = 0,1$ $\lambda = 22,5\%$ $S_S = 37,94$ m/s

$f_1 = 0,16$ Hz

From the power spectra results $S(f_1) = 64,3$ cm/S²)²Hz

The values of spectra accelerations from the power spectra of acceleration were obtained from the equation (LNEC, 1985):

$$s(f) = 0,2\lambda A^2 f^{-1,4} \quad (8.65)$$

it results for A

$A = 7,54$ cm/s²

$S_{a1} = 1.5 \times 7.54 = 11.31$ cm/s²

$(\gamma_m)_{eq} = 0,0015$

2nd iteration

$G/G_{máx} = 0.23$ $\lambda = 18\%$ $S_S = 57.5$ m/s

$f_1 = 0.24$ Hz

$S(f1) = 97.7$ (cm/s²)² Hz

$A = 19.2$ cm/s²

$S_{a1} = 28.8$ cm/s²

$(\gamma_m)_{eq} = 0.17$

3rd iteration

$G/G_{máx} = 0.21$ $\lambda = 18.5\%$ $S_S = 55$ m/s

$f_1 = 0.23$ Hz

$S(f1) = 93.7$ (cm/s²)² Hz

$A = 17.98$ cm/s²

$S_{a1} = 26.98$cm/s²

$(\gamma_m)_{eq} = 0.174$

Calculation of seismic displacement at ground level

The value of maximum displacement can be obtained by the equation:

$$d_{máx} = (\gamma)_{eq} h = (\gamma)_{eq} /0{,}65) \text{ x } h \qquad (8.66)$$

$$d_{máx} = (h^2 / S_s^2) S_{al} (\phi_1 ´.)_m \qquad (8.67)$$

The value of maximum displacement at the ground level is:

$d_{máx} = 0.02$ m

14.5 – PILE SEISMIC ANALYSIS

For piles under lateral loads the equation can be written:

$$E_p I_p \frac{d^4\rho}{\delta z^4} + k_h \, d\rho = 0 \qquad (8.68)$$

where:

E_p – elasticity modulus of the pile

I_p – moment of inertia of the pile

z - depth of the ground

d - pile diameter

ρ - horizontal displacement

k_h – subgrade modulus

The equation 8.67 can be solved analytical or numerical

Considering the pile head free and submitted by a lateral load the rotation can be obtained:

$$\theta = \frac{2\,H\,\beta^2}{k_h\,d}\left(\frac{1}{\text{sen}\,h^2\beta\,L - \text{sen}^2\beta\,L}\right) x$$
$$(\text{sen h}\,\beta\,L[\text{sen}\,\beta\,z\cos h\,\beta(L - z) + \cos\beta\,z\,\text{sen h}\,\beta(L - z)] + \text{sen}\,\beta\,L\,[\text{sen h}\,\beta\,z\,x \qquad (8.69)$$
$$x\cos\beta(L - z) + \cos h\,\beta\,z\,\text{sen}\,\beta(L - z)] = \frac{2\,H\,\beta^2}{k_h\,d}K_{\theta\,H}$$

Considering a moment M_o applied results:

$$\theta = \frac{4\,M_o\beta^3}{k_h\,d}\;x\;\frac{[\text{sen h}\,\beta\,L\cos h\,\beta(L - z)\cos\beta\,z + \text{sen}\,\beta\,L\cos h\,\beta\,z\cos\beta(L - z)]}{\text{sen}\,h^2\beta\,L - \text{sen}^2\beta\,L} = \frac{4\,M_o\beta^3}{k_h\,d}K_{\theta\,M} \qquad (8.70)$$

For the pile head fixed by the cap results

$$M = -\left(\frac{H}{2\,\beta}\right)\left[\frac{k_{\theta\,H}}{k_{\theta\,M}}\right] \qquad (8.71)$$

For a pile free and submitted to a horizontal load the horizontal displacement can be obtained by the equation:

$$\rho = \frac{2\,H\,\beta}{k_h\,d}\ x\ \left[\frac{\text{sen h}\,\beta\,L\cos\beta\,z\cos\text{h}\,\beta(L-z)\ -\ \text{sen}\,\beta\,L\cos\text{h}\,\beta\,z\cos\beta(L-z)}{\text{sen}\,h^2\beta\,L\ -\ \text{sen}^2\beta\,L}\right] = \quad (8.72)$$

$$= \frac{2\,H\,\beta}{K_h\,d} K_{\rho\,H}$$

i.e.

$$H = \frac{1}{2\,\beta}\frac{K_{h\,d}}{K_{\rho\,H}}\rho \quad (8.73)$$

from equation (8.71) results:

$$M = -\ \frac{1}{2\,\beta}\frac{K_{\theta\,H}}{K_{\theta\,M}}\ x\ \frac{1}{2\,\beta}\frac{K_h\,d}{K_{\rho\,H}}\rho = -\ \frac{1}{4\,\beta^2}\frac{K_{\theta\,H}}{K_{\theta M}K_{\rho H}} K_h\,d\,\rho \quad (8.74)$$

The distribution of the moments along the shaft of the pile results:

$$M\,(z) = -\ \frac{H}{\beta} K_{MH} + M\,K_{MM} \quad (8.75)$$

then:

$$M\,(Z) = -\ \frac{K_{MH}}{\beta}\frac{1}{2\beta}\frac{K_h\,d}{K_{\rho H}}\rho\ -\ K_{MM}\frac{1}{4\beta^2}\frac{K_{\theta H}}{K_{\theta M}K_{\rho H}} K_h\,d\,\rho = \quad (8.76)$$

$$= -\ \frac{d\,K_h}{2\beta^2}\left[\frac{K_{MH}}{K_{\rho H}} + \frac{1}{2}\frac{K_{MM}K_{\theta H}}{K_{\theta M}K_{\rho H}}\right]\rho \quad (8.77)$$

from equation (8.77) results

M (0) = 400 kNm

The value of this moment shall be added to the value transmitted by the superstructure.

It is important to stress that M= 400 kNm was computed considering a layer of mud material with 12 m of thickness. For situations of piles with 24 m long where a layer of silty clay occurred beneath the mud material values of M= 600-650 kNm will be computed.

8.3.5.10 QUALITY CONTROL

In order to make a better assessment some piles are subject to testing. The most popular tests are: i) determination of integrity; and ii) direct load testing along the pile axis.

For bored piles some inflow of soil or water can occurred. For the present situation inflow of water can not occurred but only inflow of soil. So, for all the piles integrity tests will be performed.

In general, when dealing with soil materials direct load testing along the pile's axis are performed to assess the soil behaviour.

These tests due to the equipments and staff involved are complex, high costly and in general only 1 to 2% of piles are tested.

In the present situation we believe that direct load testing along the pile axis is not necessarily due the following reasons:

a) The high extent and reliability of the site investigation. As pointed above four campaigns of field tests as laboratory tests were performed;
b) There are no particular variations in ground conditions;
c) The piles are end bearing on stiff ground material;
d) There is no detrimental effect of water;
e) The pile loads are in general low and the obtained safety factors for bearing resistance failure are high;
f) The predicted settlements are very low
h) The standard of labour and supervision on the site is good;
i) Integrity tests will be performed in all piles So any discontinuity due inflow of soil or defects will be detected.
j) The direct load tests are difficult, will demand a complex reaction frame, are costly, only 1 or 2 tests could be performed and in the present situation no additional geotechnical information will be provided.

Taking into account the above reasons we strongly recommend to perform integrity tests in all piles as direct loads tests will be useless.

8.3.5.11 DEWATERING

The dewatering scheme shall satisfy the following conditions:

- the effect of groundwater lowering shall be that the sides of the excavation remain stable at all times and that excessive heaving or rupture of the base does not occur.
- the scheme adopted shall not lead to excessive settlements.
- the dewatering scheme shall be so designed and installed as to maintain the water levels and pore pressures anticipated in the design without significant fluctuations.
- there shall be adequate margin of pumping capacity and stand by plant shall be available in the case of breakdown to facilitate maintenance.
- the effectiveness of dewatering shall be checked by monitoring the groundwater level, the pore pressures and the ground movements as necessary. Collected data shall be reviewed and interpreted frequently to determine the effects of dewatering on the ground conditions.

- As the pumping operation is to extend over a long period of time, the groundwater should be checked for the presence of dissolved salts.

8.3.5.12 LIQUEFACTION ASSESMENT

Due to the low compacity of sandy materials the likelihood of liquefaction was investigated.

It is important to stress that for borehole SP2(between depth 5-7m) there is a sandy layer of low compacity with SPT values around 11, for SP7(between depth 9-13m) there is a sandy layer of low compacity with SPT values between 6-16, for SP11(between depth 8-13m) there is a sandy layer of low compacity with SPT values around 6 and for SP15(between depth 3-7m) there is a sandy layer of low compacity with SPT values between 4-11. These sandy layers can exhibit a liquefaction potential during the occurrence of earthquakes. Due to this circumstance, it is recommended for structures located in these areas that the lateral resistance of piles, for the mentioned depths, should be neglected.

8.3.5. 13 SLOPE STABILITY

In order to fulfil the requirements for slopes of stability and limited deformation the following limit states were considered: - loss of overall stability or bearing resistance - failure due to internal erosion
- failure due to surface erosion - failure due to hydraulic uplift.

In this case the ultimate limit state design is more severe when compared with the serviceability limit state design as it is a temporary situation.

The complete method of a vibrating foundation-building system incorporates the soil and the foundation-building system in a sole model, which is usually developed by means of finite elements, and analyzed simultaneously. It is important to recognize that, as it is not feasible to cover the complete layered half space with discrete elements, an artificial boundary should be included in the model to account for the missing layered medium on the exterior of the interaction region. Artificial boundaries may reflect, into the foundation-building system, appreciable amounts of the outwardly propagating waves energy. To minimize this energy-reflection problem and at the same time to keep the model within a reasonable size, numerous energy-absorbing boundaries

Most of the theoretical developments have been implemented in computer codes. Among the most known and used to analyze soil-structure problems are FLUSH (Lysmer et al, 1975), SASSI (Lysmer et al, 1981; which use finite-element methods and CLASSI (Luco et al, 1989) that makes use of boundary elements to compute foundation-soil impedances. Wolf and Darve (1986) developed a procedure that uses boundary elements for an elastic layered far-field region together with a nonlinear model of the soil and structure near-field zone.

Note: This study was performed for the Consortium of Lares.

8.4 BUILDINGS -FOUNDATIONS

8.4.1 Case History nº 15 - Kilamba Building (Angola) – with Alexandre Pinto (JetSj)

8.4.1.1 Background

The Contractor GEO-RUMO-FDO-ABB has proposed an alternative solution for Kilamba project foundation with a diaphragm wall 0.6 m thick supported by pieces of slabs located at level 0, level –1, level –2, and a jet-grouting plug at the base of the excavation.

This solution was considered more feasible that the execution of anchors solution under water level proposed by DAR designer.

In addition, the jet grouting plug, located 1.8 m deep the level of excavation, was considered a better solution due to the geotechnical scenario of sandy materials. This plug was materialized by jet grouting columns 1.8 m diameter and 3.0 m long distributed in quinconce and 1.3 m apart.

Under the last cave a bottom slab with 0.40m thick and reinforcements of 1.2 m minimum high were proposed. A drainage system was installed to pump the water percolate through the foundation and diaphragm wall.

The loads transferred by the superstructure were supported by bored piles with 1.0 m diameter and lengths between 20.0 m to 25.0 m.

The structure was analysed by SAP 2000 code using a 3D model.

The soil –structure interaction was based in Winkler model.

Based on the geotechnical characterization the following subgrade modulus were considered:

- soil around pile: subgrade reaction modulus 40 000 kN/m^3.
- soil at the massif base: reaction modulus 6000 kN/m^3.
- soil at the bottom of the micropile: reaction modulus 8 000 kN/m^3.

The analysis has given the values of tension forces, compression forces and bending moments.

The forces and deformations of the diaphragm wall simulating the different construction phases were obtained by PLAXIS code.

Horizontal displacements of 25 mm and vertical displacements of 23 mm were computed.

The calculated values have shown that ultimate limit sates and serviceability limit sates were verified.

The bearing capacity of the piles and micropiles was defined based in the partial safety factors defined in Eurocode 7.

For the diaphragm wall the following limit states were verified: (i) loss of global safety factor; (ii) failure due insufficient resistant capacity; (iii) failure by sliding; and iv) combined failure of ground and structure.

The static water pressure causes a destabilising uplift force on the structure, which is resisted mainly by the self-weight of the structure, but there may also be some resistance from the ground around the structure due to the pile role.

It is important to stress that CPRF (Combined Pile Raft Foundation) a composite foundation of 3 elements namely pile, raft and soil has proved very successful for the tall buildings with low settlements and economic costs.

Figure 8.300 illustrates the location of the building.

Figure 8.300 Location of the building

8.4.1.2 -Geological Characteristics

GEOLOGICAL CHARACTERISTICS

- Sand landfills (C1A), with grey material and thickness less than 2.5m
- Alluvial deposits (C1B), with thickness around 6m, composed by fine sands with mud with SPT values between 3 and 11 blows
- Underlying this layer occurs fine sands and silty clay materials (unit C2A of Miocene), with SPT values between 12 and 38 blows mixed with stiff clay materials with SPT values between 13 and 33 blows
- For higher depths occur fine sands very compacted with SPT values higher than 60 blows and stiff sandy clays with SPT values higher than 24 blows classified as unit C2B of Miocene.

8.4.1.3 -Design of retaining walls

DESIGN OF RETAINING WALLS

- Behavior of gravity retaining structures during an earthquake: (i) increasing of dynamic earth pressures; (ii) variation of hydrodynamic pressure of the backfill; (iii) decreasing of stabilizing forces related with the weight of the structure; (iv) increasing of pore pressures and consequently reduction of effective pressures; and (v) soil liquefaction of backfill and/or foundation material.
- The stability of soil foundation shall be assessed for the following conditions: (i) overall stability; and (ii) local soil failure.
- Following RSA near source represents a moderate magnitude earthquake at a short focal distance with a duration of 10 seconds; (ii) far source represents a higher magnitude earthquake at a longer focal distance with a duration of 30 seconds
- Following EC 8 seismic action is associated with a probability of exceeding (PNCR) of 10 % in 50 years; or (ii) a reference return period (TNCR)= 475 years.

DESIGN OF RETAINING WALLS

MICROPILES

- loss of overall stability
- bearing resistance failure of the pile foundation
- uplift or insufficient tensile resistance of the pile foundation
- failure in the ground due to transverse loading of the pile foundation
- structural failure of the pile in compression, tension, bending or shear
- combined failure in ground and in structure
- excessive settlements
- excessive heave
- unacceptable vibrations

Figure 8. 301 illustrates the aspect of the excavation.

Figure 8.302 presents the construction of the retaining walls.

Figure 8. 301 Aspect of the excavation

Figure 8.302 Construction of the retaining walls

8.4.1.4 -Pile tests

Figure 8.303 shows the piles test.

Figure 8.303 Pile test

8.4.1.5 Construction methodology and equipment

The following construction sequence was adopted: (i) Pre borehole; (ii) Position the drill and jetting tools; (iii) Activate high pressure pump with water to check nozzle and grout line clearance; (iv) Lower the tube into
the ground to the required depth; (v) When reaching the desired depth, activate cement slurry, adjust rotation and withdrawal rate, discharge value, following the recorded parameters, a pre-cutting with lense dense grout was used, and this methodology was repeated for the final treatment, continue withdrawal while forming the column; (vi) Shut off cement slurry line and quickly withdraw the grouting tube.

Jet grouting equipment's has included: (i) Drilling equipment LT 3nx/JTC with equipment of reading, sensors, laser set Diana equipment of placement, and software EXTIG; (ii) Grout Mixing and Injection Equipment: grout mixers, holding tanks, water tanks, air compressors and pump of high pressure 7T500J; (iii) Jet Grout pump and injection monitor with horizontal radial nozzles delivering high velocities fluids; (iv) Compressor capable of producing the pressure of 15 bar and to deliver the flow rate values; (v) Jet grouting parameters: pressure of the fluids, flow rat of the fluids, grout composition, rotational speed of the jet grouting, rate of withdrawal; (vi) Equipment- Instrumentation: pressure gauges, flow meter; (vii) Silo of 60 tf.

Table 8. 43 summarizes the results of 4 trial columns.

Table 8.44 presents the characteristics of the samples.

Figure 8.304 shows the construction methodology and equipments.

Figures 8. 305 and 8.306 presents the lay - out of the equipment's and details of Tudor equipment.

Table 8. 43 Results of 4 trial columns

Column	**1**	**2**	**3**	**4**
Pre-cut	No	No	Yes	Yes
Grouting Pressure(bar)			250	350
Grout A/C			10	10
Density			1.06	1.06
Noddles (mm)			2x4	1x5
Grouting flow (l/min)			324	299
Upward velocity (cm/min)			21	17
Rotating velocity (min)			3	5
Air pressure (bar)			15	15
Jet grouting				
Theoretic consume (kg/m3)	500	600	500	600
Grout (A/C)	1	1	0.83	0.71
Density	1.5	1.5		
Injection pressure (bar)	350	450	350	450
Noddles (mm)	2x4	1x5	2x4	1x5
Grouting flow (l/min)	323	286	315	274
Upward velocity (cm/min)	19	14	21	17
Rotating velocity (min)	3	4	3	5
Air pressure (bar)	15	15	15	15
Duration of pre-cut	19	14	10.5	8.5
Diameter (mm)	<1800	<1800	>1800	>1800
Recovering r= 900 mm (%)			100	100

Table 8.44 Characteristics of the samples

Sample	Column	Date	P_i (gf)	H_i (cm)	Di (cm)	$\sigma_{comp.max}$ (kPa)	E_{cl} (GPa)	$E_{cl}/\sigma_{comp.max}$
1	4	31-12-2010	2783.67	18.2	10.25	5557.5	4.73	852
2	4	31-12-2010	2802.45	18.8	10.26	4978.9	3.92	788
3	4	31-12-2010	3114.2	20.8	10.22	6903.8	4.69	679

The samples were submerged in water during 18 hours before the test.

JET GROUTING PLUG

- Cohesion in the soil tends to reduce the ease with which the particles are eroded. As the diameter of the grout tends to reduce as the silt and or clay content increases, the jet grouting plug was located at depths around 12m from the ground level where sandy silty materials were occurring
- As the stiffness of the cohesive soil is important and only soil with low values of SPT should be regarded as being suitable, it was not reccommended to locate the jet grouting plug at high depths where stiff Miocene clays were occurring
- Soils with high stiffness requires high pressure water jet that could be detrimental to the neighbour buildings and so it was not advisable to locate the jet grouting plug at high depths due the occurrence of materials with SPT values higher than 60 blows

CONSTRUCTION METHODOLOGY AND EQUIPMENTS

Figure 8.304 Construction methodology and equipments

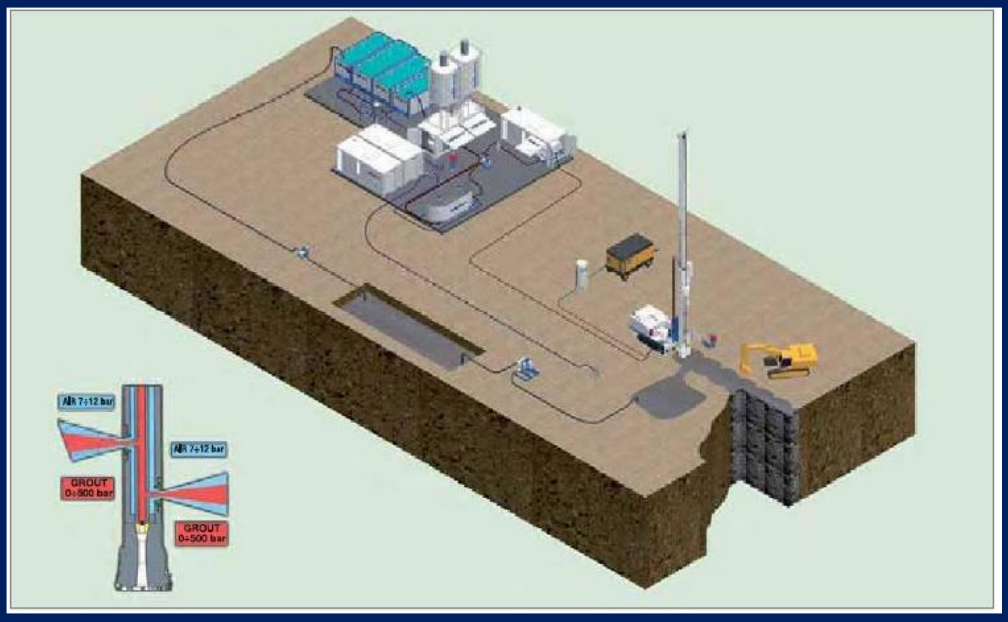

Figure 8. 305 Lay out of equipments

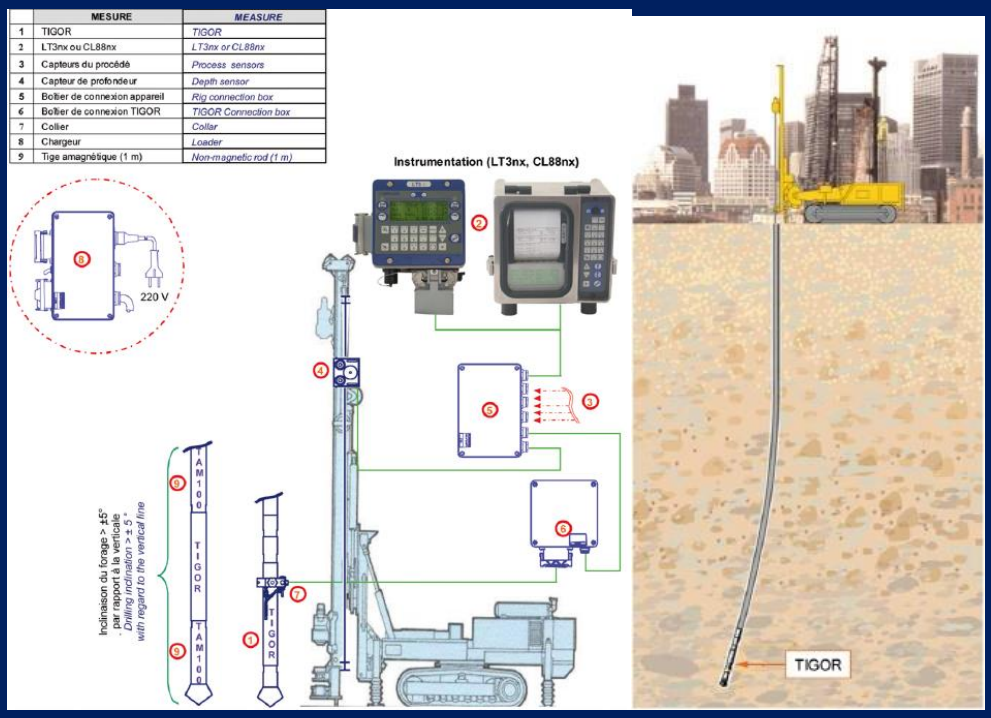

Figure 8.306 Details of Tudor equipment

8.4.1.6 MONITORING

The instrumentation plan has included piezometers, inclinometers, bench marks, fissurometers and clinometers.

Safety control has included the following tasks: (i) A visual inspection of the foundation and neighbors; (ii) Regular measurements using instrumentation; (iii) Storage of the data; (iv) Interpretation of visual observation and processed data; (v) Issue of an evaluation of the safety of the installation; (vi) Decisive actions to be taken should safety have deteriorated; (vii) Interpretation of the measurements by a comparison of the currently computed data with reference values, or their transformation into standard conditions; (viii) Definition of a criteria of alert and the reinforcement actions.

Lesson nº 15: The design of bottom slab based in partial safety of factors proposed by the Contractor was addressed. It is important to stress that the proposed solution by the Contractor that combines the role of jet grouting plug, bottom slab and piles represents a CPRF (Combined Pile Raft Foundation) i.e. a composite foundation of 3 elements, namely pile, raft and soil that has proved very successful for the tall buildings with low settlements and economic costs.

A detailed justification of the jet grouting plug position after weighting the advantages and disadvantages of its location was presented. From the analysis it was reiterate the position of jet grouting at 1.8 m beneath the excavation level.

Note: This study was done for DAR Engineering.

8.4.2 Case History nº 16 - Building Foundations -Assessment of Liquefaction

Meia Praia Bay Resort in Lagos

8.4.2.1 Introduction

The site investigation programme and geotechnical characteristics are referred, the liquefaction assessment for sites 52, 53 and 4, based in SPT tests, CPTU tests and Vs tests is addressed.

8.4.2.2 Site Investigation

The geotechnical characterization has included 3 campaigns, namely the first campaign with 17 boreholes with depths between 12.0 m and 36. 0 m, the second campaign with 7 boreholes and depths between 19.50 m and 34.5 m, 4 CPTU tests, 4 vane shear tests, the 3rd campaign with 4 boreholes and depths between 28.5m and 33.0 m, 7 CPTU tests, 12 seismic refraction tests.

Samples were collected from the boreholes for the execution of laboratory tests, namely:

a) disturbed samples for classification tests.
b) oedometer tests.
c) Direct shear tests.

The following geotechnical units were considered:

Fills with thickness of 2.0 m with sands and clay materials

Mud clay occasionally with sand bands and lenses, dark grey with thickness of 3.0 m to 13.5 m.

Yellowish brown to grey medium to coarse (occasionally fine) sand, with fine to coarse gravel (rounded to angular). Sometimes with shells and shell fragments, with thickness between 7.5 m to 24.0 m.

Plistocenic – Red sands (P)
Clays with sand component and gravel materials with thickness between 3 m and 5.5 m.

Miocenic (M)

Sands beneath the clays yellow and grey yellow.
Silts with clay materials and with sands.

8.4.2.3 Liquefaction Assessment

Subsequently, the liquefaction potential assessment of 3 sites is presented:

Analysis for Site 52

SPT Tests

The value of shear stress for earthquake type 1 (RSA) was defined considering a value r_d of 0.9.

The SPT values were modified taken into account the C_N values.

The shear stress value was increased by the factor 1.25 based in Eurocode 8-Part 5.

Considering a % of fines of 10%, following the Seed proposal liquefaction can occur.

A new proposal presented by Cetin et al. (2001) is shown considered advanced in relation with the previous ones, as integrates: (i) data of recent earthquakes; (ii) corrections due the existence of fines; (iii) experience related a better interpretation of SPT test; (iv) local effects; (v) cases histories related more than 200 earthquakes; (v) Bayesian theory.
Following Cetin et al proposal the occurrence of liquefaction is 85%.

Following the same methodology for earthquake type 2 (RSA) also following Seed proposal liquefaction can occur and following Cetin proposal the occurrence of liquefaction is 100%.

CPTU tests

The value of shear stress for earthquake type 1 (RSA) was defined considering a value r_d of 0,9.

The CPT values were modified taken into account the C_Q values.

The shear stress value was increased by the factor 1.25 based in Eurocode 8-Part 5.

Considering a % of fines of 10%, following the Seed proposal liquefaction can not occur.

The value of shear stress for earthquake type 2 (RSA) was defined considering a value r_d of 0.9.

The CPT values from CPTU 3A were modified taken into account the C_Q values.

The shear stress value was increased by the factor 1.25 based in Eurocode 8-Part 5.

Considering a % of fines of 10%, following the Seed proposal liquefaction can not occur.

Liquefaction Analysis based in Vs

Considering the Vs values registered in CPTUS 2B between 220 to 415m/s, and the Vs values registered in CPTU 14B between 201 to 389 m/s (with the exception of the value 158.7 m/s between 6 and 7 m) liquefaction can not occur.

Displacements Values

Considering the SPT modified values for earthquake type 1, and an increase factor of 1.25 a displacement value of 60 mm is obtained, considering a layer of 5 m thick.

For the earthquake type 2 a value of 75 mm is obtained.

It is important to stress;

i) The positive effect of a raft foundation with jet columns, known as "pile –raft foundation", with the capacity to absorb total displacements and differential displacements without damages to the superstructure. It is also used as a mitigation measure for ground liquefaction.

ii) Taking into account the dilatant behavior of sand materials observed in CPT tests, a safety factor of 1.1. can be considered sufficient. Nevertheless, a safety factor of 1.25 was considered to follow the EC8 recommendations.

iii) The displacements values observed in recent earthquakes, due to liquefaction, are 60 to 70 % of the calculated values (Towhata, 2009).

iv) The thickness of the layers susceptible to liquefy is less than 5 m, without continuity, so the consequences are limited, due to the lateral confinement.

v) Considering the SPT modified values for earthquake type 1, and an increase factor of 1.25 a displacement value of 60 mm is obtained, considering a layer of 5 m thick.
For the earthquake type 2 a value of 75 mm is obtained.

<u>Analysis of site 53</u>

SPT Tests

The value of shear stress for earthquake type 1 (RSA) was defined considering a value r_d of 0,9.

The SPT values for S4A were modified taken into account the C_N values.

The shear stress value was increased by the factor 1.25 based in Eurocode 8-Part 5.

Considering a % of fines of 10%, following the Seed proposal liquefaction can occur.

Following Cetin proposal the probabilistic of liquefaction occurrence is 100%.

The value of shear stress for earthquake type 2 (RSA) was defined considering a value r_d of 0.9.

The SPT values for S4A were modified taken into account the C_N values.

The shear stress value was increased by the factor 1.25 based in Eurocode 8-Part 5.

Considering a % of fines of 10%, following the Seed proposal liquefaction can occur.

Following Cetin proposal, the probabilistic of liquefaction occurrence is 100%.

CPTU tests

The value of shear stress for earthquake type 1 (RSA) was defined considering a value r_d of 0,9.

The CPT values for CPTU 4A were modified taken into account the C_Q values.

The shear stress value was increased by the factor 1.25 based in Eurocode 8-Part 5.

Considering a % of fines of 10%, following the Seed proposal liquefaction can occur.

The value of shear stress for earthquake type 2 (RSA) was defined considering a value r_d of 0.9.

The CPT values from CPTU 3A were modified taken into account the C_Q values.

The shear stress value was increased by the factor 1.25 based in Eurocode 8-Part 5.

Considering a % of fines of 10%, following the Seed proposal liquefaction can occur.

Liquefaction Analysis based in Vs

Considering the Vs values registered in CPTUS 6B between 214 to 306 m/s (with the exception of the values 167.9 m/s between 7 and 8 m and 154 m/s between 9 and 10 m), and the Vs values registered in CPTU 4B between 204 to 367 m/s (with the exception of the value 137.7 m/s between 9 and 10 m and 174 m/s between 13-14 m liquefaction can not occur.

Displacements Values

Considering the SPT modified values for earthquake type 1, and an increase factor of 1.25 a displacement value of 90 mm is obtained, considering a layer of 5 m thick.

For the earthquake type 2 a value of 95 mm is obtained for a layer of 5 m thick.

Analysis of Site 4

SPT tests

The value of shear stress for earthquake type 1 (RSA) was defined considering a value r_d of 0,9.

The SPT values for S6A were modified taken into account the C_N values.

The shear stress value was increased by the factor 1.25 based in Eurocode 8-Part 5.

Considering a % of fines of 10%, following the Seed proposal liquefaction can occur.

Following Cetin proposal, the probabilistic of liquefaction occurrence is 85%.

For earthquake type 2, following the Seed proposal liquefaction can occur.

Following Cetin proposal, the probabilistic of liquefaction occurrence is 100%.

CPTU tests

The value of shear stress for earthquake type 1 (RSA) was defined considering a value r_d of 0.9.

The CPT values for CPTU 6A were modified taken into account the C_Q values.

The shear stress value was increased by the factor 1.25 based in Eurocode 8-Part 5.

Considering a % of fines of 10%, following the Seed proposal liquefaction can occur.

The value of shear stress for earthquake type 2 (RSA) was defined considering a value r_d of 0.9.

The CPT values from CPTU 6A were modified taken into account the C_Q values.

The shear stress value was increased by the factor 1.25 based in Eurocode 8-Part 5.

Considering a % of fines of 10%, following the Seed proposal liquefaction can occur.

Liquefaction Analysis based in Vs

Considering the Vs values registered in CPTUS 9B between 192to 398.6 m/s (with the exception of the values 174.4 m/s between 8 and 9 m and 149.8 m/s between 9 and 10 m), liquefaction can not occur.

Displacements Values

Considering the SPT modified values for earthquake type 1, and an increase factor of 1.25 a displacement value of 52 mm is obtained, considering a layer of 4 m thick.

For the earthquake type 2 a value of 68 mm is obtained for a layer of 5m thick.

Foundations Settlements

Consequently, the Structural Damage index is D1 to D2 and the Ground Failure Index is GF1.

In summary: From the liquefaction analysis it can be concluded that displacements due to liquefaction are less than 100mm and the values of rotations following the survey of Niigata (1964), Filipinas (1990), Kobe (1995), Kocaeli (1999) e Chi-Chi (1999) earthquakes are less than 1 degree.

Consequently, the Structural Damages of the building can be classified as D1 e D2, light to moderate damages and the Ground Failure Index is classified as weak.

Lesson16:

Major gaps continueto persist with regard to our ability to accurately and reliably assess the likely consequences of liquefaction. This is particularly true for situations in which structural and/or site displac ements and deformations are likely to be "small to moderate" (≤ 0.75m.). Improved analytical and design tools, related "acceptable" performance, are needed.

Note: This study was done for Jetsj.

8. 5. PORT STRUCTURES

8.5.1 Introduction

The first means for the goods of transport was over the water in comparison with other means of transport such as road, rail and air.
So, the first waterborne trade developed in the great river-based civilizations like those of the Nile, the Indus, the Tigris and Euphrates and the Yellow River.

There are records from Egypt, Crete and later Phoenicia. Trading between Egypt and Crete, some 6,000 years ago has involved the transportation by ships of grain and cattle.

The Chinese maritime trade since 5000 BC, was initially limited to the inshore, but since Zhou (770-256 BC) has expanded to the Yellow Sea.

Indian sea trade goes back as far as 3000 BC, and large dry dock was constructed of bricks in Lothal, state of Gujarat.

Alexander de Great's port located in Egypt has implemented the techniques of the Minoan of Crete.

Northern Europe has more natural harbours than the Mediterranean and with many fjords have developed with Mediterranean countries.
Subsequently to the fall of the Roman gain high movement.

In the 10th century the German and Dutch merchants appeared in England.

By the end of the 15th century great voyages were performed by Europeans. Columbus reached America in 1492. The Portuguese sail to India to obtain goods from Asia and found the route for Africa.

The 16th century was a century of great development in shipping. The Treaty of Tordesillas in 1494 with the decision of the Pope to prevent war and to spread Catholic faith the 'New world' should be divided between Spain (western half) and Portugal (eastern half).

In the Netherlands, with around 25% of the country below the sea, quay walls (along with the water defense system) play an important role to protect the cities. Many of these quay walls exhibits deteriorations due to the failure or settlements of the timber pile foundations and lack of maintenance.

The quay walls were designed as massive gravity retaining walls. The foundations of these gravity walls were conceived as massive concrete bodies, constructed within a pneumatic caisson.

For many years stone and wood were used as construction materials. It is important to refer that with those materials only compressive forces can be sustained, although wood has small tensile strength. With the use of cast iron to steel and around 1900 of reinforced concrete it was also possible to sustain bending moments. So slender structures were designed.

In general, the quay walls are designed considering a safety factor and so the uncertainties are not correctly integrated.
However, the semi-probabilistic design approach is getting more popular and so the incorporation of the uncertainties is getting increase attention.
Advance studies recommends that the concrete superstructure should be incorporated into the fault tree to reach a total probabilistic design.

The quay walls design has incorporated the reliability theory and Eurocode standard EN 1990 introduced three reliability classes (RC), based on the potential consequence of failure of the structure, and the probability of failure is linked with the reliability index (β).

The reliability theory has been introduced in the design and is recommended to select a high reliable class to prevent potential damages and to guarantee the reputation of the terminal.

People who made major contributions to develop design theories include Leonardo da Vinci, Newton, Galileo, Coulomb, Rankine, Simon Stevin, and Terzaghi. Recent design codes for quay walls demand performance-based designs. To obtain a safe and economical aseismic design, these codes require that the seismic performance of the quay walls be evaluated based on the permanent wall displacement after an earthquake exploring dynamic analyses or simplified dynamic analyses based on the Newmark sliding block. However, dynamic analyses require additional time consumer and reliable soil parameters defined by special tests.

The simplified dynamic analyses exploring the Newmark sliding block concept are very popular for the preliminary designs because they can easily evaluate the wall displacement by using basic design parameters such as the weight of the wall, the internal friction angle of the backfill, and the frictional coefficient at the bottom of the wall.

Richard and Elms and Whitman and Liao proposed simplified dynamic analyses based on the Newmark sliding block to evaluate the seismic displacement of the wall. In their methods, yield acceleration is defined as the wall acceleration, when the factor of safety of the wall for sliding becomes 1.0, the wall

displacement is presumed to occur if the ground acceleration exceeds the yield acceleration. However, these analyses cannot consider the variation of wall thrust due to the development of excess pore pressure in the backfill during earthquakes.

To overcome this situation several researchers suggested degrading yield acceleration models, in which yield acceleration decreased as a function of shear deformation of the material or with value of excess pore pressure for saturated slopes.

Simplified dynamic analyses based in the Newmark model, with the variation of the yield acceleration and incorporating the excess pore pressure for the computation of wall sliding displacement were proposed. These methodologies were calibrated by comparing the predicted displacements values with the results of shaking table tests.

The failure of quay walls induced by earthquakes has been carefully analysed exploring centrifuge model tests and it was concluded that amplification of motion effects due to the resonance may aggravate the structure response in comparison with the predicted response by a pseudo-static analysis. This resonant effect is due to the generation of excess pore pressures and consequently stiff degradation of the backfill material.

8.5.2 Case History 17 - Malabo Quay

8.5.2.1 Introduction

A synthetic description of Malabo quay is presented, the geological characteristics are described, the site characterization is referred, the stability analysis is mentioned, the stress-strain analyses are discussed and the instrumentation is addressed.

8.5.2.2 Synthetic Description

Malabo quay, situated in Guinea Equatorial, is composed by 13 reinforced caissons, with 23,65 m x 19,75 m, and cells 4,50 m x 3,50 m, with granular material. It is founded on a rockfill prism with a height 3,8 m to 9 m, with a superior layer of gravel 20/80, with a thickness of 3.0 m to 9m, and the foundation is reinforced by gravel columns with a diameter of 800 mm and variable length, built by vibroflotation, and founded in the volcanic rocks.

The level of the caissons base is –16,55m, with a height of 19,75m, and the level of the platform is 2,50.

The quay has the capacity to receive ships of 27 000 DWT, a height of 20 m and 280 m long, with 4,0 m above the minimum level of the tide.

Figure 8.307 illustrates the cross section of the quay.

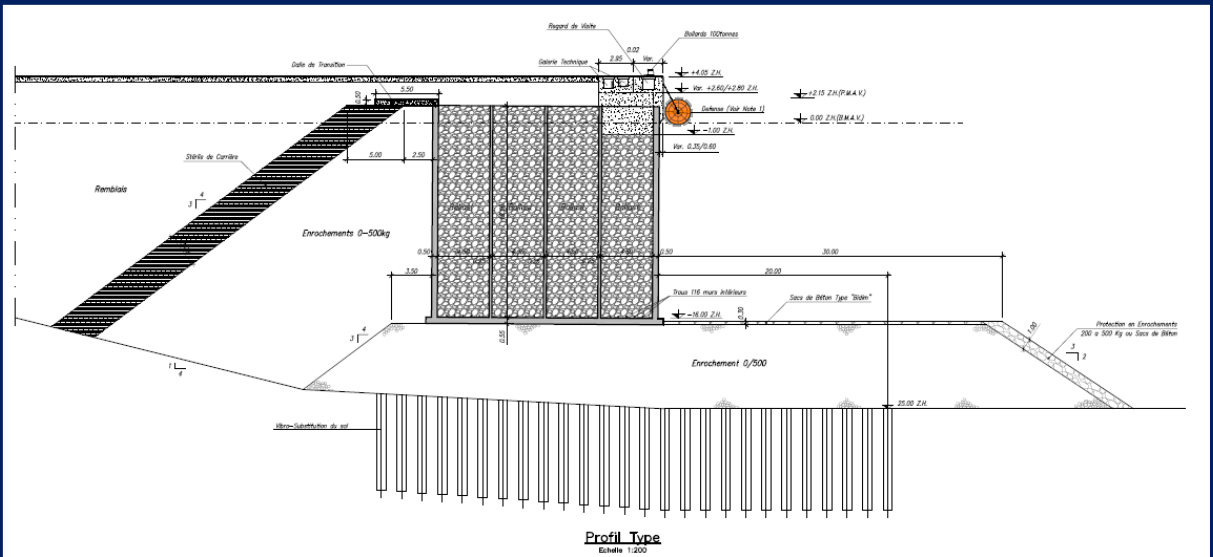

Figure 8.307 Cross section

8.5.2.3 Geological Characteristics

A) Alluvial materials:

i) sandy materials with a thickness of 3.0 m.

ii) Silty clays with a thickness of 5 to 6 m.

iii) sandy clays with gravel materials with a thickness of 5 m.

B) Vulcanic materials.

C) Weathered and fractured basalts.

8.5.2.4 Site Characterization

8 boreholes and 5 seismic reflexion profiles were performed in the west side and 6 boreholes and 3 seismic reflexion profile were performed in the south side.

In these boreholes, SPT tests, 1.5 m apart, were performed and the water level was recorded.

25 penetration tests, with depths between 5.95 (SCM20), and 40.1m (SCM1) and 20 pressuremeter tests were performed.

Identification tests (sieve analyses, Atterberg limits), density, sand equivalent, mechanical resistance tests and oedometer tests were performed.

8.5.2.5 Geotechnical Characteristics

A summary of the mechanical characteristics is given below:

i) Sandy materials

Unit weight: 19 kN/m3

Cohesion = 0

Friction angle = 25º

Elasticity modulus 8 MPa to 10 MPa.

ii) Silty clays

SPT tests with 10 to 20 blows.

Unit weight: 19 kN/m3

Cohesion = 10 kPa

Friction angle = 25º

Elasticity modulus 8 MPa to 15 MPa.

iii) Sandy clays with gravel materials

The SPT values were between 15 to 40 blows.

Unit weight: 19 kN/m3

Cohesion = 5 kPa

Friction angle = 27º

Elasticity modulus 10 MPa to 25 MPa.

iv) Vulcanic ashes

The SPT values between 20 to 50 blows.

Unit weight: 19 kN/m3

Cohesion = 30 kPa

Friction angle = 25º

Elasticity modulus 15 MPa to 40 MPa.

v) Fractured and weathered basalts

The SPT values were higher than 60 blows and the RQD values were low:

The following mechanical characteristics were considered:

Weathered materials

Unit weight: 20 kN/m3

Cohesion = 70 kPa

Friction angle = 27º

Elasticity modulus higher than 50 MPa.

Consolidated materials

Unit weight: 21 kN/m3

Cohesion = 100 kPa

Friction angle = 28º

Elasticity modulus higher than 60 MPa.

Table 8.45 summarizes the characteristics of the materials.

Table 8.45 Characteristics of the Materials

Formations	*Poids Volumique (kN/m^3)*	*Angle de Frottement (º)*	*Cohésion (kN/m^2)*
Caisson	*22,50*	*45*	*100*
Enrochement 30-70	*22,50,*	*45*	*0*
Rem Hydro	*19,00*	*35*	*0*
Enrochement 30-70	*22,50*	*45*	*0*
Sables Fins Noirâtres	*17,00*	*30*	*0*
Argiles Limoneuses Grisâtres	*19,00*	*25*	*5*
Limons Argilo-Sableux Verts-Gris	*20.00*	*27,5*	*3*
Tuf et Cendre Tourbe	*16,00*	*20*	*16*
Tuf Tendre	*22,00*	*35*	*20*
Tuf Raide	*22,00*	*40*	*500*

Table 8.46 shows the characteristics of the gravel columns.

Table 8.46 Valeurs de Calcul des Colonnes Ballastée

Matériel	*Poids Volumique (kN/m^3)*			*Angle de Frottement (º)*	*Cohésion (kN/m^2)*
Gravier	*19,00*			*45,00*	*0*

8.5.2.6 Stability Analysis

The SLOPE W code was used to define the minimum safety factor for different scenarios of water level, also different positions of the foundation's layers, and so to analyse by pseudo-static method different levels of seismic actions.

For the pseudo-static analyses the seismic coefficient values where Kc = 0.14 g and Kc = 0.186 g.

Figure 8. 308 to 8.311 shows the results for static analyses and pseudo-static analyses for horizontal layers of foundation.

Figure 8. 312 to 8.316 shows the results for static analyses and pseudo-static analyses for inclined layers of foundation.

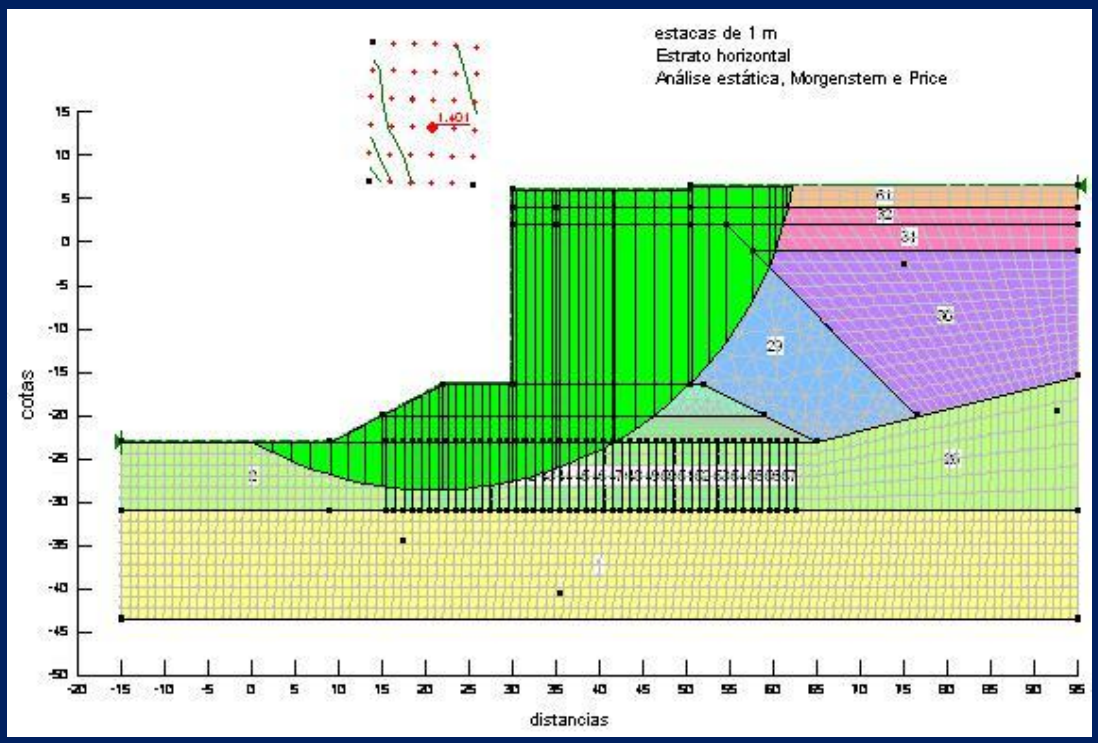

Figure 8.308 Horizontal layer – Static analysis. Critical surface

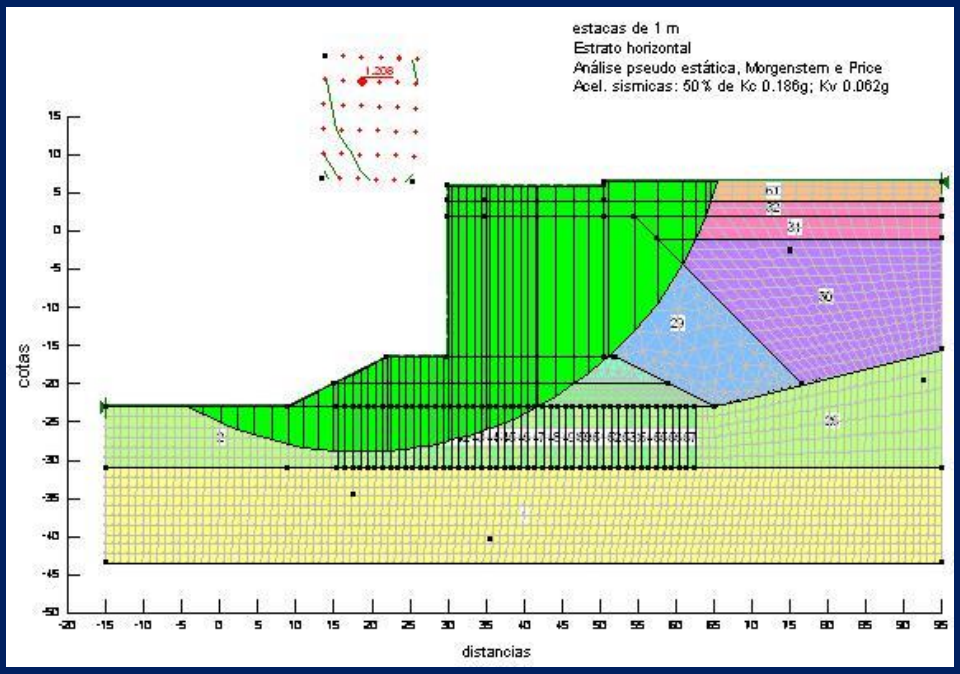

Figure 8.309 Horizontal layer – Pseudo-Static analysis. Critical surface

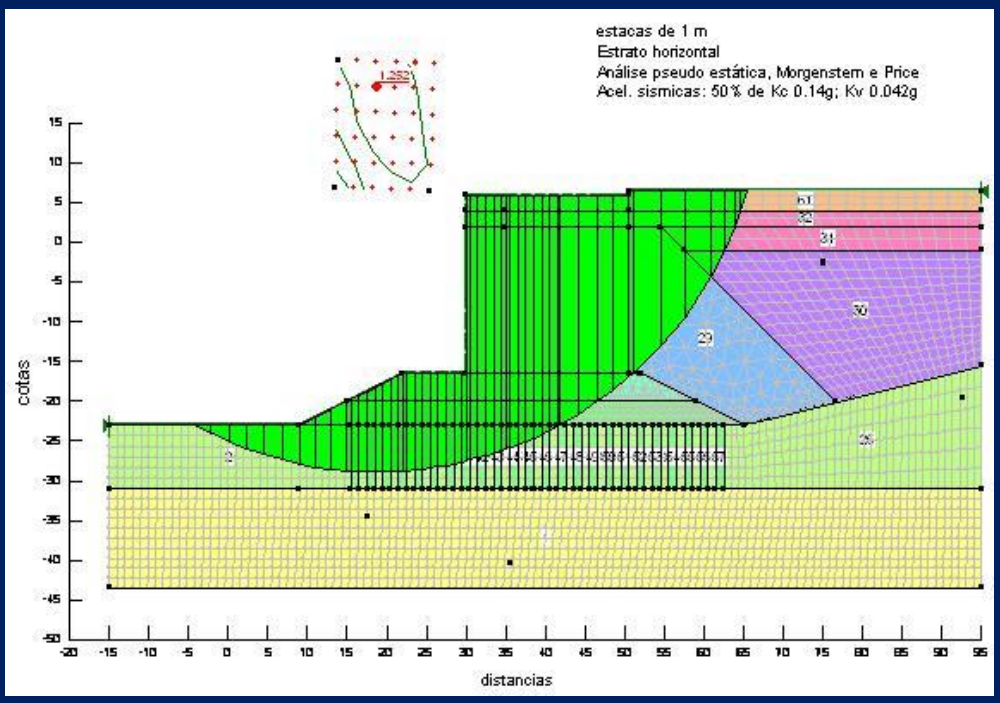

Figure 8.310 Horizontal layer – Pseudo- Static analysis. Critical surface

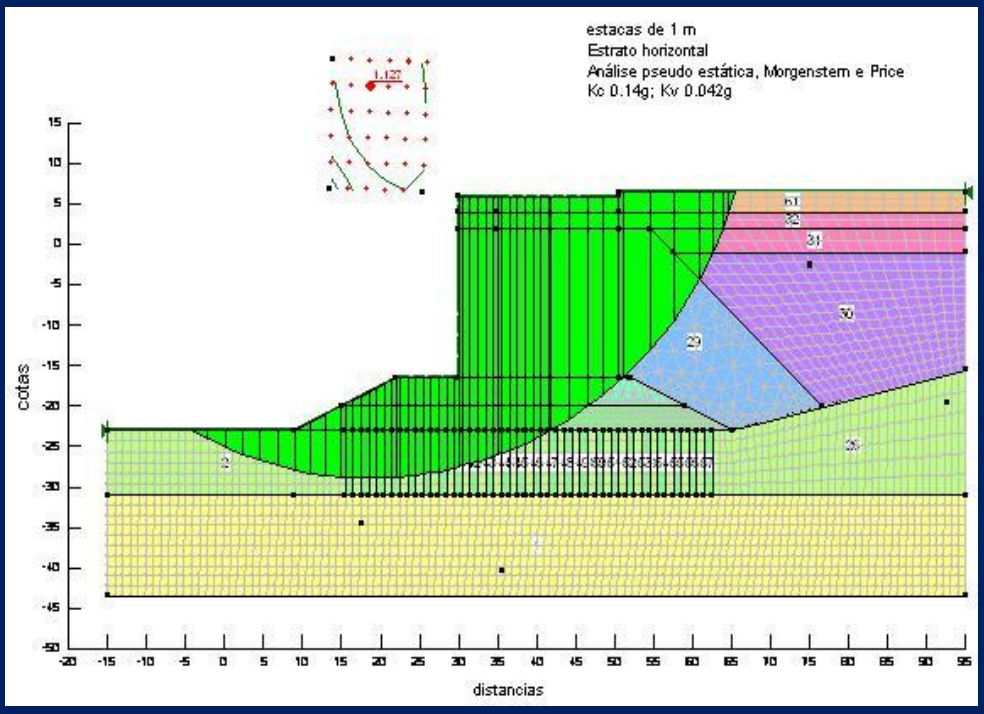

Figure 8.311 Horizontal layer – Pseudo- Static analysis. Critical surface

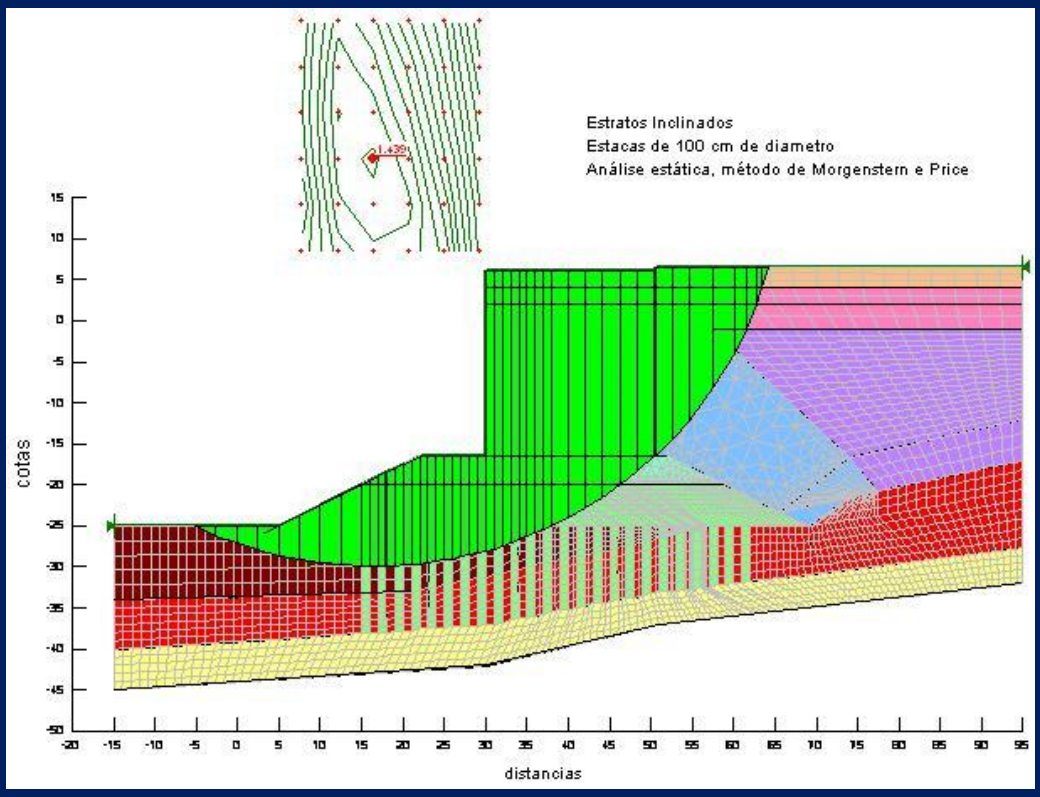

Figure 8.312 Inclined layer – Static analysis. Critical surface

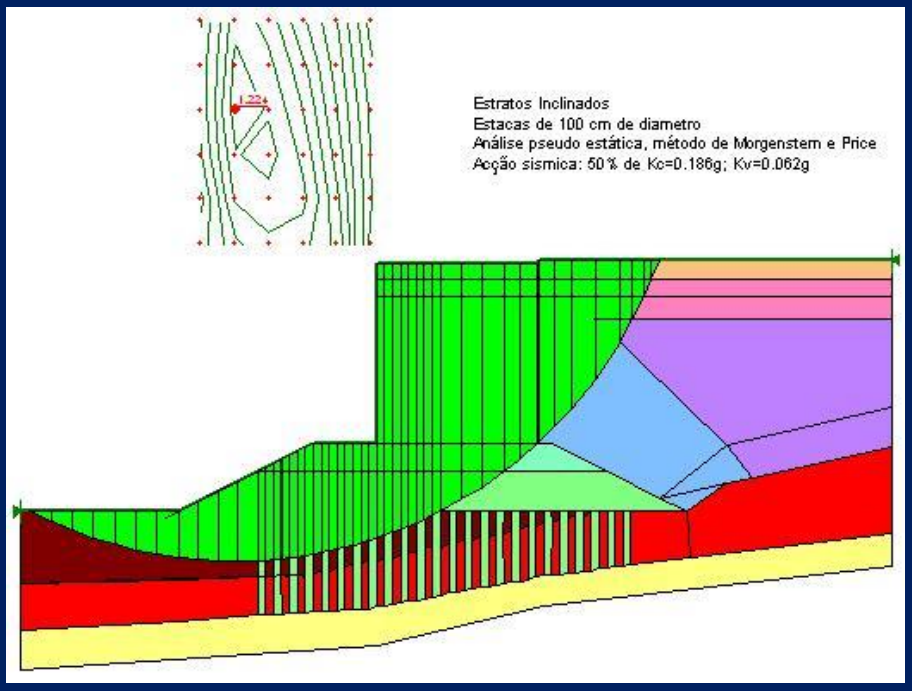

Figure 8.313 Inclined layer – Pseudo- Static analysis. Critical surface

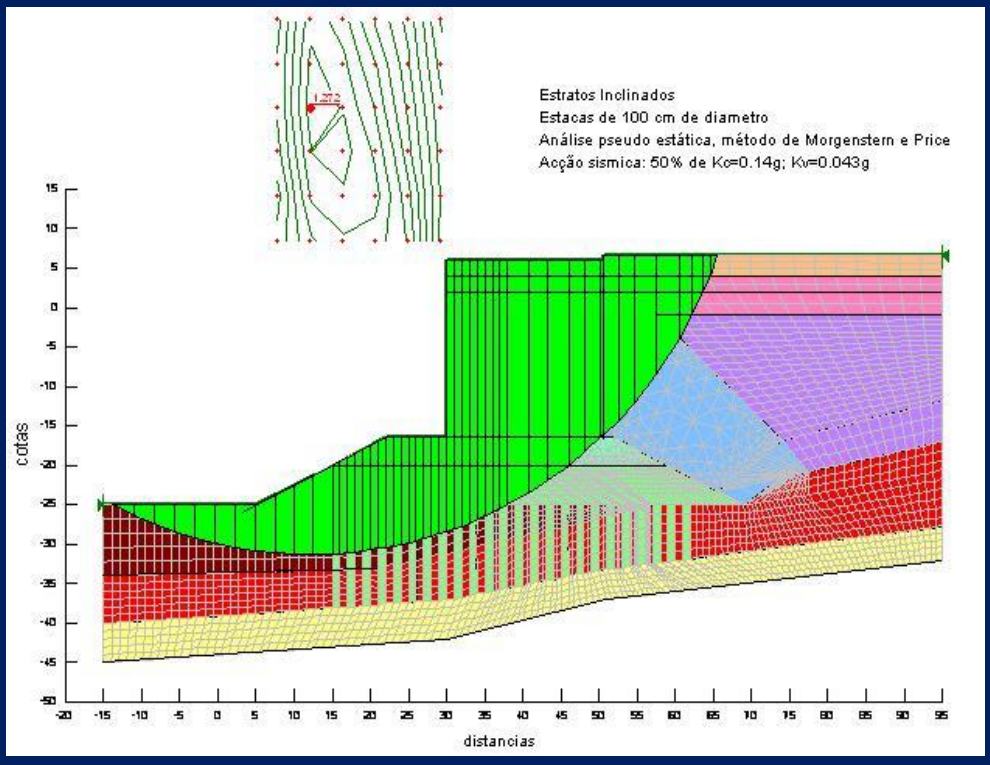

Figure 8. 314 Inclined layer – Pseudo- Static analysis. Critical surface

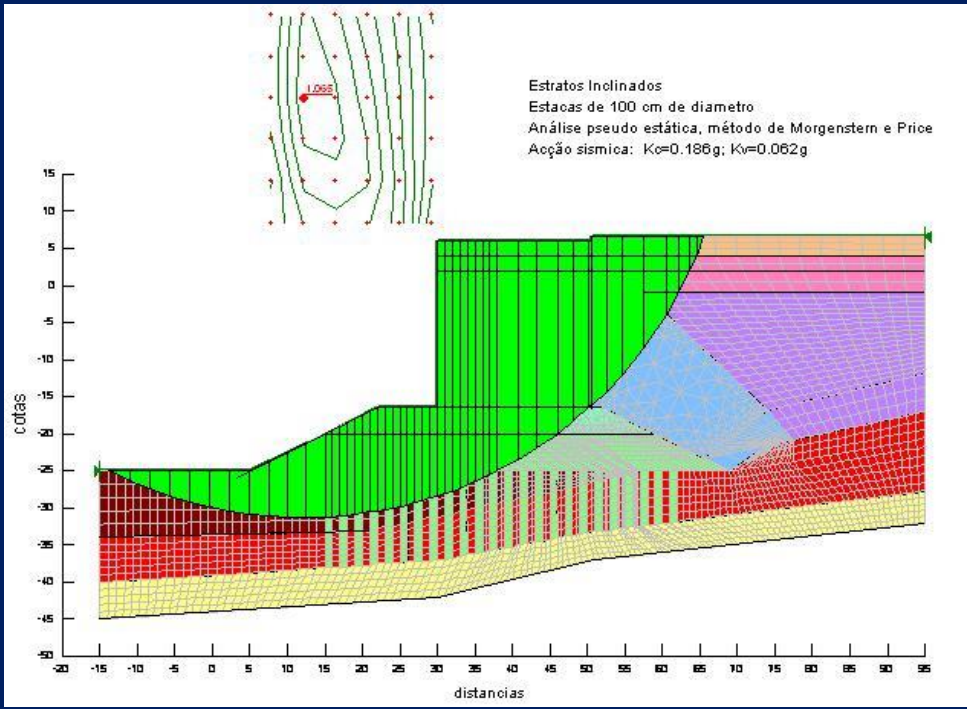

Figure 8. 315 Inclined layer – Pseudo- Static analysis. Critical surface

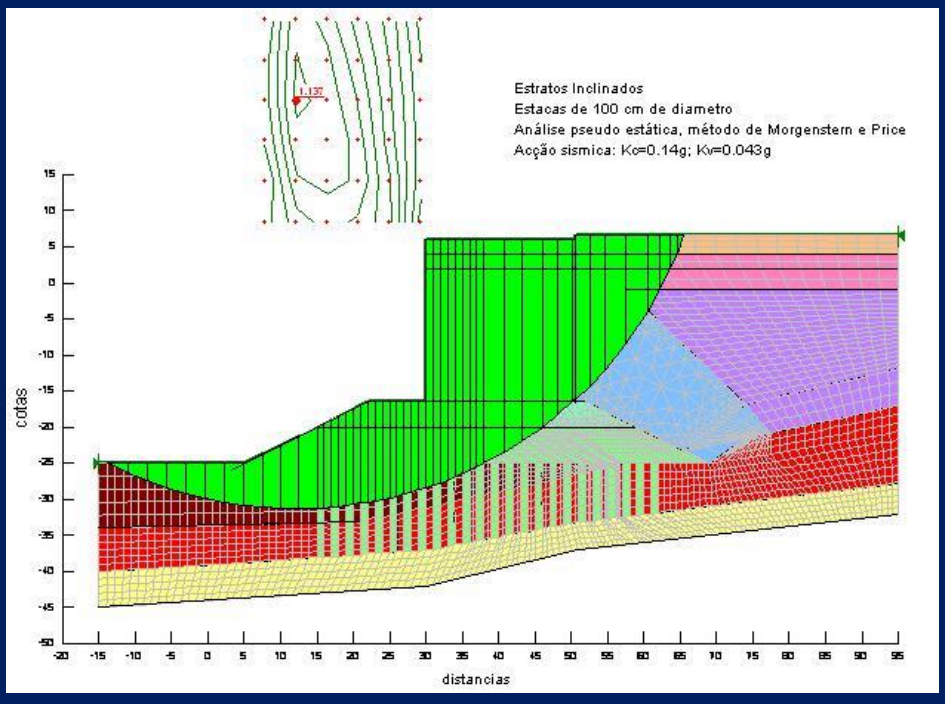

Figure 8. 316 Horizontal layer – Pseudo- Static analysis. Critical surface

Conclusion: The computed values of minimum safety factor coefficients, for static and seismic conditions, assure the stability of the quay wall.

For the different analyses the construction phase was simulated in 7 steps :

1) Placement of the lower part of the embasement after the construction of gravel columns ;
2) Placement of the superior part of the embasement with 3,0m thick to be vibrated;
3) Placement of the rockfill material 10-500 kg;
4) Placement of the caissons;
5) Placement of the fill material;
6) Placement of the final layer of the fill ;
7) Application of the surcharge of 20 kPa for the caissons and 40 kPa for the fill.

8.5.2.7 Stress-Strain Analyses

To verify serviceability limit states stress-strain analyses by SIGMA code were performed considering an elastic behaviour for the materials.

Table 8.47 summarizes the values of the modulus of elasticity for the different materials.

Table 8.47 Modulus of elasticity

Materials	E (MPa)
Caisson	
Rockfill	30
Sands	10
Silty sands	12
Clay sands	18
Sandy materials	30
Waethered and fractures basalts	60
Gravel columns	40
Rockfil in the fill	25
Fill	25

Figure 8. 317 shows the geometry and steps of loading -horizontal layers.

Figure 8. 318 illustrates the geometry - 4th step of loading for horizontal layers.
Figure 8. 319 presents the computed settlements (m)- 4th step of loading for horizontal layers.

Figure 8. 320 shows the geometry – 7th step of loading for horizontal layers.
Figure 8. 321 illustrates the computed displacements (m) - 7th step of loading – horizontal layers
Figure 8. 322 presents the computed settlements at the caissons base for the different phases – gravel columns 1.0 m diameter (horizontal layers)
Figure 8. 323 exhibits the computed settlements at the caissons base for the different phases – gravel columns 0.9 m diameter (horizontal layers)
Figure 8. 324 shows the geometry and steps of loading phases for inclined layers.
Figure 8.325 illustrates the geometry - 4th step for inclined layers.

Figure 8. 326 presents the computed settlements (m)- 4th step of loading for inclined layers.
Figure 8. 327 shows the geometry - 7th step of loading for inclined layers.
Figure 8. 328 illustrates the computed displacements (m) - 7th step of loading for inclined layers.
Figure 8. 329 presents the computed settlements at the caissons base for the different phases – gravel columns 1.0 m diameter (inclined layers).
Figure 8. 330 exhibits the computed settlements at the caissons base for the different phases – gravel columns 0.9 m diameter (inclined layers).

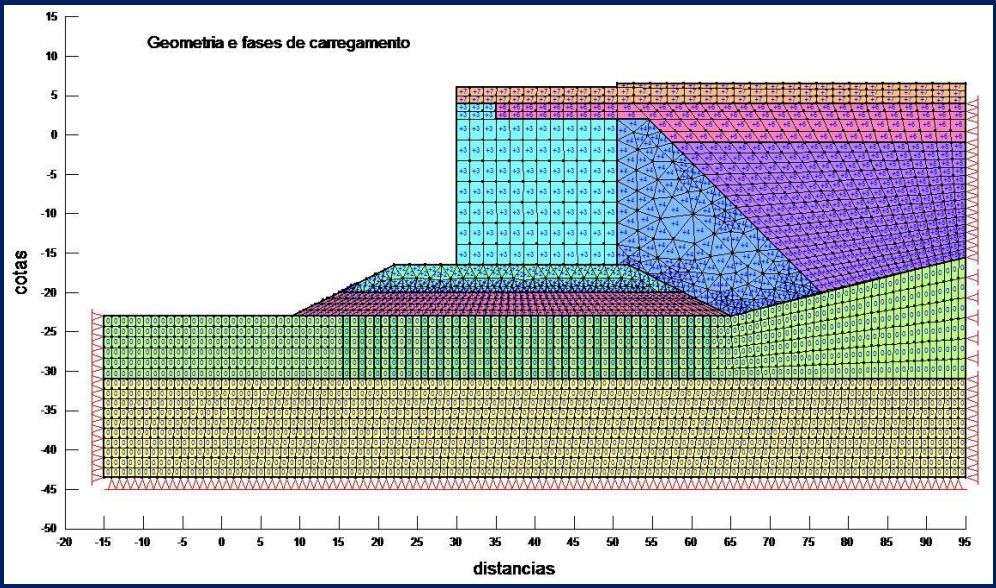

Figure 8. 317 Geometry and steps of loading -horizontal layers

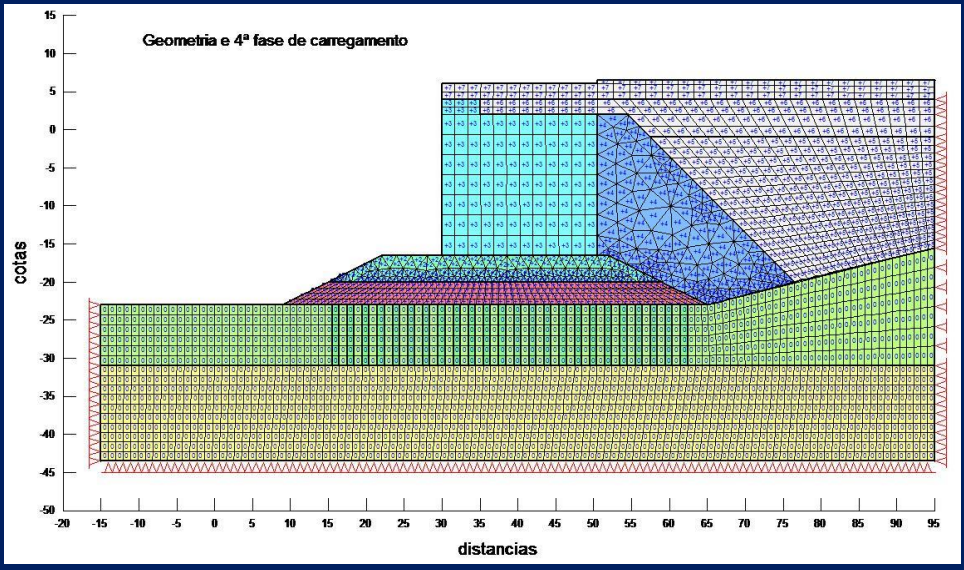

Figure 8. 318 Geometry - 4th step of loading – horizontal layers

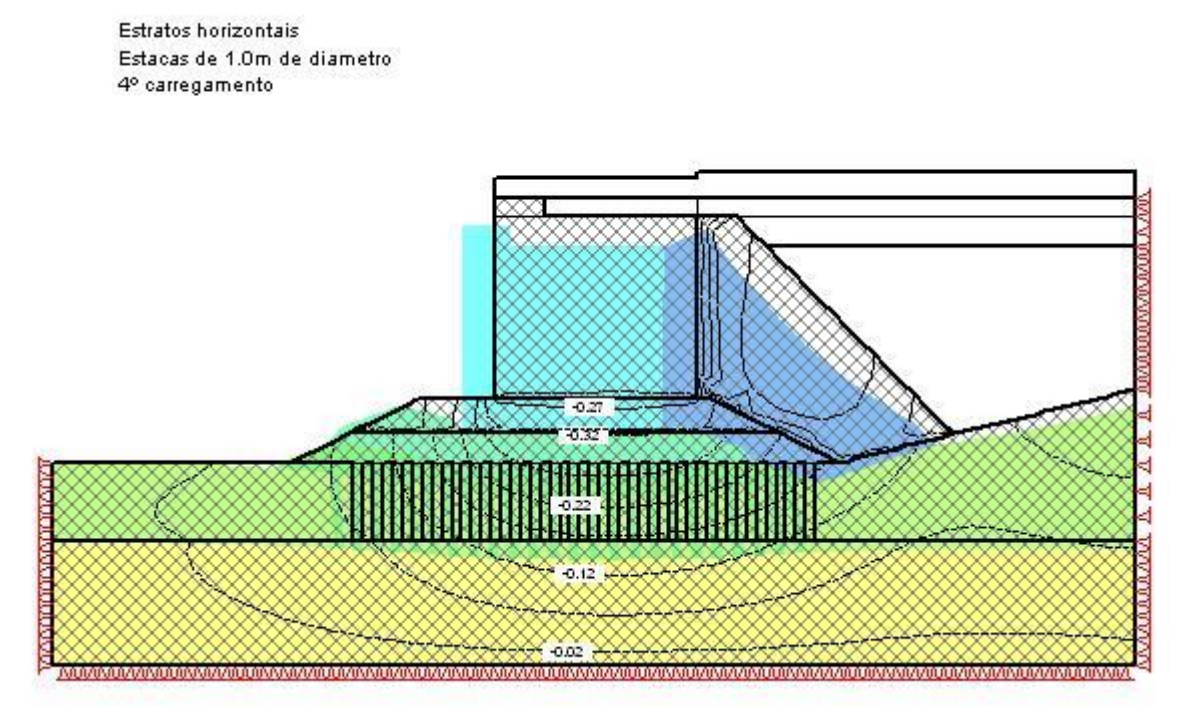

Figure 8. 319 Computed settlements (m)- 4th step of loading – horizontal layers

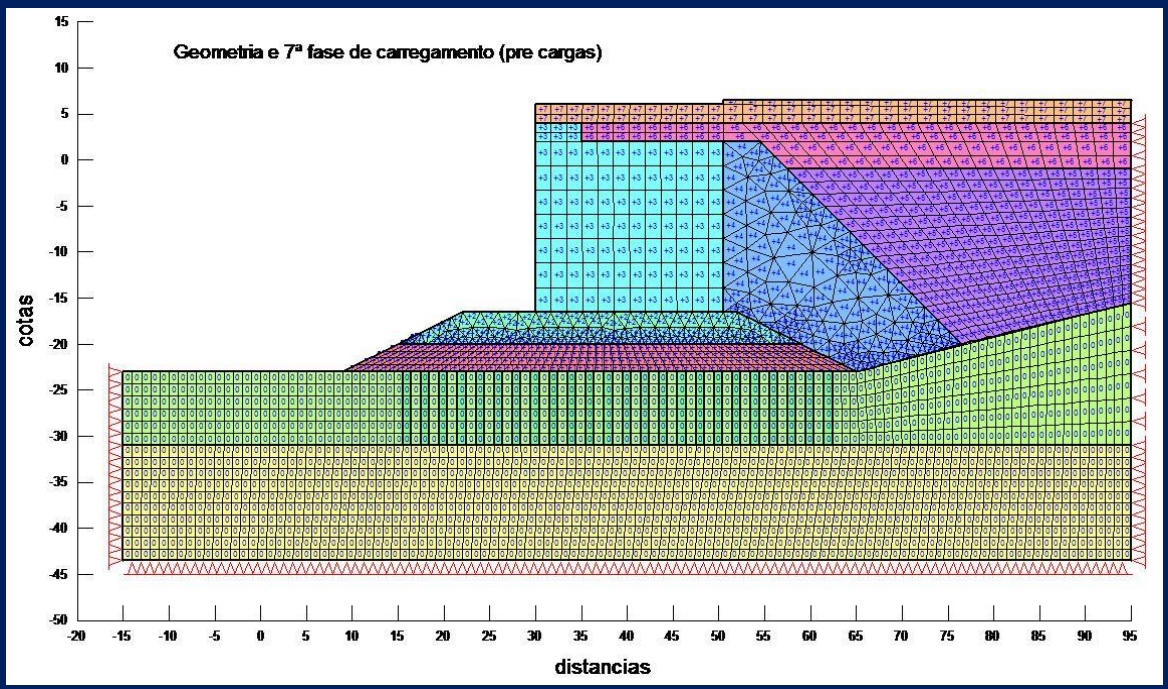

Figure 8. 320 Geometry – 7th step of loading – horizontal layers

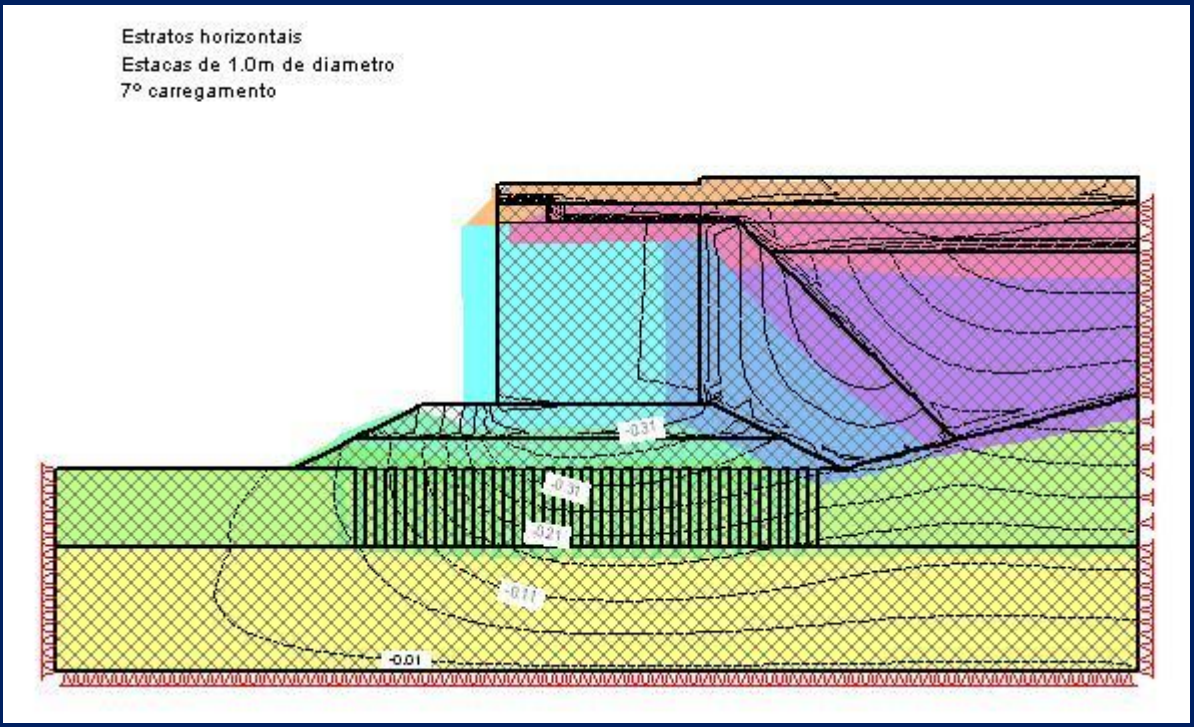

Figure 8. 321 Computed displacements (m) - 7th step of loading – horizontal layers

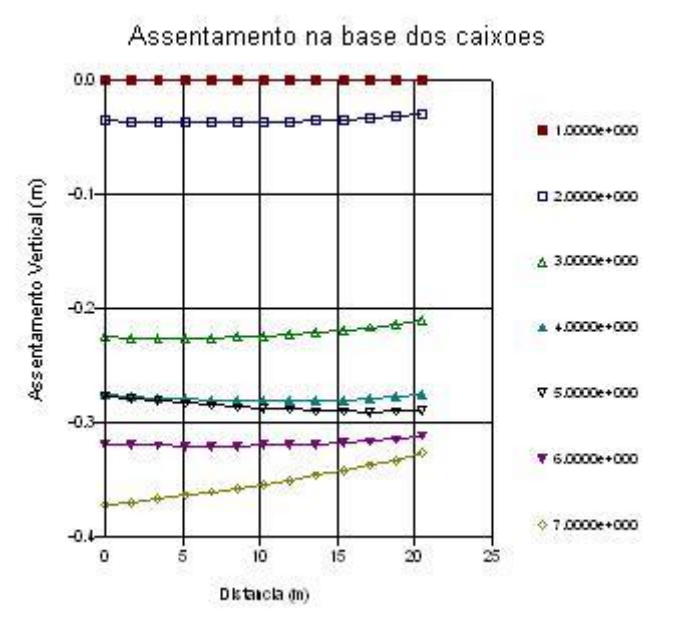

Figure 8. 322 Computed settlements at the caissons base for the different phases – gravel columns 1.0 m diameter (horizontal layers)

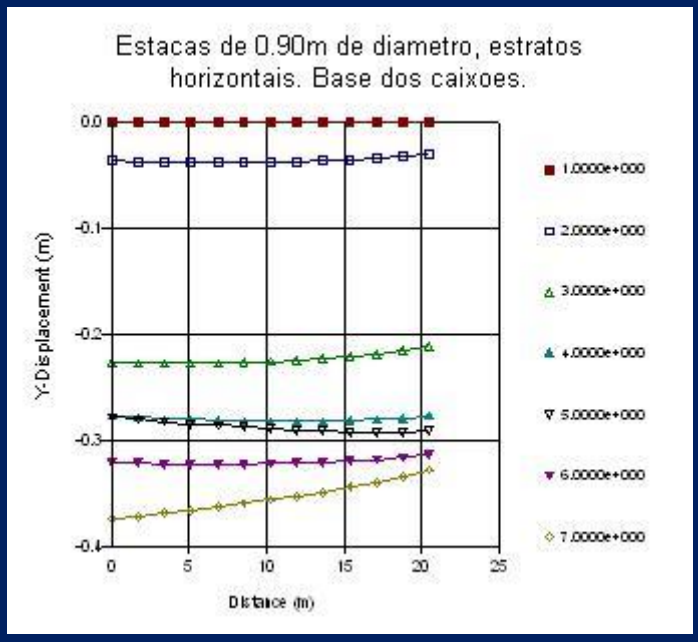

Figure 8. 323 Computed settlements at the caissons base for the different phases – gravel columns 0.9 m diameter (horizontal layers)

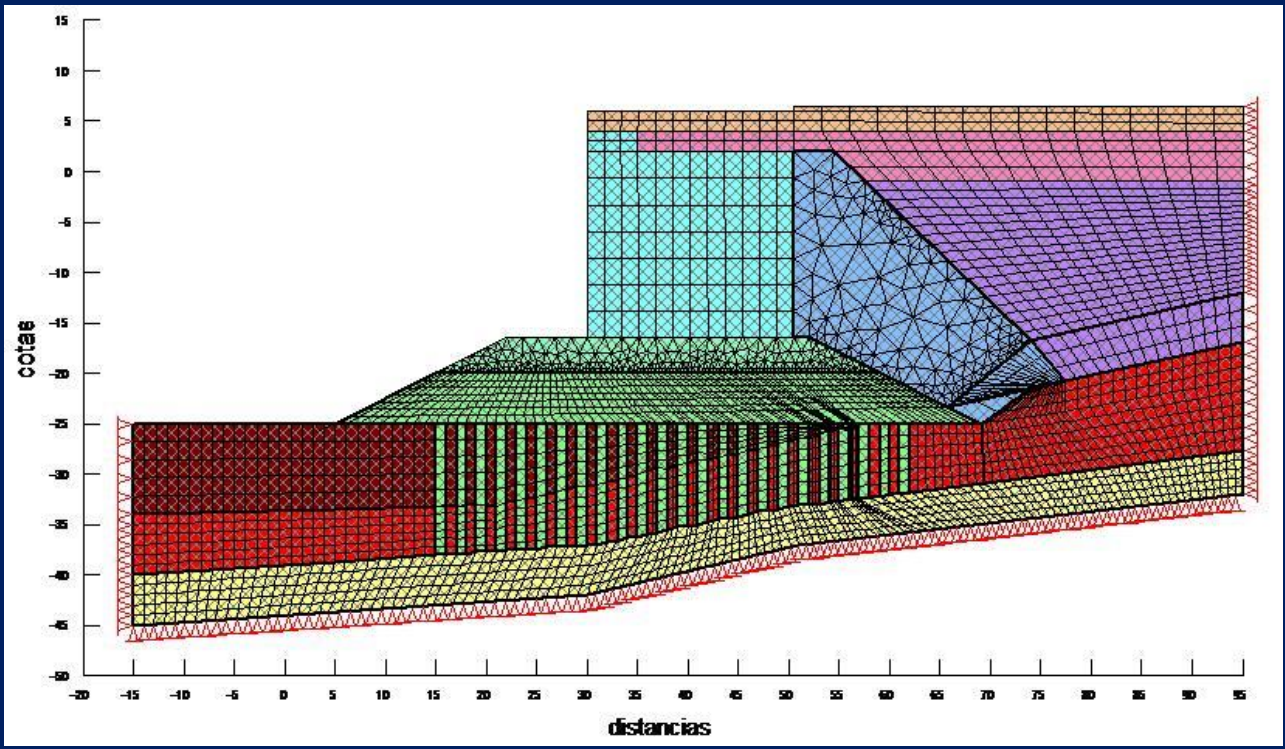

Figure 8. 324 Geometry – Loading phases-inclined layers

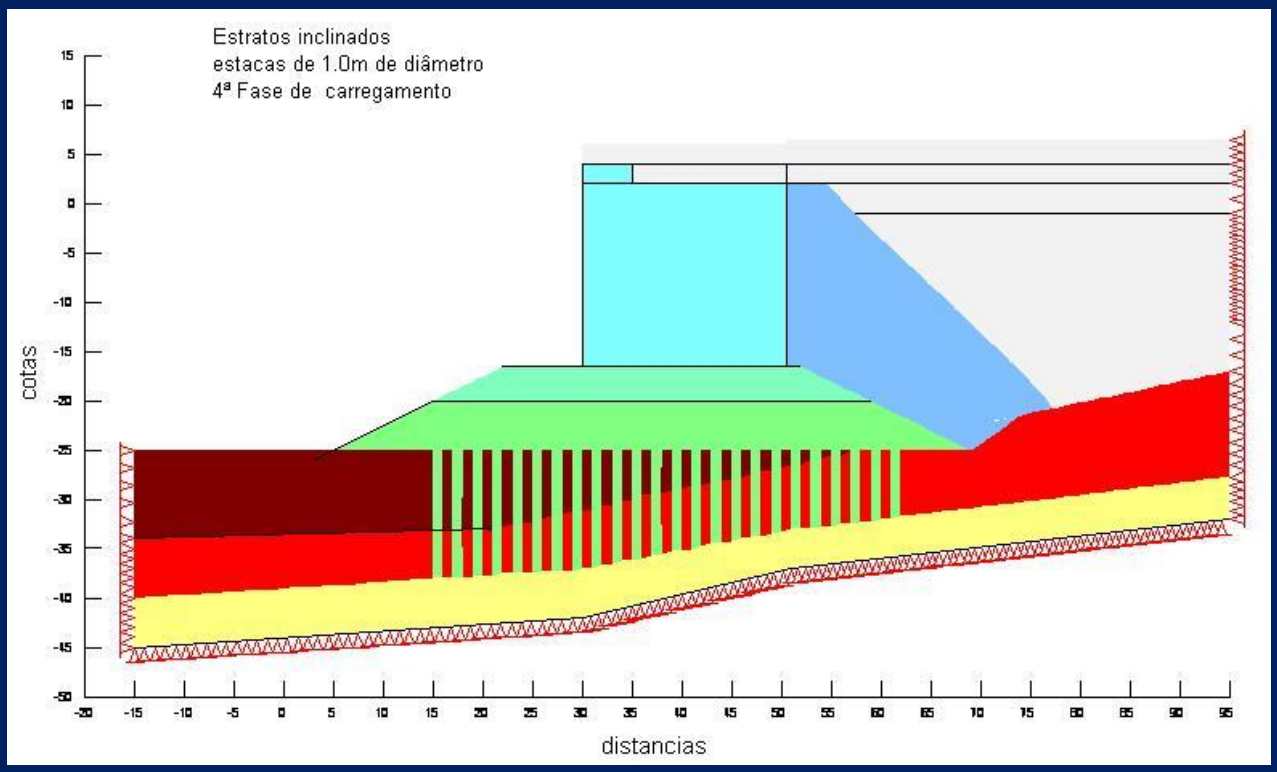

Figure 8.325 Geometry 4th step -inclined layers

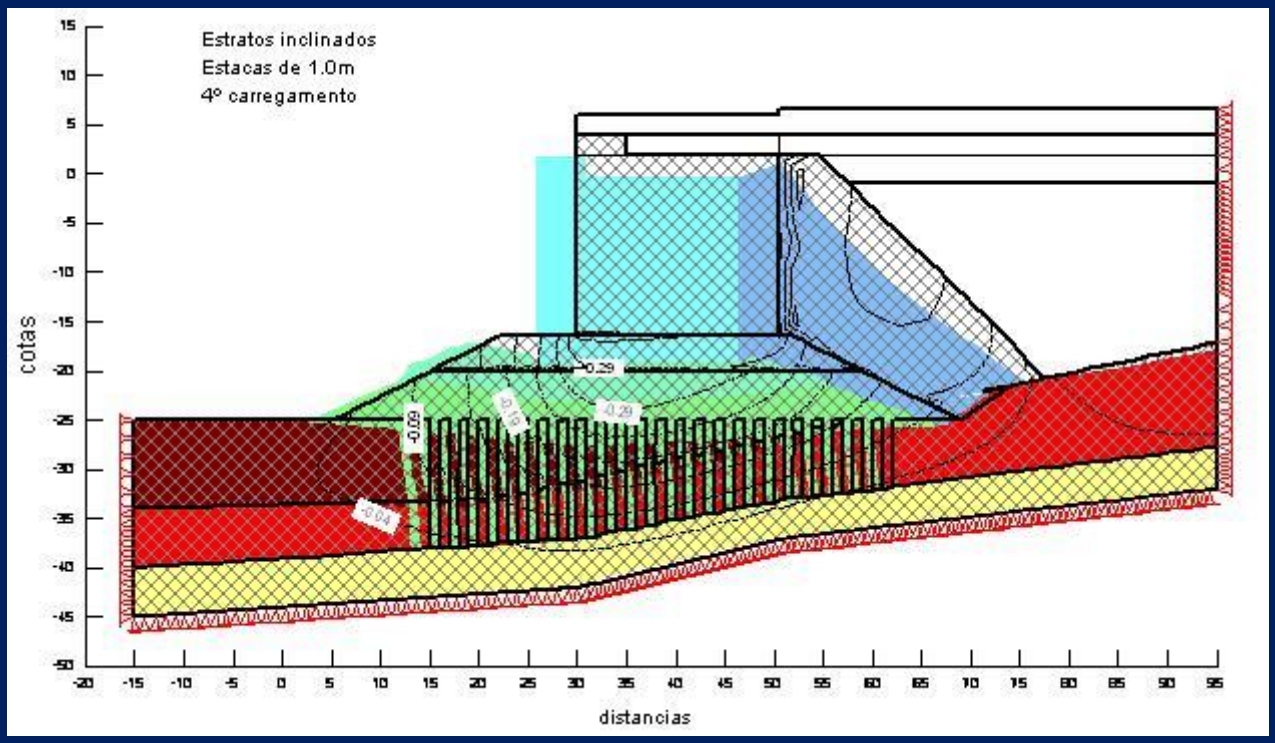

Figure 8. 326 Computed displacements (m) – 4th step- inclined layers

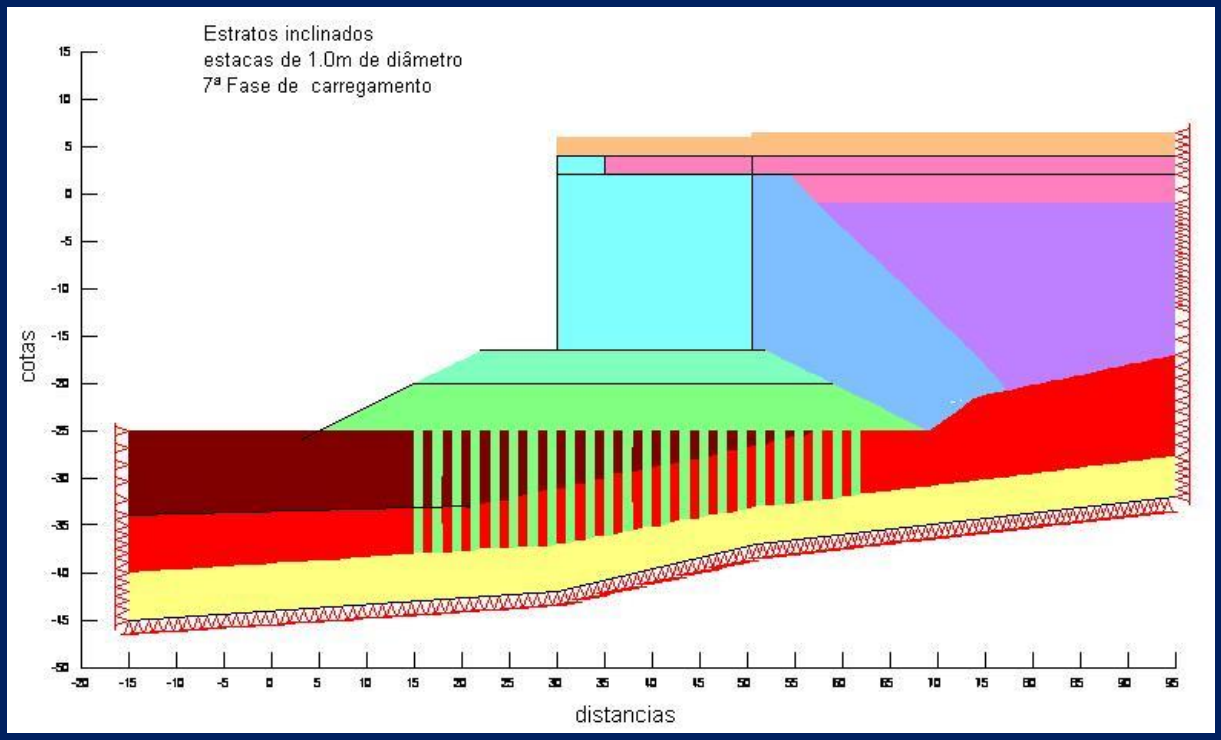

Figure 8.327 Geometry – 7th step – inclined layers

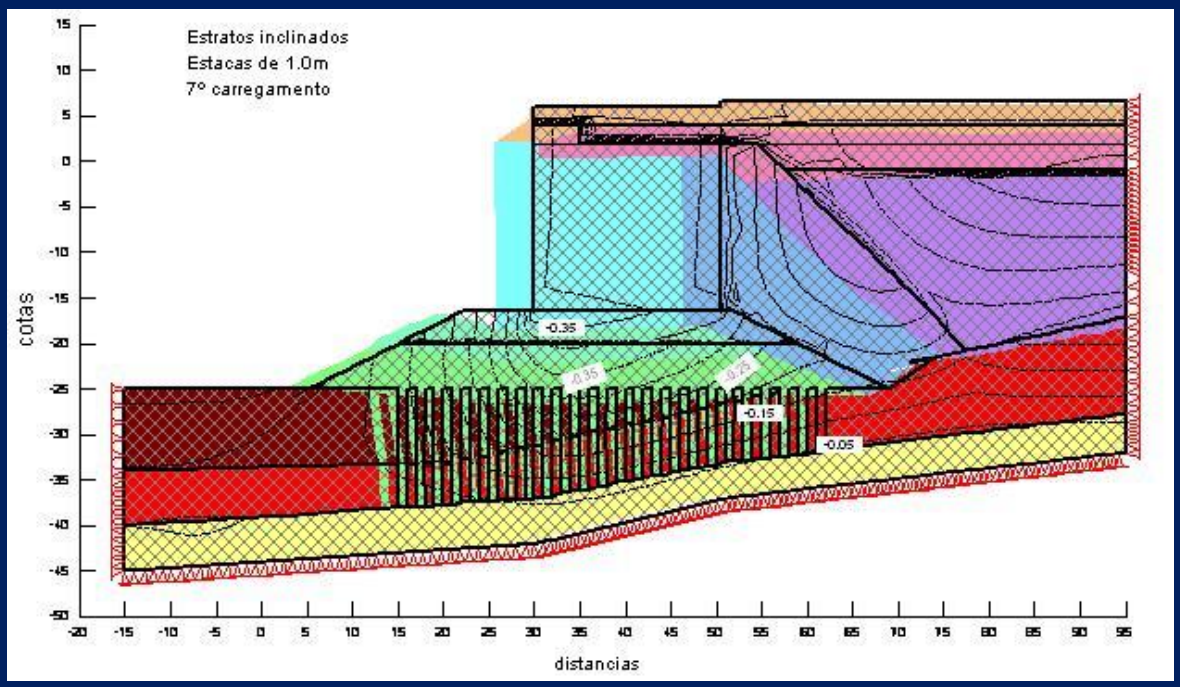

Figure 8. 328 Computed displacements (m) – 7th step- inclined layers

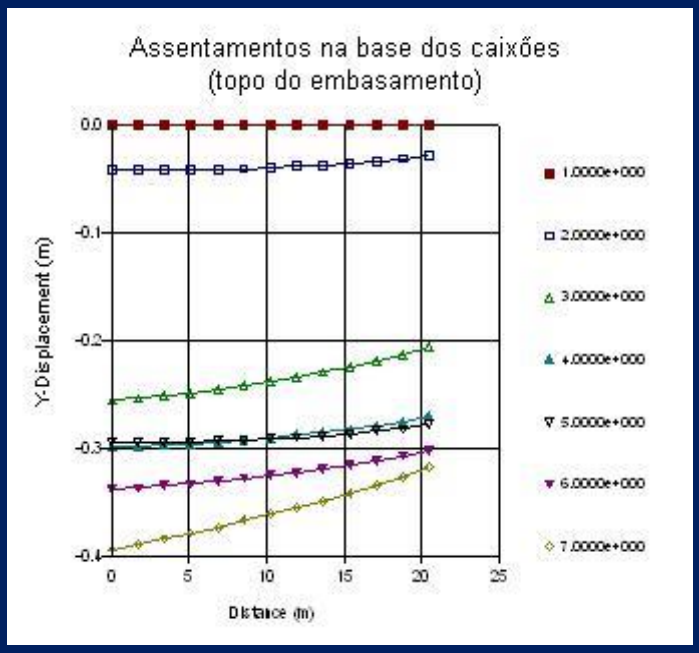

Figure 8. 329 Computed settlements at the caissons base for the different phases – gravel columns 1.0 m diameter (inclined layers)

i) The computed displacement values give a good insight, in spite the use of a linear model for the materials behavior.

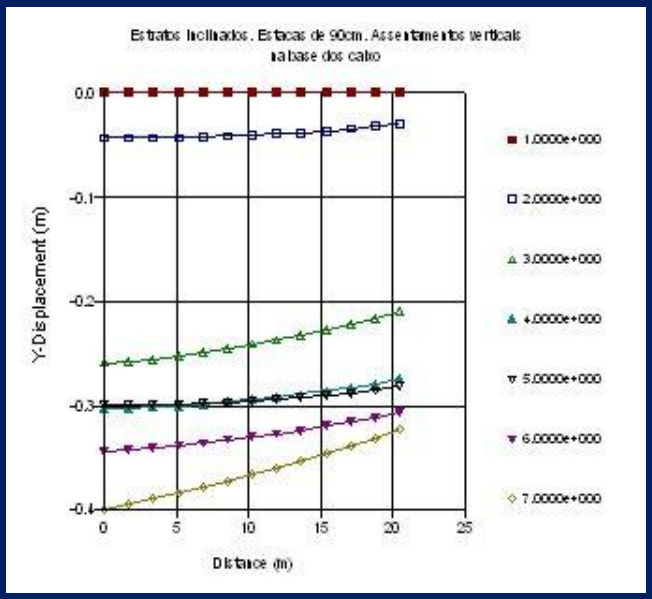

Figure 8. 330 Computed settlements at the caissons base for the different phases – gravel columns 0.9 m diameter (inclined layers)

ii) The computed displacements are independent from the diameter of the gravel columns, namely 0.9 m or 1.0 m.

iii) The computed displacements values have shown no influence related the inclination of the ground layers.

8.5.2. 8 Instrumentation

The recorded values of the settlements and the sliding for the caissons, determined weekly, were analysed. For the caisson nº 2 and for the caisson nº 10 the recorded sliding values were 28.6 cm and 61.0 cm, respectively.

The settlements of the caissons were recorded for the following phases:
- before the filling;
- after the filling with gravel material;
- after the filling with concrete;
- after the rockfill prism;
- after the pre-charge.

The settlements were recorded from the sea side and land side.

The maximum recorded settlement for the sea side was 1.72 m (caisson 9) and for the land side was 1.51m (caisson 9).

The recorded settlements have shown that the values from the sea side are 15 % higher than the recorded settlements from the land side.

When possible, the placement of hydraulic piezometers was recommended, in order to follow the consolidation process and for the interpretation of the results with the recorded displacements.

Lesson nº 17 The model does not incorporate for the computation of displacements the creep effects.
Following Lambe et al (1981) a comparison between the computed values with the observed values for the vertical displacements shows deviations between 30% to 50% and for horizontal displacements the deviations are between 50% and 100%.

The quality control of vibrocompaction by SPT tests has shown an improve of ground characteristics.

Lambe, T. W. Marr, A. W. et Silva, F. (1981) « Safety of a Constructed Facility: Geotechnical Aspects ». JGED, ASCE, vol. 107, nº GT3, pp.339-352.

Note – The study of Malabo quay was performed for Etermar.

8.5.3 Case History nº 18 - MARINA EXPO Quay (with Alexandre Pinto and R. Tomasio (JetSj)

8.5.3.1 Introduction

The lay-out of Marina Expo quay is presented, the geological characteristics are addressed, the geotechnical characteristics are referred, the proposed alternative solution is analysed, the stability analyses are presented, the construction issues jet grouting and micropiles are described and the instrumentation is addressed.

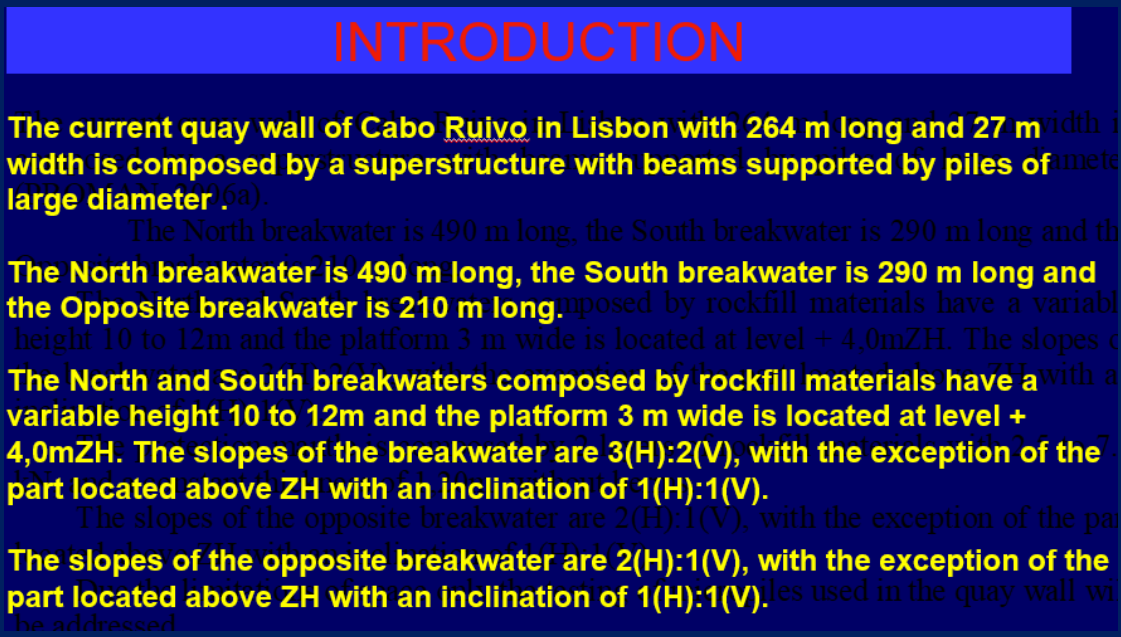

Figure 8.331 illustrates the Marina Expo view.

Figure 8. 331 General Marina Expo view

Figure 8. 332 shows the cross section of North breakwater.

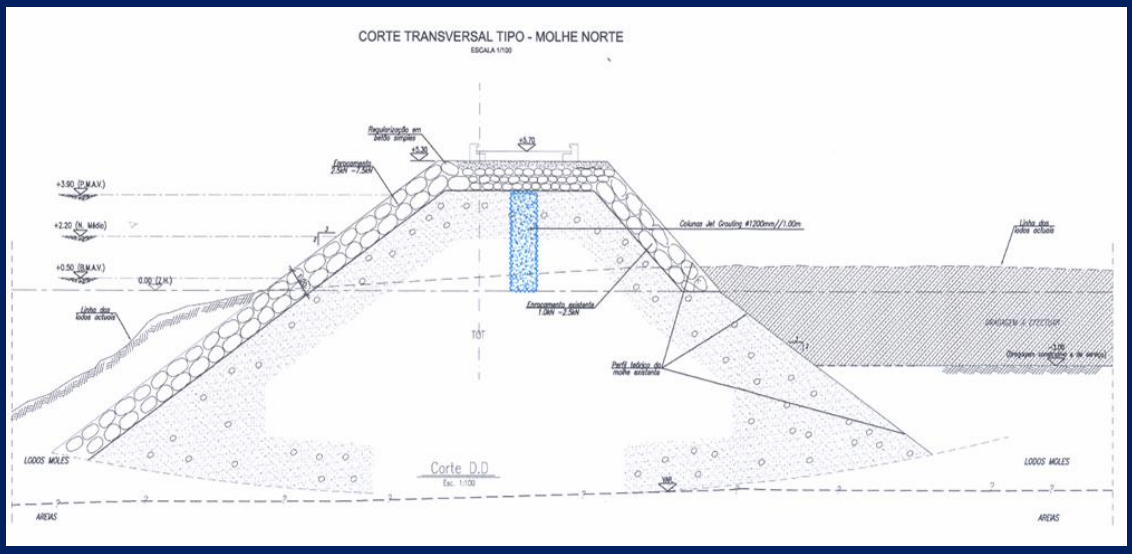

Figure 8. 332 Cross section of North breakwater

The breakwaters were designed taking into consideration limit states (Eurocode 7, 1997).

8.5.3.2. Geological Characteristics

Main Geological Characteristics

The main geological characteristics of each layer were based on the information collected from 8 borings, namely 6 borings executed from a platform and 2 borings located on the quay wall (Geocontrole, 2006).

The boreholes lengths have varied between 13.57 m and 19.60 m and the SPT tests were performed 1.5m apart.

Undisturbed samples were taken to perform triaxial tests (type CU-consolidated undrained) and oedometer tests.

In addition some inspection trenches were opened in the north breakwater

Figure 8.333 presents the inspection trench.

Figure 8.333 Inspection trench

8.5.3.3 Geotechnical Characteristics

.

The geotechnical characteristics of mud materials, silty sands and silty clays materials and Miocene complex are presented.

Geotechnical Characteristics

Mud materials

Unified classification: MH, OH-CH
% passing sieve # 200 (ASTM): 91 to 100 %
Liquid limit: 49 to 77%
Plastic index: 20 to 41%
Peak strength: 20 to 25 kPa
Residual strength 8: to 12 kPa
Young modulus less than 0.5 MPa.
SPT results were between 0 and 1 blows

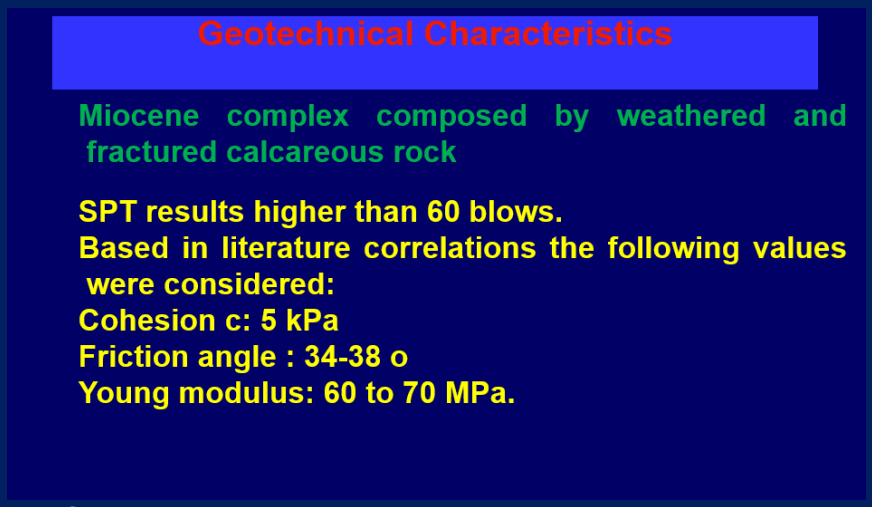

8.5.3.4 Alternative Solution

JETSJ has proposed an alternative solution for North breakwater with the use of jet-grouting columns with 1.2 m of diameter and 1.0 m apart with the purpose to turn the interior water of the marine independent of Tagus water variations. The proposed solution was reviewed and validated by Pedro Seco e Pinto.

Basis of Design

The following ultimate limit states (with severe consequences) can occur: (i) loss of overall stability; (ii) failure of a structural element such as a micropile; (iii) foundation failure; (iv) unacceptable change to the flow of groundwater; and (v) failure by sliding at the base.

The following serviceability limit states (with less severe consequences) can occur: (i) movements of the retaining structure which may affect the appearance or efficient; and (ii) excessive vibrations.

Seismic action

For the seismic action the definition of the horizontal seismic coefficient and of the vertical seismic coefficient was based in RSA (1983) and also Eurocode 8 (1998).

8.5.3.5 Stability Analyses

i) Current situation of the breakwater for low tides - analysis of external slope

Critical deep surface with FS =1.986

Critical superficial surface with FS=1.324;

ii) Current situation of the breakwater for high tides - analysis of external slope

Critical deep surface with FS =2.206

Critical superficial surface with FS=1.406;

iii) Current situation of the breakwater for low tides - analysis of internal slope

Critical deep surface with FS =1.561

Critical superficial surface with FS=1.324;

iv) Current situation of the breakwater for high tides -analysis of internal slope
Critical deep surface with FS =2.206
Critical superficial surface with FS=0.986;

v) Final situation with the maximum water level in the interior-.analysis of exterior slope
Critical deep surface with FS =2.328
Critical superficial surface with FS=1.054;

vi) Final situation with the maximum water level in the exterior - analysis of exterior slope
Critical deep surface with FS =2.983
Critical superficial surface with FS=0.989.

Figure 8.334 shows the breakwater for high tides - analysis of external slope.

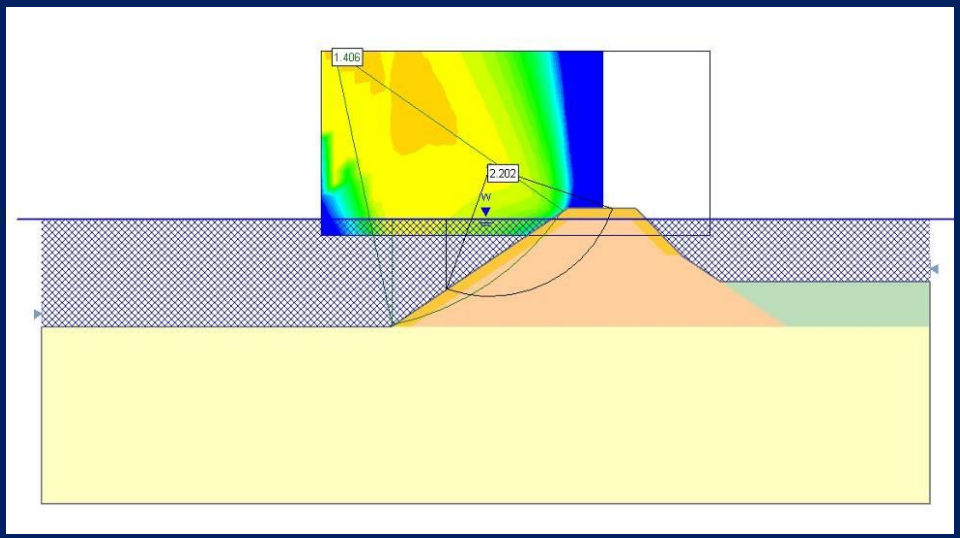

Figure 8.334 Breakwater for high tides - analysis of external slope

Figure 8.335 presents the breakwater for high tides - analysis of internal slope.

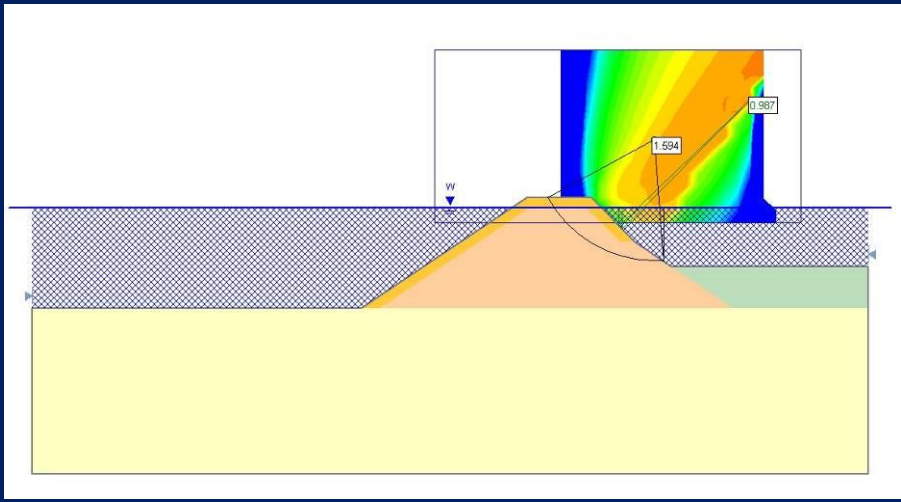

Figure 8.335 Breakwater for high tides - analysis of internal slope

8.5.3.6 Jet Grouting

i) jet-grouting columns 1.2m of diameter

Number of columns: 38

Ratio Water /Cement = 1.1 Water =600 l Cement =545 Kg

Grout pressure 400 bar Flow = 340 l

Air pressure 6 bar Flow = 3 l

Grout specific weight 1.47 t/m3

Sampling –Specific weight between 1.62 and 1.70 t/m3

Cement consumption: between 1505 and 18052 (kg/m3).

Speed rate between 30 cm/min

Rotations number 20 rpm

Boring (by rotation) 14.0m

Column inclination - 12.5º - 20º.

The jet-grouting control has included (EN 12716, 2001):
- Analysis of the mixtures with the determination of density, viscosity, decantation and hardening time.
-Definition of coefficient of permeability by laboratory and in situ tests.
- Performance of uniaxial tests and brazilian tests in samples taken from the mixtures.
- Analysis of temperature variation due to the increase of percentage of cement.

Samples taken from the jet grouting columns to perform uniaxial tests.
-Survey of site geology, control of the column's geometry, continuity of panel, calibration of manometers, injection pressures, characteristics of recycled materials, velocity of rotation and translation of the rods, inclination of the columns, foundations deformations and excavation after the execution of the columns to assess the diameter of the columns by visual inspection.
- Automatic record of jet-grouting parameters.

8.5.3.7 Micropiles

Diameter = 127mm/GEWI diameter=32 mm
-Ratio Water/Cement = 0,4 Water =400 l Cement = 1000 kg
-Sealing = Pressure 15 bar Flow = 50 l
-Air: Pressure = 6 bar Flow = 3 l
-Reinforcement: bar 32 mm, Pipe: 127 mm Thickness=9 mm
-Inclination: 20º.
-Reinforcement: Tube Gewi, Thickness 40 mm, Metallic tube N80: 127 mm Thickness=9 mm
-Specific weight: 1.93 tf/m3
-Boring by rotation = 14.65 m
-Cement consumption: 1000 (kg/ m3).

For the first cycle with a maximum load of 400 kN a displacement value of 13.22 mm was recorded and for the unloading a residual displacement value of 6.19 mm was recorded.
For the second cycle with a maximum load of 880 kN a displacement value of 26.66 mm was recorded and for the unloading a residual displacement value of 8.09 mm was recorded.
For the third cycle with a maximum load of 1100 kN a displacement value of 34.66 mm was recorded and for the unloading a residual displacement value of 10.46 mm was recorded.

Figure 8.336 illustrates the general view of tension micropile test.

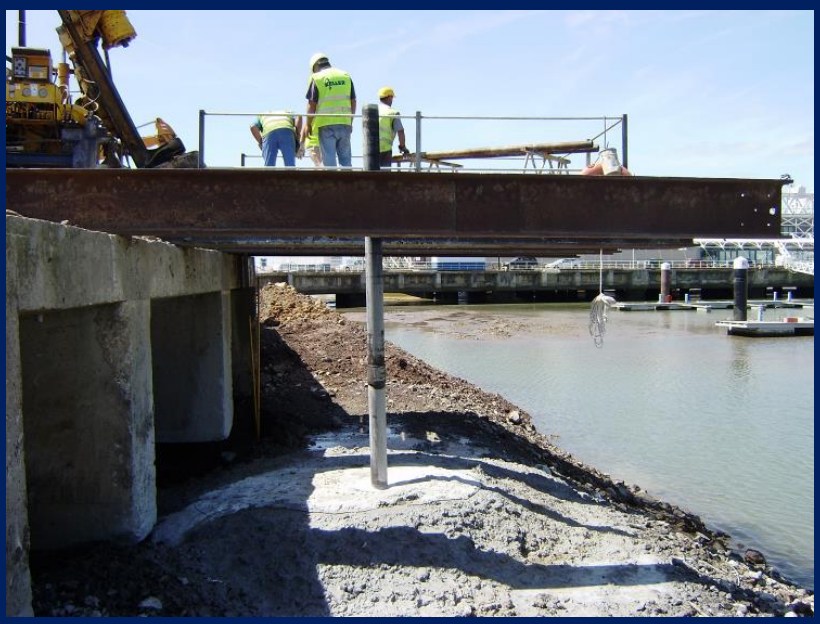

Figure 8.336 General view of tension micropile test

8.5.3.8 Monitoring

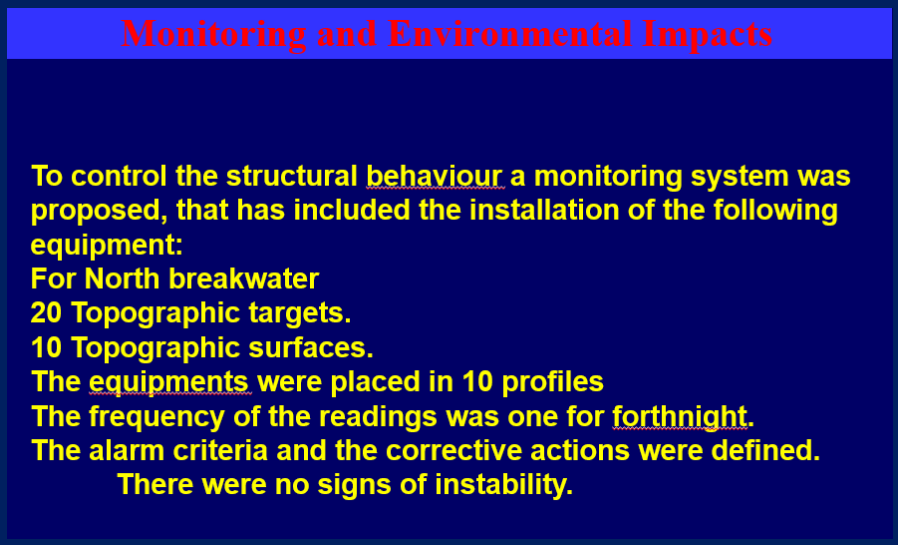

Lesson nº 18- Steel piling may be used in corrosive soil and water environments provided that adequate corrosion mitigation measures are specified. Caltrans typically includes a corrosion allowance (sacrificial metal loss) for steel pile foundations. Other corrosion mitigation measures may include coatings and/or cathodic protection. Caltrans currently uses the following corrosion rates for steel piling exposed to corrosive soil and water: Soil Embedded Zone: 0.025 mm per year Immersed Zone (salt water): 0.100 mm per year Scour Zone (salt water): 0.125 mm per year Splash Zone (salt water): 0.150 mm per year for steel piling driven into undisturbed soil, the region of greatest concern for corrosion is the portion of the pile from the bottom of the pile cap or footing down to 1 meter below the water table. This region of the soil typically has a replenishable source of oxygen needed to sustain corrosion.

A driven pile is a relatively long, slender column, provided to offer support or to resist forces, made of preformed material having a predetermined shape and size that can be physically inspected prior to and during installation, which is installed by impact hammering, vibrating or pushing into the earth.

Driven piles are a total engineering solution. The design, installation and quality assurance that are a part of each driven pile combine to eliminate guesswork and produce a known, reliable and cost effective product that can accommodate a wide variety of subsurface conditions.

Driven piles maintain their shape during installation. They do not bulge in soft soil conditions and are typically not susceptible to damage from the installation of subsequent piles. Many hollow-section piles can be visually inspected after installation to assure integrity.

The pile driving process can be easily modeled prior to installation to determine adequate and economic equipment selection. Static or Dynamic testing can confirm load carrying capacities of installed piles. Dynamic testing can easily confirm proper hammer performance and its effect on the pile. Many modern hammers have impact velocity measurement devices permanently installed, providing a very high level of quality control.

Note – The study of Marina Expo was performed for EXPO.

8.6 UNDERGROUND STRUCTURES

An Extract from the State-of-the-Art Lecture delivered by Pedro Sêco e Pinto at ICEE (International Conference on Earthquake Engineering), New Delhi-India, 2016.

8.6.1 Introduction

Tunnels were hand-dug by several ancient civilizations in the Indian and Mediterranean regions. In addition to digging tools and copper rock saws, fire was sometimes used to heat a rock obstruction before dousing it with water to crack it apart. The cut-and-cover method-digging a deep trench, constructing a roof at an appropriate height within the trench, and covering the trench above the roof (a tunneling technique still employed today)-was used in Babylon 4,000 years ago.

The first advance beyond hand-digging was the use of gunpowder to blast a 515-ft (160-m) long canal tunnel in France in 1681. The next two major advances came about 1850. Nitroglycerine (stabilized in the form of dynamite) replaced the less powerful black powder in tunnel blasting. Steam and compressed air were used to power drills to create holes for the explosive charges. This mechanization eventually replaced the manual process made famous by John Henry, the "steel-driving man," who swung a 10-lb (4.4-kg) sledge hammer with each hand for 12 hours a day, pounding steel chisels as deep as 14 ft (4.2 m) into solid rock.

Between 1820 and 1865, British engineers Marc Brunel and James Greathead developed several models of a tunneling shield that enabled them to construct two tunnels under the Thames River. A rectangular or circular enclosure (the shield) was divided horizontally and vertically into several compartments. A man working in each compartment could remove one plank at a time from the face of the shield, dig ahead a few inches, and replace the plank. When space had been dug away from the entire front surface, the shield was pushed forward, and the digging process was repeated. Workers at the rear of the shield lined the tunnel with bricks or cast-iron rings.

In 1873, American tunneler Clinton Haskins kept water from seeping into a railroad tunnel under construction below the Hudson River by filling it with compressed air. The technique is still used today, although it presents several dangers. Workers must spend time in decompression chambers at the end of their shift - a requirement that limits emergency exits from the tunnel. The pressure within the tunnel must be carefully balanced with the surrounding earth and water pressure; an imbalance causes the tunnel either to collapse or burst (which subsequently allows flooding).

Soft soil is prone to collapse and it can clog digging equipment. One way to stabilize the soil is to freeze it by circulating coolant through pipes embedded at intervals throughout the area. This technique has been used in the United States since the early 1900s. Another stabilization and waterproofing technique-widely used since the 1970s is to inject grout (liquid bonding agent) into soil or fractured rock surrounding the tunnel route.

Shotcrete is a liquid concrete that is sprayed on surfaces. Invented in 1907, it has been used as both a preliminary and a final lining for tunnels since the 1920s.

In 1931, the first drilling jumbos were devised to dig tunnels that would divert the Colorado River around the construction site for Hoover Dam. These jumbos consisted of 24-30 pneumatic drills mounted on a frame welded to the bed of a truck. Modern jumbos allow a single operator to control several drills mounted on hydraulically controlled arms.

In 1954, while building diversion tunnels for construction of a dam in South Dakota, James Robbins invented the tunnel boring machine (TBM), a cylindrical device with digging or cutting heads mounted on a rotating front face that grinds away rock and soil as the machine creeps forward. Modern TBMs are customized for each project by matching the types and arrangement of the cutting heads to the site geology; also, the diameter of TBM must be equal to the diameter of the designed tunnel (including its lining).

Tunnels have many uses: for mining ores, for transportation, including road vehicles, trains, subways, and canals and for conducting water and sewage. Underground chambers, often associated with a complex of connecting tunnels and shafts, increasingly are being used for such things as underground hydroelectric-power plants, ore-processing plants, pumping stations, vehicle parking, storage of oil and water, water-treatment plants, warehouses, and light manufacturing; also, command centers and other special military needs.

Materials

Materials used in tunnels vary with the design and construction methods chosen for each project. Grout used to stabilize soil or fill voids behind the tunnel lining may contain various materials, including sodium silicate, lime, silica fume, cement, and bentonite (a highly absorbent volcanic clay). Bentonite-and-water slurry is also used as a suspension and transportation medium for muck (debris excavated from the tunnel) and as a lubricant for objects being pushed through the tunnel (e.g., TBMs, shields). Water is used to control dust during drilling and after blasting, which is often done with a low-freezing gelatine explosive. Water and salt brine or liquid nitrogen are common refrigerants for stabilizing soft ground by freezing. The most common modern lining material, concrete reinforced by either steel or fiber, may be sprayed on, cast in place, or prefabricated in panels.

Construction Process

A tunnel's construction method is determined by several factors, including geology, cost, and potential disruption of other activities.

Site geology is evaluated by examining surface features and subsurface core samples. A pilot tunnel about one-third the diameter of the planned main tunnel may be constructed along the entire route to further evaluate the geology and to test the selected construction method.

If soil stabilization is required, it may be done by injecting grout through small pipes placed in the ground at intervals. Alternatively, a refrigerant may be circulated through pipes embedded in the ground to freeze the soil.
There are seven different methods used to remove material from the tunnel path.
The first is the immersed tube method where workers prepare an underwater tunnel site by digging a trench at the bottom of the waterway. Steel or reinforced concrete sections of tunnel shell are constructed on dry land and ballast tanks built into the section are flooded. A rubber seal between the two sections ensures a watertight connection.

In the cut-and-cover method workers dig a trench large enough to contain the tunnel and its shell. A box-shaped tube is constructed, often by in-place casting of reinforced concrete. In certain types of soil or in close proximity to other structures, tunnel walls may be built before digging begins in order to keep the trench from collapsing during excavation.

The third is the top-down method where parallel pair of walls are embedded into the ground along the tunnel's route by driving steel sheet piles or constructing slurry walls. A trench is dug between the walls to a depth equal to the planned distance from the surface to the inside of the tunnel roof. The tunnel roof is formed between the walls by framing and pouring reinforced concrete on the bottom of the shallow trench. After the tunnel roof has cured, it is covered with a waterproofing membrane and excavated soil is replaced above it. Conventional excavating machinery, such as a front-end loader, is used to dig out the soil between the diaphragm walls and under the tunnel roof. When sufficient depth has been reached, a reinforced concrete floor is poured to complete the tunnel shell.

In the drill and blast method a drilling jumbo is used to drill a predetermined pattern of holes in the rock along the tunnel's path. Carefully planned charges of dynamite are inserted in the drilled holes. The charges are detonated in a sequence designed to break away material from the tunnel's path without unduly damaging the surrounding rock. Air is circulated through the blast area to remove explosion gases and dust. Rubble dislodged by the blast is hauled away. Pneumatic drills and hand tools are used to smooth the surface of the blasted section and remove loose pieces of rock.

It is usually necessary to stabilize and reinforce the surface of the newly blasted section with a preliminary lining. One technique involves inserting a series of steel ribs connected by wood or steel braces. Another technique, called the new Austrian tunneling method (NATM), involves spraying the surface with a few inches (several centimeters) of concrete. In appropriate geologic conditions, this "shotcrete" lining may be supplemented by inserting long steel rods (rock bolts) into the rock (Figure 8.337) and tightening nuts against steel plates surrounding the head of each bolt.

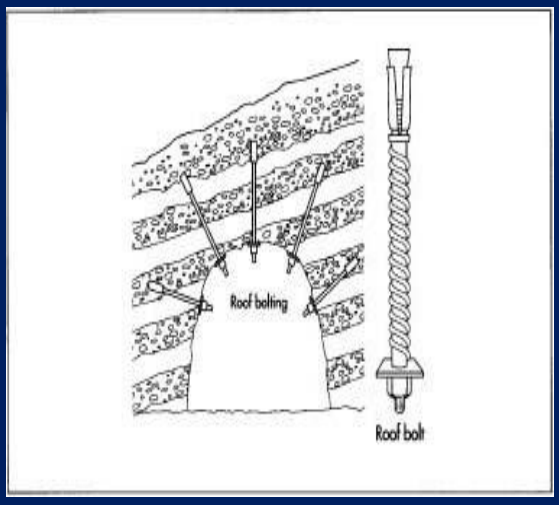

Figure 8.337 Roof bolts made of steel are secured to rock in order to support the top of the tunnel (scheme)

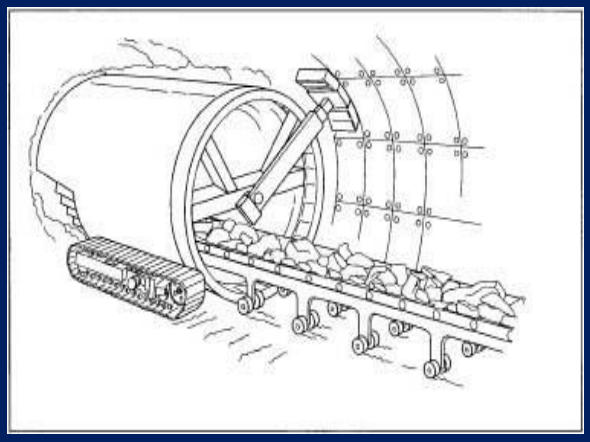

Figure 8.338 Shield Tunneling (scheme)

The shield driving or tunnel jacking method is used to remove material from the tunnel. Some tunnels are still dug using a Greathead-style shield (Figure 8.338). The top of the shield extends beyond the sides and bottom, providing a protective roof for workers digging in advance of the shield. The leading edge of the shield top is sharp so it can cut through the soil. Excavation may be done by hand or with power tools.

Tunnel jacking is a similar technique, but the shield being driven through the ground is actually a prefabricated section of tunnel lining.

In the parallel drift method, a series of parallel, horizontal holes (drifts) are bored using microtunneling machinery (microtunnels are too small for human miners to work inside of) such as augers or small versions of TBMs.

In the tunnel boring machine method, the types and arrangement of cutting devices on the face of the TBM are determined by the geology at the tunnel site. The face slowly rotates and grinds away the rock and soil in front of it. The TBM is constantly pushed forward to keep the face in contact with its target. Forward pressure may be exerted by jacks at the rear of the TBM pushing against the most recently installed section of tunnel lining. Muck is passed through holes in the face and carried by conveyor belt to the rear of the TBM, where it drops into carts that transport it out of the tunnel. Bentonite may be pumped through the TBM face to make the soil surface more workable and to carry away the muck. Some TBMs are equipped at the rear with robotic arms that position and attach segments of tunnel lining as soon as the machine has moved forward a sufficient distance. In other cases, the NATM is used to create a preliminary lining as the TBM progresses.

In some cases, the final lining is placed during the excavation process. Two examples are TBMs that install lining segments and prefabricated tunnels that are jacked into place. In other cases, a final lining must be constructed after the entire tunnel is excavated. One option is to pour a reinforced concrete lining in place. Slipforming is an efficient technique in which a section of form is slowly moved forward as the concrete is poured between it and the tunnel wall; the concrete hardens quickly enough to support itself by the time the form moves on.

A second option is to install segments of preformed concrete or steel lining, much as some TBMs do. Lining segments are constructed so that several of them can be joined to form a complete ring a few feet (a meter or two) wide. Once a ring has been bolted into place, grout is injected between it and the tunnel wall.

A third option is to spray a layer of shotcrete several inches (70 mm or more) thick onto the tunnel walls. One or two layers of wire mesh might be placed first to reinforce the shotcrete, or reinforcing fibers might be added to the concrete mixture to increase its strength.

By Products/Waste

Sometimes the earth removed from a tunnel is simply discarded into a landfill. In other cases, however, it becomes raw material for other projects. For example, it may be used to form the base course for an approach roadway or to create roadway embankments for wider shoulders or erosion control.

Quality Control

Besides maintaining ground stability around the tunnel and ensuring structural integrity of the tunnel lining, proper alignment of the excavation path must be achieved. Two valuable tools are global positioning system (GPS) sensors that receive precise locational data via satellite signals and guidance systems that project and detect a laser beam within the tunnel

Some Examples

The world's longest tunnel carries water 105 mi (170 km) to New York City from the Delaware River.

The English Channel Tunnel (Eurotunnel) between England and France, a dream for centuries envisioned and encouraged by Napoleon, was begun in 1987. Originally referred to as the Channel and now known as the Eurotunnel, it was completed in 1994 at a cost of $13 billion. The two rail tunnels (one for northbound and one for southbound traffic) and one service tunnel are each 31 mi (50 Km) in length and have an average depth of 150 ft (46 m) under the seabed. It is the first physical link between Britain and the European continent. Passenger rail service is provided, as well as the ferrying of automobiles and trucks. Travel times from London to Paris have been reduced from more than five hours (over sea) to three hours via the Eurotunnel.

The Seikan Tunnel in Japan was placed in service in 1988. The 33mi (53Km) long tunnel connects the northern tip of Japan's main island of Honshu with the island of Hokkaido, passing under the Tsugaru Strait. The Seikan Tunnel is the world's longest submarine tunnel, involving excavation 330 ft (100 m) below the seabed across a strait where the sea is up to 460 ft (140 m) in depth.

Lötschberg base Switzerland railway rail link under Lötschen Pass between Bern and Valais cantons with 34.621 Km was built in 2007.

Lærdal Norway highway carries the main cross-country highway through the mountains in central Norway with 24515 Km was built in 2000.

The Future

Exploration methods, materials, and machinery are possible areas of improvement. Sound waves transmitted through the earth can now generate a virtual CAT scan of the tunnel path, reducing the need to drill core samples and pilot tunnels. Some examples of materials research involve cutting tools that are more effective and durable, concrete with more precisely controlled hardening rates, and better processes

for modifying soil to make it easier to cut, dig, or remove. Recent developments in machine technology include multiple-headed TBMs that can bore two or three parallel tunnels simultaneously and a TBM that can turn a corner up to 90° while cutting. Better remote control capabilities for digging machinery would improve safety by reducing the amount of time people have to be underground during the digging process.

8.6.2 LESSONS FROM TUNNELS STRUCTURES BEHAVIOR DURING EARTHQUAKES

Introduction

According to Aristotle (384-322 B.C.) in his book Meteorologica earthquakes were produced by the dried exhalations (spirits or winds) in caves inside the earth which trying to escape make the earth shake.

Martin Lister in England and Nicolas Lemery in France in 17th century were the first to propose that earthquakes were produced by large explosions of inflammable material formed by a combination of sulphur, coal, nitre and other products accumulated in the interior of earth (Udias and Arroyo, 2005). The explosive theory was also proposed by Newton`s Optics (1718).

In France the world was considered a good place in which everything that happened was viewed to be "for the best" and earthquake was considered with optimism. Voltaire in his novel Candide presented a hard attack to this optimistic view point. Also, Kant and Rosseau defended the optimist position.

Recently in Japan until 19th century the fish was considered the cause of earthquake.

Failure Mechanisms

From a careful study of underground structures behaviour during the top ten earthquakes occurrences the following failure mechanisms can be selected:
-Sliding or shear distortion of surrounding massif or foundation or both.
- Compression and tension deformation.
- Longitudinal and shear deformation.
- Failure and collapse of the ceiling slab of stations.
- Subsidence of subsoils.
- Transverse and longitudinal cracks.
-Disruption of underground structure by major fault movement in foundation.
- Differential tectonic ground movements.
- Piping failure through cracks induced by ground motions.
- Large ground deformation due to liquefaction.
-Separation of construction joints on side walls at the intersection between the underground and ground surface sections in soft ground.
The damage modes listed are not necessarily independent of each other.

The tunnel would present three kinds of deformation under the seismic motion: compression and tension deformation, longitudinal deformation and shear deformation. The tunnel damage situation related to three aspects of the earthquake: the tunnel experience, the deformation character around the tunnel and the anti-seismic ability of the tunnel structure.

The Damage Grade and Damage Index

The tunnel damage grade is evaluated mainly according to the tunnel traffic function and its damage investigation. The tunnel damages are divided into five grades: no damage, minor damage, moderate damage, severe damage and collapse, and their corresponding damage index ranges are [0, 0.2], [0.2, 0.4], [0.4, 0.6], [0.6, 0.8] and [0.8, 1], and the characteristic values are 0.1, 0.3, 0.5, 0.7 and 0.9. The damage grade can be defined as: a) no damage, the lining of tunnel may have small cracks, but no falls of rock, can be safely use; b) minor damage, the road surface may sink slightly, the tunnel lining have small cracks, the fall of rock locally, and it can restore to normal use by slight repair; c) moderate damage, there are a lot of cracks in lining; many fallings of rock, the road surface may sink obviously, the traffic are blocked, it can restore to normal use after repairs; d) severe damage, there are a great deal of cracks in its lining, falls of big rocks, the road surface may sink severely, the tunnel can not be used unless thorough repairs; and e) collapse, serious crack and deformation in its lining, the tunnel structure collapsed partially, must be reconstructed.

ICOLD (2011) has presented a correlation of the estimated acceleration, using empirical relationship, and peak particle velocity with reported damage. Review of their data suggest that:
(i) *No damage* should be expected if the peak surface accelerations are less than 0.2 g and peak particle velocity less than 20 cm/s;
(ii) *Minor damage* should be experienced between 0.2 and 0.4 g, respectively 20 cm/s and 40 cm/s;
(iii) *Damage* should be forecast if peak surface accelerations are higher than 0.5 g and peak particle velocity higher than 90 cm/s.

Lessons Learned from Case Histories

Due to the myth that underground structures have a good resistance against shaking in many designs specifications aseismic design is not usually considered.

The reasons for this believe are: (i) the rock mass surrounding the tunnel has considerable stiffness to avoid tunnel shape changes; (ii) it is considered that the tunnel follow the soil movements.

The analysis of the following case histories will show that this feeling is not correct.

There are many factors governing the damage of tunnels. Generally speaking, there are three aspects: First, the earthquake motion, such as the earthquake intensity, the spectrum characteristics and so on; Second, the structure condition of the tunnel, as whether have lining, and its integrality, quality of the construction; Third, the tunnel environment condition, as rock condition, overburden layer depth, whether across the fault crushed zone and so on.

Underground structure damage in earthquake is gradually increasing with the increase of the seismic motion acceleration and the decrease of the overburden depth. The damage of underground structures in soft rock is more serious than that in hard rock. As an underground structure, tunnel should have similar rule.

Top Ten Earthquakes (courtesy from N. Sitar) (Figures 3. 339 to Figure 3.349)

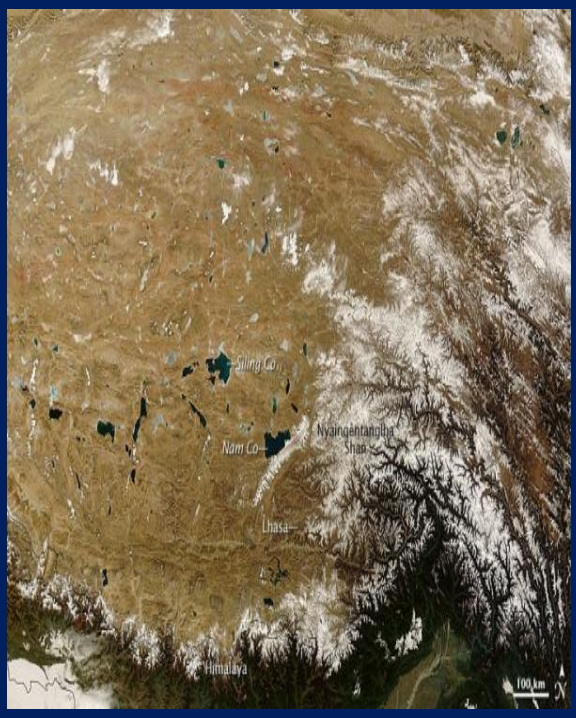

Figure 8. 339 Assam-Tibet, 1950 - Magnitude 8.6

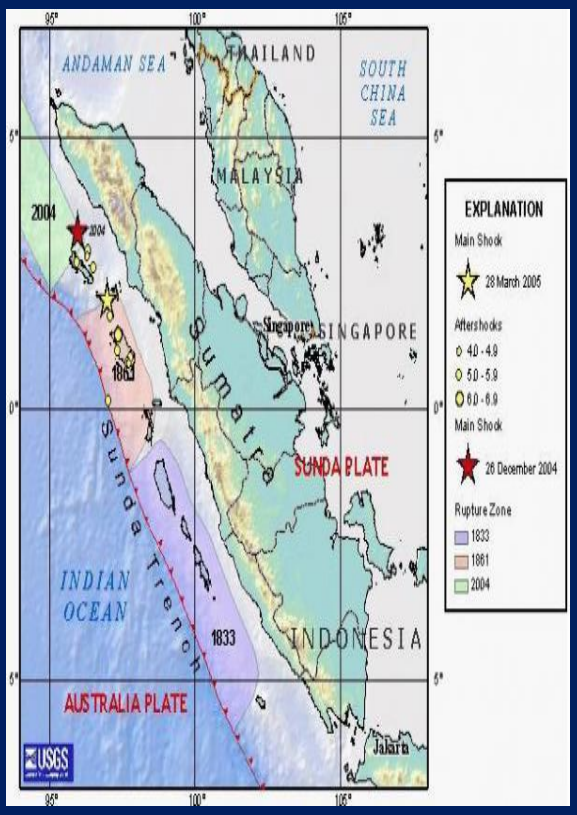

Figure 8.340 Northern Sumatra, Indonesia, 2005 –Magnitude 8.6

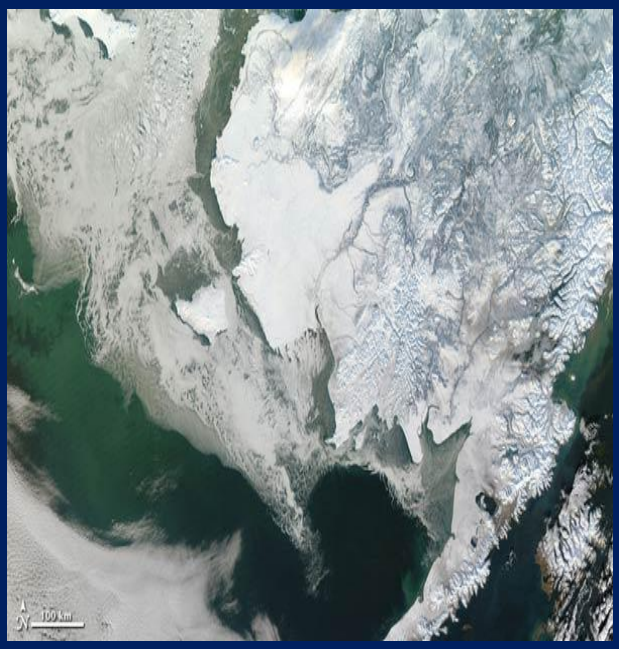

Figure 8. 341 Rat Islands, Alaska, 1965 - Magnitude 8.7

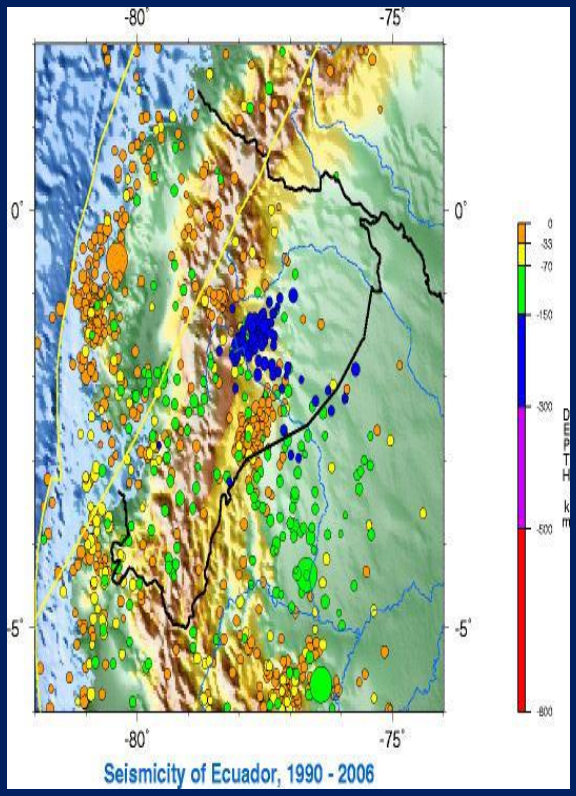

Figure 8.342 Off the Coast of Ecuador, 1906 - Magnitude 8.8

Figure 8.343 Offshore Maule, Chile, 2010 - Magnitude 8.8

Figure 8. 344 Kamchatka Peninsula, Russia, 1952 Magnitude 9.

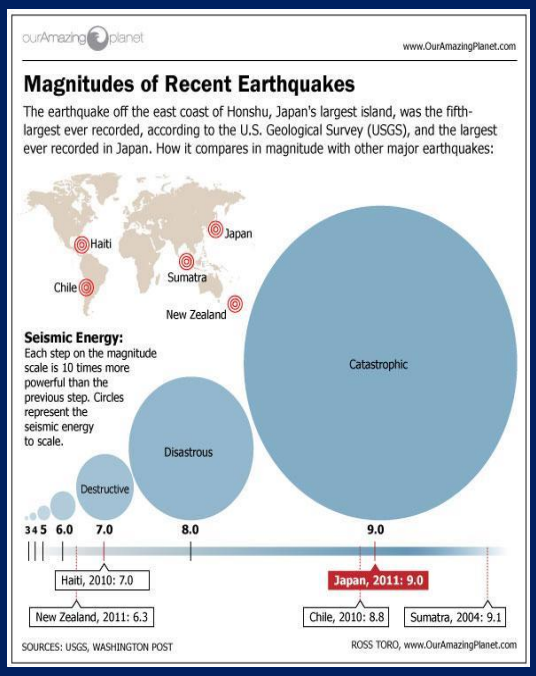

Figure 8.345 Near the East Coast of Honshu, Japan, 2011 - Magnitude *9.0*

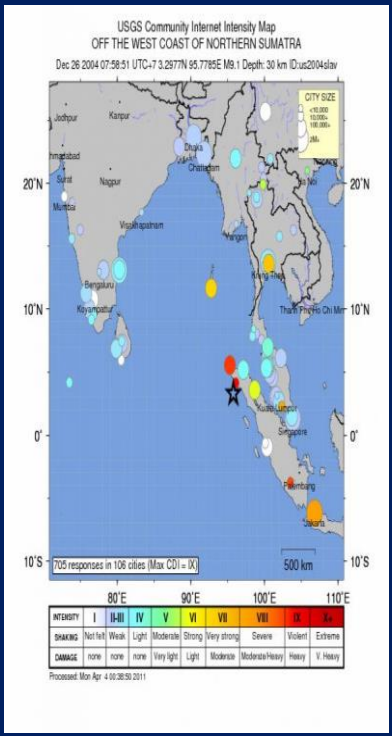

Figure 8. 346 Off the West Coast of Northern Sumatra, 2004 - Magnitude 9.1

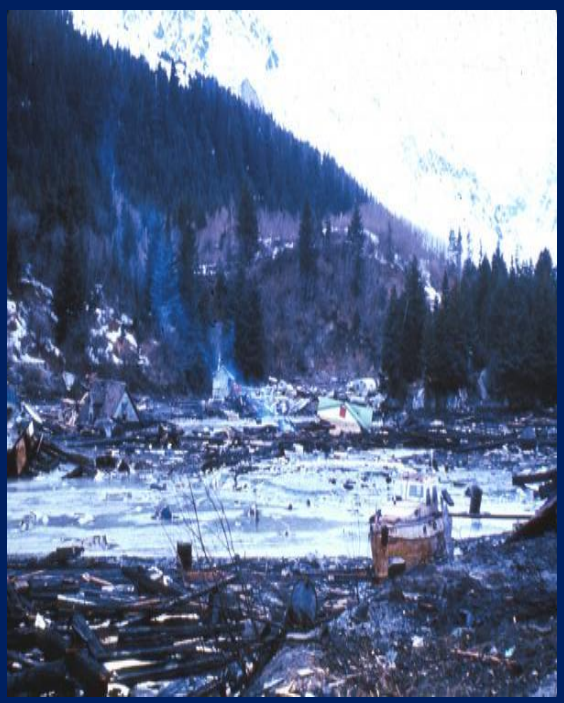

Figure 8.347 Prince William Sound, Alaska, 1964 – Magnitude 9.2

Figure 8. 348 Chile, 1960 - Magnitude 9.5

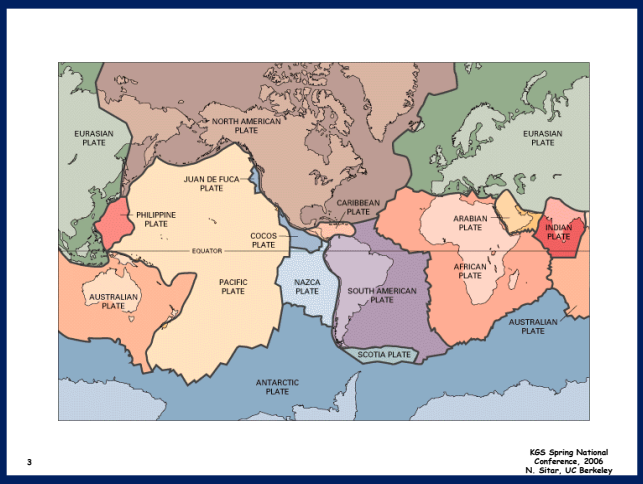

Figure 8.349 Plates world map (courtesy N. Sitar)

Figure 8.350 shows the factors governing the damage of tunnels.

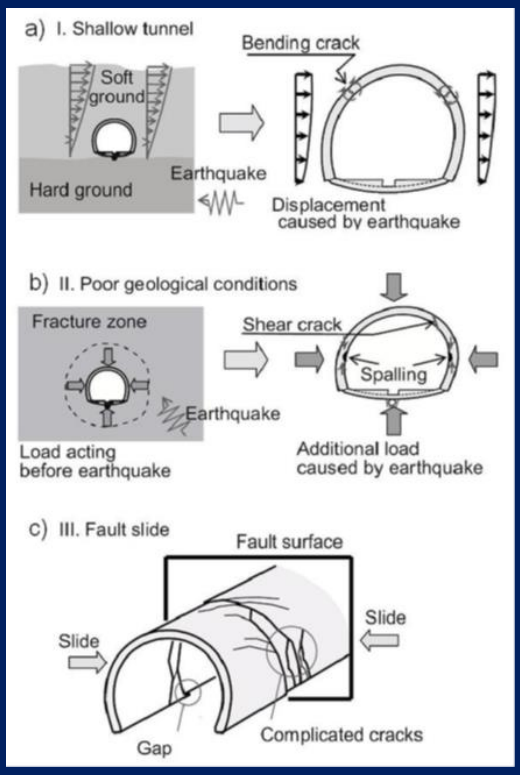

Figure 8.350 Factors governing the damage of tunnels

8.6.3 Case History nº 19 - Odelouca tunnel

8.6.3.1 Introduction

The preliminary design is addressed, the construction issues are referred.

8.6.3.2 Preliminary Design

For the design of primary lining of Odelouca tunnel Bieniaswki and Barton classifications were used.

Bieniawski's Rock Mass Rating classification (RMR) and recommendations

After analyzing the elements of the geotechnical survey, including boreholes and surface surveys, it is estimated the value of RMR (Rock Mass Rating), Bieniawski, 1989, for the 2 geotechnical areas considered.

The RMR Rock Mass Rating system is the most used for rock mass classification. It's based in the quantification of six geological and geotechnical parameters and in the attribution of the relative weights. The result of the RMR classification for a specific rock mass can range from 0 to 100, and it's obtained by the algebraic sum of the mentioned parameter weights.

The parameters considered in the classification are:

Strength of intact rock material, with rating ranging from 0 to 15;

Drill core quality (RQD), 3 to 20;

Spacing of discontinuities, 5 to 20;

Condition of discontinuities, 0 to 30;

Groundwater, 0 to 15;

Adjustment for joint orientation, -12 to 0.

For the types of ground to be crossed the recommendations of the Bieniawski classification are presented in Table 8.48.

Table 8.48 Bieniawski Classification

Rock mass class	Excavation	Rock bolts (20 mm diameter, fully grouted)	Shotcrete	Steel sets
I - Very good rock *RMR*: 81-100	Full face, 3 m advance.	Generally no support required except spot bolting.		
II - Good rock *RMR*: 61-80	Full face , 1-1.5 m advance. Complete support 20 m from face.	Locally, bolts in crown 3 m long, spaced 2.5 m with occasional wire mesh.	50 mm in crown where required.	None.
III - Fair rock *RMR*: 41-60	Top heading and bench 1.5-3 m advance in top heading. Commence support after each blast. Complete support 10 m from face.	Systematic bolts 4 m long, spaced 1.5 - 2 m in crown and walls with wire mesh in crown.	50-100 mm in crown and 30 mm in sides.	None
IV - Poor rock *RMR*: 21-40	Top heading and bench 1.0-1.5 m advance in top heading. Install support concurrently with excavation, 10 m from face.	Systematic bolts 4-5 m long, spaced 1-1.5 m in crown and walls with wire mesh.	100-150 mm in crown and 100 mm in sides.	Light to medium ribs spaced 1.5 m where required.
V – Very poor rock *RMR*: < 20	Multiple drifts 0.5-1.5 m advance in top heading. Install support concurrently with excavation. Shotcrete as soon as possible after blasting.	Systematic bolts 5-6 m long, spaced 1-1.5 m in crown and walls with wire mesh. Bolt invert.	150-200 mm in crown, 150 mm in sides, and 50 mm on face.	Medium to heavy ribs spaced 0.75 m with steel lagging and forepoling if required. Close invert.

Primary support recommendations for Bieniawski's 1989 RMR classification. In blue: for values RMR>70, in green, for values between 50 and 70, in yellow for the interval of RMR 30-50: and finally in red for RMR<30

Barton's Q-System Classification and recommendations

The Q system was developed by Barton *et al.* (1974) who, after the observation and analysis of a great number of tunnels in Scandinavia, proposed a quality index Q, for the propose of rock mass classification and evaluation of primary support requirements. The numerical value of the Q index varies in a logarithmic scale from 0.001 to a maximum of 1000, and is defined by:

$$Q = \frac{RQD}{J_n}\frac{J_r}{J_a}\frac{J_w}{SFR} \qquad (8.78)$$

RQD/Jn - Represents the structure of the rock mass, crudely measures the compartmentation of the rock mass and its block size.

- Jr/Ja - Represents the roughness and the frictional resistance of the joints.
- Jw/SRF - Represents an empirical factor related with the tensional state of the rock mass designated as "active tension"".

In the calculation of the Q value, each parameter can vary ranging between the values given in Table 8.49.

Table 8. 49 Parameters for definition of Q value

▪ Rock Quality Designation (RQD), with rating ranging from	0 to 100;
▪ Joint set number (Jn)	0.5 to 20;
▪ Joint roughness number (Jr)	0.5 to 4;
▪ Joint alteration number (Ja)	0.75 to 24;
▪ Water reduction factor (Jw)	0.05 to 1;
▪ Stress Reduction Factor (SRF)	2.5 to 10.

Picking the intervals of quality defined for the classification of the rock mass with the Bieniawski's RMR classification (boundaries with RMR =30, 50 and 70, converted to Q-System with the expression RMR=15.logQ+50, Barton, 1974; 1994), and entering them in the Grimstad and Barton, 1993 abacus, (with boundaries at Q=0.05, 1 and 20) it's possible to arrive to primary support requirements and recommendations.

Figure 8.351 illustrates the Grimstad and Barton (1993) primary support recommendations.

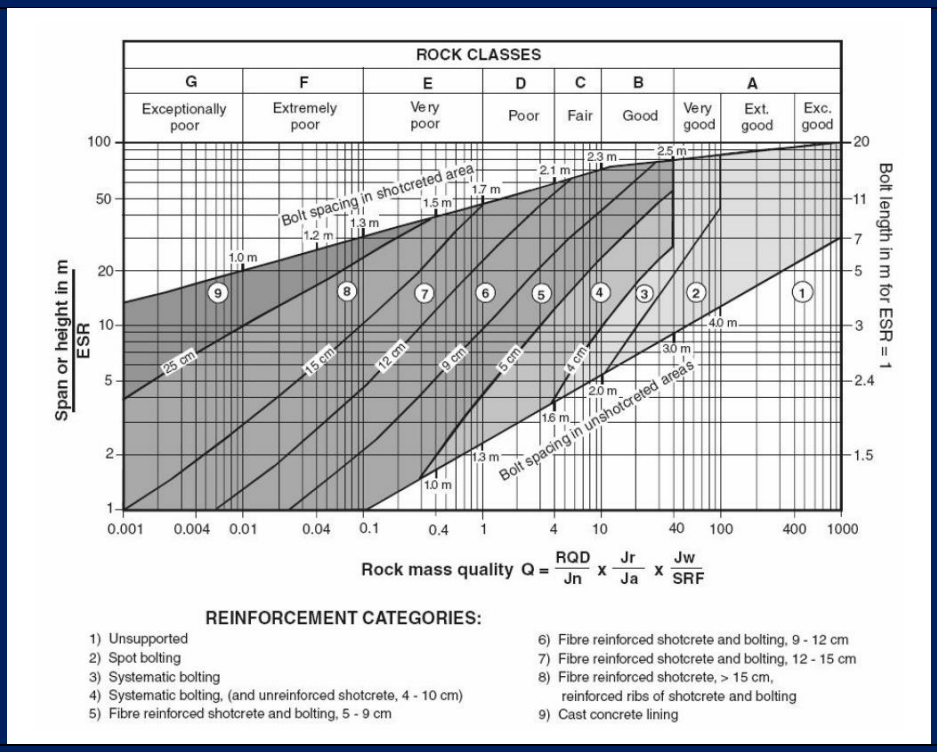

RMR=30 **RMR=50** **RMR=70**

Figure 8.351 Grimstad and Barton (1993) primary support recommendations

So, the Bieniawski interval values are directly transposed to Q values, using the correlation, other option would be to directly calculate the Q values. For a first approach to primary support and easier comparison of results, only the direct transposition is considered. For entering the abacus, also a ESR - *Excavation Support Ratio* of 1.3 is considered for an excavation around 9.6 m, which results in equivalent diameter D_e = 7.4.

For the massif with **RMR>70**, the tunnels fall in the fields 1 and 2 of the abacus, with recommendations of no support requirements and spot bolting.

In the massif quality interval with **RMR 50-70**, the primary supports recommendations for fields 3, 4 and 5 range from systematic bolting (spacing of 2.4 m) to 5 to 9 cm of reinforced shotcrete and bolting (spacing of 1.7 m).

At **RMR 30-50** rock mass quality interval, the recommended support requirements range from 9 to 15 cm of shotcrete and rock bolts with spacing between 1.25 and 1.7 m.

For **RMR<30** rock mass quality interval, the tunnel falls inside the fields 8 and 9 of the abacus, and the recommended support requirements range from reinforced shotcrete >15 cm thickness reinforced with ribs and bolting to cast concrete lining.
The recommended rock bolt length, obtained with the expression L=2+(0.15B)/ESR, where B= span, is of 3.1 m.
The maximum unsupported span can be estimated with the expression $2.ESR.Q^{0.4}$. The values obtained, at the boundaries of the geotechnical zone's intervals are of 0.78 m for Q=0.05, 2.6 m for Q=1 and 8.61 m for Q=20.

For geotechnical zone 1, with failure of blocks, a support of nailing/rock bolts for roof and side walls with 6 m long, 76mm of diameter and reinforcements of 32 mm, with concrete lining 2, 5 cm thick and metallic mesh was used.

In zone 2 with failure of blocks and slipping a primary lining with concrete of 5 cm thick, and nails 6m long, 76 mm of diameter and reinforcements of 32 mm (3m apart in current zones and 1.5 m in more critical zones) was used. Also, in some critical zones reinforcement with steel ribs was adopted.

F.E.M Analysis

A f.e.m. analysis was performed and two situations were analysed: (i) for material ZG1 (material of best quality) a tunnel was analysed with excavation in total section without support, and plastified zones in side walls were identified; (ii) for material ZG2 (material of medium quality) the tunnel was analysed and excavation was simulated in two phases. Plastification in the first phase has occurred in the opening and base of the tunnel, but no occurrence of plastification during the second phase.

Due to the occurrence of plastified zones during the opening of the tunnel a primary lining was used. For zone ZG1 gunite 7 cm thick with steel mesh, type Malhasol, was applied.
Also, for zone ZG2 application of gunite 7 cm thick with steel mesh, type Malhasol, and use of nails in the roof was recommended.

Based in f.e.m. analysis the final reinforcement was designed to face the internal and exterior pressure of decompressed rock.
For the final support reinforced concrete with 0.30 m thick was used.

8.6.3.3 Construction Issues

Figure 8.352 shows the application of sprayed concrete in Odelouca tunnel.

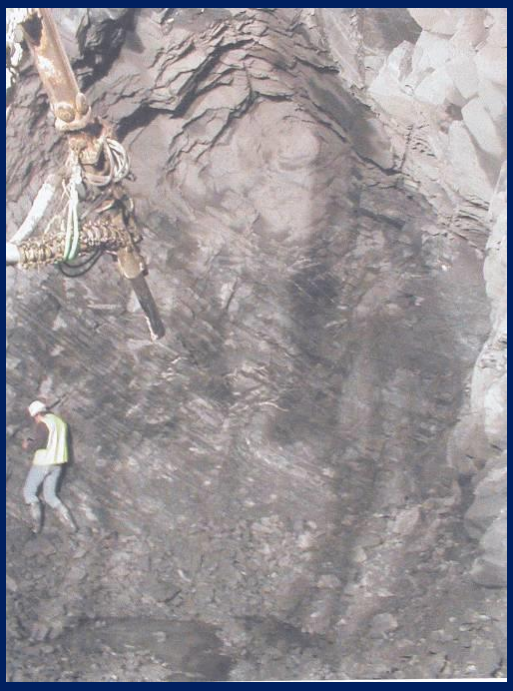

Figure 8.352 Application of sprayed concrete in Odelouca tunnel

Figure 8.353 exhibits the view of Odelouca tunnel with steel rings.
Figure 8.354 presents Odelouca tunnel entrance.

Figure 8.353 View of Odelouca tunnel with steel rings

Figure 8.354 Odelouca tunnel entrance

Lesson nº 19: Instrumentation of tunnels and underground structures to measure their response during ground shaking. These instruments would include measurement of vertical and lateral deformations along the length of the tunnel. This will be useful to understand the effect of spatial incoherency and directivity of the ground motion on tunnel response. Other instrumentation would be useful to measure differential movement between a tunnel and a portal structure,

Note: The study of Odelouca tunnel was performed for Tamega.

8.6.4 Case History nº 20 - Metro of Porto

8.6.4.1 Introduction

The author was a member of the Review Panel for Metro of Porto Project. He was involved in the revision of geotechnical projects of the tunnel and of several stations, namely: Campanhã, Heroismo, Trindade, Bulhão, Salgueiros, Av da França and 24 de Agosto.
Due to the needed restrictions only the revision of Tunnel of Porto and 24 de Agosto station will be described.

8.6.4.2 Tunnel of Porto

Introduction

Major advances have been accomplished with introduction of shields of the pressurized type which allow the construction of tunnels in all type of soils including sands under high water head.

The ITA requirements are addressed, the site investigation is described, the TBM characteristics are presented,

ITA Requirements

Following the International Tunnelling Association (ITA) the basics documents for tunnel design should include or cover:

The geological report presenting the results of the geological and geophysical survey;

The hydrogeological aspects;

The geotechnical report on site investigations, including the interpretation of the results of site and laboratory tests with respect to the tunnelling process, soil and rock classification, etc.,

Information on line, cross-section, drainage, and structural elements affecting later use of the tunnel;

Plans for and a description of the projected excavation or driving procedure, including the different cross-sections related to different ground conditions;

Design documents for the types of excavation methods and tunnel supports likely to be applied, considering, e.g. excavation advance and face support (types and number of anchors, shotcrete strength, closure length, etc.);

The programme for the in-situ monitoring of the tunnel by field measurements;

The analysis of stresses and deformations (for unlined tunnels as well as for single-or double-lined tunnels), and the dimensioning of the tunnel support for intermediate phases and final linings;

The design for waterproofing or drainage;

Structural documents for the final design of the tunnel project, including the detailing;

During and after the excavation, reports on the field measurements and interpretation of their results with respect to the response of the ground and the structural safety of the tunnel;

Documentation of the problems encountered during the excavation and measures applied, e.g. strengthening the ground or changing the projected type of support, based on monitoring results.

Concerning site investigations, the following aspects should be considered for the geological description of each zone:

Name of the geological formation in accordance with a genetic classification;

Geologic structure and fracturing of the rock mass with strike and dip orientations;

Colour, texture and mineral composition;

Degree of weathering;

Parameters of the rock mass e.g. in five classes of intervals, including:

Thickness of the layers.

Fracture intercept;

Rock classification;

Core recovery;

Uniaxial compressive strength of the rock, derived from laboratory tests;

Angle of friction of the fractures (derived from laboratory direct shear tests);

Strength of the ground in on-site situations;

Deformation properties (modulus);

Effect of water on the rock quality;

Seismic velocity. Primary stress field of the ground.

Site Investigation

The site investigation has included:

(i) Boreholes with SPT and sampling for laboratory tests;

(ii) Installation of piezometers in some boreholes to measure the water level;

(iii) Geophysical tests, namely crosshole tests and georadar survey,
(iv) Detailed investigation of the minas, wells and other manmade features;
(v) Rainfall data;
(vi) Pumping tests;
(vii) Laboratory tests, namely identification tests, oedometer tests, uniaxial compression tests and triaxial tests.

The granite material located in the upper part of the tunnel is a weathered granite W5.
The pumping tests gave results of higher permeability than the expected one.
The soil samples recovered in boreholes show values of dry unit weight very low.

The site exhibits igneous rock and the formation known as Granito do Porto consists as weathered granite with grades between W1 to W6.
The dry unit weight values are between 15.8 to 19.8 kN/m3.
Related shear strength the cohesion is between 0-20 kPa and the friction angle between 30-34º.

The severe rains that have occurred provoked saturation of the massif, washing the fines. The erosion of the materials with detrimental aspects on the residual cohesion has played an important role on the several incidents.

TBM Characteristics

The TBM S-160 allows the excavation in stiff rock, as well in soft soil.
The shear head was designed considering a strength for the Porto granite a value of 1400 kg/cm2.
The excavation will be performed in close mode.
The TBM is provided with a boring equipment that allow borings with sampling until 30 m, during the excavation operation.
The weight of the excavated material is carefully controlled.
The injection material is controlled by an adequate software.
All the received data collected during the excavation are carefully analysed in real time, in order to take immediate actions.

TBM Operation

During the TBM advance the following investigations were performed:
(i) Prove drilling from the TBM integrating the results from the surface;
(ii) Face mapping;
(iii) Systematic analysis of the muck;
(iv) Monitoring of the weight of the excavated material;
(v) TBM provided with an equipment that allows the performance of continuous boring in advance
(vi) Control of the overall monitoring system;
(vii) Monitoring of the buildings potentially at risk;
(viii) Monitoring of the water table by piezometers installed in boreholes.

The monitoring system has integrated tiltmeters, crackmeter, measurements of tunnel convergences, pressure cells, inclinometers, piezometers.
Definition of the values of Attention and Alarm.
Figure 8. 355 illustrates Porto tunnel entrance with piles with rockbolts.

Figure 8.356 shows Porto tunnel lining.
Figures 8.357 and 8.358 present Porto tunnel interior and ventilation system.
Figure 8. 359 exhibits Porto tunnel - TBM interior view.

Management of key parameters for risk mitigation

- To have practical and effective control over the face support pressure during the advance of each ring;
- For the Attention and Alarm values the following ranges were defined: 170 kPa-150 kPa and 150-130 kPa;
- To guarantee an effective pressure from the soils grains in the work chamber a minimum value of muck density of 14kN/m3 was considered;
- In addition, laboratory tests (identification tests) for the collected soil samples were recommended;
- The volume of the muck extracted from the work chamber was controlled;
- The correct grounting of the tail void was controlled to guarantee the effective confinement to the lining;
- The TBM was equipped with a device to stop the TBM if the tail void pressure was not correct;
- Control of the key parameters of the ground.

Figure 8. 355 Porto tunnel entrance with piles with rockbolts

Figure 8.356 Porto tunnel lining

Figure 8.357 Porto tunnel interior

Figure 8.358 Porto tunnel ventilation system

Figure 8. 359 Porto tunnel - TBM interior view

8.6.4.3 24 th August Metro Station

Introduction

Three geotechnical campaigns with in situ tests and laboratory test have identified 5 geomechnical groups.
Laboratory tests for soil material shave included identification tests, direct shear tests, triaxial tests.
For rock materials tests for discontinuities and uniaxial tests were performed.

The peripheral Diaphragm wall was designed respecting the ultimate limit states and the serviceability limit states.
For the verification of ultimate limit states of the diaphragm wall rotation failure, vertical failure and loss of global stability were analysed.
For the verification of serviceability limit states the displacements and distortion values of the diaphragm wall were computed.
For the last scenario circular and composite surfaces were analysed for static and pseudo-static conditions using the Bishop method and Janbu method.

The different excavations phases were simulated by Plaxis code that gives information related the applied pre-stress in the anchors, as well the diagrams of the bending moments.

For the analysis of the diaphragm wall the FLAC code was used and different scenarios were analysed related the soil parameters and the phreatic level. The values of horizontal displacements, bending moments and shear forces were computed for the different excavation phases.

In addition, PARATIE code was used to compute pre-stress forces in anchors. For the calculation of active and passive pressures the methodologies of Muller-Breslau and Caquot-Kerisel was used.
The obtained results were useful to re-analyse the risk of the buildings.

A plan for execution of the anchors has detailed the type of the anchor, the construction methodology, the orientation, the tolerances, the length of the anchor, the testing following the European standard EN 1537: 1996.

Two walls were built at entrance and exit of the gallery with size of 18x18x4.5 m by grounting a mixture of cement and bentonite in boreholes with 80 mm diameter and 1.5 m apart.
The grout mixtures have a ratio cement/water 2/1 to 1.5/1 with additives.
Unit weight 12.25 to 13.25 kN/m3;
Viscosity Marsh 30 to 40 seconds
The cement has specific surface >4500cm2/gr.
In order to assess the efficiency Lugeon tests were performed before and after the grounting.

Buildings Damages

Burland et al (1977) proposed 6 categories for damages in buildings. The categories 0, 1 and 2 are related with aesthetics damages, categories 3 and 4 are related with serviceability limit of states and category 5 with ultimate limit of states (stability).

Burland et al (1977) proposed the concept of limit tension deformation e_{lim} to define the ultimate limit state.

Boscardin and Cording (1989) developed the concept of different levels of strain and have proposed based in the analysis of 17 cases Table 4 to establish the relationship between category of damage and limiting tensile strain.

Burland (1995) proposed three levels of risk for buildings: (i) preliminary evaluation; (ii) evaluation of second level, and (iii) detailed evaluation.

For buildings of damage category 3 or higher a detailed evaluation shall be performed.

The differential settlements and relative rotations of foundations shall be established in order to avoid the occurrence of an ultimate limit state or a serviceability limit state (like cracking).

The computation of the differential settlement shall take into consideration:
- the variations of the ground properties;
- the distribution of loads;
- the construction methodology;
- the stiffness of the structure.

More details about the acceptable movements are given in Annex 3.

The damages categories in buildings following the proposals of Burland et al, (1977) and Boscarding and Cording, (1989) are also addressed in Annex 3.

The survey of the buildings located nearby the stations has identified the buildings nº 17 to 22, as the most critical.
The methodology to assess the risk has incorporated the following steps:

- Definition of a zone of influence of 30 m distance from the axis of the station;
- Structural survey of the buildings that were classified in the following categories: (i) buildings of reinforced concrete, (ii) buildings of masonry with floors in wood, (iii) buildings in masonry with floors in in reinforced concrete; (iv) mixed buildings;
- The foundations buildings were classified in: (i) shallow foundations; (ii) pile foundations; (iii) mixed foundations;

The index of vulnerability of buildings has integrated: (i) structural behavior; (ii) orientation of the building; (iii) functionality of the building; (iv) esthetic characteristics of the building, (v) conservation of the building.

- Definition of the attention and alarm values;
- Decision to be made during the execution;
- Follow-up of the situation;
- Visual inspections of the buildings with a frequency of two times per week;
- Definition of the corrective measures, e.g. compensation grouting, reinforcement by micropiles, uplift by hydraulic jacks.

For the risk evaluation the classification proposed by Burland with 6 categories was adopted.

Due to use of blasting the buildings vibrations were recorded by seismographs. In addition, a 3D triaxial vibrometer was placed near the building 21 and a uniaxial vibrometer was placed in the building near the source of the blasting.

Monitoring

For monitoring the station total pressure cells, extensometers, inclinometer, hydraulic piezometers and surface stations were installed.

The monitoring of the buildings has involved:

- Levelling devices;
- 3D optical movements measurements;
- Measurement of the cracks by fissuremeters;
- The rotations by clinometers.

The frequency of the measurements of fissuremeters, vibrometers and clinometers was two times to one time per day.
The attention values for displacements were 10 mm and for rotations 1/250.
The alarm values were 2.0 times the attention values.

Construction Issues

Some construction issues are referred:

Figure 8.360 illustrates a general view of the site.
Figures 8.361 and 8.362 show a view of the excavation.
Figure 8. 363 exhibits the piezometer installed.
Figures 8.364 8.365 present a general view and some details of the equipment for the construction of the diaphragm wall.
Figures 8.366 and 8.367 show the aspects of the neighbor's buildings.
Figure 8. 368 illustrates the monitoring of buildings cracks.

Figure 8.360 General view

Figure 8.361 View of excavation

Figure 8.362 View of excavation

Figure 8. 363 Piezometer installed

Figure 8.364 General view of the equipment for the construction of the diaphragm wall

Figure 8.365 View of the equipment

Figure 8.366 Neighbors buildings

Figure 8.367 Neighbors buildings

Figure 8. 368 Monitoring of buildings cracks

Lesson nº 20: Burland et al (1977) have proposed 6 categories for damages in buildings where categories 0, 1 and 2 are related with sthetic damages, categories 3 and 4 are related with serviceability limit of states and category 5 with ultimate limit of states (stability and introduced the concept of limit tension deformation ε_{lim} to define the ultimate limit state (see Annex 3).

Burland (1995) proposed three levels of risk for buildings: (i) preliminary evaluation; (ii) evaluation of second level; (iii) detailed evaluation.

For buildings of damage category 3 or higher a detailed evaluation shall be performed.

A limit value for deformation is related with the occurrence of an ultimate limit state or of a serviceability limit state.

The differential settlements and relative rotations of foundations shall be established in order to avoid the occurrence of an ultimate limit state or a serviceability limit state (like cracking).

The computation of the differential settlement shall take into consideration:

- the variations of the ground properties;

- the distribution of loads;

- the construction methodology;

- the stiffness of the structure.

Note: The study of Porto tunnel and 24 Agosto Station was performed for Kaiser Engineering.

8.6.5 Case History nº 21 - Albufeira Tunnel

8.6.5.1 Introduction

The preliminary studies are introduced, the geological and geotechnical studies are described, the seismic action is referred**,** the preliminary design and execution design are presented, the slope stability is analysed, the parameters to control damages are discussed, the instrumentation plan is introduced and the buildings assessment is described.

8.6.5.2 Preliminary Studies

This drainage tunnel 1460 m long is located in the west of Albufeira (Portugal), with the beginning in Albufeira lake and the end at the fisher's beach near the dyke of marine protection (see Figure 8 369).
It can reach depths of 60 m.

Figure 8. 370 illustrates the longitudinal profile.

Figure 8. 369 Tunnel crossing

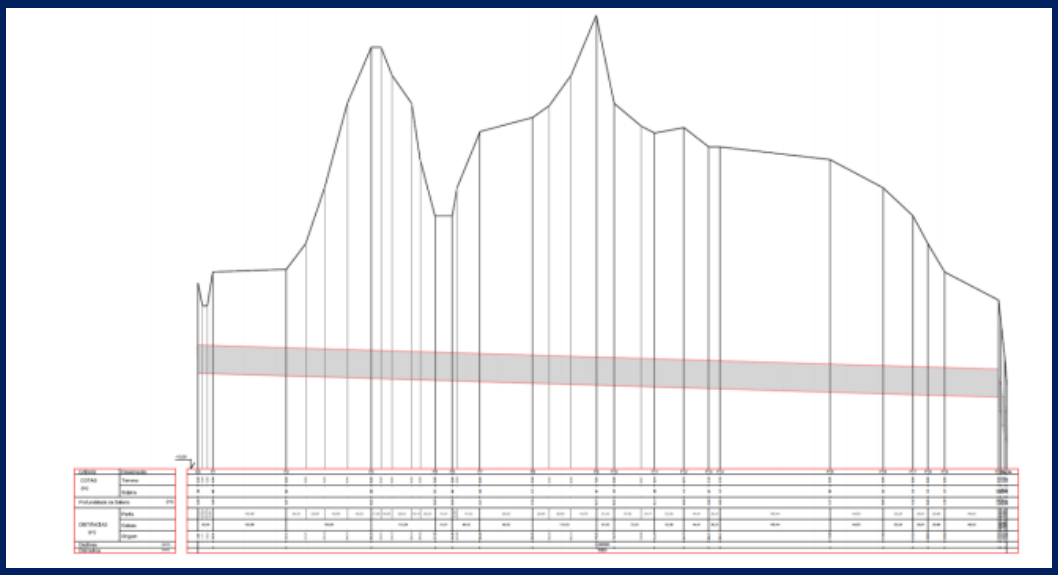

Figure 8. 370 Longitudinal profile

8.6.5.3 Geological and Geotechnical Studies

In this site there are rocks that integrate calcareous, of Jurassic and Miocenic and more recent sandy materials and carsic formations with the cavities fulfilled by siltites.

Figure 8. 371 shows the ground model (Militar Map) – Sheet 605 (Albufeira).

Figure 8. 372 illustrates the geological Map- Sheet 52-B (Albufeira).

The Geologic Map 52-B (Albufeira), identifies the following units:
- Calcareous sandy marnes

-Calcareous rocks
- Siltites.

The site investigation programme with the purpose to define the geological and geotechnical characteristics from the site has integrated:

i) 12 mechanical boreholes with SPT tests 1.5m apart;
ii) Samplers of double wall were used and in 8 boreholes hydraulic piezometers were installed. The drilling hole diameters were between 101 mm and 86 mm.

The SPT tests results were between 10 to >50 blows.

Figure 8. 373 shows the implantation of the boreholes.

The water level in the hydraulic piezometers has shown a good correlation with the tides.

Four Lugeon tests were performed in the boreholes FB-STAT2, FBT7-8, FB-STAT7-8, to assess the permeability of the rock massif.

The lay-out of the test with the borehole and the piezometers is shown in Figure 8.366.

Figure 8. 374 presents the lay -out of Lugeon test.

The disturbed samples were used for identification tests (sieve analysis and Atterberg limits) and Proctor tests.

In addition, water tests to define the aggressivity were performed.

Uniaxial compression tests performed on rock samples gave results between 16.1 to 135.2 MPa and elasticity modulus between 2.6 to 97.1 GPa.

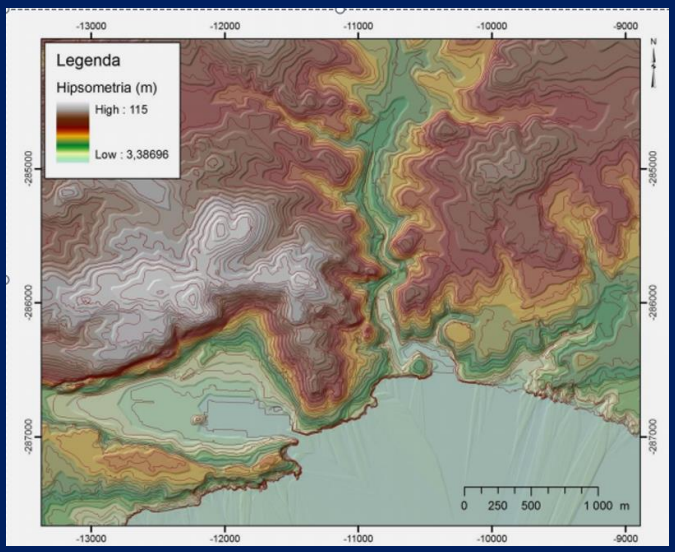

Figure 8. 371 Ground model (Militar Map) – Sheet 605 (Albufeira) (source Hidra)

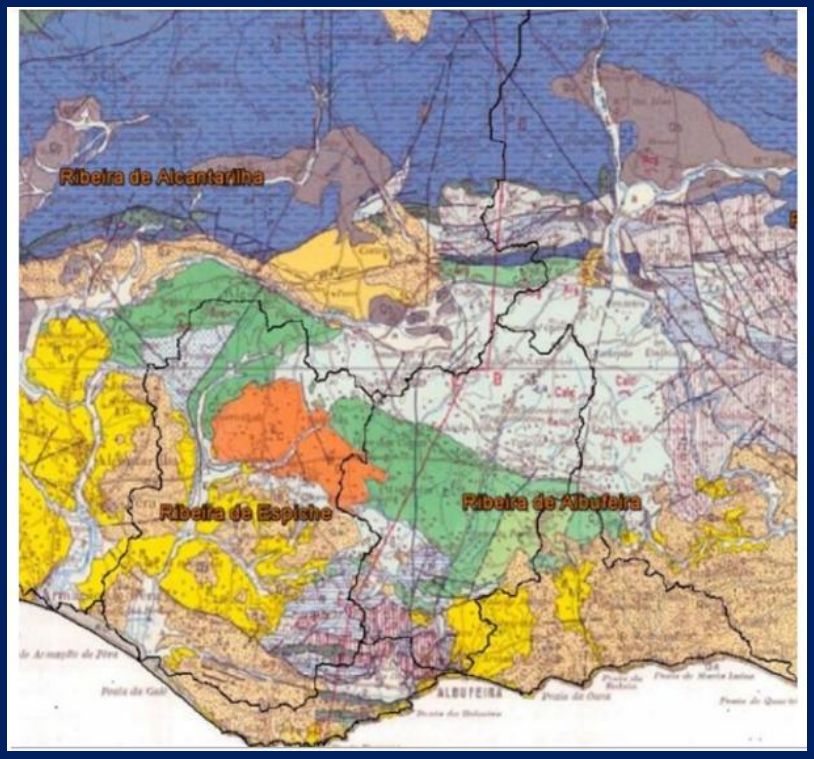

Figure 8. 372 Geological Map- Sheet 52-b (Albufeira) (source Hidra)

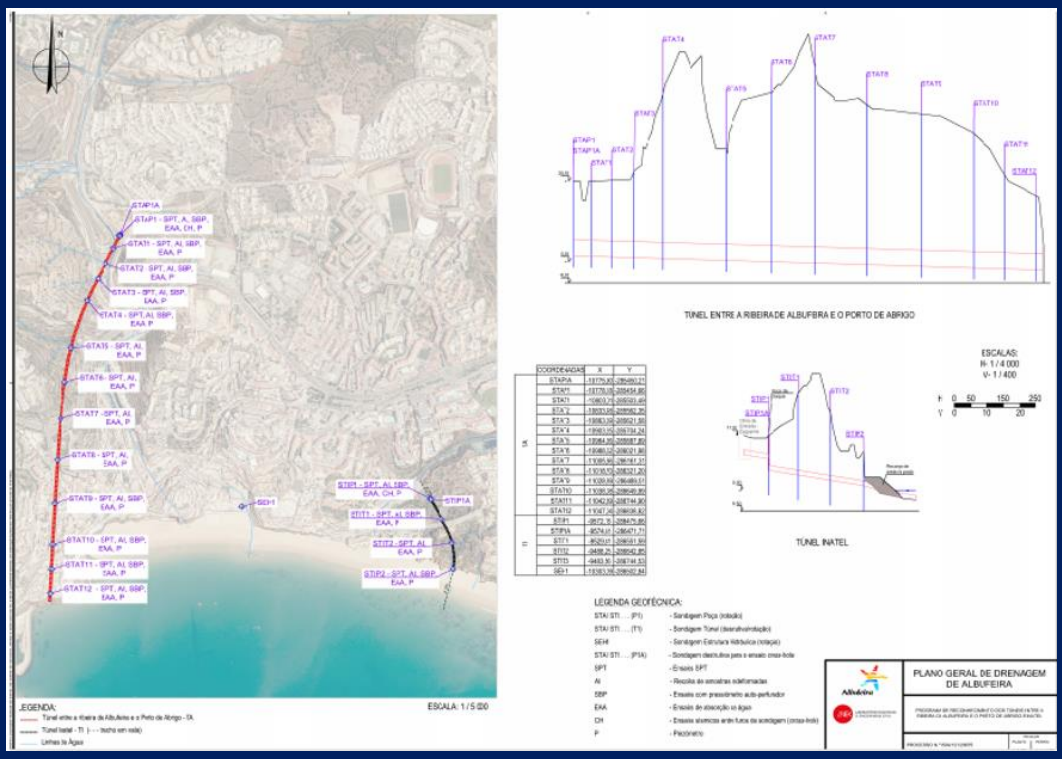

Figure 8. 373 Implantation of the boreholes

Figure 8. 374 Lay -out of Lugeon test

8.6.5.4 Seismic Action

The tunnel is located in zone A (highest risk) referred by the code- Regulamento de Segurança e Acções para Estruturas de Edifícios e Pontes-RSA (1983), and following the National Annex (Eurocode 8) the zoning for seismic Action 1 and Seismic Action 2 is presented in Figure 8.375.

The Table 8.49 shows the maximum reference acceleration a_{gr} for seismic action Type 1 (earthquakes with magnitude higher than 5.5) and seismic action Type 2 (earthquakes with magnitude less than 5.5).

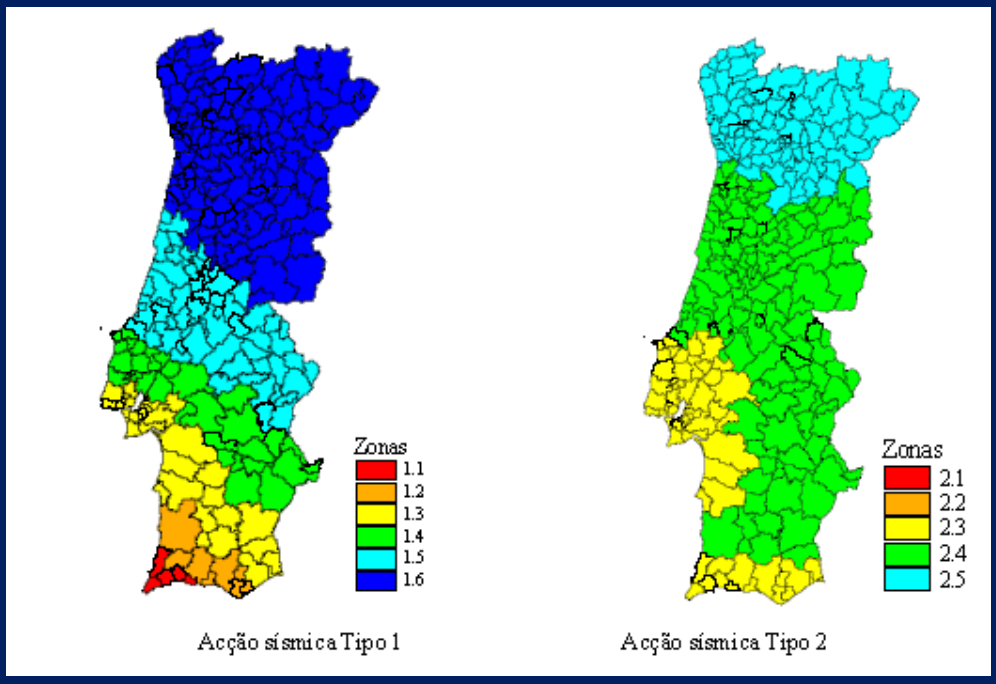

Figure 8.375 Seismic Zoning from Continental Portugal

Table 8.49 Maximum acceleration of reference a_{gr}

Acção sísmica Tipo 1		Acção sísmica Tipo 2	
Zona Sísmica	a_{gR} (m/s^2)	Zona Sísmica	a_{gR} (m/s^2)
1.1	2,5	2.1	2,5
1.2	2,0	2.2	2,0
1.3	1,5	2.3	1,7
1.4	1,0	2.4	1,1
1.5	0,6	2.5	0,8
1.6	0,35	–	–

Considering a return period of 1000 years, from the Figure8.368 for Albufeira tunnel an acceleration value of 200 gal (seismic action 1) can be considered.

It is important to stress that this acceleration value does not incorporate the local effects.

In summary, it is necessary to consider:

- the uncertainties of data;

ii) the local effects and the consequences related the attenuation;

iii) the induced seismicity for earthquakes with low epicentral distance.

So, the value of the bedrock acceleration should be multiplied by the factors 1.5 e de 1.7, for seismic action 1 and seismic action 2, respectively, to incorporate the local effects (see Figure 8.376).

For the seismic acceleration values, with the incorporation of amplification effects, were proposed:

MCE (action Type 1) = 0.285 g (horizontal component)

MCE (action Type 1) = 0.095 g (vertical component)

OBE (action Type 1) = 0.14 g (horizontal component)

OBE (action Type 1) = 0.05 g (vertical component)

MCE (action Type 2) = 0.30g (horizontal component)

MCE (action Type 2) = 0.10 g (vertical component)

OBE (action Type 2) = 0.15 g (horizontal component)

OBE (action Type 2) = 0.05 g (vertical component)

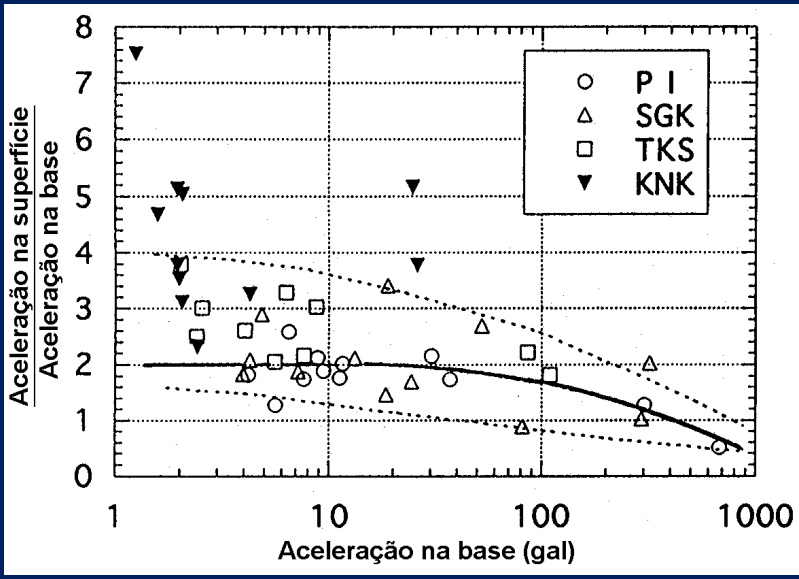

Figure 8. 376 Relationship between the maximum horizontal acceleration and the bedrock acceleration (source Kokusho and Matsumoto, 1997)

For the Detail Project the seismic action should be defined by deterministic and probabilistic methods incorporating the local effects and using a f.e.m. code in total stress (equivalent linear model) or in effective stress (non linear model). For the use of those models, it is necessary to perform dynamic laboratory tests for the definition of the variation curves G/Gmax and damping with shear strain.

8.6.5.5 Preliminary Design

For this preliminary design empirical methods like Bieniawski and Barton methods were used for the design of primary lining. Those methods have a great cumulated experience.

After analyzing the elements of the geotechnical survey, including boreholes and surface surveys, it is estimated the value of RMR (Rock Mass Rating), Bieniawski, 1989.
The RMR Rock Mass Rating system is the most used for rock mass classification, can range from 0 to 100, and it's obtained by the algebric sum of the parameter weights, namely: Strength of intact rock material, Drill core quality (RQD), spacing of discontinuities, Condition of discontinuities, Groundwater, Adjustment for joint orientation.

For the geotechnical zone 1, where failure of blocks can occur and so for the primary lining nailing or rock bolts in the ceiling and in the lateral zones 6m long, 76mm of diameter and reinforcement of 32 mm, concrete with 2,5 cm, thick and metallic mesh should be used.

For the geotechnical zone 2, where failure of blocks can occur and eventually some sliding zones, so for the primary lining nailing or rock bolts in the ceiling and in the lateral zones 6m long, 76mm of diameter and reinforcement of 32 mm, 3m apart in the current zones and eventually 1.5m apart in critical zones and concrete with 5.0 cm, thick and metallic mesh should be used.

In addition, the placement of ribs can be necessary.

For the application of the liner, it is important to respect the following steps:
1 – concrete layer with 3 to 5 cm thick;
2 – nailing;
3 – metallic mesh;

4 – metallic rings;
5 – first layer of concrete;
6 – concrete layers with metallic mesh.

For the situations where blasting is used, it is convenient to place the concrete, with 3 to 5 cm thick, with high rate of hardening, just after the excavation, in order to give to the ground a cohesion, before the application of nailing/rock bolts.

The implementation of f.e.m. codes that allows the simulation of construction phases, with the distribution of stress and strain, needs to be calibrated.

The reliability of the results, obtained by these complex codes, depends on the special laboratory tests performed to define the rheological model, in order to duplicate the real behavior.

8.6.5.6 Execution Design

For the Execution Design to simulate the construction phase it is important to use the Phase V8.0 code from Roscsience.

It is important to analyse the possibility of the formation of wedges, in the interior of the cross section, using Unwedge 3.0 code from Roscsience, and also other critical scenarios. It is important to use constitutive models non liner based in reliable tests.

In general, the analyses are 2D, but analyses 3D could be necessary to analyse the front of the tunnel and other complex geometries.

For a better analysis of the real behavior, it is important to perform:

- sensitivity analyses considering different values of Ko;

- analyses in effective stress with an elastoplastic model with hardening and the failure criteria of Mohr Coulomb;

- analyses in total stress using and elastic model with a failure criterion of Tresca, without tension resistance;

- analyses in effective stress incorporating the construction phase and the dewatering of the water with the modification of the “Hardening Soil” model and the calibration of the stress-strain curves obtained by drained triaxial tests;

- stability analyses incorporating the entrance of the tunnel.

For the safety evaluation of the tunnel the computed displacements should be compared with the observed values.

8.6.5.7 Slope Stability

The slope stability analysis was done by two methods, namely by SMR – “Slope Mass Rating”method proposed by (ROMANA 1983, 1999) and by Mora & Vahrson method.

SMR is given by the equation:

$$SMR = RMR - (F1 \times F2 \times F3) + F4 \quad (8.79)$$

A detailed explanation of these parameters and their definition is given in Volume 5.

Mora &Vahrson (1993) proposed a method to predict landslides based in failures of slopes located in South America, following the occurrence of earthquakes or intensive rains. In this method, three factors: relative relief, lithologic conditions and soil moisture, were considered as the factors influencing the susceptibility of failure. In addition, two factors, seismicity and rainfall intensity, are incorporated as triggering factors (ISSMFE, 1993).

By combining these factors, a degree of slope failure hazard was defined as follows:

$$H_l=(S_r\ S_l\ S_h) * (T_s+T_p)\ (2) \qquad (8.80)$$

where, H_l: landslide hazard index.

S_r: value of relative relief.

S_l: value of lithologic susceptibility.

S_h: value of index of influence of natural humidity of the soil.

T_s: value of influence of seismic intensity.

T_p: value of rainfall precipitation intensity.

A detailed explanation of these factors and their determination is given in Volume 5.

The RMR method proposed by Romana has identified a deficient slope, unstable, planar or big wedges failures that need corrections actions;

The methodology proposed by Mora & Vahrson shows a moderate susceptibility for sliding.

8.6.5.8 Parameters to Control Damages

As it is not possible a rigorous definition of the ground displacements horizontal and vertical displacements simplified methods were used.

The settlements depend the several factors, namely: (i) effect of the front; (ii) influence of the support; (iii) influence of the construction phases; and (iv) influence of the support.

The methods can be classified in two groups: (i) semi-empirical methods; and (ii) numerical methods.

The empirical methods depend of: (i) dimensions and depth of the excavation that define the longitudinal and transverse geometry of the influence basin; (ii) characteristic of the ground (elasticity modulus and Poisson ratio); and (iii) loss of volume in the neighboring of the excavation.

The numerical methods, namely the f.e.m. are more flexible to duplicate the construction phasing. The comparison with field observations have shown that the reliability of the predictions are linked with the quality of sampling and with the need to perform tests with imposed stress path and measurements with transducers installed in the samples.

For the risk evaluation of buildings there is a need to define the horizontal and vertical ground displacements profiles in the neighboring of the buildings, the subsidence. These profiles depend on the type of the excavation.

For simple geometries of excavations, e.g. for tunnels i tis possible to use simplified methods to predict ground displacements, namely the empirical model proposed by Peck (1969), and calibrated by the scientific biography.
It is assumed that the settlements variation follows an exponential path with the maximum value in the vertical of the tunnel axis.
The horizontal displacements are obtained from the vertical distribution.

The excavations and underground structures provoke ground movements. In a situation of no buildings "greenfield site" the shape of the basin in a transverse profile following the longitudinal axis of the tunnel, can be considered, in a simplified way, as normal distribution Gauss curve defined by equation (Peck, 1969):

$$s = s_{max} \exp(-x^2/2i^2) \quad (8.81)$$

where:

s= settlement

s_{max} = maximum settlement

i= width of the basin

For homogenous soils the width of the basin is given by the equation:

$$i = KH \quad (8.82)$$

where H is the depth of the center of the tunnel and K depends namely of the soil type, varying from 0.4 to 0.6 in clay soils and 0.25 a 0.45 in sandy soils.

8.6.5.9 Instrumentation Plan

Some preliminary recommendations for the safety control during the construction phase.

For the deformations control of the tunnel, it is important to measure the convergences and the extensometers, as well the water level by hydraulic piezometers.

Definition of attention and alert values

At the beginning the frequency of the measurements should be daily and subsequently can be two times a week or weekly, if the measurements become stable.
.
A good communication should exist among all the entities, in order to implement the corrective actions in due time.

In addition, periodical visual inspections should be performed.

Alarm criteria should be defined based in the deformation rate for the situations of stabilization, attention and alert.

Also, the values of convergences and settlements should be taken into account.

For the definition of alert values, it is important to incorporate:

i) The values of maximum estimated displacements:
ii) the geological-geotechnical model;
iii) the variation of the curve's displacements-time;
iv) comparative analysis of the values recorded in the different instrumented profiles;
v) comparative analysis between the observed values and the predicted values by the model.

The alarm criteria should base in the deformation rate and in general the following values are adopted:
0.1 mm/day: ..... stabilization
1 mm/day: ..... attention
>1 mm/day: ..... alarm

During the project phase a detailed instrumentation plan should be submitted.

8.6.5.10 Evaluation of Buildings Risk

For the building risk evaluation, the Burland et al. (1977) proposal that considers 6 risk categories and control parameter by shear deformation should be used.

The actions to be implemented for the monitoring and the rehabilitation should be presented.

The building assessment shall incorporate the buildings geometry characteristics, the settlements curves, the corner settlements and the analysis of damages.

The buildings risk evaluation shall incorporate the following aspects:

- the subsidence curves respecting the numerical computations and including the effects of the drawdown.
- risk classification for each building;
- real state of each building by the definition of vulnerability index and the correction of the initial risk.

It is important to quantify the building state by defining a vulnerability index that should characterize the building (conservation state, history of the movements, registered damages, induced ground movements by a neighboring excavation). The vulnerability index shows the deviation of the building from the ideal conservation state, i.e. his vulnerability.

Highest the building vulnerability lowest is it capacity to sustain induced damages by external factors.

Considering the vulnerability index as a basis, it is possible to define a correction for the classification of damage risk.

Report from ITA (International Tunnelling Association) –Working Group nº 2

It is important to refer the report prepared by ITA (International Tunnelling Association) –Working Group nº 2- "Identification of Risks Involved in Tunnelling", where the concept of "Unknown unknown- we do not know what we do not know" and also the following situations.

- Unknowns;

- Limited or incomplete site characterizations by time or budget;

- Hydrological conditions, seismic effects, and high permeabilities;

- Environmental risks- faults, caverns, insufficient characterization of mechanical properties;

- Interferences – buildings characterization, identification of monuments, services:

- Risks for thirds parts.

This report has the purpose to introduce: (i) to the Owners the best practices of risk management; (ii) Recommendations for the Designers about the risk identification, risk evaluation, risk analysis, elimination of the risk, and control and mitigation of risk.

These recommendations shall be introduced in the different stages of the project, namely:

Phase 1- Preliminary design (Preliminary studies and Conceptual design), responsibility from the Owner.

Phase 2- bid and contractual negotiations – responsibility of the Contractor and Owner.

Phase 3- construction phase where the Contractor has the responsibility for the risk management and the Owner is the supervisor. The Owner shall evaluate and mitigate the risks not covered by the Contractor.

Lesson nº 21 - Taking into account that the tunnel is located in the highest zone of Portugal seismic map the impact of the underground tunnel excavation on the seismic responses of the adjacent buildings need to be investigated. According to the past experience the maximum variations of the horizontal displacement of the buildings after tunnel excavation during the earthquakes changes between 1 and 3 (%) which is not of considerable value. The variations of the maximum induced bending moment changes between 2 and 10(%) which is relatively high. These values highly depend on the type of the structures and the frequency content of the earthquake.

Note: The study of Albufeira tunnel was performed for Hydra.

8.6.6 Case History nº 22 – Portinho Tunnel

8.6.6.1 Introduction

The background of Portinho tunnel is introduced, the geological characteristics are described, the design analysis is addressed and some recommendations are submitted.

8.6.6.2 Background

Portinho tunnel is an old hydraulic structure, with brick lining, cross sandy materials grey and marnes formations.

The tunnel is 523 m long and average width of 1 m and a height of 2 m.

The longitudinal profile shows a new section of 23 m long and a section with 72 m long with “donkey brick”, a section with 108.5 m long with brick and ceiling of concrete, a section with 111.6 m long without lining and the last section exhibits lateral and ceiling failures, with a part of 63. 0 m long without lining, another part with 76.0 m long without lining and with lateral failures and a final part with 40.0m long in “donkey brick”.

Figures 8. 377 and 8.378 illustrate the interior of the tunnel.

8.6.6.3 Geological Characteristics

The following units can be identified:

i) Unit geotechnical 3 of heterogenous fills, sandy materials and with construction debris, with variable thickness between 3 to 12 m.

ii) Unit geotechnical 2 with sandy materials and silty grey materials.

iii) Unit 1 composed by marnes and grey with clays.

For the first campaign 6 boreholes were performed with SPT tests 1.5 m apart and measurement of the water level.

For the second campaign 4 boreholes were performed, 2 inclinometers were placed in boreholes S1 and S2, for the control of horizontal displacements, due to the excavations.

In borehole S2 three samples were taken for the triaxial tests.

8.6.6.4 Design Analysis

(i) The Portinho tunnel was built by the Belgium methodology that allows the decompression of the massif during the construction phase.

(ii) The rock massif lightly fractured has 3 discontinuities families very pervious and with open

joints.

(iii) For the site characterization mechanical boreholes, seismic refraction tests, Lugeon test, uniaxial tests were performed

(iii) The strength and deformability characteristics of the massif were obtained by Bieniaskwi (RMR) classification and by the criteria proposed by Hoek (GSI).

(iv) The visual inspection has shown the existence of water at the tunnel ceiling and infiltrations at the tunnel walls, deteriorations of the brick material due to the construction methodology and ageing effects.

(v) Three sections of the tunnel were instrumented, one at the bridge axis and two 10 m apart from the first one. Measurements of convergences and bench marks were performed, as well measurements of the 8 inclinometers installed in the neighboring of the tunnel**.**

(vi) The definition of the lining by NTM method and AFTES recommendations point the use of concrete and nailing.

(vii) The results of the application of f.e.m. codes, that allows the simulation of the construction procedure and the knowledge of the distribution of stress and strains, need to be calibrated.

(viii) It is important to calibrate the lining obtained by NTM method and AFTES recommendations for the real conditions of the existence of voids, degradation signs and ageing effects.

(ix) The AFTES recommendations allow the incorporation of the ground, the construction conditions and environmental conditions (AFTES, 1993).

(x) The criteria related the ground behavior incorporate the rock resistance, the discontinuities, the weathering of the massif and the massif stress state.

(xi) The criteria related the construction methodology involve the dimensions, the geometry of the cavity and the excavation procedure.

(xii) The criteria related the environmental involve the ground movements, the behavior of neighbor structures the modifications of the hydrogeological equilibrium and the consequences of the ground treatment.

8.6.6.5 Recommendations

The following recommendations were submitted:

(i) Reinforcement and rehabilitation of the tunnel by nailing.

(ii) Adequate drainage of the tunnel.

(iii) Consolidation of the massif by grouting.

(iv) Measurement of the convergences, bench marks, inclinometers with a frequency of 3 weeks.

(v) Visual inspections with a frequency of 3 months.

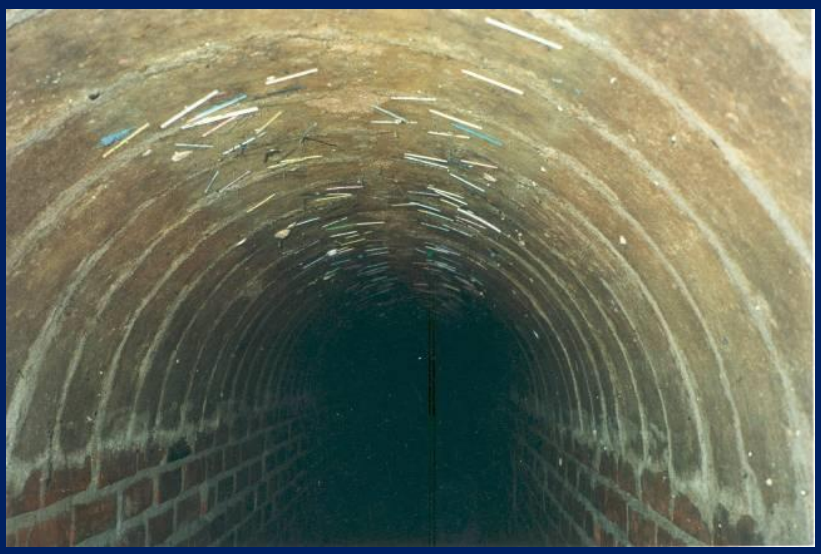

Figure 8. 377 Portinho tunnel

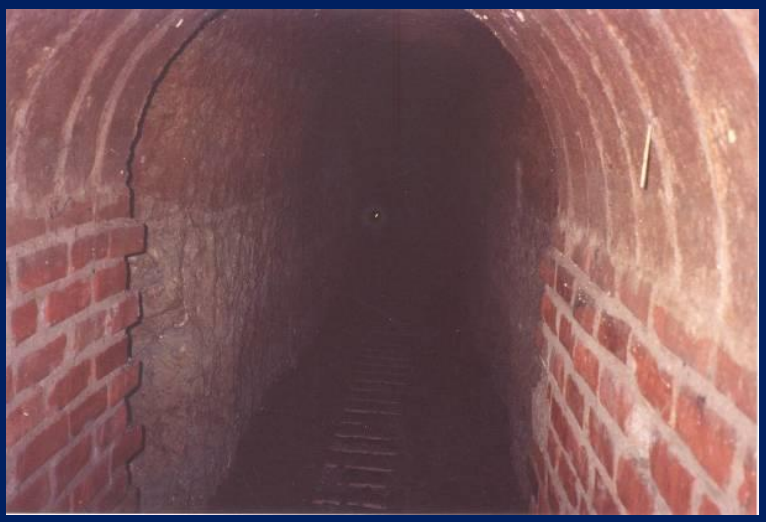

Figure 8. 378 Portinho tunnel -interior view

Due to the lack of adequate geotechnical characterization the stability assessment of the tunnel was based in empirical methods namely NMT and AFTES. For lining it was recommended concrete 10 cm thick and a metallic mesh. In some critical zones the use of metallic rings and nailing was recommended.

Lesson nº 22 - One concern for the life of a tunnel structure is the quality of contact between the liner and the surrounding geologic media. The quality of contact may be investigated by taking core samples or geophysical techniques, and may be improved by contact grouting or other means.

Earthquake effects on underground structures take the form of deformations that cannot be changed significantly by strengthening the structure. The structure should exhibit sufficient ductility to absorb the imposed deformations without losing the capacity to carry static loads.

The ground shaking may cause large curvature distortion in tunnel.

Details related with remedial works and the efficiency about the implemented actions are welcomed.

This is an interesting case history where remediation is needed to achieve the safety levels defined by the modern codes.

Note: The study of Portinho tunnel was performed for Hidra.

8.7 BRIDGES

8.7.1 History of Bridges

The bridge is a structure that provides passage over obstacles such as valleys, rough terrain, or bodies of water.

Bridge history is filled with incredible achievements and new technologies that enabled bridges to become one of the most important tools of bridging cities, countries and continents.

Ancient times

Bridges have been an essential part of human history for thousands of years. Early bridge designs using natural materials such as logs, vines, and animal hides, built by ancient civilizations in Egypt, Mesopotamia, and India, using logs and planks to create simple crossings over rivers and streams.

A tree dropped between the banks reminds us the beam bridge.

Rope bridges can be founded in in the forests of Peru or in the foothills of Himalaias and can be considered the primitive suspension bridges.

In the ancient times 6,000 years ago, Egypt could have been the first as some pseudo stone arches were found in the entrance of the great pyramid of Ghizeh, Egypt (3200 to 4200 BC) made of single sloping stones meeting over an opening.
The first evidence can be considered in Babylonia about 4000BC. With river Euphrates. spanned by a single brick arch.
In China, masonry arches were, around 2000BC, documented in the Great Wall of China.

Floating bridges in China, in 2300 BC are referred.

The Persians were great bridge builders and implemented many archs, canteliver and beam bridges.

The first record of a bridge given by Herodutus is related the bridge built across Euphrates River in ancient Babylon, around 600 BC with hundred stone piers supported by wooden beams, 200m long and 10 m wide.

The Romans have incorporated the semicircular arch about 500 to 600BC and many of them are still standing. Using this type of solution, load forces of the bridge were conveyed to move along the curve of the arch, that was connected with the ground. With this solution Romans were able to create bridges that were much lighter than before and held loads twice as heavy as the bridge itself. For aqueducts, Roman architects even managed to create water-carrying bridges with multiple arched tiers that reached incredible heights. So cheap, light, and very powerful bridges from materials they found near the project were build. The only material that had to be imported from Italy was mortar dust, which was combined with water and inserted into the bridge structure.

The Alcantara Bridge (Figure 8.379), built over the Tagus River around 100 AD, 181 m long and with the deck 62 m above water, without mortar, is an example.

The romans developed a method of constructions the foundation within a cofferdam, formed by a double ring of timber piles with clay packed and pumping the inside water.
The romans build many timber arches, but they have not resisted to the effects of time and only the stone bridges remain until now.

The most famous bridge of Renaissance is the Venice Rialto bridge, but Santa Trinita in Florence and Pont Neuf in Paris should be referred.

The timber bridges were pioneered by Switzerland, with Wettingen bridge in Zurich and later some remarkable timber bridges were constructed by the americans.

After the fall of the roman empire, bridge-building techniques in Europe and Asia were dormant until the 18th century.

Figure 8. 379 The Alcantara Bridge

Bridge building reborn in France between 1500AD and 1750AD, and in England with the construction of Westminister Bridge, in 1738.

Figure 8. 380 The remains of the Pont d'Avignon - a landmark of bridge building achievement.

For a relatively short time in history cast iron was in fashion (Figure 8.381), and substituted by structural steel, about 1890.

Suspension Bridges

Examples of suspension bridges can be found in remote villages of China, Japan, India, and Mexico and South America, using twisted vines to attach to the bridge and nearby trees.
The first modern suspension bridge arrived in 1801, connecting Uniontown to Greensburg, Pennsylvania with a span of 21m.

Analyses of stresses distribution in bridge frames are from the United States in 1847,

The Brooklyn Bridge was the first suspension bridge using steel for the wires of suspension cables in the world.

Figure 8. 381 The Coalbrookedale Bridge was the world's first bridge made entirely of cast iron.

Concrete

In Amalfi, Italy, there is a concrete bridge built in the 6th Century with 1.5 m wide, 3 m above water and 7m long, still in good condition in the current days.

Conventional concrete bridge design spread from Switzerland to United States where the railroad companies renewed old steel bridges with concrete.

Brunel was a pioneer in reinforced concrete arches, building a semi-arch of brick 18.3 m long with hoop iron bond, which supported itself through cantilever action.

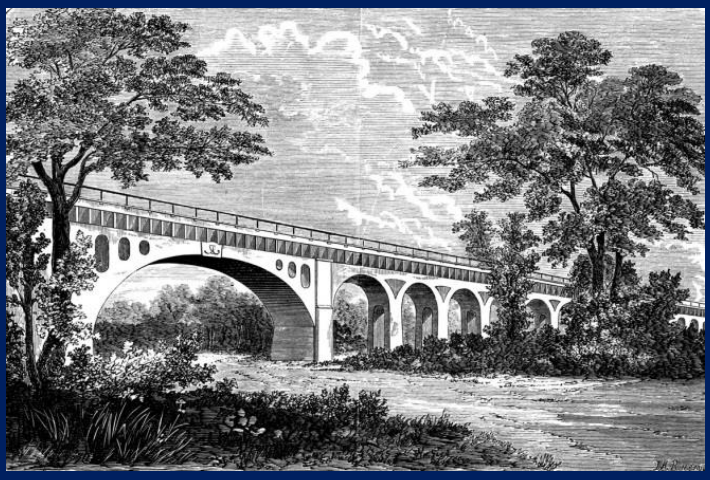

Figure 8.382 Grand Maitre Aqueduct (Source: Lehigh University Library)

The Grand Maitre Aqueduct (Figure 8.382) was one of the world's first great uses of exposed concrete.

Box Girders

In 1845 engineer Robert Stephenson design the railway bridge over the Menai Strait at Anglesey, connecting the railway between London to Holyhead. He developed an original solution of prefabrication, where the horizontal elements divided into three sections, floated out, and lifted up into position on piers.

During the 20th century, box girder design progressed into lighter weight, even longer span steel structures, often used in suspension bridges, e.g. the Severn suspension bridge, built in the 1960s and Hong Kong's Tsing Ma bridge, build in the 1990s.

Figure 8. 383 shows the Britannia Bridge, forerunner to the modern box girder.

Figure 8. 383 Britannia Bridge, forerunner to the modern box girder.

It is important to highlight that concrete has been utilized since ancient times, particularly by the Romans, who ingeniously combined it with stone in their architectural designs. The Romans were among the first to develop more advanced bridge designs, such as the stone arch bridge, which allowed for longer and more durable spans, which can be seen in instances such as the Pont du Gard in France, a Roman aqueduct that still stands today.

During the Middle Ages, bridge design continued to evolve, with advances in engineering and construction techniques. Wooden truss bridges became popular in Europe.

After the use of stone, wood, brick, steel, concrete, iron was introduced in 1775. But the iron bridges suffered failures due the vibration and dynamic loading from steam locomotive.

In the 19th century, the Industrial Revolution with its developed technologies of processing steel in mass industrial scale, allowed the construction of steel bridges.

In the 20th century with the technological it was possible to design bridges with larger spans.
One example is the suspension span structure of Akashi Kaikyo Bridge located in Japan.

In the 21st century another record with the construction of Millau Viaduct in France, the highest bridge in the world based on a cable-stayed structural system, completed in 2004.

Today, bridge design with the support of computer modeling and simulation have allowed for more precise and efficient design. The Hong Kong-Zhuhai-Macau Bridge, completed in 2018, is the world's longest sea crossing bridge, spanning 55 kilometers and featuring innovative engineering solutions to withstand typhoons and earthquakes.

Bridge design is a complex and multifaceted process that involves a range of considerations, such as load-bearing capacity, durability, functionality, environmental factors, aesthetics, and cost.

8.7. 2 Case History nº 23 - Vasco de Gama Bridge

8.7.2.1 Introduction

The 18 km Tagus bridge Lisbon, capital of Portugal, is composed by a number of structures. From the Sacavém interchange the estuary traffic will cross the North viaduct, the Expo viaduct, the Cable stayed bridge, the Central viaduct and, finally, the South viaduct (see Figure 8. 384).

Foundations for the bridge structures are a mixture of bored and driven piles.

The central viaduct, with 6.5 km long, will be supported on 648 driven piles up to 60 m long. Eight piles with a diameter of 1.7 m will be installed below each pier on all the central viaduct piers except those next to shipping channels.

The site investigation is introduced, the geological and geotechnical characteristics are described, the liquefaction assessment is addressed, the piles tests are referred, the design analysis is presented, the construction issues are described and the instrumentation is addressed.

Figure 8. 384 Vasco de Gama Bridge

8.7.2.2 Site Investigation

Figure 8.385 illustrates the site investigations platform.
Figure 8. 386 shows the execution of the vane shear tests.

Figure 8.385 Site investigations platforms

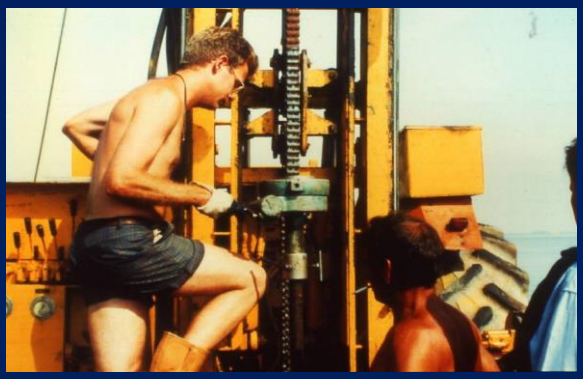

Figure 8.386 Vane shear tests

8.7.2.3 Geological Characteristics

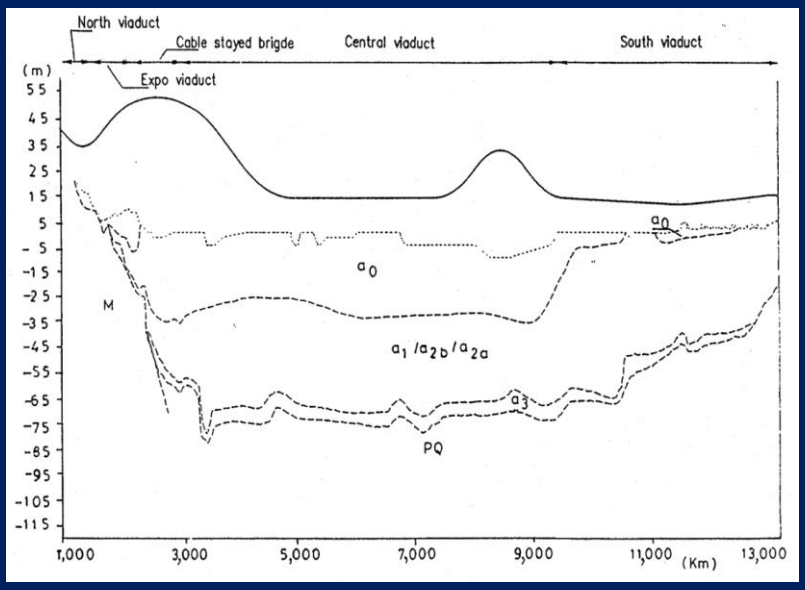

Figure 8.387 Geological profile

The general description of alluvial deposits is the following:

a_0 This unit is formed by silty to very silty clay (mud), dark grey, with maximum thickness around 35 m.
a_1 Fine to medium sand with shells and shell fragments.
a_{2a} Silty clay to clayey silt.
a_{2b} Yellowish brown to grey medium to coarse (occasionally fine) sand.
a_3 Fine to coarse gravel, rounded to angular, with sand, cobbles and occasionally some boulders.
The bedrock under the alluvial deposits consists in Plio-Pleistocene materials.

The geological profile is illustrated in Figure 8. 387.

8.7.2.4 Geotechnical Characteristics

Alluvial material (a_2)

The following results were obtained (a_{2a}):

Triaxial tests (U.U.):

Undrained strength (C_u): 40 to 42 kPa

Triaxial tests (C.U.):

Cohesion (effective) c' = 0, friction angle ϕ' = 40 to 42^o

Triaxial tests (C.D.):

Cohesion (effective) c' = 0, friction angle ϕ' = 27^o

The crosshole tests have given the following results:

Shear wave velocities V_s from 162 to 310 m/s and longitudinal wave velocities V_p from 1201 to 1674 m/s.

8.7.2.5 Liquefaction Assessment

The liquefaction potential evaluation was performed only by field tests taking into account the disturbance that occurs during sampling of sandy materials.

In this analysis attention was drawn for SPT and CPT tests as the seismic tests have only been used when soil contains gravel particles.

In a first step the shear values were computed from a total stresses model, that gave results on the conservative side using the program "SHAKE", for a second step it was performed an analysis in effective stresses using the computer program DYNAFLOW. The geotechnical profile of SR2 was used for the study of the piers belonging to the Exposition viaduct, Cable stayed bridge, the SR6 and SR7 geotechnical profiles for Central viaduct and SR10 for South viaduct.

Corrections related with SPT tests due the depth effect and the equipment were performed following the recommendations of EC8.

The sieve curves of materials a_1 and a_{2b}, have given the results presented in Table 8.50 where the symbols have the following meaning:

Table 8.50 Sieve characteristics of the materials

Structure	Material a_1			Material a_{2b}		
	F_p (%)	D50 (mm)	NCG	F_p (%)	D50 (mm)	NCG
Main Bridge	17.8	0.13	4	-	-	-
Central Viaduct	15.9	0.14	16	10	0.4	18
South Viaduct	11.2	0.14	29	2.8	0.7	4

F_p - percentage of the material that passes through the sieve # 200, D_{50} - diameter corresponding to the percentage of 50%, NCG - number of the sieve curves.

Taking into account that we are dealing with underwater materials, the sieve curves for material a_1 and material a_{2b} presented in Figure 8.388 exhibit percentages of fines lower than in reality, as a consequence of the washing effect during the sampling.

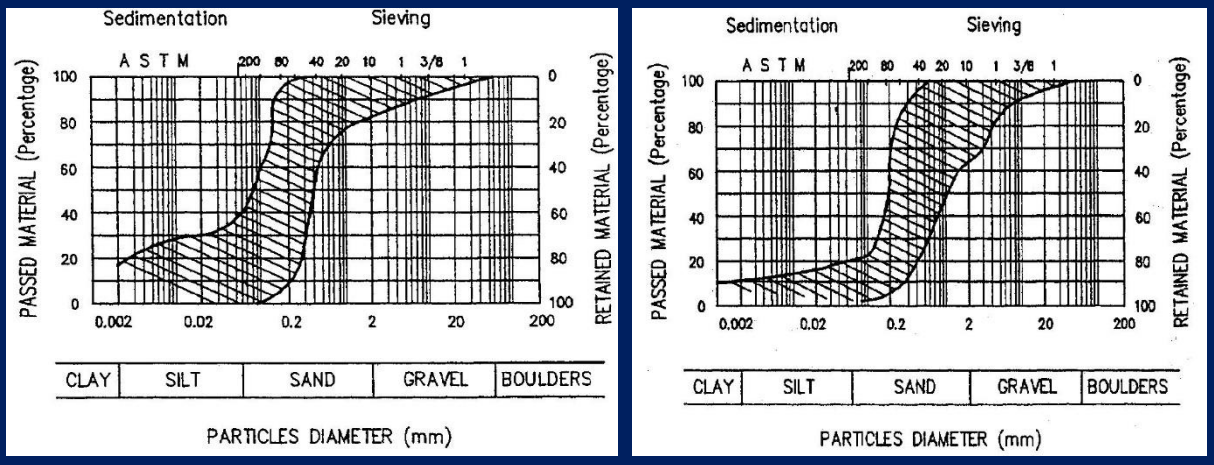

Figure 8.388 Sieve curves for material a_1 and material a_{2b}

Taking into account the dilatant behaviour of the material observed in the CPT tests and the values of the pore pressures developed in the cyclic simple shear tests and cyclic torsional shear tests, where the registered values of the pore pressures rarely reach the value of 80%, being frequently below 60%, a safety factor of 1.1 can be considered sufficient. Nevertheless, at the present case, a conservative analysis was performed, with a safety factor of 1.25 being adopted, as recommended in EC8.

Figure 8.389 shows the computation of shear stress by Shake and Dynaflow codes.

The liquefaction potential evaluation, by SPT and CPT tests, is shown in Figure 8.390.

The liquefaction susceptible zones for the different structures are shown in Table 8.51.

Table 8.51: Summary table liquefaction susceptible zones

Structure	Material a_1			Material a_{2b}		
	Treated Values	Piers Zones Susceptible to Liquefaction	Percentage	Treated Values	Piers Zones Susceptible to Liquefaction	Percentage
Exposition Viaduct	7	0	0	6	1	17
Main Bridge	27	2	7	24	1	4
Central Viaduct	291	19	7	333	14	4
South Viaduct	90	20	22	43	0	0
TOTAL	415	41	10	406	16	4

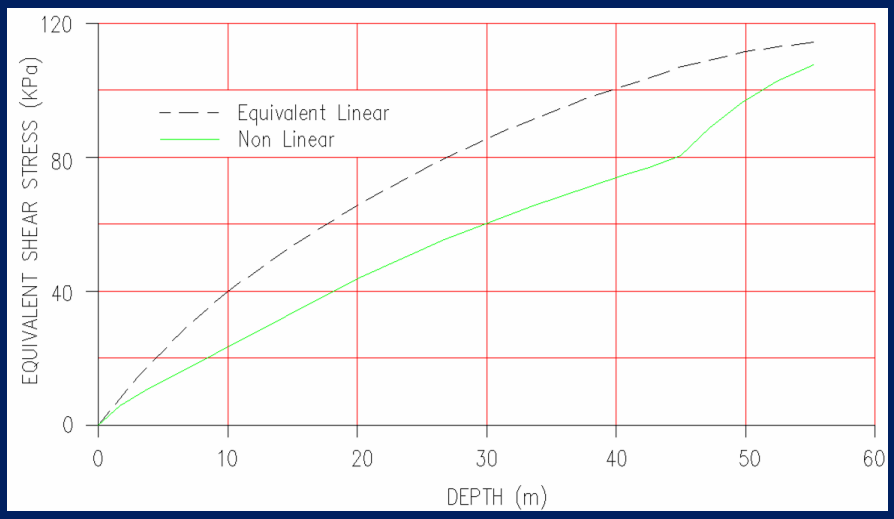

Figure 8.389 Computation of Shear Stress by Shake and Dynaflow codes

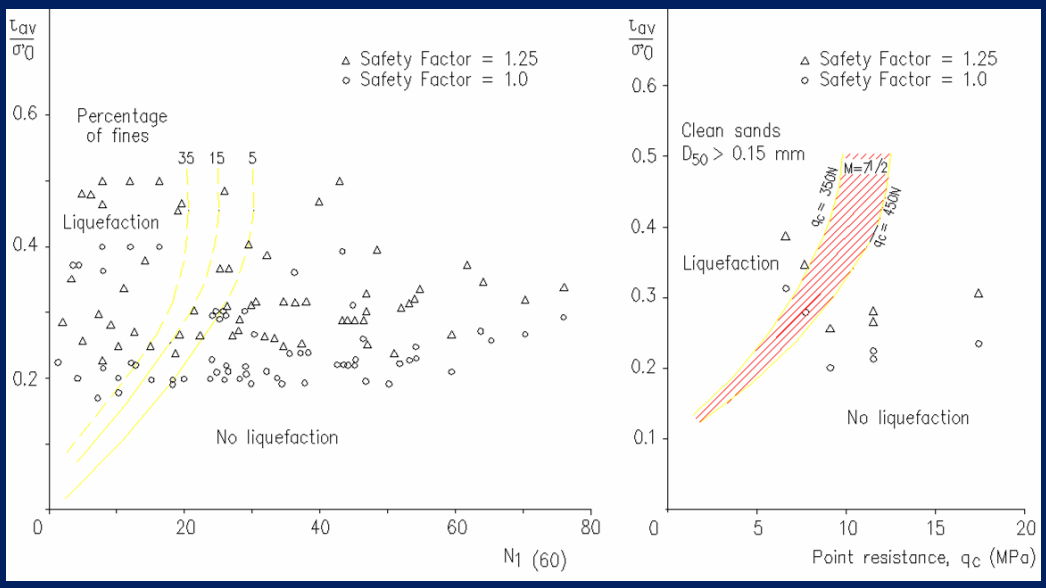

Figure 8.390 Liquefaction Assessment by SPT and CPT tests

8.7.2.6 Piles Tests

Load tests were carried out on trial piles which for test purposes before the final design.

The results of load tests were used to calibrate the design parameters and so to optimise the pile lengths, based only on the interpretation of site investigation.

Figure 8.391 Pile reinforcement

Figure 8.391 illustrates the pile reinforcement.

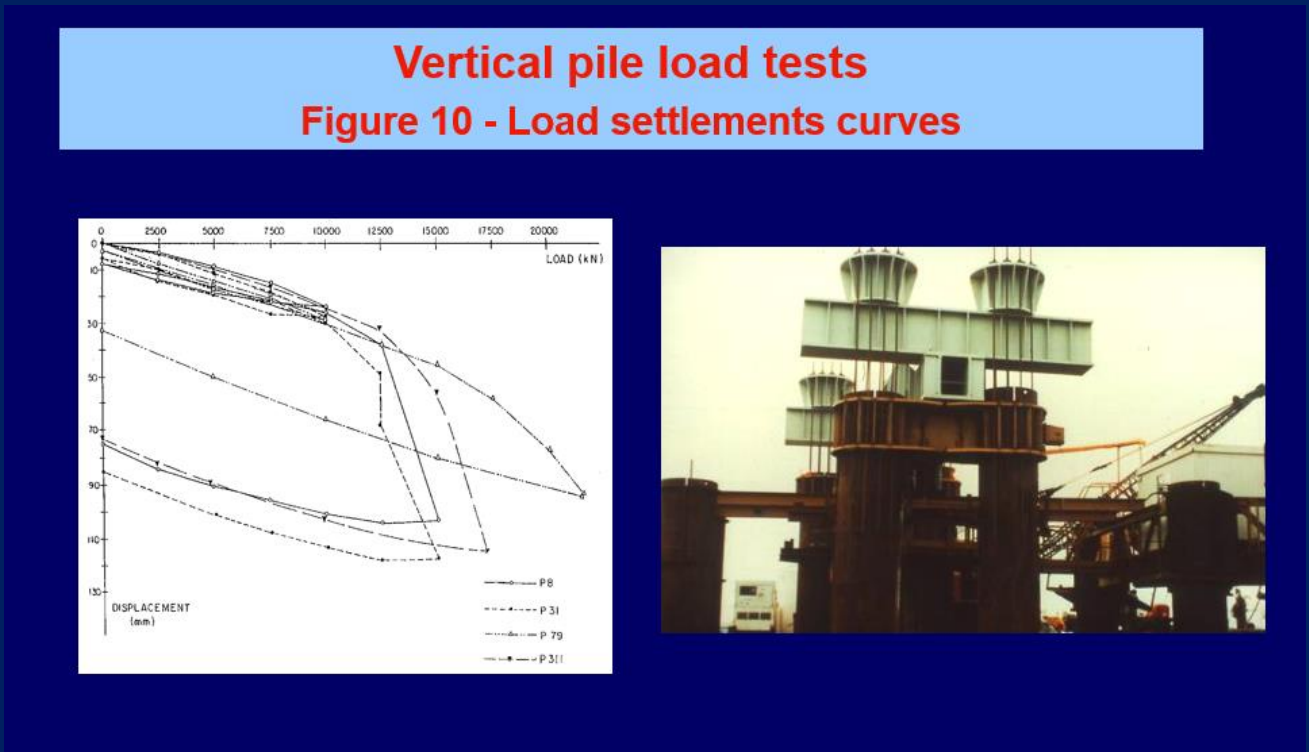

Figure 8. 392 Vertical pile loads tests

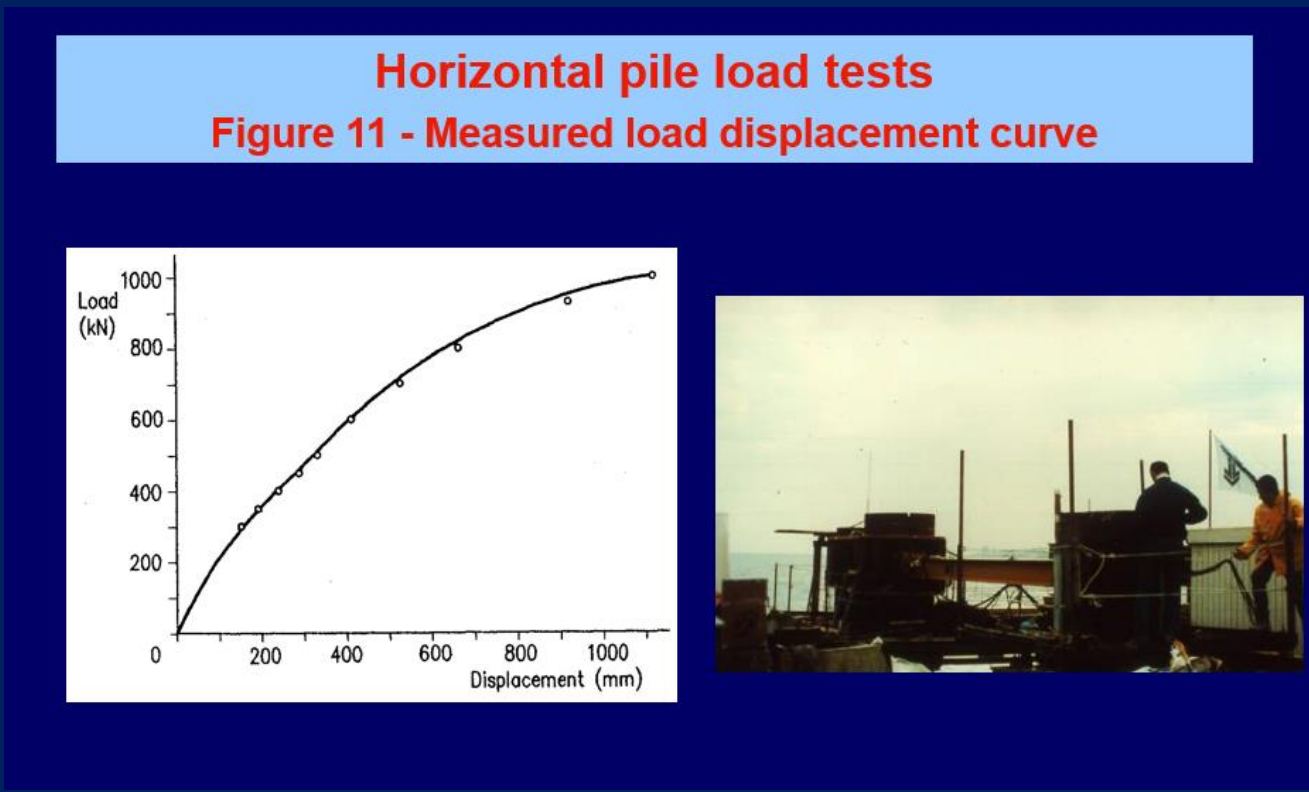

Figure 8. 393 Horizontal pile loads tests

Figure 8.394 Pile dynamic tests

Figures 8.392 and 8.393 present the results of vertical and horizontal pile load tests.

Figure 8.394 shows the lay-out of pile dynamic tests.

8.7.2.7 Design Analysis

For the seismic analysis of piles with 2.2 m of diameter the program TRIMO was used to compute the frequencies and the modes of vibration (P&V, 1994 b).

The geotechnical characteristics of the materials were selected for a value of shear strain around 1%.

For each direction 88 frequencies were computed

The displacement values, the axial forces, the shear forces and the bending moments for the piles were computed.

3D Model

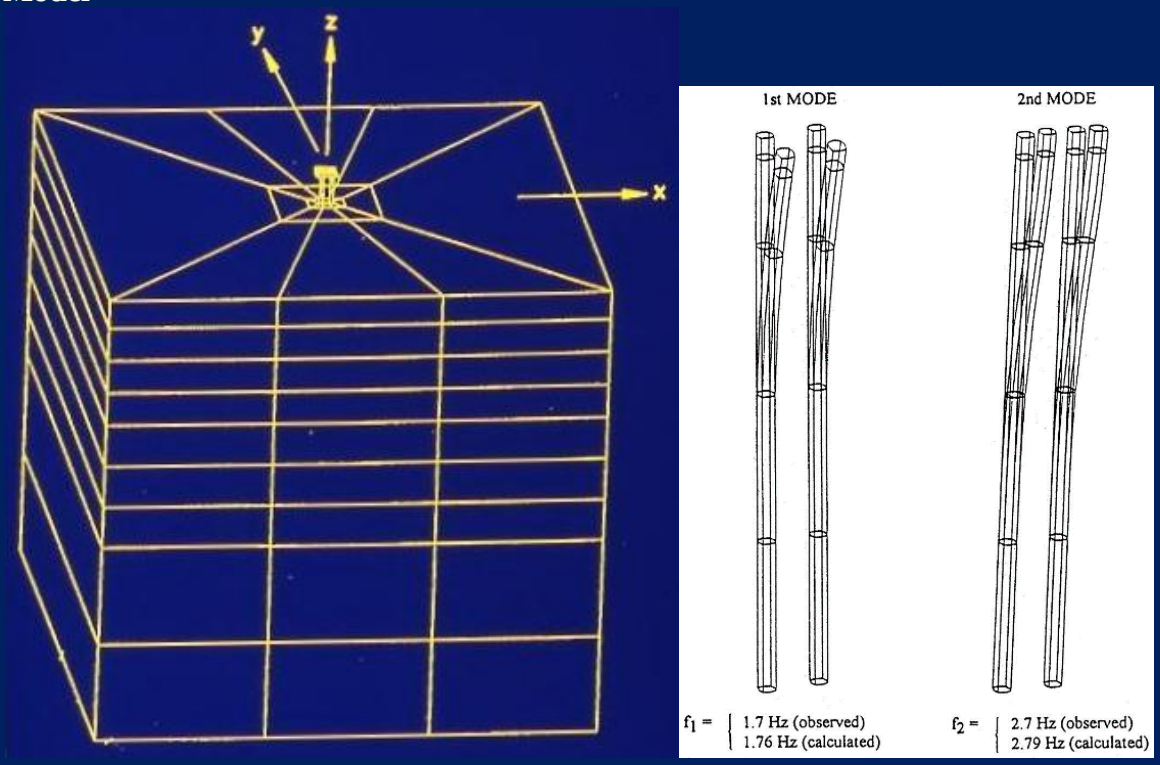

Figure 8.395 Configuration of the two first vibration modes. Observed and calculated frequencies

Table 9 - Natural Computed Frequencies

Mode	Longitudinal Direction	Transversal Direction
1	0.253	0.252
2	0.387	0.400
3	0.473	0.480
4	0.516	0.521
5	0.577	0.590
6	0.602	0.620
7	0.710	0.741
8	0.733	0.757
9	0.829	0.860
10	0.850	0.880

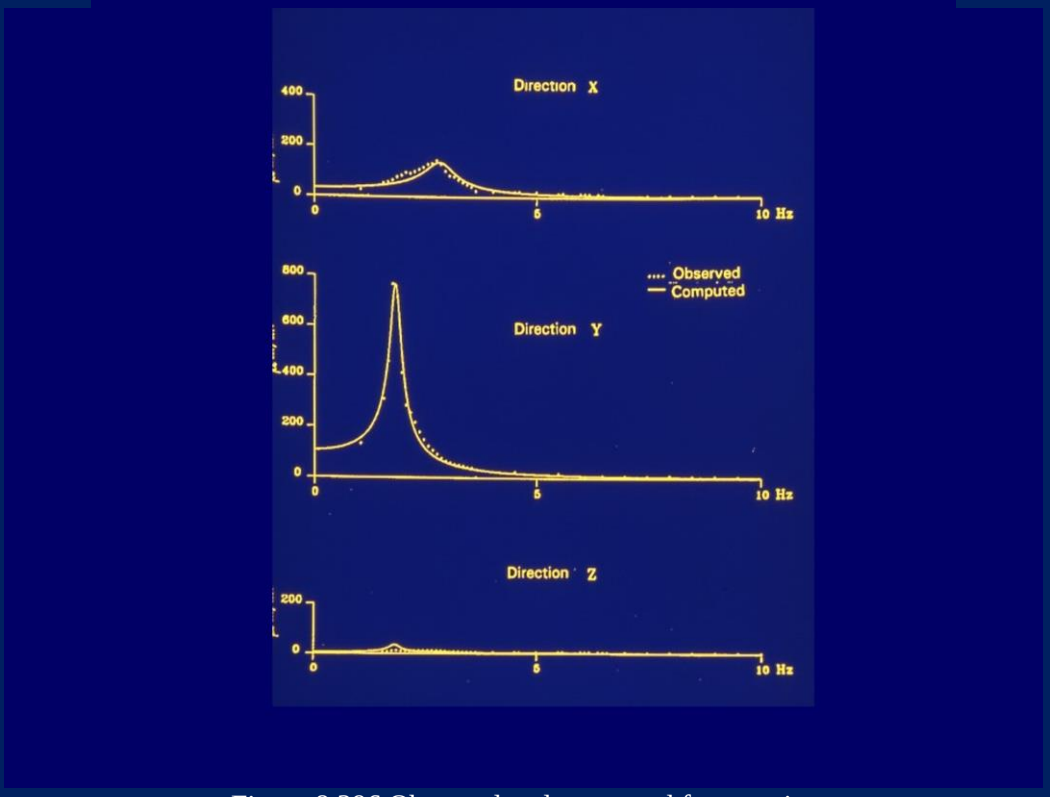

Figure 8.396 Observed and computed frequencies

Figure 8.395 shows the configuration of the two first vibration modes and the observed and calculated frequencies.

Figure 8.396 illustrates a comparison between the natural observed and computed frequencies.

8.7.2.8 Construction Issues

Figure 8. 397 Construction of Piles

Figure 8.398 Central Viaduct

Figure 8. 397 illustrates a view of the construction of piles.

Figure 8.398 shows the equipment to transport the sections of the central viaduct.

8.7.2.9 Instrumentation

Superstructure Measurements

- Piers and decks (displacements, rotations and deformations)
- Deck and stays temperatures
- Air temperature, relative humidity and wind speed
- Seismic and wind induced accelerations in the deck and piers
- Forces in stays

Infrastructure Measurements

- Pile head displacements
- Horizontal displacements along the piles
- Strain distribution of the piles
- Distribution of the accelerations

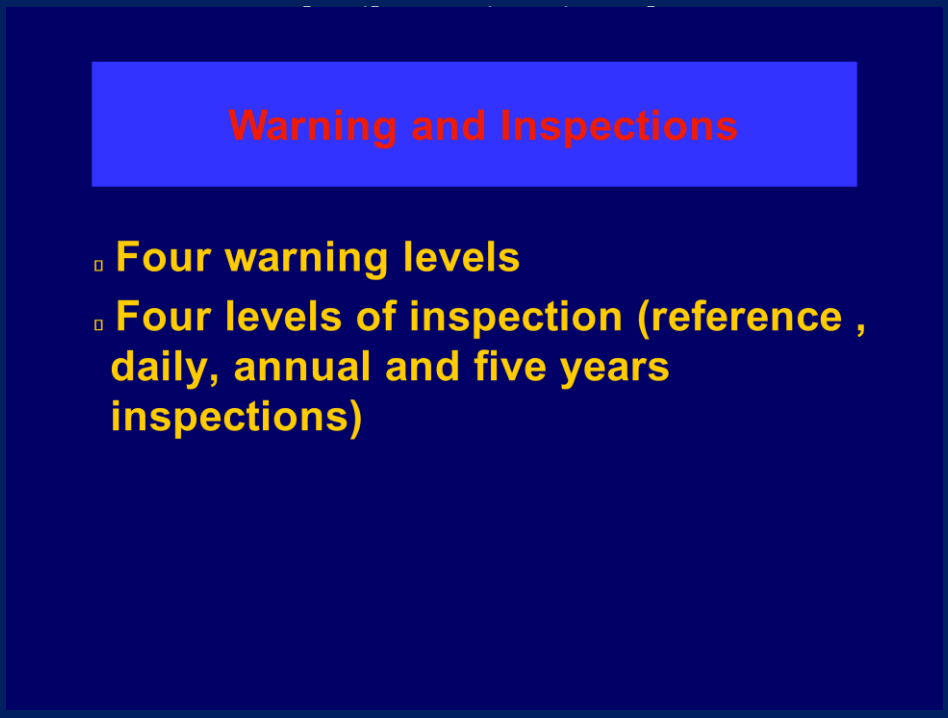

More details are given in Volume 5.

Lesson nº 23 -the axial compressive resistance of a single pile at the ultimate limit state may be teed from the results of static load, dynamic impact, or rapid load tests. The axial tensile resistance of a single p at the ultimate limit state may be determined from the results of static load tests

The settlement and transverse displacement of a piled foundation shall be determined from the results of load tests; based on the observed performance of comparable single piles or pile groups

Pile design should be validated using site-specific static load testing to confirm design parameter values, verify compressive or tensile resistance, and establish behaviour under serviceability limit state conditions.

Note: I was the co-ordinator of the geotechnical studies for the bridge design for COBA and the bridge was designed and constructed by the Consortium headed by Campenon Benard and Trafalgar House and integrating portuguese companies Teixeira Duarte, Somague, Mota-Engil.

8.7.3. Case History nº 24 - Leziria Tagus River Crossing (Portugal)

8.7.3.1 Introduction

The crossing integrates the North Viaduct, the Main Bridge and the South Viaduct.

The river, 1 km wide, runs in an alluvial plain corresponding to the Tagus valley, filled with soft sediments.

The 1695 m North Viaduct has 33 m spans. The deck is a concrete 2.0 m depth beam directed connected to 1.5 m diameter piers. There is a 62 m span to cross the railway.
The deck is 23 m above the water level.

The cross-section of the Main Bridge is composed by 3 traffic lanes, each with 3.50 m with a total width of 10.50 m
The total width of the platform is 29.95 m.

The foundations are composed by 2.20 m diameter piles. The piles were built by metallic casings 17 mm thick driven to the Miocene formations between 1m and 5.5 m depending of the gravel materials thickness.

The South Viaduct integrates a set of 22 continuous viaducts with a total length of 9230 m with a concrete deck longitudinal prestressed with current spans of 36 m and 1.5 m of diameter piles.

The geological and geotechnical characteristics are described, the seismic analysis is introduced, the liquefaction assessment is addressed, the piles tests are referred, the construction issues are described and the casing deteriorations are presented.

8.7.3.2 Geological Studies

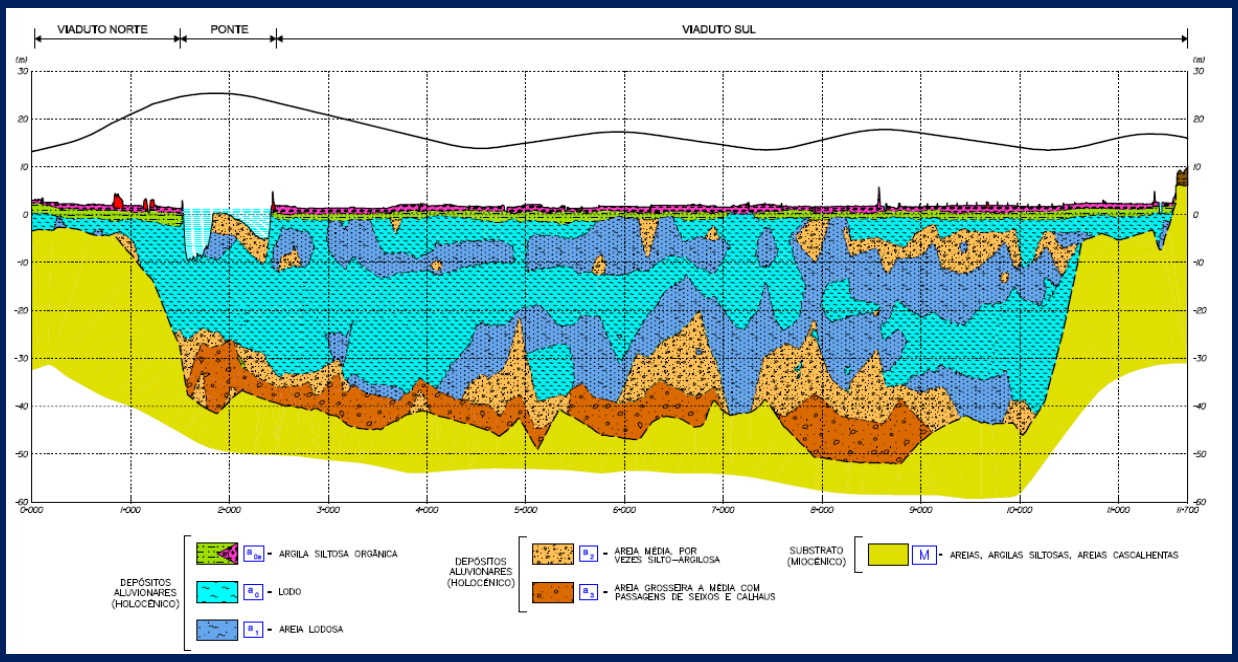

Figure 8.399 Simplified geological profile

Figure 8.399 illustrates the simplified geological profile.

8.7.3.3. Geotechnical Characteristics

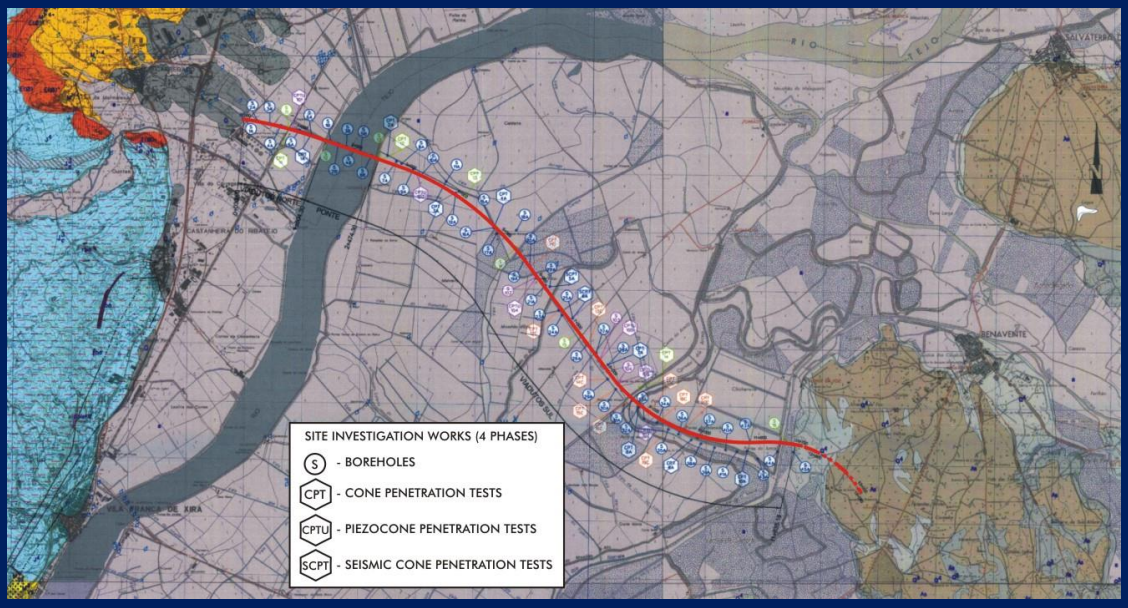

Figure 8.400 Leziria Tagus River Crossing site

Figure 8.400 shows the localization of the boreholes and other field tests of the Leziria Tagus River Crossing.

The distribution of field tests and laboratory tests by the 2 phases, namely Basis of Design and Execution Design is presented in Table 8.52 and Table 8.53.

Table 8.52 Distribution of field tests

TESTS	Base Design	Execution Design	TOTAL
BOREHOLES	58	60	118
BOREHOLES UNDISTURBED SAMPLING	0	3	3
VANE SHEAR TESTS	19	7	26
CROSSHOLE	9	6	15
CPTu/CPT	28	23 CPTu	51
SEISMIC CONE	2	4	6

Table 8.53 Distribution of laboratory tests

TESTS	Base Design	Execution Design	TOTAL
IDENTIFICATION	55	180	235
SIEVE CURVES	55	180	235
OEDOMETRE	4	18	22
TRIAXIAL	0	6	6
DIRECT SHEAR	6	13	19
PERMEABILITY	6	18	24
CHEMICAL	3	9	12
RESONANT COLUMN	0	3	3
TORSIONAL SHEAR CYCLIC	0	3	3
PARTICLE DENSITY	3	22	25

Due to the length of the bridge of 12 Km, 17 geotechnical profiles were analyzed to incorporate the variation of the geological and geotechnical characteristics.

8.7.3.4 Seismic Analysis

The Portuguese territory is affected by two seismotectonic sources: (i) near source which represents a moderate magnitude earthquake at a short focal distance with a duration of 10 seconds (action type 1); (ii) far source which represents a higher magnitude earthquake at a longer focal distance with a duration of 30 seconds (action type 2).

For the deterministic approach five artificial time histories of acceleration were produced for seismic action type 1 and seismic action type 2 and for soil type A.

For the computation of these accelerograms the validation criteria of EN (1998a) were considered.

For the stochastic approach power spectral density functions based on RSA (1983) were used.

Figure 8. 401 shows the response spectra versus code spectra.

Figure 8. 402 illustrates the response spectra acceleration km 1+500 – km 1+800 for action type 1 and action type 2.

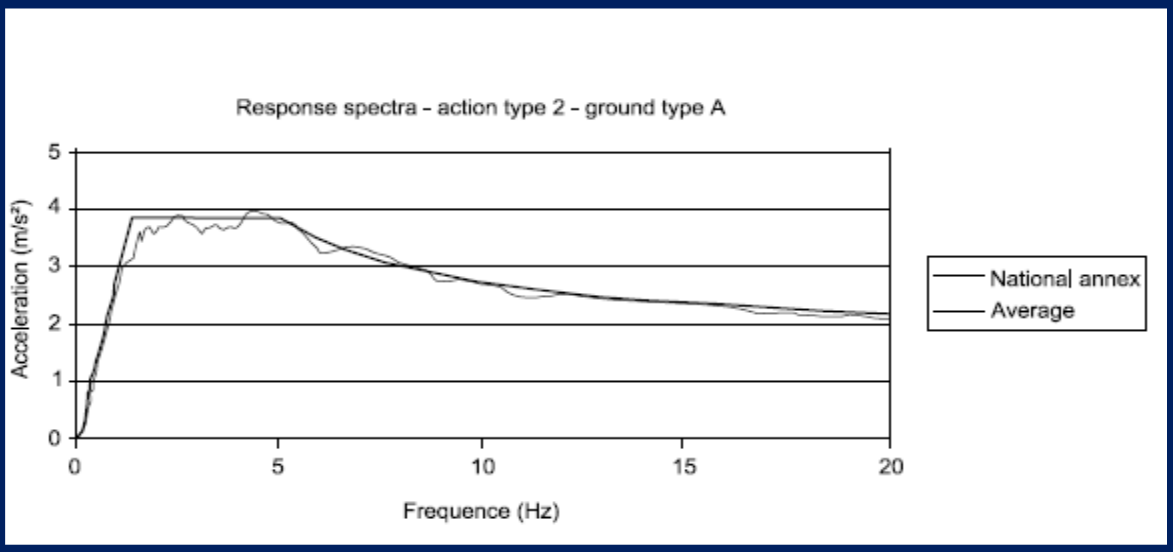

Figure 8. 401 Response spectra versus code spectra

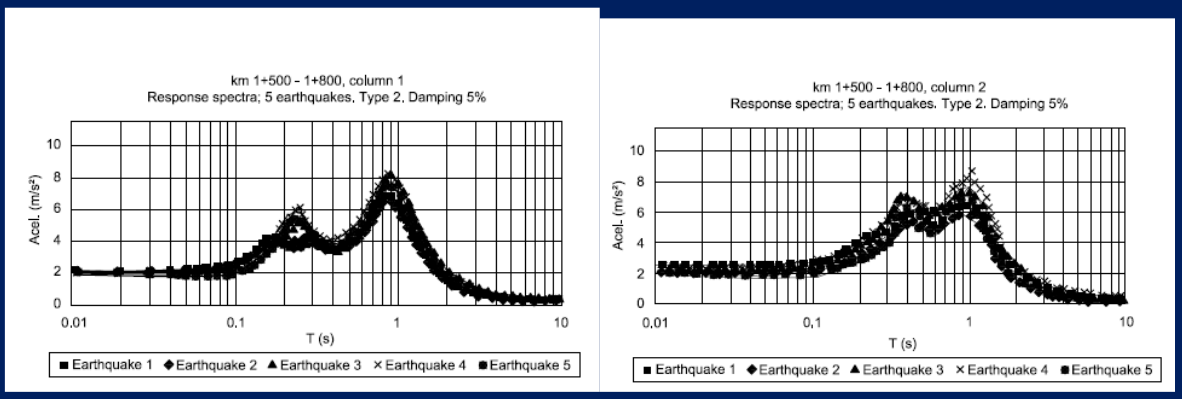

Figure 8. 402 Response spectra acceleration km 1+500 – km 1+800 action type 1 and action type 2

8.7.3.5 Liquefaction Potential Evaluation

Table 8.54 Evaluation of liquefaction potential material a_1 and material a_2

(1)	(2)	(3)	(4)	(5)	(6)	(7)	(8)	(9)	(10)	(11)	(12)	(13)	(14)	(15)	(16)
Pier	No Bore hole/ CPT	Depth (m)	Thickness (m)	N_m	$(q_c)_m$ (MPa)	σ'_o (kPa)	C_N	N_1 (60)	$(q_c)_1$ (MPa)	$\tau_{equiv.}$ (kPa)	τ/σ'_o	τ/σ'_ox 1,1	τ/σ'_o x 1,25	Mat.	Remarks

	S1B	16.8 - 25.1	8.3	44	-	139.1	0.8	37	-	39	0.29	0.36	A2	N.L
	S2B-2	24.3 - 31.3	7.0	23	-	215.4	0.7	16	-	55	0.26	0.32	A2	.L
"	S3B-1	0.0-4.2	4.2	3	0.5	33.9	1.0	3	0.5	7.6	0.22	0.28	A2	.L
"	S3B-2	4.2-7.4	3.2	6	0.52	66.4	1.2	7	0.6	19.2	0.29	0.36	A1	L
"	S3B-3	7.4-9.6	2.2	12	0.65	89.4	1.1	13	0.71	26.3	0.29	0.37	A1	L
"	S3B-4	24.6 - 27.6	3.0	26	-	200.2	0.7	18	-	52.0	0.26	0.32	A2	L
"	S4B-1	0.0-3.6	3.6	4	0.5	31.2	1.0	4	0.5	6.6	0.21	0.26	A2	L
	S4B-2	3.6-6.2	2.6	3	0.52	58.5	1.0	3	0.52	16.5	0.28	0.35	A2	L
	S5B-1	0.0-4.5	4.5	3	0.5	20.3	1.0	3	0.5	8.3	0.41	0.51	A2	L
	S5B-2	26.0 - 28.8	2.8	31	-	191.1	0.7	22	-	55.1	0.29	0.36	A2	NL
	S6B-1	0-5.4	5.4	2	0.5	24.3	1.0	2	0.5	9.7	0.40	0.50	A2	L
	S6B-2	24.1 - 25.0	0.9	5	-	164.2	0.8	4	-	48.7	0.30	0.37	A2	L
	S6B-3	25.0 - 29.2	4.2	17	-	188.1	0.7	12	-	54.4	0.29	0.36	A2	L

N_m - SPT value

N_1 (60) - Normalized SPT value

$(q_c)_m$ - CPT cone resistance value

$(q_c)_1$ - Normalized CPT cone resistance value

σ'_0 - Effective overburden pressure

$\tau_{equiv.}$ - Equivalent cyclic shear stress

C_N - Correction factor for overburden pressure

L - Liquefaction

N.L - No Liquefaction

Figure 8. 403 presents the liquefaction potential evaluation by SPT tests and CPT tests.

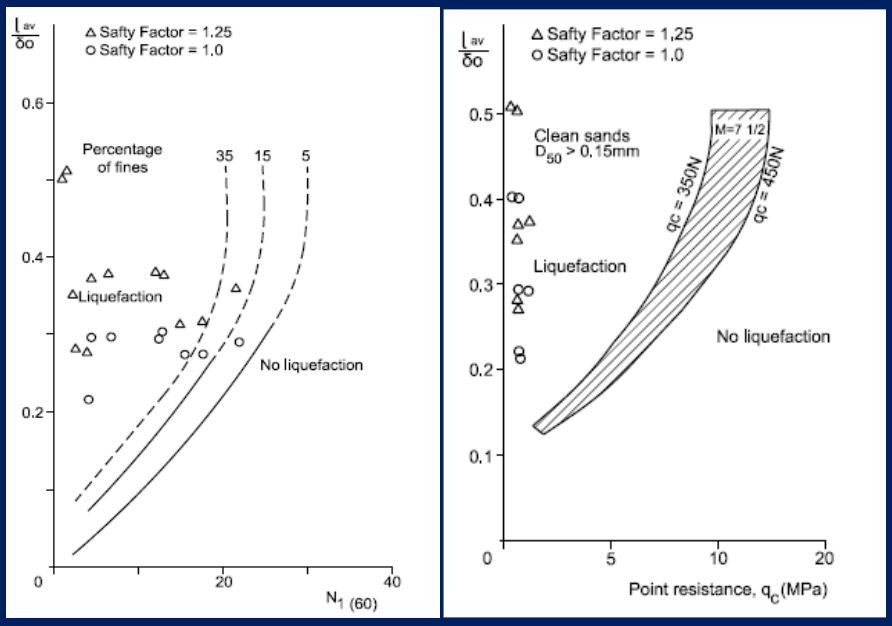

Figure 8. 403 Liquefaction potential evaluation
by SPT tests and CPT tests

8.7.3.6 Pile Testing

Figure 8.404 shows the general view for vertical pile load tests.

Figure 8.405 presents the results of horizontal pile load tests.

Figure 8. 406 illustrates the equipment used for dynamic pile test.

Figure 8.404 General view for vertical pile load tests

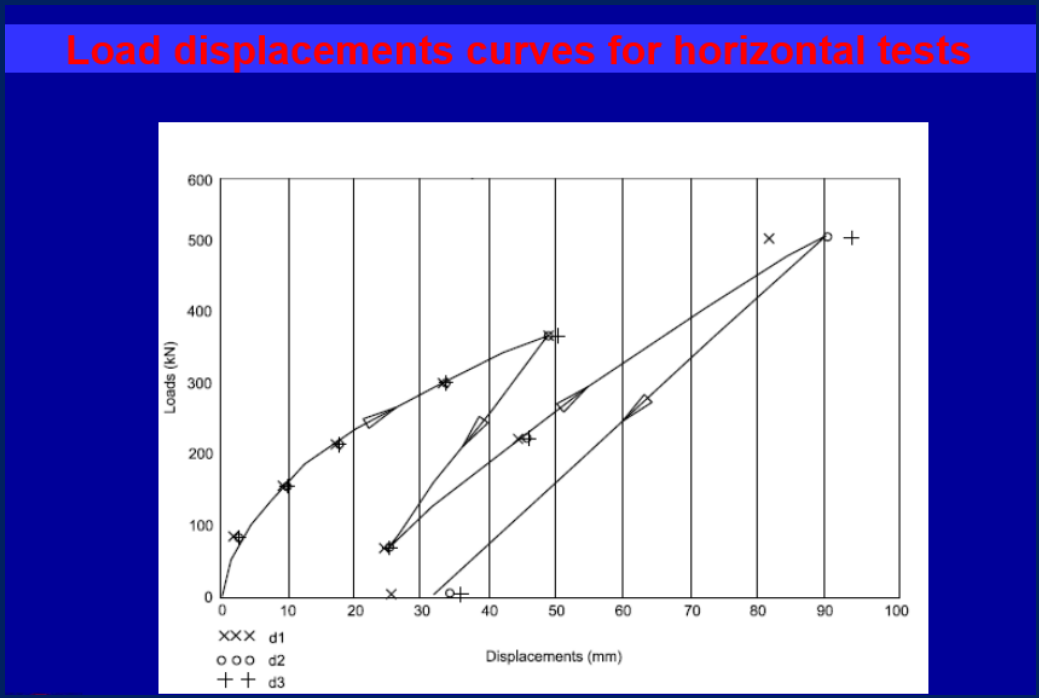

Figure 8. 405 Horizontal pile load test

Figure 8. 406 Dynamic pile test

8.7.3.7 Construction Issues

Details about the construction of South Viaduct and North Viaduct are presented in Figure 8.407 and Figure 8. 408.

Figure 8. 407 A view of South Viaduct construction

Figure 8. 408 Construction of North Viaduct

8.7.3.8 Casing Deteriorations

From the visual inspections of the metallic casings that were performed by the divers the following occurrences were recorded: (i) casings without deteriorations; (ii) light ovalization at the bottom; (iii) conic deformations at the bottom without the possibility to perform additional excavation; iv) collapse of the casing.

General speaking the deteriorations have occurred in an extension of 2 to 4 m, situated at depths between 35.3 m and 42 m, with the exception of casing P1-8 that have exhibited deteriorations in an extension of 16 m, between depths of 22.5 m and 38.4 m.
Figure 8. 409 illustrates the type of observed deteriorations.

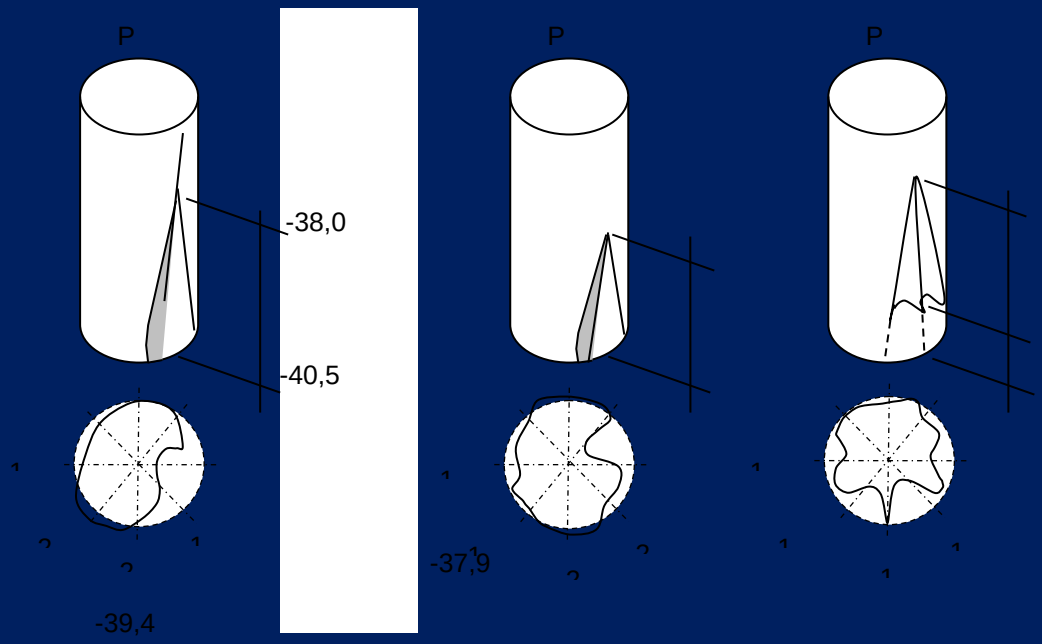

Figure 8. 409 Type of observed deteriorations

Lesson nº 24

Gravel and cobbles dimensions
Unit a_2 is composed by fine sandy materials with intercalations of silty clay material with gravel material

(ii) Unit a_3 is composed by medium sandy materials with intercalations of silty clay material with gravel material with thickness varying from 3.3m to 14.10m and SPT values between 32 to 52 blows and penetration from 11 to 29 cm for 60 blows; (iii) Unit M3 is composed by sands with intercalations of gravel materials; (iv) Unit M4 is composed by sands with intercalations of gravel materials with sand silty.

The dimensions of gravel materials are between 4.75 mm and 75 mm following the classifications of ASTM-D2487, ASTM –D653 and USCS and from 2 mm to 60 mm following the classification of LNEC E 219-1968, MIT and BS 5930:1981.

The cobbles have a size between 75mm and 300 mm following the classifications proposed by USBR (1974), US Army Engineer (1960), USCS and ASTM D 653 and from 60 mm to 300mm following the classifications of BS 5930:1981 and MIT.

In summary: Following the Geotechnical Report, it was expected the occurrence of gravel materials with dimensions between of 2 mm and 75 mm and cobbles with dimensions between 60 mm e 300mm.

The SPT values of a_3 materials between 45-60 blows are equivalent to BPT values between 60 to 80.

ORDS ORIVEABILITY OF METALLIC CASINGS

The records of driveability of metallic casings have giving the following information: (i) level of penetration: (ii) number of blows to penetrate 25 cm; (iii) energy by blow; (iv) penetration by blow; (v) time for penetration; (vi) level of top and bottom of casing; (vii) method of excavation and type of material.

- Unfortunately, the records presented by Ballast Nedam have not given the following information: (i) height of hammer fall; (ii) frequency; (iii) control of pile verticality; (iv) comparison between the driven logs of the casings and the borehole logs.

Note: The revision of the Leziria bridge project was performed for the Consortium TACE.

8.8 Retaining Walls

8.8.1 Case History nº 25 - Leixões Terminal

8.8.1.1 Introduction

The geological characteristics are addressed, the geotechnical characterization is presented, the Geological and geotechnical zoning is described, the design situations are introduced, the stability analysis is discussed, the seismic action is referred, the stress-strain analyses are presented, the construction issues are addressed and the instrumentation is introduced.

8.8.1.2 Geological Characteristics

The following geological units were considered:

-Fills with thickness of 2.0 m with sands and clay materials;

-Mud clay occasionally with sand bands and lenses, dark grey with thickness of 3.0 m to 13.5 m;

Yellowish brown to grey medium to coarse (occasionally fine) sand, with fine to coarse gravel (rounded to angular). Sometimes with shells and shell fragments, with thickness between 7.5 m to 24.0 m;

-Pleistocene – Red sands (P)
Clays with sand component and gravel materials with thickness between 3 m and 5.5 m.

Miocene (M)

Sands beneath the yellow and grey yellow clays.
Silts with clay materials and with sands.

8.8.1.3 Geotechnical Characterization

Field Tests

The geotechnical characterization of the Leixões Principal Entrance port has included 3 campaigns, namely:
- the first and second campaigns with 9 boreholes;
-Opening of 4 holes;
-Site investigation of the site where the retaining walls and special structures were located with 6 boreholes, 4 CPTU tests, 4 vane shear tests, the 3rd campaign with 4 boreholes and depths between 28.5 m and 33.0 m, 7 CPTU tests and 12 seismic refraction tests.

With the continuous sampling the values of RQD and percentage of recuperation were determined.

In the boreholes SPT tests 1.5 m apart were performed. In addition, the water level was measured.

Also 7 trenches were open for visual inspection of the material.

Laboratory Tests

The mud samples taken in boreholes VSL2 (3,90-4.50) and S3C (4.20-4.80) were used for oedometer tests and density tests.

8.8.1.4 Geological and geotechnical zoning

HG_1 – is composed by alluvial materials, with low compacity and fills with SPT values lower than 10 blows, unit weight 16 to 18 kN/m3, friction angle between 28-32º and elasticity modulus less than 20 MPa.

HG2 – is composed by alluvial materials, with medium compacity with SPT values between 10 to 30 blows, unit weight 18 to 19 kN/m3, friction angle between 32-35º and elasticity modulus between 40 to 80 MPa.

HG3 – is composed by loose materials, with medium compacity with SPT values between 30 to 50 blows, unit weight 19 to 20 kN/m3, friction angle between 35-38º and elasticity modulus between 80 to 150 MPa.

HG4 – is composed by weathered rock material W5 with SPT values higher than 60 blows, unit weight 20 to 21 kN/m3, friction angle between 40-42º e and elasticity modulus between 150 to 300 MPa.

HG5 – is composed by weathered rock material W4 with SPT values higher than 60 blows, unit weight 21 to 22 kN/m3, friction angle between 42-45º e and elasticity modulus between 300 to 500 MPa.

HG6 – is composed by rock material medium weathered W3-W2, with RQD values higher than 50%, unit weight 22 to 24 kN/m3, cohesion values higher than 100 kPa, friction angle between higher than 45 and elasticity modulus between 800 to 1500 MPa.

8.8.1.5 Design Situations

The following design situations were analysed:

- loss of global stability;
- failure due to insufficient resistance capacity;
- failure due to sliding;
- joint failure of ground and structure;
- structural failure due to foundation movement;
- excessive settlement;
- excessive swelling;
- excessive vibrations

The following actions were considered:

- soil, rock and water weights;
- in situ stress of the ground;
- free water pressures;
- ground water pressures;
- seepage forces;
- permanent loads of the structure and environmental effects;
- surcharges;
- ground excavation;
- load due to the traffic;
- displacements and accelerations due to the earthquakes, blasting, vibrations and dynamic forces;
- pre-stressed forces imposed in anchors and trusts.

8.8.1.6 Stability Analysis

i) The computed displacements values for M3 wall are 12 cm, compatible with the behavior of these type of structures and the geometry and foundations characteristics;

ii) The stability analysis for retaining wall M3 for the final situation, with ground improvement, gave a minimum safety factor of 1.383, this value is acceptable for the design situation;

v) For the pseudo-static analysis a minimum safety factor of 1.14 was computed.;

vi) The construction procedure, as well the quality control were defined.

The global equilibrium of the retaining wall and fill was analysed by the Coulomb method.

8.8.1.7 Seismic Action

Taking in to account the following factors:

i) uncertainties in data;

ii) local effects and attenuation laws;

iii) induced seismicity for earthquakes with low epicentral distance.

For the seismic analysis it was considered for the MCE a peak value of 0.15g and for OBE a value of 0.10g, taking into account that it is a low seismicity zone.

8.8.1.8 Stress-Strain Analysis

The stress and displacements of the reinforced fill were computed by the PLAXIS code, version 8.0.

The code uses triangular finite elements with 15 nodes and 12 points of Gauss.

The code incorporates the Mohr-Coulomb (MC) law, the hardening model (HM), the softening model and the softening model with creep.

The hardening model integrates the elastoplastic soil behavior, namely the cohesion, the friction angle, the elasticity modulus with loading, unloading and re-loading.

The construction phase is modelled by the code.

The initial stress state was modelled by the equations:

$$\sigma_z = \gamma_t h \quad (8.83)$$

$$\sigma_x = \sigma_z \upsilon / (1-\upsilon) \quad (8.84)$$

$$\tau_{xz} = 0.5\, \sigma_z \operatorname{sen}\beta \quad (8.85)$$

Where γ_t is the unit weight of the material, h is the height of the material between the center of the element and the layer surface, β is the angle between the superior face of the element and the horizontal.

The analyses in effective stresses have incorporated the theory of consolidation of Biot and the generation and dissipation of pore pressures.

Figure 8. 410 illustrates the mesh.

Figure 8.411 shows the deformed mesh.

Related phase 7:

Figure 8.412 and Figure 8.413 present a plot of horizontal and vertical displacements.

Figure 8.414 represents a plot of effective stress.

Figure 8.415 shows a plot of plastic points.

Related phase 9:

Figure 8.416 shows the deformed mesh.

Figure 8.417, Figure 8.418 and Figure 8.419 present a plot of total, horizontal and vertical displacements, respectively.

Figure 8.420 represents a plot of effective stress.

Figure 8.421 shows a plot of plastic points.

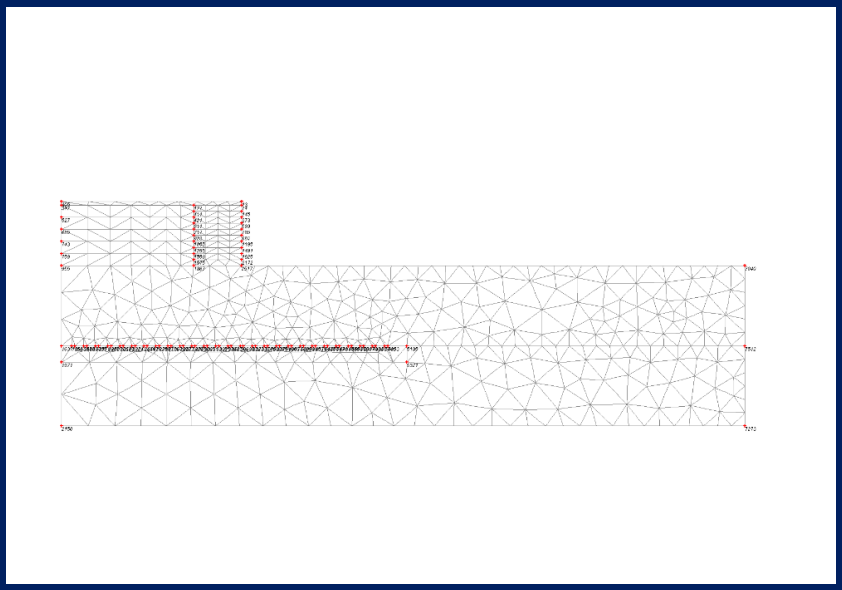

Figure 8. 410 F.E.M mesh

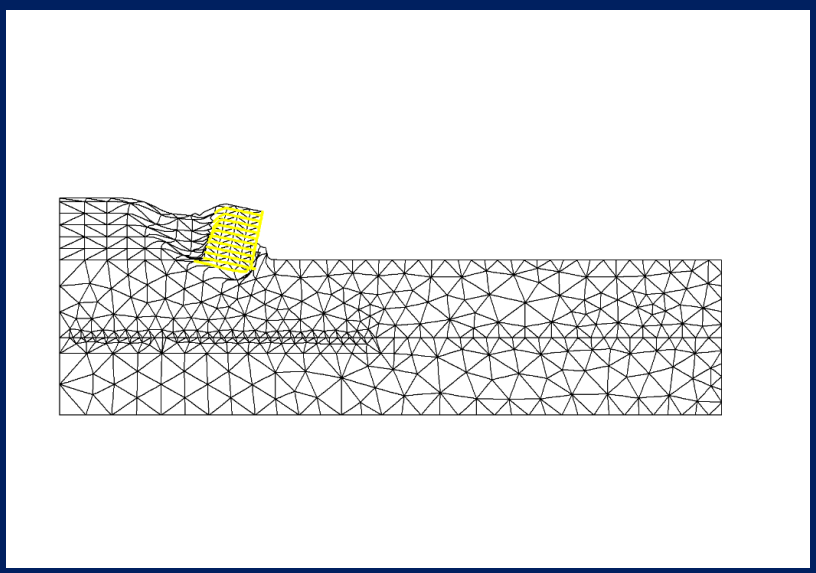

Figure 8. 411 Plot of deformed mesh
- step no: 165 - (phase: 7)

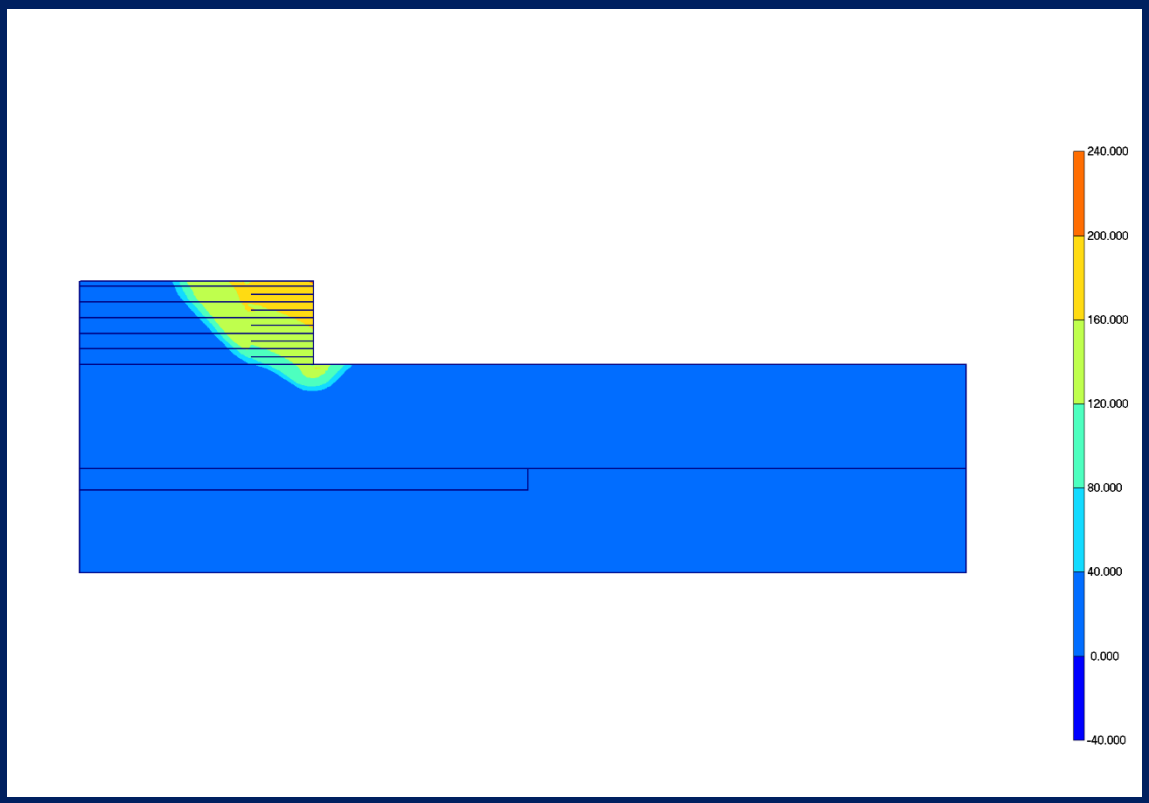

Figure 8. 412 Plot of horizontal displacements (shadings)
- step no: 165 - (phase: 7)

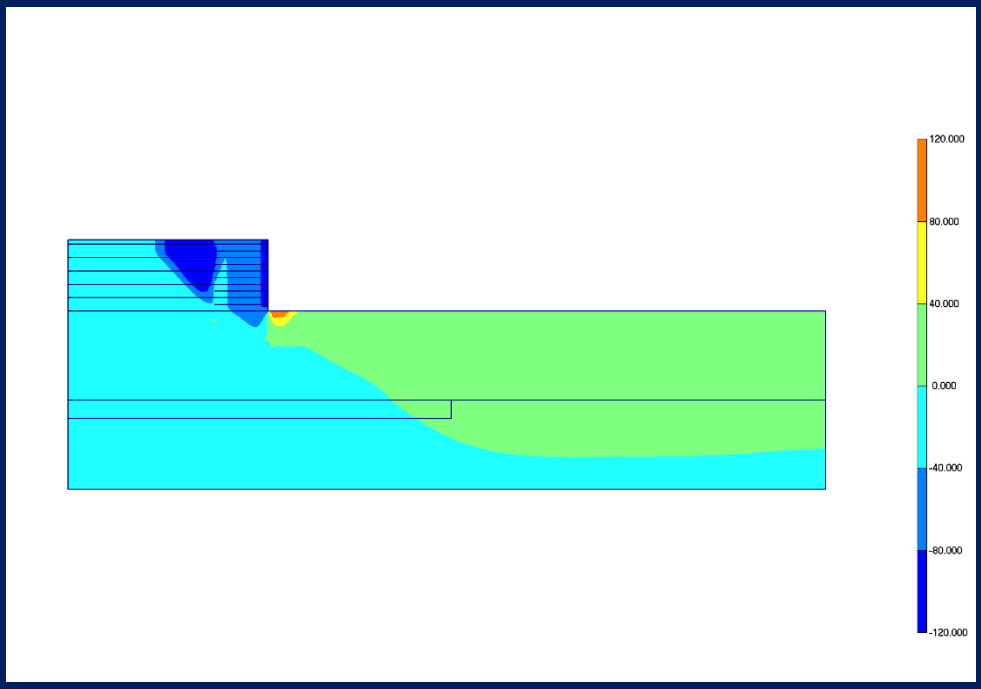

Figure 8. 413 Plot of vertical displacements (shadings)
- step no: 165 - (phase: 7)

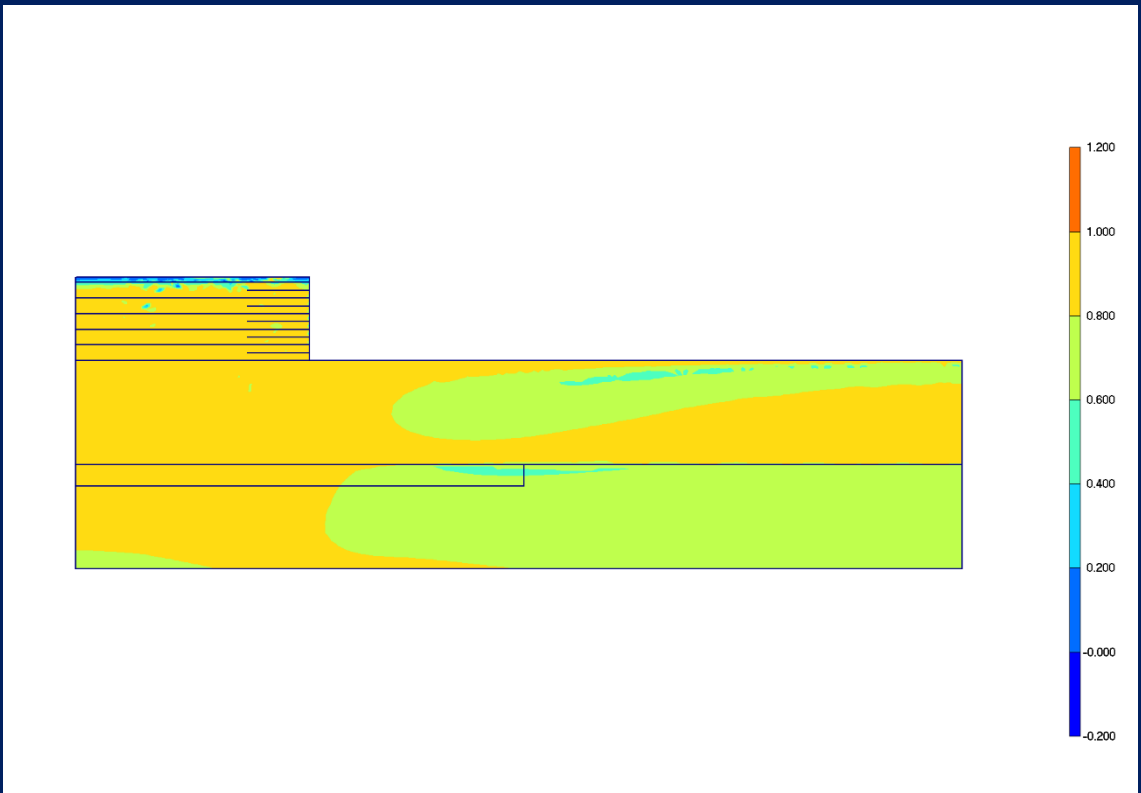

Figure 8. 414 Plot of effective stresses (relative shear shadings)
- step no: 165 - (phase: 7)

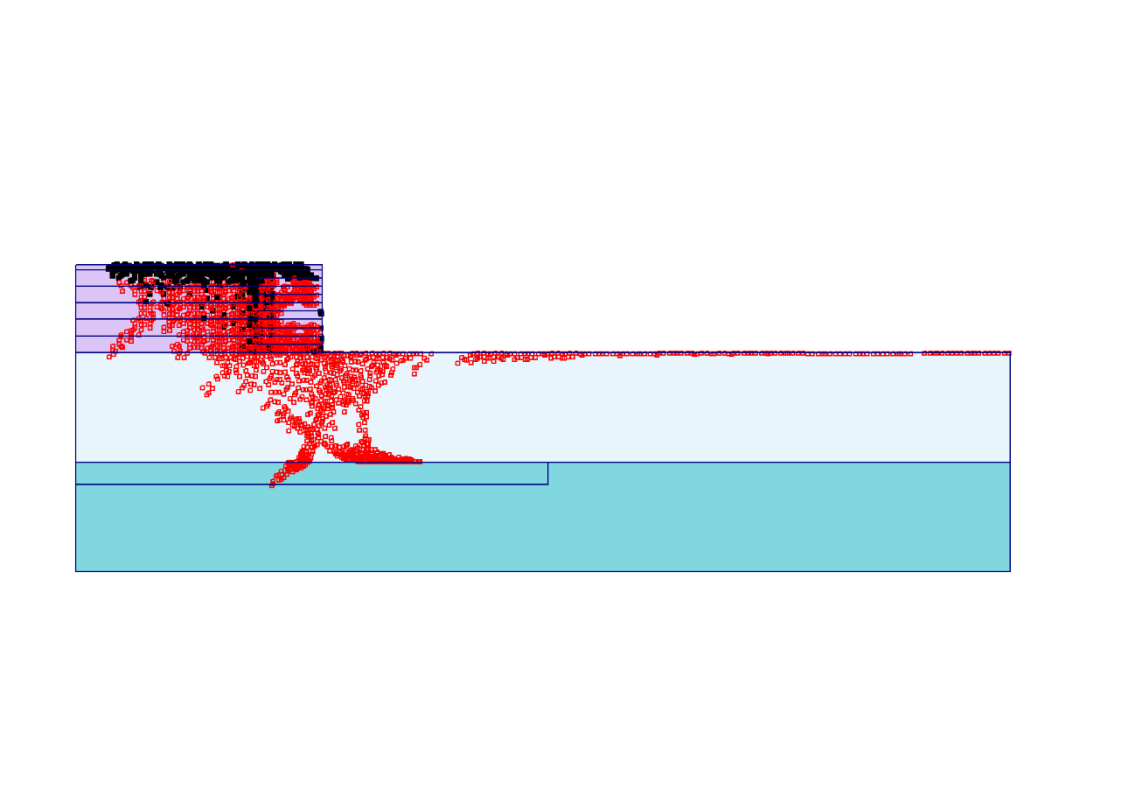

Figure 8. 415 Plot of plastic points
- step no: 165 - (phase: 7)

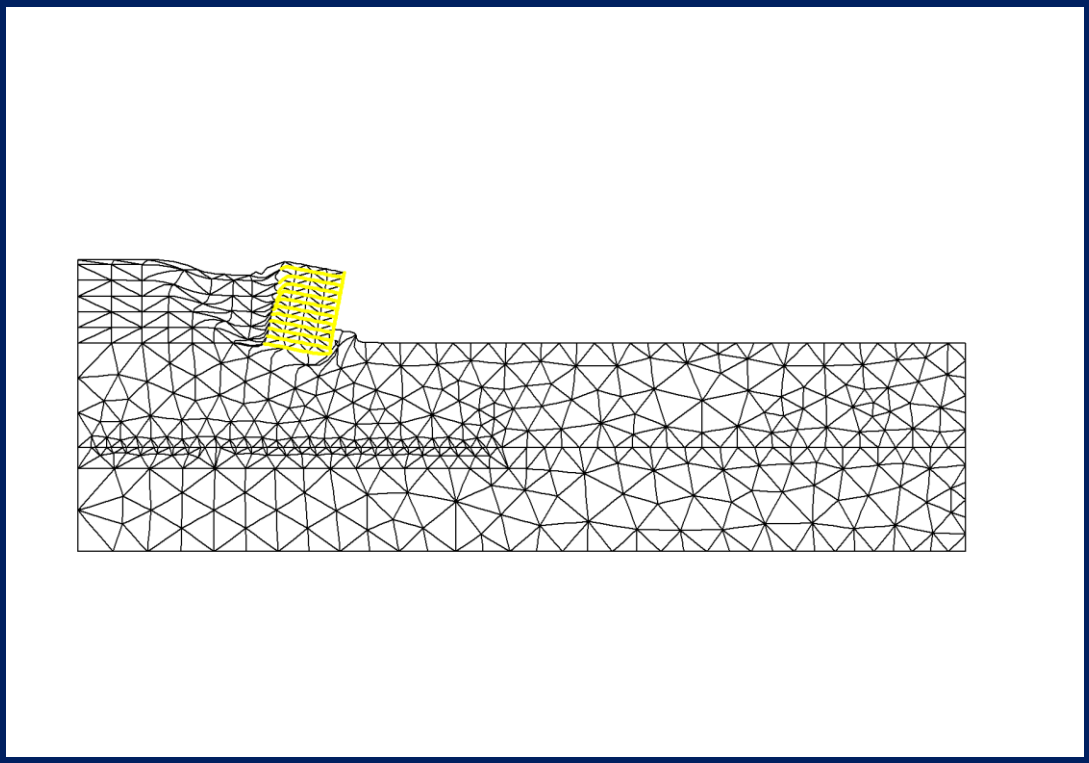

Figure 8. 416 Plot of deformed mesh
- step no: 302 - (phase: 9)

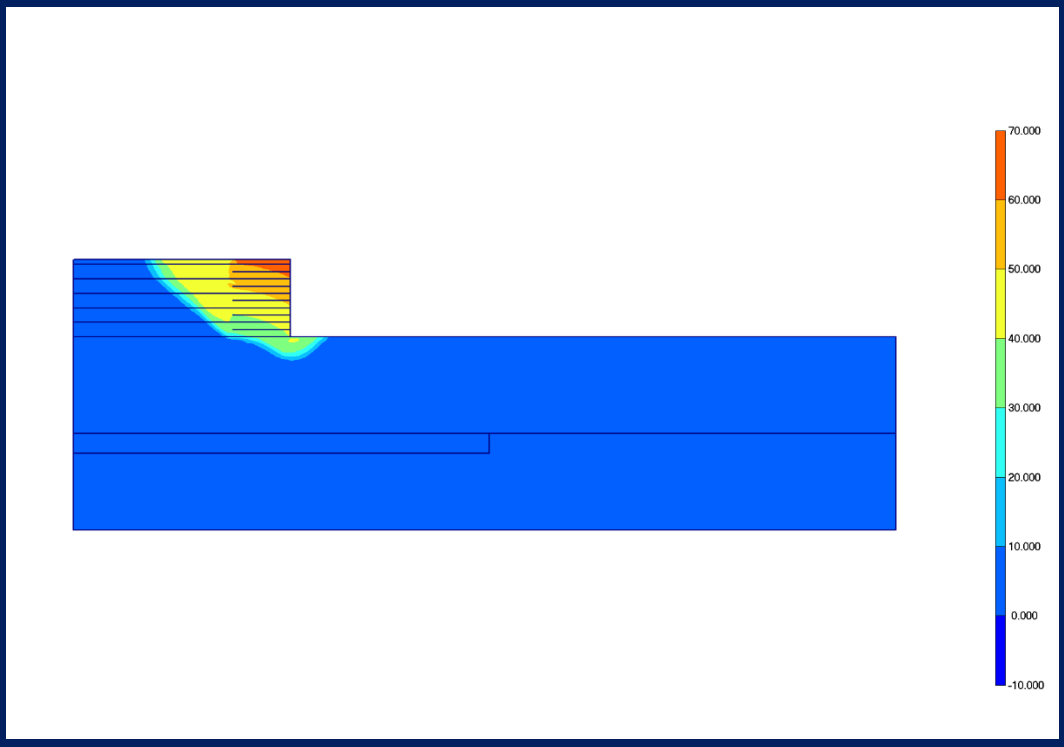

Figure 8. 417 Plot of total displacements (shadings)
- step no: 302 - (phase: 9)

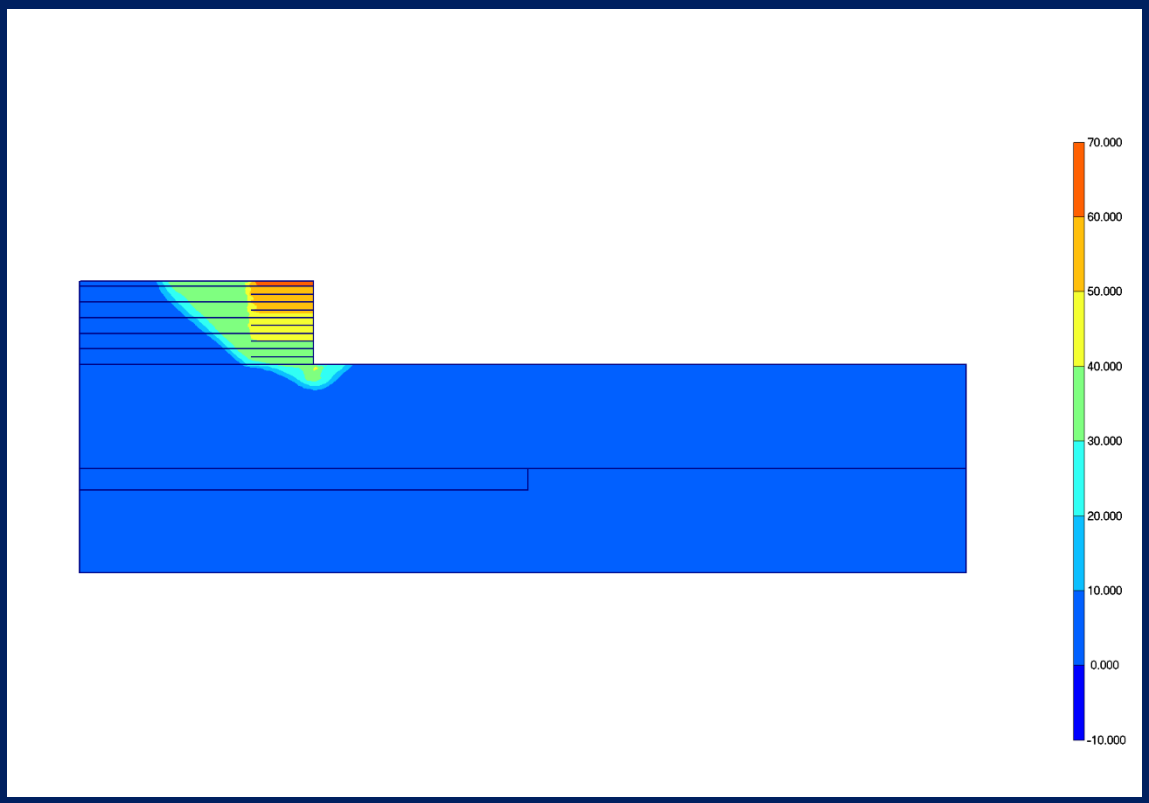

Figure 8. 418 Plot of horizontal displacements (shadings)
- step no: 302 - (phase: 9)

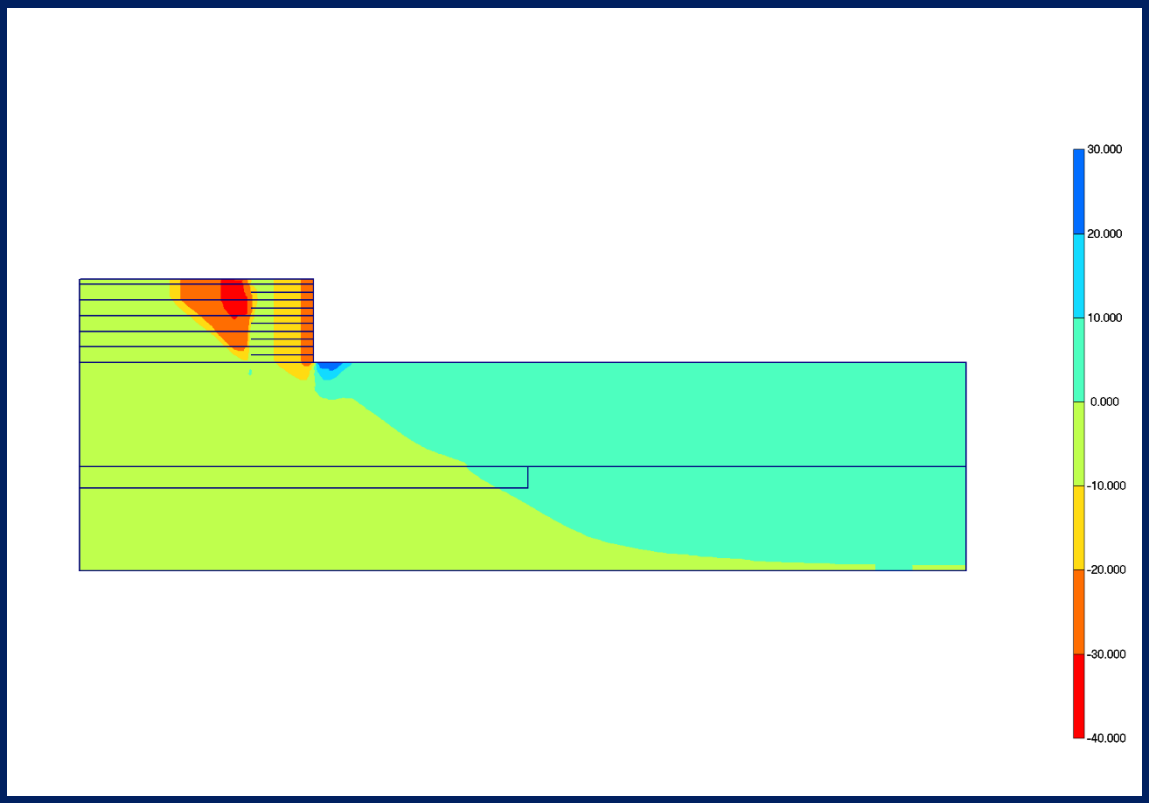

Figure 8. 419 Plot of vertical displacements (shadings)
- step no: 302 - (phase: 9)

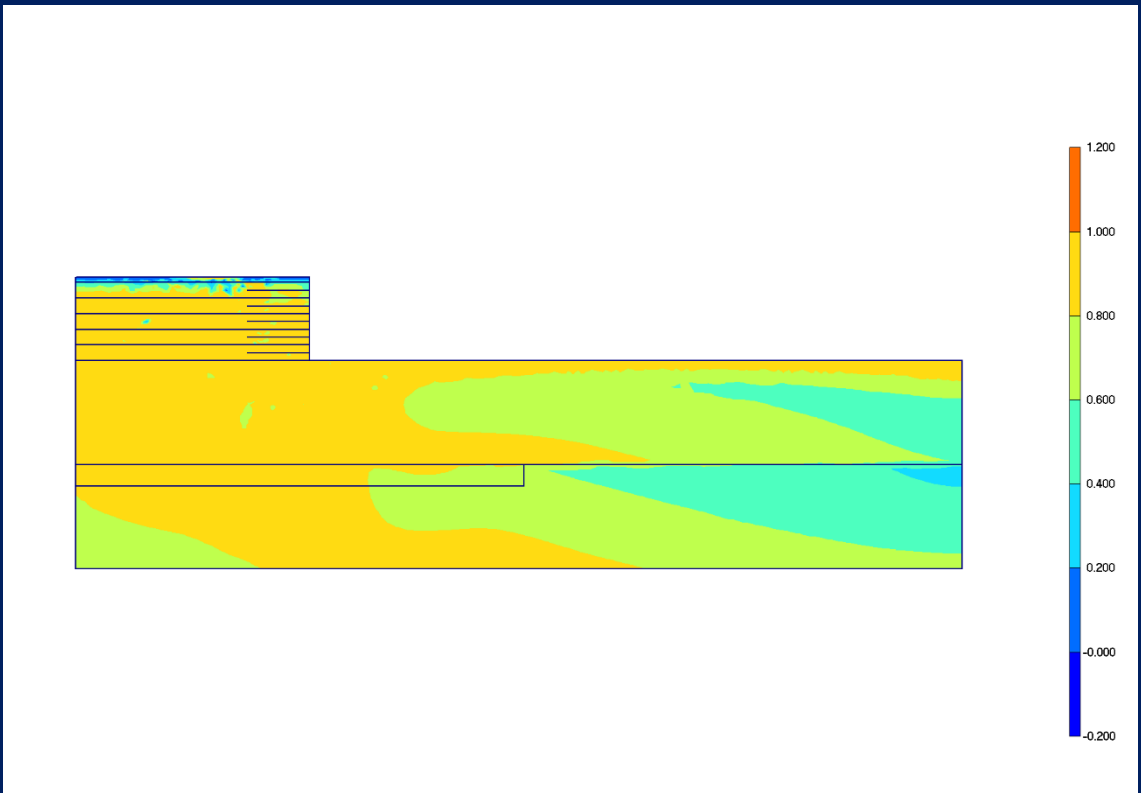

Figure 8. 420 Plot of effective stresses (relative shear shadings)
- step no: 302 - (phase: 9)

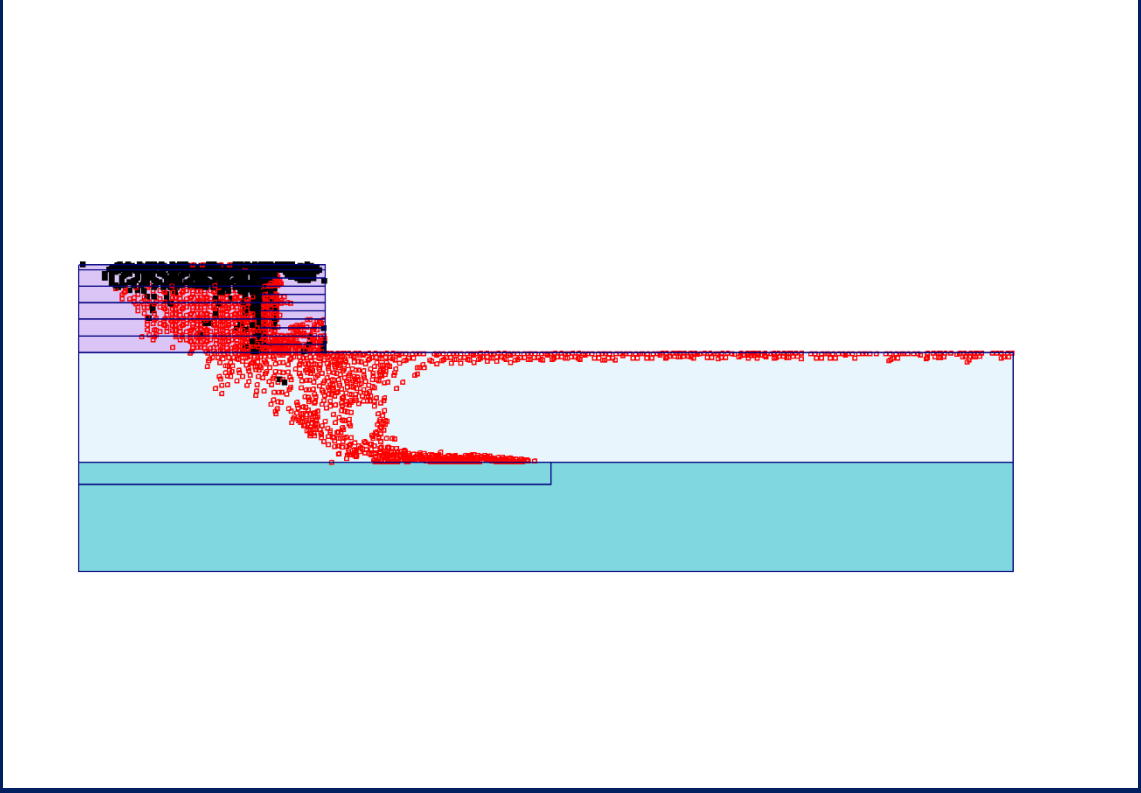

Figure 8. 421 Plot of plastic points
- step no: 302 - (phase: 9)

8.8.1.8 Construction Issues

The construction of the fills has followed the following steps:

a) Cleaning and placement of the superficial layer of 0.25 m thick;

b) Placement of 2 layers of geosynthetic to obtain a good connection with the foundation;

c) Construction of the fill by layers 0.3m thick;

d) The construction procedure should respect the Specifications.

8.8.1.9 Instrumentation

To follow the construction of the fill it was proposed the placement of 2 electric piezometers, 2 inclinometers and 10 bench marks.

It was recommended a frequency of readings weekly, during the construction phase, and more readings for the occurrence of rains.

Lesson nº 25 - There is a need of a permanent supervision during the construction phase of the wall, taking into account the uncertainties of the design parameters, the wall geometry, and the foundation characteristics. It is important a comparison between the predicted values of stress and displacements with the observed values, in order to implement, in due time, the corrective measures to assure the wall safety, if needed.

Note - The study of Leixões Terminal was performed for Somague.

8.9 Solid Waste Landfill-

8.9.1 Case History nº 26 - Grandola landfill (with Lopes, Lourdes; Agostinho Mendonça)

8.9.1.1 Introduction

The lay-out is described, the geotechnical profile of the foundation is presented, the stability analysis is addressed and the seismic analysis is introduced.

8.9.1.2 Lay-out

The Grândola landfill comprises a mixture of domestic trash, construction demolition debris and other wastes, has a maximum height of 12 m and an inclination of 2.5(H):1(V). The deck is at level 83.5m and the volume of landfill is 664 000 m3.

The cover system comprises a mineral barrier with 1.50 m of thickness and a topsoil material with 0.20 m. The bottom lining system consists of a drainage layer with 0.40 m of thickness, a geotextile (200g/m), a HDPE geomembrane (1.5 mm), another geotextile (200 g/m^2) and clay material with 0.10 m thickness.

Figure 8.422 illustrates the lay-out of the Grandola landfill.

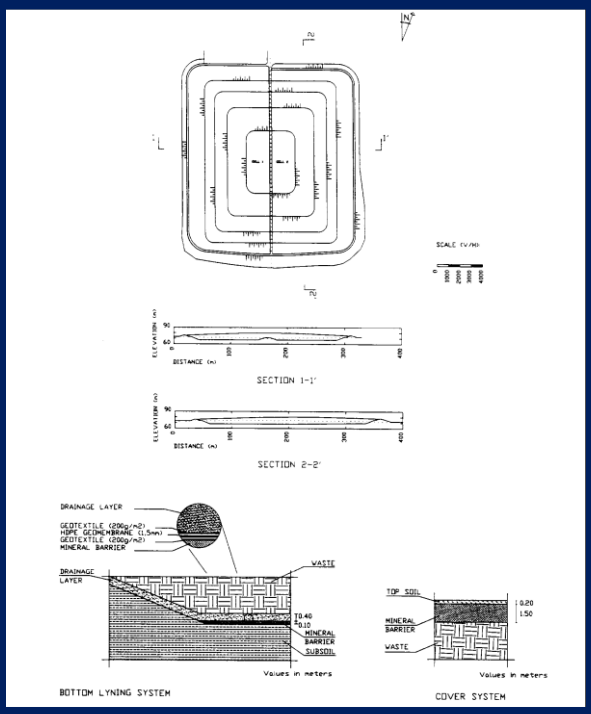

Figure 8. 422 Layout of the Grandola the landfill

8.9.1.3 Geotechnical profile

Figure 8.423 shows the geotechnical profile of the foundation.

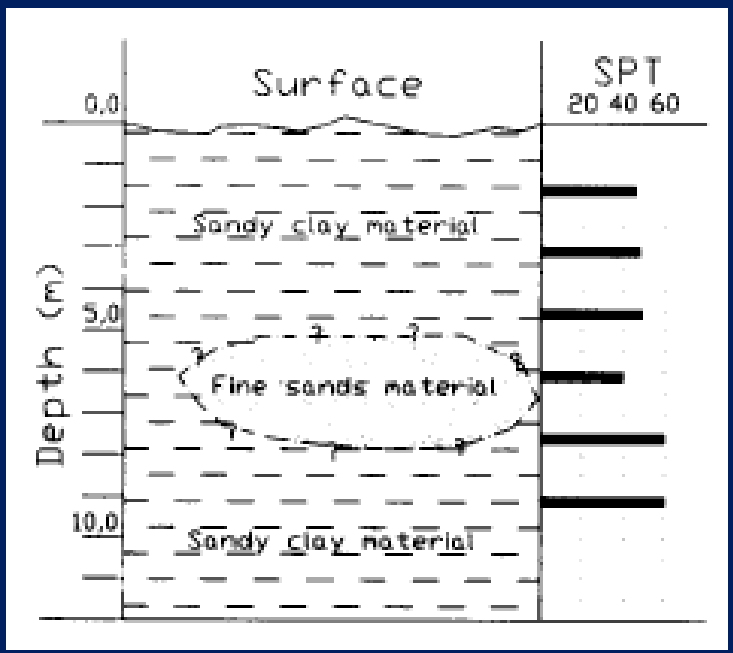

Figure 8. 423 Geotechnical profile of the foundation

The particle size distribution of Grândola landfill wastes and the particle size distribution of municipal solid wastes are presented in Figure 8.424.

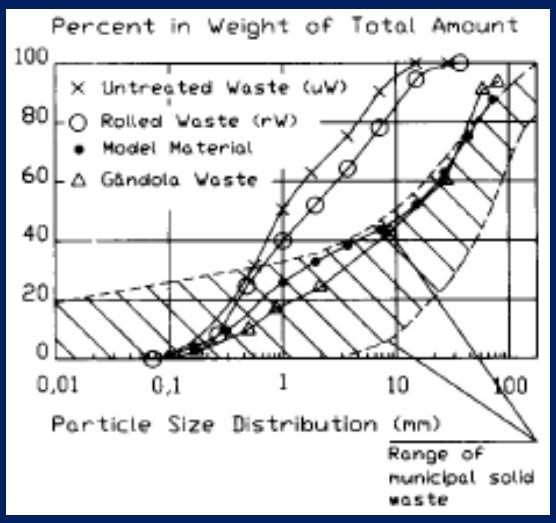

Figure 8. 424 Particle size distribution of waste

The shear wave velocities of Grândola solid wastes is illustrated in Figure 8.418.

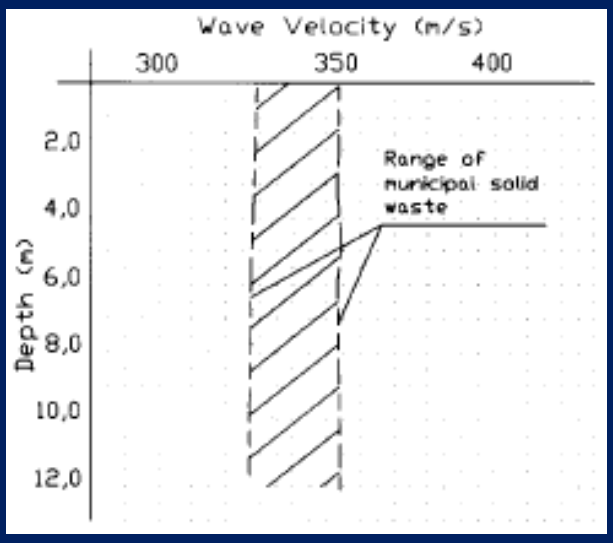

Figure 8. 425 Shear wave velocities of Grândola solid wastes

8.9.1.4 Stability Analysis

The slope stability of the waste landfill was evaluated by limit equilibrium slope stabilility analyses.

A computer code was used and the minimum static safety factor for circular surface was 2.6.

For the pseudo-static analysis, the minimum computed safety factor for circular surfaces was 1.9.

8.9.1.5 Seismic Analysis

For the Makdisi-Seed method (1977) and for the Sarma (1975) method the computed permanent displacements were lower than 10 mm.

The computed displacements values are in good agreement with the back analyses performed to analyse the solid waste landfill performance during the earhquakes and show that the Makdisi - Seed and Sarma simplified procedures for predicting permanent displacements appear to be appropriate for evaluating the seismic performance of solid waste landfills.

The seismic response was also obtained by a computer finite element program.
Input motions were incorporated by base horizontal and vertical acceleration power spectra. These can be obtained by direct records of seismic motions by response spectra or by trilogaritme diagram.
This analysis is based on the solution of the equation of motion considering a homogenous and continuous soil deposit composed by horizontal soil layers and assuming a vertical propagation of shear waves.

Figure 8. 426 represents the shear stresses distribution and Figure 8. 427 illustrates the acceleration distribution.

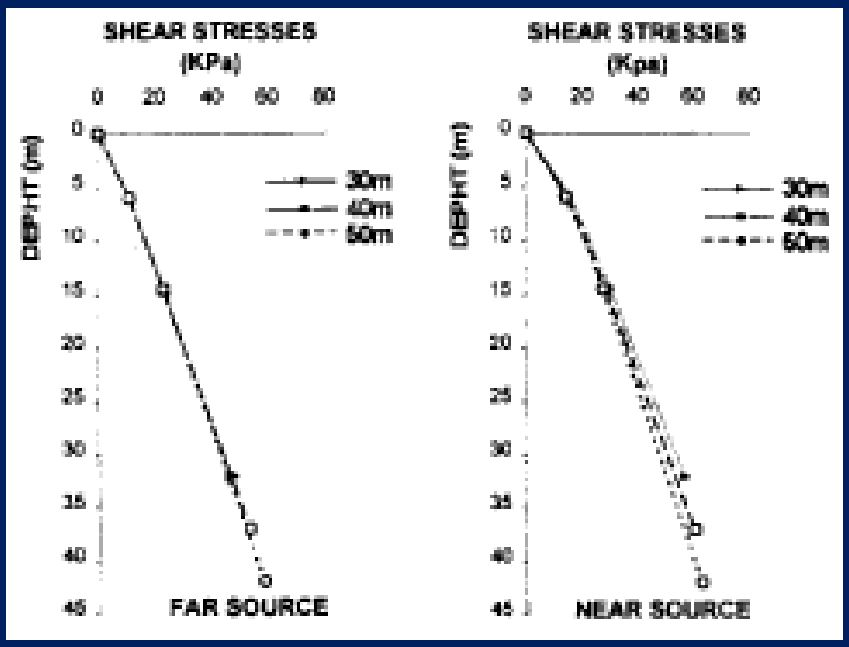

Figure 8. 426 Shear stresses distribution

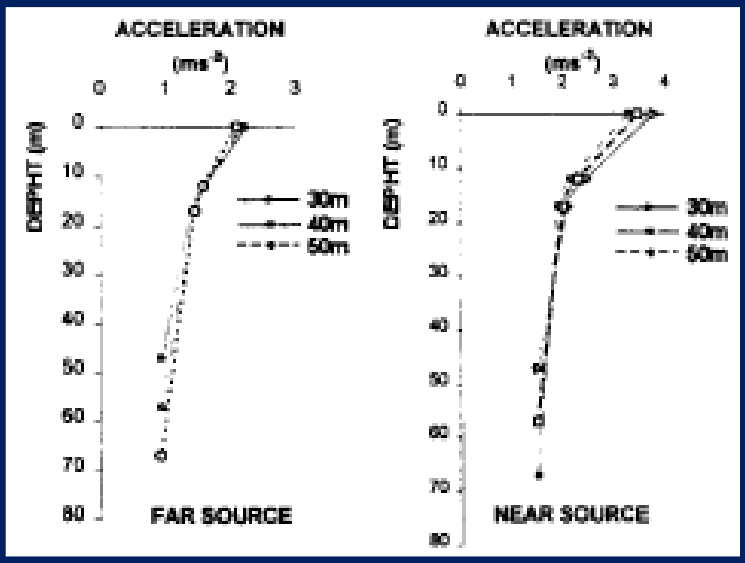

Figure 8. 427 Acceleration distribution

Lesson nº 26 - The principles of seismic design of solid waste landfill are similar to those used in the design of embankment dams. Both pseudo-static and deformational analysis methods are used. However, the major difference is that the geosynthetic elements used to cover systems and bottom lining systems are relatively less tolerant to the seismic induced permanent displacements.

It is important to stress that the shear wave velocities play an important role on the amplification effects.

Dynamic analyses of solid waste landfill use total stress and treat nonlinear behaviour by iterative linear elastic procedure.

As they can not provide information on permanent displacements and deformations strong interest has developed in nonlinear effective stress methods. For their calibration centrifuge models can be useful.

Full scale natural and man-made vibration tests accompanied by appropriate geophysical measurements can provide vital information regarding key material properties and soil dynamic characteristics of waste landfills materials.

The lessons learned from waste landfills behaviour during the occurrence of earthquakes have shown that they can withstand moderate shaking with peak accelerations up to at least 0.2 g with no harmful effects.

8.10 HIGHWAYS

8.10.1 Case History nº 27 – Highway - Evora- Estremoz branch

8.10.1.1 Introduction

The branch of the highway between Evora-Estremoz has a transverse profile with two sections of 7.5 m width, two passes of 3.75 m in each direction, a central separator with 9 m width, two left berms with 1m and two right berms of 3.5 m.

The geotechnical characterization is described and the granular base material is addressed.

8.10.1.2 Geotechnical Characterization

The geotechnical characterization has included two phases:

1. The first phase has covered a geological cartography;
2. The second phase has integrated a campaign with 103 seismic refraction profiles, 39 dynamic penetrometers, 140 trenches with depths between 0.4m and 4.0m, 106 boreholes with depths between 5.0 m and 29.9 m and 112 SPT tests 1.5 m apart.

For a longitudinal development of 29.5 Km the average spacemen of the boreholes of 280 m can be considered acceptable.

The rock samples have allowed the definition of the weathering, the fracturing and the RQD.

Based in the results of seismic refraction tests and the boreholes sampling two classes of material were identified, namely: i) category 1 – soils and rocks weathered with longitudinal waves velocities less than 2500 m/s and ii) category 2 with longitudinal waves velocities higher than 2500 m/s, classified as W3 to W2 and F3 to F2 and explored by blasting. The RQD values were around 80% and the percentage of recuperation between 90% - 100%.

Also, laboratory tests such as the identification tests (58 sieve analyses and 58 Atterberg limits), 28 Proctor tests, 21 CBR tests, 15 equivalent sand tests and 15 water content tests were performed in materials category 1.

Los Angeles tests performed in rock materials have given the following values: L.A.(F)=24% and L.A.(G) =30%.

8.10.1.3 Granular Base Material

The design has estimated a total volume of excavation of 4 300 000 m3 and has considered a volume of excavation of 530 000 m3 by blasting.

The branch Evora-Estremoz exhibits metamorphic rocks and also eruptive rocks.

The project has considered that the rock material exhibits adequate characteristics for the granular base material and so the pavement material should be explored by blasting the gneiss rocks that will generate more than 300 000 m3.

The Contractor for the blasting operation has used for the specific perforation an interval between 0.15 ml/m3 and 0.24 ml/m3 and also for the specific charge a value of gelamonite of 33% and a value of ammonite between 0.39 and 0.5 kg/m3 to obtain a good coefficient of fragmentation., following the recommendations from the experts.

The view of the rock material after blasting is shown in Figure 8.428 and Figure 8.429.
Details of the brittle central with a capacity of 300 ton/h is shown in Figure 8.430 and Figure 8.431.
Unfortunately, during the blasting works, the characterization of rock materials gave results of Los Angeles tests of 14 samples, taken from Brittle Central, between 33.9 and 48.1%, pointing a detrimental scenario in relation to the design studies.
The sand equivalent results were between 49-55 %.
The blue metile tests gave values between 0.7 and 0.9.
The index of elongation between 30, and water absorption values between 1.1 -1.9 %.
To clarify the situation a complementary geotechnical campaign was performed during the execution of the works with 8 boreholes, to assess the assumptions of the project, with depths between 8.4 m and 21.90 m.

The weathering between W3 to W4, the fracturing F3 to F4, the RQD values between 25% to 60% and the percentage of recuperation between 90% - 100% are indicated by the samples shown in Figure 8. 432 - Borehole nº 1 and Figure 8. 433 - Borehole nº 2.

The Los Angeles values performed in 16 samples between 38.2% and 62.3% have confirmed the detrimental scenario.

The additional superficial survey, and the complementary geotechnical campaign has shown that the estimated excavated volume by blasting in the project around 530 000 m3 is correct, but unfortunately only 20 % of this material will fulfil the characteristics to be used as base material for the platform.

In summary: the geotechnical survey and the characterization of rock materials for the use in base pavement, during the project phase, was limited and not adequate and this has caused substantial delays in the schedule of the construction and also additional costs.

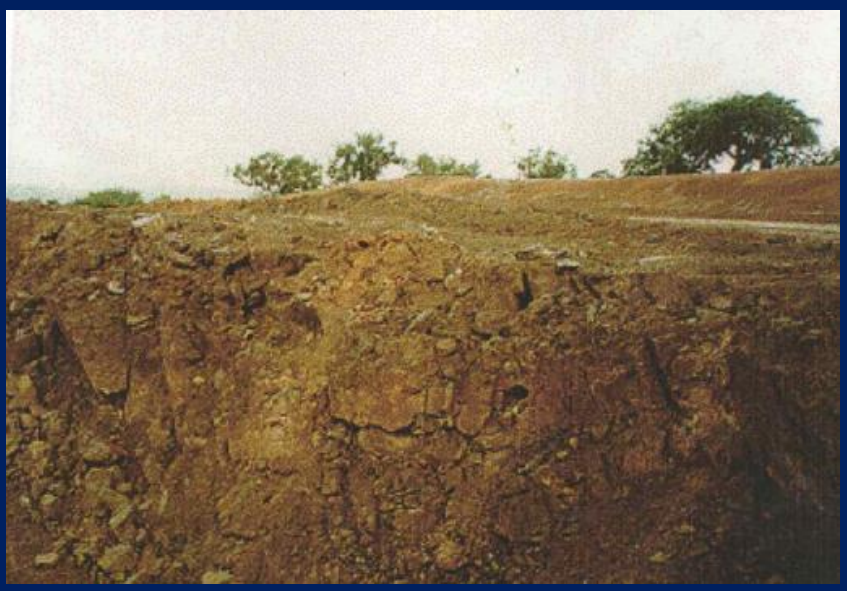

Figure 8. 428 General view of rock material after blasting in the neighboring of PS2

Figure 8. 429 General view of rock material in the neighboring of PK 10+200

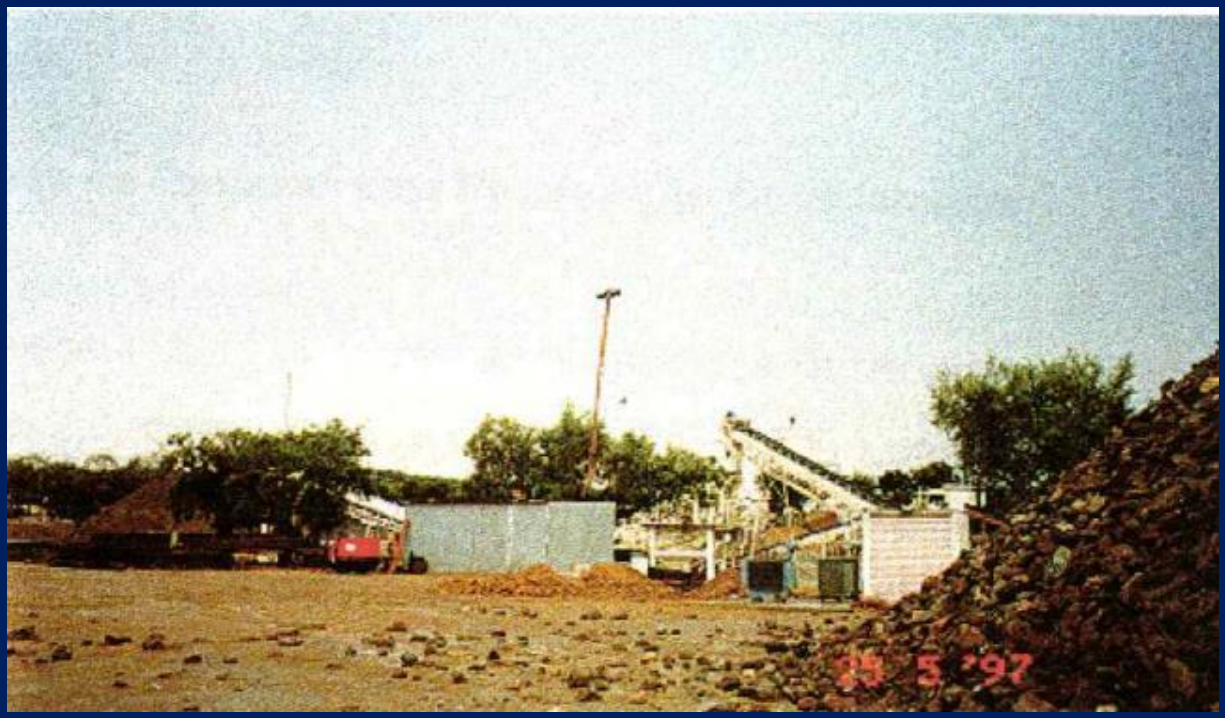

Figure 8. 430 General view of the treatment installation

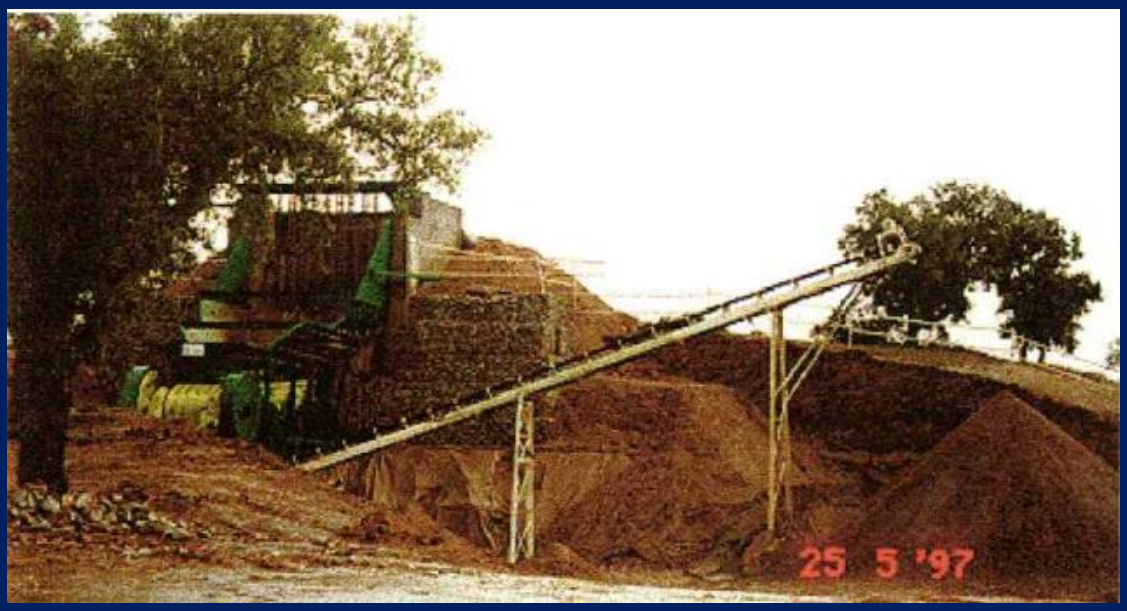

Figure 8. 431 Details of the treatment installation

Figure 8. 432 Borehole nº 1 – Samples

Figure 8. 433 Borehole nº 2- Samples

Lesson nº 27 - The ground investigation has not given the adequate attention to:

— the variability of the ground;

— the Geotechnical Category;

— the suitability of the site and the level of acceptable risks;

— the type of uncertainty of the ground investigation results and the level of acceptable risks;

— suitability for the intended use;

— the extent of deposits;

— the process to extract the materials;

— the presence of weakness zones, weathered zones, and discontinuities;

— the level of the bedrock, rockhead or transition zone between soil and rock;

— the quality, strength, and stiffness properties of the rock mass.

Note: This study was performed for ETEJE.

8.11 Station of Treatment for Residual Water

8.11.1 Case History nº 28 - ETAR-Station of Residual Water Treatment - Vila Franca

8.11.1.1 Introduction

The geological characteristics are addressed, the geotechnical characterization is presented, the ground improvement techniques are analysed, the seismic action is referred, the design of spread and raft foundations is discussed, the design of structures on pile foundations is presented, the construction specifications are addressed and the instrumentation is introduced.

8.11.1.2 General Geological Characteristics

The following units were identified:

Muddy alluvial

The results of SPT tests between 0 and 1 and vane shear tests with peak values between 28 kPa and 48 kPa and residual strength between 8 and 12 kPa have shown that these materials are very soft.

Clay sandy alluvia materials

These materials have exhibited values of SPT between 13 to 25 blows.

Quaternary complex

This unit integrates silty material with gravels and blocks, with SPT values of 60 and was considered the bedrock.

8.11.1.3 Geotechnical Characterization

For the preliminary studies the map of the materials for Lisbon District, as well the Portugal geological and the Neotectonic Portugal map were analysed.

For the second stage a campaign with 8 boreholes was performed, with boreholes length between 10.95 m to 36.5 m. In 2 boreholes hydraulic piezometers were installed.

In these boreholes SPT tests were performed 1.5 m apart, the phreatic level was measured and disturbed samples were taken for soil classification.

Also van shear tests were performed.

Laboratory tests such as the identification tests (sieve analyses and Atterberg limits), and oedometer tests were performed.

The purposes of this site investigation program were the following:

1. Definition and nature of different materials;
2. Seepage conditions through the foundation
3. Definition of soil physical indexes;
4. Determination of mechanical properties of ground materials such as strength and deformability;

5. Chemical analysis of water.

8.11.1.4 Ground Improvement of the Alluvia Materials

Considering a mud alluvial material of 25 m thick the predicted value of the settlement was around 2. 0 m, so a treatment was required.

Table 8.55 presents a summary of soil improvement techniques.

For the improvement of the alluvia materials, following a cost -benefit analysis, two assumptions were selected, namely: (i) a pre-charge fill associated to gravel columns 25 m long, 2.5 m apart in quinquonce; or pre-charge fill associated to geodrains with 5 mm diameter, a length of 25 m, in quinquonce 1.25 m apart.

The use of gravel columns requires the use of piles for the biological tank and for the digestor, due to the high settlements and also due to the past experience could not support the use of gravel columns of 28 m long.
In summary:
-The length of 28 m for the gravel columns was considered too high, based in the existent international experience;
-The alluvia unit is composed of mud material with an undrained resistance to low.
-Situations of bending could occur for gravel columns due to the weak confinement;
-For the biological tank and the digestor structure, in additional to the gravel columns there was a need to use concrete piles to satisfy the ultimate limit stets aa the behavior of gravel piles with so high length is questionable and also to respect the serviceability limit states;
-The constructive methods are not calibrated for the execution of gravel columns with the length of 28 m.

So, the use of geodrains were considered more adequate and the effects of smear were incorporated in the definition of the geodrains spacemen.

Figure 8. 434 shows the geodrain equipment, Figure 8.35 illustrates the general view of the geodrain installation and Figure 8.436 presents the instrumentation plan.

8.11.1.5 Seismic Action

The site has the influence of several seismicity mechanisms that can generate intraplate or interpolate earthquakes.

Combining the deterministic and probabilistic approaches for a return period of 1000 years for MCE (maximum credible earthquake) and for OBE (operating basis earthquake) acceleration values of 0.25 g and 0.15 g were considered.

8.11.1.6 DESIGN OF SPREAD AND RAFT FOUNDATIONS

For the verification of these foundations the following limit states were considered:

a) - Ultimate limit state design - loss of overall stability- bearing resistance failure

- failure by sliding

b) - Serviceability limit state design - settlements: immediate and delayed settlements

- excessive heave / - settlements due to vibrations.

Shallow foundations with a geometry of 2.5 m x 2.5 m and 1.5 m x 1.5 m were recommended.

The alluvial materials were consolidated with geodrains and the use of raft foundations were considered.

For Desarenador and Desengordurador – 2 tanks with 15.0 m x 4.0 m x 4.3 m the computed values were: average stress = 72.2 KPa and settlement = 40 mm.

Table 8.55 Summary of Soil Improvement Techniques

Method	Description	Type of Material	Equipment Required	Soil Improvement Characteristics	Advantages and Limitations	Costs
Light Weight Material		Soft soils		Low density	Easy to install, no ground pollution	Medium
Chemical Treatment	Chemical reactions	Silts and clays	Mixers, pumps	Increase resistance and speed consolidation	Reduction of water contents, ion exchange	High
Stone Columns and Sand Columns	Introduce of compacted stone or sand	Soft clays	Vibroflot crane	Increase strength and decrease deformations	Avoid dewatering, limited bearing capacity	Medium to High
Compaction G\\routing	The voids of the soil are filled by the grout	Loose sands and soft clay	Drilling pump, packers	Improving of strength and reducing of deformability	Treated material is no homogenous	High
Jet Grouting	Part of the soil mass is convert to soil-cement	Clays and sands	Drilling pump, packers	Increase of strength	Zones to be treated must be located with precision	High
Geotextiles in embank-ments on soft ground	Placement of geotextile	Weak foundations	Easy to install	Mechanical reinforce-ment, filtration, drainage	Economical. Tolerate deformations	Low
Geodrains	Placement of geodrains	Soft soil	Cranes	Improving of strength and reducing of deformability		**Low**

Micropiles	High contribution of shaft resistance	Soils and rocks	Drilling equipment	Improving of strength	Can be used for any type of material	High
Soil Nailing	Reinforcement by passive inclusions	Soils and rocks	Drilling equipment	Improvement of tensile stresses, shear stresses and bending moments capacity	Can not be grouted	Medium to high
Ground Anchorages	High contribution of grounting	Soils and rocks	Drilling equipment	Improving of strength	Can be used for any type of material	High
Biotechnical stabilization	Biological vegetation	Soils	Speeding equipment	Protection	Stetic aspects	Low

Table 8.56 Laboratory Tests to Assess Ground Improvement Techniques

Tests / Techniques	Bulk Density	Proctor Test	Triaxial Test	Direct Shear Test	Oedometer Test	Permeability Test	Shaking Table	Centrifuge Tests
Light Weight Materials	X	X						
Chemical Treatment			X	X	X	X		
Stone Columns and Sand Columns			X	X	X			
Compaction Grouting			X	X	X	X		
Jet Grouting			X	X	X	X		
Geotextiles			X	X	X		X	
Geodrains			X	X	X			
Micropiles							X	X
Soil Nailing							X	X
Ground Anchorages							X	X

Table 8.57 Laboratory Tests to Assess Ground Improvement Techniques

	In situ Density	SPT Test	CPT Test	Geophysical Tests	Plate load test	Pressurometer test	Permeability test
Light Weight Materials	X						
Chemical Treatment		X	X			X	
Stone Columns and Sand Columns		X	X	X	X		
Compaction Grouting		X	X	X	X	X	X
Jet Grouting		X	X	X	X	X	X
Geotextiles							
Geodrains		X	X	X			
Micropiles					X		
Soil Nailing							
Ground Anchorages							

Figure 8. 434 Geodrain equipment

Figure 8. 435 View of geodrain installation

Instrumentation

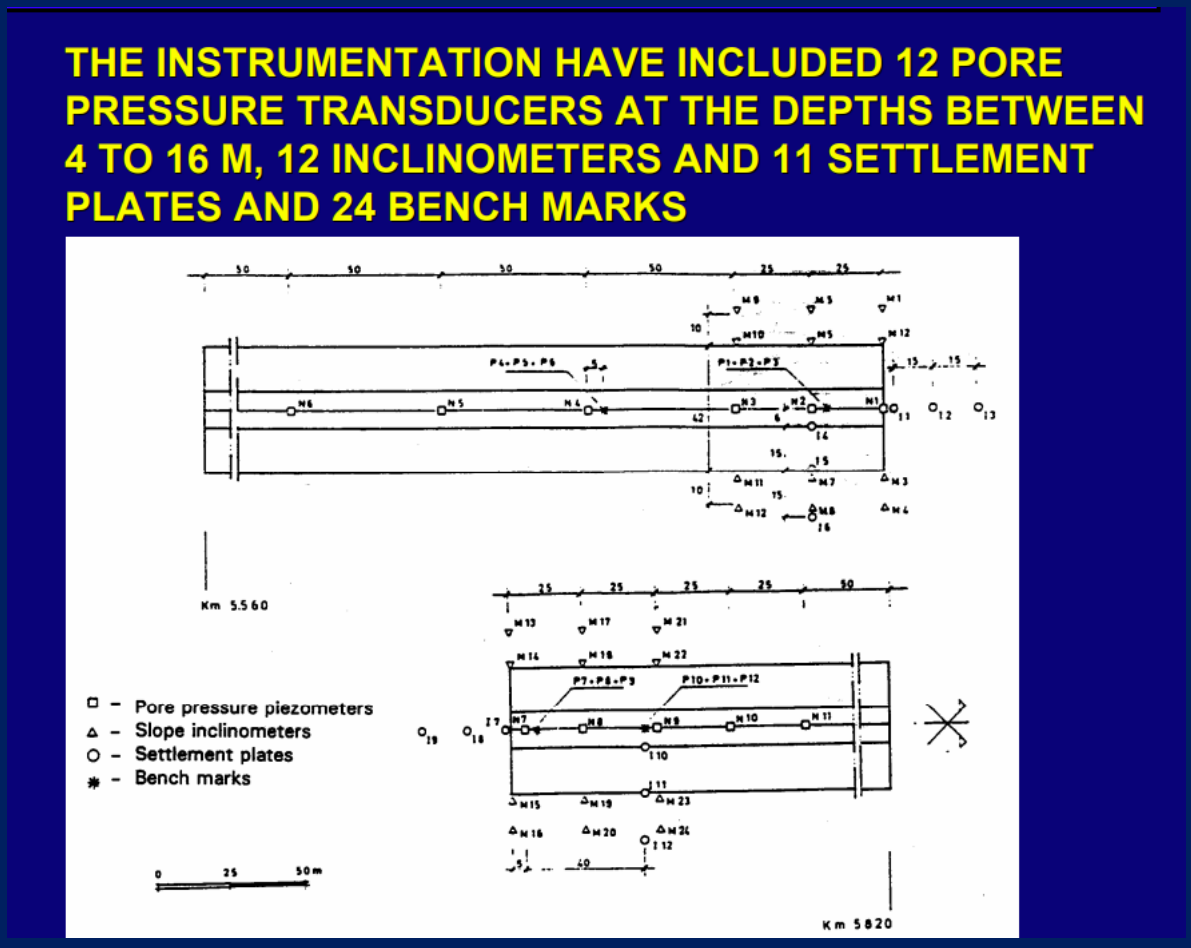

Figure 8.436 Instrumentation plan

8.11.1.7 Raft Foundations

For the Primary Decanter with 32.0m x 12.0m x 4.0m the computed values were: average stress = 75 KPa and settlement = 11 cm.

For Biological tank with 25.0m x 11.50 m x 6.7 m the computed values were: average stress = 128 KPa and settlement = 18.2 cm.

For the Secondary Decanter with 65.0 m x 7.0 m the computed values were: average stress = 46.47 KPa and settlement = 4 cm.

For the Digestor the computed values were: average stress = 280.93 KPa and settlement = 34 cm.

Settlements values until 11 cm were considered acceptable for a raft foundation.

For structures as biological tank and Digestors pile foundations were recommended.

8.11.1.8 PILE DESIGN

Piles under vertical loads

The following limit states were considered:

a) - Ultimate limit state design

- loss of overall stability - bearing resistance failure of the pile foundation

- uplift or insufficient tensile resistance of the pile foundation - failure in the ground due to transverse loading of the pile foundation / - structural failure of the pile in compression, tension, bending or shear /- combined failure in ground and in structure.

b) - Serviceability limit state design

- excessive settlements /- excessive heave / - unacceptable vibrations

Piles under horizontal loads

For the analysis of a pile under horizontal loads a value of a constant subgrade reaction or a value of subgrade reaction varying with depth, i.e the Winkler approach was considered for the calculation of the values of horizontal displacement, rotations, bending moments and shear forces, considering a beam in a domain semi-infinite, elastic, homogenous and isotropic.

Piles Seismic Design

Seismic design of piles was done using the simplified approach of Makdisi and Seed.
The kinematic computed values were considered critical for the design.

8.11.1.9 Structures in Piles Foundations

Biological tank

For this structure 49 piles of ϕ = 0.80 m and a length of 24m were recommended.
The computed settlements were less than 5 mm.
Figure 8.437 illustrates the sketch of the biological tank foundations.

Digestor

For this structure 20 piles of ϕ = 0.8 m and a length of 28 m were recommended.
Figure 8. 438 shows the sketch of the digestor foundations.

8.11.1.10 Construction Specifications

The construction specifications for the fills execution, direct foundations, pile foundations, geotextiles and geodrains were defined.

8.11.1.11 Instrumentation

To monitor the consolidation of the alluvia materials it was proposed the installation of: (i) 36 pore pressure electric cells, 15 inclinometers, 24 bench marks and 18 hydraulic piezometers in longitudinal and transverse profiles of the platform.

A complementary site investigation programme was proposed with geophysical tests, boreholes, vane shear tests, permeability tests, penetrometer tests, direct shear tests, oedometer tests, triaxial tests, water aggressivity tests.

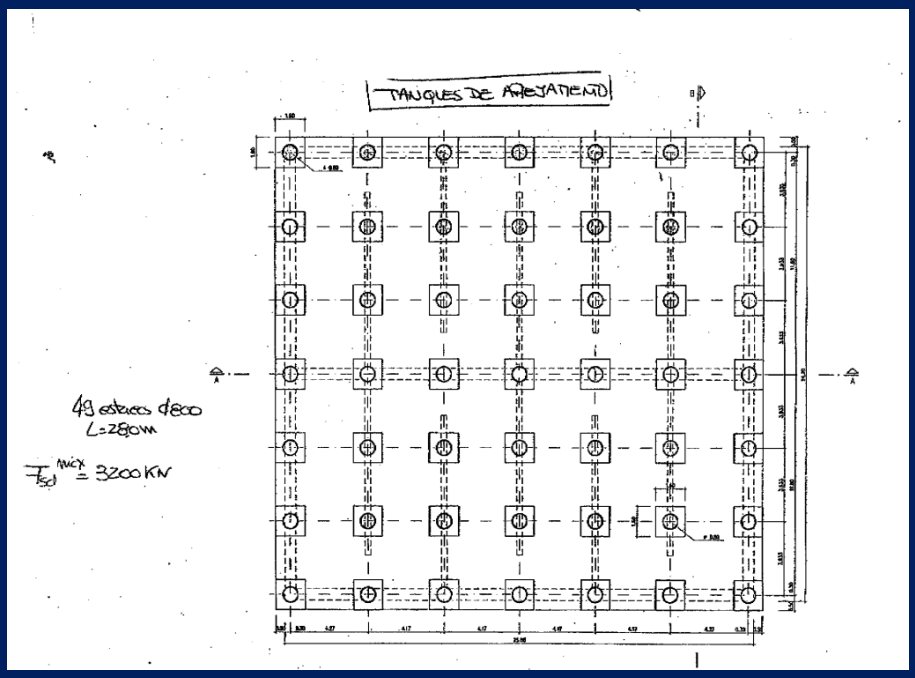

Figure 8.437 Sketch of the biological tank foundations

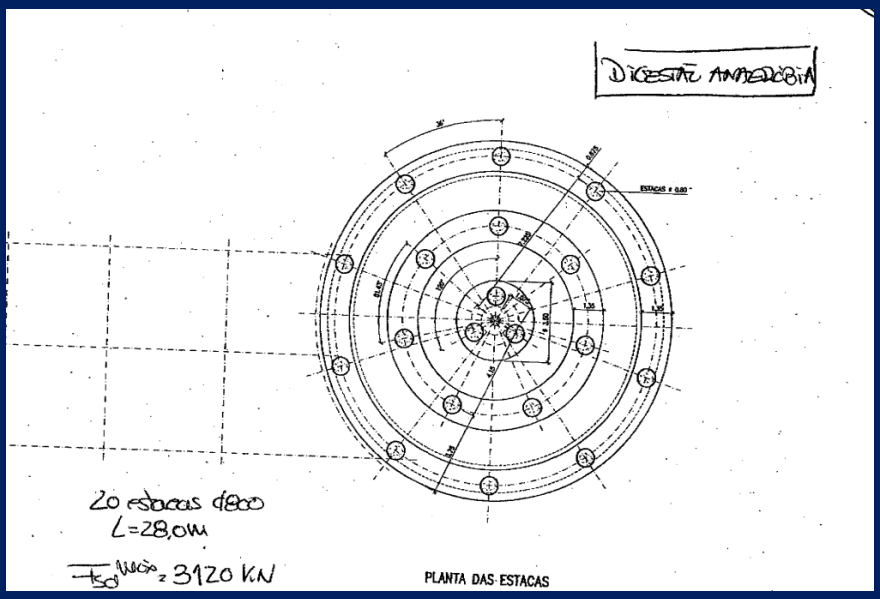

Figure 8. 438 Sketch of the digestor foundations

Lesson nº 28 The ground improvement method should be selected considering the following:

− the design situation and load variation;

− thickness and properties of the ground or fill material;

− water pressure in the various strata;

-efficiency of the technique;

- comparable past experience.

A survey related past experience of the use of gravel columns with 30 m depth was performed and has not supported the decision of this selected technique.

Note: This work was done for Hagen.

9. FINAL REMARKS

Single Reflections

It seems to me that we should cultivate the universality of the knowledge and the permanent education. It is important to communicate, to share our experiences, to compare methodologies and to monitor the results. The benefits of an open dialog between academicians, researchers, designers, contractors, decision makers and owners are huge.

We should construct bridges following the master piece of Van Gock.

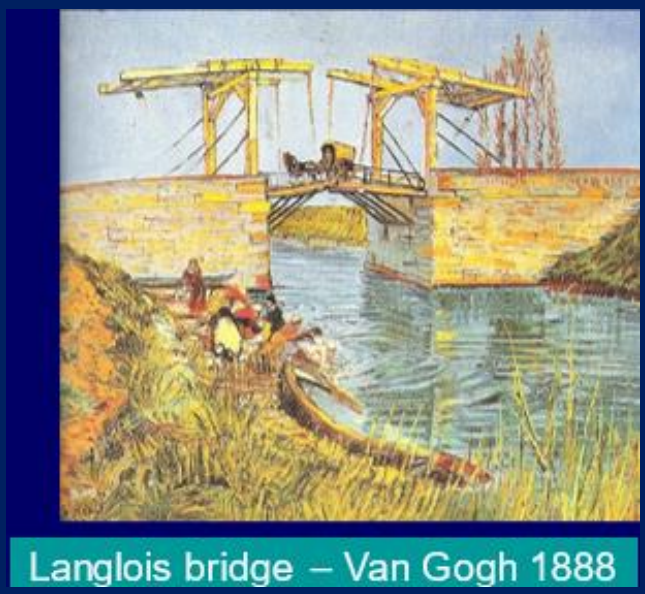

Langlois bridge – Van Gogh 1888

It is important to remember that: more important than to discover new facts is to discover new ways to think on the existent facts.

We should not forget that failure is the best ingredient for newly discovers. We can not win without leaving our safety zone and assuming calculated risks, following the example of Julius Cesar, when he crossed the Rubican.

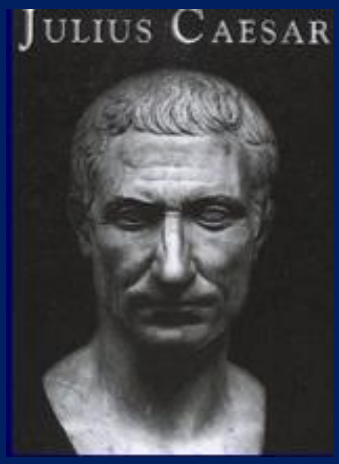

The world was built by persons that were feeling unhappy with the situation and were interest in improving it.
The greatness is achieved by persons that are not happy with the situation even if it looks good.

We should not forget the lessons of Ralf Peck "Where has all the judgement gone?

As long the myth persists that only what can be calculated constitutes engineering, engineers will lack incentive or opportunity to apply the best judgement to the crucial problems that cannot be solved by calculation.
Where has the judgment gone? It has gone where the rewards of professional recognition and advancement are greatest to the design office where the sheer beauty of analysis is often separated from reality. It has gone to the research institutions, into the fascinating effort to idealize the properties of real materials for the purposes of analyses, and into the solution of intricate problems

of stress distribution and deformation of the idealized materials. This incentive to make a professional reputation leads the best people in these directions.
To develop this judgement and to bring it to bear require a recording of our present views of what constitutes the highest form of our practice of engineering. Without detracting from the necessity for reasonable and meaningful engineering calculations and from the rewards to those who can carry them out, at least equal professional prestige and responsibility should be accorded to men of judgement, even when that judgement is not expressed in numerical form.

(Extracts from the 5th Laurits Bjerrum Memorial Lecture delivered by Ralph B. Peck in 1980)

We should address the hot topics and Case Histories with failures.
There is a need to search for the 4th dimension following Salvador Dali.

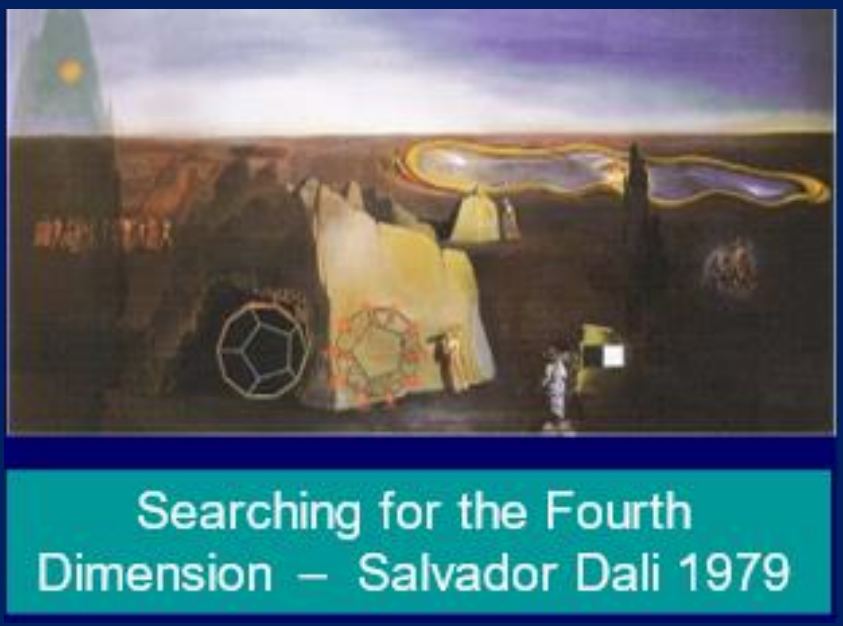

Also, the interaction with the Society is crucial following the example of the Athens School, leadered by Aristotelis, and illustrated in the master piece of Raphael.

Additional Thoughts

- Leonard de Vinci has stated that " It seems, though that those sciences which have not been born by experience the mother of all certitude, are vain and full of misconceptions".

- We should not forget that Theory without Practice is a Waste, but Practice without Theory is a Trap.

- I would stress that all the past lessons had not deserved total consideration, in order to avoid repeating the same mistakes, and we should preserve the knowledge through a careful analysis of Case Histories.

- The Predictions on Engineering are our great challenge and we should not forget that:

The Times change, as well our Wills
The Spirit changes and the Thrust changes
The entire World is continuously changing
Considering always new standards

• An engineer shall not offend the truths of the theory of material strength and the definition of the actions.

• In spite of our efforts to improve the image of the Engineer we still remain behind our colleagues of Medecine or Physics, due to the New High Tec Medecine, or Fligths to the Moon that are more spectacular.

• Geotechnical Engineers that operate below the ground surface can not compeat with Architects that are admired for their visible structures.

• We should not feel frustrated as we should explain to the Society that the concern for man and fate has been always the core interest of the geotechnical engineer.

• Remember that each day, life will send little windows of opportunity. Our destiny will ultimately be defined by how we respond to these opportunities.

As we live our days, so we craft our life.

Aristotelis, Hamurabi and Vitruvio

Aristotelis analyses the concept of Good. He is the inventor of a philosophical programme which merits and defects are extremely difficult to analyse. An open, intelligent and rigorous reader will face some profound questions of ethical life in the Book Ethics Nicomaqueia from Aristotelis

•Aristótelasanalisa a noção do que é bom para o ser. Ele é o inventorde um programa filosóficocujos méritose defeitos são extremamentedifíceisde avaliar. Um leitoraberto, cuidadoso e inteligente,enfrentará inevitavelmentealgumas das questõesmais profundas da vida éticana obra Ética Nicomaqueiade Aristóteles

Code of Hammurabi

• The Code of Hammurabi is a Babylonian legal text composed c. 17 It is the longest,best-organised,and best-preservedlegal text from the ancient Near East. It is writtenin the Old Babylonian dialectof Akkadian, purportedlyby Hammurabi, sixth king of the First Dynasty of Babylon.

The Hammurabi code of laws, a collection of 282 rules, established standards for commercial interactions and set fines and punishments to meet the requirements of justice. Hammurabi's Code was carved onto a massive, finger-shaped black stone stele (pillar) that was looted by invaders and finally rediscovered in 1901.

• 2000 years ago the Roman architect Marcus Vitruvius Pollio wrote the ten books on architecture still referred to in every European architect's education. His work has been translated into many languages and has engendered many imitations, The concept of the architectural pattern book offering design principles as well as solutions is universally familiar. This book is intended as a green pattern book for today offering advice in areas of energy, water, air and materials. The reference to green is not without its own resonance. To the Vitruvian triad of commodity, firmness and delight, with Eoin O Cofaigh we postulate the addition of a fourth ideal: restituitas or restitution, restoration, reinstatement: where the act of building enhances its immediate and the global environment in an ecological, as well as visual sense.

• Climate change mitigation may be the main driver for demands for radically higher standards of building performance, green design offers several other advantages. The continuing financial savings which energy-efficient design will achieve can be of real importance in daily life.

10. NEW CHALLENGES

• Prometheus offers the fire to the Humanity that represents the knowledge.

• Descartes in his book Methodology inspired in Prometeus has considered that the lessons are important to benefit human life and knowledge.

The geotechnical engineers should be prepared to face the new challenges of the society.

It is important to develop an independent way of thinking and capacity of decision, to develop the potentialities in order to reduce the gap between Theory and Practice, to explore the intuition and to not forget good sense and engineering judgement.

11.MY VISION – LESSONS FOR TOMORROW

1. Further discussion in recent codes related performance based design and allowable displacements for the 2 levels of seismic action.

2. Vulnerability is associated with the degree of loss or the potential loss and integrates the range of opportunities that people face in recovery. Resilience is a measure of the system`s capacity to absorb recover from a hazardous event.

3. The recognition of a better planning, early warning, quality of evacuation for extreme events. Plato (428-348 BC) in the Timaeus stressed that destructive events that happened in the past can happen again, and for prevention and protection we should followed Egyptians example and preserve the knowledge through the writing.

4. The none recognition for the engineers work is lacking since the past, e.g. the Egyptian King Cheops has his name linked with the great pyramid, a master piece engineer work, but the history does not record the name of the engineer.

5. Interaction with the Owners, Decision Makers, Society and General Public and to explain that the concern for man and fate has been always the core interest of the engineer profession.

6. The engineers should have competence, devotion and honesty.

7. The Engineers should enjoy the activities during the day, but only by performing those that will allow to sleep at the night.

8. Contribution of Voltaire and the book Candide published in 1759, after the Lisbon earthquake (1755), for the change from the intellectual optimism and potential fatalism that is a necessary condition for the construction of future scenarios in a reliability and risk analysis context.

9. 7 Pillars of Engineering Wisdom: Precedents, Practice, Principles, Prudence, Perspicacity, Professionalism and Prediction.

10. It is important to narrow the gap between the university education and the professional practice, and remember that Theory without Practice is a Waste, but Practice without Theory is a Trap. Kant has stated that *Nothing better that a good theory,* but following Seneca *Long is the way through the courses, but short through the example*.

- The wisdom to recognise the things that should be change
- The strength to change the things that can be changed and
- The tranquility to accept the things that you can not change”

Friedrich Oetinger
(1702-1782)

References and Bibliography

" Il en est des livres comme du feu dans nos foyers

On va prendre le feu chez son voison,

On l´allume chez soi,

On le communique à d`autres

Et il appartient à tous"

(Voltaire)

AFTES (1993) "Texte des recommandations relative au choix d`un type de soutènement en galerie ».

AFTES GT nº7 –*Soutènement et Revêtement. Tunnels et Ouvrages Souterrains*, pp.60-72.

Alba, P. (2004) "Residual strength after liquefaction: a rheological approach". Proc. of 3rd International Conference on Earthquake Geotechnical Engineering, Berkeley, Editors D. Doolin, A. Kammerer, T. Nogami, R.B. Seed & I. Towhata, Vol. 1 pp.740-746.

Ambraseys, N.N. (1960). "The Seismic Stability of Earth Dams". *Proc. 2nd World Conference on Earthquake Engineering*, Tokyo, Vol.II, pp. 331-336.

Ambraseys, N. N. (1998) Engineering seismology, Earthquake Engineering and Structural Dynamics, Vol.17, pp. 1-105.

Amini. F. e G. Z. Qi. (2000) “Liquefaction testing of stratified silty sands”. J.G.G.E., Vol. 126, nº: 3, pp. 208-217.

Andrus, R.D, Stokoe, K.H., II & Chung, R., M (1999) “Draft guidelines for evaluating liquefaction resistance using shear wave velocity measurements and simplified procedures”, NISTIR 6277, NIST, Gaithersburg, 121p, 1999.

Andrus, R.D. and Youd, T.L. (1989) “Penetration Tests in Liquefiable Gravels.” Proc. 12 th ICSMGE, Rio de Janeiro, Vol. 1, pp 679-682

Annakai, M. (1975) “Liquefaction of Sand in Triaxial Tests Using Uniform and Irregular Cyclic Loading”. PhD. Dissertation, University of California, Los Angeles.

ANSCOLD (Australia) - Guidelines for Dams Instrumentation in Australia, 2012.

API (1984) American Petroleum Institute Planning, Designing and Construction Fixed Offshore Platforms.

Arulanandan, K. e R.F. Scott (eds.). (1994) “Verification of Numerical Procedures for the Analysis of Soil Liquefaction Problems”. Proc. Of Int. Conf. Davis, Vols. 1 e 2, A.A. Balkema, Rotterdam, The Netherlands.

Arya, S.C., O`Neil, M.W. and Pincus, G. (!981) “Design of Structures and Foundations for Vibrating Machines, Gul Publishing Co.

Arya, S.C. and Pincus, G. (!982) “Analysis and Design of Elevated Foundations for Reciprocating Machines, Foundations for Equipment & Machinery. American Concrete Institute. CI-Publication SP-78, pp1-32.

Aristoteles (334 BC) - Ética Nicomaqueia

Aristotle – Meteorologica

ASCE (1997) “Ground Improvement, Ground Reinforcement, Ground Treatment Developments (1987-1997)”. Geotechnical Special Publication nº 69.

Australia Geomechanics Society (2000). “Landslide Risk Management Concept and Guidelines”. Australia Geomechanics Society. Sub-Committee on Landslide Risk Management. Australia Geomechanics, Vol.35, Nº1, pp.49-92.

Ayadi, Abdelhakim, (2003), “Le séisme, un danger pour la sécurité nationale: El Asnam 1980 à Zammouri 2003, où est l’état de la prévention pour la réduction du risque sismique”.

Baba, K. and Nagai, M, (1987) “Dynamic Failure Test of Model Embankment”. International Symposium on Earthquakes and Dams. Beijing, China, Vol. 1, pp 271-285.

Baecker, C.B. and Christian, J. (2003) “Reliability and Statistics in Geotechnical Engineering”. John Wiley & Sons, New York

Barton, N. (1994) “Updating the NATM”. Tunnels & Tunnelling, pp.40.

Barton, N. Grimstad, E. Palmstrom, A. (1994) “Design of Tunnel Support. Sprayed Concrete: Properties, Design and Application”, Cap. 8, pp.150-170, Londres.

Barton, N., Lien, R. & Lunde, J. (1974) “Engineering classification of rock masses for the design of tunnel support”. Rock Mech. nr. 6, pp. 189-236.

Bazant, Z.P., R.J. & Krizek. (1976) “Endochronic constitutive law for liquefaction of sand”.

JEMD, ASCE, Vol. 102, EM2, pp. 225-238.

Beaver,1972) “A History of Tunnels”, London, Peter Davies.

Benlala, A. (2003) “Le barrage de Keddara face au séisme du 21 Mai 2003 et la sécurité du Grand Alger Suite au séisme de Boumerdes du 21 Mai 2003 ». Question 83-Seismic Aspects of Dams, Montréal.

Bertram, G.E. (1940) “An Experimental Investigation of Protective Filters”. Harvard Graduate School of Engineering, Public, 267.

Bertrand, E. et Mouroux, P. (2003), “Rapport Préliminaire de la Mission AFPS”, Paris, Chap. 3.

Bertrand, E. (2003), “Rapport Préliminaire de la Mission AFPS, Paris, Chap. 2. Faure, J. et al. (1982), L’Évaluation du Risque Sismique pour la Sureté des Installations Nucléaires”. Séminaire AIEA,

Bescond, B., Bottero, A., Touzot, G. (1974) " Fondations sur sols bi-couches. Tables de Calcul des Tassements".

Bezghoud, M. et al. (1994) "Les séismes d'Algérie de 1565 à 1992". CRAAG, Alger,

Bieniawski, Z., T. (1984) "Rock mechanics design in mining and tunnelling". Pub. Balkema.

Besancon, G. and Pertusier, E. (1982) "Soil Improvement by Deep Vibration", Symposium on Recent Developments in Groun Improvement Techniques, Bangkok, Vol., pp 145-152.

Bieniawski, Z., T. (1984) "Rock mechanics design in mining and tunnelling". Pub. Balkema.

Bieniawski, Z.T. (1989) "Engineering Rock Mass Classifications". Wiley (New York), p 251.

Borcherdt, R.D. (1994). "Estimates of site dependent response spectra for design" (methodology and justification). *Earthquake Spectra*. 10: 617-653.

Boscardin, M. D. and Cording, E. G. (1989) "Building Response to Excavation Induced Settlement". Journal Geot. Eng. ASCE, Vol 115, 1 - pp. 1 - 21.

Boulanger, R. W. and Idriss, I. M. (2014) "CPT and SPT Based Liquefaction Trigging Procedures" Report No. UCD/CGM-14/01 Center for Geotechnical Modeling Department of Civil and Environmental Engineering University of California Davis, California April.

Bozozuk, M. (1981) "Tolerate Movements of Bridge Foundations". Proc. 10th Int. Conference Soil Mechanics and Foundation Engineering, Stockholm, Vol., pp 699 - 700, Balkema, Rotterdam.

Brandl, H., F. Kopf, D. Adam (2005) "Continuous Compaction Control (CCC) with Differently Excited Dynamic Rollers". Wien.

Bray, J., Sancio, R.B., Riemer, M. and Durgunoglu, H.T. (2004) "Liquefaction susceptibility of fine grained soils". Proc. of 3rd International Conference on Earthquake Geotechnical Engineering, Berkeley, Editors D. Doolin, A. Kammerer, T. Nogami, R.B. Seed and I. Towhata, Vol. 1 pp.665-662.

Bray, J.D. and Stewart, J.P. (2000) "Damage Patterns and Foundations Performance in Adapazari, Kocaeli Turkey Earthquake of August 17,1999 Reconnaissance Report", Earthquake Spectra, 16, 163-189.

Burland, J. B. (1995) “Assessment of Risk of Damage to Buildings due to Tunneling and Excavation”. Special Lecture. First International Conference on Earthquake Geotechnical Engineering, Tokyo, Japan, Vol 3, pp 1 - 14.

Burland, J. B. Broms, B. B. and De Mello, V. F. B. (1977) “Behaviour of Foundations and Structures”. Proc. 9th Int. Conference Soil Mechanics and Foundations Engineering, Tokyo, Vol. 2, pp. 495 - 546.

Burland, J. B. and Wroth, C. P. (1974) “Settlement of Buildings and Associated Damage. SOA Review. Conference Settlement of Structures, Cambridge, Pentech Press, London, pp. 611 - 654.

Building Research Institute (1965)

Byrne, P.M. e Beaty, M.H. (1999) “Assessment residual strength for embankments”. Proc. of the Second International Conference on Earthquake Geotechnical Engineering. Edited by Pedro S. Sêco e Pinto. Published by Balkema. Vol. 3, pp. 1069-1075, 1999.

Caldeira, L., Pimenta, L. and Silva Gomes, A. (2005) “Framework of Risk Analysis and their Application to Embankment Dams” (in portuguese). Seminar on Dams- Technology, Safety and Interaction with the Society, Lisbon, pp 569- 585.

Canadian Dam Safety Regulations. British Columbia, 2010.

Carter, J.P., J. R. Booker and C.P. Wroth (1982) “A critical state soil model for cyclic loading. Soil Mechanics Transient and Cyclic Loads. Constitutive Relations and Numerical Treatment. John Wiley & Sons, pp. 219-252.

Carvalho, E.C, Oliveira, C.S., Costa, A. C. and Sousa, M. L. (1999) “Definition of seismic action for the National Document of Application of Eurocode 8 (in portuguese). 4th National Congress of Seismologie and Earthquake Engineering.

Casagrande, A (1961) “Control of Seepage through Foundations and Abutments of Dams”, 1st Rankine Lecture.

CASTRO, G. (1989) "Foundations Design of Concrete Reinforced Piles” (in portuguese). Laboratório Nacional de Engenharia Civil. Bulletin nº 743. Lisboa.

Cedergreen, H.R. (1977) “Seepage, Drainage and Flow Nets”. Second Edition, John Wiley and Sons, New York.

Cetin, K.O. e Seed, R.B. Kiureghion, (2001) “Reliability Based Assessment of Seismic Soil Liquefaction Initiation. XV ICSMGE TC4 Satellite Conference on Lessons Learned from Recent Strong Earthquakes, pp. 327-332. Edited by Atilla Ansal.

Chellis, R. D. (1961) “Pile Foundations”, Mac Graw Hill, Inc, New York.

Chile Seismicity Map - 1900 to Present

Chopra, A.K. (1966) “Earthquake Effects on Dams”. Thesis submitted in Partial satisfaction of the requirements for the degree of Doctor of Philosophy. University of California, Berkeley.

Clark, R. G. (1998) “Realism in Remediation”. Theme Lecture, Proc. of the Environmental Geotechnics Congress, Vol. 4 pp. 1257- 1272. Edited by Sêco e Pinto, Published by A. Balkema.

Cristian, J.T., Ladd, C.C. and Baecher, G.B. (1994) “Reliability Applied to Slope Stability Analysis”. J. Geot. Eng. ASCE, 120(12), 2180-2207.

Clough, R.N. and Chopra, A.K. (1966) “Earthquake Stress Analysis in Earth Dams”, JEMD, ASME, Vol. 92, Nº EM2, Proc. Paper 4793, pp. 197-212

Clough, G. W., Iwabuch. S. and Kuppusamy, T. (1989) “Influence of Cementation on Liquefaction of Sands”, JGED, ASCE, Vol. 115, Nº8, pp.1102-1117.

Clough, R.W. and Zienkiewicz, O.C. (1975) “Finite Element Methods in Analysis and Design of Dams”, Ed. A.J. Naylor, K.G. Staag, O.C. Zienkiewicz.

Cook, J.B. (1984) “Progress in Rockfill Dams”, Terzaghi Lecture. ASCE Journal of Geotechnical Engineering, Vol. 110, nº 10.

Correia, A.G. (1987). “Contribution a l'etude mechanique des sols soumis a des chargements cycliques”. These de Docteur Ingenieur Ecole Nationale des Ponts et Chausses.

Cruz, P. T. (1996) “100 Brazilian Dams. Case Histories. Materials Construction, Project” (in portuguese).

CSOPT - (Conselho Superior de Obras Públicas e Transportes, Subcomissão dos Regulamentos de Barragens) (1987) - Dam Safety Code (in portuguese).

Cubrinovski, M. and Orense, R. (2010): 2010 Darfield (New Zealand) Earthquake - Impacts of liquefaction and lateral spreading, Bulletin of the International Society for Soil Mechanics and Geotechnica Engineering, Vol. 4, No. 4, pp.15-23.

Cubrinovski, M. et al. (2010): Geotechnical reconnaissance of the 2010 Darfield (Canterbury) earthquake, Bulletin of the New Zealand Society for Earthquake Engineering Inc, Vol. 43, No. 4, pp. 243-320.

Cuellar, V. (1999) "Codes and standard for Europe". Proc. of the Second International Conference on Earthquake geotechnical Engineering. Edited by Pedro S.Sêco e Pinto. Published by Balkema.Vol. 3, pp. 1129-1133.

Das, Braja (1983) "Fundamentals of Soil Dynamics". Elsevier Science Publishing, pp. 399.

Davidenkoff, R. (1955) "De la composition des filtres dans les barrages en terre". Cinquième Congrès des Grands Barrages-Paris. Vol. I, pp.385-401.

De ALBA, P. (1975). "Determination of the soil liquefaction characteristics by large-scale laboratory tests". University of California. ph D thesis.

Décret nº 2007-1735 du 11 décembre 2007 relatif à la sécurité des ouvrages hydrauliques et au comité technique des barrages hydrauliques et modifiant le code de l` environnement, 2007.

De Mello, V.F. B. (1977) "Reflections on Design Decisions of Practical Significance to Embankment Dams". 17th Rankine Lecture, Geotechnique, vol. 27, nº 3, pp.279-355.

Dibaj, M. and Penzien, J. (1969) "Response of Earrh Dams to Traveling Seismic Waves", JSMED, ASCE, Vol. 95, Nº SM2, pp. 541-560.

Drnevich, V.P. (1975) "Constrained and Shear Moduli for Finite Elements", JGED, ASCE, Vol.101, nº GT5, pp 459-473.

Duncan, J. (2000) "Factors of Safety and Reliability in Geotechnical Engineering", Journal of Geotechnical and Geoenvironmental Engineering, Vol. 126, Nº 4, .307-316.

Duncan, J.M., Dòrazio, T.B., Chang, C.S. Wong, K.S. and Namio, L.I. (1981) "CON 2D: A Finite Element Computer Program for Analysis of Consolidation". Report nº UCB/GT/81-01, University of California, Berkeley.

EARTHQUAKE SPECTRA. (1995) "Northridge Earthquake Reconnaissance Report". Vol. 1.

EERI. (1995). "Northridge Earthquake January 17, 1994". Preliminary Reconaissance Report".

EERI (1995). "The Hyogo-Ken Nanbu Earthquake Great Hanshin Earthquake Disaster" January 17.

Elms, D.(2000) “Refinements to the Newmark sliding block model”. Paper nº 2132. 12th WCEE, Auckland, New Zealand.

Elnashai, A.S. et al (2010) “The Maule (Chile) Earthquake of February 27, 2010”. MAE Centre Report Nº. 10-04.

EN 1990 Eurocode 0 – “Basis of structural design”.

EN 1991 Eurocode 1 – “Actions on structures”.

EN 1992 Eurocode 2 – “Design of Concrete Structures”

EN 1993 Eurocode 3 – “Design of Steel Structures”

EN 12716 (2001) “Execution of Special Geotechnical Works-Jet Grouting.”

EN 14199 (2001) “Execution of Special Geotechnical Work-Micropile”.

EPRI (1986) – “Inspection and Performance Evaluation of Dams”, A Guide for Managers, Engineers and Operators, Prepared by Morison-Knundsen Inc. San Francisco, California.

EUROCODE Nº 7 (1993) “Geotechnical Design, General Rules. Part 1”.

EN 1998 Eurocode 8 "Structures in Seismic Regions-Design", Part 1 - Section 1 - General information

EN 1998 Eurocode 8 "Structures in Seismic Regions-Design", Part 1 - Section 2 Basis requirements and compliance criteria applicable to buildings and civil engineering works in seismic regions

EN 1998 Eurocode 8 "Structures in Seismic Regions-Design", Part 1 - Section 5 Specific rules for concrete buildings

EN 1998 Eurocode 8 "Structures in Seismic Regions-Design", Part 4 - Specific provisions relevant to tanks, silos and pipelines

Eurocode 8. (EN1998). “Design Provisions for Earthquake Resistance of Structures” - Part 5 Foundations, Retaining Structures and Geotechnical Aspects

Evers, G. (2005) “Liquefaction mitigation implementation”. NEMISREF Seminar, CD-Rom, Athenes.

FEMA – Federal Guide Lines for Dam Safety, 2004.

Finn, W.D.L. (1987) “Finite Element Handbook - Chapter 3 - Geomechanics”. Mc. Graw-Hill Editors H. Hardestuncer.

Finn, W.D.L. and Bathia, S.K. (1981) “Prediction of Seismic Pore-Water Pressures”, Proc. 10th ICSMFE, Stockholm, Vol. 3, pp. 201-206.

Finn, W.D.L. and Vaid, Y.P. (1977) “Liquefaction Potential from Drained Constant Volume Cyclic Simple Shear Tests”. 6th WCEE, New Delhi, Vol.6, pp. 7-12.

Finn, W.D.L., M. Yogendrakumar, N. Yoshida e H. Yoshida (1986). “TARA- 3: a program to compute the response of 2D embankments and soil- structure interaction systems to seismic loadings”. Department of Civil Engineering, University of British Columbia, Canada.

Fugita, K. (!982) “Prediction of Surface Settlements Caused by Shield Tunnelling”, 7 th

Furuta and Yamamoto. (2000) “Liquefaction assessment by shear wave crosshole tomography tests”. Paper nº 831. 12 th WCEE, Auckland, New Zealand.

Gazetas, G. (2001) “The 1999 Parnitha (Athens) Earthquake: Soil Effects on Distribution of Damage” XVI ICSMGE TC4 Satellite Conference on Lessons Learned from Recent Strong Earthquakes, Istanbul, pp. 5-18, Edited by A. Ansal.

Gaziev, E. (1998) “Expert system for dam safety evaluation”. International Conference on Dams, Mexico, pp.181- 188.

GEER (2010), “Geo-engineering Reconnaissance of the 2010 Maule, Chile Earthquake,” report of NSF Sponsored GEER Association Team, J. Bray & D.
Frost, eds., http://www.geerassociation.org/

GEER (2023) “FEBRUARY 6, 2023 TÜRKIYE EARTHQUAKES: REPORT ON GEOSCIENCE AND ENGINEERING IMPACTS”.

Geodynamique et Structure (1994) “Tagus bridge, Non linear dynamic free-field response analysis”.

Golafshani, A., Bakhshi, A. & Tabeshpour, M.R. (2005) “Vulnerability and Damage Analysis of Existing Buildings”, Asian Journal of Civil Engineering (Building and Housing), 6(1-2), 85-100.

Guilloux, A. and Kastner, R. (2001) "Tunneling and Underground Space Development". Proc. of the 15th International Conference on Soil Mechanics and Geotechnical Engineering, Volume 4, pp. 2607-2628.

Hamdache, M. (1998), "Seismic hazard assessment for the main seismogenic zones in North Algeria". Pure and Applied Geophysics, 152 281-314.

Hamdache, M. et al. (2003), "Accelerations in Northern Algeria using spatially-smoothed seismicity". Fifth National Conf. on Earthquake Engineering, Istanbul, paper Ae-049.

Hamdache, M. et al. (2004), "Contribution of the Algiers earthquake (Mw 6.8) of May 21 to the probabilistic seismic hazard values in northern Algeria".

Harder, Leslie F., Jr.1, Keith I. Kelson, Tadahiro Kishida3, and Robert Kayen (2011) "Preliminary Observations of the Fujinuma Dam Failure Following the March 11, 2011 Tohoku Offshore Earthquake, Japan".

Harder, L.F. and Seed, H.B (1986) "Determination of Penetration Resistance for Coarse-Grained Soils Using the Becker Hammer Drill". Report nº UCB/EERC 86/06. University of California, Berkeley.

Harr, M.E. (1984) "Reliability-based Design in Civil Engineering", Henry M. Shaw Lecture. North Carolina State University.

Hatanaka (1955) "Fundamental Considerations on the Earthquake Resistant Properties of Earth Dams". Disaster Prevention Research Institute, Kyoto University, Bulletin nº. 11.

Hazen, A. (1911) "Discussion of Dams on Sand Foundations", Transactions, ASCE, Vol. 73, p.199.

HETENYI, M. (1946) "Beams on elastic foundations". Amy Arhor. The University of Michigan press. Scientific series. Vol. XVI.

Ho, K., Leroi, E. and Roberbs, B. (2000) "Quantitative Risk Assessment: Application, Myths and Future direction", GEO Eng, 2000, Melbourne, pp. 269 – 312.

Hoeg, K. (1978) "Deformation Computations in Geotechnical Engineering". The Second Laurits Bjerrum Lecture. Norwegian Geotechnical Institute, Publications nº 123, pp.1-19."

Holeyman, A. (1992) “Keynote Lecture: Technology of Pile Dynamic Testing”. Application of Stress- Wave Theory to Piles, F. B. J. Barends (ed).

Hosri, M.S., Biarez, J. and Hicher, P.Y. (1984) “Liquefaction characteristics of Silty clay”. 7th WCEE, S. Francisco, Vol. III, pp.277-284.

I.A.E.A. (1972) "Earthquakes Guidelines for Reactors Siting". Technical Reports Series nº 139, Vienna, Austria

IAEE (International Association of Earthquake Engineering) 1992. “Earthquake Resistant Regulations. A World List –1992, 1996”.

ICOLD. (1975). “A Review if Earthquake Resistant Design of Dams”. Bulletin 27.

ICOLD (1981). “Automated Observation for the Safety Control of Dams”. Bulletin 41.

ICOLD (1983) “Seismicity and Dam Design”. Bulletin nº 46.

ICOLD (1988) Bulletin 60, Dam Monitoring-General Considerations.

ICOLD (1988) Bulletin 61. Dam Design Criteria- Philosophy of Choice.

ICOLD (1988) Bulletin 62, “Inspection of Dams After Earthquakes-Guidelines”.

ICOLD (1988) Bulletin 68, Monitoring of Dams and Their Foundations-State of the Art.

ICOLD. (1989) “Selection Seismic Parameters for Large Dams - Guidelines”. Bulletin 72.

ICOLD (1998) “World Register of Dams and Environment”. Commission on Large Dams, Paris, France.

ICOLD (1991). “Watertight Geomembranes for Dams. State of the Art”. Bulletin nº 78.

ICOLD (1992) “Dams and environment, Socioeconomic Impacts”. Bulletin nº 86.

ICOLD (1993a). “Rock Materials for Rockfill Dams”. Bulletin nº 92.

ICOLD (1993b). “Ageing of Dams and Appurtenements Works”. Bulletin nº 93.

ICOLD (1993c). “Computer Software for Dam. Validation”. Bulletin nº 94.

ICOLD (1994b) “Embankment Dams Granular Filters and Drains. Bulletin nº 95.

ICOLD (1995). “Dam Failures, Statistical Analysis”. Bulletin nº 99.

ICOLD (1997). “Position Paper on Dams and Environment”. May.

ICOLD. (1998). “Neotectonics and Dams”. Guidelines and Case Histories. Bulletin 112.

ICOLD (1999) “Seismic Observation of Dams. Guidelines and Case Studies”. Bulletin 113.

ICOLD (2000) “Automated dam monitoring systems. Guidelines and case histories”. Bulletin nº 118.

ICOLD (2001). “Design Features of Dams to Effectively Resist Seismic Ground Motions”. Bulletin 120.

ICOLD. (2002). “Earthquake Design and Evaluation of Structures Appurtenant to Dams”. Bulletin 123, Committee on Seismic Aspects of Dam Design, ICOLD, Paris.

ICOLD (2002). “Reservoir Landslide”. Bulletin 124.

ICOLD (2005a) “Dam Foundations. Geologic Considerations. Investigation Methods. Treatment. Monitoring”. Bulletin nº 129.

ICOLD (2005b) “Risk Assessment in Dam Safety Management”. Bulletin 130.

ICOLD (2008a)” Reservoirs and Seismicity. State of Knowledge”

ICOLD (2009). “Dams Surveillance”. Bulletin 138.

ICOLD (2010) “Reservoir and Seismicity-State of Knowledge”. Bulletin 137

ICOLD (2010) “Selecting Seismic parameter for large Dams”. Guidelines, Bulletin 72 Revised (final approved Hanoi 2010).

ICOLD (“Rough Version”). “Cut off for Dams”. Bulletin 150.

ICOLD (2008b). “Inspection of Dams. Following Earthquake - Guidelines”. Bulletin nº 62. 2008 Revision.

ICOLD. (2009). “Selection Seismic Parameters for Large Dams - Guidelines”. Bulletin 72. 2009 Revision.

Idriss, I, M. (1990) “Response of soft soil during earthquakes”. Proc. H. Bolton Seed Memorial Symposium, 273-290.

Idriss, I. (1995) “An overview of Earthquake Ground Motions Pertinent to Seismic Zonation. Proceedings of the fifth International Conference on Seismic Zonation., Nice. Vol. III, pp. 2111-2126.

Idriss, I. M., and Boulanger, R. W. (2004). “Semi-empirical procedures for evaluating liquefaction potential during earthquakes”, Proceedings, 11th International Conference on Soil Dynamics and 106 Earthquake Engineering, and 3rd International Conference on Earthquake Geotechnical Engineering, D. Doolin et al., eds., Stallion Press, Vol. 1, pp. 32–56.

Idriss, I.M., Lysmer, J., Hwang, R. e Seed, H.B. (1973) “Quad-4. A Computer program for evaluating the seismic response of soil structures by variable damping finite elements”. Report nº UCB/EERC 73-16, University of California, Berkeley, 1973.

INA International Navigation Association. “Seismic Design Guidelines for Port Structure”. Publisher A. Balkema. 477 pp. (2001).

Ishihara, K. (1993). “Liquefaction and flow failure during earthquakes”, 33rd Rankine Lecture. Geotechnique 43(3), pp 351-415.

Ishihara, K. (1996) “Soil behaviour in earthquakes geotechnics”. Clarendon Press. Oxford.

Ishihara, K., Mukoi, T. and Towhata, I. (1989) “In -situ Pore Water Pressures and Ground Motions during the 1987 Chiba-Toko-Oki Earthquake. SF, Vol. 29, nº 4, pp.75-90.

Ishihara, K., Yasuda, S. and Yoshida, Y. (1990) “Liquefaction induced flow failure of embankments and residual strength of silty sands”. SF, Vol. 30, nº 3, pp. 69-80,

ISSMGE Bulletin: Volume 5, Issue 2 Page 27

ITA (2004) “Guidelines for Tunnelling Risk Management”, International Tunnelling Association, Working Group Nº 2., pp.217-237.

Itasca (2009) – “FLAC 6.0. Manuals. Dynamic Analysis”.

Iwasaki, T., Tokida, K. and Kimata, T., (1981) "Studies on Estimation of Sand Liquefaction during Earthquakes and their Application to Earthquake-Resistant Design",

Janbu, N. (1957) “Earth Pressures and Bearing Capacity Calculations by Generalized Procedure of Slices”. Proc. 4th ICSMFE. London, Vol. 2, pp. 207-212.

Janbu, N. (1963) “Soil Compressibility as determined by Oedometer and Triaxial Tests. Proc. 1st ECSMFE, Rotterdam, Vol. 1, pp. 103-107.

JCSS (Joint Committee on Structural Safety) (1981) "General Principles. General Principles on Quality Assurance for Structures; General Principles on Reliability for Structural Design” IABSE; AIPC; IVBH.

Jervis Pereira, J., Oliveira, C.S. and Duarte, R.T. (1977) “Direct and Inverse Conversation from Power Spectra”, 6th WCEE, New Delhi, Vol 2, pp.279-285.

Kant, I. (1756). “Writings on the Lisbon Earthquake”. Portuguese edition of the three essays about earthquakes published in Konigsberg, Almendina, 135 pp.

Katsikas, C.A. and Wylie, .B. (1982) “Sand Liquefaction: Inelastic Effective Stress Model”. JGED, ASCE, Vol. 108, Nº GT1, pp. 63-81.

Kenney, T.C. Chahal, E., Chu, G.I. et al. (1985) “Controlling Considerations Sizes of Granular Filters”. Canadian Geotechnical Journal, 22, pp 32-43.

Kjaernsli, B, Kvale, G., Lunde, J. and Baade, J. (1982) “Design Construction, Control, and Performance of the Svartevann Earth-Rockfill Dam”. Trans XIV ICOLD, Vol. IV, 319-337, Rio de Janeiro.

Ko, H.Y. (1988) “Summary of the State-of-the-Art in Centrifuge Model Testing”. Centrifuges in Soil Mechanics. Edited by W.H.Craig, R.G. James and A.N. Schofield.

Kokusho, T. and Matsumoto, M (1997) “Nonlinear site response during the Hyogoken-Nanbu earthquake recorded by vertical arrays in view of seismic zonation methodology”. Proc of the Discussion Special Technical Session on Earthquake Geotechnical Engineering during 14th ICSMFE, Hamburg, Edited by Pedro S. Sêco e Pinto. Published by Balkema., pp. 61-69.

Kondner, R.L. and Zelasko, J.S.C. (1963) “A Hyperbolic Stress-Strain Formulation of Sands”. Proc. 2nd PACSMFE. Brazil, Vol.1, pp 289-324.

Koppula, S.D. (1984) “Pseudo-Static Analysis of Clay Slopes Subjected to Earthquakes”. Geotechnique 34, Nº: 1, pp. 71-79.

Kramer, S.L. “Performance Based Design in Geotechnical Earthquake Engineering Practice” (2011), Proc. of 5th International Conference on Earthquake Geotechnical Engineering, Santiago de Chile, pp. 161-193.

Kramer, S.L., Arduino, P. and Shin, H. (2009) “Development of Performance Criteria for Foundations”, Proc. of the Conference, Performance Based Design in Earthquake Geotechnical Engineering, pp. 107-120.

Kutter, B.L. and James, R.G. (1989) “Dynamic Centrifuge Model Tests on Clay Embankments. Geotechnique 39, Nº1, pp.91-106.

Langefors, U. and Kihlstrom, B. (1963) "The Modern Technique of Rock Blasting". Almquist and Wikshell, Stockholm.

Lee, M.K.W. and W. D.L. Finn (1978) “DESRA-1: Program for the dynamic effective stress response analysis of soil deposits including liquefaction evaluation. Rep Nº 36, Mech. Ser. Department of Civil Engineering, University of British Columbia, Vancouver.

Lempériere, F. (1999) “Risk Analysis: What sort should be applied and to which dams?”. The International Journal on Hydropower & Dams, Vol.6, pp. 128-132.

LNEC (1985) "Concrete Reinforced Structures under seismic loads” (in portuguese). Laboratório Nacional de Engenharia Civil.

LNEC (1992) "Compilation of seismic catologes in Iberic Region” (in portuguese).

LNEC (1993) “New Tagus road crossing - Geological and geotechnical studies”. (in portuguese). Volumes nº1, 2 and 3.

Lumb, P. (1975) “Soil Variability and Engineering Design”. Proc. 2nd ICASPSSE, Aachen, Vol. 1, pp.383-397.

Lysmer, J., T. Udaka, H.B. Seed and R. Hwang (1974) "LUSH 2- A computer program for complex response analysis of soil-structure systems". Report nº UCB/EERC 75-30. University of California, Berkeley.

Lysmer, J., T. Udaka, C. Tsai and H.B. Seed (1975) "A computer program for approximate 3D analysis of soil-structure interaction problems.". Report nº UCB/EERC 74-4. University of California, Berkeley.

Lysmer, J. M.T. Raissi, F. Tajirian, S. Vahdini and F. Ostadan. (1981) SASSI – A system for analysis of soil-structure interaction. Department of Civil Engineering. University of California, Berkeley,

Majumdar, D.K. (1971) "Stability of Soil Slopes under Horizontal Earthquake Force". Geotechnique 21, nº 1, pp. 84-89.

Makdisi, F. I. and Seed. H.B. (1977). "A Simplified Procedure for Estimating Earthquake Induced Deformations in Dams and Embankments". *Report nº EERC 79-19*. University of California, Berkeley.

Marachi, D., Chan, C., Seed, H.B. and Duncan, J. (1969) "Strength and Deformation Characteristics of Rockfill Materials". University of California, Report, 139p.

Marchetti, S. (1982) "Detection of Liquefiable Sand Layers by Means of Quasi-Static Penetration Tests". Proc. Of the 2nd European Symposium on Penetrating Testing, Amesterdam, Vol.2, pp. 689-695.

Marcus Vitruvius Pollio (1st century BC)

Marsal, R. and Resendiz, D. (1975) "Presas de Tierra y Enrocamento". Editorial Limusa, México, 546 p.

Matsumoto, N. (2011), "Amended 4th Quick Report on Dams," Japanese Committee on Large Dams, April 4, 2011.

Medvedev, S.V. (1968) "Evaluation of Seismic Safety during Blasting Operations in Mines". Bulletin of the Earthquake Research Institute, Vol. 46, pp. 687-696.

Meyerhof, G. G. (1956) "Discussion on paper by Skempton, Peck and MacDonald "Settlement Analysis of Six Structures in Chicago and London". Proc. Inst. (iv. Eng. 5, nº1).

Mineiro, A.J.C. (1975) “Dynamic of Brittle Soils-Applications to Microzonation and Design of Earth Dams” (in portuguese). PhD thesis, Technical University of Lisbon.

Mineiro, A.J.C (1979) “Méthodologie pour la Prevision du Comportement Séismique du Barrage de M´jara”. 13 th ICOLD, New DelQ51, pp 1047-1075.

Mineiro, A. (1985) “Retaining Structures. Tunnels in Soft Ground (in portuguese). Report. 1st Portuguese Geotechnical Congress, pp. I-85 a I-125.

Mineiro, A.C. (1988) "Simplified Method for Evaluation of seismic loads on piles” UNL Geotechnical Bulletin nº 4.

Mizuno, M. e Hirode, T. Instrumentation and Monitoring of Dams and Reservoirs in Japan. Encyclopedia of Life Supported Systems. Water Storage Transport and Distribution.

Mononobe, N., Takata, A. e Matumura, M. “Seismic Stability of the Earth Dam” (1936). 2nd ICOLD, Washington, Vol. IV.

MOPTC(1991a) (Conselho Superior de Obras Públicas e Transportes) “Dam Design Code” (in portuguese).

MOPTC(1993a) (Conselho Superior de Obras Públicas e Transportes) “Dam Construction Code”. (in portuguese).

MOPTC(1993b) (Conselho Superior de Obras Públicas e Transportes) “Dams Exploitation Code” (in portuguese).

Mora, S. and Vahrson, W. (1993) “Macrozonation methodology for landslide hazard determination”, Bull. Int. Ass. Eng. Geology,

Mortgat, C.P. et Shah, H.C. (1978)” Seismic Hazard Analysis of Algeria”. The John A. Blume Earthquake Engineering Centre. Department of Civil Engineering Stanford University.

Mosely, M.P. (1993) “Ground Improvement”. Blackie Academic and Professional.

Moulton, L. K. (1986) “Tolerable Movement Criteria for Highway Bridges”, Report Nº FHWA - TS - 85 - 228, 86 pp. Federal Highway Administration, Washington, D.C.

Moura Esteves, J. (1993) "Vibrations Control by Blasting in Construction Industry” (in Portuguese). LNEC.

Mroz, Z., V.A. Norris and O.C. Zienkiewicz (1979) “Application of an anisotropic hardening model in the analysis of elasto-plastic deformation of soils”. Advanced Topics and New Developments in Finite Element Analysis, Portoroz, pp. 18-22.

Munfakh, G. A and Wyllie, D.C. “Ground Improvement Engineering-Issues and Selection”. GeoEng 2000, Melbourne, pp.333- 359.

Naylor D.J. (1975) “Numerical Models for Clay Core Dams”. Criteria and Assumptions for Numerical analysis of Dams. D.J. Naylor, K.G. Stagg, O.C. Zienkiiewicz (ed.), Swansea, pp.490-514.

NCEE (1997) Proc. NCCE “Workshop on Evaluation of Liquefaction Resistance of Soils, Summary Report, Edited by T. Leslie Youd and I, M. Idriss, National Center for Earthquake Engineering Research, University of Buffalo, Technical Report NCEER-97-0022.

Newmark, N.M. (1965). “Effects of Earthquakes on Dams and Embankments”. Geotechnique, Vol 15, nº2, 139-160.

Newton`s (1718) - Optics

Nobari, E.S. and Duncan, J.M. (1972) “Effect of Reservoir Filling on Stresses and Movements in Earth and Rockfill Dams”. Report Nº TE 72-1. University of California, Berkeley.

NP-2074 (83) "Limit Values for Peak Vibration Velocity Valores (mm/s)" (in portuguese).

Oliveira, C.S. (1976), "Seismology, Seismicity and Risk Seismic, Applications in Portugal”. LNEC.

Ohsaki, Y. (1966) “Niigata Earthquake, 1964 Building Damage and Conditions”, SF, Vol. 6, Nº2, pp. 14-37.

Oliveira, R. (1988) “Influence of Hydropower Construction on the Engineering Geological Environment”, Report nº 730, LNEC, Lisbon.

OSMRE Regulations (1983) "Office of Surface Mining Reclamation and Enforcement"; US. Dept. of Interior.

Paré, J.J., Cabot, L. & Garzon, M. (1982) “Large Scale Permeability and Filter Tests at LG 3”. Trans XIV ICOLD, Vol. IV, 103-123, Rio de Janeiro.

Peck, R.B. (1969) “Advantages and Limitations of the Observational Method in Applied Soil Mechanics”. 9th Rankine Lecture. Geotechnique, Vol. 19. Nº2, pp. 171-187.

Peck, R. (1972) “Influence of Nontechnical Factors on the Quality of Embankment Dams”. Embankment Dam Engineering Casagrande Volume. pp 201- 208.

Peck, R. B. (1990) “Interface between Core and Downstream Filter”. H. Bolton Seed Memorial Symposium, Proc. Vol.2, BiTech Publishers, Vancouver, pp.237-251.

Peck, R.B. (1980) “Where has All the Judgement Gone”. The Fifth Laurits Bjerrum Memorial Lecture, “Canadian Geotechnical Journal”, Vol. 17, nº 4, pp. 584-590.

Pedro, J. O. (2005) “The Revision of Portuguese Regulation on Dam Safety” (in portuguese). Seminar on Dams- Technology, Safety and Interaction with the Society, Lisbon, pp 433- 446.

Peláez, et al. (2006) “Seismic hazard in terms of spectral accelerations and uniform hazard spectra in northern Algeria”. Pure and Applied Geophysics, 163, 119-135.

Penman, A D. M. (1986) “On the Embankment Dam”, Rankine Lecture, Vol.36, Nº 3, pp.301-348.

Polshin, D. E. E Tokar, R. A. (1957) “Maximum Allowable Non-uniform Settlement of Structures. Proc. 4th Int. Conference Soil Mechanics and Foundation Engineering, London, pp. 402 - 405, Butterworths Scientific Publications.

Portela, E.T.A., Pina, C., Silva, A.R., Galahrdas, H. and Barateiro, J. (2005) “Modernization of Dams information Systems (in portuguese). Seminar on Dams- Technology, Safety and Interaction with the Society, Lisbon, pp 467- 481.

Port and Harbour Research Institute (1997) “Handbook on Liquefaction Remediation of Reclamaimed Land”, pp 312.

Post, G. (1985) “Dams and foundation monitoring”. General Report. Question 56, 15th International Conference on Large Dams. Vol. 1, Lausanne.

POULOS, H: G: and DAVIS, E: H: (1980) “Pile Foundation Analysis and Design”. John Wiley and Sons. New York.

Prevost, J. (1993). “Nonlinear dynamic response analysis of soil and soil-structure interacting systems”. Proc. of the Seminar Soil Dynamics and Geotechnical Earthquake Engineering, Lisbon, pp. 49-126. Editor P. Sêco e Pinto.

P & V (1994 b) “New Tagus bridge. Computed seismic forces for piles” (in portuguese).

REAE “Steel Structures Buildings Code” (in portuguese).

REBAP (1998) “Concrete and Pre-stressed Structures” (in portuguese)

Republique of South Africa – Department of Water Affairs, Regulation regarding the safety of dams in terms of section 1.2.3 (1. National Water Act, 1998).

Régles Parasismiques Algériennes (2003) – R.P.A.99/Version 2003, D.T.R. – B.C.2.48, Ministère de l’Habitat et l’Urbanisme.

Rocha, M. (1976) “Underground Structures” (in portuguese), Universidade Nova de Lisboa.

Roberston, P.K. and Campanella, R.G. (1985) "Liquefaction Potential of Sands Using the CPT". JGED, ASCE, Vol. 111, Nº GT3, pp. 384-403.

Roberston, P.K, B.R., List and B.A. Hofmann (1995) “CANLEX (Canadian Liquefaction Experiment): A One Year Update”, Special Presentation, Proc. 3rd. Int. Conf. Recent Advances in Geotechnical Engineering and Soil Dynamics, S. Prakash (ed.) St. Louis, Mo.,Vol. II, pp.815-823.

Roberston, P.K., D.J. Woeller and W.D. L. Finn (1992) “Seismic Cone Penetration Test for Evaluating Liquefaction Potential under Cyclic Loading. Canadian Geotechnical Journal, Vol. 29, pp.686-695.

REBAP “Reinforced Concrete and Pre-stressed Concrete Structures Code” (in portuguese).

REAE “Steel Structures Codes for Buildings” (in portuguese).

Robertson, P. K. (2009). "Interpretation of cone penetration tests – a unified approach." Canadian Geotechnical Journal, 46: 1337-1355.

Rocque, A. J. and Commissioner, Jr. (2001) - "Guidelines for Inspection and Maintenance of Dams", Connecticut Department of Environmental Protection, 2001.

Romana, M (1988) "SMR Classification. In : C. Bonnard, Editor, Landslides-Glissements de Terrains", Balkema, Rotterdam, pp.955-960

Romana M. (1993) "A Geomechanical Classification for Slopes: Slope Mass Rating". J.A. Hudson, Editor, Rock Testing and Site Characterization, Pergamon, Oxford, UK, pp.575-600.

Rodrigues, F.L. (1981). Shear wave studies by crosshole method. Proc. X Int. Conf. Soil Mec. Found. Eng. Stockholm.

Royal Decree December. New Norwegian Dam Safety Regulations, 2009.

RSA (1983) "Code of Safety and Actions for Buildings and Bridges Structures" (in portuguese). Decreto-lei nº 235/83 de 31 de Maio.

Salmon, G.M. and D. N. D., Hartford (1995b) "Risk Analysis for Dam Safety - Part II". International Water Power & Dam Construction, March, pp.38-39.

Salomome, L.A., Singh, H and Fischer, J.A. (1978) "Cyclic Shear Strength of Variably Cemented Sands". Proc. EESD, ASCE, Specialty Conference. Pasadena, Vol. II, pp.819-835.

Santana, T. (1987) "An Experimental Study of Filters for Cohesive Soils" (in portuguese). UNL. Master thesis.

Sargent, R. C. (1990] "Validation of Mathematical Models". Proc. Geoval.-90, Conf. Stockholm.

Sarma, S.K. (1973) "Stability Analysis of Embankments and Slopes". Geotechnique, Vol. 23, Nº 3, pp. 423-433.

Sarma, S.H. (1975). "Seismic Stability of Earth Dams and Embankments. Geotechnique, Vol 25, nº 4, 743-76.

Sarma, S.K. and Barbosa, M.R. (1985) "Seismic Stability Analyses for Rockfill Dams with Central Clay Cores". Geotechnique, Vol. 35, nº3, pp 319-328.

Schanable, P., Lysmer, J. and Seed, H. B (1972) “SHAKE” A Computer Program for Earthquake Response Analysis of Horizontally Layered Sites. Earthquake Engineering Center Report Nº EEAC 72-12. University of California. Berkeley.

Schneider, H.R. (1997) “Definition and Determination of Characteristics Soil Properties”. Proc. 12 ICSMFE, Hamburg, Vol. 4, pp2271-2274.

Sêco e Pinto, P. S. (1982)"Instrumentation of Embankment Dams” (in portuguese). Seminar 281, Laboratório Nacional de Engenharia Civil, Lisboa.

Sêco e Pinto, P.S. (1983) “Hydraulic Fracturing in Zoned Earth and Rockfill Dams”. Research Thesis (in portuguese). LNEC.

Sêco e Pinto, P. S. (1987a) “Finite Element Analysis of Consolidation of Embankment Dam Cores”. 2nd Int. Conf. On Education, Practice and Promotion of Computational Methods in Eng. Using Small Computers. Guangzhou China, Vol. 3, pp. 545 - 548.

Sêco e Pinto, P.S. (1987b) “Quantities to be Monitored and Measuring Devices in Embankment Dams” (in portuguese). Board of Engineers Symposium, 56 p. Report 249/87 - NF, Laboratório Nacional de Engenharia Civil, Lisboa, 1987, 56 pp.

Sêco e Pinto, P.S. (1987c) “Study of Interface Materials of Corumana Dam” (in portuguese). Ibero American Conference on Hydraulic Structures, pp B.85-B. 93.

Sêco e Pinto, P.S. (1991) “Dynamic analysis of embankment dams. New developments” (in portuguese). Research Program, LNEC, 357 pp.

Sêco e Pinto, P.S. (1993) “Dynamic analysis of embankment dams”. Soil Dynamics and Geotechnical Earthquake Engineering Seminar. Edited by Sêco e Pinto. Balkema Publisher. pp. 159-269.

Sêco e Pinto, P.S. (1996a) “Considerations on the geotechnical behavior of structures during earthquakes”. Keynote. Special Session “Lessons learned from recent earthquakes”. 11th WCEE, Acapulco, Mexico.

Sêco e Pinto, P.S. (1996b) “Seismic analysis of concrete faced rockfill. General Report of Session V: Seismic Design of Earth and Concrete Dams”. International Symposium on Seismic and Environmental Aspects of Dams Design Earth, Concrete and Tailing Dams, Chile. pp. 419 - 428.

Sêco e Pinto, P.S. (1998) “Instrumentation of embankment dams; Portuguese experience”. Invited Lecture. International Conference on Dams and Reservoirs, Mexico, pp 117-132.

Sêco e Pinto, P.S. (1999) “Slopes and embankments. General Report”. Proc. of 2nd International Conference on Earthquake Geotechnical Engineering, Lisboa. Edited by Pedro Sêco e Pinto. Published by A. Balkema, Vol. 3, pp. 1059-1068.

Sêco e Pinto, P.S. (2000) “Education in Earthquake Geotechnical Engineering. Practice and Needs”. Proc. of the 1st Int. Conference on Geotechnical Engineering Education and Training, Romania. Edited by Iacint Manoliu, Ion Antonescu & Nicoleta Radulescu. Published by A. Balkema, pp. 33-45.

Sêco e Pinto, P.S. (2001) “Dam Engineering- Earthquake Aspects”. Special Lecture. Proc. of 4th ICSDEE, San Diego, CD-Rom.

Sêco e Pinto, P.S. (2002) “Some Reflections on Instrumentation of Geotechnical Structures”. 8th Portuguese Geotechnical Congress, Lisboa.

Sêco e Pinto, P.S. (2002) “Some Reflections about Risk analysis of Geotechnical Structures”. Proc. of 12th Danube- European Conference Geotechnical Engineering, Passau pp. 41-46.

Sêco e Pinto, P. S. (2003) “Seismic Behaviour of Geotechnical Structures”. Inaugural lecture, Proc. 13 th Regional African Conference of Soil Mechanics and Geotechnical Engineering pp 3- 24., Marrakech, Edited by M.Sahli, L.Bahi & R.Khalid.

Sêco e Pinto, P. S. (2004) “Seismic Behaviour of Geotechnical Structures. What Lessons Were Learned? (in portuguese) Special Volume 100, Portuguese Society for Geotechnique.

Sêco e Pinto, P.S. (2004). “Dams, Embankment and Slopes”. General Report. *Proc. of 5th ICCHGE*, New York, CD-Rom.

Sêco e Pinto, P.S. (2006) “Dam Engineering-New Challenges”. Schezy Lecture, Budapest, 33 pages.

Sêco e Pinto, P. S. (2006) “Interaction between Eurocode 7 and Eurocode 8”. Invited Lecture. Korean Geotechnical Congress, Seoul

Sêco e Pinto, P.S. (2009a). “Interaction Between Eurocode 7-Geotechnical Design and Eurocode 8-Design for Earthquake Resistance of Geotechnical Design Concept”. Special Lecture. Proceedings of the 2nd International Symposium on Geotechnical Safety & Risk, Gifu, Editors Y. Honjo, M. Susuki, T. Hara & F. Zhang, Gifu Conference, pp 51- 66.

Sêco e Pinto, P.S. (2009b). “Seismic Behaviour of Geotechnical Structures-Past, Present and Future”. Proc. of Performance-Based Design in Earthquake Geotechnical Engineering, Tokyo, Editors T. Kokusho, Y. Tsukamoto & M. Yoshimine. pp- 341-349.

Sêco e Pinto, P.S. (2011) Dam Engineering: State of the Art and State of the practice, Observed behavior and Future Challenges. Chin Lecture, Kuala Lumpur, Malaysia.

Sêco e Pinto, P.S. (2019) “Understanding Pile Foundations Design Trough Case Histories”. 3rd Braja Das Lecture, Cairo, Egypt.

Sêco e Pinto, P.S.(2019) “Pile Fondations Design. Case Histories of New Tagus Bridge and Leziria Bridge”. 3 rd Victor de Mello Lecture, Goa, India.

Sêco e Pinto, P.S., J.P. Bilé Serra, R.J.C. Câmara and S.B.M. Oliveira (1992) “Dynamic analysis of Las Cuevas Dam”. Proc. Tenth World Conference on Earthquake Engeneering, Madrid, pp. 3585-3590.

Sêco e Pinto, P.S., L. Harder, P.C. Dakoulas, A. Chugh. and H. Watanabe (1995) “Stability of slopes and earth dams under earthquakes”. General Report - Session VI, Proc. 3rd. International Conference on Recent Advances in Geotechnical Earthquake Engineering and Soil Dynamics, St. Louis, Vol. 3, pp. 1263-1272.

Sêco e Pinto, P.S and Macedo, M.S. (1974) “Vibroflotation Process in Compaction Foundation Sand of the Main Body of Massingir Dam”. LEM Publication.

Sêco e Pinto, P.S. and Portugal, J. (1991) “Monitoring of Maranhão Dam During the Reservoir Drawdown” (in portuguese). LNEC Report.

Sêco e Pinto, P. S. and Rodrigues, L. F. (1989) “Piles Integrity Tests for Boinas Bridge“, (in portuguese). 3rd National Geotechnical Congress, Porto.

Sêco e Pinto, P.S. and Santana, T. (1989) “Filters for Clay Cores of Embankment Dams”. Proceedings 12th International Conference of Soil Mechanics and Foundation Engineering, Rio de Janeiro, Agosto, Vol. 3, pp1689-1692.

Seed, H. B. (1976) “Evaluation of Soil Liquefaction Effects on Level Ground during Earthquakes”. State-of-the-Art Paper. Symposium of Liquefaction Problems in Geotechnical Engineering, ASCE, National Convention, Philadelphia, pp.1-104.

Seed, H.B.(19799 “Considerations in the Earthquake-Resistance Design of Earth and Rockfill Dams”. Geotechnique, Vol. 29, Nº 3, pp.215-263.

Seed, H.B., Arango, I., Chan, C.K., Masso, A.G. e Ascoli, R.G. (1981) "Earthquake-Induced Liquefaction near Lake Amatitlan, Guatemala", JGED, ASCE, Vol. 107, Nº GT4, pp. 501-519.

Seed, H.B., Dickenson, S.E., Riemer, M.F., Bray, J.D., Sitar, N., Mitchell, J.K., Idriss, I.M., Kayen, R.E., Kropp, A., Harder, L.F. and Power, M.S. (1990). "Preliminary Report on the Principal Geotechnical Aspects of the October 17, 1989 Loma Prieta Earthquake". Report Nº UCB/EERE 90/05. University of California, Berkeley.

Seed, H.B., Duncan, J.M. and Idriss, I.M. (1975) “Criteria and Methods for Static and Dynamic Analysis of Earth Dams. Criteria and Assumptions for Numerical Analysis of Dams. D.J. Naylor, K.G. Stagg, O.C. Zienkiewicz(ed.) Swansea, pp 563-588.

Seed, H.B. and Harder, L.F. (1990) “SPT-based Analysis of Cyclic Pore Pressure Generation and Undrained Residual Strength”. Proc. of Memorial Symposium of H. B. Seed, Vol. 2, pp. 351-376.

Seed H. B. and Idriss, I. M. (1970) “Soil Moduli and Damping Factors for Dynamic Analysis”. Report Nº UCB / EERC70-10. University of California, Berkeley.

Seed, H.B. and Idriss, I.M. (1971) "Simplified Procedure for Evaluating Soil Liquefaction Potential". JSMFD, ASCE, Vol. 97, Nº SM9, pp. 1249-1273.

Seed, H. B. and I. M. Idriss. (1982) “Ground Motions and Soil Liquefaction during Earthquakes”. Earthquake Engineering Research Institute, Oakland, California,

Seed, H.B., Idriss, I.M. and Arango, I. (1983) "Evaluation of Liquefaction Potential Using Field Performance Data". JGED, ASCE, Vol. 109, Nº GT3, pp.458-482.

Seed, H.B. and Martin, G.R. (1966) “The Seismic Coefficient in Earth Dam Design”. JSMFD, ASCE. Vol. 92, Nº SM3, pp. 59-83.

Seed, H.B. and Peacock, W.H. (1971), "Procedures for Measuring Soil Liquefaction Characteristics", JSMFD, ASCE, Vol. 97, Nº SM8, pp. 1099-1119.

Seed, H.B., Tokimatsu, K., Harder, L.F. e Chung, R.M. (1985) "Influence of SPT Procedures in Soil Liquefaction Resistance Evaluations". JGED, ASCE, Vol. 111, Nº 12, pp. 1425-1445.

Seed, H. B., Wong, R.T., Idriss, I. M. and Tokimatsu, K. (1984) “Moduli and Damping Factors for Dynamic Analyses of Cohesionless Soils”. Report Nº UCB (EERC 84/14). University of California, Berkeley.

Seed, R.B Cetin, K.O and Moss, R.E.S (2001) “Recent Advances in Soil Liquefaction Hazard Assessment”, XV ICSMGE TC4 Satellite Conference on Lessons Learned from Recent Strong Earthquakes, Istanbul, pp. 319-326. Edited by Atilla Ansal.

Seed, R.B and R.F.S., Moss (1999) “Recent Advance in US Codes and Policy with Regard to Seismic Geotechnics”. Proc. of the Second International Conference on Earthquake Geotechnical Engineering, Lisbon, Vol. 3, pp.1111 - 1116. Edited by Pedro Sêco e Pinto. Published by A. Balkema,

“SHAKE” A Computer Program for Earthquake Response Analysis of Horizontally Layered Sites. Earthquake Engineering Center Report Nº EEAC 72-12. University of California. Berkeley

Shen, Z.J., Huang, J.D. and Wang, Z.N. (1985) “Analysis of Liquefaction and Deformation of Douhe Earth Dam during Tangshan Earthquake”. Proc. 5th ICNMG, Nagoya. Vol. 3. pp.1387-1392.

Sherard, J. L. (1973) “Contributions to Embankment Dam Engineering”. Embankment Dam Engineering Casagrande Volume, John Wiley and Sons, pp. 211-353.

Sherard, J. L. (1986) “Hydraulic Fracturing in Embankment Dams”. ASCE Journal of Geotechnical Engineering, Vol. 112, Nº 10, pp. 905 - 927.

Sherard, J. L. Dunnigan, L.P. and J.R. Talbot. (1984) “Basic Properties of Sand and Gravel Filters. JGED, ASCE, Vol. Nº 110, Nº GT 6, pp 684-699.

Singh, A. (1971) “How Reliable is the Factor of Safety in Foundation Engineering?” Proc. 1st ICASPSSE. Hong Kong, Vol. 1, pp. 390-424.

Skempton, A. W. E MacDonald, D. H. (1956) “Allowable Settlement of Buildings”. Proc. Institute of Civil Engineers, Part 3, nº 5, pp 727 - 768.

Specifications DIN 4150 (1986) "German Specifications related with Vibrations".

Specifications SN-640312 (1979) "Suisse Specifications related with Reference Values".

SRB - Subcommission of Dam Codes (1990a) “Dams Safety Code” (in portuguese).

Stokoe, K.H. II, M. B. Darendeli, R.D., Andrus and L.T., Brown (1999) “Dynamic Soil Properties: Laboratory, Field and Correlation Studies”. Theme Lecture. Proc. of 2nd International Conference

on Earthquake Geotechnical Engineering, Lisboa. Edited by Pedro Sêco e Pinto. Published by A. Balkema, Vol.3, pp. 811-845.

Stokoe, K.H. II, M. B. Darendeli, Menq, F., Y., Choi, W.K. (2004) "Comparison of the Linear and Nonlinear Dynamic Properties of Gravels, Sanda, Silts and Clays. Theme Lecture". Proc. of 3rd International Conference on Earthquake Geotechnical Engineering, Berkeley, Edited by Doolin et al., Vol.1, pp. 1-4.

Sun, J.I., Golesorkhi, R. and Seed, H.B. (1988) "Dynamic Moduli and Damping Ratios for Cohesive Soils". Report Nº UCB/EERC-88/15. University of California, Berkeley.

Tanizawa, F., Iwasaki, K., Zhou, S. and Tatsuoka, F. (1988) "Evaluation of Liquefaction Strength of Sand by Using Cone Penetration Test". Proc. 9th WCEE. Tokyo, Vol. III, pp. 201-206.

TC4 (ISSMGE). (2001). "Case Histories of Post-Liquefaction Remediation". Committee on Earthquake Geotechnical Engineering. Technical Committee for Earthquake Geotechnical Engineering,

TC4, ISSMFE, (1993) "Manual for Zonation of Seismic Geotechnical Hazards", published by the Japanese Society of Soil Mechanics and Foundation Engineering, Tokyo.

Tejoprojecto (1995) "New Road Crossing of the Tagus in Lisbon. Evaluation of Liquefaction Potential. Final report" (Volumes 1 and 2).

Terzaghi, K. and Peck, R. B. (1948) "Soft Mechanics in Engineering Practice", John, John Wiley and Sons, New - York.

Todorovska, M. I. and M. D. Trifunac (1999) "Liquefaction Opportunity Mapping via Seismic Wave Energy". J.G.G.E., Vol. 125, nº 12, pp. 1032-1042.

Tokimatsu, K., S. Kuwayama and S. Tamura (1991). "Liquefaction Potential Evaluation based on Rayleigh Wave Investigation and its Comparison with Field Behavior". Proceedings 2nd Int. Conf. On Recent Advances in Geotech. Earthquake Eng. And Soil Dynamics, March 11-15, St. Louis, Vol. I, pp. 357-364, 1991.

Tokimatsu, K. and Seed, H.B, (1984) Simplified Procedure for the Evaluation of Settlements in Clean Sands. Report nº UCB/EERC 84/16. University of California.

Tokimatsu, K. and Seed, H. B. (1987) "Evaluation of Settlements in Sands due to Earthquake Shaking", JGE, ASCE, 113, pp. 861-878.

Tohimatsu, K. and Yoshimi, Y. (1984) “Criteria of Soil Liquefaction with SPT and Fines Content”. Proc. Of 8th WCEE, Francisco, Vol.III, pp.255-262.

Towhata, I. (2008) Geotechnical Earthquake Engineering. Springer, pp.678.

Towhata, Ikuo; Goto, Hiroyuki; Kazama, Motoki; Kiyota, Takashi; Nakamura, Susumu; Wakamatsu, Kazue; Wakai, Akihiko; Yasuda, Susumu; and Yoshida, Nozomu (2011), “On Gigantic Tohoku Pacific Earthquake in Japan,” Earthquake News, Bulletin of the International Society for Soil Mechanics and Geotechnical Engineering, Volume 5, Issue 2, April.

UBC (Uniform Building Code). (1997). “International Conference of Building Officials”, Whittier, California, Vol. II.

Udias, A. and Arroyo, A.L. (2005) “The Lisbon Earthquake of 1755 in Spanish Contemporary Authors”. 250 th Anniversary of the 1755 Lisbon Earthquake, Lisbon, pp 19- 29.

United States Geological Survey (2011), “Shake Map for 2011 Tohoku Earthquake, March 13”,

Upsall, S. B. (2006) “Instrumental Intensity Scales for Geotechnical and Structural Damage”. PhD Dissertation, University of Washington, Seattle, Washington, 403 p.

U.S.A.E.C. (1973) "Design of Nuclear Powerplants". Regulatory Guide 1-60.

US Department of the Interior, Bureau of Reclamation, (1987). “Design Standards Nº 13 - Embankment Dams”. Chapter 5-Protective Filters, May.

USACE (1987) “Hydraulic Design Criteria”. United States Army Corps of Engineers.

USACE (1990) “Hydraulic Design of Spillways”. Engineer Manual 1110-2-1603. United States Army Corps of Engineers.

USACE (1994) “Standard Practice for Concrete for Civil Works Structures”. Engineer Manual 1110-2-2000. United States Army Corps of Engineers.

USACE (1995) “Gravity Dam Design. Engineer Manual 1110-2-2200”. United States Army Corps of Engineers.

USACE (2005) “Stability Analysis of Concrete Structures. Engineer”. Manual 1110-2-2100. United States Army Corps of Engineers.

USASE (2011) ER 1110 – 2 – 1156, “Engineering and Design Safety of Dams – Policy and Procedures”.

USACE (2016) “Strength Design for Reinforced Concrete Hydraulic Structures. Engineer”. Manual 1110-2-2104. United States Army Corps of Engineers.

USBR (1974). “Earth Manual”. A Water Resources Technical Publication.

USBR (1978) “Hydraulic Design of Stilling Basins and Energy Dissipators. Engineering Monograph” No. 25. United States Department of the Interior, Bureau of Reclamation

USBR (1981), “Freeboard Criteria and Guidelines for Computing Freeboard Allowances for Storage Dams”, U.S. Department of the Interior, Bureau of Reclamation

USBR (1981). “Design of Small Dams”. A Water Resources Technical Publication.

USBR (1981). “Freeboard Criteria and Guidelines for Computing Freeboard Allowances for Storage Dams”, U.S. Department of the Interior, Bureau of Reclamation.

USBR (1983) “Manual Safety of Existing Dams”-United States Department of Interior.

US Department of Homeland Security Federal Emergency Management Agency.

USBR (1987) “Design of Small Dams”. United States Department of the Interior, Bureau of Reclamation

USBR (1987) “Concrete Dams Instrumentation” United States Department of Interior.

US Department of the Interior, Bureau of Reclamation, (1987) “Design Standards Nº 13-Embankment Dams”, Chapter 5-Protective Filters, May.

US Department of the Interior Water and Power Resources Service, Denver Colorado (2004).

United States Emergency Management Agency. Federal Guidelines for Dam Safety Emergency "Action Planning for Dam Owners".

USBR (2012), "Design Standards No. 13 – Embankment Dams", Chapter 6 – Freeboard, U.S. Department of the Interior, Bureau of Reclamation

Vaid, P.Y., Byrne, P.M. and Hughes, J.M.D (1981) "Dilation Angle and Liquefaction Potential". JGED, ASCE, Vol.107, NºGT7, pp.1003-1008.

Vanmarke, E.H (1977) "Probabilistic Modeling of Soil Properties". JGED, ASCE, Vol. 103, Nº GT 11, pp.1227-1246.

Vanmarke, E.H (1984) "Risk Management to Improve Dam Safety". Proc. Of the International Conference on Safety Dams". Coimbra, Vol.2, pp.557-562.

Vaughan, P.R. and Soares, H.F. (1982) "Design of Filters for Clay Cores of Dams". JGED, ASCE, Vol. 108, Nº GT1, pp. 17-31.

Veiga Pinto, A. (1982) "Rockfill Modelation" (in portuguese). Master thesis. Universidade Nova de Lisboa.

Veiga Pinto, A. (1983) "Prediction of Structural Behavior of Rockfill Dams" (in portuguese) Doctoral thesis.

Voltaire (1759). "Candide. Oeuvres Completes", 9, vol., edit. Moland, Paris 1877.

Wang, W. (1984) "Earthquake Damages to Earth Dams and Levees in relation to Soil Liquefaction and Weakness in Soft Clays". Proc. ICCHGE, St. Louis. Vol.1, pp.511-521.

Wieland, M. (2003) "Seismic Aspects of Dams". General Report Q 83, 21 st ICOLD, Montreal.

Wilson, E. (1993) "The Essential Descartes". A Meridian Book.

Wilson, J. (2009): Canterbury region – Landscapes, Te Ara - the Encyclopaedia of New Zealand, http://www.TeAra.govt.nz/en/canterbury-region/3.

Wolski, W. Furstenberg, A. Mioduszewski, W. e Reczek, J. (1970) “Protection Against Piping of Dam Cores of Flysch Origin Cohesive Soils”. Trans. X ICOLD, Montreal. Vol. I, pp 575-585.

Wong, K.S. and Duncan, J.M. (1974) “Hyperbolic Stress -Strain Parameters for Nonlinear finite Element Analyses of Stresses and Movements in Soil Masses. Report nº TE-74-3. University of California, Berkeley.

WRPT - (Water Technical Publication) (1980) "Safety Evaluation of Existing Dams", US Department of the Interior Water and Power Resources Service, Denver Colorado.

Voltaire (1759). “Candide. Oeuvres Completes”, 9, vol., edit. Moland, Paris 1877.

Xanthakos, P. (1995) “Bridge Substructure and Foundation Design”. Prentice Hall.

Yamada, S, Orense, R., Cubrinovski, M. (2011) “Earthquake News Geotechnical Damage due to the 2011 Christchurch, New Zealand”, ISSMGE Bulletin, Vol.5, Issue 2 ISSMGE Bulletin: Volume 5, Issue 2

Yasuda, S. (1999) “Seismic Design Codes for Liquefaction in Asia”. Proc. of the Second International Conference on Earthquake geotechnical Engineering. Edited by Pedro S. Sêco e Pinto. Published by Balkema. Vol. 3, pp. 1117-1122.

Yasuda, S. (2009) “Relevant Soil Investigations and Laboratory Tests to Estimate Liquefaction-Induced Deformation of Structures”, Proc. of the Conference, Performance Based Design in Earthquake Geotechnical Engineering, pp. 259-263.

Yasuda, S. and Berril, J.B. (2000) “Observations of the Earthquake Response of Foundations in Soil Profiles Containing Saturated Sands”. Proc. Geo Eng 2000, Melbourne, pp, 1441-1470.

Yasuda, S., Irisawa, T. E, Kazami, K. (2001) “Liquefaction Induced Settlements of Buildings and Damages in Costal Areas during the Kocaeli and other Earthquakes”. XY ICSMGE Satellite Conference on Lessons Learned from Recent Strong Earthquakes, pp 33- 42.

Yelles-Chaouche, A., Boudiaff, A. Djellit, Hamou e Bracene, R., (2006) “La Tectonique Active de la Région Nord-Algérienne”. C. R. Geoscience 338 (2006) 126-139.

Youd, T. L. e S. D. Gilstrap (1999) “Liquefaction and Deformation of Silty and Fine-Grained Soils.” General Report. Proc. of 2nd International Conference on Earthquake Geotechnical

Engineering, Lisboa, Vol.3, pp. 1013-1020. Edited by Pedro Sêco e Pinto. Published by A. Balkema,

Whitman, R.V. (1984) “Evaluating Calculated Risk in Geotechnical Engineering”, JGED, ASCE, Vol. 110, nº GT2, 145-188.

Wolf, J.P. (1985). “Dynamic Soil-Structure Interaction”. Prentice- Hall.

WRPT - (Water Technical Publication) - "Safety Evaluation of Existing Dams", A Manual for the Safety Evaluation of Embankment and Concrete Dams, 1980.

Zhou, S.G. (1981) "Influence of Fines on Evaluating Liquefaction of Sand by CPT". Proc. ICRAGEESD, St. Louis, Vol. II, pp.167-172.

ANNEXES

Everything has beauty,
But not everyone sees it

Confucius

ANNEX 1

Specifications for Site Investigation Works

Testing

A.1 PLANNING OF GEOTECHNICAL CHARACTERIZATION

Geotechnical characterization is related with ground investigations;

general requirements for a number of commonly used laboratory and field tests;

interpretation and evaluation of test results;

derivation of values of geotechnical parameters and coefficients.

Prior to the carrying out of tests, the test plan will contain the objectives of the test and all specifications necessary for the selection or production of the test specimens, the execution of the tests and the test evaluation. The test plan will cover.

objectives and scope;

prediction of test results;

specification of test specimens and sampling;

loading specifications;

testing arrangement;

measurements;

evaluation and reporting of the tests.

The objective of the tests will be clearly stated, e.g. the required properties, the influence of certain design parameters varied during the test and the range of validity. Limitations of the test and required conversions (e.g. scaling effects) will be specified.
All properties and circumstances that can influence the prediction of test results will be taken into account, including:

geometrical parameters and their variability;

geometrical imperfections;

material properties;

parameters influenced by fabrication and execution procedures;

scale effects of environmental conditions taking into account, if relevant, any sequencing.

Test specimens will be specified, or obtained by sampling, in such a way as to represent the conditions of the real structure.

Factors to be taken into account include:

dimensions and tolerances;

material and fabrication of prototypes;

number of test specimens;

sampling procedures;

restraints.

The objective of the sampling procedure will be to obtain a statistically representative sample. Attention should be drawn to any difference between the test specimens and the product population that could influence the test results.

A 1.1 LOCATION OF INVESTIGATIONS POINTS

The location of investigation points and the depth of the investigations shall be selected on the basis of the geological conditions, the dimensions of the structure and the engineering problems involved.

The following will be observed:

a) "the investigation points should be arranged in such a pattern, that the stratification can be assessed across the site.

b) investigation points are arranged so that they do not present a hazard to the structure, the construction work, or the surroundings (e.g. as a result of the changes they may cause to the ground and water conditions).

c) the area considered in the design investigations extends into the neighbouring area to a distance where no harmful influence on the neighboring area is expected, for example 1,5 times the expected excavation depth. For groundwater table lowering, the affected area may be much larger.

d) for groundwater measuring points the possibility of using the equipment installed during the ground investigation for continued monitoring during and after the construction period is considered".

A1.2 RECOMMENDATIONS FOR DEPTH OF INVESTIGATIONS

For the investigation depth z_a the following values should be used as guidance. The reference level for z_a is the lowest point of the foundation of the structure or structural element, or the excavation base.

Greater investigation depths should always be selected where unfavourable geological conditions, such as weak or compressible strata below strata of higher bearing capacity, are presumed.

For dams:

$0.8\ h < z_a < 1.2\ h$

where h is the embankment height.

Boreholes

The mechanical borehole drillings with continuous sampling works shall comply with the following guidelines:

The exact location of each borehole shall be assessed by topographic implantation.

In the event of need of relocating of any work (for example, to contour an obstacle), such fact shall be immediately communicated to the Client and the Contractor shall submit a new location for approval.

A drilling report shall be prepared for each borehole, containing the following information:

The designation and location of the borehole;

The type of drilling and respective diameters used;

The type of equipment and sampling tubes used;

The ground level at the borehole mouth;

The date of commencement and completion of the borehole;

The depth and lithological description of the several geological formations encountered and the respective geological units;

Indication of the water level after completion of the borehole and after stabilization;

The weathering and fracturing degree of the rock mass;

The percentage of recovery and the RQD;

Anomalies encountered (rock mass joints, faults, cracks, etc.) and their inclination referring to the borehole axis;

Depths and results of water absorption tests;

All annotations considered relevant for a good interpretation of the boreholes.

Core samples shall be duly stored in plastic or dry wooden boxes made in carpentry, with hinges and locks or other equivalent fittings. Samples shall be arranged according to their sampling order and separated by wooden markers indicating the sampling limits. A photo report of the boxes containing the samples shall be subsequently carried out.

The name of the project, the borehole designation and the sampling limits shall be clearly identified with waterproof ink at the casing and at the top of each sample box.

Boxes' length shall be equal to 1.0 m, and their width and height shall allow the storage of four strings of cores detached by fixed separating pieces. Boxes shall be duly arranged and stored at a location sheltered from weather and ground contact.

Upon completion of the works, the boxes containing the sample cores shall be delivered to the Client at a designated location

The methodology for the execution of boreholes with core sampling, should respect the following operations:

- Correct identification of the borehole site, with the aid of a topographer;
- Placing of the sampling equipment in its respective place;
- Correct placing and adjustment of the bits to the rod and to the double core sampler;
- Beginning of the drilling with gathering of the test cores at the end of each maneuver;
- Placing of test cores in wooden boxes, approximately 1 m long, arranged from above downwards and from left to right as the drilling advances deeper;

- Identification of all the maneuvers, by separation of the respective test cores with a wooden piece where the maneuver's final depth is marked;
- Identification of the sounding boxes, with inscription of the sounding number, box number, depth of maneuvers and name of job;
- Placing of boxes in a safe place, not exposed to the sun or to large temperature variations and moisture.
- Execution, by the operator, for each borehole, of a daily record where he identifies the borehole, site, job, date and the number and length of maneuvers, lithologic description, the presence of water and its level at the beginning and at the end of the drilling, as well as other observations considered to be important.

The double wall samplers comprise an exterior tube that acts by rotary cut and which lower end is provided with hard steel jagged bit. The inner tube - sample carrier - which is maintained fixed because it adheres to the sample, is much longer than the outer tube, enabling the sample to be protected from circulating liquids.

The boxes containing the respective test cores should be the technician (Geological Engineer) in according to criteria established by the International Society for Rock Mechanics (ISRM).

Tables A1.1 and A1.2 present, respectively, the classifications for rocky massifs relative to weathering and fracture grades, defined by the ISRM.

The field geologic logs gave the information related the recovery percentage, comprises a parameter that is similarly to the RQD, represents the massif quality and corresponds to the ratio between the total length of the sampled material and the total length of the manoeuvre. The RQD only represents the total length of the test cores inside each manoeuvre with a length equal to or larger than 10 cm. Both rates, recovery and RQD, are presented as a percentage, so as to make it easier to conceive the massif quality.

Table A1.1 Weathering Grades for the Rock Mass

Term	Description	Grade
Fresh	No visible sign of rock material weathering; perhaps slight discoloration on major discontinuity surfaces	W1
Slightly weathered	Discoloration indicates weathering of rock material and discontinuity surfaces	W2
Moderately weathered	Less than thirty five per cent of the rock material is decomposed and/or disintegrated to a soil. Fresh or discoloured rock is present either as a continuous framework or as core stones.	W3

Highly weathered	More than thirty five per cent of the rock material is decomposed and/or disintegrated to soil. Fresh or discoloured rock is present either as a continuous framework or as core stones	W4
Extremely weathered	All rock material is decomposed and/or disintegrated to soil. The original mass structure is still largely intact	W5

Table A1.2 Discontinuity Spacing

Term	Spacing	Grade
Very widely spaced	Over 2 m	F1
Widely spaced	600 mm - 2 m	F2
Medium spaced	200 mm - 600 mm	F3
Closely spaced	60 mm - 200 mm	F4
Very closely spaced	Under 60 mm	F5

As from the overall analysis of the results obtained for all methods of geotechnical prospecting used: geophysics, destructive drilling and boreholes with core sampling, it is possible to establish a few comparisons.

A.1.3 QUALITY OF SOIL SAMPLES

Soil samples for laboratory tests are divided in five quality classes with respect to the soil properties that are assumed to remain unchanged during sampling and handling, transport and storage. The classes are described in Table A1.3, together with the sampling category to be used.

Table A1.3 Quality classes of soil samples for laboratory testing and sampling categories to be used

Soil properties / quality class	1	2	3	4	5
Unchanged soil properties	x	x	x	x	
particle size, water content	x	x	x		
density, density index, permeability,	x	x			
compressibility, shear strength	x				
Properties that can be determined sequence of layers	x	x	x	x	x
boundaries of strata – broad	x	x	x	x	
boundaries of strata - fine	x	x			
Atterberg limits, particle density, organic content	x	x	x	x	
water content,	x	x	x		
density, density index, porosity, permeability	x	x			
compressibility, shear strength	x				

Sampling category according to EN ISO 22475-1	**A**				
			B		
					C

A 1. 4 Static Characterization

The field investigation programme will contain:

- a plan with the locations of the investigation points including the types of investigations;
- the depth of the investigations;
- the type of samples (category, etc) to be taken including specifications on the number and
- depth at which they are to be taken;
- specifications on the ground water measurement;
- the types of equipment to be used;
- the standards that are to be applied.

The laboratory test programme depends in part on whether comparable experience exists.
The extent and quality of comparable experience for the specific soil or rock should be established.
The tests will be run on specimens representative of the relevant strata. Classification tests shall be used to check whether the samples and test specimens are representative.
This can be checked in an iterative way. In a first step classification tests and strength index tests are performed on as many samples as possible to determine the variability of the index properties of a stratum. In a second step the representativeness of strength and compressibility tests can be checked by comparing the results of the classification and strength index tests of the tested sample with entire results of the classification and strength index tests of the stratum.
The evaluation of geotechnical parameters by static field and laboratory tests are summarised in Tables A1.4 and A1.5, where the symbols are (Sêco e Pinto, 2009a):

γ = bulk density

I_d = relative density

K_o = coefficient of earth pressure at rest

G_{max} = maximum shear modulus

OCR = overconsolidation ratio

c = cohesion

S = sensivity

ϕ = friction angle

V_s = transverse wave velocity

E = elasticity modulus

V_p = longitudinal wave velocity

S_u= undrained strength

M = confined modulus

G = shear modulus

ß = damping ratio

Table A1. 4 Field tests

Test	Parameters for stress state					Strength Parameters			Parameters for deformation		
	γ	I_d	K_o	OCR	S	S_u	c	ϕ	E	G_{max}	M
CPTU	x	x	x	x	x	x	x	x	x		x
SPT		x			x	x	x	x	x		x
Vane shear			x	x	x	x	x		x		
Pressiometer			x			x	x	x	x		

Penetrometer						x	x	x	x		
Dilatometer	x	x		x		x		x	x	x	x
Plate load						x			x		

Table A1.5 Laboratory tests

Test	Strength Parameters			Deformation Parameters		
	S_u	c	ϕ	E	G_{max}	M
Direct shear		x	x			
Uniaxial compression				x		
Triaxial	x	x	x	x		
Oedoemeter						x

A.1.5 Seismic tests

The seismic test, both field tests and laboratory tests are described in item A.7.

A.2 Laboratory tests on soils and rocks

General

The laboratory test program shall be established in conjunction with the other parts of the ground investigation program (see more details in Section 2).
Whenever possible, the information obtained from field tests and soundings should be used for selecting the test samples.

General requirements for laboratory tests

The requirements given in this section should be considered a minimum.
Additional specifications, additional presentation requirements or additional interpretation, as appropriate for the ground conditions or geotechnical aspects of interest, may be required.
Details of the tests required to determine the parameters needed for design shall be specified.

Procedures, equipment and presentation

A test, for which a standard exists, should be carried out and reported according to that standard. A test, for which no standard exists, should be carried out in accordance with procedures which comply with the requirements given in the paragraphs for each test.
ISO/CEN standards, for ground investigation and testing, shall be observed and referenced, when they become available.
NOTE EN-ISO standards are under preparation for some laboratory tests.
Provided the requirements of this standard are met, alternative test methods and procedures may be selected.
NOTE The test procedures can be reported by reference to documents that are recognised internationally by the geotechnical profession.
Checks shall be made that the laboratory equipment used is adequate, fit for purpose, is calibrated and within the calibration requirements.
The reliability of the equipment and procedures should be checked by comparing the test results with data obtained on comparable soil or rock types.
The test methods and procedures used shall be reported together with the test results. Any

deviations from a standard test procedure shall be reported and justified.
If appropriate, the results of laboratory soil classification tests should be presented together with the soil profile on a plot summarising the soil description and all classification results.
If possible and required, the location of the other laboratory tests (such as oedometer and triaxial tests) should be indicated on the same figure.

Evaluation of test results

Requirements for evaluation of laboratory test results are given in 6.3.
Results of individual tests should be compared with other test results to check that no contradiction exists between the available data.
The test results should be checked with values found in the literature, correlations with index properties and comparable experience.
Laboratory tests on soils and rock prEN 1997-2: Aug 2003 47

Quality assurance and quality control
An appropriate quality assurance system shall be in place in the laboratory and engineering office, and quality control shall be exercised competently in all phases of the laboratory testing and evaluation of the test results.
Preparation of soil specimens for testing
The objective of the preparation of soil for laboratory tests is to provide test specimens that are as representative as possible of the soil from which the samples are taken.
For the purposes of preparation, five types of soil specimens may be distinguished: disturbed, undisturbed, re-compacted, remoulded and re-constituted specimens.

Requirements

The soil specimen used for testing shall be sufficiently large to take account of:
− the largest size of particles presented in significant quantity,
− the natural features such as structure and fabric (e.g., discontinuities).

Requirements of EN-ISO 22475-1 shall be observed.
All samples shall be clearly and unambiguously labelled.
Soil samples shall be protected at all times against damage and deterioration, and excessive changes in temperature. Special care shall be taken with undisturbed samples to prevent distortion and loss of water during preparation of test specimens. The material used for the sampling containers shall not react with the contained soil.
Soil shall not be allowed to dry before testing when the test results can be affected by a loss of moisture.
Undisturbed samples should be prepared under conditions of controlled humidity. If preparation is interrupted, the specimen should be protected from changes in water content.
When disaggregation processes are applied, breaking down of individual particles shall be avoided.
If special treatment of bonded and cemented soils is required, this shall be specified.
Subdivision methods shall ensure that representative portions are obtained, avoiding segregation of large particles.

Preparation of rock specimens for testing

The objective of preparing specimens for testing of rock is to provide specimens that are as representative as possible of a rock formation.
Laboratory tests on soils and rock prEN 1997-2: Aug 2003 48
It shall be specified how a rock specimen shall be prepared. If these specifications cannot be met, the specimen shall be prepared as near to the specifications as possible and it shall be reported how the specimen has been prepared.

All instruments and assemblies for determining straightness, flatness and perpendicularity of end surfaces shall be controlled on a registered regular time basis having tolerances satisfying at least the requirements of the specific rock tests
The following shall be specified:
−storage conditions for rock samples (short term and/or long term storage),
−moisture condition of the test specimens at the time of the test,
−method for preparing rock core specimens,
−method for determining dimension and shape tolerances.
Any change in water content should be avoided. If a change in the natural water content should occur, its effect shall be counteracted as part of the preparation for testing.
The cause and effect of any change in water content should be reported.
The need for recoring to a specified dimension shall be defined with reference to laboratory coring method, coolant applied and the need for re-saturation of the test specimens.
Together with the data and results for the particular test, the following should be recorded and reported:
−source of test specimen, including depth/level and orientation in space,
−dates of specimen preparation and testing,
−comments on the representativeness of the specimen(s) tested,
−all dimension and shape measurements, including conformance with requirements,
−water content of the sample/specimen (as received, during preparation, saturated),
−conditions for drying (air- or oven-drying, pressurised or partial vacuum).
The following information on the samples should be given for the interpretation of the test results:
−physical description of the specimen including rock type (such as sandstone, limestone, granite, etc.), location and orientation of inherent rock structural features and any discontinuities, and inclusions or inhomogeneities,
−sketch of the test specimen or a colour photograph for other than monotonous homogeneous rock types,
−core Recovery and Rock Quality Designation, where possible,
−data to substantiate the tolerance checks on straightness of elements on cylindrical surface, flatness of end bearing surfaces and perpendicularity of end surfaces with respect to axis of core.

Characterization of Materials

The site investigation works includes seismic refraction profiles and boreholes, identification tests (sieve analysis and Atterberg limits), density tests and compaction tests (Proctor normal).

In addition, the strength tests such as triaxial tests (CU) and direct shear tests, as well permeability tests and oedometer tests.

The geophysical parameters depend on various factors, the most significant being the type and quality of the massif, namely in terms of mineralogical composition (presence of different mineral concentrations, as well as elements with different conductivity), presence of discontinuities, namely veins, faults or other geological structures, existence or not of water levels, of voids, and material related to mine shafts, etc.

A.3 Characterization of rock materials

In this chapter an analysis of the geotechnical characterization of rock materials is presented.

USBR Practice

It is important to refer that USBR (United States Bureau of Reclamation) (1981) recommends the execution of physical, chemical and petrographic tests for the rock materials.
For the definition of physical properties of the rock materials the following tests should be performed:

- density of the particles;
- absorption tests;
- % of material passing in sieve ASTM 200;
- sieve analysis;
- Los Angeles.

The petrographic tests complement the physical tests and are of great importance. USBR proposes for the physical characterization three levels: satisfactory, reasonable and poor, based in the contribution of rocks for the strength, abrasativity and durability of concrete. The physical characterization has the purposes to analyze the chemical reaction of particles with the alkalis of the cement.

ICOLD Bulletin nº 76

It is important to mention that Bulletin nº 76 "Classic Methods for Dam Construction. Revision." Recommends for the design the rule of 6 P "Proper Prior Planning Prevents Poor Performances".
Bulletin nº 76 recommends special cares for the study and characterization of rock materials, for the concrete and fill materials for the dam and appurtenance works. The characteristics of rock materials should be defined by adequate laboratory tests and petrographic studies:
For the aggregates study it is important to consider:

- sieve analysis;
- maximum dimension;
- shape coefficient;
- contaminant products;
- mechanical strength.

.

A.4 Mechanical Rockfill properties

Some correlations between mechanical properties and crushing tests were proposed by Delgado Rodrigues et al. (1982) and presented in Figure A1.1 and Figure A1.2.
Becker et. al. (1972) have carefully evaluated the mechanical properties of rockfill materials placed in Oroville dam, Pyramid dam and Venato dam.
The results obtained by triaxial tests and plane strain tests are summarized in Figure A1.3 and can be used to calibrate the results of rockfill materials.

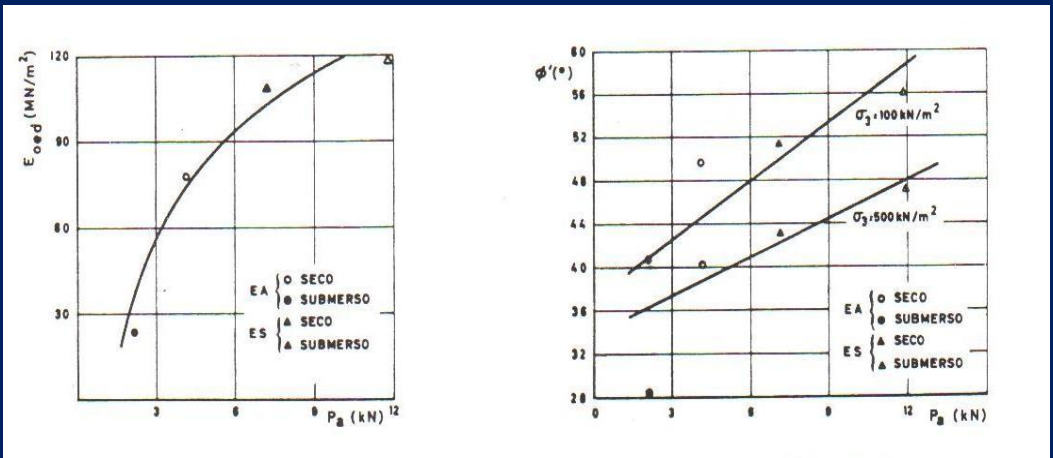

Figure A1.1 Relationship between mechanical properties and crushing test for rockfill materials (Delgado Rodrigues et al, 1982)

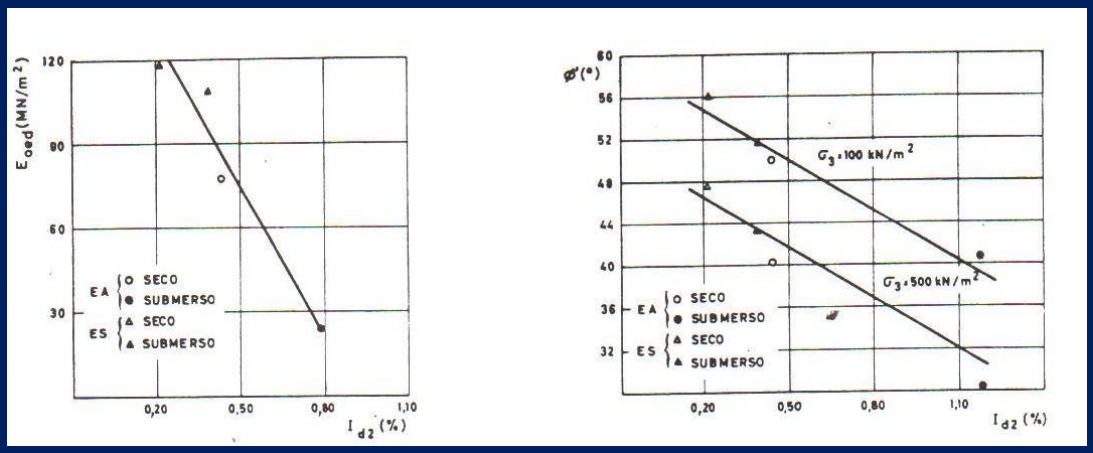

Figure A1.2 Relationship between mechanical properties and slake test for rockfill materials (Delgado Rodrigues et al, 1982)

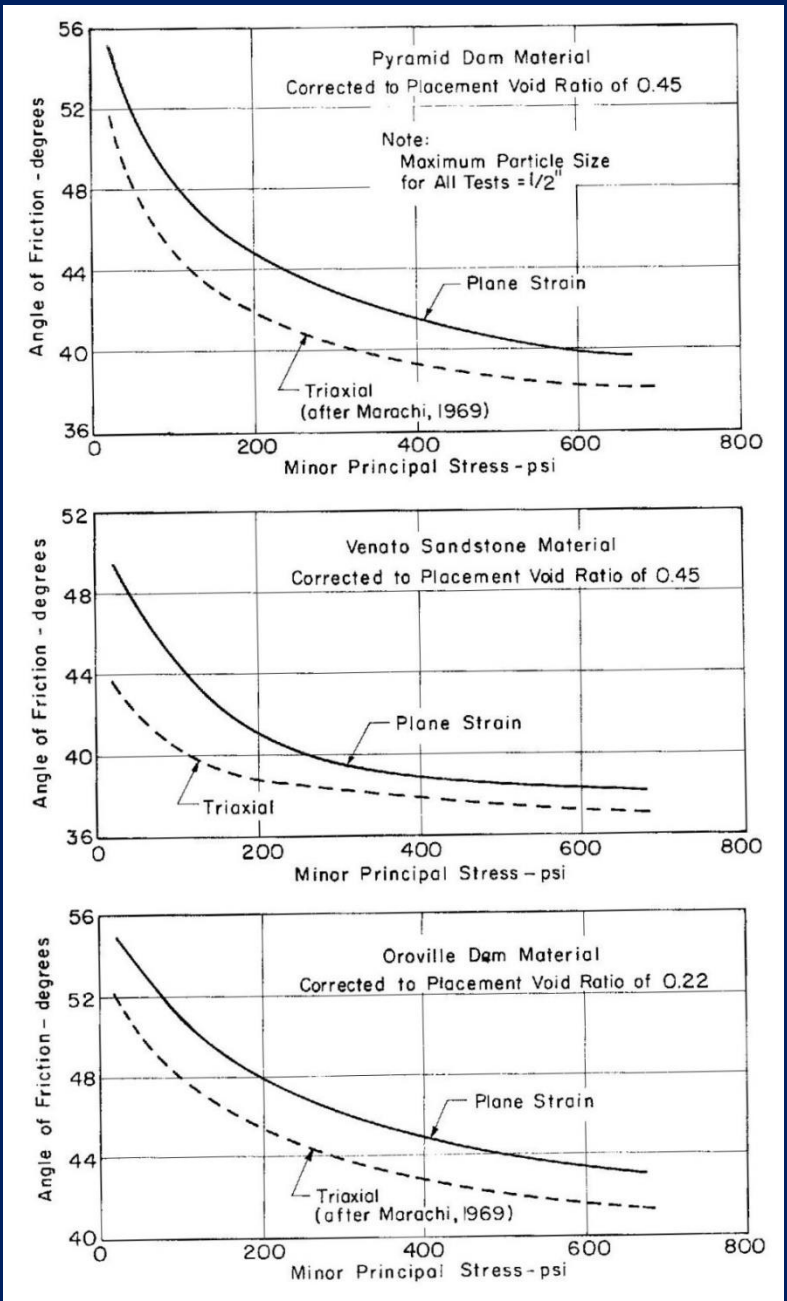

Figure A1.3 Variation of friction angle of rockfill materials in triaxial tests and plane tests (after Becker et. al. (1972).

A. 5 Ground Investigation Report

Introduction

The ground investigation report includes the presentation of Geotechnical Information and evaluation of Geotechnical Information.

Presentation of Geotechnical Information

The presentation of geotechnical information with documentation of the methods procedures and results will include all relevant reports of:

- reports on desk studies;

- the field investigations, like sampling, field tests and groundwater measurements;
- the laboratory tests.

The presentation of geotechnical information shall include:

- a factual account of all field and laboratory work;
- documentation of the methods used to carry out the field investigations and the laboratory testing;

The documentation shall be based on the test reports.
In addition, the factual account should include the following information, as relevant:

- names of all consultants and subcontractors;
- purpose and scope of the geotechnical investigation;
- dates between which field and laboratory work was performed;
- field reconnaissance of the general area of the project noting particularly:
- evidence of ground-water;
- exposures in quarries and borrow areas;
- areas of instability;
- difficulties during excavation;
- history of the site;
- geology of the site, including faulting; survey data;
- information from available aerial photographs;
- local experience in the area,
- information about the seismicity of the area.

Evaluation of Geotechnical Information

The evaluation of the geotechnical information will include:

- a review of the field and laboratory work. Any limitations in the data (e.g. defective, irrelevant, insufficient or inaccurate) shall be pointed out and commented upon. The sampling and sample transportation and storage procedures shall be considered when interpreting the test results. Any particularly adverse test results shall be considered carefully in order to determine if they are misleading or represent a real phenomenon that must be accounted for in the design;
- a review of the derived values of geotechnical parameters;
- any proposals for necessary further field and laboratory work, with comments justifying the need for this extra work. Such proposals shall be accompanied by a detailed programme for the extra investigations to be carried out with specific reference to the questions that have to be answered.

In addition, the evaluation of the geotechnical data should include the following, if relevant:

- tabulation and graphical presentation of the results of the field and laboratory work in relation to the requirements of the project and, if deemed necessary,
- histograms illustrating the range of values of the most relevant data and their distribution;
- depth of the ground-water table and its seasonal fluctuations;
- subsurface profile(s) showing the differentiation of the various formations;
- detailed descriptions of all formations including their physical properties and their deformation and strength characteristics;

- comments on irregularities such as pockets and cavities;
- the range and any grouping of derived values of the geotechnical data for each stratum.

The evaluation of the geotechnical information shall be documented and include:

- a review of the results of the site and laboratory investigations;
- a description of geometry of the strata;
- detailed description of all strata including their physical properties and their deformation and strength characteristics referring to the results of the investigations;
- comments on irregularities such as pockets and cavities.

It shall be documented that the results were interpreted taking into account the ground water table, soil and or rock type, drilling method, sampling method, transport, handling and specimen preparation the originally assumed strata subdivision were reconsidered in light of the results obtained.

The documentation of the evaluation of the geotechnical information should include as appropriate:

- tabulation and graphical presentation of the results of filed investigation and laboratory testing in cross-sections of the ground showing the relevant strata and their boundaries including the ground water table in relation to the requirements of the project;
- the values of the geotechnical parameters for each stratum;
- a review of the derived values of geotechnical parameters.

Averaging can mask the presence of a weaker zone and should be used with caution. It is important that weak zones be identified. Variations in geotechnical parameters or coefficients can indicate significant variations in site conditions.

The documentation should include comparisons of the results with, existing experience for each geotechnical parameter giving special consideration to anomalous results for a given stratum and the results of other types of laboratory and field tests capable of measuring the same geotechnical parameter if available.

The documentation of the evaluation should substantiate the following aspects:

- strata in which ground parameters differ only slightly may be considered as one stratum.
- a sequence of fine layers with greatly differing composition and/or mechanical properties may be considered as one stratum if the overall behaviour is relevant, and the behaviour can be adequately re-presented by ground parameters selected for the stratum.

When deriving the boundary between different soil layers, soil and rock and the groundwater level it may normally be assumed sufficiently accurate to interpolate linearly between the investigation points, provided the spacing is sufficiently close and the geological situation is sufficiently homogeneous. Such application of linear interpolations and the reasons should be reported.

The flow chart shown in Figure A.4 demonstrates the link between design and field and laboratory tests. The design part is covered by EN 1997-1; the parameter values part is covered by EN 1997-2.

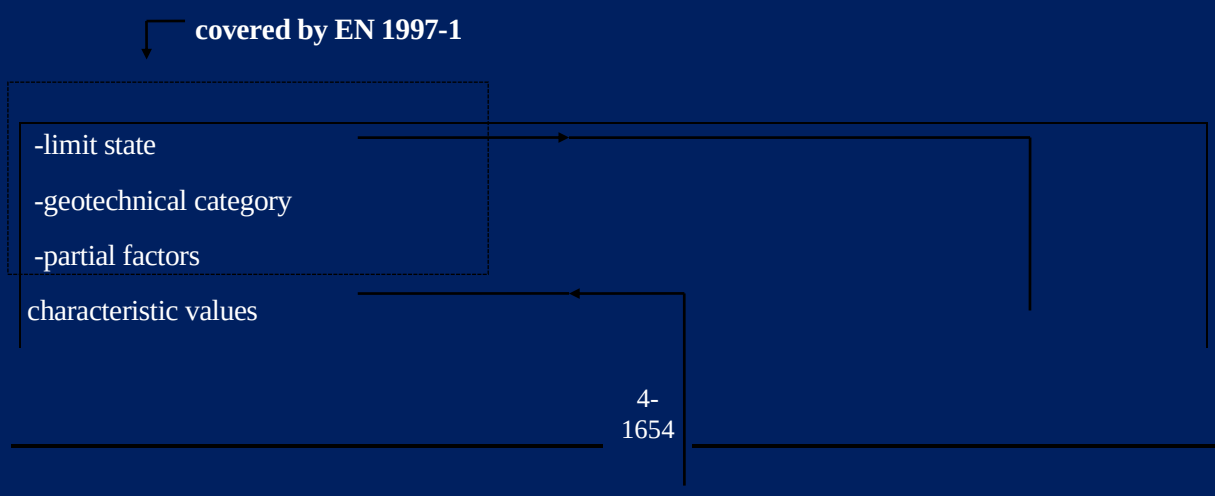

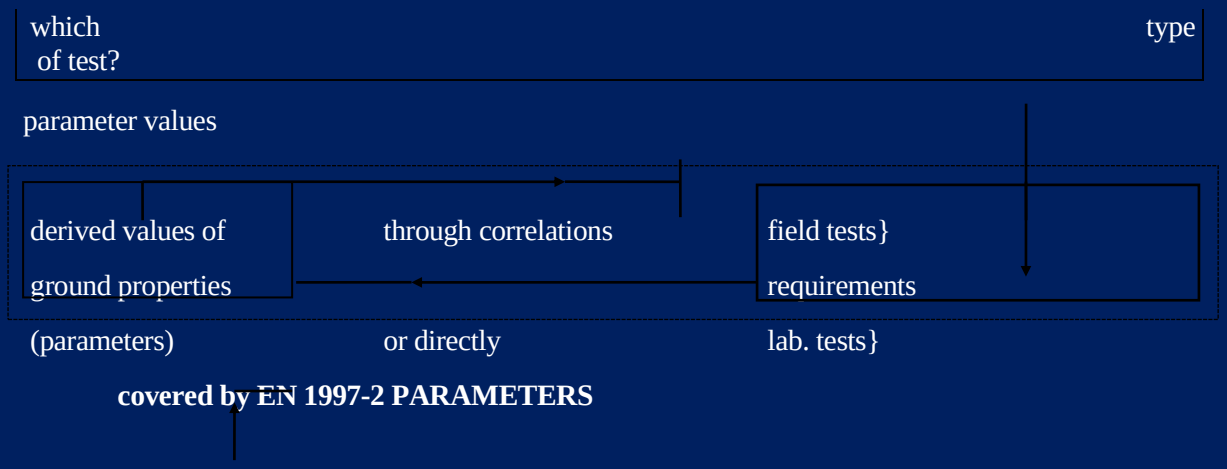

Figure A1.4 Flow chart showing the link between design and field and laboratory tests (after EN, 1997-2).

A. 6 Tests Specifications for Soils

Field Tests

CPT tests

DIN 1054: 2003-01

Lunne T., Robertson P.K., Powell J.J.M. (1997)

Cone penetration testing in geotechnical practice. Spon Press, London, New York, 312 pages.

Sanglerat, G. (1972) The penetrometer and soil exploration Elsevier Publishing Company, Amsterdam, 464 pages. Stenzel, G., Melzer, K.-J. (1978)

Flat Dilatometer

Marchetti, S. (1980) In situ test by flat dilatometer

Journal of the Geotechnical Engineering Division, Proc. ASCE, Vol. 106, N. GT3, pp 299-321.

Marchetti, S., Monaco, P., Totani, G., Calabrese, M. (2001)

The flat dilatometer test (DMT) in soil investigations. ISSMGE TC16 Report

Proc. In situ 2001, Bali, 41 pages

Pressurometer tests

Annex W Bibliography pr EN 1997-2: Aug 2003 148

Clarke B.G, Gambin M.P. (1998) Pressuremeter testing in onshore ground investigations. A report by ISSMGE Committee TC 16. Proc. 1st Int. Conf. on Site Characterization, Atlanta, Vol. 2, 1429–1468.

Clarke B.G. (1995)

Pressuremeters in Geotechnical design. Blackie Academic and Professional, Glasgow, 364 pages

Ministère de l'Equipement du Logement et des Transports (1993). Règles techniques de conception et de calcul des fondations des ouvrages de Génie civil, CCTG, Fascicule no. 62, Titre V.

SPT Tests

Burland, J.B. and Burbridge, M.C. (1985) Settlements of foundations on sand and gravel

Proceedings Inst. Civil Engineers, U.K., Part 1, 78, Dec. 1325-1381.

Canadian Foundation Engineering Manual (1992), Third Edition, Canadian Geotechnical Society,

Technical Committee on Foundations, BiTech Publishers Ltd.

Clayton C.R.I. (1995) The Standard Penetration Test (SPT): methods and use. Construction Industry Research Information Association (CIRIA), Report 143, London.143 pages

Skempton, A.W. (1986) Standard penetration test procedures and the effects in sands of overburden pressure relative density, particle size, ageing and overconsolidation Geotechnique 36, No. 3, pp 425-447.

Seismic Tests

Determination of the Maximum Shear Moduli

The maximum shear moduli may be obtained from geophysical tests or resonant column tests or by equations proposed by several authors. As stressed before the knowledge of maximum shear modulus property is required as an input parameter in finite element programs used for the dynamic analysis.

Seismic tests to measure compression and shear wave velocities were performed 5 years after the filling of Beliche dam (Sêco e Pinto, [93]). The dam is 550 m long at the crest and 55 m high. The cross-section is shown in Figure 7.49. Two holes with 20 m depth a drilling equipment were done at the crest. The position of the holes was determined by an inclinometer. Both techniques downhole and crosshole were used for the determination of compression and shear wave velocities but the latter has revealed more successful.

The obtained results for the crosshole technique are presented in Table 7. 13.

It seems from the literature survey that there is a lack of information in what concerns the knowledge of the maximum shear moduli values for embankment dam materials. Portuguese experience has privileged the cross-hole technique. Efforts should be done to analyse different techniques, the effects of time in the variation of shear velocities and also to obtain measurements in other materials.

Laboratory Tests

Notations

ASTM American Society for Testing and Materials,

BS – British Standard

DGF Dansk Geoteknisk Forening (Danish Geotechnical Society),

DIN – Deutche Industrie Normen

ETC European Technical Committee (of ISSMGE),

ISRM International Society of Rock Mechanics,

ISSMGE International Society of Soil Mechanics and Geotechnical Engineering.

NF Norme Francaise

SN Swiss Norm

SPRINT Network of Industrial Research Centres

SS Swedish Standard

Tests for classification, identification and description of soils

Classification, identification and description of soils shall be made in accordance with EN-ISO14688-1 and EN-ISO14688-2. (2) Annex L provides more details on individual classification tests and their interpretation, and a guideline for the minimum number of samples and tests in one stratum.
Laboratory tests on soils and rock prEN 1997-2: Aug 2003 49

Requirements for all classification tests
For all classification tests, special caution should be exercised when choosing the temperature for oven-drying, as too high temperatures can have detrimental effects on the value measured.

Atterberg limits determination

The Atterberg limits (consistency limits) comprise the liquid limit, plastic limit and shrinkage limit. The determination of the liquid limit and the plastic limit are covered only.
These limits are used to characterize the fine-grained fractions of soils and to specify the fine-grained fraction of construction materials.
The consistency limits are used to characterise the behaviour of clays and silty soils when the water content is changing. Classification of clays and silty soils is mainly based on the consistency limits.
The testing method to be used for determining the liquid limit (fall cone or Casagrande apparatus) shall be specified.
In general, for liquid limit, the fall cone method should be preferred to the Casagrande method. Especially for low plasticity soils, the fall cone method gives more reliable results.
The specimens should at least be of Quality Class 4, if the test results are supposed to characterise all types of soils present in the stratum.
Different geotechnical properties, for example compressibility, or optimum water content can be derived from correlations with the liquid or plastic limits.
The value of the plasticity index IP can be computed from liquid and plastic limits. IP can be used in soil classification and in correlations with some geotechnical soil properties, for example with soil strength.

The value of the consistency index IC (or the liquidity index IL) can be computed from liquid and plasticity limits and from current water content of the soil. It can be used to represent soil consistency and in correlations with some geotechnical properties.
(The activity A (activity index IA) can be computed from IP and the percentage of clay particles.
A (IA) can be used in soil classification and in correlations with different geotechnical soil properties, for example with soil strength.

This test shall be undertaken in compliance with:

Recommendations of the ISSMGE for geotechnical laboratory testing. Determination of

Atterberg limits, DIN-Beuth Verlag, Berlin.

DIN 18 122:1997 Soil, investigation and testing Consistency limits Part 1 Determination of liquid limit and plastic limit.

NF P 94-051:1993 Soils. Investigation and testing. Determination of Atterberg's limits. Liquid limit test using Casagrande apparatus. Plastic limit test on rolled thread.

NF P94-052-1 :1995 Sols : Reconnaissance et Essais – Détermination des limites

d'Atterberg – Partie 1 : Limite de liquidité – Méthode du cône de pénétration.

BS 1377:1990 Methods of test for soils for civil engineering purposes Part 2: Classification

tests Clause 4. Determination of the liquid limit.

BS 1377:1990 Methods of test for soils for civil engineering purposes Part 2: Classification

tests Clause 5. Determination of the plastic limit and plasticity index.

SN 670 345 :1959 Essais ; Limites de consistance / Versuche ; Konsistenzgrenzen.

Bulk density determination

The test is used to determine the bulk (total) mass density of a soil, including any liquid or gas contained.
The tests on fine-grained soils should be carried out and reported in accordance with the requirements given in EN 17892-2.
The test specimens should be at least of Quality Class 2.
The test method to be used shall be specified.
The evaluation of the test results should consider the possible sample disturbance.
Except in the case of special sampling methods, the laboratory determination of the density of a coarse-grained soil is generally only approximate.
The bulk density can be used in establishing design values of actions derived from soils and in processing results of other laboratory tests.
The bulk density can also be used in evaluating other soil characteristics. For example, in conjunction with the water content, in computing the density of dry soil.
Laboratory tests on soils and rock prEN 1997-2: Aug 2003 50

Determination of the density index of granular soils

The density index relates the void ratio of a soil sample to reference values determined by standard laboratory procedures. It gives an indication of the state of compaction of a free draining granular soil.
The following shall be specified or checked:
− the quantity and quality of samples,

−□the type of testing procedure to be applied,
−□the method of preparation of each test specimen.
The tested soil should contain less than 10% of fines (particles passing the 0.063 mm sieve) and less than 10% of gravel (particles retained on the 2 mm sieve).
Density index test results shall be reported together with the available particle size analysis results, natural water content, particle density, and percentage of oversize fraction (the latter if applicable).
Any deviation with respect to (3) shall be reported.
Laboratory tests on soils and rock prEN 1997-2: Aug 2003 52
When evaluating density indexes, account should be taken of the fact that the maximum and minimum densities obtained in the laboratory do not necessarily represent limiting densities. It is also generally recognised that these tests give densities with a high degree of variability.
The density index can be used to characterise the shear strength and the compressibility of coarse-grained soils.

Determination of Soil dispersibility

The objective of the tests is to identify the dispersive characteristics of clayey soils. Standard tests for classifying soils for engineering purposes do not identify the dispersive characteristics of a soil.
Tests for dispersibility are carried out on clayey soils, primarily in connection with earth embankments, mineral sealings, and other geotechnical structures in contact with water.
Four test types are considered:
−□the pinhole test which models the action of water flowing along a crack,
−□the double hydrometer test which compares the dispersion of clay particles in plain water without mechanical stirring with that obtained using a dispersant solution and mechanical stirring,
−□the crumb test which shows the behaviour of crumbs of soil placed in a dilute solution of sodium hydroxide,
−□the determination of soluble salts in the pore water which allows the correlation of percent sodium to the total dissolved salts in saturation extract.

The following shall be specified:
−□the storage of samples such that the samples are not allowed to dry before testing,
−□the testing procedures to be applied,
−□the specimen preparation method.
The results from the dispersibility tests shall be linked to the grain size distribution and consistency limits of the sample.
For the pinhole test, the compaction conditions of the soil specimens, e.g. wet or dry of optimum, and the mixing water (e.g. distilled versus reservoir water) should be specified.
For the double hydrometer test, a third hydrometer test may be specified if it appears necessary to study the effect of reservoir water on the soil in suspension.
For the crumb test, the use of distilled water may be requested in addition to the sodium hydroxide solution.

This test aims at identifying the dispersive characteristics of clay soils that are to be used in the dam's construction. ASTM D4647 standard must be complied with.

Dispersibility tests for Corumana dam

Dispersibility tests were conducted in Corumana dam with 45 m high and 2533 m long and 8 x 10^{6} m 3. The core is with clay material and the shells are with clay sandy materials and materials from excavations.

Figure A1.5 illustrates a spillway view and a crest view of Corumana dam.

Dispersibility tests, namely crumb tests, chemical tests, double sedimentation and pinhole tests were performed (Sêco e Pinto, 1987).

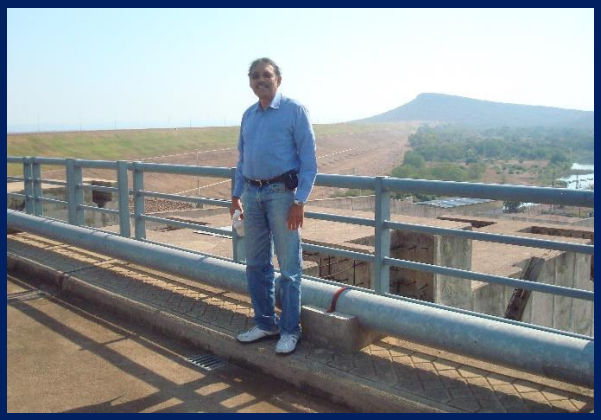

Figure A1.5a Corumana dam – spillway view

Figure A1.5b Corumana dam-crest view

The results of the crumb tests, following Sherard et al (1981) proposal, are shown in Table A1.6.

Table A1.6 Summary of the crumb tests

Samples	Distilled water	Solution NaOH (0.001 N)
Nº1	2	3
Nº2	3	4
Nº3	2	3
Nº4	3	4

Figure A1.6 illustrates the water samples for chemical results.

Table A1.7 summarizes the chemical tests results.

Table A1.7 Results of the Chemical tests

Sample		Soluble	salts	(meq/1)		
	Ca^{2+}	Mg 2+	K+	Na+	TDS	Na/TDS
Nº1	26.75	23.09	0.46	140.5	190.8	73.6
Nº2	2.34	14.40	0.35	90.3	107.39	84.1

Nº3	2.87	13.41	0.29	90.91	107.47	84.6
Nº4	0.56	3.18	0.14	11.6	15.48	74.9

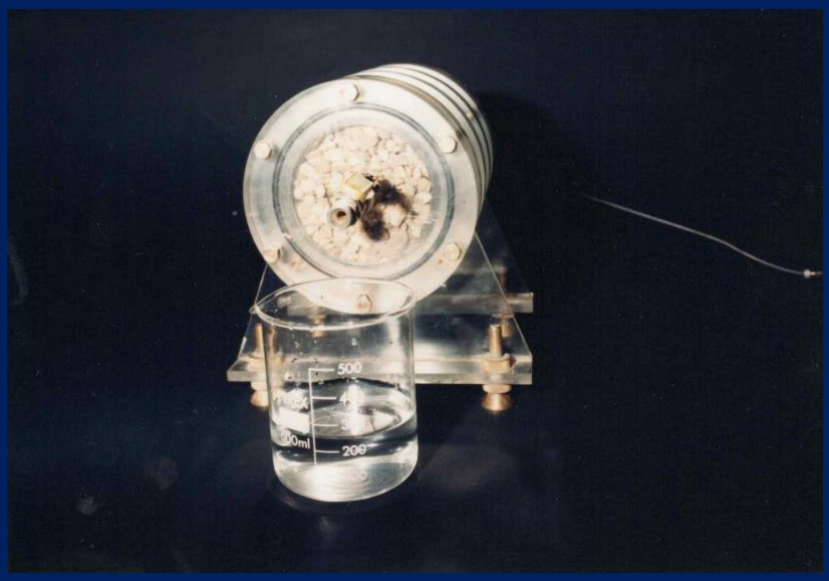

Figure A1.6 Water samples for chemical tests

Table A1.8 and Table A1.9 summarize the results of the double sedimentation tests and the interpretation following several researchers.

Table A1.8 Summary of double sedimentation tests

	Double sedimentation tests		% of fines less 0.005 mm
Samples	E LNEC-196	Without dispersive	% of dispersive PD=A/B x100
Nº1	63	24	38
Nº2	72	23	31.9
Nº3	48	30.5	63.5
Nº4	67	28	41.8

Table A1.9 Interpretation of double sedimentation tests

		Criteria	
Samples	Sherard	Decker	Ryker
Nº 1	Medium dispersive 33<PD<67	No dispersive PD<40	Dispersive PD>35
Nº 2	No dispersive 0<PD<3	No dispersive PD<40	No dispersive PD<35
Nº 3	Medium dispersive 33<PD<67	Dispersive PD>40	Dispersive PD>35
Nº 4	Medium dispersive 33<PD<67	Dispersive PD>40	dispersive PD>35

The equipment to perform pinhole tests is shown in Figure A1. 7.

Figure A1.7 View of the pinhole equipment

The obtained results of the pinhole tests are summarized in Table A1.10.

Table A1.10 Summary of pinhole tests

Samples	Water color	Final hole diameter(mm)	Classification
Nº 1	Clear	3	Dispersive
Nº2	Clear	3	Dispersive
Nº3	Clear	4	Dispersive
Nº4	clear	4	Dispersive

Frost susceptibility

The frost susceptibility of soil materials plays an essential role in the design of foundations placed above the freezing front in frost susceptible soils. Roads, airport runways, railways, buildings on spread foundations, buried pipelines, dams and other structures may be subject to frost heave due to freezing of a frost-susceptible soil having access to water. Frost-susceptible soils may be used in their natural state or as a constructed base for structures.
The risk of frost heaving may be estimated from correlation with soil classification properties (particle size distribution, height of capillary rise and/or fines content) or from laboratory tests on natural, re-compacted and re-consolidated, or re-constituted samples.
Laboratory tests on soils and rock prEN 1997-2: Aug 200353

If the estimation of frost susceptibility based on classification properties of the soil does not clearly indicate the absence of risk of frost heaving, frost heaving tests in the laboratory should be run.
Examples of soil types indicating the need of laboratory tests in addition to correlations to classification properties include organic soils, peat, saline soils, artificial soils and coarse soils with a wide range of grain size.
To determine the frost susceptibility of a soil in its natural state, natural samples should be tested. To estimate the frost susceptibility of a constructed fill, frost heave tests should be run on recompacted and then re-consolidated specimens or on re-constituted specimens.
The frost susceptibility test in the laboratory is a frost heave test. If the risk of thaw weakening is to be tested, a California Bearing Ratio test should be carried out after thawing of the specimen. The re-compacted or re-constituted specimen should be subjected to one or more freeze-thaw cycles before testing.

The results should be interpreted as a function of the type of construction work, the rules used in design and the available comparable experience, considering the consequence of the frost effects.

Chemical testing of soils and groundwater

Although the detailed chemical composition of soil is often of limited interest for civil engineering purposes, the presence of certain chemical constituents in soil can be very significant, for example for the durability of the geotechnical structure.
Routine chemical testing in a soil laboratory is usually limited to organic content (loss on ignition, total organic content, organic matter), carbonate content, sulphate content, pH value (acidity or alkalinity) and chloride content. The standard deals with these five chemical tests only.
There are other chemical components that may cause an environment very aggressive to steel and concrete, for example sulphide, magnesium and ammonium. The corresponding chemical testing is not covered in this standard.
Corrosiveness to steel constructions in soil is usually evaluated by means of electrical resistivity tests and determination of the redox potential (not covered in this standard), pH, chlorides and sulphate determinations.

The purpose of the chemical tests described herein is to classify the soil and to assess the detrimental effect of the soil and groundwater on concrete, steel and the soil itself. The tests are not intended for environmentally related purposes.

The following requirements shall be specified for all chemical tests:
− samples which are to be tested,
− number of samples to be tested,
− test procedures to be applied,
− pre-treatments including treatment of oversize particles (i.e. d > 2 mm),
Laboratory tests on soils and rock prEN 1997-2: Aug 2003 54
− number of tests per stratum and number of duplicate tests,
− number of separate tests for the determination of a mean value,
− format of reporting,
− required supplementary classification tests for each test or series of tests.
The proper procedures of mixing, riffling and quartering shall be strictly followed in order to avoid inconsistent results.
Disturbed soil samples may be used for the chemical tests, but particle size and water content need to be representative of the field conditions (Quality Class 1 to 3).
For the determination of organic content, the particle size only needs to be representative (Quality Class 4).
(5) Recommended test procedures are available in W.2.

The test results shall be reviewed together with the geological description and the prevailing environment.
Where appropriate, account shall be taken of recognised classifications in terms of the parameter measured.

Organic content determination

The organic content tests are used to classify the soil. In soils with little or no clay particles and carbonate content, the organic content is often determined from the loss on ignition at a controlled temperature. Other suitable tests can also be used. For example, organic content can be determined from the mass loss on treatment with hydrogen peroxide (H_2O_2), which provides a more specific measure of organics.
The presence of organic matter can have undesirable effects on the engineering behaviour of soils. For example, the bearing capacity is reduced, the compressibility is increased, swelling and shrinkage potential is increased due to organic content. Gas can lead to large immediate settlements and affect the consolidation coefficients and shear strength derived from laboratory tests. Organic matter is detrimental for the stabilisation of soils used for roads and is usually associated with low pH and at times with presence of sulphates which can have negative effects on foundations.

The following shall be specified for each test or series of tests, in addition to the list in 5.6.1.3:
− the drying temperature,
− the ignition temperature,
− the required corrections for bound water, carbonates, etc.
− the factor used for converting carbon content into organic content.
Non-homogeneous samples require larger specimens and the appropriate apparatus.
Correspondingly larger crucibles shall be used.
The loss on ignition shall be reported as a percentage of original dry matter, giving also drying temperature, ignition temperature and drying and ignition times.
The organic content shall be reported as a percentage of original dry matter, giving also the method of determination.
Laboratory tests on soils and rock prEN 1997-2: Aug 2003 55

In clays and silty soils with moderate organic content, the errors involved in the correction for bound water or carbonates can be so large that special testing methods are necessary.

Carbonate content determination

The carbonate content is used as an index to classify natural carbonate soils and rocks or as an index to indicate the degree of cementation.
Measurement of the carbonate content depends on the reaction with hydrochloric acid (HCl) which liberates carbon dioxide. It is usually assumed that the only carbonate present is calcium carbonate ($CaCO_3$). Carbonate content is measured from the mass loss on treatment with HCl.

The soil shall be assessed visually before the selection of the appropriate pre-treatment.
When appropriate, large initial samples can be used to cope with non-homogeneous carbonate distribution in soil and rock. Representative test samples can be established by crushing and filling.
The carbonate content shall be reported as a percentage of the original dry matter.

Some carbonates, e.g. dolomite, may not dissolve using the standard solution of hydrochloric acid during the specified time. Special methods shall be used for soil or rock types containing such carbonates.

Sulphate content determination

The objective of the test is to determine the sulphate content as an index for the possible detrimental effect of the soil on steel and concrete. All naturally occurring sulphates, with rare exceptions, are soluble in hydrochloric acid. Some are soluble in water.
The acid-soluble sulphate content is referred to as the total sulphate content, as distinct from the water-soluble sulphate content. It is important to appreciate which value is relevant.
Ground water containing dissolved sulphates, especially sodium and magnesium sulphates, can attack concrete and other materials placed in the ground or on the ground surface. Classification of soil and ground water in terms of sulphate content is therefore necessary so that suitable precautionary measures can be taken, if required.

It shall be specified for each test or group of tests, whether acid- or water-soluble sulphate is required for the test, in addition to the items listed in 5.6.1.3.
Non-homogeneous soils containing visible crystals of gypsum require large samples, which shall be crushed, mixed and riffled to provide representative test specimens. A visual assessment
The content in SO_3 or SO_4 shall be reported as a percentage of dry substance or in g/dm3, relating to acid- or water-soluble sulphate.
Laboratory tests on soils and rock prEN 1997-2: Aug 2003 56.

pH value determination (acidity and alkalinity)

The pH value of ground water or solution soil in water is used to assess the possibility of excessive acidity or alkalinity.
The following shall be specified for each test or group of tests, in addition to the general requirements for chemical testing
− whether or not the soil shall be dried,
− the ratio of soil to water.
Standard buffer solutions shall be used for calibration of the pH meter.
The pH value of the soil suspensions or the groundwater shall be reported. The test method shall be stated.
The evaluation should consider that, in some soils, the measured values can be influenced by oxidation.

Chloride content determination

The objective of the test is the determination of the water-soluble or acid-soluble chloride content so that the salinity of the pore water or soil can be assessed. The results provide an index for the possible effect of the ground water towards concrete, steel, other materials and soils.

The following shall be specified for each test or group of tests

whether water-soluble or acid-soluble chlorides shall be determined,
whether or not the soil shall be dried.
After drying the soil shall be mixed thoroughly to redistribute any salts which may have migrated to form a surface crust.
The chloride content in g/dm3 or as a percentage by dry mass of the soil shall be reported.
The test procedures used shall state whether water-soluble or acid-soluble chlorides have been determined.

Water Soluble Sulphate, chloride and total soluble salts content - Chemical analysis of soil shall be undertaken in order to determine water soluble sulphate, chloride and total soluble salts content.

BS 1377:1990 Methods of test for soils for civil engineering purposes: Part 3. Chemical and electrochemical tests.

BS 1377:1990 Methods of test for soils for civil engineering purposes: Part 3. Chemical and electrochemical tests. Clause 4. Determination of the mass loss on ignition or an equivalent method. Annex W Bibliography prEN 1997-2: Aug 2003 154

ASTM D2974:1987 Test methods for moisture, ash, and organic matter of peat and other organic soils.

NF P 94-055 : 1993 Sols : Reconnaissance et Essais – Détermination de la teneur

pondérale en matières organiques d'un sol – Méthode chimique.

XP P94-047 : 1998 Sols : Reconnaissance et Essais – Détermination de la teneur pondérale en matière organique – Méthode par calcination.

BS 1377:1990 Methods of test for soils for civil engineering purposes: Part 3. Chemical and electrochemical tests. Clause 6 Determination of the carbonate content.

DIN 18129: Soil, investigation and testing - Determination of lime content. Head Vol 1:1992 (see annex Z.2.13).

NF P 94-048 : 1996 Sols : Reconnaissance et Essais – Détermination de la teneur en carbonate – Méthode du calcimètre.

BS 1377:1990 Methods of test for soils for civil engineering purposes: Part 3. Chemical and electrochemical tests. Clause 5. "Determination of the sulphate content of soil and ground water".

BS 1377:1990 Methods of test for soils for civil engineering purposes: Part 3. Chemical and electrochemical tests. Clause 9. "Determination of the pH value".

BS 812: Part 118: 1988 Testing aggregates. Methods for determination of sulphate content.

BS 1377:1990 Methods of test for soils for civil engineering purposes: Part 3. Chemical and electrochemical tests. Subclause 7.2 / subclause 7.3.

Classification

BS 5930:1999, Code of practice for site investigations.

Compaction tests

These standard cover compaction tests (Proctor tests) and the California Bearing Ratio test.

Compaction tests

Soil compaction tests (Proctor tests) are used to determine the relationship between dry density and water content when a given compaction effort is applied.
The following shall be specified or checked:
−handling of soils with oversize fractions,
−treatment of stiff fine grained soils,
−specimen preparation and maturing,
−testing procedures and compaction effort to be applied,
−whether the equipment (moulds and rammers) used is as specified in the standard(s).
The option of carrying out in situ tests instead of laboratory tests should be considered for special types of soils.

The compaction characteristics of soils shall be reported together with grain size distribution curves and proportion of oversize material by dry mass with correction, if appropriate.
The optimum water content wopt, and the corresponding maximum dry density achieved under the applied compaction effort _max can be used in evaluating the quality of compacted fills.
Laboratory tests on soils and rock prEN 1997-2: Aug 2003 64

California Bearing ratio (CBR) test

This test is used to evaluate the potential strength of subgrade, subbase, and base course materials, for use in the design of road pavements.

The objective of the test is to determine the California Bearing Ratio (CBR) of a compacted or undisturbed sample.
The CBR value is obtained as the percentage of the standard load corresponding to the standard penetration, when a cylindrical plunger of a standard cross-sectional area is made to penetrate into the soil material.

The following shall be specified or checked:
−method of preparation of each test specimen,
−how many tests are to be run in a set of test specimens,
−handling of soils with oversize fractions (D > 16 mm),
−maturing of specimens,
−whether or not specimen is to be subjected to soaking,
−if soaking is used, whether swelling is to be measured,
−surcharge to be applied for soaking and for testing,
−water content at which compacted specimens are to be prepared,
−specimen dry density or compactive effort,
−whether equipment (moulds and rammers) used is as specified in standard,
−whether or not the test is to be carried out on one end or both ends of the specimen. **Evaluation**
The CBR test results shall be reported together with grain size distribution and proportion of oversize material by dry mass, if relevant.
The CBR value can be used as a basic parameter for the design of flexible pavements. It can be used to evaluate the potential strength of subgrade, subbase, and base course materials (including recycled materials) for supporting road, railways and airfield pavements.

This test shall be undertaken in compliance with:

BS 1377:1990 Methods of test for soils for civil engineering purposes: Part 4: Compaction related tests: Clause 3. Determination of dry density/moisture content relationship.

BS 1377:1990 Methods of test for soils for civil engineering purposes: Part 4: Compaction related tests: Clause 7 “Determination of California Bearing Ratio (CBR)”.

[Note: ASTM D-698-78, D-1557-78 and AASHTO /99 and T180 might be used for compaction tests

ASTM D1883-94and AASHTO T193 might be used for the California Bearing Ratio Determination.

However, BS 1377:1990 have minor deviations from the specification in the US Recommendations, which are used in most road laboratories.]

SS027109 Geotechnical tests – Compaction properties – Laboratory compaction.

NF P 94- 078 :1997 Sols : Reconnaissance et Essais - Indice CBR après immersion – Indice CBR immédiat - Indice Portant Immédiat - Mesure sur échantillon compacté dans le moule CBR.

NF P 94- 093 :1999 Sols : Reconnaissance et Essais - Détermination des références de

compactage d'un matériau - Essai Proctor normal - Essai Proctor modifié.

Consolidation Tests

This standard covers the requirements for measurement of deformation characteristics of soils in the triaxial apparatus and in the oedometer.

Oedometer compressibility testing

One-Dimensional Consolidation test (Oedometer test) - The data from the consolidation test are used to estimate the magnitude and rate of both differential and total settlement of the earthfill dam. These estimates are of key importance in its design and evaluation of performance

In the oedometer, the cylindrical specimen is confined laterally, and is subjected to discrete increments of vertical axial loading or unloading and allowed to drain axially. Oedometer compression and swelling tests and evaluation of the collapse potential of a soil are covered.

Alternatively, a test with continuous loading (constant rate of strain) may be carried out.

The objective of the oedometer incremental compression and swelling tests is to determine the compression, consolidation and swelling characteristics of soils.

The objective of the collapse potential test is to establish compressibility parameters for the soil in its unsaturated state, and to evaluate the additional compression upon inundation due to structural collapse of the soil.

For the determination of the compressibility of a stratum of clay, silt or organic soils, undisturbed samples (Quality Class 1) shall be used.

NOTE Small strain moduli of soils (e.g. moduli at less than 1% strain for soft to medium clays) are very sensitive to all perturbations during sampling. According to 3.4.3 (3) specific sampling equipment and method may be used, for example block sampling or stationary piston sampling or any other method known to give the best results for the soils to be tested.

For re-compacted specimens, the composition, density and water content of the prepared specimens relevant to the in-situ conditions and the specimen preparation method shall be specified.

When determining the compressibility characteristics of a soil stratum, the following items shall be taken into account:

- existing results of field investigations,
- existing settlement measurements from neighbouring sites,
- number and quality of samples,
- number and type of field tests,

−□special consideration needed for sensitive and cemented samples,
−□specimen preparation,
−□orientation of the specimen,
−□need for additional classification tests.

For complex loading or unloading conditions and/or for difficult subsoil conditions, carrying out alternative tests to the incremental oedometer test, for example constant rate of strain oedometer tests, may be considered.

The initial vertical stress shall not exceed the in-situ vertical effective stress.

NOTE: For example, for strain-softening clays, an initial stress of one fourth of the in situ vertical effective stress can be considered an appropriate value.

In a compression test, the highest vertical stress applied should be well in excess of the maximum effective vertical stress likely to occur in-situ. In a swelling test, the range of decrements of vertical stress to be applied during the test should include the range of stresses likely to be applied insitu.

Laboratory tests on soils and rock prEN 1997-2: Aug 2003 62

When testing the collapse potential, the test specimens shall be selected with adequate consideration of existing knowledge on the behaviour of the soil when subjected to inundation. The stress on the specimen at which inundation is applied shall be related to the range of vertical stresses likely to occur in-situ.

The tests should be carried out and reported in accordance with the requirements given in EN ISO 17892-5.

The oedometer test results may be used to estimate the yield stress (preconsolidation pressure) for clays, organic soils and silty soils.

It should be taken into account that the preconsolidation pressure determined by the oedometer test can be greatly affected by sampling disturbance.

The most common values to characterise compressibility are the oedometer modulus Eoed, the coefficient of compressibility mv, the compression index Cc, modified compression index Cc_, and preconsolidation pressure _p‘. Unloading and recompression can be represented by the swelling index. All these quantities are derived directly from the appropriate parts of the compression curves.

Settlements due to creep can be computed using the coefficient of secondary compression C_.

The coefficient of consolidation cv can be derived using the one-dimensional consolidation theory.

Any parameter in (4) can be used for simple analyses of the settlement of spread foundations.

If the sample methods of F.1 and F.2 of EN 1997-1, are applied, the oedometer modulus may be used.

Laboratory procedures shall comply with:

Recommendations of the ISSMGE for geotechnical laboratory testing. Incremental loading oedometer test on water-saturated soil, DIN-Beuth Verlag, Berlin.

BS 1377:1990 Methods of test for soils for civil engineering purposes: Part 5: Compressibility, permeability and durability tests.

NS 8017:1991 Geotechnical testing - Laboratory methods - Determination of one-dimensional consolidation properties by oedometer testing - Method using incremental loading. Annex W Bibliography prEN 1997-2: Aug 2003- 156

ASTM D2435:1996 Test method for One-Dimensional Consolidation Properties of Soils.

XP P94-090-1:1997 Sols : Reconnaissance et Essais - Essai œdométrique -Partie 1 : Essai de compressibilité sur matériaux fins quasi saturés avec chargement par paliers.

XP P 94-091 :1995 Sols : Reconnaissance et Essais - Essai de gonflement à l'oedomètre - Détermination des déformations

Determination of density

ETC-5-N94.48 Laboratory determination of density of cohesive (fine-grained) soil, DIN-Beuth Verlag Berlin.

DIN 18 125:1997 Soil, investigation and testing Determination of density of soil Part 1

Laboratory tests.

NF P 94-053:1991 Soils. Investigation and testing. Determination of density of fine soils.

Cutting curb, mould and water immersion methods. Sols : Reconnaissance et Essais –

Annex W Bibliography prEN 1997-2 : Aug 2003 -152

Détermination de la masse volumique des sols fins en laboratoire – Méthodes de la trousse coupante, du moule et de l'immersion dans l'eau.

BS 1377:1990 Methods of test for soils for civil engineering purposes Part 2 Classification tests.

SN 670 335 :1960 Versuche ; Raumgewicht ; Sandersatz-Methode / Essais ; Poids spécifique apparent ; Méthode du sable.

BS 1377:1990 Methods of test for soils for civil engineering purposes: Part 4: Compaction related tests; Clause 4, Determination of maximum and minimum dry densities for granular soils".

NF P 94-059 : 2000 Sols : Reconnaissance et Essais – Détermination des masses volumiques minimale et maximale des sols non cohérents.

Consolidated direct shear box tests

The tests should be carried out and reported in accordance with the requirements given in EN ISO 17892-10.
The location and orientation of the specimen shall be considered carefully so as to duplicate as closely as possible the in situ conditions. In the translational shear box and ring shear tests, failure is forced to occur on or near a horizontal plane in the middle of the test specimen.
Negative or positive pore water pressures due to shear shall be avoided during the test as they cannot be measured and accounted for in the interpretation of the test. To maintain drained conditions, the rate of shearing shall be slow enough so that pore water pressures may dissipate.
The results of standard shear box tests represent the strength under drained conditions. The values are effective friction angle and effective cohesion (see NOTE in 5.8.1(3)).
The values can be used in stability analyses (EN 1997-1, annex D).
Laboratory tests on soils and rock prEN 1997-2: Aug 200361

Mineralogical Analysis

This test shall be performed by X-Ray Diffraction (XRD) which is a non-destructive technique that reveals detailed information about the chemical composition and crystallographic structure of soils

Organic matter content determination test

Laboratory test used to determine percent organic matter in soil. This test shall be undertaken in compliance with ASTM D2974 – 14 standard.

Particle density determination

The aim of the test is to determine by a conventional method the density of solid soil particles. The tests should be carried out and reported in accordance with the requirements given in EN ISO 17892-3.

The choice of the test method to be used shall account for the soil type.
If for a particular stratum the measured values do not fall within the normally expected range of 2500 to 2800 kg/m3, the mineralogy of the soil, its organic matter and its geological origin shall be checked.

Particle Density

Particle density determination test – this test is useful for determining degree of soil compaction. Densities (unit weights) of remoulded/reconstituted specimens are commonly used to evaluate the degree of compaction of earthen fills, embankments, etc. Dry density values are usually used in conjunction with compaction curve values. Density (unit weight) is one of the key components in determining the mass composition/phase relations of soil. The test shall be undertaken in compliance with:

Recommendations of the ISSMGE for geotechnical laboratory testing. Determination of

density of solid particles, DIN-Beuth Verlag Berlin.

DIN 18 124: 1997 Soils, investigation and testing - Determination of density of solid particles - Capillary pycnometer, wide mouth pycnometer.

NF P 94-054 :1991 Sols : Reconnaissance et Essais – Détermination de la masse

volumique des particules solides des sols – Méthode du pycnomètre à eau.

.BS 1377:1990 Methods of test for soils for civil engineering purposes Part 2: Classification tests.

SN 670 335 :1960 Versuche ; Raumgewicht ; Sandersatz-Methode / Essais ; Poids specifique apparent ; Méthode du sable.

ASTM D854:1992 Test Method for Specific Gravity of Soils.

ASTM D4404:1984 Determination of pore volume and pore volume distribution of soil and rock by mercury intrusion porosimetry.

Particle size analysis

Particle size distribution by wet sieving - laboratory test used to assess the particle size distribution of granular materials.
The objective of the test is to express the mass percentage of individual particle size ranges found in the soil.
The tests should be carried out and reported in accordance with the requirements given in EN ISO 17892-4.
Two methods shall be used for particle size analysis, according to the size of the particles:
the sieve method for particles > 63 □m (or closest sieve available), the sedimentation method using a hydrometer, or pipette, for particles ≤□63 □m (or closest sieve available).
Equivalent methods may be used, provided that they are calibrated against the two methods mentioned in.
Prior to sedimentation, the specimens of fine-grained soils shall not be dried.
Procedures for the removal of organics, salts and carbonates prior to sieving and sedimentation or for corrections to account for the presence of carbonates, salts and organic material should be used, if appropriate.
NOTE Carbonates and organic matter can have a cementing or coagulating effect and influence the particle size distribution.
Account should be taken that for some soils, for example chalky soils, treatment for

carbonate removal is unsuitable.
The report shall mention the following:
− drying method used,
− whether organics, salts and carbonates have been removed and by which method,
− carbonate and/or organic content if relevant,
− whether the mass fractions are reported with respect to the total mass (including carbonate and organic matter).
The particle size such that n% of particles by weight are smaller than the size can be denoted Dn. The particle sizes D10, D30 and D60, can be used in definitions of the coefficient of uniformity and coefficient of curvature.
Laboratory tests on soils and rock prEN 1997-2: Aug 2003 51
The particle sizes D15 and D85 can be used in filter criteria for soils.

This test shall be undertaken in compliance with the ASTM D6913-04(2009) standard.

Permeability Tests of Soils

The objective of the test is to establish the coefficient of permeability (hydraulic conductivity) for water flow through water-saturated soil.
The tests should be carried out and reported in accordance with the requirements given in EN ISO 17892-11.
When determining the coefficient of permeability of a soil stratum, the following items shall be considered:
− preferred test type for permeability determination,
− orientation of the specimen,
− need for additional classification tests.
Depending on the conditions where the test results will be used, the following shall be specified:
a) in clay, silt and organic soils:
− stress conditions under which specimen is to be tested,
− criterion for achieving and maintaining the steady-state flow condition,
− direction of flow through specimen,
Laboratory tests on soils and rock prEN 1997-2: Aug 2003 65
− hydraulic gradient under which specimen is to be tested,
− need for back-pressure and required degree of saturation,
− the chemistry of percolating fluid.
b) in sand and gravel:
− density index to which specimen is to be prepared,
− hydraulic gradient under which specimen is to be tested,
− need for back-pressure and required degree of saturation.
The hydraulic gradient in the laboratory should be close to that in the field, unless otherwise required for a particular problem.
When selecting the hydraulic gradient, it shall be checked that the gradient in the laboratory test and the gradient in situ lie within the domain of application of Darcy's law.
The report should indicate any known deviation from the standard testing procedure, for example in degree of saturation of the test specimens, testing procedures, composition of the specimen or in any other aspect.
For permeability tests on clay, silt or organic soils, only soil specimens of Quality Class 1 or 2 should be used.
For sand and gravel materials, specimens of Quality Class 3 and remoulded or re-compacted soil samples may be used.
It should be checked that the volume changes due to the consolidation of the specimen shall only negligibly affect the measured permeability.
The evaluation should assess:

the extent to which the boundary conditions (degree of saturation, direction of flow, hydraulic gradient, stress conditions, density and layering, side leakage and head loss in filter and tubings) affect the test results, how well these conditions match the situation in the field.
For partially saturated soils, much smaller values may be relevant than the values measured in the case of full saturation.
Due consideration should be given to whether a temperature correction should be applied.
The coefficient of permeability can be computed from the test data under the assumption that Darcy's law is valid.
(5) POS The coefficient of permeability can be used in design of excavations and earth dams to estimate the amount of seepage, to assess the feasibility of ground water level management (lowering), to design the sheet pile walls, to estimate seepage pressures, etc

Recommendations of the ISSMGE for geotechnical laboratory testing. Determination of soil permeability by constant and falling head, DIN-Beuth Verlag Berlin.

BS 1377:1990 Methods of test for soils for civil engineering purposes: Part 5. Compressibility, permeability and durability tests.

DIN 18130-1:1998 Soil. Investigation and testing. Determination of the coefficient of water permeability. Part 1 Laboratory tests.

ISO/DIS 17313 Soil quality – Determination of hydraulic conductivity of saturated porous materials using flexible wall permeameter. ISO/TC 190/SC 5.

[Note: ISO/DIS17313 Soil quality relates to environmental testing and includes some very strict normative clauses not necessary for normal geotechnical purposes.]

Sand Equivalent value of soils

Laboratory test procedure to quantify the relative abundance of sand versus clay in soils. This test shall be undertaken in compliance with the ASTM D2419-14 standard.

Sedimentation Analysis

Laboratory test used to determine the distribution of particle sizes in soils. The distribution of particle sizes larger than 75 micrometers (retained on the No. 200 sieve) is determined by sieving, while the distribution of particle sizes smaller than 75 micrometers is determined by a sedimentation process using a hydrometer. This test shall be undertaken in compliance with the ASTM D422 - 63 standard.

Recommendations of the ISSMGE for geotechnical laboratory testing. Particle size analysis, DIN-Beuth Verlag, Berlin.

DIN 18 123:1996 Soil, investigation and testing - Determination of grain-size distribution.

NF P 94-056 :1996 Sols : Reconnaissance et Essais – Analyse granulométrique – Méthode

par tamisage à sec après lavage. (in French)

XP P 94-041 :1995 Sols : Reconnaissance et Essais – Identification granulométrique –

Méthode de tamisage par voie humide. (in French)

BS 1377:1990 Methods of test for soils for civil engineering purposes Part 2: Classification tests; 9.2 Wet sieving method.

BS 1377:1990 Methods of test for soils for civil engineering purposes Part 2: Classification tests; Subclause 9.5 Sedimentation by the hydrometer method.

BS 1377:1990 Methods of test for soils for civil engineering purposes Part 2: Classification tests; 9.4 Sedimentation by pipette method.

SN 670 810c : 1986 Granulats minéraux et sols ; Analyse granulométrique par tamisage /

Mineralische Baustoffe und Lockergesteine; Siebanalyse.

SN 670 816 :1964 Matériaux pierreux; Sédimentométrie par la méthode de l'aréomètre /

Gesteinsmaterialien; Schlämmversuch nach der Araeometermethode.

ASTM D2217:1985 Wet preparation of soil samples for particle size analysis and

determination of soil constants.

Annex W Bibliography prEN 1997-2: Aug 2003 -153

ASTM D422:1963 Test method for particle size analysis of soils.

Strength Index Tests

The purpose of strength index tests is to determine in a rapid and simple manner the undrained

shear strength cu of clayey soils.
This standard covers the following strength index tests:
− laboratory vane test,
− fall cone test.
Laboratory tests on soils and rock prEN 1997-2: Aug 2003 57
The tests shall be performed on undisturbed specimens of Quality Class 1.
The fall cone test should be carried out and reported in accordance with the requirements given in EN-ISO/TS 17892-6.
It should be considered that the values of cu represent the undrained shear strength of the soil at its state in the laboratory. They need not represent the undrained strength of the soil in situ.
Depending on the characteristics of the soil and on the particular strength index test selected the test results can be only an approximate estimate of cu.
Strength index tests should only be used for design where well documented comparable experience with similar soils exists.
If well documented comparable evidence exists, the undrained shear strength derived form the strength index tests may be used when the sample analytical method of EN 1997-1, D.3 is applied.
The test results may be used to check variability of undrained shear strength within a stratum.

Strength testing of soils

The objective of the tests is to establish the drained and/or undrained shear strength parameters.
The following strength tests are covered;
− unconfined compression test;
− unconsolidated undrained triaxial compression tests;
− consolidated triaxial compression test;
− translational shear box test and torsional shear box (ring shear) test.
Translational and ring shear box tests should be used for testing soils under drained conditions.

NOTE Under quick strain rate, clays of very low permeability may be sometimes considered loaded undrained in both types of the shear box apparatus. The test then gives an indication of the undrained strength.
In this section, only strength tests on fully saturated or dry soils are dealt with.

For the determination of the shear strength of clay, silt and organic soils, undisturbed samples (Quality Class 1) should be used. For certain soils or special purposes, tests can be carried out on re-constituted or remoulded specimens.
For coarse silts and sands, the test specimens may be re-compacted or re-constituted. Care should be taken to select a preparation method that reproduces as closely as possible the structure and density relevant for the design at hand.
For re-compacted or re-constituted specimens, the composition, density and water content of the prepared specimens relevant for the in situ conditions and the specimen preparation method shall be specified.
Laboratory tests on soils and rock prEN 1997-2: Aug 2003 58
For a strength test, the following shall be evaluated or specified:
− number of tests required,
− selection of location of test specimens in the recovered samples,
− required quality of sample,
− specimen preparation method,
− orientation of specimen,
− type of test,
− classification tests that need to be done,
− consolidation stresses (if applicable),
− time for consolidation increments (if applicable),
− shearing rate,
− failure criteria,
− criteria for terminating tests (e.g., strain at which the test shall be stopped),
− acceptability criteria (e.g. saturation, scatter),
− accuracy of measurements,
− format for presentation of test results,
− any procedure used in addition to those referenced in an accepted standard.
The shear strength of a sample should be determined by a set of three tests, or more, under different normal stresses.
When determining the shear strength of a soil stratum, the following shall be taken into account:
− type of shearing,
− specimen preparation method,
− need for additional classification tests.
If samples of Quality Class 2 are tested, the effects of the sample disturbance should be considered in the interpretation of the results.

The presentation of the test results shall include, where applicable:
− the effective stress paths,
− the Mohr circles,
− the stress-strain curves,
− the pore pressure-strain curves,
− the pore pressure parameters.
NOTE: Linear extrapolation of the test results can give erroneous values of the strength of the soil as the failure envelope is generally not a straight line, especially at low normal stresses. The stress range over which the strength parameters have been determined shall be given.
There are several methods to obtain the stress-strain and strength parameters of soils in the laboratory and in situ. If appropriate, the results from these different tests should be compared when evaluating the test results.
The results should be evaluated taking into account the strain rate used for testing.
The compression and direct shear tests provide commonly accepted strength parameters

which may be applied to routine design methods, but which are not necessarily applicable to other analyses.
It should be considered that especially unconfined compression and unconsolidated undrained compression tests need not represent the undrained strength of the soil in situ.
Laboratory tests on soils and rock prEN 1997-2: Aug 2003 59

Unconfined compression test

The unconfined compression test should be carried out on specimens of soils of sufficiently low permeability to maintain undrained conditions during the test.
Delays between trimming and testing should be avoided to prevent change of water content of specimens.
test should be carried out and reported in accordance with the requirements given in EN-ISO 17892-7.

The test result is the approximate value of the unconfined compressive strength of the tested soil.
The undrained shear strength cu may be determined as one half of the measured unconfined compressive strength.
The effective stresses within the laboratory specimen may deviate from the effective stresses in situ. Due to the difference the test result need not represent the undrained strength of the soil in situ.

Unconsolidated undrained triaxial compression test

The test shall be carried out without allowing any drainage from the specimens.
During preparation and testing soil specimens shall not be given access to water (e.g., from the drainage leads or pore pressure transducers, etc).
Water content before and after the test and bulk density before the test shall be determined for each specimen.
The test should be carried out and reported in accordance with the requirements given in EN ISO/TS 17892-8.
The test result is the undrained shear strength cu of the tested soil.
The effective stresses within the laboratory specimen may deviate from the effective stresses in situ. Due to the difference the test result need not represent the undrained strength of the soil insitu.

Consolidated Undrained Triaxial Compression Test (CU+U)

This test aims to determine the shear strength of saturated soils through triaxial compression which depends on the stresses applied, time of consolidation, strain rate, and the stress history experienced by the soil. During the test pore water pressures shall be measured. Laboratory procedures shall comply with ASTM D4767 – 11 standard.

Consolidated triaxial compression test

The tests should be carried out and reported in accordance with the requirements given in EN ISO 17892-9.
For a consolidated triaxial compression test, the following shall be evaluated or specified:
− saturation method and saturation criterion,
− back-pressure required,
− any procedure used in addition to those referenced in an accepted standard (e.g. lubricated ends, local measurements of strains or pore pressure).
Laboratory tests on soils and rock prEN 1997-2: Aug 200360

For consolidated undrained triaxial tests, the requirements on measuring pore pressures, and the total stress path for shearing shall be specified.
For consolidated drained tests, the volume change measurement device and the stress path for shearing shall be specified.
Water content before and after the test and bulk density before the test shall be determined for each specimen.
One Atterberg limit determination and particle size analysis should be done per set of triaxial tests in one stratum.
The results shall state clearly the type of test that was carried out, which strength parameters are given, the shearing rate and the failure criterion used to select the shear strength (e.g. peak deviator stress, maximum stress ratio).
The report shall indicate any known deviation from the standard testing procedure, for example in degree of saturation of the test specimens, testing procedures, composition of the specimen or in any other aspect.
In compliance with 2.4.2.3 (4), more advanced laboratory strength tests, such as triaxial extension test, simple shear test, plane strain compression and extension test, true triaxial tests, directional shear test, all with the possibility of anisotropic instead of isotropic consolidation, should be considered.
The evaluation of the test results should take into account that undrained shear strength, pore pressure parameters and stress-strain relationships are affected by sample disturbance to a greater extent than the drained strength parameters.
NOTE: Reliable stress-strain modulus values, especially in the case of stiff soils, can only be obtained from advanced tests with special procedures to measure strains and axial force accurately
Depending on the type of test, drained or undrained strength of the soil may be derived.
Accordingly, the values are effective friction angle and effective cohesion c‘, or undrained shear strength cu.
The values can be used in both drained and undrained stability analyses (EN 1997-1, annex D).

Triaxial deformability testing

The objective of the triaxial deformability testing of soils is to determine the deformation moduli (stiffness parameters).
Depending on the loading path, various stiffnesses can be measured.
According to the drainage conditions, drained or undrained moduli E’ or Eu can be determined.
Due to the non-linearity of soil behaviour, various moduli, e.g. tangent and/or secant moduli may be defined at different stress or strain levels.

For the determination of the stiffness of a stratum of a soil, undisturbed samples (Quality Class 1) shall be used.
NOTE: Small strain moduli of soils (e.g. moduli at less than 1% strain for soft to medium clays) are very sensitive to all perturbations during sampling. According to 3.4.3 (3) specific sampling equipment and method may be used, for example block sampling or stationary piston sampling or any other method known to give the best results for the soils to be tested.
Laboratory tests on soils and rock prEN 1997-2: Aug 2003 63
The stiffness may be characterised by a complete curve, or by some arbitrary values. For example, by the initial elastic Young’s modulus E0 or by E50 corresponding to 50% of maximum shear stress, etc.
A special instrumentation capable of measuring stresses and strains with high resolution shall be used for stiffness determination at the strain level below 0.1%.
NOTE For determination of very small strain moduli the techniques based on propagation of shear waves or other dynamic methods can be used.
Young’s modulus and stress-strain curves of soft, normally consolidated soils may in some cases be determined from the standard triaxial strength tests.

When determining the stiffness characteristics of a soil stratum, the following items shall be considered:

- quality of samples,
- sensitivity, saturation, state of consolidation and cementation of soils,
- specimen preparation,
- orientation of the specimen.

Recommendations of the ISSMGE for geotechnical laboratory testing. Recommended test methods for unconfined compression tests on cohesive soil, DIN-Beuth Verlag Berlin.

NF P 94-077 :1997 Sols : Reconnaissance et Essais - Essai de compression uniaxiale. Annex W Bibliography prEN 1997-2: Aug 2003 155

Recommendations of the ISSMGE for geotechnical laboratory testing. Method for unconsolidated triaxial compression test on saturated cohesive soil, DIN-Beuth Verlag Berlin.

NF P 94-070 :1994 Sols : Reconnaissance et Essais - Essais à l'appareil triaxial de révolution - Généralités, définitions

NF P 94-074 :1994 Sols : Reconnaissance et Essais - Essai à l'appareil triaxial de révolution - Appareillage - Préparation des éprouvettes - Essais (UU) non consolidé non drainé – Essai (CU + u) consolidé non drainé avec mesure de pression interstitielle - Essai (CD) consolidé drainé.

Recommendations of the ISSMGE for geotechnical laboratory testing Method for consolidated triaxial compression tests on water-saturated soil, DIN-Beuth Verlag Berlin.

BS 1377:1990 Methods of test for soils for civil engineering purposes: Part 8.

NF P 94-070 :1994 Sols : Reconnaissance et Essais - Essais à l'appareil triaxial de révolution - Généralités, définitions.

NF P 94-074:1994 Sols : Reconnaissance et Essais - Essai à l'appareil triaxial de révolution - Appareillage - Préparation des éprouvettes - Essais (UU) non consolidé non drainé - Essai (CU + u) consolidé non drainé avec mesure de pression interstitielle - Essai (CD) consolidé drainé.

Recommendations of the ISSMGE for geotechnical laboratory testing, Method for Direct Shear Testing on Water-Saturated Soil, DIN-Beuth Verlag Berlin.

BS 1377:1990 Methods of test for soils for civil engineering purposes Part 7 Shear strength test.

ASTM D 3080:1990 Test method for direct shear test of soils under consolidated drained conditions.

SS027127 Geotechnical tests - shear strength – Direct shear test, CU- and CD- tests –Cohesive soils.

NF P94-071-1 :1994 Sols : Reconnaissance et Essais - Essai de cisaillement rectiligne à la boîte - Partie 1 : Cisaillement direct.

NF P94-071-2 :1994 Sols : Reconnaissance et Essais - Essai de cisaillement rectiligne à la boîte - Partie 2 : Cisaillement alterné.

Water Contents

Moisture content - laboratory determination of the water (moisture) content by mass of soil. This test shall be undertaken in compliance with:

ETC5-N94.47, 1995 Laboratory method for determination of water content of soil, DIN-Beuth Verlag Berlin

DIN 18 121:1998 Subsoil; testing procedures and testing equipment, water content, determination by drying in oven.

NF P 94-050:1995 Soils: Investigation and testing. Determination of moisture content. Oven drying method.

BS 1377:1990 Methods of test for soils for civil engineering purposes Part 2: Classification tests.

SN 670 340:1959 Essais; Teneur en eau / Versuche; Wassergehalt.

ASTM D2216:1992 Test method for laboratory determination of water (moisture) content of soil, rock, and soil-aggregate mixtures.

ASTM D2974:1987 Test methods for moisture, ash, and organic matter of peat and other

organic soils.

ASTM D4542:1995 Test methods for pore water extraction and determination of the soluble salt content of soils by refractometer.

Water content determination

The objective of the test is to determine the gravimetric water content of a soil material. The gravimetric water content is defined as the ratio of the mass of „free“water to the mass of dry“ soil. The tests should be carried out and reported in accordance with the requirements given in EN ISO/TS 17892-1.

Soil specimens for measuring the water content should be at least of Quality Class 3.

If a sample contains more than one soil type, water contents should be determined on the specimens representing the different soil types.

When evaluating the results, the presence of significant amounts of gypsum, highly organic soils, materials in which the pore water contains dissolved solids and soils with closed pores filled with water, shall be accounted for, when relevant.

The extent to which the water content measured in the laboratory on the soil ‘as received’ is representative of the ‘in situ’ value should be checked. The effects of the sampling method, transport and handling, specimen preparation method and laboratory environment, should be taken into account in this assessment.

For the soils meant in (1)P. a drying temperature of approximately 50°C may be more appropriate than the usually prescribed, but the results obtained should be considered with caution.

A7. Seismic Testing

Laboratory Tests

It is impossible to construct a laboratory apparatus which would subject a soil specimen to the conditions experienced by an element of soil in the field during dynamic excitation. Some laboratory tests are designed to measure specific basic soil properties like shearing strength or shear modulus, while others are designed to determine soil behaviour in a simulated dynamic environment. Prior to laboratory testing a field exploration and sampling program must be conducted. The techniques employed to obtain samples depends of type of soil and existing data.

Cyclic Simple Shear Test

The cyclic simple shear test most nearly duplicates the loading conditions thought to occur during an earthquake (10). The device used by LNEC is shown in Figure A1.8 and consists of (9): (1) the sample assembly; (2) the vertical load unit; (3) the horizontal load unit. The sample assembly consists of a pedestal, the lower and upper filter holders and a plastic container. The pedestal contains a mechanism for clamping and releasing the lower filter holder.

Figure A1.8 LNEC Cyclic Simple Shear Equipment •

The vertical load unit consist of the base, the tower, the lever arm, the load gauge, the piston, the dial gauge and the adjusting mechanism. The horizontal unit for constant rate of strain consists of a gear-box, the load gauge, a precision ball bushing, a connection fork and the sliding box. The gearbox which has three different speeds is designed for interchangeable synchron motors with reduction gears. The gearbox has two end switches which limit the horizontal movement 10 rom on both sides of the neutral position. A constant volume test can be performed by keeping the height at the sample constant through adjustment of the applied vertical stress by means of the height controller. In such test the change of vertical stress required to maintain constant volume is equal to the change in pore pressure in a comparable undrained test. The height of the specimen is observed on displacement transducer placed between the pedestal and the slide box. The vertical load is determined by the vertical load gauge (transducer) adjusted by means of the adjusting mechanism operated by the servomotor. The cyclic loading system consists of the following parts: (1) pneumatic tension/compression actuator; (2) load cell for tension/compression; (3) cabinet with pneumatic parts + power source to shear apparatus and transducers. For adjusting a decided load

pulse, it is necessary to program the function generator to the desired period and to select the pulse direction and the waveform. The multicorder is provided of four independent channels and allows the record of vertical and horizontal forces and vertical and horizontal displacements. The shear modulus G is defined as the equivalent linear secant modulus, the slope of the line drawn through the end points of the hysteresis loop. By measuring the area within the loop (energy dissipated during the cycle) and the area beneath the "skeleton" curve (potential energy stored during tile cycle), the equivalent linear damping ratio D can be calculated.

Cyclic Triaxial Test

In the cyclic triaxial test the specimens can be consolidate under isotropic k 1,0=1.0, or the anisotropic I c ~1.0 stresses, where k'c is defined as the ratio of the major (jlc' to the minor (j 3c effective principal stress. Normally three different confining pressures are required with the highest near the maximum effective overburden pressure existing in the embankment. A general view of the apparatus used by LNEC is shown in Figure A1.9.

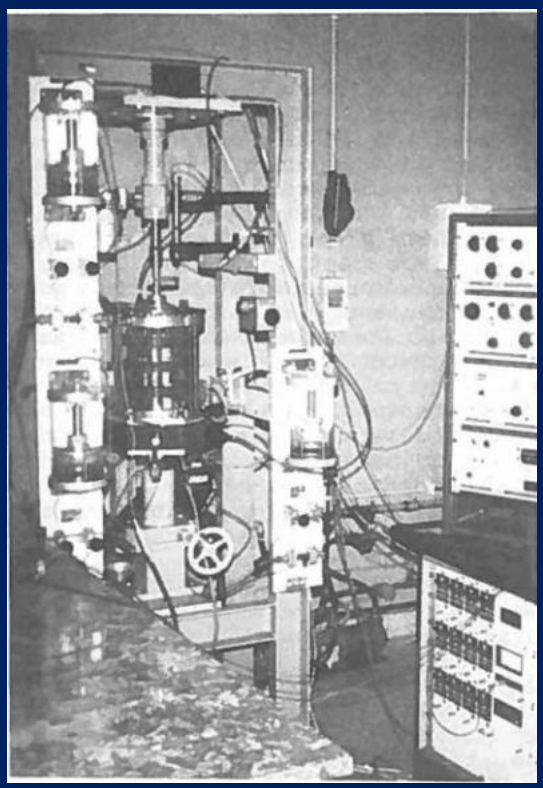

Figure A1.9 LNEC Cyclic triaxial equipment

The system allows the application of deviator and lateral stresses. The flow demands of an individual rig are low and a single small hydraulic pump can power two or three rigs working independently. Each rig comprises a loading frame housing a triaxial cell placed co-axially beneath a hydraulic ram which supplies the deviator stress. The lateral stress is generated by another

hydraulic ram connected to a Bellofram- sealed piston filled with de-aired water and connected to the triaxial cell. Electrical transducers fixed inside and outside the triaxial cells are used to measure applied loads, deformations, pore water pressures and lateral pressures. An electronic control unit supplies a command signal to the servo-valve which controls the flow of the pressurized oil to the ram. The d.c. voltage load component of the command signal causes the hydraulic ram to generate a standing force (or pressure) level and the a. c. component determines the required forces variations. To adjust the phase lag between the two actuators and their assemblies, both actuators are driven from two variable phase outputs on the same waveform generator so that a phase advance may be built into the confining stress signal relative to the deviator stress control signal. In the load - controlled mode of operation the negative electrical feedback is supplied by the load cell transducer housed in the base of the triaxial cell, directly beneath the sample. The feedback source could otherwise be a linear variable differential transformer (LVDT), the test then operating in the deformation control mode. By using the LVDT output signal to drive the gain of an amplifier, control of the stress applied to the sample is accomplished. The amplifier gain is increased proportionally to the decrease in sample height, and hence proportionally to the increase in sample cross-sectional area (assuming uniform sample deformation). The input to this amplifier is the summed a.c. and d.c. command signals, so that the amplifier output, Le. the servo-value driver voltage and hence the force applied by the ram, is increased by the same proportion. The automatic stress control is based on the assumption that tests are done undrained with no volume change. In case of drained tests manual correction is provided to compensate for the change in volume caused by drainage, to maintain a constant stress. In view of the fact that the actual seismic shear stress involves changes in direction the true triaxial test apparatus in which three principal stresses can be applied independently on a cubical specimen is recommended.

Cyclic Torsional simple shear

To overcome the disadvantages inevitable in conventional type of simple shear test which has end boundaries, torsional simple shear devices have been developed in which hollow cylindrical specimens are used. Since a hollow cylindrical specimen has no end boundaries, the specimen can be considered free from stress concentration problems. For long hollow cylindrical devices, specimen preparation is more difficult. "Undisturbed" specimens can be formed more easily for short hollow cylinder specimen rather than tall hollow cylindrical apparatus. While the initial shearing stress conditions in a short hollow cylinder specimen were described as uniform it is noted that because the shearing stresses on each boundary are not the same, all initial stresses cannot be uniform throughout the sample. Figure A1.10 shows a view of LNEC torsional simple shear device. A pneumatic cyclic loading systems was employed. cyclic linear motion of the piston of a

double-action Bellofram cylinder is converted to cyclic rotational movement of the vertical loading ram through a stretched wire, four pulleys and a wheel. The other single action Bellofram cylinder is placed on the top plate of the device for providing a vertical load to the specimen. A hydrostatic confining pressure is provided to confine a hollow cylindrical specimen the outside and inside faces of which is enclosed with conventional rubber membranes. The hollow cylindrical specimen is 100 rom in outer diameter, 60 rom in inner diameter and 100 rom high. six 1.5 rom high stainless; Steel Wire Cyclic 100d- Wheel Load cell for axial load and torque vertical displacement transducer Bellofram cylinder - Regulated air pressure Thrust bearing and loading device Stroke bearing Rotational displacement transducer Stroke bearing Btaring houst (0.04 mm GAP) Hollow cylindrical specimen. Torsional Simple Shear Device blades are fixed on the surface of porous stone of the top cap and the bottom pedestal to prevent slippage of the sand. After consolidating the specimens under the stress condition, a cyclic undrained test was performed. For an isotropically consolidated specimen, the vertical loading ram was free to move vertically during torsional cyclic loading. Since during the cyclic test both the vertical and volumetric strains are zero, the change in cross area of the specimen was also zero during cyclic loading. It is not unreasonable to assume that the outside and inside diameters were constant during cyclic loading. In this case, no change in the cross area results in no radial strain in a specimen. This is similar to the in situ plane strain condition in level ground during earthquake shaking. •

Resonant Column Tests

The resonant column test for determination modulus and damping characteristics of soil is based on the theory of wave propagation. Either compression waves or shear waves can be propagated through the soil specimen from which either Young I s modulus or shear modulus can be determinated. In a resonant column apparatus, the excitation frequency is adjusted until the specimen experience resonance. The modulus is computed from the resonant frequency and the geometric properties of the specimen and driving apparatus. A measure of the damping ratio can be obtained by either of two methods, amplitude decay or magnification factor. In the amplitude decay method, a soil specimen is forced to vibrate, and after the driving power is turned off the decay in vibration amplitude is recorded. The logarithmic decrement and damping ratio can be computed by measuring the amplitude prior to and at different numbers of cycles following the interruption of power. The magnification factor method involves the measurement of the vibration amplitude of the specimen at the resonant frequency and at the square root of two times the resonant frequency. This latter method is preferred because it is simpler of the two and provides a measure of damping as a function of strain amplitude.

Shaking Table

In view of the limitations of small-scale tests (the specimen configuration, the boundary conditions and the loading conditions) it has been suggested that improved results might be obtained by tests on large specimens, with which the behaviour of a natural soil mass could be more closely approximated, and where a "free field" zone, removed from the effects of

Figure A1.10 LNEC Cyclic torsional simple shear

boundaries, might be created. This can be done placing a large container of saturated soil on a shaking table and subjecting it to cyclic loading. To assure that the central part of the specimen would be as nearly as possible in a "free field" condition the test specimen was 90" by 42"tapering to 74" by 30" at the top and 4" height (Figure A1. 11). All specimens were prepared by pluvial deposition, using the sand spreader system that consists essentially of a Section sand hopper mounted on a self-propelled gantry moving at constant speed. The acceleration was provided by attaching the rail mounted specimen chamber to an MTS electro-hydraulic actuator system. This actuator could be programmed to reproduce various displacement patterns and actual earthquake records, a sinusoidal excitation was selected as most appropriate, considering that a specific earthquake record would provide information on only one special case, whereas earthquake records could always be reduced to equivalent sinusoidal motions, and more generally applicable results would be obtained.

Finally, in choosing the frequency of motion, a compromise was sought between high accelerations, which required high operating frequencies for the actuator system, and the

reproduction of a frequency characteristic of a strong motion earthquake. Accordingly, an operating frequency of four Hz was chosen, which was in the strong motion earthquake range and for which accelerations in excess of 3 g could be obtained.

Figure A1.12 illustrates a view of LNEC shaking table.

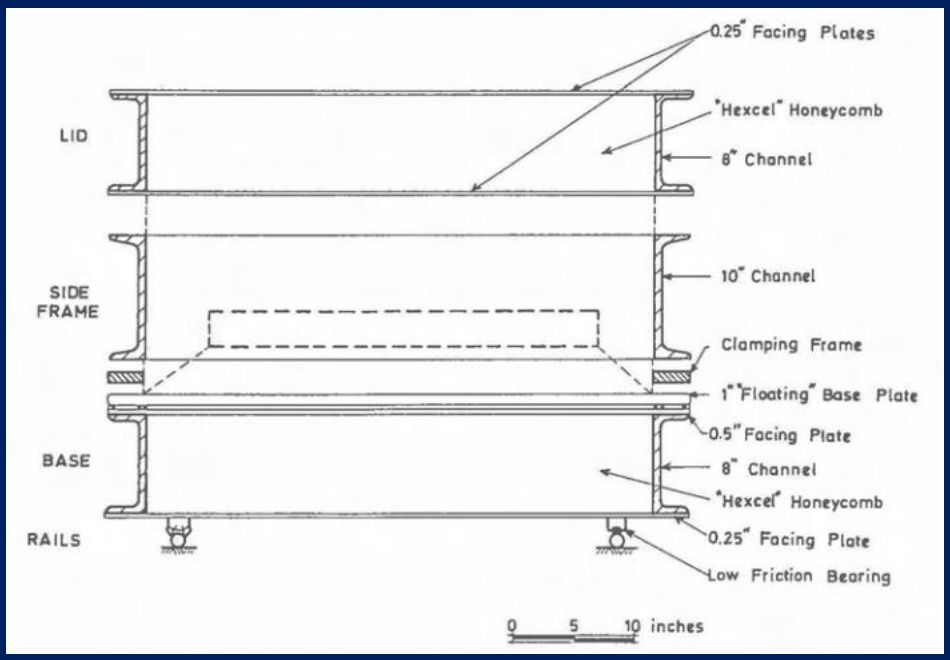

Figure A1.11 Cross section of Shaking Table System.

Figure A1.12 View of LNEC shaking table

Centrifuge Tests

Experimentation on a centrifuge presumes the knowledge of: (i) how to impose artificial boundaries that do not seriously influence the experimental results and (ii) the requirements of similitude which have a non-trivial effect on the prototype problem at the geometric scale chosen for the model test. There are three principal ways in which ground motion simulation experiments aboard a centrifuge are potentially of considerable value within the near future: (i) to provide data concerning motions, stresses etc, against which predictive theories and simpler methods of testing may be checked; (ii) to observe general patterns of response and behaviour in poorly understood situations; and (iii) to develop further the theory and practice of dynamic centrifuge modelling.

Figure A1.13 illustrates a view of LNEC centrifuge equipment.

Figure A1.13 View of LNEC centrifuge equipment

Preparation of Specimens

In general, three different specimen preparation methods are adopted: (i) the air pluviation method; (ii) the wet tamping method; and (iii) the wet vibration method. The air pluviation method consists of pluviating air dry sand into a mold from a tube keeping the height of fall constant. Densification

of the specimens is accomplished by increasing the height of fall. The wet tamping is a method of compacting moist coarsed grained material in which the material is placed in layers with each layer compacted to a prescribed dry unit weight. The density of each layer is controlled by adjusting the height of the layer. To assure the vertically uniform specimen the number of tamping for each layer is increased properly for higher layers and the compacted surface of each layer is scarified. In the wet vibration method, each layer is compacted by tapping the mold with a wooden hammer until the height of the layer is reduced to a prescribed value. The compacted surface of each layer is scarified.

Summary of the Laboratory Testing Techniques

The available laboratory techniques were presented in Figure 7.48 where the specified properties or characteristics measured by each were indicated. The clear consensus of those researchers performing dynamic soil tests in the laboratory is that there is no "perfect" laboratory test. The cyclic triaxial test has the following limitations: a) Shearing strain measurements below 10-2 percent are difficult to achieve.

The extension and compression phases of each cycle produce different results; therefore, hysteresis loops are not symmetric in strain-controlled tests and samples tend to neck in stress-controlled tests. c) stress concentrations occur at the cap and base of the specimen. d) Void ratio redistribution occurs within the specimen during cyclic testing. A major drawback of most of the cyclic simple shear apparatus is that they do not permit measurement or control of the lateral confining pressure during cyclic loading. The strains produced by a strong motion earthquake are greater than those applied in the resonant column apparatus. An advantage of the resonant column test is that the low strain levels correspond to those produced in geophysical tests. This makes it possible to investigate effects of sample disturbance, remoulding, removal of large size particles, etc. Because, of its versatility and potential range of shearing strain amplitudes, the torsional shear technique possesses superior capabilities for many kinds of dynamic soil testing and avoids some of the difficulties associates with cyclic simple shear tests. However, there are valid arguments against the hollow cylinder torsional shear tests compared to the cyclic simple shear test because of the sample size and shape. The shaking table has been used in attempts to avoid some difficulties associated with other simple shear tests. Because of the potential stress concentrations, I nonuniform stress conditions I and void ratio variations which occur in small scale simple shear tests many researchers suggested the use of large-scale simple shear test using, a shaking table for excitation. The centrifuge tests require a knowledge of similitude laws but provide data to check theories and other methods of testing.

Field Techniques

Geophysical in situ investigations methods are used to obtain the in situ shear wave velocity from which the shear modulus is calculated. A number of different geophysical explorations methods for determining in situ shear velocity (Vs) have been developed and employed over the last 20 years. Attempts have been made by several investigators to obtain damping characteristics of soils in situ. However, because the field tests are generally expensive and the results are of uncertain reliability, design engineers presently prefer to rely on laboratory determined damping values.

Seismic reflection

In the reflection method, an explosive charge is detonated and the surface geophones pick up the shear or Rayleigh wave reflected from subsurface layers of sufficient velocity contrast. In general, the reflection method is not used shear wave velocity measurements; however, under certain circumstances, shear and or Rayleigh wave reflections can be discriminated on a standard reflection seismogram.

Shear wave - crosshole

The method basically consists in generating seismic waves at a particular level in one borehole and recording their arrivals at the same level in one or more neighbouring boreholes (7). Once the distance travelled is known wave velocities are calculated by dividing that distance by the travel time. A brief description of the equipment developed at LNEC is outlined hereafter. The mechanical energy source or shear wave hammer (Figure A1.14) has been designed to generate vertically polarized shear waves and to allow the reversal of the input energy. This source is basically composed of a fixing system and a percussion system. The fixing system has a hydraulic pump, which makes two plates to expand or contract in order to clamp the source to the borehole walls and to remove it as the test has been performed.

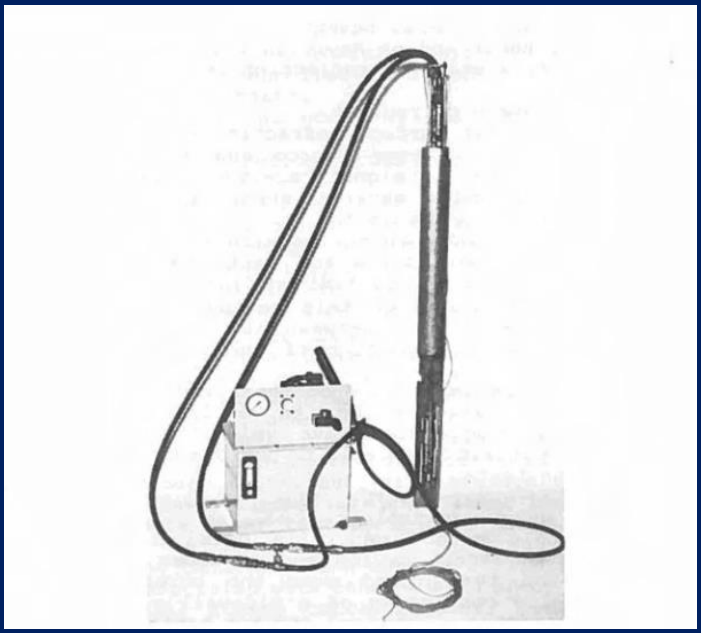

Figure A1.14 LNEC shear wave hammer

The percussion system is composed of a cable operated weight placed inside the cylinder, the energy being originated by the falling weight and transmitted to the ground through the plates in the expanded position. The slide weight is designed so that impacts in upward direction are also possible. The waves produced at the source are received by a triaxial geophone, specially designed for the tests. This geophone incorporates transducers that record the three components of particle vibration and is clamped to the borehole walls by a mechanical device operated from the surface. The recording system is composed of a set of ABEM amplifiers and of a TEKTRONIX oscilloscope, all fed by batteries. To the screen of the oscilloscope a TEKTRONIX camera with POLAROID film is couple. The oscilloscope is triggered by the signal transmitted by a velocity transducer placed inside the source, near the ·p application of the impact. For crosshole seismic tests generally three boreholes 3 to 4 m spaced are drilled and provided with iron casing, which is cemented to the surrounding soil to prevent voids. In order to know the exact distances between boreholes at tests elevations the verticality of each cased boreholes is systematically determined through an inclinometer survey. To perform a test the following procedure is adopted: a) After the source and the geophones have been clamped to the borehole walls a downward impact is produced by the falling weight and simultaneously the oscilloscope is triggered. h) The seismic signals are received at the two neighbouring geophones, amplified and then displayed on the oscilloscope and photographed on the upper half of the display screen. cJ Once this has been done an impact in the upward direction is produced and the seismic signals are now photographed on the lower half of the display screen.

Shear wave - downhole

The downhole method generally uses an energy source consisting of an impact device and a wooden plank or steel plate placed on the ground near the borehole. A signal receiver, usually consisting of a sidewall clamped velocity borehole probe with one vertical and two horizontal geophones in an orthogonal arrangement is positioned at various selected depth intervals in the borehole. Best results are obtained when using an uncased borehole drilled with thick gel mud. Plastic and steel-cased boreholes are satisfactory if the casing makes good contact with the embankment material.

Shear wave – refraction.

The conventional surface refraction survey is performed utilizing an impact energy source and a linear array of horizontal geophones as signal receivers. The geophones are arranged in a line and to generate shear waves a sledge hammer or other impact device is used. Since this method does not require the use of boreholes it is relatively inexpensive and fast; however, its depth penetration capabilities are limited. The major drawbacks of this method are that it cannot detect low velocity layers between high velocity layers and that it samples only a portion of the material in a thick layer. Because of the importance of shear moduli of soils, and the difficulties associated with estimating shear wave velocities from compression wave velocities and Poisson I s ratio, it is important to be able to perform high quality shear wave refraction tests.

Shear wave - uphole

The uphole method is usually performed by placing geophones on the ground surface near the shot-hole. Generally, a low yield explosive charge such as one or two seismic electric blasting caps, is detonated in the mud-filled borehole and the signal trace is picked up by the surface geophones.

Seismic CPT tests

- Seismic CPT The seismic cone penetration test (SCPT) allows the in situ determination of shear wave velocity with the advantage of low cost on the other in situ seismic tests which require one or more boreholes (6). The introduction of seismic measurements into the cone penetration test procedures enables the specific determination of the dynamic shear modulus (Gm~). To obtain the measurement of dynamic shear modulus, a small rugged velocity seismometer has been incorporated into the cone penetrometer. The miniature seismometer is a Geospace GSC-14-L3 (1.7 cm diameter) with a nominal natural frequency of 28 Hz. The seismometer is placed in the horizontal direction and orientated transverse to the signal source to detect the horizontal component of the shear wave arrivals. suitable seismic signal source should preferentially generate large amplitude shear waves with little or no compression wave component. The shear waves travel through the soil skeleton and are thus related to the soil shear modulus. The seismic CPT is,

however, considerably less expensive, and a more rapid procedure than the crosshole technique, especially if CPT procedures are employed as part of the standard site investigation

Standard penetration test (SPT)

Schmertmann (1977) suggests that we can hope to measure with the SPT only those dynamic properties for which the SPT provides either a direct model of the phenomenon, or the factors which control the behaviour of the SPT also similarly control the dynamic behaviour with which we wish to correlate. Advantages of the SPT in evaluating dynamic effects as pointed out (8) are: The SPT is a dynamic test modelling a dynamic phenomenon; The SPT is essentially undrained for each blow; The SPT generates principally shearing energy.

Summary of field Test

Seismic reflection method had in the past a very limited application at shallow depths for reasons related with laborious processing procedures and noise problems. In recent years, however, with the proliferation of the micro-computers, processing of digital data became cheaper and faster and new equipment was designed to account for the stringent problem of the noise contamination of the data. Seismic reflection is now being regarded as an alternative of the seismic refraction method. Although measurements performed with the downhole or the uphole method require only a single test hole, the extra holes required for the crosshole method are well worth the effort to provide comparison of the test results. The corroborative information thus obtained from this basically independent source (e.g. crosshole in addition to downhole) assures reliable shear wave velocity values. The cross-hole data are expected to be the most reliable because of better control over and knowledge of the wave path. The downhole or uphole techniques do not permit a precise resolution because travel times in any layer are averages over the layer. The use of penetration tests avoids judgments on the part of the engineer concerning the representativeness of soil samples. While the SPT has been widely used for many years in many cases it may be more expedient to use the static cone penetration test (CPT). The main advantages of this procedure are that it provides data much more rapidly than does the SPT, it provides a continuous record of penetration resistance in any borehole, and it is less vulnerable to operator error than the SPT. Some important areas for research involve eliminating disturbance developing performance. or the effects of disturbance in field sampling, uniformity in lab specimen preparation, and consistency in laboratory and field tests.

Summary

Table A1.11 and Table A1.12 summarize the most frequent field tests and laboratory tests.

γ = bulk density	I_d = relative density
K_o = coefficient of earth pressure at rest	G_{max} = maximum shear modulus
OCR = overconsolidation ratio	c = cohesion
S = sensivity	ϕ = friction angle

V_s = transverse wave velocity

E = elasticity modulus

V_p = longitudinal wave velocity

S_u= undrained strength

M = confined modulus

G = shear modulus

□ = damping ratio

Table A1.11 Field tests

Tests	Parameters		
	V_p	V_s	G_{max}
Refraction	x	x	x
Uphole	x	x	x
Downhole	x	x	x
Crosshole	x	x	x

Table A1.12 Laboratory tests

Tests	Parameters			
	G	E	□	G_{max}
Resonant Column	x	x	x	x
Cyclic Triaxial	x	x	x	
Cyclic simple shear	x	x	x	
Cyclic torsional shear	x	x	x	

In Figure A1.15 is shown the variation of shear modulus and damping ratio with shear strain for gravels materials (GW), sandy soils ((SW), clay materials of low plasticity (CL) and clay materials of high plasticity (CH) (Stokoe et al. 1999; 2004).

A.8 Rock Testing

Laboratory Tests

Laboratory tests upon rock samples from borehole cores are envisaged. The samples shall be carefully chosen in terms of their representativeness of the materials intercepted by the hydraulic structures under study.

Laboratory tests should be conducted in compliance with the Standards of the American Society for Testing and Materials (ASTM) or according to the recommendations of the International Society for Rock Mechanics (ISRM) or any other international standards acclaimed in the bibliography of specialty, when applicable. The technical specification or standard under which the test was based must be duly mentioned.

ASTM D4543:1985 Preparing Rock Core Specimens and Determining Dimensional and Shape Tolerances
Annex W Bibliography prEN 1997-2 Aug 2003 -157

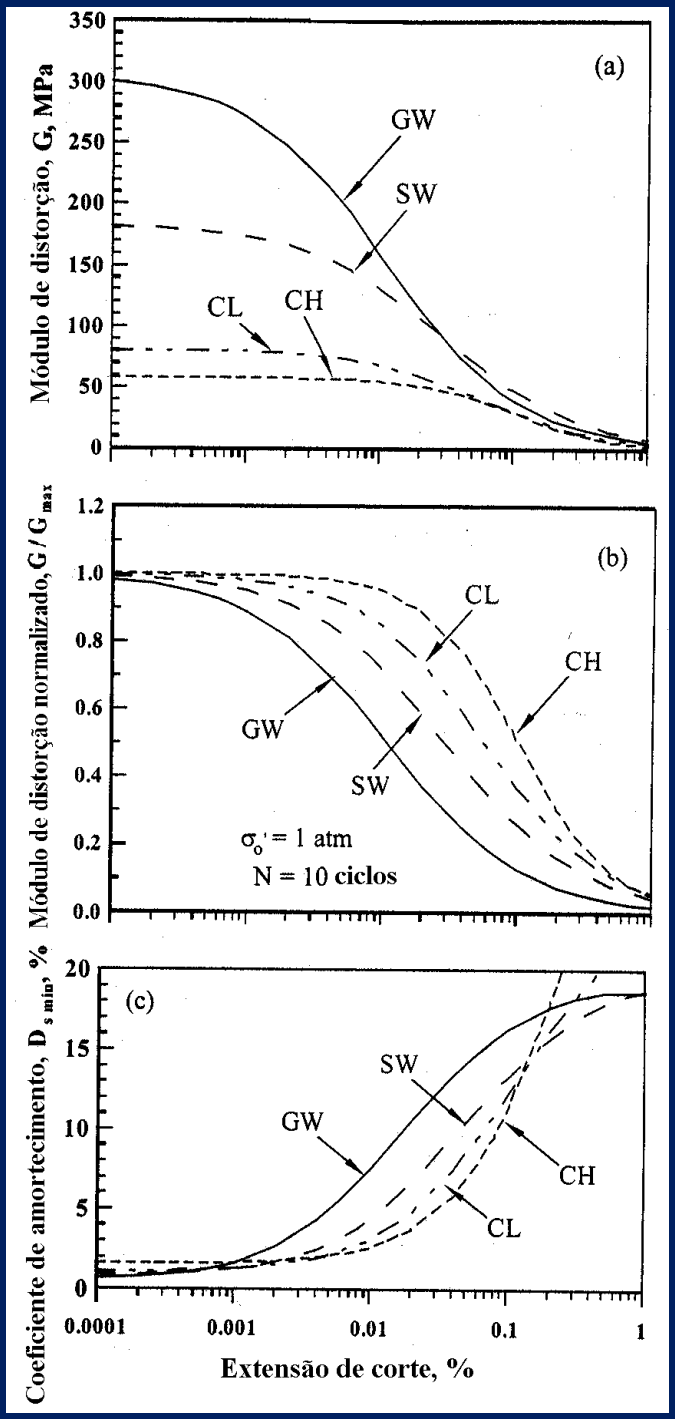

Figure A1.15 Variation of shear modulus and damping ration with shear strain for (GW), ((SW) (CL) and (CH) materials (after Stokoe et al. 2004)

General

BS 5930:1981, Code of practise for site investigation Section 8 Description and classification of rocks for engineering purposes

ISRM Suggested Methods for Rock Characterisation, Testing and Monitoring, Part I Site

ISO/DIS 14699:1995 Geotechnics in civil engineering. Identification and description of rock.

EN ISO/DIS 14689.2 Geotechnical engineering – Identification and description of rock.

Brazilian Test

Test specimens should be cut with specimen diameters not less than the NX core size, (about 54 mm), with a thickness of approximately equal to the specimen radius. The cylindrical surface should be free from obvious tool marks. Any irregularities across the thickness of the specimen should not exceed 0,025 mm. End faces should be flat within 0.25 mm and parallel to within 0.25 degree

The Brazil test is intended to measure indirectly the uniaxial tensile strength of a cylindrical rock specimen.
The following shall be specified in addition to the requirements:
− test specimen orientation and dimensions,
− testing method.
Due to the variability of the test results, duplicate testing of test specimens cut in parallel shall be performed.
For shales and other anisotropic rock, it is recommended to cut test specimens parallel to and perpendicular to bedding. For specimens cut parallel to bedding the direction of the load related to bedding should be specified.
The test specimens shall be prepared from cores taken with Category A sampling.
Recommendations for testing given in V.5 should be followed.
The test procedure given in W.2.12.5 may be applied.
The evaluation of tensile strength should take in consideration that the presence of hidden weakness planes in the test specimen may disturb the result and the failure plane should be sketched after test and evaluated.
The test provides an indirect determination of the tensile strength T in a forced rupture plane.
The tensile strength T may be used as a classification parameter for the intact rock quality and it may be used in a Mohr diagramme at a corresponding maximal stress σ1 together with Mohr circles from undrained or triaxial compression tests to define the Mohr-Coulomb rupture parameters ϕ (friction angle) and c (internal cohesion).
The test is intended for strength classification and characterisation of intact rock and should not be used without geological correlation and rock classification for field conditions.

Cerchar AbrasionTtest

This test provides a rock abrasion index “Cerchar Abrasivity Index (CAI)” that estimates the hardness of the rock. The CAI vary between values inferior to 0,5 for weak rocks and values greater than 5 for hard rock.

This test shall be undertaken in compliance with the recommendations of the “*Centre d’Études et Recherches des Charbonnages de France (1986)*”.

Crushing Value

This test aims at the determination of the aggregate crushing value (ACV) which gives a relative measure of the resistance of an aggregate to crushing under a gradually applied compressive load. It shall be performed in accordance with BS 812:1990. Testing Aggregates: Part 110 - Method of determination of the aggregate crushing value Marsal-Resendiz

$$Pa = \eta D\lambda \qquad \text{(A1.1)}$$

Where

Pa – crushing strength in kgf;

D - average dimension (d1 + d2 + d3)/3), in cm;

λ, η - coefficients, λ no dimension, η in kgf/cm2.

Some correlations between mechanical properties and crushing tests were proposed by Delgado Rodrigues et al. (1982) and presented in Figure A.1.

Density and Porosity

Density of a rock corresponds to the weight of particles per unit volume, including all voids, and reflects the composition of the rock or constituents of its grains and its porosity. The porosity characterizes the relative ratio of solids and voids.

The density and porosity should be integrated in the reporting of rock description and established strength and deformation characteristics of the rock types in boreholes and at test sites.
The density and porosity results should be used for comparison of rock strength and deformation properties and to establish correlations for the different rock types.
The existence of closed pores can influence the porosity. The determination of the total pore volume should be based on the density of solids of a powdered. However, the determination of the amount of open and closed pores calls for specialized analysis.

ISRM Part 1 Suggested methods for determining water content, porosity, density, absorption – Section 2: Suggested method for porosity/density determination using saturation and calliper techniques

ISRM Part 1 Suggested methods for determining water content, porosity, density, absorption - Section 3: Suggested method for porosity/density determination using saturation and buoyancy techniques.

This test shall be undertaken in compliance with the ISRM (1977) guidelines.

Direct Shear Test

The direct shear test measures peak and residual direct shear strength as a function of the stress normal to the plane of shearing.

If the surface characteristics of a discontinuity that controls the shear strength are determined, an accurate description should be done, including type and roughness of the joint, type and thickness of fill material, and presence of water in the joint.

The direct shear test measures peak and residual direct shear strength as a function of the stress normal to the plane of shearing.

This standard deals with the laboratory testing for the determination of the basic shear strength parameters and the surface characteristics of a discontinuity that controls the shear strength.

If the surface characteristics of a discontinuity that controls the shear strength are determined, an accurate description should be done, including type and roughness of the joint, type and thickness of fill material, and presence of water in the joint.

The following shall be specified in addition to the requirements in 5.14.2(1)P:

− test specimen orientation and dimensions,

− specifications of the testing machine,

− rate of shear displacement during test,

− selection of normal stress to be maintained during the single shear tests.

The test specimens shall be prepared from cores taken with Category A sampling or from blocks taken in a pit using at least Category B sampling.

Recommendations for testing given in V.4 should be followed.

The test procedure given in W.2.12.4 may be applied.

The evaluation of test results of shear strength versus stress perpendicular to the rupture plane should include a study of the shearing plane in order to take into account bedding and schistosity or cleavage of the rock specimen or the interface properties between rock and concrete, whatever tested.

Shear strength parameters ϕ (friction angle) and c (cohesion) may be established using a number of shear tests on specimens taken from a rock stratum or using multiple testing on an established rupture plane, the latter defines residual parameters mainly.

The test measures the shear strength in a forced rupture plane under certain stresses perpendicular to the rupture plane. Peak strength and residual shear strength after some shear deformation can be established. It is possible that the rupture plan is intendently established along a known discontinuity.

Laboratory tests on soils and rock prEN 1997-2: Aug 2003 73

The test is intended for strength classification and characterisation of intact rock and should not be used without geological correlation

The following shall be specified test specimen orientation and dimensions, specifications of the testing machine, rate of shear displacement during test, selection of normal stress to be maintained during the single shear tests.

The following amendments should be made to the ISRM procedure:

a) The testing machine should have a travel greater than the amount of dilatation or consolidation expected, and should be able of maintaining normal load to within 2% of a selected value throughout the test. Dilation should be measured during the test with the same accuracy as the shear displacements.

b) The rate of shear displacement should be less than 0,1 mm/min in the 10 min. period before taking a set of readings. If automatic data logging is used, there may be no need for a reduction of the rate of shear displacements to 0,1 mm/min.

c) The specimen should be reconsolidated under each new normal stress, and shearing continued according to criteria given in ISRM. If sample surfaces are cleaned before beginning a new testing phase, or the samples are unloaded before repositioning, this should be noted in the test report.

The appearance of the material removed by cleaning should be described.

The direct shear strength may also be determined by field tests. This requires a detailed assessment of the field characteristics of the discontinuities.

The results are utilised in, for example, equilibrium analysis of slope stability problems or for the stability analysis of dam foundations, tunnels and underground openings.

A shear strength determination should preferably comprise at least five tests on the same test horizon or from the same joint family, with each specimen tested at a different but constant normal stress in the applicable stress range.

The following specifications shall be followed:

- ASTM D 2938-86 Standard Test Method for Unconfined Compressive of Intact Rock Core Specimens.

- ASTM D 3148-86 – Standard Test Method for Elastic Module of Intact Rock Core Specimens in Uniaxial Compression.

ISRM Suggested Method for Determining Shear Strength, Part 2: "Suggested Method For Laboratory Determination of Direct Shear Strength".

Expansibility of Rocks

Index of expansibility

ISRM Suggested Methods For Determining Swelling and Slake-Durability Index Properties. Test 1:

"Suggested Method for Determination of the Swelling Pressure Index of Zero Volume Change".

Index of deformability

ISRM Suggested Methods For Determining Swelling and Slake-Durability Index Properties. Test 2:

"Suggested Method for Determination of the Swelling Strain Index for a Radially Confined Specimen with Axial Surcharge".

ISRM Suggested Methods For Determining Swelling and Slake-Durability Index Properties. Test 3:

"Suggested Method f

Los Angeles Test – characterizes the resistance of rock materials to abrasion, that is, it is a test for abrasion between the rock material under study and another element (steel spheres).

This test shall be undertaken in compliance with the ISRM (1978) guidelines.

Petrographic Analysis

This test shall follow the RILEM AAR-1 method (RILEM TC 191-ARP: 'Alkali-reactivity and prevention - Assessment, specification and diagnosis of alkali-reactivity' RILEM Recommended Test Method AAR-1: Detection of potential alkali-reactivity of aggregates – Petrographic method, I. Sims and P. Nixon, Materials

Point Load Test

The test can be run with portable equipment or using a laboratory testing equipment, and may be conducted either in the field or in the laboratory.
Rock specimens in the form of either core (the diametrical and axial tests), cut blocks (the block test), or irregular lumps (the irregular lump test) may be used for testing provided the reference (e.g. ISRM) specifications of shape and dimensions are followed.
The mean value of the Point Load Strength Index is used to classify samples or strata. To get a representative mean value, the minimum number of single tests should be 5.

For rock characterisation and predictions of other strength parameters, a higher number of tests are necessary. Generally, at least 10 separate tests per stratum should be carried out

The point load test is intended as a strength index test for the classification of rock materials.
The test results can also be used for estimating the strength of a group of rocks of the same range of competence.
The point load test is not a direct way to measure rock strength but an index test. The
correlation between point load test results and strength should be documented in each case.
In addition to the requirements in 5.14.2(1)P, the testing methods with reference to cores, blocks and irregular lumps shall be specified.
The test specimens shall be prepared from cores taken with Category A sampling.
Test specimens of blocks and irregular lumps taken in pits may be used provided it is reported accordingly and the rock specimens are taken using Category B sampling.
Laboratory tests on soils and rock prEN 1997-2: Aug 2003 72
Recommendations for testing given in V.3 should be followed.
The test procedure given in W.2.12.3 can be applied.
Because of large variability the evaluation of rock characterisation and predictions of other strength parameters shall be based on statistical approach. From the test data consisting of at least 10 single tests, the two highest and two lowest values shall be deleted before calculating the mean from the remaining.
In order to classify samples or strata using a mean value of Point Load Strength Index the minimum number of tests should be 5.
The test measures the Point Load Strength Index of rock specimens, and their Strength
Anisotropy Index, which is the ratio of the Point Load Strengths in directions which give the greatest and least values.
This test determines the tensile strength of the rock material to be tested and shall be undertaken in compliance with the ISRM (1985) guidelines - Point load test

ISRM Suggested Method for Determining Point Load Strength; revised version has been published in International Journal for Rock Mechanics. Min. SCI. & Geomech. Abstr. Vol 22, No. 2, pp. 51-60, 1985.; or with the ASTM D 5731 Standard

or Determination of the Swelling Strain Developed in an Unconfined Rock Specimen.

and Structures / Matériaux et Constructions, Vol. 36, August-September 2003, pp 480-496.

Potential Reactivity Test (alkali-aggregate)

This test enables to assess the suitability of excavated materials considering their reuse as concrete aggregates.

This test shall be undertaken in compliance with the ASTM C 1260 Standard.

Slake Durability Test

This test intends to determine the slake durability index after two drying and wetting cycles with abrasion. It shall be performed in accordance with ASTM D4644-87: 1998. Standard test method for Slake durability of shale and similar weak rocks or in alternative ISRM Suggested methods for rock characterisation, testing and monitoring, Part 2, Suggested methods for determining swelling and Slake-durability index properties (1977).

Slake durability tests are important to define the strength and durability of rock materials.

The slake durability test on wet side will be performed following the specification of IRSM, 1979, or equivalent, considering a period of 10 min and 200 rotations for two cycles.

An alternative procedure considering 1000 rotations for a period of 50 minutes was proposed by Delgado Rodrigues (1986).

Swelling testing of rock material

This standard deals with the following tests for determination of swelling potential exposed to wetting and drying or unloading in an aqueous environment:
−□swelling pressure index under conditions of zero volume change,
−□swelling strain index for radially confined specimen with axial surcharge,
−□swelling strain developed in unconfined rock specimen.
Note Some rock materials, notably those with high clay content, are prone to swelling, weakening and disintegration when exposed to wetting and drying or unloading in an aqueous environment. The index tests provide an indication to estimate swelling properties under well controlled conditions. The tests are usually done on softer rock materials like claystone and shale. The tests can be used for the characterisation of harder rocks subjected to weathering. Rocks that disintegrate during the tests should be further classified using relevant soil classification tests such as the shrinkage, liquid and plastic limits, particle size distribution and the type and content of clay minerals.
The specimens should conform closely to the practice recommended for right cylinders or for rectangular prisms according to W.2.9. The sample size should allow for preparation of test specimens by recoring and/or machining in a lathe, with the axis for one direction of the swell measurement perpendicular to a bedding or foliation.
The following shall be specified:
−□selection of test samples,
−□test specimen preparation, orientation and dimensions,
−□numbers of test per formation required,
−□test method, equipment and calibrations,
−□water to be used (natural or distilled water, water chemistry),
−□recording period,
−□need for curves of swell pressure or displacement as a function of time elapsed since flooding,
−□selection of required additional parameters,
−□reporting requirements.

The results shall be reviewed in the light of the description, and classification parameters shall be established.
The value used in design derived from laboratory tests should be compared with field experience with comparable rock types under similar climatic, loading and wetting conditions.
The short and especially long term weathering processes of swelling, weakening or disintegration due to wetting and drying may only be partly mirrored by the laboratory tests, even for similar conditions of loading and water content, because of the influence of among others natural fissuring, stress, drainage and pore water chemistry.
Laboratory tests on soils and rock prEN 1997-2: Aug 2003 69
The test is intended to measure the pressure necessary to constrain an undisturbed rock specimen at constant volume when immersed in water.
The test may be used to estimate the swell pressure in situ by comparison to documented experience for the rock stratum.
The test specimen shall be cored using Category A sampling methods.
The test can be carried out following the recommendation given in U.2.

The applied force to maintain the condition of zero volume change shall be corrected for the deformation in the test cell system itself (ball bearings, bedding of filter stones and filter paper towards the end platens) and the rock specimen under the appropriate stress conditions.
The maximum swell pressure under zero volume change should be used as an upper limit of swell pressure under the specified laboratory conditions.
Before use of laboratory determined maximum swell pressure in design field evidences should be taken in consideration related to short and especially long term weathering processes of swelling, weakening or disintegration due to wetting and drying, loading conditions, water content and pore water chemistry.
The test is intended to measure the axial swelling strain developed against a constant axial surcharge, when a radially confined undisturbed rock specimen is immersed in water.
The test specimen shall be cored using Category A sampling methods.
The test can be carried out following the recommendation given in U.3.

The measured strain under the applied force during the test stages shall be corrected for the deformation in the test cell system itself (ball bearings, bedding of filter stones and filter paper towards the end platens) and the rock specimen.
The axial swelling strain under constant axial surcharge should be used to estimate the swell potential in situ taking into account the documented experience for the rock stratum.
Depending on the applied vertical stress, the test provides background for the evaluation of the vertical heave or the lateral deformation of a rock/structure interface.
The test is intended to measure the swelling strain developed when an unconfined undisturbed rock specimen is immersed in water.
The test shall only be applied to specimens prepared from at least Category B sampling methods that do not change their geometry appreciably during testing.
Laboratory tests on soils and rock prEN 1997-2: Aug 2003 70
It is advised that slaking, less durable rocks more adequately should be tested using a confined swelling test.
The test may be carried out following the recommendation given in U.4.
The report shall clearly indicate that the specimen was not radially confined during the swelling test.
The test may be used to estimate the swell potential in situ by comparison to documented experience for the rock stratum.
Unconfined swelling strains and their directions with respect to bedding or foliation should be used only as an estimate of in situ swelling potential.

Triaxial

Strength testing of rock material

This standard includes five laboratory methods for determining the strength of rock:
−uniaxial compression and deformability test,
−point load test,
−direct shear test,
−Brazil test,
−triaxial compression test.
. The following shall be specified:
−the samples that are to be tested,
−the specimen preparation,
−the number of tests per formation,
−any required additional parameters,
−the testing methods.

Annex V provides a guideline for the minimum number of test specimens to be tested for one formation for uniaxial compression tests, Brazil tests and triaxial tests for projects of Geotechnical Category 2 with respect to standard deviations of measured strength and comparable experience.
The evaluation of the test results should include comparison with recognised data bases to help screen the data for anomalous results, while accounting for the natural range in compressive strength and deformation parameters in rock, and correlations with the results of classification tests All test results should be grouped and analysed with respect to the geological description and classification properties using statistical methods when appropriate.
The values can be used to evaluate in situ strength and deformation properties and to classify rock element and rock mass properties.

Triaxial compression

The triaxial compression test is intended to measure the strength of cylindrical rock specimens subjected to triaxial compression. A number of tests provide the values necessary to determine the strength envelope in a Mohr-Coulomb diagramme. From this envelope, the angle of shearing resistance and the cohesion intercept may be determined.
NOTE No provisions are usually made for drainage of the pore water, nor for the measurement of pore water pressure. In certain rock types (e.g. shales and porous limestone and chalk) and under certain conditions, the pore water pressure may influence the results. For such rock types advanced triaxial test systems allowing for measuring pore water pressure and volumetric strains are necessary. Such testing may include similar measuring techniques as used for uniaxial compressive strength according to V.2 and W.2.12.2
The following shall be specified in addition to the requirements in 5.14.2(1)P:
−□test specimen orientation and dimensions,
−□testing method.
Laboratory tests on soils and rock prEN 1997-2: Aug 2003

ISRM Suggested Method for Determining the Strength of Rock Materials in Triaxial Compression.

Ultrasound propagation test

This test consists in determining the velocity of propagation of compressive and shear waves, between two points of measurement, aiming to obtain information about the mechanical characteristics, such as elastic constants, the homogeneity and the presence of micro-fractures in a rock specimen. The test shall be carried out in accordance with the ASTM D2845 – 08 standard

Uniaxial Compressive Strength and Deformability

The test procedure should follow the example for uniaxial compressive strength testing and deformability testing. In addition, the modifications prescribed in the present standard should be used.

The test procedure described in ISRM contains two levels of testing:

−Part 1. Method for determining the uniaxial compressive strength of rock materials

−Part 2. Method for determining deformability of the rock materials in compression

The first method provides the compressive strength, the second method gives in addition the axial deformation modulus (Young’s modulus) and Poisson's ratio. The second method is preferred.

The procedures suggested by the reference ISRM are extremely difficult to conform to, especially with respect to sample preparation and geometrical tolerances. The practice recommended in this standard is less strict. Although the procedures recommended by ISRM are desirable, a set of minimum requirements is given herein. It is considered more important to run a greater number of tests than fewer tests on higher quality specimens.

The uniaxial compression strength should be determined as the maximum vertical stress obtained during the compression test.

The elasticity modulus defined as the ratio of the axial stress change to axial strain produced by the stress change should be determined using one of the three methods below:

tangent Young's modulus measured at a fixed percentage of ultimate strength (i.e. 50%), average Young's modulus of linear portion of axial strees-strain curve,

secant modulus measured from zero stress to some fixed percentage of ultimate strength (i.e. 50%)

The Poisson's ratio should be determined as the slope of the radial strain versus axial strain curve

Young's elasticity modulus and Poisson's ratio should be calculated within the same interval of vertical stress.

Test results should be evaluated with respect to rock classification properties and the rupture pattern illustrated by a sketch of the tested rock specimen.

The unconfined compression strength □C can be used as a classification parameter for the intact rock quality and it could be used in combination with triaxial compression test results in a Mohr diagramme to define the Mohr-Coulomb rupture parameters ϕ□(friction angle) and c (internal cohesion).

Test specimens should be right circular cylinders having a height to diameter ratio between 2 and 3 and a diameter not less than 50 mm. The diameter of the specimen related to the largest grain.

The following specifications shall be followed:

ASTM D 2938-86 Standard Test Method for Unconfined Compressive of Intact Rock Core Specimens.

ASTM D 3148-86 – Standard Test Method for Elastic Moduli of Intact Rock Core Specimens in Uniaxial Compression.

Water Absorption

This test establishes the relationship between the amount of water absorbed and the total volume of the sample and provides a direct correlation with the effective porosity.

This test shall be undertaken in compliance with the ISRM (1977) guidelines.

..

Water Content

ISRM Part 1 Suggested methods for determining water content, porosity, density, absorption - Section 1: Suggested method for determination of the water content of a rock sample

Laboratory Characterization of rock materials

.

A great number of rock properties can be defined by the index properties. These properties show the reaction of the rock for the exterior actions and can be used for design purposes.

The index properties are easily defined by conventional laboratories, allow the classification of rock materials and are useful for design purposes. The index properties are very attractive for the researchers and practitioners due its simplicity.
The index properties are defined by the following tests: porosity, density, absorption water content, velocity of elastics waves, compression tests, crushing tests, point load strength test, slake durability test and expansibility test.

Direct shear tests

The shear strength of rock discontinuities is important focusing on the influence of the length of discontinuities with the shear strength. It is important to stablish a relationship between the shear strength of discontinuities of laboratory scale to in-situ scale and to define the variation of the peak shear strength of the discontinuity with the discontinuity length.

Field Tests

Dilatometer test

The dilatometer is a radially expandable borehole probe used to determine in situ the deformability of rock mass and the creep properties of very soft rock. The dilatometer test is performed in cycles of loading-unloading inside a borehole with a radially expandable cylindrical probe.

Flat jack test

This test is based on the release of the stress in a small area of a structure by a plane cut perpendicular to its surface. The flat jack is then loaded in the cut and the pressure is gradually increased by a hydraulic pump until the state of strain is equal to the previously existing condition before the cut. Measurement between the reference points, glued symmetrically about the cut, are taken at various pressures. The pressure is increased in increments until the point of non linearity is reached in the load strain curve to avoid damage in the structure

Lugeon tests

Lugeon Water Tests shall be undertaken for each borehole in rock mass, in consecutive 5 m-long sections, with 5 pressure thresholds (3 ascending and 2 descending), stabilized during 10 minutes, as indicated in Table A1.13.

Table A1.13 Pressure Thresholds for Lugeon Water Tests

Ascending	**Descending**
$P_{max}/4$	$P_{max}/2$
$P_{max}/2$	$P_{max}/4$
P_{max}	—

The maximum pressure (Pmax) of the test shall be defined accordingly to the depth of the section tested following the criteria shown in Table A1.14.

Table A1.14 Criteria for definition of the maximum pressure in Lugeon water tests

Depth (m)	< 10	10 – 20	> 20
P_{max} (MPa)	0,3	0,5	1,0

The Lugeon water tests should be performed at the same time as the boreholes drilling progress, using shutters of sealed length superior to 0.7 m- -Single packer test.

In the execution of the tests the first 5 m of the borehole shall not be considered and the tests shall begin at 5 m depth being repeated every

Rock stress measurement

The borehole deformation type of rock stress measuring instrument measures radial displacements in the direction of one or more diameters of the borehole in which it is installed for the purpose of determining the stresses in the rock borehole.
The stresses are calculated from the changes in borehole diameter using equations based on the theory of elasticity.

Hydraulic fracturing technique

Based in laboratory and theoretical analyses it is possible to conclude that hydraulic fractures propagate in a plane perpendicular to the least-principal stress. The magnitude of this stress can be determined from pressure in the fracture immediately after pumping has stopped (the shutdown pressure). In general, is considered a vertical fracture propagating from a vertical well-bore and the principal stress is essentially vertical and results from the overburden pressure.

A.9 Tests on Concrete

Chloride, soluble sulphates and total sulphur determination

These tests shall follow EN 1744-1:2009+A1:2012 - Tests for chemical properties of aggregates - Part 1: Chemical analysis.

Determination of volumetric stability of concrete (including and mixing of concrete and shrinkage)

This test intents the determination of the thermic properties of concrete aggregates as well as its weathering susceptibility. The test method shall follow EN 1367-4:2008 - Tests for thermal and weathering properties of aggregates - Part 4: Determination of drying shrinkage

The determination of components affecting concrete curing and concrete resistance shall also follow EN 1744-1:2009+A1:2012 - Tests for chemical properties of aggregates - Part 1: Chemical analysis.

ANNEX 2 - ANCHOR TESTS

Nature to be mastered, must be obeyed

Francis Bacon (1620)

Ulisse's hero of Homero poem

has appointed the responsibility

of Man in chosen his own
Destiny

A2.1 Experimental Tests

Three types of on-site anchorage tests are usually considered: (i) investigation tests; (ii) suitability tests; and (iii) acceptance tests.

Investigation tests are needed to establish for the designer, in advance of the installation of the working ground anchorages, the ultimate load resistance in relation to the ground conditions and materials used.

Suitability tests are carried out to confirm the acceptable creep and load characteristics at proof and lock-off load levels, following the procedure recommended in CEN EN 1537.

Acceptance tests (simplified or detailed tests) shall be submitted to all the anchors.

The test programme shall confirm the free apparent length and that the relaxion anchor force is small after blocking.

For the determination of the anchorage characteristic load value R_{ak}, from R_{am} values measured in one or more suitability tests, a reduction factor is used to take into account the variability of ground and the constructive procedure. As minimum both conditions a) and b) from Table A2.1 shall satisfy using equation:

$$R_{ak} = R_a / \zeta \rightarrow \quad \text{(A2.1)}$$

The calculation of the anchorage strength R_{am}, obtained from suitability tests considers the two modes of failure and the creep limit load.

The design value R_a, is given by equation:

$$R_a = R_{ak} / \gamma_m \quad \text{(A2.2)}$$

where γ_m = [1.25] for temporary ground anchorages and γ_m = [1.5] for permanent ground anchorages.

The detailed acceptance tests, to be performed in 10 % of the anchors, shall confirm an adequate strength corresponding to the proof load (Tp), where Tp = 1.25 Ts (service load), the creep characteristics or loss of the load of the anchor system defined for several levels of load and unload of Tp and the free anchor length.

Table A2.1 Coefficient ξ for determination of R_{ak} (Eurocode 7, 1997)

Number of suitability tests	1	2	> 2
a) coefficient ξ applied to the mean value R_{am}	[1.5]	[1.35]	[1.3]
b) coefficient ξ applied to the minimum value R_{am}	[1.5]	[1.25]	[1.1]

A2.2. Suitability Tests

For the suitability tests should be performed with at least 6 cycles of load and unload and for the maximum load of each cycle the load should be maintain for a time step pre-defined.

The reference tension value T_o, (initial tension value of each cycle) shall be 0.1 T_{max}, where $T_{máx}$ is the maximum tension value that shall be less than {0.80 T_{tk}; 0.95 $T_{t0,1k}$}, where T_{tk} and $T_{t0,1k}$ represent the ultimate tension and the limit tension proportional to 0,1 % of the extension permanent of the reinforcement, respectively.

The maximum tension for each cycle should be:

1st cycle: $T_{1'}$= 0.18 $T_{máx}$ and T_1 = 0.25 $T_{máx}$
2nd cycle: T_1 = 0.25 $T_{máx}$ and T_2 = 0.40 $T_{máx}$
3rd cycle: T_2 = 0.40 $T_{máx}$ and T_3 = 0.55 $T_{máx}$
4th cycle: T_3 = 0.55 $T_{máx}$ and T_4 = 0.70 $T_{máx}$
5th cycle: T_4 = 0.70 $T_{máx}$ and T_5 = 0.85 $T_{máx}$
6th cycle: T_5 = 0.85 $T_{máx}$ and T_6 = 1.00 $T_{máx}$

Notes:

i) The minimum period at the end of each step is 1 minute.
ii) For the initial five cycles the times of load application are the following: t_1= 1 min., t_2 = 2 min., t_3= 3 min., t_4= 5 min, t_5 = 10 min. e t_6 = 15 min. Based on the measured values the value of Ks is computed.
iii) For the 6th cycle:
t_1= 1 min., t_2 = 2 min., t_3= 3 min., t_4= 5 min, t_5 = 10 min, t_6 = 15 min, t_7 = 20 min, t_8 = 30 min, t_9 = 45 min e t_{10} = 60 min.
Based on the measured values the value of Ks is computed.
iv) The referred minimum period of time shall be increased to reach a constant rate for observed displacements.

.

A2.3 Acceptance tests (simplified tests)

The anchors shall be submitted to tension, since the reference force to until the maximum force of the test $T_{máx}$, in 3 increments of loads at least, with records of force-displacements for each increment.

For the definitive or temporary anchors, the following loads shall be applied:

T_o = 0.1 $T_{máx}$; T_1 = 0.25 $T_{máx}$; T_2 = 0.50 $T_{máx}$; T_3 = 0.75 $T_{máx}$; T4 = 1.00 $T_{máx}$. $T_{máx}$, equal to the detailed acceptance tests ($T_{máx}$ Є [1.25 T_p; Minor {0.90 $T_{t0,1k}$; 0.80 T_{tk}}]).

After reaching the value $T_{máx}$, 6 loads-displacements measurements should be done for: t_1= 1 min., t_2 = 2 min., t_3= 3 min., t_4= 5 min, t_5 = 10 min. e t_6 = 15 min. Based on the measured values the value of Ks is computed= 1 min., t_2 = 2 min., t_3= 3 min., t_4= 5 min., t_5=10 min. e t_6 = 15 min.

Based on the measured values, the value of Ks is computed which should satisfy the following limits:

a) for the step corresponded to the tension of the tests, $T_{máx}$

Ks ≤ 0.8 mm, when previous tests were performed or Ks ≤ 1.0 mm if during the previous tests an ultimate limit state has not reached by creep, Ks ≥ 2.0 mm.

b) for the step related with the design tension T_p

$Ks \leq 0.5$ mm.

After reaching the creep level, initiates the unloading of $T_{máx}$ to T_o in order to compute plastic displacements and the elastic displacements related to $T_{máx}$ and the free apparent length l_r, of the anchor. The unloading shall be performed in increments of loads in the sequence T_3-T_2-T_1-T_o, with measurements of forces-displacements in each load step.

A2.4 Acceptance tests (detailed tests)

The tests shall be performed in at least 5 cycles of load-unload, and a creep step shall be performed in the maximum load of the cycle.

The reference tension values, T_o, (initial tension in each cycle) shall be 0.1 T_{max}, where $T_{máx}$ is a tension value predefined and belonging to the interval [1,25 T_p; Minor {0,90 $T_{t0,1k}$; 0,80 T_{tk}}], where T_p and $T_{t0,1k}$ represent the design tension, the limit tension proportional to 0.1 % of the permanent extension of the reinforcement and the ultimate tension of the reinforcement, respectively.

The values of the maximum tension in each cycle are:

1st cycle: $T_{1'} = 0.25\ T_{máx}$ and $T_1 = 0.40\ T_{máx}$

2nd cycle: $T_1 = 0.40\ T_{máx}$ and $T_2 = 0.55\ T_{máx}$

3rd cycle: $T_2 = 0{,}55\ T_{máx}$ and $T_3 = 0.70\ T_{máx}$

4th cycle: $T_3 = 0.70\ T_{máx}$ and $T_4 = 0.85\ T_{máx}$

5th cycle: $T_4 = 0.85\ T_{máx}$ e $T_5 = 1.00\ T_{máx}$.

After the analysis of the results of the acceptance test, if the instrumentation of the anchor is programmed the dynamometric cell shall be installed for tension measurements.

If the instrumentation of the anchor is not programmed the blocking of the anchor shall be performed.

During the installation of the cell or of the blocking, the percentage of variation ρ, corresponding to the immediate loss of pre-stressed T_p, shall be checked, in order to estimate the residual value of tension blocking, to define the effective tension of service.

A2.5 Complementary comments

i) The minimum period at the end of each step is 1 minute.
ii) For the initial four cycles the times of load application are the following: t_1= 1 min., t_2 = 2 min., t_3= 3 min., t_4= 5 min, t_5 = 10 min. e t_6 = 15 min. Based on the measured values the value of Ks is computed.
iii) For the 5th cycle the minimum period of observation is 60 min:
t_1= 1 min., t_2 = 2 min., t_3= 3 min., t_4= 5 min, t_5 = 10 min, t_6 = 15 min, t_7 = 20 min, t_8 = 30 min, t_9 = 45 min e t_{10} = 60 min.

Based on the measured values the value of Ks is computed.

iv) The referred minimum period of time shall be increased to reach a constant rate for observed displacements.

The acceptable limits for Ks are the following:

a) In the step corresponded to the tension of the test, $T_{máx}$

Ks = 0.8 mm, or

Ks = 1.0 mm, if previous tests were performed and a limit creep state was not reached (Ks<2,0 mm).

b) In the step corresponded to the tension design, T_p

Ks ≤ 0,5 mm

A2.6 Case History – Rossio Railway Station (Lisbon)

A2.6.1 Background

Due to the crossing of the Rossio railway station building (1886) by an underground gallery (for the Lisbon Metro), a careful study was performed for this station in order to avoid unacceptable damages. The building had originally three levels: ground floor (+11.86), 1st floor (+19.93) and 2nd floor (+25.96). For the installation of a Commercial Centre two new floors were built: intermediate first floor (+15.21) and intermediate second floor (+22.79). For the construction of the underground with 13 m in height and a thickness around 3m. Both walls sustain an embankment on which the railways platforms were built (Seco e Pinto et al., 2008).

The underground gallery was built underneath the whole extension of the north-south retaining wall and part of the east-west retaining wall.

The enlargement of the station including two new underground halls connected by mechanical and fixed stairways with each other.

A cross section of the tied back wall is shown in Figure A2.1.

For the underpinning of the retaining walls, more than a dozen large reinforced concrete frames were erected, side by side, under the base of the walls. This simple but massive structures allowed the excavation of the space for the installation of the Metro gallery (Figure A2. 2), under the beam of each frame.

Other parts of the station building had also to be underpinned, by means of r.c. frames, micro-piles and jet-grout columns.

In the design phase of the underpinning of the retaining walls, it was recognized that the walls didn't verify the safety conditions required by Eurocodes 7 and 8 and Portuguese Actions Code, especially in what concerns the rotational failure scenario for both static and seismic actions.

Therefore, it was decided to reinforce both walls by :(i) definitive anchorages and a grid of r.c. beams, in the case of the north-south wall; and (ii) micropiles going through the body of the wall and into the ground behind and under it, in the case of the east-west wall (Seco e Pinto et al., 2008).

A2.6.2 Main Geological Characteristics

Based in the results collected from borings executed at Rossio site, the following units were considered as shown in Figure A2.2.

Landfill: composed by sandy clayey material with a thickness varying from 3.5 to 20 meters.

Estefânia Areolas: composed by sandy materials or silty sandy materials with thickness around 3 meters.

Clays and calcareous rocks from Prazeres: composed by dark grey to dark brown clay, with layers of sandy material, up to the depth which is significant to the design of the structures of the Rossio station.

After an evaluation of the results of the field investigation (boreholes, trenches, vane shear tests, pressurometer tests, penetrometer tests and Lefranc tests) and the laboratory tests (chemical tests, oedometer tests, triaxial tests, the geotechnical characteristics adopted are shown in Table 1 (Consortium, 1996a).

Table A2.2 Geotechnical Properties

Properties	Landfill	Estefania Areolas	Clays and calcareous rocks	Masonory retaining wall
Unified classification:	CL, CH		CL, CH	
% passing sieve # 200 (ASTM)	28 to 100		32 to 75	
Liquid limit (%)	18 to 47		28.3 to 43.4	
Plastic index (%)	3.4 to 26.7		4.3 to 21	
Unit weight (kN/m3)	17.6			22
Strength (C_u) (kPa)	32.7 to 169.7			
Cohesion c` kPa	0	0	33	1000
Friction angle ϕ`:	30^o	33	35	45
k: (m/s)	10^{-9}	10^{-5}	10^{-6} to 10^{-7}	
Poisson ratio:	0.35		0.25	0,2
SPT values	4 to 18.	6 to 39	10 to 60	
CPT values (MPa)	0.2 to 5.			

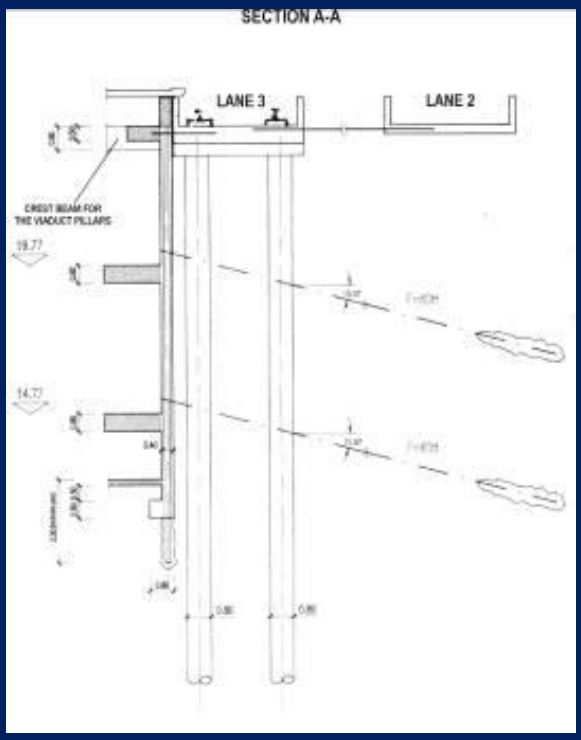

Figure A2.1 Cross section of the tied back wall
70

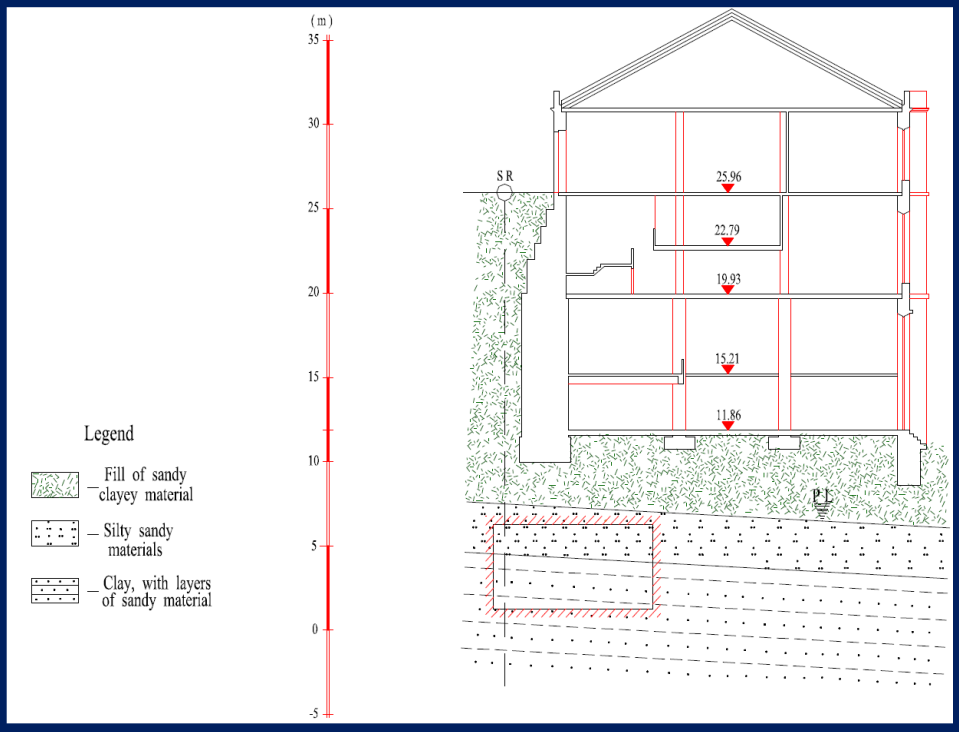

Figure A2.2 Geological profile (adopted from Consortium, 1996a)

A.2.6.3 Anchor tests

The total length of the permanent anchorages is 18 m with a tendon free length of 9 m and a fixed tendon length bonded to the ground by grout of 9 m measured in one or more suitability tests. The 6 steel cables tendon has a cross sectional area of 592.2 mm^2.

For each load test the anchorages were loaded in 4 incremental cycles from a datum load to a maximum test load, with measurement of displacements of the anchorage head. Displacement values due to creep were also determined.

The results of investigation tests of anchor A16F1 are shown in Figures A2.3 to A2.6.

Figures A2.7 to A2.10, related to the anchor A02, show the applied loads versus anchorage head displacements, the applied loads versus elastic and permanent displacements, the displacement values versus time and the Ks values for the evaluation of creep, for the suitability test.

Measurement of electrical resistance between an anchorage and the surrounding soil or structure to determine the effectiveness of the applied corrosion protection system was also performed.

The results of some of the anchorage tests are summarized in Table A2.3.

The results of acceptance tests of anchor A6F2 are shown in Figures A2.11 to A2.14.

TABLE A 2.3 ANCHOR TESTS

Anchorage	Max. Force (kN)	Maximum Disp. (mm)	Permanent Disp. (mm)	Test Method.	Initial Free Length (m)	Calculated Free Length (m)	Maximum Ks (mm)
MP02	457.5	69.60	14.54	Accep. T	15.3	15.6	0.39
MP14	453.0	89.19	14.05	Accep. T	21.3	21.2	0.60
MP21	459.0	86.27	14.97	Accep. T	21.3	20.3	0.91
MP35	456.0	77.33	16.16	Accep. T	21.3	17.9	0.70
MBA2F3	619.8	127.50	19.18	Accep. T	21.0	20.8	0.64
MBA6F2	621.6	116.05	10.19	Accep. T	21.0	20.2	0.41
MBA8V	728.1	130.33	16.87	Accep. T	21.0	17.6	0.58
MBA13F1	581.7	189.50	65.52	Accep. T	25.6	25.6	0.53
MBA16F1	673.9	149.49	32.89	Inv. T.	21.0	20.0	0.32
MBA18V	642.5	122.27	5.79	Accep. T.	21.0	20.8	1.07
MBA19F3	631.8	119.14	22.73	Accep. T	21.0	17.7	0.48

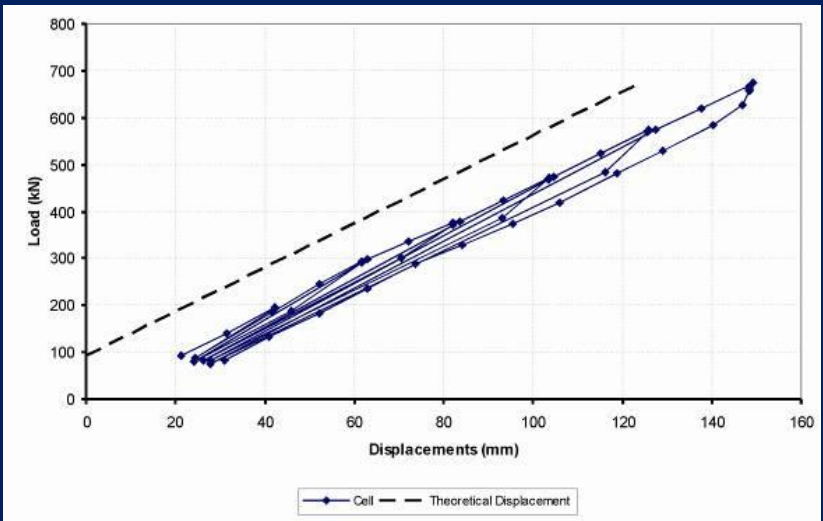

Figure A2.3 Applied loads versus displacement for Bairro Alto Wall (MB) anchor A16F1

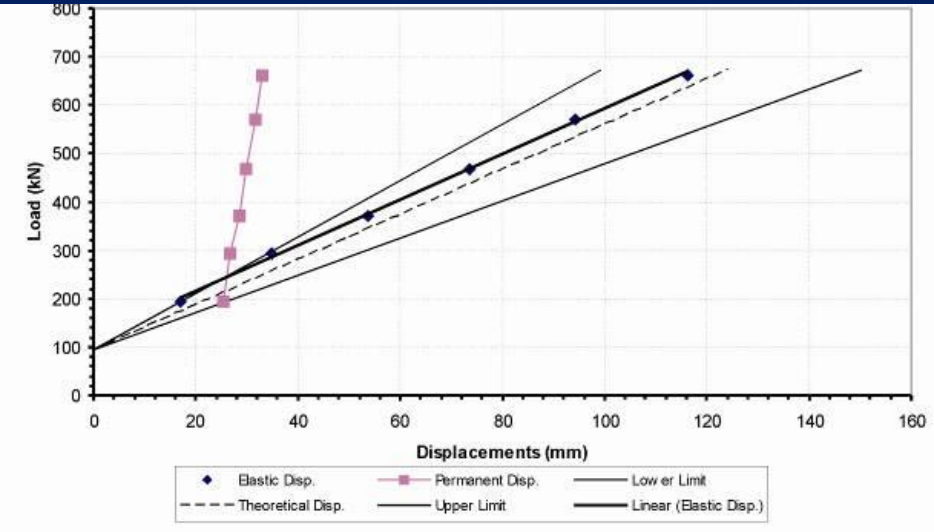

Figure A2.4 Applied loads versus elastic and permanent displacements Bairro Alto Wall anchor A16F1

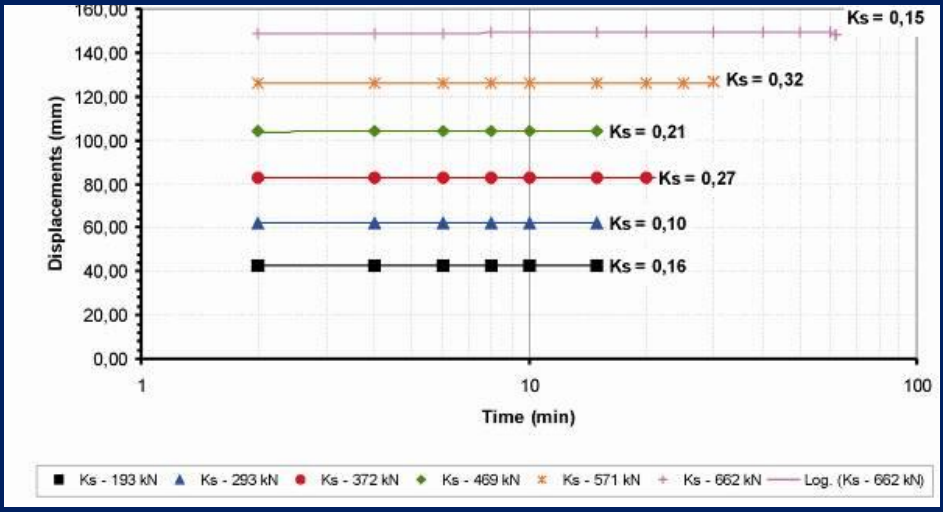

Figure A2.5 Displacements versus time Bairro Alto Wall anchor A16F1

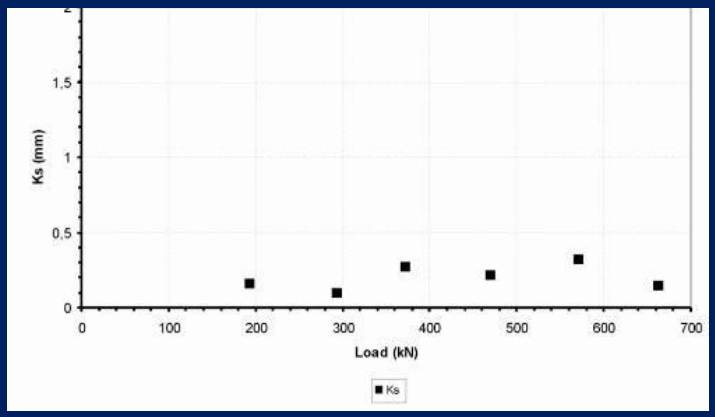

Figure A2.6 Values of Ks for Bairro Alto Wall anchor A16F1

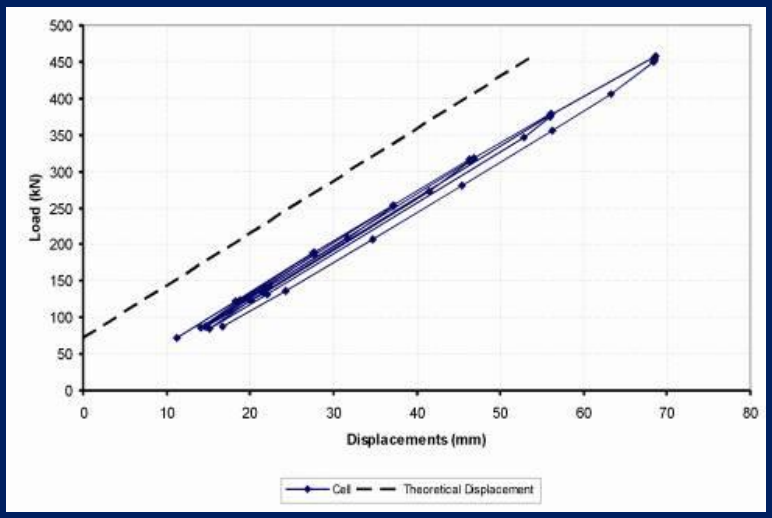

Figure A2.7 Applied loads versus displacement for Principal Wall (MP) anchor A02

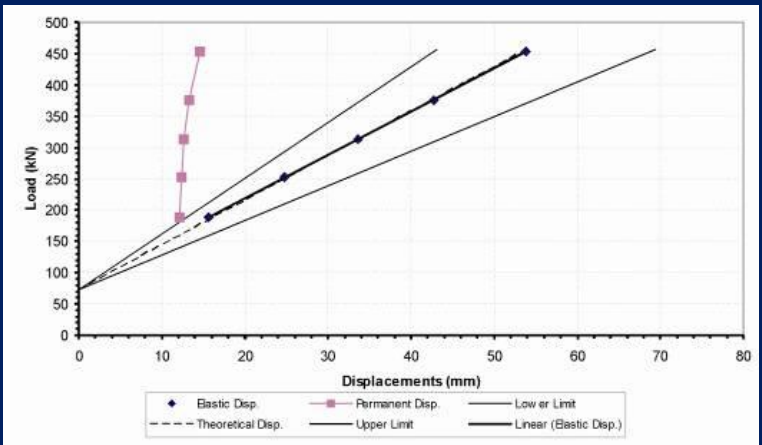

Figure A2.8 Applied loads versus elastic and permanent displacements for Principal Wall anchor A02

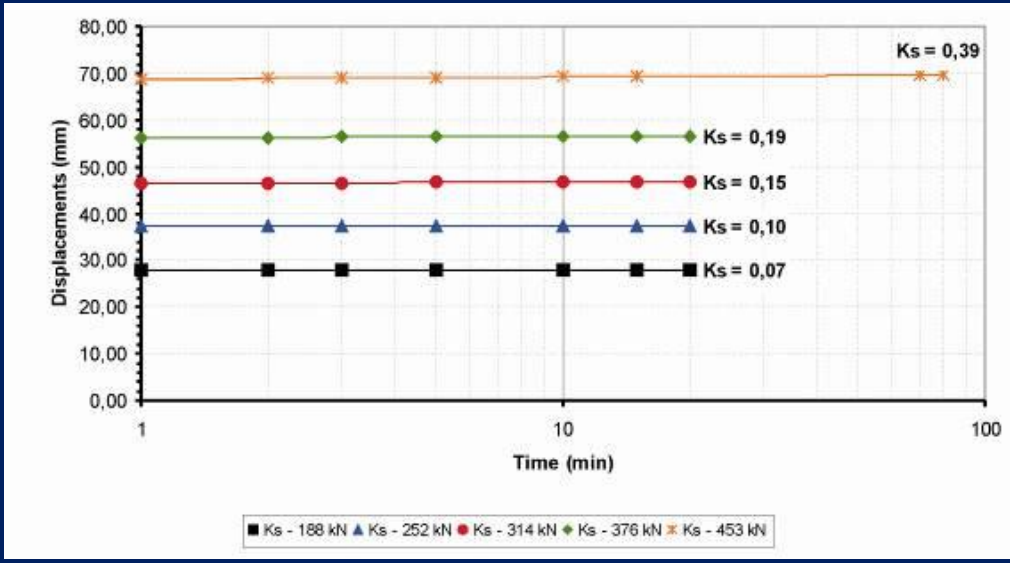

Figure A2.9 Displacements versus time for Principal Wall anchor A02

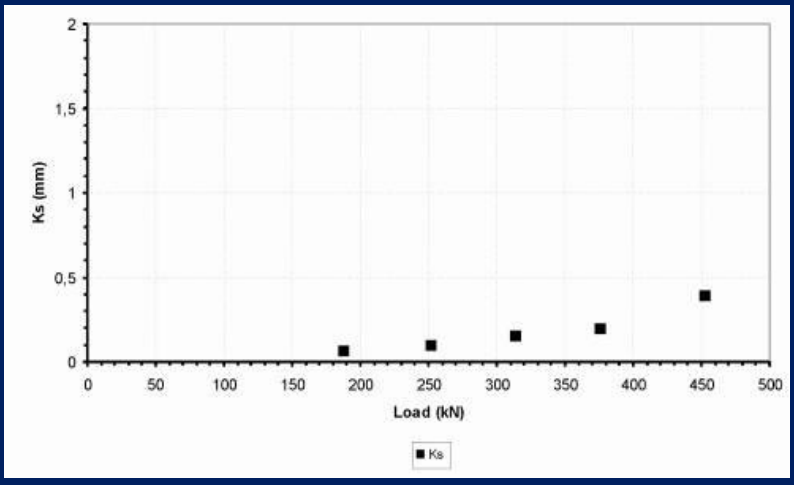

Figure A2.10 Values of Ks for Principal Wall anchor A02

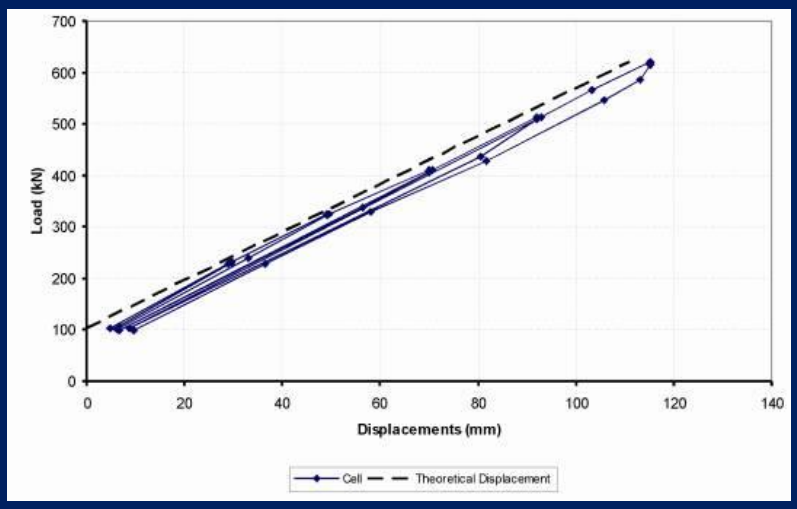

Figure A2.11 Applied loads versus displacement for Bairro Alto (MB) Wall anchor A6F2

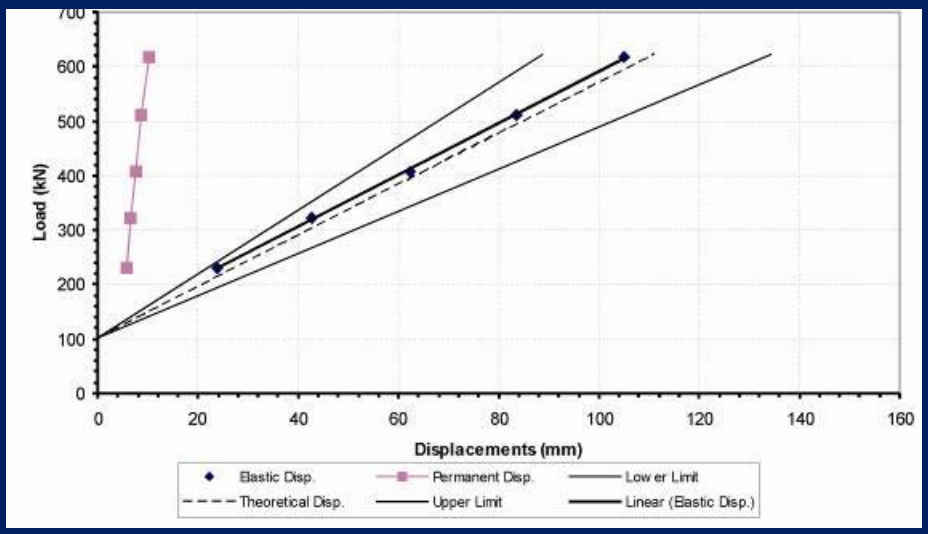

Figure A2.12 Applied loads versus elastic and permanent displacements for Bairro Alto Wall anchor A6F2

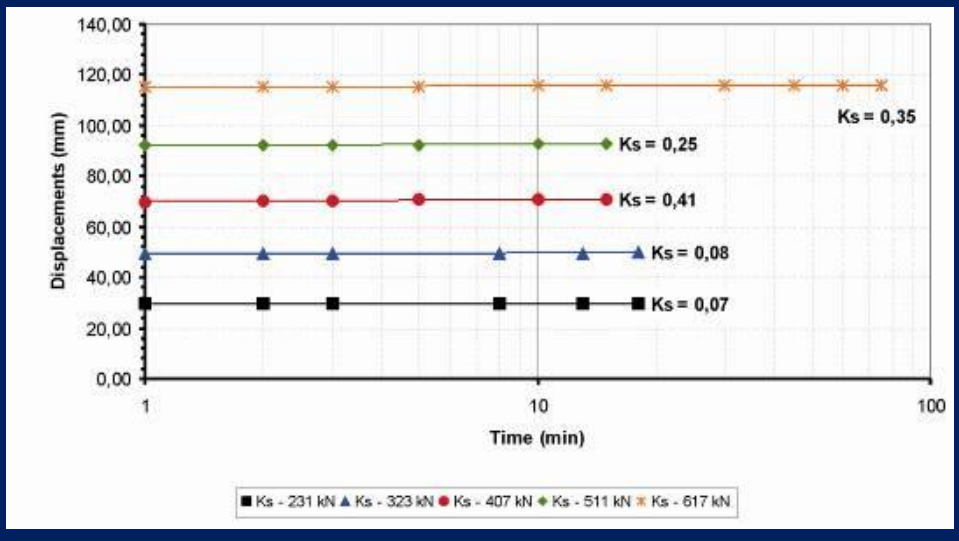

Figure A2.13 Displacements versus time for Bairro Alto Wall anchor A6F2

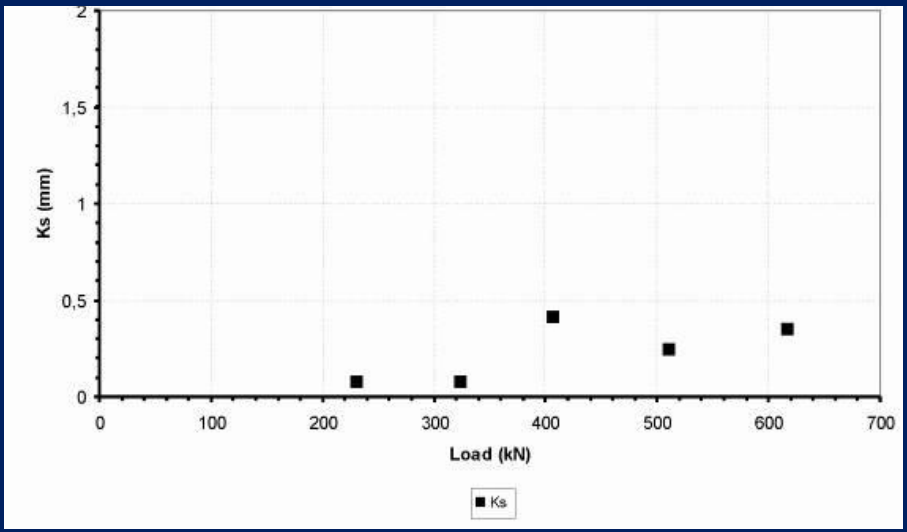

Figure A2.14 Values of Ks for Bairro Alto Wall anchor A6F2

A2.6.4 Corrosion protection tests (System tests)

In permanent anchors the integrity of the pre-grouted encapsulation shall be proven in order to detect:

i) The existence of voids

ii) The existence of longitudinal fissures;

iii) The existence of transverse fissures.

The lack of results of system tests to evaluate the long term behavior of anchorages of the type which was intended to be used in Rossio station also required a test of this type to be performed in one anchorage. According to standard CEN EN 1537 "Execution of special geotechnical work - Ground Anchorages", a test of this type requires the excavation of the anchorage after the load protocol has been carried out, and so this anchorage had to be built outside the station.

Following EN 1537(1994): (i) in the encapsulation zone a minimum cover of 5 mm shall be provided; (ii) exterior to corrugated duct a minimum cover of 20 mm shall be provided; (iii) anti-corrosive protection of tendons shall be provided.

In addition, electrical resistivity tests shall provide a minimum value of 100 kΩ between tendon and ground.

Water samples shall be taken for the determination of pH value and concentration of ionic sodic, magnesium and potassium.

In summary, the corrosion protection systems tests aim to test the corrugated duct and the internal and external protections.

A detailed suitability test shall also be performed.

The check list includes:
- thickness of the grout and behaviour of the spacers;
- position of the tendon.

The properties of grouts such as density, viscosity, decantation and setting time shall be verified.
During grouting, grouting pressure and grouting volume shall be controlled.

The results of the suitability tests are shown in Figures A2.15 to A2.18.

After the anchor load test the anchor shall be excavated and the different elements anchor namely head, tendon and grout body shall be observed.

The measurements of electrical resistivity allow the checking of the protective barrier of the steel tendon from the ground and the protection of the anchor head.

Figures A2.19 to A2.22 show photos representatives of the steel tendon protection different phases of the test.

The visual inspections have shown:

i) a good encapsulation;
ii) no direct contact between anchor head and reinforcement steel of the anchored structure;
iii) in some sections there was no minimum cover of 5 mm between the duct and bar.
iv) No cracks were observed in the grout body exterior to the manchette tube.

The tests have shown a good overall electrical isolation of the anchor from ground and structure.

A2.6.5 Monitoring and Environmental Impacts

To control the structure behaviour a monitoring system was installed, including the following types of instruments: clinometers, extensometers, surface movement points and inclinometers. Some anchorages were also instrumented with load cells.

To minimize the environmental impacts the following actions were taken: (i) protection of anchorage tendons and micro pile reinforcements against electric currents; (ii) control of vibrations due to drilling works.

As an example of the monitoring readings, obtained to build the underground walls referred in Figure A2.1 some results are presented in Figures A2. 23 to A2.26.

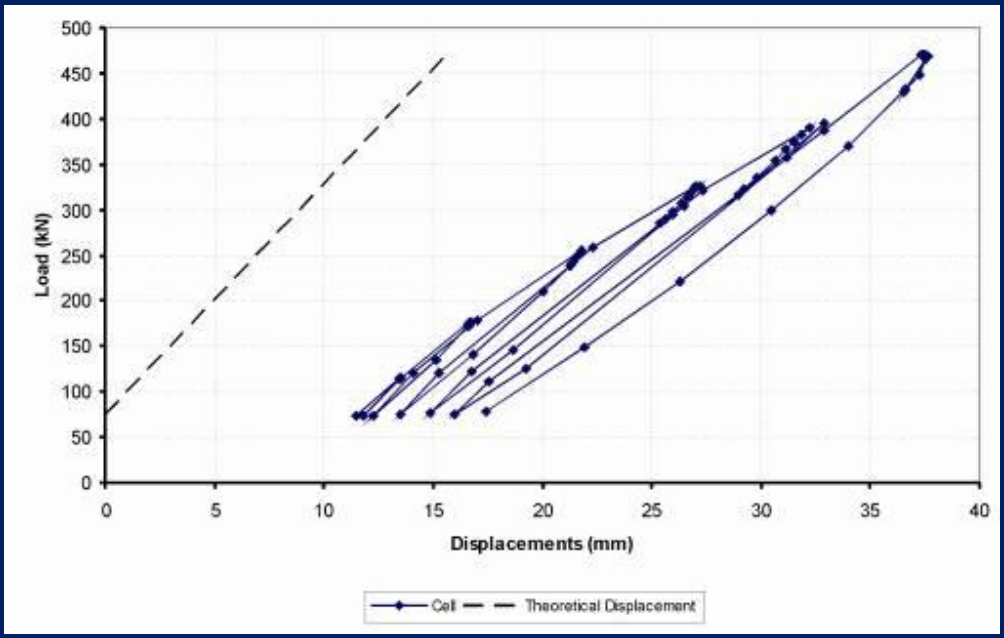

Figure A2.15 Applied loads versus displacement

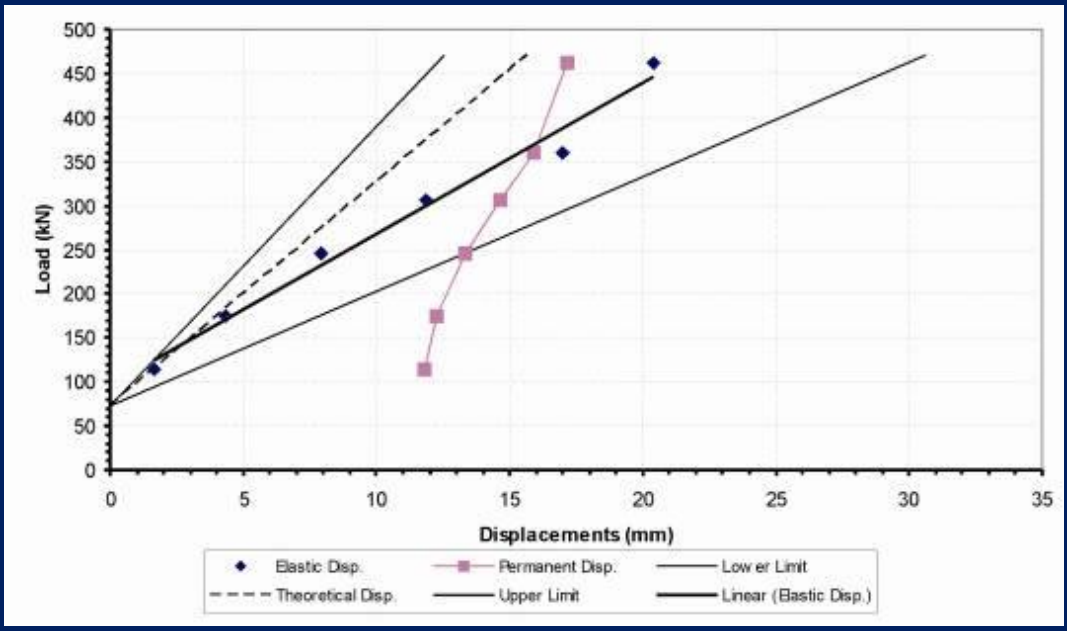

Figure A2.16 Applied loads versus elastic and permanent displacements

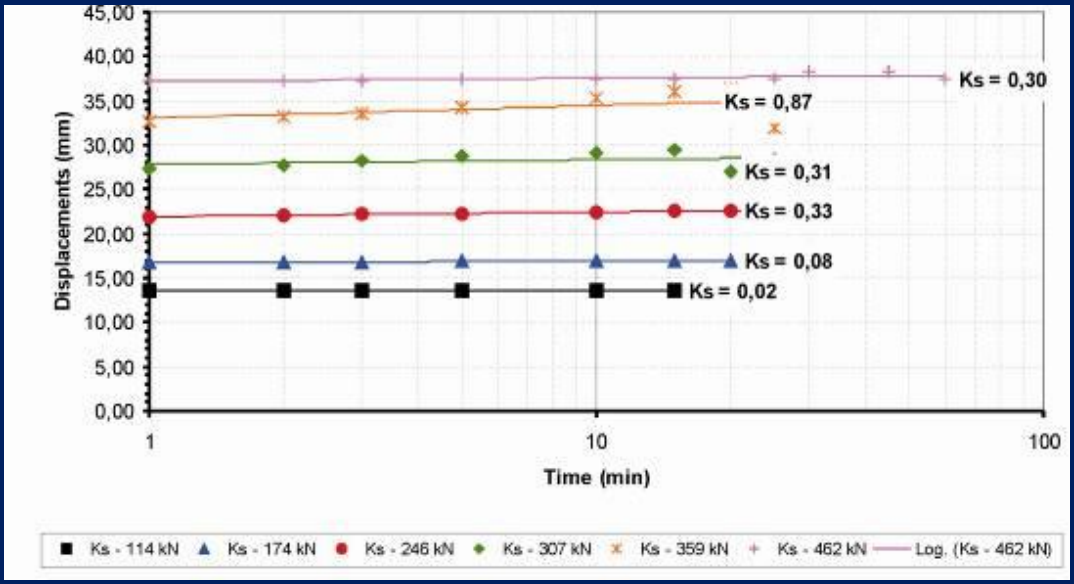

Figure A2.17 Displacements versus time

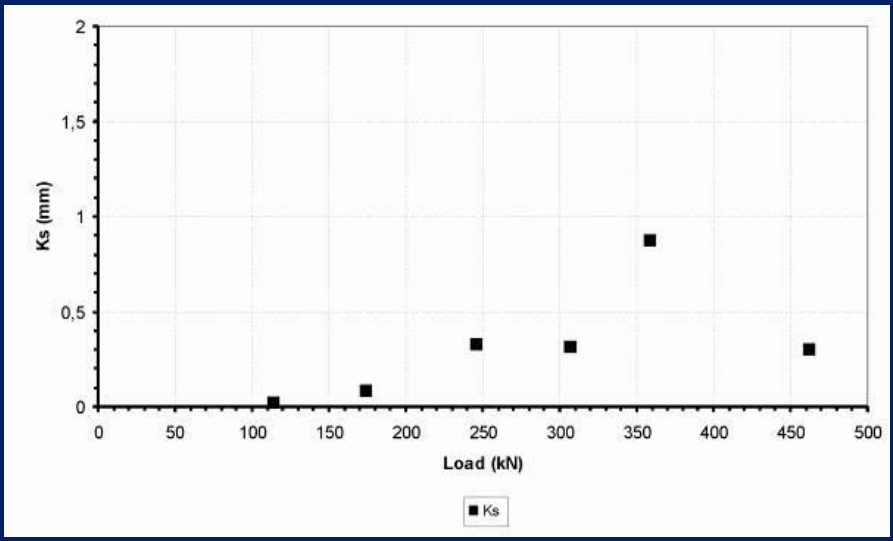

Figure A2.18 Values of Ks

Figure A2.19 Anchor excavation

Figure A2.20 Close view of anchor excavation

Figure A2.21 Transverse section of the anchor

Figure A2.22 Longitudinal section of the anchor

For the monitoring of anchors the instrumentation included a logger. In Figure A2.23 and Figure A2. 24 details of the logger are shown. The results measured by the logger are shown in Figure A2. 25.

Figure A2.23 Logger

Figure A2.24 General view of equipment

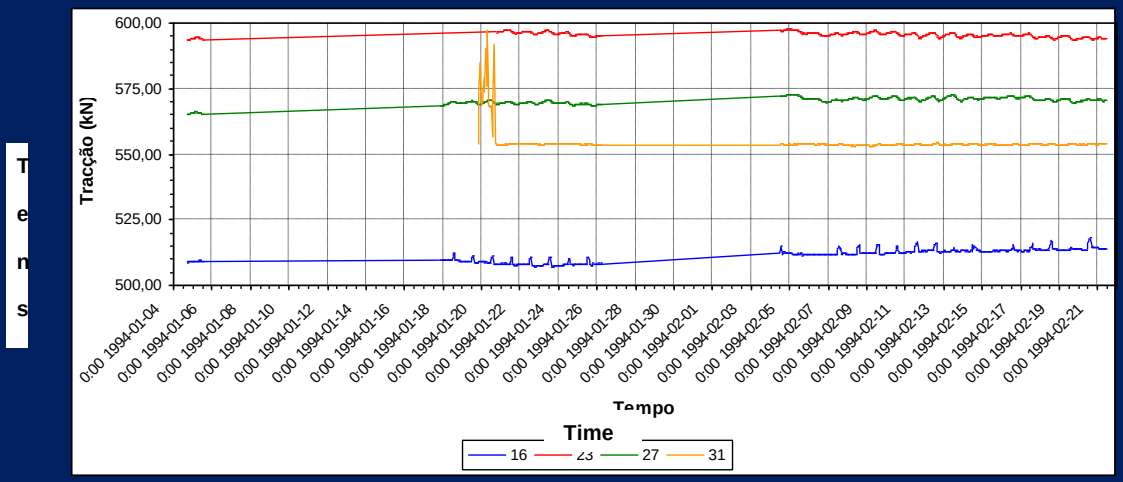

Figure A2.25 Values of anchor loads measured by the logger

Consortium 1996a. Section 60 - Restauradores-Baixa/Chiado. Geological and Geotechnical Report. (in portuguese), Doc. RT - 02.3-0238.

Consortium 1996b. Section 60 - Restauradores-Baixa/Chiado. Crossing under CP-Rossio. Numerical Analysis of the Principal Retaining Wall. (in portuguese), Doc. RT - 02.3-0168.

Seco e Pinto, P.S. Barradas, J. and Sousa, A. 2008. Lessons Learned from Two Case Histories of Retaining Structures. *5th International Conference on Case Histories in Geotechnical Engineering*, Arlington.

ANNEX 3 – Foundations Movements

So be course not to be commanded by the crowd, but to follow your hearts and your consciences. Big risks, big life. Small risks, small life.

Icarus wax Wings conceived by
Daedalus

A3.1 STATIC CONDITIONS

The foundation movements shall not reach certain limit values to avoid the occurrence of an ultimate limit state or a serviceability limit state.

Burland and Wroth (1974) proposed a consistent set of definitions based on the displacements, that are illustrated in Figure A3.1:

rotation (θ) is the change in gradient of a line joining two reference points;

the angular strain (α), defined in Figure (A3.1a), is positive for upward concavity (sagging) and negative for downward concavity (hogging);

relative deflection (Δ) is the displacement of a point relative to the line connecting two reference points on either side (see Figure A3.1.(b)).

deflection rate Δ/L, where L is the distance between the two reference points defining Δ;

tilt (w) describes the rigid body rotation;

relative rotation ($\Re$) – is the rotation of the line joining two points;

average horizontal strain (e_n) is defined as the change of length δ_L over the length L.

vi)

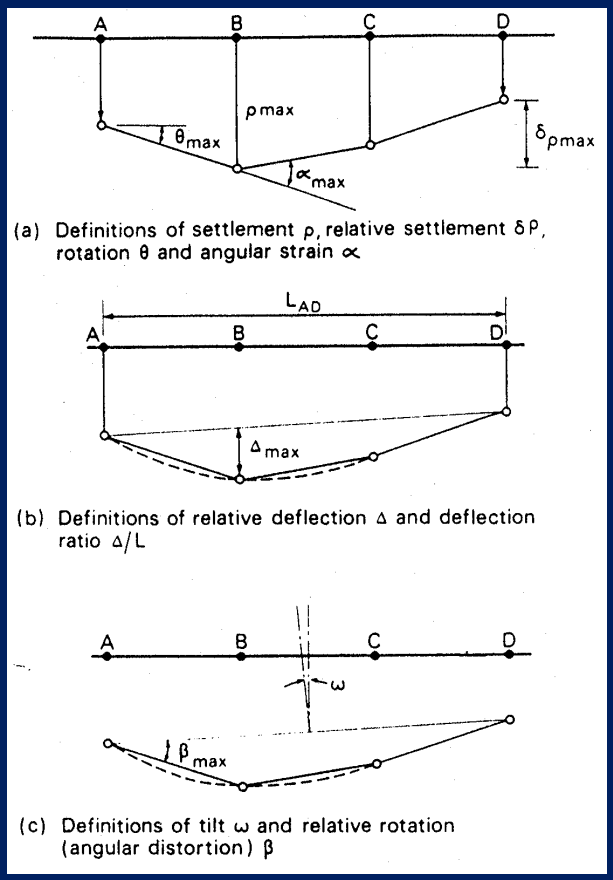

Figure A3.1 Definition of foundation movements

The selection of design values for limiting movements shall take account of the following:

- the confidence with which the acceptable value of the movement can be specified;
- the type of structure;
- the type of construction material;
- the type of foundation;
- the type of ground;
- the mode of deformation;
- the proposed use of the structure.

Table A3.1 presents a summary of allowable deformations proposed by different authors and EC7.

The allowable displacements for shallow foundations and raft foundations for sand and clay materials are summarised in Tables A3.2 and A3.3.

EC7 recommends that settlements for pile foundations for ultimate limit of states and serviceability limit of states shall include:

-the settlement of a single pile;

-the additional settlement due to group of action.

Bozozuk (1981), based on a study related with the allowable displacements in foundation bridges (piles) after the observation of 150 cases has proposed the limits for vertical settlement S_v and horizontal S_H defined in Table A3.4.

A recent study performed by Moulton (1986) based on 314 bridges located in United States and Canada has confirmed the proposal of Bozozuk (1981).

Burland et al (1977) have proposed 6 categories for damages in buildings related with Table 5 where categories 0,1 and 2 are related with stetic damages, categories 3 and 4 are related with serviceability limit of states and category 5 with ultimate limit of states (stability).

Burland et al (1977) the concept of limit tension deformation e_{lim} to define the ultimate limit state.

Boscardin and Cording (1989) develop the concept of different levels of strain and have proposed based in the analysis of 17 cases the Table 6 to establish the relationship between category of damage and limiting tensile strain.

Burland (1995) proposed three levels of risk for buildings: (i) preliminary evaluation; (ii) evaluation of second level; (iii) detailed evaluation.

For preliminary evaluation of buildings a value of less than 1/500 or settlement less than 10 mm are considered of degree of severity negligible.

For buildings of damage category 3 or higher a detailed evaluation shall be performed.

A limit value for deformation is related with the occurrence of an ultimate limit state or of a serviceability limit state.

The differential settlements and relative rotations of foundations shall be established in order to avoid the occurrence of an ultimate limit state or a serviceability limit state (like cracking).

The computation of the differential settlement shall take into consideration:

- the variations of the ground properties;

- the distribution of loads;

- the construction methodology;

- the stiffness of the structure.

Table A3.1 Allowable deformations

A – Concrete buildings and reinforced walls

Allowable values for rotations	Skempton and MacDonald (1956)	Meyerhof (1956)	Polshin et Tokar (1957)	Bjerrum (1963)	EC7 (1994)
Structural Damages and cracks	1/150 1/300	1/250 1/500	1/200 1/500	11/150 /1/500	11/150 11/300

B – Wall without reinforcement

Deflection ratio Δ/L	Meyerhof (1956)	Polshin & Tokar (1957)	Burland & Wroth (1975)
Deformation ∪	1/2500	L/H < 3 1/3500 to 1/2500; L/H > 5 1/2000 to	1/2500 L/H = 1 1/1250 L/H = 5

		1/1500	
Deformation	∩-	--	1/5000 L/H = 1 1/2500 L/H = 5

Table A3.2 Allowable settlements (in mm)

for isolated foundations

Allowable values for isolated foundations	Burland et al. (1977)	Skempton & MacDonald (1956)	EC7 (1994)
Total settlements in sands Differential settlements in sands	25 20	40 25	50 20
Total settlements in clays Differential settlements in clays	45 25	65 40	High values

Table A3.3 Allowable values for raft foundations settlements (mm)

Allowable values for raft foundations settlements	Terzaghi and Peck (1948)	Skempton and MacDonald (1956)	Burland et al (1977)	EC7
Sandy soils	50	40 to 60	High values	50
Clay soils		65 to 100		

Table A3.4 Allowable values for bridge foundations

Damage classification	Limit values
Allowable or acceptable	S_V < 50 mm S_H < 25 mm
With acceptable damages	50 mm = S_V = 100 mm 25 mm = S_H = 50 mm
Non acceptable	S_V < 100 mm S_H > 50 mm

Table A3.5 Damages categories in buildings (after Burland et al, 1977)

Damage category	Degree of severity	Description of damage
0	Negligible	Hairline cracks 0,1 mm
1	Very light	Fine cracks, easily treated
2	Light	Cracks easily filled
3	Moderate	Cracks required some opening
4	Severe	Extensive repair working involving breaking and replacement
5	Very Severe	Major repair involving partial or complete rebuilding

TableA3.6 Categories of damages in buildings (after Boscarding and Cording, 1989)

Category of damage	Degree of severity	Limiting tensile strain (%)
0	Negligible	0 - 0,05
1	Very slight	0,05 - 0,075
2	Slight	0,075 - 0,15
3	Moderate	0,15 - 0,3
4 to 5	Severe to very severe	>0,3